Springer Series in Vision Research

Gábor Horváth *Editor*

Polarized Light and Polarization Vision in Animal Sciences

Second Edition

Springer Series in Vision Research

Volume 2

For further volumes:
http://www.springer.com/series/10633

Gábor Horváth
Editor

Polarized Light and Polarization Vision in Animal Sciences

Second Edition

Springer

Editor
Gábor Horváth
Environmental Optics Laboratory,
Dept. Biological Physics
Eötvös University
Budapest, Hungary

Originally published as "Polarized Light in Animal Vision: Polarization Patterns in Nature" by Gábor Horváth and Dezső Varjú (2004)

Videos to this book can be accessed at
http://www.springerimages.com/videos/978-3-642-54717-1

ISBN 978-3-642-54717-1 ISBN 978-3-642-54718-8 (eBook)
DOI 10.1007/978-3-642-54718-8
Springer Heidelberg New York Dordrecht London

Library of Congress Control Number: 2014948469

Printed on acid-free paper

Springer is part of Springer Science+Business Media (www.springer.com)

Preface to the Series

The Springer Series in Vision Research is a comprehensive update and overview of cutting-edge vision research exploring current breakthroughs at a conceptual level. It details the whole visual system from molecular processes to anatomy, physiology and behaviour and covers both invertebrate and vertebrate organisms from terrestrial to aquatic habitats. Each book in the series is aimed at all individuals with interests in vision including advanced graduate students, post-doctoral researchers, established vision scientists and clinical investigators. The series editors are N. Justin Marshall (Queensland Brain Institute, The University of Queensland, Australia) and Shaun P. Collin (Neuroecology Group within the School of Animal Biology and the Oceans Institute at The University of Western Australia).

This volume on polarisation vision is the second in the Springer Series in Vision Research and exemplifies the broad range and appeal we are aiming for in this series. It includes some aspects of review and collation of ideas but is largely concerned with recent advances in this field. Terrestrial and aquatic systems are considered, and both vertebrate and invertebrate visual systems are discussed. Invertebrate retinal design is, for reasons explained in some of the chapters, more conducive to polarisation vision, and as a result, most of the work contained in the volume is around our advancing knowledge in these taxa. Polarisation vision, or more strictly polarisation sensitivity, in animals is rapidly expanding to take up a level of importance alongside colour vision. We are learning that several species communicate with polarisation patterns for mate choice and that there may be an 'arms races' in the evolution of this visual modality, where predator and prey compete. Some animal groups, such as cephalopods and crustaceans may, in fact, glean more information from their environment using polarisation cues rather than colour cues. This is an exciting new world for us, as humans are largely insensitive to polarised light (but see Chaps. 14 and 25). We need filters, such as polarising

sunglasses, or polarisation-sensitive cameras to join the animals in their use of this property of light. Several of the chapters also touch on different technical engineering aspects, suggesting some of the ways that polarisation vision may be bio-inspirational for creating our own imaging systems.

Perth, Australia — Shaun P. Collin
Brisbane, Australia — N. Justin Marshall

Preface to the Volume

This book provides a much needed update on the Springer volume entitled *Polarized Light in Animal Vision—Polarization Patterns in Nature* (Horváth and Varjú 2004). Much has happened in this field in the last 10 years. The main goal of this volume is to summarise new results but also place these in the context of past work. Each of the chapters is written by relevant experts in each field and includes a thorough literature survey and explores future research directions. Literature prior to 2004 is also extensively cited here; however, we focus mainly on the results obtained in the last decade. Other useful reviews of the field that have appeared in this period include the special issue 'New directions in biological research on polarized light' in the *Philosophical Transactions of the Royal Society B* edited by Marshall et al. (2011) and the review by Wehner and Labhart (2006) on polarisation vision in the book entitled *Invertebrate Vision* edited by Warrant and Nilsson. The book of Können (1985) entitled *Polarized Light in Nature* and the booklet of Pye (2001) entitled *Polarised Light in Science and Nature* introduce the reader to the world of light polarisation and some of its applications.

This book is intended for anyone interested in animal vision, environmental optics, polarised light and polarisation sensitivity, including biologists, physiologists, ecologists and physicists. In particular, the recent advances in imaging polarimetry, which translate the parameters of polarisation into colour, allow the reader to understand the information within the polarisation patterns of the optical environment not directly accessible to the human visual system. Such instrumentation has also allowed polarisation research to advance rapidly, as we can now glimpse this previously hidden world.

Part I of the book deals with the polarisation vision in animals and humans. Chapter 1 gives an overview on the historical perspective of polarisation vision research. The subject of Chap. 2 is polarisation vision and orientation of ball-rolling dung beetles, which is governed partly by sky polarisation. Dung beetles, unlike most insect navigators, do not need to locate a stationary nest at the end of their foraging journey. Their main task is to roll their dung ball from the dung source as quickly and as far from potential competitors as possible. That is along a straight line to avoid the attack of other dung beetles that might steal the ready-made ball.

During their straight-line orientation, they rely on celestial compass cues to move along straight paths and can even achieve this at night using both moon and starlight. Chapter 3 summarises recent knowledge regarding polarisation vision in the most extensively studied groups such as ants, bees and wasps, using behavioural, anatomical and physiological approaches. Chapter 4 deals with polarisation-based behaviour, polarisation detectors and polarised-light processing in the brains of desert locusts, Monarch butterflies, crickets, houseflies and fruit flies. Polarisation sensitivity is also considered in the context of colour vision.

The topic of Chap. 5 is polarisation vision in aquatic insects. The recently discovered polarisation sundial of these insects explains why they fly at low and/or high sun elevations at different times of the day or evening. Polarisation-based water detection and positive polarotaxis (attraction to horizontally polarised light) in non-biting midges, dragonflies, mayflies and tabanid flies are surveyed. It is shown that the polarotaxis in egg-laying yellow fever mosquitoes is odour masked. Finally, it is demonstrated how negative polarotaxis in desert locusts can hinder flying over the sea.

Chapter 6 deals with the potential for circular polarisation vision of scarab beetles. The appearance of circular polarisation in the abiotic and biotic optical environment is surveyed, and the polarisation characteristics of circularly polarising scarab beetle cuticle, as measured by imaging polarimetry, are presented. Finally, behavioural evidence for the lack of circular polarisation sensitivity in four scarab species with a circularly polarising exocuticle—*Anomala dubia*, *A. vitis* (Coleoptera, Scarabaeidae, Rutelinae) and *Cetonia aurata*, *Protaetia cuprea* (Coleoptera, Scarabaeidae, Cetoniinae)—is presented. Previously suggested circular polarisation sensitivity in the scarab species *Chrysina gloriosa* is considered and criticised.

Chapter 7 is about the polarisation vision of crustaceans. It surveys the polarised light sources for crustaceans, the structural basis and neural processing of polarisation sensitivity and polarisation-based behaviours in crustaceans. Chapter 8 details polarisation sensitivity and its functions in cephalopods. Chapter 9 summarises the recent results about the structural and neural mechanisms of polarisation sensitivity in fishes, the functions of which are object recognition, navigation and camouflage. Chapter 10 is devoted to polarisation sensitivity in amphibians. It describes amphibian photoreception, the pineal complex, the use of polarisation sensitivity in orientation and the possible connection between polarisation sensitivity and magnetoreception. Chapter 11 surveys the photoreceptors and mechanisms underlying polarisation sensitivity in crocodiles, lizards and snakes. It also considers the possible use of polarisation sensitivity for orientation in reptilian migration. Chapter 12 examines polarisation vision in birds. It deals with avian celestial orientation and migration, the importance of skylight polarisation in avian compass calibration and the behavioural evidence for polarisation sensitivity in birds.

Chapter 13 examines some of the possible interactions between colour vision and polarisation vision. It is shown how polarisational false colours could help

visual discrimination between smooth (shiny) and rough (matte) leaf surfaces but cannot unambiguously code surface orientation. This chapter also demonstrates how uniformly polarisation-sensitive retinas can perceive polarisation-induced false colours. Chapter 14 reviews the available knowledge of human polarisation sensitivity. It deals with Haidinger's and Boehm's brushes and the potential mechanisms underlying these visual phenomena. Some applications of human polarisation sensitivity are also considered.

Part II of the book concerns mainly descriptions of the physics of polarised light in nature but with specific reference to animal polarisation vision. Chapter 15 is about underwater polarisation induced by scattering hydrosols. It considers the sources of polarised light in the ocean, the transmission (refraction) of polarised light at the air–water interface, the attenuation of polarisation by scattering and absorption, the effect of water turbidity on polarisation, measurements and modelling of polarisation in clear and turbid waters and the polarisation-based response of animals living in turbid waters.

Chapter 16 presents polarisation patterns of freshwater bodies and their likely role in guiding water detection in aquatic insects. Polarisation visibility of water surfaces is also measured and calculated as a function of the solar elevation angle, which explains why water-seeking polarotactic aquatic insects might fly at low and/or high sun elevations.

Chapter 17 presents the polarisation characteristics of forest canopies and shows how the azimuth of the foliage-occluded sun can be determined from the pattern of the direction of polarisation of sunlit foliage canopies. Why dusk-active cockchafers sense downwelling polarisation in the green part of the spectrum is also explored.

Chapter 18 demonstrates the robustness of the celestial E-vector pattern, which is the basis of orientation of many polarisation-sensitive animals and the basis for hypothetical sky-polarimetric Viking navigation. It is shown how well the Rayleigh model describes the pattern of the angle of polarisation of clear and cloudy skies. The polarisation characteristics of foggy, partly cloudy, overcast, twilight and eclipsed skies are also revealed including fogbows and the 'water-skies' above arctic open waters. The anomalous sky polarisation due to forest fire smoke is also presented as a way of explaining why some polarisation-sensitive insects disorient under smoky skies. Similarly, the changed sky polarisation during total solar eclipses is discussed with respect to its influence on the orientation of honeybees. Finally, it is shown how skylight polarisation is transmitted through Snell's window on flat water surfaces.

Chapter 19 surveys the linearly and circularly polarised signals from terrestrial and aquatic animals, such as butterflies, beetles, flies, dragonflies, spiders, fiddler crabs, birds, stomatopods, cephalopods and fishes.

Chapter 20 is devoted to anthropogenic polarisation and polarised light pollution (PLP), which induces polarised ecological traps for polarotactic insects, such as water beetles, aquatic bugs, dragonflies, mayflies, caddisflies and stoneflies. It is shown that the maladaptive attractiveness of solar panels to polarotactic insects can

be reduced by surface fragmentation due to white grid patterns. The PLP of asphalt surfaces, black horizontal agricultural plastic sheets, glass surfaces, shiny black gravestones and dark car bodies is considered in detail. The insectivorous animals (birds, spiders and bats) lured by the polarotactic insects attracted to polarised-light-polluting artificial surfaces are also surveyed. The questions of why vertical glass panes attract polarotactic insects and why these insects remain on such glass surfaces after landing are answered. It is shown how the vertically polarised mirror image of bridges on the water surface can deceive flying mayflies and what are the ecological consequences. Finally, it is explained why strongly polarising black and burnt stubble fields do not attract polarotactic aquatic insects.

Part III of the book summarises several practical applications of polarisation vision and patterns. Chapter 21 surveys existing knowledge about polarisation as a guiding cue for oviposition in non-biting midges (chironomids) and mosquitoes. Chapter 22 presents recent research about linearly polarised light and its use as a guiding cue for water detection and host finding in tabanid flies. It is shown that bright animal coats are only weakly attractive to polarotactic tabanids. A new explanation of the evolutionary advantage of zebra stripes and spotty fur patterns is also presented. We show that stripes and spots make ungulates unattractive to host-seeking female tabanid flies, and stripes disrupt the odour attractiveness of host animals to tabanids.

Chapter 23 surveys novel polarisation-based insect traps. Polarisation chironomid traps are initially considered, followed by three different polarisation tabanid traps, which are presented as a new technique of horsefly control to capture host- and water-seeking tabanids.

Chapter 24 is devoted to polarisation cloud detection with imaging polarimetry. It reviews the full-sky photometric imagers and photometric cloud detection algorithms and examines the airborne PARASOL and POLDER polarisation cloud detectors. The applications of polarisation cloud detection for the determination of cloud distribution, cloud-base height, solar forecasting, aerosol characterisation, Viking navigation and the study of animal orientation are also presented.

Chapter 25 examines the possibility and the atmospheric prerequisites of hypothetical sky-polarimetric Viking navigation. Modern sky-polarimetric navigation, the medieval Norse sailing routes, the climatic conditions in the Viking era and the presumed nature of the enigmatic Viking sunstone are initially considered. Then, the possibility of sky-polarimetric Viking navigation under various weather conditions is discussed. The hypothesised Viking solar navigation instruments (horizon board, Viking sun compass, twilight board, medieval twilight navigation toolkit, sun-shadow board with a sundial and millennium-old carved schedule) are all surveyed. Some atmospheric-optical phenomena providing alternative navigation cues are also summarised.

Additional photographs, polarisation patterns, tables, graphs and video films are provided electronically.

We dedicate this book to the late Professors Talbot H. Waterman and Dezso Varju and to Professor Rudiger Wehner on the occasion of his 75th birthday.

The oeuvre of Waterman was appreciated recently by Cronin, Marshall and Wehling (2011). Dezső Varjú, the mentor of the editor of this volume, Gábor Horváth, and one of the authors of the book *Polarized Light in Animal Vision—Polarization Patterns in Nature*, unfortunately died in August 2013. Finally, we greet Professor Rudiger Wehner on the occasion of his 75th birthday.

Budapest, Hungary — Gábor Horváth
Perth, Australia — Shaun Collin
Brisbane, Australia — Justin Marshall
January 2014

References

Cronin TW, Marshall J, Wehling MF (2011) Dedication: Talbot H. Waterman. Philos Trans R Soc B 366: 617–618

Horváth G, Varjú D (2004) Polarized light in animal vision—polarization patterns in nature. Springer, Heidelberg, p 447

Können GP (1985) Polarized light in nature. Cambridge University Press, Cambridge

Marshall J, Cronin T, Wehling MF (2011) New directions in the detection of polarized light. Philos Trans R Soc B 366:615–616

Pye JD (2001) Polarised light in science and nature. Institute of Physics Publishing, London

Wehner R, Labhart T (2006) Polarization vision. In: EJ Warrant, DE Nilsson (eds) Invertebrate vision. Cambridge University Press, Cambridge, pp 291–348

Acknowledgements

My financial support to write this book was given by the Alexander von Humboldt Foundation, providing a 3-month research fellowship (3.3-UNG/1073032 STP) from 1 June to 31 August 2013 in the Zoological Institute of the University of Regensburg in Germany. I am thankful for the kind hospitality of Professors Jürgen Heinze and Stephan Schneuwly at Regensburg University and also appreciate the secretarial and technical assistance of Sonja Dörfner and Eva Köppl (secretaries) and Stephan Buchhauser (computer expert) at the departments of Professors Heinze and Schneuwly.

My researches were supported by (1) the grant TabaNOid 232366 (Trap for the Novel Control of Horse-flies on Open-air Fields) funded by the European Commission under the 7th Framework Programme, (2) the grant OTKA K-105054 (Full-Sky Imaging Polarimetry to Detect Clouds and to Study the Meteorological Conditions Favourable for Polarimetric Viking Navigation) from the Hungarian Science Foundation, (3) the grant OTKA K-68462 (Polarotaxis in Caddis Flies and Tabanid Flies) from the Hungarian Science Foundation, (4) equipment donation from the Alexander von Humboldt Foundation and (5) financial support from the Forest Paper Ltd (Ferenc Bodrogai, Drs. László Horváth and Viktor Horváth). Many thanks to Csaba Viski (Szokolya, Hungary) and István Simon (Göd, Hungary), who allowed our tabanid experiments to be performed on their horse farms. We are grateful to Mónika Gyurkovszky and Prof. Róbert Farkas (Department of Parasitology and Zoology, Faculty of Veterinary Science, Szent István University, Budapest) and to Prof. József Majer (Department of Hydrobiology, University of Pécs, Hungary) for the taxonomic identification of the tabanid species captured in our field experiments. The management of the Hungarian patents of different polarisation tabanid traps by Györgyi Antoni (director of the Center for Innovation and Grant Affairs, Eötvös University, Budapest) is also acknowledged.

I am grateful to my Hungarian colleagues, co-authors and students for their indispensable contributions to the results summarised in this book: Professors György Dévai, Róbert Farkas, József Majer; Doctors András Barta, Balázs Bernáth, László Péter Bíró, Pál Boda, Zoltán Csabai, Gábor Fekete, József Gál, Ramón Hegedüs, Tibor Hegedüs, Tamás Herczeg, Ákos Horváth, György Kriska, Szabolcs

Lengyel, Ákos Molnár, Arnold Móra, László Neumann, István Pomozi, István Seres, Győző Szél, Ildikó Szivák, Miklós Tóth; Mrs. Lea Báhidszki, Orsolya Buza, Alexandra Farkas, Mónika Gyurkovszky, Júlia Jósvai, Éva Prill, Csenge Sinkovics, Brigitta Sipőcz, Nikolett Tarjányi and Mr. Pál Barta, Miklós Blahó, László Czinke, Ádám Egri, László Fogl, István Gubek, Ottó Haiman, András Havasi, Loránd Horváth, Sebestyén Lénárd Horváth, Krisztián Kertész, Péter Malik, Kristóf Málnás, László Polyák, András Sándor, Bence Suhai, and Dénes Száz. Special thanks are to Sándor Hopp (Mechanical Workshop, Physical Institute, Eötvös University, Budapest) for producing the mechanical equipments used in the Hungarian field experiments with tabanids and horses.

Thank you for the possibility to participate on the following expeditions and polarimetric measuring campaigns: (1) August–October 2005: Beringia 2005 international polar research expedition on the Arctic through the North Pole (organised by the Swedish Polar Research Secretariat, Stockholm; in cooperation with Prof. Susanne Åkesson, Department of Biology, Centre for Animal Movement Research, University of Lund, Sweden). (2) August 2006: Oulu, Finland (in cooperation with Prof. Benno Meyer-Rochow, University of Oulu, Finland). (3) September–October 2008: Lund, Sweden (in cooperation with Prof. Susanne Åkesson). (4) October–November 2010: expedition ANT-XXVII/1 onboard research vessel Polarstern from Bremerhaven through the Atlantic Ocean up to Cape Town (in cooperation with Prof. Andreas Macke and Dr. Ákos Horváth, Leibniz Institute for Tropospheric Research, Leipzig, Germany, and Dr. Karl Bumke, Helmholtz Center for Ocean Research, Kiel, Germany).

Mária Horváth-Fischer and János Horváth, my parents, rendered indispensable help and support during the Hungarian field experiments in Kiskunhalas and Kunfehértó. I am very grateful to my wife, Zsuzsanna Horváth-Tatár, who ensured the ideal, quiet and familiar atmosphere, which was one of the most important prerequisites of my work.

Ramón Hegedus acknowledges the financial support of the German Science Foundation (Deutsche Forschungsgemeinschaft) within the Emmy Noether project IH 114/1-1. He is also grateful to the Alexander von Humboldt Foundation for receiving a Humboldt Fellowship for Experienced Researchers.

Last, but not least, we are also very much indebted to Springer-Verlag, especially to Verena Penning, Jutta Lindenborn, Sylvia Gschwilm-Drees, Melissa Higgs and Lars Koerner, who initiated the publication of this book and provided the editors and co-authors with valuable advice and technical support while preparing the manuscript. I also thank the series editors, Professors Shaun P. Collin and N. Justin Marshall, for their continuous help during the writing of this volume.

Budapest, Hungary Gábor Horváth

Contents

Part I
Polarization Vision in Animals and Humans

Chapter 1
Polarization Vision: A Discovery Story

Rüdiger Wehner

Abstract During the last half a century, polarization vision has become a flourishing field of multidisciplinary research in neuroethology and sensory ecology spanning the full methodological range from membrane biophysics and photoreceptor optics to behavioural analyses in the laboratory as well as in the field. It comprises a multitude of behavioural tasks accomplished by various groups of animals in both terrestrial and aquatic environments. The fact that this richness of behaviours mediated by naturally occurring polarized light has come to the fore only rather recently is certainly due to our own inability to perceive these polarized light phenomena without the aid of special optical devices. While in the present book the chapters are arranged according to animal taxa, so that questions are posed and arguments are presented within the branching pattern of the phylogenetic tree, this introductory chapter retraces the time arrow of discovery. For example, immediately after Karl von Frisch had demonstrated that bees can perceive the polarization of skylight, the 1950s were dominated by the search for the polarization analyser in arthropod eyes. The 1970s and early 1980s became high noon for the behavioural experimental analysis of the bee's and ant's skylight compass, followed in the 1990s by the advent of forceful neurobiological investigations of the polarization vision network residing in the insect (especially locust) brain. At about the same time polarized reflections from water surfaces were recognized as cues used by flying aquatic insects on dispersal. In the late 1980s vertebrates, mainly fish and birds, appeared on the polarization vision scene as well. Since the turn of the millennium long-standing studies of various aspects of underwater polarization vision have received an enormous boost, especially by including small-field, close-range polarization signalling, and now advance at an ever increasing pace. Most recently, with new technologies at hand, the interest in the basic mechanisms of polarization sensitivity comes full circle when now a closer and

R. Wehner (✉)
Brain Research Institute, University of Zurich, Winterthurerstrasse 190, CH-8057 Zurich, Switzerland
e-mail: rwehner@zool.uzh.ch

G. Horváth (ed.), *Polarized Light and Polarization Vision in Animal Sciences*,
Springer Series in Vision Research 2, DOI 10.1007/978-3-642-54718-8_1,

more sophisticated look can be taken at the molecular mechanisms of how dichroism is generated within the photoreceptor membrane.

1.1 Introduction

The story of polarization vision started with an observation that appeared mysterious at the time. In 1914 Felix Santschi showed that ants were able to maintain their straight homeward courses even if they could see only a patch of unobscured sky offered to them via an open-topped cardboard cylinder. While this cylinder was carried along with the moving ant, it continuously screened off the sun. Even though Santschi tested only a few specimens of ants belonging to some *Messor*, *Monomorium*, *Cataglyphis* and *Camponotus* species, the results were clear-cut: The sun-free sky had presented the ants with sufficient compass information. Unaware of the phenomenon of polarized light, Santschi hypothesized that light intensity gradients perceived by the ants within the circular skylight window might have provided the decisive cues, or that the ants endowed with heavily shielded small-field light detectors (ommatidia) in their compound eyes might have been able to see the stars in the daytime sky, 'just as Aristotle had surmised that a person sitting at the bottom of a deep well could perceive the stars in the blue diurnal sky'. Even though Santschi did not draw the right conclusion from his startling discovery, which he published only many years later (Santschi 1923), he was the first to show that insects could derive compass information not only from the direct light of the sun but also from the scattered light in the sky (for a biographical account on Felix Santschi published on the occasion of the 50th anniversary of his death, see Wehner 1990).

Several decades later, in 1947, Karl von Frisch not knowing of Santschi's early account did an experiment in bees that was almost identical to the one Santschi had performed in ants, with the only difference that he studied the bees while they were performing their recruitment dances in the hive rather than their foraging journeys in the field. When he provided the dancing bees with a small patch of cloudless sky, he got the same result and asked the same question which Santschi had pondered on, but in contrast to Santschi—and advised by the physicist Hans Benndorf—he checked for polarized light. Next summer he did the crucial experiment. He placed one of the polaroid sheets which had just become commercially available above a bee dancing on a horizontal comb. As he rotated the polarizer, the bee changed the direction of its dance accordingly (von Frisch 1949). On the one hand, this discovery stimulated quite a number of scientists to place polarizing sheets above walking insects and other arthropods and to demonstrate that the animals changed their courses when the polarizer was rotated (e.g. ants: Vowles 1950; Carthy 1951; Jander 1957; flies: Wellington 1953; beetles: Papi 1955a; amphipod crustaceans: Pardi and Papi 1952; spiders: Papi 1955b; Görner 1958). On the other hand,

Karl von Frisch's discovery immediately raised two major questions: First, where are the polarization analysers in the insect's eye, and second, what neural mechanisms and behavioural strategies do the animals employ in using polarized skylight as a compass cue?

1.2 Search for the Analyser

The obvious hypothesis that the polarization analysers were located as some kind of optical polarizing filters in front of the photoreceptors, i.e. somewhere within the dioptric systems of the compound eyes, had indeed been proposed (e.g. Berger and Segal 1952; Stephens and Fingerman 1953), but could be refuted. Careful optical measurements provided clear evidence that neither the corneal lenses nor the crystalline cones of the individual ommatidia exhibited any dichroic properties in the direction of incident light, and hence could not serve as polarization analysers (Stockhammer 1956). Later, simultaneous intracellular recordings from pairs of photoreceptor cells located within the same ommatidium and thus receiving light via the same dioptric apparatus revealed cells that differed in their E-vector tuning axes (Shaw 1967). These findings provided compelling evidence for the proposal of Hansjochem Autrum and Hessel de Vries that the sensitivity of insect photoreceptors to linearly polarized light was an intrinsic property of the photoreceptors themselves and resulted from the dichroism of the visual pigment (rhodopsin) molecules and their preferential alignment within the photoreceptor membrane (Autrum and Stumpf 1950; de Vries et al. 1953). Note that the rhodopsin molecules get activated only when the electric (E-)vector of light vibrates within the plane of the excitable double bond of the molecule (the 11-cis bond of the chromophore retinal). Just a few years after the receptor-analyser hypothesis had been proposed, Humberto Fernández-Morán performed the first electron microscopic study of an insect retina. Indeed, in his 2-page *Nature* paper he was able to present the most likely structural basis of the intrinsic dichroism of photoreceptor cells. He showed that the light-absorbing parts of these cells, the rhabdomeres, consisted of stacks of microvillar tubes arranged in parallel to each other and perpendicularly to the optical axis of the cell, and already interpreted these microvillar stacks as the very polarization analysers that had been searched for since Karl von Frisch's discovery (Fernández-Morán 1956). Immediately thereafter, an upsurge of electron microscopic analyses of photoreceptors in *Musca*, *Sarcophaga* and *Drosophila* flies (Danneel and Zeutzschel 1957; Goldsmith and Philpott 1957; Wolken et al. 1957), and a little later in honey bees (Goldsmith 1962), provided further evidence for the fine structure of insect rhabdomeres. When finally the first intracellular recordings were performed in insect photoreceptors, the polarization sensitivity of these cells became immediately apparent (in *Lucilia* and *Calliphora* flies: Kuwabara and Naka 1959; Burkhardt and Wendler 1960). In conclusion, by the end of the 1950s sufficient anatomical and physiological evidence supported the hypothesis that the intrinsic dichroism of rhabdomeric photoreceptors of insects—and other

arthropods (*Limulus*: Miller 1957)—formed the basis of the polarization sensitivity of photoreceptor cells.

After these 'roaring fifties' in the early research on polarization vision—research including the first anatomical, electrophysiological and behavioural investigations on the perception of polarized light—more than a decade passed until the dichroism and polarization sensitivity of photoreceptors became the focus of detailed studies, both theoretically and experimentally. For example, the question was raised why vertebrate photoreceptors were apparently insensitive to polarized light. Spectroscopic measurements performed at Harvard University (Brown 1972; Cone 1972) led to the conclusion that in the rod outer segments of frogs, the rhodopsin dipoles were free to rotate within the photoreceptor membrane, so that at any one time no preferred orientation of absorption axes would prevail (for lateral diffusion in addition to rotational diffusion, see Poo and Cone 1974). This view was soon extended to vertebrate photoreceptors in general. Even though we now know, and shall see later, that such generalizations were premature, at the time it was taken for granted that the staggered sheets of vertebrate photoreceptor membranes were characterized by a random distribution of pigment absorption axes rendering these stacks of membranes insensitive to any particular E-vector of on-axis incident light. Under this assumption it was soon realized that if such photoreceptor membranes were rolled into narrow tubes (as is the case in the microvilli of rhabdomeric photoreceptors), these tubes would already exhibit some, though low, dichroism for the simple geometrical reason that the randomly distributed molecular dipoles at the side flanks of the tubes could be activated only by light polarized parallel to the axis of the tubes. What resulted was a dichroic ratio of maximally 2 (Moody and Parriss 1961). Furthermore, when whole stacks of microvilli were considered, these periodically packed structures were found to generate what has been called form dichroism (Laughlin et al. 1975; Israelachvili and Wilson 1976). However, both geometrical effects could not explain the high polarization sensitivities (PS = 5–19) usually recorded from insect photoreceptors. Soon the literature about PS recordings in insect photoreceptor cells increased substantially (revs. Wehner 1983; Wehner and Labhart 2006), so that in the present context it might suffice to mention that the first high PS values lying within the range mentioned above were recorded in dragonflies by Simon Laughlin (Laughlin 1976), to whom we also owe important theoretical considerations about dichroism and polarization sensitivity in rhabdomeric photoreceptors in general (e.g. Laughlin et al. 1975).

High polarization sensitivities could only result from some alignment of the rhodopsin molecules along the microvillar axes and in addition, of course, from the alignment of the microvilli within the rhabdomere. Photopigment alignment was directly demonstrated in studies of light-induced dichroism (photodichroism: Goldsmith and Wehner 1977) and bump-frequency measurements (Lillywhite 1978). As to the molecular basis of this alignment, membrane-associated cytoskeletal elements have been discussed from early on in *Drosophila*, squid and crayfish photoreceptors (Blest et al. 1982; Saibil 1982; Stowe 1983; Decouet et al. 1984), but it has been only most recently that this field of research in membrane biophysics and biochemistry gathered momentum. For example, work in *Drosophila* led to the idea

that the entire phototransduction signalling complex is linked to the cytoskeleton (Montell 1999), and crystallization studies performed in squid rhodopsin made it most likely that the dimerization of rhodopsin molecules within the membrane and certain linkages of the rhodopsin dimers across the membranes of adjacent microvilli contributed to a paracrystalline membrane structure (Murakami and Kouyama 2008). In principle, such protein–protein contacts, as they occur within and across photoreceptor membranes, might be involved not only in increasing the polarization sensitivity of rhabdomeric photoreceptors, but also in rendering certain types of vertebrate photoreceptors (e.g. cones) sensitive to polarized light (Roberts and Needham 2007; Roberts et al. 2011; Chap. 9).

Before further elaborating on the functional significance of these recent studies in membrane biochemistry, let us return to the 1970s. At that time another startling discovery was made: the twist of the photoreceptor cells in the eyes of the honey bee—obviously a means of secondarily reducing or completely destroying the intrinsic polarization sensitivity of the cells (Wehner et al. 1975). The finding that in the bee retina the rhabdoms and with them the entire photoreceptor cells were twisted in a corkscrew-like way was greeted with disbelief. Based on apparent counter-evidence, the photoreceptor twist was claimed to be an artefact caused by improper preparation or fixation procedures (Ribi 1979, 1980). However, further detailed anatomical studies clearly established the twist as an in vivo trait of the bee's compound eyes (Wehner and Meyer 1981) and in addition showed that ontogenetically the twist of the photoreceptors occurred already in an early pupal stage, long before the rhabdomeric microvilli were formed (Wagner-Boller 1987; rev. Wehner 1994). Soon thereafter a similar kind of rhabdomeric twist was found and systematically studied in *Calliphora*, *Musca* and *Drosophila* flies (Smola and Tscharntke 1979; Smola and Wunderer 1981). In the latter, a start has even been made to analyse the molecular and cell biological events that lead to rhabdomeric twisting (Baumann and Lutz 2006).

Based on optical analysis it was assumed already in the original twist paper that the observed rate of twist (about 1°/μm) would completely destroy the polarization sensitivity of a bee's twisted retinular cell, if it were combined with low values of effective birefringence (Wehner et al. 1975). This assumption could finally be confirmed by intracellular recordings. In twisted and straight photoreceptor cells (the latter occur at the dorsal rim of the bee's eye, see below) polarization sensitivities amount to $PS < 2$ and $PS > 10$, respectively (Labhart 1980). Beyond this demonstration, however, the functional question remained: why did honey bees go to quite some length to abolish their polarization sensitivity by twisting their photoreceptors? The answer provided almost two decades later and based on spectroscopic measurements and computational analyses lent support to the hypothesis that the photoreceptor twist protects the insect's colour vision system from getting severely contaminated by polarization-induced false colours. This protection is necessary, because light reflected from mirror-like surfaces such as those of plants that are coated with waxy and thus shiny epicuticles gets partially polarized. If the input channels of the colour vision system picked up this polarized glare, the system would generate a wide and variable spectrum of 'false colours', which

would make it difficult to detect the real colours of the flowers to be visited by the bees (Wehner and Bernard 1993; Horváth et al. 2002; Chap. 33 of Horváth and Varjú 2004, pp. 362–380; Chap. 13). After the discovery of twisted photoreceptors, other kinds of rhabdomeric disorders were recognized (e.g. 'wobbling' of microvillar stacks in *Cataglyphis* ants: Räber 1979; Meyer and Domanico 1999), and several additional ways of reducing the polarization sensitivity of a photoreceptor cell such as self-screening within long rhabdomeres, electrical coupling of receptor cells with phase-shifted E-vector tuning axes and neural summation of the outputs of such cells were discussed and in some cases experimentally demonstrated (rev. Wehner 1983), but recently these issues have received little attention.

Towards the end of this section, let us return to the beginning, to what had been discarded as the primary source of the polarization sensitivity in insect compound eyes: extraretinal polarization analysers. A striking example of such an extraretinal analyser had been described in humans about a century before polarization vision was discovered in other animals. (As in vertebrates the retina is part of the brain, both ontogenetically and functionally, in this case 'extraretinal' means 'outside the receptor layer'.) The example to which I refer is the faint phenomenon of Haidinger's brush, a small bowtie-like pattern, which appears in the centre of the visual field and changes its orientation as an E-vector is rotated in the outside world (Haidinger 1844). It is caused by a radial analyser sitting in front of the foveal photoreceptors and consisting of the radial arrangement of the axons of cone photoreceptors in connection with dichroic macula pigment molecules (see Chap. 14). Moreover, even in eyes equipped with rhabdomeric and hence intrinsically dichroic photoreceptors, extraretinal structures have been found which enhance polarization sensitivity. Such a polarization enhancer was discovered in the single-lens (postero-median) eyes of a gnaphosid spider, *Drassodes cupreus* (Dacke et al. 1999). There a *tapetum lucidum* (a multilayer interference mirror) acts as a specular reflector that polarizes light just parallel to the microvillar orientation of the overlying photoreceptors. Nearly a decade later Tsyr-Huei Chiou, Tom Cronin, Justin Marshall and their collaborators at the University of Maryland and the Queensland Brain Institute made the most stunning discovery in this respect. Stomatopods—predatory and visually highly gifted marine crustaceans—employ a special set of ommatidia to detect circularly polarized light and to differentiate its handedness (Chiou et al. 2008). This remarkable sensory capacity is due to a quarter-wavelength plate (retarder) located on top of the photoreceptors and converting incoming circularly polarized into linearly polarized light, which is then analysed in the usual way by rhabdomeric photoreceptors underneath. The particular highlight of this mechanism is that the retarder itself consists of a photoreceptor cell (R8), which is designed in a way that the quarter-wavelength retardation results in the most efficient stimulation of the underlying receptors (R1–R7). Interestingly, the circularly polarized signals that these receptors are supposed to detect on certain body parts of conspecific animals are produced in a similar way. As most recently demonstrated, the dichroic carotinoid astaxanthin embedded in the stomatopod's cuticle causes reflected light to become linearly polarized

(Chiou et al. 2012). These reflections are then converted into circularly polarized light by an overlying quarter wave retardation layer (see Chap. 19).

The story of polarization vision started in invertebrates, and for about four decades invertebrates endowed with rhabdomeric photoreceptors have been considered the top and sometimes even the only candidates for perceiving and using polarized light. However, from the late 1980s onwards vertebrates, mainly birds (Phillips and Waldvogel 1988; Helbig 1990) and fish (Hawryshyn and Bolger 1990; Hawryshyn 1992; see also Sect. 1.3), have started to appear on the polarization scene. The behavioural data, on which claims about various kinds of polarization vision in these groups of animals have been based, are often ambiguous and leave many questions open (for fish, see Lerner et al. 2011 and Chap. 9; for birds, see Muheim 2011 and Chap. 12). However, at least in fish the search for the analyser has been significantly intensified in the last decade. As already reported in 1978, certain regions in the retina of anchovies (*Anchoa* and *Engraulis* species) contain cone photoreceptors with transversely oriented outer segments, so that the lamellar stacks of photoreceptor membrane are hit by light side on (Fineran and Nicol 1978; rev. Novales-Flamarique 2011). Furthermore, it is now widely agreed that internal reflections in double cones can provide the fish retina with polarization sensitivity (Cameron and Pugh 1991; Novales-Flamarique et al. 1998). A similar mechanism has been proposed for birds. In this case light scattered in a polarization-dependent way by a transparent oil droplet in the inner segment of the principal member of a double cone is thought to illuminate the outer segment of the associated cone sideways (Young and Martin 1984). Both hypotheses are based on the fact known since the classical work of the zoologist Wilhelm Josef Schmidt on the optical polarization properties of various biological tissues that vertebrate photoreceptors are highly dichroic when illuminated from the side (Schmidt 1924, 1951; see also Hárosi and MacNichol 1974).

Besides these cellular idiosyncrasies, so to speak, more general mechanisms of polarization sensitivity exhibited even by on-axis illumination may involve a number of ways of increasing the ordering of visual pigment molecules and leading to aligned arrays of dimers and oligomers of these molecules within the membranes of cone photoreceptors as well as slower diffusion times than previously suggested (see above). In goldfish, *Carassius auratus*, it could be directly shown that double cone (but not rod) photoreceptors display remarkable intrinsic axial polarization sensitivity (Roberts and Needham 2007). These recent studies, which benefit from an arsenal of modern technologies including atomic force microscopy and most elegantly a multi-trap laser tweezer system, are brilliantly portrayed by Roberts et al. (2011). It is in this area of multidisciplinary inquiry that the search for the vertebrate polarizer will become most exciting.

1.3 Unravelling the Polarization Compass

After Karl von Frisch's discovery the immediate interest in the polarization analyser had relegated studies on the functional design of the polarization compass into the background. Two decades had to pass until in the 1970s all of a sudden and completely independently of each other several Swiss (Wehner and Duelli 1971), German (Kirschfeld 1972; von Helversen and Edrich 1974), Russian (Zolotov and Frantsevich 1973), Dutch (van der Glas 1976) and American (Brines and Gould 1979) research groups started to inquire about the compass strategies employed by honey bees and desert ants during their foraging journeys. Within a few years quite a number of hypotheses were generated. For example, one hypothesis proposed that the insects would first determine the E-vector orientation in particular (at least two) points in the sky and in the second step apply spherical geometry to determine the position of the hidden sun—just as the rules of Rayleigh scattering in the atmosphere would predict (Kirschfeld et al. 1975). According to another hypothesis, the insects were considered to be able to locate the rotation pole of the celestial E-vector pattern and use this north pole as some kind of diurnal Polaris reference (Brines 1978). Finally, it was surmised that bees would transform the E-vector pattern in the sky into a trichromatic colour pattern (van der Glas 1976). However, all these authors had to consistently struggle for providing sufficient experimental evidence supporting their claims. A breakthrough came when in desert ants and a few months later in honey bees a small specialized dorsal rim area (DRA) was discovered anatomically (Herrling 1975; Schinz 1975; Wehner et al. 1975), analysed optically and electrophysiologically (Labhart 1980, 1986; Wehner 1982) and recognized behaviourally as being necessary and sufficient for detecting polarized skylight (Wehner 1982; Fent 1985; Wehner and Strasser 1985). Subsequently, a painstaking survey showed that DRAs of one kind or another occurred in various groups of insects (Labhart and Meyer 1999). A tiny DRA has even been found in the extremely miniaturized compound eyes of the microlepidopteran species *Phyllonorycter medicaginella*, in which the eyes are only 160 μm in diameter and contain no more than 149 ommatidia (Fischer et al. 2014).

However exciting the discovery of the DRA had been, in principle it only meant that the compass problem had been anatomically narrowed down from the entire dorsal compound eye as previously suggested to a small region at the uppermost dorsal rim of the eye. The compass strategy employed by bees and ants became apparent only after long series of sophisticated behavioural experiments had been performed, in which the animals were presented with limited views of the sky and had their compound eyes covered with light-tight paint except for limited parts of the eye. The overall result derived from the systematic navigation errors that occurred under these experimental conditions was that the ants and bees always tried to determine the angular position of the symmetry plane of the E-vector pattern (the solar vertical)—or what they considered to be the symmetry plane—relative to their direction of travel. In doing so they assumed that to the left and right of the symmetry plane, the E-vectors were distributed homogeneously, as they are

when the sun is at the horizon (for details and summaries see Rossel and Wehner 1984a, 1986; Wehner 1997; Wehner and Müller 2006).

As regards the neural machinery mediating this compass behaviour, an experimental chimera problem emerged. In bees and ants, in which the polarization compass had been unravelled behaviourally, it turned out to be extremely difficult to record electrophysiologically from polarization-sensitive interneurons, so that almost all such research was—and still is—done in larger and neurophysiologically more easily accessible insects, mainly in crickets and locusts. Drawing upon this work, which started in the late 1980s (Labhart 1988) and then advanced rapidly due to the beautiful studies of Uwe Homberg and his group at the University of Marburg, Germany, we now have a quite complete picture of the polarization vision network in the locust brain (Homberg 2004; Heinze and Homberg 2007; Homberg et al. 2011). As extensively described and referenced in Chap. 4, polarized light information is processed and passed on from the retinal DRA via a number of relay stations (optic lobes, anterior optical tubercle, lateral accessory lobe) to the central complex. There, in the protocerebral bridge, the entire 0°–180° range of E-vectors is represented in each hemisphere (Heinze and Homberg 2007, 2009). This is in accordance with Nicholas Strausfeld's hypothesis that the central complex provides a self-centred multimodal representation of azimuthal space (Strausfeld 1999, see also Homberg 2008), to which Stanley Heinze, Uwe Homberg and their collaborators have now masterly added the celestial E-vector gradient as a decisive component. It is easy to understand how this system could work as a skylight compass, if the animal referred to the E-vector in the zenith, because there the solar vertical always runs at right angles to this E-vector. *Cataglyphis* ants, however, do not use the zenithal skylight polarization, but read compass information preferentially from the frontal part of their DRA visual field, and in trying to do so they somersault backward when presented with an E-vector in the zenith (Duelli 1975; Wehner et al. 2014). If one wanted to use the locust's polarization vision network to simulate the navigational errors induced in bees and ants under particular skylight conditions (when the animals would compute an angular position of the celestial symmetry plane that did not coincide with the real position of this plane), one could determine the L0°–180°/R0°–180° response modulations of the protocerebral bridge that resulted when the animal rotated about its vertical body axis under these particular skylight conditions. As the mid-line neuropils of the central complex share the same basic architectural features in most insect species examined so far (Strausfeld 2012, pp. 310–352), using the polarization vision network of locusts for understanding the behaviourally dissected polarization compass of bees and ants might be justified, at least as a first attempt.

It was also in the early 1980s, i.e. at the time when the decisive work on the hymenopteran skylight compass was done, that in the ocelli of *Cataglyphis bicolor* the photoreceptors were found to be polarization sensitive (electrophysiological recordings: Mote and Wehner 1980) and to mediate E-vector compass responses (behavioural analysis: Fent and Wehner 1985). A quarter of a century passed until this topic was taken up again, this time in Australian desert ants, *Melophorus bagoti* (Schwarz et al. 2011a, b). In the wake of this new interest in ocellar function, the

spatial arrangement of ocellar rhabdoms across the retina was recently studied histologically in *Myrmecia* ants and several bee and wasp species (see Chap. 3). Certainly, the integration of information from the ocelli and the compound eyes will now open new avenues of inquiry. This is all the more challenging as even within the compound eyes of bees and ants celestial compass information is picked up not only by the polarization-sensitive DRA (polarization gradients in the sky) but also by the polarization-insensitive or weakly sensitive adjacent dorsal retina (spectral gradients in the sky) (Rossel and Wehner 1984b; Wehner 1994, 1997). The sun characterized by zero polarization and causing the highest green/UV receptor response ratio is a distinct point in either gradient. As studies in *Cataglyphis* ants have shown, the celestial compass system is quite versatile. For example, the ants can receive and store information by one celestial compass cue and later retrieve it by using another one (Wehner 1997; Lebhardt and Ronacher 2014). A possible neural substrate for the confluence of polarization and spectral information has been described in the locust brain (Kinoshita et al. 2007).

These different sensory inputs raised the question as to the salience of the various compass cues that insects derive from the sky. As it turns out, in contrast to ambient light intensity, spectral stimuli and the degree of polarization, the orientation of the E-vectors is by far the most robust cue being least affected by haze, dust and other atmospheric disturbances. Certainly, the most exciting recent discovery resulting from full-sky imaging polarimetry was that in the sunlit sky underneath the clouds (Pomozi et al. 2001) and even under moderate overcast conditions (Hegedüs et al. 2007a) and in light fog (Hegedüs et al. 2007b) quite robust E-vector patterns prevailed, in which the degree of polarization could be high enough to be detected by insects (see Chap. 18). In the latter cases these patterns are caused by the scattering of light by water droplets. The previous (classical) view was that skylight polarization resulted only from the primary (Rayleigh) scattering of sunlight by the air molecules (oxygen and nitrogen molecules), which are much smaller than the wavelength of light. Multiple scattering by larger particles, e.g. water droplets, was considered to depolarize the light so much that insects could not perceive it any longer.

The highest overall degree of polarization is reached in the clear sky when the sun is at the horizon and the band of maximum polarization extends across the zenith. At dusk the degree of polarization decreases in a slightly stepwise way until the E-vector pattern completely vanishes at the end of astronomical twilight, when the sun is 18° below the horizon and does not directionally illuminate the earth's outer atmosphere any longer. Depending on the local inclination of the sun's path, this occurs at about 1–1.5 h after sunset. The reverse happens during dawn (Rozenberg 1966; Coulson 1988; Cronin et al. 2006). It was already in one of the first studies on desert ant navigation that *Cataglyphis bicolor*, which naturally does not forage after sunset and before sunrise, could be experimentally shown to rely on its polarization compass during the twilight period (Wehner and Duelli 1971). Then this celestial compass governed the ants' directional responses until about 35 min after sunset (at dusk) and before sunrise (at dawn). At lower elevations of the sun, the polarization compass was smoothly superseded by the ants' wind compass (for

the latter, see also Müller and Wehner 2007). Forty years after these results had been obtained, another ant species, the night-active Australian bull ant, *Myrmecia pyriformis*, was described to use polarized skylight alongside landmark panoramas as a twilight compass cue (Reid et al. 2011), and South African dung beetles, *Scarabaeus zambesianus*, which are active during crepuscular times, were found to stabilize their straight running courses by the twilight pattern of polarization (Dacke et al. 2003a). Furthermore, just after the turn of the millennium, full-sky imaging polarimetry was applied to demonstrate the obvious: Due to light scattering in the atmosphere moonlight, like sunlight, generates a celestial pattern of polarization, which in its geometrical structure does not differ from the pattern generated by the sun, but is more than six orders of magnitude dimmer (Gál et al. 2001). Already two years after this demonstration, the very same species of dung beetle mentioned above was shown to rely on this dim E-vector pattern in the moonlit sky for maintaining its straight-line running courses (Dacke et al. 2003b; see Chap. 2). Even in birds it has been claimed, though not fully proven yet, that during migration the twilight periods are of special importance, because then the azimuthal position of the band of maximum polarization is potentially used for recalibrating the birds' magnetic compass (Muheim 2011; Chap. 12).

We cannot end this section without mentioning, at least in passing, that recently even *Drosophila* became the focus of exciting studies on E-vector orientation. In one study a portable flight arena was used in which magnetically tethered flies were flying under the open sky, where they adjusted their courses by means of the natural E-vector patterns perceived by the fly's DRA (Weir and Dickinson 2012). In another study, Mathias Wernet and his co-workers generated transgenic flies, in which the output of each class of photoreceptor could be inactivated. They showed that in the DRA the UV receptors R7 and R8 sufficed for polarotaxis, while the newly discovered ventral polarotactic response was mediated by the combined activity of weakly twisted UV and green receptors R7, R8 and R4, R5, R6, respectively (Wernet et al. 2012). Sure enough, genetic tools have entered the polarization vision arena.

1.4 Detecting Polarized Cues and Signals

In the 1980s, when the behavioural analysis of the hymenopteran skylight compass and work on the dorsal rim area of the bee's and ant's compound eye were in full swing, Rudolf Schwind from the University of Regensburg, Germany, discovered a polarotactic response mediated by the ventral retina of a water-seeking insect, the backswimmer *Notonecta glauca* (Schwind 1983, 1984). While flying on dispersal in search for bodies of water, these insects take advantage of the horizontally polarized light reflected from water surfaces. Note that in nature polarized light is generated not only by scattering, as described above, but also by reflection, i.e. by transmitting incoming light not in all directions (diffuse, Lambert reflection), but in one direction only (specular, Fresnel reflection). The horizontal polarization

resulting from the specular reflection of light at water surfaces is used by *Notonecta* and many other flying aquatic insects as a cue that indicates a body of water underneath. This behaviour is so robust that the insects get attracted even if the horizontally polarized reflections arise from polarizing shiny black sheets on the ground (Schwind 1991; Horváth and Varjú 2004; Horváth et al. 2008), asphalt roads (Kriska et al. 1998), waste oil lakes (Horváth and Zeil 1996; Horváth et al. 1998) or other kinds of liquid traps (Kriska et al. 2009). The higher the degree of polarization in the reflected light, the stronger is the response of the aquatic insects. Unpolarized light is ineffective, even if its intensity is substantially increased. As already indicated by a number of detailed analyses (e.g. Csabai et al. 2006), polarotactic water detection will provide a rich source for studies in sensory ecology (see Chaps. 5, 16 and 20–23).

Furthermore, polarized reflections are used not only as cues, but also as signals employed by various (mainly aquatic) animals in a number of behavioural contexts. This is a field of research in polarization vision that emerged only most recently. It started in the late 1990s when some marine invertebrates were shown to display patterns of reflected polarized light: cuttlefish (Shashar et al. 1996; Mäthger and Denton 2001) and stomatopod as well as brachiopod crustaceans (Marshall et al. 1999; Zeil and Hofmann 2001). Stomatopods, the best studied group of animals in this respect, display a variety of polarized signals alongside colour patterns on distinct body parts such as antennal scales, maxillipeds and uropods. These signals are either linearly polarized, and are generated, e.g. by reflections from dichroic carotinoid molecules (Chiou et al. 2012), or they can be polarized even circularly (Chiou et al. 2008, see Sect. 1.1). In cephalopods, in both cuttlefish and squid, it is an arsenal of iridophores that polarizes light by reflection. Together with other chromatophores these iridophores constitute the building blocks of the polarizing arm stripes of these animals (Chiou et al. 2007; Mäthger and Hanlon 2007).

For obvious physical reasons, polarized signals might be more effective in aquatic than in terrestrial environments. On the one hand, the low refractive index difference between water and natural objects markedly reduces the ‘polarization noise’ (Wehner and Bernard 1993) in underwater environments as compared to terrestrial ones, and thus renders polarization signals more conspicuous in the aquatic world (Cronin et al. 2003). On the other hand, the angle and degree of polarization do not substantially change with increasing distance from the water surface, but the spectral content of light does. Hence, in close-range social interactions, cephalopods and crustaceans seem to have swapped colour for polarization signals (see Chaps. 7, 8 and 19). Moreover, in an operant conditioning paradigm stomatopods could even be trained to discriminate between different states of linear and circular polarization (Marshall et al. 1999; Chiou et al. 2008). Nearly 40 years earlier this had already been shown, with respect to linear polarization, for cephalopods (Moody and Parriss 1961). However fascinating and flourishing the current research on such polarized ‘signals’ is, we still have much to learn about the signaling function of these structures. Certainly, depending on behavioural context, the polarized arm stripes of squid, *Loligo pealeii*, can be turned off and on by neural

control (Mäthger and Hanlon 2007), and communication studies in cuttlefish, *Sepia officinalis*, and more directly in one species of stomatopod crustacean, *Haptosquilla trispinosa*, have indicated that polarization signals are most likely involved in intraspecific encounters (Boal et al. 2004; Chiou et al. 2011), but full behavioural evidence has still to be obtained.

This problem is even exaggerated in the terrestrial world, in which insects display a vast variety of polarized 'signals', of which we do not know, or only recently have started to examine, whether there is any receiver around adapted to respond to these polarized reflections. Iridescence and specular reflections from insect cuticles have been studied for more than a century. For example, four years after he had received the Nobel Prize in Physics, Albert Abraham Michelson, the 'Dean of American Optics', as he was entitled (Bennett et al. 1973), presented a detailed study of the optics of such 'metallic colouring' and described circularly polarized reflections from the cuticle of a scarab beetle, *Chrysina* (=*Plusiotis*) *resplendens* (Michelson 1911). Recently, this phenomenon was investigated intensively and found to exist in almost 20,000 species and subspecies of scarab beetles (Scarabaeoidea) from the collections of the Natural History Museum in London (Pye 2010). In another recent and marvelously detailed study, in which ellipsometric polarimetry was applied, some of the investigated species exhibited elliptic polarization that changed from linear to circular even in different body areas (Arwin et al. 2012) (see Chap. 6). Notwithstanding the beauty of these photonic structures (Vukusic and Sambles 2003), at present we must confess that we know nearly nothing about their functional significance. The possibility cannot be excluded yet that they are just by-products of the inner structure of insect cuticles and do not serve any specific signaling function. At least for the time being there is no terrestrial animal that has been convincingly shown to be able to perceive circularly polarized light (e.g. Blahó et al. 2012). Of course, this is different when it comes to visual signals that contain linearly polarized components. In this case the males of certain rainforest butterflies, *Heliconius cydno*, have been reported to recognize their sexual partners by polarized iridescent reflections from female wings (Sweeney et al. 2003), and in swordtail butterflies, *Graphium sarpedon*, optical studies have provided clear evidence that the ventral sides of the wings display strongly direction-dependent polarized reflections, which during flight might result in a flashing polarized signal (Stavenga et al. 2012). With these two recent studies from the insect realm—hopefully the starting point for investigations into the promising field of polarized signalling—we end this short excursion into the terrestrial world and return to the underwater environment.

In freshwater lakes and oceans polarized signals must be detected against the scattered and hence polarized background space light. The natural polarization patterns, which in the hydrosphere cover a full sphere rather than only a hemisphere, have been studied long before polarized signals became a focus of research (Waterman 1954, 1955; Timofeeva 1962; Jerlov 1968; Ivanoff 1974). They result from scattering by water molecules (Rayleigh scattering) and—previously underrated—by larger particles suspended in water such as silt and plankton (Mie scattering) (see Chap. 15). Even though in limnic and marine environments

the degree of polarization is usually less than 50–60 % (Waterman 1981; Cronin and Shashar 2001), underwater polarization is almost everywhere and thus constitutes an omnipresent part of the visual scenery to which aquatic animals are inescapably exposed. In this situation, in which the scattering of light also considerably decreases the contrast between any particular object and its background, it has been proposed from early on that polarization sensitivity helps an animal to cut through the 'veil of brightness' of the underwater space light by enhancing the contrast between any object and its surroundings for the simple reason that the background space light is much more scattered and hence polarized than the light between the object and the observer (Lythgoe and Hemmings 1967; Lythgoe 1971). After these early advances, this field of research was left lying largely fallow, until in the last decade due to the new measurement and modelling approaches of Thomas Cronin, Nadav Shashar, Amit Lerner and their collaborators studies on underwater polarimetry and polarization vision gathered momentum again (Shashar et al. 2004, 2011; Lerner et al. 2011), e.g. in helping to understand how polarization-sensitive predators could detect otherwise camouflaged prey (Shashar et al. 1998, 2000).

Let me end this section with a short digression on potential navigation of aquatic animals by polarized skylight. Inspired by a lecture, which Karl von Frisch gave at Yale University about his discoveries in honey bees, Talbot Waterman, who had already developed an early interest in underwater vision (Cronin et al. 2011), performed the first experiments on skylight navigation in teleost fish (Waterman and Forward 1970; Forward et al. 1973)—a topic which was taken up again only two decades later (Hawryshyn et al. 1990; Hawryshyn 1992). The physical basis of this potential navigational ability is that the entire sky can also be perceived under water. Due to refraction at the air/water interface, the celestial hemisphere is compressed into a conical window, the so-called Snell's window, which has a constant, depth-independent angular width of 97.2°. Under certain conditions, e.g. under a totally clear sky, in clear waters and with no surface waves present, this refracted celestial E-vector pattern can still be recorded at several metres below the water surface (Horváth and Varjú 1995; Cronin and Shashar 2001; Sabbah et al. 2006), and as it is now generally agreed, navigation by underwater polarization might well be confined to such restricted conditions (Lerner et al. 2011; Chap. 9). However, even then strong evidence in the way as it has been obtained on land in the analysis of the hymenopteran polarization compass (Sect. 1.2) is hard to come by. For example, juvenile rainbow trouts, *Oncorhynchus mykiss*, have been reported to use the E-vector pattern within this aerial window as a compass cue (Hawryshyn 1992; Novales-Flamarique et al. 1992), and at the same time a decapod crustacean, the grass shrimp *Palaemonetes vulgaris*, has been described to steer its 'shore-flight' courses—a potential escape response from shore-living predators—by exactly this overhead E-vector pattern (Goddard and Forward 1991); but major questions about important features of such an underwater polarization compass remain to be elucidated. After more than 40 years of work on this subject, the late Talbot Waterman, the doyen of underwater polarization vision, finally concluded

his very last paper by remarking that underwater visual navigation is an 'unusually difficult task' (Waterman 2006).

1.5 Outlook

Polarization vision comes in various guises, and so does the research done on this remarkable sensory capacity. Indeed, studies on polarization vision advanced at different times at different fronts and at different paces. They dealt and still deal with different topics investigated by different experimental strategies. These multifaceted approaches favoured by different research groups, both conceptually and experimentally, somehow reflect the different tasks that are subsumed under the term 'polarization vision'. Certainly, polarization vision is not a uniform sensory capacity (Wehner 2001). So-called 'true polarization vision' (Nilsson and Warrant 1999), in which the animal is credited with the ability to determine the angle of polarization (E-vector orientation) independently of variations in radiant intensity and spectral content of a visual stimulus, might not have been the goal that evolution has aimed at in each single species and under all environmental conditions. The ant's and bee's celestial polarization compass based on scattered skylight has indeed been shown to rely on E-vector information alone, but in other cases, especially in the detection of objects that reflect polarized light—as it occurs in female butterflies searching for particular leaf structures to deposit their eggs—polarization and colour information are combined (Kelber 1999; Kelber et al. 2001; but see also Horváth et al. 2002; Hegedüs and Horváth 2004a,b; Chap. 13). While in this case the photoreceptors themselves are sensitive to both the spectral and polarization component of the stimulus to be detected, in the hymenopteran skylight compass spectral and polarization information are picked up by separate types of receptor and combined only at some later stage of information processing (Wehner 1997). One of the most pressing questions for future research will be to unravel the neural pathways along which several aspects of visual information, e.g. information about polarization and spectral content, travel separately—and if so, how far—or in combination. Such studies should be tightly linked with inquiries into the environmental setting, within which an animal species accomplishes its particular visual task, because it is this setting that has defined the task in the first place.

Irrespective of the final tasks, the most common characteristics shared by polarization vision systems bear on the peripheral sensors, the dichroic photoreceptor membranes. However, even in the functional design of the photoreceptor cells and their light-guiding structures, task-specific and environment-dependent modifications occur. For example, in the dorsal rim area of the strictly diurnal desert ants, genus *Cataglyphis*, the retinular rhabdoms are wide, but short (first described by Herrling 1975), so that the reduction of polarization sensitivity due to self-screening is minimized, but in aquatic crustaceans inhabiting dim-light environments the need for sufficiently high rates of quantum catch requires the rhabdoms to

be long and, in order to avoid the otherwise inevitable effect of self-screening, to be composed of interdigitated, orthogonally arranged slabs of microvilli (first described by Eguchi 1965). At the systems level there are certain striking commodalities. For example, the 'cross-analyser' arrangement of rhabdomeres, which enhances polarization sensitivity and renders the system intensity invariant, and the homochromacy of the polarization-sensitive photoreceptors are well established in the polarization vision systems of cephalopods, crustaceans and insects. However, in the underlying neural processing systems particular network structures might strongly depend on the task to be accomplished. Just to mention an example, the task might already differ in the use which a species makes of skylight polarization: either to compute a time-compensated compass direction or just to stabilize a straight course. The different anatomical designs of the dorsal rim areas found in various groups of insects (Labhart and Meyer 1999) are certainly matched to such particular tasks. For studying such task-specific peculiarities, there is even more variety, more challenging research potential ahead, more beauty and lustre when one moves into the rich underwater world of polarization.

At present, we have many technical tools at hand to address the major questions raised in the last half a century about the multifold aspects of polarization vision. As in the past, various research groups will use these tools according to their own needs. They might march separately in their particular terrestrial and aquatic worlds by taking advantage of the biodiversity of species and visual life styles, but hopefully they will strike together in understanding what role polarized light information plays in the visually guided behaviour of one species or another. These roles might be subtle and might come to the fore only in the context of other aspects of the animal's visual world. Hence, rather than headily trying to characterize and isolate polarization vision as an animal's distinct ability of 'seeing the third quality of light' we should always keep Jared Diamond's *caveat* in mind—the question, which this eminent biologist raised in the context of evolutionary physiology (Diamond 1991): 'How much is enough, but not too much?'

References

Arwin H, Magnusson R, Landin J, Järrendahl K (2012) Chirality-induced polarization effects in the cuticle of scarab beetles: 100 years after Michelson. Philos Mag 92:1583–1599

Autrum H, Stumpf H (1950) Das Bienenauge als Analysator für polarisiertes Licht. Z Naturforsch 5b:116–122

Baumann O, Lutz K (2006) Photoreceptor morphogenesis in the *Drosophila* compound eye: R1-R6 rhabdomeres become twisted just before eclosion. J Comp Neurol 498:68–79

Bennett JM, McAllister DT, Cabe GM (1973) Albert A. Michelson, Dean of American Optics—life, contributions to science, and influence on modern-day physics. Appl Opt 12:2253–2279

Berger P, Segal MJ (1952) La discrimination du plan de polarisation de la lumière par l'oiel de l'abeille. C R Acad Paris 234:1308–1310

Blahó M, Egri Á, Hegedüs R, Jósvai J, Tóth M, Kertész K, Biró LP, Kriska G, Horváth G (2012) No evidence for behavioral responses to circularly polarized light in four scarab beetle species with circularly polarizing exocuticle. Physiol Behav 105:1067–1075

Blest AD, Stowe S, Eddey W (1982) A labile Ca^{2+}-dependent cytoskeleton in rhabdomeral microvilli of blowflies. Cell Tissue Res 223:553–573

Boal JG, Shashar N, Grable MM, Vaughan KH, Loew ER, Hanlon RT (2004) Behavioral evidence for intraspecific signaling with achromatic and polarized light by cuttlefish (Mollusca: Cephalopoda). Behaviour 141:837–861

Brines ML (1978) Skylight polarization patterns as cues for honey bee orientation: physical measurements and behavioural experiments. PhD thesis, Rockefeller University, New York

Brines ML, Gould JL (1979) Bees have rules. Science 206:571–573

Brown PK (1972) Rhodopsin rotates in the visual receptor membrane. Nat New Biol 236:35–38

Burkhardt D, Wendler L (1960) Ein direkter Beweis für die Fähigkeit einzelner Sehzellen des Insektenauges, die Schwingungsrichtung polarisierten Lichtes zu analysieren. Z Vergl Physiol 43:687–692

Cameron DA, Pugh EN (1991) Double cones as a basis for a new type of polarization vision in vertebrates. Nature 353:161–164

Carthy JD (1951) The orientation of two allied species of British ants. Behaviour 3:275–381

Chiou TH, Mäthger LM, Hanlon RT, Cronin TW (2007) Spectral and spatial properties of polarized light reflections from the arms of squid (*Loligo pealeii*) and cuttlefish (*Sepia officinalis*). J Exp Biol 210:3624–3635

Chiou TH, Kleinlogel S, Cronin TW, Caldwell R, Loeffler B, Siddiqi A, Goldizen A, Marshall JN (2008) Circular polarization vision in a stomatopod crustacean. Curr Biol 18:429–434

Chiou TH, Marshall NJ, Caldwell RL, Cronin TW (2011) Changes in light-reflecting properties of signalling appendages alter mate choice behaviour in a stomatopod crustacean, *Haptosquilla trispinosa*. Mar Freshw Behav Physiol 44:1–11

Chiou TH, Place AR, Caldwell RL, Marshall NJ, Cronin TW (2012) A novel function for a carotinoid: astaxanthin used as a polarizer for visual signalling in a mantis shrimp. J Exp Biol 215:584–589

Cone RA (1972) Rotational diffusion of rhodopsin in the visual receptor membrane. Nat New Biol 236:39–43

Coulson KL (1988) Polarization and intensity of light in the atmosphere. A. Deepak Publishing, Hampton, VA

Cronin TW, Shashar N (2001) The linearly polarized light field in clear, tropical marine waters: spatial and temporal variation of light intensity, degree of polarization and e-vector angle. J Exp Biol 204:2461–2467

Cronin TW, Shashar N, Caldwell RL, Marshall J, Cheroske AG, Chiou TH (2003) Polarization vision and its role in biological signaling. Integr Comp Biol 43:549–558

Cronin TW, Warrant EJ, Greiner B (2006) Celestial polarization patterns during twilight. Appl Opt 45:5582–5589

Cronin TW, Marshall J, Wehling MF (2011) Dedication: Talbot H. Waterman. Philos Trans R Soc Lond B 366:617–618

Csabai Z, Boda P, Bernáth B, Kriska G, Horváth G (2006) A 'polarization sun-dial' dictates the optimal time of day for dispersal by flying aquatic insects. Freshw Biol 51:1341–1350

Dacke M, Nilsson DE, Warrant EJ, Blest AD, Land MF, O'Carroll DC (1999) Built-in polarizers form part of a compass organ in spiders. Nature 401:470–473

Dacke M, Nilsson DE, Scholtz CH, Byrne M, Warrant EJ (2003a) Insect orientation to polarized moonlight. Nature 424:33

Dacke M, Nordström P, Scholtz CH (2003b) Twilight orientation to polarized light in the crepuscular dung beetle *Scarabaeus zambesianus*. J Exp Biol 206:1535–1543

Danneel R, Zeutzschel B (1957) Über den Feinbau der Retinula bei *Drosophila melanogaster*. Z Naturforsch 12b:580–583

de Vries H, Spoor A, Jielof R (1953) Properties of the eye with respect to polarized light. Physica 19:419–432

Decouet H, Stowe S, Blest A (1984) Membrane-associated actin in the rhabdomeral microvilli of crayfish photoreceptors. J Cell Biol 98:834–846

Diamond J (1991) Evolutionary design of intestinal nutrient absorption: enough but not too much. Physiology 6:92–96
Duelli P (1975) A fovea for e-vector orientation in the eye of *Cataglyphis bicolor* (Formicidae, Hymenoptera). J Comp Physiol 102:43–56
Eguchi E (1965) Rhabdom structure and receptor potentials in single crayfish retinular cells. J Cell Comp Physiol 66:411–429
Fent K (1985) Himmelsorientierung bei der Wüstenameise *Cataglyphis bicolor*: Bedeutung von Komplexaugen und Ocellen. PhD thesis, University of Zürich
Fent K, Wehner R (1985) Ocelli: a celestial compass in the desert ant, *Cataglyphis*. Science 228: 192–194
Fernández-Morán H (1956) Fine structure of the insect retinula as revealed by electron microscopy. Nature 177:742–743
Fineran BA, Nicol JAC (1978) Studies on the photoreceptors of *Anchoa mitchilli* and *A. hepsetus* (Engraulidae) with particular reference to the cones. Philos Trans R Soc Lond B 283:25–60
Fischer S, Meyer-Rochow VB, Müller CHG (2014) Compound eye miniaturization in Lepidoptera: a comparative morphological analysis. Acta Zool. doi:10.1111/azo.12041
Forward RB, Horch KW, Waterman TH (1973) Evidence for e-vector and light intensity pattern discrimination by the teleost *Demogenys*. J Comp Physiol 87:189–202
Gál J, Horváth G, Barta A, Wehner R (2001) Polarization of the moonlit clear night sky measured by full-sky imaging polarimetry at full moon: comparison of the polarization of moonlit and sunlit skies. J Geophys Res D 106:22647–22653
Goddard SM, Forward RB (1991) The role of the underwater polarized light pattern in sun compass of the grass shrimp, *Palaemonetes vulgaris*. J Comp Physiol A 169:479–491
Goldsmith TH (1962) Fine structure of the retinulae in the compound eye of the honeybee. J Cell Biol 14:489–494
Goldsmith TH, Philpott DF (1957) The microstructure of the compound eyes of insects. J Biophys Biochem Cytol 3:429–440
Goldsmith TH, Wehner R (1977) Restrictions of rotational and tranlational diffusion of pigment in the membranes of rhabdomeric photoreceptors. J Gen Physiol 70:453–490
Görner P (1958) Die optische und kinästhetische Orientierung der Trichterspinne *Agelena labyrinthica*. Z Vergl Physiol 41:111–153
Haidinger W (1844) Über das direkte Erkennen des polarisirten Lichts und die Lage der Polarisationsebene. Ann Physik Chemie (Poggendorf Annalen) 63:29–39
Hárosi FI, MacNichol EF (1974) Visual pigments of goldfish cones: spectral properties and dichroism. Gen Physiol 63:279–304
Hawryshyn CW (1992) Polarisation vision in fish. Am Sci 80:164–175
Hawryshyn CW, Bolger AE (1990) Spatial orientation of trout to partially polarized light. J Comp Physiol A 167:691–697
Hawryshyn CW, Arnold MG, Bowering D, Cole RL (1990) Spatial orientation of rainbow trout to plane-polarized light: the ontogeny of e-vector discrimination and spectral characteristics. J Comp Physiol A 166:565–574
Hegedüs R, Horváth G (2004a) Polarizational colours could help polarization-dependent colour vision systems to discriminate between shiny and matt surfaces, but cannot unambiguously code surface orientation. Vis Res 44:2337–2348
Hegedüs R, Horváth G (2004b) How and why are uniformly polarization-sensitive retinae subject to polarization-related artefacts? Correction of some errors in the theory of polarization-induced false colours. J Theor Biol 230:77–87
Hegedüs R, Åkesson S, Horváth G (2007a) Polarization patterns of thick clouds: overcast skies have distribution of the angle of polarization similar to that of clear skies. J Opt Soc Am A 24: 2347–2356
Hegedüs R, Åkesson S, Wehner R, Horváth G (2007b) Could Vikings have navigated under foggy and cloudy conditions by skylight polarization? On the atmospheric optical prerequesites of

polarimetric Viking navigation under foggy and cloudy skies. Proc R Soc Lond A 463: 1081–1095
Heinze S, Homberg U (2007) Map-like representation of celestial E-vector orientations in the brain of an insect. Science 315:995–997
Heinze S, Homberg U (2009) Linking the input to the output: new sets of neurons complement the polarization vision network in the locust central complex. J Neurosci 29:4911–4921
Helbig AJ (1990) Depolarization of natural skylight disrupts orientation of an avian nocturnal migrant. Experientia 46:755–758
Herrling PL (1975) Topographische Untersuchungen zur funktionellen Anatomie der Retina von *Cataglyphis bicolor* (Formicidae, Hymenoptera). PhD thesis, University of Zürich
Homberg U (2004) In search of the sky compass in the insect brain. Naturwissenschaften 91:199–208
Homberg U (2008) Evolution of the central complex in the arthropod brain with respect to the visual system. Arthropod Struct Dev 37:347–362
Homberg U, Heinze S, Pfeiffer K, Kinoshita M, el Jundi B (2011) Central neural coding of sky polarization in insects. Philos Trans R Soc Lond B 366:680–687
Horváth G, Varjú D (1995) Underwater refraction-polarization patterns of skylight perceived by aquatic animals through Snell's window of the flat water surface. Vis Res 35:1651–1666
Horváth G, Varjú D (2004) Polarized light in animal vision – polarization patterns in nature. Springer, Heidelberg – Berlin
Horváth G, Zeil J (1996) Kuwait oil lakes as insect traps. Nature 379:303–304
Horváth G, Bernáth B, Molnár G (1998) Dragonflies find crude oil visually more attractive than water: multiple-choice experiments on dragonfly polarotaxis. Naturwissenschaften 85: 292–297
Horváth G, Gál J, Labhart T, Wehner R (2002) Does reflection polarization by plants influence colour perception in insects? Polarimetric measurements applied to a polarization-sensitive model retina of *Papilio* butterflies. J Exp Biol 205:3281–3298
Horváth G, Majer J, Horváth L, Szivák I, Kriska G (2008) Ventral polarization vision in tabanids: horseflies and deerflies (Diptera: Tabanidae) are attracted to horizontally polarized light. Naturwissenschaften 95:1093–1100
Israelachvili JN, Wilson M (1976) Absorption characteristics of oriented photopigments in microvilli. Biol Cybern 21:9–15
Ivanoff A (1974) Polarization measurements in the sea. In: Jerlov NG, Nielsen ES (eds) Optical aspects of oceanography. Academic, London, pp 151–175
Jander R (1957) Die optische Richtungsorientierung der roten Waldameise (*Formica rufa*). Z Vergl Physiol 40:162–238
Jerlov NG (1968) Optical oceanography. Elsevier, Amsterdam
Kelber A (1999) Why 'false' colours are seen by butterflies. Nature 402:251
Kelber A, Thunell C, Arikawa K (2001) Polarisation-dependent colour vision in *Papilio* butterflies. J Exp Biol 204:2469–2480
Kinoshita M, Pfeiffer K, Homberg U (2007) Spectral properties of identified polarized-light sensitive interneurons in the brain of the desert locust *Schistocerca gregaria*. J Exp Biol 210:1350–1361
Kirschfeld K (1972) Die notwendige Anzahl von Rezeptoren zur Bestimmung der Richtung des elektrischen Vektors linear polarisierten Lichtes. Z Naturforsch 27c:578–579
Kirschfeld K, Lindauer M, Martin H (1975) Problems of menotactic orientation according to the polarized light of the sky. Z Naturforsch 30c:88–90
Kriska G, Horváth G, Andrikovics S (1998) Why do mayflies lay their eggs *en masse* on dry asphalt roads? Water-imitating polarized light reflected from asphalt attracts Ephemeroptera. J Exp Biol 201:2273–2286
Kriska G, Bernáth B, Farkas R, Horváth G (2009) Degrees of polarization of reflected light eliciting polarotaxis in dragonflies (Odonata), mayflies (Ephemeroptera) and tabanid flies (Tabanidae). J Insect Physiol 55:1167–1173

Kuwabara M, Naka K (1959) Response of a single retinua cell to polarized light. Nature 184: 455–456
Labhart T (1980) Specialized photoreceptors at the dorsal rim of the honeybee's compound eye: polarizational and angular sensitivity. J Comp Physiol 141:19–30
Labhart T (1986) The electrophysiology of photoreceptors in different eye regions of the desert ant, *Cataglyphis bicolor*. J Comp Physiol A 158:1–7
Labhart T (1988) Polarization opponent interneurons in the insect visual system. Nature 331: 435–437
Labhart T, Meyer EP (1999) Detectors for polarized skylight in insects: a survey of ommatidial specializations in the dorsal rim area of the compound eye. Microsc Res Tech 47:368–379
Laughlin SB (1976) The sensitivities of dragonfly photoreceptors and the voltage gain of transduction. J Comp Physiol 111:221–247
Laughlin SB, Menzel R, Snyder AW (1975) Membranes, dichroism and receptor sensitivity. In: Snyder AW, Menzel R (eds) Photoreceptor optics. Springer, Heidelberg, pp 237–259
Lebhardt F, Ronacher B (2014) Transfer of direction information between the polarization compass and the sun compass in desert ants. J Comp Physiol A (submitted)
Lerner A, Sabbah S, Erlick C, Shashar N (2011) Navigation by light polarization in clear and turbid waters. Philos Trans R Soc Lond B 366:671–679
Lillywhite PG (1978) Coupling between locust photoreceptors revealed by a study of quantum bumps. J Comp Physiol A 125:13–27
Lythgoe JN (1971) Vision. In: Woods JD, Lythgoe JN (eds) Underwater science. Oxford University Press, Oxford, pp 103–139
Lythgoe JN, Hemmings CC (1967) Polarized light and underwater vision. Nature 213:893–894
Marshall NJ, Cronin TW, Shashar N, Land M (1999) Behavioural evidence for polarisation vision in stomatopods reveals a potential channel for communication. Curr Biol 9:755–758
Mäthger LM, Denton EJ (2001) Reflective properties of iridophores and fluorescent 'eyespots' in the loliginid squids *Alloteuthis subulata* and *Loligo vulgaris*. J Exp Biol 204:2103–2118
Mäthger LM, Hanlon R (2007) Malleable skin coloration in cephalopods: selective reflectance, transmission and absorbance of light by chromatophores and iridophores. Cell Tissue Res 329: 179–186
Meyer EP, Domanico V (1999) Microvillar orientation in the photoreceptors of the ant *Cataglyphis bicolor*. Cell Tissue Res 295:355–361
Michelson AA (1911) On the metallic colouring in birds and insects. Philos Mag 21:554–567
Miller WH (1957) Morphology of the ommatidia in the compound eye of *Limulus*. J Biophys Biochem Cytol 3:421–428
Montell C (1999) Visual transduction in *Drosophila*. Annu Rev Cell Dev Biol 15:231–268
Moody MF, Parriss JR (1961) The discrimination of polarized light by *Octopus*: a behavioral and morphological study. Z Vergl Physiol 44:268–291
Mote MI, Wehner R (1980) Functional characteristics of photoreceptors in the compound eye and ocellus of the desert ant, *Cataglyphis bicolor*. J Comp Physiol 137:63–71
Muheim R (2011) Behavioural and physiological mechanisms of polarized light sensitivity in birds. Philos Trans R Soc Lond B 366:763–771
Müller M, Wehner R (2007) Wind and sun as compass cues in desert ant navigation. Naturwissenschaften 94:589–594
Murakami M, Kouyama T (2008) Crystal structure of squid rhodopsin. Nature 453:363–368
Nilsson DE, Warrant EJ (1999) Seeing the third quality of light. Curr Biol 9:R535–R537
Novales-Flamarique I (2011) Unique photoreceptor arrangements in a fish with polarized light discrimination. J Comp Neurol 519:714–737
Novales-Flamarique I, Hendry A, Hawryshyn CW (1992) The photic environment of a salmonid nursery lake. J Exp Biol 169:121–141
Novales-Flamarique I, Hawryshyn CW, Hárosi FI (1998) Double-cone internal reflection as a basis for polarization detection in fish. J Opt Soc Am A 15:349–358

Papi F (1955a) Orientamento astronomico in alcuni Carabidi. Atti Soc Tosc Sci Nat Pisa Mem 62B:83–97
Papi F (1955b) Ricerche sull'orientamento astronomico di *Arctosa* (Araneae Lycosidae). Pubbl Staz Zool Napoli 27:76–103
Pardi L, Papi F (1952) Die Sonne als Kompass bei *Talitrus saltator*, Amphipoda, Talitridae. Naturwissenschaften 39:262–263
Phillips JB, Waldvogel JA (1988) Celestial polarized patterns as a calibration reference for sun compass of homing pigeons. J Theor Biol 131:55–67
Pomozi I, Horváth G, Wehner R (2001) How the clear-sky angle of the polarization pattern continues underneath clouds: full-sky measurements and implications for animal orientation. J Exp Biol 204:2933–2942
Poo MM, Cone RA (1974) Lateral diffusion of rhodopsin in the photoreceptor membrane. Nature 247:438–441
Pye JD (2010) The distribution of circularly polarized light reflections in the Scarabaeoidea (Coleoptera). Biol J Linn Soc 100:585–596
Räber F (1979) Retinatopographie und Sehfeldtopologie des Komplexauges von *Cataglyphis bicolor* (Formicidae, Hymenoptera). PhD thesis, University of Zürich
Reid SF, Narendra A, Hemmi JM, Zeil J (2011) Polarized skylight and the landmark panorama provide night-active bull ants with compass information during route following. J Exp Biol 214:363–370
Ribi WA (1979) Do the rhabdomeric structures in bees and flies really twist? J Comp Physiol 134:109–112
Ribi WA (1980) New aspects of polarized light detectors in the bee in view of non-twisting rhabdomeric structures. J Comp Physiol 137:281–285
Roberts NW, Needham MG (2007) A mechanism of polarized light sensitivity in cone photoreceptors of the goldfish *Carassius auratus*. Biophys J 93:3241–3248
Roberts NW, Porter ML, Cronin TW (2011) The molecular basis of mechanisms underlying polarization vision. Philos Trans R Soc Lond B 366:627–637
Rossel S, Wehner R (1984a) How bees analyse the polarization patterns in the sky. J Comp Physiol A 154:607–615
Rossel S, Wehner R (1984b) Celestial orientation in bees: the use of spectral cues. J Comp Physiol A 155:605–613
Rossel S, Wehner R (1986) Polarization vision in bees. Nature 323:128–131
Rozenberg GV (1966) Twilight. A study in atmosheric optics. Plenum, New York
Sabbah S, Barta A, Gál J, Horváth G, Shashar N (2006) Experimental and theoretical study of skylight polarization transmitted through Snell's window of a flat water surface. J Opt Soc Am A 23:1978–1988
Saibil HR (1982) An ordered membrane-cytoskeleton network in squid photoreceptor microvilli. J Mol Biol 158:435–456
Santschi F (1923) L'orientation sidérale des fourmis, et quelques considérations sur leurs differentes possibilités d'orientation. Mém Soc Vaud Sci Nat 4:137–175
Schinz RH (1975) Structural specialization in the dorsal retina of the bee, *Apis mellifera*. Cell Tissue Res 162:23–34
Schmidt WJ (1924) Die Bausteine des Tierkörpers im polarisierten Licht. F. Cohen, Bonn
Schmidt WJ (1951) Polarisationsoptische Analyse der Verknüpfung von Protein- und Lipidmolekülen, erläutert am Aussenglied der Sehzellen der Wirbeltiere. Pubbl Staz Zool Napoli 23(Suppl):158–183
Schwarz S, Albert L, Wystrach A, Cheng K (2011a) Ocelli contribute to the encoding of celestial compass information in the Australian desert ant *Melophorus bagoti*. J Exp Biol 214:901–906
Schwarz S, Wystrach A, Cheng K (2011b) A new navigational mechanism mediated by ant ocelli. Biol Lett 7:856–858
Schwind R (1983) A polarization-sensitive response of the flying water bug *Notonecta glauca* to UV light. J Comp Physiol 150:87–91

Schwind R (1984) Evidence for true polarization vision based on a two-channel analyzer system in the eye of the water bug, *Notonecta glauca*. J Comp Physiol A 154:53–57
Schwind R (1991) Polarization vision in water insects and insects living on a moist substrate. J Comp Physiol A 169:531–540
Shashar N, Rutledge PS, Cronin TW (1996) Polarization vision in cuttlefish: a concealed communication channel? J Exp Biol 199:2077–2084
Shashar N, Hanlon RT, Petz AD (1998) Polarization vision helps detect transparent prey. Nature 393:222–223
Shashar N, Hagen R, Boal JG, Hanlon RT (2000) Cuttlefish use polarization sensitivity in predation on silvery fish. Vis Res 40:71–75
Shashar N, Sabbah S, Cronin TW (2004) Transmission of linearly polarized light in seawater: implications for polarization signaling. J Exp Biol 207:3619–3628
Shashar N, Johnsen S, Lerner A, Sabbah S, Chiao CC, Mäthger LM, Hanlon RT (2011) Underwater linear polarization: physical limitations to biological functions. Philos Trans R Soc Lond B 366:649–654
Shaw SR (1967) Simultaneous recordings from two cells in the locust retina. Z Vergl Physiol 55:183–194
Smola U, Tscharntke H (1979) Twisting of blowfly (*Calliphora erythrocephala*; Diptera: Calliphoridae) rhabdomeres: an *in vivo* feature unaffected by preparation or fixation. J Insect Morphol Embryol 10:331–344
Smola U, Wunderer H (1981) Fly rhabdomeres twist *in vivo*. J Comp Physiol 142:43–49
Stavenga DG, Matsushita A, Arikawa K, Leertouwer HL, Wilts BD (2012) Glass scales on the wing of the swordtail butterfly *Graphium sarpedon* act as thin film polarizing reflectors. J Exp Biol 215:657–662
Stephens GC, Fingerman M (1953) The orientation of *Drosophila* to plane polarized light. Ann Entomol Soc Am 46:75–83
Stockhammer K (1956) Die Wahrnehmung der Schwingungsrichtung linear polarisierten Lichtes bei Insekten. Z Vergl Physiol 38:30–83
Stowe S (1983) Light-induced and spontaneous breakdown of the rhabdoms in a crab at dawn: depolarisation versus calcium levels. J Comp Physiol 153:365–375
Strausfeld NJ (1999) A brain region in insects that supervises walking. Prog Brain Res 123: 273–284
Strausfeld NJ (2012) Arthropod brains. The Belknap Press of Harvard University Press, Cambridge
Sweeney A, Jiggins C, Johnsen S (2003) Insect communication: polarized light as a butterfly mating signal. Nature 423:31–32
Timofeeva VA (1962) Spatial distribution of the degree of polarization of natural light in the sea. Bull Acad Sci USSR Geophys Ser 12:1160–1164
van der Glas HW (1976) Polarization induced colour patterns: a model of the perception of the polarized skylight. II. Experiments with direction trained dancing bees, *Apis mellifera*. Neth J Zool 26:383–413
von Frisch K (1949) Die Polarisation des Himmelslichts als orientierender Faktor bei den Tänzen der Bienen. Experientia 5:142–148
von Helversen O, Edrich W (1974) Der Polarisationsempfänger im Bienenauge: ein Ultraviolettrezeptor. J Comp Physiol 94:33–47
Vowles DM (1950) Sensitivity of ants to polarized light. Nature 165:282–283
Vukusic P, Sambles JR (2003) Photonic structures in biology. Nature 424:852–855
Wagner-Boller E (1987) Ontogenese des peripheren visuellen Systems der Honigbiene (*Apis mellifera*). PhD thesis, University of Zürich
Waterman TH (1954) Polarization patterns in submarine illumination. Science 120:927–932
Waterman TH (1955) Polarization of scattered sunlight in deep water. Deep Sea Res 3(Suppl): 426–434

Waterman TH (1981) Polarization sensitivity. In: Autrum H (ed) Handbook of sensory physiology, vol VII/6B. Springer, Heidelberg, pp 281–469
Waterman TH (2006) Reviving a neglected celestial underwater polarization compass for aquatic animals. Biol Rev 81:111–115
Waterman TH, Forward RB (1970) Field evidence for polarized light sensitivity in the fish *Zenarchopterus*. Nature 228:85–87
Wehner R (1982) Himmelsnavigation bei Insekten. Neurophysiologie und Verhalten. Neujahrsbl Naturforsch Ges Zürich 184:1–132
Wehner R (1983) The perception of polarized light. Symp Soc Exp Biol 36:331–369
Wehner R (1990) On the brink of introducing sensory ecology: Felix Santschi (1872-1940)—Tabib-en-Neml. Behav Ecol Sociobiol 27:295–306
Wehner R (1994) The polarization-vision project: championing organismic biology. In: Schildberger K, Elsner N (eds) Neural basis of behavioural adaptations. G. Fischer, Stuttgart, pp 103–143
Wehner R (1997) The ant's celestial compass system: spectral and polarizational channels. In: Lehrer M (ed) Orientation and communication in arthropods. Birkhäuser, Basel, pp 145–185
Wehner R (2001) Polarization vision—a uniform sensory capacity? J Exp Biol 204:2589–2596
Wehner R, Bernard GD (1993) Photoreceptor twist: a solution to the false-color problem. Proc Natl Acad Sci USA 90:4132–4135
Wehner R, Duelli P (1971) The spatial orientation of desert ants, *Cataglyphis bicolor*, before sunrise and after sunset. Experientia 27:1364–1366
Wehner R, Labhart T (2006) Polarization vision. In: Warrant E, Nilsson DE (eds) Invertebrate vision. Cambridge University Press, Cambridge, pp 291–348
Wehner R, Meyer EP (1981) Rhabdomeric twist in bees—artefact or *in vivo* structure? J Comp Physiol 142:1–17
Wehner R, Müller M (2006) The significance of direct sunlight and polarized skylight in the ant's celestial system of navigation. Proc Natl Acad Sci USA 103:12575–12579
Wehner R, Strasser S (1985) The POL area of the honey bee's eye: behavioural evidence. Physiol Entomol 10:337–349
Wehner R, Bernard GD, Geiger E (1975) Twisted and non-twisted rhabdoms and their significance for polarization vision in the bee. J Comp Physiol 104:225–245
Wehner R, Cheng K, Cruse H (2014) Visual navigation strategies in insects: lessons from desert ants. In: Werner J, Chalupa JL (eds) New visual neurosciences. MIT Press, Cambridge, MA, pp 1153–1163
Weir PT, Dickinson MH (2012) Flying *Drosophila* orient to sky polarization. Curr Biol 22:21–27
Wellington WG (1953) Motor responses evoked by the dorsal ocelli of *Sarcophaga aldrichi*, and the orientation of the fly to plane polarized light. Nature 172:1177–1179
Wernet M, Velez MM, Clark DA, Baumann-Klausener F, Brown JR, Klovstad M, Labhart T, Clandinin TR (2012) Genetic dissection reveals two separate retinal substrates for polarization vision in *Drosophila*. Curr Biol 22:12–20
Wolken JJ, Capenos J, Turano A (1957) Photoreceptor structures. J Biophys Biochem Cytol 3: 441–448
Young SR, Martin GR (1984) Optics of retinal oil droplets: a model of light collection and polarization detection in the avian retina. Vis Res 24:129–137
Zeil J, Hofmann M (2001) Signals from 'crabworld': cuticular reflections in a fiddler crab colony. J Exp Biol 204:2561–2569
Zolotov V, Frantsevich L (1973) Orientation of bees by the polarized light of a limited area of the sky. J Comp Physiol 85:25–36

Chapter 2
Polarized Light Orientation in Ball-Rolling Dung Beetles

Marie Dacke

Abstract Many dung beetles, unlike most insect navigators, do not need to locate a stationary nest at the end of their foraging journey. This makes the nature of their orientation task fundamentally different, and in the case of straight-line orientation, the beetles appear to rely single-handedly on celestial compass cues to move along straight paths. With a focus on the sky, diurnal dung beetles rely on the sun and the skylight cues that span the entire sky. These cues include the linear polarization pattern of skylight. As day turns to night, crepuscular and nocturnal dung beetles start to fly at around sunset. At this time, the full sky is polarized in one single direction, and the ball-rolling beetles can be observed to turn sharply when rolling under a linear polarizer placed with its E-vector oriented 90° to that of skylight. When the moon has risen, the beetles continue to orient along straight paths well after sunset, guided by the celestial polarization pattern created by the scattered moonlight. The intensity of this relatively dim polarization pattern will gradually decline as the moon wanes. Remarkably, even the extremely dim celestial polarization pattern formed around a crescent moon is sufficient to guide the nocturnal beetles along straight paths. Moreover, straight-line orientation on these dark nights is performed with the same precision and speed as in dung beetles orienting under the much brighter polarization pattern of the sun or full moon. So strong is their desire to roll their balls of dung that nocturnal beetles can be made to roll at day and diurnal beetles can be compelled to roll in the middle of the night. This incredible flexibility opens up the possibility to perform a new set of experiments directed towards an understanding of how celestial compasses have been adapted to the visual environment in which the insect is normally active.

M. Dacke (✉)
Department of Biology, Lund Vision Group, Lund University, 221 00 Lund, Sweden
e-mail: marie.dacke@biol.lu.se

G. Horváth (ed.), *Polarized Light and Polarization Vision in Animal Sciences*,
Springer Series in Vision Research 2, DOI 10.1007/978-3-642-54718-8_2,

2.1 Introduction

A freshly made dung pile on the African savannah attracts visitors from near and far. Ball-rolling dung beetles fly in from kilometres away and gather at this food source to feed and mate. Once the foraging beetles have climbed onto the dung pile, they begin to sculpt the dung into a transportable package of food. Using their flat heads and legs, they quickly form even the sloppiest excrement into a ball and start to push it away. The beetles exit the pile in different directions (Fig. 2.1a) (Dacke et al. 2003a, 2013a, b, 2014) in search of a suitable (but not predetermined) place to bury and consume their smelly meal. Newly arriving beetles are hot from flying (and therefore faster and stronger than colder beetles) and will try to steal a ready-made ball from the exiting beetles, rather than making one of their own (Bartholomew and Heinrich 1978). To protect its nutritional prize from these competitors at and around the dung pat, a beetle must roll its ball away as swiftly and efficiently as possible, that is, along a straight line.

Despite their peculiar style of food transport—rolling a large ball backwards while keeping their heads close to the ground (Fig. 2.1b)—the dung beetles manage to move along near-perfect straight paths whilst traversing over flat terrain. When analysed over a distance of 120 cm, the paths are on average no more than 127 ± 3 cm long (mean $\pm$ standard deviation, $n = 11$), (Fig. 2.1a) (Dacke et al. 2013b). The extra distance of 7 cm is an unavoidable consequence of the slight side-to-side rocking motion made by the beetles as they push the ball along an overall constant rolling direction.

It is unclear what makes the beetles choose their departure bearings from the dung pat, but it appears as if the process of making a new ball provides the behavioural circumstance necessary for choosing an exit direction (Baird et al. 2010). Once the bearing has been selected, the beetle keeps steadfastly to it. Forcing a beetle off course by placing obstacles in its way, making it fall from a ramp or even spinning it around on a rotating platform will only temporarily deflect the beetle in a different direction (Byrne et al. 2003; Dacke et al. 2003b; Baird et al. 2012). When negotiating a barrier, the beetles are forced to move around it, but as soon they reach its edge, they take a course that is parallel to the desired direction of travel (Fig. 2.2). A similar manipulation on a homing animal would result in a new intermediate course to compensate for the sideways movement, but since a ball-rolling beetle does not navigate towards a particular location, it simply continues along its original direction of travel. This simplifies the task of orientation, while still effectively taking the beetle away from the busy dung pile.

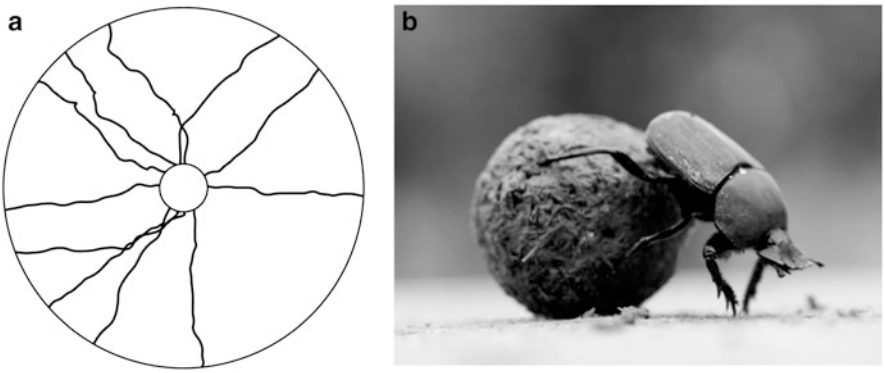

Fig. 2.1 (**a**) Paths of the ball-rolling beetle *Scarabaeus lamarcki* rolling outwards from the centre of a 3 m diameter circular arena (as seen from *above*) on a clear day. The tracking of the beetle began once it rolled out from the inner, 60 cm diameter circle. A perfectly straight track will thus be 120 cm long. The paths made by the 11 beetles in the figure are on average no more than 127 ± 3 cm long (mean ± standard deviation). (**b**) The diurnal dung beetle *Scarabaeus lamarcki* rolling its ball of dung [modified after Dacke et al. (2013b), photo: Emily Baird]

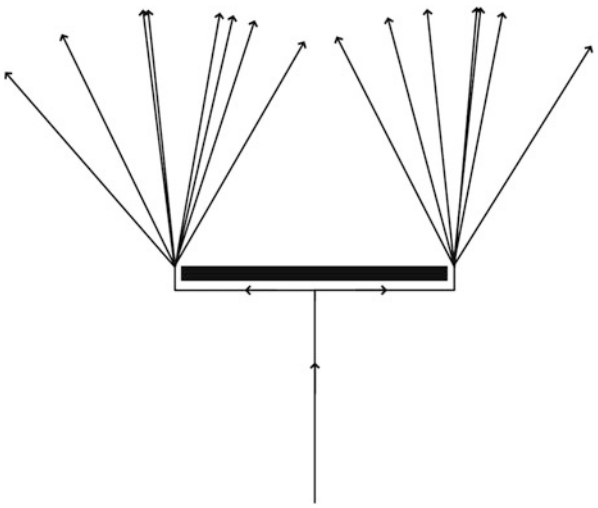

Fig. 2.2 Schematic drawing of the orientation of 15 ball-rolling dung beetles (*Scarabaeus lamarcki*) before and after encountering a barrier. *Arrows* mark the direction of movement. The absolute mean angle of deviation from the original course is 16.9° [modified after Dacke (et al. 2003b)]

2.2 Polarized Light Orientation During the Day

Navigating insects use a number of compass cues to find their way to a food source and back home again. These include the sun, the pattern of polarized skylight and landmarks (for reviews see Wehner 1992; Wehner and Srinivasan 2003; Collett and Collett 2009). Dung beetles, however, seem to rely exclusively on celestial compass cues for orientation. The sudden removal of visual landmarks, such as bushes, trees or the centrally placed dung pile, has no effect on orientation precision (Dacke et al. 2013b). Under a heavily overcast sky when the sun is no longer visible and the degree of skylight polarization is greatly reduced (Pomozi et al. 2001; Hegedüs et al. 2007; see also Chap. 18), the skydome and the surrounding landmarks are the only sources of directional information. Nonetheless, ball-rolling dung beetles do not make use of this information, since the tracks of beetles rolling over 80 cm under a completely overcast sky become curved and significantly longer (116 ± 4 cm, $n = 7$) than when rolling under a clear sky (84 ± 0 cm) (Dacke et al. 2013b) (Fig. 2.3). Thus, when the beetles can no longer see the celestial compass cues, their straight-line orientation performance is significantly impaired (Dacke et al. 2003a, 2011, 2013b).

To our knowledge, ball-rolling dung beetles are the only animals with a visual compass system that ignore the extra orientation precision that landmarks can offer. These beetles, unlike most insect navigators, do not need to locate a stationary nest at the end of their foraging journey. This makes the nature of their orientation task fundamentally different, and in the case of the straight-line orientation, celestial compass cues appear to provide the precision these beetles need to ensure a safe exit from the dung pile. That is, for as long as the sky is not completely overcast, but this is a rare event in the life of the South African beetle.

With a focus on the sky, diurnal dung beetles can rely on the skylight cues that span the entire sky. These cues include the pattern of polarized skylight and gradients of colour and intensity (Edrich et al. 1979; Brines and Gould 1982; Rossel and Wehner 1984; Horváth and Varjú 2004; Ugolini et al. 2009). Beetles rolling under a linearly polarizing filter, placed with its E-vector (direction of polarization) oriented 90° to that of skylight, will turn by a mean angle of 77 ± 6° ($n = 30$) (el Jundi et al. 2014) (Fig. 2.4a, black circles). In these experiments, the sun was hidden from view and the 90° rotation of the E-vector direction did not allow the beetles to discriminate between an apparent left rotation or a right rotation of the polarization direction. As a result, 17 beetles turned to the left and 13 beetles turned to the right. Conversely, the beetles maintained their rolling direction under the polarizer, if it was instead placed with its E-vector parallel to that of skylight (mean change in bearing 18 ± 6°, $n = 30$, Fig. 2.4a, white circles). This clearly shows that dung beetles are able to orient by using the celestial polarization pattern as a compass cue, while the role of the other skylight cues remains to be tested.

Artificially changing the apparent position of the sun by 180°, in a classical experiment using a mirror while blocking the view of the sun with a board

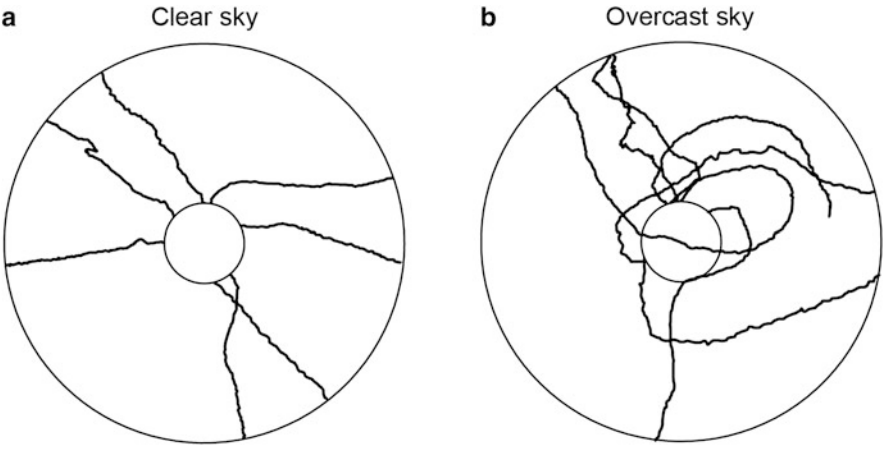

Fig. 2.3 Paths of the ball-rolling dung beetle, *Scarabaeus lamarcki*, rolling outwards from the centre of a 2 m diameter circular arena (as seen from *above*) under a clear (**a**) and an overcast sky (**b**). Tracking of the beetle began once it rolled out from the inner, 40 cm diameter circle. A perfectly straight track will thus be 80 cm long. The tracks are significantly longer when orienting under the overcast sky (116 ± 4 cm, mean ± SD) than under the clear sky (84 ± 0 cm) (*t*-test, $p < 0.01$). Thus, when the beetles can no longer see the celestial compass cues, their straight-line orientation performance is significantly impaired [modified after Dacke et al. (2013b)]

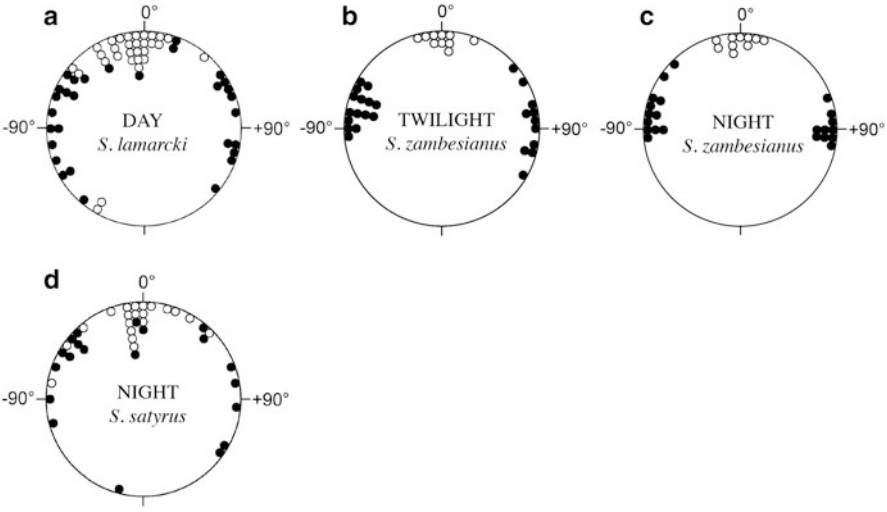

Fig. 2.4 Circular diagram of turns made by ball-rolling dung beetles in response to a polarization pattern rotated by 90° (*black circles*) or 0° (*white circles*), during the day (**a**), at twilight (**b**) or during the night (**c**, **d**). In these experiments, the sun and the moon were hidden from view and the 90° change in the E-vector direction did not allow the beetles to discriminate between an apparent left rotation or a right rotation of the direction of polarization. As a result, some of the beetles turned to the left and some of others turned to the right. The data is binned in 5° intervals and the species tested in each condition is indicated in the *centre of the diagram* [modified after el Jundi et al. (2014): **a**; Dacke et al. 2003b: **b**; Dacke et al. 2003a: **c**]

(Santschi 1911), caused the beetles to change their bearing by 128 ± 6° ($n = 60$) (Dacke et al. 2014). This indicates that the primary cue for orientation is the sun, rather than the pattern of polarized skylight, which remains unaffected by this treatment. If the same experiment was repeated at solar elevations below 30°, rather than above 75° as in the first set of experiments, the beetles changed their bearing by no more than 104 ± 7° ($n = 60$). As the sun draws closer to the horizon, the degree of polarization in the zenith of the sky increases (Brines and Gould 1982), and it is likely that the observed decrease in the relative influence of the sun at low solar elevations is a consequence of the increased input to the polarized light compass.

2.3 Polarized Light Orientation During Twilight

As day turns to night, diurnal dung beetles cease their activity, while crepuscular dung beetles just start to wake up (Caveney et al. 1995). The beetle *Scarabaeus zambesianus* starts to fly at around sunset and can be seen in dim light at our experimental dung piles some 30 min after sunset. The setting of the sun, and the drastic decrease in surrounding light levels, is a phenomenon of twilight that is clearly perceptible to the human observer. At the same time, though invisible to us, the sunset also generates the simplest celestial polarization pattern—the full sky is polarized in one single direction. This is also the time of the day with the highest degree of polarization in the zenith of the sky (between 70 and 80 %; Brines and Gould 1982). This provides us with ideal conditions to manipulate the celestial polarization pattern as it appears to the ball-rolling dung beetles. Like their diurnal relatives, *S. zambesianus* can be made to turn by 81 ± 16° when rolling under a linear polarizer placed with its E-vector oriented 90° to that of skylight (Fig. 2.4b) (Dacke et al. 2003b).

The degree of polarization in the zenith of the sky decreases to 50 % when the sun is between 8° and 12° below the horizon, and from 15 % to near zero when the sun is between +16° and −18° (Dave and Ramanathan 1955; Rozenberg 1966). When the sun is more than 18° below the horizon, sunlight no longer influences the night sky and the celestial polarization pattern vanishes. Since night has now succeeded day, *S. zambesianus* beetles behave as if the sky were overcast; unable to extract any relevant compass input from the sky they start to roll in circles (Dacke et al. 2003a). This is true, however, only for nights when the moon has not yet risen.

2.4 Polarized Light Orientation at Night

As a celestial body reflecting sunlight, the moon emits roughly the same spectrum of light as direct sunlight, but obviously with a much lower luminance (Lythgoe 1979). Moonlight, like sunlight, scatters in the earth's atmosphere, and a celestial pattern of polarized light is also present around the moon. On a full moon night, this pattern shows no significant difference in its structure from that of the pattern of polarized light formed around the sun, although it is at least a million times dimmer (Gál et al. 2001).

When the moon has risen, *S. zambesianus* can continue to orient along straight paths well after sunset. If the rising moon is hidden from view, and a linear polarizer is placed with its transmission axis perpendicular to the dominant E-vector in the sky, the beetles can again be observed to change their direction of rolling by close to 90° ($80 \pm 3°$, $n = 22$) (Dacke et al. 2003a) (Fig. 2.4c). For almost 10 years, *S. zambesianus* was the only animal that had been observed to orient using the dim polarization pattern of the moonlit sky. Recently, we demonstrated that the nocturnal dung beetle *Scarabaeus satyrus* also uses this cue to orient (el Jundi et al. 2014) (Fig. 2.4d). The main difference between the dim light activity of these two species is that *S. zambesianus* will only remain active on nights when the moon has risen in conjunction with the setting sun, while *S. satyrus* can function on every night of the lunar month.

The intensity of the relatively dim celestial polarization pattern will gradually decline as the moon wanes. On nights with a crescent moon, the intensity of the polarization pattern is almost 100 times dimmer than on a full moon night (Land 1981; Lynch and Livingston 2001). Remarkably, even the extremely dim celestial polarization pattern formed by a crescent moon is sufficient to guide the nocturnal ball-rolling dung beetles along a straight path. Moreover, straight-line orientation on these dark nights is performed with the same precision and speed as in beetles orienting under the much brighter polarization pattern of the sun or full moon (Dacke et al. 2011) (Fig. 2.5a–c).

When the moon leaves the sky, the tracks made by the ball-rolling dung beetles become curved and significantly longer than on moonlit nights (Fig. 2.5d). However, beetles pushing their balls on these dark nights are not lost, and many of them still travel along relatively straight paths. To investigate the importance of celestial cues on the nocturnal orientation behaviour of these beetles, we occluded the dorsal visual field (and therefore all celestial input) using an opaque cap taped to the dorsal thorax (Fig. 2.5f). Tracks made by beetles wearing a cap are curved and significantly longer than when they have a full view of the sky (Fig. 2.5e) (Dacke et al. 2013a). Experiments in the field and in the planetarium reveal that on these moonless nights the nocturnal beetles still have one more ace to play: celestial orientation to the Milky Way (Dacke et al. 2013a). Since the moon is potentially visible for only half of all nights, the stars and more importantly the Milky Way, provide an additional celestial cue for orientation to keep the beetles on track. An

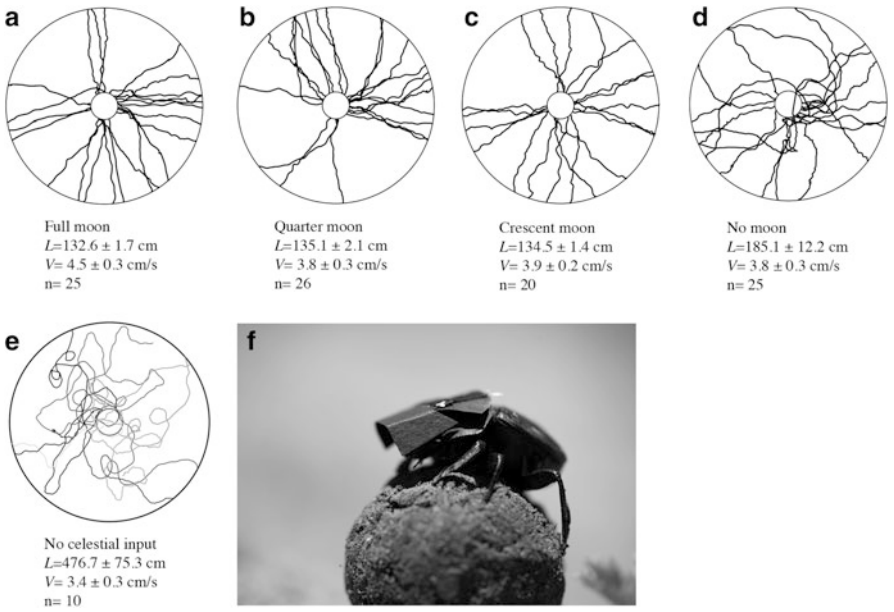

Fig. 2.5 Paths of the ball-rolling beetle, *Scarabaeus satyrus*, rolling outwards from the centre of a 3 m diameter circular arena (as seen from *above*) under a sky lit by the full moon (**a**), quarter moon (**b**), new moon (**c**), on a moonless night (**d**) or with an occluded view of a moonless starry sky (**e**). To block the view of the sky, small "caps" were attached to the thorax of the beetle (**f**). The tracking of the beetle began once it rolled out from the inner, 60 cm diameter circle. The average length of the tracks ($L \pm$ standard deviation) and rolling speed ($V \pm$ standard deviation) under each condition are given next to each figure. The orientation performance—as measured by these two parameters—remained consistent for as long as there was a moon present in the sky (ANOVA, L: $p = 0.33$, V: $p = 0.14$). The tracks did, however, become significantly longer (more curved), if the beetles rolled on a moonless night (ANOVA, $p < 0.001$). On these nights there was no polarization pattern present in the sky to guide the beetles along a given route and their orientation along a straight line became significantly impaired. If the night sky was occluded from view by the use of a cap, the tracks became significantly longer again (t-test, $p > 0.001$). Thus, the straight-line orientation of *S. satyrus* was significantly impaired if they were prevented from seeing the starlit sky [modified after Dacke et al. (2011: **a**–**d**, 2013a: **e**); photo: Emily Baird]

orientation to the Milky Way for straight-line travel is another "first" for the celestially fixated South African dung beetles.

2.5 The Morphology and Physiology of Polarized Light Analysis

As the previous sections indicate, ball-rolling dung beetles can be observed to push their spherical treasures of dung along straight paths on bright sunny days, under the reddish sunset sky as well as on dark moonless nights. The ability to successfully range across almost the complete range of light intensity habitats is made possible

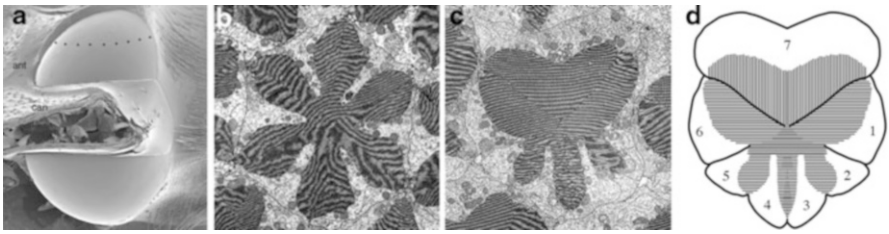

Fig. 2.6 (**a**) Scanning electron micrograph of the dorsal and ventral eye of *Scarabaeus zambesianus*. A lateral view of the head of the beetle shows the canthus (*can*) that completely separates the eye into a dorsal and a ventral part. *The stars* mark the border of the dorsal rim area (DRA). (**b**, **c**) Electron micrographs of the rhabdoms in the ventral eye (**b**) and in the DRA (**c**). (**d**) Schematic drawing of a rhabdom in DRA. The rhabdoms are all formed by seven receptor cells (1–7), but differ in their shape and microvillar orientation. The rhabdoms of the DRA are *heart-shaped* with orthogonal microvilli, while the rhabdoms in the rest of the dorsal eye and in the ventral eye are *flower-shaped* with a variety of microvillar orientations [modified after Dacke et al. (2003b)]

through differences in the morphology of the eyes of nocturnal and diurnal dung beetles (Dacke et al. 2002, 2003b; Byrne and Dacke 2010). Here, we will focus on differences in the parts of the dung beetle eyes devoted to the analysis of celestial polarization.

In dung beetles, as in most other polarization-sensitive insects (Labhart and Meyer 1999), the photoreceptors for celestial polarization analysis are restricted to the dorsal rim area (DRA) of the eye. The location of this area is revealed by the structure of its rhabdoms, in which two sets of receptors with parallel microvilli are oriented 90° to each other (Fig. 2.6d). With a maximum sensitivity to light polarized parallel to the direction of the microvilli (Israelachvili and Wilson 1976; Goldsmith and Wehner 1977; Hardie 1984), this arrangement tunes the two groups of receptors to orthogonal planes of polarization. The straighter and better aligned the microvilli are, the greater the cell's sensitivity to light that is polarized parallel to the main microvillar direction (Wehner et al. 1975; Nilsson et al. 1987). Polarization contrast can be enhanced by a comparison between receptors tuned to different directions of polarization (Labhart 1988; Nilsson and Warrant 1999), and an orthogonal arrangement of the two sets of receptors thus meet the requirement for a polarization-opponent analyser.

The best described polarization analyser of dung beetles is that of *S. zambesianus* (Dacke et al. 2003b). The eyes of this crepuscular species, as in most other ball-rolling beetles, are divided into dorsal and ventral eyes by a cuticular ridge, the canthus (Fig. 2.6a). In the ventral eye, and the ventral half of the dorsal eye, the microvilli form a flower-shaped rhabdom (Fig. 2.6b). In these rhabdoms, the microvilli of the seven receptor cells run in different directions, making these parts of the eye unsuitable for the detection of light polarization. In the dorsal region of the eye (the area above the stars in Fig. 2.6a), the microvilli run in only two directions, forming miniature heart-shaped rhabdoms in cross section (Fig. 2.6c, d). This, together with the finding that these rhabdoms do not twist along

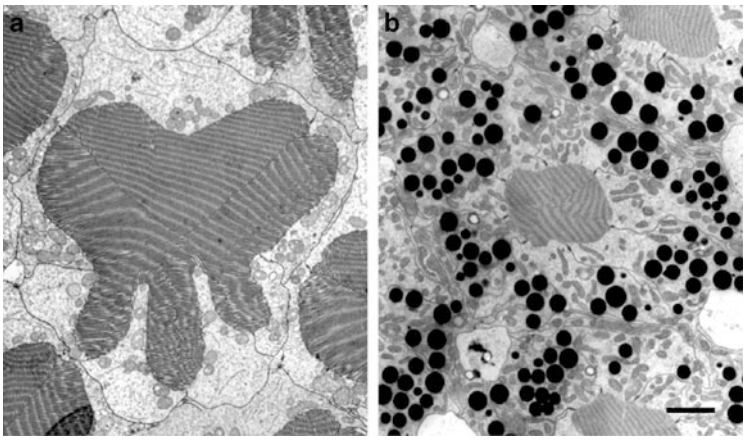

Fig. 2.7 Cross sections of DRA-rhabdoms in the crepuscular dung beetle *Scarabaeus zambesianus* (**a**) and the diurnal beetle *Pachysoma striatum* (**b**). Note the difference in the size of the rhabdom and amount of pigmentation, both morphological adaptations to the time of activity. Scale bar: 2 μm [modified after Dacke et al. (2003b)]

their length, makes them well suited for detection and analysis of polarization. Intracellular recordings show that the receptor cell in the DRA of *S. zambesianus* is at least ten times more sensitive to light polarized parallel to the microvilli than perpendicular to them (Dacke et al. 2004). In other words, they have a polarization sensitivity of at least 10, which is similar to that recorded for other insects (Labhart 1980, 1986; Blum and Labhart 2000; Dacke et al. 2002).

The ability of all visual systems to reliably detect visual information, such as the polarization of light, decreases with falling light intensities. This is because of the random variance of photon arrival on the retina: a photoreceptor that absorbs N photons will experience an uncertainty of $(N)^{1/2}$ associated with this sample (Land 1981; Warrant and McIntyre 1993). This uncertainty, or noise, will reduce the reliability of any visual measurement as light intensity decreases. The photoreceptors themselves also add to this noise by producing spontaneous electrical events that cannot be distinguished from the response to a photon. This means that the darker it gets, the increasing relative noise levels will gradually make it more difficult for the crepuscular and nocturnal dung beetles to reliably detect the direction of skylight polarization.

One possible way for an eye to improve vision in low light levels is to catch more of the available photons. Compared to the diurnal dung beetle *Pachysoma striatum*, the rhabdom in *S. zambesianus* is much longer and three times as wide (Fig. 2.7). This allows the receptors to catch more light and, thus, makes them more sensitive in dim light. In addition, a tracheal *tapetum lucidum* (biological multi-layer mirror) at the base of the retina of *S. zambesianus* reflects light back through the rhabdom, giving it a second opportunity to collect light and effectively doubling its length. Photon catch can also be improved neurally by summing photons in time and space

(Warrant 1999), but this very likely possibility remains to be investigated among the ball-rolling dung beetles.

The nocturnal dung beetles *Scarabaeus deludens* and *Scarabaeus goryi* also have an orthogonal microvilli arrangement of the large photoreceptors in the dorsal part of their eyes. Combined with a need to roll in straight lines, it is more than likely that these beetles, like all their nocturnal relatives, orient to the polarization pattern of the night sky. Laboratory experiments strongly suggest that crickets and tenebroid beetles can also make use of the celestial polarization pattern formed by scattered moonlight (Herzmann and Labhart 1989; Bisch 1999), but behavioural studies in the field at night are inherently difficult in these species. Thus, 10 years after the first demonstration of the use of a nocturnal polarization compass, ball-rolling dung beetles are still the only animals described to possess this ability.

2.6 Conclusions

Few insects, perhaps with the exception of ants, are so ideally suited for the study of celestial orientation as the dung beetles. Their purely celestially based orientation system helps us to avoid confounding orientation effects of landmarks, and when given a ball of dung (or even a golf ball!), these insects will immediately start to roll it along a set compass direction. So strong is their desire to roll that nocturnal beetles can be made to roll at day and diurnal beetles can be compelled to roll in the middle of the night. This incredible flexibility opens up the possibility to perform a new set of experiments directed towards understanding how the celestial compasses can be adapted to the environment in which the insect is normally active. The ball-rolling dung beetles are thus predicted to retain their crown as the best experimental model for nocturnal polarized light orientation for many years to come.

References

Baird E, Byrne MJ, Scholtz CH, Warrant EJ, Dacke M (2010) Bearing selection in ball-rolling dung beetles: is it constant? J Comp Physiol A 196:801–806

Baird E, Byrne MJ, Smolka J, Warrant EJ, Dacke M (2012) The dung beetle dance: an orientation behaviour? PLoS One 7:e30211. doi:10.1371/journal.pone.0030211

Bartholomew GA, Heinrich B (1978) Endothermy in African dung beetles during flight, ball making, and ball rolling. J Exp Biol 73:65–83

Bisch S (1999) Orienterungsleistungen des nachtaktiven Wüstenkäfers *Parastizopus aramaticeps* Peringuey (Coleoptera: Tenebrionidae). Doctoral thesis, Zoologisches Institut, Rheinischen Friedrich-Wilhems-Universität Bonn

Blum M, Labhart T (2000) Photoreceptor visual fields, ommatidial array, and receptor axon projections in the polarisation-sensitive dorsal rim area of the cricket compound eye. J Comp Physiol A 186:119–128

Brines ML, Gould JL (1982) Skylight polarization patterns and animal orientation. J Exp Biol 96:69–91

Byrne MJ, Dacke M (2010) The visual ecology of dung beetles. In: Simmons LW, Ridsdill-Smith TJ (eds) Ecology and evolution of dung beetles. Wiley-Blackwell, Oxford, pp 177–198
Byrne M, Dacke M, Nordström P, Scholtz CH, Warrant EJ (2003) Visual cues used by ball-rolling dung beetles for orientation. J Comp Physiol A 189:411–418
Caveney S, Scholtz CH, McIntyre P (1995) Patterns of daily flight activity in onitine dung beetles (Scarabaeinae: Onitini). Oecologia 103:444–452
Collett M, Collett TS (2009) Local and global navigational coordinate systems in desert ants. J Exp Biol 212:901–905
Dacke M, Nordström P, Scholtz CH, Warrant EJ (2002) A specialized dorsal rim area for polarized light detection in the compound eye of the scarab beetle *Pachysoma striatum*. J Comp Physiol A 188:211–216
Dacke M, Nilsson DE, Scholtz CH, Byrne M, Warrant EJ (2003a) Insect orientation to polarized moonlight. Nature 424:33
Dacke M, Nordström P, Scholtz CH (2003b) Twilight orientation to polarised light in the crepuscular dung beetle *Scarabaeus zambesianus*. J Exp Biol 206:1535–1543
Dacke M, Byrne M, Scholtz CH, Warrant EJ (2004) Lunar orientation in a beetle. Proc Biol Sci 271:361–365
Dacke M, Byrne M, Baird E, Scholtz CH, Warrant EJ (2011) How dim is dim? Precision of the celestial compass in moonlight and sunlight. Philos Trans R Soc B 366:697–702
Dacke M, Baird E, Byrne M, Scholtz CH, Warrant EJ (2013a) Dung beetles use the Milky Way for orientation. Curr Biol 23:1–3
Dacke M, Byrne M, Smolka J, Warrant EJ, Baird E (2013b) Dung beetles ignore landmarks for straight-line orientation. J Comp Physiol A 199:17–23
Dacke M, el Jundi B, Smolka J, Byrne, M, Baird E (2014) The role of the sun in the celestial compass of dung beetles. Philos Trans R Soc B 369: 20130036
Dave JV, Ramanathan KR (1955) On the intensity and polarisation of the light from the sky during twilight. Proc Indian Acad Sci A 43:67–68
Edrich W, Neumeyer C, von Helversen O (1979) "Anti-sun orientation" of bees with regard to a field of ultraviolet light. J Comp Physiol A 134:151–157
el Jundi B, Smolka J, Baird E, Byrne, M, Dacke, M (2014) Diurnal dung beetles use the polarization pattern and intensity gradient of the sky for orientation. J Exp. Biol doi:10.1242/jeb.101154
Gál J, Horváth G, Barta A, Wehner R (2001) Polarization of the moonlit clear night sky measured by full-sky imaging polarimetry at full moon: comparison of the polarization of moonlit and sunlit skies. J Geophys Res D 106:22647–22653
Goldsmith TH, Wehner R (1977) Restrictions on rotational and translational diffusion of pigment in the membranes of a rhabdomeric photoreceptor. J Gen Physiol 70:453–490
Hardie RC (1984) Properties of photoreceptors R7 and R8 in dorsal marginal ommatidia in the compound eyes of *Musca* and *Calliphora*. J Comp Physiol A 154:157–165
Hegedüs R, Akesson S, Horváth G (2007) Polarization patterns of thick clouds: overcast skies have distribution of the angle of polarization similar to that of clear skies. J Opt Soc Am A 24: 2347–2356
Herzmann D, Labhart T (1989) Spectral sensitivity and absolute threshold of polarization vision in crickets: a behavioral study. J Comp Physiol A 165:315–319
Horváth G, Varjú D (2004) Polarized light in animal vision—polarization patterns in nature. Springer, Heidelberg
Israelachvili JNJ, Wilson MM (1976) Absorption characteristics of oriented photopigments in microvilli. Biol Cybern 21:9–15
Labhart T (1980) Specialized photoreceptors at the dorsal rim of the honeybee's compound eye: polarizational and angular sensitivity. J Comp Physiol A 141:19–30
Labhart T (1986) The electrophysiology of photoreceptors in different eye regions of the desert ant, *Cataglyphis bicolor*. J Comp Physiol A 158:1–7

Labhart T (1988) Polarization-opponent interneurons in the insect visual system. Nature 331: 435–437
Labhart T, Meyer EP (1999) Detectors for polarized skylight in insects: a survey of ommatidial specializations in the dorsal rim area of the compound eye. Microsc Res Tech 47:368–379
Land M (1981) Optics and vision in invertebrates. In: Autrum H (ed) Handbook of sensory physiology. Springer, Heidelberg, pp 133–280
Lynch DK, Livingston W (2001) Color and light in nature, 2nd edn. Cambridge University Press, Cambridge
Lythgoe JN (1979) The ecology of vision. Oxford University Press, New York
Nilsson DE, Warrant EJ (1999) Visual discrimination: seeing the third quality of light. Curr Biol 9: R535–R537
Nilsson DE, Labhart T, Meyer E (1987) Photoreceptor design and optical properties affecting polarization sensitivity in ants and crickets. J Comp Physiol A 161:645–658
Pomozi I, Horváth G, Wehner R (2001) How the clear-sky angle of polarization pattern continues underneath clouds: full-sky measurements and implications for animal orientation. J Exp Biol 204:2933–2942
Rossel S, Wehner R (1984) Celestial orientation in bees: the use of spectral cues. J Comp Physiol A 155:605–613
Rozenberg GV (1966) Twilight: a study in atmospheric optics. Plenum, New York
Santschi F (1911) Observations et remarques critiques sur le mécanisme de l'orientation chez les fourmis. Rev Suisse Zool 19:303–338
Ugolini A, Galanti G, Mercatelli L (2009) Difference in skylight intensity is a new celestial cue for sandhopper orientation (Amphipoda, Talitridae). Anim Behav 77:171–175
Warrant EJ (1999) Seeing better at night: life style, eye design and the optimum strategy of spatial and temporal summation. Vis Res 39:1611–1630
Warrant EJ, McIntyre PD (1993) Arthropod eye design and the physical limits to spatial resolving power. Prog Neurobiol 40:413–461
Wehner R (1992) Arthropods. In: Papi F (ed) Animal homing. Chapman and Hall, London, pp 45–144
Wehner R, Srinivasan MV (2003) Path integration in insects. In: Jeffery JK (ed) The neurobiology of spatial behaviours. Oxford University Press, Oxford, pp 9–30
Wehner R, Bernard GD, Geiger E (1975) Twisted and non-twisted rhabdoms and their significance for polarization detection in the bee. J Comp Physiol A 104:225–245

Chapter 3
Polarisation Vision in Ants, Bees and Wasps

Jochen Zeil, Willi A. Ribi, and Ajay Narendra

Abstract We review here what is known from behavioural, anatomical and physiological studies about polarisation sensitivity in the hymenopteran insect groups of ants, wasps and bees. We briefly summarise the behavioural evidence for the use of polarised skylight in orientation and navigation, including some lesser known or less accessible older work, and then review our state of knowledge of the polarisation sensitivity and the arrangement of photoreceptors in compound eyes and in ocelli. We note in particular how little we know about the role of ocelli in polarisation vision.

3.1 Introduction

As central place foragers, hymenopteran insects, such as ants, bees and wasps, routinely return home to their nest, hive or burrow at the end of each foraging trip. To achieve this, they employ two distinct navigational mechanisms: landmark guidance and path integration. The degree to which insects rely on landmark guidance or path integration depends on the navigational information content of their specific habitat (e.g. Cheung et al. 2012). In landmark-poor, featureless environments, such as salt pans, the desert ants of the genus *Cataglyphis* have to rely exclusively on path integration (Wehner and Wehner 1986). During path integration, insects monitor two components of their foraging path in order to

J. Zeil (✉) • A. Narendra
Research School of Biology, The Australian National University, Bld 46, Biology Place, Canberra ACT0200, Australia
e-mail: jochen.zeil@anu.edu.au

W.A. Ribi
Research School of Biology, The Australian National University, Bld 46, Biology Place, Canberra ACT0200, Australia

The Private University of Liechtenstein, Dorfstrasse 24, Triesen FL-9495, Liechtenstein

G. Horváth (ed.), *Polarized Light and Polarization Vision in Animal Sciences*, Springer Series in Vision Research 2, DOI 10.1007/978-3-642-54718-8_3,

compute the direct line home (a home vector; reviewed by Cheung and Vickerstaff 2010; Vickerstaff and Cheung 2010): the distance travelled and their heading direction relative to an external compass reference. The distance component is estimated in walking insects by some form of a stride integrator (Wittlinger et al. 2006) and in flying insects by monitoring the amount of optic flow they experience as they move (Esch and Burns 1996; Srinivasan 2003). Insects are known to monitor heading direction by referring to magnetic (Wajnberg et al. 2010) and visual cues, whereby the latter involve terrestrial information such as the landmark panorama (Graham and Cheng 2009; Reid et al. 2011; Narendra et al. 2013a) and celestial cues such as the sun, the moon, the milky way and the pattern of polarised skylight (Wehner 2001; Dacke et al. 2003, 2004, 2013; Reid et al. 2011).

Here we review what is known from behavioural, anatomical and physiological studies about polarisation sensitivity in the hymenopteran insect groups of ants, wasps and bees. We briefly summarise the behavioural evidence for the use of polarised skylight in orientation and navigation, including some lesser known or less accessible older work, and then review our state of knowledge of the polarisation sensitivity and the arrangement of photoreceptors in compound eyes and in ocelli. We note in particular how little we know about the role of ocelli in polarisation vision.

3.2 Behavioural Evidence

With the exception of some hints that wasps make use of celestial compass cues (Ugolini 1987; Ugolini and Samoggia 1991) there is—to our knowledge—no published behavioural work on polarisation vision in wasps. We will therefore in the following concentrate on what is known in this respect for bees and ants.

The first behavioural evidence that insects can derive directional information from polarised skylight came from the experiments of von Frisch (1949, 1950) showing that the orientation of honeybee waggle dances on horizontal surfaces can be predictably influenced by a rotating linear polariser (summarised by von Frisch 1967; Horváth and Varjú 2004). A large body of work since then has unravelled the computational structure and the sensory and neural basis of this ability (reviewed by Horváth and Varjú 2004; Wehner and Labhart 2006). Bees that are trained to visit a feeder typically signal the direction and the distance of the feeder through their waggle dance. When such foragers are made to dance on a horizontal surface in the presence of linearly polarised light from above, the orientation of a bee's waggle dance changes as the direction of polarisation is changed (Fig. 3.1a) in a way that indicates that the bees employ a simplified template of the pattern of polarised skylight (Rossel and Wehner 1984, 1986). By analysing this response in honeybees, in which different parts of the compound eyes were occluded, Wehner and Strasser (1985) showed that the ommatidia of the dorsal rim area (DRA) of the compound eye, but not those of the rest of the eye or the ocelli, are necessary and sufficient for mediating the bees' orientation relative to the direction of polarisation (Fig. 3.1).

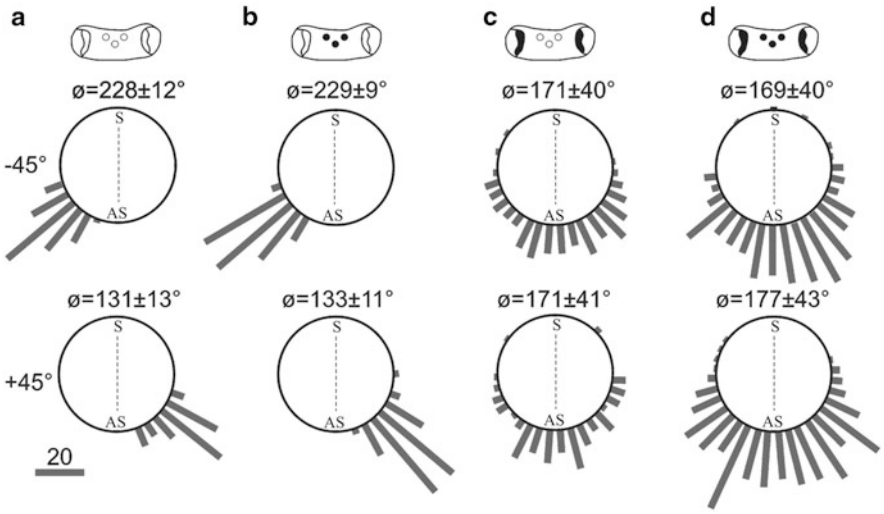

Fig. 3.1 Orientation of honeybee waggle dances. Waggle dance orientation of bees when presented with ±45° E-vector orientation. (**a**) Controls, (**b**) with ocelli occluded, (**c**) with DRA (dorsal rim area) occluded, (**d**) with DRA and ocelli occluded. The data indicate where the bees expect these E-vector directions to occur in the sky relative to the solar meridian (*vertical dashed lines*) with S marking the solar and AS the antisolar half of the sky. Ø—means of the circular distribution of waggle run directions. Scale: 20 waggle runs; $N = 24$ bees, 1,343 waggle runs [modified after Rossel and Wehner (1984)]

Similar experiments in bumblebees, *Bombus terricola occidentalis*, provided contradictory results (Wellington 1974). Wellington (1974) showed that bumblebees are able to orient with reference to polarised skylight at dusk using only their ocelli. During this period of the day, ambient light levels become so low that the photoreceptors in normal apposition compound eyes cease to provide reliable signals (e.g. Warrant 2008).

Until very recently, most behavioural experiments on honeybee polarisation vision were conducted on walking bees or bees dancing in the hive. It remained to be shown that foraging bees actually do use the pattern of polarised skylight to decide where to go. Experiments by Kraft et al. (2011) now have gone some way to demonstrate that indeed they do. The authors trained honeybees to find food in a four-armed maze with sheets of linear polarisers on top of each of the arms that had axially or transversely oriented transmission axes (Fig. 3.2). The clearest results were obtained when bees had to learn to choose an arm of the maze that was illuminated by a transverse direction of polarisation and that branched off to the right, perpendicular to the direction of the entrance tunnel. In this case, bees that were tested with transverse direction of polarisation over the maze arm straight ahead or to the left clearly based their decision where to search for the feeder on the direction of polarisation of overhead light.

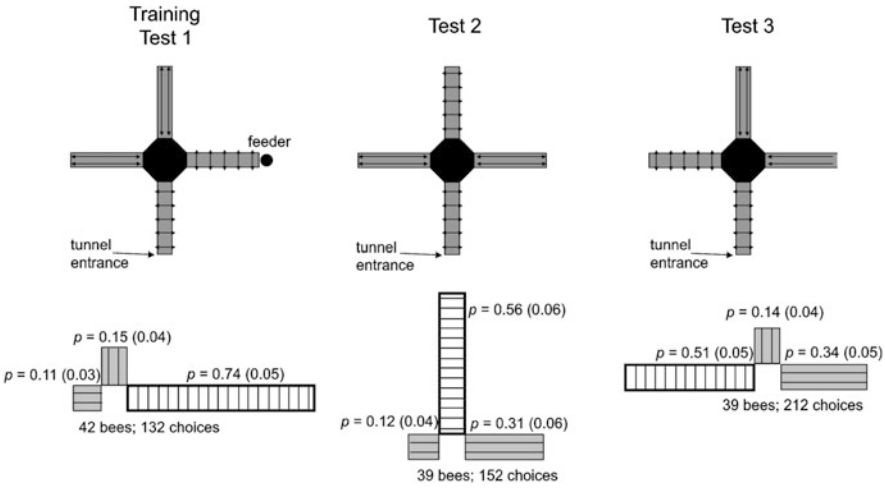

Fig. 3.2 Honeybees detect change in polarisation illumination. Bees were trained to enter a tunnel with transversely polarised light and to choose the right-hand tunnel, which also had transversely polarised illumination. Bees tested with the same configuration (Test 1) chose the right arm over the other two arms, which had axially polarised illumination. In Tests 2 and 3, trained bees chose the arm that had the transversely polarised illumination, which they were trained to. Shown are here mean choice probabilities and standard errors of the means (*in parentheses*) for each exit tunnel. *Stripes* denote the direction of polarisation of the illumination in each tunnel. *White*: tunnel with the same illumination as during the training [modified after Kraft et al. (2011)]

It turned out to be easier to demonstrate that foraging ants attend to the directional information provided by polarised skylight, and we review here briefly some early experiments that are not widely known (reviewed by Waterman 1981). Vowles (1950), studying *Myrmica ruginodis*, repeated experiments first conducted by Santschi (quoted in Wehner 1990) where a cylinder screen that only allowed view of the sky was placed over ant foragers returning to the nest. A large proportion of ants were able to maintain their direction of heading. Vowles (1950) then specifically tested whether this ability was due to the ants' sensitivity to skylight polarisation by observing the change in direction of heading of ants on a horizontal platform that was illuminated from above through a sheet of linear polariser that could be turned through defined angles. Ants changed their direction of heading in response to a change of polariser orientation (Fig. 3.3a). Carthy (1951) trained *Lasius niger* ants to collect larvae in an artificially lit arena and measured the path length of ants in the arena with and without linearly polarised light from above. He found that ants were more directed in the presence of polarised light from above and that their path length became longer when the direction of polarisation was changed. Finally, Jander (1957) conducted an extensive set of experiments under more natural conditions with *Formica rufa*. In one of his experiments, he recorded the heading directions of homing ants in a situation where a sheet of linear polariser was rotated 50° to the left or to the right of the dominant direction of skylight polarisation they had experienced during normal

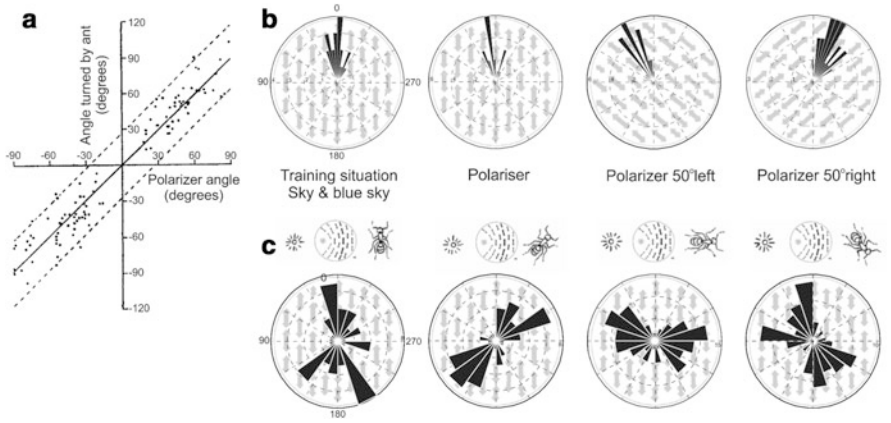

Fig. 3.3 Responses of ants to changes in the direction of polarisation of light from above. (**a**) Heading direction of ants (*y*-axis) on a horizontal platform that was illuminated from above through a sheet of linear polariser that could be turned through defined angles (*x*-axis) [modified after Vowles (1950)]. (**b**) Polarised skylight and polariser orientation are indicated by fields of *double arrows* [modified after Jander (1957)]. (**c**) Ants were trained under open sky to forage in different directions relative to the pattern of polarised skylight (indicated by *pictograms* above *circular histograms*) and subsequently tested under a sheet of linear polariser with a constant orientation as indicated by fields of *double arrows*. Note that depending on their training situation, ants orient appropriately under the polariser, but are unable to discriminate between the solar and the antisolar half of the sky [modified after Jander (1957)]

foraging. The ants' heading direction changed accordingly, but by less than 50° (Fig. 3.3b). Jander (1957, p. 177) repeated these experiments with similar results with a number of other ant species (*Formica fusca*, *Lasius niger*, *Myrmica ruginodis*, *Tetramorium caespitum* and *Tapinoma erraticum*). In an additional experiment Jander's (1957) ants were trained into different compass directions with unobstructed view to sun and sky, and then tested under a linear polariser. The ants in about equal numbers headed either into the appropriate training direction relative to the direction of polarisation or in the opposite direction (Fig. 3.3c), because they were unable to distinguish between the solar and the antisolar hemisphere of the sky in this experimental situation.

Following these early experiments, work on polarisation vision in ants has mainly concentrated on the desert ant *Cataglyphis* that in its featureless desert habitat has to rely heavily on celestial compass information and path integration during foraging (reviewed by Wehner and Srinivasan 2003; Horváth and Varjú 2004; Wehner and Labhart 2006). In fact, these ants employ similar to bees, a template of the pattern of polarised skylight as it is present when the sun is at the horizon and they rely predominantly on a polarisation compass, regardless of whether they can see the sun or not (Wehner and Müller 2006). However, even in *Cataglyphis*, landmark guidance takes precedence over path integration when the ants' habitat provides navigational information in the form of landmarks (Wehner et al. 1996). This was again demonstrated in another desert ant species, the

Australian *Melophorus bagoti* that inhabits comparatively landmark-rich environments and relies only partially on path integration. Homing ants when captured and released in an unfamiliar location travel only half the distance indicated by the path integrator (Narendra 2007; Cheung et al. 2012). The strongest evidence of path integration in these ants came from experiments where ants learnt to reach a food source at the end of an L-shaped channel. When displaced to an unfamiliar location, homing ants walked into a direction that would lead them to the fictive nest as indicated by path integration. However, we do not know at present whether path integration in these ants does rely on the pattern of skylight polarisation as a compass cue. Finally, slave-making ants, *Polyergus rufescens,* when displaced follow a home vector direction, indicating the use of celestial compass information (Grasso et al. 1996), and are disoriented when they cannot perceive the UV component of skylight (Grasso et al. 1997). Considering that polarisation vision in bees (von Helversen and Edrich 1974) and in ants (Duelli and Wehner 1973) depends on UV receptors and that the polarisation-sensitive photoreceptors in the DRA of many insect compound eyes are indeed UV sensitive (Labhart 1986; Wehner and Labhart 2006), this is an indication that these ants do rely on the pattern of polarised skylight for compass information.

Most of the evidence showing that ants use a celestial compass and more specifically the pattern of polarised skylight comes from day-active ants. However, a large number of ant species are active at night, and they also require an external compass reference for navigation. At this stage, only one study (Reid et al. 2011) has shown that the heading direction of foragers of the crepuscular/nocturnal Australian bull ant, *Myrmecia pyriformis,* is influenced by the direction of skylight polarisation. Outbound ants that travel to nest-specific trees during the evening twilight change direction when walking underneath a linear polariser that is rotated $\pm 45^{\circ}$ relative to the dominant direction of polarisation of the sky at dusk (Fig. 3.4a). During twilight, the pattern of skylight polarisation is particularly simple with uniform direction of polarisation approximately parallel to the north–south axis. Many insects are known to use this twilight pattern to derive directional information (Cronin et al. 2006).

Interestingly, the path integrator does not process distance information when there is no simultaneous input of celestial compass information (Sommer and Wehner 2005). Desert ants, *Cataglyphis fortis*, were trained to walk in straight channels with alternating open and covered roofs that partially blocked access to celestial compass information. Homing ants when displaced travelled only the sum of the distance under the open sky they had experienced on their food-ward journey. *Cataglyphis fortis* ants on their outbound journey indeed interpret changes in the perceived direction of polarisation of overhead light as a change in heading direction and integrate such a change into a home vector direction (Lebhardt et al. 2012). In one of the experiments, ants were trained to forage in straight channels that were covered by linear polarisers, with a change in the direction of polarisation halfway along the channel. Ants that were ready to return home were released in an open field. Their heading direction clearly demonstrated that they perceived the change in direction of polarisation in the channel as a change in heading direction, which was incorporated into the computation of their home vector.

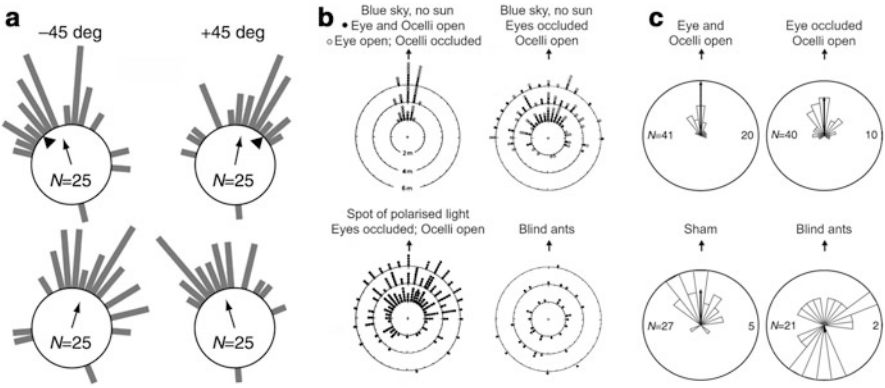

Fig. 3.4 Orientation of ants to change in the dominant direction of polarised skylight. (**a**) Polarisation compass in night-active ants, *Myrmecia pyriformis*. *Top circular histograms* show that ants respond predictably to ±45° rotation of a linear polariser (indicated by *arrow head*) and *bottom histograms* that they reorient after exiting the polariser. *Arrow*: mean vector (from Reid et al. 2011). (**b**) Heading direction of *Cataglyphis bicolor* ants following occlusion of eye and/or ocelli. *Black arrow* indicates true homeward direction [modified after Fent and Wehner (1985)]. (**c**) Role of ocelli in the Australian desert ant, *Melophorus bagoti*. *Circular histograms* show heading direction of ants 2, 4 and 6 m after release in an unfamiliar location. *Short arrow* indicates true nest direction and *arrows* attached to *centre of circles* are the mean vectors [modified after Schwarz et al. (2011a)]

Behavioural evidence for the involvement of the DRA of the compound eye is still lacking in ants (Rüdiger Wehner, personal communication), although the DRA is well developed at least in *Myrmecia* (see below) and in *Cataglyphis*, where it has first been described for ants (Herrling 1976). However, there is evidence that in some ant species the ocelli can provide directional information when the compound eyes are occluded. Fent and Wehner (1985) and Fent (1986) trained *Cataglyphis bicolor* foragers to visit a food source. They then displaced and tracked the paths of homing ants under three conditions: (1) with compound eyes open and ocelli occluded, (2) with compound eyes occluded and ocelli open or (3) as blind animals (Fig. 3.4b). Ants with covered compound eyes and open ocelli headed towards their fictive nest when viewing an annulus-shaped celestial window of polarised skylight and when presented with a 40° diameter spot of linearly polarised light at 45° elevation (Fent and Wehner 1985). Similar experiments were recently carried out by Schwarz et al. (2011a, b) with the Australian desert ant *Melophorus bagoti*, demonstrating that ocelli do indeed provide compass information (Fig. 3.4c), but in this case it remains unclear whether the directional information from *Melophorus bagoti* ocelli makes use of the pattern of skylight polarisation, the sun or the non-uniform brightness and spectral distribution of skylight.

3.3 Anatomical and Physiological Evidence

3.3.1 Dorsal Rim Area

The pattern of skylight polarisation is viewed in most hymenopteran insects by a specialised set of ommatidia in the dorsal-most part of the compound eye, the DRA (Fig. 3.5). The DRA constitutes about 7.6 % of the ommatidia found in *C. bicolor* (100 specialised ommatidia out of a total of 1,300 ommatidia per eye: Labhart 1986). The proportion is substantially smaller in nocturnal bees and ants (2.5 % of 4,800 ommatidia per eye in *Megalopta genalis*: Greiner et al. 2007; 1.7 % of 3,593 ommatidia per eye in *Myrmecia pyriformis*: Reid 2010). In the ommatidia of the DRA, the cross sections of rhabdoms tend to be rectangular (Fig. 3.5) and the directions of the cross-sectional long axes of these rhabdoms change systematically from one ommatidium to the next resulting in a fan-like arrangement in the DRA ommatidial array (Fig. 3.5).

The following specialisations are commonly found in the DRA of hymenopteran insects (following Labhart and Meyer 1999): (a) The optical axes of the DRA ommatidia are directed upwards. (b) The rhabdoms are shorter but have a larger and often distinctly rectangular cross-sectional area compared to the rest of the eye. (c) The microvilli of retinular cells contributing to the fused rhabdom within one ommatidium are oriented 90° to each other (Fig. 3.6). (d) Microvilli alignment is constant throughout the length of the rhabdom. (e) Light-scattering pore canals in the cornea increase the acceptance angle of the photoreceptors (see below). This is thought to reduce ambiguities caused by clouds, for example (Meyer and Labhart 1981; Labhart and Meyer 1999).

Microvilli orientation is an indication of the polarisation sensitivity of a photoreceptor, because the absorption of linearly polarised light is maximal when the E-vector is parallel to the long axis of the microvilli (reviewed by Roberts et al. 2011). Moreover, in the rectangular DRA rhabdoms of many insects, microvilli are oriented parallel and perpendicular to the long axis of the rhabdom cross sections (Fig. 3.6). The orientation of these rhabdoms in the array of DRA ommatidia thus allows us to predict the distribution of polarisation sensitivity across the array, as shown in the black and white histograms in Fig. 3.5.

The structure and organisation of the rhabdoms in the DRA have only been described in a few hymenopteran insect species (*C. bicolor*: Herrling 1976; *C. bicolor* and *Apis mellifera*: Labhart and Meyer 1999; *Megalopta genalis*: Greiner et al. 2007; *Polyrhachis sokolova*: Narendra et al. 2013b). To our knowledge, the spatial distribution of DRA rhabdoms and their viewing directions have only been mapped in *C. bicolor* (Wehner 1982). The rhabdoms in the DRA are typically formed by nine long retinular cells, while elsewhere in the eye each ommatidium contains eight long retinular cells and one short basal retinular cell number 9. In the DRA of the nocturnal *Megalopta genalis,* facet diameters are smaller and the cornea is thinner than in the rest of the compound eye (Fig. 3.7). The crystalline cone has a cylindrical shape while in the rest of the eye it is cone-shaped and

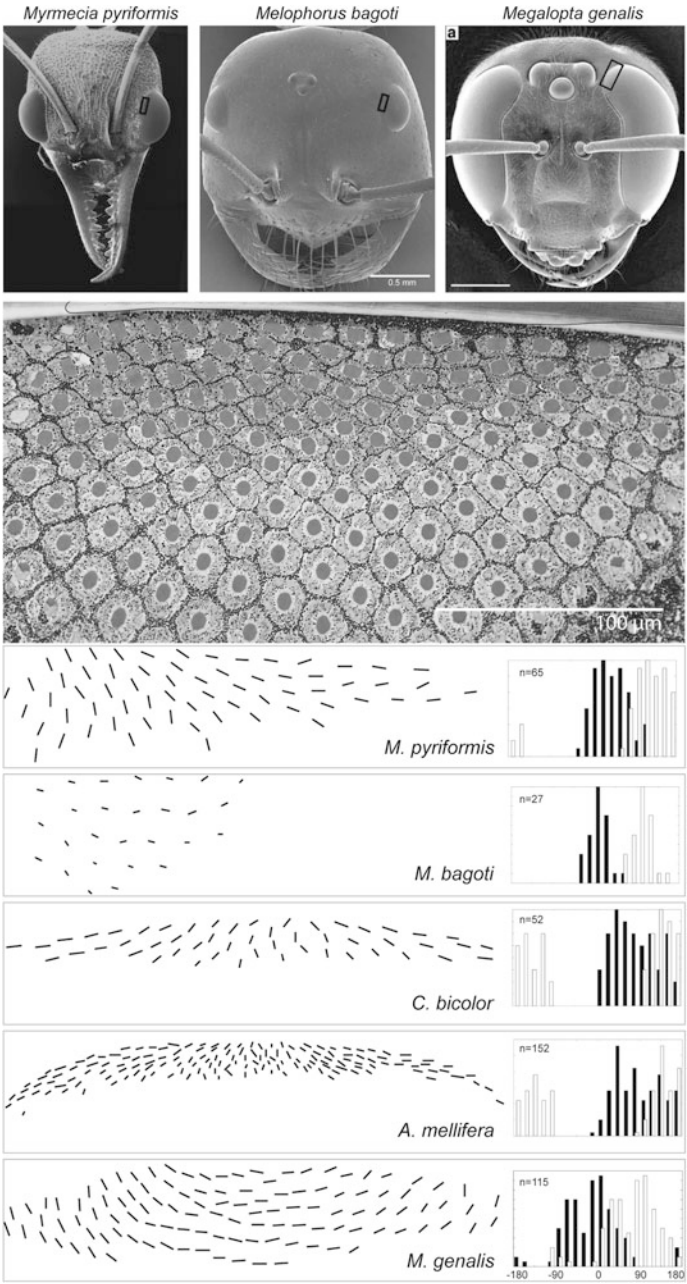

Fig. 3.5 Orientations of the long axis of rhabdoms in the dorsal rim area (DRA) of hymenopterans. *First row*: Scanning electron microscopy images of dorso-frontal views of the heads of *Myrmecia pyriformis*, *Melophorus bagoti* and *Megalopta genalis* indicating the DRA on the left eye. *Second row*: Light microscopy image of a cross section through the distal rhabdoms of the bull ant, *Myrmecia pyriformis*. Specialised rhabdoms appear *rectangular* in shape and are found in the dorsal-most 3–4 rows of ommatidia. *Bottom rows*: Maps illustrating the orientation of the

tapering towards the distal tip of the rhabdom in both bees (*A. mellifera*: Aepli et al. 1985; *Megalopta genalis*: Greiner et al. 2007) and wasps (*Sphex cognatus*: WA Ribi unpublished). This specialisation appears to be absent in ants (*Myrmecia gulosa*, *Paraponera clavata*: E Meyer unpublished; *Myrmecia pyriformis*, *Polyrhachis sokolova*: A Narendra unpublished). Figures 3.5 and 3.6 provide a comparative overview of rhabdom cross sections in the DRA of a number of hymenopteran insects.

Even less is known about the physiology of DRA retinular cells, although early behavioural experiments indicated that UV receptors play a crucial role in the detection of skylight polarisation (Mote and Wehner 1980). *C. bicolor* ants appear to be disoriented when wavelengths below 430 nm are cut off in the skylight they see, but are well oriented when they see the sky through a UV window only (<400 nm, Duelli and Wehner 1973). Menzel and Snyder (1974) did find UV cells with high polarisation sensitivity in the honeybee, but unfortunately did not report where in the compound eye they recorded these cells. The same is true for high polarisation sensitivities recorded by Menzel (1975) in photoreceptors of the bulldog ant *Myrmecia gulosa* that were most sensitive at wavelengths of 500 nm. The UV cells in the DRA of *C. bicolor* are much larger in size compared to the green cells (Labhart 1986). Electrophysiological evidence shows that the polarisation sensitivity (PS) of the UV cells is higher in the DRA (PS = 6.3) compared to elsewhere in the eye (PS = 2.9, Labhart 1986). In bees the UV cells in the DRA alone provide the input channels to the E-vector detection system (Labhart 1980). In the case of the nocturnal bee *Megalopta genalis,* polarisation-sensitive photoreceptors are present only in the DRA (Greiner et al. 2007). The photoreceptors in the DRA exhibit a very high polarisation sensitivity (PS = 21.2 ± 7.5) compared to elsewhere in the eye (PS = 1.4 ± 0.4). It is also notable that DRA retinular cells have acceptance functions that are consistently about twice as wide compared to those of retinular cells in the rest of the eye (*C. bicolor*: Labhart 1986): $\Delta\rho_{DRA} = 5.4^{o} \pm 1.25$ ($n = 13$) vs. $\Delta\rho_{Rest} = 3.0°–4.3°$ ($n = 48$); *Megalopta genalis* (Greiner et al. 2007): $\Delta\rho_{DRA} = 13.8° \pm 3.6°$ ($n = 15$) vs. $\Delta\rho_{Rest} = 5.9° \pm 1.7°$ ($n = 20$), with $\Delta\rho$ values indicating the half-width of the acceptance function.

Fig. 3.5 (continued) cross-sectional long axis of the specialised rhabdoms in the DRA of *Myrmecia pyriformis*, *Melophorus bagoti*, *Cataglyphis bicolor*, *Apis mellifera* and *Megalopta genalis*. *Black bars*: distribution of the long-axis orientation of rhabdom cross sections relative to the horizontal at 0°. *Open bars*: distribution of the short-axis orientation of rhabdom cross sections. Note that *histograms* indicate the distribution of likely polarisation sensitivities. Scanning electron microscopy of *Myrmecia pyriformis*: courtesy of Rainer Foelix. Scanning electron microscopy of *Megalopta genalis*: courtesy of Eric Warrant

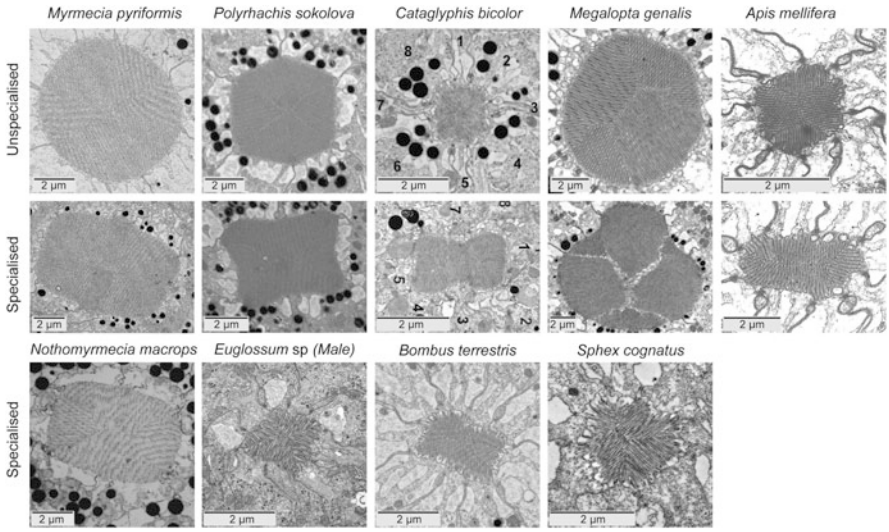

Fig. 3.6 Transmission electron micrographs of cross sections through rhabdoms of hymenopteran insects, all female except for *Euglossum* sp. *First row*: unspecialised rhabdoms with at least four different orientations of microvilli. *Second and third rows*: specialised rhabdoms in the dorsal rim area (DRA) with microvilli oriented in two directions, opposite to each other. Image courtesy: Labhart and Meyer (1999)—*Cataglyphis bicolor*, Narendra et al. (2013b)—*Polyrhachis sokolova*, Wehner (1982)—*Nothomyrmecia macrops*, Warrant et al. (2004) and Greiner et al. (2007)—*Megalopta genalis*

3.3.2 Ocelli

In addition to the compound eyes, many hymenopterans possess single lens eyes called ocelli on the dorsal surface of the head. An ocellus consists of a lens, a vitreous body, an iris, a corneageneous cell layer, a retina and a neuropil (Fig. 3.8) (Goodman 1981; Ribi et al. 2011). Three ocelli are typically placed in a triangular arrangement on the head (ants: male and female alates; bees: *Apis*, *Bombus*, *Megalopta*, *Trigona*, *Xylocopa*; wasps: *Polistes*, *Vespa*, *Sphex*). In the worker ants (see http://www.antweb.org) ocelli are either absent (most ants) or present only in certain castes (e.g. *Gesomyrmex chaperi*). Some species possess only the median or lateral ocellus (e.g. *Polyrhachis ypsilon*, *Polyrhachis bihamata*) and others have all three ocelli (e.g. *Cataglyphis*, *Formica*, *Harpegnathos*, *Melophorus*, *Myrmecia*). The size of the ocelli, as first noted by Kerfoot (1967), is larger in nocturnal hymenopterans compared to crepuscular and diurnal animals (Warrant et al. 2006; Somanathan et al. 2009; Narendra et al. 2011), suggesting that the ocelli due to their superior optical sensitivity gain in importance under low light conditions. Indeed, ocelli appear to allow bumblebees to extend their foraging activity well into the dim-lit dusk periods (Wellington 1974).

As first noted by Kral (1978), ocellar rhabdoms in *A. mellifera* and in *Vespa vulgaris* must be polarisation sensitive due to their sheet-like elongated shape in

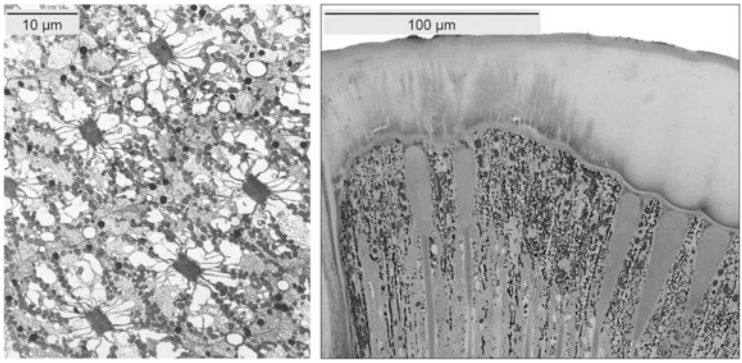

Fig. 3.7 *Left*: TEM cross section of the dorsal rim area (DRA) in the honeybee, *Apis mellifera*. *Right*: light micrograph of a longitudinal section of the DRA in the night-active bee, *Megalopta genalis*. The cornea in the DRA is thinner, and the crystalline cone has a *cylindrical shape* [see also Greiner et al. (2007)]

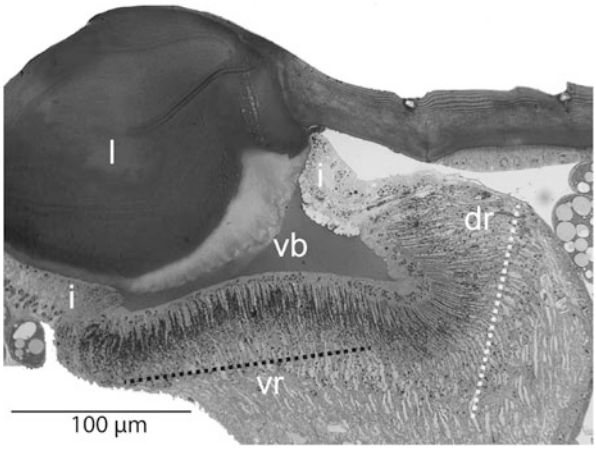

Fig. 3.8 Longitudinal section of the median ocellus of the blue-banded bee, *Amegilla holmessi*, illustrating the dipartite ocellar retina and typically found structures. l: lens, i: iris, vb: vitreous body, vr: ventral retina, dr: dorsal retina

cross sections. Two paired retinular cells contribute microvilli that are oriented perpendicular to the long axis of the rhabdom cross section, with microvilli mostly aligned in a single direction, making it very likely that ocellar rhabdoms are sensitive to the direction of polarisation (Fig. 3.9). Indeed, the few electrophysiological investigations of ocellar photoreceptors (*C. bicolor*: Mote and Wehner 1980; *A. mellifera*: Geiser and Labhart 1982) have reported high polarisation sensitivities. Interestingly, Berry et al. (2011) when recording from ocellar photoreceptors in night-active bees, *Megalopta genalis*, found them not to be polarisation sensitive, most probably because only a few rhabdoms appear straight in cross sections in

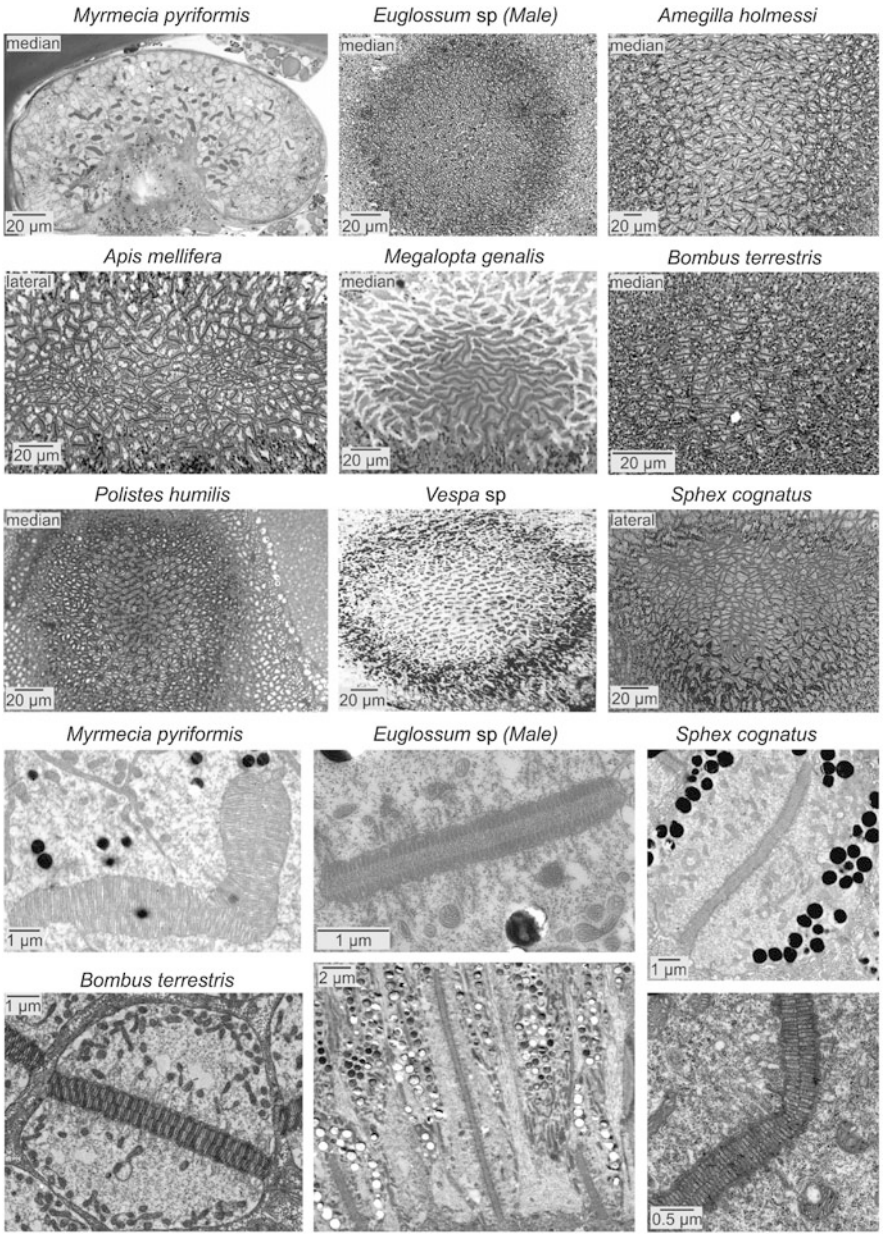

Fig. 3.9 The anatomy of the ocellar retina in hymenopteran insects. *Rows 1–3*: Light micrographs of cross sections of the median and lateral ocelli in ants, bees and wasps. *Rows 4–5*: Transmission electron micrographs of individual ocellar rhabdoms in the ant *Myrmecia pyriformis*, the bumble bee *Bombus terrestris*, the orchid bee *Euglossum* sp. (*centre image* in *bottom row* is a longitudinal section through the dorsal ocellar retina) and the digger wasp *Sphex cognatus* (right image in bottom row is a longitudinal section through the dorsal ocellar retina). Images courtesy: Berry et al. (2011)—*Megalopta genalis*, Ribi et al. (2011)—*Apis mellifera*

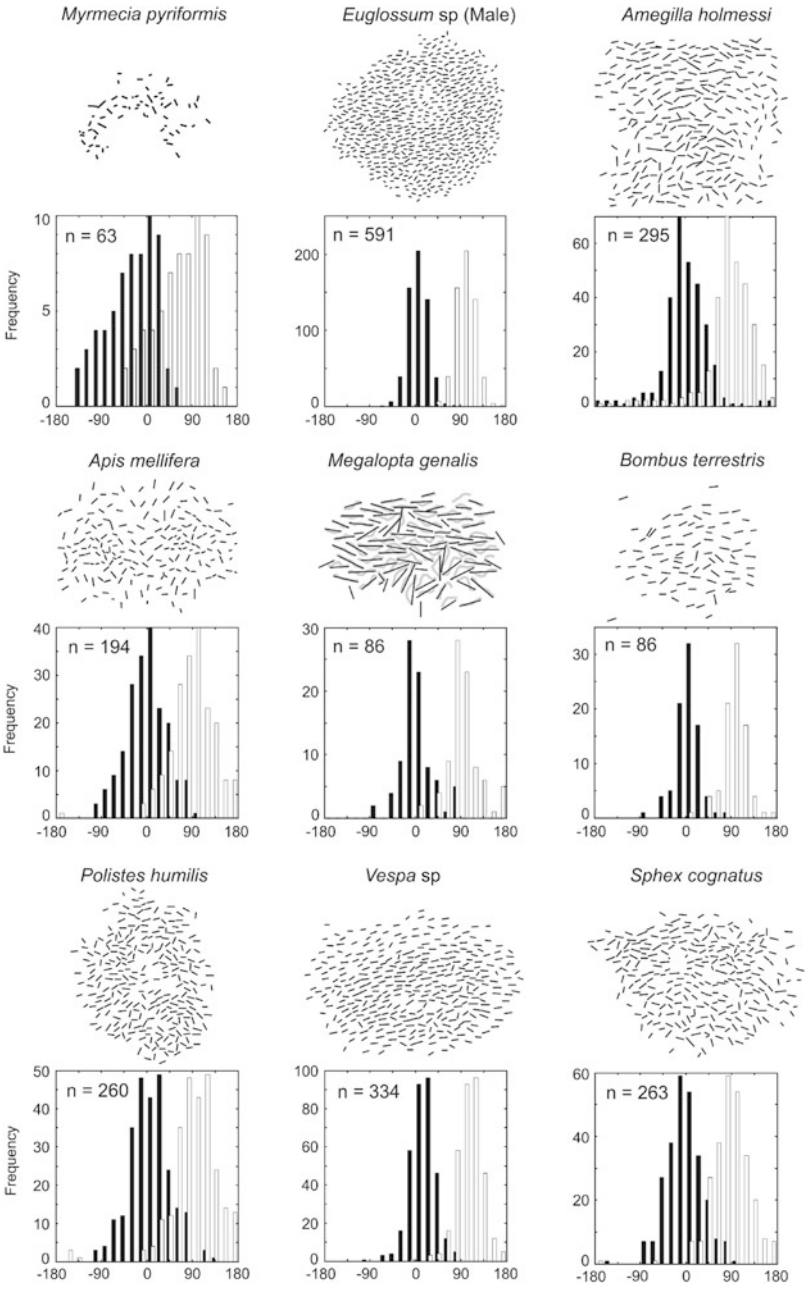

Fig. 3.10 *Maps and orientation histograms* of the long axis of ocellar rhabdom cross sections in ants, bees and wasps, corresponding to light micrographs shown in Fig. 3.9, *rows 1–3*. Rhabdom maps are not to scale. *Black bars*: distribution of rhabdom cross-section orientation relative to horizontal at 0°; *white bars*: predicted distribution of polarisation sensitivity of ocellar photoreceptor arrays

these bees compared to a majority of straight rhabdoms in the day-active honeybee, *A. mellifera* (Fig. 3.10) (Warrant et al. 2006; Ribi et al. 2011).

Comparing the organisation of the ocellar retina in different species, three features are notable that have a bearing on the possible role of ocelli in the processing of polarised light information (Figs. 3.9 and 3.10; see also Ribi et al. 2011): (1) In most cases (*Euglossum*, *Amegilla*, *Apis*, *Bombus*, *Polistes*, *Vespa* and *Sphex*) the rhabdoms are elongated and straight in cross section, while in the night-active bee *Megalopta genalis* most rhabdom cross sections are curved, thus destroying polarisation sensitivity (Fig. 3.9). (2) The overall cross-section alignment of the elongated rhabdom sheets tends to be horizontal, and the sheets do not twist along their length (Fig. 3.8 and centre image, bottom row in Fig. 3.9), making most of the rhabdoms sensitive to vertically polarised light (Fig. 3.10). This arrangement has interesting consequences for the possible function of ocelli. Consider an insect with one forward-looking and two sideways-looking ocelli, each with an array of photoreceptors with predominantly vertically aligned microvilli. When the sun is at the horizon, the photoreceptor arrays in the three ocelli will be in very different states of activation, because skylight is always horizontally polarised along the solar-antisolar meridian and vertically polarised at right angles to the sun. When an insect is pointing away from the sun (toward the antisolar meridian), for instance, the forward-looking ocellus would receive mainly horizontally polarised skylight, and the photon absorption probability in its photoreceptor array would be low. The lateral ocelli, however, would view predominantly vertically polarised skylight, and the photon absorption probability of their photoreceptor arrays would be high. The relative absorption of photons in the three ocelli would change dramatically as the orientation of the insect around the yaw axis changes. At dawn and dusk, the ocelli would thus provide signals that could help to maintain a compass bearing and/or contribute to head stabilisation around the yaw axis (e.g. Parsons et al. 2006, 2010). Note that the non-uniform stimulation of ocellar photoreceptors will become less and less pronounced as the sun rises to higher elevations. During midday, with skylight being predominantly horizontally polarised throughout the celestial hemisphere, photon absorption will be low in the photoreceptor arrays of all three ocelli, irrespective of the yaw (azimuth) orientation of the insect. This raises the interesting possibility that ocellar function may vary with the time of day and, as far as celestial compass information is concerned, will be restricted to mornings and evenings (e.g. Wellington 1974). It is also worth exploring to what extent the horizontally aligned ocellar rhabdom arrays can provide control signals for roll and pitch stabilisation of the head (e.g. Stange 1981). (3) We also note that the number of rhabdoms and the patterns of ocellar rhabdom alignment differ significantly between species (Fig. 3.10).

The only ant in which the ocellar retina has been investigated is the night-active ant *Myrmecia pyriformis*. The rhabdoms in this nocturnal ant are large, but significantly fewer and less straight compared to the ones described in bees and wasps (Figs. 3.9 and 3.10). In both bees and wasps the microvilli of the two retinular cells that make up the ocellar rhabdoms are aligned in the same direction, whereas this is not the case in *Myrmecia pyriformis*. It remains to be seen whether microvillar

organisation is different in diurnal ants. Thus, the anatomical evidence suggests that as in nocturnal bees, in the nocturnal ant *Myrmecia pyriformis* only some ocellar retinular cells may be polarisation sensitive. We know, unfortunately, very little about the ocellar organisation in those ants (*C. bicolor* and *Melophorus bagoti*), where there is behavioural evidence for ocellar involvement in the detection of light polarisation.

3.4 Future Directions

Work on polarisation vision in ants, bees and wasps has exclusively concentrated on the use of celestial compass information, yet the extent to which these insects make use of the additional information content of reflection polarisation, such as from water surfaces, from moist surfaces and from shiny leaves, is completely unknown (e.g. Grant et al. 1993; Horváth et al. 2002; Nicolson 2009). However, electrophysiological recordings from photoreceptors in different eye regions of the honeybee *A. mellifera* (Labhart 1980), sweat bee *Megalopta genalis* (Greiner et al. 2007) and the desert ant *C. bicolor* (Labhart 1986) did not find significant polarisation sensitivities of photoreceptors outside the DRA, suggesting that reflection-polarisation signals may not be important at least for these three species.

Evidence of polarisation vision has been restricted to a handful of hymenopteran insects and we know surprisingly little about polarisation vision in wasps. Behavioural evidence shows that both day-active and night-active ants and bees use the pattern of skylight polarisation as a compass cue. However, it remains to be explored to what extent polarisation-sensitive photoreceptors are also involved in attitude control and in landmark guidance. Polarisation sensitivity can potentially provide increased contrast between the terrestrial landmark panorama and the sky and thus may contribute robust signals in the context of roll, pitch and yaw control, but also in the use of canopy patterns for orientation.

Lastly, the role of ocelli in the context of polarisation vision still remains to be investigated. While the behavioural evidence from diurnal honeybees confronted with individual E-vectors indicates that ocelli are not polarisation sensitive (Rossel and Wehner 1984; Wehner and Strasser 1985), the anatomical evidence suggests the contrary (Ribi et al. 2011). In ants, there is behavioural evidence for ocellar involvement in the polarisation compass when they can view large parts of the sky (Fent and Wehner 1985; Fent 1986; Schwarz et al. 2011b), but anatomical, and most crucially, physiological, evidence is lacking. Behavioural experiments are thus needed on the potentially multiple roles of ocelli comparing walking and flying animals, animals with and without ocelli and diurnal and nocturnal animals together with comparative anatomical and physiological investigations of ocellar photoreceptors.

Acknowledgements We acknowledge funding support from the Australian Research Council's (ARC) Centre of Excellence Scheme (CE0561903), an ARC Discovery Project and Australian

Postdoctoral fellowship (DP0986006), an ARC Discovery Early Career Researcher Award (DE120100019), Hermon Slade Foundation and the GO8-DAAD Germany Australia Research Cooperation Scheme. We thank Eric Meyer, Eric Warrant, Rüdiger Wehner and Tom Labhart for generously providing TEM and SEM images. We thank Rüdiger Wehner for comments on the draft manuscript and Matthias Flötenmeyer MPI Tübingen for his support and the use of the EM-facilities.

References

Aepli F, Labhart T, Meyer EP (1985) Structural specializations of the cornea and retina at the dorsal rim of the compound eye in hymenopteran insects. Cell Tissue Res 239:19–24

Berry RP, Wcislo WT, Warrant EJ (2011) Ocellar adaptations for dim light vision in a nocturnal bee. J Exp Biol 214:1283–1293

Carthy JD (1951) The orientation of two allied species of British ant. 1. Visual direction finding in *Acanthomyops* (Lasius) *niger*. Behaviour 3:275–303

Cheung A, Vickerstaff R (2010) Finding the way with a noisy brain. PLoS Comput Biol 6: e1000992

Cheung A, Hiby L, Narendra A (2012) Ant navigation: fractional use of the home vector. PLoS One 7:e58801

Cronin TW, Warrant EJ, Greiner B (2006) Celestial polarization patterns during twilight. Appl Opt 45:5582–5589

Dacke M, Nordström P, Scholtz CH (2003) Twilight orientation to polarised light in the crepuscular dung beetle *Scarabaeus zambesianus*. J Exp Biol 206:1535–1543

Dacke M, Byrne MJ, Scholtz CH, Warrant EJ (2004) Lunar orientation in a beetle. Proc R Soc B 271:361–365

Dacke M, Baird E, Byrne M, Scholtz CH, Warrant EJ (2013) Dung beetles use the milky way for orientation. Curr Biol 23:298–300

Duelli P, Wehner R (1973) The spectral sensitivity of polarised light orientation in *Cataglyphis bicolor* (Formicidae, Hymenoptera). J Comp Physiol A 86:37–53

Esch HE, Burns JE (1996) Distance estimation by foraging honeybees. J Exp Biol 199:155–162

Fent K (1986) Polarized skylight orientation in the desert ant *Cataglyphis*. J Comp Physiol A 158:145–150

Fent K, Wehner R (1985) Ocelli—a celestial compass in the desert ant *Cataglyphis*. Science 228:192–194

Geiser FX, Labhart T (1982) Electrophysiological investigations on the ocellar retina of the honeybee (*Apis mellifera*). Verhandlungen der Deutschen Zoologischen Gesellschaft 75:307

Goodman LJ (1981) Organisation and physiology of the insect dorsal ocellar system. In: Autrum H (ed) Handbook of sensory physiology, vol VII/6C. Springer, Berlin, pp 201–286

Graham P, Cheng K (2009) Ants use the panoramic skyline as a visual cue during navigation. Curr Biol 19:R935–R937

Grant L, Daughtry CST, Vanderbilt VC (1993) Polarized and specular reflectance variation with leaf surface features. Physiol Plant 88:1–9

Grasso DA, Ugolini A, Le Moli F (1996) Homing behaviour in *Polyergus rufescens* Latr (Hymenoptera, Formicidae). Ethology 102:99–108

Grasso DA, Ugolini A, Visicchio R, Le Moli F (1997) Orientation of *Polyergus rufescens* (Hymenoptera, Formicidae) during slave-making raids. Anim Behav 54:1425–1438

Greiner B, Cronin T, Ribi WA, Wcislo W, Warrant EJ (2007) Anatomical and physiological evidence for polarisation vision in the nocturnal bee *Megalopta genalis*. J Comp Physiol A 193:591–600

Herrling PL (1976) Regional distribution of three unltrastructural retinula types in the retina of *Cataglyphis bicolor* Fabr. (Formicidae, Hymenoptera). Cell Tissue Res 169:247–266

Horváth G, Varjú D (2004) Polarized light in animal vision—polarization patterns in nature. Springer, Heidelberg

Horváth G, Gál J, Labhart T, Wehner R (2002) Does reflection polarization by plants influence colour perception in insects? Polarimetric measurements applied to a polarization-sensitive model retina of *Papilio* butterflies. J Exp Biol 205:3281–3298

Jander R (1957) Die optische Richtungsorientierung der roten Waldameise (*Formica rufa* L.). Zeitschrift für vergleichende Physiologie 40:162–238

Kerfoot WB (1967) Correlation between ocellar size and the foraging activities of bees (Hymenoptera; Apoidea). Am Nat 101:65–70

Kraft P, Evangelista C, Dacke M, Labhart T, Srinivasan MV (2011) Honeybee navigation: following routes using polarized-light cues. Philos Trans R Soc B 366:703–708

Kral K (1978) The orientation of the rhabdoms in the ocelli of *Apis mellifera carnia* Pollm. and of *Vespa vulgaris* L. Zoologisches Jahrbuch Physiologie 82:263–271

Labhart T (1980) Specialized photoreceptors at the dorsal rim of the honeybee's compound eye: polarizational and angular sensitivity. J Comp Physiol 141:19–30

Labhart T (1986) The electrophysiology of photoreceptors in different eye regions of the desert ant, *Cataglyphis bicolor*. J Comp Physiol A 158:1–7

Labhart T, Meyer EP (1999) Detectors for polarized skylight in insects: a survey of ommatidial specializations in the dorsal rim area of the compound eye. Microsc Res Tech 47:368–379

Lebhardt F, Koch J, Ronacher B (2012) The polarization compass dominates over idiothetic cues in path integration of desert ants. J Exp Biol 215:526–535

Menzel R (1975) Polarisation sensitivity in insect eyes with fused rhabdoms. In: Snyder AW, Menzel R (eds) Photoreceptor optics. Springer, Berlin, pp 372–387

Menzel R, Snyder A (1974) Polarised light detection in the bee *Apis mellifera*. J Comp Physiol 88: 247–270

Meyer EP, Labhart T (1981) Pore canals in the cornea of a functionally specialized area of the honey bee's compound eye. Cell Tissue Res 216:491–501

Mote MI, Wehner R (1980) Functional characteristics of photoreceptors in the compound eye and ocellus of the desert ant, *Cataglyphis bicolor*. J Comp Physiol 137:63–71

Narendra A (2007) Homing strategies of the Australian desert ant *Melophorus bagoti* I. Proportional path-integration takes the ant half-way home. J Exp Biol 210:1798–1803

Narendra A, Reid SF, Greiner B, Peters RA, Hemmi JM, Ribi WA, Zeil J (2011) Caste-specific visual adaptations to distinct daily activity schedules in Australian *Myrmecia* ants. Proc R Soc B 278:1141–1149

Narendra A, Gourmaud S, Zeil J (2013a) Mapping the navigational knowledge of individually foraging ants, *Myrmecia croslandi*. Proc R Soc B 208:20130683

Narendra A, Alkaladi A, Raderschall CA, Ribi WA, Robson SKA (2013b) Compound eye adaptations for diurnal and nocturnal lifestyle in the intertidal ant, *Polyrhachis sokolova*. PLoS One 8(11):e76015

Nicolson SW (2009) Water homeostasis in bees, with the emphasis on sociality. J Exp Biol 212: 429–434

Parsons MM, Krapp HG, Laughlin SB (2006) A motion-sensitive neurone responds to signals from the two visual systems of the blowfly, the compound eyes and ocelli. J Exp Biol 209: 4464–4474

Parsons MM, Krapp HG, Laughlin SB (2010) Sensor fusion in identified visual interneurons. Curr Biol 20:624–628

Reid SF (2010) Life in the dark: vision and navigation in the nocturnal bull ant. PhD thesis. The Australian National University, Canberra

Reid SF, Narendra A, Hemmi JM, Zeil J (2011) Polarised skylight and the landmark panorama provide night-active bull ants with compass information during route following. J Exp Biol 214:363–370

Ribi WA, Warrant EJ, Zeil J (2011) The organization of honeybee ocelli: Regional specializations and rhabdom arrangements. Arthropod Struct Dev 40:509–520

Roberts NW, Porter ML, Cronin TW (2011) The molecular basis of mechanisms underlying polarization vision. Philos Trans R Soc B 366:627–637
Rossel S, Wehner R (1984) Celestial orientation in bees: the use of spectral cues. J Comp Physiol 155:605–613
Rossel S, Wehner R (1986) Polarization vision in bees. Nature 323:128–131
Schwarz S, Albert L, Wystrach A, Cheng K (2011a) Ocelli contribute to the encoding of celestial compass information in the Australian desert ant *Melophorus bagoti*. J Exp Biol 214:901–906
Schwarz S, Wystrach A, Cheng K (2011b) A new navigational mechanism mediated by ant ocelli. Biol Lett 7:856–858
Somanathan H, Kelber A, Borges R, Wallen R, Warrant EJ (2009) Visual ecology of Indian carpenter bees II: adaptations of eyes and ocelli to nocturnal and diurnal lifestyles. J Comp Physiol A 195:571–583
Sommer S, Wehner R (2005) Vector navigation in desert ants, *Cataglyphis fortis*: celestial compass cues are essential for the proper use of distance information. Naturwissenschaften 92:468–471
Srinivasan MV (2003) Honeybee navigation. Current biology 13: R894
Stange G (1981) The ocellar component of flight equilibrium control in dragonflies. J Comp Physiol 141:335–347
Ugolini A (1987) Visual information acquired during displacement and initial orientation in *Polistes gallicus* (L) (Hymenoptera, Vespidae). Anim Behav 35:590–595
Ugolini A, Samoggia M (1991) Workers of *Polistes dominulus* (Christ): influence of the landscape on initial orientation. Ethol Ecol Evol 3:247–255
Vickerstaff RJ, Cheung A (2010) Which coordinate system for modelling path integration? J Theor Biol 263:242–261
von Frisch K (1949) Die Polarisation des Himmelslichtes als orientierender Faktor bei den Tänzen der Bienen. Experientia 5:142–148
von Frisch K (1950) Die Sonne als Kompass im Leben der Bienen. Experientia 6:210–221
von Frisch K (1967) The dance language and orientation of bees. Harvard University Press, Cambridge, MA
von Helversen O, Edrich W (1974) Der Polarisationsempfänger im Bienenauge: ein Ultraviolettrezeptor. J Comp Physiol 94:33–47
Vowles DM (1950) Sensitivity of ants to polarized light. Nature 165:282–283
Wajnberg E, Acosta-Avalos D, Alves OC, De Oliveira JF, Srygley RB, Esquivel DM (2010) Magnetoreception in eusocial insects: an update. J Roy Soc Interface 7:S207–S225
Warrant EJ (2008) Seeing in the dark: vision and visual behaviour in nocturnal bees and wasps. J Exp Biol 211:1737–1746
Warrant EJ, Kelber A, Gislen A, Greiner B, Ribi WA, Wcislo WT (2004) Nocturnal vision and landmark orientation in a tropical halictid bee. Curr Biol 14:1309–1318
Warrant EJ, Kelber A, Wallen R, Wcislo W (2006) Ocellar optics in nocturnal and diurnal bees and wasps. Arthropod Struct Dev 35:293–305
Waterman TH (1981) Polarization sensitivity. In: Autrum H (ed) Handbook of sensory physiology, vol VII/6B. Springer, Berlin, pp 281–469
Wehner R (1982) Himmelsnavigation bei Insekten. Neurophysiologie und Verhalten, Neujahrsblatt der Naturforschenden Gesellschaft Zürich, pp 1–132
Wehner R (1990) On the brink of introducing sensory ecology: Felix Santschi (1872-1940) Tabib-en-Neml. Behav Ecol Sociobiol 27:295–306
Wehner R (2001) Polarization vision: a uniform sensory capacity? J Exp Biol 204:2589–2596
Wehner R, Labhart T (2006) Polarization vision. In: Nilsson DE, Warrant EJ (eds) Invertebrate vision. Cambridge University Press, Cambridge, pp 291–348
Wehner R, Müller M (2006) The significance of direct sunlight and polarized skylight in the ant's celestial system of navigation. Proc Natl Acad Sci USA 103:12575–12579
Wehner R, Srinivasan MV (2003) Path integration in insects. In: Jeffry K (ed) The neurobiology of spatial behaviour. Oxford University Press, Oxford, pp 9–30

Wehner R, Strasser S (1985) The Pol area of the honey bee's eye: behavioral evidence. Physiol Entomol 10:337–349
Wehner R, Wehner S (1986) Path integration in desert ants: approaching a long-standing puzzle in insect navigation. Monitore Zoologico Italiano 20:309–331
Wehner R, Michel B, Antonsen P (1996) Visual navigation in insects: coupling of egocentric and geocentric information. J Exp Biol 199:129–140
Wellington WG (1974) Bumblebee ocelli and navigation at dusk. Science 183:550–551
Wittlinger M, Wehner R, Wolf H (2006) The ant odometer: stepping on stilts and stumps. Science 312:1965–1967

Chapter 4
Polarized-Light Processing in Insect Brains: Recent Insights from the Desert Locust, the Monarch Butterfly, the Cricket, and the Fruit Fly

Stanley Heinze

Abstract The pattern of linearly polarized light in the sky can be used for orientation behavior by many insects. Although such behavioral responses have been well described in bees and ants over several decades, until recently it remained largely elusive how polarized-light information is processed in the insect brain. However, over the last decade, substantial advances in understanding polarized-light processing have been made, based on behavioral, electrophysiological, and anatomical data. Particularly, progress was made in the desert locust, but based on comparative work in the field cricket, the monarch butterfly, and the fruit fly broader conclusions about how polarized-light information is encoded in the insect brain in general begin to emerge. After polarized light is detected by photoreceptors of specialized parts of the compound eye, this information passes through the optic lobe, the anterior optic tubercle, and the central complex. In these brain regions, detailed neural responses to polarized light have been characterized in a large set of anatomically defined neurons that together comprise the polarization vision network. This work has begun to unravel how polarized light is integrated with unpolarized light, and how response characteristics of involved neurons are modulated in context-dependent ways. Eventually, all skylight cues appear to be combined to generate a neural representation of azimuthal space around the animal in the central complex of the brain, which could be used as a basis for directed behavior. Polarized-light information is likely contributing to such a representation in many insects and thus this modality could be crucial for illuminating how the insect brain in general encodes the position of the animal in space, a task that all animal brains have to master.

Electronic supplementary material is available in the online version of this chapter at 10.1007/978-3-642-54718-8_4. Color versions of the black and white figures as well as a supplementary figure can also be found under http://extras.springer.com

S. Heinze (✉)
Department of Biology, Lund University, Sölvegatan 35, 22362 Lund, Sweden
e-mail: stanley.heinze@biol.lu.se

G. Horváth (ed.), *Polarized Light and Polarization Vision in Animal Sciences*,
Springer Series in Vision Research 2, DOI 10.1007/978-3-642-54718-8_4,

4.1 Introduction

It has long been known that the sun can be used by insects for orienting in their environment. Surprisingly, early experiments on harvester ants (*Messor barbarus*) revealed that the animals were still properly orienting on the homebound journey of a foraging trip even though the direct view of the sun had been blocked (Santschi 1923). However, this orientation was abolished when the patch of blue sky visible to the ants was covered with a ground glass plate. Although Felix Santschi could not interpret his results at the time, we now know that the depolarizing effect of the ground glass disturbed the ant's navigation. Karl von Frisch (1949) eventually showed several decades later through work in the honey bee (*Apis mellifera*) that the polarization pattern of the blue sky can be used by insects to determine the position of the sun, even when the direct view of the sun is obscured. This pattern is invisible to the human eye and is produced through scattering of sunlight in the atmosphere. Importantly, the plane of polarization—oscillation direction of the electric field vector (*E*-vector)—is always perpendicular to the scattering plane determined by the sun, the observer, and the observed celestial point. Therefore, the position of the sun can be directly inferred from analyzing the distribution of *E*-vectors in a patch of blue sky.

Extensive work has been done with honey bees and desert ants over the course of several decades, during which the behavioral responses of these animals to polarized light have been characterized in detail (e.g., Rossel and Wehner 1987; Wehner 1997). But how does the brain of insects process these *E*-vector signals and transform them into motor commands? Two competing theories were proposed at the time that had very different demands on the nervous system: First, the simultaneous method, in which an animal can immediately determine any *E*-vector at the sky by combining three parallel analyzer channels and can therefore perceive individual *E*-vectors (Kirschfeld 1972). Second, the scanning method, in which the animal compares all *E*-vectors in the sky with a single matched filter (Rossel and Wehner 1986). The output value of this matching can be used to determine the plane of mirror symmetry of the sky (i.e., the solar–antisolar meridian), when the animal rotates around its own body axis by 360° and compares the output over time. While the first method is quite demanding on the nervous system, the second one is much simpler, albeit providing much less information for the animal.

As bees and ants were not easily accessible for electrophysiological recordings, it was the pioneering work of Thomas Labhart on field crickets (*Gryllus campestris*) that gave the first evidence of how polarized light is processed in the insect brain. He discovered and characterized neurons that responded with changes in their spiking activity in response to different *E*-vectors (Labhart 1988, 1996; Labhart and Petzold 1993; Labhart and Meyer 2002). These cells (POL1 neurons) were maximally excited at one *E*-vector orientation, and were maximally inhibited by the orthogonal *E*-vector angle. This response pattern was called polarization opponency and is found in most polarization-sensitive neurons in the insect nervous system. The fact that the tuning of these cells fell into one of three groups, and

therefore POL1 neurons could act as three analyzer channels, was strong support for the hypothesis of instantaneous *E*-vector detection. A decade later, it was shown by work from the laboratory of Uwe Homberg that the cricket was not the only species in which polarization-sensitive neurons could be analyzed (Homberg and Würden 1997; Vitzthum et al. 2002). In the desert locust (*Schistocerca gregaria*), several types of neurons were described that also responded to changes in *E*-vector orientation. Most of these cells were located in the center of the brain in a region called the central complex. It therefore became evident that the complexity of the neural network involved in processing of polarized light was substantial, and much effort was since put into the task of describing additional neural elements that together constitute the polarization vision network of the insect brain.

The main scope of this chapter is to summarize the work over the last decade that immensely widened our knowledge about how polarized light is processed in the brain of insects, particularly in the desert locust, but also in the cricket, in the monarch butterfly (*Danaus plexippus*), and—very recently—in the fruit fly *Drosophila melanogaster*. The earlier literature on polarization vision has been reviewed by Horváth and Varjú (2004) and Wehner and Labhart (2006).

4.2 The Skylight Polarization Pattern

To understand the neural and behavioral responses of insects to polarized-light stimuli, we have to briefly outline the main features of the skylight polarization pattern. In the behavioral and neurophysiological studies considered in this chapter, a simplified version of the natural sky is used, which is based on the single-scattering Rayleigh model (Coulson 1988) (Fig. 4.1). In this approximation to the natural situation, the skylight polarization pattern is described with two variables: the *E*-vector angle and the degree of linear polarization. The *E*-vector angles are distributed along concentric circles around the sun, and the degree of polarization is maximal at angles 90° away from the sun. Although the Rayleigh model results in degrees of polarization between 0 and 100 %, the maximal values measured in the clear sky do not exceed 75 % (Brines and Gould 1982; Horváth and Varjú 2004). Hence, in studies dealing specifically with models of the degree of polarization (Heinze and Reppert 2011; Pfeiffer et al. 2011), a correction factor of 0.75 was applied to adapt the Rayleigh equations to the empirical skylight conditions.

Importantly, the *E*-vector pattern in the sky is not stationary, but moves across the sky according to the apparent movement of the sun (Fig. 4.1b, c). This results in the fact that the overall degree of polarization in the sky is the highest at the lowest solar elevations (i.e., in the morning and evening), when the *E*-vectors are nearly all oriented in parallel in a wide band passing the zenith perpendicular to the solar–antisolar meridian, while high degrees of polarization can only be found near the horizon at the antisolar half of the sky if the sun is located at high elevations.

The polarization characteristics of real skies (clear, partly cloudy, overcast, foggy, smoky, canopied, moonlit) were investigated both theoretically (Coulson 1988; Schwind and Horváth 1993; Barta and Horváth 2004; Hegedüs et al. 2006)

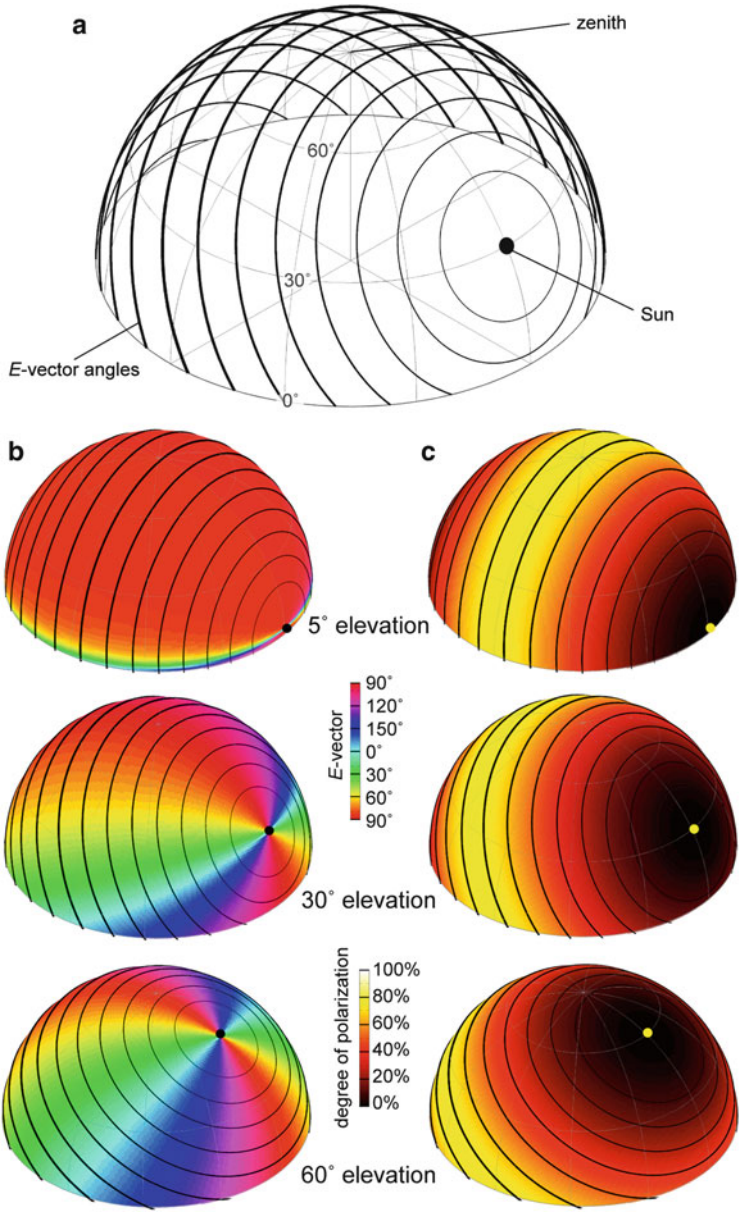

Fig. 4.1 Single-scattering Rayleigh model of skylight polarization. (**a**) Pattern of electric field vectors (*E*-vectors) in the sky. Orientation of *black lines* indicate *E*-vector angles, while their *thickness* indicates the degree of linear polarization. *Numbers* represent elevation above the horizon. (**b**) *E*-vector angles during different solar elevations; 0° is defined as an *E*-vector parallel to the solar meridian. (**c**) Degree of polarization at different solar elevations

and experimentally (Coulson 1988; Horváth and Wehner 1999; Gál et al. 2001a, b; Pomozi et al. 2001; Horváth et al. 2002a; Hegedüs et al. 2007a, b, c, d) using full-sky imaging polarimetry. These characteristics may considerably differ from the single-scattering Rayleigh model (Suhai and Horváth 2004). The biological implications of these were summarized by Horváth and Varjú (2004) and are discussed in Chaps. 17, 18, 24 and 25.

4.3 Behavior that Utilizes Linearly Polarized Light

Behavioral experiments with bees and ants were central to discovering that animals can use linearly polarized light and remain the optimal method for describing a species' ability to use this sensory cue. Additionally, precise behavioral data are extremely valuable as they allow relating electrophysiological data to the biology of a species and thus give relevance to otherwise isolated observations of neuronal responses. In the following sections, a brief overview will be provided over the evidence showing that the species covered in this chapter utilize linearly polarized light.

4.3.1 Cricket

The best studied species with respect to its ability to use linearly polarized light is the field cricket, *G. campestris* (Fig. 4.2a). In the used experimental paradigm, a tethered cricket is placed on a small sphere, which can rotate freely in all directions and the movement of which can be precisely tracked (Brunner and Labhart 1987). When the animal walks on top of this sphere, the direction as well as the speed of walking can be monitored (Fig. 4.2b).

When a linear polarizer is slowly rotated around its vertical axis above the walking cricket, the animal shows approximately sinusoidal walking tracks (Fig. 4.2c). This "polarotactic" behavior suggests that the animals possess a preferred *E*-vector orientation, with which they try to align themselves. Turning tendencies are consequently induced by the mismatch between the preferred orientation and the currently displayed *E*-vector angle. Consistent with the cricket being a central place forager that uses polarized light for orienting during foraging trips (Beugnon and Campan 1989), the population of all tested animals has no consistently preferred orientation and individual animals even change their preferred *E*-vector angle between trials. Although on average there is a tendency of either aligning themselves in parallel or perpendicular to the *E*-vector stimulus (Brunner and Labhart 1987), the preferred directions cover all possible angles with respect to the stimulus, suggesting that the observed behavior is not merely an alignment response. The orientation behavior is completely abolished when the dorsal rim

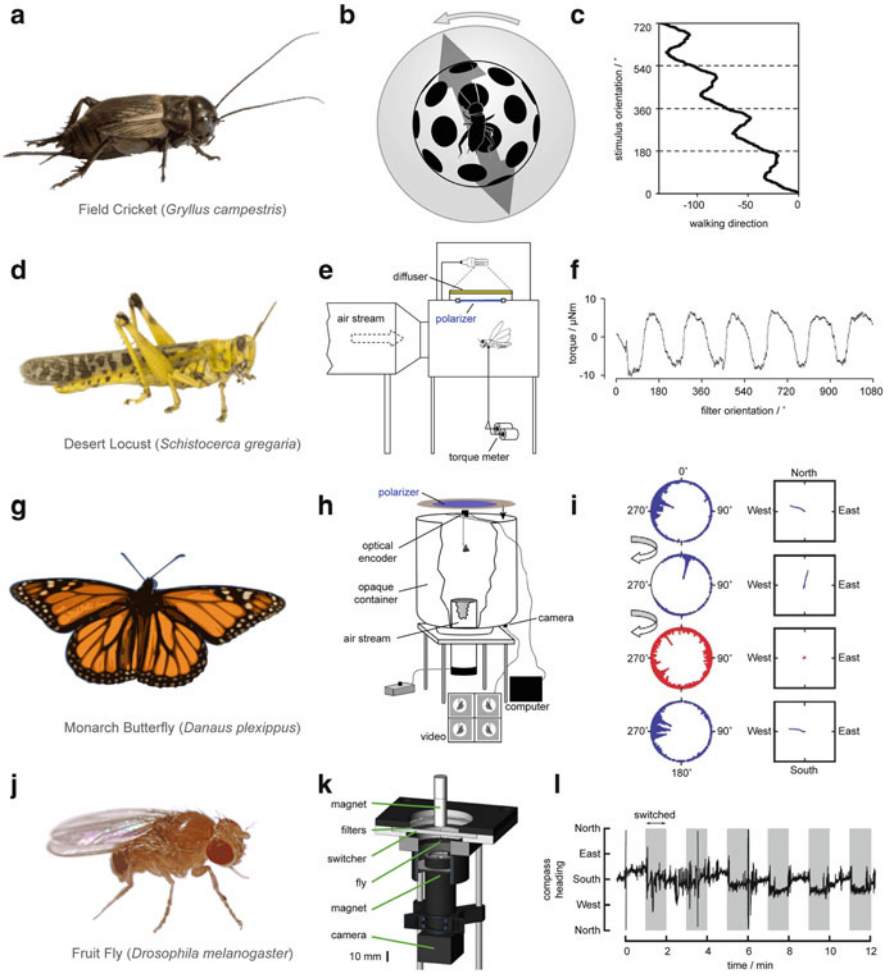

Fig. 4.2 Behavioral experiments to illuminate polarization vision. (**a**–**c**) Crickets. (**d**–**f**) Desert locusts (*Schistocerca gregaria*). (**g**–**i**) Monarch butterflies (*Danaus plexippus*). (**j**–**l**) Fruit flies (*Drosophila melanogaster*). (**b**, **e**, **h**, **k**) Behavioral assays for testing polarized-light orientation responses in the respective species. In **b** a linear polarizer is slowly rotated above the tethered cricket, which walks on an air-suspended ball, the movements of which are tracked. In **e** the tethered locust is placed in front of a wind tunnel and its turning tendencies in response to a rotating linear polarizer are measured by a torque meter. In **h** the monarch butterfly is tethered inside a flight simulator placed outdoors with clear view of the sky. It can freely rotate and its angular orientation is monitored by an optical encoder. A polarizer can be placed above the simulator to rotate the current *E*-vector pattern in the sky by 90°. In **k** a tethered fly is placed inside an outdoor flight arena with clear view of the sky. The fly can rotate freely and its angular orientation is monitored. The current skylight polarization pattern can be switched by 90° by a liquid-crystal-based device, which preserves all skylight features except the polarization angles. (**c**, **f**, **i**, **l**) Examples of data obtained with the respective assay in each species. All examples show changes in walking or flight direction in response to changing *E*-vector angles shown from dorsal

area (DRA) of the compound eye is painted over, revealing that this specialized part of the eye is required for the detection of the *E*-vector orientation of polarized light.

Over the last two decades, this behavioral response has been studied in more detail and was characterized with respect to absolute sensitivity, spectral tuning, response to low degrees of polarization, and under limited visibility conditions (Herzmann and Labhart 1989; Henze and Labhart 2007). These experiments have shown that the spectral tuning of the behavior matches the spectral tuning of the blue receptors in the DRA of the eyes (Herzmann and Labhart 1989). It has been suggested that the blue sensitivity might benefit species that are active not only during the day but also during crepuscular periods (e.g., crickets), as the absolute radiance of the sky is highest in the blue part of the spectrum at these daytimes (Barta and Horváth 2004). In tune with this argument, the absolute sensitivity of the behavior is remarkably high, with the threshold (2.5×10^7 photons/cm^2/s) being below the light levels of a moonless night (Herzmann and Labhart 1989). More recent work determined the abilities of crickets to use polarized light under more natural conditions (Henze and Labhart 2007). This work takes into account that within the natural habitats of these animals, the visibility of the sky is often limited to small patches and that the degree of polarization is much lower than the 100 % used in previous experiments. Remarkably, the behavior is very robust and can be sustained to average degrees of polarization as low as 7 %, both with small polarized-light stimuli embedded in a large unpolarized stimulus (simulating cloud cover with patches of blue sky) as well as homogeneously low degrees of polarization (simulating haze, fog, or overcast sky). Also, the size of the stimulus can be reduced to 1° without abolishing the response of the animals (Henze and Labhart 2007).

4.3.2 Desert Locust

Very similar to the cricket, polarotactic behavior has been used in desert locusts (*S. gregaria*) to verify their ability to perceive and use polarized light (Fig. 4.2d–f). Hereby, the animals were tethered in front of a wind tunnel, so that the airflow induced sustained bouts of flight. The lateral torque produced by intended turning responses of the locust was used to monitor the direction of flight (Mappes and Homberg 2004). Similar to crickets, the locusts showed approximately sinusoidal

Fig. 4.2 (continued) directions. In **i**, the *arrows* indicate 90° rotations of the polarizer. The *highlighted circle* represents a trial with a UV-interference filter placed above the polarizer. *Left column*: circular plots of flight orientations accumulated over time. *Right column*: virtual flight paths calculated from orientation data. Images reproduced with permission from Henze and Labhart (2007) (**b**, **c**); Mappes and Homberg (2004) (**e**, **f**); Mouritsen and Frost (2002) (Copyright (2002) National Academy of Sciences, USA) (**h**); Sauman et al. (2005) (**i**); Weir and Dickinson (2012) (**k**, **l**)

flight tracks when a polarizer was slowly rotated above the animals, indicating that the locusts initiate turning responses when the *E*-vector orientation of the stimulus does not match an internal preferred orientation (Fig. 4.2f). The preferred orientations of the examined locust population were randomly distributed, showing that locusts can orient in all possible angles relative to the *E*-vector stimulus, but do not have an overall shared orientation (Mappes and Homberg 2004). Although a common orientation would be expected for a long distant migratory animal such as the desert locust, the lack of finding it in laboratory-raised animals indicates that the common orientation observed in wild locust swarms might be learned, induced by the dynamics of the swarm itself or that polarized light does not play a decisive role in choosing the migratory direction.

As in the cricket, the DRA of the compound eye is also required for polarotaxis in the desert locust (Mappes and Homberg 2004). Additionally, surgically induced lesions in the anterior optic tract completely abolished this behavior as well (Mappes and Homberg 2007), showing that this pathway of the brain is required for a response to polarized light.

4.3.3 Monarch Butterfly

The migration of the monarch butterfly (*Danaus plexippus*) is one of the prime examples for long-distance migrations in the animal world, and magnificent swarms of millions of these butterflies fly each year from northeastern North America to their overwintering grounds in central Mexico. Behavioral experiments using a flight simulator have been carried out over the last decade and have shown that monarchs use a time-compensated sun compass to keep a southerly bearing (Mouritsen and Frost 2002; Froy et al. 2003; Reppert et al. 2010). In this simulator, the butterfly is tethered but can rotate freely around its vertical body axis (Fig. 4.2h). The direction of flight can thus be chosen by the animal and is recorded by an optical encoder to calculate virtual flight paths (Fig. 4.2i). While the lateral view of the landscape is obscured by the simulator walls, the natural sky is freely visible to the animal. The question whether monarchs can use polarized skylight for orienting has been addressed in three studies, two of which produced strong evidence that these animals have the capacity for polarized-light guided navigation. Nevertheless, the sun itself must still be regarded as the primary source of information for orientation purposes in these animals, as polarized light is clearly not necessary for time-compensated sun compass orientation (Stalleicken et al. 2005).

The studies showing *E*-vector-dependent orientation were carried out in situations with low solar elevation, i.e., when the sun was not visible for the butterfly inside the simulator, and the polarization pattern was more or less uniform across the sky. The visible part of the sky was covered with a polarizer, the transmission direction of which was aligned with the dominant *E*-vector orientation in the sky. While animals flying under this condition did not change their behavior with respect to the control without the polarizer, they changed their flight direction by 90° in

either direction, when the polarizer was turned by 90° (Reppert et al. 2004) (Fig. 4.2i). In a subsequent study, a spectral filter that blocked all light below wavelengths of 400 nm (ultraviolet light) was placed above the polarizer. This resulted in complete loss of polarized-light-induced turning responses and reveals that monarch butterflies perceive the polarization pattern of the sky in the UV range (Sauman et al. 2005) (Fig. 4.2i).

4.3.4 Houseflies and Fruit Flies

Two species of flies have been examined behaviorally with respect to polarized-light orientation: the fruit fly, *Drosophila melanogaster*, and the housefly, *Musca domestica*. Early studies investigated responses to polarized light in tethered walking or flying flies (flying *Drosophila*: Wolf et al. 1980; walking *Musca*: Philipsborn and Labhart 1990). The housefly was examined in a setup very similar to the one used for crickets, and results were comparable. The flies showed sinusoidal modulations of their walking direction when a linear polarizer was slowly rotated above the animal (Philipsborn and Labhart 1990). Interestingly, the preferred *E*-vector orientations were highly significantly clustered around the axis perpendicular to the body length axis of the flies, i.e., flies avoided to align themselves parallel to the *E*-vector orientation of the stimulus. Furthermore, repeating the experiments with UV and yellow light resulted in the full response amplitude for UV stimuli, while yellow led to no response. This means that UV light was fully sufficient for the observed response.

In *Drosophila*, orientation responses to rotating *E*-vectors were examined by recording yaw-torque responses of tethered flies (Wolf et al. 1980). During flight orientation in closed loop conditions (i.e., the flight orientation of the fly generates immediate feedback that controls the stimulus), the flies tended to either align themselves in parallel or perpendicular to the *E*-vector angle of the stimulus. Surprisingly, significant responses were observed not only in the UV range but also in green light. Moreover, the response was not restricted to the dorsal visual field, but extended into the ventral visual field as well, albeit with reduced amplitude.

Very recently, and after almost three decades of no research, work on polarization vision was revived in *Drosophila*. Two different behavioral assays were developed that either looked at alignment responses in fly populations (Wernet et al. 2011), or investigated orientation responses of single tethered flies in a flight simulator (Weir and Dickinson 2012) (Fig. 4.2k). In the latter work the flies were stimulated with natural skylight while flying. It revealed that the animals could maintain a straight course over prolonged periods of time and initiated course correction when the flight arena was rotated with respect to the stimulus. This response was abolished by inserting a circular polarizer into the light path, but surprisingly it was maintained under blue light (Weir and Dickinson 2012). Additionally, a second experiment used a liquid-crystal-based polarization-switching

device with which the natural skylight *E*-vector pattern was switched by 90° at 1 min intervals. Importantly, this manipulation only switches the *E*-vector pattern, but leaves all other skylight cues intact. Also in this setup the flies adjusted their flight direction according to the changing polarization pattern (Fig. 4.2i). This study clearly shows that *Drosophila* is able to use natural polarization patterns for controlling its flight direction and suggests that, unlike previously thought, the UV receptors of the DRA are not the only means of detecting orientation-relevant *E*-vectors. These results are strongly supported and expanded by the previously mentioned population assay (Wernet et al. 2011). In this assay, flies generally aligned their body axis parallel to the *E*-vector. When stimulated with linearly polarized light dorsally, this alignment response was restricted to UV light, while ventral stimulation was also observed for blue and green stimulation. With genetic manipulations the authors showed elegantly that the dorsal response was mediated exclusively by the UV receptors of the DRA. The ventral response, on the other hand, requires a complex interaction of inner (R7/R8) and selected outer photoreceptors (R4–R6) to mediate the observed green, blue, and UV responses (Wernet et al. 2011).

4.3.5 Polarized Light in the Context of Color Vision

At last, polarized light cannot only be used for orientation behavior. For most purposes, high polarization sensitivity in the main retina of insects would interfere with other visual tasks such as color vision (Horváth and Varjú 2004, pp 362–380, see also Chapter 13 of this book). Polarization sensitivity has therefore been actively reduced in large parts of the eyes in most insects by introducing rhabdomeric twist or bent rhabdomes (Wehner and Bernard 1993). However, some species, particularly *Papilio* butterflies, have retained moderate degrees of polarization sensitivity in the entire compound eye. In these cases polarized light could be used to enhance the salience of attractive features of the environment for solving specific, species-dependent problems. The ability to distinguish polarized-light-induced false colors and the ability to distinguish isoluminant stimuli of identical color but distinct polarization angles have been revealed through learning paradigms in *Papilio* butterflies under controlled laboratory conditions (Kelber 1999; Kelber et al. 2001; Kinoshita et al. 2011).

In ovipositing choice experiments in female *Papilio* butterflies, horizontally polarized green light was strongly preferred over vertically polarized light (Kelber et al. 2001). This choice preference was dependent on the spectrum of the presented stimuli and the authors concluded that the different polarization angles are perceived by the butterfly as having different colors, as they are likely processed by the same neural substrate. In choice experiments involving feeding responses, the animals could also be trained to prefer stimuli of either vertical or horizontal *E*-vector orientation (Kelber et al. 2001). Whether *Papilio* perceive different *E*-vector angles as apparent changes in brightness or changes in color during foraging behavior was examined in a recent study (Kinoshita et al. 2011). During foraging, these animals possess a strong innate preference for vertically polarized

light. Choice experiments in this context showed that the dynamics of the learning process resembled that of intensity choices much more closely than that of color-based learning. Hence during foraging, different *E*-vectors are likely perceived as different intensities rather than different colors (Kinoshita et al. 2011). Whether these laboratory-based findings indeed translate into the natural world and bear behavioral relevance remains hypothetical. Although the described experiments clearly reveal potential interactions between color and polarization processing pathways, the effective crosstalk between both channels is expected to be rather weak, due to the low PS values of the involved photoreceptors (~2). Indeed, modeling combined with imaging polarimetry showed that the color of specularly reflecting leaf surfaces is masked by white glare, which may prevent the perception of polarization-induced hue shifts (Horváth et al. 2002b). Additionally, light reflected from matte flower surfaces can be colorful, but is only weakly polarized or even unpolarized. Modeling degree and angle of polarization of reflections on different surfaces and their dependence on wavelength showed that polarization-induced false colors could help polarization-dependent color vision systems to discriminate between shiny and matte surfaces, but might not be suited to unambiguously encode surface orientation (Hegedüs and Horváth 2004a, b; Chap. 13). However, even if the described experimental results from *Papilio* butterflies do not fully translate into biologically relevant contexts, they might eventually be highly valuable for disentangling the complex wiring downstream of the multiple spectral types of butterfly photoreceptors.

4.4 The Detectors of Polarized Light

The sensory periphery for polarization vision has been studied for a long time and consequently has been described in many insect species. As briefly mentioned above, a specialized region of the compound eye called the DRA is generally thought to mediate the detection of linearly polarized light. Fundamental for polarization sensitivity is the alignment and orientation of the microvilli in the rhabdom of DRA ommatidia. In all polarization-sensitive ommatidia, microvilli of the individual photoreceptors are aligned for the entire lengths of the receptor, i.e., the rhabdom is not twisted around its length axis. Second, within each ommatidium the microvilli of one group of photoreceptors are oriented orthogonally to the microvilli of another group of photoreceptors, resulting in two analyzer channels optimized to detect orthogonal *E*-vector orientations (Fig. 4.3a). Additionally, rhabdoms are often shortened to reduce self-screening, while the area of the cross section is widened to maintain high absolute sensitivity. Also, receptors within the DRA are generally homochromatic, a feature that renders the polarized-light responses indifferent to the spectral composition of the stimulus. Additional anatomical specializations like enlarged receptive fields, lack of screening pigments, or degraded optics are often present as well, but depend on the species studied (summarized by Labhart and Meyer 1999).

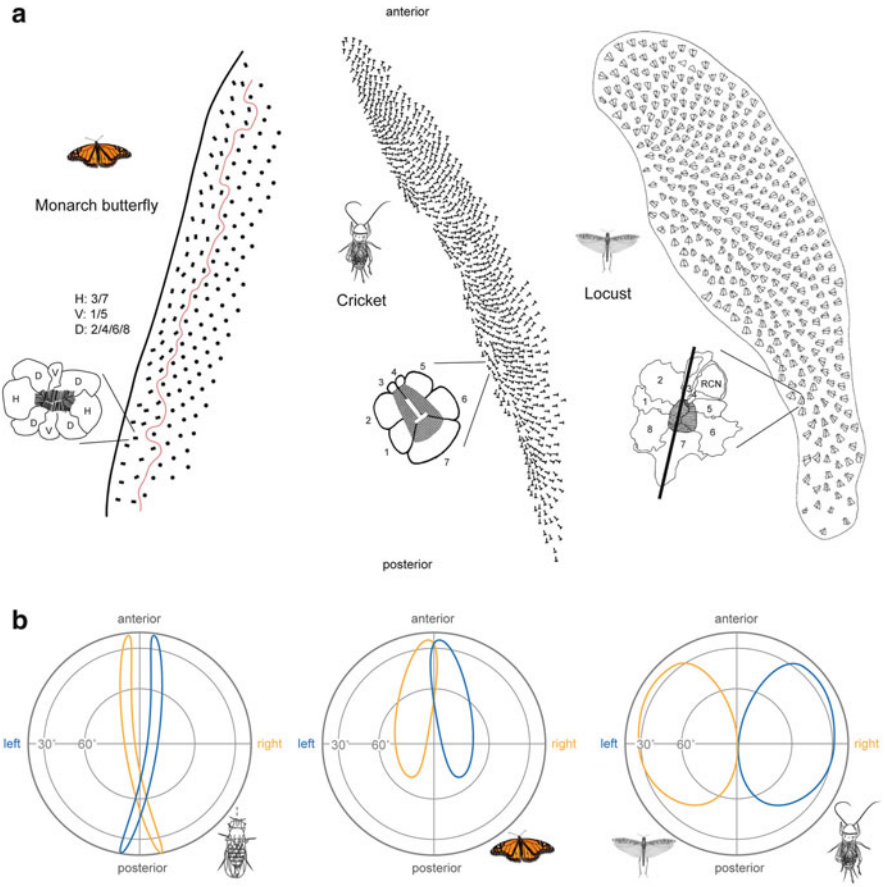

Fig. 4.3 The dorsal rim areas (DRAs) of the compound eyes across insect species. (**a**) Anatomical layout of the DRA in the monarch butterfly, the cricket, and the desert locust. Shown for each species are the outlines of a single ommatidium with the microvilli orientation of the individual retinula cells. The dominant microvilli orientations are shown for all ommatidia of the DRA in the overview images. Note the fan-shaped organization of the ommatidial arrays in all species. Images reproduced with permission from Labhart et al. (2009) (monarch butterfly); Blum and Labhart (2000) (cricket); Homberg and Paech (2002) (locust). (**b**) Estimated region of sky viewed by the DRA in *Drosophila*, the monarch butterfly, and the locust/cricket. The area of sky viewed by the left eye is indicated in *blue (dark)*, while the area viewed by the right eye is shown in *yellow (light)*. Estimates are based on data from Henze (2009) (*Drosophila*); Stalleicken et al. (2006), Labhart et al. (2009) (monarch butterfly); Blum and Labhart (2000) (cricket); Homberg and Paech (2002) (locust). Cartoons of cricket and *Drosophila* adapted from Henze (2009)

The four species considered in this chapter show several differences in the organization of their DRAs (Fig. 4.3a). These differences are particularly strong in the overall layout and orientation of the DRA. As the direction of view and size of the DRA, combined with the receptive field size of the photoreceptors, determine

which part of the sky can be viewed and analyzed by an animal (Fig. 4.3b), these features are exceptionally important for interpreting the characteristics of later-stage neural responses to polarized light. Only when the information available to the animal is known, it can be combined with behavioral observations to reveal the algorithms operating on a neuronal level that transform sensory information into motor commands.

4.4.1 *Which Part of the Sky Is Viewed by the DRAs of the Different Species?*

In principle, two types of DRA can be distinguished in the four species covered in this chapter: First, crickets and locusts possess short but wide DRAs directed towards a large, elliptical region of the contralateral sky, centered at an elevation of around 60° (Blum and Labhart 2000; Homberg and Paech 2002). Second, elongated and narrow DRAs are found in monarch butterflies and *Drosophila*. These long DRAs are directed towards a narrow strip of sky approximately parallel to the body length axis of the animal (Stalleicken et al. 2006; Henze 2009; Labhart et al. 2009) (Fig. 4.3b). In all species the microvilli orientations of the ommatidia are arranged in a fan-like manner across the DRA (Fig. 4.3a). While the acceptance angle of individual ommatidia is large in crickets (ca. 20°, Labhart et al. 1984) and locusts (ca. 30°, Eggers et al. 1993), it is small in monarch butterflies and *Drosophila* (ca. 4°, Stalleicken et al. 2006; Henze 2009). Consequently, the receptive fields of individual ommatidia overlap substantially in locusts and crickets, so that each part of the sky within the acceptance range of the DRA is viewed by many ommatidia at the same time. Due to the fan-shaped nature of microvilli orientations, all possible *E*-vector angles can be simultaneously detected at each point of sky within the receptive field of the DRA. In contrast, in monarchs and *Drosophila* the stretched out, narrow fan of microvilli orientations, combined with the small acceptance angles of individual ommatidia, implicates that each part of the DRA is optimized to perceive a different *E*-vector angle. Thus, the information transmitted from the overall DRA is expected to differ substantially between locusts and crickets on the one hand, and monarchs and flies on the other hand, even in identical skylight situations.

4.4.2 *Which DRA Photoreceptors Are Involved in Polarized-Light Perception?*

The answer to this question depends strongly on which of the four species covered in this chapter is considered. Most similar is the situation in the cricket and the locust. In both species, the majority of DRA photoreceptors is blue sensitive, while

a small proportion is UV sensitive (Labhart et al. 1984; Eggers et al. 1993). The major blocks of orthogonal microvilli are produced by the R7 and the R1, R2, R5, R6 receptors, all of which are blue sensitive and thus together provide two homochromatic polarization analyzers. Interestingly, one microvilli orientation (R1, R2, R5, R6) contributes considerably more area to the cross section of the rhabdom than the orthogonal one (R7) (Blum and Labhart 2000; Homberg and Paech 2002) (Fig. 4.3a). While the R8 receptor is a fully developed receptor cell in the locust, it is much shorter in the cricket and is restricted to the proximal part of the rhabdom. In both species it contributes microvilli to the R1, R2, R5, R6 group of photoreceptors. Recent data from the cricket surprisingly show that the R8 cell expresses UV opsin (Henze et al. 2012), suggesting that this might also be the case in locusts, for which similar data do not yet exist. At last, R3, R4 receptors lack microvilli in the cricket and are substantially reduced in the locust as well (Blum and Labhart 2000; Homberg and Paech 2002). Whereas the majority of receptors target the lamina in both species, a few receptors target the medulla. While no further detail is known in the locust, dye fills in the cricket suggest that the long projections to the medulla originate from the R7, R8 cells (Blum and Labhart 2000). Overall, both species possess a photoreceptor organization in the DRA that indicates a high degree of specialization for the detection of polarized light. With the partial reduction of the R8 receptor and the complete lack of microvilli in the R3, R4 receptors, the cricket DRA ommatidia appear slightly more specialized than their locust counterparts.

In the monarch butterfly, all eight DRA receptor cells in each ommatidium ubiquitously express UV opsins and thus comprise a completely homochromatic system for polarization vision (Sauman et al. 2005). Receptors R3 and R7 comprise one analyzer channel, while R1, R2, R4, R5, R6, R8 cells constitute the orthogonal channel (Labhart et al. 2009). Similar to locusts and crickets, the area of cross section allocated to the R3, R7 channel is considerably smaller than the area taken up by the orthogonal analyzers, indicating that this finding might bear functional significance. Dye fills into the DRA of the monarch suggest that all projections terminate in the medulla, as known for UV-opsin-expressing photoreceptors in other species (Sauman et al. 2005).

In *Drosophila* the existence of neural superposition eyes with their unfused rhabdomes precludes orthogonal analyzer channels to which all photoreceptors of one ommatidium contribute, as the optical axes of the individual receptor cells are not aligned. Here, the two only receptors with identical optical axes are the inner receptors, i.e., R7 and R8. In the DRA, these cells express exclusively UV opsins and show orthogonal microvilli orientations with respect to one another (Wernet and Desplan 2004; Wernet et al. 2011). As in the monarch butterfly, the UV-sensitive receptors possess long projections that target the medulla (Fischbach and Dittrich 1989).

4.4.3 A Second Specialized Area for Detecting Polarized Light?

Recently, data has accumulated suggesting that the DRA is likely not the only region in the eye specialized for detecting polarized light. The most direct evidence results from data in *Drosophila*. Here, the existence of a ventral alignment response to polarized light has led to a thorough investigation of ventral photoreceptors (Wernet et al. 2011). Although no clearly defined ventral region could be identified, in which ommatidia were as highly specialized as in the DRA, the rhabdomeres of individual receptors showed only low to moderate twist compared to surrounding receptors, a crucial prerequisite for detecting polarized light. These untwisted receptor cells were either UV-opsin-expressing R7 or blue-opsin-expressing R4, R5, consistent with the above-described behavioral data. Additionally, the microvilli orientation of R7 cells was highly aligned across neighboring ommatidia, allowing extraction of *E*-vector information even from only moderately polarization-sensitive receptors by means of spatial integration (Wernet et al. 2011). Green-opsin-expressing R8 receptors might be needed in conjunction with outer receptors to mediate a behavioral response to green stimuli, although the mechanism remains unclear. As the R8 receptor is highly twisted (and expresses a different opsin than R7), no crossed analyzers exist in the ventral eye.

In crickets, in situ hybridization data revealed that blue opsins are not only expressed in the DRA as previously thought but also occur in a band-like region of the ventral eye (Henze et al. 2012). Other than in the DRA, the involved receptors are likely only R1, R3, R5, R7, while the remaining R2, R4, R6, R8 cells express green opsins. Although the ultrastructure of this eye region is unknown and no behavioral data exist in crickets that suggest the use of ventral sources of polarized light, such data exist for the closely related desert locusts. These animals have been reported to avoid extended bodies of water (Shashar et al. 2005). As such behavior is likely mediated via detection of horizontally polarized light (Schwind 1985; Horváth and Varjú 2004; Chaps. 5 and 16), a ventral band of specialized photoreceptors for polarized-light detection might be a shared feature among orthopteran insects. Indirect evidence for this speculation was found through anatomical and physiological data in the locust brain. First, in the medulla, two neuron types that arborize in the dorsal rim medulla possess a second arborization tree in a ventral part of the medulla, either ipsilaterally or contralaterally (el Jundi et al. 2011). Second, the lateral extent of receptive fields of polarization-sensitive neurons in the optic lobe, as well as in the central brain, extends to sky regions close to the horizon, and thus cannot solely result from the activation of DRA photoreceptors. This includes optic lobe neurons (el Jundi et al. 2011), several types of central-complex neurons (Heinze et al. 2009), and descending neurons of the ventral nerve cord (Träger and Homberg 2011).

These findings in orthopteran insects and flies are in tune with long-standing observations in aquatic insects (e.g., water beetles, water bugs, dragonflies, tabanid flies, mayflies, stoneflies, caddisflies), which are attracted to bodies of water and use

horizontally polarized light for this task (Horváth and Varjú 2004; Chaps. 5, 16, and 22). The backswimmer, *Notonecta glauca*, indeed possesses a ventral eye region specialized for detecting polarized light and might be an extreme example of a more general principle applicable to many insects (Schwind 1983, 1985).

4.4.4 Polarization Sensitivity in the Main Retina

For the main retina outside the DRA, moderate polarization sensitivity has been described in some insects, particularly in butterflies (Kelber et al. 2001; Pirih et al. 2010) but also in the cricket (Labhart et al. 1984). The values of polarization sensitivity (PS) range from 2 to 5, as opposed to much higher values in the DRA (up to 40). In crickets the strongest polarization sensitivity for non-DRA photoreceptors was found in UV receptors, while in *Papilio* butterflies all spectral classes of photoreceptors possess PS values of around 2 (Kelber et al. 2001; Kinoshita et al. 2011). In the eastern pale clouded yellow butterfly (*Colias erate*), the highest polarization sensitivity was found for blue and red receptors (Pirih et al. 2010). Interestingly, in both butterfly species fixed sets of photoreceptors possess specific microvilli orientations, which are 0°, 90°, 35°, and 145° (Kelber et al. 2001; Pirih et al. 2010; Kinoshita et al. 2011), possibly providing a substrate for the described innately preferred *E*-vector orientations.

Additionally in *Drosophila*, polarization sensitivity in the dorsal eye outside the DRA is suggested by behavioral experiments (Weir and Dickinson 2012). Hereby, the ability of the fly to respond to the skylight polarization pattern with changes in flight direction was not affected, when only blue light was available and thus the UV part of the spectrum was excluded from the stimulus. As the polarization-sensitive inner receptors of the DRA are exclusively UV sensitive, the behavior is either mediated by the outer receptor cells of the DRA (expressing *rh1* blue opsins) or by ommatidia of the dorsal eye outside the DRA, both of which would be surprising findings.

4.5 The Optic Lobe

Like all visual information detected by the compound eyes, polarized-light information is first processed in the optic lobes. The layout of these large structures on either side of the central brain can be described as a series of stacked, retinotopically organized neuropils adjacent to the retina (Fig. 4.4). In all species, the outermost neuropil region is the lamina, which is proximally followed by the medulla. The third region, the lobula complex, varies considerably between locusts and crickets on the one hand and butterflies and flies on the other hand. In flies and monarchs it consists of the actual lobula and the posteriorly located lobula plate, whereas in locusts and crickets, the lobula complex comprises four subunits, none of which can be easily homologized to the lobula and lobula plate of the other group. The last neuropil of the optic lobe is the accessory medulla, a small,

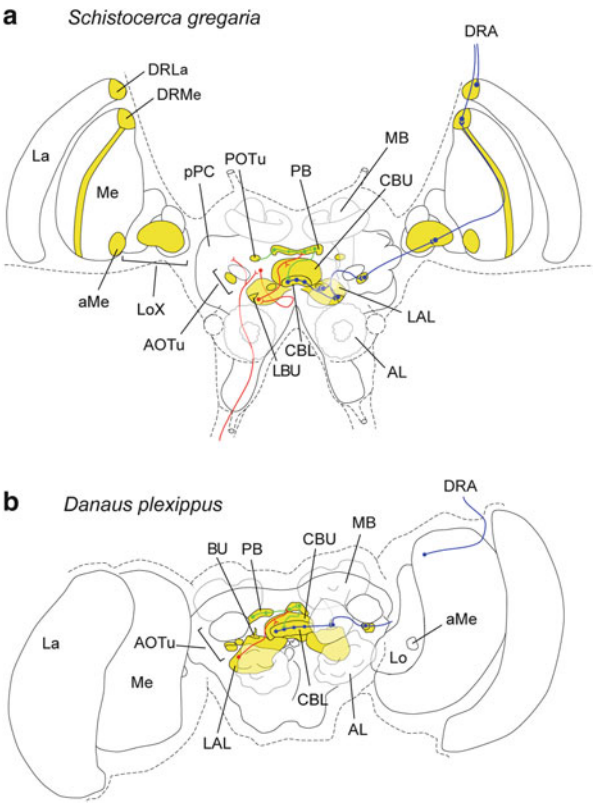

Fig. 4.4 Polarization vision pathway in the brain of the desert locust (**a**) and the monarch butterfly (**b**). Brain regions involved in polarization vision are *highlighted*. Known neural elements are illustrated by *lines*. Proposed output regions are symbolized by *filled circles*, while proposed input areas are represented by *open half circles*. Note that input elements of the polarization vision pathway are shown on the left brain hemisphere (as viewed by the animal), while output elements are shown on the right hemisphere. The mushroom body pedunculus and lobes have been eliminated on the right hemisphere for clarity. *DRA* dorsal rim area, *DRLa* dorsal rim lamina, *DRMe* dorsal rim medulla, *La* lamina, *Me* medulla, *aMe* accessory medulla, *LoX* lobula complex, *Lo* lobula, *MB* mushroom body, *AOTu* anterior optic tubercle, *LAL* lateral accessory lobe, *BU* bulbs, *AL* antennal lobe, *CBL* lower unit of the central body, *CBU* upper unit of the central body, *PB* protocerebral bridge, *POTu* posterior optic tubercle, *pPC* posterior protocerebrum. Figure reproduced with permission from Merlin et al. (2012)

spherical brain area that lies just anterior of the medulla and has been shown to house the circadian clock in cockroaches and *Drosophila* (Helfrich-Forster et al. 1998). Although its role is not known in the locust, anatomical similarity suggests a circadian function as well (Homberg et al. 1991). In monarchs, fibers stained for the clock protein CRYPTOCHROME-1 connect this region to the pacemaker cells in the *pars lateralis* and therefore also implicate a circadian function for the accessory medulla in that species (Sauman et al. 2005).

The photoreceptors of the DRA terminate either in the lamina (majority of receptors in locusts and crickets) or in the medulla (all other receptors). In the locust, these projections form specialized regions at the dorsal rims of both neuropils that are clearly distinct from the main lamina and medulla (Homberg and Paech 2002) (Fig. 4.4a). Unfortunately, to date no neurons directly postsynaptic to DRA photoreceptors have been physiologically described.

Nearly all neurons of the brain that respond to polarized light exhibit a feature called polarization opponency, i.e., they are maximally excited when the animal is stimulated at one particular *E*-vector orientation, while they are maximally inhibited at the perpendicular *E*-vector orientation. This behavior, first described by Labhart (1988) for neurons of the cricket optic lobe, has led to a model that describes how photoreceptors could transmit signals to their postsynaptic partner neurons (Labhart 1988). Hereby, the two blocks of photoreceptors with orthogonally oriented microvilli converge on a common neuron. While one would inhibit the neuron, the other one would excite it. As all insect photoreceptors contain histamine as transmitter (leading to postsynaptic inhibition; Nässel 1999), the excitatory pathway must comprise an indirect connection. This model additionally suggests that polarized-light perception is independent of the stimulus intensity, a feature confirmed by several studies in the cricket as well as the locust (Labhart 1988; Herzmann and Labhart 1989; Kinoshita et al. 2007; el Jundi and Homberg 2012).

An alternative model of how polarization opponency could be produced has been proposed recently by Pfeiffer et al. (2011). In this model, the release of histamine inhibits the postsynaptic neuron, but additionally leads to rebound excitation. Therefore, at moderately spaced bouts of transmitter release (at nonoptimal *E*-vectors), the postsynaptic cell would be excited due to rebound excitation in between transmitter release events. At higher activation levels of the photoreceptors, the transmitter release would become contiguous and thus the postsynaptic neuron would only be inhibited. This model predicts otherwise difficult to explain behavior of certain locust neurons in response to different degrees of polarization and to unpolarized light (see below). Additionally, the same neurons also show higher activation at higher light intensities and therefore are not intensity insensitive, a feature easier to explain with the second model.

The neurons that likely receive input from the dorsal rim medulla have only been described anatomically in the locust. These neurons, termed transmedulla neurons (formerly line-tangential neurons), possess input fibers in the dorsal rim medulla, as well as a single input neurite that runs vertically through the medulla (Homberg et al. 2003; el Jundi et al. 2011) (Fig. 4.5a). Thus, each of these cells should be responsive to polarized light and to unpolarized light from one vertical row of ommatidia, i.e., to illumination from a specific azimuth angle. The axonal projections of these cells are located within a small region of the anterior lobula and in the lower division of the anterior optic tubercle (AOTu). Overall, the population of these cells is suited to transmit polarized-light information from the dorsal rim medulla to the central brain and combine it with information about

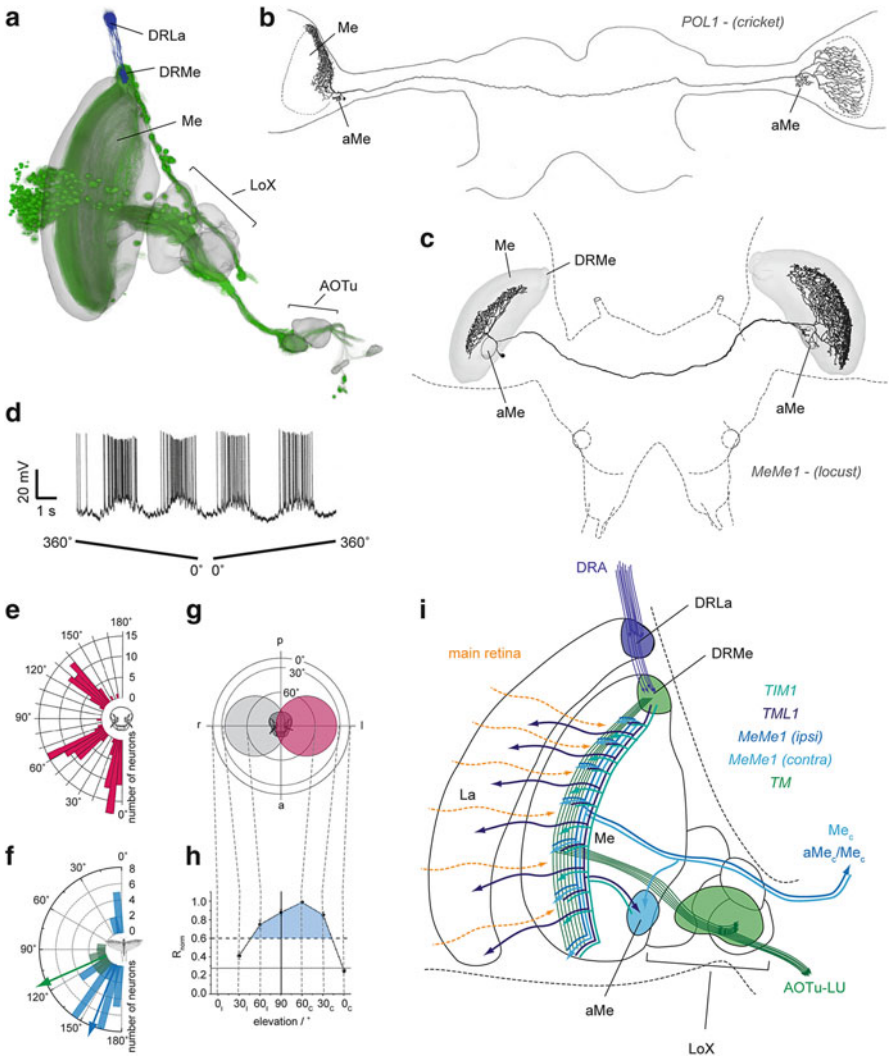

Fig. 4.5 Polarization-sensitive neurons of the optic lobe. (**a**) Photoreceptor projections and transmedulla neurons revealed from dye injections in the desert locust (data from el Jundi et al. 2011). (**b**) Frontal reconstruction of a cricket POL1 neuron. (**c**) Frontal reconstruction of a locust MeMe1 neuron (data from el Jundi et al. 2011). (**d**) Neural activity in response to a rotating linear polarizer in a cricket POL1 neuron. Shown are two successive 360° rotations of the polarizer (*black lines* below spike trace). (**e**, **f**) Distribution of *E*-vector tunings in POL1 neurons of the cricket (**e**) and in MeMe1 neurons (*blue/light*) as well as TIM1 neurons (*green/dark*) of the locust (**f**). Mean orientations of the locust neurons are illustrated by *arrows*. Note that in the cricket angles are plotted clockwise, while in locusts they are plotted counterclockwise (see Supplementary Fig. 4.1). (**g**, **h**) Receptive fields of cricket POL1 neurons (**g**; schematic illustration) and locust MeMe1 neurons (**h**). Data in **h** show the lateral extent of the receptive field orthogonal to the body length axis. *Plotted* is the normalized response amplitude against the elevation of the stimulus (data from el Jundi et al. 2011). (**i**) Schematic illustration of neural elements involved in polarization vision in the optic lobe of the locust. All neurons converge in an individual layer of

unpolarized light from all possible azimuth angles. Whether similar neurons exist in the other species covered in this chapter is still unclear, as is the proof that these neurons are indeed polarization sensitive in locusts.

The single vertical neurites of the transmedulla neurons are confined to one layer of this neuropil. Interestingly, all polarization-sensitive neurons of the locust medulla are equally confined to the identical layer, implying that this layer provides the neural substrate for processing of polarized-light information in the optic lobe (el Jundi et al. 2011) (Fig. 4.5i). These neurons all possess large tangential arborization trees that cover a large number of medulla cartridges (Homberg and Würden 1997; el Jundi and Homberg 2010; el Jundi et al. 2011). Additionally, they fall into one of two groups, as they either possess input and output fibers within the ipsilateral optic lobe, or they possess a midline crossing neurite that connects ipsilateral dendrites with contralateral axonal endings. Three types of locust neurons fall into the first group (TIM1, TIM2, and TML; names from el Jundi et al. 2011), all of which appear to receive input from the dorsal rim medulla. While the TIM1 neuron possesses input and output fibers throughout the innervated medulla layer, the TIM2 neuron receives input only in the dorsal medulla (including the dorsal rim medulla) and projects to ventral parts of the same layer. The TML neuron receives input throughout the medulla, but possesses its output fibers in the lamina. Whereas the TIM1 neuron appears to receive additional input from the accessory medulla, the TML neuron possesses potential output fibers in this neuropil (Fig. 4.5i). The second group of cells comprises two types of intermedulla neurons (MeMe1 and MeMe2). MeMe1 cells receive input from large parts of the ipsilateral medulla and project to equally big areas of the same layer in the contralateral medulla, while giving rise to additional output fibers in the contralateral accessory medulla (Fig. 4.5c). Surprisingly, this cell type does not arborize in the dorsal rim medulla. MeMe2 cells receive input from dorsal parts of the medulla (including the dorsal rim medulla), while projecting to ventral parts of the contralateral medulla. Additionally, these cells project to extensive areas within the median, posterior protocerebrum (el Jundi et al. 2011).

Although the set of polarization-sensitive neurons of the optic lobe has been most extensively described in the locust, a cell type similar to locust MeMe1 cells has been long known in the cricket and in fact was the first polarization-sensitive neuron discovered in any insect (Labhart and Petzold 1993; Labhart 1996; Labhart et al. 2001) (Fig. 4.5b). These POL1 neurons have long been viewed as the

Fig. 4.5 (continued) the medulla. Neuron types are color-coded and named in *italics*. Target neuropils (not included in the image) are named in normal font. Note that TIM2 and MeMe2 neurons have been omitted for clarity. *DRLa* dorsal rim lamina, *DRMe* dorsal rim medulla, *Me* medulla, *aMe* accessory medulla, *LoX* lobula complex, *AOTu* anterior optic tubercle, *La* lamina, *DRA* dorsal rim area, *LU* lower unit; *c* contralateral. Images reproduced/adapted with kind permission from: Springer Science + Business Media (Labhart and Petzold 1993) (**b**); Cambridge University Press (Wehner and Labhart 2006) (**d**); Labhart and Meyer (2002) (**e**); Journal of Experimental Biology (Labhart et al. 2001) (**g**); el Jundi et al. (2011) (**h**)

prototype of all polarization-sensitive insect neurons, and indeed share many features with all other polarization-sensitive cells in different brain areas and in other insect species. The defining feature of POL1 neurons is a tonic change of action potential frequency in response to changing *E*-vector orientations presented to the animal from the zenith. When a linear polarization filter is slowly rotated above the animal, this leads to a sinusoidal modulation of firing frequency (Fig. 4.5d). Thus, characteristics of this sine function can be used to describe the neurons in detail. First, the activity peak is defined as the preferred *E*-vector orientation (Φ_{max}-value), while the activity trough is called the Φ_{min}-value. Additionally, the summed amplitude of frequency modulation is defined as the response strength (R). This term is calculated by summing up all absolute deviations from the mean activity during a rotation of the polarization filter in bins of 20° (Labhart 1996, modified by Heinze et al. 2009). As the background frequency, i.e., the activity of the cell without any stimulation, lies in between maximal and minimal activity during stimulation, the neuron is excited at Φ_{max} and inhibited at Φ_{min}, a behavior termed polarization opponency. At last, the receptive field of the neuron is defined as the spatial region in which stimulation leads to at least 25 % of maximal excitation.

The recorded population of POL1 neurons can be divided into three groups, which are distinguished by their Φ_{max}-values. These distinct tuning directions are roughly 10°, 60°, and 130° for neurons with the soma in the left optic lobe (Labhart et al. 2001) and suggest that POL1 neurons occur as three individual neurons per brain hemisphere (Fig. 4.5e). The receptive fields of these cells are large and centered at around 60° elevation in the contralateral sky hemisphere, suggesting that around one-third of all DRA ommatidia converge on each POL1 neuron (Labhart et al. 2001) (Fig. 4.5g). The *E*-vector tuning does neither depend on the position within the receptive field nor on the degree of polarization or the stimulus intensity (Labhart and Petzold 1993; Labhart 1996; Labhart et al. 2001). Importantly, POL1 neurons do not respond to unpolarized light stimuli, but are extremely sensitive to polarized light, even at very low degrees of polarization (threshold 5 %) (Labhart 1996).

How do the polarization-sensitive neurons of the locust optic lobe compare to the described cricket POL1 neurons? First, only one of the five neuron types of the locust medulla shows polarization opponency (el Jundi et al. 2011). While all cell types respond with sinusoidal modulation of spiking frequency, responses are generally exclusively excitatory. The receptive fields for polarized-light stimulation were tested for TIM1, MeMe1, and TML neurons. Whereas TIM1 and MeMe1 cells possess receptive fields comparable to cricket POL1 neurons (Fig. 4.5h), the TML neurons (innervating the lamina) possess an ipsilaterally centered receptive field. Interestingly, all three neuron types respond exclusively to stimulation from the ipsilateral eye for zenithal stimulation (el Jundi et al. 2011). The combination of input from the ipsilateral eye and an ipsilateral receptive field in TML neurons suggests that information from the main retina outside the DRA is responsible for the polarization sensitivity of this neuron, as the DRA is directed towards the contralateral sky hemisphere. Another interesting difference between locusts and crickets is found in the distribution of *E*-vector tunings. In no single cell type of the

locust, one finds the characteristic three tuning groups of the cricket POL1 neurons. Nevertheless, individual cell types possess distinct *E*-vector tunings. Sufficient numbers of recordings only exist for TIM1 and MeMe1 neurons, of which the first is tuned to 113°, while the second is tuned to 160° (el Jundi et al. 2011) (Fig. 4.5f). In this context it has to be noted that in crickets Φ_{max}-angles have been plotted clockwise, while in locusts they have been plotted counterclockwise (Supplementary Fig. 4.1). Considering this, the tuning groups found in the locust cells coincide remarkably well with two of three tuning groups of the cricket POL1 neurons (in cricket coordinates: TIM1 = 67° and MeMe1 = 20°). As for these cells the receptive fields are also similar between the species, one could speculate that the function of cricket POL1 neurons is distributed over several cell types in the locust. On the other hand, a detailed anatomical analysis of the cricket optic lobe has not yet been performed, so that the existence of locust-like cell types in the cricket cannot be ruled out.

Maybe the most fundamental difference between locust and cricket neurons is that in the locust unpolarized light also results in neuronal responses, whereas cricket POL1 neurons are insensitive to unpolarized light. When an unpolarized light spot is rotated around the animal at constant elevation, all described locust neurons show excitation when the stimulus is present at a specific azimuth (el Jundi et al. 2011). This so-called "azimuth tuning" occurs independent of the used spectral range of the stimulus, and tuning is largely identical for UV and green light. Interestingly, the distribution of these tunings within the population of medulla neurons depends on whether laboratory-raised animals are used or animals that have been raised with a clear view of the sky. In laboratory-raised locusts, the distribution of preferred azimuth angles is random, implying that the observed excitation can be mediated by both eyes. On the other hand, in the second locust group, all neurons showed an identical tuning at an azimuth of ca. 100°, i.e., on the left side of the animal (ipsilateral to the soma of the recorded cell) (el Jundi et al. 2011). This means that the sensory experience of the locust during development shapes the response properties of the studied neurons in the optic lobe. Thus, data obtained from animals raised under laboratory conditions allow drawing conclusions about the genetically determined default state of these cells. The detailed comparison of these polarization-sensitive neurons in animals with and without sensory experience of skylight cues could therefore provide an excellent model for studying experience-dependent modulation of neural networks.

4.6 The Anterior Optic Tubercle

The first processing stage of polarized-light information in the central brain of insects is the anterior optic tubercle (AOTu) (Fig. 4.4). This relatively small neuropil is composed of several subunits and receives input from the optic lobe through fibers of the anterior optic tract, while fibers originating in the AOTu project to the lateral accessory lobes (LALs) and to the contralateral AOTu. Generally, one can distinguish a large subunit and either a single (locust) or several

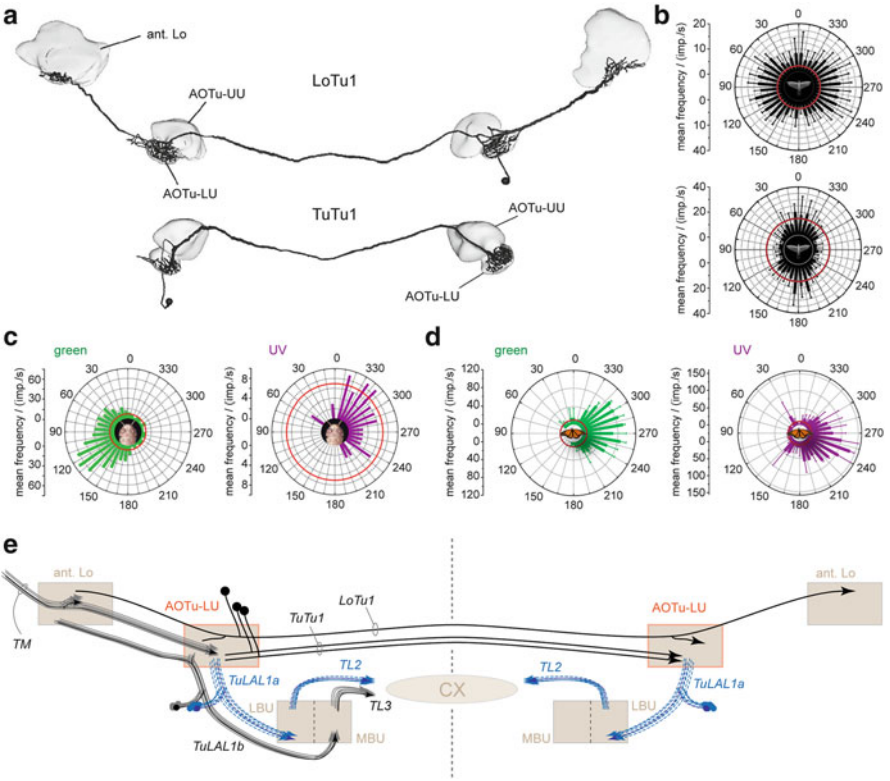

Fig. 4.6 Polarization-sensitive neurons in the anterior optic tubercle. (**a**) Reconstructions of the intertubercle neurons of desert locusts (*top*: LoTu1; *bottom*: TuTu1; data from el Jundi and Homberg 2012). (**b**) Circular plots of mean activity during rotations of a linear polarizer above the locust for LoTu1 (*top*) and TuTu1 (*bottom*) neurons (modified from el Jundi and Homberg 2012). (**c**) Circular plots of mean spiking activity of a locust LoTu1 neuron during stimulation with an unpolarized light spot moving around the locust at constant elevation. (**d**) As **c**, but data from a monarch butterfly TuLAL neuron. Lines in **b**–**d** indicate background firing frequency of the respective neurons. (**e**) Schematic illustration of polarization-sensitive neural connections of the anterior optic tubercle of the locust. Input is drawn on the *left side* of the image. *Highlighted (blue/dashed) neurons* have been shown to receive input from both eyes. While the number of LoTu1 and TuTu1 cells is shown accurately, all other cell types occur in large, but unknown numbers. Somata of TL2 and TL3 cells have been omitted for clarity. *ant. Lo* anterior lobula, *AOTu* anterior optic tubercle, *UU* upper unit, *LU* lower unit, *LBU* lateral bulb, *MBU* medial bulb, *CX* central complex. Images reproduced with permission from: Pfeiffer and Homberg (2007) (**c**); Heinze and Reppert (2011) (**d**)

(monarch) small subunits (Homberg et al. 2003; Heinze and Reppert 2012). Polarization-sensitive neurons have only been described in the small subunits. These neurons belong to one of two groups: First, neurons projecting from the AOTu to specialized regions of the LAL (TuLAL neurons), and second, neurons interconnecting the AOTu's of both brain hemispheres (intertubercle neurons; Fig. 4.6a). The latter cell types from the locust (LoTu1 and TuTu1 cells) are

probably the best studied polarization-sensitive neurons in the central brain of any insect (Pfeiffer et al. 2005, 2011; Kinoshita et al. 2007; Pfeiffer and Homberg 2007; el Jundi and Homberg 2012). As these cells occur only once (LoTu1) or as a single pair (TuTu1) per brain hemisphere, they can be uniquely identified and the same individual neurons were studied in hundreds of recordings. They have been examined with respect to their response to different *E*-vector angles (Pfeiffer et al. 2005), degrees of polarization (Pfeiffer et al. 2011), and stimulus intensities (Kinoshita et al. 2007; el Jundi and Homberg 2012). Additionally, their spectral response properties have been described (Kinoshita et al. 2007), as well as the lateral extent of their receptive fields for polarized-light stimuli (el Jundi and Homberg 2012). Some of these characteristics have been compared between laboratory-raised animals and animals reared with clear view of the sky (Pfeiffer and Homberg 2007), as well as between the solitary and gregarious forms of the desert locust (el Jundi and Homberg 2012). Furthermore, these cells respond to unpolarized light stimuli in a complex way as well, both in locusts and in monarch butterflies (Kinoshita et al. 2007; Pfeiffer and Homberg 2007; Heinze and Reppert 2011).

4.6.1 Polarized-Light Responses of AOTu Neurons

In response to polarized light, all types of locust AOTu neurons (LoTu, TuTu, and TuLAL) show strong modulations of their firing frequency when the animal is stimulated with a rotating linear polarizer, resulting in a preferred *E*-vector orientation at the point of maximal excitation (Φ_{max}) typical for each cell type (Fig. 4.6b). Except for LoTu1 neurons, all cell types show polarization opponency, thus suggesting converging inhibitory and excitatory channels with opposite *E*-vector preference. Contrary, *E*-vector responses of LoTu1 neurons lack an inhibitory component and are excited by all *E*-vector orientations, i.e., maximally excited at Φ_{max} and minimally excited at Φ_{min} (Pfeiffer et al. 2005). As expected from the spectral sensitivity of the locust DRA photoreceptors, the polarization response is most pronounced in the blue range (tested for intertubercle neurons) (Kinoshita et al. 2007). LoTu and TuTu cells receive signals almost exclusively from the ipsilateral eye, and, in tune with the geometry of the DRA, the receptive fields of these cells are located in the contralateral sky hemisphere. They are centered at around 60° elevation and have a diameter of ca. 120° (el Jundi and Homberg 2012). Although TuLAL neurons are much more numerous, they have been studied much less due to their smaller fiber diameters. The available data suggest that their receptive fields are variable both in lateral extension as well as in the location of the receptive field center. Based on a single recording, TuLAL1a neurons receive input from both eyes, while the ocular dominance of TuLAL1b cells remains unknown (el Jundi and Homberg 2012) (Fig. 4.6e).

4.6.2 Stimulus Intensity

The polarized-light responses of TuTu neurons as well as TuLAL projection neurons are remarkably indifferent with respect to the presented light intensity. The full amplitude of the frequency modulation is maintained over several orders of magnitude of decreasing light levels and breaks down completely within one to two orders of magnitude below levels of 10^{10} photons/cm^2/s (Kinoshita et al. 2007; el Jundi and Homberg 2012). This means that these neurons are not suited to encode stimulus intensity, but possess an all-or-nothing response pattern above their sensitivity threshold. Differently, LoTu1 neurons possess an intensity-response curve with a shallower slope and therefore respond with stronger frequency modulations at more intense light levels over at least four orders of magnitude (Kinoshita et al. 2007; el Jundi and Homberg 2012). Additionally, very bright light levels comparable to midday conditions lead to a reduction in the response amplitude of LoTu cells, resulting in a uniquely bell-shaped intensity-response curve (el Jundi and Homberg 2012). Together with a described increase in response amplitude towards the end of the day (el Jundi and Homberg 2012), these characteristics suggest that LoTu1 cells may constitute a polarization channel specialized for dim light conditions around sunset.

4.6.3 E-Vector Tuning

In laboratory-raised locusts, the single LoTu1 cell in the right hemisphere is tuned to ~45° and the one in the left hemisphere to ~135°, i.e., their tuning is mirror symmetrical with respect to the midline of the brain. Similarly, TuTu cells (two per hemisphere) are tuned to ~45° and ~0° in the right hemisphere and ~135° and ~0° in the left hemisphere (Pfeiffer et al. 2005). While the tunings of LoTu neurons were confirmed in a second study, the same study showed no significant tuning groups for TuTu cells (el Jundi and Homberg 2012), indicating that there might be differences in the characteristics of these neurons between different locust populations. Interestingly, in animals that have been raised with clear view of the sky, the described distinct tunings change for both cell types, and the distributions become much broader (TuTu1) or even completely random (LoTu1) (Pfeiffer and Homberg 2007). Similarly, when solitary locusts are compared to gregarious locusts, the same broadening to the point of randomness was also observed in the solitary animals (el Jundi and Homberg 2012). This shows that the *E*-vector tunings of intertubercle neurons can be influenced by a variety of factors, including behavioral state and sensory experience. Together with the pronounced change of *E*-vector tuning in response to the time of day (see section "Time Compensation"), this raises the question of how the different *E*-vector tunings of these neurons are generated from the presumably constant photoreceptor input in a fixed receptive field.

For TuLAL neurons, *E*-vector tunings were randomly distributed in all studies, in line with the large number of these cells (ca. 60 per hemisphere) and their variable receptive fields. The latter suggests that different sets of ommatidia from the locust DRA are integrated by different TuLAL neurons, with the resulting *E*-vector tuning reflecting the average orientation of the input ommatidia.

4.6.4 Degree of Polarization

Interestingly, LoTu neurons are exclusively excited when presented with polarized light from dorsal directions, but are strongly inhibited by unpolarized light from the same direction (Pfeiffer et al. 2005; Kinoshita et al. 2007). As unpolarized light is merely a blend of polarized light with all possible *E*-vector orientations, this seems a paradox. When these neurons were presented with successively reduced degrees of polarization *d*, the purely excitatory response became polarization opponent at intermediate *d*-values and purely inhibitory at low *d*-values (Pfeiffer et al. 2011). This means that the mean spiking activity is correlated with the degree of polarization. Additionally, the response amplitude linearly decreased with smaller values of *d* and became indistinguishable from background variability at *d*-values of ca. 30 %. Importantly, this limits the area of the sky containing useful information for these cells (and for the locust) to the region further away than 50° from the sun (and the anti-sun). For TuTu neurons, lower *d*-values also lead to decreased response amplitudes as well as to lower mean spiking rates, albeit not reaching near total inhibition as in LoTu neurons. Although lower response amplitudes at lower *d*-values are intuitive (more *E*-vector noise), the reduction in overall activity found for both neurons when adding unpolarized light to a polarized-light stimulus is more difficult to explain. Pfeiffer et al. (2011) addressed this neuronal behavior in an elegant model and proposed that the release of well-spaced bouts of inhibitory transmitter (histamine) from photoreceptors in response to polarized light allows for rebound excitation in the postsynaptic lamina cells, and therefore leads to the observed excitatory responses. In contrast, when stimulated with unpolarized light or very high intensities of polarized light (el Jundi and Homberg 2012), transmitter release from photoreceptors would become contiguous and is thus increased to a level that does no longer allow for rebound excitation, which consequently leads to an inhibitory response. The *E*-vector tuning of LoTu neurons would result from combining all ommatidia of the DRA while considering the asymmetry of rhabdom area devoted to one of the two dominant microvilli orientations within each ommatidium. Estimating from the microvilli orientation of R7 photoreceptors across the DRA, the resulting tuning of 35° is reasonably close to the observed 45° in laboratory-raised animals (Pfeiffer et al. 2011).

4.6.5 Integration of Unpolarized Skylight Cues

Neurons of the AOTu also respond to unpolarized light (Pfeiffer et al. 2005; Kinoshita et al. 2007). Experiments in which unpolarized light spots were moved around the animal at constant elevation showed that these cells are strongly excited when the stimulus passes through a specific azimuth (Pfeiffer and Homberg 2007; Heinze and Reppert 2011) (Fig. 4.6c, d). This azimuth tuning has been shown for all recorded AOTu neuron types in locusts and monarch butterflies (locusts: TuTu1, LoTu1, TuLAL1a; monarch: TuLAL1a, TuLAL1b). In monarchs, the color of the unpolarized light does not affect the responses, and a strong response is found with UV, blue, and green light. The tuning for all three colors is indistinguishable (Heinze and Reppert 2011) (Fig. 4.6d). In locusts on the other hand, the neurons show color opponency with green stimuli being excitatory and UV stimuli being inhibitory (Fig. 4.6c). Consequently, the monarch cells appear to encode the azimuth of the brightest spot in the sky across all wavelengths, and thus likely provide direct information about the position of the sun, whereas the locust neurons are suited to encode the spectral gradient of the sky, another sun-derived skylight cue. As longer wavelengths dominate the solar hemisphere of the sky, while short wavelengths are more evenly distributed, the ratio of green to UV light in each point in the sky indicates the angular distance of that point from the sun. Thus, for example, if a locust neuron has a preferred azimuth lying directly ahead of the animal, the cell would be activated when the locust faces towards the solar sky hemisphere, but would be inhibited when facing in the opposite direction, whereas zenithal *E*-vector information is identical in both situations. Thus, Pfeiffer and Homberg (2007) suggest that these response characteristics are well suited to provide an unambiguous direction signal in polarization-sensitive neurons. This disambiguation of the *E*-vector information is necessary due to the axial symmetry of zenithal *E*-vectors, which allow finding the solar meridian, but cannot be used to distinguish the solar from the antisolar hemisphere of the sky.

An interesting question arises when one asks how the locust neurons would respond to direct illumination by the sun. As the sun is the brightest source of UV light as well as of green light, the described opponent response to both wavelengths would block an activation of the neuron. Remarkably, a reversal in the response from inhibition to excitation has been observed for some LoTu1 neurons between low and high intensities of UV light (Kinoshita et al. 2007). This suggests that when the sun is not visible, low intensity UV light received from the sky would inhibit the neuron and thus facilitate encoding of the spectral gradient, while during times of visibility of the sun, high intensity UV light from the sun itself would activate the neuron and lead to a response like the one described for the monarch butterfly. As responses to unpolarized light were mostly stronger than the responses to polarized light in both species (Pfeiffer and Homberg 2007; Heinze and Reppert 2011), the sun as the most prominent skylight cue would dominate the neuron's response when it is present in the sky. Only when the sun is not available as orientation cue, the spectral gradient of the sky and the polarization pattern would dominate the

neuronal response and thus guarantee a robust encoding of the solar azimuth under more difficult sky conditions. Behavioral data from the monarch butterfly strongly support such an hierarchy of skylight cues by showing that although these animals have the capacity for using polarized light for navigation, the sun is used as the primary orientation cue (Mouritsen and Frost 2002; Froy et al. 2003; Reppert et al. 2004; Sauman et al. 2005; Stalleicken et al. 2005).

Another interesting difference between locusts and monarchs becomes apparent when one compares the distribution of azimuth tunings in these neurons. In locusts, this distribution depends on the cell type. LoTu1 neurons recorded from the left brain hemisphere share a common excitatory azimuth tuning of 90°, i.e., on the left side of the animal, while TuTu neurons show a double peaked tuning distribution centered contralaterally with a strong inhibitory component ipsilaterally (Pfeiffer and Homberg 2007). In the UV range, this reverses and TuTu neurons share one ipsilateral excitatory peak, while LoTu neurons show a broad distribution with a shared ipsilateral, inhibitory azimuth tuning. At last, TuLAL neurons show no shared common azimuth tuning at all (Pfeiffer and Homberg 2007). On the contrary, all recorded neuron types in the monarch butterfly possess a tuning distribution for all tested colors with a highly significant maximum near 270°, i.e., on the right side of the animal (for neurons recorded in the left brain hemisphere) (Heinze and Reppert 2011). Although the functional significance of this finding is not yet known, it clearly suggests species-dependent differences in polarized-light processing at the level of the AOTu.

4.7 The Central Complex

The final processing stage for polarized-light information in the brains of all examined animals to date is the central complex (CX) (Homberg et al. 2011; Merlin et al. 2012) (Fig. 4.4). This midline-spanning group of neuropils is located at the center of the brain. It consists of four major compartments: the upper and lower divisions of the central body (CBU, CBL; called fan-shaped body and ellipsoid body in flies), the protocerebral bridge (PB), and the paired noduli. Although the overall orientation of the CX within the brain differs substantially between locusts and crickets on the one hand, and butterflies and flies on the other hand, its components are highly conserved (Williams 1975; el Jundi et al. 2010; Heinze and Reppert 2012; Ito et al. 2014). Moreover, their internal neuroarchitecture appears to be remarkably well conserved down to the level of single cell types (Hanesch et al. 1989; Heinze and Homberg 2008; Heinze et al. 2013; Lin et al. 2013). In all analyzed species these cell types can be divided into three major classes of neurons: tangential neurons, columnar neurons, and pontine neurons (in most detail described in the desert locust, the monarch butterfly, and *Drosophila*).

Tangential neurons connect a variety of brain regions outside the CX with complete layers of either one of the CX-compartments, generating a characteristic stratified layout in the central body and in the noduli. These cells, of which many

different types have been found, are generally thought to constitute the principal input to the CX (Hanesch et al. 1989; Li et al. 2009; el Jundi et al. 2010; Heinze et al. 2013).

In contrast, columnar neurons connect small, well-defined regions between several CX-compartments. As these cell types generally occur in isomorphic sets of 16 individual neurons, the arborization trees of which are evenly distributed across the width of the innervated CX-compartment, they generate a repetitive neuroarchitecture consisting of 16 "columns" or "slices" (Williams 1975; Hanesch et al. 1989; Heinze and Homberg 2008; Heinze et al. 2013; Ito et al. 2014). While existing in a linear array in the unlayered PB, in the central body, the columns orthogonally intersect with the layers generated by tangential neurons. Ultimately, many columnar cell types converge with their proposed output arborizations in the LALs, paired neuropils on either side of the central body. These neurons are thought to constitute the major output pathway from the CX (Heinze and Homberg 2008; el Jundi et al. 2010; Heinze et al. 2013).

Cells of the third group, the pontine neurons, connect individual columns on either side of the midline with one another. They only occur in the CBU and also exist as isomorphic sets of cells (Heinze and Homberg 2008; Siegl et al. 2009; Heinze et al. 2013). Thus, these cell types provide the basis for complex, interhemispheric information flow within the CBU. Similarly, sets of tangentially oriented, multicolumnar neurons of the PB provide another, even more complex way of information exchange between CX-regions on either side of the midline (Heinze and Homberg 2007; Heinze et al. 2013). In some species, these neurons additionally arborize in the posterior optic tubercle, a small neuropil near the posterior brain boundary, and are therefore considered tangential neurons of the PB. As these fibers are lacking in other species (Homberg 1985; Hanesch et al. 1989; Young and Armstrong 2010; Lin et al. 2013), only the intrinsic arborizations restricted to columns of the PB appear to be a commonly shared feature of the CX in many insects.

The vast majority of the mentioned types of neuron have been reported to respond to linearly polarized light and together form the CX-polarization vision network. However, most knowledge about how this information propagates through this intricate network is indirect, i.e., either derived from anatomical data or from comparisons of response characteristics between individual cell types. Nevertheless, a substantial amount of evidence has accumulated over the recent years that indicates that, in principle, there are three processing stages present in the CX neuronal network: First, the input stage, represented by tangential neurons of the CBL (Fig. 4.7); second, an intermediate stage, represented by special types of columnar neurons, as well as multicolumnar neurons of the PB (Fig. 4.8); and third, the output stage, represented by a group of large columnar neurons projecting to the LALs (Fig. 4.9). In the following subsections, all three stages will be examined in detail.

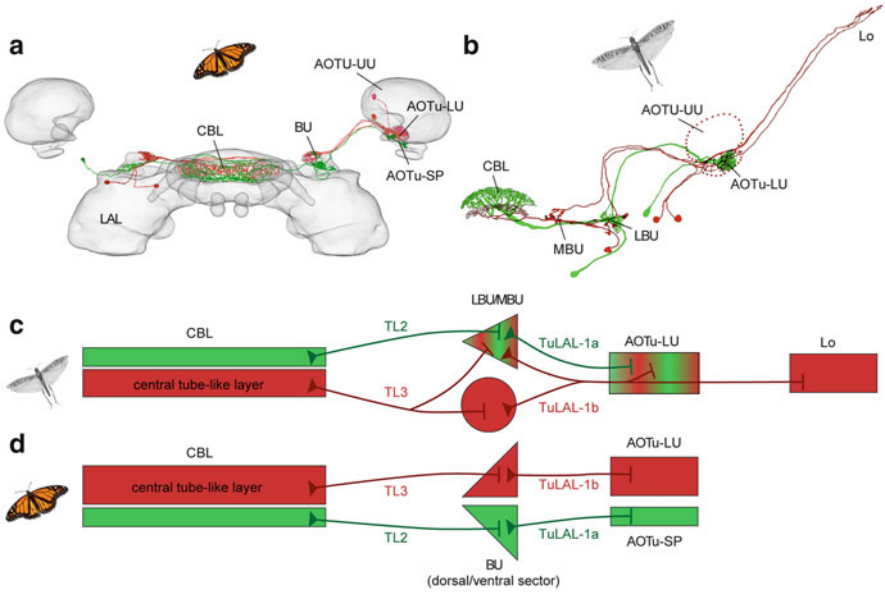

Fig. 4.7 The input stage of polarized-light processing in the central complex. (**a**) TuLAL neurons and their likely postsynaptic tangential neurons of the lower division of the central body (CBL) registered into the standardized compass neuropils of the monarch butterfly (data from Heinze et al. 2013). The pathway originating in the lower unit of the anterior optic tubercle (AOTu-LU) is shown in *red (dark)*, while the pathway originating in the strap region (SP) of the AOTu is shown in *green (light)*. Pathway 1 passes through the dorsal sector of the bulbs (BU) and ends in a central layer of the CBL. Pathway 2 passes through the ventral sector of the BU and ends in peripheral layers of the CBL. (**b**) Frontal reconstructions of TuLAL neurons and tangential neurons of the CBL in the desert locust. Likely parallel pathways are illustrated in *red (dark)* and *green (light)*. Pathway 1 passes predominantly through the medial bulb (MBU) and ends in a central layer of the CBL, while pathway 2 passes through the lateral bulb (LBU) and ends in a peripheral layer of the CBL (reconstructions modified after Pfeiffer et al. 2005; Träger et al. 2008). (**c**, **d**) Schematic illustrations of the input pathways to the CBL from the AOTu in the locust (**c**) and the monarch butterfly (**d**). Names of cell types are shown next to the lines illustrating the neurons. Colors as in A/B. *LAL* lateral accessory lobe, *Lo* lobula, *UU* upper unit

4.7.1 The Input Stage of the Central-Complex Network

How does polarized-light information reach the CX? The output neurons of the AOTu (TuLAL cells) carry polarized-light information to a specialized part of the LAL, which is characterized by a microglomerular structure and strong GABA (γ-aminobutyric acid) immunoreactivity. This region serves as a relay between the AOTu and the CX and is now referred to as the bulb (in previous literature: lateral triangle; Hanesch et al. 1989; Träger et al. 2008; Heinze and Reppert 2012) (Fig. 4.7a, b). It is divided into two distinct parts in the locust (called the lateral bulb [lateral triangle] and the medial bulb [median olive]), whereas it consists of two to three fused compartments in *Drosophila*, the monarch butterfly, and the

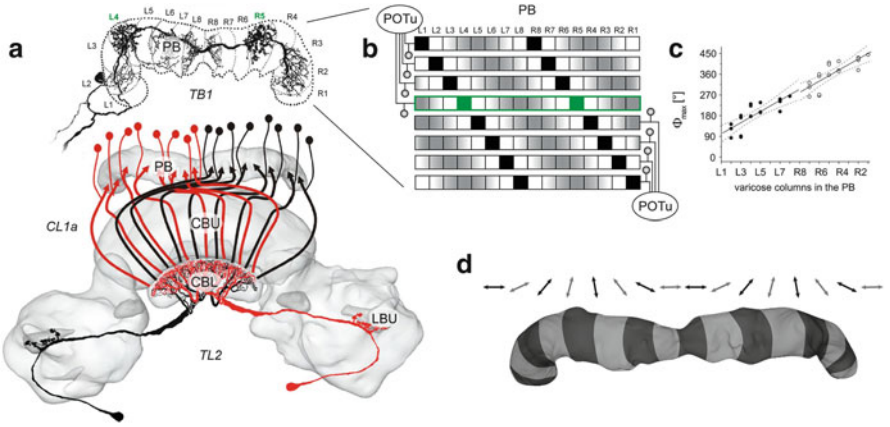

Fig. 4.8 The intermediate stage of polarized-light processing in the central complex of the desert locust. (**a**) Proposed information flow to the intermediate stage neurons of the protocerebral bridge (PB). Based on receptive field organization, information from input neurons of the right side of the midline (black TL2 neurons) appears to be passed on to CL1a neurons of the contralateral brain side (*black*), and vice versa for information from the *left side* (*red*/*gray neurons*). Within the PB (*top*), TB1 neurons are suited to integrate information from both hemispheres with their bilateral input fibers and generate zenith-centered receptive fields. TB1 and TL2 neurons are shown as frontal reconstructions (neurite to posterior optic tubercle POTu in TB1 cells has been omitted for clarity), while CL1a neurons are drawn schematically. Nomenclature for PB-columns is shown on *top*. (**b**) Arborization scheme of TB1 neurons in the locust brain. *Each row* represents one individual neuron, with *black squares* indicating varicose (output) fibers and *gray squares* indicating smooth (input) fibers. The example shown in **a** is highlighted. (**c**) Preferred *E*-vector tuning of TB1 neurons plotted against the position of the output fibers along the PB. As each TB1 neuron possesses two columns filled with output fibers at a distance of eight columns, the analysis was restricted to one hemisphere and the dataset was shown twice for illustration purposes. Note that *E*-vector tunings of the neurons change linearly with the position of the arborization tree along the PB. (**d**) Schematic illustration of the linear regression data shown in **c**. Each column of the PB is associated with a particular *E*-vector tuning, overall covering all possible *E*-vectors (180°) once per PB hemisphere. *CBL* lower division of the central body; *CBU* upper division of the central body, *BU* bulb. Images were reproduced with permission from: Heinze et al. (2009) (**a**); Heinze and Homberg (2007) (**b**, **c**)

cricket. Its microglomerular structure originates from very large synapses formed between the AOTu-projection neurons and tangential neurons of the CBL (TL neurons). Here, large, cup-shaped presynaptic terminals (TuLAL neurons) engulf tangles of very fine postsynaptic endings (TL neurons) (Träger et al. 2008; Heinze et al. 2013). These synaptic complexes have been particularly well described in the locust and are reminiscent of the specialized giant synapses (Calyx of Held) in the vertebrate auditory pathway. Their function within the polarization vision pathway remains elusive, but both pre- and postsynaptic neurons are tightly tuned to particular *E*-vectors when the animal is stimulated with a rotating linear polarizer in locusts and monarchs (Vitzthum et al. 2002; Pfeiffer et al. 2005; Heinze and Reppert 2011). Träger et al. (2008) speculate that the anatomical resemblance with the Calyx of Held might reflect a functional

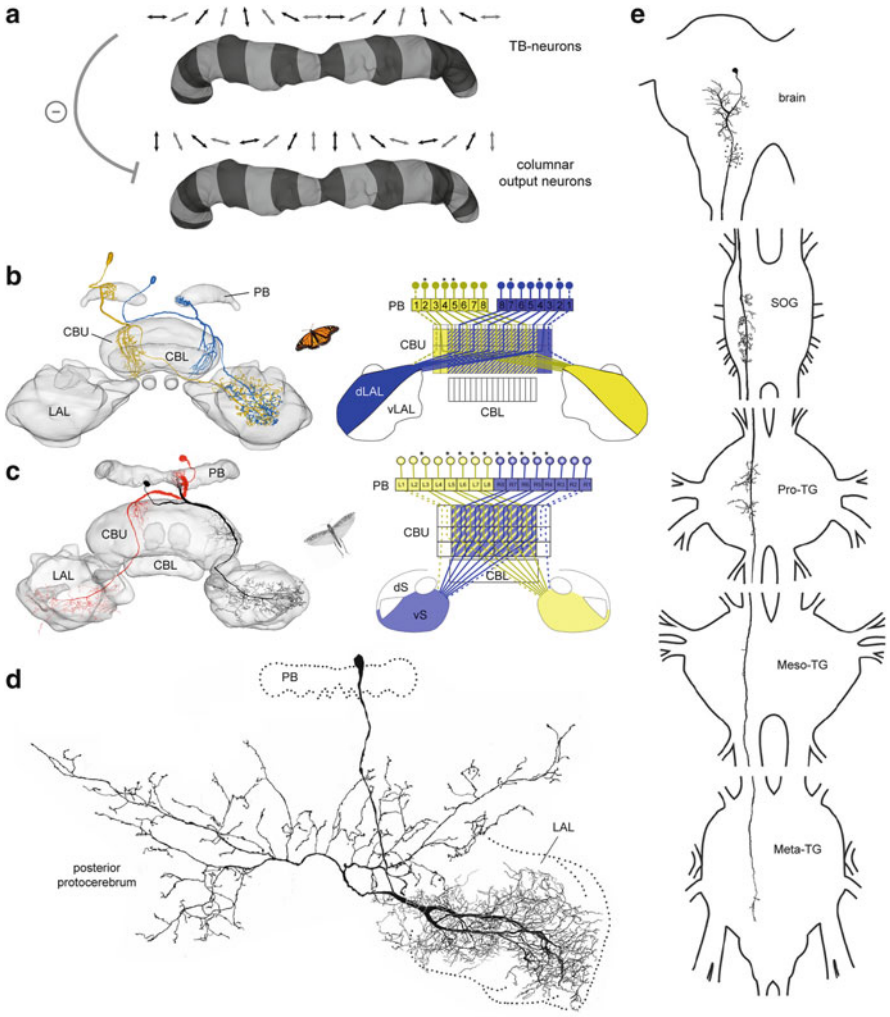

Fig. 4.9 The output stage of the central-complex and polarization-sensitive downstream connections. (**a**) Schematic illustration of the systematic *E*-vector tunings in the protocerebral bridge (PB) in columnar neurons as opposed to TB1 neurons. The 90° shift in tunings between TB1 and columnar neurons indicates an inhibitory connection. (**b**, **c**) Anatomy of major output neurons of the central complex (CPU1 neurons) in the monarch butterfly (**b**) and the desert locust (**c**). The *left panels* show two individual neurons (registered into the standardized central complex in the monarch; frontal reconstructions projected onto 3D reconstruction of neuropils in the locust), while the *right panel* shows the heterolateral connectivity scheme for these neurons. The *asterisks* indicate actually identified neurons. Note the similarity between the species, despite 360 million years of separated evolutionary history. (**d**) Reconstruction of a polarization-sensitive neuron with input fibers in the lateral accessory lobes (LAL), providing a potential link to descending pathways. (**e**) Reconstruction of a polarization-sensitive descending neuron with input fibers in the posterior protocerebrum and output arborizations in the subesophageal ganglion (SEG) and in all three thoracic ganglia (TG). *CBU* upper division of the central body, *CBL* lower division of the

similarity, suggesting a role of these synapses in ensuring the precise timing of *E*-vector signals provided by the right and the left eye, before these signals reach the CX as central integration center.

Tangential neurons of the CBL (TL neurons) are the principal input for polarized-light information into the CX. They receive signals from projection neurons of the AOTu and project to individual layers of the CBL (Träger et al. 2008; Heinze et al. 2009; Heinze and Reppert 2011). Depending on which CBL layer is innervated, several types of these cells can be distinguished (Fig. 4.7). First defined for the locust (Müller et al. 1997), these neuronal subtypes have also been identified in the monarch butterfly (Heinze et al. 2013), and similar polarization-sensitive cells exist also in the cricket (Sakura et al. 2008). In *Drosophila*, the ring neurons of the ellipsoid body are the homologous counterparts to these neurons (Hanesch et al. 1989), but have so far not been shown to respond to polarized light. Interestingly, anatomical data suggest that the different subtypes of TL neurons receive input from different types of AOTu-projection neurons in monarchs and locusts, and hence constitute at least two parallel pathways which carry information about polarized light from early processing stages to the CX (Träger et al. 2008; Heinze et al. 2013) (Fig. 4.7c, d). In locusts, these pathways have been examined in most detail and can be distinguished by the response characteristics of the involved neurons: TL2 neurons respond to stimuli from both eyes, while TL3 neurons only receive ipsilateral input (Vitzthum et al. 2002; Heinze et al. 2009). Although the ocular dominance of these cells has not been examined in other species to date, the striking anatomical similarity, particularly between the monarch butterfly and the locust, suggests that two parallel input pathways carrying nonredundant *E*-vector information are a fundamental computational element found in the polarization vision network of the central brain of insects.

4.7.2 *The Intermediate Stage of the Central-Complex Network*

How is the information arriving in the CX via TL neurons processed through further stages? The most likely target neurons are a group of columnar cells, called CL1 neurons (Heinze and Homberg 2009). These cells connect individual columns of the CBL with columns of the PB, while also projecting to a small region of the LAL. Interestingly, the detailed structure of the neuronal terminals suggests that there are

Fig. 4.9 (continued) central body, *vLAL* ventral LAL, *dLAL* dorsal LAL, *dS* dorsal shell, *vS* ventral shell, *MBU* medial bulb, *LBU* lateral bulb. Images have been reproduced with permission from: Heinze et al. (2013) (**b**); Heinze and Homberg (2008) (**c**); Heinze and Homberg (2009) (**d**); Träger and Homberg (2011) (**e**)

two subtypes of these cells with opposite polarity: the first with input regions in the CBL and output regions in the PB and the second with input regions in the PB and output regions in the CBL (Hanesch et al. 1989; Heinze and Homberg 2008, 2009; Heinze et al. 2013; Lin et al. 2013). The LAL projections appear to be output areas in all types. This complex anatomy has been described in all examined species (locusts, monarchs, and *Drosophila*) and thus the possibility for bidirectional information flow between the PB and the CBL appears to be a shared feature of the insect CX. The input arborizations of these cells in the CBL coincide with the location of the output fibers of major TL neurons in locusts and monarchs, and indeed CL1 cells exhibit exquisite polarization sensitivity (Heinze and Homberg 2009; Heinze et al. 2009; Heinze and Reppert 2011). In fact, in locusts these neurons are most narrowly tuned to their preferred *E*-vector compared to all other cell types. As for TL-neurons, the tuning of each individual CL1 neuron is not correlated with its anatomical characteristics (Vitzthum et al. 2002; Heinze and Homberg 2009). This is remarkable and difficult to explain for the columnar neurons, as each individual cell can be uniquely identified based on the location of its columnar arborization tree along the width of the CBL/PB. Either different sets of these neurons possess different tuning directions in identical columns or the tuning of each cell is dynamically adjusted over time (or between individual animals).

Intriguingly, the potentially postsynaptic partners of CL1 cells show a precise correlation between their *E*-vector tuning and the position of their arborization trees along the width of the PB (Heinze and Homberg 2007). These cells, called TB1 cells, possess two columnar output arborizations, filling two of the 16 PB-columns at a distance of eight columns apart. The space not covered by these arborization trees is largely filled with smooth input fibers, while only the columns directly adjacent to the output fibers remain devoid of terminals (Fig. 4.8a). As at least one TB neuron exists for each PB-column (Fig. 4.8b), the location of the output fiber trees can be correlated to the zenithal *E*-vector tuning of the cell. When this was performed in the locust, a significant relation between the physiology and the morphology of the neurons emerged (Fig. 4.8c). Moreover, the *E*-vector tunings of these neurons are distributed in such a way along the PB that all possible *E*-vectors (range from 0° to 180°) are mapped precisely on each PB hemisphere (Heinze and Homberg 2007) (Fig. 4.8d). This means that when a given *E*-vector is shown to the locust from the zenith, two activity maxima are produced along the length of the PB, and the location of these maxima changes systematically with the orientation of the animal. That is, the readout of these activity maxima can serve as a predictor of body orientation relative to the zenithal *E*-vector. Given the fact that the zenithal *E*-vector orientation depends strictly on the azimuth of the sun, this population of neurons can act as an ordered array of head direction cells within the global frame of reference provided by the sun, i.e., they can serve as an internal sun compass.

The question of how this *E*-vector map is computed remains one of the major questions related to polarization vision. The complex interplay of CL1 and TB1 neurons may be suited to perform the necessary computations, especially as these neuron types are highly conserved in many insect species. An additional piece in the

puzzle, however, is provided by neurons described in the locust that interconnect the posterior optic tubercles on either side of the midline (el Jundi and Homberg 2010). As these small neuropils are also innervated by TB1 neurons (Heinze and Homberg 2007), a potentially closed loop between TB1 cells on either hemisphere of the PB is created that might play a role in shaping and stabilizing activity peaks within the PB through mutual inhibition (U. Homberg, personal communications).

4.7.3 The Output Stage of the Central-Complex Network

How is the information stored in the azimuth representation of the PB transmitted to the motor system? Judged by anatomical data as well as their physiological response characteristics, the most likely candidates for this task are columnar neurons that receive their input in the PB and project to different areas of the LALs. Among these, found in all insects studied so far, is a group of cell types called CPU1 neurons, which likely constitute the major output pathway from the CX in general (Homberg 1985; Hanesch et al. 1989; Vitzthum et al. 2002; Heinze and Homberg 2008; Heinze et al. 2009, 2013; el Jundi et al. 2010; Heinze and Reppert 2011; Phillips-Portillo 2012; Lin et al. 2013) (Fig. 4.9b, c). Aside from input fibers in the PB, these cells have additional input-type branches propagating through the layers of the CBU, whereas their output terminals cover large regions of the contralateral LAL. Detailed analyses in the locust and the monarch revealed several subtypes of these neurons, all of which were shown to respond to polarized light in both species (Heinze and Homberg 2008; Heinze et al. 2013). In locusts, the *E*-vector tunings of these cells are arranged in a systematic way and depend on the PB-column in which each neuron receives its input (Heinze and Homberg 2007). As for TB1 neurons, this map-like *E*-vector representation covers a range of 180° in each PB hemisphere, but is shifted by 90° with respect to TB1 cells (Fig. 4.9a). This means that in PB-columns in which TB1 neurons exhibit maximal activity at a given *E*-vector, the corresponding CPU1 cell shows minimal activity (i.e., maximal inhibition). If CPU1 neurons are indeed postsynaptic to TB1 cells, this implies an inhibitory connection between those two types of neuron. Although TB1 cells are not GABAergic, the presence of serotonin and several neuropeptides (shown through immunocytochemistry) in these cells in the locust does at least permit such inhibitory effects (Heinze and Homberg 2007). Preliminary data in the monarch butterfly reveal a very similar correlation between *E*-vector tuning and location of arborization trees along the PB in that species and suggest that systematic representations of *E*-vector angles are not a specialization of the desert locust (S. Heinze, unpublished observation; J. Phillips-Portillo, personal communications).

In the locust, two more columnar cell types with input-type fibers in the PB have been consistently shown to respond to polarized light: CP1 and CP2 neurons (Vitzthum et al. 2002; Heinze et al. 2009). These cells project to small regions of the LAL, closely associated (but likely not overlapping) with the lateral and medial bulbs (lateral triangle and median olive). The tuning angles of these neurons follow the same pattern as CPU1 neurons with respect to the position of the input

arborization in the PB, i.e., they might also receive inhibitory input from TB1 neurons (Heinze and Homberg 2007). Unlike CPU1 cells though, these cell types have not been reported in any other insect to date.

A separate possible output pathway is present in the LAL projections of CL1 neurons. This projection is very small (and even missing in one subtype of these cells) in the locust (Heinze and Homberg 2008, 2009), but is much more prominent in the monarch butterfly (Heinze et al. 2013). In the monarch these cells show an increased fiber diameter and higher numbers of axonal terminals in the LAL. Additionally, the CL1 projection area in the monarch LAL stands out as a distinct region (called anterior loblet) not found in the locust. Importantly, this pathway does not necessarily receive input from the PB, and could thus mediate a direct route between tangential input neurons of the CBL and LAL cells serving as input to the motor system.

At last, a group of neurons found in many insects, but physiologically examined only in the locust, shows a behavior termed "conditional polarization sensitivity" (Heinze and Homberg 2009). These cells, which are all columnar neurons of the PB that project either to the noduli (CL2, CPU4) or to bilateral regions of the LAL (CPU2), do not consistently respond to polarized-light stimulations, but appear to be recruited to the polarized-light processing network of the CX in a context-dependent manner. What might trigger the switch in their responsiveness is unknown. Also the question of whether homologous neurons show similar behavior in other insects remains to be solved. However, the presence of these cells underlines the potential complexity and dynamic nature of the polarization vision network of the CX at least in the desert locust. The striking anatomical resemblance of the locust neurons to those in other insects (particularly in the monarch butterfly; Heinze et al. 2013) across extremely wide evolutionary distances makes it likely that the described network is not only a specialization of the locust brain but also exists in other insect species, possibly exhibiting similar functions.

4.7.4 Physiological Evidence for Proposed Information Flow

Aside from anatomical data and the fact that all described neurons respond to polarized light, what is the evidence supporting the laid out polarization vision network of the CX? Despite the fact that *E*-vector response curves appear to be similar between different cell types at first sight, detailed analysis in the locust has revealed characteristics that systematically vary from "early stage" to "late stage" neurons of the POL network in the CX (Heinze et al. 2009). This includes the signal-to-noise ratio of the neurons, their background activity, and the size and orientation of their receptive fields. In detail, tangential neurons of the CX (input stage) possess comparably small receptive fields centered in the contralateral hemisphere (in tune with the viewing direction of the ipsilateral DRA), while exhibiting low background activity and high signal-to-noise ratios (Fig. 4.10b). On the other hand, all neurons participating in the map-like *E*-vector representation

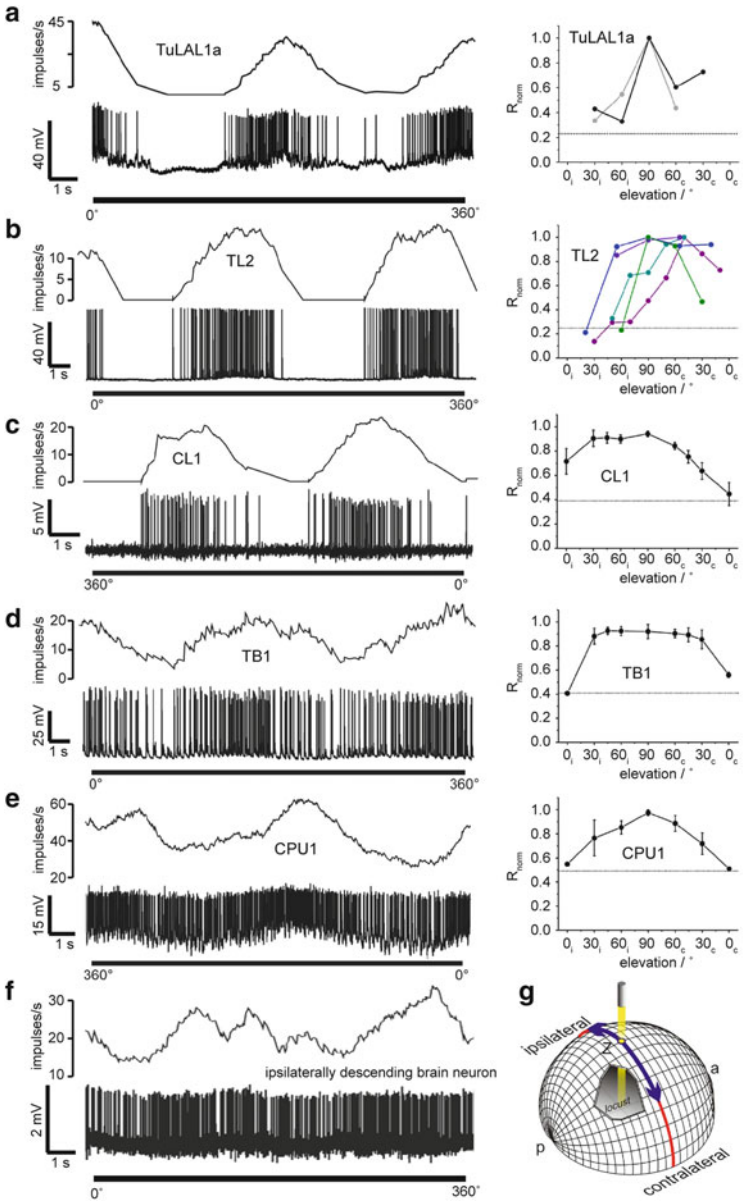

Fig. 4.10 Physiology of polarization-sensitive neurons across processing stages in the desert locust. *Left column:* Activity of neurons during one rotation of a linear polarizer above the animal. *Top trace* shows mean activity (gliding average); *bottom trace* shows voltage trace of intracellular recording. Counterclockwise rotations: 0°–360°; clockwise rotations: 360°–0°. *Right column*: Lateral extent of receptive fields for stimulation with polarized light. Plotted is the normalized response amplitude against the elevation of the stimulus along the meridian orthogonal to the body length axis of the animal. The *line* indicates background variability of the neuron type without stimulation. Neuron types are arranged from early to late processing stages: (**a**) TuLAL1a neurons

of the PB show zenith-centered, very large receptive fields, high background activity, and lower signal-to-noise ratios (Fig. 4.10d, e). Furthermore, columnar neurons of the CBL, which are proposed to serve as the link between the input stage and the later stages, possess intermediate physiological characteristics. Their receptive fields are larger compared to tangential input stage cells, but are not zenith-centered as in later processing stages (Fig. 4.10c). In fact, the observed slight shift in receptive field center towards the ipsilateral hemisphere in these neurons suggests that information present in TL neurons from one side of the brain is transmitted to only those CL neurons projecting to the contralateral hemisphere of the PB (CL1 cell bodies are located close to the PB, i.e., contralaterally to TL neurons). Therefore, information from each sky hemisphere would be projected to the ipsilateral half of the PB (Fig. 4.8a). The previously described multiglomerular neurons of the PB (TB neurons) would then be ideally suited to integrate this information with their bilateral input fibers to generate the observed very large, zenith-centered receptive fields (Heinze et al. 2009).

The most direct evidence for the directionality of signal flow in neurons of the POL network are intracellular recordings from several types of columnar neurons from either the PB or the LAL. When recorded in the PB (their proposed input region), postsynaptic potentials were frequently observed in CPU1 and CP2 neurons (locusts; CPU1 also in monarchs), while recordings from the same cell types in the LAL (proposed output region) revealed no such potentials (Heinze et al. 2009). These observations are strongly supporting the direction of signal flow within the output stage of the CX-POL network. Interestingly, and despite large numbers of recorded cells, no such clear distinction could be made for CL1 neurons, supporting the idea of bidirectional information flow between the PB and the CBL.

4.8 Beyond the Central Complex

In order to guide an insect's behavior, the information about polarized light represented in the central brain has to reach the motor centers of the thorax. Indeed, intracellular recordings performed in the locust have demonstrated the presence of

Fig. 4.10 (continued) (modified after el Jundi and Homberg 2012). (**b**) TL2 neurons. (**c**) CL1 neurons. (**d**) TB1 neurons. (**e**) CPU1 neurons. (**f**) Ipsilaterally descending neuron. No receptive field data exist for this cell type. Receptive field data show data from individual neurons in **a** and **b**, while showing mean ± standard error for **c**–**e**. Note that receptive fields change from small, variable, often contralaterally centered fields (TuLAL1a, TL2) to broad, ipsilaterally centered fields in CL1 neurons, to zenith-centered, very wide fields (TB1, CPU1). Within spike trains, comparison between cell types reveals that signal-to-noise ratio decreases the further the cell type is removed from the sensory periphery, while background activity and variability increase. (**g**) Illustration of stimulus delivery for measuring lateral extent of receptive fields. *a* anterior, *p* posterior, *Z* zenith. Images are reproduced with permission from: Heinze et al. (2009) (**b**–**e**, **g**); Träger and Homberg (2011) (**f**)

such a polarization-sensitive descending pathway (Träger and Homberg 2011) (Fig. 4.9e). Two pairs of neurons, one descending through the ipsilateral neck connective and the other one descending through the contralateral connective, possess proposed input fibers in the posterior protocerebrum of the brain and have their proposed output fibers in the subesophageal and thoracic ganglia. These cells respond with modulations of their spiking frequency when the animal is presented with a rotating linear polarizer (Fig. 4.10f). The responses are relatively weak and are imposed on a high background variability and variable background firing frequency (Träger and Homberg 2011). However, such behavior is expected for neurons many synapses away from the sensory input and is in line with the increasing variability and decreasing signal-to-noise ratio in late processing stages of the CX (Heinze et al. 2009) (Fig. 4.10). Both neurons also show strong, direction-selective responses to moving gratings, indicating that information from more than one sensory system has converged onto these cells. As responses to these motion stimuli were much stronger than responses to polarized light, the latter might carry less behavioral relevance. Indeed, so far it has not been shown that locusts use polarized-light information for flight orientation in a natural setting, and potentially only use it as a backup system or in particular behavioral contexts.

Where do these descending neurons receive their information from, and which cells might be their postsynaptic targets? A conclusive answer for these questions remains yet to be found, but candidate neurons for both tasks have been identified in the locust. As the described descending neurons do not have input fibers in the LAL, they cannot receive information directly from the CX output cells. So far, two types of polarization-sensitive neurons have been found that could be postsynaptic to CX output cells (Heinze and Homberg 2009). The first one projects from the ipsilateral LAL to large bilateral regions of the posterior protocerebrum (Fig. 4.9d) and has also been anatomically identified in the monarch butterfly (Heinze and Reppert 2011). It is therefore the most promising candidate for integrating information from CX-output cells and relaying it to descending neurons. The second cell connects the ipsilateral LAL to its contralateral counterpart. Although it cannot contact the described descending neurons directly, it might provide an intermediate step in integrating CX-output signals.

Within the ventral nerve cord, one type of neuron has been described that shows remarkably robust polarization sensitivity. It projects from the ipsilateral hemisphere of the subesophageal ganglion to the contralateral hemisphere of the first thoracic ganglion and might be suited to link polarization-sensitive descending neurons to motor neurons, if the descending brain neurons do not directly target motor neurons themselves (Träger and Homberg 2011). Interestingly, the polarization sensitivity of these neurons is much more pronounced than in the potentially presynaptic descending cells. Also, the found motion sensitivity in these cells is not direction selective and weaker than the polarized-light response. This either suggests that there is another unidentified polarization-sensitive descending pathway converging onto these neurons, or that there is substantial local processing of information within the networks of the ventral cord ganglia, which amplifies the descending polarized-light signals. Altogether, this underlines that there are still

significant gaps in our understanding of the pathways that carry polarized-light information from the neural circuits of the central brain to the thoracic motor circuits.

4.9 Time Compensation and Circadian Input

Two of the three species that have been most extensively studied in the context of polarization vision, the desert locust and the monarch butterfly, are both insects that perform spectacular long-distance migrations. This implies that these animals are capable of maintaining a straight course over prolonged periods of time. If they indeed use the sun and the sun-derived polarization pattern of the sky as major orientation cues, these insects must compensate for the changing solar position over the course of the day. That means they have to adjust their desired heading with respect to the sun by using information about the time of day derived from the circadian clock. To perform this task, a neural connection between the circadian clock and the polarization vision network of the central brain is necessary.

Two parameters about solar position change differentially over the course of the day: solar elevation and solar azimuth. As compass information can be exclusively derived from the solar azimuth, only changes in this parameter have to be compensated to maintain a steady course over the duration of the day ("azimuth compensation"). Additionally, however, when polarized-light cues are used to derive the solar azimuth, another problem occurs: Changes in solar elevation strongly influence the interrelation between skylight polarization within the receptive fields of the DRA photoreceptors and solar azimuth. As the information content of detected polarized light consequently depends on how high the sun is up in the sky, reliable information about solar azimuth can only be derived from polarized-light information, when the animal accounts for the current solar elevation (Fig. 4.11a). This process ("elevation compensation") is needed independent of whether the compass information will be used for long-distance migration or local foraging, as it is required to generate an intrinsically consistent representation of the current solar azimuth from more than one skylight compass cue. The fact that elevation compensation is needed by all insects that use polarized light to detect the solar azimuth, while azimuth compensation is only required by long-distance migrants to maintain a steady course, suggests that these processes are distinct from each other. In the following, both processes and their potential neural substrates will be discussed in more detail.

4.9.1 Elevation Compensation

The concept of elevation compensation was first introduced by Pfeiffer and Homberg (2007) through work in the desert locust. The authors recorded from neurons of the AOTu and determined the cell's *E*-vector tuning as well as their

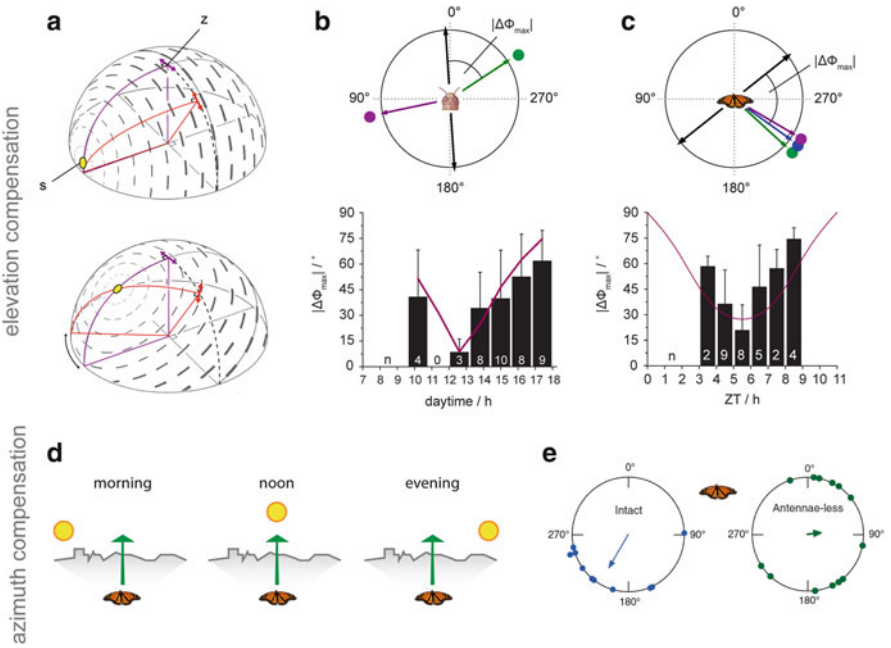

Fig. 4.11 Time compensation of skylight compass cues. (**a**) Relation between solar elevation and skylight polarization pattern. At low solar elevations (*top*), all *E*-vectors (*short gray lines*) are arranged in parallel, so that the correct solar azimuth is always indicated when a 90° relation between *E*-vector and solar azimuth is assumed. When the solar elevation is higher, the 90° relation between the solar azimuth and the *E*-vector angle is only valid in the zenith. Outside the zenith, assuming a 90° relation results in a large error (*black double arrow*) in the solar azimuth estimate. Therefore, when *E*-vectors outside the zenith are used for detecting the solar azimuth, the current solar elevation has to be accounted for. (**b**) Tuning of locust neurons from the anterior optic tubercle to polarized light from the zenith (*black*) and unpolarized light spots moving around the animal at constant elevation (green light, ultraviolet light). The difference between the azimuth tuning in response to green light and the *E*-vector tuning is termed $\Delta\Phi_{max}$. This $\Delta\Phi_{max}$ value is plotted in the *bottom panel* against the time of recording of the neurons (bins of 72 min). The data are fitted with a function that describes the angular difference between solar azimuth and *E*-vector orientation for individual points of the sky over the course of the day. The fit is calculated for August 1 (within the rearing period of the used animals) and 60° elevation above the horizon according to the visual axis of the DRA. The fit line is calculated for the coordinates of Tropic of Cancer (23.4°N), which is in the natural habitat of the locusts. (**c**) As **b**, but data for neurons recorded from the bulbs of the monarch butterfly (AOTu neurons and TL neurons). $\Delta\Phi_{max}$ is defined as the difference of *E*-vector tuning to the mean of the azimuth tunings of all tested colors. The *line* in the *bottom panel* represents the mean perceived *E*-vector in the region of sky viewed by the dorsal rim of the monarch over the course of the day, calculated for the location and date of capture of the used animals. Data are binned in 1 h bins and plotted against the Zeitgeber time (0 = light on). Note that in both species, the angular difference between azimuth and *E*-vector tuning is large in the evening and morning (at low solar elevations) and small around noon (at high solar elevations). Thus, the *E*-vector tuning of the neurons changes over the course of the day to match the skylight situation in the region of sky viewed by each species' dorsal rim area, a process called elevation compensation. (**d**) The principle of azimuth compensation. When an animal has to maintain a constant flight bearing over the course of the day by using a sun compass, it has to adjust

azimuth tuning to unpolarized light points. As the polarized-light stimuli were presented from the zenith, the expectation was that, within an individual neuron, the difference between azimuth tuning and *E*-vector tuning would be 90° (*E*-vectors in the zenith are perpendicular to the solar azimuth). However, it was found that this difference varied greatly and, surprisingly, its absolute value depended on the daytime of the recording (Fig. 4.11b). Large values (close to 90°) occurred in the morning and evening, while during midday small values dominated. This behavior could be explained by taking into account that the locust DRA has a receptive field centered at around 60° elevation on either side of the animal. In this region of the sky, the *E*-vector orientation of skylight strongly depends on the solar elevation: For any given solar azimuth, the *E*-vector orientation in the DRA receptive field changes when the sun is located at different heights above the horizon. In other words, the identical solar azimuth is indicated by different *E*-vectors depending on the solar elevation, which itself depends on the time of day. If the correct solar azimuth should be derived from the detected *E*-vectors, they have to be interpreted differently according to the current time of day. Pfeiffer and Homberg (2007) related the rate of change of the *E*-vector tuning in the recorded neurons to the rate of change of celestial *E*-vectors in the center of the receptive field of the DRA and found them to be virtually identical. The match was particularly strong when the skylight conditions of the locust's native habitat (latitude of northern Africa) were taken into account (Fig. 4.11b). Several conclusions can be drawn from these results: First, the zenithal *E*-vectors presented in the experiments are likely interpreted as if they came from the complete DRA, i.e., that information from all parts of the DRA is pooled before reaching the recorded cells. Second, the neurons anticipate the changing interrelation of celestial *E*-vectors and solar azimuth by adjusting their *E*-vector tuning in a way that ensures that it encodes the correct solar azimuth throughout the day (consistent with the azimuth obtained from the presented unpolarized stimuli). Third, this correction function is optimized to match the sensory periphery of the locust (i.e., shape and orientation of the DRA), as well as the skylight conditions of the native habitat of the animals.

Recent work in the AOTu of migratory monarch butterflies has led to very similar results in this species (Heinze and Reppert 2011). Here, the *E*-vector tuning is also changing according to the time of day, so that the difference between *E*-vector tuning and tuning to the azimuth position of unpolarized light spots follows a function similar to the locust neurons (Fig. 4.11c). However, the function

Fig. 4.11 (continued) its orientation with respect to the sun, i.e., keep the sun on the left in the morning, while keeping it on its right in the evening. (**e**) Behavioral data revealing that the antennae are required for a time-compensated sun compass in the monarch butterfly. *Left*: Circular plot of flight directions of a population of butterflies in a flight simulator. All animals maintain a steady southwesterly bearing. *Right*: When antennae are clipped, the butterflies still show directed flight; however, they become disoriented as a group. This implies that the timing information needed to adjust flight direction according to the daytime is housed within the antennae (modified after Merlin et al. 2009)

derived from the locust neurons did not match the monarch data precisely, but needed to be modified in a way that accounted for the different receptive fields of the monarch DRA and the date and location that the animals had been caught from the wild. This underlines the fundamental importance of the elevation-compensation process: Both species modify the *E*-vector tuning of their AOTu neurons according to the time of day to consistently combine otherwise ambiguous skylight compass cues into a consistent representation of the solar azimuth. To reach this identical outcome, both species have optimized the correction function in a way that accounts for their different eye shapes and habitats.

Where in the brain is timing information combined with *E*-vector information? A conclusive answer to this question has not been found to date. However, the location must occur upstream of the AOTu neurons that exhibit the described response features. Therefore, polarization-sensitive neurons of the optic lobe are promising candidates for integrating timing information. The source of this information would likely be the circadian clock of the animals. Whether the daytime-dependent change of neural tuning is truly circadian or is merely a response to rhythmic lighting conditions remains to be shown by repeating recordings in animals kept in constant darkness.

The pacemaker of the circadian clock in the monarch brain is located within few neurons in the *pars lateralis* (Reppert 2006; Zhu et al. 2008). Through tracing neurons expressing the clock protein CRYPTOCHROME-1, fibers have been identified that might colocalize with projections from DRA photoreceptors in the medulla and this way provide a possible interaction site between the circadian system and polarization-sensitive neurons (Sauman et al. 2005; Reppert et al. 2010; Merlin et al. 2012). In locusts, the seat of the clock is unknown, but through anatomical comparison with data from cockroaches is postulated to be located in the accessory medulla, a small neuropil of the optic lobes. Indeed, several polarization-sensitive neurons have been found in the optic lobe of locusts and crickets that possess side branches in this neuropil. As some of these likely serve as input fibers, they would be suited to transfer timing information from the clock to the compass system (Labhart and Petzold 1993; Homberg and Würden 1997; el Jundi and Homberg 2010; el Jundi et al. 2010).

4.9.2 Azimuth Compensation

Much less is known about the neural mechanisms of azimuth compensation (Fig. 4.11d, e). Through behavioral experiments with clock-shifted animals, this process has only been conclusively shown to exist in the monarch butterfly to date (Mouritsen and Frost 2002; Froy et al. 2003). Interestingly, this behavior depends on the presence of the antennae, particularly of functional antennal clocks (Merlin et al. 2009) (Fig. 4.11e). When the antennal clocks become interrupted or desynchronized by either cutting them or blocking their exposure to light, the

animals lose their ability for time-compensating their flight direction (Merlin et al. 2009; Guerra et al. 2012). How timing information from the antenna feeds into the polarization-sensitive network of the brain remains one of the major questions of the field. A promising candidate region of the brain is the LAL, where the output of the CX-polarization vision network converges and which, in moths, receives indirect input from the antennal lobes, while it also appears to play a crucial role in guiding steering movements (Iwano et al. 2010). Whether this mechanism is a specialization of lepidopteran insects, or whether it is applicable for insects in general, remains to be shown.

In the desert locust, a connection between the accessory medulla, the presumed seat of the clock, and the posterior optic tubercle has been anatomically identified (Homberg and Würden 1997; el Jundi and Homberg 2010). As the posterior optic tubercle is an intrinsic part of the locust polarization vision network (Heinze and Homberg 2007; el Jundi and Homberg 2010), the authors hypothesize that timing information needed to compensate for the changing solar azimuth over the course of the day might be transmitted through this connection. However, no physiological evidence supporting this hypothesis exists to date. Interestingly, the *E*-vector tunings of descending brain neurons of the locust are linearly correlated with the time of day of the recording (Träger and Homberg 2011). As alternate explanations for this correlation still cannot be ruled out and no evidence exists for time-dependent changes of flight direction in locust behavioral experiments, it remains to be confirmed whether this is the first direct observation of daytime-dependent alterations of *E*-vector tunings downstream of the CX. If these data indeed show azimuth-compensated *E*-vector tunings in premotor command neurons, it is puzzling that this does not manifest itself in the behavior of the animals.

4.10 Putting Polarized Light Into Context

Polarized light cannot be viewed as an isolated sensory cue, as it is used by the animal in conjunction with other available skylight cues. Together they provide the animal with a global frame of reference, in which it can embed sensory information that is of immediate behavioral relevance. Moreover, detecting and perceiving directional skylight cues does not provide the insect with any useful information, unless they are combined with features of the environment that have to be either avoided (e.g., predators) or approached (e.g., food, mating partners, nest). Additionally, whether features are attractive or repulsive depends on the behavioral context. For example, the nest of a central place forager is only attractive on the inbound journey after a foraging trip. Hence, modulating factors, like the motivational state of the animal or the current time of day, have to be integrated when transforming sensory signals into motor commands. An animal constantly has to evaluate whether its current direction of movement does match its desired heading.

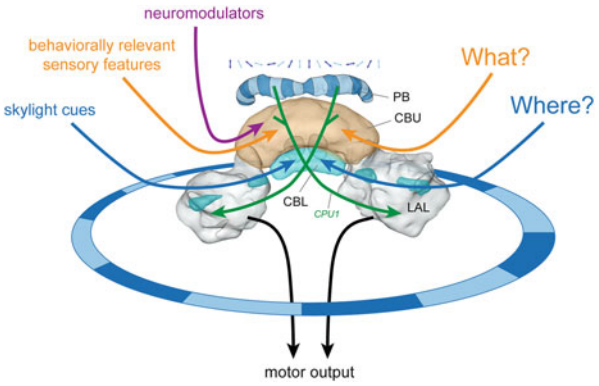

Fig. 4.12 Polarized-light perception in the context of central-complex function. In summary, the data accumulated over the last decade suggest that polarized light is one of several skylight cues that helps to establish a global frame of reference in the central complex. The neural basis of this is an ordered array of neurons in the protocerebral bridge (PB), which encodes the body orientation of the animal with respect to the sun, i.e., they provide an internal representation of the azimuthal space around the animal. This information is reaching the PB through specialized regions of the lateral accessory lobes (*blue*/*dark*: lateral bulb and medial bulb) and the lower division of the central body (CBL) (the "Where-pathway"). Behaviorally relevant features of the environment, e.g., conspecifics, food, obstacles, etc., are thought to be represented in the upper division of the central body (CBU), a neuropil that receives input from many areas of the brain (the "What-pathway"). Additionally, the CBU contains a large variety of neuromodulatory substances, which potentially confer information about the motivational state of the animal or its arousal level. At last, output neurons of the central complex (CPU1 cells) that receive input from the azimuth representation of the PB as well as from the CBU are ideally suited to combine information about body orientation with interesting features of the environment and thereby produce signals that may be used to induce motor commands guiding the behavior of the animal

Any discrepancy has to be translated into compensatory movements. If the behavior of the animal involves prolonged straight segments or a central point to which it has to return, having a global frame of reference is of great importance for ensuring accuracy. It is in this context, in which the sun and other celestial features like polarized skylight can provide most valuable orientation cues (Lambert et al. 2011).

Through the described data from desert locusts and monarch butterflies, it became evident that, early in the system, information about the skylight polarization pattern is combined with information obtained from observing the sun itself or the skylight spectral gradient. This way, a more robust signal is produced that reliably encodes head direction even if one of the cues is noisy or missing. This implies, however, that the activity of the involved neurons does not serve the perception of polarized light as such, as action potentials in these cells are generated by all skylight cues and cannot be separated according to which sensory cue caused them. Rather, these cells are suited to encode body orientation with respect to the solar azimuth. Later in the system, this information is used to generate an ordered representation of azimuthal space in the CX, for which polarized skylight is likely only one of many contributing factors (Fig. 4.12). One could speculate that this

azimuth representation provides the frame of reference in which behaviorally relevant features of the environment are associated with directional information. This process of combining a "Where-pathway" (azimuth representation) with a "What-pathway" (behaviorally relevant aspects of the sensory world) could provide the basis for generating motor commands. Promising candidate neurons have been identified that occur in all insects studied and likely receive input from the CBU as well as from the azimuth representation of the PB (CPU1, CPU2 cells; Figs. 4.9b, c and 4.12). As the CBU receives neural connections from many brain areas (Heinze et al. 2013) and has been implicated in memory formation of acutely relevant visual stimuli (Liu et al. 2006), it could indeed be the endpoint of a "What-pathway." Exceptionally rich supply of neuromodulatory substances (Homberg 2002; Nässel and Homberg 2006; Kahsai et al. 2010; Kahsai and Winther 2011) together with the observation of context-dependent switches in sensory responses (conditionally polarization-sensitive cells; Heinze and Homberg 2009) additionally suggest that modulating factors required to direct behavior are also integrated within the CX.

4.11 Conclusions

In summary, despite remaining gaps in understanding, a more and more complete picture of the neural pathways involved in the processing of polarized-light information has emerged recently, especially through work in the desert locust. This extensive neuronal network spans nearly all processing stages from photoreceptors of the retina to neurons in the thorax that are potentially directly involved in controlling steering movements of the animal. The significant challenge that lies ahead is to verify the proposed links between these neural elements to combine them to a comprehensive network that performs the computations needed to explain an animal's behavior in response to polarized-light stimuli.

To extract general computational principles and to find the key shared elements that define the polarization vision network in the insect brain, work is needed in species other than the desert locust and the monarch butterfly. Particularly, species that do not share the migratory behavior of these animals will give important insights into how widely applicable the findings from locusts and monarchs are. The rich behavior described in bees, as well as the already extensive knowledge from crickets, makes these species ideal for expanding electrophysiological studies. Additionally, the powerful genetic methods available in *Drosophila*, combined with the recent description of well-defined behavioral responses to linearly polarized light, open up a new line of research, which will enable us to examine polarization vision on completely new levels.

Importantly, all this will not only be relevant for the understanding of polarized-light orientation of insects, but will shed light on more general principles of how the brain transforms sensory signals into motor commands that guide an animal's behavior.

Acknowledgments I am grateful to Basil el Jundi, Almut Kelber, and Gábor Horváth for valuable comments on earlier drafts of this chapter.

References

Barta A, Horváth G (2004) Why is it advantageous for animals to detect celestial polarization in the ultraviolet? Skylight polarization under clouds and canopies is strongest in the UV. J Theor Biol 226:429–437

Beugnon G, Campan R (1989) Homing in the field cricket, *Gryllus campestris*. J Insect Behav 2: 187–198

Blum M, Labhart T (2000) Photoreceptor visual fields, ommatidial array, and receptor axon projections in the polarization-sensitive dorsal rim area of the cricket compound eye. J Comp Physiol A 186:119–128

Brines ML, Gould JL (1982) Skylight polarization patterns and animal orientation. J Exp Biol 96:69–91

Brunner D, Labhart T (1987) Behavioural evidence for polarization vision in crickets. Physiol Entomol 12:1–10

Coulson KL (1988) Polarization and intensity of light in the atmosphere. A. Deepak Publishing, Hampton, VA, USA

Eggers A, Gewecke M, Wiese K, Popov AV, Renninger G (1993) The dorsal rim area of the compound eye and polarization vision in the desert locust (*Schistocerca gregaria*). In: Wiese K (ed) Sensory systems in arthropods. Birkhäuser, Basel, pp 101–109

el Jundi B, Homberg U (2010) Evidence for the possible existence of a second polarization-vision pathway in the locust brain. J Insect Physiol 56:971–979

el Jundi B, Homberg U (2012) Receptive field properties and intensity-response functions of polarization-sensitive neurons of the optic tubercle in gregarious and solitarious locusts. J Neurophys 108:1695–1710

el Jundi B, Heinze S, Lenschow C, Kurylas AE, Rohlfing T, Homberg U (2010) The locust standard brain: a 3D standard of the central complex as a platform for neural network analysis. Front Syst Neurosci 3:21

el Jundi B, Pfeiffer K, Homberg U (2011) A distinct layer of the medulla integrates sky compass signals in the brain of an insect. PLoS One 6:e27855

Fischbach KF, Dittrich APM (1989) The optic lobe of *Drosophila melanogaster*. I.: a Golgi analysis of wild-type structure. Cell Tissue Res 258:441–475

Froy O, Gotter AL, Casselman AL, Reppert SM (2003) Illuminating the circadian clock in monarch butterfly migration. Science 300:1303–1305

Gál J, Horváth G, Barta A, Wehner R (2001a) Polarization of the moonlit clear night sky measured by full-sky imaging polarimetry at full moon: comparison of the polarization of moonlit and sunlit skies. J Geophys Res D 106:22647–22653

Gál J, Horváth G, Meyer-Rochow VB, Wehner R (2001b) Polarization patterns of the summer sky and its neutral points measured by full-sky imaging polarimetry in Finnish Lapland north of the Arctic Circle. Proc R Soc A 457:1385–1399

Guerra PA, Merlin C, Gegear RJ, Reppert SM (2012) Discordant timing between antennae disrupts sun compass orientation in migratory monarch butterflies. Nat Commun 3, article no 958

Hanesch U, Fischbach KF, Heisenberg M (1989) Neuronal architecture of the central complex in *Drosophila melanogaster*. Cell Tissue Res 257:343–366

Hegedüs R, Horváth G (2004a) How and why are uniformly polarization-sensitive retinae subject to polarization-related artefacts? Correction of some errors in the theory of polarization-induced false colours. J Theor Biol 230:77–87

Hegedüs R, Horváth G (2004b) Polarizational colours could help polarization-dependent colour vision systems to discriminate between shiny and matt surfaces, but cannot unambiguously code surface orientation. Vis Res 44:2337–2348

Hegedüs R, Horváth Á, Horváth G (2006) Why do dusk-active cockchafers detect polarization in the green? The polarization vision in *Melolontha melolontha* is tuned to the high polarized intensity of downwelling light under canopies during sunset. J Theor Biol 238:230–244

Hegedüs R, Åkesson S, Horváth G (2007a) Polarization patterns of thick clouds: overcast skies have distribution of the angle of polarization similar to that of clear skies. J Opt Soc Am A 24: 2347–2356

Hegedüs R, Åkesson S, Horváth G (2007b) Anomalous celestial polarization caused by forest fire smoke: why do some insects become visually disoriented under smoky skies? Appl Opt 46: 2717–2726

Hegedüs R, Åkesson S, Wehner R, Horváth G (2007c) Could Vikings have navigated under foggy and cloudy conditions by skylight polarization? On the atmospheric optical prerequisites of polarimetric Viking navigation under foggy and cloudy skies. Proc R Soc A 463:1081–1095

Hegedüs R, Barta A, Bernáth B, Meyer-Rochow VB, Horváth G (2007d) Imaging polarimetry of forest canopies: how the azimuth direction of the sun, occluded by vegetation, can be assessed from the polarization pattern of the sunlit foliage. Appl Opt 46:6019–6032

Heinze S, Homberg U (2007) Maplike representation of celestial E-vector orientations in the brain of an insect. Science 315:995–997

Heinze S, Homberg U (2008) Neuroarchitecture of the central complex of the desert locust: intrinsic and columnar neurons. J Comp Neurol 511:454–478

Heinze S, Homberg U (2009) Linking the input to the output: new sets of neurons complement the polarization vision network in the locust central complex. J Neurosci 29:4911–4921

Heinze S, Reppert SM (2011) Sun compass integration of skylight cues in migratory monarch butterflies. Neuron 69:345–358

Heinze S, Reppert SM (2012) Anatomical basis of sun compass navigation I: the general layout of the monarch butterfly brain. J Comp Neurol 520:1599–1628

Heinze S, Gotthardt S, Homberg U (2009) Transformation of polarized light information in the central complex of the locust. J Neurosci 29:11783–11793

Heinze S, Florman J, Asokaraj S, el Jundi B, Reppert SM (2013) Anatomical basis of sun compass navigation II: the neuronal composition of the central complex of the monarch butterfly. J Comp Neurol 521:267–298

Helfrich-Forster C, Stengl M, Homberg U (1998) Organization of the circadian system in insects. Chronobiol Int 15:567–594

Henze MJ (2009) Two facets of insect vision: polarization sensitivity and visual pigments. PhD thesis, Universität Zürich, Zürich, Switzerland

Henze MJ, Labhart T (2007) Haze, clouds and limited sky visibility: polarotactic orientation of crickets under difficult stimulus conditions. J Exp Biol 210:3266–3276

Henze MJ, Dannenhauer K, Kohler M, Labhart T, Gesemann M (2012) Opsin evolution and expression in arthropod compound eyes and ocelli: insights from the cricket *Gryllus bimaculatus*. BMC Evol Biol 12:163

Herzmann D, Labhart T (1989) Spectral sensitivity and absolute threshold of polarization vision in crickets: a behavioral study. J Comp Physiol A 165:315–319

Homberg U (1985) Interneurones of the central complex in the bee brain (*Apis mellifera*, L.). J Insect Physiol 31:251–264

Homberg U (2002) Neurotransmitters and neuropeptides in the brain of the locust. Microsc Res Tech 56:189–209

Homberg U, Paech A (2002) Ultrastructure and orientation of ommatidia in the dorsal rim area of the locust compound eye. Arthropod Struct Dev 30:271–280

Homberg U, Würden S (1997) Movement-sensitive, polarization-sensitive, and light-sensitive neurons of the medulla and accessory medulla of the locust, *Schistocerca gregaria*. J Comp Neurol 386:329–346

Homberg U, Würden S, Dircksen H, Rao K (1991) Comparative anatomy of pigment-dispersing hormone-immunoreactive neurons in the brain of orthopteroid insects. Cell Tissue Res 266: 343–357

Homberg U, Hofer S, Pfeiffer K, Gebhardt S (2003) Organization and neural connections of the anterior optic tubercle in the brain of the locust, *Schistocerca gregaria*. J Comp Neurol 462: 415–430

Homberg U, Heinze S, Pfeiffer K, Kinoshita M, el Jundi B (2011) Central neural coding of sky polarization in insects. Philos Trans R Soc Lond B 366:680–687

Horváth G, Varjú D (2004) Polarized light in animal vision—polarization patterns in nature. Springer, Heidelberg

Horváth G, Wehner R (1999) Skylight polarization as perceived by desert ants and measured by video polarimetry. J Comp Physiol A 184:1–7 [Erratum 184: 347-349 (1999)]

Horváth G, Barta A, Gál J, Suhai B, Haiman O (2002a) Ground-based full-sky imaging polarimetry of rapidly changing skies and its use for polarimetric cloud detection. Appl Opt 41: 543–559

Horváth G, Gál J, Labhart T, Wehner R (2002b) Does reflection polarization by plants influence colour perception in insects? Polarimetric measurements applied to a polarization-sensitive model retina of *Papilio* butterflies. J Exp Biol 205:3281–3298

Ito K, Shinomiya K, Ito M, Armstrong JD, Boyan G, Hartenstein V et al (2014) A systematic nomenclature for the insect brain. Neuron 81(4):755–765

Iwano M, Hill ES, Mori A, Mishima T, Mishima T, Kei Ito K, Kanzaki R (2010) Neurons associated with the flip-flop activity in the lateral accessory lobe and ventral protocerebrum of the silkworm moth brain. J Comp Neurol 518:366–388

Kahsai L, Winther AME (2011) Chemical neuroanatomy of the *Drosophila* central complex: distribution of multiple neuropeptides in relation to neurotransmitters. J Comp Neurol 519: 290–315

Kahsai L, Martin J-R, Winther AME (2010) Neuropeptides in the *Drosophila* central complex in modulation of locomotor behavior. J Exp Biol 213:2256–2265

Kelber A (1999) Why "false" colours are seen by butterflies. Nature 402:251

Kelber A, Thunell C, Arikawa K (2001) Polarisation-dependent colour vision in *Papilio* butterflies. J Exp Biol 204:2469–2480

Kinoshita M, Pfeiffer K, Homberg U (2007) Spectral properties of identified polarized-light sensitive interneurons in the brain of the desert locust *Schistocerca gregaria*. J Exp Biol 210:1350–1361

Kinoshita M, Yamazato K, Arikawa K (2011) Polarization-based brightness discrimination in the foraging butterfly, *Papilio xuthus*. Philos Trans R Soc Lond B 366:688–696

Kirschfeld K (1972) The number of receptors necessary for determining the position of the E-vector of linearly polarized light. Z Naturforsch B 27:578–579

Labhart T (1988) Polarization-opponent interneurons in the insect visual system. Nature 331: 435–437

Labhart T (1996) How polarization-sensitive interneurons of crickets perform at low degrees of polarization. J Exp Biol 199:1467–1475

Labhart T, Meyer EP (1999) Detectors for polarized skylight in insects: a survey of ommatidial specializations in the dorsal rim area of the compound eye. Microsc Res Tech 47:368–379

Labhart T, Meyer EP (2002) Neural mechanisms in insect navigation: polarization compass and odometer. Curr Opin Neurobiol 12:707–714

Labhart T, Petzold J (1993) Processing of polarized light information in the visual system of crickets. In: Wiese K (ed) Sensory systems in arthropods. Birkhäuser, Basel, pp 158–169

Labhart T, Hodel B, Valenzuela I (1984) The physiology of the cricket's compound eye with particular reference to the anatomically specialized dorsal rim area. J Comp Physiol A 155: 289–296

Labhart T, Petzold J, Helbling H (2001) Spatial integration in polarization-sensitive interneurones of crickets: a survey of evidence, mechanisms and benefits. J Exp Biol 204:2423–2430
Labhart T, Baumann F, Bernard GD (2009) Specialized ommatidia of the polarization-sensitive dorsal rim area in the eye of monarch butterflies have non-functional reflecting tapeta. Cell Tissue Res 338:391–400
Lambert A, Furgale P, Barfoot TD, Enright J (2011) Visual odometry aided by a sun sensor and inclinometer. In: 2011 I.E. aerospace conference, 5–11 March 2011, Big Sky, MT, pp 1–14
Li W, Pan Y, Wang Z, Gong H, Gong Z, Liu L (2009) Morphological characterization of single fan-shaped body neurons in *Drosophila melanogaster*. Cell Tissue Res 336:509–519
Liu G, Seiler H, Wen A, Zars T, Ito K, Wolf R, Heisenberg M, Liu L (2006) Distinct memory traces for two visual features in the *Drosophila* brain. Nature 439:551–556
Mappes M, Homberg U (2004) Behavioral analysis of polarization vision in tethered flying locusts. J Comp Physiol A 190:61–68
Mappes M, Homberg U (2007) Surgical lesion of the anterior optic tract abolishes polarotaxis in tethered flying locusts, *Schistocerca gregaria*. J Comp Physiol A 193:43–50
Merlin C, Gegear RJ, Reppert SM (2009) Antennal circadian clocks coordinate sun compass orientation in migratory monarch butterflies. Science 325:1700–1704
Merlin C, Heinze S, Reppert SM (2012) Unraveling navigational strategies in migratory insects. Curr Opin Neurobiol 22:353–361
Mouritsen H, Frost BJ (2002) Virtual migration in tethered flying monarch butterflies reveals their orientation mechanisms. Proc Natl Acad Sci USA 99:10162–10166
Müller M, Homberg U, Kühn A (1997) Neuroarchitecture of the lower division of the central body in the brain of the locust (*Schistocerca gregaria*). Cell Tissue Res 288:159–176
Nässel DR (1999) Histamine in the brain of insects: a review. Microsc Res Tech 44:121–136
Nässel DR, Homberg U (2006) Neuropeptides in interneurons of the insect brain. Cell Tissue Res 326:1–24
Pfeiffer K, Homberg U (2007) Coding of azimuthal directions via time-compensated combination of celestial compass cues. Curr Biol 17:960–965
Pfeiffer K, Kinoshita M, Homberg U (2005) Polarization-sensitive and light-sensitive neurons in two parallel pathways passing through the anterior optic tubercle in the locust brain. J Neurophys 94:3903–3915
Pfeiffer K, Negrello M, Homberg U (2011) Conditional perception under stimulus ambiguity: polarization- and azimuth-sensitive neurons in the locust brain are inhibited by low degrees of polarization. J Neurophys 105:28–35
Philipsborn A, Labhart T (1990) A behavioural study of polarization vision in the fly, *Musca domestica*. J Comp Physiol A 167:737–743
Phillips-Portillo J (2012) The central complex of the flesh fly, *Neobellieria bullata*: recordings and morphologies of protocerebral inputs and small-field neurons. J Comp Neurol 520:3088–3104
Pirih P, Arikawa K, Stavenga DG (2010) An expanded set of photoreceptors in the Eastern pale clouded yellow butterfly, *Colias erate*. J Comp Physiol A 196:501–517
Pomozi I, Horváth G, Wehner R (2001) How the clear-sky angle of polarization pattern continues underneath clouds: full-sky measurements and implications for animal orientation. J Exp Biol 204:2933–2942
Reppert SM (2006) A colorful model of the circadian clock. Cell 124:233–236
Reppert SM, Zhu H, White RH (2004) Polarized light helps monarch butterflies navigate. Curr Biol 14:155–158
Reppert SM, Gegear RJ, Merlin C (2010) Navigational mechanisms of migrating monarch butterflies. Trends Neurosci 33:399–406
Rossel S, Wehner R (1986) Polarization vision in bees. Nature 323:128–131
Rossel S, Wehner R (1987) The bee's E-vector compass. In: Menzel R, Mercer A (eds) Neurobiology and behaviour of honeybees. Springer, Heidelberg, pp 76–93
Sakura M, Lambrinos D, Labhart T (2008) Polarized skylight navigation in insects: model and electrophysiology of E-vector coding by neurons in the central complex. J Neurophys 99: 667–682

Santschi F (1923) L'orientation siderale des fourmis, et quelques consideration sur leurs differentes possibilites d'orientation. Mem Soc Vaudoise Sci Nat 4:137–175
Sauman I, Briscoe AD, Zhu H, Shi D, Froy O, Stalleicken J, Yuan Q, Casselman A, Reppert SM (2005) Connecting the navigational clock to sun compass input in monarch butterfly brain. Neuron 46:457–467
Schwind R (1983) Zonation of the optical environment and zonation in the rhabdom structure within the eye of the backswimmer, *Notonecta glauca*. Cell Tissue Res 232:53–63
Schwind R (1985) Sehen unter und über Wasser, Sehen von Wasser. Naturwissenschaften 72:343–352
Schwind R, Horváth G (1993) Reflection-polarization pattern at water surfaces and correction of a common representation of the polarization pattern of the sky. Naturwissenschaften 80:82–83
Shashar N, Sabbah S, Aharoni N (2005) Migrating locusts can detect polarized reflections to avoid flying over the sea. Biol Lett 1:472–475
Siegl T, Schachtner J, Holstein GR, Homberg U (2009) NO/cGMP signalling: L-citrulline and cGMP immunostaining in the central complex of the desert locust *Schistocerca gregaria*. Cell Tissue Res 337:327–340
Stalleicken J, Mukhida M, Labhart T, Wehner R, Frost B, Mouritsen H (2005) Do monarch butterflies use polarized skylight for migratory orientation? J Exp Biol 208:2399–2408
Stalleicken J, Labhart T, Mouritsen H (2006) Physiological characterization of the compound eye in monarch butterflies with focus on the dorsal rim area. J Comp Physiol A 192:321–331
Suhai B, Horváth G (2004) How well does the Rayleigh model describe the E-vector distribution of skylight in clear and cloudy conditions? A full-sky polarimetric study. J Opt Soc Am A 21: 1669–1676
Träger U, Homberg U (2011) Polarization-sensitive descending neurons in the locust: connecting the brain to thoracic ganglia. J Neurosci 31:2238–2247
Träger U, Wagner R, Bausenwein B, Homberg U (2008) A novel type of microglomerular synaptic complex in the polarization vision pathway of the locust brain. J Comp Neurol 506:288–300
Vitzthum H, Müller M, Homberg U (2002) Neurons of the central complex of the locust *Schistocerca gregaria* are sensitive to polarized light. J Neurosci 22:1114–1125
von Frisch K (1949) Die Polarisation des Himmelslichtes als orientierender Faktor bei den Tänzen der Bienen. Experientia 5:142–148
Wehner R (1997) The ant's celestial compass system: spectral and polarization channels. In: Lehrer M (ed) Orientation and communication in arthropods. Birkhäuser, Basel, pp 145–186
Wehner R, Bernard GD (1993) Photoreceptor twist: a solution to the false-color problem. Proc Natl Acad Sci USA 90:4132–4135
Wehner R, Labhart T (2006) Polarization vision. In: Warrant E, Nilsson DE (eds) Invertebrate vision. Cambridge University Press, Cambridge, UK, pp 291–348
Weir PT, Dickinson MH (2012) Flying *Drosophila* orient to sky polarization. Curr Biol 22:21–27
Wernet MF, Desplan C (2004) Building a retinal mosaic: cell-fate decision in the fly eye. Trends Cell Biol 14:576–584
Wernet MF, Velez MM, Clark DA, Baumann-Klausener F, Brown JR, Klovstad M, Labhart T, Clandinin TR (2011) Genetic dissection reveals two separate retinal substrates for polarization vision in *Drosophila*. Curr Biol 21:1–9
Williams JLD (1975) Anatomical studies of the insect central nervous system: a ground-plan of the midbrain and an introduction to the central complex in the locust, *Schistocerca gregaria* (Orthoptera). J Zool 176:67–86
Wolf R, Gebhardt B, Gademann R, Heisenberg M (1980) Polarization sensitivity of course control in *Drosophila melanogaster*. J Comp Physiol A 139:177–191
Young JM, Armstrong J (2010) Structure of the adult central complex in *Drosophila*: organization of distinct neuronal subsets. J Comp Neurol 518:1500–1524
Zhu H, Sauman I, Yuan Q, Casselman A, Emery-Le M, Emery P, Reppert SM (2008) Cryptochromes define a novel circadian clock mechanism in monarch butterflies that may underlie sun compass navigation. PLoS Biol 6:e4

Chapter 5
Polarization Vision of Aquatic Insects

Gábor Horváth and Zoltán Csabai

Abstract In this chapter we show that primary aquatic insects fly predominantly in mid-morning, and/or around noon and/or at nightfall. We describe the different types of their diurnal flight activity rhythm characterised by peaks at low and/or high solar elevations. We present here experimental evidence that the polarization visibility $Q(\theta)$ of water surfaces is always maximal at the lowest (dawn and dusk) and highest (noon) angles of solar elevation θ for dark waters, while $Q(\theta)$ is maximal at dawn and dusk (low solar elevations) for bright waters both under clear and partly cloudy skies. The θ-dependent reflection-polarization patterns, combined with an appropriate air temperature, clearly explain why polarotactic aquatic insects disperse to new habitats in mid-morning, and/or around noon and/or at dusk. This phenomenon is called the "polarization sundial" of dispersing aquatic insects. We also show that non-biting midges (Chironomidae, Diptera) are positively polarotactic and like many other aquatic insects, their females are attracted to horizontally polarized light. We present here measured thresholds (i.e., the minimum degrees of linear polarization of reflected light that can elicit positive polarotaxis) of the ventral polarization sensitivity in mayflies, dragonflies and tabanid flies. The mayflies *Palingenia longicauda* swarm exclusively over the river surface; thus, they need not search for water. It could be assumed that this species is not polarotactic. We show here that also *P. longicauda* has positive

Electronic supplementary material is available in the online version of this chapter at 10.1007/978-3-642-54718-8_5. Colour versions of the black and white figures can also be found under http://extras.springer.com.

G. Horváth (✉)
Environmental Optics Laboratory, Department of Biological Physics, Physical Institute, Eötvös University, Pázmány sétány 1, 1117 Budapest, Hungary
e-mail: gh@arago.elte.hu

Z. Csabai
Department of Hydrobiology, University of Pécs, Ifjúság útja 6, 7624 Pécs, Hungary
e-mail: csabai@gamma.ttk.pte.hu

G. Horváth (ed.), *Polarized Light and Polarization Vision in Animal Sciences*, Springer Series in Vision Research 2, DOI 10.1007/978-3-642-54718-8_5,

polarotaxis, which, however, can be observed only when the animals are displaced from the water and then released above artificial test surfaces. *P. longicauda* is the first species in which polarotactic water detection was demonstrated albeit it never leaves the water surface, and thus, a polarotactic water detection seems unnecessary for it. The yellow fever mosquito, *Aedes aegypti*, has been thought to locate its breeding habitats exclusively by chemical cues. We demonstrate here that horizontally polarized light can also attract ovipositing *Ae. aegypti* females when they are deprived of chemical cues. *Aedes aegypti* is the first known water-associated species in which polarotaxis exists, but does not play a dominant role in locating water bodies and can be constrained in the presence of chemical cues. Finally, we deal with the negative polarotaxis in the desert locust, *Schistocerca gregaria*, the ventral eye region of which detects the horizontally polarized water-reflected light, and thus can navigate towards or away from large water surfaces.

5.1 The Polarization Sundial of Aquatic Insects: Why Do Water Insects Fly at Low and/or High Sun Elevations?

The seasonal and diel flight activity of aquatic insects (Fernando 1958; Popham 1964; Zalom et al. 1990; Behr 1993) and the influence of environmental variables on their dispersal flight (Landin 1968; Nilsson and Svensson 1992; Weigelhofer et al. 1992) have been studied by light trapping at night, when insect phototaxis dominates (Nowinszky 2003). However, daily changes in the flight activity of aquatic insects cannot be assessed by 24-h light trapping, because the attraction of light traps to insects is considerably reduced by day due to the higher ambient light intensity. While suction traps may be of use for monitoring small, weakly flying insects, assessment of the diel pattern of a wide range of aquatic insects needs a method that is similarly efficient by day and night.

Both primary (where both adults and larvae are aquatic) and secondary (where only the larvae live in water) aquatic insects recognise their habitat by means of the horizontal polarization of light reflected from the water surface (Schwind 1991, 1995; Horváth and Varjú 2004). The higher the degree of linear polarization of reflected light, the more attractive is a reflecting surface to aquatic insects. Thus, a horizontal shiny black plastic sheet is an ideal trap for aquatic insects, because it always polarizes the reflected light strongly and horizontally (Horváth and Varjú 2004). Csabai et al. (2006) observed in the field that in mid-morning, near noon and at dusk the rattling noise caused by thousands of primary aquatic insects crashing into such shiny black plastic sheets created the impression of an intense “rain” of aquatic insects.

Csabai et al. (2006) explored the diel flight activity patterns of primary aquatic insects and assessed the most important factors governing their daily activity rhythm. Using aspirators and nets, they captured aquatic insects landing on shiny black plastic sheets (9 m × 3 m) laid on the ground in a Hungarian wetland from

March to July, when hourly insect samplings happened continuously for 24 h once every week. A strongly and horizontally polarizing plastic sheet is as attractive to polarotactic aquatic insects as is a natural dark water surface. Thus, such an insect trap is similarly efficient both by day and night.

Using 180° field-of-view imaging polarimetry, Bernáth et al. (2004) measured the reflection-polarization patterns of a black and a grey horizontal reflector (imitating a dark and a bright water body) as a function of the solar elevation angle θ from sunrise to sunset under clear and partly cloudy skies (see Sect. 16.2). Dark waters reflect a small amount of light, because they are deep, and/or their water contains dark suspended particles, and/or their bed is dark, while bright waters reflect a large amount of light, because their water contains bright suspended particles, and/or their water is clear and shallow and the bed is bright (Bernáth et al. 2002).

Polarotactic aquatic insects trying to find water are attracted to any surface, if the degree of linear polarization d of reflected light is higher than the threshold d^* of polarization sensitivity, and if the deviation $\Delta\alpha$ of the angle of polarization α (measured clockwise from the vertical) of reflected light from the horizontal is smaller than a threshold $\Delta\alpha^*$ in that part of the spectrum in which the polarization of reflected light is perceived (Horváth and Varjú 2004). Thus, a polarotactic insect in flight senses as water those areas of the ground from which light is reflected with the following two criteria: (1) $d > d^*$ and (2) $|\alpha - 90°| < \Delta\alpha^*$. The polarization visibility Q of waters is the angular proportion of all viewing directions (relative to the angular extension of 2π steradians of the whole lower hemisphere of the field of view of the insect) for which both criteria are satisfied. Q gives the relative proportion of the entire ventral field of view in which reflecting surfaces are sensed/detected polarotactically as water. The higher the Q-value for a water surface in a given visual environment, the larger its polarization visibility, that is, the higher the probability that insects seeking water can find it by polarotaxis.

Csabai et al. (2006) found that primary aquatic insects belonging to 99 taxa (78 Coleoptera, 21 Heteroptera) fly predominantly in mid-morning, and/or around noon and/or at nightfall, and there are at least four different types of diurnal flight activity rhythm in aquatic insects, characterised by peak(s) (1) in mid-morning, (2) in the evening, (3) both in mid-morning and the evening, and (4) around noon and in the evening (Figs. 5.1, 5.2 and 5.3). These activity maxima are quite general and cannot be explained exclusively by daily fluctuations of air temperature, air humidity, wind speed and risk of predation.

Figure 5.4 shows the polarization visibility $Q(\theta)$ of dark and bright waters by aquatic insects as a function of the solar elevation angle θ measured in the blue, green and red parts of the spectrum, under clear and partly cloudy skies (see Sect. 16.2). The shorter the wavelength λ, the higher the $Q(\theta)$. Independently of λ and the weather conditions (clear or partly cloudy), $Q(\theta)$ is maximal at the lowest θ (sunrise and sunset) as well as at the highest θ (noon) for dark waters, while $Q(\theta)$ is maximal at the lowest θ (sunrise and sunset) for bright waters.

From the temporal coincidence between peaks in the diel flight activity of primary aquatic insects (Figs. 5.1, 5.2 and 5.3) and the polarization visibility

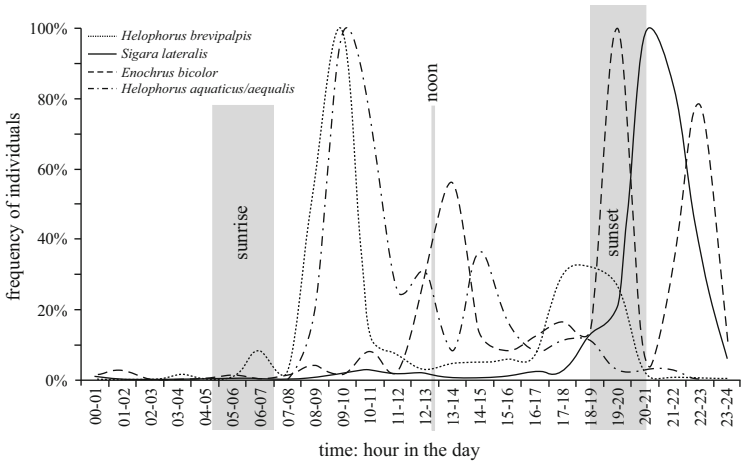

Fig. 5.1 Four different typical daily rhythms of dispersal by aquatic insects. Frequency of *Helophorus brevipalpis*, *Sigara lateralis*, *Enochrus bicolor* and *Helophorus aquaticus/aequalis* landed *en masse* on a horizontal shiny black plastic sheet as a function of the hour in the day (local summer time = UTC + 2 h). Frequency is calculated as the total number N of insects captured in any 1 h, summed over the 18 sampling days, divided by the maximum N_{max}. The temporal shifts of sunrise (from 04:50 to 07:01), noon (from 12:47 to 12:41) and sunset (from 18:33 to 20:33) from the beginning to the end of the 4-month monitoring of aquatic insects are marked by *vertical grey bands* [after Fig. 1 on page 1343 of (Csabai et al. 2006)]

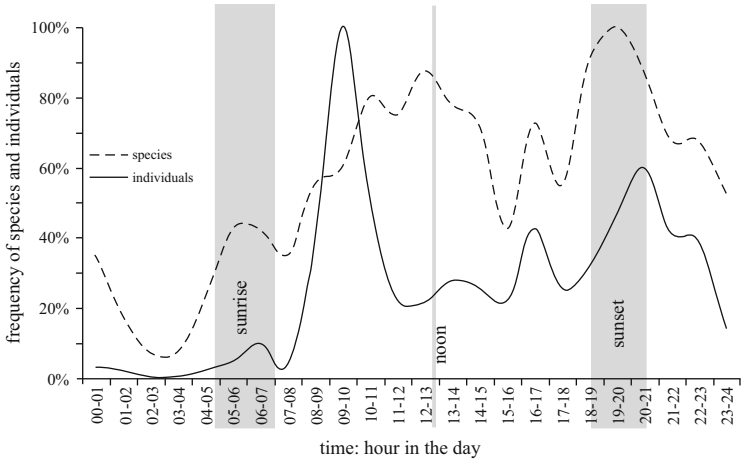

Fig. 5.2 Frequency of species (*dashed*) and individuals (*continuous*) of dispersing aquatic insects landed *en masse* on a horizontal shiny black plastic sheet as a function of the hour in the day. Other conventions as in Fig. 5.1 [after Fig. 2 on page 1343 of (Csabai et al. 2006)]

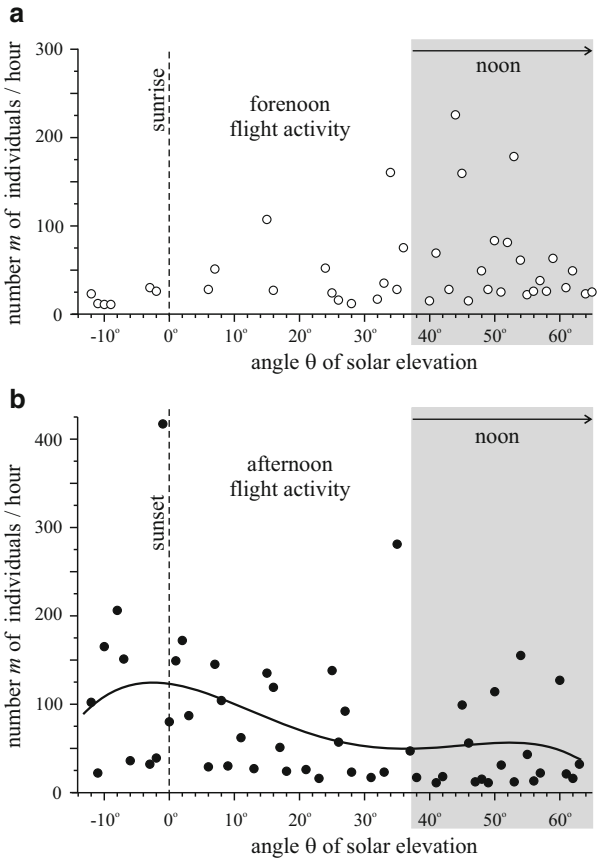

Fig. 5.3 Number m of aquatic insects per hour landing on a shiny black plastic sheet in the forenoon (**a**) and afternoon (**b**) as a function of the angle θ of solar elevation. $m = N/t$, where N is the total number of individuals caught during the total sampling time t (measured in hour) when the solar elevation was between θ and $\theta + \Delta\theta$ ($\Delta\theta = 1°$) in the whole sampling period (18 days). The angular shift of solar culmination (noon) from the beginning to the end of the 4-month monitoring of aquatic insects is marked by *vertical grey bands*, where *horizontal arrows* show the shift direction. The polynomial in (**b**) was fitted to the data points for the afternoon ($r^2 = 0.169$; SD = 68.329; $n = 74$; $p = 0.012$) period by means of the method of least squares [after Fig. 3 on page 1344 of (Csabai et al. 2006)]

$Q(\theta)$ of water surfaces (Fig. 5.4) it was concluded that the optimal times of day for aquatic insects to disperse by flight are the periods of low and high solar elevations θ. The θ-dependent reflection-polarization patterns, combined with an appropriate air temperature, clearly explain why polarotactic aquatic insects disperse to new habitats in mid-morning, and/or around noon and/or at dusk. This phenomenon is called the polarization sundial of dispersing aquatic insects (Csabai et al. 2006).

The pattern of the daily flight activity of aquatic insects depends on species (Fig. 5.1) and is surely governed partly by air temperature, relative air humidity and

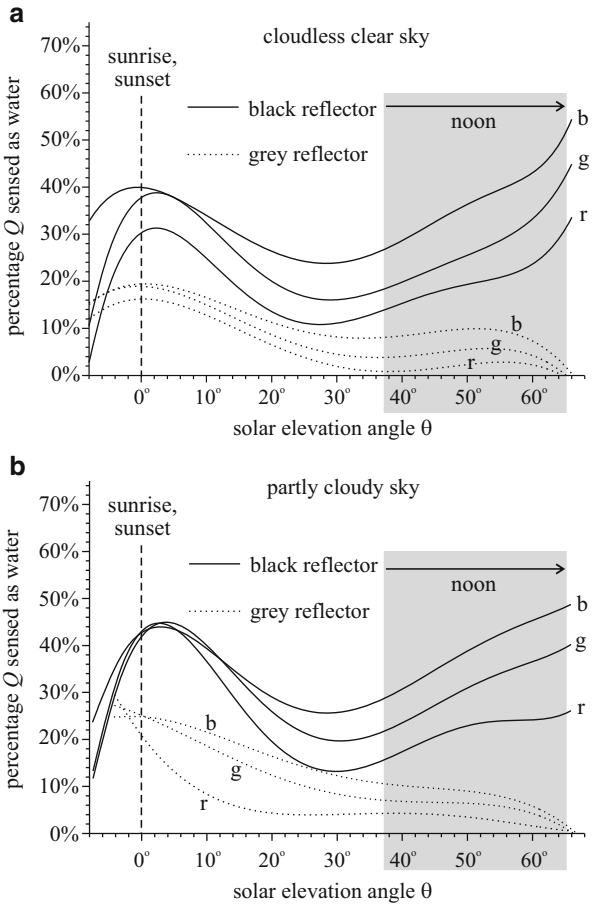

Fig. 5.4 Polarization visibility Q, that is, the percentage (%) of *black (continuous)* and *grey (dashed)* horizontal reflectors that would be sensed as water by water-seeking polarotactic aquatic insects as a function of the solar elevation angle θ in the blue (b, 450 nm), green (g, 550 nm) and red (r, 650 nm) parts of the spectrum under clear (**a**) and partly cloudy (**b**) sky. The angular shift of solar culmination (noon) from the beginning to the end of the 4-month monitoring of aquatic insects is marked by *vertical grey bands*, where *horizontal arrows* show the shift direction [after Fig. 4 on page 1344 of (Csabai et al. 2006)]

wind velocity. These environmental factors, however, strongly vary with the weather: generally, the higher the air temperature, the lower the air humidity. Thus, humidity is usually low at noon and in the early afternoon, when air temperature is generally maximal, while humidity is generally high in the morning and at nightfall, when air temperature is usually low. Since higher humidity is advantageous for flying aquatic insects, due to the reduced risk of dehydration, dawn and dusk are optimal for flight. However, peak flight activity was observed around noon and in the afternoon (Figs. 5.1 and 5.2) when low humidity is very disadvantageous, as is the high risk of visual predation (e.g. by birds and dragonflies). Dawn and dusk offer a lower risk of visual predation, although the risk of predation from echolocating bats is usually high. High wind speeds reduce the flight activity of aquatic insects (Csabai and Boda 2005). Around noon the wind speed is usually much greater than that after dusk and before dawn due to intense thermal convection currents in the air near noon (Landin and Stark 1973). Therefore, flying at noon and in the afternoon in wind is more disadvantageous to

aquatic insects than flying at dawn and dusk in still air. However, since a high enough air temperature is necessary for the efficient functioning of insect flight muscles, flying near dawn is disadvantageous due to the usually lowest air temperature.

From the above it is clear that the three daily maxima in the flight activity of aquatic insects observed in mid-morning, around noon and around nightfall (Figs. 5.1, 5.2 and 5.3) cannot be explained solely on the basis of daily variations in air temperature, air humidity, wind speed and/or risk of predation. Daily changes in these environmental factors are rather stochastic, due to the chaotic weather fluctuations. Csabai et al. (2006) suggested that the most important factor for the flight of aquatic insects is the polarization visibility $Q(\theta)$ of water bodies, while air temperature, air humidity, wind and predation risks are secondary. Sufficiently, high $Q(\theta)$-values are a prerequisite for the polarotactic detection of water by dispersing aquatic insects: if $Q(\theta)$ is too low, it is not worth flying, because the surface of water bodies cannot be polarotactically detected, despite other secondary advantages (such as low wind velocity, for example). The first temporal peak in dispersal is in mid-morning rather than at sunrise, when the solar elevation θ is minimal (zero) and the polarization visibility $Q(\theta)$ of waters is maximal. The reason for this is that the air temperature must increase from its minimum at dawn so that the insects can fly. Thus, the flight maximum in mid-morning (09:00–10:00 h, Figs. 5.1 and 5.2) is a compromise between polarization visibility and air temperature.

Hence, mid-morning and nightfall are two optimal periods of the day for aquatic insects to disperse, due to the high (morning) or maximum (nightfall) polarization visibility $Q(\theta)$ of dark and bright waters (Fig. 5.4), and because air temperature is usually sufficient. Around noon/early afternoon is a further optimal period for dispersal by insects that are looking for dark waters, because then the polarization visibility $Q(\theta)$ of dark waters is always maximal (Fig. 5.4). This explains the third flight activity maximum of certain aquatic insects around noon.

These three optimal periods for dispersal by polarotactic aquatic insects, governed by the reflection-polarization pattern of the water surface, can be easily and reliably identified on the basis of the solar elevation θ (polarization sundial for dispersing aquatic insects), even under the water where neither air temperature and humidity, nor wind velocity can be perceived.

Since the polarization sundial theory (Csabai et al. 2006) was based on a 4-month study (from the beginning of March to the beginning of July), Csabai et al. (2012) and Boda and Csabai (2013) repeated these field investigations spanning the whole period that is appropriate for dispersal flight during a year. Using the same method and the same study site as Csabai et al. (2006), they performed weekly samplings during a 7-month period (from the beginning of April to the end of October). On the basis of 2,000 samples, 720 h of field work and flight data of more than 45,000 individuals of primary aquatic insects belonging to 92 taxa, Csabai et al. (2012) found that generally there is no particular time of the day which would be totally inappropriate for water insects to rise into the air, but

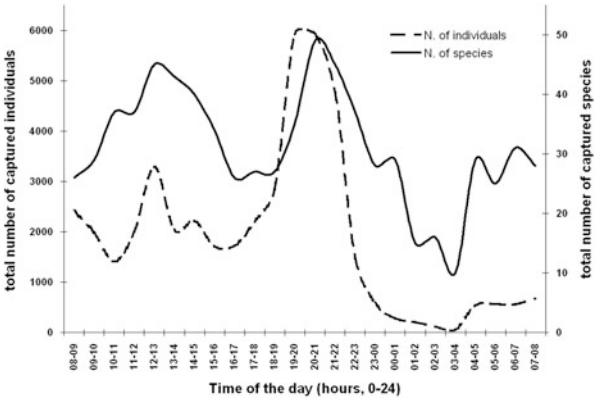

Fig. 5.5 Variations in the total numbers of captured individuals (*dashed line*) and species (*solid line*) based on pooled dataset of the 7-month sampling period of Csabai et al. (2012). Changes of the numbers of individuals and species clearly follow the three optimal periods for flying determined by polarization visibility of water surfaces: highest numbers can be seen at morning, noon and evening hours [after Fig. 1 on page 756 of (Csabai et al. 2012)]

the law of the three optimal period of the day (discovered by Csabai et al. 2006) for flying and seeking new water habitats remained valid. The peaks of the hourly captured total numbers of individuals and species clearly follow the three optimal periods for flying determined by the polarization visibility of water surfaces: highest numbers occur in the morning, noon and evening hours (Fig. 5.5).

According to Boda and Csabai (2013), a given group of aquatic insect species can be characterised by different yearly rhythms of dispersal flight due to the different reproductive cycle, phenology or any external pressure: Nine different and clearly separable annual strategies were detected including some exclusively spring, summer or autumn flyers and flyers utilising various combinations of seasons (Fig. 5.6). The meteorological and other environmental circumstances are highly different among the seasons. Thus, it would not be practical to follow the same diurnal flight pattern for a species that is active all year round or at least in two seasons. Indeed, Csabai et al. (2012) found that most of the studied water insect species flew at different hours of the day in different seasons; the daily dispersal activity changed remarkably in the second half of the year (Fig. 5.7). This phenomenon occurred also on the assemblage level: the hourly composition of the flying insect assemblages was significantly different among the seasons (Fig. 5.8). Csabai et al. (2012) registered 12 frequent species that flew in more than one season, but only one species which followed the same diurnal dispersal pattern during its entire flying period. Consequently, seasonally separated analyses of the diurnal dispersal pattern are needed.

Based on the results of a three-season weekly monitoring separated by species and seasons, Csabai et al. (2012) confirmed and completed the formerly published information about the diurnal flight dispersal activity of primary aquatic insects. They observed again the four formerly known patterns described by Csabai

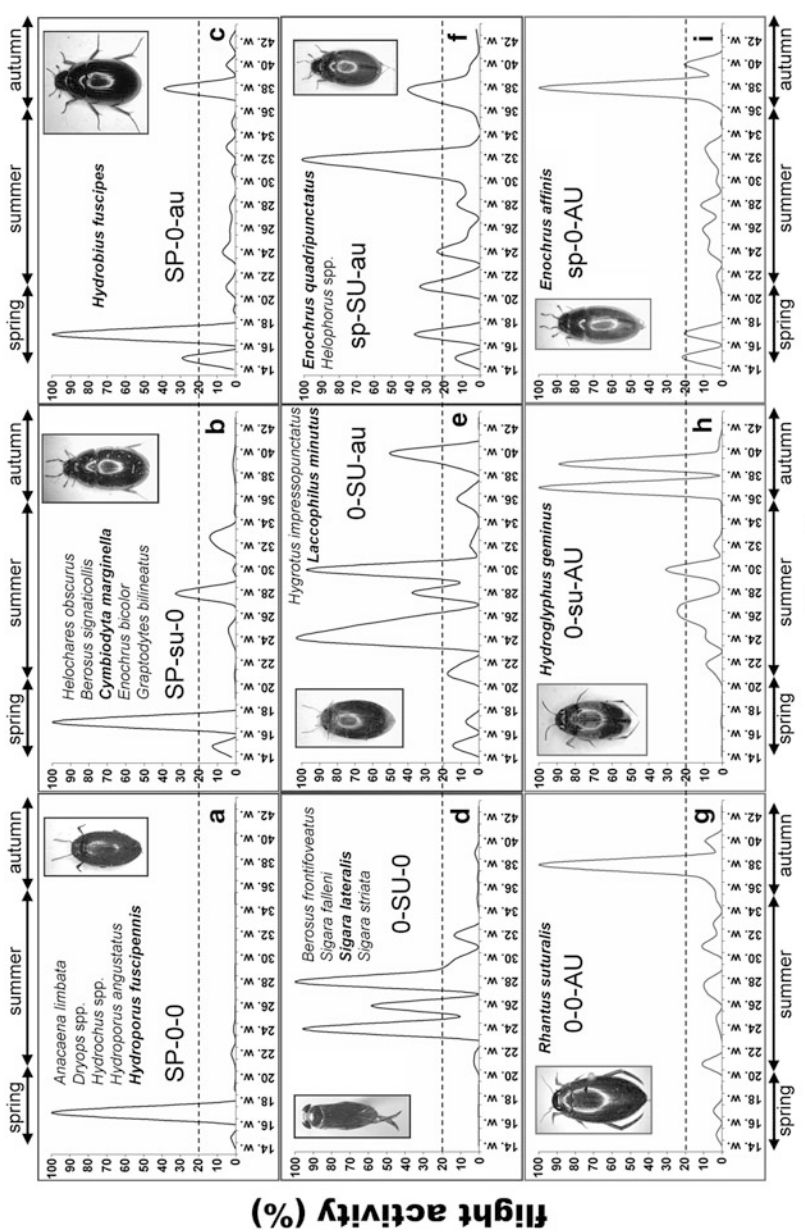

Fig. 5.6 Seasonal dispersal patterns and sub-patterns of typical species highlighted in *bold* and shown in the *inset pictures*. (**a**–**c**) Spring main pattern (SP). (**a**) Spring sub-pattern (SP-0-0). (**b**) Spring–summer sub-pattern (SP-su-0). (**c**) Spring–autumn sub-pattern (SP-0-au). (**d**–**f**) Summer main pattern (SU). (**d**): Summer sub-pattern (0-SU-0). (**e**) Summer–autumn sub-pattern (0-SU-au). (**f**) Summer–spring–autumn sub-pattern (sp-SU-au). (**g**–**i**) Autumn main pattern (AU). (**g**) Autumn sub-pattern (0-0-AU). (**h**) Autumn–summer sub-pattern (0-su-AU). (**i**) Autumn–spring sub-pattern (sp-0-AU). 20 % of the maximal flight activity is shown by the *horizontal broken lines* as the boundary of the sub-pattern level [after Fig. 2 on page 140 of (Boda and Csabai 2013)]

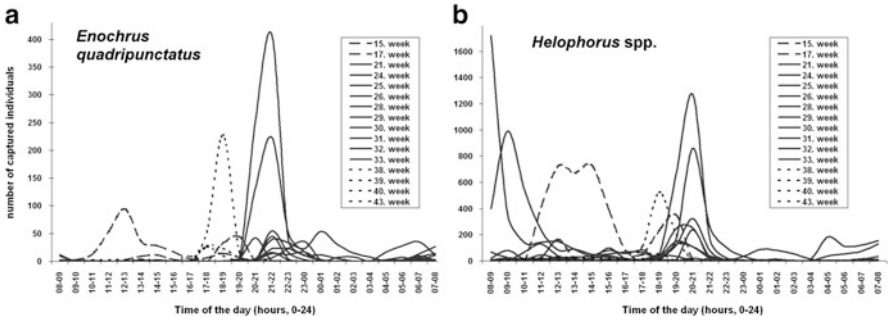

Fig. 5.7 The timing of the mass dispersal activity of *Enochrus quadripunctatus* (**a**) and *Helophorus* spp. (**b**) on certain sampling days shows high differences among seasons: timing in spring totally differs from that in other seasons, while between summer and autumn a forward shift in time can be seen for the evening dispersal peak [after Fig. 2 on page 757 of (Csabai et al. 2012)]

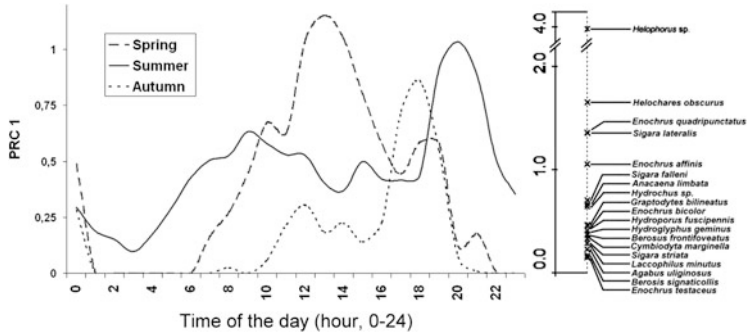

Fig. 5.8 Results of a principal response curve (PRC) analysis: the differences between the averaged response curves for the days of the seasons prove the differences among seasons on assemblage level, too. The contributions of species to the curves figured out by the eigenvalues on the right diagram show that the most frequent taxa have the main role in forming differences on assemblage level. All species characterised with measurable contribution were captured in at least 60 individuals during the whole sampling period [after Fig. 3 on page 757 of (Csabai et al. 2012)]

et al. (2006) (Fig. 5.1) and added four new ones. Seven of the eight recognised dispersal patterns followed the general rule, that is peaks at morning, and/or noon and/or evening: higher or lower but distinct dispersal peaks can be seen (1) exclusively in the morning, (2) morning and noon, (3) morning and noon and evening, (4) morning and evening, (5) exclusively around noon, (6) noon and evening, and (7) exclusively in the evening hours.

Theoretically, species could follow all the possible patterns in every season. However, in reality, not all of them are utilised by species in each season. In summer six patterns were used by aquatic insects, but in spring and autumn they displayed neither of the four "morning patterns" (Fig. 5.9). Changes in the environmental conditions may considerably affect the flight, and thus induce the change of the diel dispersal pattern among seasons (Fig. 5.10).

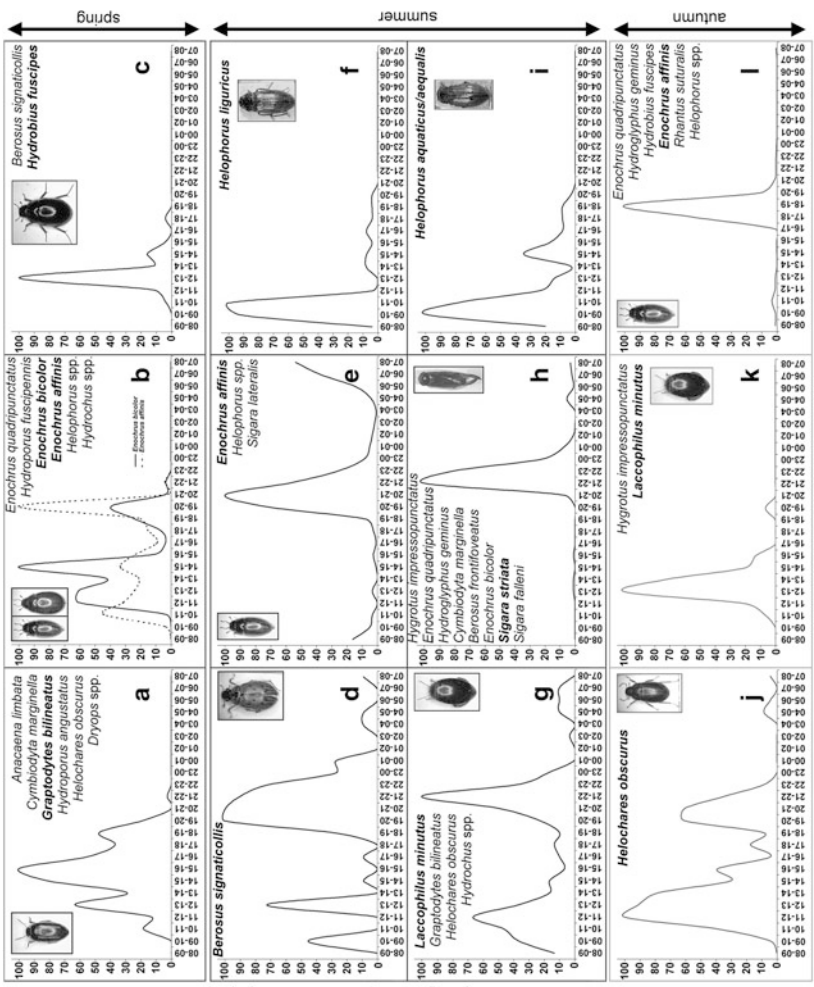

Fig. 5.9 Diel dispersal flight activity patterns of typical species highlighted in **bold** and shown in the *inset pictures*. (**a**–**c**) Diel patterns for spring. (**a**) Daytime (DT). (**b**) Noon-Evening (NE). (**c**) Noon (N). (**d**–**i**) Diel patterns for summer. (**d**) Morning-Noon-Evening (MNE). (**e**) Morning-Evening (ME). (**f**) Morning (M). (**g**) Noon-Evening (NE). (**h**) Evening (E). (**i**) Morning-Noon (MN). (**j**–**l**) Diel patterns for autumn. (**j**) Noon-Evening (NE). (**k**) Noon (N). (**l**) Evening (E) [after Fig. 4 on page 758 of (Csabai et al. 2012)]

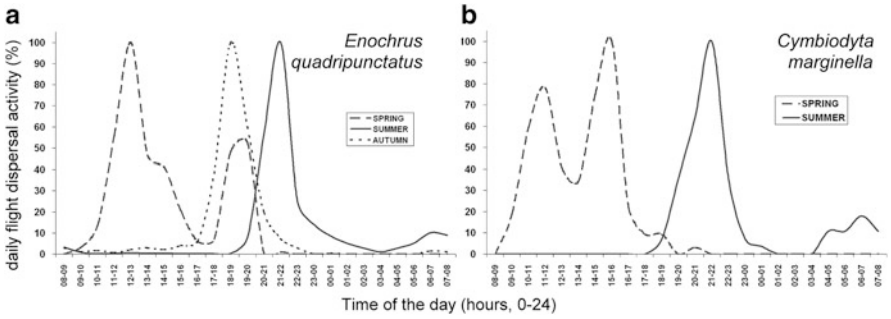

Fig. 5.10 Typical changes in the diel flight dispersal activity patterns among the seasons in the case of a three- (**a**) and a two-season (**b**) species based on seasonally pooled data [after Fig. 6 on page 760 of (Csabai et al. 2012)]

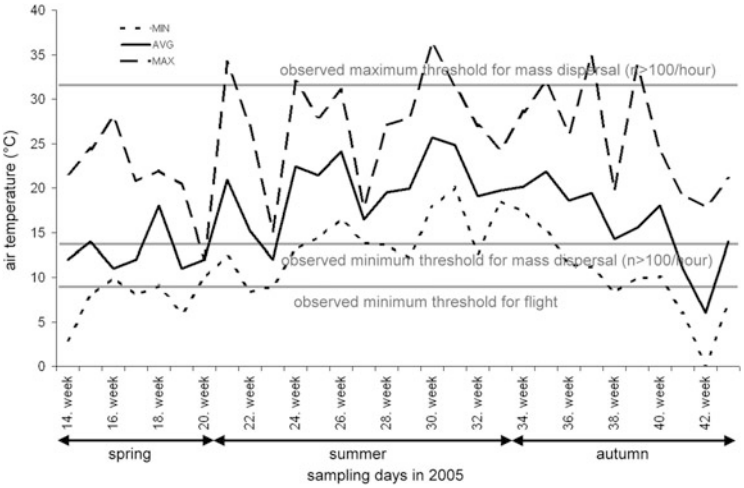

Fig. 5.11 Change of maximum, minimum and average air temperature during the whole sampling period of Csabai et al. (2012) in 2005 with the thresholds for flight and mass dispersal. It is clearly visible that in spring and autumn, the minimum daily air temperature (occurring in the morning hours) did not exceed the observed lower threshold of mass dispersal (sometimes not even the minimum threshold for flight), which caused that the morning patterns were absent in these seasons. MIN: minimum air temperature. AVG: average air temperature. MAX: maximum air temperature [after Fig. 7 on page 762 of (Csabai et al. 2012)]

As emphasised above, the air temperature has a global effect on the diurnal dispersal flight pattern and partly governs the flight activity during the entire year. According to Csabai et al. (2012), the air temperature is a minimum–maximum factor for the dispersal flight. Temperature thresholds for flying were detected: No insects flew below 9 °C and none probably over 35 °C, but mass dispersals occurred between 14 and 31 °C (Fig. 5.11). In spring and autumn the minimum (manifesting in the early morning) and average air temperature did not exceed the threshold of

mass dispersal (Fig. 5.11). In the morning, beetles and bugs have no chance to fly due to coolness, so the morning dispersal patterns were absent. Moreover, the evening peaks during summer time manifested between 19 and 23 h (Fig. 5.9d, e, g, h), but in the two other seasons they occurred earlier, between 18 and 20 h in spring and between 18 and 21 h in autumn (Fig. 5.9b, j, l). The starting hours of the evening dispersal wave shifted earlier, because the earlier nightfall in autumn and spring caused higher polarization visibility of water surfaces at early evening (Bernáth et al. 2004). On the other hand, the earlier ceasing of the dispersal flight was most likely caused by the lower late evening air temperature in these seasons (Fig. 5.11). In the morning hours, the later sunrise might have caused an opposite shift, but also due to the low air temperature in these morning hours this was not visible (the morning patterns were absent in spring and autumn). Furthermore, aquatic insects tended not to follow the pattern with exclusively noon peak in summer, whereas this pattern was used by insects in other seasons. Csabai et al. (2012) found water insects in the air at noon, but without exceptions these species showed a higher peak at morning and/or evening. In summer, at noon and early afternoon, the air temperature can be extremely high; thus, it is not beneficial to fly only during this period because of the high risk of dehydration.

There is a pattern being an exception to the general rule, in which case remarkable dispersal activity was found through a longer period in daytime, from 10 to 19 h with variously manifested peaks. The highest peak occurred usually around noon, but high peaks were present, for example, at 10 or 16 h, too. This pattern was exclusively bounded to spring flyers and could not be observed in other seasons. The reason for this pattern with extended flying to the less optimal periods was also the lower air temperature. In spring, due to the shorter warm period these species may have to take a risk of lower polarization visibility of waters. Then the air temperature exceeds the threshold for mass dispersal for a short period per day or just remains below this value (Fig. 5.11).

According to Csabai and Boda (2005), high wind speeds block the dispersal flight with a threshold of about 12 km/h. There is a strong negative correlation between wind speed and number of flying individuals for speeds between 6 and 12 km/h, but no remarkable influence of wind speed on flight was observed between 0 and 6 km/h. High- or low-intensity rainfalls also fully hinder the dispersal flight of aquatic insects (Csabai et al. 2012).

5.2 Polarotaxis in Non-biting Midges: Female Chironomids Are Attracted to Horizontally Polarized Light

The family Chironomidae (Diptera) is the most widely distributed, most diverse and often the most abundant of all aquatic insect families (Cranston 1995). The short-living chironomid species (non-biting midges) swarm in large numbers above water surfaces, and are sometimes considered as nuisance pests. Swarming non-biting

midges may also play a role as vector species transferring bacteria (e.g. *Vibrio cholerae*, Halpern et al. 2006) from infected water bodies to clear ones. On the other hand, non-biting midges have a key role in freshwater benthic ecosystems (Cranston 1995). Huge masses of their aquatic larvae serve as a basis of benthic food webs. Emerging adults remove significant amounts of biomass from natural water bodies, which facilitates the natural cleaning of waters by reducing their total carbon amount and phosphorus content. Moreover, their carcasses transfer surplus organics present in water to nearby areas, increasing also the fertility of arable land.

Optical cues including reflection polarization were found to be important in three Mediterranean freshwater chironomid species (Lerner et al. 2008, 2011; Meltser et al. 2008; see Chap. 21), and polarized light was regarded as one of the possible factors in breeding habitat selection by the females of these chironomids. The role of positive polarotaxis in finding places for oviposition by chironomids could be modified by habitat availability and density of specimens, for example (Lerner et al. 2011).

Information on the generality of attraction to horizontally polarized light (positive polarotaxis) in chironomids is important to assess the applicability of polarized-light traps or the measures affecting the reflection-polarization characteristics of water surfaces. In their multiple-choice field experiments studying chironomid polarotaxis, Horváth et al. (2011) used four test surfaces: weakly horizontally polarizing matte black cloth, unpolarizing matte white cloth, strongly horizontally polarizing black oil-filled tray (at the Brewster angle $\theta_{\text{Brewster}} = 33.7^\circ$ from the horizontal for salad oil with an index of refraction $n = 1.5$), and weakly vertically polarizing white oil-filled tray. These test surfaces were put on a weakly and horizontally polarizing dry asphalt road, or on a strongly and horizontally polarizing car roof (150 cm from the ground), because in a pilot experiment it was observed that numerous chironomid species were attracted to the roof, where they performed sexual behaviour (nuptial dance, surface touching and copulation) being typical in chironomids only above water surfaces. From the numbers of chironomids trapped by the oil traps or the touchdowns of chironomids on the dry cloths, the attractiveness of the test surfaces was deduced.

Horváth et al. (2011) showed that the females of the temperate-zone chironomid species *Chironomus riparius*, *Micropsectra atrofasciata*, *M. notescens*, *Rheocricotopus atripes* are positively polarotactic, being attracted to horizontally polarized light. These chironomids were attracted practically only to the strongly and horizontally polarizing black oil trap (Fig. 5.12), independently of the height of the test surfaces. This finding, supporting the generality of polarotaxis in chironomids, is important in the visual ecology of chironomids and useful in the design of traps for these insects. Field entomologists studying the biology and ecology of these insects can design new chironomid traps reflecting or emitting strongly and horizontally polarizing light, and thus attracting these insects.

The above-mentioned chironomids were attracted to the strongly and horizontally polarizing test surfaces placed on the ground or at a height of 150 cm above the ground. Jäch (1997), Nilsson (1997), Kriska et al. (1998), van Vondel (1998), Bernáth et al. (2001) and Kriska et al. (2006) have observed a similar attraction of aquatic insects to car roofs. Aquatic insects (e.g. Coleoptera and Heteroptera)

Fig. 5.12 Photograph of chironomid specimens (*Chironomus riparius*, *Micropsectra atrofasciata*, *Micropsectra notescens*, *Rheocricotopus atripes*) trapped by the black oil-filled tray used in the choice experiments of Horváth et al. (2011) [after Fig. 3 on page 1013 of (Horváth et al. 2011)]

often swarm in large numbers, mate in air and land on the roofs, bonnets and boots of black or red cars; Ephemeroptera and Odonata females, moreover, often lay their eggs *en masse* on these car surfaces (Kriska et al. 2006). Dragonflies have also been observed to swarm above cars (Wyniger 1955; Svihla 1961; Watson 1992; Wildermuth 1998; Stevani et al. 2000a, b; Bernáth et al. 2001; Günther 2003; Torralba-Burrial and Ocharan 2003; Wildermuth and Horváth 2005). All these observations demonstrate that horizontally polarizing surfaces attract numerous aquatic insect species, even if these surfaces are elevated above the ground. This is remarkable, since flying, water-seeking polarotactic tabanid flies, for example, are attracted to horizontally polarizing surfaces only if these surfaces are on the ground level (Egri et al. 2012, 2013; see also Chap. 22 and Sect. 23.2).

5.3 Degrees of Linear Polarization of Reflected Light Eliciting Polarotaxis in Dragonflies, Mayflies and Tabanid Flies

Insects with aquatic larvae detect water by means of the horizontal polarization of light reflected from the water surface (Schwind 1991, 1995; Horváth and Varjú 2004; Lerner et al. 2008). Polarotactic aquatic insects are attracted to sources of

horizontally polarized light. The consequence of this positive polarotaxis is that aquatic insects can be deceived by artificial surfaces reflecting strongly and horizontally polarized light. Such surfaces are, for example, crude and waste oil lakes (Horváth and Zeil 1996; Horváth et al. 1998; Bernáth et al. 2001), asphalt roads (Kriska et al. 1998), black plastic sheets (Wildermuth 1998; Kriska et al. 2007), black, red or dark-coloured cars (Wildermuth and Horváth 2005; Kriska et al. 2006), polished black gravestones (Horváth et al. 2007), dark glass surfaces (Kriska et al. 2008; Malik et al. 2008), shiny black photovoltaic solar panels and sun collectors (Horváth et al. 2009, 2010; Blahó et al. 2012). These human-made shiny dark surfaces may act as polarized ecological traps for polarotactic insects, because such surfaces are inappropriate for the development of eggs laid onto them by the deceived and attracted insects, which can also perish due to exhaustion or dehydration (Horváth and Varjú 2004; Horváth and Kriska 2008).

All adverse effects of such artificial surfaces on polarotactic aquatic insects are summarised in the term polarized light pollution (Horváth et al. 2009; see also Chap. 20). The extent of polarized light pollution of a given human-made surface depends on the surface characteristics, illumination conditions, direction of view and the threshold d^* of polarization sensitivity of a given aquatic insect species. d^* means the minimum degree of linear polarization d of reflected light that can elicit positive polarotaxis from a given species.

Species-specific values of d^* may also have a deep ecological meaning: In aquatic environments turbidity and plant density are constraints on predator–prey interactions involving aquatic invertebrates (Van de Meutter et al. 2005). These physical parameters are not directly accessible to flying aquatic insects searching for suitable places for their offsprings. However, the degree of polarization d of reflected light is a remotely perceivable and reliable physical predictor of aquatic oviposition sites (Bernáth et al. 2002). The higher the d^* of an aquatic insect, the more probable that it will prefer darker, deeper or clearer water bodies—reflecting light with higher d-values—and avoid brighter, shallow, turbid or eutrophic ones—reflecting light with lower d (Bernáth et al. 2004). Schwind (1995) hypothesised that the value of d^* for the ventral polarization-sensitive eye region in aquatic beetles and bugs studied by him may be much higher ($d^* \approx 35$ %) than that of the polarization-sensitive dorsal rim area of the eye in the field cricket, *Gryllus campestris* ($d^* \approx 5$ % for blue light; Labhart 1996), and the honeybee, *Apis mellifera* ($d^* \approx 11$ % for ultraviolet light; von Frisch 1967; Rossel and Wehner 1984).

In multiple-choice field experiments, Kriska et al. (2009) measured the threshold d^* of ventral polarization sensitivity in mayflies, dragonflies and tabanid flies, the positive polarotaxis of which has been shown earlier (mayflies: Kriska et al. 1998, 2007; dragonflies: Wildermuth 1998; Horváth et al. 1998, 2007; Bernáth et al. 2002; tabanids: Horváth et al. 2008). Kriska et al. (2009) captured dragonflies, mayflies and tabanids with white, light grey, medium grey, dark grey and black salad oil-filled trays reflecting horizontally polarized light with different degrees of linear polarization d (Fig. 5.13). Using imaging polarimetry, they measured the

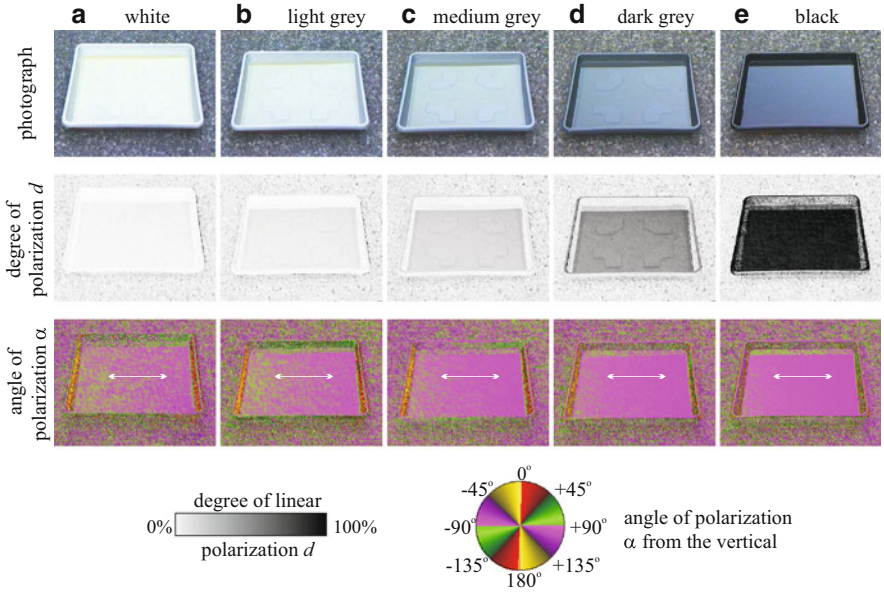

Fig. 5.13 Reflection-polarization characteristics of shady salad oil-filled white (**a**), light grey (**b**), medium grey (**c**), dark grey (**d**) and black (**e**) trays used in the choice experiments of (Kriska et al. 2009) and measured by imaging polarimetry in the blue (450 nm) part of the spectrum. The optical axis of the polarimeter viewed towards the antisolar meridian at the Brewster angle $\theta_{\text{Brewster}} = \arctan(n) \approx 56.3^\circ$ from the vertical calculated for the refractive index $n \approx 1.5$ of salad oil. At the Brewster angle the surface-reflected ray of light is perpendicular to the refracted ray penetrating into the oil, resulting in the highest possible degree of polarization d of reflected light. Thus, the measured polarization data belonging to this angle of view are the maximum d-values a polarotactic insect approaching these traps can ever perceive. In the α-patterns *double-headed arrows* show the horizontal direction of polarization of reflected light. Quite similar patterns were obtained in the *red* (650 nm) and *green* (550 nm) parts of the spectrum, and if the trays were sunlit [after Fig. 2 on page 1168 of (Kriska et al. 2009)]

reflection-polarization characteristics of these insect traps in the red (650 nm), green (550 nm) and blue (450 nm) parts of the spectrum. From the numbers of trapped insects and the degrees of polarization d of trap-reflected light, they determined the lower (d_{min}) and upper (d_{max}) limits of d^* in the investigated positively polarotactic insect species (Table 5.1).

Kriska et al. (2009) observed that the darker a colourless (black, grey, white), shiny, horizontally polarizing test surface, the higher the degree of polarization d of reflected light (Fig. 5.13), and the larger the attractiveness to dragonflies, mayflies and tabanids, if the reflected light is horizontally polarized. In the blue (450 nm) spectral range, for example, they obtained the following thresholds (Table 5.1): Dragonflies: *Enallagma cyathigerum* ($0\ \% < d^* \leq 17\ \%$), *Ischnura elegans* ($17\ \% \leq d^* \leq 24\ \%$). Mayflies: *Baetis rhodani* ($32\ \% \leq d^* \leq 55\ \%$), *Ephemera*

Table 5.1 Lower (d_{min}) and upper (d_{max}) limits of the polarization sensitivity threshold d^* eliciting positive polarotaxis from polarotactic dragonflies, mayflies and tabanid flies estimated on the basis of the choice experiments and reflection-polarization measurements of (Kriska et al. 2009) with the assumption that their polarization sensitivity functions in the red, green or blue part of the spectrum

		$d_{min} \leq d^* \leq d_{max}$ (%)		
Species		Red (650 nm)	Green (550 nm)	Blue (450 nm)
Dragonflies	*Enallagma cyathigerum*	0–6.8	0–7.3	0–17.0
	Ischnura elegans	6.8–11.0	7.3–11.1	17.0–23.5
Mayflies	*Baetis rhodani*	23.2–47.7	20.7–45.7	31.8–55.4
	Ephemera danica	47.7–90.3	45.7–88.7	55.4–91.9
	Epeorus sylvicola (recent name: *E. assimilis*)			
	Rhithrogena semicolorata			
Tabanid flies	*Tabanus bovinus*	23.2–47.7	20.7–45.7	31.8–55.4
	Tabanus tergestinus			
	Tabanus maculicornis	47.7–90.3	45.7–88.7	55.4–91.9

We would like to emphasise that here the values of d^* are given for the red, green and blue spectral ranges, because the wavelength ranges of polarization sensitivity of the ventral eye region in the investigated dragonfly, mayfly and tabanid species are still unknown

danica, *Epeorus sylvicola* (recent name: *E. assimilis*), *Rhithrogena semicolorata* ($55\ \% \leq d^* \leq 92\ \%$). Tabanids: *Tabanus bovinus*, *T. tergestinus* ($32\ \% \leq d^* \leq 55\ \%$), *T. maculicornis* ($55\ \% \leq d^* \leq 92\ \%$). The knowledge of d^* in aquatic insects allows the measurement and monitoring of the extent of polarized light pollution of artificial surfaces in the human-made optical environment.

Insects orienting on the basis of the celestial polarization pattern use the direction of polarization of skylight, because it is the most stable optical variable of the sky (Horváth and Varjú 2004; see also Chaps. 17 and 18). Insects most probably do not rely on the degree of polarization d of skylight for navigation, because it is highly susceptible, even to minor atmospheric disturbances (Coulson 1988; see also Chap. 18). On the other hand, the brightness (intensity of light coming from water) of a water body cannot be perceived at small angles relative to the water surface, because the light coming from water is then overwhelmed by the light reflected from the water surface. Thus, from a remote distance the brightness of water bodies can be guessed only from the degree of polarization d of water-returned light. This characteristic d of water-reflected light correlates with the depth and turbidity (Bernáth et al. 2002), which affect the predator–prey interactions, and are closely related with nutrient concentration and oxygen balance in lake ecosystems. Thus, the degree of polarization d of water-reflected light is highly useful for water-seeking flying aquatic insects, the larvae of which develop in water.

Strongly and horizontally polarized light is a quite stable optical cue of dark/deep water bodies; thus, positive polarotaxis with a high threshold d^* of the degree of polarization can guide aquatic insects to dark/deep waters in most cases. On the other hand, shallow and bright (e.g. alkaline) water bodies reflect weakly polarized light (with low d), because the large amount of light coming from the water

(scattered back from the bottom, or the suspended particles) is vertically polarized due to refraction at the water surface and thus reduces the effect of the horizontally polarized light reflected from the water surface. Aquatic insects bound to find such bright water bodies may possess a lower threshold d^* and/or fly predominantly at sunset or sunrise to exploit the decrease of the depolarizing backscattered light component coming from water (Csabai et al. 2006; see also Sect. 5.1).

A decrease of d^*, for instance, can dramatically increase the chance to reliably locate bright waters by polarotactic aquatic insects that prefer bright water bodies (e.g. *Enallagma cyathigerum* and *Ischnura elegans*, the larvae of which live in small, bright alkaline lakes; see Table 5.1). On the other hand, a low d^* also increases their susceptibility to polarized light pollution induced by horizontally polarizing artificial reflectors (Horváth et al. 2009; see also Chap. 20).

5.4 Polarotaxis in a Mayfly that Never Leaves the Water Surface: Polarization-Based Water Detection in *Palingenia longicauda*

Mayflies (Ephemeroptera) develop as larvae in water for 0.5–3 years. After emergence they swarm and copulate mid-air, and then lay eggs into the water. The mayfly species *Ephemera danica*, *Ecdyonurus venosus*, *Epeorus sylvicola* (recent name: *E. assimilis*), *Baetis rhodani*, *Rhithrogena semicolorata* and *Habroleptoides confusa* detect water by means of the horizontal polarization of light reflected from the water surface and thus are positively polarotactic (Kriska et al. 1998). These mayflies have been frequently observed to swarm above dry asphalt roads and to oviposit onto the dry horizontal asphalt surface. The reason for this strange behaviour is that near sunset, when the mentioned mayflies swarm, the degree of linear polarization of light reflected from asphalt is high (often higher than that of light reflected from water surfaces), and the direction of polarization of asphalt-reflected light is approximately horizontal (see Sect. 20.2). Thus, at sunset the strongly and horizontally polarizing asphalt surface can be more attractive than the water surface to water-seeking polarotactic mayflies.

According to Brodskiy (1973), on the basis of their swarming site mayflies can be sorted into three groups: (1) species swarming immediately over water and never moving away horizontally from the water surface; (2) species swarming over the shore (littoral), but maintaining visual contact with the water; and (3) species swarming horizontally far (maximum about 500–1,000 m) from the water without visual contact with its surface. The six above-mentioned mayfly species studied by Kriska et al. (1998) belong to groups 2 and 3. Do also mayflies belonging to group 1 detect water by the horizontal polarization of water-reflected light?

The mayfly, *Palingenia longicauda*, is a typical representative of group 1. It swarms exclusively over the river surface (Andrikovics and Turcsányi 2001).

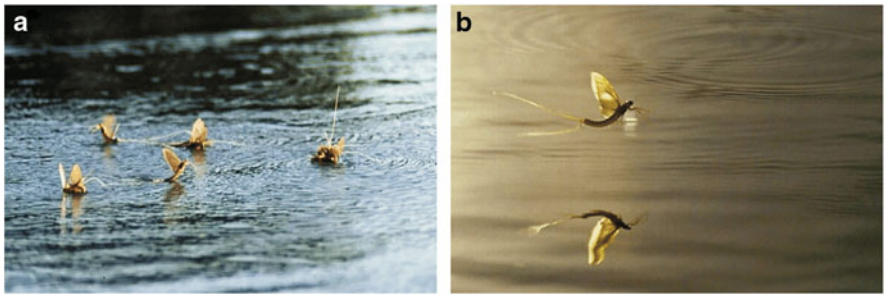

Fig. 5.14 *Palingenia longicauda* mayflies swarm immediately above the river surface. The photographs were taken by Sándor Zsila [after Fig. 1 on page 149 of (Kriska et al. 2007)]

During swarming, *P. longicauda* mayflies fly immediately above the river (Fig. 5.14) in such a way that their cerci touch frequently the water or sweep its surface. This continuous close connection with the water surface results in that these mayflies never move away horizontally from the water; consequently, they need not search for water.

As mentioned above, several Ephemeroptera species move away horizontally far from water and return to it guided by the horizontal polarization of water-reflected light. One could imagine that also *P. longicauda* mayflies use the polarization of water-reflected light to recognise the water and stay over it rather than drift to shore. However, they fly so near the water (Fig. 5.14) that they can recognise it by their tactile organs and hygroreceptors of their cerci and wings (Fink and Andrikovics 1997) as well as by the intensity of light reflected from the water surface. Consequently, they might not need an extra sensitivity to polarization for water recognition. Furthermore, *P. longicauda* mayflies need not possess polarization vision to stay over water, because they never drift to shore by wind, and because they never swarm/fly under windy conditions. Hence, it is not obvious that also *P. longicauda* needs positive polarotaxis.

In a field experiment during the very short (a few days) swarming period of *P. longicauda*, Kriska et al. (2007) tested whether this species is or is not polarotactic. They showed that also *P. longicauda* has positive polarotaxis, which however can be observed only under unnatural conditions, when these mayflies are displaced from the water and then released above horizontally polarizing artificial test surfaces, from which the river is not visible. When released above such test surfaces, *P. longicauda* mayflies stayed over a strongly and horizontally polarizing shiny black plastic sheet for short periods following the plastic like water surfaces (Fig. 5.15). The mayflies flew along nearly straight or zigzag paths above the plastic surface at an altitude of 40–80 cm rising occasionally, but never higher than 120 cm. Individuals stayed above the plastic only until they kept low altitude (i.e. saw the plastic surface under sufficiently wide angles). They followed the black plastic sheet and turned back several times at its edges. Figure 5.16 shows

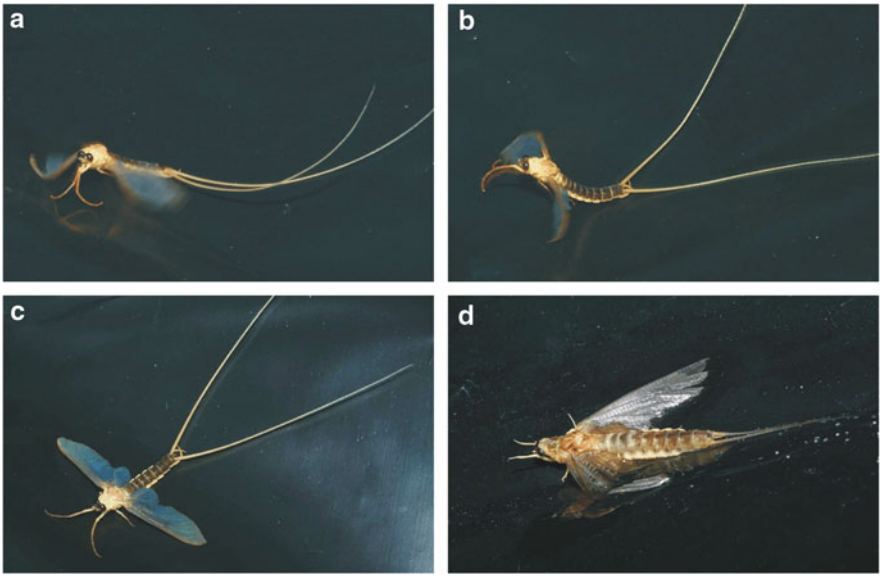

Fig. 5.15 (**a**, **b**) Male *Palingenia longicauda* mayflies flying immediately above a horizontal shiny black plastic sheet. (**c**) A male *P. longicauda* settling down onto the black plastic sheet. (**d**) A female *P. longicauda* laying eggs onto the black plastic sheet [after Fig. 2 on page 151 of (Kriska et al. 2007)]

some typical paths of individuals performing this water-following flight over the plastic sheets. In average, the path length of flying *P. longicauda* mayflies was about 42 ± 15 m over the black plastic sheet, which is nearly 2 times as large as the 23 ± 15 m path length over the white plastic. From this significant difference, it was concluded that *P. longicauda* preferred the black plastic against the white one. A weakly or not always horizontally polarizing aluminium foil, matte black cloth and matte white cloth laid on the ground did not induce such polarotactic water-following flight from *P. longicauda*. Thus, *P. longicauda* has a positive polarotaxis (Kriska et al. 2007).

Over the black plastic sheet Kriska et al. (2007) observed two different flying behaviours of *P. longicauda*: (1) water-seeking flight and (2) water-following flight. The former reaction occurs when the mayflies seek for water, and the latter reaction is the very same as the flight over real water surfaces. The water-seeking flight may allow individuals emerging accidentally in fresh backwaters and narrow branches to join the swarm above the main river branch.

P. longicauda is the first species in which polarotactic water detection was demonstrated albeit it never leaves the water surface and thus a polarotactic water detection seems unnecessary for it. This demonstrates that polarization-based water detection is an ancient, conservative ability among Ephemeroptera. The polarotactic behaviour of *P. longicauda* explains the observation that these mayflies

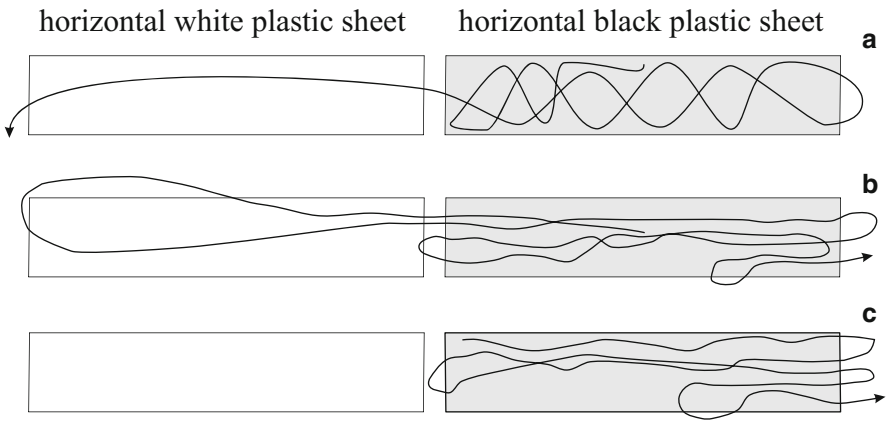

Fig. 5.16 Three typical flight trajectories of male *Palingenia longicauda* mayflies released in the field experiment of (Kriska et al. 2007) and flying immediately above horizontal shiny black and white plastic sheets laid onto the shore of river Tisza, from which the river surface was not visible. (**a**) This mayfly was released at the middle of the black plastic. It flew above the black plastic slowly along a zigzag path for about 1 min. Finally, it flew straight over the white plastic and left it. (**b**) This mayfly was released at the middle of the black plastic. It flew above the white plastic in an elongated, straight loop and after turning back at the edge of the white plastic it flew above the black plastic where it remained for about 40 s flying along a nearly straight path with some zigzagging until leaving the black plastic. (**c**) This mayfly was released near to the neighbouring border of the black and white plastics. It started to fly towards the black plastic. It flew exclusively above the black plastic for about 20 s slowly and not higher than about 40 cm, turning back when reaching the edges. Finally, it flew away rising high above the ground [after Fig. 2 on page 151 of (Kriska et al. 2007)]

anomalously swarmed above wet asphalt roads (polarizing reflected light strongly and horizontally) running next to river Tisza (Ladócsy 1930, p. 29).

5.5 Odour-Masked Polarotaxis in Egg-Laying Yellow Fever Mosquitoes

Biting mosquitoes are vectors of the pathogens of numerous diseases and are also a nuisance. Gravid female mosquitoes have to find suitable water bodies in which their aquatic larvae can develop. Responses of mosquitoes elicited by visual, chemical and tactile stimuli and involved in the location and selection of oviposition sites are continuously studied in the hope of developing efficient egg traps to monitor mosquito populations and increasing efficacy of control methods. Different chemical compounds, e.g. pentatonic and tridecanoic carboxylic acids, have been reported to influence the ability of mosquitoes to locate water bodies (Bentley and Day 1989; Mendki et al. 2000; Ganesan et al. 2006; Navarro-Silva et al. 2009).

Simple water vapour is also known to be a mosquito attractant (Clements 1999; Yokohari 1999).

Chemical cues are, however, reliable only over relatively short distances, and mosquitoes in flight are known to depend also on visual inputs for orientation (Allan et al. 1987). Optical characteristics of water surfaces influence oviposition site location by mosquitoes (Muirhead-Thompson 1940; Kennedy 1942; Belton 1967; McCrae 1984). Sporadic studies on polarization sensitivity in mosquitoes failed to prove reactions to polarization signals while excluding reactions to light intensity and chemical cues, or used insufficient numbers of mosquito individuals, and thus led to unconvincing conclusions (Kalmus 1958; Kovrov and Monchadskiy 1963; Wellington 1974; Clements 1999; Bernáth et al. 2008; see also Chap. 21).

The yellow fever mosquito, *Aedes (Stegomyia) aegypti*, is found throughout subtropical and tropical areas of the world and considered the major vector for the transmission of dengue and yellow fever. It is a largely diurnal-biting species (Chadee 1988) that apparently uses chemical and visual cues to locate its host (Kawada et al. 2005). Female *Ae. aegypti* lay their eggs into small and inconspicuous water bodies, such as tree holes, and in urban areas, containers, flower vases, discarded tyres, cans, bottles and paper cups, for example (Seng and Jute 1994).

Relying on reflection polarization in detecting water bodies is considered to be a likely asset of all flying aquatic insect species (Schwind 1991, 1995; Horváth and Varjú 2004). After a laboratory study (Bernáth et al. 2008) finding no evidence for positive polarotaxis in the yellow fever mosquito, *Aedes aegypti* (Fig. 5.17), this water-associated insect species has been thought to be an exception, locating its breeding habitats by chemical cues like odour of conspecifics, their eggs or water vapour. Later, in a more thorough dual-choice experiment, Bernáth et al. (2012) showed that horizontally polarized light can also attract ovipositing *Ae. aegypti* females if they are deprived of chemical cues. *Ae. aegypti* is the first known aquatic insect in which polarotaxis exists, but does not play a dominant role in locating water bodies and can be constrained in the presence of chemical cues.

Bernáth et al. (2012) performed dual-choice laboratory experiments to test the attractiveness of gravid, blood-fed *Ae. aegypti* females to horizontally polarized light. They used an experimental design (Fig. 5.18) that allowed testing the attractiveness of egg trays solely on the basis of light polarization in the ultraviolet and visible spectral ranges ($300\ \text{nm} < \lambda < 700\ \text{nm}$; the ventral UV and green photoreceptors of *Ae. aegypti* are maximally sensitive at 370 and 520 nm, respectively; Muir et al. 1992): the only difference between egg trays was the state of polarization (totally linearly polarized or unpolarized) of the emitted light, while their emission spectra and intensities were identical (Fig. 5.19). Any diluted infochemicals in the egg trays originating from eggs or females were either removed through continuous rinsing (with a water flow of 0.7 ml/s in each egg tray to continuously wash away any infochemicals originating from ovipositing females, eggs or carcasses) or allowed to accumulate (both egg trays filled by clear dechlorinated tap water with a water flow lower than 0.01 ml/s being sufficiently slow to allow an accumulation of infochemicals).

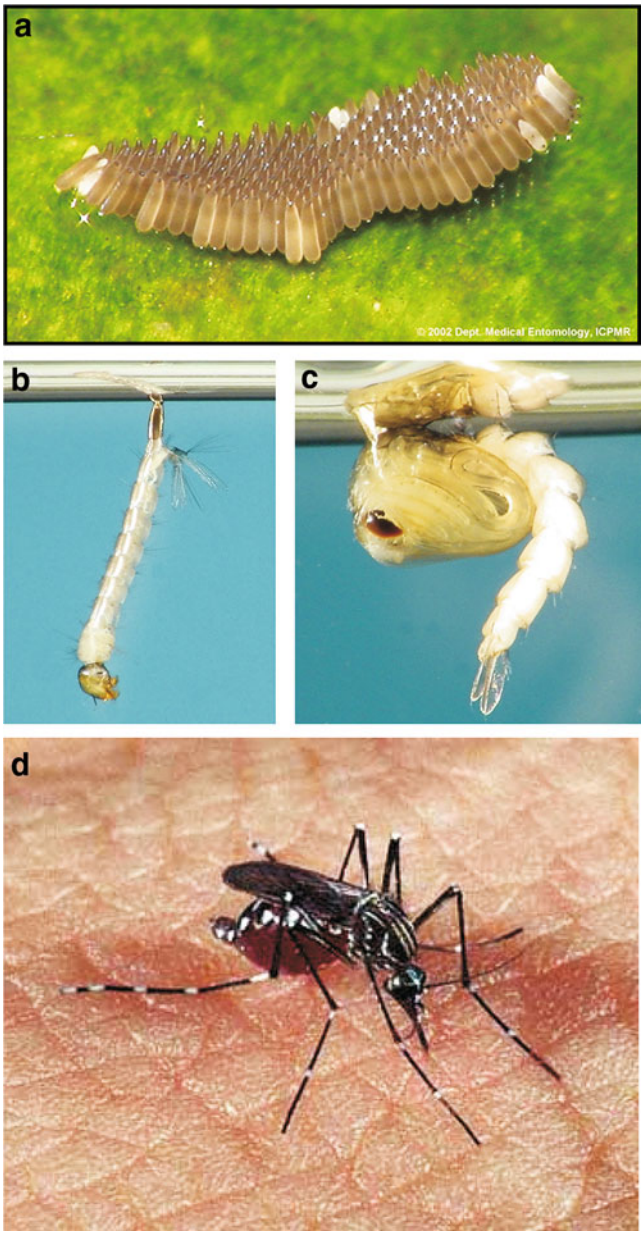

Fig. 5.17 Eggs (**a**), a larva (**b**), a pupa (**c**) and a female adult (**d**) of *Aedes aegypti* (http://www.hudsonregional.org)

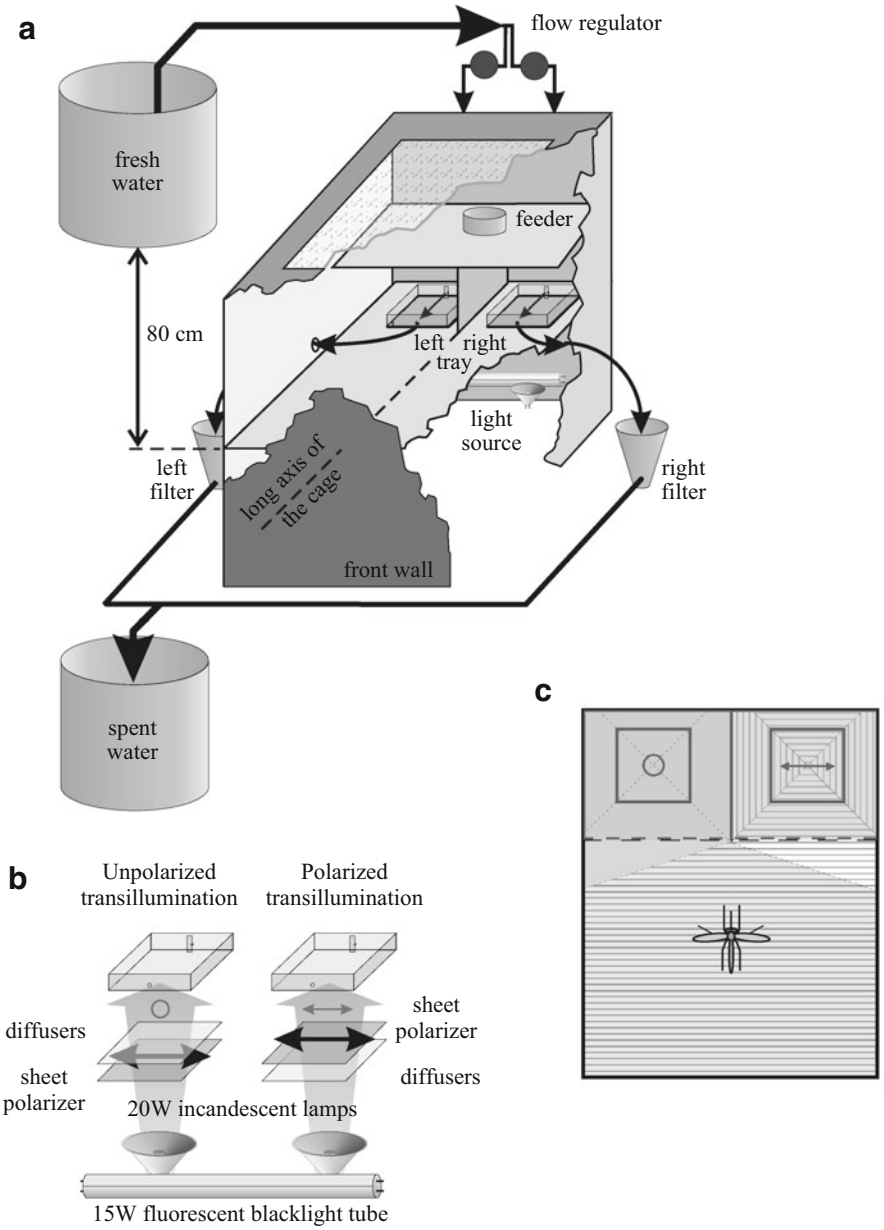

Fig. 5.18 Arrangement of the dual-choice experiment performed by Bernáth et al. (2012) with gravid female *Aedes aegypti*. (**a**) Geometry of the test cage with rinsable egg trays and transilluminating windows. (**b**) Production of unpolarized and totally linearly polarized transilluminations. (**c**) The egg trays were shielded by plates forming cubes of 20 cm × 15 cm × 15 cm open only from the side facing the front. This arrangement ensured that mosquitoes flying in the cage (seen from above in the figure) perceived only unpolarized light (on the *left*) or horizontally polarized (on the *right*), rather than vertically or obliquely polarized light [after Fig. 1 on page 1002 of (Bernáth et al. 2012)]

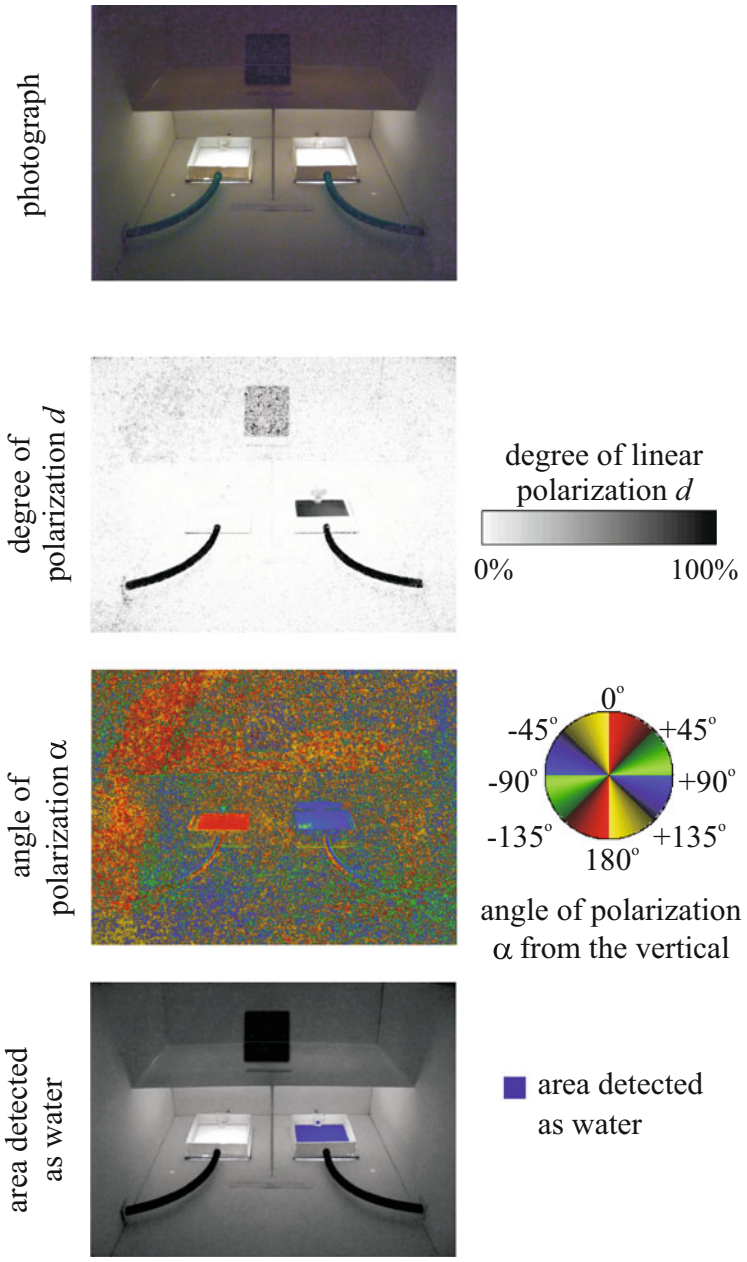

Fig. 5.19 Photograph and patterns of the degree of linear polarization d and angle of polarization α (clockwise from the vertical) and area detected as water (for which the following two conditions are satisfied: $d > 20$ % and $80° < \alpha < 100°$) for the transilluminated egg trays in the test cage of *Aedes aegypti* measured by imaging polarimetry in the *green* (550 nm) part of the spectrum. The *left*/*right window* was transilluminated by unpolarized/totally horizontally polarized light. *Left* or *right positions* of unpolarized and linearly polarized transillumination were arranged randomly [after Fig. 2 on page 1003 of (Bernáth et al. 2012)]

A significant difference occurred between rinsed and non-rinsed choice experiments: once water-dissolved chemical substances were removed by rinsing, the egg tray that emanated horizontally polarized light gained about 94 % higher total number of eggs than the unpolarized light-emanating tray. Bernáth et al. (2012) concluded that (1) *Ae. aegypti* can detect water visually by means of horizontally polarized light reflected from the water surface, but (2) vision is not the sense that dominates the search for water, the selection of oviposition sites and oviposition itself. *Ae. aegypti* females possess a polarotactic capacity that can facilitate remote water detection, but the sequels of polarotaxis are masked in the presence of stimulants indicative of conspecifics and/or their eggs or larvae in the water. This overwhelming effect of infochemicals is the reason why in earlier studies (e.g. Bernáth et al. 2008), positive polarotaxis in *Ae. aegypti* had remained completely hidden.

A possible structural basis for polarization sensitivity in the eyes of yellow fever mosquitoes, as with the eyes of other Diptera closely related to mosquitoes (Sato 1959; Meyer-Rochow and Waldvogel 1979; Hardie 1985), is provided by the orthogonally directed microvilli of retinula cells 7 and 8, which are arranged in a tandem position in the centre of each ommatidium. These two cells have separate second-order neuronal channels (Wolf and Ready 1993), and thus could reliably relay information on the linear polarization to the brain of the insect. Polarization-sensitive ommatidia are expected to be located in the ventral eye region of *Ae. aegypti* with neurons responsible for processing the polarization information.

Aedes aegypti typically breed in small and covered waters (e.g. water-filled tree/rock holes, man-made small containers/bottles/old tyres containing water), the detection of which may be difficult. Recognising dark patches is useful in detecting entrances to cavities, but being sensitive to horizontally polarized stimulation in the lower visual field is helpful in identifying water surfaces whether in cavities or in the open (Fig. 5.20). These optical cues are perceptible for mosquitoes also under low light intensities, not requiring high spatial resolution. Mosquito species ovipositing on open water surfaces (e.g. *Anopheles* sp., *Culex* sp.) or dropping eggs while hovering over water (some species of the genera *Anopheles*, *Sabethes*, *Toxorhynchites* and *Wyeomyia*) would benefit even more from perceiving the horizontally polarized light reflected from water surfaces (Clements 1999). *Ae. aegypti* is probably not the only mosquito species, which may display masked polarization sensitivity.

The positive polarotaxis hidden by infochemicals in yellow fever mosquitoes may also help to reinterpret some contradictory results in mosquito ecology: Constrained polarotaxis of any mosquito species can influence the results of bioassays involving water-filled egg trays and strongly and horizontally polarizing smooth black surfaces to test the effectiveness of chemical attractants or repellents in ovipositing females. Brightness contrasts are usually controlled to avoid artefacts originating from the preference of gravid female mosquitoes for dark oviposition sites and water surfaces against bright ones (Clements 1999). However, polarization contrasts are usually not addressed, and the separation of intensity contrasts

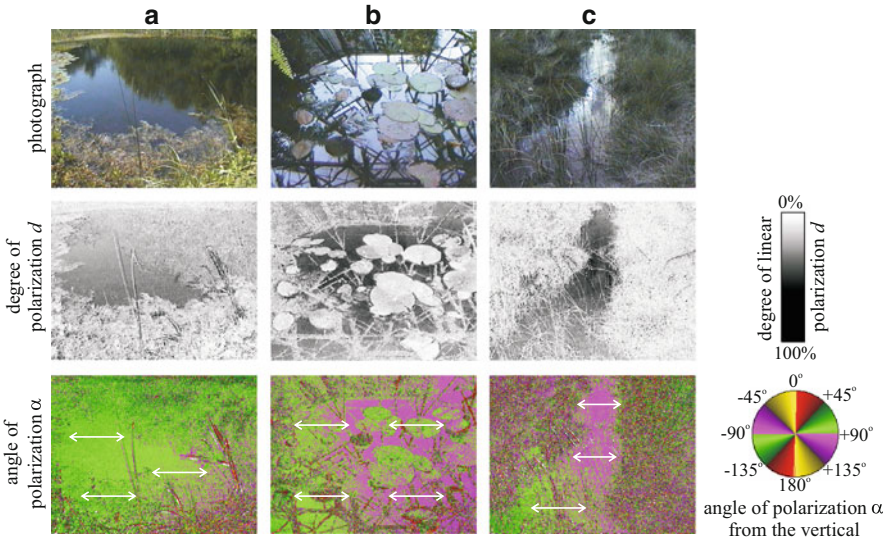

Fig. 5.20 Photographs and patterns of the degree of linear polarization d and angle of polarization α of three typical oviposition sites of *Aedes aegypti* measured by imaging polarimetry in the *green* (550 nm) part of the spectrum. In the *third row double-headed arrows* show the local direction of polarization of reflected light. (**a**) A lake with water plants close to the shore. (**b**) A small lake with dense growth of water lilies on the water surface. (**c**) A shiny wet mud surface of a grassy field in a marshy area [after Fig. 4 on page 1453 of (Bernáth et al. 2008)]

from polarization contrasts in choice experiments is not trivial (Horváth and Varjú 2004, pp. 381–383).

Polarization sensitivity of the dorsal eye region in *Ae. aegypti* may conceivably serve as a skylight-polarization compass. Early behavioural tests by Kalmus (1958) and Wellington (1974) may support this hypothesis, although further information is required because of their methodological shortcomings.

5.6 Negative Polarotaxis in Desert Locusts Hinders Flying Over the Sea

Aquatic insects have positive polarotaxis, that is they are attracted to linearly polarized light. On the one hand, they find their aquatic habitat by detecting the horizontal polarization of light reflected from the water surface (Schwind 1991, 1995; Horváth and Varjú 2004). On the other hand, blood-sucking female tabanid flies find their host animals partly by means of the degree of linear polarization of light reflected from the body of the host, independently of the direction of polarization (Horváth et al. 2008; Egri et al. 2012, 2013). Both kinds of positive

polarotaxis help the concerned insects to detect and approach targets (water, host) that are important for their survival.

In certain circumstances, it could be important to detect water by means of reflected polarization in order to avoid water, rather than to be attracted to it. Larger or smaller water surfaces can be dangerous for terrestrial insects, which would perish if they crash into water. In this case negative polarotaxis, that is a repellence by the horizontal polarization of water-reflected light, would be an adequate reaction. Shashar et al. (2005) reported on such a negative polarotactic behaviour in migrating desert locusts.

The desert locust *Schistocerca gregaria* is a migrating insect, travelling long distances in swarms containing millions of individuals. Shashar et al. (2005) observed that a locust swarm reached the northern coast of the Gulf of Aqaba, coming from the Sinai desert towards the southeast. Upon reaching the coast, they avoided flying over the water surface of the 3–5 km wide gulf and instead flew north along the coast. Only after passing the tip of the gulf they turned east again. The insects rarely flew over water, and if blown over it rapidly turned back towards the shore. However, *Schistocerca gregaria* is well capable of crossing large bodies of water when flying high, often at a height of hundreds of metres, or when carried by strong winds.

Experiments with tethered locusts showed that they avoided flying towards a horizontal mirror laid on the ground and reflecting partially linearly polarized light (Shashar et al. 2005). The average flight direction in the control position without a mirror (above the sandy soil) tended to coincide with the direction from which the wind was blowing. When tethered locusts could select between a weakly polarizing horizontal test surface (matte black felt on the ground) and a strongly and horizontally polarizing reflector (shiny black plastic on the ground), they preferred to fly over the former (Shashar et al. 2005). These results suggest that desert locusts can detect the polarized reflections of water bodies and avoid crossing them.

Schistocerca gregaria is sensitive to linearly polarized light and possesses a specialised group of ommatidia in the dorsal rim of its compound eyes (Eggers and Gewecke 1993; Mappes and Homberg 2003; Homberg et al. 2004), which are designed to analyse the polarized skylight as a navigational cue (Homberg 2004). The results of Shashar et al. (2005) showed that the ventral eye region of desert locusts should also be sensitive to linear polarization. By this polarization-sensitive ventral eye region, the locusts detect the upwelling horizontally polarized water-reflected light, and thus can navigate towards or away from large water surfaces.

For migrating desert insects, water presents a potential hazard and large bodies of water, such as the sea, are especially dangerous. Therefore, detecting and avoiding such surfaces with the help of ventral polarization vision is beneficial to them. This capacity can be most relevant to desert locusts when they are flying at low altitudes and when other weather conditions, such as wind speed and direction, permit flying in specific directions (Shashar et al. 2005).

References

Allan SA, Day JF, Edman JD (1987) Visual ecology of biting flies. Annu Rev Entomol 32: 297–316

Andrikovics S, Turcsányi I (2001) Tisza mayfly—ecology of an endangered species. Booklet of Tisza Club 10:1–69 (in Hungarian)

Behr H (1993) Wiederfangergebnisse aus Markierungsexperimenten an fünf in einem Moorgewässer koexistierenden Hydroporus-Arten (Coleoptera; Dytiscidae: Imagines). Zoologisches Jahrbuch der Systematik 120:201–214

Belton P (1967) The effect of illumination; pool brightness on oviposition by *Culex restuans* (Theo.) in the field. Mosq News 27:66–82

Bentley MD, Day DF (1989) Chemical ecology and behavioural aspects of mosquito oviposition. Annu Rev Entomol 34:401–421

Bernáth B, Szedenics G, Molnár G, Kriska G, Horváth G (2001) Visual ecological impact of "shiny black anthropogenic products" on aquatic insects: oil reservoirs and plastic sheets as polarized traps for insects associated with water. Arch Nat Conserv Landsc Res 40(2):89–109

Bernáth B, Szedenics G, Wildermuth H, Horváth G (2002) How can dragonflies discern bright and dark waters from a distance? The degree of polarization of reflected light as a possible cue for dragonfly habitat selection. Freshw Biol 47:1707–1719

Bernáth B, Gál J, Horváth G (2004) Why is it worth flying at dusk for aquatic insects? Polarotactic water detection is easiest at low solar elevations. J Exp Biol 207:755–765

Bernáth B, Horváth G, Gál J, Meyer-Rochow VB (2008) Polarized light and oviposition site selection in the yellow fever mosquito: No evidence for positive polarotaxis in *Aedes aegypti*. Vis Res 48:1449–1455

Bernáth B, Horváth G, Meyer-Rochow VB (2012) Polarotaxis in egg-laying yellow fever mosquitoes *Aedes* (*Stegomyia*) *aegypti* is masked due to infochemicals. J Insect Physiol 58: 1000–1006

Blahó M, Egri Á, Barta A, Antoni G, Kriska G, Horváth G (2012) How can horseflies be captured by solar panels? A new concept of tabanid traps using light polarization and electricity produced by photovoltaics. Vet Parasitol 189:353–365

Boda P, Csabai Z (2013) When do beetles and bugs fly? A unified scheme for describing seasonal flight behaviour of highly dispersing primary aquatic insects. Hydrobiologia 703:133–147

Brodskiy AK (1973) The swarming behavior of mayflies (Ephemeroptera). Entomol Rev 52:33–39

Chadee DD (1988) Landing periodicity of the mosquito *Aedes aegypti* in Trinidad in relation to the timing of insecticidal space-spraying. Med Vet Entomol 2:189–192

Clements AN (1999) The biology of mosquitoes. Cambridge University Press, Cambridge, UK

Coulson KL (1988) Polarization and radiance of light in the atmosphere. A. Deepak, Hampton, VA

Cranston PS (1995) Introduction. In: Armitage P, Cranston PS, Pinder LCV (eds) The chironomidae. The biology and ecology of non-biting midges. Chapman Hall, London, pp 1–7

Csabai Z, Boda P (2005) Effects of the wind speed on the migration activity of aquatic insects (Coleoptera, Heteroptera). Acta Biologia Debrecina Supplementum Oecologica Hungarica 13:37–42

Csabai Z, Boda P, Bernáth B, Kriska G, Horváth G (2006) A 'polarisation sun-dial' dictates the optimal time of day for dispersal by flying aquatic insects. Freshw Biol 51:1341–1350

Csabai Z, Kálmán Z, Szivák I, Boda P (2012) Diel flight behaviour and dispersal patterns of aquatic Coleoptera and Heteroptera species with special emphasis on the importance of seasons. Naturwissenschaften 99:751–765

Eggers A, Gewecke M (1993) The dorsal rim area of the compound eye and polarization vision in the desert locust (*Schistocerca gregaria*). In: Wiese K, Gribakin FG, Popov AV, Renninger G (eds) Sensory systems of arthropods. Birkhäuser Verlag, Basel, pp 101–109

Egri Á, Blahó M, Sándor A, Kriska G, Gyurkovszky M, Farkas R, Horváth G (2012) New kind of polarotaxis governed by degree of polarization: Attraction of tabanid flies to differently polarizing host animals and water surfaces. Naturwissenschaften 99:407–416 + electronic supplement

Egri Á, Blahó M, Száz D, Barta A, Kriska G, Antoni G, Horváth G (2013) A new tabanid trap applying a modified concept of the old flypaper: linearly polarising sticky black surfaces as an effective tool to catch polarotactic horseflies. Int J Parasitol 43:555–563

Fernando CH (1958) The colonization of small freshwater habitats by aquatic insects. 1. General discussion, methods and colonization by the aquatic Coleoptera. Ceylon J Sci 1:117–154

Fink TJ, Andrikovics S (1997) The presumed role of wing sensory structures in the unique mating behaviour of the endangered European mayflies *Palingenia lomgicauda* (Olivier) and *Palingenia fuliginosa* (Georgi) (Insecta, Ephemeroptera). In: Landolt P, Sartori M (eds) Ephemeroptera and plecoptera: biology-ecology-systematics. MTL, Fribourg, pp 326–331

Ganesan K, Mendki MJ, Suryanarayana MV, Prakash S, Malhotra RC (2006) Studies on *Aedes aegypti* (Diptera: Culicidae) ovipositional responses to newly identified semiochemicals from conspecific eggs. Aust J Entomol 45:75–78

Günther A (2003) Eiablage von *Sympetrum vulgatum* auf ein parkendes Auto (Odonata: Libellulidae). Libellula 22:19–23

Halpern M, Raats D, Lavion R, Mittler S (2006) Dependent population dynamics between chironomids (nonbiting midges) and *Vibrio cholerae*. FEMS Microbiol Ecol 55:98–104

Hardie RC (1985) Functional organization of the fly retina. In: Ottoson D (ed) Progress in sensory physiology, vol 5. Springer, Heidelberg, pp 1–79

Homberg U (2004) In search of the sky compass in the insect brain. Naturwissenschaften 91:199–208

Homberg U, Hofer S, Mappes M, Vitzthum H, Pfeiffer K, Gebhardt S, Müller M, Paech A (2004) Neurobiology of polarization vision in the locust *Schistocerca gregaria*. Acta Biol Hung 55:81–89

Horváth G, Kriska G (2008) Polarization vision in aquatic insects and ecological traps for polarotactic insects. In: Lancaster J, Briers RA (eds) Aquatic insects: challenges to populations. CAB International Publishing, Wallingford, Oxon, pp 204–229, Chapter 11

Horváth G, Varjú D (2004) Polarized light in animal vision—polarization patterns in nature. Springer, Heidelberg

Horváth G, Zeil J (1996) Kuwait oil lakes as insect traps. Nature 379:303–304

Horváth G, Bernáth B, Molnár G (1998) Dragonflies find crude oil visually more attractive than water: multiple-choice experiments on dragonfly polarotaxis. Naturwissenschaften 85:292–297

Horváth G, Blahó M, Egri Á, Kriska G, Seres I, Robertson B (2010) Reducing the maladaptive attractiveness of solar panels to polarotactic insects. Conserv Biol 24:1644–1653

Horváth G, Malik P, Kriska G, Wildermuth H (2007) Ecological traps for dragonflies in a cemetery: the attraction of *Sympetrum* species (Odonata: Libellulidae) by horizontally polarizing black gravestones. Freshw Biol 52:1700–1709

Horváth G, Majer J, Horváth L, Szivák I, Kriska G (2008) Ventral polarization vision in tabanids: horseflies and deerflies (Diptera: Tabanidae) are attracted to horizontally polarized light. Naturwissenschaften 95:1093–1100

Horváth G, Kriska G, Malik P, Robertson B (2009) Polarized light pollution: a new kind of ecological photopollution. Front Ecol Environ 7:317–325

Horváth G, Móra A, Bernáth B, Kriska G (2011) Polarotaxis in non-biting midges: female chironomids are attracted to horizontally polarized light. Physiol Behav 104:1010–1015 + cover picture

Jäch MA (1997) Daytime swarming of rheophilic water beetles in Austria (Coleoptera: Elmidae, Hydraenidae, Haliplidae). Latissimus 9:10–11

Kalmus H (1958) Responses of insects to polarized light in the presence of dark reflecting surfaces. Nature 182:1526–1527

Kawada H, Takemura SY, Arikawa K, Takagi M (2005) Comparative study on nocturnal behavior of *Aedes aegypti* and *Aedes albopictuts*. J Med Entomol 42:312–318

Kennedy JS (1942) On water finding and oviposition by captive mosquitoes. Bull Entomol Res 32:279–301

Kovrov BG, Monchadskiy AS (1963) About the possibility of using polarized light to attract insects. Entomol Rev 62(1):49–55, in Russian, see a review in English in Entomological Review of Washington 42:25–28

Kriska G, Horváth G, Andrikovics S (1998) Why do mayflies lay their eggs *en masse* on dry asphalt roads? Water-imitating polarized light reflected from asphalt attracts Ephemeroptera. J Exp Biol 201:2273–2286

Kriska G, Csabai Z, Boda P, Malik P, Horváth G (2006) Why do red and dark-coloured cars lure aquatic insects? The attraction of water insects to car paintwork explained by reflection-polarization signals. Proc R Soc B 273:1667–1671

Kriska G, Bernáth B, Horváth G (2007) Positive polarotaxis in a mayfly that never leaves the water surface: polarotactic water detection in *Palingenia longicauda* (Ephemeroptera). Naturwissenschaften 94:148-154 + cover picture

Kriska G, Malik P, Szivák I, Horváth G (2008) Glass buildings on river banks as "polarized light traps" for mass-swarming polarotactic caddis flies. Naturwissenschaften 95:461–467

Kriska G, Bernáth B, Farkas R, Horváth G (2009) Degrees of polarization of reflected light eliciting polarotaxis in dragonflies (Odonata), mayflies (Ephemeroptera) and tabanid flies (Tabanidae). J Insect Physiol 55:1167–1173

Labhart T (1996) How polarization-sensitive interneurones of crickets perform at low degrees of polarization. J Exp Biol 199:1467–1475

Ladócsy K (1930) The mating flight of the Tisza mayfly (*Palingenia longicauda*, Oliv.) in 1929 in Szeged, part 2. Fishery 31(7–8):28–30, in Hungarian

Landin J (1968) Weather and diurnal periodicity of flight by *Helophorus brevipalpis* Bedel (Col. Hydrophilidae). Opusc Entomol 33:28–36

Landin J, Stark E (1973) On flight thresholds for temperature and wind velocity, 24-hour flight periodicity and migration of the water beetle *Helophorus brevipalpis*. J Zool Upps Univ Suppl 1:105–114

Lerner A, Meltser N, Sapir N, Erlick C, Shashar N, Broza M (2008) Reflected polarization guides chironomid females to oviposition sites. J Exp Biol 211:3536–3543

Lerner A, Sapir N, Erlick C, Meltser N, Broza M, Shashar N (2011) Habitat availability mediates chironomid density-dependent oviposition. Oecologia 165:905–914

Malik P, Hegedüs R, Kriska G, Horváth G (2008) Imaging polarimetry of glass buildings: Why do vertical glass surfaces attract polarotactic insects? Appl Opt 47:4361–4374

Mappes M, Homberg U (2003) Behavioral analysis of polarization vision in tethered flying locusts. J Comp Physiol A 190:61–68

McCrae AWR (1984) Oviposition by African malaria vector mosquitoes. II. Effect of site tone, water type and conspecific immatures on target selection by freshwater *Anopheles gambiae* Giles, *sensu lato*. Ann Trop Med Parasitol 78:307–318

Meltser N, Kashi Y, Broza M (2008) Does polarized light guide chironomids to navigate toward water surfaces? Bol Mus Munic Funchal (História Natural) 13(Suppl):141–149

Mendki MJ, Ganesan S, Prakash MVS, Suryanarayana RC, Malhotra KM, Rao KM, Vaidyanathawamy R (2000) Heneicosane: an oviposition-attractant pheromone of larval origin in *Aedes aegypti* mosquito. Curr Sci 78:1295–1296

Meyer-Rochow VB, Waldvogel H (1979) Visual behaviour and the structure of dark and light-adapted larval and adult eyes of the New Zealand glowworm *Arachnocampa luminosa* (Mycetophylidae, Diptera). J Insect Physiol 25:601–613

Muir LE, Thorne MJ, Kay BH (1992) *Aedes aegypti* (Diptera, Culicidae) vision: spectral sensitivity and other perceptual paramteres of the female eye. J Med Entomol 29:278–281

Muirhead-Thompson RC (1940) Studies on the behaviour of *Anopheles minimus* II: The influence of water movement on the selection of the breeding place. J Malar Inst India 3:295–322

Navarro-Silva MA, Marques FA, Duque LJE (2009) Review of semiochemicals that mediate the oviposition of mosquitoes: a possible sustainable tool for the control and monitoring of Culicidae. Rev Bras Entomol 53(1):1–6

Nilsson AN (1997) On flying *Hydroporus* and the attraction of *H. incognitus* to red car roofs. Latissimus 9:12–16
Nilsson AN, Svensson BW (1992) Taking off in cold blood—*Dytiscus marginalis* flying at 6.4 °C. Balfour-Browne Club Newslett 50:1–2
Nowinszky L (2003) The handbook of light trapping. Savaria University Press, Szombathely, Hungary
Popham EJ (1964) The migration of aquatic bugs with special reference to the Corixidae (Hemiptera, Heteroptera). Archiv für Hidrobiologie 60:450–496
Rossel S, Wehner R (1984) How bees analyse the polarization patterns in the sky. J Comp Physiol A 154:607–615
Sato S (1959) Structure and development of the compound eye of *Culex* (*Lutzia*) *vorax* Edwards. (Morphological studies on the compound eye in the mosquito, no. VI). Scientific Reports of the Tohoku University (Series 4) 25:99–110
Schwind R (1991) Polarization vision in water insects and insects living on a moist substrate. J Comp Physiol A 169:531–540
Schwind R (1995) Spectral regions in which aquatic insects see reflected polarized light. J Comp Physiol A 177:439–448
Seng CM, Jute N (1994) Breeding of *Aedes aegypti* (L.) and *Aedes albopictus* (Skuse) in urban housing of Sibu town, Sarawak. Southeast Asian J Trop Med Public Health 25:543–548
Shashar N, Sabbah S, Aharoni N (2005) Migrating locusts can detect polarized reflections to avoid flying over the sea. Biol Lett 1:472–475
Stevani CV, Porto JS, Trindade DJ, Bechara EJH (2000a) Automotive clearcoat damage due to oviposition of dragonflies. J Appl Polym Sci 75:1632–1639
Stevani CV, Faria DLA, Porto JS, Trindade DJ, Bechara EJH (2000b) Mechanism of automotive clearcoat damage by dragonfly eggs investigated by surface enhanced Raman scattering. Polym Degrad Stab 68:61–66
Svihla A (1961) An unusual ovipositing activity of *Pantala flavescens* Fabricius. Tombo 4:18
Torralba-Burrial A, Ocharan FJ (2003) Coches como hábitat para libélulas? Algunos machos de *Crocothemis erythraea* creen que sí. Boletin de la Sociedad Entomologia Aragonesa 32: 214–215
Van de Meutter F, De Meester L, Stoks R (2005) Water turbidity affects predator-prey interactions in a fish-damselfly system. Oecologia 144:327–336
van Vondel BJ (1998) Another case of water beetles landing on a red car roof. Latissimus 10:29
von Frisch K (1967) The dance language and orientation of bees. Harvard University Press, Cambridge, MA, USA
Watson JAL (1992) Oviposition by exophytic dragonflies on vehicles. Notulae Odonatologicae 3: 137
Weigelhofer G, Weissmair W, Waringer J (1992) Night migration activity and the influence of meteorological parameters on light-trapping for aquatic Heteroptera. Zool Anz 229:209–218
Wellington WG (1974) Change in mosquito flight associated with natural changes in polarized light. Can Entomol 106:941–948
Wildermuth H (1998) Dragonflies recognize the water of rendezvous and oviposition sites by horizontally polarized light: a behavioural field test. Naturwissenschaften 85:297–302
Wildermuth H, Horváth G (2005) Visual deception of a male *Libellula depressa* by the shiny surface of a parked car (Odonata: Libellulidae). Int J Odonatol 8:97–105
Wolf T, Ready DF (1993) Pattern formation in the Drosophila retina. In: Bate M, Arias AM (eds) The development of *Drosophila melanogaster*, vol II. Cold Spring Harbor Laboratory Press, Cold Spring Harbor, NY, pp 1277–1325
Wyniger R (1955) Beobachtungen über die Eiablage von *Libellula depressa* L. (Odonata, Libellulidae). Mitteilungen der Entomologischen Gesellschaft Basel NF 5:62–63
Yokohari F (1999) Hygro- and thermoreceptors. In: Eguchi E, Tominaga Y (eds) Atlas of Arthropod sensory receptors. Springer, Berlin, pp 191–210
Zalom FG, Grigarick AA, Way MO (1990) Diel flight periodicities of some Dytiscidae (Coleoptera) associated with California rice paddies. Ecol Entomol 5:183–187

Chapter 6
Circular Polarization Vision of Scarab Beetles

Gábor Horváth, Miklós Blahó, Ádám Egri, Ramón Hegedüs, and Győző Szél

Abstract In this chapter the occurrence of circularly polarized (CP) light in nature (both in the abiotic and biotic optical environment) is surveyed. We deal with the reason and the possible adaptive significance of CP light reflected from the exocuticle of many beetle species belonging to the Scarabaeoidea. This unique feature of the insect exocuticle seems to have evolved only in scarabaeoids. The imaging polarimetry of circularly polarizing scarab beetles and its results are reviewed. The alleged CP sensitivity in *Chrysina gloriosa* scarabs is briefly discussed. Finally, the experimental evidence for the lack of CP vision in the scarab species *Anomala dubia*, *A. vitis* (Coleoptera, Scarabaeidae, Rutelinae), *Cetonia aurata*, and *Protaetia cuprea* (Coleoptera, Scarabaeidae, Cetoniinae) with circularly polarizing exocuticle is presented.

Electronic supplementary material is available in the online version of this chapter at 10.1007/978-3-642-54718-8_6. A colour version of a black and white figure as well as supplementary figures can also be found under http://extras.springer.com

G. Horváth (✉) • M. Blahó • Á. Egri
Environmental Optics Laboratory, Department of Biological Physics, Physical Institute, Eötvös University, Pázmány sétány 1, 1117 Budapest, Hungary
e-mail: gh@arago.elte.hu; majkl2000@gmail.com; adamp39@gmail.com

R. Hegedüs
Max Planck Institute for Informatics, Campus E1.4, 66123 Saarbruecken, Germany

INRIA Sud-Ouest Bordeaux, 200, Avenue de la Vieille Tour, 33400 Talence, France

Laboratoire Photonique, Numérique et Nanosciences (L2PN), UMR 5298, CNRS IOGS University Bordeaux, Institut d'Optique d'Aquitaine, 33405 Talence, France
e-mail: ramon.hegedus@gmail.com

G. Szél
Coleoptera Collection, Department of Zoology, Hungarian Natural History Museum, 1088 Budapest, Baross utca 13, Hungary
e-mail: szel@nhmus.hu

G. Horváth (ed.), *Polarized Light and Polarization Vision in Animal Sciences*, Springer Series in Vision Research 2, DOI 10.1007/978-3-642-54718-8_6,

6.1 Introduction: Circular Polarization in the Abiotic and Biotic Optical Environment

Throughout this chapter we use consequently the following nomenclature: A left-circular (LC) polarizer transmits left-circularly polarized (LCP) light and blocks right-circularly polarized (RCP) light, while a right-circular (RC) polarizer transmits RCP light and blocks LCP light. A circular polarization (CP) filter is the complement of a circular polarizer: An LCP filter blocks (i.e. filters) LCP light and transmits RCP light. Similarly, an RCP filter blocks RCP light and transmits LCP light.

The occurrence of circularly polarized (CP) light in nature is rare relative to the partially linearly polarized light (Horváth and Varjú 2004). In the abiotic optical environment, the three most important sources of CP are the light originating from certain stars and nebulae (Coulson 1974), the light reflected from some optically active stones and ground/soil surfaces (Wolstencroft 1974) and the underwater light total reflected from the air–water interface outside the Snell window (Waterman 1954; Ivanoff and Waterman 1958; Können 1985, p. 149). The light from the turbid sky also has a weak CP component due to the scattering of sunlight on special anisotropic aerosol particles (Hannemann and Raschke 1974; Hitzfelder et al. 1976).

In the biotic optical environment, the larvae of the fireflies, *Photuris lucicrescens* and *P. versicolor*, can be mentioned, the left and right lanterns of which emit weak LCP and RCP bioluminescent light at a peak wavelength of 540 nm (Wynberg et al. 1980), the function of which (if any) is, however, unknown. The birefringent cuticle of certain crustaceans reflects CP light (Neville and Luke 1971; see also Chap. 7), and the light passing through the semi-transparent body of certain dinoflagellates is also circularly polarized (Horváth and Varjú 2004, pp. 100–103; see also Chap. 19).

The Nobel laureate American physicist Albert Abraham Michelson (1852–1931) discovered in 1911 that the light reflected from the metallic coloured body surface of the golden scarab beetle *Chrysina* (formerly *Plusiotis*) *resplendens* had an LCP component (Fig. 6.1a, b). Robinson (1966), investigating the chemical structure and optical properties of cholesteric liquid crystals and observing CP light reflected from them, became fascinated by the studies of Michelson (1911) and obtained a variety of beetles, with which he repeated Michelson's investigations. He found that the light reflected from many beetle species belonging to the Scarabaeoidea was LC polarized. He emphasized that it would be of interest to consider what survival value can account for the occurrence of this most unusual property in so many species.

The LCP of light reflected from the exocuticle of certain scarabs can be easily demonstrated by observing them through an RC polarizer, when the body appears more or less dark (Fig. 6.2). The CP gloss spreads all over the body of some scarabs and is retained after the death of the animals. According to Können (1985, pp. 83–85) and Kattawar (1994), some mutant specimens may reflect not LCP but RCP light. Some specimens of *Chrysina resplendens*, for example, showed

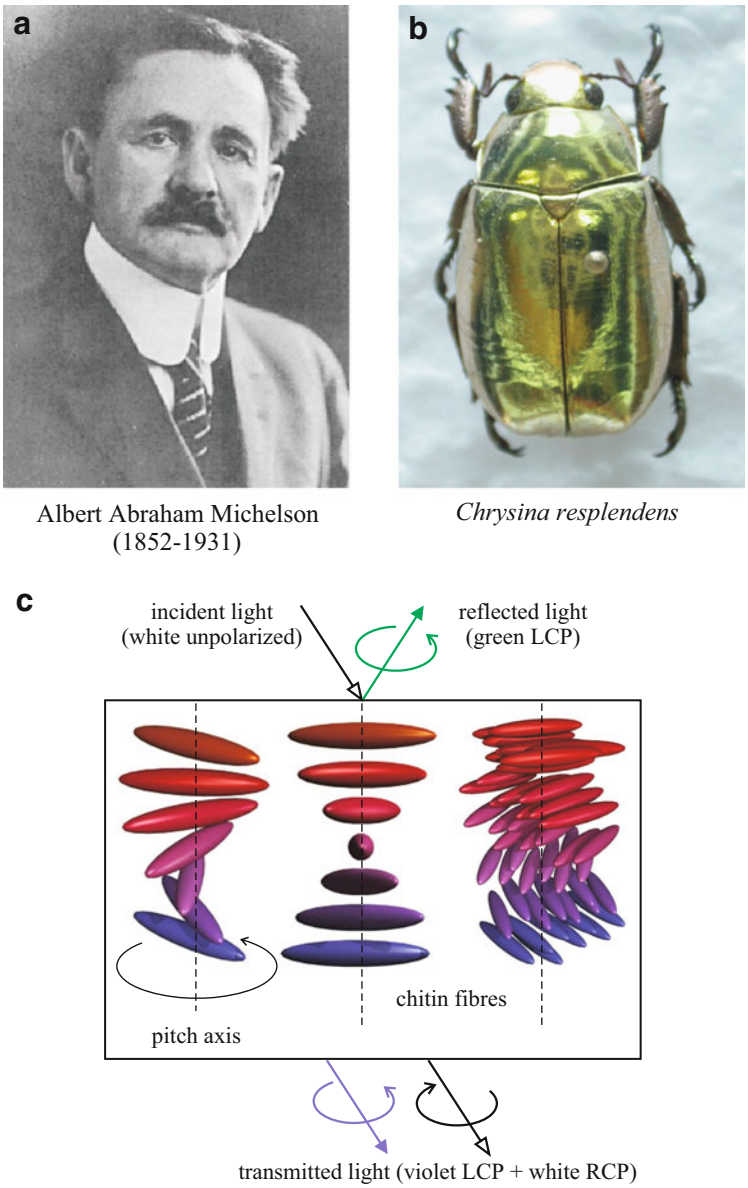

Fig. 6.1 (**a**) Portrait of the Nobel laureate American physicist, Albert Abraham Michelson (1852–1931), who discovered in 1911 that the light reflected from the exocuticle of the golden scarab beetle *Chrysina resplendens* is left-circularly polarized. (**b**) *Chrysina resplendens*. (**c**) The structure of the left-circularly polarizing exocuticle of scarabs is optically analogous to that of the cholesteric liquid crystals composed of layers in which the chitin fibres are ordered more or less parallel to each other, and the fibre direction turns continuously and evenly from layer to layer (the fibres of which have the same colour here) with a constant pitch. Due to this helicoidal structure, a white unpolarized incident light becomes green LC polarized after reflection, while the transmitted light is a combination of violet LCP and white RCP light

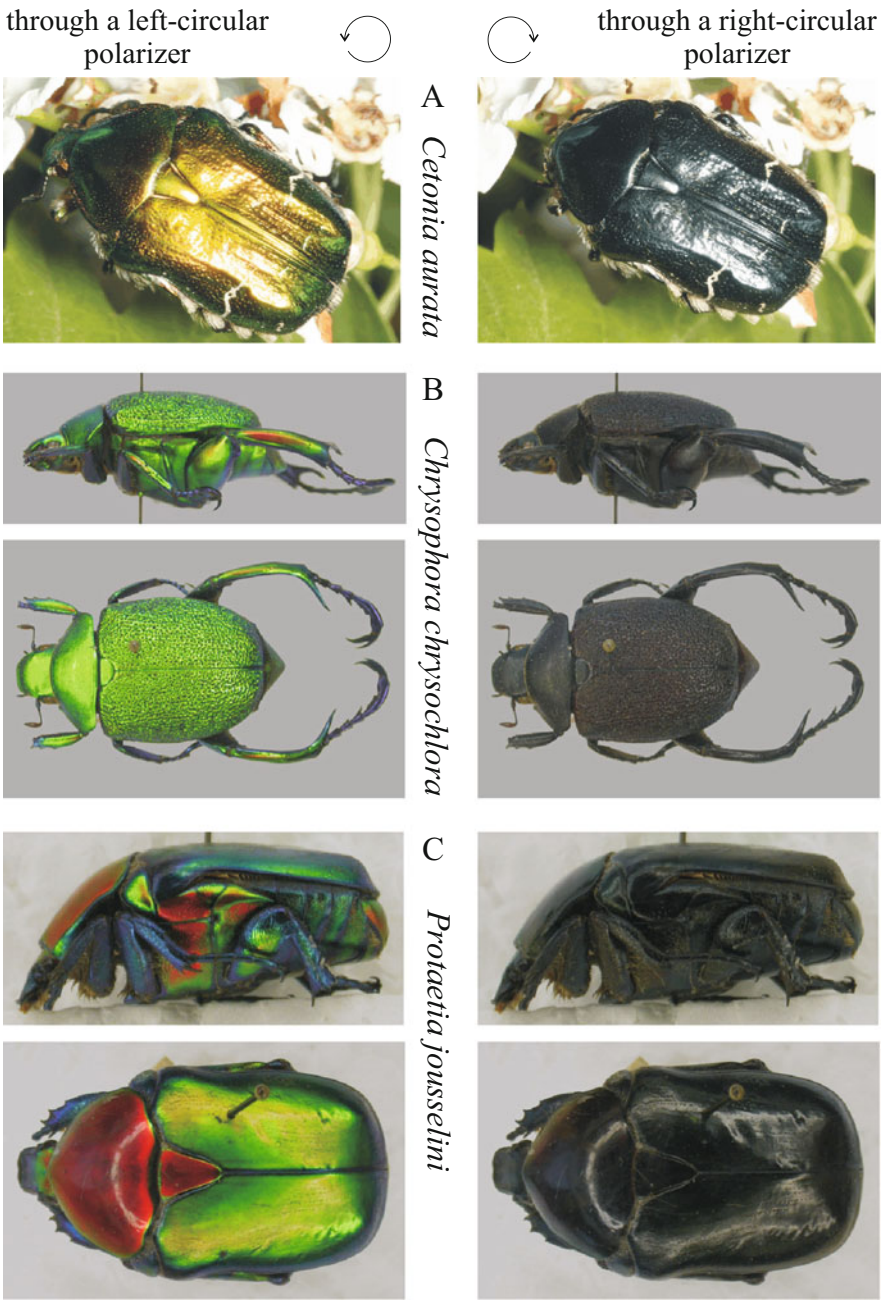

Fig. 6.2 Photographs of the scarab beetles *Cetonia aurata* (rose chafer) (**a**), *Chrysophora chrysochlora* (longleg scarab beetle) (**b**) and *Protaetia* (formerly *Cetonischema*, *Potosia*) *jousselini* (flower chafer) (**c**) taken through a right-circular and a left-circular polarizer. The *circular arrows* show the handedness of CP light transmitted by the polarizers

uniquely reversed handedness of reflected CP light, that is, RCP instead of LCP (Pye 2010a).

Pye (2010a) surveyed approximately 1,500 genera and more than 19,000 species/subspecies of scarab beetles (Scarabaeoidea) in the collection of the Natural History Museum, London, with LCP and RCP filters. He made more than 1,100 measurements of the degree of circular polarization d_c, in some cases registering $d_c = 97$ %. He experienced much intra- and interspecific variabilities: some scarab species were unpolarized or only weakly circularly polarized, but many were strongly circularly polarized. Such high d_c-values are unique in nature, since other phenomena generally produce less than 1 % CP. According to Pye (2010a), many circularly polarizing scarab species are strikingly metallic shiny in appearance, but many others are completely matte. Some metallic shiny scarabs do not polarize circularly. There are many examples of variation in CP associated with different colour morphs within a given scarab species: strongest with green, red and bronze colours, but almost invariably weaker with blue. CP may not even be consistent within a scarab species, because some subspecies, or even some individuals, show CP, whereas others do not. It is, however, remarkable that the handedness of CP is always the same uniformly on the body and appendages of scarabs, irrespective of normal bilateral symmetry (Pye 2010a).

Circular polarization had been previously described from four subfamilies of Scarabaeidae: Coprinae, Cetoniinae, Rutelinae and Melolonthinae. Pye (2010a) found CP in three further subfamilies: Phaenomeridinae, Dynastinae and Euchirinae, as well as in the subfamily Ceratocanthinae of the family Hybosoridae, comprising the first records outside the Scarabaeidae. Hence, reflected LCP light is common but not universal in one subfamily of the Hybosoridae and seven subfamilies of the Scarabaeidae. It is imaginable that CP reflection might be useful as a new, cladistic character in taxonomy (Pye 2010a). Nevertheless, the survey of Pye (2010a) did not suggest the presence of any cryptic species separable only by CP characteristics.

The selective reflection of LCP light is due to a special structure of the outer cuticle (exocuticle) being optically analogous to the cholesteric liquid crystals (Neville and Caveney 1969; Caveney 1971; Können 1985, pp. 139–140) (Fig. 6.1c). The direction of rotation of the electric field vector (E-vector) of reflected CP light depends on the sense of rotation of the helicoidal arrangement of parallel microfibrils in the exocuticle that show a steady rotation. The pitch of the helix determines the spectrum of the reflected CP light. In living organisms, the capability to produce a given helicoidal microfibril array is restricted to one sense of rotation, which has been fixed at a very early stage in evolution. Thus, apart from some mutants, this sense may be the same for all living organisms. Since the exoskeletons of all beetles reflecting CP light consists of the same substance, the sense of rotation of the E-vector of reflected light is the same, left-handed, for all of them (Können 1985, pp. 83–85). Since 1911 LC polarizing exocuticles (Fig. 6.2) have been reported in many scarab species (Neville and Caveney 1969; Können 1985, pp. 83–85; Wolken 1995, p. 189; Goldstein 2006; Hegedüs et al. 2006; Jewell et al. 2007; Pye 2010a).

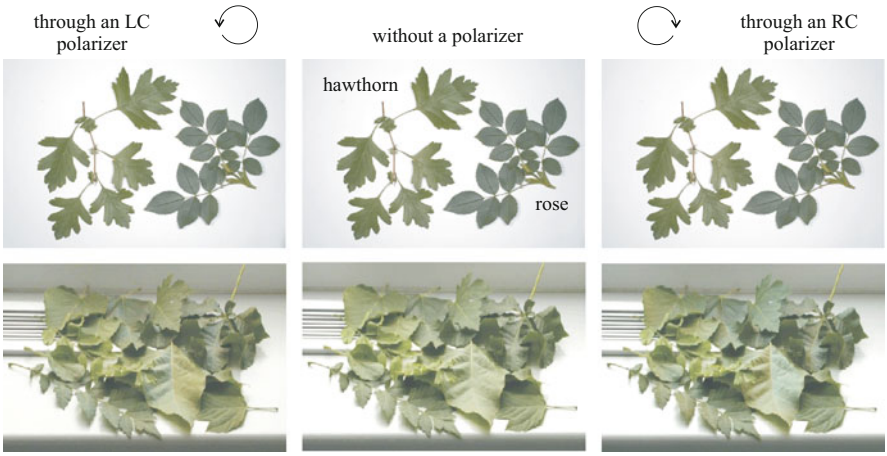

Fig. 6.3 *Row 1*: Photographs of hawthorn (*Crataegus monogyna*) and wild rose (*Rosa canina*) leaves (host plants of rose chafers and other scarab species) taken without a polarizer (*middle column*) and through a right-circular polarizer and a left-circular polarizer. In the *left* and *right columns* the *circular arrows* show the handedness of circularly polarized light transmitted by the polarizers. *Row 2*: As *row 1* for the following 12 different green plant leaves (host plants of many scarab species): black poplar (*Populus nigra*), London plane (*Platanus acerifolia*), common whitebeam (*Sorbus aria*), field maple (*Acer campestre*), small-leaved lime (*Tilia cordata*), European rowan (*Sorbus aucuparia*), wild cherry (*Prunus avium*), staghorn sumac (*Rhus typhina*), common elm (*Ulmus campestris*), pagoda tree (*Sophora japonica*), sweet chestnut (*Castanea sativa*), European birch (*Betula pendula*) [after Fig. 1 on page 1068 of Blahó et al. (2012)]

Earlier, the potential biological functions of CP light emitted, transmitted or reflected by different organisms have been enigmatic, because it was unknown whether these animals are at all able to perceive CP. Although Shurcliff (1955) observed that the human eye stimulated by CP light can perceive a visual illusion similar to the Haidinger's brushes (see Chap. 14) induced by linearly polarized light (Haidinger 1844), the discovery of a species being sensitive to CP happened only in 2008, when Chiou et al. (2008) and Kleinlogel and White (2008) showed that the stomatopod shrimp *Gonodactylus smithii* is able to detect CP light at the receptor level. Chiou et al. (2008) reported that the carapace of this marine shrimp has sexually dimorphic circularly polarizing reflective patches; furthermore, they also demonstrated behaviourally that these crustaceans can also be conditioned to CP light stimuli when foraging (see Chap. 7).

Since the discovery of Michelson (1911), it has been supposed that the scarab beetles possessing LC polarizing metallic shiny exocuticle (Fig. 6.2) in a vegetation environment being poor in CP light (Fig. 6.3) may also perceive CP. This could constitute a new form of covert intraspecific communication (Warrant 2010): For instance, the CP signals could allow identification of conspecifics at a distance that is too far for olfaction to be effective. A possible biological advantage of CP light is that there is no preferential viewing direction from which to detect CP (Brady and Cummings 2010), as is the case with linearly polarized light reflected from water surfaces, for instance (Horváth and Varjú 2004). Thus, animals using CP light to

communicate could send and receive signals regardless of their respective orientations. Cuttlefish (Shashar et al. 1996) and certain butterflies (Sweeney et al. 2003) are examples for invertebrates that use linearly polarized light signals in such covert conspecific visual interactions. Brady and Cummings (2010) claimed that jewel scarabs, *Chrysina gloriosa*, may be sensitive to CP. Warrant (2010) explained how beetles and other invertebrates could perceive CP light (see Chap. 7). On the other hand, Blahó et al. (2012) found no evidence for behavioural responses to CP light in the scarabs *Anomala dubia* (Scopoli 1763, Rutelinae), *Anomala vitis* (Fabricius 1775, Rutelinae), *Cetonia aurata* (Linnaeus 1761, Cetoniinae) and *Protaetia* (formerly *Potosia*) *cuprea* (Fabricius 1775, Cetoniinae) possessing strongly circularly polarizing exocuticle. Similarly, Miao et al. (2014) found no evidence for CP vision in the scarab beetle *Anomala corpulenta*. In behavioural choice experiments they showed that CP light does not influence the mating behaviour of *A. corpulenta* scarabs.

Thus, the question remains: What is the adaptive significance of LCP light reflected from the exocuticle, which seems to have evolved only in scarabaeoids. Blahó et al. (2012) suggested that the CP of reflected light may only be a by-product of the helicoidal structure of the scarab exocuticle. The function of this helicoidal structure could be a mechanical and/or chemical one in order to enhance the resistance of the exocuticle against mechanical stresses and/or acidic/alkaline damages. However, in the opinion of Pye (2010a), '*it is unlikely to have a mechanical function, such as increasing the strength of the cuticle; the sporadic distribution within each group, the variation in position on the body, and the extreme variability of the degree of [circular] polarization all appear to counter such a view. The [circular] polarization occasionally occurs in patterns (patches, stripes or edgings) and may occur only, or especially strongly, on the scutellum as in some melolonthines. It does not appear to be related to the varied ornamentations, excrescences or sculpturing of the surface*'.

The evolutionary significance of LCP reflection in scarabs is unknown and is therefore open to speculation. Pye (2010a, b) suggested that the LCP light of scarabs may be simply the equivalent of another colour—which demands an eye that can detect it. It is widely supposed that the bright colours of scarab beetles might provide camouflage in their forest environments: green for leafy backgrounds and metallic colours to imitate dappled sunlight. An ability to detect CP could break this camouflage, allowing beetles of the same species to identify each other at some distance, thereby aiding social interaction (Pye 2010a, b). Nevertheless, the truth of this hypothesis is drastically reduced by the findings of Blahó et al. (2012).

6.2 Imaging Polarimetry of Circularly Polarizing Scarab Beetles

In the literature sporadic photographs taken from certain scarab species (e.g. *Chrysina resplendens*, *Chrysina woodi*, *Cetonia aurata*, *Pelidnota sumptuosa* and *Pelidnota cyanitarsis*) through LC and RC polarizers are available (e.g. Können 1985, p 83; Kattawar 1994; Pye 2010a, b). Through an RC polarizer

these beetles appear more or less dark. This demonstration is, however, inadequate to quantitatively investigate the spatial distribution and the wavelength dependency of CP reflected from the metallic shiny exocuticle of scarabs. Hegedüs et al. (2006) developed a portable, rotating-analyser imaging polarimeter by which the linear and circular polarization patterns of scarabs can be quantitatively measured in the red, green and blue parts of the spectrum. This polarimeter consists of a digital camera, one RC and three LC polarizers mounted on a rotatable filter wheel (Fig. 6.4a). The first three polarizers mounted normally in front of the camera function as linear analysers with different angles of the transmission axis relative to the radius of the filter wheel, while the fourth polarizer is mounted reversed and functions as a circular analyser (Fig. 6.4b, c). The target insect is illuminated uniformly and omnidirectionally by rotationally symmetric two concentric, circular light tubes (Fig. 6.4d–f) emitting white light. The four polarization pictures of a given insect target are evaluated with an appropriate computer program resulting in the components S_0, S_1, S_2 and S_3 of the Stokes vector $\underline{S}$ of light reflected from the target towards the polarimeter. Component S_0 is the intensity; components S_1 and S_2 describe the linear polarization, while component S_3 characterizes the CP. Then the intensity I, degree of linear polarization d_L, angle of polarization α (measured from an arbitrary reference direction), ellipticity ε and degree of circular polarization d_c are calculated from the Stokes vector $\underline{S}$ as follows (Collett 1993):

Intensity:

$$I = S_0,$$

Degree of linear polarization:

$$d_L = \frac{\sqrt{S_1^2 + S_2^2}}{S_0},$$

Angle of polarization:

$$\alpha = \frac{1}{2}\arctan\left(\frac{S_2}{S_1}\right),$$

Ellipticity:

$$\varepsilon = \frac{1}{2}\arcsin\left(\frac{S_3}{S_0}\right),$$

Degree of circular polarization:

$$d_c = \sin\varepsilon \tag{6.1}$$

Finally, the patterns of I, d_L, α and d_c are visualized in the red (650 nm), green (550 nm) and blue (450 nm) spectral ranges.

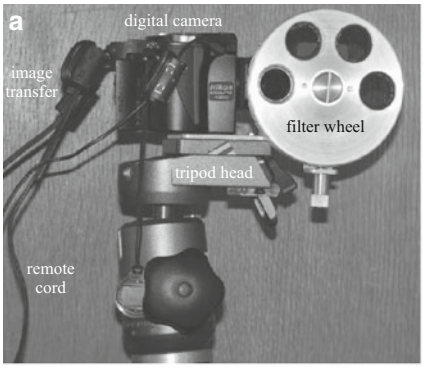

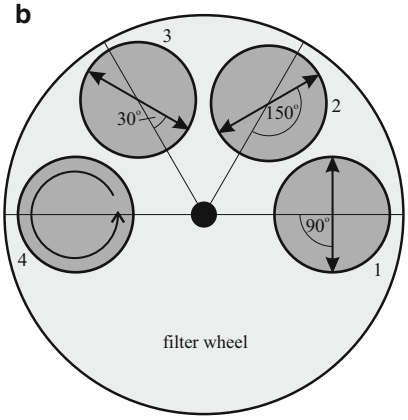

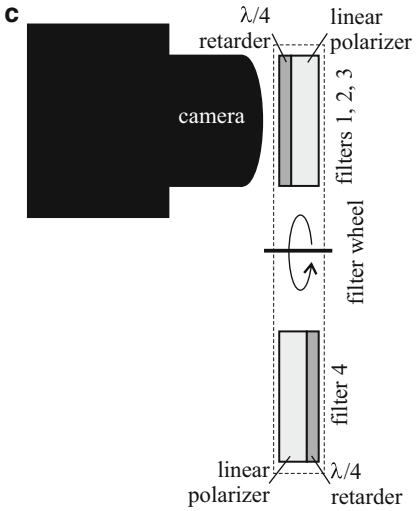

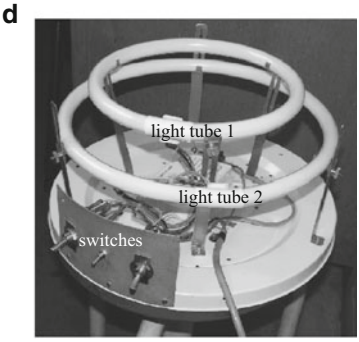

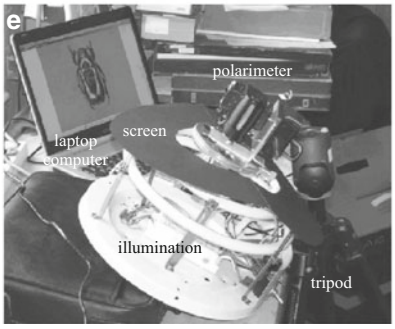

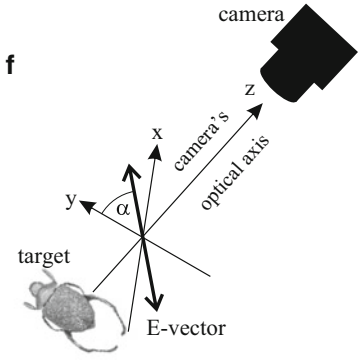

Fig. 6.4 (**a**) The portable, rotating-analyser, linear-circular imaging polarimeter of Hegedüs et al. (2006). (**b**) Filter wheel of the polarimeter with the four polarizers as seen by the camera. Filters 1–3 are LC polarizers, while filter 4 is a reversely mounted RC polarizer. Filters 1–3 function as linear analysers, the transmission axes of which are represented by *double-headed arrows*. Angles 90°, 150° and 30° are measured from the radius of the filter wheel. Filter

Hegedüs et al. (2006) measured the linear and circular polarization patterns of some air-dried specimens from the Coleoptera Collection of the Hungarian Natural History Museum in Budapest. They experienced that about 20 % of the species in both Rutelinae and Cetoniinae subfamilies (formerly families) have entirely or partially metallic shiny body. Beetles with circularly polarizing cuticles occur among these metallic shiny insects. However, not all metallic body parts reflect CP light. Hegedüs et al. (2006) found the wavelength- and species-dependent CP patterns to be of a rather complex nature.

Left-circularly polarizing scarabs become darker and brighter relative to the background when seen through an RC and an LC polarizer, respectively (Figs. 6.2, 6.5 and 6.6). The intensities of light passing through an RC and an LC polarizer are $I_{RC} = (S_0 - S_3)/2$ and $I_{LC} = (S_0 + S_3)/2$, where S_0 and S_3 are the components of the Stokes vector of light passing through the polarizer. Consequently, those parts of the exocuticle brighten through an LC polarizer which darken through an RC polarizer, and vice versa. This brightening and darkening effect depends on the degree and handedness of CP characterized by S_3.

As examples, Figs. 6.5 and 6.6 show the reflection-polarization patterns of the flower chafer, *Protaetia jousselini*, from above and the side. The head and the elytra of this beetle are metallic green, while the thorax and the scutellum (= triangular shield) are metallic red. In the green spectral range, the green head and elytra reflect strong LCP light, but in other spectral ranges they are only weakly circularly polarizing (Fig. 6.5m–o). Both the red thorax and red shield are strongly LC polarizing in the red, while weakly RC polarizing in the green and blue (Fig. 6.5m–o). This explains why the beetle appears completely black when seen through an RC polarizer (Figs. 6.5c and 6.6c): then both the LCP green light reflected from the head and elytra and the LCP red light reflected from the thorax and shield are filtered out. In Fig. 6.6 we can see in both the green and red spectral ranges the entire ventral side, while in the blue only some ventral areas of *Protaetia jousselini* are strongly LC polarizing. There is no significant contrast in CP between the dorsal and ventral sides of the beetle. The linear and circular polarization patterns of the metallic shiny *Chrysophora chrysochlora*, *Chrysina resplendens*, *Chrysina macropus*, *Ischiopsopha lucivorax*, *Calomacraspis haroldi*, *Protaetia jousselini* and a tropical flower scarab beetle are presented in the online-only Extra Materials.

Fig. 6.4 (continued) 4 functions as a circular analyser, in which the transmission axis of the linear polarizer component is arbitrarily aligned (and therefore is not displayed). The *circular arrow* represents the handedness of the circular polarizer 4. (**c**) Arrangement of the filters in front of the camera from the side. (**d**) Annular light source composed of two concentric, circular light tubes illuminating the target (scarab beetle) positioned along the axis of rotation of the tubes. These tubes produce a rotationally symmetric omnidirectional illumination. (**e**) Set-up of the measurement. (**f**) Reference system of coordinates for the description of light polarization. The *x*–*y* plane corresponds to the plane of the piece of paper. The angle of polarization α (that is the alignment of the E-vector of linearly polarized light) is measured from the *y*–*z* plane, which is the plane of reference of the Stokes vector [after Fig. 1 on page 2788 of Hegedüs et al. (2006)]

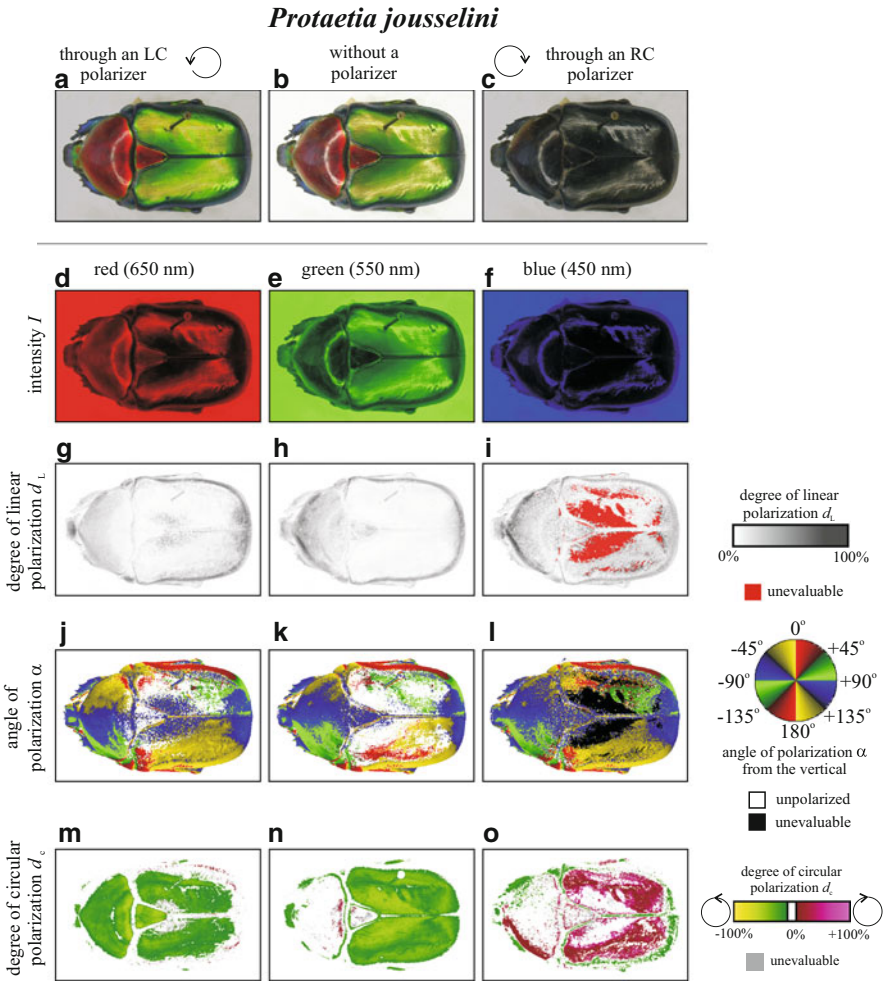

Fig. 6.5 Linear and circular polarization patterns of the flower chafer, *Protaetia jousselini*, measured by imaging polarimetry in the *red* (650 nm), *green* (550 nm) and *blue* (450 nm) parts of the spectrum. The *upper row* shows the appearance through an LC polarizer (**a**), an RC polarizer (**c**) and without a polarizer (**b**). The *circular arrows* here show the handedness of CP light transmitted by the polarizers. Below **a**–**c**, the *panels* are sorted by wavelength (650, 550, 450 nm). Rows **d**–**f**, **g**–**i**, **j**–**l**, **m**–**o** display the intensity I, degree of linear polarization d_L, angle of polarization α (measured clockwise from the vertical) and degree of circular polarization d_c. The illumination of the beetle was omnidirectional due to two circular light tubes [after Fig. 4 on page 2792 of Hegedüs et al. (2006)]

Michelson (1911) found that in his specimen of *Chrysina resplendens,* the LCP was strongest in the blue, diminished in yellow and was absent in the orange, while in the red spectral range he found RCP-reflected light rather than LCP light. Gaubert (1924) confirmed that relationship in *Chrysina amoena*. Hegedüs et al. (2006) investigated the problem with imaging polarimetry in *Chrysophora*

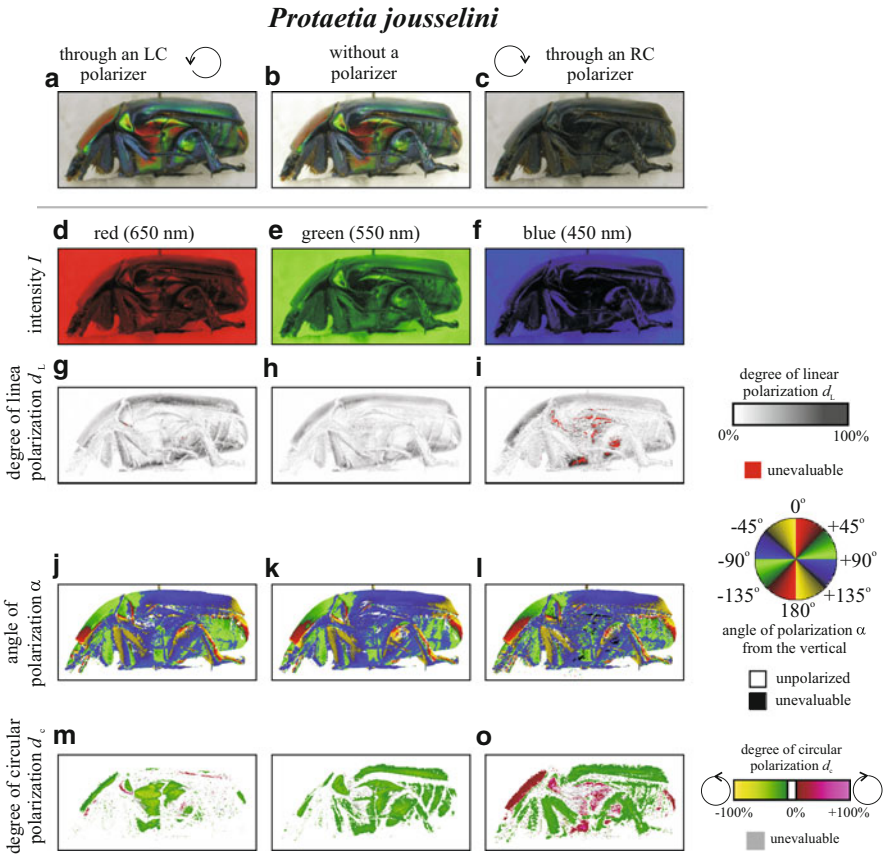

Fig. 6.6 As Fig. 6.5 from the side [after Fig. 5 on page 2793 of Hegedüs et al. (2006)]

chrysochlora, *Chrysina resplendens* and *Protaetia jousselini*. They found examples of RCP within certain wavelength ranges but concluded that the situation is complicated. Goldstein (2006) found that in *Chrysina resplendens* 'there are scarabs for which the hand of the circular polarization reverses from the blue end of the spectrum to the red'. Pye (2010a) has also found wavelength-dependent handedness of CP in certain scarab species. He concluded that the problem of spectrally dependent handedness of CP reflection clearly deserves much more detailed study.

6.3 Circular Polarization Sensitivity in *Chrysina gloriosa*?

Brady and Cummings (2010) tested for phototactic response and differential flight orientation of *Chrysina gloriosa* and *Chrysina woodi* scarab beetles towards different light stimuli. They performed double- and triple-choice experiments with each beetle in an experimental chamber presenting two or three different optical stimuli simultaneously. These stimuli were unpolarized (UP), vertically linearly polarized (LP), left-circularly polarized (LCP) and right-circularly polarized (RCP) light. All polarized stimuli were more intense by 15–19 % than the UP stimulus. Each beetle was tested up to four flights recorded per trial. A bright versus dark phototaxis experiment was used to establish positive phototaxis as a basis for the rest of the experiments. The UP versus LCP versus RCP experiment studied sensitivity to CP. The LP stimuli were used to establish the relative relationship between CP and LP reactions.

Chrysina gloriosa displayed significant nonrandom orientation towards specific stimuli in all choice experiments of Brady and Cummings (2010): (1) In the phototactic experiments, *C. gloriosa* exhibited a differential response towards the brighter unpolarized stimulus, indicating a simple positive phototaxis. (2) In the LP versus LCP versus RCP experiment, *C. gloriosa* displayed differential orientation among stimuli polarization with a graded response between the LP versus the CP stimuli being consistent with the differences in stimuli intensities. (3) In the LP versus LCP experiment between LP and CP light stimuli of equal intensities, a differential response was observed for *C. gloriosa*, while no discrimination was found in flight orientation for *C. woodi*. (4) In the UP versus RCP versus LCP experiment, where UP was 15–19 % lower in intensity, *C. gloriosa* favoured the less intense UP stimulus. Hence, *C. gloriosa* exhibited positive phototaxis, differential flight orientation between LP and CP stimuli of equal intensities and discrimination between CP and UP lights of different intensities. From their results Brady and Cummings (2010) concluded that *C. gloriosa* has linear and/or circular polarization sensitivity, while *C. woodi* cannot detect CP. This conclusion of Brady and Cummings (2010) is, however, not convincing and weakened by the following problems:

1. Although LCP light was slightly more preferred by *C. gloriosa* than RCP light, this could be simply explained by the fact that the RCP stimulus was slightly less intense than the LCP stimulus in the choice experiments of Brady and Cummings (2010): $\log I = 0.914$ for LCP and 0.872 for RCP, meaning a flux difference of 5 % between the two CP stimuli.
2. Although Brady and Cummings (2010) were aware of the serious problem caused by the blackness of the walls of any test box used in the study of polarization sensitivity[1], the inner covering of their test chamber was black,

[1] Brady and Cummings (2010, p. 616) wrote: *We used a matte black box to reduce experimental noise associated with phototaxis. A potential problem with using black backgrounds for polarization experiments is the Umow effect, where black backgrounds reflect higher percentages of polarized light than white backgrounds, increasing the chance of spurious polarized signals*

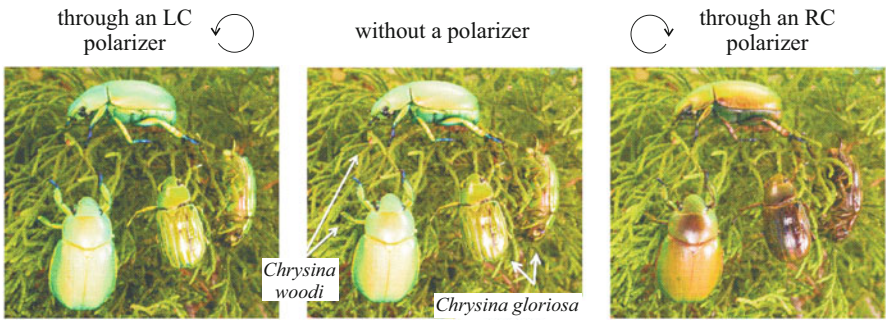

Fig. 6.7 Photographs of *Chrysina gloriosa* and *Chrysina woodi* scarab beetles on juniper branches photographed without a polarizer and through an LCP and an RCP polarizer. The *circular arrows* show the handedness of circularly polarized light transmitted by the polarizers. Photographs by John C. Abbott with the permission of Parrish Brady and Molly Cummings [after Fig. 1 on p. 615 of Brady and Cummings (2010)]

which can result in reflection-polarization-induced intensity patterns. These possible artefacts should be eliminated by matte white surfaces in all experiments investigating polarization vision. This has been reviewed in detail in Chapter 34 (entitled 'A Common Methodological Error: Intensity Patterns Induced by Selective Reflection of Linearly Polarized Light from Black Surfaces') of the book of Horváth and Varjú (2004, pp 381–383). Note that exactly such a methodological error resulted in an experimental artefact, from which the polarization sensitivity of homing pigeons (*Columba livia*) has been erroneously concluded (see the story in Horváth and Varjú 2004, pp. 342–348), for example. In the choice experiments of Blahó et al. (2012) the inner covering of the choice boxes was matte white or matte light brown to eliminate this artefact.

3. In the first choice experiment of Brady and Cummings (2010, Fig. 3b, p. 617), the numbers of responses of *C. gloriosa* were the following: to LP, LCP and RCP light 20, 10 and 3 responses, respectively. In their second experiment (Fig. 3d, p. 617 of Brady and Cummings 2010) the numbers of responses were 16, 3 and 1 to UP, LCP and RCP light, respectively. Statistically, no convincing conclusions can be drawn from such limited numbers (1, 3, 10, 16, 20) of scarab responses. In the choice experiments of Blahó et al. (2012), who concluded that *Cetonia aurata*, *Protaetia cuprea*, *Anomala vitis* and *A. dubia* scarabs do not perceive CP, conclusions were drawn from several hundreds of responses of the tested scarabs: in the third experiment 120 responses of *Cetonia aurata*; in the fourth experiment 468 responses of *Cetonia* and 100 responses of each *Protaetia cuprea*, *Anomala vitis*, *A. dubia*; in the fifth experiment 100 responses of each

(Horváth and Varjú 2004). These effects are not likely to significantly affect our results because of our box configuration. Reflected light off of the sides of the box will be at angles that will have minimal polarized Fresnel reflection relative to the test subject. Also, the light from the stimulus will be several orders of magnitude brighter than light reflected off the sides of the box.

Cetonia aurata, *Protaetia cuprea*, *Anomala vitis*, *A. dubia*; in the sixth experiment 869, 382, 415, 47 responses of *Anomala vitis*, *A. dubia*, *Cetonia aurata*, *Protaetia cuprea*, respectively; in the seventh and eighth experiments 100 responses of each *Cetonia aurata*, *Protaetia cuprea*, *Anomala vitis*, *A. dubia*.

4. According to Brady and Cummings (2010), *Chrysina gloriosa* with strongly circularly polarizing exocuticle (Fig. 6.7) responded differentially to CP light, while *C. woodi*, a close relative with reduced CP reflection (Fig. 6.7), exhibited no phototactic discrimination between LP and CP light. Brady and Cummings (2010) hypothesized that CP sensitivity may allow *C. gloriosa* to perceive and communicate with conspecifics that remain cryptic to predators, reducing indirect costs of communication. However, it is clear from Fig. 6.7 that the exocuticle of *C. woodi* reflects light with medium (rather than weak) degrees of CP; thus, along this logic this species could also possess CP sensitivity.
5. Brady and Cummings (2010) '*used a vertically oriented LP filter because the polarized field that these beetles would be exposed to would be from leaves, and vertical polarized light will be a dominating orientation of polarized light in this environment*'. However, it is a well-known fact that the direction of polarization of light reflected from sunlit vegetation is always perpendicular to the plane of reflection determined by the sun, the observer and the leaf observed (Horváth and Varjú 2004, pp. 374–375). Thus, the direction of polarization of foliage-reflected light generally differs from the vertical. It is approximately vertical only at sunset and sunrise when the sun is near but still above the horizon. On the other hand, horizontal direction of polarization of foliage-reflected skylight is typical prior to sunrise and after sunset, or under a totally overcast sky, when the vegetation is illuminated by scattered skylight, rather than direct sunlight.

Due to the above problems, the choice experiments aiming to test the response of *Chrysina gloriosa* scarabs to CP light should be repeated with a more appropriate methodology.

6.4 Lack of Circular Polarization Vision in Four Scarab Species with Circularly Polarizing Exocuticle

Cetonia and *Anomala* scarab beetles reflecting LCP light (Fig. 6.8) are common worldwide and are usually serious pests in the horti- and agriculture (Hill 2009). Blahó et al. (2012) performed choice experiments with several hundred individuals of the scarab species *Anomala dubia*, *A. vitis* (Coleoptera, Scarabaeidae, Rutelinae), *Cetonia aurata* and *Protaetia cuprea* (Coleoptera, Scarabaeidae, Cetoniinae) to decide whether they are attracted to CP light in different behavioural contexts:

- **Preliminary choice experiment 1** was performed in the field, where large (130 cm × 50 cm) vertical RC and LC polarizers were offered next to blooming hawthorn bushes (*Crataegus monogyna*, Rosaceae), where female and male *Cetonia aurata* scarabs swarmed. The reactions of flying *Cetonia aurata* to the

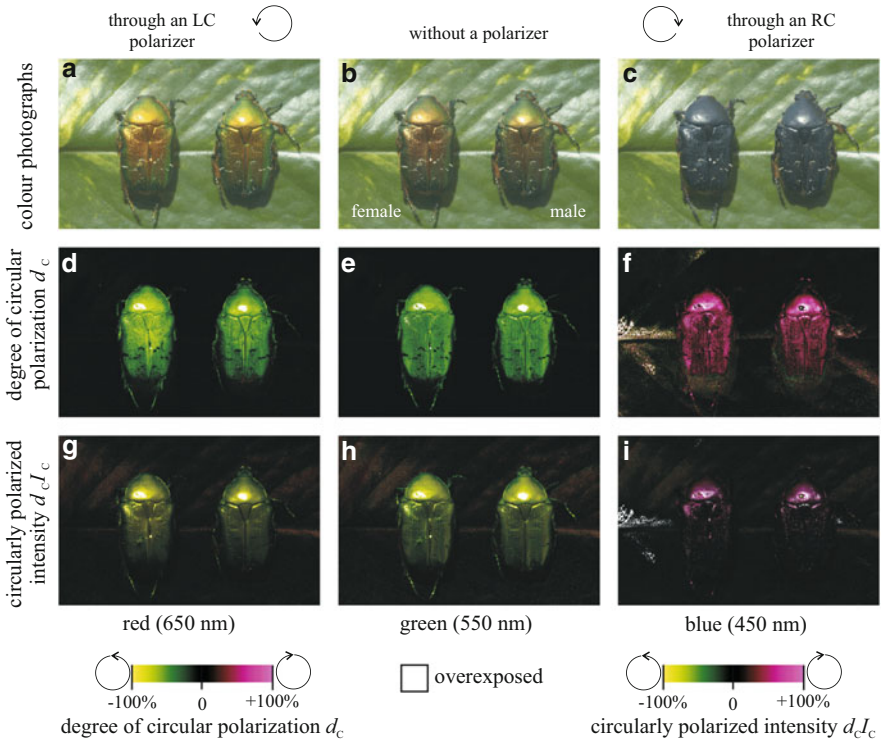

Fig. 6.8 *Row 1*: Photographs of *Cetonia aurata* scarab beetles (*left*: female, *right*: male) on a centipede tongavine (*Epipremnum pinnatum*) leaf taken without a polarizer and through an LC and an RC polarizer. The *circular arrows* show the handedness of circularly polarized light transmitted by the polarizers. *Row 2*: Patterns of the degree of circular polarization d_c of light reflected from the beetles and leaf measured by imaging polarimetry in the *red*, *green* and *blue* spectral ranges. *Row 3*: As *row 2* for the circularly polarized intensity I_c. Here luminance encodes I_c, while colour hue is given by the degree of circular polarization d_c with the same colour coding as in *row 2*. The background of the beetles in patterns **d–i** is almost totally *black*, because the leaf reflects practically circularly unpolarized light [after Fig. 1 on page 1068 of Blahó et al. (2012)]

circular polarizers were observed 10 times at different blossoming hawthorn bushes.

- **For preliminary choice experiment 2** five female and five male *Cetonia aurata* were collected from blossoming hawthorn bushes and released one by one from the grassy ground 2 m apart from the large vertical RC and LC polarizers. Again, the reactions of the released and flying *Cetonia* scarabs to the circular polarizers were observed 10 times at different blossoming hawthorn bushes.

In these preliminary experiments, *Cetonia aurata* displayed no reaction to the LCP and RCP stimuli: the released scarabs simply flew away without any approach towards the CP stimuli.

- **Experiment 1** was conducted with 120 *Cetonia aurata* (65 females, 55 males). The test chamber had two vertical test windows: one covered with an LCP filter and the other with an RCP filter. The outer surface of the polarizers was covered by a white diffuser.
- **Experiment 2** was done with the scarab species *Cetonia aurata* (196 individuals), *Protaetia cuprea* (100), *Anomala vitis* (100) and *A. dubia*. (100). The choice box presented 12 vertical colour pictures of the same scene (a *Cetonia aurata* sitting on a *Crataegus monogyna* hawthorn flower, hawthorn flowers and leaves, a blooming hawthorn bush) covered alternating with an LC and an RC polarizer.
- **Experiment 3** was performed with 100 individuals of each *Cetonia aurata*, *Protaetia cuprea*, *Anomala dubia* and *A. vitis*. The choice box offered two optical stimuli (Fig. 6.9): (1) one female and one male scarab carcass (illuminated by ultraviolet and visible light) of the same species as the test beetle seen directly and (2) one female and one male dead scarab of the same species as the test beetle seen through a plane glass-silver mirror tilted at 45° from the horizontal. The function of this mirror was to convert the LCP light originating from the shiny metallic green exocuticle of the stimulus beetles to RCP light after reflection (Fig. 6.10). This mirror effect has been discovered by the French crystallographer Gaubert (1924), who observed that the handedness of rotation of LCP light reflected from a scarab beetle was reversed (became RCP) when viewed in a mirror (Pye 2010a, b).
- **Experiment 4** was conducted to see whether the LCP light from dead adult scarabs evokes attraction from three feral scarab populations in the field. Two trapping experiments were conducted: one with *Anomala vitis* and *A. dubia* and the second with *Cetonia aurata*. CSALOMON® VARb3 traps (Schmera et al. 2004) with transparent upper funnels were used. Treatments included (1) Traps with dead beetles (without semiochemicals) glued to the inside of the transparent funnel of the trap. (2) Unbaited traps for negative control. (3) Traps baited with sex attractants (Tóth et al. 1994), or floral attractants (Vuts et al. 2010) for positive control.
- **In pilot experiments** it was tested with all scarab individuals investigated in experiments 5 and 6 whether a positive phototaxis can be elicited from them. The beetles could choose between a dark and a bright unpolarized white light. For experiments 5 and 6 only those scarabs were used that evidently were positively phototactic.
- **Experiment 5** was performed with 100 individuals of each *Cetonia aurata*, *Protaetia cuprea*, *Anomala vitis* and *A. dubia*. In all six sectors of the choice box the same picture, a blooming hawthorn bush, was seen through an LC polarizer (the quarter-wavelength retarder layer of which faced the test beetle and the linear polarizing sheet of which faced the colour picture) in the left window, and through a reversed LC polarizer (with its quarter-wavelength retarder layer facing the colour picture, while its linear polarizing sheet facing the test beetle) in the right window. Thus, the intensity and colour characteristics of both stimuli were the same, and only their polarization characteristics (LCP and LP with angle of polarization of 45° from the horizontal) were different.

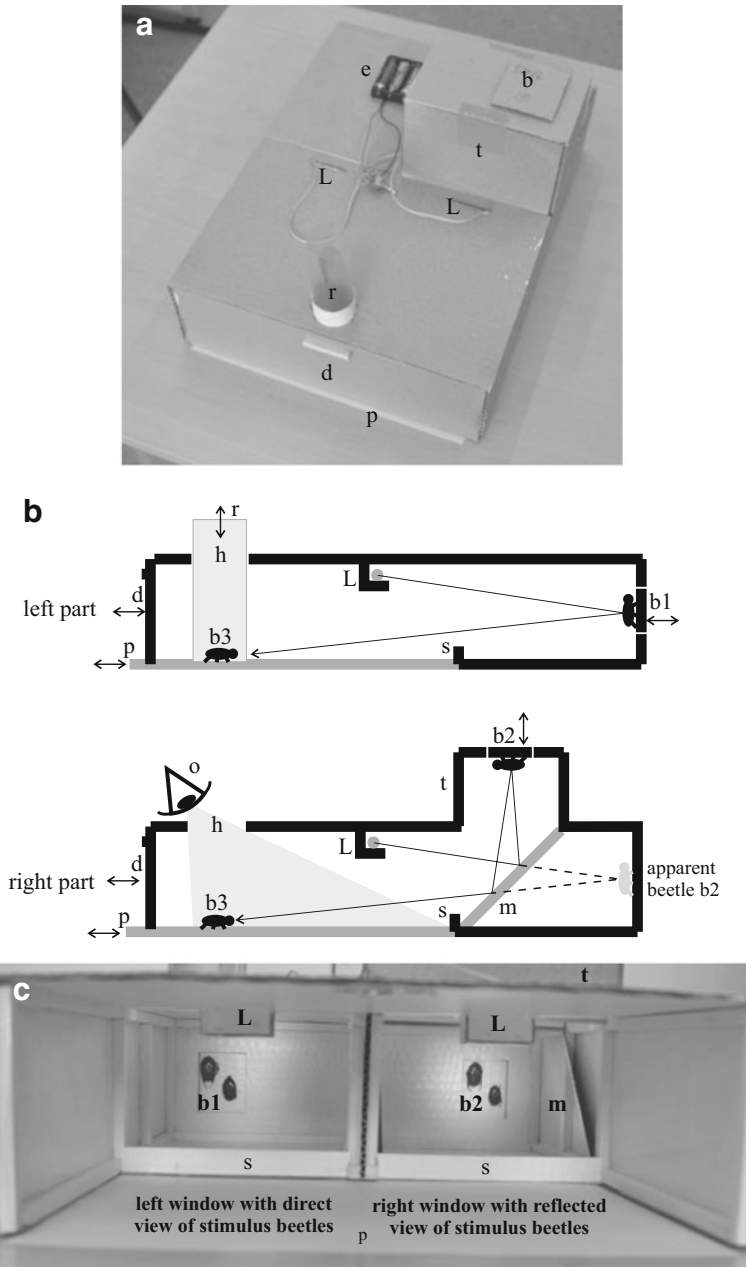

Fig. 6.9 Structure of the choice box used in experiment 3 of Blahó et al. (2012). (**a**) Photograph of the choice box taken from above. d: door, p: paper sheet, r: release cylinder, L: light-emitting diodes, e: electrical batteries as power supplies for the diodes, t: tower and b: holder of dead beetles. (**b**) Cross section of the *left* and *right parts* of the choice box showing the inner structure. *Double-headed arrows* represent that the concerned component is removable. h: circular hole through which the test beetle can be observed; b3: test beetle; s: a bar of cardboard closing the

- **Experiment 6** was conducted with 100 individuals of each *Cetonia aurata*, *Protaetia cuprea*, *Anomala vitis* and *A. dubia*. In the choice box one of the windows transmitted LCP white light and the other window transmitted unpolarized (UP) white light.

In all these experiments the test beetles could select from two different optical stimuli with the same intensity, towards which they crawled or flew. The order of the two stimuli was randomized between test runs. The inner surfaces of the choice boxes were painted by matte white to eliminate any disturbing polarization of wall-reflected light. Each individual beetle was tested 1–3 times. The possible influence of odour marks left by the scarabs tested was appropriately eliminated. Furthermore, the experimental conditions excluded the possibility that the test beetles would lose their motivation to look for mate/conspecifics and/or host plants: during these experiments the scarabs were active and motivated, being obviously in mating and/or foraging mood.

The whole cuticle (both dorsal and ventral) of *Cetonia aurata*, *Protaetia cuprea* and *Anomala vitis* is metallic shiny green and reflects intense LCP light (Fig. 6.8). In the case of *A. Dubia* the brownish elytra reflect weak LCP light, while other parts of the cuticle reflect intense LCP green light. The reflection spectra of the LC polarizing exocuticle of *Anomala vitis*, *A. dubia*, and *Cetonia aurata* have a single peak in the green (*Anomala vitis*: 562 nm, *A. dubia*: 614 nm, *Cetonia*: 574 nm) part of the spectrum, while *Protaetia cuprea* possesses a main peak in the red (670 nm) and a secondary peak in the green (549 nm) (Fig. 6.11). The only peak results in the metallic green colour of *Anomala* and *Cetonia*, and the two peaks result in the brownish green colour of *Protaetia cuprea*. Due to the green CP peak of the exocuticle in *Anomala vitis*, *A. dubia* and *Cetonia aurata* and the green and red CP peaks in *Protaetia cuprea* (Fig. 6.11), it could be expected that these scarabs would perceive CP in the visible part of the spectrum, rather than in the UV.

The light reflected from the host plants (hawthorn: *Crataegus monogyna*, wild rose: *Rosa canina*, black poplar: *Populus nigra*, London plane: *Platanus acerifolia*, common whitebeam: *Sorbus aria*, field maple: *Acer campestre*, small-leaved lime: *Tilia cordata*, European rowan: *Sorbus aucuparia*, wild cherry: *Prunus avium*, staghorn sumac: *Rhus typhina*, common elm: *Ulmus campestris*, pagoda tree: *Sophora japonica*, sweet chestnut: *Castanea sativa*, European birch: *Betula pendula*) of these scarabs is circularly unpolarized (Fig. 6.3).

In the above experiments of Blahó et al. (2012), there were no statistically significant choice differences between the two differently polarized (LCP versus

Fig. 6.9 (continued) choice arena; b1: holder of dead beetles seen directly; o: observer; m: tilted plane mirror; b2: holder of dead beetles seen through the tilted mirror. (**c**) The view seen by a test beetle. L: box of the light-emitting diodes; b1: left holder of dead scarab beetles seen directly, presenting LCP light stimuli originating from the beetles' exocuticle; b2: right holder of dead scarabs seen through the tilted plane mirror, presenting RCP light stimuli originating from the exocuticle of beetles being in the tower [after Fig. 2 on page 1071 of Blahó et al. (2012)]

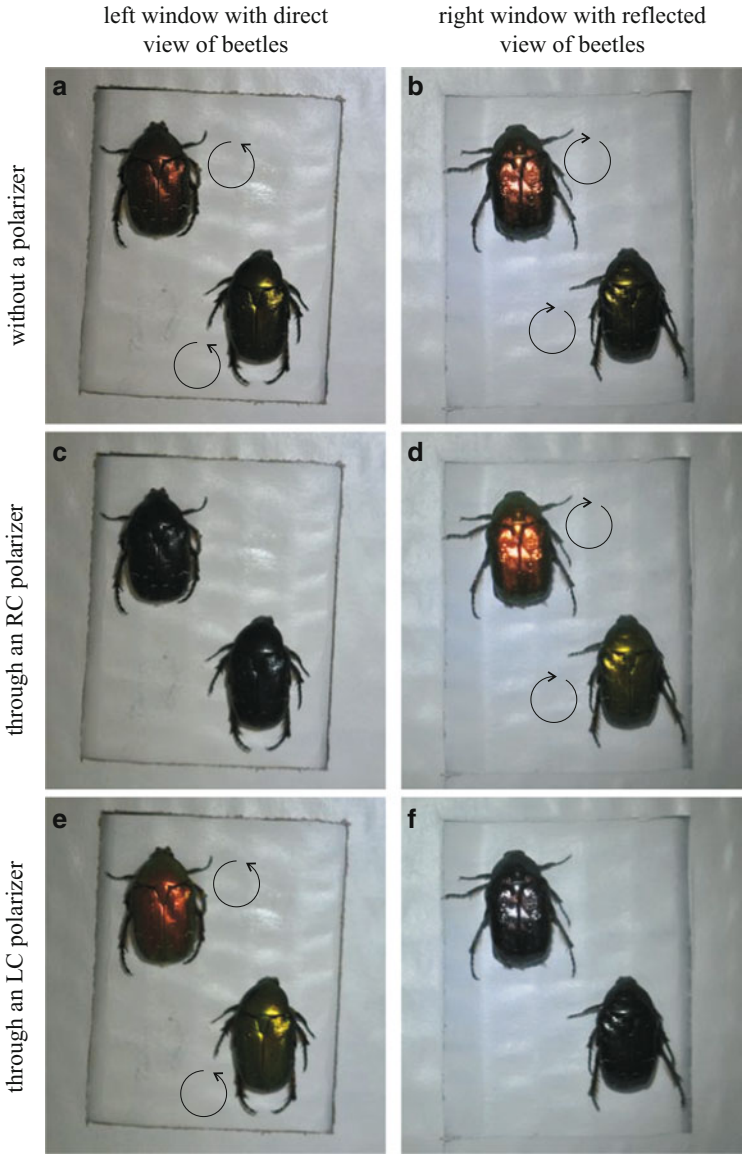

Fig. 6.10 Photographs of the stimulus beetles (*Cetonia aurata*) in the *left* and *right windows* of the choice box used in experiment 3 of Blahó et al. (2012) taken without a polarizer (**a**, **b**), and through an RC polarizer (**c**, **d**) and an LC polarizer (**e**, **f**), respectively. In the *left window* the dead scarabs were seen directly, presenting LCP light stimuli originating from their exocuticle. In the *right window* the dead scarabs were seen through a tilted plane mirror, presenting RCP light stimuli. The *circular arrows* show the handedness of CP light transmitted by the polarizers. In C the beetles are *black*, because the RC polarizer absorbed the LCP light originating directly from the beetles' exocuticle. In F the beetles are *black*, because the LC polarizer absorbed the RCP light originating from the exocuticle and reflected from the mirror. The sides of the rectangular windows of the stimulus beetles were horizontal and vertical. Here, they are tilted due to the slight tiltness of the photographic camera [after Supplementary Fig. S5 of Blahó et al. (2012)]

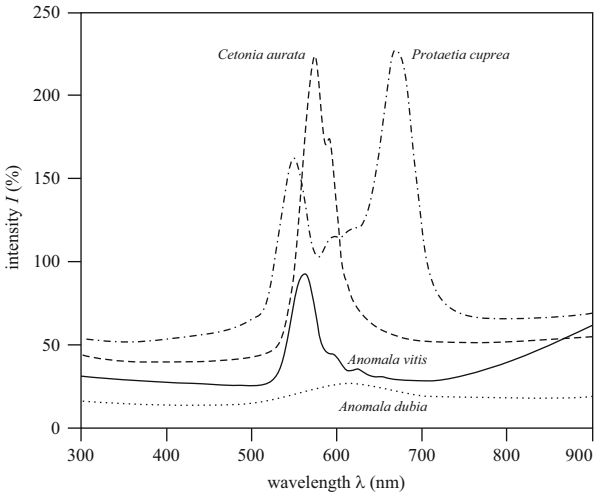

Fig. 6.11 Typical reflection spectra of the metallic shiny, LC polarizing exocuticle of *Anomala vitis*, *A. dubia*, *Cetonia aurata* and *Protaetia cuprea* scarab beetles measured at normal reflection. The value of reflected intensity *I* is measured relative to the diffuse reference reflection standard of the instrument. *I*-values can be larger than 100 %, if a surface reflects a greater amount of light than the diffuse reference standard [after Fig. 3 on page 1072 of Blahó et al. (2012)]

RCP, LCP versus LP, LCP versus UP) stimuli for *Cetonia aurata*, *Protaetia cuprea*, *Anomala dubia* and *A. vitis*. The reactions of these scarabs practically corresponded to a random choice between the two stimuli presented. The traps with sex attractant caught a high number of *Anomala dubia* and *A. vitis*, significantly different from all other treatments. On the other hand, single or no *Anomala* specimens were captured by traps with dead *Anomala* scarabs and by unbaited traps. The floral-attractant-baited traps caught significantly more *Cetonia aurata* and *Protaetia cuprea* than the traps with dead *Cetonia* or the unbaited traps.

From the results of these experiments, Blahó et al. (2012) concluded that *Cetonia aurata*, *Protaetia cuprea*, *Anomala vitis* and *A. dubia* scarabs are not attracted to CP light when looking for food or mate/conspecifics. The LC polarizing ability of scarab cuticles has been discovered by Michelson (1911). For a century, one could have believed that this CP could be an optical cue for scarabs. One hundred years after Michelson's discovery, Blahó et al. (2012) showed that CP light reflected from the mentioned four scarab species has no visual function.

In experiment 4 of Blahó et al. (2012) the scarabs found each other by means of pheromones, rather than by visual cues, e.g. the exocuticle-reflected LCP light. If these scarabs can find each other by means of odours, they do not need visual cues to find mate/conspecifics. Thus, Blahó et al. (2012) suggested that the CP of exocuticle-reflected light may only be a by-product of the helicoidal structure of scarab exocuticle. Instead, the major function of this helicoidal structure could be, for example, a mechanical or chemical one (in order to enhance the resistance of the exocuticle against mechanical stresses and/or acidic/alkaline damages), rather than optical (to produce LCP light for visual communication). This mechanical/chemical hypothesis should be tested in the future.

Recently, Miao et al. (2014) showed that the mating behaviour of *Anomala corpulenta* scarabs, close relatives of *A. dubia* and *A. vitis*, is not influenced by circular polarization. Thus, in three species (*Anomala vitis*, *A. dubia*, *A. corpulenta*) of the subfamily Rutelinae and in two species (*Cetonia aurata*, *Protaetia cuprea*) of the subfamily Cetoniinae in the family Scarabaeidae (Coleoptera), all possessing LC polarizing exocuticle, no evidence has been found for behavioural responses to CP light. Furthermore, there are no sexual differences in the polarization characteristics of exocuticular reflections, and attraction by pheromones seems more important than vision in finding mate/conspecifics. Since the visual system of scarab beetles shares basic optical and anatomical features (Gokan and Meyer-Rochow 2000), these results might be generalized among scarabs.

6.5 Outlook: Conclusion and Future Research

On the basis of the review performed in this chapter, our main conclusion is that despite the intensive research and the hypotheses/speculations of many scientists over the last hundred years, the sensitivity to CP of the visual system of scarab beetles possessing LC polarizing exocuticle and the function (if any) of the helicoidal structure of the exocuticle of these beetles (inducing reflected LCP light) remain henceforward elusive.

The anatomical prerequisite for perception of CP is a quarter-wavelength ($\lambda/4$) retarder in front of photoreceptors with orthogonal microvilli being sensitive to linear polarization (LP) (Warrant 2010). The whole system operates as a circular polarizer: The $\lambda/4$ retarder converts CP light into LP light that could be detected (transmitted or absorbed) by the underlying two LP filters L1 and L2. If the incoming light is LC polarized, the $\lambda/4$ retardation results in LP light with a direction of polarization that maximally stimulates subsystem L1, which thus has LCP sensitivity, but if the incoming light is RC polarized, subsystem L2 is maximally stimulated, which thus has RCP sensitivity (for further details about such a CP visual system in stomatopod crustacenas see Chap. 7). Whether jewel scarabs, *Chrysina gloriosa*, with their alleged CP sensitivity surmised by Brady and Cummings (2010), employ a similar mechanism remains to be (re)investigated. Furthermore, considering CP vision in scarab beetles, the following topics are worthy of future research:

- **Survey of CP reflection from scarab exocuticles**: The pioneering and thorough survey of the distribution of CP light reflection in the Scarabaeoidea performed by Neville and Caveney (1969) and Pye (2010a) could be continued and extended to scarab species not investigated until now.
- **Structural and optical investigation of the circularly polarizing exocuticle in scarabs**: The fine anatomical details of the helicoidal structure of different scarab exocuticles and the induced spectral and polarization characteristics of exocuticle-reflected light could be revealed with the methods used by Robinson

(1966), Caveney (1971), Neville and Luke (1971), Goldstein (2006), Hegedüs et al. (2006), Jewell et al. (2007), for example.

- **Behavioural tests of CP sensitivity in scarabs**: The sensitivity to CP of the eyes in scarab species not investigated yet could be studied with similar choice experiments as performed by Brady and Cummings (2010), Blahó et al. (2012) and Miao et al. (2014).
- **Anatomical and receptor(electro)physiological studies of CP sensitivity in scarab retinae**: If behavioural tests proved really convincingly the CP sensitivity in a scarab species, its retinal anatomy could be investigated, and more importantly, the CP sensitivity of photoreceptors should be directly demonstrated by electrophysiology, as performed by Chiou et al. (2008) and Kleinlogel and White (2008) in stomatopod crustaceans.

References

Blahó M, Egri Á, Hegedüs R, Jósvai J, Tóth M, Kertész K, Biró LP, Kriska G, Horváth G (2012) No evidence for behavioral responses to circularly polarized light in four scarab beetle species with circularly polarizing exocuticle. Physiol Behav 105: 1067–1075 + electronic supplement

Brady P, Cummings M (2010) Differential response to circularly polarized light by the jewel scarab beetle *Chrysina gloriosa*. Am Nat 175:614–620

Caveney S (1971) Cuticle reflectivity and optical activity in scarab beetles: the role of uric acid. Proc R Soc Lond B 178:205–225

Chiou TH, Kleinlogel S, Cronin T, Caldwell R, Loeffler B, Siddiqi A, Goldizen A, Marshall J (2008) Circular polarization vision in a stomatopod crustacean. Curr Biol 18:429–434

Collett E (1993) Polarized light—fundamentals and applications. Marcel Dekker, New York

Coulson KL (1974) The polarization of light in the environment. In: Gehrels T (ed) Planets, stars and nebulae studied with photopolarimetry. University of Arizona Press, Tucson, AZ, pp 444–471

Gaubert P (1924) Sur la polarisation circulaire de la lumière réfléchie par les Insectes. Compte rendu hebdomadaire des séances de l'Académie des sciences de Paris 179:1148–1150

Gokan N, Meyer-Rochow VB (2000) Morphological comparisons of compound eyes in Scarabaeoidea (Coleoptera) related to the beetles' daily activity maxima and phylogenetic positions. J Agric Sci 45:15–61

Goldstein DH (2006) Polarization properties of Scarabaeidae. Appl Opt 45:7944–7950

Haidinger W (1844) Über das direkte Erkennen des polarisierten Lichts und der Lage der Polarisationsebene. Annalen der Physik und Chemie 63:29–39

Hannemann D, Raschke E (1974) Measurements of the elliptical polarization of sky radiation: preliminary results. In: Gehrels T (ed) Planets, stars and nebulae studied with photopolarimetry. University of Arizona Press, Tucson, AZ, pp 510–513

Hegedüs R, Szél G, Horváth G (2006) Imaging polarimetry of the circularly polarizing cuticle of scarab beetles (Coleoptera: Rutelidae, Cetoniidae). Vis Res 46:2786–2797

Hill DS (2009) Pests of crops in warmer climates and their control. Springer, Heidelberg

Hitzfelder SJ, Plass GN, Kattawar GW (1976) Radiation in the earth's atmosphere: its radiance, polarization, and ellipticity. Appl Opt 15:2489–2500

Horváth G, Varjú D (2004) Polarized light in animal vision—polarization patterns in nature. Springer, Heidelberg

Ivanoff A, Waterman TH (1958) Elliptical polarization of submarine illumination. J Mar Res 16: 255–282

Jewell SA, Vukusic P, Roberts NW (2007) Circularly polarized colour reflection from helicoidal structures in the beetle Plusiotis boucardi. New J Phys 9: Art. No. 99
Kattawar GW (1994) A search for circular polarization in nature. Opt Photonics News Sept 1994: 42–43
Kleinlogel S, White AG (2008) The secret world of shrimps: polarisation vision at its best. PLoS One 3(5):1–8, e2190. doi:10.1371/journal.pone.0002190
Können GP (1985) Polarized light in nature. Cambridge University Press, Cambridge
Miao J, Wu YQ, Li KB, Jiang YL, Gong ZJ, Duan Y, Li T (2014) Evidence for visually mediated signal in mate choice in the scarab beetle *Anomala corpulenta*. J Insect Behav (in press)
Michelson AA (1911) On metallic colouring in birds and insects. Philos Mag 21:554–567
Neville AC, Caveney S (1969) Scarabaeid beetle exocuticle as an optical analogue of cholesteric liquid crystals. Biol Rev 44:531–562
Neville AC, Luke BM (1971) Form optical activity in crustacean cuticle. J Insect Physiol 17: 519–526
Pye JD (2010a) The distribution of circularly polarized light reflection in the Scarabaeoidea (Coleoptera). Biol J Linn Soc 100:585–596
Pye JD (2010b) Left-handed beetles. Phys World August 2010: 52
Robinson C (1966) The cholesteric phase in polypeptide solutions and biological structures. Mol Cryst 1:467–494
Schmera D, Tóth M, Subchev M, Sredkov I, Szarukán I, Jermy T, Szentesi Á (2004) Importance of visual and chemical cues in the development of an attractant trap for *Epicometis* (*Tropinota*) *hirta* Poda (Coleoptera: Scarabaeidae). Crop Prot 23:939–944
Shashar N, Rutledge PS, Cronin TW (1996) Polarization vision in cuttlefish: a concealed communication channel? J Exp Biol 199:2077–2084
Shurcliff WA (1955) Haidinger's brushes and circularly polarized light. J Opt Soc Am 45:399
Sweeney A, Jiggins C, Johnsen S (2003) Polarized light as a butterfly mating signal. Nature 423: 31–32
Tóth M, Leal WL, Szarukán I, Lesznyák M, Szőcs G (1994) 2-(E)-Nonen-1-ol: male attractant for chafers *Anomala vitis* Fabr. and *A. dubia* Scop. (Coleoptera: Scarabaeidae). J Chem Ecol 20: 2481–2487
Vuts J, Imrei Z, Tóth M (2010) New co-attractants synergizing attraction of *Cetonia aurata aurata* and *Potosia cuprea* to the known floral attractant. Zeitschrift für angewandte Entomologie 134:9–15
Warrant EJ (2010) Polarisation vision: beetles see circularly polarised light. Curr Biol 20(14): R610–R612
Waterman TH (1954) Polarization patterns in submarine illumination. Science 120:927–932
Wolken JJ (1995) Light detectors, photoreceptors, and imaging systems in nature. Chapter 13. Polarized light in nature: detection by animals. Oxford University Press, Oxford
Wolstencroft RD (1974) The circular polarization of light reflected from certain optically active surfaces. In: Gehrels T (ed) Planets, stars and nebulae studied with photopolarimetry. The University of Arizona Press, Tucson, AZ, pp 495–499
Wynberg H, Meijer EW, Hummelen JC, Dekkers HPJM, Schippers PH, Carlson AD (1980) Circular polarization observed in bioluminescence. Nature 286:641–642

Chapter 7
Polarisation Vision of Crustaceans

Justin Marshall and Thomas Cronin

Abstract The photoreceptor design of crustaceans, often containing regular arrays of intrinsically polarisation-sensitive microvilli, has had a profound influence on the visual biology of this subphylum. The land-based arthropods (insects and arachnids) also construct photoreceptors from ordered microvilli; however while in many species polarisation sensitivity results, a general overview of these groups suggests a major difference. With notable exceptions discussed in this chapter, many crustaceans seem to have "invested" in polarisation vision more than colour vision. This may be the result of the relatively limited spectral environment found in much of the aquatic world or due to the information content in polarisation being as useful as colour. The terrestrial arthropods are generally trichromatic with specialised visual areas for polarisation-specific tasks. Crustaceans are mostly di- or monochromats and most of their visual field displays polarisation sensitivity. This chapter examines the anatomical, neurophysiological and behavioural evidence for polarisation vision in a few of the many crustacean groups. Common themes are emerging such as the possession of vertical and horizontal E-vector sensitivity. This two-channel orthogonality is carried through the neural processing of information and reflected in behavioural capability. A few groups such as the stomatopods possess both complex colour and polarisation sensitivity, and particularly in this group, the evolutionary pressures responsible are centred on unique

Electronic supplementary material is available in the online version of this chapter at 10.1007/978-3-642-54718-8_7. Colour versions of the black and white figures can also be found under http://extras.springer.com

J. Marshall (✉)
Sensory Neurobiology Group, Queensland Brain Institute, University of Queensland, St Lucia, Brisbane, QLD 4072, Australia
e-mail: justin.marshall@uq.edu.au

T. Cronin
Department of Biological Sciences, University of Maryland, Baltimore County, 1000 Hilltop Circle, Baltimore, MD 21 250, USA
e-mail: cronin@umbc.edu

G. Horváth (ed.), *Polarized Light and Polarization Vision in Animal Sciences*, Springer Series in Vision Research 2, DOI 10.1007/978-3-642-54718-8_7,

polarisation signalling structures used in social interaction. Other functions of polarisation sensitivity in crustaceans include navigation, phototaxis and potentially increasing visual range through de-hazing in a turbid world.

7.1 Introduction

Crustaceans are numerous, with more than 67,000 known species exhibiting a great variety of body plans from metre long lobsters and crabs to tiny, sub-millimetre planktonic organisms. They inhabit all of the available aquatic niches from lakes, rivers and coastlines to ocean depths beyond 7,000 m. A few, like the oniscid isopods, woodlice or pill-bugs, for example, have truly ventured onto land, while littoral species, such as mud-flat dwelling fiddler crabs or beach-bound ghost crabs, are best thought of as conducting vision mostly in air rather than water. The physical and optical challenges of living in and around water have driven the evolution of a great variety of eye designs, as Mike Land (1984) notes: "*Although one usually thinks of the Crustacea as linked to the insects by the presence of an exoskeleton and compound eyes, there is actually a much greater diversity of eye types in the Crustacea than the insects or any other invertebrate group*."

Paired, lateral apposition or superposition compound eyes are found in most crustacean groups, being stalked and mobile in the decapods, euphausids and mysids, and sessile or essentially embedded in the heads of amphipods and isopods. The copepods possess single element "simple eyes" with a variety of, in fact rather complex, lens arrangements and others like the ostracod *Gigantocypris* have even branched out into reflective optics (Land 1984; Land and Nilsson 2012). This diversity is largely centred around modifications in optical design and it is perhaps surprising to find that beneath the dioptrics the construction of crustacean photoreceptors and their optic neuropils is relatively conservative (Land 1984; Strausfeld and Nässel 1981; Marshall et al. 1999a). Within each ommatidium, most possess a central fused rhabdom constructed from eight cells, very often arranged with a distal cell named "R8" in a tier above the remaining seven "R1–R7" cells (Fig. 7.1). The smaller members of the subphylum, particularly the copepod and related lineages, may diverge from this typical photoreceptor arrangement and, in truth, there are many crustacean eyes that we know little about.

In common with many arthropods, crustacean rhabdoms are constructed from microvilli and are therefore inherently sensitive to the direction of the electric vector (E-vector henceforward) of linearly polarised light, which is maximally absorbed if the E-vector is parallel to the long axis of the membrane tubules (Fig. 7.1 and Chap. 4; Snyder 1973). With a few exceptions, the crustaceans investigated so far are less interested in colour than their aquatic neighbours, the fish. Many possess one or at most two visual pigments, and, paralleling the also largely colour-blind cephalopods, crustaceans have developed polarisation vision more than colour sense (Marshall and Messenger 1996; Marshall et al. 1999a, b).

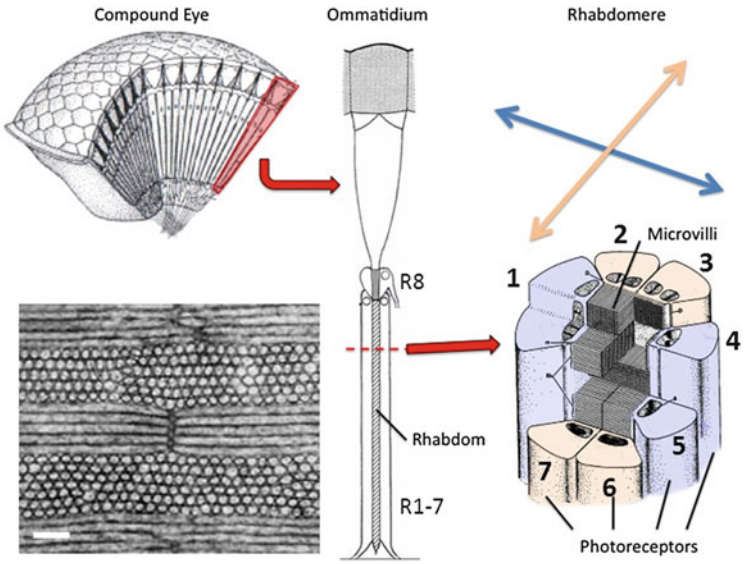

Fig. 7.1 Rhabdom construction in crustaceans. (**a**) Generalised apposition compound eye, ommatidium and diagrammatic three-dimensional transverse section through rhabdomere (in part after Kirschfeld 1976; Stowe 1977 and courtesy of Mike Bok). R1–R7 cells numbered and orthogonal microvilli made by opposite rhabdomeres and resultant E-vector sensitivities (*double-headed arrows*) coloured *yellow* and *blue*. (**b**) Transmission electron micrograph detail of orthogonal microvilli in longitudinal section from stomatopod. Scale 0.2 μm

The convergence of both cephalopods (Chap. 8) and crustaceans on polarisation sensitivity (PS) is interesting in that both are highly successful aquatic invertebrate groups that have found as much use from this form of light as colour. As humans are essentially polarisation blind (however, see Chap. 14), we are only just beginning to understand the advantages and information contained in this photic realm.

Like many of the invertebrates and vertebrates with PS, crustacean photoreceptors usually contain or combine two major orthogonal directions of E-vector sensitivity (Rutherford and Horridge 1965). A theme that this book emphasises is that, although three directions of PS are theoretically needed to fully disambiguate E-vectors (Bernard and Wehner 1977; How and Marshall 2014), many animals including the crustaceans stop short at two. While in some animals, such as fish or spiders, this involves comparison of different photoreceptors or even eyes, the crustaceans generally possess orthogonal microvilli within one rhabdom. Very often our knowledge of PS in the crustaceans is based only on correlations from structure to presumed function. Behavioural evidence of PS is certainly an area ripe for study. What has been termed true polarisation vision (PV), where E-vector and/or degree (%) of polarisation discriminations are made, has only been demonstrated in one of the many species available, a stomatopod (Marshall et al. 1999a, b).

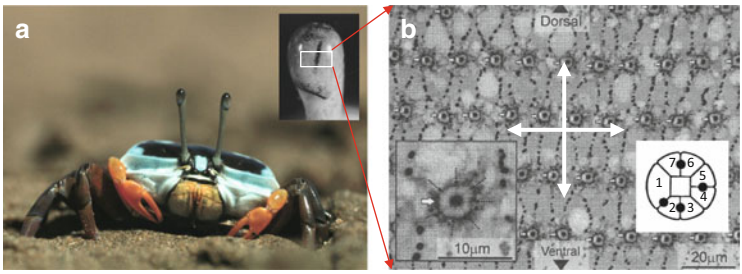

Fig. 7.2 Orientation of crustacean microvilli relative to outside world is maintained horizontal and vertical. (**a**) Fiddler crab female *Uca vomeris* (Photograph, Martin How) and inset close-up of fiddler crab eye (Photograph, Jochen Zeil). Note although body is tilted, eyes remain vertical to local substrate. (**b**) Light micrograph transverse section through equatorial R1–R7 rhabdoms of fiddler crab with insets showing enlarged single rhabdom (*left*) and diagrammatic representation of single rhabdom (*right*) [after Alkaladi et al. (2013) and Marshall et al. (1991a)]. *White arrows* denote E-vector sensitivity directions and microvillar directions

7.2 The Structural Basis of PS

A two-tiered construction, having a distal R8 cell placed over a proximal R1–R7 block, is found in the eyes of most of the malacostracan crustaceans, whether of apposition or superposition type (Fig. 7.1). Cell nomenclature, as originally determined by Waterman and others (Eguchi and Waterman 1966; Waterman and Horch 1966; Waterman 1981; and summarised in Marshall et al. 1991a), is important for consistency when describing PS. Presumably, in an effort to maximise microvillar area in each of the two orthogonal directions, many crustacean rhabdoms have a square cross-sectional profile (Figs. 7.1 and 7.2). Usually cells R1, R4 and R5 construct microvilli in one direction, while cells R2, R3, R6 and R7 construct microvilli in the orthogonal direction. Comparison of the relative excitations of these three versus four cells is what underlies PS at the opponent level. R8 cell rhabdoms often contain disorganised or well-ordered but orthogonal microvilli. Only those few known with unidirectional microvilli may show PS; the other two arrangements are presumably adaptations for PS destruction (Fig. 7.3).

The main rhabdom of crustaceans differs from the insect design in that, instead of rhabdomeres projecting a single cake-slice-shaped block of microvilli towards the centre of the rhabdom and stopping when they meet, microvilli in crustaceans form interdigitating layers (Fig. 7.1). The microvilli from rhabdomeres opposite each other still stop at the rhabdom mid-line but intersperse with the microvilli from adjacent cells. A few insects, with examples from butterflies, beetles and flies, also adopt this design (Meyer-Rochow 1971; Kolb 1977), an adaptation to prevent self-screening that would otherwise reduce PS as light travels down the rhabdom (Snyder 1973; Snyder and Laughlin 1975). Found throughout most of the malacostracan lines, this optical innovation allows the construction of rhabdoms up to several hundred microns long, enabling greater sensitivity while still retaining high PS.

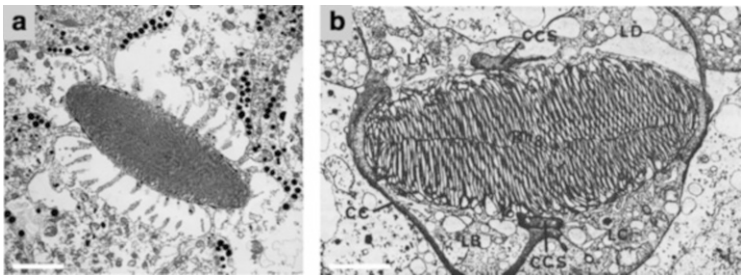

Fig. 7.3 R8 rhabdoms in transverse section showing unidirectional microvilli perpendicular to long axis of the ovid. (**a**) Stomatopod *Pseudosquilla ciliata* mid-band row 6. Scale 5 μm. (**b**) Crayfish *Procambarus* (from Eguchi and Waterman unpublished, in Waterman 1977). Scale 3 μm. The crayfish *Astacus leptodactylus* also shows similar R8 microvilli

The filtering effect of R8 cells may also influence the PS of the R1–R7 cells below by selective screening. In fact, R8s generally possess relatively short, or in some e.g. squilloid stomatopod species, almost vestigial rhabdoms that probably have little influence on the absorption of light in the proximal photoreceptors (Marshall et al. 1991a). In a few species, however, including other gonodactyloid stomatopods (Marshall et al. 1991a) and some of the deep-sea decapods (Gaten et al. 1992; Shelton et al. 1992; Frank and Widder 1994) the R8 cell may contribute up to a third of the total rhabdom length. The precise geometry of R8 microvilli and that of the proximal rhabdom is important here. Some crayfish (*Procambarus* and *Astacus*, Waterman 1981; Krebs and Lietz 1982) R8 rhabdoms as well as the R8 rhabdoms from rows 5 and 6 of the stomatopod mid-band region exhibit unidirectional microvilli (Figs. 7.3 and 7.4). In the crayfish, the R8 microvillar orientation is horizontal and is also aligned with the underlying microvilli of R1–R7 cells R1, R4 and R5. Arrayed thus, the screening effect of the R8 microvilli may enhance the PS of the other cells (R2, R3, R6 and R7); however, this currently remains theoretical. In stomatopods the R8 cells are arranged with microvilli at 45° to those of the underlying R1–R7s, equalling out any filtering of photoreceptors located below. At least in some species, the 45° angle is an important part of their circular polarisation sensitivity, as explained below.

The spectral sensitivity of R8 and R1–R7 tiers differs, with R8 cells containing violet or ultraviolet (UV) visual pigment (360–440 nm), while the main rhabdom is generally blue/green sensitive around 480–540 nm (Marshall et al. 1999a). Differential spectral absorption will reduce any filtering effects, and the intriguing possibility of separate PS channels, one in the UV/violet (R8) and one in the blue/green (R1–R7), exists in a few crab and crayfish species and the stomatopods (Waterman 1981; Eguchi et al. 1982; Krebs and Lietz 1982; Kleinlogel and Marshall 2006, 2009). The optical properties of aquatic environments generally produce the highest degree of polarisation in the blue/green (450–550 nm) range and it is no surprise therefore to find most crustacean PS systems clustering around 500 nm (Cronin et al. 1994b, c; Marshall et al. 1999a, b). However, polarisation in

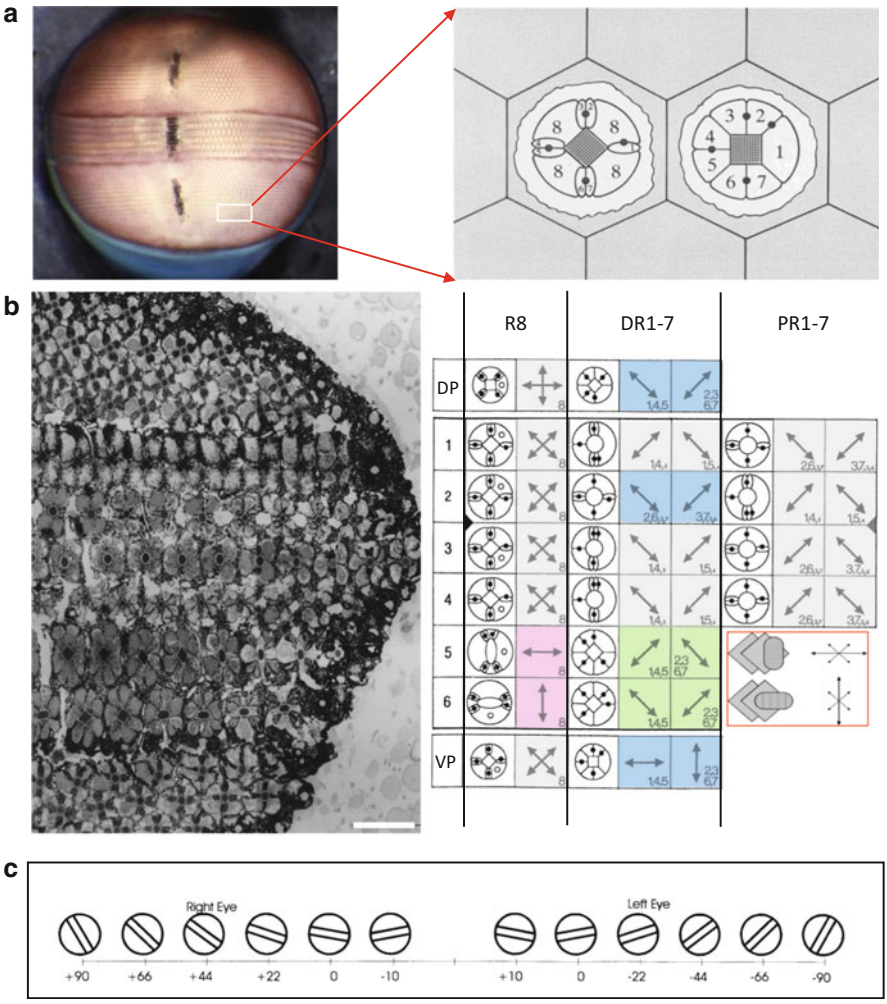

Fig. 7.4 Orientation of microvilli relative to outside world in stomatopod eye with mid-band oriented horizontal. (**a**) Right eye of *O. scyllarus* showing expanded portion of ventral periphery with diagrammatic transverse sections through R8 (*left*) and R1–R7 (*right*) cell rhabdom levels. (**b**) Semi-thin (2 μm) transverse section through mid-band and peripheral retina in *Coronis excavatrix* at transition between R8 and R1–R7 cell level and diagrammatic representation of rhabdoms (*right*) and microvillar directions/E-vector sensitivities (*double-headed arrows*) in various eye regions. *Grey shaded areas*: R8 cell and microvillar orthogonality in rows 1–4 reduces PS. *Green shaded area*: CPS cells in *Odontodactylus* species and LPS in, e.g., *Gonodactylus chiragra*. *Blue shaded areas*: 500 nm *blue/green LPS cells*. *Violet shaded area*: UV-sensitive R8 cells. Inset: *red bounded diagram* is erroneous representation of three-directional rhabdomal unit previously published (Marshall 1988). VP: ventral periphery, DP: dorsal periphery, DR1–R7: distal R1–R7 cells, PR1–R7: proximal R1–R7 cells. Scale 100 μm. (**c**) Extensive rotational eye movements of *O. Scyllarus* eye in diagrammatic form. Eyes are most often held close to 40°

water may be quite variable (Cronin and Shashar 2001), and depending on the task it may be more adaptive to pick a wavelength range that does not transmit far (Chap. 19). UV is rapidly scattered and absorbed in most coastal and reef waters, making it a good choice for not broadcasting messages in these relatively turbid habitats. Given that the cephalopods, some of the crustaceans' most successful predators, also possess 500 nm-centred PS, for those crustaceans signalling with polarisation, this may be particularly important.

In fact, many terrestrial animals and fish preferentially chose UV as a polarisation waveband (the reason of which was explained by Barta and Horváth 2004 for terrestrial animals using sky polarisation), and at least crayfish and stomatopods may employ UV/violet-sensitive R8 cells for PS tasks. Below the retina, the axonal termination of R8 cells bypasses the first neural relay station, where R1–R7 cells terminate, to synapse deeper in the optic neuropils (Fig. 7.5, and see the later Sect. 7.5), suggesting two spectrally distinct subsystems that may or may not show PS (Strausfeld and Nässel 1981). The optimum position for PS in the spectrum has resulted in some confusion in the literature and is also reviewed in Chapter 10 of Horváth and Varjú (2004, pp. 53–73; see also Hegedüs et al. 2006). Rather than drawing broad ecological conclusions it is more constructive to consider the behavioural needs of each animal separately.

Most crustacean R8 cells seem designed specifically not to impinge upon R1–R7 PS function. As well as being short or spectrally isolated, in other crustaceans and in certain stomatopod eye regions, R8s may contain jumbled microvilli or orthogonal interdigitated bands. This latter pattern is noted in a variety of crabs (e.g. *Palinurus* and *Grapsus*: Waterman 1981; *Petro listhes*: Eguchi et al. 1982; *Uca vomeris*: Alkaladi et al. 2013) and in the R8 cells of most of the stomatopod eye (Marshall et al. 1991a; Fig. 7.4). Either arrangement would lead to cancellation or reduction of PS within the single R8 and an overall neutral polarising filtering effect below. PS destruction may be important for the R8 cell's correct function, perhaps disambiguating colour from polarisation information. Several insects use a number of strategies and a variety of microvillar arrangements to reduce PS for similar reasons, while some butterflies (Kelber et al. 2001) and fish (Hawryshyn 1992, 2000) seem to deliberately mix the polarisation and colour message for specific behavioural tasks (Chaps. 4, 9 and 13).

A number of different arrangements to the usual R8/R1–R7 square profile rhabdom exist, both in species from the malacostracans and outside this group. Many seem designed to reduce PS. For example, the proximal section of the rhabdoms in the lobsters *Panulirus longipes* (Meyer-Rochow 1975) and *Jasus edwardsii* (Meyer-Rochow and Tiang 1984) expands to form elaborate multi-fingered shapes in transverse sectional profile. The microvillar directions are multiple and the neat orthogonal banding of the distal rhabdom breaks down. While it is not certain how such length-wise changes to organisation influence PS, if the rhabdomere is read from as a single unit, it will be reduced (Meyer-Rochow 1975). The porcellanid crab, *Petrolisthes*, also expands its proximal rhabdom, but here retains neat microvillar orthogonal banding. On close examination, however, the cells contributing layers rearrange to reduce rather than enhance PS (Eguchi et al. 1982).

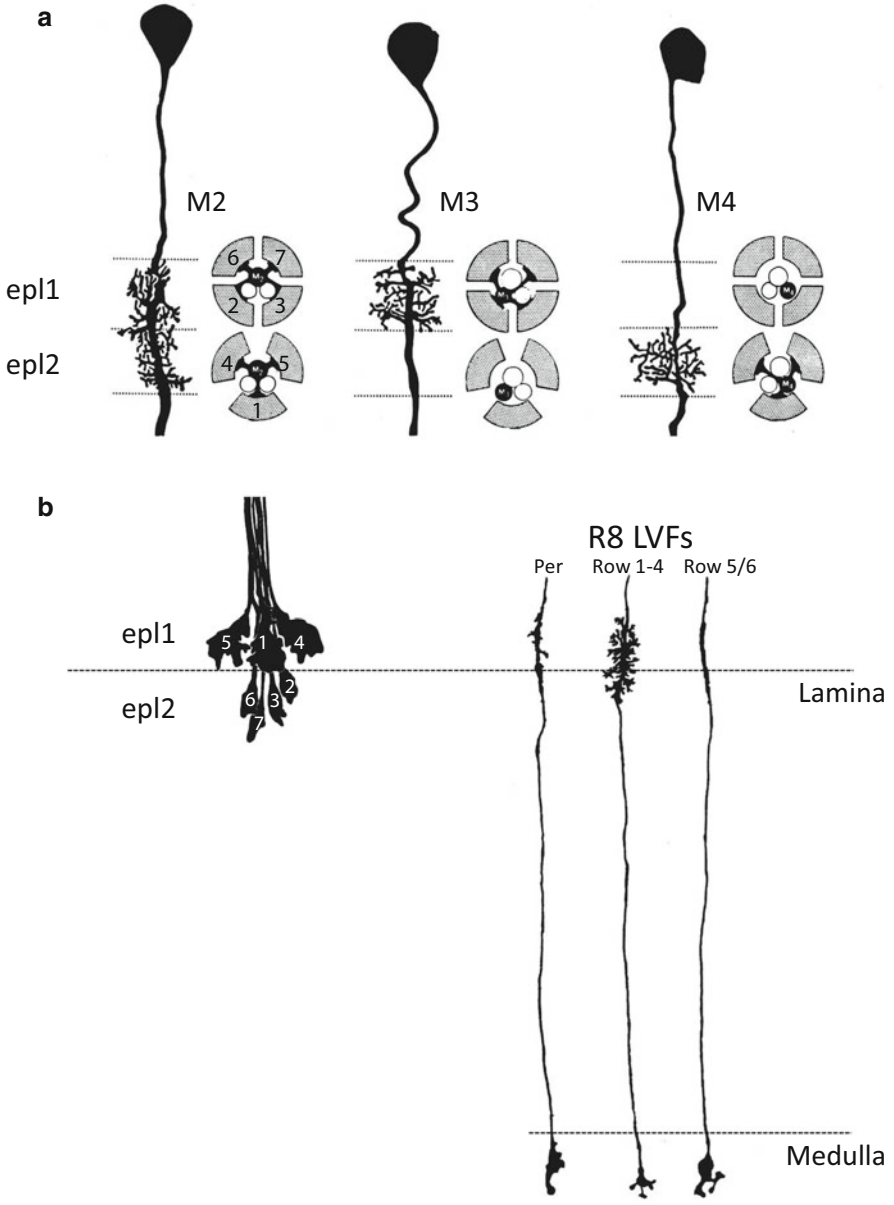

Fig. 7.5 Arborisations of monopolar cells and photoreceptor terminations in a crayfish showing tracings of Golgi stains of likely luminance channel M2 arborising over both *lamina* layers, epl1 and epl2, and E-vector-specific channels M3 and M4 arborising in distal and proximal layers, respectively. Diagrams to right of each monopolar cell show photoreceptor connectivity to centrally placed monopolar endings. Cells R2, R3, R6 and R7 synapse in distal layer and R1, R4 and R5 in proximal layer, while in stomatopods b and other crustaceans investigated, photoreceptor terminations (*left*) terminate with cells R1, R4 and R5 in distal and cells R2, R3, R6 and

Copepods, amphipods and isopods may possess four or generally five rather than eight retinular cells forming relatively short rhabdoms, some of which appear to contain orthogonal microvilli, while others construct pentamerous structures more like the insects (Waterman 1981; Meyer-Rochow 1982). The status of PS in these smaller groups is generally obscure, even from anatomical inference only (Meyer-Rochow 1982). Hyperiid amphipods have been examined in some detail (Land 1981) and construct rhabdoms from five cells that, although showing alternate banding of microvilli, may twist or combine directions to eliminate PS (Ball 1977; Meyer-Rochow 1978).

The water flea *Daphnia* has a single medial compound eye consisting of only 22 ommatidia, formed by the fusion of lateral eyes. Short, rectangular rhabdoms are constructed from eight cells that produce orthogonal microvilli, but these are arranged along the cell edge (three cells) or with interdigitations (four cells) that traverse the entire rhabdom. The eighth cell contributes to the rhabdom more proximally (Macagno et al. 1973). Although different from the typical malacostracan design, the overall result is still two sets of cells with orthogonal E-vector sensitivity (Waterman and Horch 1966; Waterman 1981). The relatively small numbers of ommatidia align their rectangular profiles together and coincident with the transverse and sagittal planes of the animal. They mediate polarotactic and possibly other behaviours (Fig. 7.6) as well as four-channel colour vision (Waterman 1981; Smith and Macagno 1990).

How *Daphnia* segregates colour and polarisation information is still an emerging story, as both drive a variety of behaviourally overlapping phototaxes (Smith and Macagno 1990; Novales-Flamarique and Browman 2000). The stomatopods, on the other hand, provide a clear example of a system that goes to some length not to mix the visual modalities. The stomatopod eye is divided into three areas, dorsal and ventral hemispheres, or peripheral eye regions, and the mid-band. Mid-band ommatidia are often larger or differently shaped to those of the periphery, betraying a different function, and it is in the six rows of the mid-band that most of the stomatopods' 16 photoreceptor types are found (Marshall 1988; Cronin and Marshall 1989; Marshall et al. 1991a, b; Marshall and Land 1993). Functionally there are in fact more than 20 information channels, 12 for colour from 300 to 710 nm (mid-band rows 1–4), 6–10 for linear polarisation (dorsal and ventral peripheral regions, R2, R3, R6 and R7 cells in mid-band row 2, in mid-band rows 5 and 6 the R8 cells and R1–R7 cells in some species), 2 for circular polarisation (in mid-band rows 5 and 6 the R1–R7 cells in some species) and a luminance channel, presumably also the function of the peripheral ommatidia (Fig. 7.4).

Fig. 7.5 (continued) R7 in proximal *lamina* layers. Stomatopod R8 cell long visual fibre (LVF) tracings (*right*) illustrate *en passant* arborisations in *lamina* from different retinal regions on the way to terminate in *medulla externa* [modified from Nässel and Waterman (1977) and Kleinlogel and Marshall (2005)]

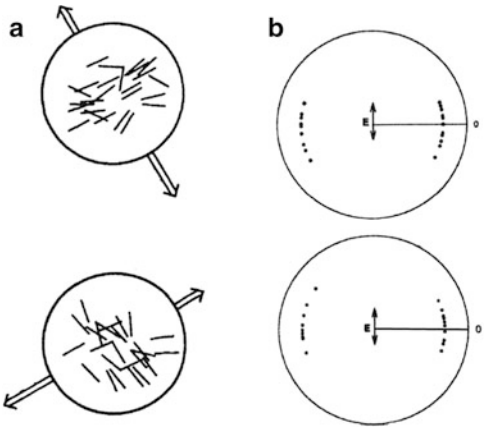

Fig. 7.6 Polarotaxis in small crustaceans swimming under a linearly polarised light field. (**a**) The perpendicular swimming orientation (25 observations) of the mysid shrimp *Mysidium* to overhead beam of polarised light as indicated by underlying *double-headed arrow* [after Bainbridge and Waterman (1957)]. (**b**) The perpendicular orientation of *Daphnia magna* (*top*) and *D. pulex* (*bottom*) to downwelling polarised light, central *double-headed arrow*, as well as sidewelling white light [after Novales-Flamarique and Browman (2000)]

Aside from R8 cells in rows 5 and 6, all other stomatopod eye region R8s contain orthogonal microvilli to cancel or remove PS; important are R8 cells in mid-band rows 1–4 as these cells contain four different UV sensitivities from 300 to 400 nm (Cronin et al. 1994a; Marshall and Oberwinkler 1999). This forms part of the 12-channel continuous spectral sampling system that stomatopods have evolved, replacing colour vision through analogue comparison (Marshall et al. 1991b, 2007; Neumeyer 1991; Thoen et al. 2014). In the peripheral eye regions, the R8s are also UV sensitive and polarisation insensitive; however, their function is not known. As well as possessing orthogonal microvilli within one cell, the square cross-sectional profile these cells present is arranged at 45° to the square of the R1–R7 cells (Fig. 7.4). This would minimise any residual filtering influence that the two selective E-vector absorptions of the R8 microvilli might have on the R1–R7s below.

R1–R7 cells in rows 1–4 in stomatopods have become secondarily tiered and show further PS removal adaptations. The "normal crustacean" interdigitations have un-interdigitated and each ommatidium exhibits three over four cells (R1, R4, R5 over R2, R3, R6, R7) in rows 1, 3 and 4 and four over three cells (R2, R3, R5, R6 over R1, R4, R5) in row 2 (Marshall et al. 1991a). Each of these secondary tierings carries a different visual pigment for the 400–700 nm part of the colour vision system (Cronin and Marshall 1989; Marshall et al. 2007). Oddly enough, in longitudinal section each tier still reveals orthogonal microvillar arrangements; however, these function to destroy PS in order to keep the colour information clean (Marshall et al. 1991a; Kleinlogel and Marshall 2006). Two mechanisms operate here: Some cells, particularly R1, clearly produce bidirectional microvilli, as R8 cells do, cancelling PS within one cell. The second mechanism relies on the

synaptic termination and information combination of the cells in the cartridges of the *lamina ganglionaris*. Each chromatic channel combines input and therefore orthogonal E-vector sensitivities, by synapsing on common monopolar cells in different layers (Fig. 7.5) which therefore carry colour-only information (Kleinlogel et al. 2003; Kleinlogel and Marshall 2005; Marshall et al. 2007). Theoretically, any of the crustaceans so far described could also do this for specific eye regions beneath the retina; however, such interneuronal detail is rarely investigated.

Finally, in this section on the reduction of PS, it is worth noting that the cross-sectional profile of the stomatopod rhabdoms in rows 1–4 is round rather than square, also suggesting that PS is less critical in these rows. The regularity of microvillar layering also degrades in all areas of these rows (aside from the distal tier of R1–R7s in row 2), again suggesting that extracting an evenly balanced PS signal is not important here. This relationship between microvillar layering proportions and PS has now also been investigated in fiddler crabs as detailed below (Alkaladi et al. 2013).

Considering now stomatopod retinal regions that appear specifically designed to enhance PS, the following list and Fig. 7.4 summarise our knowledge so far:

(a) R1–R7 cells of the peripheral areas in all species conduct linear polarisation sensitivity (LPS) close to 500 nm with four directions of E-vector sensitivity, orthogonal within dorsal (±45°) or ventral (0° and 90°) periphery. These angles may differ with eye position and species, but there are always four overall (Marshall et al. 1991a).

(b) R8 cells in rows 5 and 6 in all species are adapted for UV LPS. Their rhabdoms are oval in transverse section with unidirectional microvilli orthogonal to the long axis of the oval and arranged orthogonally between rows (Fig. 7.4). Currently, we assume comparison of sensitivities between rows to achieve UV LPS (Kleinlogel and Marshall 2009).

(c) R1–R7 cells in rows 5 and 6 achieve circular polarisation sensitivity (CPS) in some *Odontodactylus* species. The mechanism for this, which also involves the R8 cells of these rows, is described below (Chiou et al. 2008; Roberts et al. 2009). In other species like *Gonodactylus chiragra*, LPS is found in these cells (Kleinlogel and Marshall 2006). Very recent evidence also demonstrates a class of PS between CPS and LPS, exhibiting elliptical sensitivity, is found in some species (Chiou and Marshall unpublished).

(d) Row 2 of the mid-band is certainly involved in colour vision, bearing coloured intrarhabdomal filters (Marshall 1988; Cronin et al. 1994b) and sensitivity in the yellow to orange (500–650 nm) range. Electrophysiological recordings from this row forced a re-examination of its capabilities as high PS-values around 6 or 7 were returned from the distal R1–R7 cells (Kleinlogel and Marshall 2006; Marshall et al. 2007, and see Sect. 7.5 for details). Row 2 is upside down compared to other rhabdoms in rows 1–4, with cells R2, R3, R6 and R7 distal to R1, R4 and R5 and it may be that this anatomical re-organisation is associated with high PS. In fact, these evenly matched cells do retain the "normal" crustacean orthogonal arrangement (with cells R2 and R6 opposing R3 and R7) and a regular layering of microvilli associated with PS

in other eye regions and other crustacean species. It is possible that, like certain butterflies (Kelber et al. 2001; but see Horváth et al. 2002b; Hegedüs and Horváth 2004a, b), stomatopods have recognised a specific advantage in mixing colour and polarisation information; however, more evidence is required here before further speculation.

Both PS enhancement and reduction mechanisms described are found so far in the lysiosquilloid and gonodactyloid superfamilies only. The eyes of squilloid and other minor superfamilies have a reduced mid-band with only two rows of ommatidia, or in the deeper living species, no mid-band at all. In squilloids, at least this is a derived state (Ahyong and Harling 2000; Porter et al. 2010) and in the squilloid species examined, the whole eye shows similar rhabdoms possessing rudimentary R8s and orthogonal R1–R7 cells with opposing sets at 0° and 90°. Very little is known about the PS capability of squilloids (but see Yamaguchi et al. 1976); however, interestingly, some species show distinct polarisation reflections that may be visible to conspecifics (Cronin et al. 2009; Chap. 19).

Gonodactyloid stomatopods from the genus *Odontodactylus* are the first animals known with sensitivity to circularly polarised light (Chiou et al. 2008). This is a remarkable optical feat that relies upon a secondary characteristic of the R8 cells in rows 5 and 6, separate from their UV LPS capability. The CPS system is tuned to around 500 nm, by the spectral sensitivity of the R1–R7 cells in these rows. The extreme regularity and unidirectionality of microvilli in these R8s, possibly along with other anatomical features such as cell length, aspect ratio and refractive index, make these cells 1/4 wave retarders (Chiou et al. 2008; Roberts et al. 2009; Fig. 7.7). This is critical for CPS as, so far, no cell is known that is intrinsically able to detect or discriminate circular polarisation of either handedness. The full story contains structural, optical, electrophysiological, behavioural and signal production elements, described in each section below. Here the structure and optics are described, and for a better understanding of the physics of elliptical polarisation, the reader is recommended to Hecht (2001).

Before further description of CPS, a second correction relative to past literature must be made, to add to our row 2 mistake. A notable feature of the R8 cells in rows 5 and 6 is their oval or ellipsoidal profile in transverse section (Marshall 1988; Figs. 7.3 and 7.4). The long axis of the oval is oriented at 45° to the underlying R1–R7 cell profile and their orthogonal microvilli. This led to the idea of a single rhabdom in both rows 5 and 6 possessing three directions of E-vector sensitivity and perhaps removing the null points inherent in a two-directional system (Bernard and Wehner 1977; Marshall 1988; How and Marshall 2014; and inset in Fig. 7.4). As we have already noted here, due to spectral sensitivity difference, neural termination differences between R8 and R1–R7 cells and now this CPS function, we no longer view this as likely.

The 45° relationship of R8 to R1–R7 in these rows is in fact critical to their CPS, as this is precisely the geometrical requirement of the 1/4 wave retarder, if it is to convert circularly polarised light (CPL) to linearly polarised light (LPL) at the angles optimally absorbed by the R1–R7 microvilli below (Fig. 7.7). All 1/4 wave retarders have a fast and a slow axis and as CPL passes through the structure, it

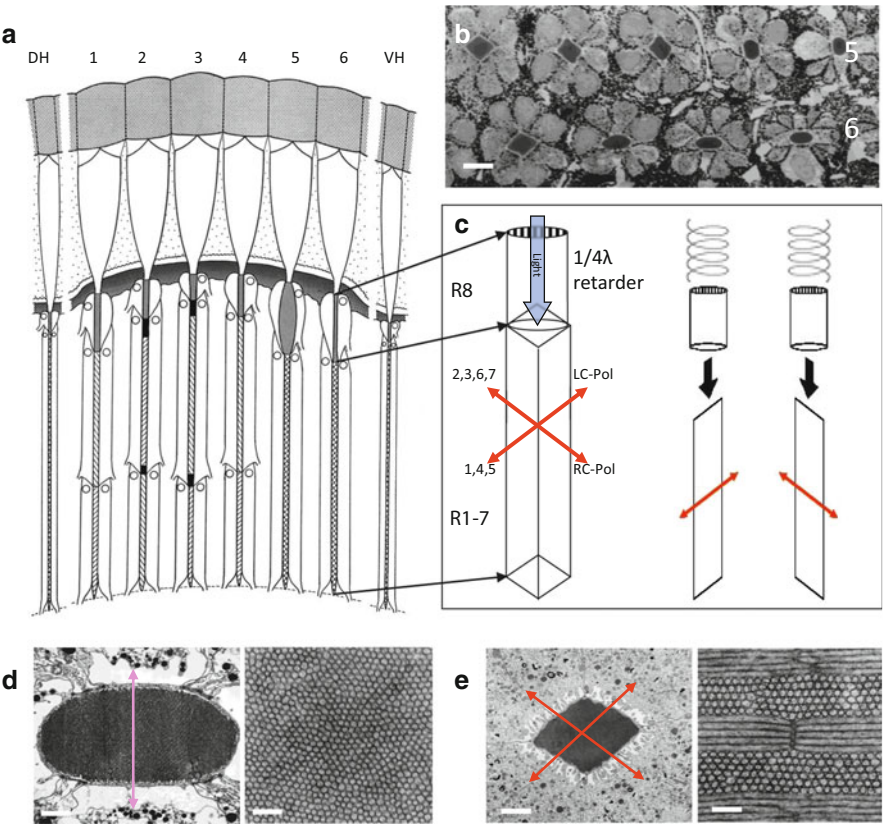

Fig. 7.7 Aspects of circular polarisation vision in stomatopods. (**a**) Diagram of longitudinal section through stomatopod ommatidia including *mid-band rows* 1–6 and representative ommatidia from dorsal and ventral hemispheres (DH, VH) or peripheral regions. (**b**) Rows 5 and 6 that construct CPS in semi-thin section at transition between oval profile R8 cells and diamond profile R1–R7 cells. Scale 10 μm. (**c**) Diagrammatic representation of row 6 rhabdom. As circular polarised light passes through R8 cells, it is converted through 1/4 wave retardation to linearly polarised light in one of two directions, depending on CPL handedness. The R1–R7 cells of these rows are in the correct orientation to absorb this ongoing light, being set at 45° to the R8 cell's fast axis [after Chiou et al. (2011)]. (**d**) Transmission electron micrograph of R8 cell in row 6 in transverse (*left*) and longitudinal section (*right*) showing unidirectional microvilli. This cell has dual function as 1/4 wave retarder and UV linear PS as shown by *violet double-headed arrow* (Fig. 7.11). Scale 1 μm at *left*, 0.2 μm at *right*. (**e**) Transmission electron micrograph of R1–R7 cells in row 6 in transverse (*left*) and longitudinal section (*right*) showing orthogonal microvilli that are sensitive to CPL in *Odontodactylus* species and LPL in *Gonodactylus chiragra*. Scale 2 μm at *left*, 0.2 μm at *right*

emerges at 45° to this with left-handed orthogonal to right-handed, due to the relative delays in each vector component of the light (Hecht 2001). The R1–R7 cells in rows 5 and 6 therefore only "see" CPL as it has been converted to the LPL form that their microvilli can absorb, and their microvilli are positioned at just the right angle to do this (Chiou et al. 2008; Roberts et al. 2009; Fig. 7.7).

It is worth asking why two rows are needed for CPS and what their specific geometry relative to one another achieves? When the anatomy of the system was first described (Marshall 1988; Marshall et al. 1991a), it was recognised that the rhabdoms in row 5 were rotated along their entire length through 90° relative to row 6, as seen most clearly through the orientation of the R8 oval shapes (Figs. 7.4 and 7.7). As just described, a single row could theoretically distinguish left- and right-handed CPL through opponent comparison of its R1, R4, R5 and R2, R3, R6, R7 cell sets. By rotating row 5 90° to row 6, the UV LPS function of the R8s is enabled, allowing the R8s to provide another channel of LPS input in a spectral region that many aquatic creatures operate within. By maintaining rotation of the whole rhabdom, and not just the R8 cells, the handedness of the CPS also remains similar between R1–R7 cells with R1, R4 and R5 sensitive to left-handed CPL and R2, R3, R6 and R7 sensitive to right-handed CPL in both rows (Chiou et al. 2008).

A feature of crustacean microvillar construction and PS that is often overlooked is their remarkable plasticity and seeming response to light. For example, during a 24 h day/night cycle, rhabdom size in several crab species increases by up to 20 times at night, chiefly the result of microvilli increasing and decreasing in length. In fact, the original works on PS in crustaceans noted this turnover (Eguchi and Waterman 1968; Nässel and Waterman 1979) and Stowe (1980, 1981, 1983) examined the phenomenon in some detail. While this is generally thought to allow the capture of more photons at night, it will likely have some effect on PS, although this has yet to be quantified (Stowe 1980). The Norwegian lobster *Nephrops* and other deep-living crustaceans show considerable rhabdomal damage to bright light with severe disruption of microvilli (Loew 1976). It has also been noted in the stomatopods that there seems to be an inverse relationship between the amount of light reaching a photoreceptor subcategory and microvillar size and neatness (Marshall et al. 1991a, b). Particularly deep-dwelling gonodactyloid stomatopods are in fact known to discard the tiers in mid-band row 3 or even the whole row, apparently as the long wavelength light that these photoreceptors are sensitive to is not present at such depths (Cronin et al. 1994a). With PS in mind, it would be interesting to determine to what extent the banding pattern and structure of rhabdoms is a fixed process and to what extent it is determined by polarised light level (Meyer-Rochow 1982; Marshall et al. 1991a; Alkaladi et al. 2013).

7.3 Polarised Light Sources for Crustaceans

Having detailed the anatomy of individual rhabdoms in crustacean eyes, the next important step is to place these photoreceptors within the overall geometry of the eye and animal as a whole and determine how this array samples the polarised light available in the world. Before this, however, it is worth briefly reviewing the sort of polarised light, both LPL and CPL, that might be available to crustaceans. Chapters 15, 18 and 19 describe this in more detail; however, here we take a specifically crustacean eye view.

Two broad categories of polarised light exist: large-field or extended sources, and smaller discrete sources such as might come from reflections off individual objects. These drive different types of behaviour, for example, polarisation navigation and polarotaxis derived from the former category, and intraspecific or sexual signalling from the latter. Large-field sources, by definition, most likely fall on several ommatidia at once and require an integrated signal from this array, while small polarising signals may stimulate only a few ommatidia at a time. The following list of examples describes the light source and possible crustacean behaviours associated with it. Some of these are expanded upon in Sect. 7.6.

7.3.1 Large-Field Sources

7.3.1.1 The Celestial Polarisation Pattern

This reliable pattern relative to the sun and caused by particle scatter has been well described by Wehner (1983) and others (Horváth and Wehner 1999; Pomozi et al. 2001; Gál et al. 2001a, b; Horváth et al. 2002a, b; Suhai and Horváth 2004; Hegedüs et al. 2007a, b, c, d; Sipőcz et al. 2008) and may be utilised by insects and other animals for orientation or navigation (Chaps. 2–4, 9–12, 18 and 25). An upward directed dorsal rim area (DRA) of specialised ommatidia is often associated with such behaviour (Wehner 1983; Wehner and Labhart 2006). Crustaceans that inhabit terrestrial or mainly terrestrial environments may also utilise this polarisation cue, and some evidence suggests that fiddler crabs could utilise a DRA-like area in the eye for this purpose (Zeil and Layne 2002).

7.3.1.2 The Celestial Polarisation Pattern Compressed into Snell's Window

As studied in detail by Horváth and Varjú (1995, 2004) and Sabbah et al. (2006), the 180° celestial panorama is visible under calm water through a 97° refracted cone defined by Snell's window. Crustaceans looking into the window, particularly those in close association with the water surface, may therefore still utilise the sun compass. Surface ripples or waves rapidly confuse or pollute the pattern; however, there are many, particularly still freshwater habitats, where it remains a strong feature for animals with PS. The polarisation of the sky overhead at dawn and dusk also provides a highly polarised backdrop against which certain objects may be more visible.

7.3.1.3 Water Surface Reflections and Wet Surfaces

Reflection, in fact a special form of scatter itself, is the other main source of polarised light in the environment (Schwind and Horváth 1993; Horváth 1995;

Horváth and Varjú 1997, 2004; Gál et al. 2001c; Wehner 2001; Bernáth et al. 2004). While many insects associate with and even live on this surface (Chaps. 5, 16 and 20–23), the more heavy-bodied crustaceans tend to sink through it; however, for littoral species it is a source of polarisation that may help with navigation or "flight" towards or away from water. Mud flats and other wet shorelines provide a similar large-field reflective surface and Zeil and Hemmi (2006) suggest the importance of this in the ecology of fiddler crabs from the *Uca* genus, among others.

7.3.1.4 Water Surface Reflections Under Water

For aquatic animals looking up at the water surface, internal reflection may also provide a strong linear polarising signal. Any animal living in sight of the surface and looking up will see two polarised sources, the transmission of the celestial pattern within Snell's window, as just described, and then beyond the critical angle of around 48.5° from vertical, total internal reflection delivers a partially polarised view of the aquatic field beneath the critical angle. This reflection of upwelling and sidewelling light is usually substantially dimmer than the light through Snell's window and in still conditions a sharp boundary exists. Although one aquatic insect (*Notonecta glauca*: Schwind 1983) and some fish (Munk 1970) construct specialised eye regions that utilise the polarisation and other features of this zone, it is not known if any crustaceans also make use of it. Almost all crustaceans undergo a larval developmental stage for dispersal. During this larval period, or even as adults in some species, the animals inhabit the nektonic zone just beneath the water surface, which is rich in linear polarisation information. This habitat and the PS of crustaceans that live there deserve more attention.

Waterman (1954) and Ivanoff and Waterman (1958a, b) demonstrated the presence of elliptically polarised light (EPL) derived from internal reflection of partially LPL (derived from volume scatter in water) beyond the critical angle. We recently demonstrated that some stomatopod crustaceans can discriminate CPL; however, it is not known if they make use of this broad EPL field as well as the discrete CPL reflections from other stomatopods (Fig. 7.8).

7.3.1.5 Polarised Background Space Light Underwater

The dominant large-field polarisation source for most aquatic animals comes from the scatter of light entering water (Waterman 1954; Ivanoff and Waterman 1958a, b; Hawryshyn 1992; Cronin and Shashar 2001; and see Chap. 15). Any animal looking horizontally into the water around it sees what is termed *background space light*, the combination of absorption and scatter (Jerlov 1976). In clear waters, the degree of polarisation of this source may reach over 50 % but rapidly degrades with increased turbidity and is usually closer to 30 % in relatively clear reef waters (Cronin and Shashar 2001). With the sun overhead, or close to overhead (a condition through much of the day due to refraction), this scattered light is oriented horizontally, or largely so, relative to the observer (Chap. 15). Close to

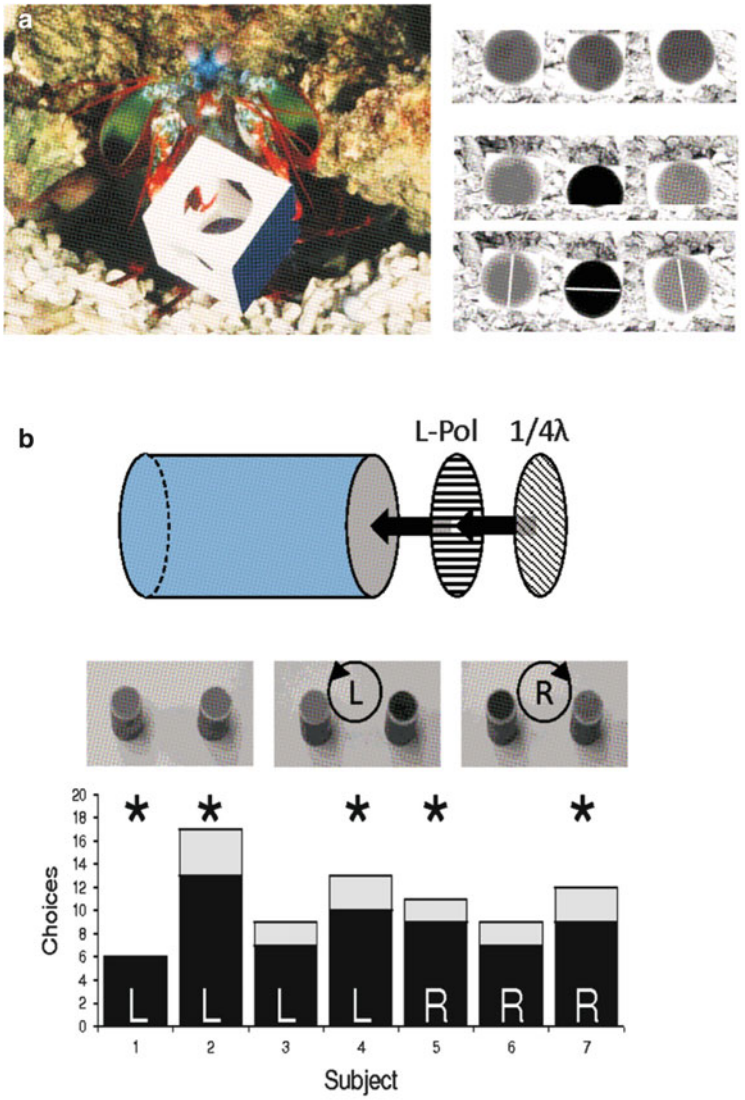

Fig. 7.8 Behavioural tests showing E-vector and CPL handedness discrimination in stomatopod *Odontodactylus scyllarus*. (**a**) Experimental paradigm to demonstrate linear E-vector discrimination in *O. scyllarus* from cube-shaped food containers with polarising filters glued to one side, *top*: no camera filter, *mid*: vertical polarising filter to show different feeding cubes and *bottom* with E-vector lines drawn on photograph. Stomatopods can learn to choose vertically polarised from horizontally polarised food containers. *Left*: stomatopod reaching inside a smashed open feeding container (after Marshall et al 1999). (**b**) Details of CPL paradigm. *Top*: construction of feeding containers with polarising filter and 1/4 wave plate glued to end. Other end is sealed with coverslip after food is placed inside and animal must choose and break open tube with handedness of CPL trained to. *Middle*: Feeding containers photographed through left- and right-handed CP filters and no filter (as we see them). *Bottom*: Graph of choices (*correct black* and *incorrect grey* out of an array of three feeding tubes where one was correct choice) of 7 animals trained to left- or right-handed CP feeding containers. *Stars* indicate statistical significance [after Chiou et al. (2008)]

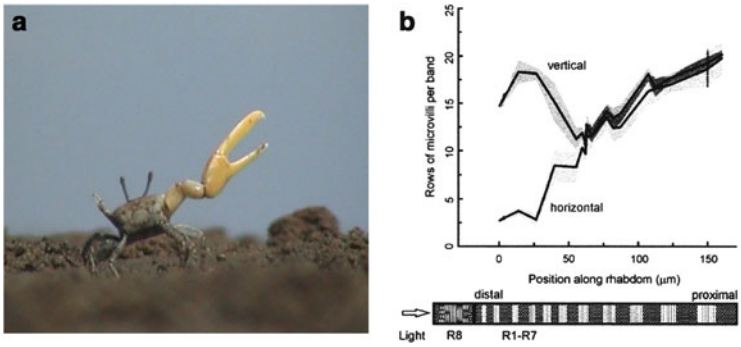

Fig. 7.9 Animals living in close association with horizontal reflective surfaces, such as fiddler crabs *Uca* sp., may experience and utilise a strong horizontally polarised large field. (**a**) Waving coloured and possibly polarised claw. (**b**) In the ventral part of the eye of *Uca signata*, more vertical than horizontal microvilli are found per band and may reduce glare from horizontal mud flat habitat [after Alkaladi et al. (2013)]

dawn and dusk, the angle does tilt, but for most of the day, polarised light from this source is mostly horizontal. As such it provides a predictable and largely constant LPL backdrop.

Behavioural observations do exist suggesting the use of horizontally polarised space light to determine polarotaxis as detailed below (Siebeck 1968; Novales-Flamarique and Browman 2000). Other uses of this large polarised curtain, including contrast enhancement, have been suggested (Lythgoe and Hemmings 1967; Johnsen et al. 2011). This is discussed relative to crustaceans PS after we consider the small sources of polarised light they may be exposed to.

7.3.2 Small-Field Signals

7.3.2.1 Reflections from Wet or Other Reflective Surfaces

A wet crab or one with a naturally specular carapace will present a small area of polarisation with the E-vector direction dependent on the orientation of the surface or body area. Terrestrial or littoral crustaceans may use PS to detect or discriminate such small sources of LPL and it has been suggested that fiddler crabs use polarisation, as well as colour and motion, as part of their agonistic or mating behaviours (Zeil and Hofmann 2001). The mostly horizontal carapace of these and other crabs may also be important in polarisation camouflage on an also horizontal polarising large-field wet mud flat, disguising them from potential aerial predators, for example (Hemmi et al. 2006). A fiddler crab erecting a vertical display claw (Fig. 7.9) would present a vertically polarised specular surface from certain directions of view against the largely horizontally polarised background, perhaps providing extra contrast to the PS systems of conspecifics (Fig. 7.9).

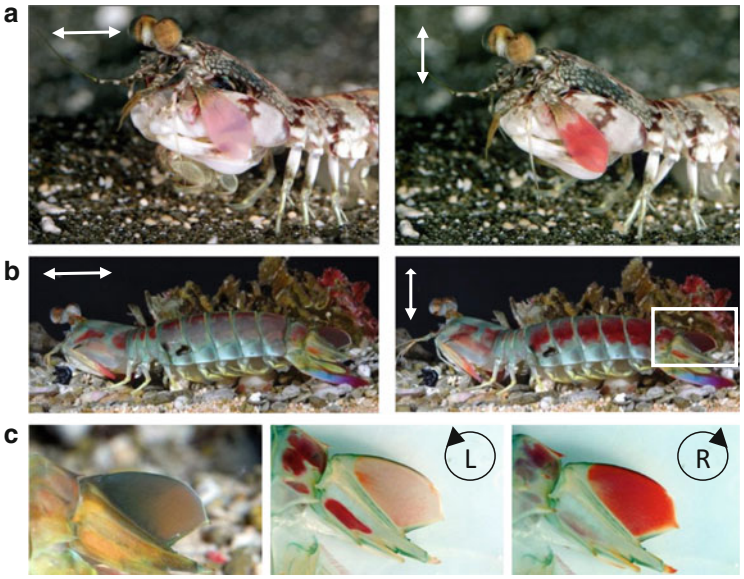

Fig. 7.10 Polarisation signals from stomatopod cuticle. (**a**) The antennal scales of *Odontodactylus latirostris* photographed through horizontal and vertical polarising filter as denoted by *double-headed arrows*. Polarisation activity is astaxanthin based. (**b**) The thoracic and abdominal carapace of the stomatopod *Odontodactylus cultrifer* is also strongly linearly polarised (*arrows* as **a**). Note the lack of change in the telson carina (*white box*). (**c**) In male *O. cultrifer* the central carina of the telson, *inset* in (**b**) and enlarged below, is circularly polarised. L and R circular polarised filters reveal activity not apparent with linear polarising filters (**b**). Photographs courtesy of Roy Caldwell

7.3.2.2 Intrinsic Polarisation Signals

It is becoming increasingly apparent that a number of animals are able to construct polarisation signals in their skin or cuticle derived from the scattering, dichroic or interference properties of the materials used. Among the Crustacea, it has been known for some time that the cuticular articulations of some lobsters reflect CPL, but these areas are usually hidden from view (Neville and Luke 1971). Also dinoflagellates induce CPL as light passes through their bodies via unknown mechanisms (Shashar et al. 1995), but again, the possible relevance of these signals is unknown. Likely polarising signals are constructed in the stomatopod crustaceans, reflecting both CPL and LPL, and importantly, these are located on body areas, such as uropods, antennal scales and maxillipeds, used specifically in display (Caldwell and Dingle 1976). This supports the notion that their polarisation content is used somehow in a way akin to colour communication in other animals (Cronin et al. 2003a, b). Stomatopod polarisation signalling mechanisms are examined in some detail in Chap. 19 and are therefore only described briefly here.

Three varieties of polarising signals are made by stomatopods, categorised according to the physics of the production mechanism. Firstly, pink or red colouring, such as that in *Odontodactylus* species (Fig. 7.10), is indicative of

polarisation produced by the dichroic molecule astaxanthin. Astaxanthin is a ketocarotenoid found in many crustacean tissues and is strongly dichroic, a bit like the chromophore in visual pigments. The specific length of the molecule makes it to sit in membranes perpendicular to the surface, and the antennal scales of *O. scyllarus*, for example, contain many membrane layers with highly oriented astaxanthin embedded within. This gives the overall structure a strong (80 %), directional polarising signal (Chiou et al. 2012).

The second type of polarising signal from stomatopods emerges from the unique circular polarising areas, such as the keel of the uropod in *O. cultrifer* (Fig. 7.10). Although the details of this process are still being worked out, it most likely starts with an astaxanthin-rich layer, like the one just described, that on its own would reflect linearly polarised light. A second translucent layer is found on top of this that acts as a 1/4 wave retarder. The linearly polarised light that passes through this zone is converted to circular, in fact the reverse of the way the light is detected by the photoreceptors (Cronin et al. 2003b; Fig. 7.7).

The third type of polarising tissue from stomatopods is quite different and is found on the maxillipeds of *Haptosquilla trispinosa* and other related species. Again, these areas are shown in social interaction and are known in this case to be critical in mate choice (Chiou et al. 2011). In courtship displays, females prefer males with normal and not depolarised maxillipeds. The blue colour and linear polarisation reflected from these structures are produced from layers that contain elongated vesicles, neatly arranged in rows. A resonant photonic scattering process is thought to produce polarised light in this case, determined by the size and orientation of the vesicles (Chap. 19).

Small-field polarising signals may be of particular use in aquatic habitats for two reasons. With increasing depth and over horizontal distance in water, colour is filtered out and becomes an unreliable signal (Lythgoe 1979). Polarisation is also degraded rapidly over distance by scatter, so that even in clear, oceanic waters just two metres of water is enough to reduce the degree of polarisation of an object by close to 50 % (Cronin and Shashar 2001). As a result, like colour, polarisation communication probably works best over short distances. Polarisation is different from colour, however, as it retains the same information, in terms of angle or degree, at depth as it does near the surface. This does not solve the problem of signal degradation with distance from the observer, but it does mean that over depth, polarisation signals may be more reliable than colours. In this context, it is interesting that *Odontodactylus* stomatopod species living at moderate depth seem to swap colour for polarisation signals, both linear and circular.

The second special characteristic of polarisation signals underwater is that they may be notably conspicuous relative to background, again making for an efficient communication channel. Due to the refractive index similarity of water and many of the water-containing objects in water, such as animals, algae, plants and substrate, there is very little specular reflective polarisation in underwater environments compared to land. In fact, this source of reflective “polarised light pollution” has been noted a number of times on land (Horváth et al. 2009, 2010; Chap. 20), and may drive some of the adaptations to reduce PS in terrestrial arthropods

(Wehner 1983). Clearly defining contrast mechanisms from polarised light underwater is worthwhile and four circumstances that crustaceans might experience seem likely:

1. The low-polarisation substrate underwater will provide strong contrast for a polarising object and conversely camouflage for a non-polarising object. Specially constructed polarisation signals, such as those from stomatopods, or indeed cephalopods (Chap. 19), will therefore be particularly contrasting against the substrate.
2. The relatively high (20–50 %) and consistently mostly horizontally polarised background space light (Chap. 15) will contrast against unpolarised objects or against vertically polarised objects. Polarisation camouflage against such a backdrop requires the object to intrinsically polarise horizontally, or transmit or reflect the local polarisation light field. This, and the breaking of such camouflage, is more rare in nature than previously thought (Chap. 19; Johnsen et al. 2011; Jordan et al. 2012).
3. Crustaceans looking up through Snel's window can use the refracted celestial E-vector pattern to contrast objects against. Particularly at dawn and dusk, when there may be a strong (80 %) band of polarisation overhead as the sun reaches the horizon, the same set of circumstances as just described for horizontal polarisation field applies. The difference is that to align photoreceptor analysers to this light field requires the animal to be able to rotate eye or body while looking up.
4. The removal of polarised haze underwater is another contrast-increasing mechanism crustaceans may utilise. This is distinct from the previous three in that it does not rely on target and background differences in one plane, but rather removes a source of image degradation between the observer and the subject. In brief, this idea recognises that the veil that frequently obscures objects underwater and that results from forward scattered light is partially linearly polarised. Lythgoe and Hemmings (1967) suggested that some clarity could be regained using a single tunable polarising mechanism to remove some of this light. More recently, Schechner and Karpel (2005) have taken this a step further, suggesting that a pair of orthogonally arranged analysers might largely strip away the veil, increasing object detection distance underwater dramatically (Chap. 15).

All four of the above contrast-increasing mechanisms remain theoretical for crustaceans and indeed any animal; however, a very strong correlative argument exists in that a two-channel orthogonal system is the most practical to achieve the required result in each case. This is precisely the pattern found in most crustaceans, cephalopods (Talbot and Marshall 2011) and indeed in the eyes of many other animals with PS. Where an object reflecting polarisation requires analysis, it may be that considerable analyser rotation is required to align the eye's two sampling directions relative to an arbitrarily placed polarising object. Interestingly, stomatopods, which as we have seen may be specifically interested in each other's

polarising patterns, exhibit eye rotations of more than 90° in some species (Land et al. 1990; Fig. 7.4). It is tempting to speculate that this degree of freedom is related to their formidable LPS ability and the need to extracting polarising information from specific body areas.

So far we have considered the relative E-vector sensitivities of individual receptors to the polarisation stimuli outside the animal. Bearing in mind both the large and small field of the various polarising light stimuli that crustaceans may visualise, we now go on to examine whole photoreceptor arrays.

7.4 Mapping the Internal Eye on the External World

Talbot Waterman (1981) introduced the idea of a "collaborative pattern" of photoreceptors to underline the need to understand not just the E-vector sensitivities of individual receptors, but how the whole array samples the world. This is not a trivial task and is often bypassed. In principle, rotation along the long axis of adjacent rhabdoms could be used to alter or cancel PS; however, so far this is not observed in crustaceans. Instead, where examined, for instance in terrestrial crabs (Zeil and Hemmi 2006; Alkaladi et al. 2013), *Daphnia* (Waterman 1981) and crayfish (Glantz 2007), at least the equatorial sections of the eye possess rhabdoms that all contain vertical and horizontal microvilli relative to their principal body axis. Similar patterns exist in cephalopods (Talbot and Marshall 2010, 2011), fish (Hawryshyn 2000; Novales-Flamarique 2011) and several insect species (Labhart et al. 2001; Wehner 2001), which also suggests a general principle and likely matched filter to the horizontal aspects of the outside world (Wehner 1987).

Away from the equatorial portion of the eye, ommatidia wrap around to sample different directions, and the distribution of ommatidial axes and E-vector sensitivity may vary between species, potentially associated with lifestyle (Land 1984; Zeil et al. 1986; Marshall et al. 1991a; Glantz 2007). Crayfish, for example, allow E-vector sensitivity directions to depart from horizontal and vertical in dorsal eye regions, while fiddler crabs do not (Glantz 2007; Alkaladi et al. 2013). A recent careful anatomical analysis of PS and eye region in the fiddler crabs (*Uca vomeris* and *U. signata*) confirmed the generally horizontal and vertical E-vector arrangement over the whole eye (Fig. 7.2), but also revealed unusual microvillar banding patterns (Alkaladi et al. 2013). In all eye regions, along the length of R1–R7, the banding thickness increased from distal to proximal rhabdomal zones. In the equatorial regions, horizontal microvillar layers increased from 3 to 20 per band, while vertical bands went from around 20 to 10 and back to 20 again over the length of the rhabdom. Dorsally placed, more upward looking rhabdoms showed horizontal microvilli that occupied half the cross-sectional area of the vertical bands. These patterns achieve three things: (a) constant photon absorption and therefore relative PS signal along the rhabdom length, (b) matched filtering to the polarisation content of the external world between dorsal and equatorial eye and (c) a glare reduction or polarising sunglasses-like preferential filtering of horizontally polarised light in

equatorial regions (Fig. 7.9). This adjustment of microvilli to reduce those in the horizontal direction is also found in the *Gerris* waterstriders, insects also inhabiting a world full of bright horizontally polarised light (Schneider and Langer 1969; Chapters 18.4 and 27.5 of Horváth and Varjú 2004, pp. 181–183 and 278–287). This may also be a polarising sunglasses-like response to block possibly saturating light reflected from water surfaces, or for crabs, from wet mud flats. Hemmi et al. (2006) interpret the difference on microvilli in the upward looking ommatidia as a mechanism to increase the contrast of predators against a polarised sky, along the lines of polarisation contrast enhancement mechanism (c) above.

The stomatopods are again unusual and (as already noted), instead of keeping their eyes locked to a single orientation, rotate them along their eyestalk axis by more than 90° (Fig. 7.4). While some of this may be to allow the unique scanning eye movements of stomatopods to progress orthogonal to the mid-band (Land et al. 1990), it will also modulate the polarisation information coming into the eye (Marshall et al. 1991a). With the mid-band horizontal, the stomatopod, *Odontodactylus scyllarus*, has two R1–R7 orthogonal subset arrangements, one at 0°, 90° and one at ±45°, placed in ventral and dorsal peripheral eye regions, respectively (Fig. 7.4). The precise angle relative to the mid-band does vary between species (Marshall et al. 1991a); however, the end result for all stomatopods so far examined is that between the dorsal and ventral ommatidia, E-vector sensitivities exist at four angles separated by 45°. How the substantial eye rotations noted may influence LPS from these and other eye regions remains a mystery.

The eyes of most stomatopod species are most often positioned with mid-bands around 45° and show some mid-band angle dependence with eye position (Land et al. 1990; Fig. 7.4). In trying to interpret this complexity, it is important to remember that the eye does not look at a two-dimensional array as most eyes do (Marshall and Land 1993). Both the polarising channels just described and the 12 colour channels sweep over objects temporally and the current hypothesis treats the whole array as an object-analysing device with each point in space receiving simultaneous parallel input from the 20 information channels that the eye provides (Marshall et al. 1991b, 2007; Thoen et al. 2014). How or if adjacent channels or elements of this matrix of information are compared is still under investigation, but for polarisation at least, there are parallels with a Mueller matrix examination of objects. All components of the matrix are provided (0°, +45°, 90° and −45° L and R circular) and the Stokes vector calculations in each element are like those possible from simple neural opponency. Although seemingly far-fetched, this element-by-element examination of objects seems to be the design "rationale" or evolutionary driver for the stomatopod system (Thoen et al. 2014). In the same way as a 12-dimensional colour space is unlikely, the alternative of a full description of polarisation space as may be represented by the Poincaré sphere (Goldstein 2003; Hecht 2001), as suggested by Kleinlogel and White (2008), also seems out of the question. The more pertinent remaining question for stomatopods is, what is the information they glean with this remarkable system useful for?

7.5 Neural Processing and Electrophysiology

As should be clear from the previous sections, having the structural potential for PS, with unidirectional microvilli in a cell or cell subpopulation, does not guarantee PS at the behavioural level. Physiological recordings and neural connectivity of potential PS channels beneath the retina are a required next step, although also of themselves, still not a guarantee that the whole organism uses polarised light. In malacostracan crustaceans there are three neuropils or information integration levels beneath the retina: the *lamina*, the *medulla externa* and then the *lobula* complex, part of which has been termed the *medulla interna*. Entomostracan crustaceans possess only the first two of these (Strausfeld and Nässel 1981; Strausfeld 2005).

7.5.1 Electrophysiology in Crustaceans

Intracellular and extracellular recordings of PS have been made in a few crustacean species such as crabs, crayfish and stomatopods, at a number of levels including at the photoreceptors, optic neuropils and optic nerve (Yamaguchi et al. 1976; Waterman 1981). Electroretinograms (ERG) of land crab (*Cardisoma*) demonstrated 90° different response modulation to flashes of rotating polarised light (Waterman and Horch 1966). Shaw (1966) recorded the intracellular responses of a crab (*Carcinus maenas*) to linearly polarised light at different E-vector angles. He found two cell populations with preferred E-vector orientation orthogonal to each other and corresponding to the microvillar directions within the rhabdom. This was confirmed in *C. maenas* and the blue crab *Callinectes sapidus* by Mote (1974) who measured PS-values of 3.2–9.0 with a mean of 4.5. Leggett (1976) recorded intracellular photoreceptor and extracellular responses from the *medulla externa* of the swimming crab, *Scylla serrata*. The photoreceptors had a PS-value of 10, around the theoretical average for a crustacean (Stowe 1983), and two classes of interneurons were described: I—that responded to E-vector rotation but not rotation direction and II—that responded to both E-vector rotation and its direction. Leggett (1976) suggested that these PS interneurons might play a role in three ways: (a) contrast enhancement of objects relative to a polarised background as described above, (b) stabilisation of swimming direction through maintaining a constant PS output relative to a polarised background or (c) navigation by using the changing underwater polarisation pattern as the sun alters angle. These behavioural speculations have yet to be confirmed in this species.

The shore crab *Leptograpsus variegatus* has also been investigated with intracellular photoreceptor recording (Doujak 1984). PS in this species varies from 1.8 to 7.5 with an average around 5.0, considerably lower than *S. serrata*, but corresponding to the dichroic ratio of these photoreceptors estimated structurally. More recently, Berón de Astrada et al. (2009) described sustaining and dimming

fibres in the *medulla* of the crab *Chasmagnathus granulatus* that respond best to vertical and horizontal E-vectors, respectively. This system appears identical to the crayfish.

Crayfish are the most thoroughly studied crustacean using electrophysiological techniques. In an intracellular study of *P. clarkii* photoreceptors Muller (1973) found two cell populations with orthogonal E-vector responses. He suggested electrical coupling between cells with the same E-vector orientation, while Eguchi et al. (1982) also found electrical coupling between cells in the eyes of the porcellanid crab *Petrolisthes*, but between unidentified cells. This potential for PS signal combination at the photoreceptor level requires further investigation. In other early work, Waterman and Fernandez (1970) and Yamaguchi et al. (1984) recorded both violet (440 nm) and yellow (594 nm) sensitive cells in *Procambarus clarkii* using intracellular and extracellular optic nerve recordings (Waterman 1985; Figs. 7.11 and 7.12). Both cell classes also show E-vector sensitivity maxima to vertical and horizontal polarised light (PS = 1.2–11.9 and averaging 3.1). These presumably correspond to R8 and R1–R7 cells, the vertical 440 nm sensitivity showing some discrepancy with what is known anatomically, as only horizontally oriented R8 microvilli are described (Fig. 7.3; Waterman 1981).

Intracellular recordings and Lucifer Yellow dye labelling of photoreceptors in *P. clarkii* have revealed where different retinular cells terminate in the *lamina* (Sabra and Glantz 1985). Horizontally sensitive cells R1, R4 and R5 terminate in the distal plexiform layer (epl_1) and vertically sensitive cells R2, R3, R6 and R7 terminate in the proximal plexiform layer (epl_2). Monopolar cells are the first interneurons with which photoreceptors synapse in the *lamina*. Different classes of these, M3 and M4, divide their dendrites between epl_1 and epl_2, respectively (Strausfeld and Nässel 1981; Fig. 7.5). As a result, M3 carries only horizontal PS information and M4 vertical PS, setting up the foundation for opponent processing, and these cell classes seem ubiquitous to all malacostracans investigated.

Glantz (1996a) has extended the crayfish study considerably in recent years using large-field stimuli to excite both receptors and a variety of interneurons in *P. clarkii* and *Pacifastacus leniusculus*. More than three-quarters of monopolar cells recorded from (presumably M3 and M4) possess PS in the same direction as photoreceptors and exhibit properties consistent with the initiation of an opponency mechanism (Glantz 1996a). Interneurons from the *medulla externa*, including tangential, dimming and sustaining fibres, showed PS, including evidence of opponent interaction within and between neurons (Fig. 7.12). Sustaining fibres, for example, are maximally stimulated by vertical E-vectors, while dimming fibres respond best to horizontal E-vectors and are inhibited by vertical ones (Glantz 1996b, 2001; Glantz and McIsaac 1998). Interestingly, there is considerable interaction between PS- and intensity-driven responses in the crayfish, both spatially and time varying, leading to the suggestion that PS contributes to motion detection and contrast enhancement in low-contrast environments (Glantz 2001, 2008; Glantz and Schroeter 2006). An important result from these studies, relevant to possible PS-driven behaviours, is that polarisation contrast on its own is enough to drive motion detection (Glantz and Schroeter 2006). This supports the notion that large-

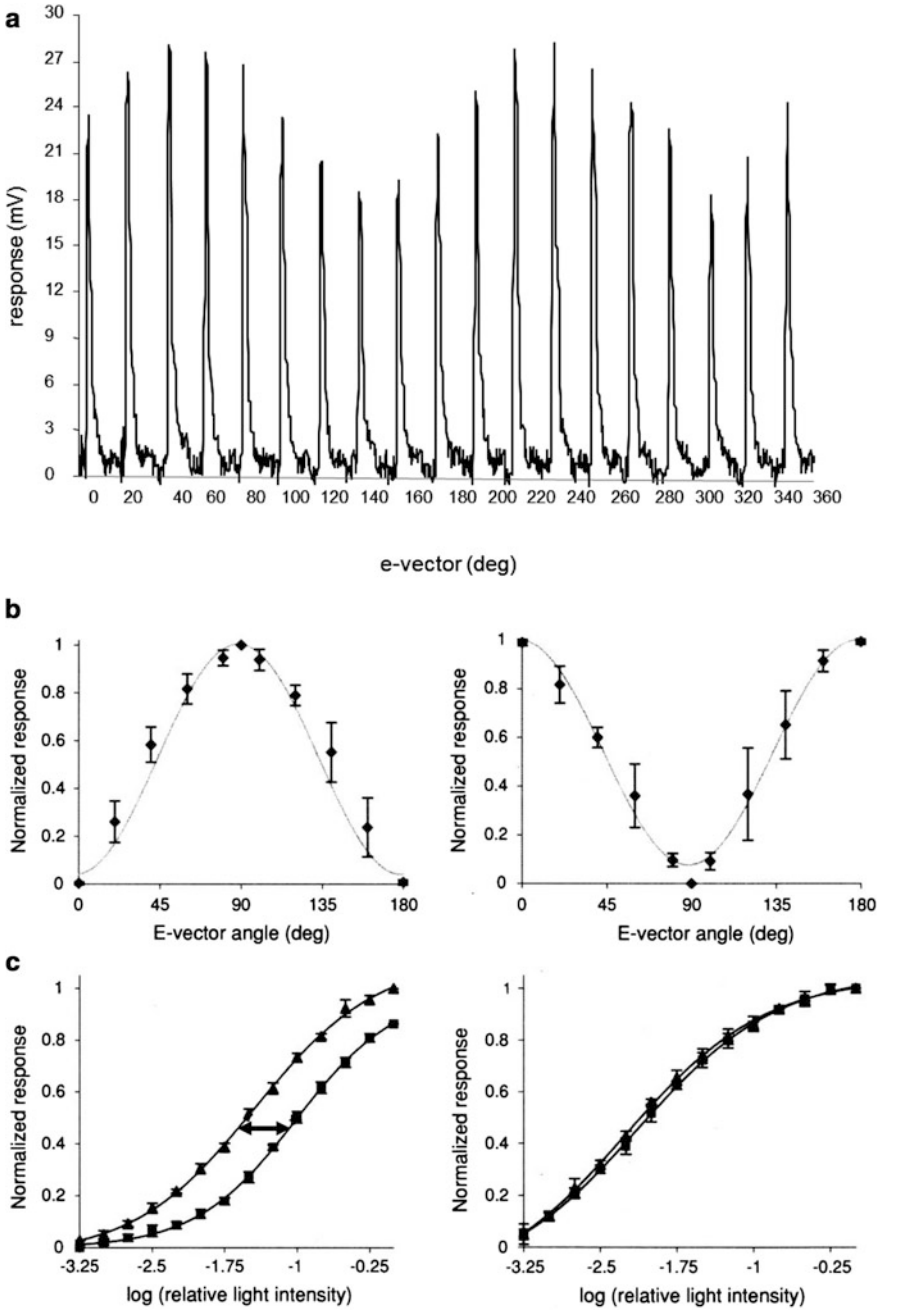

Fig. 7.11 Intracellular electrophysiological recordings from stomatopod photoreceptors. (**a**) Different depolarisation levels from a single cell as flashes of light are delivered through a rotating polarising filter from 0–360°. (**b**) Normalised E-vector versus response amplitude for UV-sensitive R8 cells from *row 5* (*left*) and *row 6* (*right*) showing orthogonal relationship as predicted from

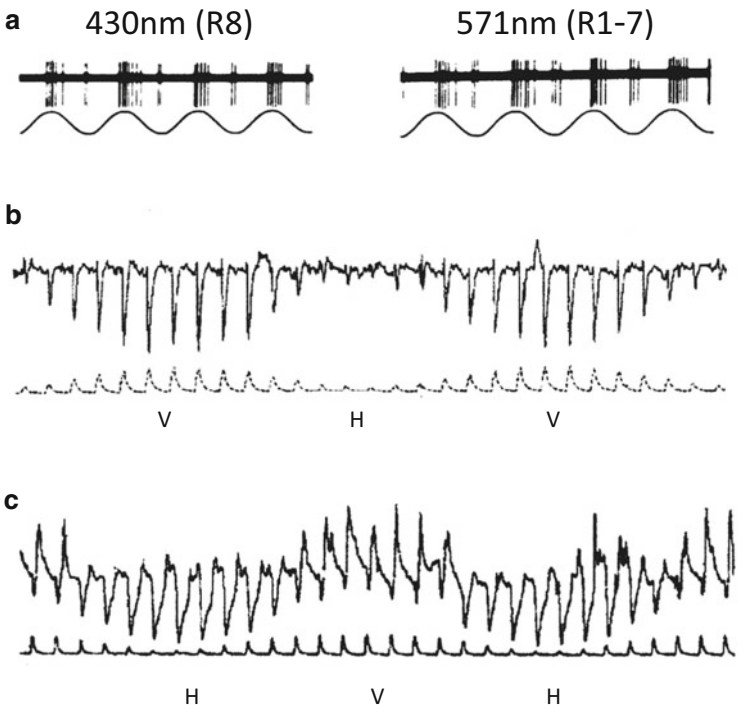

Fig. 7.12 PS recorded from interneuron recordings in crayfish. (**a**) Extracellular recordings from optic nerve in *Procambarus* at two different wavelengths close to spectral sensitivities of R1–R7 and R8 cells to a rotating polarised filter as denoted by sinusoidal curve with maxima at 180°. It is remarkable that both cell types show similar orthogonal response even though the R8 cell only possesses horizontal microvilli (Fig. 7.3). (**b**) Response of crayfish *lamina* monopolar cell to variable E-vector orientation indicated by lower trace and marked V: vertical and H: horizontal [after Glantz (1996a)]. (**c**) Response of crayfish tangential cell recorded in *medulla externa* to variable E-vector as in **b**. Note clear opponent response (after Glantz 2001)

field underwater polarisation may drive animal orientation, taxes and navigation, whether or not the same cells also respond to intensity (Glantz 1996a, b).

A careful intracellular study of *P. clarkii* photoreceptor PS and E-vector angle in different areas of the crayfish eye showed largely horizontal and vertical PS in equatorial regions (Glantz 2007). As detailed in Fig. 7.2 and Alkaladi et al. (2013),

Fig. 7.11 (continued) anatomy. (**c**) Peak response versus relative light intensity for R8 cell in row 6 (*left*) and R8 cell in row 2 (*right*). Curves measured at maximum (*triangles*) and minimum (*squares*) response angle. Polarisation sensitivity is calculated from the difference in intensity curves at half-maximal response and indicated by *double-headed arrow*. PS = 3.3 for R8 in row 6 and PS = 1.15 or negligible as expected for the mixed microvillar direction for R8 in row 2 [after Kleinlogel and Marshall (2009)]

this is what might be expected from the direction of microvilli in many crustacean eyes, including crayfish (Waterman 1981), and as already discussed probably represents a matched filter to outside large-field E-vector sources. In the dorsal eye area, however, maximum PS responses exhibit modes at 0°, 45° and 90° (Glantz 2007). While this may be a result of ommatidial packing as the hexagonal array becomes compressed at the edges of the eye, this three-angle PS bears striking resemblance to the dorsal rim areas (DRAs) of compound eyes in insects and their use in navigation (Labhart et al. 2001). Such a three-channel polarisation analyser may also overcome the null-point limits of a two-channel system (Bernard and Wehner 1977); however, a solid behavioural connection from physiology to behaviour needs to be established for this eye region. This second population of receptors may account for the early optic nerve spike recordings of Waterman and Horch (1966) that showed sensitivity at 45° and 135° as well as 0° and 90°.

Responses to polarised light have also been recorded from stomatopod photoreceptors and interneurons. Recording from photoreceptors in the squilloid species, *Oratosquilla oratoria*, Yamaguchi et al. (1976) noted two populations of cells with orthogonal maximal PS corresponding to the horizontal and vertical axis of the eye and correlating with the microvillar arrangement within (Schiff 1963; Marshall et al. 1991a). Extracellular recordings from sustaining fibres in the optic nerve also demonstrated modulation to E-vector angle at 90° intervals, supporting the idea that the PS information is passed to the brain after the optic neuropils.

Stomatopod photoreceptors from many retinal regions in several gonodactyloid species have been recorded with intracellular micro-electrodes (Marshall and Oberwinkler 1999; Kleinlogel and Marshall 2006, 2009; Chiou et al. 2008). Approximate PS-values generally follow predictions from microvillar directions (Fig. 7.4) and show some intraspecific variation in CPS. The linear PS, CPS and spectral sensitivities (SS) of two species, *Gonodactylus chiragra* and *Odontodactylus scyllarus*, are compared in Table 7.1.

The range of PS for *G. chiragra* was divided into three averaged categories by Kleinlogel and Marshall (2006): low (PS = 2.3) in most of mid-band rows 1–4, medium (PS = 3.8) in the periphery and high (PS = 6.1) for R1–R7 in rows 5 and 6, and for DR1–R7 in row 4. Notable from these data is the similarity of DR1–R7 spectral sensitivities in rows 5 and 6 and row 2, both in terms of their PS and spectral sensitivities. This might be advantageous if polarisation information from these areas is combined at a later integration stage; however, if this occurs in this species is unknown. Although the PS of many of the R8 cells in *G. chiragra* was not determined, the close relative *Neogonodactylus oerstedii* exhibited variable UV sensitivity in these cells (Marshall and Oberwinkler 1999) and low PS-values close to 1.0, as would be expected from their mixed orthogonal microvilli (Fig. 7.4). Optical estimates of UV PS in *N. oerstedii* rows 5 and 6 gave values of 3.0, close to those measured electrophysiologically (Cronin et al. 1994c).

A specific intracellular study of R8 cells in *O. scyllarus* (Kleinlogel and Marshall 2009) demonstrated a similar pattern of variable UV spectral sensitivities noted for *N. oerstedii* (Marshall and Oberwinkler 1999) and PS-values as shown in Table 7.1.

Table 7.1 Linear polarisation sensitivities (PS) and circular polarisation sensitivities (CPS) along with spectral sensitivities were relevant to PS in *Odontodactylus scyllarus* and *Gonodactylus chiragra* (Kleinlogel and Marshall 2006; Chiou et al 2008)

Receptors		*Gonodactylus chiragra*	*Odontodactylus scyllarus*
Peripheral	R8	PS = unknown	PS = 1.2 SSN = 311 nm
	R1–R7	PS = 1–7 (average: 3.8) SSB = 450–550 nm	
Mid-Band Row 1	R8	PS = unknown	PS = 1.6 SSN = 381 nm
	DR1–R7	PS = 1–3 (average: 2.3)	
	PR1–R7	PS = 1	
Mid-Band Row 2	R8	PS = unknown	PS = 1.4 SSN = 330 nm
	DR1–R7	PS = 4–8 (average: 6.1) SSN = 565 nm	
	PR1–R7	PS = 2–4 (average: 2.8)	
Mid-Band Row 3	R8	PS = unknown	PS = unknown
	DR1–R7	PS = 2–4 (average: 2.8)	
	PR1–R7	PS = 1.5	
Mid-Band Row 4	R8	PS = unknown	PS = 1.0 SSN = 311 nm
	DR1–R7	PS = 1–4 (average: 2.2)	
	PR1–R7	PS = 2.5	
Mid-Band Rows 5 and 6	R8	PS = unknown	PS = 2.75 SSN = 335 nm
	R1–R7	PS = 4–12 (average: 6.1) SSN = 565 nm	CPS = 10.2 SSN = 500 nm

Distal and proximal tiers in rows 1–4 denoted DR1–R7 and PR1–R7, respectively. SSN: narrow spectral sensitivity, SSB: broad spectral sensitivity

Peripheral and mid-band R8 cells possess low PS, around or slightly above 1.0, while PS of R8 cells in rows 5 and 6 was on average 2.75. While clearly more sensitive than other R8 cells, a PS of 2.75 is in the same "low PS = 2.3" range as some of the supposedly weakly PS mid-band R1–R7 cells from *G. chiragra* (Table 7.1; Kleinlogel and Marshall 2006). Other crustaceans including crabs and crayfish as detailed above also exhibit relatively low PS-values just over 3.0. The dichroic ratio of orthogonal channels determines PS-values (Snyder 1973; Stowe 1983) and it is not clear how variability in this value between species is related to polarisation task (Waterman 1981; Leggett 1976). It is more clear between functional areas in stomatopods and using the R8 data a fourth PS category of very low PS, close to 1.0, may be defined. Also recall that, while individual cells in rows 1–4 might show some "low PS", spectrally similar cells with orthogonal microvilli (R1, R4 and R5 or R2, R3, R6 and R7) combine at the level of the *lamina*. This presumably eliminates the relatively low PS, already set up by uneven microvillar layering in these cells (Marshall et al. 1991a), in favour of spectral information (Kleinlogel and Marshall 2005; Marshall et al. 2007).

The optical mechanism for CPS in stomatopods relies on the second function of the R8 cells in rows 5 and 6, 1/4 wave retardation of CPL on the way to being absorbed by the R1–R7 cells below (Fig. 7.7). The conversion of CPL to LPL means the light can be absorbed as normal by the dichroic receptors below. CPS has only been found so far in *Odontodactylus* species and intracellular recordings from R1–R7 in rows 5 and 6 showed both CPS to left-handed (cells R1, R4 and R5) and right-handed (cells R2, R3, R6 and R7) stimuli in both rows. A high CPS of 10.2 was measured and calculated, as with LPS, from the differential between maximal and minimal response, this time to left- and right-handed light (Fig. 7.7). Importantly, the lack of LPS in these cells was also shown (Chiou et al. 2008). Any linearly polarised light passing through the R8 1/4 wave retarder is converted to CPL and therefore the R1–R7 cell beneath cannot absorb left or right CPL generated in this manner. As a result, rotating a linear polariser in front of these cells results in no or minimal modulation relative to angle (Chiou et al. 2008; Roberts et al. 2009).

The difference in CPL sensitivity between the species *G. chiragra* and *O. scyllarus* is striking. It relies on the precise anatomy and resulting retardation characteristics of the R8 cells in rows 5 and 6, and recent recordings from other species indicate that some, such as *Haptosquilla trispinosa*, are maximally sensitive to elliptically polarised light of a specific retardation state between circular and linear. The details of this and the ecological consequence or explanation for individual species' potential ellipticity preference is an area of current research. It is worth speculating, however, that such differences may encode a "spectrum" of communication we are just beginning to quantify.

7.5.2 Neuro-Architecture and Polarisation Information Channelling

Recording PS in photoreceptors and interneurons is indicative that polarisation may be behaviourally useful. However, tracing the combination of E-vector sensitivities to the brain and motor output of the organism is necessary to complete the story. Despite the efforts of Glantz and co-workers, who worked with crayfish, our knowledge of polarisation information channels in crustaceans is less complete than in the insects (Wehner and Labhart 2006; Chaps. 3 and 4). Most malacostracan crustaceans and insects show general similarity in optic neuropil gross morphologies. Crabs, crayfish and stomatopods, for example, possess *lamina ganglionaris*, *medulla externa* and two further integration levels (the *lobula* and *lobula* plate, parts of which were previously termed *medulla interna* and *terminalis*, Strausfeld and Nässel 1981; Strausfeld 2005). One ommatidium projects to one *lamina* cartridge, and while there are chiasmata, or reversals of order, between successive neuropils, retinotopicity is maintained through each level (Strausfeld and Nässel 1981).

In lobsters (Hámori and Horridge 1966a, b), decapod shrimp (*Pandalus borealis*: Nässel 1975, 1976), crayfish (*Pacifastacus leniusculus*: Nässel 1976, 1977; Nässel and Waterman 1977), crabs (Stowe 1977; Sztarker et al. 2009) and stomatopods

(*Squilla mantis*: Strausfeld and Nässel 1981, and gonodactyloid stomatopods of several species: Kleinlogel and Marshall 2005) retina-*lamina* projections and *lamina* cartridge structures are remarkably similar (Strausfeld and Nässel 1981). In all species, three information streams are found: One integrated luminance channel receiving input from all R1–R7 cells and two E-vector-specific channels as mentioned above (Figs. 7.5 and 7.13). Also across species, the R1–R7 cells synapse with usually five or six monopolar cells that extend dendrites into two distinct layers, epl_1 and epl_2. The retinular cell complement in each layer may differ between species. For example, the crayfish *P. leniusculus* possesses four retinular cells, R2, R3, R6 and R7, terminating in epl_1 and three, R1, R4 and R5, in epl_2 (Nässel and Waterman 1977), while in other species such as stomatopods (Kleinlogel et al. 2003; Kleinlogel and Marshall 2005) and shrimp (Nässel 1975) this is reversed so cells R2, R3, R6 and R7 terminate in epl_2 and R1, R4 and R5 in epl_1. In the crabs *Hemigrapsus oregonensis* and *Chasmagnathus granulatus*, photoreceptor terminations are also in two layers, but less precisely stratified (Sztarker et al. 2009).

In crayfish (Nässel 1976, 1977; Strausfeld and Nässel 1981), monopolar cells are labelled M1–M6. M3 and M4 stratify dendrites in only epl_1 and epl_2, respectively (Fig. 7.5), while M1 and M2 extend dendrites into both layers. M5 is found in a fraction of the cartridges, but synapses between many of them, and M6 is a small monopolar cell not found in all species. Most important for PS, in all species retinular cells R1, R4 and R5 synapse in a different plexiform layer to those from cells R2, R3, R6 and R7, segregating horizontal and vertical E-vector information between M3 and M4 (Sabra and Glantz 1985). M2 cells possess dendrites in both plexiform layers, receive input from all R1–R7 cells combining horizontal and vertical E-vectors input and most likely form a polarisation-insensitive intensity information channel. M1 cells of two categories also synapse in both layers, but in a segregated way that makes it unclear if they carry E-vector-specific information.

From the *lamina*, monopolar cells send axons to the *medulla externa*, and tangential fibres originating in the *medulla externa* also convey information from several *lamina* cartridges to this second neuropil (Nässel 1975; Strausfeld and Nässel 1981). Some of the tangential and other cells within the *medulla externa* show polarisation opponency (Glantz 1996b, 2001; Glantz and McIsaac 1998), presumably enabled by interaction between epl_1 and epl_2.

R8 cells in all species send long axons through the *lamina* to terminate, also retinotopically, in the distal layer of the *medulla externa*, segregating UV/violet from blue/green spectral information. R8 cells are mostly polarisation insensitive, aside from crayfish and in stomatopod ommatidia in rows 5 and 6 (Fig. 7.11). In *P. Leniusculus* the R8 cell has horizontally oriented microvilli (Fig. 7.2), while stomatopod R8 microvilli are oriented parallel (row 5) or orthogonal (row 6) to the mid-band and vary in space according to angle of eye rotation (Figs. 7.4 and 7.7). As a result, UV/violet polarisation projects to the *medulla*, while blue/green polarisation meets its first interneurons in the *lamina* in these species. It is interesting to note that several of the navigational/large-field PS tasks in many animals rely on UV PS, and this early segregation of information may be behaviourally significant in this respect.

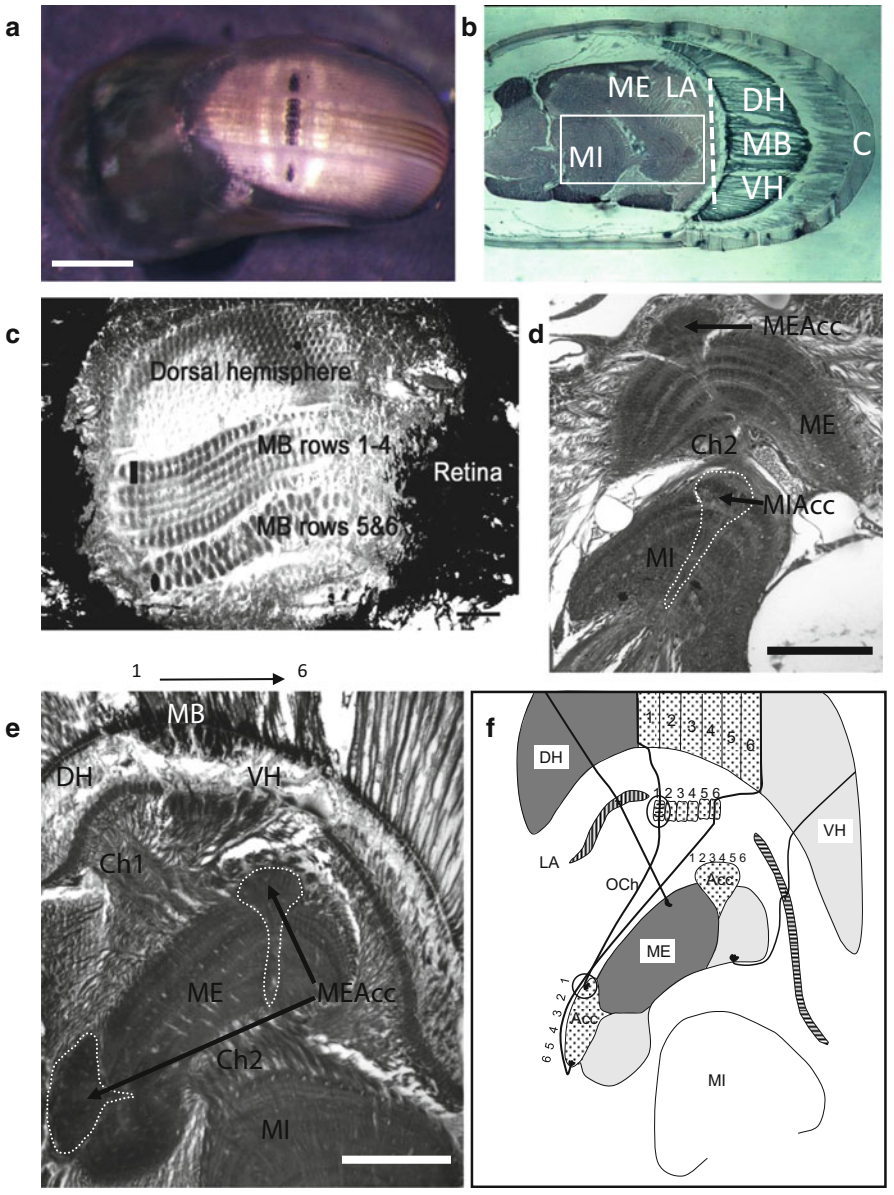

Fig. 7.13 Gross morphology of chloral hydrate stained stomatopod optic neuropils showing partition of colour and polarisation. (**a**) The eye of a gonodactyloid stomatopod. Scale 1 mm. (**b**) Semi-thin section of eye in same orientation as **a**. (**c**) Transverse section at *lamina* cartridge level (*dotted line* in **b** showing segregation of *lamina* under each retinal subsection and differing cartridge morphologies). Scale 70 μm. (**e**) Enlargement of area *boxed* in **b** showing separate accessory lobes of ME and MI dedicated to MB. Scale 100 μm. (**e**, **f**) Section and drawing of section of proximal portion of retina and neuropils, mapping of *mid-band rows* and separation of polarisation information. The single accessory lobe in ME appears in two areas due to its curvature

In crayfish and crabs there appear to be no synaptic connections as the long R8 fibre passes through the *lamina* plexiform layers to the distal *medulla*, and this arrangement is also found in stomatopod R8s in mid-band rows 5 and 6 (Strausfeld and Nässel 1981; Kleinlogel and Marshall 2005; Sztarker et al. 2009). Conversely, stomatopod colour R8 cells in rows 1–4 show extensive *en passant* arborisations in both *lamina* strata, and this may allow R1–R7/R8 cell interaction at this level, setting up trichromatic or dichromatic UV interactions. The stomatopod peripheral eye region R8 axons arborise to a small extent in the *lamina*, again implying chromatic interaction with R1–R7 cells early on. As R8s in the peripheral rows and in rows 1–4 are polarisation insensitive, and crayfish and stomatopod R8 cells in rows 5 and 6 show PS, it appears specifically advantageous for UV/violet PS information to bypass the *lamina*. Conversely, polarisation-insensitive R8 axons in the shrimp, *P. borealis*, also show no arborisations on the way through the *lamina* (Nässel 1975), and in other crustaceans the situation is not well described.

The stomatopod retina is divided into three subsections and each projects to its own optic neuropil subsection (Fig. 7.13; Strausfeld and Nässel 1981; Kleinlogel et al. 2003; Kleinlogel and Marshall 2005; Marshall et al. 2007). At the light-microscope level, the *lamina* cartridges of dorsal and ventral periphery, rows 5 and 6, and rows 1–4 do look different to each other and are well segregated in space (Fig. 7.13). This spatial information separation also projects to mid-band lobes in the *medulla externa* and *lobula*, also maintaining a rows 1–4/5 and 6 division (Kleinlogel et al. 2003). While *Squilla mantis* may present some structural differences in the *lamina*, including an "insect-like" arrangement of three rather than two stratifications (Strausfeld and Nässel 1981), the gonodactyloid species conform more exactly to the basic malacostracan design. It is remarkable that, aside from the gross morphological differences, gonodactyloid stomatopod neuropils, *lamina* cartridge structure and monopolar cells are essentially identical to other malacostracans (Figs. 7.5 and 7.13; Kleinlogel and Marshall 2005). It seems that, whether it is linear polarisation, circular polarisation or colour processing that is required, the pre-existing interneuronal wiring design works.

The optic neuropil structure in non-malacostracan crustaceans is partially known in Branchiopods such as *Daphnia* and *Artemia*, among others, and is generally a simplified version of that of malacostracans (reviewed in Strausfeld and Nässel 1981; Strausfeld 2005). *Lamina* stratifications are present, and analogues of M3 and M4 monopolar cells that may carry separate E-vector information are also present. Given the clear behavioural response of several of these smaller crustacean groups to polarised light (Waterman 1981), there remains much worth learning regarding PS neural circuitry in these "simplified" groups.

Fig. 7.13 (continued) in and out of section plane. *Lines* show representative R8 cell axonal projections. Scale 100 μm. c: cornea, MB: mid-band retina, DH, VH: dorsal and ventral hemispheres or peripheral retina, LA: *lamina*, ME: *medulla externa*, MI: *medulla interna* = part of lobular complex, Ch1,Ch2: chiasmata between neuropils, Acc: Accessory lobes of ME or MI from mid-band [modified from Kleinlogel et al. (2003), and Marshall et al. (2007)]

7.6 Polarisation Behaviour

Although it remains true to say that few crustaceans have had their PS capability examined behaviourally, by 1973 Waterman had collated information from 70 behavioural studies in crustaceans (Waterman 1981; Horváth and Varjú 2004). These mostly examine behaviours under broad-field E-vector illumination from above. Polarotaxis under a large field such as this involves the coordination of E-vector information from many photoreceptors. More recent studies have studied learning or innate behaviours to discrete polarised objects, bringing polarisation sensitivity into a similar category to colour vision.

7.6.1 Taxes, Navigation, Optokinetic and Large-Field Responses

Crustaceans, including several cladocerans (Verkhovskaya 1940; Baylor and Smith 1953; Waterman 1981; Novales-Flamarique and Browman 2000), mysid shrimp (Bainbridge and Waterman 1957), copepods (Umminger 1968a; Manor et al. 2009), larval crabs (Via and Forward 1975; Bardolph and Stavn 1978) and grass shrimp (Goddard and Forward 1991) swim or locomote at a predictable angle, perpendicular or parallel to the E-vector, in a polarised light field. In nature, these may be responses to the celestial E-vector pattern entering Snell's window, or to the intrinsic pattern of largely horizontal polarisation in water. Baylor and Smith (1953) suggested that such swimming behaviour in *Daphnia* might allow them to find food in brighter areas, possibly close to the surface. Cladoceran taxes are also complicated by particular colour preferences (Smith and Baylor 1953; Storz and Paul 1998), and the polarisation responses themselves are both wavelength and species dependent. *Daphnia pulex*, for example, employs two photoreceptor types with spectral sensitivities in the mid- (525 nm) and long- (608 nm) wavelength parts of the spectrum, whereas *D. magna* polarotaxis is wavelength independent, relying on a single middle-wavelength visual pigment (Novales-Flamarique and Browman 2000). *Daphnia* in fact possess four spectral sensitivities including UV (Smith and Macagno 1990). It is interesting that some crustaceans conduct PS at the mid- and long-wavelengths, rather than in the blue or UV, like other crustaceans and indeed many other animals.

E-vector orientation in the freshwater copepod, *Cyclops vernalis*, is thought to drive diurnal vertical migrations (Umminger 1968a). The simple single lens nauplius eye of this crustacean is capable of PS, and Umminger (1968b) found orthogonal microvilli in the two dorsally directed ocelli of this copepod. Also present is a reflective *tapetum lucidum*, which like that of the spider, *Drassodes cupreus*, may increase the PS efficiency (Dacke et al. 1999). The marine copepod, *Pontella karachiensis*, also possesses orthogonal microvilli within its dorsal ocelli and showed polarotaxis within certain illumination thresholds (Manor et al. 2009). These authors also suggest that PS in such planktonic species may allow detection

of other planktonic neighbours through one of the contrast mechanisms discussed above. Diurnal vertical migration is common in planktonic crustaceans and its potential ecological functions to find food or avoid predators and possibly damaging UV illumination are the most frequently cited as an explanation (reviewed in Horváth and Varjú 2004).

Novales-Flamarique and Browman (2000) tested *Daphnia* species in both downwelling and sidewelling polarised light. Where both were present, *D. pulex* showed a preference to swim towards sidewelling horizontally and away from sidewelling vertically polarised light. *D. magna* preferred to orient perpendicularly to an overhead polarised stimulus, even if there was sidewelling polarisation also present. This behaviour is interpreted as a crepuscular displacement mechanism. Previously, the natural attraction towards the horizontal E-vector of deeper water was interpreted as an escape or "shore flight" ("uferflucht" in Siebeck 1968) from potential predators along the shore (Schwind 1999; Fig. 7.6).

Predator avoidance is also suggested for the away-from shore movements of the grass shrimp *Palaemonetes vulgaris*, although in this case the response is driven by the overhead celestial E-vector pattern entering the water, as well as a number of other cues (Goddard and Forward 1991; Ritz 1991). The shrimp modify the angle of escape relative to moving celestial cues, so this behaviour is perhaps best categorised as adjustable orientation rather than navigation. Similarly, on land, beach-dwelling isopods and amphipods orient relative to the shore and may flee towards the water, apparently using the celestial compass, among other cues, for direction (Pardi 1957; Menzel 1975; Hartwick 1976; Ugolini et al. 2002).

Orientation using the celestial light field has been suggested in other littoral crustaceans. The mangrove crab, *Goniopsis cruentata*, can orient to varying E-vector in a manner corresponding to the change in celestial E-vector and suggestive of a time-compensated celestial compass (Schöne 1968). The ball-rolling crab, *Dotilla wichmanni*, centres its feeding excursions on a home hole, in part using the celestial E-vector for orientation, and thus avoids feeding over the same area (Luschi et al. 1997). Fiddler crabs may also orient and find their home burrow using the celestial sky pattern, potentially employing a dorsal rim area (DRA) at the tip of the compound eye analogous to that of insects (Chaps. 3 and 4; Labhart 1980; Alkaladi et al. 2013). Their ability to navigate in fact relies on multiple cues such as landmarks and substrate slope, but direction finding is diminished if the celestial pattern is removed. In this instance, navigation with complexity approaching that of the insects is apparent (Chiussi and Diaz 2002; Zeil and Layne 2002; Zeil and Hemmi 2006).

Further evidence that large-field E-vector patterns may be utilised for orientation comes from polarisation optomotor or optokinetic (eye movement) experiments. The ghost crab, *Ocypode quadrata*, will tilt eyestalks relative to a rotating E-vector sheet (Schöne and Schöne 1961), and at the time this was interpreted as evidence for PS without a mechanism or biological significance attached. A substantial amount of work now suggests that crabs living in semi-terrestrial "flat-world" environments specifically align their eyes to the local horizontal in order to match resolution and distance (Zeil et al. 1986; Nalbach 1990; Zeil and Hemmi 2006).

Reflections from wet mud or sand are partially linearly polarised and it may be also important for crabs to align their E-vector sensitivities relative to the horizon, as discussed for fiddler crabs above (Figs. 7.2 and 7.9; Alkaladi et al. 2013).

The potential to use the underwater E-vector light field for orientation and swimming attitude, rather than directional movement, has been suggested a number of times (Waterman 1985; Horváth and Varjú 2004). Glantz and Schroeter (2006) used pitch, roll and yaw optomotor responses in the crayfish *P. leniusculus* to clearly disambiguate polarisation from brightness as a cue for motion detection. A response specifically to E-vector angle differences of around 15° was shown, and this may be interpreted as attention to the pattern of polarised light in different sections of the visual field. They went on to demonstrate a clear dorsal light reflex to E-vector contrast in crayfish (Glantz and Schroeter 2007). While also suggestive of the importance of the E-vector contrast information in the underwater light field for orientation, this sort of reaction is distinct from optokinetic or optomotor behaviours that rely on global motion (Miller et al. 2002). Both reactions, however, are driven by the polarisation-sensitive sustaining fibres discussed above (Glantz and McIsaac 1998; Glantz and Schroeter 2006, 2007) and both may allow the animal to orient relative to E-vector in the absence of other cues.

The dorsal light reaction and optomotor responses in crayfish position the eye such that its photoreceptor array E-vector directions are arranged vertically and horizontally. Unlike semi-terrestrial crabs, the largely underwater life of crayfish implies no obvious ecological reason to maintain this eye to an external E-vector frame of reference. However, as already discussed, with two rather than three angles of E-vector analysis (Bernard and Wehner 1977), maintaining this angle optimises the ability to detect or discriminate polarisation differences in angle or degree (Glantz and Schroeter 2007).

7.6.2 Discrete Polarised Objects and Small-Field Responses

While large-field behaviours rely on the stimulation of a large number of ommatidia, a few crustaceans have also been shown capable of responding to small polarised objects. This use for PS is akin to object detection or discrimination using colour vision and therefore invokes a number of potentially different constraints on the viewing system. The swamp crayfish *P. clarkii* can detect and retreat from a moving birefringent and otherwise transparent object that is presented as a looming threat (Tuthill and Johnsen 2006). While this clearly demonstrates that PS in this species functions to visualise an object that would be essentially invisible without PS, the ecological significance of the reaction is not clear. Transparent zooplankton may be made more visible with PS at very short range, although this rapidly degrades with distance (Johnsen et al. 2011). As a predator, *P. clarkii* might increase the contrast of potentially transparent prey against a polarising background using correctly aligned PS detectors. The startle response seen is, however, best interpreted as a reaction to an object that provides polarisation contrast to the

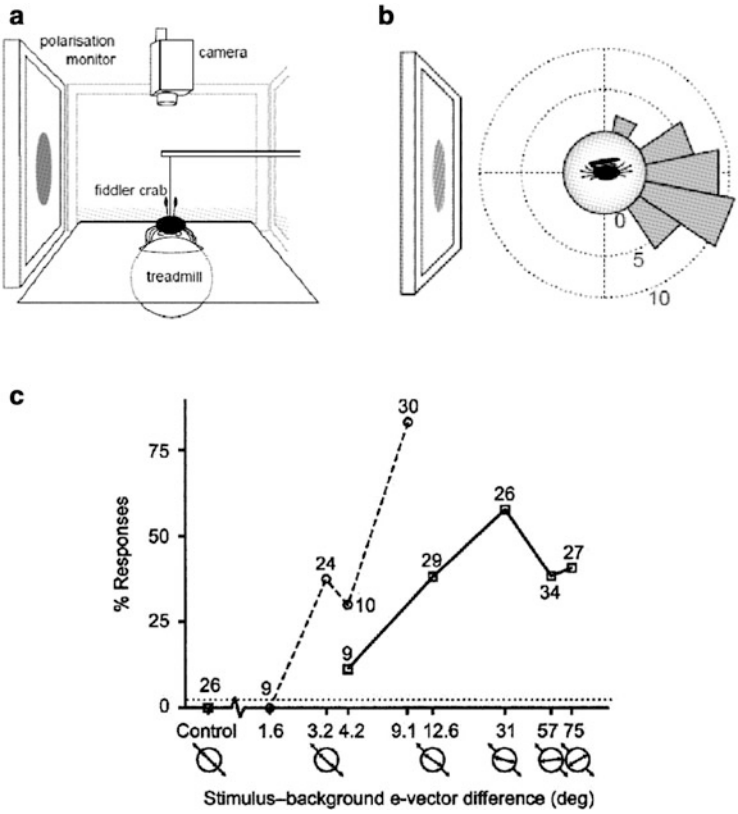

Fig. 7.14 (**a**) Behavioural tests exploiting the startle response of fiddler crabs when presented a looming stimulus on a modified LCD screen. (**b**) Experimental set-up from side and top, respectively. The expanding circle shown on screens can only be seen by animals with PS as the front polarising filter of screens has been removed. Crabs run on a floating polystyrene ball while fixed in one place from above. Behaviour is running in opposite direction as graphed in polar histogram of responses in each binned direction. (**c**) E-vector acuity to fast (*dotted line*) and slow (*solid line*) presentations of looming stimuli. E-vector difference between stimulus and background is plotted on log scale and represented below with *arrows* within *circle*. Number of stimulus presentation beside each point; E-vector discrimination of at least 3.2 is reached, the highest known for any crustacean currently [after How et al. (2012)]

crayfish but is one that would not normally occur in nature. The results are consistent with the idea proposed by Glantz (1996b) that crayfish use PS independent of intensity to enhance motion detection.

Fiddler crabs (*Uca vomeris*) also show a startle response to a rapidly looming polarisation-only stimulus displayed on a modified LCD screen (Fig. 7.14; How et al. 2012). The method exploits the fact that, once the front polaroid filter from a LCD screen is removed, the only way to see the contrast generated on the screen by the voltage-sensitive nematic crystals it contains is to use PS (Glantz and Schroeter 2006; Pignatelli et al. 2011). Operated normally, black and white are generated with

crystals perpendicular and parallel to the front polarising filter, and in the modified case, relative to the animal's PS system. The contrast of the object on the screen can be varied by changing the crystal angle relative to the background. E-vector discrimination of the crabs to a looming polarised stimulus produced in this way is remarkably fine, with flight reactions still present at a ~3° difference in E-vector (Fig. 7.14; How et al. 2012). Fiddler crabs are very sensitive to movement, and rapidly advancing objects, such as avian predators, are a major threat (Zeil and Hemmi 2006). As birefringent transparent birds or other predators are not known, the ecological significance of this reaction is also obscure; however, it does reveal the capabilities of the system. The display claw and other areas of carapace of fiddler crabs may reflect polarised information (Zeil and Hofmann 2001) and being able to detect fine variations in these signals may be important for agonistic or sexual display.

Stomatopods are the only crustaceans so far shown able to learn E-vector orientation, and it can be argued that this elevates their PS to true polarisation vision (PV, Marshall et al. 1999b; Fig. 7.8). This slightly semantic distinction aside, their interest in polarisation is already clear from the morphology of the eye alone (Fig. 7.4 and Marshall et al. 1991a). In operant conditioning feeding tests, both linear and circular polarisation discrimination have been demonstrated in *O. scyllarus* (Marshall et al. 1999b; Chiou et al. 2008). This paradigm exploits the animal's naturally violent prey capture and dismemberment mechanism (Caldwell and Dingle 1976) as they are asked to break into feeding containers with different polarising filters stuck to the outside (Fig. 7.8).

Again, it is not clear if this is behaviourally relevant in itself, for as far as we know, stomatopods do not specifically target prey that reflect polarised light. More likely, the small polarising objects that stomatopods are interested in are reflections from their own bodies as detailed above (Fig. 7.10) and expanded upon in Chap. 19. Polarising appendages and regions on stomatopods are often used in display and contest between and within species and are shown during both agonistic competition for dwellings and in mating (Chiou et al. 2011). This does not exclude the use of PS for other tasks, and given the array of polarisation detectors in stomatopods, several uses for PS seem likely. It is interesting, however, that at a cognitive level, they seem able to transfer an object discrimination ability evolved for inter- and intraspecific signalling to feeding.

The information content in polarisation signals, compared to colour communication, for example, is an area we are only beginning to understand. In feeding trials stomatopods were tested for vertical versus horizontal and left- versus right-handed CPL and the acuity of discrimination was not examined. Unpublished results in fact indicate that they fail to discriminate below E-vector differences of 20°, a finding supported by their also coarse discrimination of E-vector difference in startle tests (Roberts et al. unpublished). Tests of both E-vector and degree of polarisation acuity, analogous to wavelength discrimination (Neumeyer 1998), are needed in stomatopods if we are to begin to understand their formidable PS ability. Future work should also concentrate on looking for small-field polarisation stimuli that are important in the lives of other crustaceans.

References

Ahyong ST, Harling C (2000) The phylogeny of the stomatopod Crustacea. Aust J Zool 48:607–642

Alkaladi A, How M, Zeil J (2013) Systematic variations in microvilli banding patterns along fiddler crab rhabdoms. J Comp Physiol A 199:99–113

Bainbridge R, Waterman TH (1957) Polarized light and the orientation of two marine crustacea. J Exp Biol 34:342–364

Ball EE (1977) Fine structure of the compound eyes of the midwater amphipod *Phronima* in relation to behavior and habitat. Tissue Cell 9:521–536

Bardolph M, Stavn RH (1978) Polarized light sensitivity in the stage I zoea of the mud crab *Panopeus herbstii*. Mar Biol 46:327–33

Barta A, Horváth G (2004) Why is it advantageous for animals to detect celestial polarization in the ultraviolet? Skylight polarization under clouds and canopies is strongest in the UV. J Theor Biol 226:429–437

Baylor ER, Smith FE (1953) The orientation of cladocera to polarized light. Am Nat 87:97–101

Bernard GD, Wehner R (1977) Functional similarities between polarization vision and color vision. Vis Res 17:1019–1028

Bernáth B, Gál J, Horváth G (2004) Why is it worth flying at dusk for aquatic insects? Polarotactic water detection is easiest at low solar elevations. J Exp Biol 207:755–765

Berón de Astrada M, Tuthill J, Tomsic D (2009) Physiology and morphology of sustaining and dimming neurons of the crab *Chasmagnathus granulatus* (Brachyura: Grapsidae). J Comp Physiol A 195:791–798

Caldwell RL, Dingle H (1976) Stomatopods. Sci Am 234(1):80–89

Chiou TH, Kleinlogel S, Cronin TW, Caldwell R, Loeffler B, Siddiqi A, Goldizen A, Marshall J (2008) Circular polarization vision in a stomatopod crustacean. Curr Biol 18:429–434

Chiou TH, Marshall NJ, Caldwell RL, Cronin TW (2011) Changes in light-reflecting properties of signalling appendages alter mate choice behaviour in a stomatopod crustacean *Haptosquilla trispinosa*. Mar Freshw Behav Physiol 44:1–11

Chiou TH, Place AR, Caldwell RL, Marshall NJ, Cronin TW (2012) A novel function for a carotenoid: astaxanthin used as a polarizer for visual signalling in a mantis shrimp. J Exp Biol 215:584–589

Chiussi R, Diaz H (2002) Orientation of the fiddler crab, *Uca cumulanta*: responses to chemical and visual cues. J Chem Ecol 28:1787–96

Cronin TW, Marshall NJ (1989) A retina with at least ten spectral types of photoreceptors in a mantis shrimp. Nature 339:137–140

Cronin TW, Shashar N (2001) The linearly polarized light field in clear, tropical marine waters: spatial and temporal variation of light intensity, degree of polarization and e-vector angle. J Exp Biol 204:2461–2467

Cronin TW, Marshall NJ, Caldwell RL (1994a) The intrarhabdomal filters in the retinas of mantis shrimps. Vis Res 34:279–291

Cronin TW, Marshall NJ, Caldwell RL, Shashar N (1994b) Specialization of retinal function in the compound eyes of mantis shrimps. Vis Res 34:2639–2656

Cronin TW, Marshall NJ, Quinn CA, King CA (1994c) Ultraviolet photoreception in mantis shrimp. Vis Res 34:1443–1452

Cronin TW, Shashar N, Caldwell RL, Marshall J, Cheroske AG, Chiou TH (2003a) Polarization signals in the marine environment. In: Shaw JA, Tyo JS (eds) Polarization science and remote sensing, vol 5158, Proceedings of the Society of Photo-Optical Instrumentation Engineers (SPIE), pp 85–92

Cronin TW, Shashar N, Caldwell RL, Marshall J, Cheroske AG, Chiou TH (2003b) Polarization vision and its role in biological signaling. Integr Comp Biol 43:549–558

Cronin TW, Chiou TH, Caldwell RL, Roberts N, Marshall J (2009) Polarization signals in mantis shrimps. In: Shaw JA, Tyo JS (eds) Polarization science and remote sensing, vol 7461, Proceedings of SPIE

Dacke M, Nilsson DE, Warrant EJ, Blest AD, Land MF, O'Carroll DC (1999) Built-in polarizers form part of a compass organ in spiders. Nature 401:470–473

Doujak FE (1984) Electrophysiological measurement of photoreceptor membrane dichroism and polarization sensitivity in a Grapsid crab. J Comp Physiol 154:597–605

Eguchi E, Waterman TH (1966) Fine structure patterns in crustacean rhabdoms. In: Bernard GC (ed) The functional organisation of the compound eye. Pergamon, Oxford, pp 105–124

Eguchi E, Waterman TH (1968) Cellular basis for polarized light perception in the spider crab, *Libinia*. Z Zellforsch Mik Ana 84:87–101

Eguchi E, Goto T, Waterman TH (1982) Unorthodox pattern of microvilli and intercellular junctions in regular retinular cells of the porcellanid crab *Petro listhes*. Cell Tissue Res 222:493–513

Frank TM, Widder EA (1994) Evidence for behavioral sensitivity to near-UV light in the deep-sea crustacean *Systellaspis debilis*. Mar Biol 118:279–284

Gál J, Horváth G, Barta A, Wehner R (2001a) Polarization of the moonlit clear night sky measured by full-sky imaging polarimetry at full moon: comparison of the polarization of moonlit and sunlit skies. J Geophys Res D 106:22647–22653

Gál J, Horváth G, Meyer-Rochow VB, Wehner R (2001b) Polarization patterns of the summer sky and its neutral points measured by full-sky imaging polarimetry in Finnish Lapland north of the Arctic Circle. Proc R Soc A 457:1385–1399

Gál J, Horváth G, Meyer-Rochow VB (2001c) Measurement of the reflection-polarization pattern of the flat water surface under a clear sky at sunset. Remote Sens Environ 76:103–111

Gaten E, Shelton PMJ, Herring PJ (1992) Regional morphological variations in the compound eyes of certain mesopelagic shrimps in relation to their habitat. J Mar Biol Assoc UK 72:61–75

Glantz RM (1996a) Polarization sensitivity in crayfish lamina monopolar neurons. J Comp Physiol A 178:413–425

Glantz RM (1996b) Polarization sensitivity in the crayfish optic lobe: peripheral contributions to opponency and directionally selective motion detection. J Neurophysiol 76:3404–3414

Glantz RM (2001) Polarization analysis in the crayfish visual system. J Exp Biol 204:2383–2390

Glantz RM (2007) The distribution of polarization sensitivity in the crayfish retinula. J Comp Physiol A 193:893–901

Glantz RM (2008) Polarization vision in crayfish motion detectors. J Comp Physiol A 194:565–575

Glantz RM, McIsaac A (1998) Two-channel polarization analyzer in the sustaining fiber dimming fiber ensemble of crayfish visual system. J Neurophysiol 80:2571–2583

Glantz RM, Schroeter J (2006) Polarization contrast and motion detection. J Comp Physiol A 192:905–914

Glantz RM, Schroeter J (2007) Orientation by polarized light in the crayfish dorsal light reflex: behavioral and neurophysiological studies. J Comp Physiol A 193:371–384

Goddard SM, Forward RB (1991) The role of the underwater polarized light pattern, in sun compass navigation of the grass shrimp, *Palaemonetes vulgaris*. J Comp Physiol A 169:479–491

Goldstein D (2003) Polarized light. Dekker, Basel

Hámori J, Horridge GA (1966a) The lobster optic lamina I. General organization. J Cell Sci 1:249–256

Hámori J, Horridge GA (1966b) The lobster optic lamina II. Types of synapse. J Cell Sci 1:257–269

Hartwick RF (1976) Beach orientation in talitrid amphipods: capacities and strategies. Behav Ecol Sociobiol 1:447–458

Hawryshyn CW (1992) Polarization vision in fish. Am Sci 80:164–175

Hawryshyn CW (2000) Ultraviolet polarization vision in fishes: possible mechanisms for coding e-vector. Philos Trans R Soc Lond B Biol Sci 355:1187–1190
Hecht E (2001) Optics. Addison-Wesley, Reading, MA, USA
Hegedüs R, Horváth G (2004a) How and why are uniformly polarization-sensitive retinae subject to polarization-related artefacts? Correction of some errors in the theory of polarization-induced false colours. J Theor Biol 230:77–87
Hegedüs R, Horváth G (2004b) Polarizational colours could help polarization-dependent colour vision systems to discriminate between shiny and matt surfaces, but cannot unambiguously code surface orientation. Vis Res 44:2337–2348
Hegedüs R, Horváth Á, Horváth G (2006) Why do dusk-active cockchafers detect polarization in the green? The polarization vision in *Melolontha melolontha* is tuned to the high polarized intensity of downwelling light under canopies during sunset. J Theor Biol 238:230–244
Hegedüs R, Åkesson S, Horváth G (2007a) Polarization patterns of thick clouds: overcast skies have distribution of the angle of polarization similar to that of clear skies. J Opt Soc Am A 24:2347–2356
Hegedüs R, Barta A, Bernáth B, Meyer-Rochow VB, Horváth G (2007b) Imaging polarimetry of forest canopies: how the azimuth direction of the sun, occluded by vegetation, can be assessed from the polarization pattern of the sunlit foliage. Appl Opt 46:6019–6032
Hegedüs R, Åkesson S, Horváth G (2007c) Anomalous celestial polarization caused by forest fire smoke: why do some insects become visually disoriented under smoky skies? Appl Opt 46:2717–2726
Hegedüs R, Åkesson S, Wehner R, Horváth G (2007d) Could Vikings have navigated under foggy and cloudy conditions by skylight polarization? On the atmospheric optical prerequisites of polarimetric Viking navigation under foggy and cloudy skies. Proc R Soc A 463:1081–1095
Hemmi JM, Marshall J, Pix W, Vorobyev M, Zeil J (2006) The variable colours of the fiddler crab *Uca vomeris* and their relation to background and predation. J Exp Biol 209:4140–4153
Horváth G (1995) Reflection-polarization patterns at flat water surfaces and their relevance for insect polarization vision. J Theor Biol 175:27–37
Horváth G, Varjú D (1995) Underwater refraction-polarization patterns of skylight perceived by aquatic animals through Snell's window of the flat water surface. Vis Res 35:1651–1666
Horváth G, Varjú D (1997) Polarization pattern of freshwater habitats recorded by video polarimetry in red, green and blue spectral ranges and its relevance for water detection by aquatic insects. J Exp Biol 200:1155–1163
Horváth G, Varjú D (2004) Polarized light in animal vision—polarization patterns in nature. Springer, Heidelberg
Horváth G, Wehner R (1999) Skylight polarization as perceived by desert ants and measured by video polarimetry. J Comp Physiol A 184:1–7, Erratum 184: 347-349 (1999)
Horváth G, Barta A, Gál J, Suhai B, Haiman O (2002a) Ground-based full-sky imaging polarimetry of rapidly changing skies and its use for polarimetric cloud detection. Appl Opt 41:543–559
Horváth G, Gál J, Labhart T, Wehner R (2002b) Does reflection polarization by plants influence colour perception in insects? Polarimetric measurements applied to a polarization-sensitive model retina of *Papilio* butterflies. J Exp Biol 205:3281–3298
Horváth G, Kriska G, Malik P, Robertson B (2009) Polarized light pollution: a new kind of ecological photopollution. Front Ecol Environ 7:317–325
Horváth G, Kriska G, Malik P, Hegedüs R, Neumann L, Åkesson S, Robertson B (2010) Asphalt surfaces as ecological traps for water-seeking polarotactic insects: how can the polarized light pollution of asphalt surfaces be reduced? Environmental remediation technologies, regulations and safety. Nova Science Publishers, Inc., Hauppauge, NY
How MJ, Marshall NJ (2014a) Polarization distance: a framework for modelling object detection by polarization vision systems. Proc R Soc B Biol Sci 281(1776):20131632
How MJ, Pignatelli V, Temple SE, Marshall NJ, Hemmi JM (2012) High e-vector acuity in the polarisation vision system of the fiddler crab *Uca vomeris*. J Exp Biol 215:2128–2134

Ivanoff A, Waterman TH (1958a) Elliptical polarization of submarine illumination. J Mar Res 16:255–282
Ivanoff A, Waterman TH (1958b) Factors, mainly depth and wavelength, affecting the degree of underwater light polarization. J Mar Res 16:283–307
Jerlov NG (1976) Marine optics, Elsevier oceanography series. Elsevier, Amsterdam
Johnsen S, Marshall NJ, Widder EA (2011) Polarization sensitivity as a contrast enhancer in pelagic predators: lessons from in situ polarization imaging of transparent zooplankton. Philos Trans R Soc B 366:655–670
Jordan TM, Partridge JC, Roberts NW (2012) Non-polarizing broadband multilayer reflectors in fish. Nat Photonics 6:759–763
Kelber A, Thunell C, Arikawa K (2001) Polarisation-dependent colour vision in *Papilio* butterflies. J Exp Biol 204:2469–2480
Kirschfeld K (1976) The resolution of lens and compound eyes. In: Zettler F, Weiler R (eds) Neural principles in vision. Springer, Heidelberg, pp 354–370
Kleinlogel S, Marshall NJ (2005) Photoreceptor projection and termination pattern in the lamina of gonodactyloid stomatopods (mantis shrimp). Cell Tissue Res 321:273–284
Kleinlogel S, Marshall NJ (2006) Electrophysiological evidence for linear polarization sensitivity in the compound eyes of the stomatopod crustacean *Gonodactylus chiragra*. J Exp Biol 209:4262–4272
Kleinlogel S, Marshall NJ (2009) Ultraviolet polarisation sensitivity in the stomatopod crustacean *Odontodactylus scyllarus*. J Comp Physiol A 195:1153–1162
Kleinlogel S, White AG (2008) The secret world of shrimps: polarisation vision at its best. PLoS One 3(5):e2190
Kleinlogel S, Marshall NJ, Horwood JM, Land MF (2003) Neuroarchitecture of the color and polarization vision system of the stomatopod haptosquilla. J Comp Neurol 467:326–342
Kolb G (1977) Structure of eye of *Pieris brasicae* L. (Lepidoptera). Zoomorphologie 87:123–146
Krebs W, Lietz R (1982) Apical region of the crayfish retinula. Cell Tissue Res 222:409–415
Labhart T (1980) Specialized photoreceptors at the dorsal rim of the honeybees compound eye—polarizational and angular sensitivity. J Comp Physiol 141:19–30
Labhart T, Petzold J, Helbling H (2001) Spatial integration in polarization-sensitive interneurones of crickets: a survey of evidence, mechanisms and benefits. J Exp Biol 204:2423–2430
Land MF (1981) Optics of the eyes of *Phronima* and other deep-sea amphipods. J Comp Physiol 145:209–226
Land MF (1984) Crustacea. In: Ali MA (ed) Photoreception and vision in invertebrates. Plenum, New York, pp 401–438
Land MF, Nilsson DE (2012) Animal eyes. Oxford University Press, Oxford
Land MF, Marshall JN, Brownless D, Cronin TW (1990) The eye-movements of the mantis shrimp *Odontodactylus scyllarus* (Crustacea: Stomatopoda). J Comp Physiol A 167:155–166
Leggett LMW (1976) Polarized light-sensitive interneurones in a swimming crab. Nature 262:709–711
Loew ER (1976) Light and photoreceptor degeneration in the Norway lobster, *Nephrops norvegicus* L. Proc R Soc Lond B 193:31–44
Luschi P, Seppia CD, Crosio E (1997) Orientation during short-range feeding in the crab *Dotilla wichmanni*. J Comp Physiol A 181:461–468
Lythgoe JN (1979) The ecology of vision. Clarendon, Oxford
Lythgoe JN, Hemmings CC (1967) Polarized light and underwater vision. Nature 213:893–895
Macagno ER, Lopresti V, Levinthal C (1973) Structure and development of neuronal connections in isogenic organisms: Variations and similarities in the optic system of *Daphnia magna*. Proc Natl Acad Sci 70:57–61
Manor S, Polak O, Saidel WM, Goulet TL, Shashar N (2009) Light intensity mediated polarotaxis in *Pontella karachiensis* (Pontellidae, Copepoda). Vis Res 49:2371–2378
Marshall NJ (1988) A unique color and polarization vision system in mantis shrimps. Nature 333:557–560

Marshall NJ, Land MF (1993) Some optical features of the eyes of stomatopods 2. Ommatidial design, sensitivity and habitat. J Comp Physiol A 173:583–594
Marshall NJ, Messenger JB (1996) Colour-blind camouflage. Nature 382:408–409
Marshall J, Oberwinkler J (1999) The colourful world of the mantis shrimp. Nature 401:873–874
Marshall NJ, Land MF, King CA, Cronin TW (1991a) The compound eyes of mantis shrimps (Crustacea, Hoplocarida, Stomatopoda) 1. Compound eye structure—the detection of polarized light. Philos Trans R Soc Lond B 334:33–56
Marshall NJ, Land MF, King CA, Cronin TW (1991b) The compound eyes of mantis shrimps (Crustacea, Hoplocarida, Stomatopoda) 2. Color pigments in the eyes of stomatopod crustaceans—Polychromatic vision by serial and lateral filtering. Philos Trans R Soc Lond B 334:57–84
Marshall NJ, Kent J, Cronin TW (1999a) Visual adaptations in crustaceans. In: Archer SN, Djamgoz MBA, Lowe E, Partridge JC, Vallerga S (eds) Adaptive mechanisms in the ecology of vision. Kluwer, London, pp 285–328
Marshall J, Cronin TW, Shashar N, Land M (1999b) Behavioural evidence for polarisation vision in stomatopods reveals a potential channel for communication. Curr Biol 9:755–758
Marshall J, Cronin TW, Kleinlogel S (2007) Stomatopod eye structure and function: a review. Arthropod Struct Dev 36:420–448
Menzel R (1975) Polarised light sensitivity in arthropods. In: Evans GC (ed) Light as an ecological factor II. Blackwell, Oxford, pp 289–303
Meyer-Rochow VB (1971) A crustacean-like organization of insect rhabdoms. Cytobiologie 4:241–249
Meyer-Rochow VB (1975) Larval and adult eye of the western rock lobster (*Panulirus longipes*). Cell Tissue Res 162:439–457
Meyer-Rochow VB (1978) The eyes of mesopelagic crustaceans: II. *Streetsia challengeri* (Amphipoda). Cell Tissue Res 186:337–349
Meyer-Rochow VB (1982) The divided eye of the isopod *Glyptonotus antarcticus*: effects of unilateral dark adaptation and temperature elevation. Proc R Soc Lond B Biol Sci 215:433–450
Meyer-Rochow VB, Tiang KM (1984) The eye of *Jasus edwardsii* (Crustacea, Decapoda): electrophysiology, histology and behaviour. Zoologica 45:1–61
Miller CS, Johnson DH, Schroeter JP, Myint LL, Glantz RM (2002) Visual signals in an optomotor reflex: systems and information theoretic analysis. J Comput Neurosci 13:5–21
Mote M (1974) Polarization sensitivity. J Comp Physiol 90:389–403
Muller KJ (1973) Photoreceptors in the crayfish compound eye: electrical interactions between cells as related to polarized light sensitivity. J Physiol Lond 232:573–595
Munk O (1970) On the occurrence and significance of horizontal band-shaped retinal areae in teleosts. Videnskabelige Meddelelser Dansk Naturhistorisk Forening 133:85–120
Nalbach HO (1990) Visually elicited escape in crabs. In: Wiese K, Krenz WD, Tautz J, Reichert H, Mulloney B (eds) Advances in life sciences: frontiers in crustacean neurobiology. Birkhauser, Basel
Nässel DR (1975) The organization of the *lamina ganglionaris* of the prawn, *Pandalus borealis* (Kröyer). Cell Tissue Res 163:445–464
Nässel DR (1976) Retina and retinal projection on *lamina ganglionaris* of crayfish *Pacifastacus leniusculus* (Dana). J Comp Neurol 167:341–359
Nässel DR (1977) Types and arrangements of neurons in crayfish optic lamina. Cell Tissue Res 179:45–75
Nässel DR, Waterman TH (1977) Golgi em evidence for visual formation channeling in crayfish *lamina langlionaris*. Brain Res 130:556–563
Nässel DR, Waterman TH (1979) Massive diurnally modulated photoreceptor membrane turnover in crab light and dark adaptation. J Comp Physiol 131:205–216
Neumeyer C (1991) Evolution of colour vision. In: Cronly-Dillon JR, Gregory RL (eds) Vision and visual dysfunction: evolution of the eye and visual system, vol 2. Macmillan, London, pp 284–305

Neumeyer C (1998) Color vision in lower vertebrates. In: Backhaus WGK, Kliegl R, Werner JS (eds) Color vision—perspectives from different disciplines. Walter de Gruyter & Co., Berlin, pp 149–162
Neville AC, Luke BM (1971) Form optical activity in crustacean cuticle. J Insect Physiol 17:519–526
Novales-Flamarique I (2011) Unique photoreceptor arrangements in a fish with polarized light discrimination. J Comp Neurol 519:714–737
Novales-Flamarique I, Browman HI (2000) Wavelength-dependent polarization orientation in *Daphnia*. J Comp Physiol A 186:1073–1087
Pardi L (1957) L'orientamento astronomico degli animali: risultati e problemiattuali. Bolletino di zoologia 24:473–523
Pignatelli V, Temple SE, Chiou TH, Roberts NW, Collin SP, Marshall NJ (2011) Behavioural relevance of polarization sensitivity as a target detection mechanism in cephalopods and fishes. Philos Trans R Soc B 366:734–741
Pomozi I, Horváth G, Wehner R (2001) How the clear-sky angle of polarization pattern continues underneath clouds: full-sky measurements and implications for animal orientation. J Exp Biol 204:2933–2942
Porter ML, Zhang Y, Desai S, Caldwell RL, Cronin TW (2010) Evolution of anatomical and physiological specialization in the compound eyes of stomatopod crustaceans. J Exp Biol 213:3473–3486
Ritz DA (1991) Polarised light responses in the shrimp *Palaemonetes vulgaris* (Say). J Exp Mar Biol Ecol 154:245–250
Roberts NW, Chiou TH, Marshall NJ, Cronin TW (2009) A biological quarter-wave retarder with excellent achromaticity in the visible wavelength region. Nat Photonics 3:641–644
Rutherford DJ, Horridge GA (1965) The rhabdom of the lobster eye. Q J Microsc Sci 106:119–130
Sabbah S, Barta A, Gál J, Horváth G, Shashar N (2006) Experimental and theoretical study of skylight polarization transmitted through Snell's window of a flat water surface. J Opt Soc Am A 23:1978–1988
Sabra R, Glantz RM (1985) Polarization sensitivity of crayfish photoreceptors is correlated with their termination sites in the *lamina ganglionaris*. J Comp Physiol A 156:315–318
Schechner YY, Karpel N (2005) Recovery of underwater visibility and structure by polarization analysis. IEEE J Ocean Eng 30:570–587
Schiff H (1963) Dim light vision of *Squilla mantis* L. Am J Physiol 205:927–940
Schneider L, Langer H (1969) Die Struktur des Rhabdomes im "Doppelauge" des Wasserläufers *Gerris lacustris*. Z Zelforsch 99:528–559
Schöne H (1968) Agonistic and sexual display in aquatic and semi-terrestrial Brachyuran crabs. Am Zool 8:641–645
Schöne H, Schöne H (1961) Eyestalk movements induced by polarized light in the ghost crab, *Ocypode quadrata*. Science 134:675–676
Schwind R (1983) Zonation of the optical environment and zonation in the rhabdom structure within the eye of the backswimmer, *Notonecta glauca*. Cell Tissue Res 232:53–63
Schwind R (1999) *Daphnia pulex* swims towards the most strongly polarized light: a response that leads to 'shore flight'. J Exp Biol 202:3631–3635
Schwind R, Horváth G (1993) Reflection-polarization pattern at water surfaces and correction of a common representation of the polarization pattern of the sky. Naturwissenschaften 80:82–83
Shashar N, Addessi L, Cronin TW (1995) Polarization vision as a mechanism for detection of transparent objects. In: Gulko D, Jokiel V (eds) Ultraviolet radiation and coral reefs. HIMB Technical Report 41, pp 207–2211
Shaw SR (1966) Polarized light responses from crab retinula cells. Nature 211:92–93
Shelton PMJ, Gaten E, Herring PJ (1992) Adaptations of tapeta in the eyes of mesopelagic decapod shrimps to match the oceanic irradiance distribution. J Mar Biol Assoc UK 72:77–88
Siebeck O (1968) "Uferflucht" und optische Orientierung pelagischer Crustaceen. Arch Hydrobiol Suppl 35:1–118

Sipőcz B, Hegedüs R, Kriska G, Horváth G (2008) Spatiotemporal change of sky polarization during the total solar eclipse on 29 March 2006 in Turkey: polarization patterns of the eclipsed sky observed by full-sky imaging polarimetry. Appl Opt 47(34):H1–H10

Smith FE, Baylor ER (1953) Color responses in the cladocera and their ecological significance. Am Nat 87:49–55

Smith KC, Macagno ER (1990) UV photoreceptors in the compound eye of *Daphnia magna* (Crustacea, Branchiopoda): a 4th spectral class in single ommatidia. J Comp Physiol A 166:597–606

Snyder AW (1973) Polarisation sensitivity of individual retinula cells. J Comp Physiol 83:331–360

Snyder AW, Laughlin SB (1975) Dichroism and absorption by photoreceptors. J Comp Physiol 100:101–116

Storz UC, Paul RJ (1998) Phototaxis in water fleas (*Daphnia magna*) is differently influenced by visible and UV light. J Comp Physiol A 183:709–717

Stowe S (1977) The retina-lamina projection in the crab *Leptograpsus variegatus*. Cell Tissue Res 185:515–525

Stowe S (1980) Rapid synthesis of photoreceptor membrane and assembly of new microvilli in a crab at dusk. Cell Tissue Res 211:419–440

Stowe S (1981) Effects of illumination changes on rhabdom synthesis in a crab. J Comp Physiol 142:19–25

Stowe S (1983) A theoretical explanation of intensity-independant variation of polarisation sensitivity in crustacean retinular cells. J Comp Physiol 153:435–441

Strausfeld NJ (2005) The evolution of crustacean and insect optic lobes and the origins of chiasmata. Arthropod Struct Dev 34:235–256

Strausfeld NJ, Nässel DR (1981) Neuroarchitecture of brain regions that subserve the compound eyes of crustacea and insects. In: Autrum H (ed) Handbook of sensory physiology, vol VII(6). Springer, Heidelberg, pp 357–344

Suhai B, Horváth G (2004) How well does the Rayleigh model describe the E-vector distribution of skylight in clear and cloudy conditions? A full-sky polarimetric study. J Opt Soc Am A 21:1669–1676

Sztarker J, Strausfeld NJ, Andrew D, Tomsic D (2009) Neural organization of first optic neuropils in the littoral crab *Hemigrapsus oregonensis* and the semiterrestrial species *Chasmagnathus granulatus*. J Comp Neurol 513:129–150

Talbot CM, Marshall J (2010) Polarization sensitivity in two species of cuttlefish—*Sepia plangon* (Gray 1849) and *Sepia mestus* (Gray 1849)—demonstrated with polarized optomotor stimuli. J Exp Biol 213:3364–3370

Talbot CM, Marshall JN (2011) The retinal topography of three species of coleoid cephalopod: significance for perception of polarized light. Philos Trans R Soc B 366:724–733

Thoen HH, How MJ, Chiou T-H, Marshall J (2014) A different form of color vision in Mantis shrimp. Science 343:411–413

Tuthill JC, Johnsen S (2006) Polarization sensitivity in the red swamp crayfish *Procambarus clarkii* enhances the detection of moving transparent objects. J Exp Biol 209:1612–1616

Ugolini A, Tiribilli B, Boddi V (2002) The sun compass of the sandhopper *Talitrus saltator*: the speed of the chronometric mechanism depends on the hours of light. J Exp Biol 205:3225–3230

Umminger BL (1968a) Polarotaxis in copepods I. An endogenous rhythm in polarotaxis in *Cyclops vernalis* and its relation to vertical migration. Biol Bull 135:239–251

Umminger BL (1968b) Polarotaxis in copepods II. The ultrastructural basis and ecological significance of polarized light sensitivity in copepods. Biol Bull 135:252–261

Verkhovskaya IN (1940) The influence of polarised light upon the phototaxis of certain organisms. Bull Moscow Nat Hist Soc Biol Sec 49:101–113 (in Russian)

Via SE, Forward RB Jr (1975) The ontogeny and spectral sensitivity of polarotaxis in larvae of the crab *Rhithropanopeus harrisi* (Gould). Biol Bull 149:251–266

Waterman TH (1954) Polarization patterns in submarine illumination. Science 120:927–932

Waterman TH (1977) The bridge between visual input and central programming in crustaceans. In: Hoyle G (ed) Identified neurons and behaviour of arthropods. Plenum, New York
Waterman TH (1981) Polarisation sensitivity. In: Autrum H (ed) Handbook of sensory physiology, vol VII/6B. Springer, Heidelberg, pp 283–469
Waterman TH (1985) Natural polarised light and vision. In: Ali MA (ed) Photoreception and vision in invertebrates. Plenum, New York, pp 63–113
Waterman TH, Fernandez HR (1970) E-vector and wavelength discrimination by retinular cells of the crayfish *Procambarus*. Zeitschrift für Vergleichende Physiologie 68:154–174
Waterman TH, Horch KW (1966) Mechanism of polarized light perception. Science 154:467–475
Wehner R (1983) The perception of polarized light. Symp Soc Exp Biol 36:331–369
Wehner R (1987) 'Matched filters'—neural models of the external world. J Comp Physiol A 161:511–531
Wehner R (2001) Polarization vision—a uniform sensory capacity? J Exp Biol 204:2589–2596
Wehner R, Labhart T (2006) Polarisation vision. In: Warrant EJ, Nilsson DE (eds) Invertebrate vision. Cambridge University Press, Cambridge
Yamaguchi T, Katagiri Y, Ochi K (1976) Polarised light responses from retinular cells and sustaining fibres of the mantis shrimp. Biol J Okayama Univ 17:61–66
Yamaguchi T, Okada Y, Nakatani K, Ohta N (1984) Functional morphology of visual interneurons in the crayfish central nervous system. In: Aoki K (ed) Animal behaviour: neurophysiological and ethological approaches. Science Society Press, Tokyo, pp 109–122
Zeil J, Hemmi JM (2006) The visual ecology of fiddler crabs. J Comp Physiol A 192:1–25
Zeil J, Hofmann M (2001) Signals from 'crabworld': cuticular reflections in a fiddler crab colony. J Exp Biol 204:2561–2569
Zeil J, Layne J (2002) Path integration in fiddler crabs and its relation to habitat and social life. In: Weise K (ed) Crustacean experimental systems in neurobiology. Springer, Heidelberg
Zeil J, Nalbach G, Nalbach HO (1986) Eyes, eye stalks and the visual world of semi-terrestial crabs. J Comp Physiol A 159:801–811

Chapter 8
Polarization Vision in Cephalopods

Nadav Shashar

Abstract Polarization sensitivity, namely sensitivity to linearly polarized light, has been known in cephalopods for over 50 years. So far our neurological understanding of this polarization sensitivity has remained at the level of the retina, and our knowledge of how polarization information is processed is lacking. However, when examining function, a range of tasks in which polarization vision plays a role have been identified. These include, but are not limited to, detailed examination of the environment, target (including both prey and predator) detection and recognition, short range navigation, image stabilization and most likely communication. Neurological examination of the processing of polarization information and its integration with other sensory inputs on the one hand, along with a physical understanding of the propagation of the polarization signals under various conditions, are needed for a better understanding of the function of polarization vision in the lives of cephalopods.

8.1 Introduction

Polarization sensitivity, or sensitivity to the E-vector orientation of linearly polarized light, was first discovered in cephalopods half a century ago by Moody and Parriss (1960, 1961), who were able to train octopuses to prefer light of a given E-vector orientation over another. This finding was reached just 12 years after von Frisch (1949) reported the existence and use of polarization sensitivity in honeybees. However, over time the direction, in which the study and our understanding of

N. Shashar (✉)
Department of Life Sciences, Marine Biology and Biotechnology Program, Ben Gurion University, Eilat Campus, P.O.B. 653, Beer Sheva 84105, Israel
e-mail: nadavsh@bgu.ac.il

G. Horváth (ed.), *Polarized Light and Polarization Vision in Animal Sciences*, Springer Series in Vision Research 2, DOI 10.1007/978-3-642-54718-8_8,

polarization sensitivity in cephalopods developed, greatly differed from its profound understanding in the visual systems of a range of insects.

The anatomical basis for polarization sensitivity in insects as well as in cephalopods is similar, relying on the rhabdomeric structure of the photoreceptors in their retina. This structure, in which the microvilli of each photoreceptor cell are aligned parallel to each other, renders the cell with increased sensitivity to a given polarization orientation (Goldsmith 1991). In insects this alignment often occurs along three different orientations, set approximately 60° from one another (reviewed in Horváth and Varjú 2004). Although in cephalopods two orthogonal orientations are common (Talbot and Marshall 2011), a middle third orientation has been reported (Shashar et al. 2002). A somewhat deeper examination shows that the alignment of visual pigment molecules within the microvillar membrane is such that the photoreceptor cell absorbs light most efficiently in one orientation of polarization over a perpendicular orientation (Young 1971; Goldsmith 1991). In squid, recordings from the optic nerve fibers have shown differential activity of photoreceptor cells, when exposed to changes in the orientation of polarization of incoming light, and that this information is conveyed to the brain in the form of a spike activity code (Saidel et al. 1983, 2005).

However, here ends the similarity in our understanding of coding and processing of polarization information in insects versus cephalopods. Unlike the former, so far there is no knowledge as to specific centres or even areas in the brain of cephalopods where polarization information is decoded and processed; nor is there knowledge of how this information interacts with other sensory inputs. Is polarization information perceived as a separate mode of visual information (as is colour information in humans for example), or is it a mere modulation of the intensity information? Even, this most basic question is not yet answered. Several studies have attempted to answer it in an indirect way (Cartron et al. 2013a, b and references within), but a true neurological examination is still missing. Indeed, the neuro-anatomical mapping of tracts and centres in cephalopod brains that are involved in processing polarization information may well be the next challenge facing the study of polarization vision in cephalopods.

Lacking a comparative neurological approach, researchers have focused on behavioural studies, mainly looking at the function of polarization sensitivity, or even polarization vision to the animals. In parallel studies researchers have been examining the function of polarization patterns that are created by a range of cephalopods, by specific light-reflecting cells, and in particular examining the function as a communication channel (Mäthger et al. 2009). The earlier literature on cephalopod polarization vision has been reviewed by Horváth and Varjú (2004, Chapter 26, pp. 267–275). In this chapter, we survey the new results about the polarization sensitivity in cephalopods obtained in the last decade (Table 8.1).

Table 8.1 Tasks involving polarization sensitivity in cephalopods

Task	Details	References	Comments
High-resolution vision	The ability to see differences as small as 1° in orientation of polarization	Temple et al. (2012)	Resolution of partial polarization yet unknown
Short-scale navigation	Using polarization patterns as landmarks and as guides on short scale	Cartron et al. (2012)	The ability for long-scale navigation or the use of the sky's polarization pattern is yet unknown
Object detection	Detection of transparent planktonic prey	Shashar et al. (1998)	
	Detection of grass shrimp	Darmaillacq et al. (2006), Temple et al. (2012)	
	Detection of looming targets through a scattering medium	Pignatelli et al. (2011), Cartron et al. (2013a, c)	
Object recognition	Recognition of prey	Shashar et al. (2000), Darmaillacq et al. (2006)	
	Recognition of potential predators	Cartron et al. (2013a, c)	
	Recognition of artificial targets	Moody and Parriss (1960, 1961)	
Image/scene stabilizing	Positive response	Cartron et al. (2013c), Talbot and Marshall (2010)	Tested by optomotor responses
	Negative response	Darmaillacq and Shashar (2008)	
Communication	Anatomical evidence	Chiou et al. (2007), Mäthger and Hanlon (2006)	
	Behavioural evidence	Shashar et al. (1996), Hanlon et al. (1999), Boal et al. (2004)	

8.2 Functions of Polarization Sensitivity

The original work of Moody and Parriss (1960, 1961) identified two possible functions for polarization sensitivity: (1) discriminating between objects and (2) target recognition. The idea is that a target is transmitting or reflecting a known pattern

of polarization that allows the observer to recognize it, for example, as a possible food item. This function has been repeatedly examined and examples of it were suggested to include recognition of fish by their polarization reflection and of crabs hidden among other objects (Shashar et al. 2000). Subsequent studies (Darmaillacq et al. 2006) demonstrated that even young cuttlefish use polarization as a cue of identifying preferred and non-preferred prey items.

Detection of targets based on the polarization of light transmitted through them was demonstrated for squid hatchlings feeding on transparent yet polarization-optically active copepods (Shashar et al. 1998). However, Johnsen et al. (2011) calculated that polarization-based target detection in the open sea will increase detection range by only a short distance, less than doubling it. Nonetheless, such polarization-based prey detection was also demonstrated in cuttlefish hunting for grass shrimp (Darmaillacq et al. 2006; Temple et al. 2012).

In addition to prey and food items, another type of target that needs to be detected are approaching predators. Using the modification of flat screens, in such a way that the screen delivers a polarized pattern, Pignatelli et al. (2011) demonstrated a strong response to a looming predator, simulating image by three species of cephalopods, namely the mourning cuttlefish (*Sepia plangon*), the striped pyjama squid (*Sepioloidea lineolata*) and the big fin squid (*Sepioteuthis lessoniana*). This response occurred to both grey-scale images with no polarization content (delivered through Cathode Ray Tube computer screens) and to linearly polarized images that could not be detected without a polarization imaging system. Cartron et al. (2013a, c), using a modification of the mentioned stimulus system, showed a similar startling response of two species of cuttlefish to a range of looming objects, and specifically to images of approaching predatory fish, both in the intensity and the polarization domains. It is worth noting that under clear water conditions, the responses towards both types of targets were similar. However, when examined under increasingly turbid conditions, the polarized target elicited a stronger response than the intensity-only target, suggesting a stronger transmission of the polarization information through turbid media.

Stabilizing one's field of view is a basic task or near a reflex behaviour of visual systems. Optomotor systems, in which an animal is placed inside a rotating, patterned arena, use this function to examine the ability of animals to see different types of patterns, or rotating at different rates, testing things such as colour vision, flicker fusion and visual acuity. Talbot and Marshall (2010) used this approach to detect polarization sensitivity in *Sepia plangon* and *S. mestus*. However, examining the elongated cuttlefish *S. elongata*, Darmaillacq and Shashar (2008) did not find such scene-stabilizing optomotor response to polarized patterns, although a strong optomotor response to black and white stripes was noted. Nonetheless, polarization sensitivity was found in this species using a different assay (Cartron et al. 2013c). Cartron et al. (2013b), examining the common European cuttlefish, *S. officinalis*, have taken this assay forward to examine the development of optomotor responses in hatchlings and young cuttlefish. Cartron and colleagues found that polarization sensitivity develops later than intensity sensitivity and that the polarization-based visual acuity lagged after the intensity-based acuity. In their study, Cartron

et al. (2013b) provided supportive evidence to the notion that polarization information has its unique properties as it is processed in cephalopods' brains.

One of the most important tasks of any visual system is to identify the details of its surroundings. Towards this task animals have large eyes, high density of photoreceptors, special high-resolution areas such as a fovea, and other means to increase sensitivity to details. One requirement for detecting details is the ability to differentiate between them, such as by detecting differences in brightness, hue, etc. Until recently, it was believed that cephalopod resolution in polarization was limited as compared to the resolution in the intensity domain. However, Temple et al. (2012) have demonstrated that cuttlefish (*Sepia plangon*) possess high-resolution polarization vision in that they can discriminate between differences in orientation of linear polarization as small as 1°. Detailed examination of objects relevant to the cuttlefish, such as fish and grass shrimp, showed that when examined on such a fine scale, otherwise hidden details of the object, as well as differences between the object and its background, come to view. Assuming this high resolution is common in cephalopods, it may well increase the advantage of using polarization vision for detecting transparent prey, since much of the limitations described by Johnsen et al. (2011) lead to small differences in linear polarization.

In a wide range of terrestrial and marine organisms, polarization plays an important role in their navigation ability, often through the examination of the celestial polarization pattern or as part of a sun compass. So far, no such navigation or even orientation according to the polarization of downwelling illumination has been detected in cephalopods. This is despite the fact that squid and cuttlefish are well known of making long journeys onto their breeding grounds. Cartron et al. (2012) examined another mode of short-term navigation: using landmarks to identify the preferred direction in which to go. Using a specially designed T maze, Cartron et al. (2012) trained cuttlefish (*Sepia officinalis*) to turn to the direction in which a linearly polarized pattern was presented. This was contrasted with a different orientation of polarization marked by a perpendicular pattern. To ensure that the cuttlefish are not trained on external signals, the entire system was rotated during the experiments. In doing so, Cartron et al. (2012) have demonstrated that polarization signals or patterns can provide cues in spatial orientation of cephalopods.

8.3 Communication

Ever since the accidental discovery of patterns of polarized light reflected off the arms of *Sepia officinalis* cuttlefish nearly 20 years ago (Shashar et al. 1996), the suggestion that cephalopods have their own mode of communication that is undetectable to animals that are not polarization sensitive intrigued and challenged researchers (Mäthger et al. 2009). To date, unique patterns of polarization have been found not only in cuttlefish but also in octopus and squid (see also Chap. 19). Detailed anatomical examination revealed that these linearly polarized reflections

arise from a special type of reflecting cells that are present in the skin: the elongated iridophores (Mäthger and Hanlon 2006). It was also found that the polarized signal can be transmitted regardless of the colour pattern produced by the overlaying chromatophores. Furthermore, the polarization reflection is not sensitive to the direction from which it is viewed (Chiou et al. 2007). Indeed, the polarization patterns coming off *Loligo pealei* squid, for example, are so distinctive that Hanlon et al. (1999) were able to create an ethogram of these polarization patterns and correlate them to a more generalized ethogram of the body patterns and postures of the squid. All these are strongly suggesting the existence of a unique capacity of producing a changing polarized pattern, which could be controlled by the animal. But, is this polarization pattern really used for communication? (Mäthger et al. 2009).

Up until now, the strongest support of the notion of a polarization-based communication channel is a study by Boal et al. (2004). In it, Boal and colleagues found that female *Sepia officinalis* cuttlefish behaved differently when they observed other cuttlefish through a transparent filter that distorted only the polarization component of light, as compared to when viewing the very same animals through a regular glass. In general, the response of females towards the distorted images could be described as less accepting of these polarization-lacking animals. In addition, when examining the amount of time cuttlefish present a polarized pattern when viewing other cuttlefish, it was found that this polarization presentation was correlated to the relevant social status of the animals involved. In general, cuttlefish tended to present a linearly polarized pattern to animals that were lower than themselves on the dominant-timid scale and to reduce them when facing a dominant animal. An interesting finding was that cuttlefish presented the polarized pattern even when they were alone, yet this presentation was not constant but was carried out for only approximately 40 % of the time.

As much as the behavioural findings of Boal et al. (2004), along with the anatomical and optical measurements and knowledge gained by subsequent studies, we are far from understanding what information, if any, is conveyed in the polarization channel as well of its understanding. Future behavioural experiments using classical ethological approaches combined with advanced imaging systems are needed to decipher the enigmas of the function of polarization patterns and the meaning of polarization communication in cephalopods.

8.4 Outlook

The polarization of light, being mostly unseen to humans (but see Chap. 14), presents us with a challenge of understanding its potential use and of combining it into our visual world. The multiple tasks, in which polarization sensitivity is part of, suggest that for this group of animals polarization is simply a part of the visual scenery. As such, it may well be that polarization is an integrated part of all visual function in cephalopods, not having any unique role by itself. To address this issue,

neuro-anatomical studies are needed to identify overlays of regions used for processing intensity information and polarization information. Such studies will also allow us to connect polarization inputs to behavioural outputs.

When considering polarization sensitivity and polarization signals, one must bear in mind that these signals propagate in the scattering medium of the sea. The physical limitations towards the generation and propagation of mentioned signals set limitations as to their functionality (Shashar et al. 2011). Understanding these limitations and with them the potential advantages of polarization sensitivity under different optical conditions (Cartron et al. 2013c) is another significant challenge facing the scientific community.

References

Boal JG, Shashar N, Grable MM, Vaughan KH, Loew ER, Hanlon RT (2004) Behavioral evidence for intraspecific signaling with achromatic and polarized light by cuttlefish (Mollusca: Cephalopoda). Behaviour 141:837–861

Cartron L, Darmaillacq AS, Jozet-Alves C, Shashar N, Dickel L (2012) Cuttlefish rely on both polarized light and landmarks for orientation. Anim Cogn 15:591–596

Cartron L, Shashar N, Dickel L, Darmaillacq AS (2013a) Effects of stimuli shape and polarization in evoking deimatic patterns in the European cuttlefish, *Sepia officinalis* under varying turbidity conditions. Invertebr Neurosci 13:19–26

Cartron L, Dickel L, Shashar N, Darmaillacq AS (2013b) Maturation of polarization and luminance contrast sensitivities in cuttlefish (*Sepia officinalis*). J Exp Biol 216:2039–2045

Cartron L, Josef N, Lerner A, McCusker SD, Darmaillacq AS, Dickel L, Shashar N (2013c) Polarization vision can improve object detection in turbid waters by cuttlefish. J Exp Mar Biol Ecol 447:80–85

Chiou TH, Mäthger LM, Hanlon RT, Cronin TW (2007) Spectral and spatial properties of polarized light reflections from the arms of squid (*Loligo pealeii*) and cuttlefish (*Sepia officinalis* L.). J Exp Biol 210:3624–3635

Darmaillacq AS, Shashar N (2008) Lack of polarization optomotor response in the cuttlefish *Sepia elongata* (d'Orbigny, 1845). Physiol Behav 94:616–620

Darmaillacq AS, Chichery R, Shashar N, Dickel L (2006) Early familiarization overrides innate prey preference in newly-hatched *Sepia officinalis* cuttlefish. Anim Behav 71:511–514

Goldsmith TH (1991) Photoreception and vision. In: Prosser CL (ed) Neural and integrative animal physiology. Wiley-Liss, New York, pp 171–245

Hanlon RT, Maxwell MR, Shashar N, Loew ER, Boyle KL (1999) An ethogram of body patterning behavior in the biomedically and commercially valuable squid *Loligo pealei* of Cape Cod, Massachusetts. Biol Bull 197:49–62

Horváth G, Varjú D (2004) Polarized light in animal vision—polarization patterns in nature. Springer, Heidelberg

Johnsen S, Marshall NJ, Widder EA (2011) Polarization sensitivity as a contrast enhancer in pelagic predators: lessons from *in situ* polarization imaging of transparent zooplankton. Philos Trans R Soc Lond B 366:655–670

Mäthger LM, Hanlon RT (2006) Anatomical basis for camouflaged polarized light communication in squid. Biol Lett 2:494–496

Mäthger L, Shashar N, Hanlon RT (2009) Do cephalopods communicate using polarized light reflections from their skin? J Exp Biol 212:2133–2140

Moody MF, Parriss JR (1960) Discrimination of polarized light by *Octopus*. Nature 186:839–840

Moody MF, Parriss JR (1961) Discrimination of polarized light by *Octopus*: A behavioral and morphological study. Z Vergl Physiol 44:268–291

Pignatelli V, Temple SE, Chiou TH, Roberts NW, Collin SP, Marshall NJ (2011) Behavioural relevance of polarization sensitivity as a target detection mechanism in cephalopods and fishes. Philos Trans R Soc Lond B 366:734–741

Saidel WM, Lettvin JY, McNichol EF (1983) Processing of polarized light by squid photoreceptors. Nature 304:534–536

Saidel WM, Shashar N, Schmolesky MT, Hanlon RT (2005) Discriminative responses of squid (*Loligo pealeii*) photoreceptors to polarized light. Comp Biochem Physiol A 142:340–346

Shashar N, Rutledge PS, Cronin TW (1996) Polarization vision in cuttlefish: a concealed communication channel? J Exp Biol 199:2077–2084

Shashar N, Hanlon RT, Petz AM (1998) Polarization vision helps detect transparent prey. Nature 393:222–223

Shashar N, Hagan R, Boal JG, Hanlon RT (2000) Cuttlefish use polarization sensitivity in predation on silvery fish. Vis Res 40:71–75

Shashar N, Milbury CA, Hanlon RT (2002) Polarization vision in cephalopods: neuroanatomical and behavioral features that illustrate aspects of form and function. Mar Freshwat Behav Physiol 35:57–68

Shashar N, Johnsen S, Lerner A, Sabbah S, Chiao CC, Mathger LM, Hanlon RT (2011) Underwater linear polarization: physical limitations to biological functions. Philos Trans R Soc B 366:649–654

Talbot CM, Marshall NJ (2010) Polarization sensitivity in two species of cuttlefish—*Sepia plangon* (Gray 1849) and *Sepia mestus* (Gray 1849)—demonstrated with polarized optomotor stimuli. J Exp Biol 213:3364–3370

Talbot CM, Marshall NJ (2011) The retinal topography of three species of coleoid cephalopod: significance for perception of polarized light. Philos Trans R Soc B 366:724–733

Temple S, Pignatelli V, Cook T, How M, Chiou TS, Roberts N, Marshall NJ (2012) High-resolution polarisation vision in a cuttlefish. Curr Biol 22:R121–R122

von Frisch K (1949) Die Polarisation des Himmelslichts als orientierender Faktor bei dem Tanzen der Bienen. Experientia 5:142–148

Young JZ (1971) The anatomy of the nervous system of *Octopus vulgaris*. Oxford University Press, Oxford

Chapter 9
Polarisation Vision of Fishes

Nicholas William Roberts

Abstract Since the first edition of this book, our understanding of vertebrate polarisation vision has increased significantly. Much of this work has concentrated on a number of species of fish, and the aim of this updated chapter is to highlight some of the new discoveries and new directions this area of animal polarisation vision has seen. Three distinctive research directions stand out and form the main sections of this chapter update: (1) mechanisms of polarisation sensitivity, (2) neural processing of polarisation information and (3) behavioural evidence of polarisation vision and associated visual ecology. The new additions to this chapter bring together work on molecular mechanisms of dichroism in cone photoreceptors and new evidence that questions the original measures of the levels of diffusion of the visual pigment in outer segment membranes. Advances in our understanding of how intra-retinal feedback influences the neural coding of polarisation information are also considered. Finally, several studies into the ability of fish to react to dynamic polarisation-based stimuli are also presented in conjunction with evidence that some fish also manipulate the degree of polarisation in the light that they reflect. However, it is still clear that this area of research lacks depth in much of the evidence, leaving many questions still wide open for future studies.

Electronic supplementary material is available in the online version of this chapter at 10.1007/978-3-642-54718-8_9. Colour versions of the black and white figures can also be found under http://extras.springer.com

N.W. Roberts (✉)
Bristol Life Science Building, University of Bristol, 24 Tyndall Avenue, Bristol, BS8 1TQ, United Kingdom
e-mail: nicholas.roberts@bristol.ac.uk

G. Horváth (ed.), *Polarized Light and Polarization Vision in Animal Sciences*, Springer Series in Vision Research 2, DOI 10.1007/978-3-642-54718-8_9,

9.1 Introduction

Over the last 10 years, the vast majority of new research into vertebrate polarisation vision has been conducted on fish (see Hawryshyn 2010 and Kammermans and Hawryshyn 2011 for reviews; the earlier literature on fish polarisation sensitivity has been reviewed by Horváth and Varjú 2004, Chapter 28, pp. 293–316). As with all areas of sensory ecology, studies into fish polarisation vision have focused on the three main sensory themes: mechanisms, neural processing and behavioural studies. Work has been undertaken in a variety of species including cyprinids, engraulids, pomacentrids and salmonids. Protein–protein interaction of the visual pigment providing a mechanism of dichroism for vertebrate photoreceptors has proved one new avenue of research (Govardovskii et al. 2009; Roberts et al. 2011). Similarly, advances in our understanding of how intra-retinal feedback influences the neural coding of polarisation information have also considerably furthered our knowledge (Ramsden et al. 2008). However, the lack of depth to the evidence in most cases still means polarisation vision in fish remains an area wide open for further study.

9.2 Structural Mechanism of Polarisation Sensitivity

For all animals, both vertebrate and invertebrate, intrinsic dichroic absorbance at a molecular level provides the foundation of polarisation sensitivity. In rhabdomeric photoreceptors there is a degree of orientational order where the chromophore is preferentially aligned relative to the long axis of the microvillus (Snyder 1973; Roberts et al. 2011 and see Chap. 7). Coupled with low effective birefringence within the individual cells (Roberts et al. 2009), the straight and aligned microvilli along the length of the cell provide a well-understood mechanism of cellular polarisation sensitivity.

In fish, only anchovies seem to display a similar clear microscopic mechanism of geometric order that results in significant cellular dichroism (Fineran and Nicol 1978; Novales-Flamarique and Hárosi 2002). One of the three cone formations in the retina have longitudinally oriented lamellae in their outer segments that, coupled with the transmembrane visual pigment, display clear microscopic evidence of a mechanism of orientational order; see Fig. 9.1a–h (Fineran and Nicol 1978; Novales-Flamarique and Hárosi 2002). Since the first edition of this book (Horváth and Varjú 2004), Novales-Flamarique (2011) has further extended our knowledge of this unusual retinal architecture. In *Engraulis mordax*, the retina displays significant and characteristic spatial variability in all the three different cone assemblies. (1) *E. mordax* has long and short (bilobed) cones ordered in continuous rows. The outer segments of these photoreceptors have perpendicularly arranged longitudinal lamellae. (2) Short cones with longitudinally oriented lamellae are positioned in rows of long and short cones. (3) Triple cones are comprised of

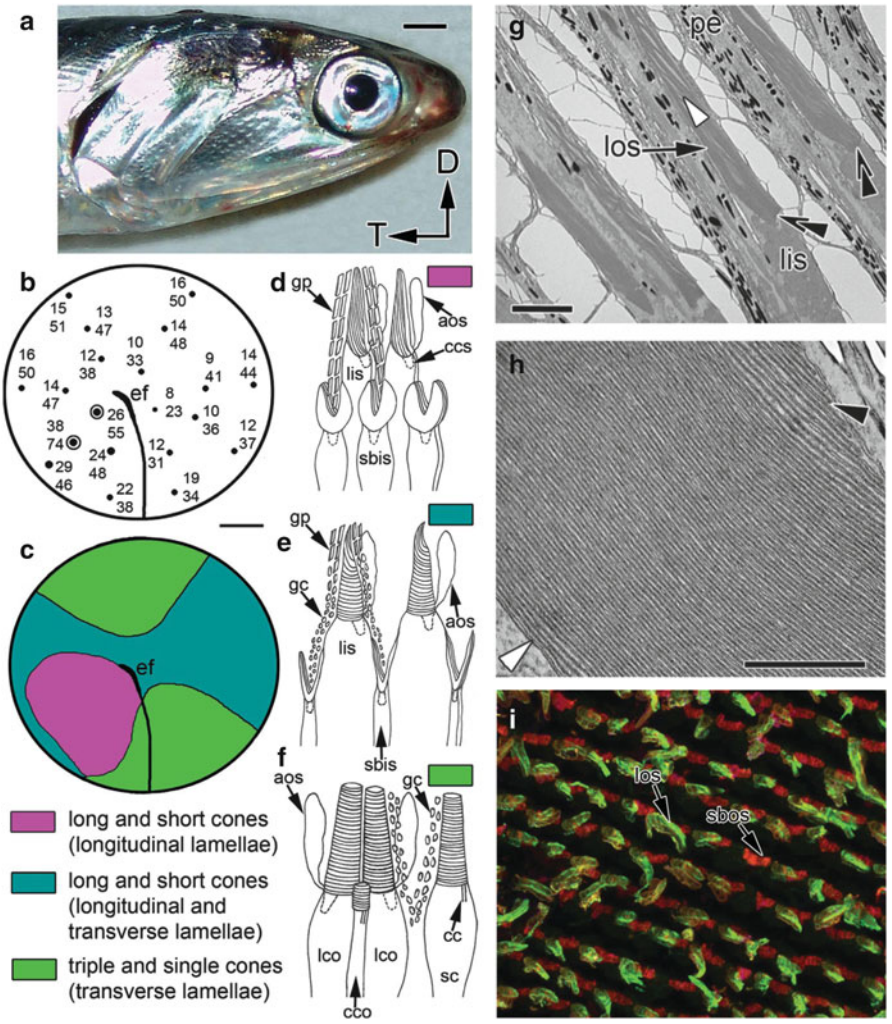

Fig. 9.1 The retinal specialisation in the northern anchovy, *Engraulis mordax*. (**a**) The right eye with the *arrows* D and T depicting the dorsal and temporal directions, respectively (scale bar = 2.2 mm). (**b**) Cone densities [$\times 10^3$ mm^{-2}] across the retina (*top number*) and percentage packing (*bottom number*). (**c**, **d**, **e**, **f**) Schematic of the cone type distributions in the retina colour matched with cartoons of the cone morphology. (**g**) The anchovy long cones with vertically oriented lamellae (scale bar = 5 μm). Note that the base of the outer segment is laterally displaced towards the temporal side of the inner segment (*double black arrowheads*). (**h**) Higher magnification view of the vertically orientated lamellae from a long cone outer segments (scale bar = 0.5 μm). At this level, the *black arrowhead* shows the closed ends of the lamellae on the right (temporal) side of the outer segment. On the other side (*white arrow head*) the membranes run parallel to the plasma membrane. (**i**) Confocal images from whole-mount retina showing opsin expression in the rows of alternating long and short (bilobed) cones. The outer segments of long cones label with two types of M/LWS opsin antibodies (*dark grey colour*), but the bilobed outer segments label exclusively with the mouse rod opsin antibody (*light grey colour*) [adapted from Novales-Flamarique (2011)]

two lateral cones flanking a small central cone. These cells have transversely oriented lamellae. The flattened outer segments, bilobed nature of the cones and the alternating continuous rows of rods and cones make the anchovy retina remarkably different from most other vertebrates.

The study of Novales-Flamarique (2011) has also been the first to label against the specific opsins that occur in each cone type; see Fig 9.1h. He discovered that all the long type cones and lateral cones in the triple cell type are labelled with the MWS (middle-wavelength-sensitive) and LWS (long-wavelength-sensitive) antibodies. The bilobed short outer segments and the central member of the triple cones are labelled with the rod opsin antibody. As all three of these different cone types occupy different areas of the retina, this suggests each cell type may contribute to a particular visual function. The long and short cones that both have longitudinal lamellae occupy the forward most looking area of the retina and occur here in the highest density of all the cone types. Novales-Flamarique (2011) proposed that this is consistent with polarisation vision being used for prey detection, in line with the previous electrophysiological evidence of polarisation sensitivity. As yet, however, no species of anchovy have been shown behaviourally to display polarisation sensitivity; this remains an important study for the future. Moreover, the signal-to-noise ratio in any polarisation contrast enhancement of transparent prey against the open water background was shown to be considerably less than previously believed. Johnsen et al. (2011) cautioned against the assignment of behavioural importance of an environmental cue before actually determining the information that is actually there for a relevant viewer. Specifically related to polarisation, Johnsen et al. (2011) suggested that the contrast threshold for the degree of polarisation in an image is not as low as the threshold for radiance. They also suggested that because many aquatic animals have a contrast threshold of around 1 % (reviewed by Douglas and Hawryshyn 1990), it is unlikely that a polarisation image of a transparent animal would be detectable from a further distance than the intensity-based image of that same animal.

Intra-retinal specialisation is in fact common across the vertebrates, whether in terms of cone ordering (particularly in the sensory context of colour vision). Fish (Levine et al. 1979; Reckel et al. 2003; Temple et al. 2010), amphibians (Firsov et al. 1994), birds (Maldonado et al. 1988) and mammals (Lukáts et al. 2005) have all been shown to possess such spectral type specialisation. Kondrashev et al. (2012) recently expanded on this idea, proposing that anchovies may use the spatial segregation of cone types in order to disentangle polarisation and spectral information.

A second idea that has, in general, become accepted about the anchovy visual system concerns the function of the guanine crystals that surround the outer segments. These have been suggested to play a role in enhancing polarisation sensitivity in the cones through the anisotropy in the Fresnel reflection coefficients. However, one classic study (Denton and Nicol 1965) and two more recent (Jordan et al. 2012; Brady et al. 2013) have demonstrated that guanine reflectors in fish can exhibit some unusual polarisation properties, effectively acting as a polarisation neutral reflector. Nothing is known about the guanine crystal type in anchovy retina or the true polarisation properties of the crystals. The complex three-dimensional

structure acting as either a polarising or polarisation neutral reflector could in theory either enhance or confound the polarisation signal reaching the cell depending on specific properties. An investigation combining experimental measurements and optical modeling is a particularly important future study.

Whilst the transversely orientated lamellae in anchovy cone outer segments provide a clear mechanism of polarisation sensitivity, a similar mechanism in morphologically typical cones is not so evident. This applies to all fish species, and for that matter, other vertebrates as well. A lack of dichroism in cones has always been attributed to the fluidity of the membranes and the rotational diffusion of the visual pigment. Measurements of the diffusion constants of rhodopsin in rods came from several studies, including Cone (1972), Poo and Cone (1973, 1974), Liebman and Entine (1974), Liebman et al. (1982) and Gupta and Williams (1990). Here it is worth being clear that the measurements of rotational diffusion were from rods of *Rana pipiens*, a cell type not involved in polarisation detection and in a species not known to possess polarisation sensitivity (Cone 1972). Throughout the literature, these results have been generalised, possibly incorrectly, to all cone types in all vertebrates.

Lateral diffusion is inferred from simultaneous absorbance measurements taken at each side of the outer segment. When a short bleaching flash is applied to one side of the outer segments, the equilibrating movement of the visual pigment is measured by monitoring how the difference in absorbance between both sides lessens. All studies to date have only measured lateral movement across the outer segment, i.e. in the plane of the membranes. Recently, Govardovskii et al. (2009) have re-examined the results of these studies by making new measurements of the lateral diffusion of rhodopsin in rods of several amphibian species and a gecko. Interestingly, they pinpointed two mistakes in several of the original works, experimental and computational: (1) Previous diffusion measurements were made at a single wavelength, and the results were affected by the production of photoproducts. The new full absorbance spectra obtained by Govardovskii et al. (2009) indicate that there is no "safe" wavelength where an absorbing contribution from photoproducts, principally meta-rhodopsin III, is excluded. Whilst changing the pH of the samples could affect this conclusion, no details of the sample preparation were provided in any of the original works (Poo and Cone 1973, 1974; Liebman and Entine 1974; Liebman et al. 1982; Gupta and Williams 1990), suggesting that the pH was not manipulated and the measurements would have been confounded. (2) Not correctly accounting for the effect of the photoproducts would have increased the measured diffusion constant. However, an arithmetic correction factor, which accounts for the fissured morphology of the rod membranes, was also used incorrectly. This fortuatively increased the diffusion constant back to approximately 5×10^{-9} cm^2 s^{-1} or 0.5 μm^2 s^{-1}. Govardovskii et al. (2009) measured the lateral diffusion constant to be closer to $4 \pm 0.4 \times 10^{-9}$ cm^2 s^{-1} (mean ± 1 standard error on the mean, SEM), values more similar to 3.2×10^{-9} cm^2 s^{-1}, that was found in bleaching experiments on catfish cones (Gupta and Williams 1990), earlier fluorescence photobleaching and recovery data on bullfrog rods (Wey and Cone 1981) and experiments that are insensitive to formation of metaproducts. From these values the viscosity of disc membrane is estimated to be around 2 poise.

A notable result in this study is a significant proportion of the rhodopsin that exhibits slower diffusion times, with much of it appearing immobile. *Ambystoma mexicanum*, *Rana temporaria* and *Bufo bufo* showed a mean immobile rhodopsin fraction of 0.27 ± 0.03 (mean $\pm$ SEM). A much higher value of 0.69 ± 0.06 (mean $\pm$ 1 SEM) was found in *Geck gecko*. G-coupled protein receptors (GCPRs), of which opsin proteins are some of the best studied, are now well understood to form homodimers, heterodimers and higher ordered oligomeric arrays (also termed micro-phase separation or protein rafts) (for reviews see Kroeger et al. 2003; Palczewski 2006, 2010). For rhodopsin specifically, evidence of in-membrane ordering has been provided through atomic force microscopy, see Fig. 9.2a, (Fotiadis et al. 2003; Liang 2003), powder sample X-ray scattering (Fotiadis et al. 2003), transmission electron microscopy (TEM), see Fig. 9.2b (Corless et al. 1994, 1995), fluorescence recovery energy transfer (FRET) (Kota et al. 2006) and gel electrophoresis (Shukolyukov 2009). The powder diffraction measurements in particular confirmed the double row and axial repeat periodicities of the rhodopsin dimers to be 8.4 and 4.2 nm^{-1}, respectively (Fotiadis et al. 2003). The TEM studies by Corless et al. (1994, 1995) showed extensive areas of order within the membranes—not only in the membrane plane but also between bilayers, where the interdiscal space seemed expanded, with processes linking across the extra- and interfaces of the membranes. These studies show remarkable similarities with the work described above by Saibil (1982) of the actin-based linkages between rhabdomeric microvilli. Further evidence of ordered arrays of rhodopsin has been obtained by Ryba and Marsh (1992) using recombinant membranes via saturation-transfer spin-label electron spin resonance. Their key finding was that the composition of different synthetic membranes changed the level of rhodopsin oligomerisation, and this was correlated with a reduction of rotational diffusion. They found that greater levels of protein aggregation take place with longer lipid chain lengths in these artificial membranes. Botelho et al. (2006) concurred with this; their FRET evidence showed that particular membrane lipid compositions could induce the oligomerisation of rhodopsin.

Two significant questions, however, remain: (a) To what extent does the oligomerisation of homodimers occur in native outer segment membranes? The majority of measurements have been made in membranes that are either in mechanically or biochemically non-native conditions, although it is worth noting though that dimerisation appears to be a fundamental property of many GCPRs (George et al. 2002; Park et al. 2004; Palczewski 2010). (b) It is unclear as to the effect ordered paracrystalline arrays would have on transduction. Based on the theory that the interactions between rhodopsin and transducin are mediated by the mobility of rhodopsin, paracrystalline arrays of rhodopsin dimers would inhibit phototransduction; see Fig. 9.2c. However, if transducin itself is the mobile dynamic control of extent, then the order in oligomers could be an additional way to regulate the transduction cascade. This agrees with the result of Bruckert et al. (1992) that transducin diffuses in the membrane plane faster than rhodopsin. The rate of transducin activation was largely independent of rhodopsin mobility. Most recently, Dell-Orco (2013) reviewed how the formation of transient rhodopsin dimer/

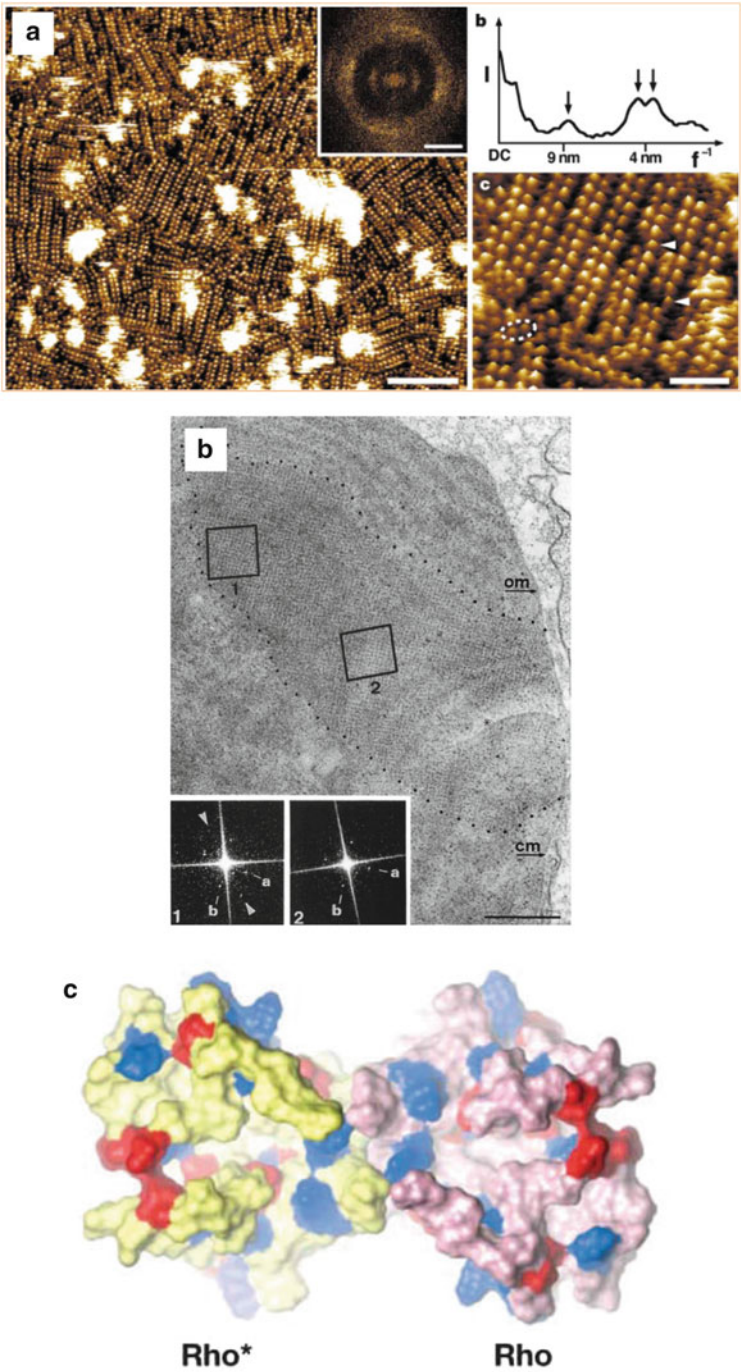

Fig. 9.2 Rhodopsin dimerisation in photoreceptor membranes. (**a**) Atomic force microscopy image of rod outer segment discs illustrating the homodimer ordering of rhodopsin into a paracrystalline array. Insets are X-ray diffraction profiles with the peaks detailing the protein–

transducin complexes in the dark was a simple mechanism that ensures a high-speed activation of the transduction cascade.

If dimerisation and high-order oligomeric arrays are a common feature of vertebrate photoreceptors, could this be a mechanism of dichroism in morphological typical cells? Two experimental studies in the past 10 years have suggested that both single and double cones do indeed display a level of axial dichroism, whereas rods do not. Roberts and Needham (2007) used laser tweezers to axially orientate and rotate goldfish (*Carassius auratus*) photoreceptors whilst measuring the polarisation absorbance of the cell. Laser tweezers are constructed with a laser beam focused by a high numerical aperture objective lens. For objects larger than the wavelength of light, both refraction and scattering within the area of the beam waist exert a net attractive force on any non-absorbing dielectric object. This traps the object close to the focal area. Laser tweezers are commonly used to manipulate and study biological cells including photoreceptors (Townes-Anderson et al. 1998; Molloy and Padgett 2002). With the correct choice of laser trapping wavelength and power, cells can be trapped without altering their properties or causing cellular damage. The first study to trap rod photoreceptors was by Townes-Anderson et al. (1998) and proved that the cells were unaffected by the trapping and could be deposited with the re-interconnection of intracellular process occurring between adjacently placed cells. Roberts and Needham (2007) used a 1,064 nm laser as the trap so that it did not bleach the visual pigment. They found that individual cells "stood up" parallel to the laser beam's propagation direction, allowing a linearly polarised second beam of 514 nm to be passed into the outer segment to measure the absorbance. By circularly polarising the trapping laser, the trapped object experienced a transfer of angular momentum, causing the photoreceptor to rotate around its long axis. This provided a simple means by which the absorbance of polarised light at different in-plane angles could be measured, thus providing a measure of any levels of dichroism; see Fig. 9.3a–d.

Roberts and Needham (2007) studied two cell types: goldfish rods and the MWS member of the double cones. In this species, rods are not believed to mediate polarisation information, whereas the MWS outer segment of the double cone does (Hawryshyn and McFarland 1987). They found that the rods showed no dichroism, with the axially measured dichroic ratio $= 1.04 \pm 0.03$. However, the dichroic ratio of the MWS member of the double cone was 1.20 ± 0.09; see Fig. 9.3e. This equates to a polarisation contrast of 9.2 ± 0.4 %. After each measurement the cell was bleached with high-intensity white light, and then the measurement was repeated in order to be sure that just rotating the cell in the measurement beam did not cause the modulation in the absorbance. For both the

Fig. 9.2 (continued) protein interaction distances [adapted from Fotiadis et al. (2003)]. (**b**) Similar evidence of phase separation in the plane of the discs taken by a transmission electron microscope [adapted from Corless et al. (1994)]. (**c**) A calculated *top view* of a photoactivated rhodopsin dimer taken from the cytoplasmic side. This cytoplasmic surface of photoactivated rhodopsin, Rho*, and rhodopsin, Rho, interacts with the G protein transducin [adapted from Palczewski (2006)]

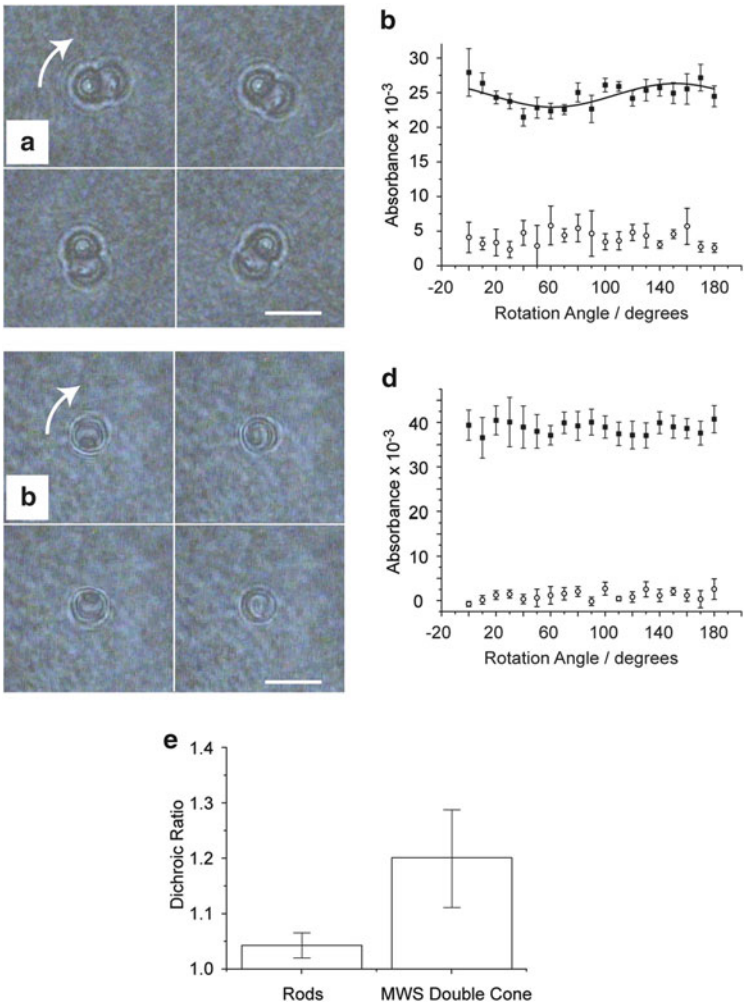

Fig. 9.3 Axial dichroism in vertebrate double cones. (**a**) A time series of video images illustrating a 180° rotation of an axially orientated double cone photoreceptor. The rotation is centered on the mid-wavelength sensitive (MWS) outer segment (scale bar = 10 μm). (**b**) A typical set of axial absorbance measurements from an MWS outer segment indicating the axial dichroism of the cell type. (**c**) A time series of video images illustrating a 360° rotation of an axially orientated rod photoreceptor (scale bar = 5 μm). (**d**) The corresponding constant axial absorbance measurements from a rotating rod photoreceptor. In *panels* **b** and **d**, the *solid symbols* represent the absorbance, and the *open symbols* show the post-bleach baseline. (**e**) The mean axial dichroic ratios from all measured rods and MWS cones. The mean values are significantly different between cell types ($N = 9$; $p < 0.05$; one-way ANOVA). *Error bars* represent mean ± 1 SD [adapted from Roberts and Needham (2007)]

rods and cones the post-bleach absorbance was both independent of rotation angle and not significantly different from zero. These data, combined with the square cone mosaic of double cones in the retina, suggest that intrinsic axial dichroism could be a mechanism of polarisation sensitivity.

In a second study, Roberts et al. (2004) used polarised microspectrophotometry to investigate the transverse dichroic ratios of all five spectral cell types in coho salmon (*Oncorhynchus kisutch*). They found that when outer segments were illuminated transversely with linearly polarised light, rods and cones absorbed the light differently. In rods, the maximum absorbance occurred when the direction of polarisation was perpendicularly across the outer segment, parallel to the plane of the membrane discs. However, in cones the angle varied, from zero degrees up to approximately 20° relative to the plane of the membranes. These results do match previous measurements of dichroic ratios in vertebrate photoreceptors that show the general rule that the dichroic ratios of cones are less than rods. Typically, dichroic ratios are 2–3 in cones compared to 3–5 for rods (see Table 2 in Roberts and Gleeson 2004).

There could be several reasons for this difference between rods and cones: Either the membranes in the cones' outer segments show a distribution in their tilt relative to the axes of the outer segment. Or the visual pigment may not have the same coefficient of rotational diffusion as rods, with the chromophores displaying a degree of alignment, as indicated above in the discussion of dimers and oligomerisation. The rotational degree of freedom of the whole cell itself would provide the distribution, and the maximum tilt angle measured would be a measure of the chromophore angle within the binding pocket. This agrees with the original measurements of Jäger et al. (1997), showing that the tilt angle of the chromophore is 16°.

Roberts et al. (2004) further suggested that the explanation for the difference between rods and cones could be due to the different membrane morphologies and compositions, rods having separate disc-shaped flattened vesicles compared to the membranes of cones being continuous infoldings of the outer cell membrane. It has been shown that rod membranous discs and the outer cell membrane differed significantly in both lipid composition and chemical properties. Higher levels of cholesterol exist in the outer cell membrane compared with the levels in the rod disc membranes (Boesze-Battaglia and Schimmel 1997), and different molecular compositions of membranes create different orientations of the constituent lipids. Murari et al.(1986), MacIntosh (1973) and Brzustowicz et al. (1999) showed the tilt of lipids and cholesterol in a membrane as a function of the bilayer composition. This further agrees with many of the studies described above, illustrating how different membrane compositions affect the levels of oligomerisation of rhodopsin.

In two other studies, Roberts and Gleeson (2004) and Roberts (2006) went on to calculate the optics of the outer segment structures from first principles, solving Maxwell's equations for the intrinsic and form birefringent lamellar structure. Various other researchers (Liebman et al. 1974; Israelachvili et al. 1975; Laughlin et al. 1975; Liebman 1975; Hárosi 1981) have attempted to theoretically calculate the optics of photoreceptors investigating the form birefringence; however, none

had previously taken into account the effect of intrinsic birefringence. Complete solutions to Maxwell's equations are important, as simplified theoretical descriptions such as Israelachvili et al. (1975) and Hárosi (1981) predicted a strong form birefringence component for the membrane volume fraction equal to zero. If there are no membranes and the system is isotropic, there can be no form birefringence. Using a 4×4 transfer matrix technique commonly used to calculate the optics of layered liquid crystal systems, both these newer studies concluded that when cones are illuminated axially, the measured tilt in the chromophore and degree of alignment would produce a dichroic ratio of approximately 10 %. This matches the values measured experimentally in the goldfish double cones (Roberts and Needham 2007).

As a final note, and taking this section back to where it started with the transversely orientated membranes of anchovies, Roberts (2006) also showed how form dichroism increases the dichroic levels of the transversely illuminated membranes. However, the gains in dichroism, and thus increases in polarisation sensitivity, come from decreasing the volume fraction of the outer segment occupied by the bilayers. This would therefore decrease the optical density and overall sensitivity. Consequently, a balance must exist between efficiency of photon detection and the level of polarisation contrast.

9.3 Neural Processing of Polarisation Information

The majority of our knowledge regarding fish polarisation vision lies with the spectral input channels and the retinal processing. Studies have continued to probe the initial stages of processing (electroretinograms, ERGs) and at later stages in the optic nerve (compound action potentials, CAPs). At both these points, two characteristic patterns have emerged in the data: see Fig. 9.4a–d: (1) Hawryshyn et al. (2010) tested the polarisation sensitivity of Atlantic salmon (*Salmo salar*). The early stage ERG recordings exhibited a complex angular sensitivity, showing peak sensitivities to light polarised at 0°, 45°, 90°, 135° and 180°. This mirrors the results the same group has obtained in green damsel fish (*Chromis viridis*) using ERGs (Hawryshyn et al. 2003). (2) The polarisation sensitivity obtained in Atlantic salmon using CAP recordings showed a simpler W-shaped sensitivity curve, with peaks at 0°, 90° and 180°. Again this corroborates other findings in Salmonids, and the frequency halving of the sensitivity function is still believed to provide optimal discrimination for light polarised either vertically or horizontally. One point that should be made here for future works relates to Nyquist's limit. The measured angles should be sampled at least twice the frequency of the modelled periodic signal. Only having a data point at each maxima and minima of the function does not preclude multiples of that period from describing the data equally as well.

Hawryshyn et al. (2010) went on to investigate the chromatic bias in the polarisation information being conveyed by the optic nerve. By chromatically adapting the LWS cone mechanism, the maximum polarisation sensitivity in the

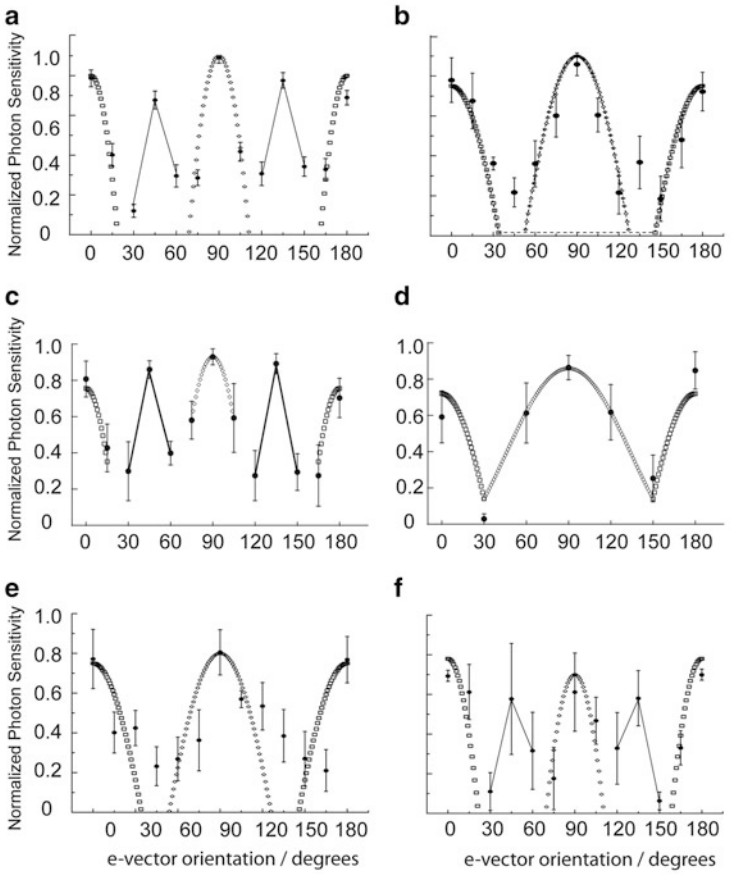

Fig. 9.4 Electrophysiological recording of ultraviolet (UV) polarisation sensitivity (PS) in rainbow trout and Atlantic salmon. (**a**, **b**) Mean UV PS (±1 SD) of rainbow trout. (**a**) UV PS determined using ERG recording ($N = 21$, *filled circles*). The vertical detector mechanism (*open squares*) and the horizontal mechanism (*open diamonds*) are shown. The *solid line* connects the sensitivity points representing the intermediary peaks [adapted from Ramsden et al. (2008)]. (**b**) UV PS determined using CAP recording ($N = 5$, *filled circles*). The vertical detector mechanism (*open squares*) and the horizontal mechanism (*open diamonds*) are shown [adapted from Ramsden et al. (2008)]. (**c**, **d**) Mean PS (±1 SD) of Atlantic salmon. (**c**) UV PS determined using ERG recording ($N = 3$, *filled circles*). The vertical detector mechanism (*open squares*) and the horizontal mechanism (*open diamonds*) are shown. The *solid line* connects the sensitivity points representing the intermediary peaks [adapted from Hawryshyn (2010)]. (**d**) UV PS determined using CAP recording ($N = 3$, *filled circles*). The vertical detector mechanism (*open squares*) and the horizontal mechanism (*open diamonds*) are shown [adapted from Hawryshyn (2010)]. For **a**, **b**, **c** and **d**, a 360 nm linearly polarised stimulus in 15° E-vector increments was used. Note the differences in sensitivity between **a** and **b** as well as between **c** and **d** curves at 45° and 135°. (**e**) UV PS of rainbow trout recorded using an ERG treated with cobalt chloride (intraocular concentration ~0.275 mmol l^{-1}, $N = 3$). (**f**) Comparative control measurements using an intraocular injection of saline ($N = 3$). Note again the differences in sensitivity between E and F curves at 45° and 135° demonstrating the negative feedback contribution at these angles

CAP recordings shifted towards the horizontal (90° from the vertical). Conversely, by adapting the UVS (ultraviolet-sensitive) cone mechanisms, the maximum sensitivity shifts to the vertical (0° and 180° from the vertical). Therefore, the 90° peak is dominated by the LWS cone mechanism, and the 0° and 180° peaks are dominated by the UVS cone mechanism.

In previous studies by the same group, rainbow trout (*Oncorhynchus mykiss*) had been shown to lose their polarisation sensitivity as they transformed from parr to migratory smolts. With the idea that salmonids could use celestial polarisation patterns for orientation, the loss of polarisation sensitivity has always seemed somewhat of a puzzle. Why loose a sensory ability at the development stage when it would be most useful. Recently, Sabbah et al. (2013) used CAP recordings to find that polarisation sensitivity does not disappear. Instead, the polarisation sensitivity shifts from the ventral retina in parr to the dorsal retina in smolts. They proposed that this change allows the parr to use overhead polarisation information and the deeper living migratory smolts to use the underwater scattered light field.

The study of Sabbah et al. (2013) went on to suggest further details of processing involved in producing the characteristic polarisation sensitivity. Using a cascade model to fit to the data, it was suggested that two perpendicular channels were differentially compared and coupled with feedback from horizontal cells. This was sufficient to explain measured polarisation sensitivity. The proposal was that gain and tuning by the retinal network would allow the retina to unambiguously process this information in parallel with colour and intensity. Parts of this explanation were supported by the study of Ramsden et al. (2008), where feedback from the horizontal cells was chemically blocked. Cobalt has previously been shown to block horizontal cell-mediated feedback on cones in goldfish retina (Thoreson and Burkhardt 1990; Fahrenfort et al. 2004). The high-pass characteristics of the synapse are chemically inhibited with the characteristic evidence being a temporally broader b-wave contribution in the ERG. In rainbow trout, the intermediary peaks at 45° and 135° appear to function from feedback activity, as they disappeared with the cobalt treatment and the decrease in horizontal cell feedback; see Fig. 9.4e–f. The network interaction is described as the MWS/LWS opponency affecting the negative feedback of the horizontal cells onto UVS cones. The UVS cones in turn affect the negative feedback from the horizontal cells onto the MWS/LWS cones. These all imply that the 45° or 135° peaks in the polarisation sensitivity are therefore produced by the opponent interaction of MWS/LWS cones reducing the negative feedback on UVS cones.

A final significant point that deserves a mention is the comparative phylogenetics of Atlantic and Pacific species of salmon and other members of the Salmoninae. Hawryshyn et al. (2010) highlighted how the details of the UV polarisation sensitivity in Atlantic salmon are common across this group. Both the ERG and CAP record function of polarisation sensitivity match throughout the Salmoninae, as do the chromatic aspects in both the UVS and MWS/LWS polarisation-sensitive channels (Parkyn and Hawryshyn 2000). The SWS polarisation-insensitive single cone channel is similarly common, one that is possibly a light level monitor, maybe used to define the gain of the retinal neural

network (Marc and Sperling 1976). Furthermore, the ontogeny and organisation of photoreceptors in the retinas of Atlantic salmon and other salmonids are very similar. The characteristics of UV polarisation sensitivity we see in the Atlantic salmon are also very homologous to those described for cyprininds (Hawryshyn and McFarland 1987) and pomacentrids (Hawryshyn et al. 2003; Mussi et al. 2005).

9.4 Seeing the Polarisation of Light and a Behavioural Advantage for Fish

Despite almost 50 years of investigations into fish polarisation sensitivity, there is still no obvious natural behaviour that fish use polarisation information for. It has been proposed that the ability to view polarised light differently depending on the angle of polarisation and/or the degree of polarisation could be used in a variety of ways (reviewed by Horváth and Varjú 2004): (1) Improving object contrast, either directly using the polarisation properties of an object or by cutting out the scattered horizontally polarised space light. (2) Polarisation could be used for orientation and navigation by the celestial polarisation patterns. (3) There are suggestions that fish could also use polarisation information for short-range signals, whether in a shoaling scenarios or perhaps in combination with iridescent colour as a sexual signal. However, all these theories have yet to receive any direct evidence and over the last 10 years, behavioural experiments have still been restricted to tank-based investigations of simple sensitivity and discrimination.

9.4.1 Object Recognition

There are three main directions in which behavioural work has progressed since the first edition of this book (Horváth and Varjú 2004). The first is object recognition via polarisation information, which has been investigated in two main studies: One investigated the abilities of green chromis (*Chromis viridis*) to learn to choose between two different polarisation targets (Mussi et al. 2005). The second was an investigation of an innate response to either a polarisation-based scare/looming stimulus or interest in simulated "polarisation prey" (Pignatelli et al. 2011). In the first study, green chromis were successfully trained to choose a particular direction of polarisation in a two-alternative forced choice test; see Fig. 9.5a. The fish ($N = 4$) were able to discriminate between either horizontally or vertically polarised light. The intensity was varied between the choices by 90 % (1 ND), indicating that this choice was made independently of brightness; see Fig. 9.5b. The same fish were further tested for the minimum difference in angle between two different polarisations. Two of the fish were tested relative to the horizontal polarisation and could differentiate 25° but not 20°. Similarly, the other two fish discerned 25° for the vertical polarisation, but again, not 20°; see Fig. 9.5c–f. In agreement with

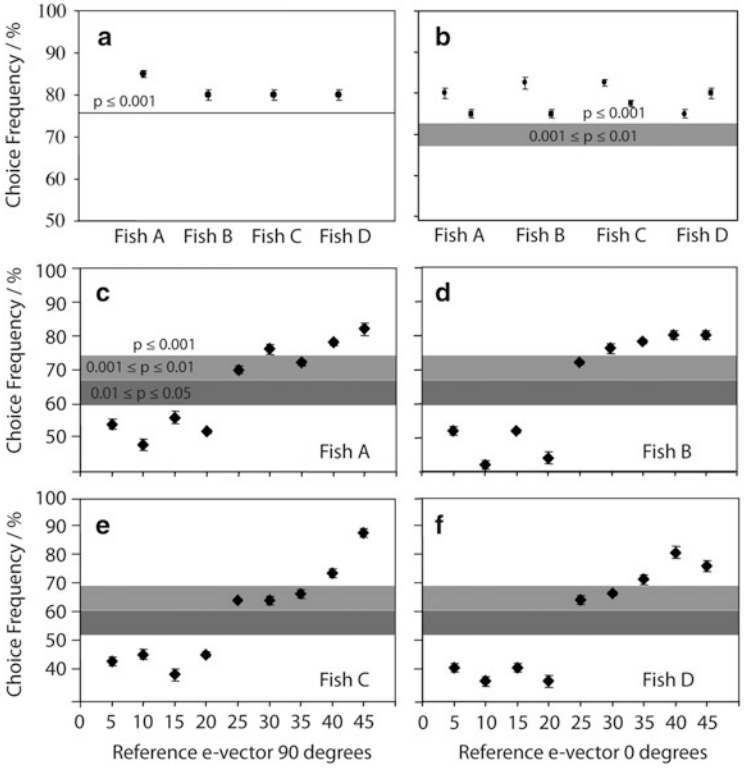

Fig. 9.5 Behavioural discrimination between different polarisations of light by *Chromis viridis*. (**a**) *C. viridis* could discriminate between 0° and 90° E-vector orientations ($p < 10^{-4}$ in each case). Each point represents the percentage of correct choice frequency (mean ± SEM) when 0° and 90° E-vector orientations were presented. The *horizontal line* represents the choice frequency value for a significance level of $p = 0.001$ compared with chance for 40 Bernoulli trials calculated using the binomial probability function. Fish A and C were trained to swim towards 90° E-vector orientation (85 and 80 % correct choice frequency, respectively). Fish B and D were trained to select 0° E-vector orientation (80 % correct choice frequency in both fish). (**b**) The percentage of correct choice frequency (mean ± SEM) (80 trials per fish, $N = 4$) when 0° was dimmer than 90° (*circles*) and when 90° was dimmer than 0° (*squares*). The reference E-vector for fish A and C was 90°, whereas the reference E-vector for fish B and D was 0°. (**c**–**f**) The percentage of correct choice frequency at various angular differences between the reference E-vector and the comparison E-vector (ΔE-vector) (mean ± SEM) (40 trials per fish, $N = 4$). The smallest ΔE-vector was approximately 25° in all four fish [adapted from Mussi et al. (2005)]

the earlier electrophysiology on this species (Hawryshyn 2010), the behaviour was driven by UV wavelengths. The ability to correctly select between two different angles of polarisation completely disappeared when the UV wavelength was removed from the target illumination. The conclusion here was: this is further evidence that the presence of UV light is critical for E-vector discrimination by fish.

Pignatelli et al. (2011) more recently assessed whether several species of fish would react to a computer-generated looming and prey stimulus on a liquid crystal

display (LCD) screen. By removing the front polariser from a twisted nematic type LCD (TN-LCD), images that normally exhibit intensity contrast change to display contrast in the angle of polarisation. In this work, the authors used a difference in angle of polarisation between the stimulus and background of approximately 37.5°. All four species, goldfish (*C. auratus*), zebrafish (*Danio rerio*), green chromis (*C. viridis*) and Ambon damselfish (*Pomacentrus amboinensis*), responded with a strong startle response when shown a black on white looming stimulus. Two of these species, green chromis and Ambon damselfish, also showed tracking behaviour to a simulated black on white moving prey item. However, none of these species showed any response at all to any of the polarised versions of these stimuli. The experimental set-up contained sufficient power in the UV part of the spectrum, ruling out the lack of UV as an explanation for these findings. This left the authors to conclude that the polarisation information of a moving object may not be used in escape or targeting behaviour of these species. This conclusion further matches that of a study by Browman et al. (2006) which found that UV and polarised light did not have an effect on the growth rate in the larval stages of several marine species of fish, turbot (*Scophthalmus maximus*), Atlantic cod (*Gadus morhua*) and Atlantic herring (*Clupea harengus*) when reared under typical aquaculture conditions.

9.4.2 Navigation

Navigation is the second behavioural area that has seen a small level of interest in recent years. Parkyn et al. (2003) demonstrated that both rainbow trout and steelhead could learn to orientate to a particular celestial angle of polarisation. Naive fish showed no significant preferential orientation. However, once fish had been conditioned to a particular direction of polarisation in an indoor L-shaped tank setup, they generally repeated this orientation in both artificially lit indoor aquaria and under natural skylight outside. These tests were conducted at sunset when the plane of maximally polarised skylight was near zenith along a compass bearing of approximately 131°/311° (corrected for magnetic declination). At the onset of testing, the maximum recorded degree of polarisation in the sky was 59 % and was 67 % on the 2 days when the tests were conducted. Waterman (2006) revisited the subject with a concept paper aiming to re-invigorate the field of polarisation-based navigation in aquatic animals. His conclusions were that there is sufficient and constant polarisation information for a compass heading to be used over a range of depths in clear oceanic waters. This was somewhat backed up by Lerner et al. (2011) and their experimental and theoretical study. They theoretically calculated the underwater polarisation patterns and compared these with measurements made under a variety of environmental conditions: At two depths (2 and 5 m), over different sea floor depths (6 and 28 m) and in clear and semi-turbid conditions. They found that a direct correlation between the degree of polarisation underwater and the solar elevation only occurred in clear waters. Furthermore, the compass information where the orientation of the polarisation angle matches the

angle of refraction was most reliable in a horizontal viewing direction and without interference from the floor, i.e. in deeper water. Ultimately, polarisation information used for a skylight-based compass, as it is in many insects, seems only possible under a specific set of conditions.

9.4.3 Camouflage

The third area of fish behaviour relating to polarisation vision is camouflage. The study of Pignatelli et al. (2011) showed that four fish species did not use the polarisation information they were given for prey detection. However, others such as cephalopods may use the polarisation of the reflections from fish for prey detection (Shashar et al. 2000). When unpolarised light is normally incident on a flat surface, the polarisation of reflected light remains also unpolarised. However, as the angle of incidence increases, the reflected light becomes more and more polarised parallel to the surface until it reaches a maximum at Brewster angle (53° from the normal vector of the air–water interface). If the incident light is already polarised parallel to the surface, then that polarisation will always be reflected to some degree. If the light is polarised parallel to the plane of incidence, then at Brewster angle there is no reflected light at all. This common effect (Born and Wolf 1999) is normally particularly apparent from highly reflective, flat objects.

The first studies to investigate the degree of polarisation of reflections from fish were actually published in the 1960s, as part of Eric Denton's remarkable body of work. One set of results in Denton and Nicol (1965) hinted at a reflection effect not consistent with the above description of the Brewster effect. Figure 9.6a shows that there is no angle of incidence in the range of 10° to 80° at which the reflection becomes predominantly polarised. Jordan et al. (2012) recently revisited this question by analyzing the polarisation of reflections from two species of silvery fish, *Clupea harengus* (Atlantic herring) and *Sardina pilchardus* (European sardine). The silvery reflective sides of these species do not have a typical Brewster effect, but reflected the light with a similar degree of polarisation as the incident ray. Brady et al. (2013) showed something similar occurring in the lookdown (*Selene vomer*), a highly silvered fish. With a detailed experimental and theoretical treatment, they concluded that over a range of solar elevation angles, the "polarisation signature" of the fish was at a minimum. This advantage was not just static, their analysis also suggested that under modeled movements, the lookdown has a specific advantage in continuing to match the polarised visual background. From these results, they put forward the term polarocrypsis, suggesting that this could be a camouflaging adaption against polarisation-sensitive predators. It should be noted here that these examples are specific to these species of silvery broadband-reflecting fish. Many fish act more as diffuse reflectors and these fish depolarise the light and stand out more against a polarised background.

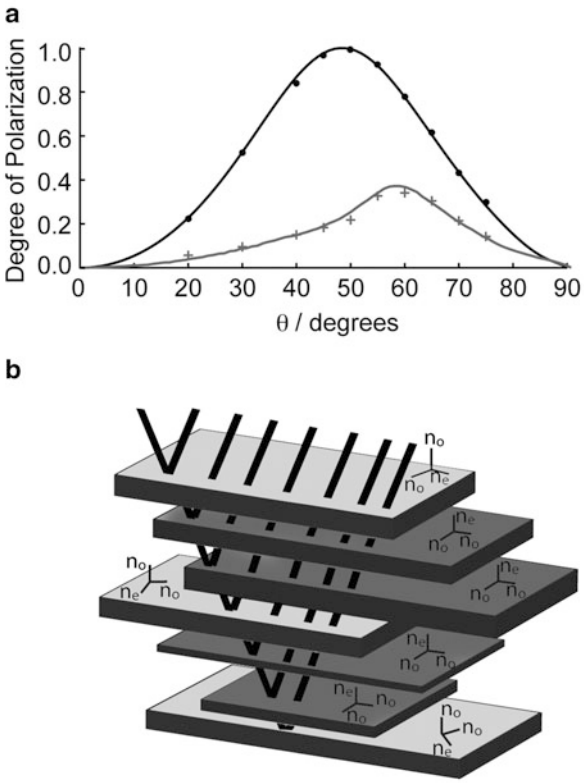

Fig. 9.6 Weakly polarising guanine-based multilayer reflectors in fish. (**a**) Measurements of the degree of polarisation at $\lambda = 600$ nm for azimuthal (dorsoventral; *grey cardinal crosses*) angles of illumination from *Clupea harengus*. *Solid grey line* is a parametric best fit for multilayer model with a mixture of 75 % Type 1 and 25 % Type 2 crystals. The model explained 95 % of the variation in the data, assessed by the R^2 from linear regression. There was no systematic difference between model and data (mean pairwise difference and standard deviation $= 0.0044 \pm 0.0132$, $t = 0.7512$, d.f. $= 9$, $p = 0.472$). The best fit parameters are $N = 37$ crystal layers in each multilayer structure, with sampling intervals for guanine and cytoplasm thicknesses of [55, 110] nm and [30, 300] nm, respectively. *Black solid circles* and *black line* represent a positive control and are experimental data and a theoretical curve for a double surface Fresnel reflection (front and back reflection) from a glass microscope slide with a refractive index of 1.5, in air. (**b**) Schematic illustrating the multilayer model used and the two populations of guanine crystals: Type 1 crystals (*dark grey*) and Type 2 crystals (*light grey*). The orientation of the principle refractive indices' coordinate axes in each crystal layer are indicated [adapted from Jordan et al. (2012)]

The work by Jordan et al. (2012) showed the mechanism by which fish can control the degree of polarisation in their reflections: Silvery reflections from fish are produced by multilayer "stacks" of high-refractive-index guanine-based crystals separated by low-refractive-index cytoplasm gaps. Whilst multilayer reflectors are common in nature, the majority use materials that have isotropic optical properties. The crystals here are different, as within the material, light passing

through a single crystal can experience one of two possible refractive indices depending on the direction it is traveling. The crystals are a mixture of pure guanine and hypoxanthine, which have refractive indices of 1.93, 1.91, 1.47 and 1.85, 1.78, 1.42, respectively. These materials are termed birefringent and with three different refractive indices are biaxial. The reflections that Jordan et al. (2012) measured were from the *stratum argenteum*, a silvery layer in the skin. For the first time, two optically different types of crystal were found in this layer and were termed Type 1 and Type 2. Type 1 crystals have the low refractive index value aligned with the direction the light traverses, whereas the low refractive index in the plane of the crystal in Type 2. The authors went onto solve Maxwell's equations for this composite structure and found that particular mixes of these two different optical types caused the structure to have unusual low polarising properties. A model of 75 % Type 1 and 25 % Type 2 crystals resulted in the best fit to the experimental data (Fig. 9.6a, b).

Regarding the central question of: are low-polarising broadband reflectors an adaptation for polarisation-based camouflage, Jordan et al. (2012) made one further important point. For a normal highly reflective polarising reflector, any weakly polarised incident light will be reflected at a much lower intensity. The limiting case is incident unpolarised light. Only half the intensity will come back at Brewster angle from a perfect 100 % reflective structure. Thus, a non-polarising mirror is also a more efficient reflector over all angles of incidence, and the discovered mixing ratio of the two types of guanine-based crystal seems optimal to maximise the reflected intensities over all angles of incidence. Thus, the very nature of a high degree of polarisation neutrality for reflections over all angles of incidence ensures a greater total reflected intensity that more closely matches the open water background light field. This implies that non-polarising type structures significantly benefit intensity matching the background. For optimal concealment, the reflecting structures must produce both spectrally broadband and high-percentage, non-polarising reflectivity over all angles of incidence. Furthermore, polarisation information defining a visual contrast, or lack of it, should not be taken in isolation. Any viewer will always receive a convolved signal of intensity and polarisation, and for a system that cannot process these dimensions of visual information independently, the combined perception is the one that is ecologically relevant.

9.5 Summary

Overall, the subject area of fish polarisation vision has continued to move forward in the last 10 years. However, significant challenges remain and the main questions of mechanism and behaviour are still largely unanswered. These outstanding questions certainly require new input from diverse areas of membrane biophysics,

optics, and behavioural biology to bring our knowledge of this interesting subject to the current level of understanding of invertebrate polarisation vision. Perhaps with further insight from these new approaches, the mechanism of polarisation sensitivity may turn out to be not so different from rhabdomeric systems.

References

Boesze-Battaglia K, Schimmel RJ (1997) Cell membrane lipid composition and distribution: implications for cell function and lessons learned from photoreceptors and platelets. J Exp Biol 200:2927–2936

Born M, Wolf E (1999) Principles of optics, 7th edn. Cambridge University Press, Cambridge, UK

Botelho A, Wang Y, Gibson N, Brown M (2006) Membrane bilayer properties influence photoactivation of rhodopsin. Biophys J 78:198–210

Brady PC, Travis KA, Maginnis T, Cummings ME (2013) Polaro-cryptic mirror of the lookdown as a biological model for open ocean camouflage. Proc Natl Acad Sci USA 110:9764–9769

Browman HI, Skiftesvik AB, Kuhn P (2006) The relationship between ultraviolet and polarized light and growth rate in the early larval stages of turbot (*Scophtalmus maximus*), Atlantic cod (*Gadus morhua*) and Atlantic herring (*Clupea harengus*) reared in intensive culture conditions. Aquaculture 256:296–301

Bruckert F, Chabre M, Vuong TM (1992) Kinetic analysis of the activation of transducin by photoexcited rhodopsin: influence of the lateral diffusion of transducin and competition of guanosine diphosphate and guanosine triphosphate for the nucleotide site. Biophys J 63:616–629

Brzustowicz MR, Stillwell W, Wassall SR (1999) Molecular organization in polyunsaturated phospholipid membranes: a solid state 2H NMR investigation. FEBS Lett 451:197–202

Cone RA (1972) Rotational diffusion of rhodopsin in visual receptor membrane. Nat New Biol 236:39–43

Corless JM, Worniallo E, Fetter RD (1994) 3-dimensional membrane crystals in amphibian cone outer segments. I. Light-dependent crystal-formation in frog retinas. J Struct Biol 113:64–86

Corless J, Worniallo E, Schneider T (1995) 3-dimensional membrane crystals in amphibian cone outer segments. II. Crystal type associated with the saddle-point regions of cone disks. J Struct Biol 61:335–349

Dell-Orco D (2013) A physiological role for the supramolecular organization of rhodopsin and transducin in rod photoreceptors. FEBS Lett 587:2060–2066

Denton EJ, Nicol JAC (1965) Polarization of light reflected from the silvery exterior of the bleak, *Alburnus alburnus*. J Mar Biol Assoc UK 45:705–709

Douglas RH, Hawryshyn CW (1990) Behavioural studies of fish vision: an analysis of visual capabilities. In: Douglas RH, Djamgoz MBA (eds) The visual system of fish. Chapman and Hall, New York, pp 373–418

Fahrenfort I, Sjoerdsma T, Ripps H, Kamermans M (2004) Cobalt ions inhibit negative feedback in the outer retina by blocking hemichannels on horizontal cells. Vis Neurosci 21:501–511

Fineran BA, Nicol JAC (1978) Studies on the photoreceptors of *Anchoa mitchilli* and *A. Hepsetus* (Engraulidae) with particular reference to the cones. Philos Trans R Soc Lond B 283:25–60

Firsov ML, Govardovskii VI, Donner K (1994) Response univariance in bull-frog rods with two visual pigments. Vis Res 34:839–847

Fotiadis D, Liang Y, Filipek S, Saperstein D, Engel A, Palczewski K (2003) Atomic-force microscopy: rhodopsin dimers in native disc membranes. Nature 421:127–128

George S, O'Dowd B, Lee S (2002) G-protein-coupled receptor oligomerization and its potential for drug discovery. Nat Rev Drug Discov 1:808–820

Govardovskii VI, Korenyak DA, Shukolyukov SA, Zueva LV (2009) Lateral diffusion of rhodopsin in photoreceptor membrane: a reappraisal. Mol Vis 15:1717–1729
Gupta BD, Williams TP (1990) Lateral diffusion of visual pigments in toad (*Bufo marinus*) rods and in catfish (*Ictalurus punctatus*) cones. J Physiol 430:483–496
Hárosi FI (1981) Microspectrophotometry and optical phenomena: birefringence, dichroism and anomalous dispersion. In: Enoch JM, Tobey FL (eds) Vertebrate photoreceptor optics. Berlin, Springer, pp 337–399
Hawryshyn CW (2010) Ultraviolet polarization vision and visually guided behavior in fishes. Brain Behav Evol 75:186–194
Hawryshyn CW, McFarland WN (1987) Cone photoreceptor mechanisms and the detection of polarized light in fish. J Comp Physiol A 160:459–465
Hawryshyn CW, Moyer HD, Allison WT, Haimberger TJ, McFarland WN (2003) Multidimensional polarization sensitivity in damselfishes. J Comp Physiol A 189:213–220
Hawryshyn CW, Ramsden SD, Betke KM, Sabbah S (2010) Spectral and polarization sensitivity of juvenile Atlantic salmon (*Salmo salar*): phylogenetic considerations. J Exp Biol 213:3187–3197
Horváth G, Varjú D (2004) Polarized light in animal vision—polarization patterns in nature. Springer, Heidelberg
Israelachvili JN, Sammut RA, Snyder AW (1975) Birefringence and dichroism of photoreceptors. Vis Res 16:47–52
Jäger S, Lewis JW, Zvyaga TA, Szundi I, Sakmar TP, Kliger DS (1997) Chromophore structural changes in rhodopsin from nanoseconds to microseconds following pigment photolysis. Proc Natl Acad Sci USA 94:8557–8562
Johnsen S, Marshall NJ, Widder EA (2011) Polarization sensitivity as a contrast enhancer in pelagic predators: lessons from in situ polarization imaging of transparent zooplankton. Philos Trans R Soc B 366:655–670
Jordan TM, Partridge JC, Roberts NW (2012) Non-polarizing broadband multilayer reflectors in fish. Nat Photonics 6:759–763
Kammermans M, Hawryshyn C (2011) Teleost polarization vision: how it might work and what it might be good for. Philos Trans R Soc B 366:742–756
Kondrashev SL, Gnyubkina VP, Zueva LV (2012) Structure and spectral sensitivity of photoreceptors of two anchovy species: *Engraulis japonicus* and *Engraulis encrasicolus*. Vis Res 68:19–27
Kota P, Reeves PJ, RajBhandary UL, Khorana HG (2006) Opsin is present as dimers in COS1 cells: identification of amino acids at the dimeric interface. Proc Natl Acad Sci USA 103:3054–3059
Kroeger K, Pfleger KDG, Eidne KA (2003) G-protein-coupled receptor oligomerization in neuroendocrine pathways. Front Neuroendocrinol 24:254–278
Laughlin SB, Menzel R, Snyder AW (1975) Membranes, dichroism and receptor sensitivity. In: Menzel R (ed) Photoreceptor optics AW Snyder. Springer, Berlin, pp 237–259
Lerner A, Sabbah S, Erlick C, Shashar N (2011) Navigation by light polarization in clear and turbid waters. Philos Trans R Soc B 366:671–679
Levine JS, MacNichol EF Jr, Kraft T, Collins BA (1979) Intraretinal distribution of cone pigments in certain teleost fishes. Science 204:523–526
Liang Y (2003) Organization of the G-protein-coupled receptors rhodopsin and opsin in native membranes. J Biol Chem 278:21655–21662
Liebman PA (1975) Birefringence, dichroism and rod outer segment structure. In: Snyder AW, Menzel R (eds) Photoreceptor optics. Springer, Berlin, pp 199–214
Liebman PA, Entine G (1974) Lateral diffusion of visual pigment in photoreceptor disk membranes. Science 185:457–459
Liebman PA, Jagger WS, Kaplan MW, Bargoot FG (1974) Membrane structure changes in rod outer segments with rhodopsin bleaching. Nature 251:31–36

Liebman PA, Weiner HL, Drzymala RE (1982) Lateral diffusion of visual pigment in rod disk membranes. Methods Enzymol 81:660–668
Lukáts A, Szabó A, Röhlich P, Vígh B, Szél A (2005) Photopigment coexpression in mammals: comparative and developmental aspects. Histol Histopathol 20:551–574
MacIntosh TJ (1973) The effect of cholesterol on the structure of phosphatidycholine bilayers. Biochim Biophys Acta 513:43–58
Maldonado PE, Maturana H, Varela FJ (1988) Frontal and lateral visual system in birds: frontal and lateral gaze. Brain Behav Evol 32:57–62
Marc RE, Sperling HG (1976) The chromatic organization of the goldfish cone mosaic. Vis Res 16:1211–1224
Molloy JE, Padgett MJ (2002) Lights, action: optical tweezers. Contemp Phys 43:241–258
Murari R, Murari MP, Baumann WJ (1986) Sterol orientations in phosphatidylcholine liposomes as determined by deuterium NMR. Biochemistry 25:1062–1067
Mussi M, Haimberger TJ, Hawryshyn CW (2005) Behavioural discrimination of polarized light in the damselfish *Chromis viridis* (family Pomacentridae). J Exp Biol 208:3037–3046
Novales-Flamarique I (2011) Unique photoreceptor arrangements in a fish with polarized light discrimination. J Comp Neurol 519:714–737
Novales-Flamarique I, Hárosi FI (2002) Visual pigments and dichroism of anchovy cones: a model system for polarization detection. Vis Neurosci 19:467–473
Palczewski K (2006) G protein-coupled receptor rhodopsin. Annu Rev Biochem 75:743–767
Palczewski K (2010) Oligomeric forms of G protein-coupled receptors (GPCRs). Trends Biochem Sci 35:595–600
Park PSH, Filipek S, Wells JW, Palczewski K (2004) Oligomerization of G protein-coupled receptors: past, present, and future. Biochemistry 43:15643–15656
Parkyn DC, Hawryshyn CW (2000) Spectral and ultraviolet-polarisation sensitivity in juvenile salmonids: a comparative analysis using electrophysiology. J Exp Biol 203:1173–1191
Parkyn DC, Austin JD, Hawryshyn CW (2003) Acquisition of polarized-light orientation in salmonids under laboratory conditions. Anim Behav 65:893–904
Pignatelli V, Temple SE, Chiou TH, Roberts NW, Collin SP, Marshall NJ (2011) Behavioural relevance of polarization sensitivity as a target detection mechanism in cephalopods and fishes. Philos Trans R Soc B 366:734–741
Poo M, Cone RA (1973) Lateral diffusion of rhodopsin in *Necturus* rods. Exp Eye Res 17:503–510
Poo MM, Cone RA (1974) Lateral diffusion of rhodopsin in the photoreceptor membrane. Nature 247:438–441
Ramsden SD, Anderson L, Mussi M, Kamermans M, Hawryshyn CW (2008) Retinal processing and opponent mechanisms mediating ultraviolet polarization sensitivity in rainbow trout (*Oncorhynchus mykiss*). J Exp Biol 211:1376–1385
Reckel F, Hoffman B, Melzer RR, Horppila J, Smola U (2003) Photoreceptors and cone patterns in the retina of the smelt *Osmerus eperlanus* (L.) (Osmeridae: Teleostei). Acta Zool (Stockholm) 84:161–170
Roberts NW (2006) The optics of vertebrate photoreceptors: anisotropy and form birefringence. Vis Res 46:3259–3266
Roberts NW, Gleeson HF (2004) The absorption of polarized light by vertebrate photoreceptors. Vis Res 44:2643–2652
Roberts NW, Needham MG (2007) A mechanism of polarized light sensitivity in cone photoreceptors of the goldfish *Carassius auratus*. Biophys J 93:3241–3248
Roberts NW, Gleeson HF, Temple SE, Haimberger TJ, Hawryshyn CW (2004) Differences in the optical properties of vertebrate photoreceptor classes leading to axial polarization sensitivity. J Opt Soc Am A 21:335–345
Roberts NW, Chiou TH, Marshall NJ, Cronin TW (2009) A biological quarter-wave retarder with excellent achromaticity in the visible wavelength region. Nat Photonics 3:641–644
Roberts NW, Porter ML, Cronin TW (2011) The molecular basis of mechanisms underlying polarization vision. Philos Trans R Soc B 366:627–637

Ryba N, Marsh D (1992) Protein rotational diffusion and lipid protein interactions in recombinants of bovine rhodopsin with saturated diacylphosphatidylcholines of different chain lengths studied by conventional and saturation-transfer electron-spin-resonance. Biochemistry 31:7511–7518

Sabbah S, Habib-Nayany MF, Dargaei Z, Hauser FE, Kamermans M, Hawryshyn CW (2013) Retinal region of polarization sensitivity switches during ontogeny of rainbow trout. J Neurosci 33:7428–7438

Saibil HR (1982) An ordered membrane-cytoskeleton network in squid photoreceptor microvilli. J Mol Biol 158:435–456

Shashar N, Hagan R, Boal JG, Hanlon RT (2000) Cuttlefish use polarization sensitivity in predation on silvery fish. Vis Res 40:71–75

Shukolyukov SA (2009) Aggregation of frog rhodopsin to oligomers and their dissociation to monomer: application of BN-and SDS-PAGE. Biochem Mosc 74:599–604

Snyder AW (1973) Polarization sensitivity of individual retinula cells. J Comp Physiol 83:331–360

Temple S, Hart NS, Marshall NJ, Collin SP (2010) A spitting image: specializations in archerfish eyes for vision at the interface between air and water. Proc R Soc B 277:2607–2615

Thoreson WB, Burkhardt DA (1990) Effects of synaptic blocking agents on the depolarizing responses of turtle cones evoked by surround illumination. Vis Neurosci 5:571–583

Townes-Anderson E, St Jules RS, Sherry DM, Lichtenberger J, Hassanain M (1998) Micromanipulation of retinal neurons by optical tweezers. Mol Vis 4:12

Waterman TH (2006) Reviving a neglected celestial underwater polarization compass for aquatic animals. Biol Rev 81:111–115

Wey CL, Cone RA (1981) Lateral diffusion of rhodopsin in photoreceptor cells measured by fluorescence photobleaching and recovery. Biophys J 33:225–232

Chapter 10
Polarization Sensitivity in Amphibians

Victor Benno Meyer-Rochow

Abstract Polarization sensitivity (PS) in amphibians has been examined in some species of anurans and urodelans. Gymnophiones, on account of their tiny eyes and fossorial or aquatic lifestyles, are considered unlikely candidates for PS. Some anura and urodela have been shown to detect the direction of polarization with photoreceptors of the pineal organ rather than their lateral eyes. An ordered array of light-absorbing visual molecules is paramount for PS, but an ordered array of radical pairs generated through photo-induced electron transfer is also essential for magnetoreception, which suggests that there is some interaction between the two senses. An anatomical requirement for PS is a constant and characteristic orientation of the photoreceptor's disc membranes. A closer look at ultrastructural modifications in different retinal regions of species deemed polarization sensitive seems warranted. Polarization sensitivity may help to relocate breeding sites in philotropic species and to improve visibility of prey in predatory larval and adult urodeles plus those few anurans that hunt under water. Furthermore, it could possibly be of assistance in separating overlapping shadows and play a role during courtship in species with distinct sexually dimorphic colouration.

V.B. Meyer-Rochow (✉)
Department of Biology, University of Oulu, Oulu, P.O. Box 3000, FIN-90014 Oulu, Finland

Hachijojima Geothermal Energy Museum, P.O. Box 2872, Nakanogo, Hachijojima, Tokyo, 100-1623, Japan
e-mail: vmr@cc.oulu.fi; meyrow@gmail.com

G. Horváth (ed.), *Polarized Light and Polarization Vision in Animal Sciences*, Springer Series in Vision Research 2, DOI 10.1007/978-3-642-54718-8_10,

10.1 Introduction

Amphibians are a class of vertebrate animals with three extant orders: Urodela, Anura and Gymnophiona. The latter are also known as 'caecilians'. Adult urodeles like newts and salamanders always possess tails as adults; anurans like frogs and toads are tailless as adults and gymnophiones, lacking legs, are aquatic or terrestrial worm-like species of the tropics. All adult amphibians, without exception, are carnivorous and feed on insects, slugs, worms or indeed anything that is not too big and therefore can be swallowed. Although the adults all have very tiny teeth, no amphibian is known to chew. Most of the adult species are visual hunters, but in aquatic species or larval forms olfaction can play a major role as well. However, even then a pair of eyes is always present except in some strictly troglobitic species like, for instance, *Typhlotriton spelaeus* and *Proteus anguinus* (Stone 1964; Durand 1976).

Largely dependent on freshwater bodies for reproduction, many species possess larvae (in anurans termed 'tadpoles', in urodeles sometimes referred to as 'efts') that develop in water until they metamorphose to acquire the adult body and begin to live their postlarval lives. The aquatic larvae of the urodeles and gymnophiones are usually carnivorous chasing and consuming water fleas and other small aquatic invertebrates; those of the anurans, on the other hand, are more omnivorous and apart from consuming algae, leaves and other plant material can also be seen to feed on corpses or slow invertebrates like earthworms that ended up in the water.

There are species of anurans, especially but not exclusively in the tropics, in which reproductive strategies have evolved that do not require eggs to be laid into the water. The eggs are instead carried around by the adults, mostly the females, but, e.g. in the midwife toad, sometimes also by the males, until the tadpoles hatch and then need water for the continuation of their development. There are even species of anurans in which the entire froglet or toadlet develops in the egg or on the body of the adult (Greven and Richter 2009), making reproduction either totally independent of water and/or skipping the tadpole stage (Callery et al. 2001). Very few species are live-bearing. Amongst the anurans the African toad *Nectophrynoides viviparus* should be mentioned (Channing and Howell 2006) and amongst the urodeles the black Alpine salamander *Salamandra atra* is a live-bearing species (Greven 2003).

Since most amphibian species, nevertheless, do need to find freshwater in order to lay their eggs in, they must be able to locate suitable water bodies and get there before the reproductive season is over or the water body has dried up. It is well known that amphibians often return to the same breeding site year after year and that migrations of several kilometres can be involved (Sinsch 2006). It is also known that during the reproductive season, adult anurans as well as urodeles often change morphologically and develop bright colour patterns for courtship displays, especially in the males (Fig. 10.1).

A variety of senses have been suggested to be involved in the task of locating suitable water bodies and in orienting towards previously visited breeding sites.

Fig. 10.1 Male *Rana arvalis* in *blue courtship colouration*, which it displays only under bright sunny conditions. Female individuals remain *brown-coloured*, which is also the colour of the males outside their breeding season (photo credit: Dr. Hans-Bert Schikora, Bremen)

The opposite, namely escape from the water and colonization of the land surrounding the breeding site, is a task of the metamorphosing larvae ready to lead their terrestrial lives. For them it is important to locate the shoreline from deeper water and to radially move away from the place they had spent their larval phase in, so as to avoid competition for food with conspecifics. To what extent polarization sensitivity can assist in these tasks, i.e. (a) location and migration to water and escape from it and (b) communication with conspecifics, will be examined further below. Another task in which polarization sensitivity could possibly be involved lies in the detection of prey. The earlier literature on amphibian polarization sensitivity has been reviewed by Horváth and Varjú (2004, Chapter 29, pp. 317–323).

10.2 Photoreception in Amphibians

There is no doubt that vision plays a dominant role for adult terrestrial anurans and urodeles in procuring food, but not probably in fossorial gymnophiones (Badenhorst 1978). Under water larval urodeles (and those few amphibians remaining aquatic as adults) use vision in their hunt for prey. Even phytophagous tadpoles that alternate between feeding sites and shelters and respond sensitively to shadows, be it by an approaching fish or a bird from above, possess sensitive eyes: they immediately scuttle for safety when a shadow falls on them. It therefore should not come as a surprise that vision in amphibians has been the subject of a large number of optical, anatomical, ultrastructural, biochemical and electrophysiological studies. Since amphibians can perceive light not only with their lateral (lens) eyes but also possess a photosensitive pineal body with its frontal organ (Vigh and Vigh-Teichmann 1986) and may even possess a dermal light sense (Daniolos et al. 1990), photoreception in amphibians is a complicated issue and requires separate investigations of at least the lateral eyes and the pineal complex.

Structurally, the amphibian lateral eye (even that of the most archaic leiopelmatid frogs: Meyer-Rochow and Pehlemann 1990) differs little from that

of other vertebrates. A transparent cornea is separated from a transparent but cellular lens by a space known as the anterior chamber containing aqueous humour. The lens, which lies in front of the posterior chamber with its vitreous humour, is usually more spherical than that of higher vertebrates and consequently less capable of accommodating to near and far objects. The retina is made up of the characteristic cell layers and cell types through which light rays have to pass in order to reach the outer segment discs with the photopigments in their membranes. Rods are usually the dominating photoreceptive cells and can possess huge diameters (up to 15 μm in *Leiopelma hamiltoni*: Meyer-Rochow and Pehlemann 1990). Because of their large diameters, frog rod outer segments as well as those of urodeles have prominent incisures (Corless 1986), of which there can be more than 20 seen in a transversely sectioned outer segment profiles (Mariani 1986). Cones may also be present, but since frogs can have two types of rods (green and red), which according to Tsukamoto (1987) can be distinguished on the basis of the number of incisures, cones do not appear to be an essential element of the amphibian retina to see the world in colours.

Evidence for colour vision in amphibians comes from behavioural as well as electrophysiological and biochemical studies. There has been consensus that four types of photoreceptors occur in the anura: two types of rhodopsin rods termed red ($\lambda_{max} = 502$ nm) and green ($\lambda_{max} = 433$ nm) and two kinds of cone. Large single cones and principal members of double cones have been reported to have $\lambda_{max} = 575$ nm, while the smaller accessory members of double cones have been reported to be more blue sensitive. A third type of short-wavelength-sensitive cone has been reported to peak at $\lambda_{max} = 431$ nm (Koskelainen et al. 1994) and may correspond to the one immunocytochemically detected by Röhlich and Szel (2000) in the *Xenopus* retina, but termed 'UV-sensitive cone' by them. The same conclusion was earlier reached by Zhang et al. (1994), who likened the small cone to UV-sensitive cells known from the tiger salamander retina (Perry and McNoughton 1991). It ought to be mentioned though that peak spectral sensitivities of retinal photoreceptor cells can differ between different species, age groups and perhaps even males and females (this latter aspect has not been studied to any extent and neither have seasonal effects been examined).

Fish have evolutionarily preceded amphibians, and since many species possess some UV-receptors in their retinae (at least for some time during their juvenile life: Kunz et al. 1994; Miyazaki et al. 2011) and furthermore have been shown to possess polarization sensitivity (e.g. Flamarique and Hawryshyn 1998; Flamarique and Browman 2001), aquatic amphibians may be more likely candidates than adults, in which to find both UV- and polarization sensitivity either together as a package or separately. Seasonal effects, as numerous publications on fish photopigments have shown (summarized in Meyer-Rochow and Coddington 2003), will also have to be considered for amphibians. In the European salamander *Salamandra salamandra*, colour vision was demonstrated by Himstedt (1972), but the perception of ultraviolet light in *S. salamandra* according to Przyrembel et al. (1995) does not require a separate UV-receptor, since this is possible with tri-chromatic vision based on photoreceptor types maximally sensitive to lights of around 450, 500 and

570 nm. Przyrembel et al. (1995) concluded that UV sensitivity in *S. salamandra* was due to the short wavelength flank of a photoreceptor type maximally sensitive to around 500 nm.

Turning to aquatic amphibians, *Rana temporaria* tadpoles have different photopigments from those of metamorphosed individuals and exhibit red-shifted maxima on account of their greater porphyropsin content (Reuter 1969). UV sensitivity and/or indisputable electrophysiological evidence for polarization sensitivity in tadpoles, however, is not known (although it has been reported that behaviourally tadpoles of the bullfrog apparently use compass orientation: Justin and Taylor 1976). Yet, neotenic larval and adult aquatic *Ambystoma mexicanum* do possess UV photoreception and Deutschlander and Phillips (1995) suggest that this property could be used in prey detection and polarized light perception. However, in the few cases of amphibians in which orientation with respect to the direction of polarization had been demonstrated not the lateral but the pineal photoreceptors seemed involved (Taylor and Adler 1978).

10.3 The Pineal Complex

Spectrally, different receptors are not only present in the retinae of the lateral eyes, but in fish (e.g. Ekström and Meissl 1997; Meyer-Rochow et al. 1999) and amphibians (Vigh et al. 1985; Vigh-Teichmann and Vigh 1990) they have also been shown to exist in the pineal complex made up of frontal organ and pineal organ. Both of these organs contain photoreceptive cells, and the pineal complex as a whole is situated in the skull in such a way that a horizontally located frog or salamander receives light on discs of its intracranial pineal receptors that are parallel to the incident light. This should make them more polarization sensitive to light—that is polarized through scattering in the atmosphere (e.g. Rayleigh scattering in the air), or passing through dichroic filters, or getting reflected from shiny surfaces—than receptor cells in the retinas of the lateral eyes, in which the outer segment discs are basically oriented perpendicularly to the incident light (Marshall and Cronin 2011). Although no electrophysiological evidence has been available to demonstrate polarization sensitivity in amphibians, be they larvae or adults, a number of behavioural observations exist, which show that at least some species can perceive linear polarization and will use this information.

Focusing on extraocular perception, Adler and Taylor (1973) could show that tiger salamanders (*Ambystoma tigrinum*) were able to orientate bi-modally and perpendicularly to the direction of polarization (E-vector) without the lateral eyes being involved. When the skull of these animals was covered by opaque plastic between the eye sockets and from immediately behind the nostril to the posterior of the skull, irrespective of whether seeing or blinded, orientation was random under linearly polarized light. When transparent plastic was used to cover the skull, bidirectional orientation perpendicular to the E-vector was again present. This kind of extraocular perception of polarization has also been demonstrated in eyeless

cricket frogs *Acris gryllus* (Taylor and Ferguson 1970) and the newt *Notophthalmus viridescens*, but it vanished when the pineal organ was covered (Demian and Taylor 1977; Taylor and Adler 1978; Hershey and Forester 1980; Hairston 1994; Stebbins and Cohen 1995).

10.4 Use of Polarization Sensitivity in Orientation

One of the tasks in which polarization sensitivity can be of use is in the context of orientation. However, polarization would be just one of many visual cues available to an amphibian (spectral quality and intensity of the light are others), and there are also acoustic, magnetic, mechanical and olfactory signals that can be integrated into a 'redundant-multisensory system' (Ferguson 1971). Sinsch (2006) has summarized the extent to which each of the cues might contribute to terrestrial urodele and anuran species. With regard to visual cues he distinguishes fixed landmarks 'like shorelines or forest silhouettes from periodically "moving" celestial cues like sun, moon, stars and skylight polarization patterns'.

While for metamorphosing aquatic amphibian larvae it is important to reach the shoreline without delay, it is important for the reproductive adults to reach the breeding site via as short a way as possible to save energy and to prevent dehydration and the likelihood of being attacked by predators. For the frog *Rana pipiens* (King and Conner 1996) and the toad *Rhinella arenarum* (Daneri and Casaneve 2011) body-centred cues like turning responses seemed to be more important than visual cues. On the other hand, it could be shown by Ferguson and Landreth (1966) that some diurnal anurans, e.g. *Bufo fowleri* (seen by them as diurnal), the bullfrog *Rana catesbeiana* (Ferguson et al. 1968) and the southern cricket frog *Acris gryllus* (Taylor and Ferguson 1970), use the position of the sun in combination with an endogenous clock for orientation. A similar ability was shown for some urodeles: newts were tested by Landreth and Ferguson (1967) and the tiger salamander *Ambystoma tigrinum* was investigated by Adler and Taylor (1973) as well as Taylor and Adler (1978). In larval *Rana catesbeiana* Justin and Taylor (1976) were able to demonstrate compass orientation on the basis of extraocular photoreception.

In an attempt to show whether tadpoles exhibited 'philopatry', Patrick et al. (2007) translocated 400 *Rana sylvatica* tadpoles to an area 55 km away from their original habitat and observed the direction the tadpoles chose in their new environment. The result suggested that the tadpoles relied on indirect cues, perhaps linearly polarized light, for orientation. Emigration orientations were studied for the marbled salamander *Ambystoma maculatum*, the red-spotted newt *Notophthalmus viridescens* and the wood frog *Rana sylvatica* over a period of four years by Timm et al. (2007), whose results revealed that emigration orientation of the newly metamorphosed juveniles of all of the species examined was consistently non-uniform 'across ponds, years and species'. This result shows that conclusions based on data from a single year or observation cannot be extrapolated to other years or used to predict long-term orientation.

On the other hand, for at least 13 species of urodeles and 16 species of anurans, homing and orientation to breeding ponds have been demonstrated (cf. review by Russell et al. 2005), but true navigation from outside their natural migratory range has only been shown for *Taricha rivularis* newts, even when released in excess of 30 km from their natural home range (Phillips 1986) and for the salamander *Notophthalmus viridescens* (Phillips 1998). Although the use of celestial cues in orientation tasks requires the presence of an internal clock to compensate for the apparent motion (rotation around the star Solaris) of the celestial pattern (and circadian clocks have indeed been shown to operate in amphibians that use the position of the sun: cf. review by Sinsch 1990), toads and many other amphibians migrate preferentially during the night or on overcast and rainy days. Conditions favouring migration are thus not those in which sky polarization signals could provide the easiest of optimal cues (but see Chaps. 18 and 25).

Some criticism was voiced by Horváth and Varjú (2004, pp. 317–323), who explained that 'the major problem with the experimental apparatus used by Adler and Taylor (1973) is that they used black plastic covers around the training and testing tanks. The entire training tank, including the area directly above it, was enclosed with opaque black plastic curtains such that no light penetrated from the outside. The test arena, a circular pale blue plastic pool, was also completely surrounded by an opaque black plastic curtain. No differences in light intensity were measured directly beneath the polarizing filter when its transmission axis was rotated by 90° from its original direction. However, the brightness distribution around the training tank and test arena was not measured. Thus, it cannot be excluded that the salamanders utilized brightness patterns induced by selective reflection of polarized light from these black coverings. According to Taylor and Adler (1978), the utilization of such brightness patterns is unlikely because "Ambystomatids typically are negatively phototactic and, as such, their typical response should have been parallel, not perpendicular, to the E-vector since the region of maximum reflection and thus brightness are perpendicular to the E-vector". However, this argument loses its validity if both in the training and testing situation, reaching the shore by positive phototaxis towards the brightest region of the optical environment (perpendicular to the E-vector) was more important for the salamanders than finding a shelter by negative phototaxis towards the darkest region (parallel to the E-vector). Hence, the observed reaction of salamanders, bidirectional orientation perpendicularly to the E-vector, can also be explained exclusively by a response to the brightness pattern, i.e. bimodal orientation towards the brightest directions associated with the shore during training, the directions of which are always perpendicular to the E-vector.

In the red-spotted newt *Notophthalmus viridescens* orientation behaviour was studied in larvae of the eft stage and in adult individuals by Taylor and Auburn (1978). Training occurred in outdoor elongated tanks under clear skies allowing adult newts to swim back to the deeper water and efts to swim from the deep water to the shallow end. Testing of the efts took place outdoors in a circular arena filled with shallow water and surrounded by an opaque wall. Only the sky could be viewed by the animals, which were tested in an arena with completely black

surroundings and also with white panels placed over opposite quarters of the test arena, either perpendicularly or parallel to the celestial E-vector at the zenith. Efts were oriented in the predicted direction under clear skies after sunset, but randomly after sunset under overcast skies.

Controls with white panels placed either perpendicularly or parallel to the E-vector suggested that the efts were responding to the E-vector and not to the brightness pattern induced by selective reflection of polarized light. Tests with adult newts trained to two different compass directions responded as predicted relative to the imposed E-vector, i.e. responded as if the E-vector was the primary celestial E-vector outdoors at that time of day. The conclusion from this series of experiments reached by Taylor and Adler (1978) was that larval and adult *Notophthalmus viridescens* can perceive the linear polarization of light and use it for orientation purposes. Further tests with aquatic tadpoles of the bullfrog *Rana catesbeiana* not only confirmed that also these larval amphibians use celestial cues, but furthermore showed that the linear polarization of light was responsible for the tadpoles to orient towards or away from the shoreline. Additional experiments showed that not the lateral eyes but the receptors of the pineal complex (either frontal organ or pineal body or both) were involved in the observed polarization-sensitive responses (Auburn and Taylor 1979).

Summarizing structural and functional properties of frog pineal bodies and frontal organs, Vigh and Vigh-Teichmann (1986) had earlier reported the presence of one rod and two cone-like photoreceptive cell types in both pineal and frontal organs of the frogs *Rana esculenta* and *R. temporaria*, so that one could assume that *R. catesbeiana* would also possess these receptors in its pineal complex. Spectral sensitivity peaks of 500/570 nm and 425/525 nm were given by Vigh and Vigh-Teichmann (1986) for the pineal organ and 355/515 nm and 570 nm for the frontal organ of the frog pineal complex.

10.5 Possible Additional Uses of Polarization Sensitivity

Since under water scattered light is nearly always at least partially polarized (Sabbah et al. 2005), the polarization could provide valuable cues not only for the purpose of orientation in aquatic amphibians but could also improve the visibility of prey organisms to predatory larval and adult urodeles and those few aquatic anurans that hunt under water. A search for polarization-sensitive amphibians is therefore deemed to be most likely successful, if aquatic species were to be investigated. Another and hitherto somewhat ignored aspect is that polarization sensitivity might be of assistance in separating and contrasting overlapping shadows. That shadow separation is almost impossible with conventional imaging, but is achievable through illumination with linearly polarized light (Lin and Yemelyanov 2006), is a feature, which could be of considerable use for amphibians both under water and on land, but which to date has not been explored in any species.

Fig. 10.2 Male *Triturus alpestris* in *blue courtship colouration*, which it displays only under water in spring. Females remain *dark brown-coloured*, as is also the colour of the males outside their breeding season on land (photo credit: Mr Dieter Florian, Leipzig)

Nilsson and Warrant (1999) compared colour vision and polarization vision and concluded that polarization vision is potentially as powerful as colour vision and that one does not exclude the other. A beautiful example underscoring this statement is provided by the butterflies of the genus *Heliconius*, in which linearly polarized light reflected from the colourfully iridescent wings of females is used as a signal in mate recognition (Sweeney et al. 2003). Given that numerous species of amphibians turn into exceptionally colourful individuals during the mating season (Figs. 10.1 and 10.2) and often have colour change accompany their courtship displays, be that under or above water, one might wonder if polarization in addition to colour, acoustic and olfactory signals could not also be involved. For example, males of the newt *Triturus alpestris*, for which Himstedt (1979) has shown the importance of colour vision, court and display under water by making undulating, rapid movements with their tails that sport silvery-blue flanks (Fig. 10.2). Whether the integument of the displaying individuals reflects polarized light has never been investigated, and polarization photographs or imaging polarimetry of amphibians apparently are non-existent. However, some male frogs like those of the species *Rana arvalis* become so strikingly blue when croaking in full sunlight (Fig. 10.1) that in addition to their acoustic mating signal an optical one (with or without a polarization component) is at least a possibility that ought to be checked out—especially since Marshall and Cronin (2011) highlight that linear polarization sensitivity could be used in 'camouflage breaking of transparent or silvery animals in the ocean'. One might add, 'and freshwater most likely as well' (see also Chap. 19).

Although polarization sensitivity in the lateral eyes of amphibians has yet to be conclusively demonstrated, it should not be ruled out that at least some part of the retina could possess a certain degree of polarization sensitivity. Just like different regions of the retina in vertebrates have different spectral sensitivities (Temple 2011), some regions may possess a certain amount of polarization sensitivity over others, especially if one considers that the retina in frog eyes is curved and not all discs are strictly perpendicular to the incident light. Compared with the rather flat urodeles with more dorsally placed eyes or toads which mostly move around

horizontally and rarely climb, frogs, however, are much more mobile, and during climbs frequently change their positions and, consequently, that of their eyes as well. For them polarization signals, if at all perceived, might be less reliable than for the aforementioned urodeles and toads.

10.6 Polarization Sensitivity and Magnetoreception: Possible Mechanisms

True navigation has so far been analysed only in the aquatic salamander *Notophthalmus viridescens*, and according to Phillips (1998) and Phillips et al. (2001) this ability to navigate is based on magnetoreception and not the detection of linearly polarized light. That magnetoreception in birds and other vertebrates is light dependent has been amply demonstrated by Wiltschko and Wiltschko (1995, 2005), Wiltschko et al. (2000a, b) and others (cf. review by Ritz et al. 2002). Wavelength dependency in orientation responses was implicated in newts, birds and fruit flies, but not mole rats, turtles and mealworm beetles (cf. review by Ritz et al. 2002). It has therefore become obvious that in amphibians, the two sensory modalities (magnetoreception and polarization sensitivity) must not be seen to operate in total isolation from each other, so that Phillips et al. (2001) concluded that 'the amphibian pineal organ mediates orientation to both the E-vector of plane polarized light and the magnetic field' and went on to explain parallels between the detection of polarized light and the light-dependent detection of magnetic fields. They suggested that the short-wavelength-sensitive receptors of the pineal complex (implicated in the polarization response) also provided an input to the magnetic compass of the newt.

The search for the mechanism of polarization sensitivity in amphibians has to be seen as an attempt to understand polarization sensitivity generally, because the prerequisites for the detection of polarized light in amphibians are not expected to be unique for this class of vertebrates. Nevertheless, casting more light on this kind of interaction between the two sensors in amphibians would seem a promising and exciting task for the future as more and more species including salamanders, newts and some frogs are shown to use magnetic cues (Russell et al. 2005). Ever since Schmidt (1938) had first discovered that light was absorbed preferentially when polarized parallel to the transverse axis of the photoreceptor outer segment, numerous studies were carried out to measure and calculate ratios of the dichroic absorption parallel and perpendicular to the transverse axis of the photoreceptor (Roberts and Gleeson 2004). One consistent finding in all of these dichroism measurements of vertebrate photoreceptors was that cones usually exhibited a lower dichroism than rods (Roberts and Gleeson 2004).

An ordered array of light-absorbing molecules is paramount for polarization sensitivity to occur, but an ordered array of radical pairs, generated through a photo-induced electron transfer (Ritz et al. 2002), is also regarded as an essential feature

of magnetoreception if we accept the resultant change in spin states of the radical products as suggested by Schulten et al. (1978), updated in Schulten (1982). Thus, the earlier demonstrated links between magnetoreception and photoreception are becoming more and more understandable, and the recently discovered class of photopigments known as cryptochromes has become a strong candidate for the generation of potentially magnetosensitive radical pairs (Foley et al. 2011). Photopigments of this nature are expressed in the ganglion cells and inner nuclear layer of the vertebrate eye and play a pivotal role in the regulation of circadian rhythms. Circadian rhythmicity, on the other hand, has long been known to be controlled by the cells of the pineal complex, which was shown to be responsible for the polarization sensitivity proved to guide *Ambystoma tigrinum* and tadpoles of *Rana catesbeiana* in orientation tasks given to them by Taylor and Adler (1978) and Auburn and Taylor (1979), respectively.

There are other theories that can be used to explain the link between polarization sensitivity and magnetoreception, and Phillips et al. (2001) explain on the basis of suggestions first put forward by Edmonds (1996) that aligned carotenoid molecules with single-domain particles of magnetite could be affected by mechanical strain resulting from the rotation of the particles in the geomagnetic field. Because the absorption of light by carotenoid molecules is strongly anisotropic, transmission of light through such magnetite-containing material would vary with the alignment of the magnetic field. Magnetic fields aligned perpendicularly to the long axis of the receptor would result in a lower light intensity reaching the outer segment than if the carotenoid molecules with their magnetite particles were aligned parallel to the long axis. An accompanying effect would be differences in the transmission of polarized light with different E-vectors. As with the case of a radical-pair-based mechanism (Ritz et al. 2002), the mechanism proposed by Edmonds (1996) would lead to both magnetic and polarization sensitivity. The problem is that to date no magnetic particles in retinal cells of either lateral or pineal photoreceptive cells have been discovered. Another unrelated problem is that the fundamental requirements to detect the E-vector may exist in the retina, but that the visual centres of the brain lack the ability to sort and integrate the information on the degree of polarization arriving from the retina. Only close collaboration between biochemists, biophysicists, anatomists and ethologists can solve the question of polarization sensitivity and its likely function(s) in the lives of amphibians.

Irrespective of the theory behind polarization sensitivity, the single most basic requirement as mentioned already is an ordered alignment of dipole photopigment molecules in the membranes of the receptor cells. The photoreceptors of the lateral eye of the mudpuppy (*Necturus maculosus*), an amphibian, were used in an early study by Hárosi (1975), who measured absorption spectra and linear dichroism of this amphibian's photoreceptive cells by microspectrophotometry and biochemical analyses. Numerous additional (cf. Roberts and Gleeson 2004) studies confirmed and expanded Hárosi's findings, but without arriving at a consensus on what was actually driving the molecular order. Very recently, however, investigations by Roberts et al. (2011) brought together a diverse range of biochemical and biophysical investigations to explain polarization sensitivity in both vertebrate and invertebrate

animals. The authors concluded that in polarization-sensitive vertebrates, photoreceptors were involved that contained carefully balanced cholesterol in their membranes responsible for the formation of liquid-ordered L_o and L_α micro-domains (Roberts et al. 2011). Cone opsins were thought to affiliate with the L_α micro-domains allowing protein–protein interactions to occur. Associations like these would then permit rhodopsin to oligomerize, causing alignments of the chromophores 'into a cellular-scale polarization detector, producing the higher levels of dichroism measured experimentally than predicted theoretically'. Whether or not this is the last word in explaining the mechanisms of molecular alignments and in permitting the formulation of conclusions in connection with the link between polarized light perception and magnetoreception, future will tell.

Acknowledgements I wish to thank Prof. Hong Yang Yan (Taiwan National Academy of Science) for valuable hints on relevant literature and President James Jin Kyung Kim of Pyongyang University of Science and Technology for his support and for allowing me time to complete this chapter during my sabbatical semester in North Korea (DPRK). I am grateful to Dr. Hans-Bert Schikora and Mr Dieter Florian for making available the photographs in Figs. 10.1 and 10.2 and furthermore to Prof. G. Horváth for inviting me to contribute this chapter to this book.

References

Adler K, Taylor DH (1973) Extraocular perception of polarized light by orienting salamanders. J Comp Physiol 87:203–212

Auburn JS, Taylor DH (1979) Polarized light perception and orientation in larval bullfrogs *Rana catesbeiana*. Anim Behav 27:658–668

Badenhorst A (1978) The development and the phylogeny of the organ of Jacobson and the tentacular apparatus of *Ichthyophis glutinosus* (Linne). Ann Univ Stellenbosch Ser 2AI:1–26

Callery EM, Fang H, Elinson RP (2001) Frogs without polliwogs: evolution of anuran direct development. BioEssays 23:233–241

Channing A, Howell KM (2006) Amphibians of East Africa. Cornell University Press, Ithaca, NY

Corless JM (1986) A minimum diameter limit for retinal rod outer segment disks. In: Sheffield JB, Hilfer SR (eds) Development of order in the visual system. Springer, Heidelberg, pp 127–142

Daneri MF, Casaneve E (2011) Control of spatial orientation in terrestrial toads (*Rhinella arenarum*). J Comp Psychol 125:296–307

Daniolos A, Lerner AB, Lerner MR (1990) Action of light on frog pigment cells in culture. Pigment Cell Res 3:38–43

Demian JJ, Taylor DH (1977) Photoreception and locomotor rhythm entrainment by the pineal body of the newt *Notophthalmus viridescens* (Amphibia, Urodela, Salamandridae). J Herpetol 11:131–139

Deutschlander ME, Phillips JB (1995) Characterization of an ultraviolet photoreception mechanism in the retina of an amphibian, the axolotl (*Ambystoma mexicanum*). Neurosci Lett 197: 93–96

Durand J (1976) Ocular development and involution in the European cave salamander *Proteus anguinus* Laurenti. Biol Bull 151:450–466

Edmonds DT (1996) A sensitive optically-detected magnetic compass for animals. Proc R Soc Lond B 263:295–298

Ekström P, Meissl H (1997) The pineal organ of teleost fishes. Rev Fish Biol Fisher 7:199–284

Ferguson DE (1971) The sensory basis of orientation in amphibians. Ann N Y Acad Sci 188:30–36

Ferguson DE, Landreth HF (1966) Celestial orientation of Fowler's toad, *Bufo fowleri*. Behaviour 26:105–123
Ferguson DE, McKeown JB, Bosarge OS, Landreth HF (1968) Sun-compass orientation of bullfrogs. Copeia 1968:230–235
Flamarique IN, Browman MI (2001) Foraging and prey-searching behaviour of small juvenile rainbow trout (*Oncorhynchus mykiss*) under polarized light. J Exp Biol 204:2415–2422
Flamarique IN, Hawryshyn CW (1998) Photoreceptor types and their relation to the spectral and polarization sensitivities of clupeid fishes. J Comp Physiol A 182:793–803
Foley EL, Gegear RJ, Reppert SM (2011) Human cryptochrome exhibits light-dependent magnetosensitivity. Nat Commun 2:356. doi:10.1038/ncomms1364
Greven H (2003) Larviparity and pueriparity. In: Sever DM (ed) Reproductive biology and phlogeny of urodela. Science Publications, Enfield, Plymouth, pp 447–475
Greven H, Richter S (2009) Morphology of skin incubation in *Pipa carvalhoi* (Anura; Pipidae). J Morphol 270:1311–1319
Hairston NGS (1994) Vertebrate zoology: an experimental field approach. Cambridge University Press, Cambridge
Hárosi FI (1975) Absorption spectra and linear dichroism of some amphibian photoreceptors. J Gen Physiol 66:357–382
Hershey JL, Forester DC (1980) Sensory orientation in *Notophthalmus v. viridescens* (Amphibia; Salamandridae). Can J Zool 58:266–276
Himstedt W (1972) Untersuchungen zum Farbensehen von Urodelen. J Comp Physiol 81:229–238
Himstedt W (1979) The significance of color in partner recognition of the newt *Triturus alpestris*. Copeia 1979:43–47
Horváth G, Varjú D (2004) Polarized light in animal vision—polarization patterns in nature. Springer, Heidelberg
Justin CS, Taylor DH (1976) Extraocular photoreception and compass orientation in larval bullfrogs *Rana catesbeiana*. Copeia 1976:98–105
King JR, Conner CM (1996) Visually elicited turning behavior in *Rana pipiens:* comparative organization and neural control of escape and prey capture. J Comp Physiol A 178:293–305
Koskelainen A, Hemilä S, Donner K (1994) Spectral sensitivities of short- and long-wavelength sensitive cone mechanisms in the frog retina. Acta Physiol Scand 152:115–124
Kunz YW, Wildenburg G, Goodrich L, Callaghan E (1994) The fate of ultraviolet receptors in the retina of the Atlantic salmon (*Salmo salar*). Vis Res 34:1375–1383
Landreth HF, Ferguson DE (1967) Newts: sun-compass orientation. Science 158:1459–1461
Lin S, Yemelyanov KM (2006) Separation and contrast enhancement of overlapping cast shadow components using polarization. Opt Express 14:7099–7107
Mariani AP (1986) Photoreceptors of the larval tiger salamander retina. Proc R Soc Lond B 227: 483–492
Marshall J, Cronin TW (2011) Polarisation vision. Curr Biol 21:R101–R105
Meyer-Rochow VB, Coddington PE (2003) Eyes and vision of the New Zealand torrentfish *Cheimarrichthys fosteri* von Haast (1874): histology, photochemistry and electrophysiology. In: Val AL, Kapoor BG (eds) Fish adaptations. Science Publications, Enfield, Plymouth, pp 337–381
Meyer-Rochow VB, Morita Y, Tamotsu S (1999) Immunocytochemical observations of the pineal organ and retina of the Antarctic teleosts *Pagothenia borchgrevinki* and *Trematomus bernacchii*. J Neurocytol 28:125–130
Meyer-Rochow VB, Pehlemann FW (1990) Retinal organization in the native New Zealand frogs *Leiopelma archeyi, L. hamiltoni*, and *L. hochstetteri* (Amphibia: Anura; Leiopelmatidae). J Roy Soc NZ 20:349–366
Miyazaki T, Iwami I, Meyer-Rochow VB (2011) The position of the retinal area centralis changes with age in *Champsocephalus gunnari* (Channichthyidae), a predatory fish from coastal Antarctic waters. Polar Biol 34:117–1123
Nilsson D, Warrant EJ (1999) Seeing the third quality of light. Curr Biol 9:R535–R537

Patrick DA, Calhoun AJK, Hunter ML (2007) Orientation of juvenile wood frogs, *Rana sylvatica*, leaving experimental ponds. J Herpetol 41:158–163
Perry RJ, McNoughton PA (1991) Response properties of cones from the retina of the tiger salamander. J Physiol 433:561–587
Phillips JB (1986) Magnetic compass orientation in the Eastern red spotted newt (*Notophthalmus viridescens*). J Comp Physiol A 158:103–109
Phillips JB (1998) Magnetoreception. In: Heatwole H (ed) Amphibian biology 3: sensory perception. Surrey Beatty & Sons Pty Ltd, Chipping Norton, pp 954–964
Phillips JB, Deutschlander ME, Freake MJ, Borland SC (2001) The role of extraocular photoreceptors in newt magnetic compass orientation: parallels between light-dependent magnetoreception and polarized light detection in vertebrates. J Exp Biol 204:2543–2552
Przyrembel C, Keller B, Neumeyer C (1995) Trichromatic colour vision in the salamander (*Salamandra salamandra*). J Comp Physiol A 176:575–586
Reuter T (1969) Visual pigments and ganglion cell activity in the retinae of tadpoles and adult frogs (*Rana temporaria* L.). Act Zool Fenn 122:1–64
Ritz T, Dommer DH, Phillips JB (2002) Shedding light on vertebrate magnetoreception. Neuron 34:503–506
Roberts NW, Gleeson HF (2004) The absorption of polarized light by vertebrate photoreceptors. Vis Res 44:2643–2652
Roberts NW, Porter ML, Cronin TW (2011) The molecular basis of mechanisms underlying polarization vision. Philos Trans R Soc B 366:627–637
Röhlich P, Szel A (2000) Photoreceptor cells in the *Xenopus* retina. Microsc Res Tech 50:327–337
Russell AP, Bauer AM, Johnson MK (2005) Migration in amphibians and reptiles. In: Bewa AMT (ed) Migration of organisms: climate, geography, ecology. Springer, Heidelberg, pp 151–203
Sabbah S, Lerner A, Erlick C, Shashar N (2005) Underwater polarization vision—a physical examination. Recent Res Dev Exp Theor Biol 1:123–176
Schmidt WJ (1938) Doppelbrechung, Dichroismus und Feinbau des Aussengliedes der Sehzellen vom Frosch. Z Zellforsch 22:485–522
Schulten K (1982) Magnetic field effects in chemistry and biology. Adv Solid State Phys 22:61–83
Schulten K, Swenberg C, Walter A (1978) A biomagnetic sensory mechanism based on magnetic field-modulated coherent electron spin motion. Z Phys Chem NF111:1–5
Sinsch U (1990) Migration and orientation in anuran amphibians. Ethol Ecol Evol 2:65–79
Sinsch U (2006) Orientation and navigation in amphibian. Mar Freshw Behav Physiol 39:65–71
Stebbins RC, Cohen NW (1995) A natural history of amphibians. Princeton University Press, Princeton, NJ
Stone LS (1964) The structure and visual function of the eye of larval and adult cave salamanders *Typhlotriton spelaeus*. J Exp Zool 156:201–218
Sweeney A, Jiggins C, Johnsen S (2003) Polarized light as a butterfly mating signal. Nature 423:31
Taylor DH, Adler K (1978) The pineal body: site of extraocular perception of celestial cues for orientation in the tiger salamander (*Ambystoma tigrinum*). J Comp Physiol A 124:357–361
Taylor DH, Auburn JS (1978) Orientation of amphibians by linearly polarized light. In: Schmidt-Koenig K, Keeton WT (eds) Animal migration, navigation and homing. Springer, Heidelberg, pp 334–346
Taylor DH, Ferguson DE (1970) Extraoptic celestial orientation in the southern cricket frog *Acris gryllus*. Science 168:390–392
Temple SE (2011) Why different regions of the retina have different spectral sensitivities: a review of mechanisms and functional significance of intraretinal variability in spectral sensitivity in vertebrates. Vis Neurosci 28:281–293
Timm BC, McGarigal K, Jenkins CL (2007) Emigration orientation of juvenile pond-breeding amphibians in western Massachusetts. Copeia 3:658–698
Tsukamoto Y (1987) The number, depth and elongation of disc incisures in the retinal rod of *Rana catesbeiana*. Exp Eye Res 45:105–116

Vigh B, Vigh-Teichmann I (1986) Three types of photoreceptors in the pineal and frontal organs of frogs: ultrastructure and opsin immunoreactivity. Arch Histol Jap 49:495–518
Vigh B, Vigh-Teichmann I, Oksche A (1985) Sensory cells of the 'rod' and 'cone' type in the pineal organ of *Rana esculenta* as revealed by immunoreaction against opsin and by the presence of an oil (lipid) droplet. Cell Tissue Res 240:143–148
Vigh-Teichmann I, Vigh B (1990) Opsin immunocytochemical characterization of different types of photoreceptors in the frog pineal organ. J Pineal Res 8:323–333
Wiltschko W, Wiltschko R (1995) Magnetic orientation in animals. Springer, Heidelberg
Wiltschko W, Wiltschko R (2005) Magnetic orientation and magnetoreception in birds and other animals. J Comp Physiol A 191:675–693
Wiltschko W, Wiltschko R, Munro U (2000a) Light-dependent magnetoreception: does directional information change with light intensity? Naturwissenschaften 87:36–40
Wiltschko W, Wiltschko R, Munro U (2000b) Light-dependent magnetoreception in birds: the effect of intensity of 565 nm green light. Naturwissenschaften 87:366–369
Zhang J, Kleinschmidt J, Sun P, Witkovsky P (1994) Identification of cone classes in *Xenopus* retina by immunocytochemistry and staining with lectins and vital dyes. Vis Neurosci 11: 1185–1192

Chapter 11
Polarization Sensitivity in Reptiles

Victor Benno Meyer-Rochow

Abstract Somewhat questionable evidence in support of reptilian polarization sensitivity (PS) has come from field and laboratory observations on the behaviour of a few species of marine and freshwater turtles. More convincing are conclusions based on PS-aided orientation in the lizards *Uma notata*, *Tiliqua rugosa* and *Podarcis sicula*. It is suggested that submersed hunters like, for instance, sea snakes ought to be included in examinations for PS since contrast enhancement by PS under water could bestow some benefits to them during food procurement. Courtship displays in certain species of lizards could also contain signals for which the presence of PS would be advantageous, but as yet polarization signals have not been demonstrated in any species. Results based on electrophysiological recordings to demonstrate PS in photoreceptors of the lateral eyes or pineal organs are scant and a connection between PS and magnetoreception is regarded as likely.

11.1 Introduction

Reptiles represent a class of amniotic vertebrates. Most taxonomists distinguish four reptilian orders, namely the Crocodilia, the Sphenodontia, the Squamata (which include the worm-like amphisbaenids, the lizards and the snakes) and the Testudines (turtles and tortoises). Being ectothermic, reptiles generally cannot tolerate cold climates or, in case we deal with aquatic species, cold water and are therefore poorly represented in regions of high latitude or altitude. The few species that do manage to

V.B. Meyer-Rochow (✉)
Department of Biology, University of Oulu, Oulu, P.O. Box 3000, FIN-90014 Oulu, Finland

Hachijojima Geothermal Energy Museum, P.O. Box 2872, Nakanogo, Hachijojima, Tokyo, 100-1623 Japan
e-mail: vmr@cc.oulu.fi; meyrow@gmail.com

G. Horváth (ed.), *Polarized Light and Polarization Vision in Animal Sciences*, Springer Series in Vision Research 2, DOI 10.1007/978-3-642-54718-8_11,

Fig. 11.1 Head of a male *Lacerta viridis* during courtship. Note the *metallic blue coloration* of the head (photo credit: Prof. Dr. Peter Stoeckl)

survive in such regions usually survive the winter in hibernation. Relatively short- or medium-distance migrations to hibernation sites, feeding locations or nesting areas can occur, but long-distance migrations over hundreds and thousands of kilometres are only common in some species of marine turtles and perhaps sea snakes of the family Laticaudinae (Russell et al. 2005; Southwood and Avens 2010).

Unlike amphibians (Meyer-Rochow 2014: Chap. 10), no reptile requires water bodies to lay its eggs in; sandy beaches, on the other hand, are a necessity for marine turtles. Although the remainder of the egg-laying reptiles (there are also viviparous species of lizards and snakes) usually choose their oviposition sites carefully, they rarely seem to exhibit the kinds of migrations known from the marine reptiles. Courtship displays, colour change and colour variations are not uncommon in lizards (Fig. 11.1) and snakes, but an involvement of polarization signals has yet to be shown.

Polarization sensitivity, however, has been suspected and even been shown in some species of marine and freshwater turtles that seek identical oviposition sites year after year or that need to relocate earlier shelters. A capacity for homing, in which polarization sensitivity seems involved, appears to be displayed by some crocodilians, tortoises, a few species of snakes and some lizards. The earlier literature on reptilian polarization sensitivity has been reviewed by Horváth and Varjú (2004, Chapter 30, pp. 324–327).

11.2 Possible Use of Polarization Sensitivity in Reptilian Migrators

Reviewed by Russell et al. (2005) and Southwood and Avens (2010), reptilian migration involves relatively few species. The prime reasons for those that do migrate are responses to seasonal habitat changes, to reach feeding places, or to find suitable terrestrial nesting sites in the case of aquatic species. Some of the best

studied migratory animals generally, and reptiles in particular, are the marine turtles. Often their nesting sites are on small islands or beaches remote from the turtles' feeding areas.

Of the seven or so recognized species of marine turtle, members of the Ascension Island population of *Chelonia mydas* undertake one of the most spectacular migrations of any non-flying animal. Feeding off the coast of Brazil for at least 10 years until sexually mature, they then take off in an easterly direction to reach the sandy beaches of Ascension Island, an island measuring 20 km in diameter 2,200 km away. A journey takes a turtle around 6 weeks and is undertaken every 2–3 years. Confirmed through mitochondrial DNA analyses, females usually return to their natal beach, lay their eggs and make their way back to the Brazilian coastal waters. How they can possibly locate and reach this mere speck in the vastness of the Southern Atlantic that Ascension Island represents has puzzled and intrigued generations of researchers, but the ability of the hatchlings to unerringly run towards the sea and then orient across "spans of seemingly featureless ocean" (Russell et al. 2005) is no less amazing and suggests the presence of a sophisticated orientation system.

Turning to the hatchlings first, it is well known that they are guided by the brightest light around, which is usually the horizon over the sea. A preference of blue over red light has been noticed in *Chelonia mydas* (Ehrenfeld 1968), and it was suggested that polarized light might be involved. Imprinting on the natal beach has been linked to the turtles' presumed sensitivity to the earth's magnetic field's angle of inclination and strength in such a way that a bi-coordinate map is created (Lohmann et al. 1996). This map and the ability to use it are thought to be retained into adulthood for the purpose of orientation and navigation. Magnetoreception (as with other vertebrates, in which magnetoreception has been shown to exist: Wiltschko and Wiltschko 1995) may require a visual input and observations on freshwater turtles indicated that the latter might well use surface-reflected polarized light to detect and orient towards water (Yeomans 1995; Zug et al. 2001).

Note, however, that unlike in flying aquatic insects (see Chap. 5), in turtles such polarization-based water detection could function only at very small distances from the water body, because from a remote distance the angle of view of the water body relative to the horizontal is so small that the water-reflected light reaching the turtle's eye is practically unpolarized (degree of linear polarization $d \approx 0$). When a turtle crawling on the ground approaches the water, its angle of view together with the degree of linear polarization d gradually increases. Water can be detected polarotactically only if d is higher than the threshold d^* of polarization sensitivity of the turtle. The condition $d > d^*$ may be satisfied only in the immediate vicinity of water where other (e.g. olfactorial) cues would make unnecessary polarization sensitivity to detect water. Aquatic insects flying at large enough heights from the ground can always detect the horizontally and maximally polarized light reflected from the water surface at or near the Brewster angle already from a remote distance from the water body, which guides them to water (see Chap. 5). Would aquatic insects crawl on the ground, it would be questionable, as in the case of freshwater turtles, whether they could detect water by reflection polarization at all.

Experiments with freshwater turtles of the genera *Terrapene* and *Chrysemys* have demonstrated the use of sun compass orientation in combination with an internal clock (Emlen 1969; Yeomans 1995) and magnetic cues (Mathis and Moore 1988). Other contributing senses like olfaction, geotaxis and even wave noise cannot totally be ruled out (Graham et al. 1996), but tests with loggerhead sea turtles in which various cues were disrupted that could have been of use in the turtle's orientation response have shown that solar cues were more important than any other (Avens and Lohmann 2003). Tortoises, being terrestrial, have also been shown to display some forms of orientation and use olfactory as well as visual cues based on landmarks and topography. Polarization sensitivity, however, has not been demonstrated convincingly in any tortoise.

Since scattered light is almost always more polarized under water than above (Sabbah et al. 2005), polarization sensitivity would not only be useful for a turtle above water to detect the surface of a water body, but perhaps even more so for submerged individuals, feeding and moving around underwater. The extent to which light is polarized under water depends on both depth and suspended particles (see Chapter 15 of this book), and since marine turtles, being air-breathing vertebrates, have to reach the surface at regular intervals, they would be able to access both aerial and aquatic polarization patterns. The linkage between polarization sensitivity, magnetoreception and ultraviolet vision has come under scrutiny by Mäthger et al. (2011), who used loggerhead sea turtle hatchlings (*Caretta caretta*) to test whether they had the ability to orient by using linearly polarized light. In a carefully conducted series of experiments, their turtles did not show any evidence that allowed the conclusion that they perceive polarized light let alone use it for orientation purposes. This result confirms an earlier conclusion reached by Ehrenfeld and Carr (1967), but is at odds with others. However, as Mäthger et al. (2011) point out, ontogenetic changes are possible and perhaps polarization sensitivity becomes apparent only after the animals have matured.

11.3 Polarization Sensitivity in Crocodiles, Lizards and Snakes

Crocodiles like turtles spend most of their activities in and under water, but need to come ashore for reproduction and basking. Homing behaviour and true navigational skills have been demonstrated in several crocodilian species (Rodda 1984, 1985; Ouboter and Nanhoe 1988; Pough et al. 2002), but the cues they use and the mechanisms involved have yet to be determined.

The situation for certain species of snakes and lizards is different. Although there is no evidence that nocturnally active snakes utilize lunar or stellar cues for orientation (Chelazzi 1992), or that snakes moving from summer feeding locations to hibernation sites in autumn use polarization cues (Russell et al. 2005), garter snakes (*Thamnophis sirtalis*) have at least been shown to make use of celestial cues

(Lawson and Secoy 1991) and are known to possess selective sensitivity to light in the near ultraviolet region (Sillman et al. 1997). Since garter snakes are aquatic predators and possibly use their UV sensitivity to improve contrasts between prey and environment, they would be a good candidate to examine polarization sensitivity in. Other good candidates for polarization sensitivity in snakes would be sea serpents, especially those of the family Laticaudinae, which in contrast to the pelamid sea snakes are not viviparous but reproduce on tropical beaches and, moreover, may exhibit special courtship coloration (Mehrtens 1987). Yet, once again, the cues they use for orientation are still unknown and for the time being remain speculative.

In lizards migratory behaviour is a rare phenomenon and has been observed, for example, in *Sceloporus jarrovi*, for which Ellis-Quinn and Simon (1991) could show that the time-compensated celestial compass responsible for the behaviour was disrupted when the parietal eye was occluded. Convincing evidence for polarization sensitivity is available for only the three lizard species *Uma notata*, *Tiliqua rugosa* and *Podarcis sicula* (Horváth and Varjú 2004, pp. 324–327). Individuals of *Uma notata*, known as the Fringe-toed Lizard, were trained by Adler and Phillips (1985) to orient in a predictable direction under natural skylight in elongated outdoor enclosures. Experimental phase-shifting by −6 and +6 h caused the expected 90° clockwise and counter-clockwise shifts, under the assumption that a time-compensated celestial compass was involved. In indoor tests under a totally linearly polarized light source, a bimodal E-vector-dependent (i.e. dependent on the direction of polarization) orientation response was observed. Care was taken that possible room-specific cues like brightness patterns associated with differential reflection of polarized light from the arena walls or geomagnetic signals were absent and the results therefore show that the lizard can use skylight polarization in a way that compensates for the regular daily rotation of the celestial E-vector pattern.

The usefulness of detection of sky polarization in this species of burrowing lizard is likely to be related to the habitat it occurs in. As a desert creature in sand-blown terrain with few landmarks, it can become easy prey to terrestrial and aerial predators. It is therefore of paramount importance for the lizard not only to be vigilant, but to be able to flee in as straight a line as possible to its burrow if attacked. For such escape movements the almost constantly available and reliable solar direction and celestial E-vector pattern would be of considerable help, so that Horváth and Varjú (2004, pp. 324–327) likened this lizard to some desert ants and called it “the vertebrate analogue of the desert ant *Cataglyphis*”.

Another lizard from semi-arid areas in which polarization sensitivity has been demonstrated is the Australian Sleepy Lizard *Tiliqua rugosa*. Training adult individuals to move in a particular direction under natural skylight in outdoor arenas, Freake (1999) recorded symmetrical bimodal orientation along the trained directions when the animals were tested under clear skies at late afternoon. To confirm that the lizards really oriented according to the celestial polarization pattern and were not using sky coloration or light intensity or geomagnetic cues, animals were trained indoors under totally linearly polarized light and when tested oriented

bimodally along the trained direction. Room-specific cues had been eliminated and the results showed that this lizard could use the E-vector direction of skylight as a compass. In field tests with lizards displaced from their homes by up to 800 m, individuals that had their field of vision restricted to just the sky and no other landmarks; still their homeward orientation was as good as that of lizards displaced with no such visual restriction. However, if the parietal eye of the pineal complex was covered, orientation following displacement was random. This observation showed the importance of the parietal eye in the response and provided support for the suggestion first expressed by Adler and Phillips (1985) that in E-vector orientating lizards the cues were received by the parietal eye.

The third species for which not only polarization sensitivity has been shown, but furthermore that the parietal eye was involved in the behavioural reaction, is the ruin lizard *Podarcis sicula*. Beltrani et al. (2010, 2012), following up work by Foa et al. (2009) on the same species and on the role of the parietal eye in sun compass orientation, were able to prove through tests conducted in a water maze under red, green, cyan and blue linearly polarized lights that "perception of linear polarization in the blue is necessary and sufficient for a proper functioning of the sky polarization compass of ruin lizards" (Beltrani et al. 2012). Since painting over the parietal eyes with opaque black completely disoriented the lizards despite the presence of intact lateral eyes, Beltrani et al. (2010) concluded that the pineal complex' parietal eye must play a central role in mediating the orientation response to polarized light. That this result does not come as a total surprise is evident from several earlier suggestions (e.g. Ellis-Quinn and Simon 1991; Zug et al. 2001) that had implicated the pineal complex, albeit without definitive proof.

Apart from the purpose of orientation and navigation, the perception of linear polarization could have other uses and especially in aquatic species could improve contrast visibility of prey (Sabbah et al. 2005). It could also be involved in separating overlapping shadows (Lin and Yemelyanov 2006) and in courtship displays in species that exhibit visual signalling as, for example, in tropical anolis lizards or have individuals that differ in coloration (Vercken et al. 2008) or are able to change colour as in chameleons. Males of the European green lizard (*Lacerta viridis*) develop a bluish nuptial throat coloration (Fig. 11.1), the UV component of which females of the species find attractive (Bajer et al. 2011). However, until now no polarization photographs or imaging polarimetry of any lizard appear to have been taken.

11.4 Photoreception and Photoreceptors in Reptiles

Apart from dermal photoreceptors involved in the basking behaviour of the lizard *Podarcis muralis* (Tosini and Avery 1996), photoreceptive cells in reptiles are known from the lateral eyes and the parietal eye of the pineal complex. More than 70 years ago, Walls (1942) could show that the basic organization of the lateral eye in reptiles varied little between the different orders. Ultrastructural studies on

the cone-dominated retina of the evolutionary relict and phylogenetically ancient but extant tuatara (*Sphenodon punctatus*) by Meyer-Rochow et al. (2005) have shown that its photoreceptors are morphologically virtually identical to those of other and more modern reptiles (Kolb and Jonas 1987; Ammermüller and Kolb 1996; Sillman et al. 1997). A similar high degree of structural conservancy has also been noted for the reptilian vomeronasal organ by Hillenius and Rehorek (2005). That tuatara are unable to locate live mealworms by their odour or crawling sounds (Meyer-Rochow 1989), but require a light intensity of at least 0.006 lx, was shown by Meyer-Rochow and The (1991). Tuatara, however, do return to their underground burrows irrespective of whether they had been away from their burrow at night or during the day and they possess the perhaps most developed parietal eye of all reptiles (Ung and Molteno 2004). This should make them a prime candidate to investigate polarization sensitivity and magnetoreception.

Microspectrophotometrically determined characteristics of the visual cells in reptiles also show little variation between the different species except for UV-sensitive cells. For instance, in the diurnal gecko *Gonatodes albogularis,* microspectrophotometric analysis revealed at least three kinds of visual pigments peaking around 542 nm in the green, 475 nm in the blue-green and 362 nm in the UV (Ellingson et al. 1995). Although UV-sensitive visual pigments were not identified from alligator eyes (Sillman et al. 1991), they were not ruled out in ruin lizards by Beltrani et al. (2012) and they were clearly identified in the eyes of three species of gecko by Loew et al. (1996), in the retina of the turtle *Trachemys dorbignii* by Ventura et al. (1999) and in the eye of the garter snake *Thamnophis sirtalis* by Sillman et al. (1997). Intracellular recordings from seven morphologically distinct photoreceptive cells in the eye of the Chinese pond turtle *Geoclemys reevesii* by Ohtsuka (1985), however, did not reveal any UV-sensitive cells, but sensitivity to the red, i.e. long wavelength end of the visual spectrum, which was in agreement with earlier ERG recordings from the eye of the turtle *Chrysemys picta picta* by Sokol and Muntz (1966).

Electroretinogram recordings from the parietal eye of the Desert Night Lizard *Xantusia vigilis* by Solessio and Engbretson (1999) demonstrated two sensitivity peaks, one in the green and one in the blue. These observations, although stemming from a different species, would add support to the finding by Beltrani et al. (2012) on the ruin lizard *Podarcis sicula*, that only the linear polarization of the blue skylight was involved in the parietal eye's perception of the E-vector. To what extent these results are applicable to the other species of lizards and reptiles, in which polarization sensitivity has been demonstrated or has been suspected to exist, remains to be seen.

11.5 The Mechanism Underlying Polarization Sensitivity in Reptiles

Mechanisms unique to reptiles that possess polarization sensitivity have not been suggested by anyone. In fact, compared with amphibians, polarization sensitivity in reptiles has received much less attention and therefore it is not surprising that no research on E-vector detecting mechanisms in this group of vertebrates seems to have been carried out. The possibility that vision and magnetoreception could be linked exists for reptiles as much as it does for amphibians (cf., Meyer-Rochow 2014: Chap. 10). Another similarity between the two classes of vertebrates is that the photoreceptors of the pineal complex rather than those of the lateral eyes seem involved. But while in amphibians no relationship to a particular spectral colour was demonstrated, in the lizard *Podarcis sicula* orientation was shown to require only linearly polarized blue light (and an intact parietal eye of the pineal complex). The possible E-vector detecting mechanisms, which are discussed by Meyer-Rochow (2014, Chap. 10) in connection with amphibians, are not expected to differ from those that might operate in reptiles.

Acknowledgements I wish to thank Prof. Hong Yang Yan (Taiwan National Academy of Science) for valuable hints on relevant literature and Jacobs University Bremen for the support I received while on sabbatical. I am grateful to Dr. Peter Stoeckl (Vienna, Austria) for having made available the photograph in Fig. 11.1, and I thank Professor G. Horváth for having invited me to contribute to this book.

References

Adler K, Phillips JB (1985) Orientation in a desert lizard (*Uma notata*): time-compensated compass movement and polarotaxis. J Comp Physiol A 156:547–552

Ammermüller J, Kolb H (1996) Functional architecture of the turtle retina. Prog Retin Eye Res 15:393–433

Avens L, Lohmann KJ (2003) Use of multiple orientation cues by juvenile loggerhead sea turtles (*Caretta caretta*). J Exp Biol 206:4317–4325

Bajer K, Molnár O, Török J, Herczeg G (2011) Ultraviolet nuptial colour determines fight success in male European green lizards (*Lacerta viridis*). Biol Lett 7:866–868

Beltrani G, Bertolucci C, Parretta A, Petrucci F, Foa A (2010) A sky polarization compass in lizards: the central role of the parietal eye. J Exp Biol 213:2048–2054

Beltrani G, Parretta A, Petrucci F, Buttini P, Bertolucci C, Foa A (2012) The lizard celestial compass detects linearly polarized light in the blue. J Exp Biol 215:3200–3206

Chelazzi G (1992) Reptiles. In: Papi F (ed) Animal homing. Chapman and Hall, London, pp 235–255

Ehrenfeld DW (1968) The role of vision in the sea-finding orientation of the green turtle (*Chelonia mydas*). 2. Orientation mechanism and range of spectral sensitivity. Anim Behav 16:281–287

Ehrenfeld DW, Carr A (1967) The role of vision in the sea-finding orientation of the green turtle (*Chelonia mydas*). Anim Behav 15:25–36

Ellingson JM, Fleishman LJ, Loew ER (1995) Visual pigments and spectral sensitivity of the diurnal gecko *Gonatodes albogularis*. J Comp Physiol A 177:559–567

Ellis-Quinn BA, Simon CA (1991) Lizard homing behaviour: the role of the parietal eye during displacement and radio-tracking, and time-compensated celestial orientation in the lizard *Sceloporus jarrovi*. Behav Ecol Sociobiol 28:397–407
Emlen ST (1969) Homing ability and orientation in the painted turtle, *Chrysemys picta marginata*. Behaviour 33:58–76
Foa A, Basaglia F, Beltrani G, Carnacina M, Moretto E, Bertolucci C (2009) Orientation of lizards in a Morris water-maze: roles of the sun compass and the parietal eye. J Exp Biol 212: 2918–2994
Freake MJ (1999) Homing behaviour in the sleepy lizard (*Tiliqua rugosa*): the role of visual cues and the parietal eye. Behav Ecol Sociobiol 50:563–569
Graham T, Georges A, Mc Elhinney N (1996) Terrestrial orientation in the eastern long-necked turtle, *Chelodina longicollis*, from Australia. J Herpetol 30:467–477
Hillenius WJ, Rehorek SJ (2005) From the eye to the nose: ancient orbital to vomeronasal communication in tetrapods? Chem Signal Vert 10:228–241
Horváth G, Varjú D (2004) Polarized light in animal vision—polarization patterns in nature. Springer, Heidelberg
Kolb H, Jonas J (1987) The distinction by light and electron microscopy of two types of cone containing oil droplets in the retina of the turtle. Vis Res 27:1445–1458
Lawson PA, Secoy DM (1991) The use of solar cues as migratory orientation guides by the plains garter snake, *Thamnophis radix*. Can J Zool 69:2700–2702
Lin S, Yemelyanov KM (2006) Separation and contrast enhancement of overlapping cast shadow components using polarization. Opt Express 14:7099–7107
Loew ER, Govardovskii VI, Röhlich P, Szel A (1996) Microspectrophotometric and immunocytochemical identification of ultraviolet photoreceptors in geckos. Vis Neurosci 13:247–256
Lohmann KJ, Witherington BE, Lohmann CMF, Salmon M (1996) Orientation, navigation, and natal beach homing in sea turtles. In: Lutz PL, Musick JA (eds) The biology of sea turtles. CRC Press, Boca Raton, pp 107–136
Mäthger LM, Lohmann KJ, Limpus CJ, Fritsches KA (2011) An unsuccessful attempt to elicit orientation responses to linearly polarized light in hatchling loggerhead sea turtles (*Caretta caretta*). Philos Trans R Soc Lond B 366:757–762
Mathis A, Moore FR (1988) Geomagnetism and the homeward orientation of the box turtle, *Terrapene carolina*. Ethology 78:265–274
Mehrtens JM (1987) Living snakes of the world in color. Sterling, New York
Meyer-Rochow VB (1989) Behaviour of young tuatara (*Sphenodon punctatus*) in total darkness. Tuatara 30:36–38
Meyer-Rochow VB (2014) Polarization sensitivity in amphibians. In: Horváth G (ed) Polarized light and polarization vision in animal sciences. Springer Series in Vision Research (eds: S. Collin, J. Marshall). Springer, Heidelberg, Chapter 10
Meyer-Rochow VB, The KL (1991) Visual predation by tuatara (*Sphenodon punctatus*) on the beach beetle (*Chaerodes trachyscelides*) as a selective force in the production of distinct colour morphs. Tuatara 31:1–8
Meyer-Rochow VB, Wohlfahrt S, Ahnelt PK (2005) Photoreceptor cell types in the retina of the tuatara (*Sphenodon punctatus*) have cone characteristics. Micron 36:423–428
Ohtsuka T (1985) Spectral sensitivities of seven morphological types of photoreceptors in the retina of the turtle, *Geoclemys reevesii*. J Comp Neurol 237:145–154
Ouboter PE, Nanhoe LM (1988) Habitat selection and migration of Caiman crocodiles in a swamp and swamp-forest habitat in northern Suriname. J Herpetol 22:283–294
Pough HF, Janis CM, Heiser JB (2002) Vertebrate life. Prentice Hall, New Jersey
Rodda GH (1984) The orientation and navigation of juvenile alligators: evidence of magnetic sensitivity. J Comp Physiol A 154:649–658
Rodda GH (1985) Navigation in juvenile alligators. Z Tierpsychol 68:65–77
Russell AP, Bauer AM, Johnson MK (2005) Migration in amphibians and reptiles. In: Bewa AMT (ed) Migration of organisms: climate, geography, ecology. Springer, Heidelberg, pp 151–203

Sabbah S, Lerner A, Erlick C, Shashar N (2005) Underwater polarization vision—a physical examination. Recent Res Dev Exp Theor Biol 1:123–176

Sillman AJ, Ronan SJ, Loew ER (1991) Histology and microspectrophotometry of the photoreceptors of a crocodilian, *Alligator mississippiensis*. Proc R Soc Lond B 243:93–98

Sillman AJ, Govardovskii VI, Röhlich P, Southard JA, Loew ER (1997) The photoreceptors and visual pigments of the garter snake (*Thamnophis sirtalis*): a microspectrophotometric, scanning electron microscopic and immunocytochemical study. J Comp Physiol A 181:89–101

Sokol S, Muntz WRA (1966) The spectral sensitivity of the turtle *Chrysemys picta picta*. Vis Res 6:285–292

Solessio E, Engbretson GA (1999) Electroretinogram of the parietal eye of lizards: photoreceptor, glial, and lens cell contributions. Vis Neurosci 16:895–907

Southwood A, Avens L (2010) Physiological, behavioral, and ecological aspects of migration in reptiles. J Comp Physiol A 180:1–23

Tosini G, Avery RA (1996) Dermal photoreceptors regulate basking behavior in the lizard *Podarcis muralis*. Physiol Behav 59:195–198

Ung CY, Molteno AC (2004) An enigmatic eye: the histology of the tuatara pineal complex. Clin Exp Ophthalmol 32:614–618

Ventura DF, DeSouza JN, Devoe RD, Zana Y (1999) UV responses in the retina of the turtle. Vis Neurosci 16:191–204

Vercken E, Sinervo B, Clobert J (2008) Colour variation in female common lizards: why we should speak of morphs, a reply to Cote et al. J Evol Biol 21:1160–1164

Walls GL (1942) The vertebrate eye and its adaptive radiation. Crembrook, Bloomfield Hills

Wiltschko W, Wiltschko R (1995) Magnetic orientation in animals. Springer, Heidelberg

Yeomans RS (1995) Water-finding in adult turtles: random search or oriented behaviour. Anim Behav 49:977–987

Zug JR, Vitt LJ, Caldwell JP (2001) Herpetology. Academic, San Diego, CA

Chapter 12
The Ecology of Polarisation Vision in Birds

Susanne Åkesson

Abstract Birds have evolved a mobile lifestyle in which vision is of major importance when controlling movements, avoiding predators, finding food and selecting mates. Birds have extraordinary colour vision and have been suggested to perceive the linear polarisation of light. Behavioural experiments support this idea, but still the exact physiological mechanism involved is not known. The twilight period, when the sun is near the horizon at sunrise and sunset, is of crucial importance for migrating birds. At this time millions of songbirds initiate migration when the degree of skylight polarisation is the highest and all compass cues are visible in a short range of time. The biological compasses are based on information from the stars, the sun and the related pattern of skylight polarisation, as well as the geomagnetic field, and may be recalibrated relative to each other. The celestial polarisation pattern near the horizon has been shown to be used in the recalibration of the magnetic compass, but conflicting results have been obtained in experiments with different bird species. For the future we should understand the physiological mechanisms of avian polarisation vision and investigate the interrelationship and calibrations between the different compasses, including the one based on the pattern of skylight polarisation. A conditioning paradigm may be fruitful, but the risk of introducing optical artefacts needs to be minimised in behavioural experiments, as well as in cage experiments with migratory birds.

S. Åkesson (✉)
Department of Biology, Centre for Animal Movement Research, Lund University, Ecology Building, 223 62 Lund, Sweden
e-mail: susanne.akesson@biol.lu.se

G. Horváth (ed.), *Polarized Light and Polarization Vision in Animal Sciences*, Springer Series in Vision Research 2, DOI 10.1007/978-3-642-54718-8_12,

12.1 Introduction

Birds are highly aerial animals and in their everyday life they are largely dependent on their vision. Some birds may use their vision while diving several hundreds of metres in cold oceanic waters, while others are climbing to 3,000 m altitude and navigate across continents by relying on celestial and magnetic compasses. Others inhabit dense tropical forests where they display to find a mate. On the outermost branches in tall trees, tiny warblers feed on insects and spiders, optimising their foraging efforts and locating their prey by vision. Some birds are only active at night or hide in caves. The width of avian visual adaptations to cope with these varying ecological situations is large (Goldsmith 1991). Bird eyes show an allometric relationship with brain and body size (Burton 2008). At the same time they constitute a major part of the head, and correspondingly, the optical lobes are a substantial part of the brain (Martin 1985; de Brooke et al. 1999). Birds have especially high temporal resolution measured as flicker fusion frequency (FFF) extending up to 100 Hz in domestic fowl (Lisney et al. 2011), and varying with light levels (average FFF: 20–87 Hz), underlining the visual adaptation to a highly mobile life, where fast aerial movements through forested habitats and detection of predators have been important selective forces involved in shaping the form and function of the birds' visual system.

Birds have been shown to possess extraordinary colour vision (Bowmaker 1980; Goldsmith 1991; Finger and Burkhardt 1994), involving at least four classes of visual cone pigments with specific maximum sensitivity to different parts of the spectrum and an additional long-wavelength-sensitive double cone (Bowmaker et al. 1997; Bowmaker 1991; Hart et al. 1998). Associated with the single and double cones in birds, a number of oil droplets have been described. Absorbing in different parts of the 300–700 nm range, they function as cut-off filters (e.g. Bowmaker 1977; Lythgoe 1979; Partridge 1989; Hart et al. 1998, 1999, 2000; Beason and Loew 2008). The colourless oil droplets, on the other hand, seem to have a light-gathering function (Baylor and Fettiplace 1975). It has been found that a certain type of oil droplets is associated with one type of cone pigments (Bowmaker 1991, 2008), and most of them contain carotenoid pigments (Wald and Zussman 1937; Goldsmith et al. 1984). The dimensions of oil droplets for pigeons are typically 2–4 μm (Muntz 1972). The combination of cones and oil droplets provides an arsenal of different types of optical sensors which can be important in colour and hue discrimination as well as possibly in polarisation vision (Fig. 12.1). The colour vision in birds is used in a number of tasks including mate choice (e.g. Andersson and Amundsen 1997; Hunt et al. 1998), foraging (e.g. Church et al. 1998) and orientation (Able 1982, 1989), where detection of the pattern of skylight polarisation and linearly polarised light may be one of these tasks. Still we need to understand the mechanism behind polarisation vision in birds.

The visible spectrum typically extends into the ultraviolet (UV) range (300–400 nm) in birds (Fig. 12.2), while this UV spectral part is invisible to humans (Burkhardt 1982; Bennett and Cuthill 1994). Within this range of vision, maximum

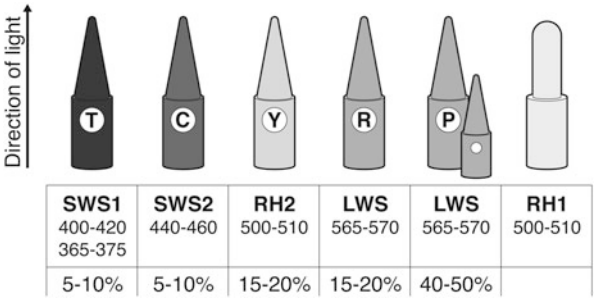

Fig. 12.1 Schematic diagram of photoreceptors found in the avian retina of diurnal songbirds. Below the schematic photoreceptors, the λ_{max} of the visual pigments of the four spectral classes of single cone (SWS1, SWS2, RH2, LWS), double cones (LWS) and rods (RH1) is shown. In the UV/UVS cone class (SWS1) the maximal sensitivity is either in the UV close to 370 nm or in the violet between 400 and 420 nm. Both members of the double cones contain the same LWS (long-wavelength-sensitive) pigment as the R-type single cones. The oil droplets associated with the photoreceptors are pale (principal: P) in double cones and Red (R), Yellow (Y), Clear (C) and Transparent (T) in single cones. Given below each cone and double cone are the approximate relative percentages of the different cone types in the bird's retina [from Bowmaker (2008)]. Visualised are "red" LWS, "green" RH2, "blue" SWS2 (short-wavelength-sensitive) and "violet or ultraviolet" SWS1 single cones. Double cones contain a red-sensitive LWS cone pigment in both members, with the principal member containing a large pale yellow, P-type droplet that cuts off at about 460 nm and the accessory member having low concentration of carotenoids that may or may not be contained in a small droplet [modified after Bowmaker (2008)]

sensitivity has been found at 470 nm for 15 bird species (Chen et al. 1984; Chen and Goldsmith 1986) and at 480 nm for the red-billed leiothrix (*Leiothrix lutea*; Burkhardt and Maier 1989; Maier 1992; Maier and Bowmaker 1993). In the UV range (<400 nm), birds have five times higher sensitivity compared to the human visual range (400–700 nm), and they can discriminate between nearby wavelengths differing by only 7–16 nm (Emmerton and Delius 1980). It is, thus, most likely that here we will find some of the most specialised adaptations and important functions within the most sensitive range of the avian visual system. However, so for experimentation studying, for example, the polarisation sensitivity in birds has mainly been concentrated outside this range of the visible spectrum (400–700 nm), since the polarisers used in the behavioural experiments absorb strongly or completely in the UV (<400 nm; Horváth and Varjú 2004, pp. 328–354).

Birds have been indirectly shown to be able to perceive linear polarisation in behavioural experiments studying avian orientation (Able and Able 1990, 1993; Muheim et al. 2006a), but the photoreceptors and specific mechanism(s) involved in this process in the bird eyes are still not described (Horváth and Varjú 2004, pp. 328–354). Behavioural evidence has further provided conflicting results, which, in part, can be attributed to erroneous experimental design and lack of complete control of the manipulated cues (Horváth and Varjú 2004, pp. 328–354, and references therein). Differences may also be explained by species-specific adaptations in the avian visual system and differential use of cues for orientation between

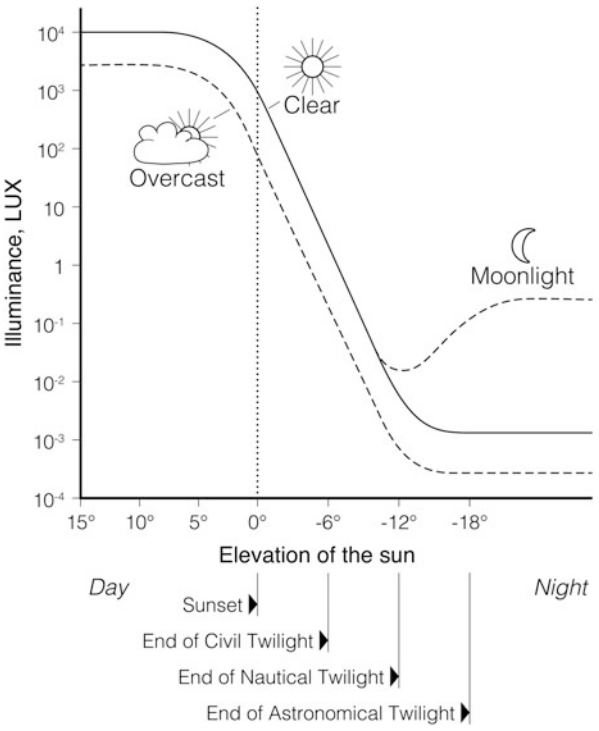

Fig. 12.2 Light intensity during the twilight period (measured as illuminance in lux on a horizontal surface) at different elevations of the sun. Given are sunset (highlighted by a *vertical dotted line*) and ends of civil, nautical and astronomical twilight periods [from Åkesson et al. (1998); modified after Dusenbery (1992), see also Rozenberg (1966)]

bird species. In this chapter I intend to review the most recent findings of polarisation vision and associated behaviours in birds, which have mainly been published after the in-depth review by Horváth and Varjú (2004, pp. 328–354), and put the avian polarisation vision in an ecological perspective.

12.2 Polarisation Vision in Birds

A proposed mechanism for avian polarisation vision has been suggested to involve a double cone (Young and Martin 1984; Cameron and Pugh 1991) with an associated transparent oil droplet, the optical functional characteristics of which have been extensively outlined by Horváth and Varjú (2004, pp. 328–354). In this mechanism the oil droplet significantly enhances the photon capture rate in the outer segment of the photoreceptor. The lack of melanin as a screening pigment in the outer segments of the double cones further facilitates that light may pass from one cell to the one nearby. The mechanism would allow light to scatter when passing the oil droplet located in the principal cone and then to pass the outer segment of the associated cone sideways. The polarisation characteristics of light passing the oil droplet will retain those of the incoming light, and since the outer

segment of vertebrate photoreceptors is dichroic when illuminated from the side (Hárosi and MacNichol 1974), the accessory cone signals would have the inherited characteristics to vary with the E-vector orientation of scattered light, oriented parallel or perpendicular to the disc membranes as was pointed out by Horváth and Varjú (2004, pp. 328–354). If this promising mechanism is indeed used in the avian visual system for detecting light polarisation, however, still remains to be shown.

12.3 Celestial Orientation and Migration

Migratory birds have adapted their phenotype to cope with long migration flights, fuelling and orientation (Åkesson and Hedenström 2007). Three biological compasses have been described for birds, based on information from (1) the geomagnetic field (Wiltschko and Wiltschko 1972, 1995), (2) the stars (Emlen 1967a, b, 1970, 1975) and (3) the sun and the related pattern of skylight polarisation (Wiltschko 1980, 1981; Able 1982, 1989; Schmidt-Koenig 1990). The linearly polarised skylight is expected to be used for compass orientation as the E-vector of first-order-scattered skylight is always perpendicular to the scattering plane determined by the sun, the observer and the celestial point observed (Chaps. 17 and 18). The pattern of skylight polarisation is, thus in theory, providing birds with an additional cue to pinpoint the position of the sun when the sun itself may be occluded by clouds or landmarks or is below the horizon (Horváth and Varjú 2004). In insects and spiders the polarisation pattern of the sky may provide the most important compass used during navigation (von Frisch 1949; Wehner 1989), and polarised skylight may be used also to guide certain dung beetles during dusk orientation (Chap. 2).

The avian magnetic compass is based on the angle of inclination and not on the polarity of the Earth's magnetic field (Wiltschko and Wiltschko 1972). The magnetic field is most likely perceived by specialised photoreceptors in the bird's eyes, involving cryptochrome molecules and a radical-pair process (for review, see Mouritsen and Hore 2012). In a neuroanatomical study, Niessner et al. (2011) discovered bands of cryptochrome 1a molecules along the membrane discs of the outer segments of UV/violet cones in the retinas of the domestic chicken (*Gallus gallus*) and the European robin (*Erithacus rubecula*), a migratory songbird. The discovery is suggestive and supports the possible involvement of these visual receptor cells in avian magnetoreception. Furthermore, the sensitivity of the magnetic compass in birds is tuned to the ambient magnetic field (25,000–68,000 nT) expected to be met during migration, but may be modified also outside the range of intensities occurring at different regions of the Earth (15,000 and 150,000 nT, respectively; for review see Wiltschko and Wiltschko 2010). It will be interesting to find out if the mechanism for polarisation vision in birds, possibly involving the

double cones (Young and Martin 1984), is somehow integrated in the retina with the magneto-sensitive photoreceptors.

A population-specific orientation relative to the geomagnetic field has been shown to be inherited in songbirds, in which experience from a combination of the geomagnetic field and the rotational centre of the night sky during development is crucial (Weindler et al. 1996). In addition, the necessary 180° shift in relation to the angle of inclination for two bird species, the garden warbler, *Sylvia borin*, and the bobolink, *Dolichonyx oryzivorus*, crossing the magnetic equator on migration has been demonstrated (Beason 1992; Wiltschko and Wiltschko 1992). The stellar compass is also inherited, but for functionality a rotating stellar sky needs to be experienced during development (Emlen 1970, 1975). The stellar compass provides birds with a direction relative to the geographic North, which is given by the rotation centre and may be memorised based on stellar patterns. This compass does not seem to be connected to an internal time sense in birds as the sun compass, which completely depends on this internal time-keeping mechanism in order to work (Schmidt-Koenig 1990). The sun compass in homing pigeons (*Columba livia*) further seems to be finely tuned to local azimuthal movement of the sun during the day (Wiltschko et al. 2000).

During long-distance flights the time-compensated sun compass has been suggested to be the major compass mechanism at work (Alerstam et al. 2001). At these long flights across longitudes, the bird's internal time sense is thought not to be adjusted to local time during flights, but remains at the local time from the site where the bird departed (Alerstam et al. 2001). When applying such a mechanism, the flight trajectories will lead the birds along great circle routes, i.e. shortest-distance routes between two points on the globe. This hypothesis has rendered some support from the long flights by arctic waders flying along approximate great circle routes in autumn from the high Arctic to wintering sites in the southern hemisphere (Alerstam et al. 2001). However, not all migrating birds are following such routes between start and end positions during extensive migration flights (e.g. Gudmundsson et al. 1995; Åkesson et al. 2012), and it is still open how these deviating routes may be explained and what compass mechanism(s) may be used during these flights.

The majority of songbirds migrate at night, and these nocturnal migrations involve impressive numbers of birds crossing continents and seas. For instance, the autumn avian migration between Europe and Africa has been estimated to involve more than 2.6 billion birds (Haan et al. 2009). For successful migration, the birds rely on the functionality of their biological compasses in flight, but they need also to be able to pinpoint their species-specific and endogenously encoded geographical goal by additional cues. Nocturnal songbird migrants have been shown to predominantly initiate their nocturnal flights shortly after sunset (Fig. 12.3; e.g. Åkesson et al. 1996, 2001), but it has also been shown that the decision to start migration at night may be triggered by the visibility of a clear night sky (Åkesson et al. 1996). In addition to the visibility of celestial cues, also the wind situation will be important for departure decision (Åkesson and Hedenström 2000).

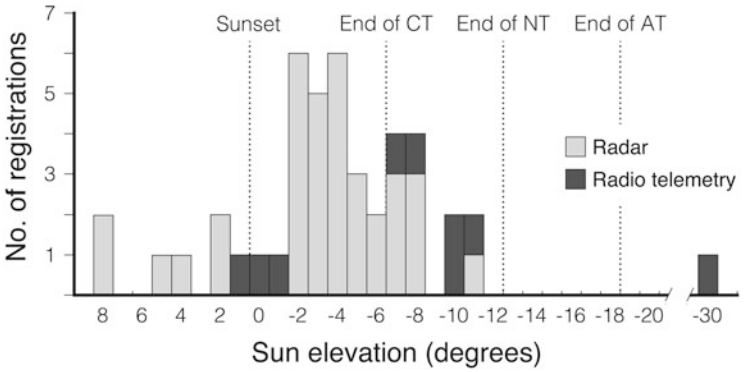

Fig. 12.3 Time of departure flights where individual songbirds initiated migration during the twilight and night period in south Sweden. Given is the number of registrations of birds departing on nocturnal migration flights in relation to sun elevation at departure. Sun elevations at Sunset, Civil (CT), Nautical (NT) and Astronomical Twilights (AT) are given by vertical dotted lines. *Light grey* refers to flocks or single birds recorded by radar and *dark grey* to radio-tracked birds [from Åkesson et al. (1998)]

For songbirds the time of transition between day and night is critical for migration departure, and at this time migratory songbirds have been shown to climb into trees and bushes and to sit quietly observing the surroundings (Palmgren 1949), probably observing the sky conditions, compass cues as well as weather situations before migration departures. Thus, the orientation information available during the twilight period is most likely of great importance for the departing songbirds (Emlen 1975; Moore 1987; Åkesson et al. 1996), and one or several of the available cues will further provide guidance during the upcoming nocturnal migration flight.

12.4 Importance of the Twilight Period for Orientation

The twilight period involves the entire complex of atmospheric optical phenomena that takes place when the sun is near the horizon (from +6° to −18°) and when the transition between daylight illumination and darkness occurs (Rozenberg 1966; Fig. 12.4). At the twilight period, the celestial cues related to the sun, i.e. azimuthal position of the sun, horizon glow and colour gradients and the pattern of skylight polarisation, are clearly visible (Rozenberg 1966; Brines and Gould 1982; Cronin et al. 2006), and in the end of the civil twilight period (when the sun reaches below −6°) the first stars become visible. Furthermore, at sun elevations near the horizon the highest (up to 80 %) degrees of polarisation of skylight occur. The twilight provides the possibility to put different orientation cues into conformity by their coordinated presence, and based on this, the departing bird may decide on the particular course to select for the upcoming nocturnal flight (Åkesson et al. 1996).

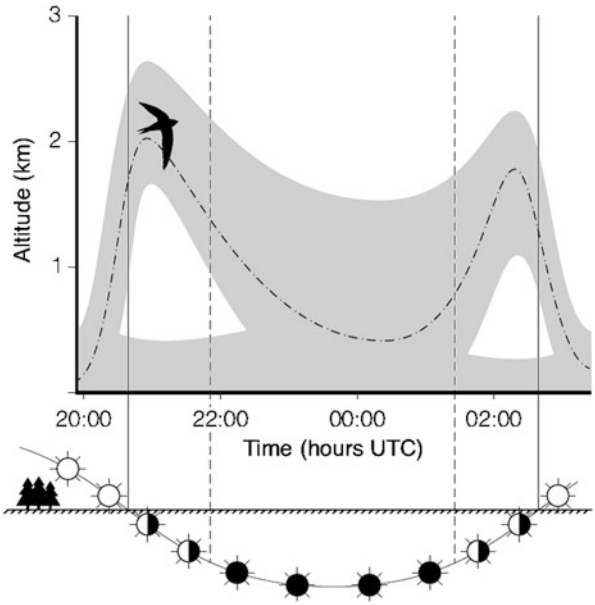

Fig. 12.4 Schematic flight altitude profile based on a reflectivity profile collected from a Doppler weather radar located at De Bilt in The Netherlands and visualised for the night of 12 June 2009, showing twilight ascents of common swifts *Apus apus*. The altitude profile in *grey* shows that the swifts are engaged in both dusk and dawn ascent flights to similarly high altitudes of 2,500 and 2,000 m at both times. The displayed time series started at sunset and ended at sunrise. *Solid vertical black lines* indicate the transition between civil twilight and nautical twilight, when the sun has reached −6° below the horizon. *Dotted vertical lines* indicate the transition between night and nautical twilight [sun elevation −12°; modified after Dokter et al. (2013)]

A similarly important period occurs at sunrise, when birds migrating predominantly at daytime initiate their migrations.

It has recently been shown (Dokter et al. 2013) that the highly aerial common swift, *Apus apus*, makes ascent flights to high altitudes at times symmetrical to the time of local sunset and sunrise, when the sun shows the same elevation relative to the horizon at both times (Fig. 12.5). These high-altitude ascent flights have been demonstrated by weather Doppler radar for common swifts spending the night on the wings during the summer months and may extend up to 2,000–2,500 m altitudes (Dokter et al. 2013). The highest altitude was reached at both sunset and sunrise at solar elevations ranging between −6° and −8° relative to the horizon, when the maximum degree of polarisation of the twilight sky is visible, horizon glow (i.e. radiance and spectral gradients) is present and stars are also visible in the sky.

The occurrence of the two symmetric twilight high-altitude flights was unexpected and could not be explained by the presence of foraging insects, because the birds were aiming for altitudes above those where insects were present at night, and also the swifts reached higher altitudes than other bird species present in the same region at night (Dokter et al. 2013). The authors therefore concluded that the flights

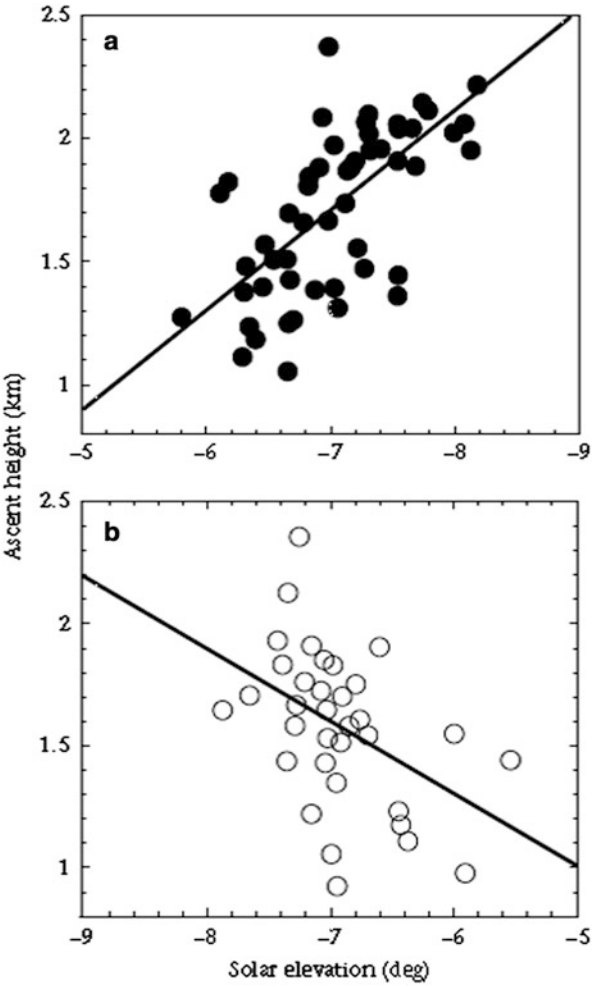

Fig. 12.5 Maximum ascent flight altitude and solar elevation at the time when the common swifts reached the maximum altitude during (**a**) dusk ascent and (**b**) dawn ascent. Data are given for days with limited cloud cover. The *solid lines* show the linear least-square regressions [from Dokter et al. (2013)]

may instead be explained by other factors. One previously suggested possibility is that the common swifts may climb to high altitudes for nocturnal roosting (Weitnauer 1952; Bruderer and Weitnauer 1972; Tarburton and Kaiser 2001). However, the symmetrical climbing flights occurring in early morning could not be explained by this, since the swifts were shortly after reaching the highest altitude initiating slow descending flights to lower altitudes where they forage in daytime. Dokter et al. (2013) suggested that the ascent flights in early morning may be related to the probing for flight and foraging conditions during upcoming daytime, and/or facilitation to detect visual information for navigation such as distant landmarks and celestial information, in which the skylight polarisation pattern may be one cue of importance. Detection of the skylight polarisation pattern at nearby sunset and sunrise times has further been proposed to be important for compass calibration (Muheim et al. 2006a).

Symmetrical spike dives to deep waters in relation to sunset and sunrise times have further been observed for southern bluefin tunas (*Thunnus maccoyii*) in the ocean, at similar times as the swifts, and one possible explanation to these deep dives has been the relatively smooth temporal variations of the geomagnetic field at this time of the day, and thus facilitation to detect orientation cues such as the geomagnetic field (Willis et al. 2009). These two observations of the symmetrically timed twilight ascent in common swifts and spike dives in southern bluefin tunas call for further attention and suggest that the behaviour might be present also in other aerial species or long-distance migrating animals in the ocean, and may possibly be explained by the reading of orientation cues present in this time period, when in particular the pattern of skylight polarisation is especially pronounced due to the highest degrees of polarisation, and the temporal variations of the geomagnetic field are relatively smooth.

12.5 Importance of Skylight Polarisation Pattern in Compass Calibration

The functional characteristics of the biological compasses used by birds have been described in some detail, and the compasses based on celestial and geomagnetic information have been shown to be present in a number of songbird species. However, the integration between compass cues is much less understood, and cue-conflict experiments have rendered varying results (Åkesson 1994; Muheim et al. 2006a). Both the celestial and magnetic compasses may be recalibrated if their directional information is set into conflict (Able and Able 1990, 1993, 1995), and it is not completely clear why one or the other of the compasses is recalibrated (Åkesson 1994; Muheim et al. 2006a). In some studies performed with birds before migration, the birds seem to give precedence to celestial information and recalibrate the magnetic compass, while in other studies performed during migration the magnetic compass is used to instead recalibrate the celestial compass (Muheim et al. 2006a). Recalibration of compasses may be adaptive in songbirds, especially at high latitudes, where the magnetic declination (i.e. angular difference between geomagnetic and geographic North) may largely vary between nearby sites (Åkesson et al. 2002). Birds inhabiting these regions have to cope with variations in declination during their migrations. Free-flying migratory songbirds studied by radio-telemetry in North America have been shown to recalibrate their magnetic compass daily based on celestial twilight cues (Cochran et al. 2004). This suggests the importance of twilight sunset cues as a reference and possible involvement of the pattern of skylight polarisation in the recalibration process.

In a study (Muheim et al. 2006b) performed with Savannah sparrows (*Passerculus sandwichensis*) in late summer and during autumn migration, the skylight polarisation pattern near the horizon at sunset and sunrise has been shown to be crucial for recalibration of the magnetic compass (Fig. 12.6). The

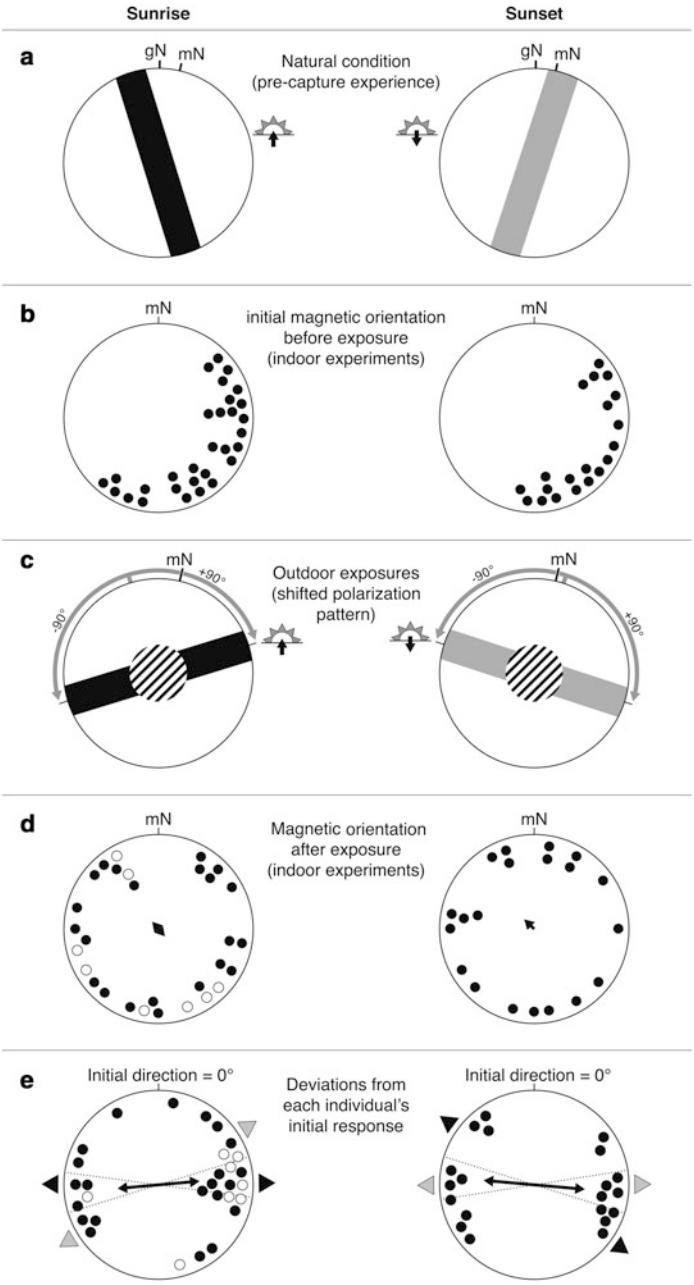

Fig. 12.6 The magnetic orientation of Savannah sparrows exposed to a polarisation pattern shifted ±90° at sunrise (*left*) and sunset (*right*) has been measured in circular cages for birds migrating in Alaska in autumn. (**a** and **c**) 360° view of sky under natural and experimental conditions (gN: geographic north, mN: magnetic north). *Black* and *grey bars* indicate mean position of the band of maximum polarisation (BMP) at sunrise and sunset, respectively; *hatched central zones* indicate which areas of sky were not visible to the birds during exposure. (**a**) Outline

experiments were performed in circular cages with young and adult *P. sandwichensis* caught at the site of experiments in south-western Alaska. The experimental birds were held indoors without access to celestial cues, within the local geomagnetic field, and with possibility to experience the natural photoperiod. The orientation cage experiments were performed indoors in the local geomagnetic field at sunset and after, but without access to visual cues. Prior to the registration of the preferred orientation, the experimental birds had experienced a cue-conflict situation for one hour at sunrise or sunset, in which the celestial polarisation pattern was shifted ±90° relative to the pattern available at respective time of the day. Some birds were exposed to a cue conflict both at sunrise and sunset, and thereafter tested in circular Emlen cages. At exposure to the cue conflict, the Savannah sparrows were given access to the surrounding sky down to the horizon.

The experimental birds that have previously expressed meaningful migratory directions towards south-east relative to the magnetic field were shown to recalibrate their magnetic course on the basis of the shifted celestial polarisation pattern (Muheim et al. 2006b). It became clear from these experiments that the Savannah sparrows had paid extra attention to the polarisation pattern near the horizon for these recalibrations, and that there were no differences in response between birds with or without previous experience from migration or tested at different times of the autumn period. Also in this part of the sky is the highest degree of polarisation under foggy and partly or completely cloudy conditions (Hegedüs et al. 2007a, b).

These cue-conflict experiments with Savannah sparrows were performed at high latitudes in the Arctic (Muheim et al. 2006b, 2007), but they have been proven difficult to repeat with other species of migratory birds and in other geographical areas (Muheim et al. 2008; Wiltschko et al. 2008; Gaggini et al. 2010; Schmaljohann et al. 2013), except in one species of songbird, the white-throated sparrow (*Zonotrichia albicollis*), studied during spring and autumn migration at a location in the transition zone between the breeding and wintering areas in North America (Muheim et al. 2009). Just like the Savannah sparrows described above,

Fig. 12.6 (continued) of the natural relationship between sunrise/sunset celestial cues and the direction to magnetic North according to the local geomagnetic field where the experiments were performed. (**b**) Mean orientation of Savannah sparrows selected for exposure to cue conflict. (**c**) Alignment of ±90°-shifted polarisation axis using filters during exposure to cue conflict. (**b** and **d**) Magnetic orientation of birds tested indoors, plotted relative to mN and the individually preferred orientation prior to cue-conflict exposure (=0°). Savannah sparrows for which the disc of the Sun was visible during exposure are depicted by *open symbols*. *Arrowheads* show mean angle or axis of orientation. The length of the vector is a measure of concentration, being inversely related to scatter and drawn relative to the radius of the circle ($r = 0 - 1$). (**d**) Bird orientation relative to the magnetic field after cue-conflict exposure. (**e**) Angular deviations from each individual's initial orientation before exposure [initial direction (**b**) of each individual set to =0°]. *Arrows* show mean axial distribution; *dashed lines* denote 95 % confidence intervals according to Batschelet (1981); *triangles outside the circles* give predicted responses for a ±90° shift in band of maximum polarisation relative to the natural sunrise (*black*) or sunset (*grey*) position [from Muheim et al. (2006b)]

the white-throated sparrows were recalibrating their magnetic compass based on the pattern of skylight polarisation at both sunrise and sunset (Muheim et al. 2009). In the latter experiments, both the magnetic field and the polarised skylight pattern were manipulated to set the two cues into conflict, suggesting that the polarisation filters did not cause an unnatural situation to the birds (Muheim et al. 2009), which has previously been proposed. In other studies, however, the experimental birds that were given similar access to horizontal skylight cues have not been shown to recalibrate their magnetic compass on the basis of the celestial information from the pattern of skylight polarisation (Wiltschko et al. 2008; Gaggini et al. 2010; Schmaljohann et al. 2013). All of these non-responding cage experiments have been performed with migratory songbirds in Australia (Wiltschko et al. 2008) and Europe (Gaggini et al. 2010; Schmaljohann et al. 2013; Åkesson et al. unpublished), and one possible explanation for the discrepancies in the results may be local adaptation in migratory birds to the geometry of the geomagnetic and celestial compass information present in different geographical areas and to which area specific birds have evolved to migrate. However, this possibility needs to be investigated further.

12.6 Behavioural Evidence for Polarisation Vision in Birds

Conditioning experiments have been used to study the perception of polarisation in birds, and the first experiments were performed with homing pigeons, *C. livia* (Kreithen and Keeton 1974; Delius et al. 1976). Montgomery and Heinemann (1952) had previously investigated the response in homing pigeons to linearly polarised light by conditioning to a two-choice situation with a polarisation pattern orthogonally rotated relative to each other, and found no response to this manipulation, but a response to difference in brightness. Later, it has turned out to be very difficult to train birds to respond to artificial polarised stimuli (Coemans et al. 1990, 1994; Vos et al. 1995; Greenwood et al. 2003), and it has been pointed out that the difficulty may be related to optical artefacts in the experimental set-up and the difficulty to create an experimental situation where birds may be responding naturally to artificial manipulations (Horváth and Varjú 2004; Muheim 2011). The negative results of conditioning experiments designed to study polarisation sensitivity in birds have extensively been covered by Horváth and Varjú (2004, pp. 328–354).

12.7 Outlook

Despite the fact that birds are highly visual animals, we still lack crucial understanding of how their visual system is adapted to perceive light polarisation. A promising physiological mechanism in the bird's eye involving a double cone has

been proposed as the key mechanism in polarisation detection, but it still needs to be investigated if this is the case. It has further been hard to condition birds to polarisation detection tasks, and it might at least partly be explained by the difficulty to create a relevant artificial experimental situation where this can be tested by birds held in captivity. The twilight period involving the complete transition between day- and night-time, when the highest degree of polarisation is available in the sky, is central for migratory birds as it plays a key role in timing of migratory departures and selection of migration courses. Birds have access to several compasses and two celestial compasses based on information from the sun (and the related pattern of sky polarisation), and the stars are combined with a magnetic compass. The three compass mechanisms guide birds during flights across continents and seas, but still we lack understanding on which compass is used by migrants during the flights. Contradictory experiments with songbirds suggest a different compass hierarchy between bird species, and therefore this area needs further experimentation to fully understand the pattern observed. Because of several still unanswered questions, we should look forward to exciting discoveries on avian polarisation vision during the coming years.

References

Able KP (1982) Skylight polarization patterns at dusk influence migratory orientation in birds. Nature 299:550–551

Able KP (1989) Skylight polarization patterns and the orientation of migratory birds. J Exp Biol 141:241–256

Able KP, Able MA (1990) Ontogeny of migratory orientation in the Savannah sparrow, *Passerculus sandwichensis*: calibration of the magnetic compass. Anim Behav 39:905–913

Able KP, Able MA (1993) Daytime calibration of magnetic orientation in a migratory bird requires a view of skylight polarization. Nature 364:523–525

Able KP, Able MA (1995) Interactions in the flexible orientation system of a migratory bird. Nature 375:230–232

Åkesson S (1994) Comparative orientation experiments with different species of long-distance migrants: effect of magnetic field manipulation. Anim Behav 48:1379–1393

Åkesson S, Hedenström A (2000) Selective flight departure in passerine nocturnal migrants. Behav Ecol Sociobiol 47:140–144

Åkesson S, Hedenström A (2007) How migrants get there: migratory performance and orientation. Bioscience 57:123–133

Åkesson S, Alerstam T, Hedenström A (1996) Flight initiation of nocturnal passerine migrants in relation to celestial orientation conditions at twilight. J Avian Biol 27:95–102

Åkesson S, Walinder G, Karlsson L, Ehnbom S (2001) Reed warbler orientation: Initiation of nocturnal migratory flights in relation to visibility of celestial cues at dusk. Anim Behav 61:181–189

Åkesson S, Morin J, Muheim R, Ottosson U (2002) Avian orientation: effects of cue-conflict experiments with young migratory songbirds in the high Arctic. Anim Behav 64:469–475

Åkesson S, Klaassen R, Holmgren J, Fox JW, Hedenström A (2012) Migration routes and strategies in a highly aerial migrant, the common swift *Apus apus*, revealed by light-level geolocators. PLoS One 7(7):e41195

Alerstam T, Gudmundsson GA, Green M, Hedenström A (2001) Migration along orthodromic sun compass routes by arctic birds. Science 291:300–303
Andersson S, Amundsen T (1997) Ultraviolet colour vision and ornamentation in bluethroats. Proc R Soc Lond B 264:1587–1591
Batschelet E (1981) Circular statistics in biology. Academic, New York
Baylor ER, Fettiplace D (1975) Light path and photon capture in turtle photoreceptors. J Physiol 248:433–464
Beason RC (1992) You can get there from here: responses to simulated magnetic equator crossing by the Bobolink (*Dolichonyx oryzivorus*). Ethology 91:75–80
Beason RC, Loew ER (2008) Visual pigment and oil droplet characteristics of the bobolink (*Dolichonyx oryzivorus*), a new world migratory bird. Vis Res 48:1–8
Bennett ATD, Cuthill IC (1994) Ultraviolet vision in birds: what is its function? Vis Res 34:1471–1478
Bowmaker JK (1977) The visual pigments, oil droplets and spectral sensitivity of the pigeon. Vis Res 17:1129–1138
Bowmaker JK (1980) Colour vision in birds and the role of oil droplets. Trends Neurosci 3:196–199
Bowmaker JK (1991) Photoreceptors, photopigments and oil droplets. In: Gouras P (ed) Vision and visual dysfunction, vol 6, The perception of colour. Macmillan, London, pp 108–127
Bowmaker JK (2008) Evolution of vertebrate visual pigments. Vis Res 48:2022–2041
Bowmaker JK, Heath LA, Wilkie SE, Hunt DM (1997) Visual pigments and oil droplets from six classes of photoreceptor in the retinas of birds. Vis Res 37:2183–2194
Brines M, Gould J (1982) Skylight polarization patterns and animal orientation. J Exp Biol 96:69–91
Bruderer B, Weitnauer E (1972) Radarbeobachtungen über Zug und Nachtflüge des Mauerseglers (*Apus apus*). Rev Suisse Zool 79:1190–1200
Burkhardt D (1982) Birds, berries and UV. Naturwissenschaften 69:153–157
Burkhardt D, Maier EJ (1989) The spectral sensitivity of a Passerine bird is highest in the UV. Naturwissenschaften 76:82–83
Burton RF (2008) The scaling of eye size in adult birds: relationship to brain, head and body sizes. Vis Res 48:2345–2351
Cameron DA, Pugh EN (1991) Double cones as a basis for a new type of polarisation vision in vertebrates. Nature 353:161–164
Chen DM, Goldsmith TH (1986) Four spectral classes of cone in the retinas of birds. J Comp Physiol A 159:473–479
Chen DM, Collins JS, Goldsmith TH (1984) The ultraviolet receptor of bird retinas. Science 225:337–340
Church SC, Bennett AT, Cuthill IC, Partridge JC (1998) Ultraviolet cues affect the foraging behaviour of blue tits. Proc R Soc Lond B 265:1509–1514
Cochran WW, Mouritsen H, Wikelski M (2004) Migrating songbirds recalibrate their magnetic compass daily from twilight cues. Science 304:405–408
Coemans MAJM, Vos Hzn JJ, Nuboer JFW (1990) No evidence for polarization sensitivity in the pigeon. Naturwissenschaften 77:138–142
Coemans MAJM, Vos Hzn JJ, Nuboer JFW (1994) The orientation of the e-vector of linearly polarized light does not affect the behaviour of the pigeon, *Columba livia*. J Exp Biol 191:107–123
Cronin TW, Warrant EJ, Greiner B (2006) Celestial polarization patterns during twilight. Appl Opt 45:5582–5589
de Brooke ML, Hanley S, Laughlin SB (1999) The scaling of eye size with body mass in birds. Proc R Soc B 266:405–412
Delius JD, Perchard RJ, Emmerton J (1976) Polarized light discrimination by pigeons and an electroretinographic correlate. J Comp Physiol Psychol 90:560–571

Dokter AM, Åkesson S, Beekhuis H, Bouten W, Buurma L, van Gasteren H, Holleman I (2013) Twilight ascents by common swifts, *Apus apus*, at dawn and dusk: acquisition of orientation cues? Anim Behav 85:545–552

Emlen ST (1967a) Migratory orientation in the indigo bunting, *Passerina cyanea*. Part II: mechanism of celestial orientation. Auk 84:463–489

Emlen ST (1967b) Migratory orientation in the indigo bunting, *Passerina cyanea*. Part I: evidence for use of celestial cues. Auk 84:309–342

Emlen ST (1970) Celestial rotation: its importance in the development of migratory orientation. Science 170:1198–1201

Emlen ST (1975) Migration: orientation and navigation. Avian Biol 5:129–219

Emmerton J, Delius JD (1980) Wavelength discrimination in the "visible" and UV spectrum by pigeons. J Comp Physiol A 141:47–52

Finger E, Burkhardt D (1994) Biological aspects of bird colouration and avian colour vision including ultraviolet range. Vis Res 34:1509–1514

Gaggini V, Baldaccini N, Spina F, Giunchi D (2010) Orientation of the pied flycatcher *Ficedula hypoleuca* cue-conflict experiments during spring migration. Behav Ecol Sociobiol 64:1333–1342

Goldsmith TH (1991) Optimization, constraint and history in the evolution of eyes. Q Rev Biol 65:281–322

Goldsmith TH, Collins JS, Licht S (1984) The cone oil droplets of avian retinas. Vis Res 24:1661–1671

Greenwood VJ, Smith EL, Church SC, Partridge JC (2003) Behavioural investigation of polarisation sensitivity in the Japanese quail (*Coturnix coturnix japonica*) and the European starling (*Sturnus vulgaris*). J Exp Biol 206:3201–3210

Gudmundsson GA, Alerstam T, Benvenuti S, Papi F, Lilliendahl K, Åkesson S (1995) Examining the limits of flight and orientation performance: satellite tracking of brent geese migrating across the Greenland ice-cap. Proc R Soc Lond B 261:73–79

Haan S, Bauer S, Liechti F (2009) The natural link between Europe and Africa—2.1 billion birds on migration. Oikos 118:624–626

Hárosi FI, MacNichol EF Jr (1974) Visual pigments of goldfish cones: spectral properties and dichroism. J Gen Physiol 63:279–304

Hart NS, Partridge JC, Cuthill IC (1998) Visual pigments, oil droplets and cone photoreceptor distribution in the European starling (*Sturnus vulgaris*). J Exp Biol 201:1433–1446

Hart NS, Partridge JC, Cuthill IC (1999) Visual pigments, cone oil droplets, ocular media and predicted spectral sensitivity in the domestic turkey (*Meleagris gallopavo*). Vis Res 39:3321–3328

Hart NS, Partridge JC, Cuthill IC, Bennett AT (2000) Visual pigments, oil droplets, ocular media and cone photoreceptor distribution in two species of passerine bird: the blue tit (*Parus caeruleus* L.) and the blackbird (*Turdus merula* L.). J Comp Physiol A 186:375–387

Hegedüs R, Åkesson S, Wehner R, Horváth G (2007a) Could Vikings have navigated under foggy and cloudy conditions by skylight polarization? On the atmospheric optical prerequisites of polarimetric Viking navigation under foggy and cloudy skies. Proc R Soc A 463:1081–1095

Hegedüs R, Åkesson S, Horváth G (2007b) Polarization patterns of thick clouds: overcast skies have distribution of the angle of polarization similar to that of clear skies. J Opt Soc Am A 24:2347–2356

Horváth G, Varjú D (2004) Polarized light in animal vision: polarization patterns in nature. Springer, Heidelberg

Hunt S, Bennett AT, Cuthill IC, Griffiths R (1998) Blue tits are ultraviolet tits. Proc R Soc Lond B 265:451–455

Kreithen ML, Keeton WT (1974) Detection of polarized light by the homing pigeon, *Columba livia*. J Comp Physiol A 89:83–92

Lisney TJ, Rubene D, Rózsa J, Lovlie H, Håstad O, Ödeen A (2011) Behavioural assessment of flicker fusion frequency in chicken *Gallus gallus domesticus*. Vis Res 51:1324–1332

Lythgoe JN (1979) The ecology of vision. Oxford University Press, Oxford
Maier EJ (1992) Spectral sensitivities including the UV of the passeriform bird *Leiothrix lutea*. J Comp Physiol A 170:709–714
Maier EJ, Bowmaker JK (1993) Colour vision in the passeriform bird, *Leiothrix lutea*: correlation of visual pigment absorbance and oil droplet transmission with spectral sensitivity. J Comp Physiol A 172:295–301
Martin GR (1985) Eye. In: King AS, McLelland J (eds) Form and function in birds, vol 3. Academic, London, pp 311–373
Montgomery KC, Heinemann EG (1952) Concerning the ability of homing pigeons to discriminate patterns of polarized light. Science 116:454–456
Moore FR (1987) Sunset and the orientation behaviour of migrating birds. Biol Rev 62:65–86
Mouritsen H, Hore P (2012) The magnetic retina: light-dependent and trigeminal magnetoreception in migratory birds. Curr Opin Neurobiol 22:343–352
Muheim R (2011) Behavioural and physiological mechanisms of polarized light sensitivity in birds. Philos Trans R Soc B 366:763–771
Muheim R, Moore FR, Phillips JB (2006a) Calibration of magnetic and celestial compass cues in migratory birds: a review of cue-conflict experiments. J Exp Biol 209:2–17
Muheim R, Phillips JB, Åkesson S (2006b) Polarized light cues underlie compass calibration in migratory songbirds. Science 313:837–839
Muheim R, Åkesson S, Phillips JB (2007) Magnetic compass of migratory Savannah sparrows is calibrated by skylight polarization at sunrise and sunset. J Ornithol 148:485–494
Muheim R, Åkesson S, Phillips JB (2008) Response to R. Wiltschko et al. (*Journal für Ornithologie*): contradictory results on the role of polarized light in compass calibration in migratory songbirds. J Ornithol 149:659–662
Muheim R, Phillips JB, Deutschlander ME (2009) White-throated sparrows calibrate their magnetic compass by polarized light cues during both autumn and spring migration. J Exp Biol 212:3466–3472
Muntz WRA (1972) Inert absorbing and reflecting, pigments. In: Dartnall HJA (ed) The handbook of sensory physiology, vol WII/l. Springer, Berlin, pp 529–565
Niessner C, Denzau S, Gross JC, Peichl L, Bischof HJ, Fleissner G, Wiltschko W, Wiltschko R (2011) Avian ultraviolet/violet cones identified as probable magnetoreceptors. PLoS One 6: e20091
Palmgren P (1949) On the diurnal rhythm of activity and rest in birds. Ibis 91:561–576
Partridge JC (1989) The visual ecology of avian cone oil droplets. J Comp Physiol A 165:415–426
Rozenberg GV (1966) Twilight. A study in atmospheric optics. Plenum, New York
Schmaljohann H, Rautenberg T, Muheim R, Naef-Daenzer B, Bairlein F (2013) Response of a free-flying songbird to an experimental shift of the light polarization pattern around sunset. J Exp Biol 216:1381–1387
Schmidt-Koenig K (1990) The sun compass. Experientia 46:336–342
Tarburton MK, Kaiser E (2001) Do fledgling and pre-breeding common swifts *Apus apus* take part in aerial roosting? An answer from a radiotracking experiment. Ibis 143:255–264
von Frisch K (1949) Die Polarisation des Himmelslichtes als orienterender Faktor bei den Tänzen der Bienen. Experientia 5:142–148
Vos HJJ, Coemans M, Nuboer J (1995) No evidence for polarization sensitivity in the pigeon electroretinogram. J Exp Biol 198:325–335
Wald G, Zussman H (1937) Carotenoids of the chicken retina. Nature 140:197
Wehner R (1989) Neurobiology of polarization vision. Trends Neurosci 12:353–359
Weindler P, Wiltschko R, Wiltschko W (1996) Magnetic information affects the stellar orientation of young bird migrants. Nature 383:158–160
Weitnauer E (1952) Übernachtet der Mauersegler, *Apus apus* (L.), in der Luft? Ornithologische Beobachtungen 49:37–44
Willis J, Phillips J, Muheim R, Diego-Rasilla FJ, Hobday AJ (2009) Spike dives of juvenile southern bluefin tuna (*Thunnus maccoyii*): a navigational role? Behav Ecol Sociobiol 64:57–68

Wiltschko R (1980) Die Sonnenorientierung der Vögel. 1. Die Rolle der Sonne im Orientierungssystem und die Funktionsweise des Sonnenkompass. J Ornithol 121:121–143
Wiltschko R (1981) Die Sonnenorientierung der Vögel. 2. Entwicklung des Sonnenkompass und sein Stellenwert im Orientierungssystem. J Ornithol 122:1–22
Wiltschko W, Wiltschko R (1972) Magnetic compass of European robins. Science 176:62–64
Wiltschko W, Wiltschko R (1992) Migratory orientation: magnetic compass orientation of garden warblers, *Sylvia borin*, after a simulated crossing of the magnetic equator. Ethology 91:70–74
Wiltschko R, Wiltschko W (1995) Magnetic orientation in animals. Springer, Heidelberg
Wiltschko R, Wiltschko W (2010) Avian magnetic compass: its functional properties and physical basis. Curr Zool 56:265–276
Wiltschko R, Walker M, Wiltschko W (2000) Sun-compass orientation in homing pigeons: compensation for different rates of change in azimuth? J Exp Biol 203:889–894
Wiltschko R, Munro U, Ford H, Wiltschko W (2008) Contradictory results on the role of polarized light in compass calibration in migratory songbirds. J Ornithol 149:607–614
Young SR, Martin GR (1984) Optics of retinal oil droplets: a model of light collection and polarization detection in the avian retina. Vis Res 24:129–137

Chapter 13
Polarization-Induced False Colours

Gábor Horváth and Ramón Hegedüs

Abstract If the photoreceptors of a colour vision system are polarization sensitive, the system detects polarization-induced false colours. It has been hypothesized that egg-laying *Papilio* butterflies could use these polarizational colours as a cue to detect leaf orientation and to discriminate between shiny and matte leaves. In this chapter, we show that a shiny green surface with any orientation can possess almost any polarizational false colour under any illumination condition (for different solar elevations and directions of view with respect to the solar azimuth as well as for sunlit and shady circumstances under clear skies). Consequently, polarizational colours cannot unambiguously code surface orientation. Polarization sensitivity is even disadvantageous for the detection of surface orientation by means of colours. On the other hand, the colour changes due to retinal rotation can be significantly larger for shiny surfaces than for matte ones. Thus, polarizational colours could help polarization-dependent colour vision systems to discriminate between shiny and matte surfaces. Earlier it has been believed that a uniformly polarization-sensitive retina (UPSR)—in which receptors of all spectral types have the same polarization sensitivity ratio and microvilli direction—cannot detect polarization-induced false colours. Here we show that, contrary to this belief, a colour vision

Electronic supplementary material is available in the online version of this chapter at 10.1007/978-3-642-54718-8_13. The videos can also be accessed at http://www.springerimages.com/videos/978-3-642-54717-1.

G. Horváth (✉)
Environmental Optics Laboratory, Department of Biological Physics, Physical Institute, Eötvös University, Pázmány sétány 1, 1117 Budapest, Hungary
e-mail: gh@arago.elte.hu

R. Hegedüs
Max Planck Institute for Informatics, Campus E1.4, 66123 Saarbruecken, Germany

INRIA Sud-Ouest Bordeaux, 200, Avenue de la Vieille Tour, 33400 Talence, France

Laboratoire Photonique, Numérique et Nanosciences (L2PN), UMR 5298, CNRS IOGS University Bordeaux, Institut d'Optique d'Aquitaine, 33405 Talence, France
e-mail: ramon.hegedus@gmail.com

G. Horváth (ed.), *Polarized Light and Polarization Vision in Animal Sciences*, Springer Series in Vision Research 2, DOI 10.1007/978-3-642-54718-8_13,

based on a UPSR is subject to polarization-related artefacts, because both the degree and the angle of polarization of light reflected from natural surfaces depend on wavelength. These findings are of general importance for polarization-dependent colour vision systems.

13.1 Polarizational False Colours and Visual Discrimination Between Smooth (Shiny) and Rough (Matte) Leaf Surfaces

According to Wehner and Bernard (1993), the interference of colour vision and polarization vision has to be avoided; otherwise polarizational (i.e. polarization-induced) false colours are induced if both visual qualities are mixed. They showed that the function of the photoreceptor twist in the eyes of honeybees (*Apis mellifera*) is to avoid the polarizational false colours of leaves and flower petals reflecting partially linearly polarized light. The degree and direction of polarization of plant-reflected light depend strongly on the roughness and orientation of the plant surface (Horváth et al. 2002). For flower visitors these reflection-polarization characteristics could cause serious problems, because the photopigments underlying colour vision are in photoreceptors with different microvilli orientations. Thus, each receptor gives a signal that depends not only on the intensity and the wavelength but also on the direction and the degree of polarization of plant-reflected light. If the receptors of a colour vision system are polarization sensitive, the system generates false colours that may obscure the real colours determined by the spectral characteristics of flowers and leaves and perceived by polarization-insensitive (-blind) colour vision systems.

Kelber (1999) and Kelber et al. (2001) demonstrated that *Papilio* butterflies perceive polarization-induced false colours if their photoreceptors are stimulated by artificially strongly polarized and unnaturally quasi-monochromatic light under laboratory conditions, because their colour-sensitive receptors are weakly polarization sensitive. However, polarizational false colours have been believed to be disadvantageous, and are usually eliminated in insect eyes by a proper photoreceptor twist (Wehner et al. 1975), or by random microvilli orientations, or by colour blindness (monochromacy) of the polarization-sensitive receptors (Wehner and Bernard 1993). Thus, there may be some selective advantages to *Papilio* butterflies that have retained the polarization sensitivity of their colour vision (Kelber 1999; Kelber et al. 2001). Female *Papilio* butterflies lay eggs on the shiny, smooth leaves of plants in the Rutaceae or *Citrus* family. Kelber and her collaborators suggested that the polarizational false colours perceived by these butterflies may be relevant during oviposition.

Kelber (1999) hypothesized that horizontal leaves could be more attractive than vertical or tilted leaves to an ovipositing butterfly, because the former could provide a better landing for the butterfly and offer more protection for the eggs and young larvae. The reflection-polarization characteristics of plant surfaces depend strongly

on their orientation, the illumination conditions and the direction of observation (Horváth et al. 2002; Hegedüs and Horváth 2004a; Horváth and Varjú 2004). In the opinion of Kelber et al. (2001), an approaching female *Papilio* butterfly could select a horizontal leaf from the differently oriented leaves on the basis of the polarizational false colours.

Kelber (1999) and Kelber et al. (2001) also assumed that the detection of polarization-induced false colours could help *Papilio* butterflies to discriminate between shiny (smooth) and matte (rough) leaves before landing on them. Since leaves with different surface roughnesses reflect differently polarized light, the polarization-induced false colours of smooth (shiny) and rough (matte) leaves could look different to a *Papilio* butterfly, and the false colour could change when the butterfly passes by. This property might serve as a visual indicator of the leaf smoothness coding the quality of a leaf as a food source for the caterpillars.

The above hypotheses raise the following two questions: (1) Can the orientation of a leaf surface be unambiguously coded by the polarizational false colours perceived by polarization-sensitive colour vision systems? (2) Are the changes in the polarization-induced false colours due to retinal rotation (relative to the plant surface seen) significantly different between shiny (smooth) and matte (rough) leaf surfaces?

Hegedüs and Horváth (2004a) answered both questions. Using imaging polarimetry, they measured the reflection-polarization characteristics of a shiny (smooth) green hemisphere (upper half of a billiard ball) in the red, green and blue spectral ranges under 60 different illumination conditions (at solar elevation angles $\varepsilon_S = 2°$, 11°, 19°, 26°, 30°, 32° and viewing directions $\gamma = 0°, 45°, 90°, 135°, 180°$ from the solar azimuth as well as for sunlit and shady circumstances) under clear skies (Fig. 13.1a–d). Since different points of the continuously curving surface of the hemisphere represent different surface orientations (Fig. 13.1b), the hemisphere modelled numerous differently oriented leaf surfaces (Fig. 13.1a). Using the polarization- and colour-sensitive retina model of Horváth et al. (2002), Hegedüs and Horváth (2004a) computed the polarizational false colours of this green hemisphere (Fig. 13.1e–g). They studied the correlation between these false colours and the local surface orientation of the hemisphere (Fig. 13.2). They also calculated the maximal changes of the polarizational false colours of a shiny (smooth) and a matte (rough) green hemisphere induced by retinal rotation (Fig. 13.1g).

Hegedüs and Horváth (2004a) found that a surface with any orientation can possess almost any polarizational false colour under any illumination condition. This graphically means that in Fig. 13.2 in any row (belonging to angle θ of a plant surface, where θ is the direction of the normal vector $\underline{n}$ of the surface from the vertical, Fig. 13.1a, b) of the polarizational false colour occurrence matrix $\underline{\underline{M}}$ practically all possible colours m (counting the columns of the matrix) occur. An element $M_{m,\theta}$ of this matrix gives how many times a colour m occurs at the interval of points with zenith angle $\theta \pm 1.5°$ on the hemisphere (Fig. 13.1f). Consequently, polarization-induced false colours cannot unambiguously code the orientation of a leaf surface. In fact, depending on the microvilli directions of photoreceptors, the polarization sensitivity of colour vision can even degrade the efficiency of detecting

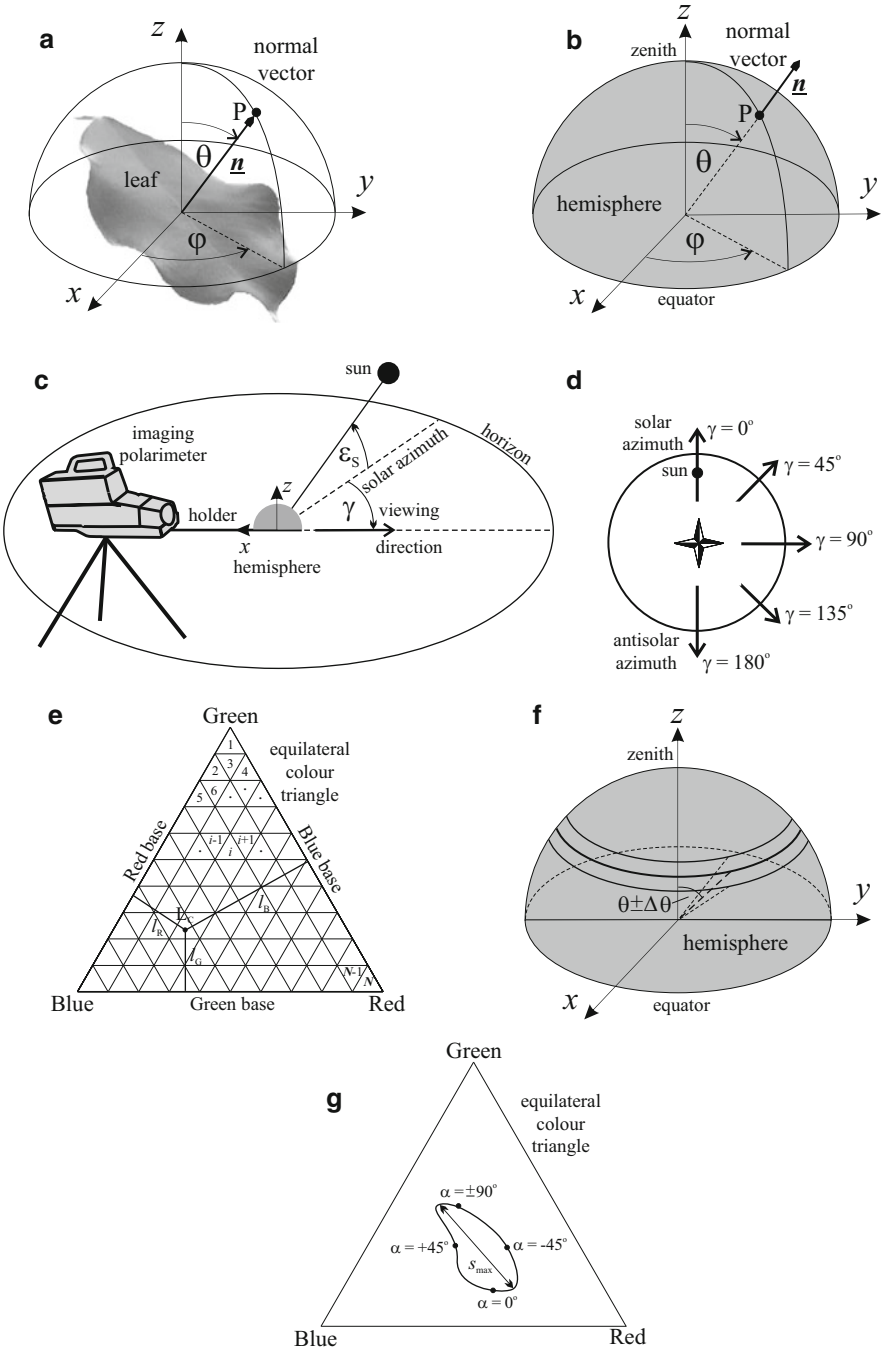

Fig. 13.1 (**a**) A leaf blade with a given orientation is described by the zenith angle θ and azimuth angle φ of the normal vector $\underline{\boldsymbol{n}}$ of its surface. (**b**) A hemisphere, the surfacial points of which model numerous differently oriented leaf surfaces in the following ranges of θ and φ: $0^\circ \leq \theta \leq 90^\circ$,

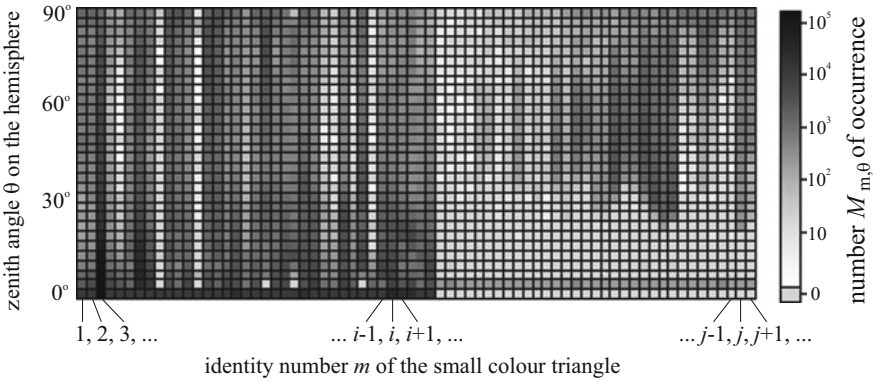

Fig. 13.2 An example for a small fragment of the normalized net polarizational false colour occurrence matrix $\underline{\underline{M}} = \sum_{i=1}^{60} \underline{\underline{M}}(H_i)$ calculated for a shiny green hemisphere (modelling numerous differently oriented shiny green leaves) by summing up the polarizational colour occurrence matrices $\underline{\underline{M}}(H_i)$ belonging to 60 different illumination situations (Fig. 13.1c, d). An element $M_{m,\theta}$ of this matrix gives how many times a colour m occurs at the interval of points with zenith angles $\theta \pm 1.5°$ on the hemisphere. The numerical values of the matrix elements $M_{m,\theta}$ are *grey coded* in such a way that *darker grey codes* larger $M_{m,\theta}$-value. $M_{m,\theta} = 0$ is coded by a *dotted pattern*

surface orientation by means of colours (Hegedüs and Horváth 2004a). Another counterargument against detecting the surface orientation by means of polarizational false colours is that a butterfly should memorize too many (millions) different colours which code the optimal surface orientations. It is questionable whether butterflies are able to memorize so many different colours and can learn the association between these colours and the optimal surface orientations (if any).

On the other hand, the maximal colour changes s_{max} (Fig. 13.1g) induced by retinal rotation and/or translation are significantly larger for shiny (smooth) leaves than for matte (rough) ones (Hegedüs and Horváth 2004a). The locus of the

Fig. 13.1 (continued) $-90° \leq \varphi \leq +90°$. (**c**) Arrangement of the measurement of reflection-polarization characteristics of the hemisphere at a given solar elevation angle ε_S and direction of view γ with respect to the solar azimuth. (**d**) Viewing directions γ of the polarimeter seen from above. (**e**) The three coordinates ℓ_R, ℓ_G and ℓ_B of the spectral locus $L_C(\ell_R, \ell_G, \ell_B)$ of a perceived colour C is displayed in the equilateral, unit-sided red-green-blue colour triangle, which is divided into N small triangles with an identity number n ranging from 1, 2, 3, ... through $i-1$, i, $i+1$, ... to $N-1$, N. (**f**) A horizontal band with an angular width of $2 \times \Delta\theta$ on the hemisphere at zenith angle θ (called the θ-zone), representing a possible optimal zone for butterfly egg laying. (**g**) The locus of the polarizational false colour of a point of the hemisphere moves along a closed loop in the equilateral colour triangle as the retina makes a half rotation, i.e. the angle α of the eye's dorso-ventral meridian (measured from the vertical) changes from $-90°$ to $+90°$. The maximal spectral distance s_{max} between the points of this loop is the measure of the maximum difference in the polarizational false colours due to retinal rotation. Four colour loci are shown for $\alpha = \pm 90°$, $-45°$, $0°$ and $+45°$ along the loop, the dimensions of which are extremely enlarged for the sake of a better visualization [after Fig. 1 on page 2339 of Hegedüs and Horváth (2004a)]

polarizational false colour of a point of the hemisphere (leaf) moves along a closed loop in the equilateral colour triangle (Fig. 13.1g) as the retina makes a half rotation, i.e. the angle α of the eye's dorso-ventral meridian (measured from the vertical) changes from $-90°$ to $+90°$. The maximal spectral distance s_{max} between the points of this loop is the measure of the maximum difference in the polarizational false colours due to retinal rotation/translation (Fig. 13.1g). Such rotations and/or translations of the retina or movements of the image of plant surfaces relative to the retina occur when an insect approaches a plant surface on wing. According to Hegedüs and Horváth (2004a), if the colour discrimination ability of *Papilio* butterflies were in the range of that of honeybees (Neumeyer 1991), these butterflies could probably perceive the polarizational false colour differences due to retinal rotation/translation, thus enabling them a possible way of visual discrimination between shiny (smooth) and matte (rough) surfaces. Consequently, polarizational false colours can help the discrimination between smooth and rough leaves. Hence, question 1 mentioned above was answered negatively, while question 2 positively (Hegedüs and Horváth 2004a): Egg-laying *Papilio* butterflies cannot use polarizational false colours as a cue to detect leaf orientation, but could use polarization-induced false colours to discriminate between smooth and rough leaves.

On the basis of the above, one can draw the general conclusion that polarizational false colours (which tend to obscure the real colours rather randomly due to the random temporal and/or spatial changes of the degree and the direction of polarization along plant surfaces) are useless for polarization-dependent colour vision systems to identify a particular/preferred surface orientation, e.g. for butterflies to find optimally (e.g. horizontally) oriented leaves for oviposition. In fact, the lack of unambiguous correlation between colour and surface orientation renders the identification of surface orientation much more difficult than it is for a polarization-blind colour vision system. A possible advantage polarization-dependent colour vision systems could gain is the detection of the magnitude of changes in polarizational false colours due to retinal rotation/translation, since these changes are primarily determined by the surface roughness and are not subject to further major temporal or spatial ambiguities (Hegedüs and Horváth 2004a).

13.2 Uniformly Polarization-Sensitive Retinas and Polarization-Induced False Colours

If the photoreceptors of a colour vision system are polarization sensitive, the system detects polarization-induced false colours, which differ from the real colours determined by the spectral characteristics of objects (Wehner and Bernard 1993). In a uniformly polarization-sensitive retina (UPSR) the microvilli of receptors of different spectral types are uniformly oriented with the same angle β (e.g. $\beta_{UltraViolet} = \beta_{Blue} = \beta_{Green} = \beta$) relative to the eye's dorso-ventral meridian, and the polarization sensitivity ratios P of receptors of different spectral types are also

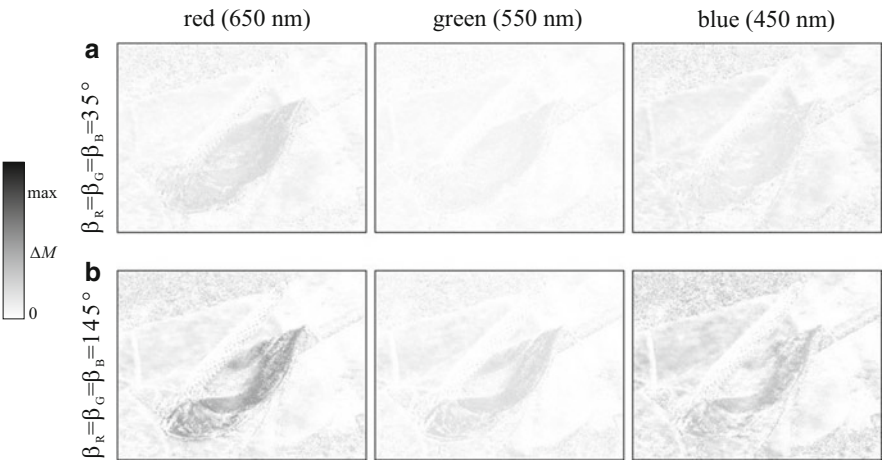

Fig. 13.3 Patterns of the difference $\Delta M_r = |M_r^{UPSR} - M_r^{PBR}|$ ($r = R, G, B$) between the components (M_R, M_G, M_B) of colours of *Epipremnum aureum* (the reflection-polarization patterns of which are shown in Fig. 13.4) detected by a uniformly polarization-sensitive retina (UPSR, with polarization sensitivity ratios $P_R = P_G = P_B = 10$, and microvilli directions $\beta_R = \beta_G = \beta_B = \beta = 35°$ or 145°) and a polarization-blind retina (PBR, with $P_R = P_G = P_B = 1$ and β_R, β_G, β_B = arbitrary). The ΔM_r-values are normalized to the maximal difference ΔM^{max} (shaded by *dark grey*) obtained throughout all difference patterns [after Fig. 5 on page 82 of Hegedüs and Horváth (2004b)]

identical (e.g. $P_{UV} = P_B = P_G = P$). Based on the functional similarities between polarization vision and colour vision, earlier it has been believed that a UPSR cannot detect polarization-induced false colours (Kelber et al. 2001). However, Hegedüs and Horváth (2004b) showed that a UPSR (independently of the dimension of the colour space: tri-, tetra-, penta-, etc., chromaticism) can detect polarizational false colours, because both the degree and the direction (angle) of polarization of light reflected from natural surfaces usually depend on the wavelength λ.

If the degree $d(\lambda)$ and/or the angle $\alpha(\lambda)$ of linear polarization of the stimulus is wavelength-dependent, the colours detected by a UPSR differ from the real colours detected by a polarization-blind retina (PBR) with $P_B = P_G = P_R = 1$. Consequently, a UPSR can detect polarization-induced false colours, contrary to the earlier belief. This phenomenon is demonstrated in Fig. 13.3, based on the reflection-polarization patterns in Fig. 13.4 measured by imaging polarimetry. In the computation of Fig. 13.3, the amplitude normalized absorption functions $A_r(\lambda)$ of the *Red*, *Green* and *Blue* photoreceptors (Fig. 13.5a), the microvilli directions β_R, β_G and β_B relative to the eye's dorso-ventral meridian (Fig. 13.5b) and the polarization sensitivity ratios P_R, P_G and P_B of the R, G and B receptors were chosen according to the characteristics of photoreceptors in the butterfly *Papilio xuthus* (Kelber et al. 2001). In the computation of patterns in Figs. 13.3 and 13.4d the values of intensity I, degree of linear polarization d and angle of polarization α at a given point of the patterns were taken from the I-, d- and α-patterns in Fig. 13.4a–c.

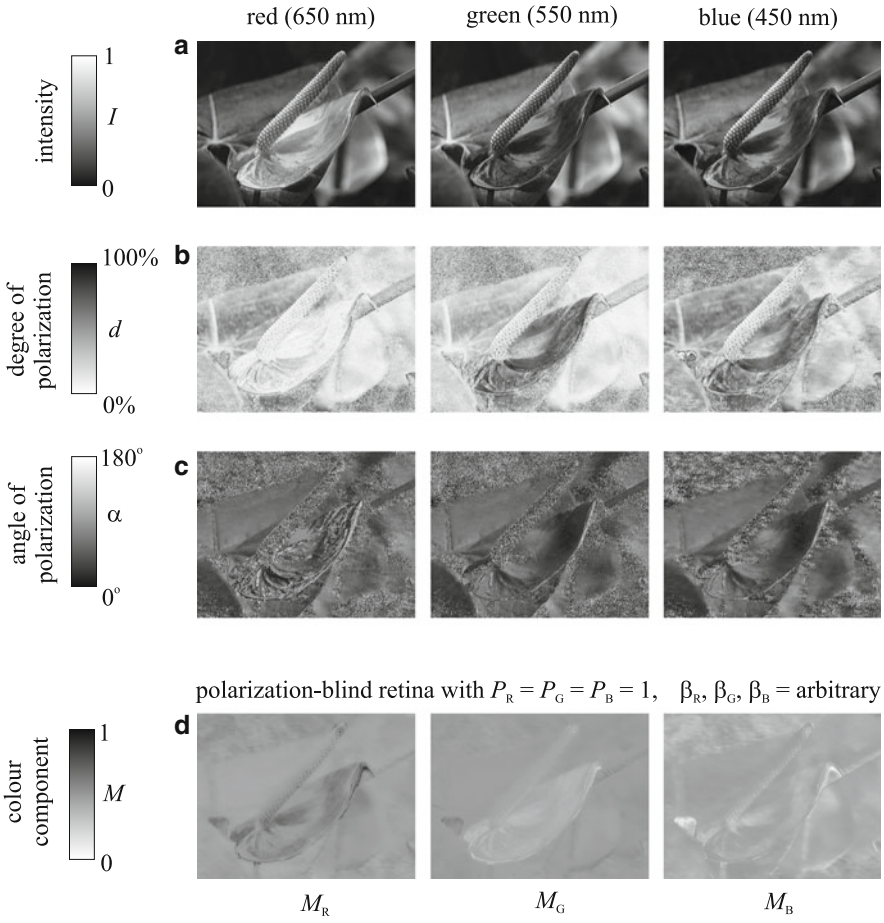

Fig. 13.4 (**a–c**) Patterns of the intensity I, degree of linear polarization d and angle of polarization α of *Epipremnum aureum* (golden pothos, Aracea)—illuminated by light from a clear sky from above through glass panes of a greenhouse—measured by imaging polarimetry at wavelengths 650, 550 and 450 nm. (**d**) Patterns of the red, green and blue components M_R, M_G and M_B of the colour of *E. aureum* detected by a polarization-blind retina with polarization sensitivity ratios $P_R = P_G = P_B = 1$ and microvilli directions β_R, β_G, β_B = arbitrary, where M_r (r = R, G, B) are the coordinates of the spectral locus in the equilateral colour triangle [after Fig. 3 on page 80 of Hegedüs and Horváth (2004b)]

Figure 13.4a–c shows the patterns of the intensity I, degree of linear polarization d and angle of polarization α of *Epipremnum aureum* (golden pothos, Aracea) measured in the red, green and blue spectral ranges. Due to the rule of Umow (1905), in a given spectral range the lower the intensity of light reflected from a plant surface, the higher the degree of linear polarization d of reflected light (Horváth et al. 2002; Horváth and Varjú 2004). This is the reason why the red

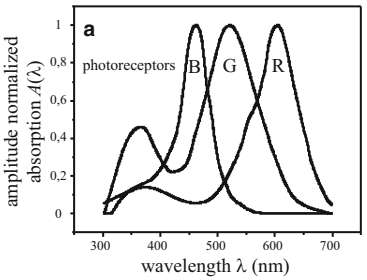

b

microvilli directions		
β_R	β_G	β_B
0°	0°	0°
0°	90°	0°
35°	0°	0°
35°	90°	0°
145°	0°	0°
145°	90°	0°

Fig. 13.5 (**a**) Absorption functions $A(\lambda)$ of the blue (**b**), green (G) and red (R) photoreceptors in the butterfly *Papilio xuthus* being maximally sensitive in the blue, green (with a secondary maximum in the ultraviolet) and red spectral ranges found by Kelber et al. (2001). (**b**) Angles β_R, β_G and β_B of the microvilli directions relative to the eye's dorso-ventral meridian of the red, green and blue photoreceptors found by Kelber et al. (2001) in *Papilio xuthus* [after Fig. 1 on page 78 of Hegedüs and Horváth (2004b)]

spathe of *E. aureum* is so weakly polarized in the red, and its green leaves in the background are least polarized in the green (Fig. 13.4b). Figure 13.4d displays the patterns of the red, green and blue components M_r (r = R, G, B) of the colour of *E. aureum* detected by a polarization-blind retina.

Figure 13.3 shows the patterns of difference $\Delta M_r = |M_r^{UPSR} - M_r^{PBR}|$ (r = R, G, B) between the components of colours of *E. aureum* (Fig. 13.4) detected by a UPSR and a PBR calculated for two different values of the uniform microvilli directions $\beta_R = \beta_G = \beta_B$ in the UPSR. Large and small ΔM_r-values mean strong and weak false colour effect, respectively. In other words, Fig. 13.3 displays how the polarization-induced false colours detected by a UPSR differ from the real colours detected by a PBR shown in Fig. 13.4e. Figure 13.3 demonstrates well that depending on the microvilli direction as well as on the spectral and polarization characteristics, a UPSR can detect weaker or stronger polarization-induced false colours.

The theoretical basis of polarization-induced false colours is to calculate the colour loci in the colour space of colour vision systems (Fig. 13.1e, g) from the quantum catches of polarization-sensitive receptors of different spectral types. Wehner and Bernard (1993) calculated the polarization-induced false colours of a dandelion leaf perceived by a hypothetical honeybee without receptor twist. They referred to a formula used by Bernard and Wehner (1977). Kelber et al. (2001) used another formula to calculate polarizational false colours. Horváth et al. (2002) presented the first detailed mathematical and receptor-physiological derivation of expressions for polarization-induced false colours. Hegedüs and Horváth (2004b) corrected some errors in the theory of polarizational false colours, showing that the polarization sensitivity function defined by Bernard and Wehner (1977) is inappropriate for calculation of polarization-induced false colours, and the formula used by Kelber et al. (2001) to describe the quantum catch for totally linearly polarized light [with degree of linear polarization $d(\lambda) = 1$ and angle of polarization $\alpha(\lambda) =$ constant, where λ is the wavelength of light] is erroneous. Polarizational false colours

can be correctly calculated from the formulae of the quantum catch derived by Horváth et al. (2002). Hegedüs and Horváth (2004b), however, emphasized that this correction does not influence the validity of experimental data and the principal conclusions drawn by Kelber et al. (2001) about the colour vision and polarization sensitivity in *Papilio xuthus* and *P. Aegeus* butterflies.

References

Bernard GD, Wehner R (1977) Functional similarities between polarization vision and color vision. Vis Res 17:1019–1028

Hegedüs R, Horváth G (2004a) Polarizational colours could help polarization-dependent colour vision systems to discriminate between shiny and matt surfaces, but cannot unambiguously code surface orientation. Vis Res 44:2337–2348

Hegedüs R, Horváth G (2004b) How and why are uniformly polarization-sensitive retinae subject to polarization-related artefacts? Correction of some errors in the theory of polarization-induced false colours. J Theor Biol 230:77–87

Horváth G, Varjú D (2004) Polarized light in animal vision—polarization patterns in nature. Springer, Heidelberg

Horváth G, Gál J, Labhart T, Wehner R (2002) Does reflection polarization by plants influence colour perception in insects? Polarimetric measurements applied to a polarization-sensitive model retina of *Papilio* butterflies. J Exp Biol 205:3281–3298

Kelber A (1999) Why 'false' colours are seen by butterflies. Nature 402:251

Kelber A, Thunell C, Arikawa K (2001) Polarisation-dependent colour vision in *Papilio* butterflies. J Exp Biol 204:2469–2480

Neumeyer C (1991) Evolution of colour vision. In: Cronly-Dillon JR, Gregory RL (eds) Vision and visual dysfunction, vol 2, Evolution of the eye and visual system. MacMillan, London, pp 285–305

Umow N (1905) Chromatische Depolarisation durch Lichtzerstreuung. Physikalische Zeitschrift 6:674–676

Wehner R, Bernard GD (1993) Photoreceptor twist: a solution to the false-color problem. Proc Natl Acad Sci USA 90:4132–4135

Wehner R, Bernard GD, Geiger E (1975) Twisted and non-twisted rhabdoms and their significance for polarization detection in the bee. J Comp Physiol 104:225–245

Chapter 14
Human Polarization Sensitivity

Juliette McGregor, Shelby Temple, and Gábor Horváth

Abstract Humans can detect the E-vector of incident polarized light using a subtle, transient visual phenomenon known as Haidinger's brush. The effect is a result of the human macula having the properties of a radial analyser with peak absorption at 460 nm. A number of mechanisms, each capable of generating radial diattenuation, have been proposed: (1) oblique light incident on cone outer segments, (2) form dichroism in the Henle fibre layer (the photoreceptor axons) and (3) a perpendicular arrangement of dichroic carotenoid pigments with respect to the radially oriented Henle fibres. A close correlation between the dichroic ratio of the macula and the optical density spectrum of liposome-bound lutein and zeaxanthin provides strong evidence that macular pigment plays a key role. Corneal birefringence can affect the contrast and perceived angle of the brush, together with the appearance of the phenomenon in circularly polarized light. When the retina is photographed between crossed polarizers, a brush-like pattern is observed; this is a result of the birefringence of the Henle fibre layer and cornea and is distinct from the radial diattenuation that generates Haidinger's brush. A secondary entoptic phenomenon that allows humans to detect the orientation of polarized light was described by Gundo von Boehm. Boehm's brush is only visible when a polarized

J. McGregor (✉)
School of Biological Sciences, University of Bristol, Woodland Road, Bristol BS8 1UG, UK

Cell Physiology and Pharmacology, College of Medicine, Biological Sciences and Psychology, University of Leicester, Maurice Shock Medical Sciences Building, University Road, Leicester, LE1 9HN, United Kingdom
e-mail: juliette.mcgregor@gmail.com

S. Temple
School of Biological Sciences, University of Bristol, Woodland Road, Bristol BS8 1UG, UK
e-mail: shelbytb@hotmail.com

G. Horváth
Environmental Optics Laboratory, Department of Biological Physics, Physical Institute, Eötvös University, Pázmány sétány 1, 1117 Budapest, Hungary
e-mail: gh@arago.elte.hu

G. Horváth (ed.), *Polarized Light and Polarization Vision in Animal Sciences*, Springer Series in Vision Research 2, DOI 10.1007/978-3-642-54718-8_14,

light source rotates in the peripheral visual field against a dark background and results from light scattering off axis into the photoreceptors. Both phenomena allow for the detection of polarized light by the unaided human eye; however, there is no evidence to suggest that such capabilities are adaptive.

14.1 Introduction

In 1844, Wilhelm Karl von Haidinger (1795–1871), an Austrian physicist, geologist and mineralogist, discovered that the human eye is able to perceive the linear polarization of light due to an entoptic phenomenon that was later given his name. This discovery of Haidinger's brush preceded, by 100 years, Karl von Frisch's (1949) discovery that honeybees (*Apis mellifera*) are sensitive to the linear polarization of skylight and use it for orientation and navigation. The ability to detect the orientation of the electric field vector (E-vector) of polarized light is surprising as human photoreceptors, like those of all vertebrates, are generally thought to be insensitive to the E-vector orientation of axially incident light (exceptions to this are detailed in Chap. 9). Human polarization sensitivity appears to be a by-product of the dichroic properties of the retinal layers; specifically the macula. To date, there has been no biological function assigned to the human ability to detect the E-vector orientation of polarized light. In 1940, Gundo von Boehm described another entoptic phenomenon that enables the human eye to perceive polarized light. 'Boehm's brush' is most visible when a small polarized light source is viewed against a dark background in the peripheral visual field and is only perceived if the E-vector of the light source is rotating. The literature on human polarization sensitivity has also been reviewed by Lester (1970), Zhevandrov (1995), Fairbairn (2001), Horváth and Varjú (2004, pp. 355–361).

14.2 Haidinger's Brush

If one gazes at a homogenous polarized white light field, a faint pattern can be seen consisting of a small yellowish bowtie or 'brush' with bluish intervening areas (Fig. 14.1). This faint entoptic image referred to as Haidinger's brush subtends approximately 5° and rotates about the fixation point as the E-vector of the incident light is rotated. If the polarized light field remains unchanged, neural adaptation causes the effect to fade within a couple of seconds.

Usually, a little practice is needed to see Haidinger's brush, but the effect can be enhanced and maintained by changing the E-vector angle of the polarized light. Looking at a white polarized light field in which the E-vector alternates between two perpendicular E-vector orientations (e.g. horizontal and then vertical) can make the effect more visible, as the afterimage of one orientation of the brush reinforces the

Fig. 14.1 An illustration of the appearance of Haidinger's brush in response to a vertically polarized light stimulus. The sensation of *blue* (vertically aligned *light blue* 8-shaped figure, the *blue part* of the Haidinger's brush) results from a simultaneous contrast effect and has been generated here by removing *yellow* from regions of an otherwise *yellow-tinted background*. The horizontally aligned *dark yellow* 8-shaped figure is the *yellow part* of the Haidinger's brush

image of the second formed at 90° to the original. Alternatively, the E-vector, or the observers head, can be rotated to continuously refresh the image. Recording the potentials evoked in the visual cortex in response to rotating a linearly polarized blue (465 nm) stimulus, Dodt and Kuba (1990) found that the electrophysiological response they measured disappeared when the E-vector rotation ceased. Similarly, no electrical response was detected in response to the rotation of a green (531 nm) stimulus, consistent with reports that if the blue component of the incident polarized light is filtered out, Haidinger's brush is not observed (Stokes 1850; von Helmholtz 1924).

Haidinger's brush has the best contrast when the degree of polarization approaches 100 %, for example looking at a white area on a liquid crystal display (LCD) computer monitor, which employs polarizers as part of the image forming technology. A practiced observer can also detect Haidinger's brush at the zenith of a clear blue sky at sunrise or sunset (or in general, 90° from the sun), where the degree of polarization reaches 75 % (see Chap. 18). For further advice on observing the effect for yourself, consult Fairbairn (2001) or Ovcharenko and Yegorenkov (2002).

14.3 Potential Mechanisms Generating Haidinger's Brush

If one were to image a linearly polarized light field (with homogeneous E-vector orientation) through a linear polarizer in which the transmission axes were oriented radially (a radial analyser) (Fig. 14.2a, b), one would see a dark bowtie-like brush resulting from light attenuation along the meridian perpendicular to the E-vector

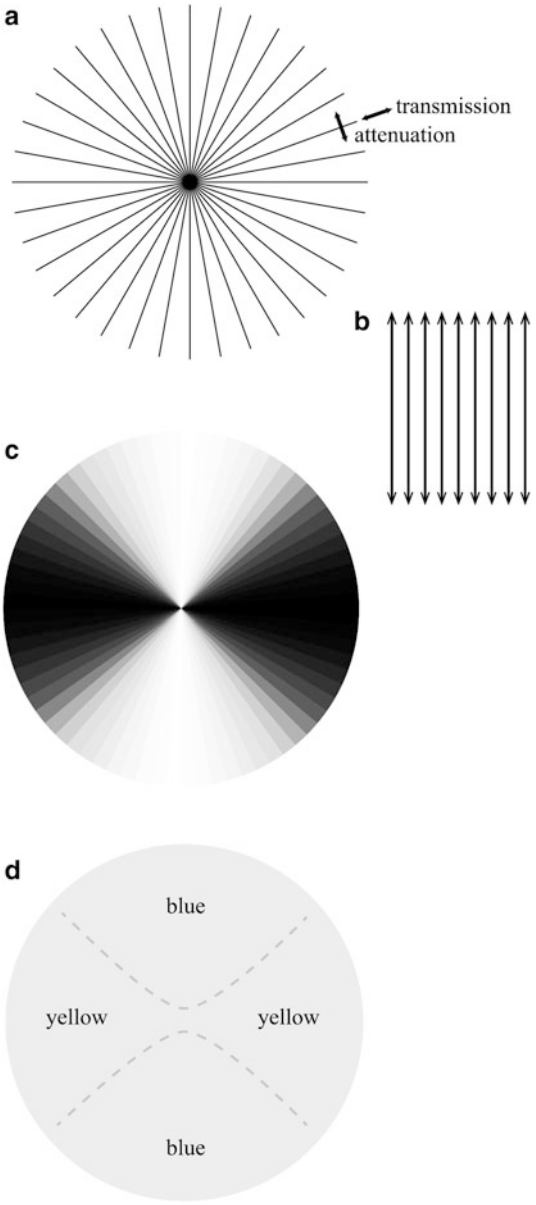

Fig. 14.2 A simple model simulating Haidinger's brush. Looking through a linear polarizer in which the transmission axes are oriented radially (**a**), at a linearly polarized light field with a homogeneous, vertically oriented E-vector (**b**), a darkened bowtie-like pattern of intensity is observed (**c**) as light is preferentially attenuated along the horizontal meridian, perpendicular to the transmission axes of the radial analyser. If the radial analyser selectively attenuates blue light, then areas that appear dark in (**c**) (where blue light has been depleted) would appear yellower than the prevailing incident light field. The resulting percept is shown in (**d**). The blue regions that flank the yellow are understood to be the result of a simultaneous contrast effect produced in response to the yellow bowtie. In this way, a structure in the retina acting as a radial analyser and selectively attenuating short wavelength light could give rise to Haidinger's brush

orientation of the polarized light field (Fig. 14.2c). If this radial analyser preferentially attenuated short wavelengths from the incident white light field, the resulting bowtie (where the blue light had been attenuated) would appear yellow (Figs. 14.1 and 14.2d). The blue-indigo regions that appear perpendicular to the yellow brush

have been attributed to a psychophysical simultaneous contrast effect (Stokes 1850) generated by blue-yellow colour opponent processing.

The possibility that a radial analyser located within the retina is generating Haidinger's brush was first proposed by Maxwell (1850), and radial dichroism has now been demonstrated by both microdensitometry experiments on excised retinas (Snodderly et al. 1984) and psychophysical tests (De Vries et al. 1953; Naylor and Stanworth 1954; Bone 1980; Bone et al. 1992). A close correlation between the optical density spectrum of the macular pigment and the dichroic ratio of the macula as a function of wavelength has provided strong support for the involvement of the macular pigment in generating this dichroism (Bone et al. 1992). Macular pigment is localized in the Henle fibre layer of the retina, which contains numerous, closely packed, cone photoreceptor axons that extend radially from the fovea towards synapses in the displaced outer plexiform layer (Figs. 14.3 and 14.4). Although other models have also been proposed (Summers et al. 1970; Hochheimer and Kues 1982; Le Floch et al. 2010), an interaction between the macular pigment and this radially symmetric fibre framework is the leading hypothesis explaining the origin of radial dichroism in the retina. However, the exact nature of this interaction is subject to debate. A number of authors (e.g. von Helmholtz 1924; De Vries et al. 1953; Naylor and Stanworth 1954; Bone 1980) have attributed Haidinger's brush to a tangential arrangement of dichroic macular pigment molecules, oriented on average, perpendicular to the Henle fibre membranes. Alternatively, the macular pigment molecules could be randomly oriented within a geometrical arrangement of Henle fibres capable of generating form dichroism (Hemenger 1982). In what remains of this section we review the proposed hypotheses in more detail.

Macular pigment is composed of the carotenoids lutein, zeaxanthin and meso-zeaxanthin (Bone et al. 1985, 1993; Schalch et al. 2009), which are extensively conjugated along their polyene chains and absorb strongly if the incident light is polarized parallel to the long axis of the molecule (Bone and Landrum 1983, 1984). If the long axes of the carotenoid pigment molecules were aligned tangentially to concentric circles centred on the fovea (Fig. 14.3), the result would be a radial analyser. Bone et al. (1992) calculated that an average molecular orientation of 54.7° or less with respect to the normal to the surface of the Henle fibres would be sufficient to generate Haidinger's brush in the correct orientation. If the carotenoids adopted a membrane spanning configuration in the lipid bilayers of the Henle fibres, this could generate the radial dichroism necessary to explain Haidinger's brush (Bone and Landrum 1984). This configuration is certainly plausible; however, as carotenoids can adopt a range of orientations within lipid bilayers (Gruszecki and Strzalka 2005), the specific orientations of the various carotenoid components of the macular pigment within the Henle fibre membranes remain uncertain. Recently, specific macular binding proteins for lutein and zeaxanthin have been identified (Bhosale et al. 2004; Li et al. 2011) and may provide another mechanism for the tangential alignment of the dichroic macular pigments.

An alternative model, proposed by Hemenger (1982), does not require the directional organization of the macular pigment molecules, but rather of the

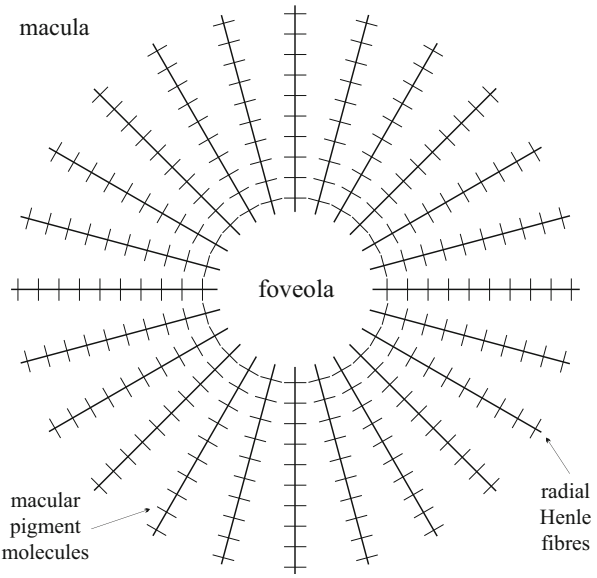

Fig. 14.3 Schematic representation of the hypothesized tangential arrangement of the macular pigment molecules bound to the radially oriented Henle fibres in the human macula [adapted from Fig. 32.3 of Horváth and Varjú (2004, p. 358)]

medium in which they are located. Form dichroism results from repeated blocks of absorbing and non-absorbing materials with a spatial frequency comparable to the wavelength of light. This could be the case in the Henle fibre layer, with pigment molecules randomly oriented between the radially arranged photoreceptor axons. Hemenger (1982) stopped short of a full model of form dichroism demonstrating only that attenuation could be increased in the local environment of a single fibre. Detractors of this hypothesis have indicated that it requires carotenoids to be present in an aqueous phase between the Henle fibres, the spectroscopic signature of which is not consistent with psychophysical measurements of dichroic ratio (Bone and Landrum 1984). Summers et al. (1970) developed a related theory that Haidinger's brush is an interference figure resulting from the illumination of an anisotropic absorbing crystal with strongly convergent polarized light. They proposed that the regular arrangement of fibrils gives rise to form birefringence, and the presence of macular pigment adds absorption to the system. A distinctive feature of this hypothesis is that it does not involve the circular symmetry of the Henle fibre layer, but rather looks to the many parallel fibres that traverse the region between the fovea and the optic disc (the retinal nerve fibre layer; Fig. 14.4b) as the potential birefringent crystal producing Haidinger's brush. Attributing polarization sensitivity to this structure is problematic as this would produce an effect that is not centred at the fixation point, which is inconsistent with all reports that Haidinger's brush is localized in the centre of the visual field (Maxwell 1850).

It has also been suggested that Haidinger's brush is produced by light impinging on the outer segments of foveal photoreceptors slightly off axis, as it is well established that photoreceptor outer segments are dichroic when illuminated transversely (Denton 1959; Liebman et al. 1974). Gribakin and Govardovskii (1975)

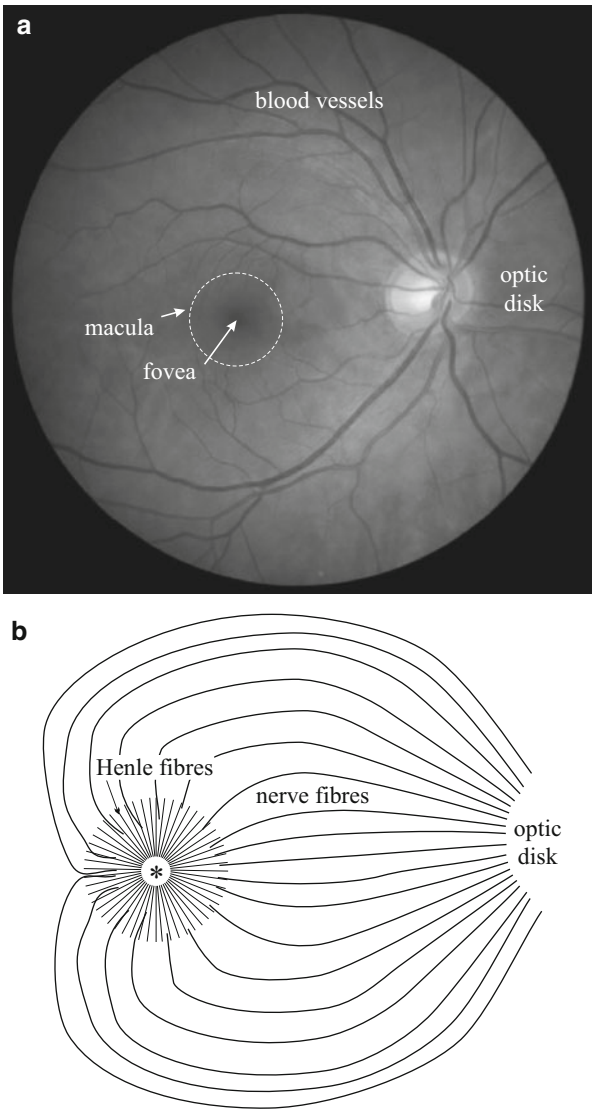

Fig. 14.4 (**a**) Photograph of a human retina with the fovea, optic disc (blind spot) and blood vessels [after Fig. 32.2a of Horváth and Varjú (2004, p. 357)]. (**b**) Schematic drawing of the retinal nerve fibre axon arrangement at the fovea (marked by an *asterisk*), which is nearly devoid of nerve fibres, includes the central 0.35 mm of the fovea (1.2° of the visual field), located 4 mm temporally and 0.8 mm inferior to the centre of the optic disc. The macula lutea (Latin for *yellow spot*) is a portion of the retina centred on the fovea containing the carotenoid pigments lutein, zeaxanthin and meso-zeaxanthin [after Fig. 32.1b of Horváth and Varjú (2004, p 356)]

suggested that any slight tilt in the cone array would provide a mechanism for detecting polarization. However, the Stiles–Crawford effect (Stiles and Crawford 1933) together with micrographic evidence (Laties et al. 1968; Fuld et al. 1979) indicates that photoreceptors in the human retina align towards the centre of the pupil to maximize photon catch; thus a systematically tilted photoreceptor array in the human eye is unlikely. Furthermore, the off axis light hypothesis could not readily explain the blue and yellow colours of the brushes. Alternatively, there may be a significant amount of non-image-forming light incident obliquely on the foveal

photoreceptor array. Polarized light differentially scattered by the Henle fibre layer could traverse the outer segments obliquely to produce brush-like effects (Weale 1976). Le Floch et al. (2010) proposed that differential attenuation arises through differential reflection of oblique polarized light from the surface of short-wavelength-sensitive cones, which have a lower density in the fovea, and therefore, it is claimed, have a greater exposure to oblique light. However, the existence of sufficient oblique light to generate this phenomenon in the retina remains speculative, and the sensitivity spectrum of macular dichroism (Bone et al. 1992) does not match the spectral sensitivity of human short-wavelength-sensitive cone photoreceptors, as would be expected if this hypothesis were the true explanation.

14.4 Corneal Birefringence, Circular Polarization and Haidinger's Brush

Shurcliff (1955) observed that circularly polarized light can also produce a brush, such that an observer can determine the handedness of circular polarization. Right-handed circularly polarized light reportedly produces a brush at approximately +45°, and left-handed circularly polarized light produces a brush at −45°. These fixed brushes have been referred to as 'Shurcliff's brushes', but this is potentially misleading as they have the same origins as Haidinger's brush. The effect can be simply explained by the presence of the birefringent cornea, acting as a quarter waveplate. Circularly polarized light incident on such a structure emerges linearly polarized at ±45° to the optical axis of the waveplate, and Haidinger's brush is perceived as before. In practice, the orientation of the optical axes and the retardation that the cornea introduces vary across the population. Knighton and Huang (2002) found that 80 % of subjects they measured had corneal retardance values in the range 0.03λ to 0.12λ for measurements taken at $\lambda = 585$ nm. Furthermore, the orientation of the fast and slow axes of the cornea varied by tens of degrees between individuals (Knighton and Huang 2002). Rigorous measurements of the angle at which a brush induced by circularly polarized light is perceived have not yet been undertaken, but the inter-individual variability in corneal parameters means that a brush fixed at exactly 45°, as would be produced by a quarter waveplate with fast and slow axes aligned horizontally and vertically, is more likely to be the exception than the rule.

The salience of Haidinger's brush is also expected to vary with orientation of the incident E-vector as a result of the birefringence of the cornea. Modelling the birefringent cornea and radially dichroic retina, Misson (2003) and Rothmayer et al. (2007) predicted an angle- and retardation-dependent contrast fluctuation with minimum contrast associated with linearly polarized light incident at 45° to the optical axes of the cornea, which introduces a retardation of a quarter of a wavelength. This is the reverse scenario to that described above: linearly polarized light is now converted to circularly polarized light and Haidinger's brush is abolished. Rothmayer et al. (2007) also predicted an increasingly nonlinear relationship between the E-vector angle of incident polarized light and the perceived angle of the brush as the retardation of the cornea approaches a quarter of a

wavelength. As a result, some observers may describe the brush 'jumping' or 'switching' as the incident E-vector rotates relative to the eye. The optical properties of the human cornea are still under investigation, with some authors reporting that it is best described as a curved dome of biaxial material (Knighton et al. 2008). If this is the case then the retardation and orientation of the optical axes will vary with position. To date, theoretical models of the dynamics of Haidinger's brush have not incorporated these more advanced models of corneal birefringence. von Helmholtz (1924) reported that when viewing linearly polarized light at various orientations, the width of Haidinger's brush changed. If the yellow brush was formed horizontally, it was narrower at its centre than when the yellow brush was vertical. Hochheimer and Kues (1982) speculated that this effect may also be due to the birefringence of the cornea.

14.5 Imaging Retinal Polarization Patterns: The Macular Cross

If the primate retina is photographed with the cornea removed and crossed linear polarizers in the stimulating and recording light paths, a 4–5° Maltese cross pattern can be observed overlying the macula, centred on the fovea (Hochheimer 1978). The macular cross pattern is produced when the illuminating polarized light is in the range 400–700 nm, but disappears for wavelengths longer than this (Hochheimer and Kues 1982). The formation of this cross pattern is due to a periodic refractive index variation between the Henle fibres and the Müller cells, which are in close apposition to them. This radial refractive index modulation produces uniaxial form birefringence with the slow optic axis directed along the length of the fibres (Brink and van Blokland 1988; Elsner et al. 2008). Macular birefringence is solely responsible for the cross pattern, but if the macula is imaged in the same way (with polarizers in the stimulating and recording light paths) but now through the birefringent cornea, then a brush-like pattern is obtained (Delori et al. 1979). The cross pattern is recovered when the E-vector of the incident light is aligned with either the slow or the fast axis of the cornea. The similar appearance of the macular cross to the entoptic phenomenon of Haidinger's brush has led to some confusion between (a) the radial birefringence and additional linear polarizer, which gives rise to the cross and (b) the radial dichroism that gives rise to the perception of Haidinger's brush.

Hochheimer and Kues (1982) tested several healthy human subjects and several patients with diseased retinae to establish whether they could see Haidinger's brush. All those who could see Haidinger's brush had an easily discernible macular cross, and those who could not see Haidinger's brush did not display any such retinal polarization pattern. If both effects are dependent on the radial arrangement of the Henle fibre layer (albeit with different physical origins), this correlation is to be expected. More recently, scanning laser polarimetry of the macular cross has been employed to identify the location of the fovea in babies and young subjects (Van Nasdale et al. 2009).

14.6 Boehm's Brush

There is another entoptic phenomenon that provides a means for the perception of polarized light, the so-called Boehm's brush, which is named after the German scientist Gundo von Boehm who first reported the effect in 1940. He described a visible rotating brush pattern of increased intensity that has its long axis oriented perpendicularly to the E-vector of a small (1–2°), rotating (1–2 Hz), linearly polarized light source, viewed in the peripheral visual field (15–20° parafoveally) against a dark background. Boehm's brush does not appear within the light source that causes it, but is perceived as a pattern of glare on either side of the image of the light source on the retina (Fig. 14.5). von Boehm (1940a, b) performed a range of tests to characterize the phenomenon and showed that the effect disappears instantly when rotation of the polarized light source stops. If the rotation is too fast, the ends of the observed brush lag behind creating a spiral-like effect. Under optimal viewing conditions, Boehm's brush may subtend an arc of up to 12° and, unlike Haidinger's brush, is perceived to be the same colour as the light source. The phenomenon is also visible when the light source is elliptically polarized, but becomes invisible as linearly polarized light becomes more circular (disappearing when ellipticity is above 0.8). It is equally salient in both right- and left-handed elliptically polarized conditions. Furthermore, von Boehm (1940a, b) showed that it is visible to people of all ages, as well as aphakics (people lacking lenses) and those suffering from various forms of colour blindness.

von Boehm (1940a, b) proposed that scattering within the retina gives rise to the phenomenon, which explains why the rotating brush pattern is oriented perpendicular to the orientation of the E-vector. When the light source is polarized, light interacting with the non-photosensitive layers of the retina will be preferentially scattered along an axis that is perpendicular to the E-vector orientation of the incoming light. Scattering should be strongest near the axis of the beam and decreases sharply with increasing angular distance. In support of his scattering hypothesis, Boehm (1940a, b) showed that the brush effect is weaker (narrower and shorter) at longer wavelengths. This would be expected if the brush is generated by a Rayleigh scattering process, which has a $1/\lambda^4$ dependence. He also showed that the brush takes on the same colour as the polarized light source, also consistent with the proposed scattering mechanism.

14.7 Applications of Human Polarization Sensitivity

Whilst human polarization sensitivity is not understood to have any direct behavioural significance, efforts have been made to make practical use of the phenomenon. A simple test based on a rotating polarized light field was developed to assess the potential clinical relevance of polarization sensitivity. The test consisted of a small light fitted with a blue filter and a rotating linear polarizer. Subjects were asked to identify the direction that the brush was rotating. Healthy

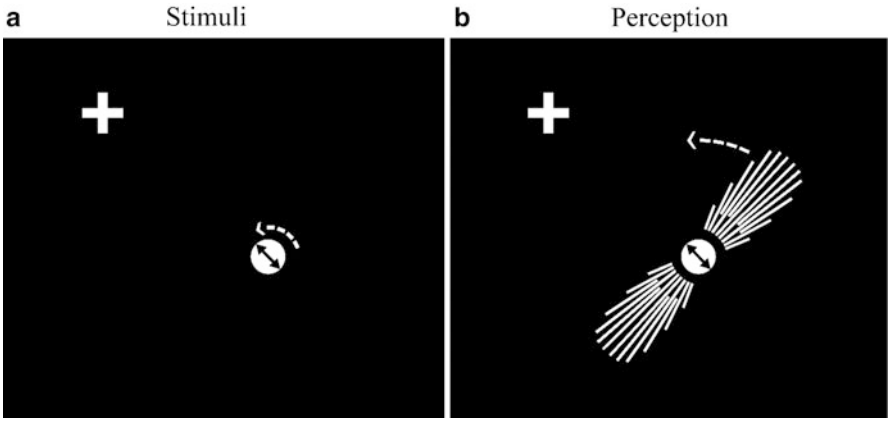

Fig. 14.5 Schematic representation of the conditions necessary to elicit the Boehm's brush phenomenon (**a**), and how it is perceived (**b**) relative to a linearly polarized light source (*circle with arrow inside*). The cross is the point of fixation. The *circle with arrow inside* represents a small (1–2°) linearly polarized light source rotating in the direction of the *broken arrow above the circle*, and positioned in the peripheral field of view. The rotating brush-like pattern in **b** has its long axis perpendicular to the E-vector of the rotating polarized light source

subjects and subjects with known existing eye diseases were tested (Schmidt 1938; Goldschmidt 1950; Forster 1954; Naylor and Stanworth 1955; Sloan and Naquin 1955). These studies revealed that perception of Haidinger's brush is normal in humans without visual defects. An inability to perceive Haidinger's brush is associated with disturbance of the macula and its surrounding structure, but this has proven to be of little use for differential diagnostic assessment. Recent studies have suggested that the human ability to perceive Haidinger's brush could be used to directly observe the optical activity of chiral molecules, the Faraday effect and the outcome of quantum entanglement experiments (Sekatski et al. 2009; Ropars et al. 2012a). Ropars et al. (2012b) suggested that the alleged sky-polarimetric Viking navigation could have been based on the perception of Haidinger's brush (see Chap. 25). Boehm's brush has been used to investigate intraocular scatter. Vos and Bouman (1964), for example, used the phenomenon to show that scatter from the retina itself accounts for between 12 and 40 % of the total scattered light inside the eye. Weale (1976) used Boehm's brush as a tool to investigate spectral aspects of the Stiles–Crawford effect.

A greater understanding of the structures and mechanisms giving rise to polarization sensitivity has the potential to generate future applications in biomedical science. It is also useful to note that the human ability to detect E-vector orientation is a great way to introduce the uninitiated to the study of polarized light!

References

Bhosale P, Larson AJ, Frederick JM, Southwick K, Thulin CD, Bernstein PS (2004) Identification and characterization of a pi isoform of Glutathione S-Transferase (GSTP1) as a zeaxanthin-binding protein in the macula of the human eye. J Biol Chem 279:49447–49454

Bone RA (1980) The role of the macular pigment in the detection of polarized light. Vis Res 20:213–220

Bone RA, Landrum JT (1983) Dichroism of lutein: a possible basis for Haidinger's brushes. Appl Opt 22:775–776

Bone RA, Landrum JT (1984) Macular pigment in Henle fiber membranes: a model for Haidinger's brushes. Vis Res 24:103–108

Bone RA, Landrum JT, Tarsis SL (1985) Preliminary identification of the human macular pigment. Vis Res 25:1531–1535

Bone RA, Landrum JT, Cains A (1992) Optical density spectra of the macular pigment in vivo and in vitro. Vis Res 32:105–110

Bone RA, Landrum JT, Hime GW, Cains A, Zamor J (1993) Stereochemistry of the human macular carotenoids. Investig Ophthalmol Vis Sci 34:2033–2040

Brink HB, van Blokland GJ (1988) Birefringence of the human foveal area assessed in vivo with Mueller-matrix ellipsometry. J Opt Soc Am A 5:49–57

De Vries HL, Spoor A, Jielof R (1953) Properties of the eye with respect to polarized light. Physica 19:419–432

Delori FC, Webb RH, Parker JS (1979) Macular birefringence. Invest Ophthalmol Vis Sci (Suppl, ARVO Abstr) 19:53

Denton EJ (1959) The contributions of the oriented photosensitive and other molecules to the absorption of the whole retina. Proc R Soc Lond B 150:78–94

Dodt E, Kuba M (1990) Visually evoked potentials in response to rotating plane-polarized blue light. Ophthalmic Res 22:391–394

Elsner AE, Weber A, Cheney MC, VanNasdale DA (2008) Spatial distribution of macular birefringence associated with the Henle fibers. Vis Res 48(26):2578–2585

Fairbairn MB (2001) Physical models of Haidinger's brush. J R Astron Soc Can 95:248–251

Forster HWJ (1954) The clinical use of the Haidinger's brushes phenomenon. Am J Ophthalmol 38:661–665

Fuld K, Wooten BR, Katz L (1979) The Stiles-Crawford hue shift following photopigment depletion. Nature 279:152–154

Goldschmidt M (1950) A new test for function of the *macula lutea*. Arch Ophthalmol 44:129–135

Gribakin FG, Govardovskii VI (1975) The role of the photoreceptor membrane in photoreceptor optics. In: Snyder AW, Menzel R (eds) Photoreceptor optics. Springer, Heidelberg, pp 215–236

Gruszecki WI, Strzalka K (2005) Carotenoids as modulators of lipid membrane physical properties. Biochim Biophys Acta 1740:108–115

Hemenger RP (1982) Dichroism of the macular pigment and Haidinger's brushes. J Opt Soc Am A 72:734–737

Hochheimer BF (1978) Polarized light retinal photography of a monkey eye. Vis Res 18:19–23

Hochheimer BF, Kues HA (1982) Retinal polarization effects. Appl Opt 21:3811–3818

Horváth G, Varjú D (2004) Polarized light in animal vision—polarization patterns in nature. Springer, Heidelberg

Knighton RW, Huang XR (2002) Linear birefringence of the central human cornea. Investig Ophthalmol Vis Sci 43:82–86

Knighton RW, Huang XR, Cavuoto LA (2008) Corneal birefringence mapped by scanning laser polarimetry. Opt Express 16:13738–13751

Laties AM, Liebman PA, Campbell CE (1968) Photoreceptor orientation in the primate eye. Nature 218:172–173

Le Floch A, Ropars G, Enoch J, Lakshminarayanan V (2010) The polarization sense in human vision. Vis Res 50:2048–2054
Lester G (1970) Haidinger's brushes and the perception of polarization: the history to the present of an on-going problem. Acta Psychol 34:106–114
Li B, Vachali P, Frederick JM, Bernstein PS (2011) Identification of StARD3 as a lutein-binding protein in the macula of the primate retina. Biochemistry 50:2541–2549
Liebman PA, Jagger WS, Kaplan MW, Bargoot FG (1974) Membrane structure changes in rod outer segments associated with rhodopsin bleaching. Nature 251:31–37
Maxwell JC (1850) Manuscript on experiments on the cause of Haidinger's brushes. The scientific letters and papers of James Clerk Maxwell. Taylor and Francis, London, pp 199–204
Misson GP (2003) A Mueller matrix model of Haidinger's brushes. Ophthalmic Physiol Opt 23:441–447
Naylor EJ, Stanworth A (1954) Retinal pigment and the Haidinger effect. J Physiol Lond 124:543–552
Naylor EJ, Stanworth A (1955) The measurement and clinical significance of the Haidinger effect. Trans Opthalmol Soc UK 75:67–79
Ovcharenko AP, Yegorenkov VD (2002) Teaching students to observe Haidinger brushes. Eur J Phys 23:123–125
Ropars G, Le Floch A, Enoch J, Lakshminarayanan V (2012a) Direct naked-eye detection of chiral and Faraday effects in white light. Europhys Lett 97:64002–64006
Ropars G, Gorre G, Le Floch A, Enoch J, Lakshminarayanan V (2012b) A depolarizer as a possible precise sunstone for Viking navigation by polarized skylight. Proc R Soc A 468:671–684
Rothmayer M, Dultz W, Frins E, Zhan Q, Tierney D, Schmitzer H (2007) Nonlinearity in the rotational dynamics of Haidinger's brushes. Appl Opt 46:7244–7251
Schalch W, Landrum JT, Bone RA (2009) The Eye. In: Britton G, Pfander H, Liaaen-Jensen S (eds) Carotenoids. Basel, Birkhäuser, pp 301–334
Schmidt WJ (1938) Polarisationsoptische Analyse eines Eiweiss-Lipoid-Systems, erlautert am Aussenglied der Sehzellen. Kolloid-Zeitschrift 85:137–148
Sekatski P, Brunner N, Branciard C, Gisin N, Simon C (2009) Towards quantum experiments with human eyes as detectors based on cloning via stimulated emission. Phys Rev Lett 103:113601–113604
Shurcliff WA (1955) Haidinger's brushes and circularly polarized light. J Opt Soc Am 45:399
Sloan LL, Naquin HA (1955) A quantitative test for determining the visibility of the Haidinger brushes: clinical applications. Am J Ophthalmol 40:393–406
Snodderly DM, Auran JD, Delori FC (1984) The macular pigment. II. Spatial distribution in primate retinas. Invest Ophthalmol Vis Sci 25:674–685
Stiles WS, Crawford BH (1933) The luminous efficiency of rays entering the eye pupil at different points. Proc R Soc Lond B 112:428–450
Stokes GG (1850) On Haidinger's brushes. British Association Reports, Edinburgh
Summers DM, Friedmann GB, Clements RM (1970) Physical model for Haidinger's brush. J Opt Soc Am 60:271–272
Van Nasdale DA, Elsner AE, Weber A, Miura M, Haggerty BP (2009) Determination of foveal location using scanning laser polarimetry. J Vis 9:1–17
von Boehm G (1940a) Über maculare (Haidinger'sche) Polarisationsbüschel und über einen polarisationsoptischen Fehler des Auges. Acta Ophthalmol (Copenhagen) 18:109–142
von Boehm G (1940b) Über ein neues entoptisches Phänomen im polarisierten Licht: "periphere" Polarisationsbüschel. Acta Ophthalmol (Copenhagen) 18:143–169
von Frisch K (1949) Die Polarisation des Himmelslichtes als orientierender Faktor bei den Tänzen der Bienen. Experientia 5:142–148
von Helmholtz H (1924) Treatise on physiological optics. In: Southall JPC (ed) Optical society of America., pp 301–308
Vos JJ, Bouman MA (1964) Contribution of the retina to entoptic scatter. J Opt Soc Am 54:95–100
Weale RA (1976) On the spectral sensitivity of the human retina to light which it has scattered. Vis Res 16:1395–1399
Zhevandrov ND (1995) Polarisation physiological optics. Physics-Uspekhi 38:1147–1166

Part II
Polarized Light in Nature with Implications to Animal Polarization Vision

Chapter 15
Underwater Polarization by Scattering Hydrosols

Amit Lerner

Abstract During more than six decades of underwater polarization research, polarization by hydrosols has got little attention. It was somewhat neglected by both optical oceanographers and marine biologists, because Rayleigh (molecular, sub-micronic) scattering was generally assumed as the main process determining the polarization field in water, similarly to the one in the atmosphere. Recent measurements and modeling have shown that the Rayleigh assumption is inaccurate, and instead Mie scattering (i.e. scattering by particles suspended in water, such as plankton and minerals of microns in size) should be considered as the dominating process, even in clear waters. This chapter focuses on the physical processes that determine the polarization in water, and presents the theoretical basis of scattering and radiative transfer which is needed to investigate and solve the effect of scattering particles of varied sizes and shapes on polarization, and the methods in use to measure it in situ. The chapter also reviews past studies on underwater polarization modeling and measurements, emphasizes the missing knowledge in the topic, and thus encourages future research.

15.1 Introduction

Polarization in water has got little attention in Horváth and Varjú (2004), who mainly concentrated on aquatic animals that perceive it, although the research in the water has been performed by optical oceanographers in parallel to the one in air along the last six decades since the pioneering polarization research of Karl von Frisch (1949, 1950, 1967) on honeybees. However, ocean optics did not always

A. Lerner (✉)
Ocean BioOptics and Vision Laboratory, Israel Oceanographic and Limnological Research, National Institute of Oceanography, Tel-Shikmona, POB 8030, Haifa 31080, Israel
e-mail: amit.lerner@ocean.org.il

G. Horváth (ed.), *Polarized Light and Polarization Vision in Animal Sciences*, Springer Series in Vision Research 2, DOI 10.1007/978-3-642-54718-8_15,

concentrate on polarization, but rather on the intensity, and has got attention mainly for the purposes of water-leaving radiance and remote sensing rather than for animal vision. Nonetheless, numerous in situ measurements of the underwater polarization field, modeling and reviews are available, most of them conducted and published in the last two decades. The knowledge about the influence of scattering hydrosols and water turbidity on the underwater polarization field is even more limited to date. It began with laboratory measurements by V.A. Timofeyeva in the 1960s (Timofeyeva 1961, 1962, 1969), who showed the striking effect of hydrosols on the polarization phase function (scattering function further on), the partial linear polarization and the electric (E-) vector orientation versus the scattering angle around the scatterer. This research has been followed by modeling by G.W. Kattawar and co-workers in the 1970s (e.g. Kattawar and Plass 1971, 1976; Kattawar et al. 1973). The research in this field did not advance much until its recent flourishing in the last decade with more in situ measurements and modeling referring to polarization under turbid conditions. This chapter summarizes the recent knowledge on the effect of water turbidity on the underwater polarization and provides insights on how and why scattering hydrosols alter the polarization state in water.

15.2 Sources for Polarized Light in Ocean

In water, light can be polarized or depolarized in many scenarios:

(1) The unpolarized direct sunlight and the partially linearly polarized skylight are further polarized by the transmission (refraction) of light at the water surface.

(2) Nearby the water surface, internal reflections polarize the upwelling partially linearly polarized light, making it partially circularly polarized (Kattawar 2013). However, this circular state does not hold for more than a few centimetres in water due to scattering by the water itself that changes the circular state to linear.

(3) In the same way, unpolarized light reflected from shiny (specular) surfaces underwater, such as fish scales, becomes partially linearly polarized by reflection, although scales of some fish were recently found to be non-polarizing due to a multi-layered structure including layers of low refractive index close to that of the water (Jordan et al. 2012).

(4) Related to the refraction effect is the polarization by surface waves that temporally alter the polarization of light below the water surface as they change the incident angle of the incoming radiation (Sabbah and Shashar 2006; Xu et al. 2011). The variability in the polarization domain is higher than that in the intensity domain, and is reduced with depth, suggesting a weakening of the wave effect on polarization with distance from the water surface.

(5) Next, the single scattering by water molecules (molecular scattering) increases the polarization in water. When multiple scattering events occur, e.g. with increasing water turbidity, the partial polarization decreases (You et al. 2011). Non-molecular scattering, i.e. scattering of ultraviolet-visible (UV–VIS: 350–650 nm) radiation by suspended hydrosol particles of micron size and

above ("large" particles) such as phytoplankton or suspended minerals/sand, will polarize and depolarize the light differently from the polarization by water molecules (Lerner et al. 2012). Therefore, the polarization field in clear water (molecular scattering assumed) will be different from that under turbid conditions (scattering by large particles assumed).

(6) Another important feature of scattering is that it is directional; that is, the amounts of energy and polarization scattered vary with the scattering angle around the scatterer. This is emphasized by the fact that the resulted polarization or depolarization of light occurs at different magnitudes at different scattering directions. This makes the underwater polarization field highly directional and non-homogeneous, a feature that may assist in navigation and orientation or avoiding predation by polarization-sensitive predators against the underwater polarized background.

(7) Finally, another source of depolarization in water is the non-spherical shape of scatterers. The fact that most of the scatterers in the water column are optically non-spherical (i.e. they possess axes that differently interact with the incoming radiation) depolarizes the light (Chang et al. 1999). As most of the suspended matter in ocean is non-spherical, this becomes an important source determining the polarization field in water.

The above scenarios can be categorized into two physical processes that alter the polarization state in water, refraction (reflection and transmission) and scattering. These two processes share a common physical entity, the refractive index. In both processes, the light is propagating through two media differing in their refractive indices: either the air and the water (transmission of light at the water surface) or the water medium and the scattering particle (e.g. plankton or suspended minerals, mainly sand in water). This is the basis of the effect of scattering and turbidity on the polarization state of light in water. Figure 15.1 shows the calculated effect of increasing difference Δm between the refractive indices of air and a medium on the maximum of partial polarization $p_{\max}$ resulted by the transmission process from air into the medium. The values of p were calculated by applying the Mueller matrix of transmission (from air into a medium of higher refractive index) to the Stokes vector of the incoming unpolarized radiation (for more details see Kattawar 1994). $p_{\max}$ increased with increasing the difference Δm between the refractive indices of the two media. However, only a change in the first digit ($\Delta m > 10$ %) of the refractive index (such as an air–water or water–plankton/sand–particles interactions) will cause a detectable effect on $p_{\max}$ of 7 % or above, which is the minimal polarization sensitivity threshold currently known for animals (Henze and Labhart 2007). Any physical parameter that changes Δm by the second digit of the refractive index ($\Delta m < 1$ %) will not have a noticeable effect on the partial polarization, at least not for the purposes of animal polarization vision. Such parameters are seawater salinity, temperature, pressure and the spectral change of seawater refractive index in the UV–VIS wavelength range, all changing the refractive index of seawater by less than 1 % (http://scubageek.com/articles/-wwwh2o.html and references therein).

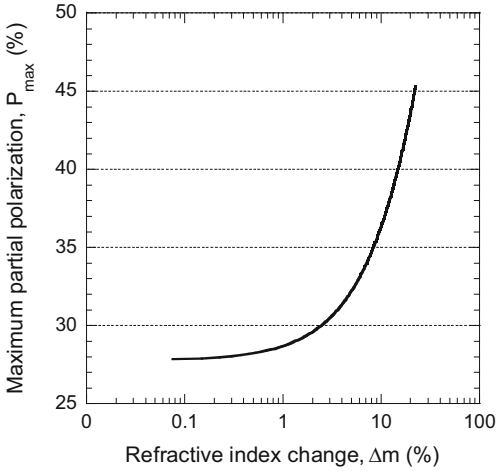

Fig. 15.1 Calculated change in the maximum partial polarization, p_{max}, by transmission of incoming unpolarized light from air to a medium with increasing change Δm of the refractive index. The angle of incidence was 90°. The value of the refractive index of the medium changed between 1.330 (water, no change) and 1.630 (22 % change) with increments of 0.001. Note that p_{max} is not changing for $\Delta m < 1$ % (second digit) and changes by 7 % (the sensitivity polarization threshold known for animals) only at $\Delta m > 10$ % (first digit)

15.3 Polarization by Transmission (Refraction)

Unpolarized sunlight or partially polarized skylight is refracted at the water surface. Figure 15.2 shows calculations (with the same method as in Fig. 15.1) of the partial polarization p and the E-vector orientation ψ for the transmission of light from air to water. The transmission (refraction) increases the polarization of unpolarized direct sunlight by up to 27 % with increasing zenith angle of incidence. This effect was found to be independent of the wavelength in the UV–VIS range as p varied by <0.5 % and ψ by <1°, which are below the polarization sensitivity threshold currently known for animals (Henze and Labhart 2007; Temple et al. 2012). For any given angle of incidence of sunlight, the E-vector orientation of light scattered in water is perpendicular to the plane of scattering defined by the underwater observer, the underwater point observed and the apparent sun seen from water through the Snell's window (see Fig. 14.1 of Horváth and Varjú 2004, p. 96). In addition, Lerner et al. (2011) confirmed theoretically and from in situ measurements that the position of the maximum value of E-vector orientation angle of light that has been refracted and singly scattered by water molecules is located at an azimuth angle that is 90° from the apparent sun bearing (90° from the azimuth angle of the sun; see Figs. 3 and 5c in Lerner et al. 2011). Furthermore, this maximum value of the E-vector orientation angle was found to be equal to the angle of transmission into the water, such that there is a correlation between the E-vector orientation and the elevation of the sun through Snell's law of refraction. The

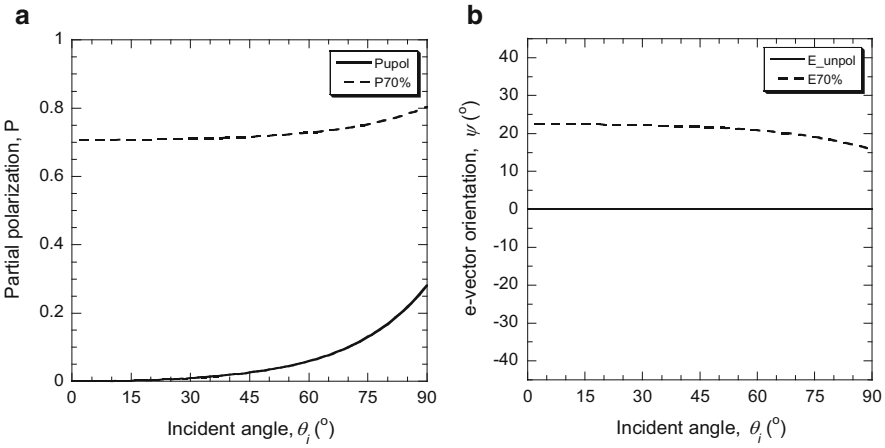

Fig. 15.2 Calculated change in the partial polarization p (**a**) and the E-vector orientation ψ (**b**) by transmission from air to water with increasing angle of incidence θ_i for unpolarized (*solid line*) and 70 % and 22.5° oriented partially polarized (*dashed line*) incoming radiation. A rotation matrix was not applied here to show the change in ψ by the transmission process. The refractive index of water was 1.335 (500 nm wavelength of pure water). p varied by <0.5 % and ψ by <1° at the UV–VIS wavelength range (350–650 nm), as the refractive index of water changed by the second digit only in that range. Note the small change in ψ of ~7° when the incoming light is 70 % partially polarized

correlation of the E-vector orientation with sun elevation allows it to be used as a sun compass for navigation (Lerner et al. 2011). However, this phenomenon was found to hold in clear waters only. Water turbidity alters the E-vector orientation of underwater scattered light, so that the E-vector orientation angle is no longer limited by the angle of transmission into the water. For partially polarized sunlight penetrating the water (e.g. skylight transmitted through Snell's window), the E-vector orientation varies as a function of both the angle of transmission and the partial polarization of the incoming light (Fig. 15.1b and see also Horváth and Varjú 1995).

15.4 Polarization by Attenuation (Scattering and Absorption): The Effect of Water Turbidity

As mentioned above, when light travels through two media, differing in their refractive indices, it becomes partially linearly polarized. The difference in the refractive indices does not relate only to the media scattering efficiency, but also to their absorption ability, as the refractive index is a complex number which represents the scattering and absorption efficiencies of the medium in its real and imaginary part, respectively. Absorption and scattering are complementary

processes in the sense that photons, being not absorbed, are scattered. This means that strong absorption can reduce the scattering effect on polarization.

In water, partially polarized light suffers scattering and absorption by water molecules and suspended contents in water (hydrosols) such as plankton or mineral particles. Note that while the water molecules are sub-micronic in size, the other scatterers can have all sizes from sub-micronic to tens and hundreds of microns and beyond. This difference in the size of scatterers relative to the wavelength impinging it dictates a difference in the light–particle interaction. To model these interactions and why and how the turbidity of water affects the light field and its polarization state, the Radiative Transfer Theory is applied. The starting point of this theory is the Beer–Lambert's (BL) law that describes the attenuation of light with distance in a medium.

15.4.1 Attenuation and the Beer–Lambert's Law

In its derivative form, the BL law states that the intensity $I(z)$ at a distance z is described by

$$\frac{\mathrm{d}I(z)}{\mathrm{d}z} = -kI(z), \tag{15.1}$$

where k is the attenuation coefficient. As one can immediately see, the light intensity I decreases with distance z, as both k and I are positive. Solving this derivative equation leads to the well-known BL exponential equation:

$$I(z) = I(z=0) \cdot e^{-kz}. \tag{15.2}$$

Equation (15.2) introduces us to a new fundamental parameter in scattering theory, the optical depth τ, which equals to $k\Delta z$, or in its integral form:

$$\tau(\lambda) = \int k(\lambda) \cdot \mathrm{d}z, \tag{15.3}$$

where λ is the wavelength of light. As one can see, $\tau(\lambda)$ depends on λ because of the dependence of k on the wavelength. This is important, because the dependence of the scattering and absorption efficiencies of each scatterer in the medium, including the water molecules themselves, varies with λ. The attenuation coefficient k depends on the number n of scatterers and absorbers and their effective cross section σ_{sca} and σ_{abs}, respectively. Then the attenuation coefficient k can be written as:

$$k = k_{\text{sca}} + k_{\text{abs}} = n_{\text{sca}}\sigma_{\text{sca}} + n_{\text{abs}}\sigma_{\text{abs}}. \tag{15.4}$$

Here the dependency on wavelength relays in the effective cross section σ, which is defined by

$$\sigma(\lambda) = \pi r^2 Q(\lambda), \tag{15.5}$$

where $Q(\lambda)$ is the scattering or absorption efficiency at wavelength λ. As one can see, σ depends not only on the geometric cross section (πr^2) but also on the scattering/absorption efficiency Q. This is why the effective cross section may be greater than 1 and can get as high as 4 for some particle-radius-to-wavelength ratios. This means that the effective area of the particles that contribute to the scattering and absorption of light is greater than its own geometric cross section. Figure 15.3 presents the dependency of the extinction (i.e. attenuation), absorption and scattering efficiencies on the radius-to-wavelength ratio. One can see that while the absorption efficiency Q_{abs} does not exceed its geometric cross section of 1, the scattering efficiency Q_{sca} does. The reason for this is that in particles with radius of the same order or higher than the impinging wavelength, new electric fields are induced inside the particle by the incoming radiation. These electric fields radiate outside the particle and interfere with the incoming radiation. This results in local maxima and minima (due to constructive and destructive waves of the impinging light) of the electric field around the particle (Fig. 15.3). Therefore, incoming photons are scattered from an area that is larger than the geometric cross section of the particle. In fact, the scattering efficiency depends on a more fundamental parameter, the size parameter $x = 2\pi r/\lambda$, where r is the scatterer's radius and λ is the wavelength of the incoming radiation. This parameter divides the scatterers to three scattering regimes named after the type of interaction of light with the scatterer (1) Rayleigh (molecular scattering: $x \ll 1$), (2) Mie ($x \approx 1$; after Gustav Mie, who first described the interaction mathematically in 1908), and (3) geometric ($x \gg 1$; as the scattering depends on the geometry of the scatterer).

Looking at the definition of x, it is clear that the relevant radius of the scatterer depends on what wavelength range we are dealing with. The Rayleigh scattering that occurs at sub-micronic scatterers for wavelength range of animal vision is characterized by a dipole distribution of the electric field radiating from the scatterer. This is why in this regime most of the radiation is scattered equally to the forward and backward directions. The partial polarization, on the other hand, is the highest (100 %) at 90° in respect to the propagation direction of light (scattering angle of 90°) and decreases to zero in the forward and backward directions. The Mie regime includes multiple dipole interactions due to the induced electric fields inside the particle. For vision purposes, the relevant Mie scatterer radii are one to few microns in size, which is relevant to many phytoplankton and small zooplankton species inhabiting the oceanic waters as well as minerals and sand particles. The Mie interaction is complex and its directionality is not trivial due to the interference effect. However, while most of the radiation is scattered forward from the Mie

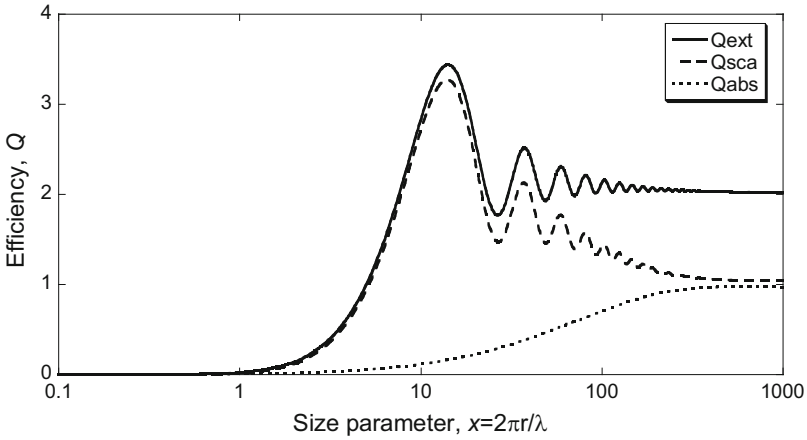

Fig. 15.3 Dependence of the scattering (Q_{sca}), absorption (Q_{abs}) and extinction (Q_{ext}, attenuation) coefficients on the size parameter $x = 2\pi/\lambda$ for a spherical particle. Particle refractive index $= 1.53 + 0.005i$ (sand), wavelength $= 450$ nm (in water), medium refractive index $= 1.337$ (water). Note the three different interactions (regimes) of Q_{ext} resulted in by the scattering efficiency Q_{sca} with x (a) increasing monotonously (Rayleigh scattering; $x < 10$; $r \ll \lambda$), (b) fluctuating due to interferences (Mie; $10 < x < 100$; $r \approx \lambda$) and (c) constant at value of 2 (geometric; $x > 500$; $r \gg \lambda$). The particle radius for $\lambda = 0.5$ μm is $r = 0.8$ μm. Note that efficiency value of 1 represents the particle geometric cross section πr^2. The data were generated using the MiePlot4.3 free software (Laven 2012)

particle, the polarization is maximally scattered to scattering angles slightly higher than 90° and relays somewhere between 90° and 100° scattering angle (You et al. 2011; Lerner et al. 2012). Surprisingly, this is what we found in polarization measurements in ocean (Sabbah et al. 2005; You et al. 2011). Therefore, it is clear now that the underwater polarization field is determined not only by the Rayleigh scattering as was broadly assumed but also by the Mie scattering. In the geometric regime (in which for vision purposes the relevant scatterer radii are of 50 μm and above) most of the radiation is scattered to the forward direction, but the highest polarization values are achieved at scattering angles lower than 90° (Lerner et al. 2012).

The nice thing about the optical depth τ is that it is more fundamental than the attenuation coefficient k or the distance z through which the light passes; therefore, it can be used to compare light attenuation at different water bodies or different depths and distances in water, respectively. So now the BL equation can be written in terms of the optical depth as

$$I(\tau) = I(0) \cdot e^{-\tau(\lambda)}. \tag{15.6}$$

Now it is clear how the depletion of radiation depends on increasing depth or distance in water (Δz) and hydrosol concentration [as k depends on the particle concentration n; see Eq. (15.4)]. The reason for dwelling on this rather simple equation is that it is now in general use by biologists and physicists looking into

polarization decay in water (Schechner and Karpel 2004; Johnsen et al. 2011; Shashar et al. 2011). However, the use of the BL equation in scattering medium is not appropriate, since it does not include scattered light reaching the sensor or the observer from directions other than the measurement optical axis (the line between the light source and the sensor). To obtain the exact amount of light propagating in scattering media, the Radiative Transfer Equation needs to be used and solved.

15.5 The Vector Radiative Transfer Equation

The Vector Radiative Transfer Equation (VRTE) is derived from the BL equation and is extensively used in modeling of the radiation field in scattering media [for review see Sabbah et al. (2005)]. Its most basic form is the following:

$$\mu \frac{\mathrm{d}\underline{I}(\tau,\mu,\phi)}{\mathrm{d}\tau} = \underline{I}(\tau,\mu,\phi) - \frac{\varpi}{4\pi}\int_0^{2\pi}\left[\int_0^1 \underline{\underline{M}}(\mu',\phi',\mu,\phi)\cdot\underline{I}(\tau,\mu',\phi')\cdot \mathrm{d}\mu'\right]\mathrm{d}\phi', \tag{15.7}$$

where $\underline{I}$ is the Stokes vector that represents the three qualities of light: intensity, colour and polarization. The four components of this vector represent the intensity, partial linear polarization, linear polarization orientation and circularity of polarization (how much the radiation is circularly polarized). The colour is represented by the fact that all parameters in the VRTE, including the four components of $\underline{I}$, are wavelength dependent. The directionality of light is represented by μ (which is the cosine of the zenith angle θ) and the azimuth angle ϕ. The tagged (by $'$) and untagged parameters represent the incoming and scattered (outgoing) directions, respectively. Therefore, μ is the cosine of the scattering angle, which is calculated from the four angles of the incoming and scattering directions (μ', ϕ', μ, ϕ) using the cosine equation. The important addition of the VRTE to the BL law is the second term on the right side of (15.7), which describes the scattering source function. The single-scattering albedo ϖ emphasizes the scattering-to-absorption ratio and ranges between 0 and 1. $\underline{\underline{M}}$ is the 4×4 Mueller matrix that describes the type of interaction (e.g. reflection, transmission or scattering) between the incoming light and the particle. It is applied to the incoming radiation as represented by the Stokes vector $\underline{I}(\tau, \mu', \phi')$. The scattering function represents information of light coming to the observer or the measuring device from other sources than the main source of light. In the ocean, the main light source can be the sunlight, while the other sources may be the downwelling light from the sky, the upwelling light from the ocean or the veiling light scattered from above and into the visual pathway between the main light source or target and the observer. The Mueller matrix can be measured in situ and in many studies it is the only feature that is being presented.

15.6 Measurements and Modeling of Polarization in Clear and Turbid Waters

Both modeling and in situ measurements of underwater polarization were scarcely performed over the years and mainly for the purposes of remote sensing which concentrated on the upwelling and water-leaving radiation at shallow depths near the water surface. The first measurements were obtained by the pioneer of underwater polarization research, Waterman (1954) together with the oceanographers Ivanoff (1956) and Jerlov (1963) [see review in Horváth and Varjú (2004) and Sabbah et al. (2005)]. In a set of measurements conducted in the 1950s, they investigated the E-vector orientation ψ and partial polarization p in water. They showed that p can reach values as high as 40 % at certain viewing directions in great depths down to 200 m. They also found that the ψ-pattern which can be used as sun compass for navigation in water is different in the upwelling and downwelling hemispheres, which could be the result of the strong attenuation and large optical depth of upwelling light. They also obtained that the ψ-patterns inside and outside the Snell's window are not similar, which was confirmed later on by Sabbah et al. (2006), who showed a resemblance between the inside pattern and the celestial E-vector pattern. The outside E-vector orientation was found by Lerner et al. (2011) to be dominated by the direct sunlight and water turbidity. In the 1960s, Timofeyeva (1961, 1962, 1969) showed in in situ and laboratory measurements that turbidity changes the p-pattern.

The next leg of measurements was reported only more than 30 years later by Shashar et al. (2004), who measured polarization in tempered clear and semi-turbid waters at shallow depths down to 15 m. They showed that the maximum polarization $p_{\max}$ near the water surface in clear water reaches 50–60 % (Sabbah et al. 2005; Sabbah and Shashar 2007; Voss and Souaidia 2010). At 15 m depth in semi-turbid waters, Cronin and Shashar (2001) reported that $p_{\max}$ ranges between 25 and 40 % and does not vary with wavelength, although later on Sabbah et al. (2006) and Sabbah and Shashar (2007) claimed for significant dependence of p and ψ on wavelength mainly outside the Snell's window. The horizontal distance (10 m) in which a fully polarized target is becoming unpolarized in turbid seawater was found to be shorter by 2/3 s of that (15 m) under clear conditions (Shashar et al. 2004).

The refractive index of phytoplankton-containing chlorophyll is about 1.43 (Stramski et al. 2001), while the refractive index of minerals (such as sand) is 1.53 (Sinyuk et al. 2003). Using numerical simulations, Lerner et al. (2012) showed that an increase in the refractive index of particle community of varied sizes including Mie particles causes a decrease in $p_{\max}$ and shifts the polarization maximum to higher scattering angles than 90°. Increasing the chlorophyll concentration in planktonic particles was also found to depolarize the light (Chami et al. 2001). These predictions were confirmed from Radiative Transfer modeling and in situ measurements conducted by Tonizzo et al. (2009) and You et al. (2011). Lerner et al. (2012) also showed that increasing the amount of Mie particles causes a decrease in $p_{\max}$, and its location is shifted to scattering angles between 90° and

100°. However, when the amount of geometric particles is increased, p_{max} is increased and its location shifts to scattering angles lower than 90°. Therefore, the Mie particles (with radii around 1–10 μm for vision purposes) depolarize the light, while Rayleigh (sub-micronic scatterers) and geometric particles (with radii above 50 μm) act to reduce the Mie scattering effect and increase the partial polarization.

15.7 Polarization-Based Response of Animals in Turbid Waters

While the common thinking is that turbidity should lower animal visual performance, some evidences exist that, as far as polarization vision is concerned, this may not always be the case. It is well known that by using linearly polarizing filters, the intensity contrast of unpolarized or weakly polarized objects (such as clouds) against the strongly polarized background (such as certain regions of the sky) can be enhanced (Pomozi et al. 2001; Suhai and Horváth 2004; Hegedüs et al. 2007a, b; see also Chap. 18). When we look at the cloudy sky at hazy days, we see the clouds better with polarizing sunglasses. However, if the sky is clear, the intensity contrast will not be increased much by polarized sunglasses.

Bainbridge and Waterman (1958) observed that the 90° orientation of Mysid crustaceans to the transmission axis of polarized stimuli was performed only under turbid conditions. In clear water, however, Mysids were disoriented. They suggested that this happened, because the Mysids could not increase the intensity contrast using their polarization analyzers in clear water, therefore could not detect the axis of transmission based on intensity differences. Supportive evidence to this phenomenon was recently presented by Cartron et al. (2013a, b) who performed object detection tests on cuttlefish in clear and turbid waters. The animals showed high detecting performance in turbid water, while their detection efficiency in clear water was low and did not differ between the intensity and polarization domains. These studies support the concept that using polarization vision to improve object detection is more relevant under turbid conditions than in clear waters. However, the positive effect of turbidity on the object detection and orientation cannot remain while turbidity continues to increase. At high turbidity levels, which were not checked in the above-mentioned studies, the turbidity will destroy the difference both in intensity and polarization between the object and its surrounding. This should diminish the contrast at the two domains and decrease the detection efficiency.

15.8 Concluding Remarks

There is no doubt that the knowledge on the effect of turbidity on underwater polarization is still in its infant stage. Although some work has been done in recent years both in modeling and measurements, many questions, mainly biologically related, await further research, for example, how polarization-sensitive aquatic animals perform under turbid conditions in terms of signaling and communication, predation and mate detection and navigation. Turbidity should have an optimal effect on animal behaviour, that is, it should improve vision up to a point where any increase in turbidity leads to a reduction in visual behaviour. However, this optimal hypothesis may not be valid to all polarization conditions or polarization-related behaviour. To date, turbidity effects were checked mainly qualitatively, while only turbid and clear conditions were applied. Instead, future studies should include quantitative investigations and several levels of turbidity to show if the above hypothesis holds or not.

On the physical side, it is still unclear how turbidity affects polarization and its distribution with wavelength, as contradictive evidences are available from modeling and measurements. It needs to be defined what is the detectable change, as it depends on the visual system perceiving the light. Different scatterers may cause different changes to the partial polarization and E-vector orientation depending on their spectral refractive efficiencies. The effect of coated particles (i.e. particles that contain layers of more than one refractive index) on polarization has been poorly studied. Although addressed by You et al. (2011), it is still not completely clear how important multiple scattering is to explain the polarization field under turbid conditions. The effect of non-sphericity of the scatterers, especially in the Mie and geometric regimes, is not fully understood. Finally, more in situ measurements at water bodies of various turbidity levels of different particles and with different depths are needed to reveal the effect of turbidity on the underwater polarization field.

Acknowledgements The author's studies were supported by the Israel Science Foundation (grants 1314/10 and 1081/10).

References

Bainbridge R, Waterman TH (1958) Turbidity and the polarized light orientation of the crustacean Mysidium. J Exp Biol 35:487–493

Cartron L, Josef N, Lerner A, McCusker SD, Darmaillacq AS, Dickel L, Shashar N (2013a) Polarization vision can improve object detection in turbid waters by cuttlefish. J Exp Mar Biol Ecol 447:80–85

Cartron L, Shashar N, Dickel L, Darmaillacq AS (2013b) Effects of stimuli shape and polarization in evoking deimatic patterns in the European cuttlefish, Sepia officinalis, under varying turbidity conditions. Invertebr Neurosci 13:19–26

Chami M, Santer R, Dilligeard E (2001) Radiative transfer model for the computation of radiance and polarization in an ocean-atmosphere system: polarization properties of suspended matter for remote sensing. Appl Opt 40:2398–2416

Chang PCY, Walker JG, Jakeman E, Hopcraft KI (1999) Polarization properties of light multiply scattered by non-spherical Rayleigh particles. Wave Random Media 9:415–426

Cronin TW, Shashar N (2001) The linearly polarized light field in clear, tropical marine waters: spatial and temporal variation of light intensity, degree of polarization and e-vector angle. J Exp Biol 204:2461–2467

Hegedüs R, Åkesson S, Wehner R, Horváth G (2007a) Could Vikings have navigated under foggy and cloudy conditions by skylight polarization? On the atmospheric optical prerequisites of polarimetric Viking navigation under foggy and cloudy skies. Proc R Soc A 463:1081–1095

Hegedüs R, Åkesson S, Horváth G (2007b) Polarization patterns of thick clouds: overcast skies have distribution of the angle of polarization similar to that of clear skies. J Opt Soc Am A 24: 2347–2356

Henze MJ, Labhart T (2007) Haze, clouds and limited sky visibility: polarotactic orientation of crickets under difficult stimulus conditions. J Exp Biol 210:3266–3276

Horváth G, Varjú D (1995) Underwater refraction-polarization patterns of skylight perceived by aquatic animals through Snell's window of the flat water surface. Vis Res 35:1651–1666

Horváth G, Varjú D (2004) Polarized light in animal vision—polarization patterns in nature. Springer, Heidelberg

Ivanoff A (1956) Degree of polarization of submarine illumination. J Opt Soc Am 46:362

Jerlov NG (1963) Optical oceanography. Oceanogr Mar Biol Ann Rev 1:89–114

Johnsen S, Marshall NJ, Widder EA (2011) Polarization sensitivity as a contrast enhancer in pelagic predators: lessons from in situ polarization imaging of transparent zooplankton. Philos Trans R Soc B 366:655–670

Jordan TM, Partridge JC, Roberts NW (2012) Non-polarizing broadband multilayer reflectors in fish. Nat Photonics 6:759–763

Kattawar GW (1994) Polarization of light in the ocean. In: Spinrad RW, Carder KL, Perry MJ (eds) Ocean optics. Oxford University Press, New York, NY, pp 202–225

Kattawar GW (2013) Genesis and evolution of polarization of light in the ocean. Appl Opt 52: 940–948

Kattawar GW, Plass GN (1971) Radiance and polarization of light reflected from optically thick clouds. Appl Opt 10:74–80

Kattawar GW, Plass GN (1976) Asymptotic radiance and polarization in optically thick media: ocean and clouds. Appl Opt 15:3166–3178

Kattawar GW, Plass GN, Guinn JA Jr (1973) Monte Carlo calculations of the polarization of radiation in the Earth's atmosphere-ocean system. J Phys Oceanogr 3:353–372

Laven P (2012) MiePlot v4.3. http://www.philiplaven.com/mieplot.htm

Lerner A, Sabbah S, Erlick C, Shashar N (2011) Navigation by light polarization in clear and turbid waters. Philos Trans R Soc B 366:671–679

Lerner A, Shashar N, Haspel C (2012) Sensitivity study on the effects of hydrosol size and composition on linear polarization in absorbing and nonabsorbing clear and semi-turbid waters. J Opt Soc Am A 29:2394–2405

Pomozi I, Horváth G, Wehner R (2001) How the clear-sky angle of polarization pattern continues underneath clouds: full-sky measurements and implications for animal orientation. J Exp Biol 204:2933–2942

Sabbah S, Shashar N (2006) Underwater light polarization and radiance fluctuations induced by surface waves. Appl Opt 45:4726–4739

Sabbah S, Shashar N (2007) Light polarization under water near sunrise. J Opt Soc Am A 24: 2049–2056

Sabbah S, Lerner A, Erlick C, Shashar N (2005) Underwater polarization vision: a physical examination. In: Pandalai SG (ed) Recent research development in experimental and theoretical biology, vol 1. Transworld Research Network, Kerala, India, pp 123–176

Sabbah S, Barta A, Gál J, Horváth G, Shashar N (2006) Experimental and theoretical study of skylight polarization transmitted through Snell's window of a flat water surface. J Opt Soc Am A 23:1978–1988

Schechner YY, Karpel N (2004) Clear underwater vision. In: Proceedings of the 2004 I.E. computer society conference on computer vision and pattern recognition, vol 1. Proceedings—IEEE computer society conference on computer vision and pattern recognition. IEEE Computer Soc, Los Alamitos, pp 536–543

Shashar N, Sabbah S, Cronin TW (2004) Transmission of linearly polarized light in seawater: implications for polarization signaling. J Exp Biol 207:3619–3628

Shashar N, Johnsen S, Lerner A, Sabbah S, Chiao CC, Mathger LM, Hanlon RT (2011) Underwater linear polarization: physical limitations to biological functions. Philos Trans R Soc B 366:649–654

Sinyuk A, Torres O, Dubovik O (2003) Combined use of satellite and surface observations to infer the imaginary part of refractive index of Saharan dust. Geophys Res Lett 30:51–54

Stramski D, Bricaud A, Morel A (2001) Modeling the inherent optical properties of the ocean based on the detailed composition of the planktonic community. Appl Opt 40:2929–2945

Suhai B, Horváth G (2004) How well does the Rayleigh model describe the E-vector distribution of skylight in clear and cloudy conditions? A full-sky polarimetric study. J Opt Soc Am A 21:1669–1676

Temple SE, Pignatelli V, Cook T, How MJ, Chiou TH, Roberts NW, Marshall NJ (2012) High-resolution polarisation vision in a cuttlefish. Curr Biol 22(4):R121–R122

Timofeyeva VA (1961) On the problem of polarization of light in turbid media. Izvestiya Akad Nauk SSSR Geophys 5:766–774

Timofeyeva VA (1962) Spatial distribution of the degree of polarization of natural light in the sea. Izvestiya Akad Nauk SSSR Geophys 6:1843–1851

Timofeyeva VA (1969) Plane of vibrations of polarized light in turbid media. Izvestiya Akad Nauk SSSR Atmos Ocean Phys 5:603–607

Tonizzo A, Zhou J, Gilerson A, Twardowski MS, Gray DJ, Arnone RA, Gross BM, Moshary F, Ahmed SA (2009) Polarized light in coastal waters: hyperspectral and multiangular analysis. Opt Express 17:5666–5683

von Frisch K (1949) Die Polarisation des Himmelslichtes als orientierender Faktor bei den Tänzen der Bienen. Experientia 5:142–148

von Frisch K (1950) Die Sonne als Kompass im Leben der Bienen. Experientia 6:210–221

von Frisch K (1967) The dance language and orientation of bees. Harvard University Press, Cambridge, MA

Voss KJ, Souaidia N (2010) POLRADS: polarization radiance distribution measurement system. Opt Express 18:19672–19680

Waterman TH (1954) Polarization patterns in submarine illumination. Science 120:927–932

Xu Z, Yue DKP, Shen L, Voss KJ (2011) Patterns and statistics of in-water polarization under conditions of linear and nonlinear ocean surface waves. J Geophys Res 116:C00H12

You Y, Tonizzo A, Gilerson AA, Cummings ME, Brady P, Sullivan JM, Twardowski MS, Dierssen HM, Ahmed SA, Kattawar GW (2011) Measurements and simulations of polarization states of underwater light in clear oceanic waters. Appl Opt 50:4873–4893

Chapter 16
Polarization Patterns of Freshwater Bodies with Biological Implications

Gábor Horváth

Abstract In this chapter we show that the polarization visibility of water surfaces is an important factor in the colonization of aquatic habitats by flying water beetles using horizontal polarization of water-reflected light to seek potential locations. After mowing of cattail (*Typha* sp.), for example, in freshwater marshes, aquatic beetles become more abundant due to the higher water temperature and the enhanced polarization visibility of the water surface. Here we also show that it is worth flying at dusk for aquatic insects, because the polarotactic water detection is easiest at low solar elevations. Polarotactic water insects interpret a surface as water if the degree of linear polarization of reflected light is higher than a threshold and the deviation of the direction of polarization from the horizontal is lower than a threshold. At sunrise and sunset the polarization visibility of water surfaces is maximal. Thus, the risk that a polarotactic insect will be unable to recognize the surface of a dark or bright water body is minimal at low solar elevations. The daily change in the reflection-polarization pattern of water surfaces is an important visual ecological factor that contributes to the preference of the twilight period for habitat searching by polarotactic water insects. Air temperature at sunrise is generally low, so dusk is one of the optimal periods for polarotactic aquatic insects to seek new habitats.

Electronic supplementary material is available in the online version of this chapter at 10.1007/978-3-642-54718-8_16. The supplementary figures can also be accessed at http://extras.springer.com, the videos at http://www.springerimages.com/videos/978-3-642-54717-1.

G. Horváth (✉)
Environmental Optics Laboratory, Department of Biological Physics, Physical Institute, Eötvös University, Pázmány sétány 1, 1117 Budapest, Hungary
e-mail: gh@arago.elte.hu

G. Horváth (ed.), *Polarized Light and Polarization Vision in Animal Sciences*, Springer Series in Vision Research 2, DOI 10.1007/978-3-642-54718-8_16,

16.1 Polarization Patterns of Freshwater Bodies Guiding the Water Detection of Aquatic Insects

Under a clear sky at a given solar elevation angle θ, the reflection-polarization characteristics of water bodies depend on two components of returned light. (1) The first component is the light reflected from the water surface. This component results in a complex reflection-polarization pattern (Schwind and Horváth 1993; Horváth 1995; Gál et al. 2001) determined by the celestial polarization pattern and the Fresnel formulae for light reflection. The direction of polarization of this first partially linearly polarized component is always horizontal except in small regions within the Brewster circle,[1] and if the angle of reflection is equal to the Brewster angle, it is totally linearly polarized (with degree of polarization $d = 100$ %). (2) The second component is the light originating from below the water surface due to reflection from the bottom of water or to backscattering from particles suspended in water. This second component is always partially vertically polarized due to refraction at the water surface (Horváth and Varjú 1995; Horváth and Pomozi 1997). The net degree and direction of polarization of light returned by a water body are determined by the states of polarization and the relative intensities of both components (Horváth and Varjú 1997; Bernáth et al. 2002, 2004; Molnár et al. 2011). Since these two components have orthogonal directions of polarization, their superposition reduces the net degree of polarization d. If the intensity of the first component is greater than that of the second one, the returned light is partially linearly polarized with horizontal direction of polarization. When the second component is more intense, the returned light is partially vertically polarized. If the intensities of these two components are approximately equal, the returned light is nearly unpolarized. In the Extra Materials for this chapter, the reflection-polarization patterns of numerous different water bodies can be seen.

The influence of the reflection-polarization patterns of open water surfaces on aquatic beetle assemblages has been demonstrated by Molnár et al. (2011), who showed the practical importance of cattail mowing that changes advantageously the relevant environmental factors determining the aerial colonization of aquatic habitats. Cattails (*Typha* spp.) often cause conservation problems, because their dense, monotypic stands exclude other wetland-dependent plant species, waterfowl (Anseriformes) and shorebirds (Charadriiformes) (Kostecke et al. 2004), due to the reduced open water surface (Ball 1990), even where cattails are native (Kercher and Zedler 2004). Previous studies predicted that cattail may exclude water beetle species from aquatic habitats for the following two main reasons:

1. Emergent vegetation, and thus also cattail stands, may shade the water from direct sunlight and thus reduce the water temperature (DeBusk and DeBusk

[1] At the Brewster angle θ_{Brewster} (=arctan $n \approx 53°$ from the vertical for the refractive index $n = 1.33$ of water), the surface-reflected ray of light is perpendicular to the refracted ray penetrating into water.

2000), the consequence of which is the increase of the larval developmental time of aquatic insects (Nilsson and Söderstrom 1988; Fairchild et al. 2003).

2. When positively polarotactic aquatic insects seek their habitats by aerial colonization flight, the horizontally polarized light reflected from the water surface provides the major optical signal for habitat detection from a remote distance (Schwind 1991, 1995; Wildermuth 1998; Horváth and Varjú 2004; Horváth and Kriska 2008). If emergent cattail cover is relatively dense, the horizontally polarized optical signal is weak, and aquatic beetles may fail to detect the water surface, whilst less screened waters may be easier to find (Nilsson and Svensson 1995; Lundkvist et al. 2001). Removing emergent vegetation strongly increases the open water surface in mowed plots, affecting the visibility. Visibility here means not simply the view of the glittering water surface, because aquatic insects generally find water by means of positive polarotaxis, rather than by the colour and intensity of reflected light (Schwind 1991, 1995). Horizontally polarized light can be reflected towards flying polarotactic water insects only from vegetation-free regions of the water surface. The optical availability of horizontally polarizing open water surfaces for flying polarotactic aquatic insects is called the 'polarization visibility' (Molnár et al. 2011).

Mowing is a conventional management technique to decrease the negative impacts of cattail (Ball 1990). Although Murkin et al. (1982) investigated the effect of cattail mowing on aquatic invertebrates, they considered it only as a food resource of waterfowl. Molnár et al. (2011) examined the response of aquatic beetle assemblages to the mowing of cattail (*Typha angustifolia* L., *T. latifolia* L.) in a freshwater marsh. Following removal of cattail by mowing at the water level in experimental plots (10 m × 10 m), aquatic beetles were sampled both in 5 mowed and 5 intact (control) plots weekly, through a month in the spring of 2008. Molnár et al. (2011) found that aquatic beetles were more abundant in mowed plots. Species richness was the same, but it showed different patterns in mowed and intact plots: 29 % of the aquatic beetles showed a strong preference for mowed plots, and 15 % preferred the control plots. Among the measured environmental factors (temperature, electrical conductivity and pH of water), water temperature was an important factor, with mowed plots having higher water temperatures because of increased solar radiation. Neither conductivity nor pH of water was affected by mowing (Molnár et al. 2011).

Polarization visibility of the water surface was also a relevant factor, since aerially colonizing (flying) aquatic beetles use horizontally polarized light reflected from the water surface to seek potential locations (see Sect. 5.1). An area of the water surface is sensed as water by a flying polarotactic aquatic insect, if (1) the degree of linear polarization d of water-reflected light is higher than a threshold d^* and (2) the deviation $\Delta\alpha = |90^\circ - \alpha|$ of the angle of polarization α from the horizontal is smaller than a threshold $\Delta\alpha^*$ (Horváth and Varjú 2004; Kriska et al. 2009). Both thresholds d^* and $\Delta\alpha^*$ may be species specific and wavelength dependent. As examples, in Figs. 16.1 and 16.2 (as well as in Supplementary Figs. 16.1, 16.2, 16.3, 16.4, 16.5, 16.6, 16.7, 16.8, 16.9, 16.10, 16.11, 16.12,

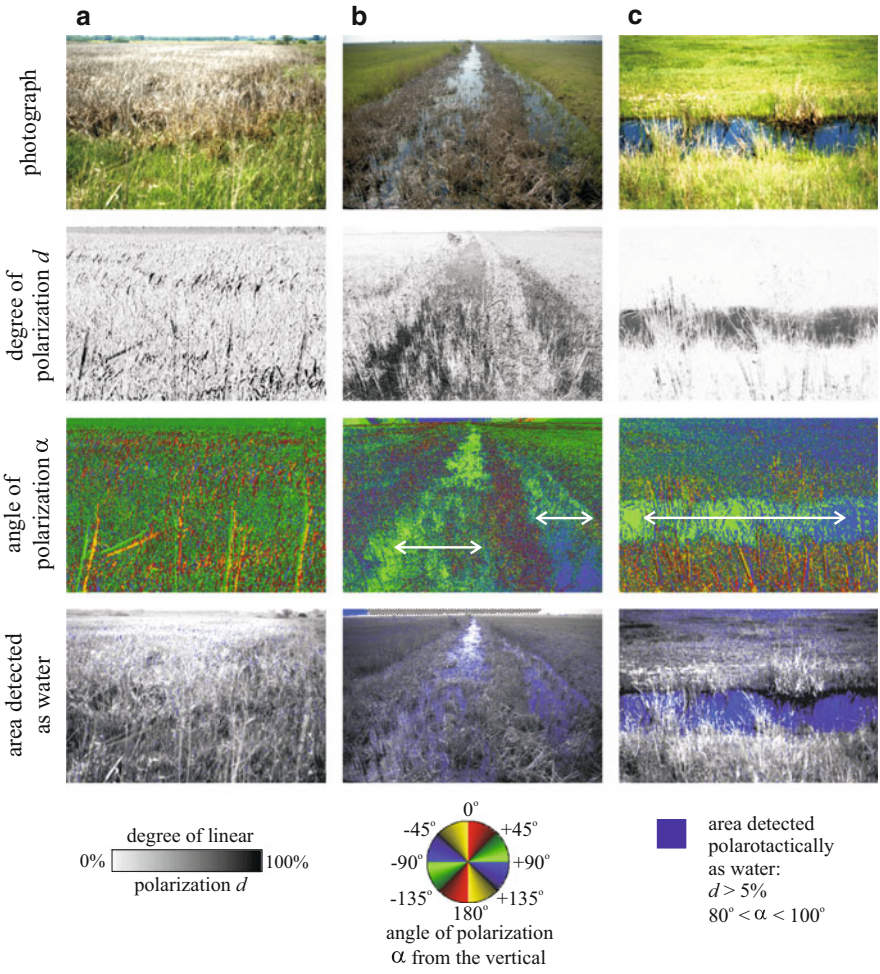

Fig. 16.1 Photographs, patterns of the degree d and angle α (clockwise from the vertical) of linear polarization and areas detected polarotactically as water (for which $d > 5$ % and $80° < \alpha < 100°$) of different water bodies measured by imaging polarimetry in the blue (450 nm) part of the spectrum. In the α-patterns *double-headed arrows* show the local and dominant directions of polarization. The angle of elevation of the optical axis of the polarimeter was $-35°$ from the horizontal. (**a**) A water surface that is totally covered by cattail. (**b**) A water channel, the surface of which is partly covered by cattail. (**c**) Another water channel, the surface of which is open (without water plants) [after Fig. 1 on page 393 of Molnár et al. (2011)]

16.13, 16.14, 16.15, 16.16, 16.17, 16.18, 16.19, 16.20, 16.21, 16.22, 16.23, 16.24, 16.25, 16.26, 16.27, 16.28, 16.29, 16.30, 16.31 and 16.32), $d^* = 10$ % and $\Delta\alpha^* = 10°$ were used. Although these threshold values are arbitrary, the use of other values does not influence qualitatively the main conclusions of Molnár et al. (2011).

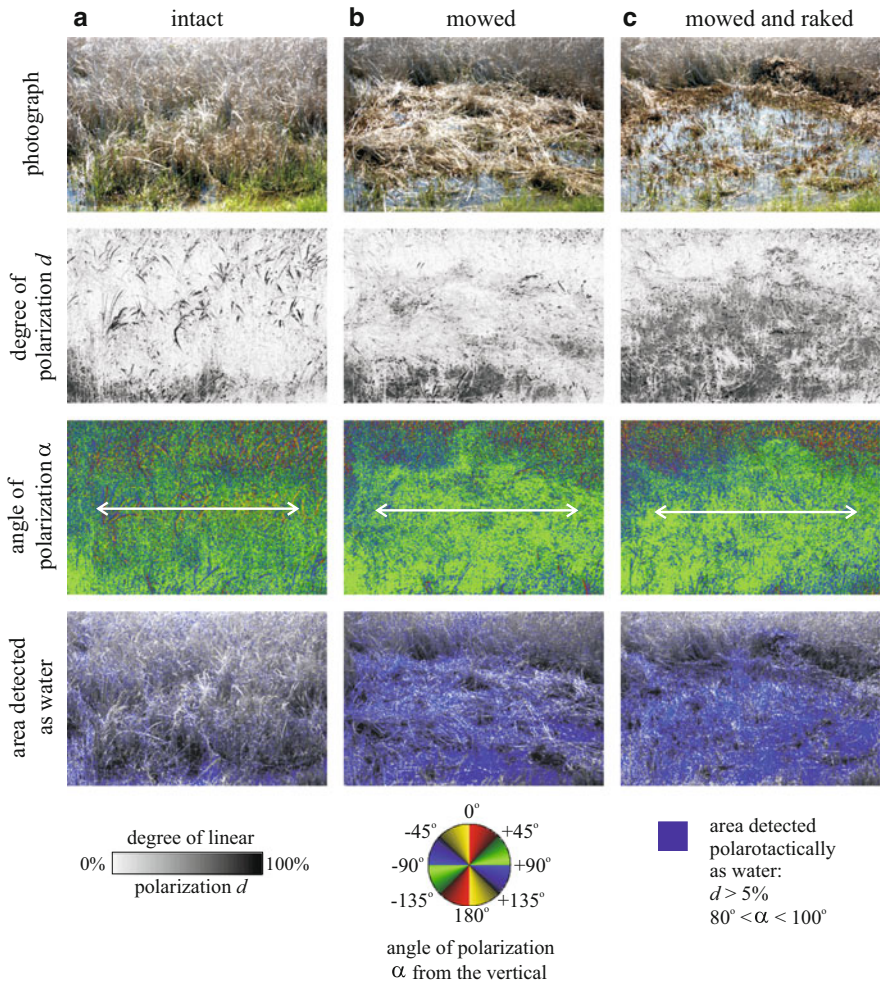

Fig. 16.2 As Fig. 16.1 for a region of a water body, when it was almost totally covered by cattail (**a**), it was covered by the mowed cattail (**b**), and the mowed cattail was raked away (**c**) [after Fig. 2 on page 394 of Molnár et al. (2011)]

The quantitative measure of polarization visibility is the proportion Q of the area (relative to a given region of the scene) detected polarotactically as water, for which $d > d^*$ and $\Delta\alpha = |90^\circ - \alpha| < \Delta\alpha^*$. Using imaging polarimetry, Molnár et al. (2011) showed that mowing strongly enhances the water-reflected polarized light signal (Figs. 16.1 and 16.2, Table 16.1), because it reduces the screening effect of cattail leaves, which makes the visual detection of water easier. Their polarimetric measurements were performed under clear sky in sunshine, in intact (control) plots, in mowed but not raked plots and in mowed and raked plots.

Table 16.1 Proportion Q (=polarization visibility) of the area (relative to the regions below the horizon) detected polarotactically as water (for which degree of polarization $d > 5$ % and angle of polarization $80° < \alpha < 100°$) for the water body in Fig. 16.2 measured by imaging polarimetry in the red, green and blue parts of the spectrum [after Table 2 on page 395 of Molnár et al. (2011)]

Spectral range	Covered by cattail (Fig. 16.2a)	Covered by mowed cattail (Fig. 16.2b)	Mowed cattail raked away (Fig. 16.2c)
Red (650 nm)	18.2 %	42.2 %	44.3 %
Green (550 nm)	20.6 %	46.0 %	47.6 %
Blue (450 nm)	24.0 %	49.5 %	51.9 %

The reflection-polarization patterns of different water bodies measured by imaging polarimetry in the blue part of the spectrum are shown in Fig. 16.1. Brown dry cattail (covering/screening totally the underlying water surface) and the green grass (on the shore of the water body) reflect weakly polarized light with directions of polarization changing strongly spatially due to the different orientations of cattail leaves (Fig. 16.1a). Such reflected light is unattractive to positively polarotactic aquatic insects (Horváth and Varjú 2004). Regions of dark water surfaces not covered by cattail reflect highly and horizontally polarized light (Fig. 16.1b), which is very attractive to polarotactic aquatic insects (Schwind 1991, 1995). Dark open water surfaces without vegetation (Fig. 16.1c) always reflect highly and horizontally polarized light when viewed at the Brewster angle.

In Fig. 16.2 the reflection-polarization patterns of a region of a water body are shown for three different conditions (1) when the water surface was almost totally covered by cattail (Fig. 16.2a), (2) when it was covered by mowed cattail (Fig. 16.2b) and (3) when the mowed cattail was raked away (Fig. 16.2c).

Depending on the wavelength of light, the proportion Q of the highly and horizontally polarizing regions of the water surface (sensed as water by flying, water-seeking polarotactic aquatic beetles) increased from about 18–24 to 42–50 % after the cattail was mowed, and Q increased further to 44–52 % after the mowed cattail was raked away. Q was highest in the blue part of the spectrum (24–52 %), and it decreased through the green (21–48 %) towards the red (18–44 %) spectral range (Table 16.1). The physical reason for this is that the water-reflected light was the blue skylight, and the light coming from under the water surface was most intense in the red spectral range. Hence, depending on its density, the cattail (and other plant) coverage can more or less reduce the polarization visibility Q (highly and horizontally polarized light signal) of the water surface (Fig. 16.2, Table 16.1) and thus can make more or less difficult the aerial colonization of waters by aquatic beetles.

Molnár et al. (2011) concluded that the considerably increased polarization visibility of water due to mowing (Table 16.1, Fig. 16.2) was the primary factor which enhanced the chance of aerial colonization by aquatic beetles and thus modified aquatic beetle assemblages. Water temperature was the secondary environmental factor that resulted in the different patterns in aquatic beetle assemblages. From a remote distance, a water-seeking flying aquatic insect cannot sense

the temperature, pH, conductivity, oxygen content, etc. of water but can perceive the horizontally polarized light reflected from open areas of the water surface (Schwind 1991). This polarized signal guides the insect to a water body. After entering into water, the insect may sense physico-chemical parameters and decide whether they are appropriate or not. If the environmental factors are appropriate, the insect may remain in the chosen water body; otherwise, it leaves the water in order to seek another, more appropriate location (Schwind 1995; Horváth and Varjú 2004).

These results show that cattail mowing is a useful method in aquatic beetle conservation: it increases the chance of aerial colonization due to the enhanced polarization visibility of the water surface and creates a habitat for more abundant assemblages otherwise excluded by the monodominant dense cattail stands. Thus, sustaining hemi-marsh conditions with vegetated and mowed areas is advisable to maximize overall aquatic beetle diversity. An important practical consequence of the work of Molnár et al. (2011) is that mowed cattail need not be raked away, if the only aim is to enhance the polarization visibility of the water surface, as it increases more after mowing than after mowed cattail is raked away (Table 16.1). Such raking is very difficult, and time and energy can be spared by leaving the mowed cattail in situ. Studying the possible negative or positive effects of mowed cattail (increased plant debris) on aquatic insects can be undertaken in the future.

16.2 Polarization Visibility of Water Surfaces as a Function of the Sun Elevation

It is a well-documented phenomenon that aquatic insects, especially the small-bodied ones, seek for new water habitats during their migration and dispersal flight generally at dusk (Popham 1964; Danilevskii 1965; Johnson 1969; Fernando and Galbraith 1973; Zalom et al. 1979, 1980; Saunders 1981; Danthanarayana 1986). From an ecological point of view, this is explained conventionally by the reduced risk of both predation and dehydration as well as by the period of calm and optimal air temperature at twilight (Landin 1968). At sunset the intensity of ambient light decreases exponentially with time (see Fig. 12.2 in Chapter 12) rendering more difficult the visual detection of flying preys by birds (King and Wrubleski 1998). Furthermore, at nightfall the lower temperature, higher humidity and calmness of air relative to those in daytime are optimal for small-bodied aquatic insects (Landin 1968), which can easily become dehydrated during flight if they cannot find a water body within about one hour. Csabai et al. (2006, 2012) showed that flying aquatic insects seek for new water bodies not only at dusk but many species also in early forenoon and/or near noon. According to their results, a ‘polarization sundial’ dictates the optimal time of day for dispersal by flying aquatic insects; furthermore, the diel flight behaviour and dispersal patterns of these insects depend on the season (see Sect. 5.1).

Hence, flying aquatic insects look for water surfaces at low and high elevation angles of the sun. Bernáth et al. (2004) showed that the polarization visibility of water surfaces, as an important visual ecological factor, contributes to the preference of low and high solar elevations for habitat searching by polarotactic insects detecting water by means of the horizontal polarization of light reflected from the water surface (Schwind 1991, 1995). They presented evidence for the phenomenon that polarotactic water detection is most efficient at low and high solar elevations. Using 180° field-of-view imaging polarimetry, they measured the reflection-polarization patterns of a dark and a bright horizontal water dummy (water-imitating artificial surface) as a function of the solar elevation angle θ in the red (650 nm), green (550 nm) and blue (450 nm) spectral ranges under clear and cloudy skies from sunrise to sunset near the summer solstice. The first water dummy consisting of a horizontal glass pane underlain by a matt black cloth imitated dark water bodies (with transparent water and black bottom, or deep waters, from the subsurface layers of which only small amount of light is returned), whilst the other dummy with a horizontal glass pane underlain by a matt light grey cloth mimicked bright water bodies (with transparent shallow water and bright bottom, or waters with bright suspended particles, from which considerable amount of light is returned in comparison with the amount of surface-reflected light). The use of such dummies was necessary to eliminate the inevitable rippling of natural water surfaces.

Bernáth et al. (2004) determined the percentage Q of the lower hemispherical visual field, in which both water dummies are considered by a flying polarotactic aquatic insect as water versus solar elevation θ. The polarization visibility Q is the angular proportion of the viewing directions for which both criteria $d > d^*$ and $\Delta\alpha = |90° - \alpha| < \Delta\alpha^*$ are satisfied relative to the angular extension of 2π steradians of the whole lower hemisphere of the field of view of a flying insect, where d^* and $\Delta\alpha^*$ are species-specific thresholds. The reflection-polarization patterns (Fig. 16.3) and polarization visibility Q were also calculated versus θ for a perfectly black horizontal reflector (modelling well flat black water surfaces without rippling) absorbing all penetrating light for both indices of refraction $n_{\text{water}} = 1.33$ and $n_{\text{glass}} = 1.5$ of water and glass, respectively. It was shown that the difference ΔQ between water and glass is smaller than 4 %, which is practically negligible. Furthermore, according to the results of Gál et al. (2001), the reflection-polarization patterns of the dark, flat (without ripples) water surface under a clear sky at sunset (Fig. 16.3f) are practically the same as those of the dark water dummy used by Bernáth et al. (2004). Thus, the conclusions drawn from the data obtained for the glass water dummy also hold for flat water surfaces. Bernáth et al. (2004) obtained (Fig. 5.4 in Chapter 5) that in the visible spectral range:

- If the sun is at the horizon, the polarization visibility Q is maximal for bright waters and has a local maximum for black waters.
- The differences in the reflection-polarization patterns and the polarization visibilities between bright and dark water bodies are minimal at near-zero solar elevations.

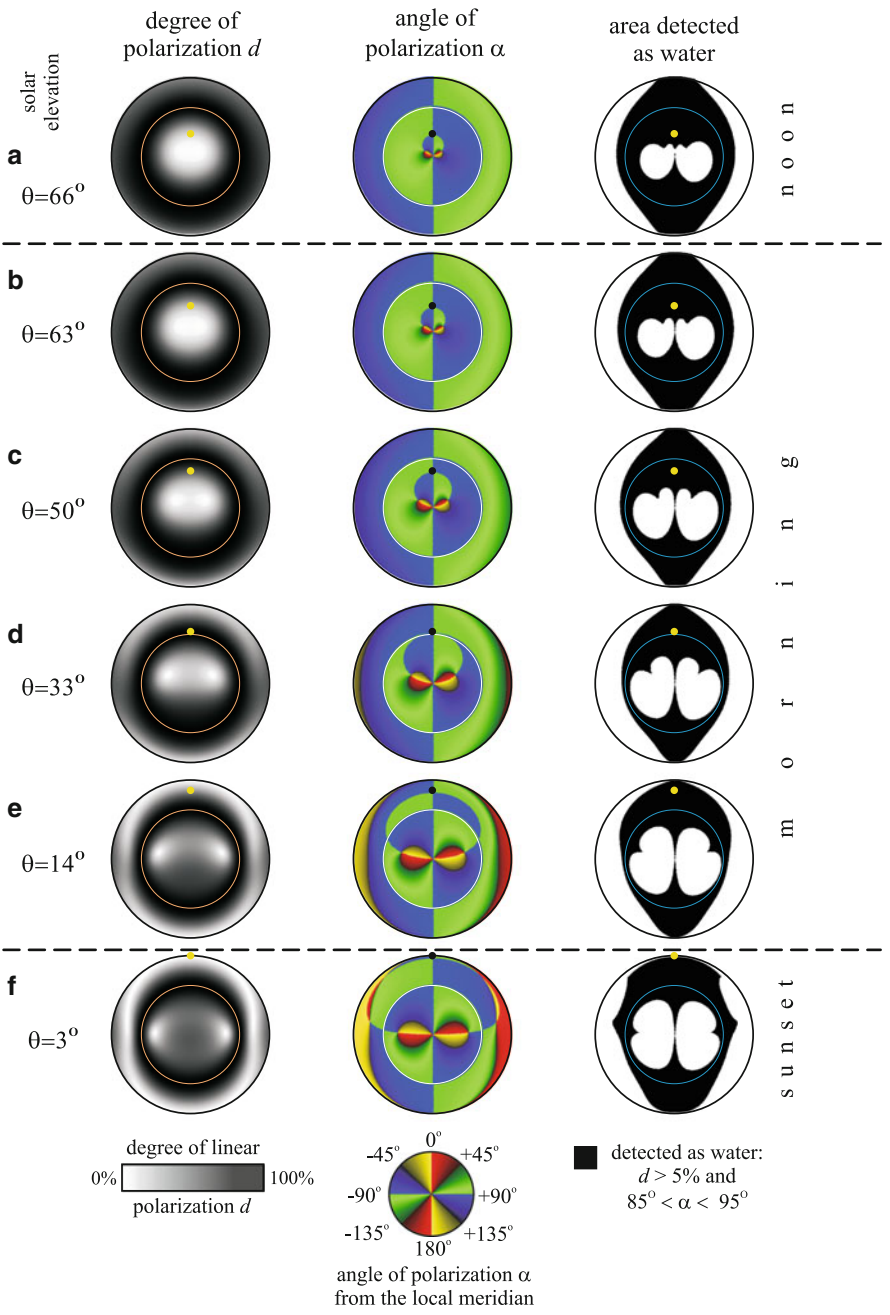

Fig. 16.3 180° field-of-view patterns of the degree d and angle α (measured from the local meridian) of linear polarization of reflected skylight and the area detected polarotactically as water as a function of the solar elevation angle θ for a perfectly black glass reflector (with an index of refraction $n_{\text{glass}} = 1.5$, absorbing all penetrating light) calculated for incident single-scattered

If the polarization of light reflected from water is analysed in the whole lower hemisphere of the visual field of a flying and water-seeking polarotactic insect, the polarization visibility Q is proportional to the chance that a water body is recognized as water in the optical environment. From these the following conclusions can be drawn:

- Polarotactic water detection of both dark and bright waters is most efficient at sunrise and sunset, when the reflection-polarization characteristics of dark and bright waters are most uniform and the risk of escaping the attention of flying polarotactic insects is minimal. Due to the lower air temperature at sunrise, the sunset period is more optimal than the sunrise period for polarotactic insects to seek for new aquatic habitats.
- Polarotactic water detection of dark waters is also advantageous near noon, at high solar elevations, when the risk of escaping the attention of flying polarotactic insects is also minimal for dark water bodies.

The reflection-polarization characteristics of water surfaces depend on the illumination conditions, material composition of the bottom, dissolved organic materials, angle of view from the nadir and the direction of observation relative to the sun. Aquatic insects can identify their water habitat by perceiving the partial linear polarization of light reflected from the water surface, if the degree of linear polarization is high enough and the direction of polarization approximates the horizontal. These two criteria are satisfied predominantly in the Brewster zone, which is continuous throughout the day at dark water bodies, but for bright waters this is true only towards the sun and anti-sun and in the time of sunrise and sunset (Bernáth et al. 2004). During the day the percentage Q detected as water is so low at bright water bodies (Fig. 5.4 in Chapter 5) that they can be easily overlooked by flying water insects. The shape and direction of the regions of bright water surfaces suitable for polarotactic water detection change considerably with the changing solar elevation (see right column in Fig. 16.3); therefore, bright aquatic habitats can be recognized polarotactically only from certain directions of view with respect to the sun.

Fig. 16.3 (continued) Rayleigh skylight with the use of the Fresnel formulae. In the *right column regions* are shaded by *black*, where $d > d^* = 5$ % and $85° \leq \alpha \leq 95°$. A polarotactic water insect is assumed to consider a surface as water, if these two conditions are satisfied for the partially linearly polarized reflected light. In the *right column* the regions where these criteria are not satisfied remained *blank*. The positions of the mirror image of the sun are shown by *dots*; the Brewster angle (56.3° from the nadir for glass with a refractive index of $n = 1.5$) is represented by an *inner circle* within the circular patterns. The centre and perimeter of the circular maps are the nadir and the horizon, respectively [after Fig. 4 on page 761 of Bernáth et al. (2004)]

References

Ball JP (1990) Influence of subsequent flooding depth on cattail control by burning and mowing. J Aquat Plant Manag 28:32–36

Bernáth B, Szedenics G, Wildermuth H, Horváth G (2002) How can dragonflies discern bright and dark waters from a distance? The degree of polarization of reflected light as a possible cue for dragonfly habitat selection. Freshw Biol 47:1707–1719

Bernáth B, Gál J, Horváth G (2004) Why is it worth flying at dusk for aquatic insects? Polarotactic water detection is easiest at low solar elevations. J Exp Biol 207:755–765

Csabai Z, Boda P, Bernáth B, Kriska G, Horváth G (2006) A 'polarisation sun-dial' dictates the optimal time of day for dispersal by flying aquatic insects. Freshw Biol 51:1341–1350

Csabai Z, Kálmán Z, Szivák I, Boda P (2012) Diel flight behaviour and dispersal patterns of aquatic Coleoptera and Heteroptera species with special emphasis on the importance of seasons. Naturwissenschaften 99:751–765

Danilevskii AS (1965) Photoperiodism and seasonal development of insects. Oliver and Boyd, Edinburgh, London

Danthanarayana W (ed) (1986) Insect flight: dispersal and migration. Springer, Heidelberg

DeBusk TA, DeBusk WF (2000) Wetlands for water treatment. In: Kent DM (ed) Applied wetland science and technology, 2nd edn. Lewis Publishers, Chelsea, MI

Fairchild GW, Cruz J, Faulds AM, Short AEZ, Matta JF (2003) Microhabitat and landscape influences on aquatic beetle assemblages in a cluster of temporary and permanent ponds. J N Am Benthol Soc 22:224–240

Fernando CH, Galbraith D (1973) Seasonality and dynamics of aquatic insects colonizing small habitats. Verhandlungen des Internationalen Vereins für Limnologie 18:1564–1575

Gál J, Horváth G, Meyer-Rochow VB (2001) Measurement of the reflection-polarization pattern of the flat water surface under a clear sky at sunset. Remote Sens Environ 76:103–111

Horváth G (1995) Reflection-polarization patterns at flat water surfaces and their relevance for insect polarization vision. J Theor Biol 175:27–37

Horváth G, Kriska G (2008) Polarization vision in aquatic insects and ecological traps for polarotactic insects. In: Lancaster J, Briers RA (eds) Aquatic insects: challenges to populations. CAB International Publishing, Wallingford, Oxon, pp 204–229

Horváth G, Pomozi I (1997) How celestial polarization changes due to reflection from the deflector panels used in deflector loft and mirror experiments studying avian navigation. J Theor Biol 184:291–300

Horváth G, Varjú D (1995) Underwater refraction-polarization patterns of skylight perceived by aquatic animals through Snell's window of the flat water surface. Vis Res 35:1651–1666

Horváth G, Varjú D (1997) Polarization pattern of freshwater habitats recorded by video polarimetry in red, green and blue spectral ranges and its relevance for water detection by aquatic insects. J Exp Biol 200:1155–1163

Horváth G, Varjú D (2004) Polarized light in animal vision—polarization patterns in nature. Springer, Heidelberg

Johnson GC (1969) Migration and dispersal of insects by flight. Methuen and Co., London

Kercher SM, Zedler JB (2004) Flood tolerance in wetland angiosperms: a comparison of invasive and noninvasive species. Aquat Bot 80:89–102

King RS, Wrubleski DA (1998) Spatial and diel availability of flying insects as potential duckling food in prairie wetlands. Wetlands 18:100–114

Kostecke RM, Smith LM, Hands HM (2004) Vegetation response to cattail management at Cheyenne Bottoms, Kansas. J Aquat Plant Manag 42:39–45

Kriska G, Bernáth B, Farkas R, Horváth G (2009) Degrees of polarization of reflected light eliciting polarotaxis in dragonflies (Odonata), mayflies (Ephemeroptera) and tabanid flies (Tabanidae). J Insect Physiol 55:1167–1173

Landin J (1968) Weather and diurnal periodicity of flight by *Helophorus brevipalpis* Bedel (Col. Hydrophilidae). Opuscula Entomologica 33:28–36

Lundkvist E, Landin J, Milberg P (2001) Diving beetle (Dytiscidae) assemblages along environmental gradients in an agricultural landscape in southeastern Sweden. Wetlands 21:48–58
Molnár Á, Hegedüs R, Kriska G, Horváth G (2011) Effect of cattail (*Typha* spp.) mowing on water beetle assemblages: changes of environmental factors and the aerial colonization of aquatic habitats. J Insect Conserv 15:389–399
Murkin HR, Kaminski RM, Titman RD (1982) Responses by dabbling ducks and aquatic invertebrates to an experimentally manipulated cattail marsh. Can J Zool 60:2324–2332
Nilsson AN, Söderstrom O (1988) Larval consumption rates, interspecific predation, and local guild composition of egg-overwintering *Agabus* (Coleoptera, Dytiscidae) species in vernal ponds. Oecologia 76:131–137
Nilsson AN, Svensson BW (1995) Assemblages of Dytiscid predators and Culicid prey in relation to environmental-factors in natural and clear-cut boreal swamp forest pools. Hydrobiologia 308:183–196
Popham EJ (1964) The migration of aquatic bugs with special reference to the Corixidae (Hemiptera Heteroptera). Arch Hydrobiol 60:450–496
Saunders DS (1981) Insect photoperiodism. In: Handbook of Behavioral Neurobiology (J Aschoff, ed) Plenum Press, New York
Schwind R (1991) Polarization vision in water insects and insects living on a moist substrate. J Comp Physiol A 169:531–540
Schwind R (1995) Spectral regions in which aquatic insects see reflected polarized-light. J Comp Physiol A 177:439–448
Schwind R, Horváth G (1993) Reflection-polarization pattern at water surfaces and correction of a common representation of the polarization pattern of the sky. Naturwissenschaften 80:82–83 + cover picture
Wildermuth H (1998) Dragonflies recognize the water of rendezvous and oviposition sites by horizontally polarized light: a behavioural field test. Naturwissenschaften 85:297–302
Zalom FG, Grigarick AA, Way MO (1979) Seasonal and diel flight periodicities of rice field Hydrophilidae. Environ Entomol 8:938–943
Zalom FG, Grigarick AA, Way MO (1980) Diel flight periodicities of some Dytiscidae (Coleoptera) associated with California rice paddies. Ecol Entomol 5:183–187

Chapter 17
Polarization Characteristics of Forest Canopies with Biological Implications

Gábor Horváth and Ramón Hegedüs

Abstract In this chapter we show that the pattern of the direction of polarization of sunlit grasslands and sunlit tree canopies is qualitatively the same as that of the clear sky. Since the mirror symmetry axis of this pattern is the solar–antisolar meridian, the azimuth direction of the sun, occluded by vegetation, can be assessed in forests from this polarization pattern. This robust polarization feature of the optical environment in forests can be important for forest-inhabiting animals that make use of linearly polarized light for orientation. Here we also present an atmospheric optical and receptor-physiological explanation of why longer wavelengths are advantageous for the perception of polarization of downwelling light under canopies illuminated by the setting sun. This explains why the upward-pointing ommatidia of the dusk-active cockchafers, *Melolontha melolontha*, detect the polarization of downwelling light in the green part of the spectrum. We show that the polarization vision in *Melolontha melolontha* is tuned to the high polarized intensity of downwelling light under canopies during sunset. This is an optimal compromise between simultaneous maximization of the quantum catch and the quantum catch difference.

Electronic supplementary material is available in the online version of this chapter at 10.1007/978-3-642-54718-8_17. The supplementary figures can also be accessed at http://extras.springer.com

G. Horváth (✉)
Environmental Optics Laboratory, Department of Biological Physics, Physical Institute, Eötvös University, Pázmány sétány 1, 1117 Budapest, Hungary
e-mail: gh@arago.elte.hu

R. Hegedüs
Max Planck Institute for Informatics, Campus E1.4, 66123 Saarbruecken, Germany

INRIA Sud-Ouest Bordeaux, 200, Avenue de la Vieille Tour, 33400 Talence, France

Laboratoire Photonique, Numérique et Nanosciences (L2PN), UMR 5298, CNRS IOGS University Bordeaux, Institut d'Optique d'Aquitaine, 33405 Talence, France
e-mail: ramon.hegedus@gmail.com

G. Horváth (ed.), *Polarized Light and Polarization Vision in Animal Sciences*, Springer Series in Vision Research 2, DOI 10.1007/978-3-642-54718-8_17,

17.1 How the Azimuth of the Foliage-Occluded Sun Can Be Determined from the E-Vector Pattern of Sunlit Forest Canopies

Polarimetric remote sensing has numerous applications in the field of agriculture (Kong 1990), and many of the methods used exploit information of polarized light reflected from vegetation (Coulson 1988). The polarization signature of vegetated surfaces can be used to distinguish different types of crops and to indicate developmental states and possible stress factors (e.g. water deficiency, disease, excessive salinity) that could affect production (Brines and Gould 1982; Vanderbilt and Grant 1985; Vanderbilt et al. 1985a, b; Grant et al. 1987a, b, 1993). The optical environment in forests has complex spatial distributions of light intensity and colour (Endler 1993), and the polarized light field is equally complex. Brines and Gould (1982) hypothesized that under certain circumstances, biologically significant Rayleigh polarization patterns may exist against overhead vegetation at ultraviolet (UV) wavelengths. Using imaging polarimetry, Shashar et al. (1998) studied the linear polarization of light in a tropical rain forest. They found that the celestial polarization pattern remains visible underneath the forest canopy, provided patches of clear (blue) sky are visible through the overhead vegetation. They characterized some distinct light environments in the forest, each having a typical linearly polarized light field. They concluded that polarization-based animal navigation would be limited to spaces exposed to several extended portions of the blue sky and that other forms of orientation throughout the forest would include remote sensing of surface features, object detection and camouflage violations. Horváth et al. (2002a) measured the polarization patterns of some plant leaves by imaging polarimetry. They showed that these patterns are complex and strongly depend on the surface characteristics of the leaf, the orientation of the leaf blade and the illumination conditions.

Since polarization patterns in the entire upper hemisphere of the visual environment of forests could be important for forest-inhabiting animals that make use of polarization patterns for orientation, Hegedüs et al. (2007a) measured the 180° field-of-view polarization patterns of the overhead foliage in a variety of forest types by full-sky imaging polarimetry. From a hot air balloon, Horváth et al. (2002b) and Hegedüs et al. (2007a) measured the polarization patterns of grasslands lit by the rising sun (at a solar elevation angle of 4.5°) at heights of 100–200 m above ground. They found that the pattern of the angle of polarization α of the upwelling light from sunlit grasslands (Fig. 17.1) and that of the downwelling light from sunlit tree canopies (Fig. 17.2) are qualitatively the same as that of the corresponding sky with the same sun position (Fig. 17.3), independently of the solar elevation and the sky conditions. They also showed that contrary to an earlier assumption, the α-pattern characteristic of the sky (Fig. 17.3) always remains

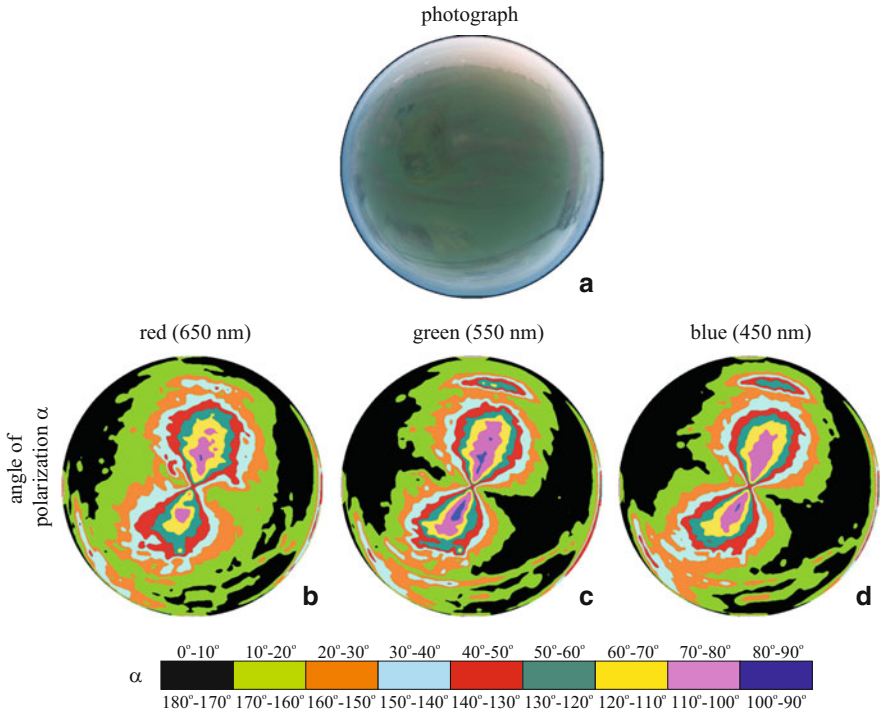

Fig. 17.1 Photograph and patterns of the angle of polarization α from the local meridian of a grassland lit by the rising sun measured by 180° field-of-view imaging polarimetry in the *red*, *green* and *blue parts* of the spectrum. The measurements were performed from a hot air balloon at an altitude of 100 m. The optical axis of the polarimeter's fish-eye lens pointed towards the nadir, which is the centre of the circular patterns [after Fig. 2 on page 6025 of Hegedüs et al. (2007a)]

visible underneath overhead vegetation, independently of the solar elevation and the sky conditions (clear or partly cloudy with visible sun's disc), provided the foliage is sunlit (Fig. 17.4) and not only when large patches of the clear sky are visible through the vegetation. Since the mirror symmetry axis of the α-pattern of the sunlit foliage is the solar–antisolar meridian, the azimuth direction of the sun occluded by vegetation can be assessed in forests from this robust polarization pattern. The α-patterns of skies and vegetations have the following characteristics (Hegedüs et al. 2007a):

- The α of *light from the clear sky* has a typical pattern (Fig. 17.3): The isolines with $\alpha =$ constant are always 8 shaped with a cross-point at the zenith and an axis of mirror symmetry coinciding with the solar–antisolar meridian in such a way that the smaller loop of the figure-8 occurs consistently in the solar half of the sky. (The crossing of the α-isolines at the zenith is purely a geometrical artefact and the consequence of the definition of α rather than a true polarization singularity.) Depending on the wavelength, solar elevation and atmospheric

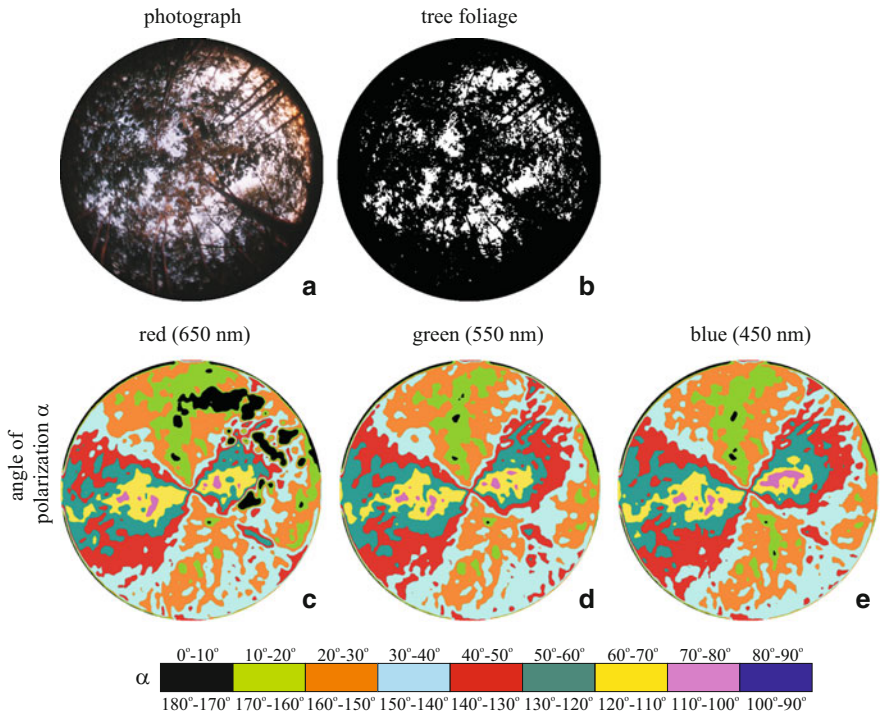

Fig. 17.2 Photograph and patterns of the angle of polarization α from the local meridian of a clear sky with the overhead vegetation of a forest composed of birch trees lit by the setting sun measured by full-sky imaging polarimetry in the *red*, *green* and *blue parts* of the spectrum. In pattern **b** *black* shows the tree foliage and *white* indicates the sky [after Fig. 3 on page 6026 of Hegedüs et al. (2007a)]

turbidity, the noisiness n of α of the clear sky (n denotes how noisy is the α-pattern compared to the white noise: $n = 0$ %, no noise; $n = 100$ %, white noise) is $2\ \% \leq n_{\text{clear}} \leq 7\ \%$. If the sky is partly cloudy or overcast, the α-pattern remains qualitatively the same (apart from heavily overcast skies) as that of the clear sky. Depending on the degree of cloudiness and the wavelength, the noisiness n of α of partly cloudy and overcast skies is $5\ \% \leq n_{\text{cloudy}} \leq 21\ \%$ and $14\ \% \leq n_{\text{overcast}} \leq 35\ \%$. Hence, as the cloudiness increases, the noisiness n of α increases, but the α-pattern remains qualitatively the same.

- Depending on the wavelength, the noisiness n of α of the *grass-reflected sunlight* ranges from 11 to 16 %, but the α-pattern of the sunlit grassland is qualitatively the same as that of the clear sky: The α-pattern is characterized by the typical figure-8 pattern, the mirror symmetry axis of which is the solar–antisolar meridian (Fig. 17.1).
- Depending on the wavelength, the sky conditions and the foliage ratio f (=percentage of vegetation in the celestial hemisphere), the noisiness n of the α-pattern of *skies with overhead vegetation* is $19\ \% \leq n_{\text{foliage}} \leq 51\ \%$. If the

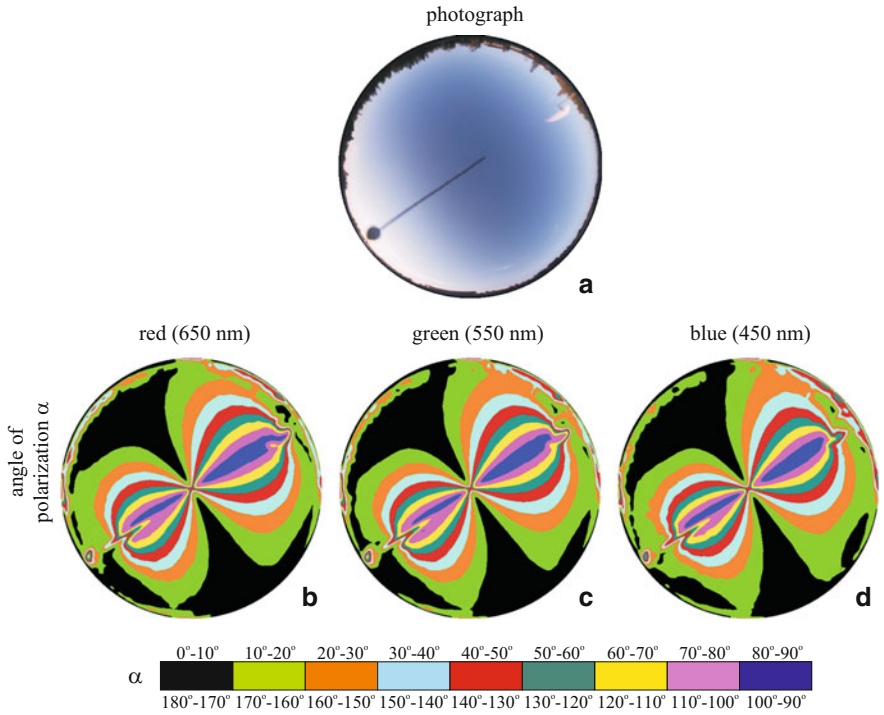

Fig. 17.3 Photograph and patterns of the angle of polarization α from the local meridian of a clear sky, measured by full-sky imaging polarimetry in the *red*, *green* and *blue parts* of the spectrum. The optical axis of the polarimeter's fish-eye lens was vertical; thus, the horizon is the perimeter, and the centre of the circular patterns is the zenith. At the perimeter of the *circular colour picture*, the dark silhouette of trees can be seen. The sun near the horizon was occluded by a *small black disc* placed on a *thin wire*, which is seen radially in the circular patterns [after Fig. 1 on page 6023 of Hegedüs et al. (2007a)]

foliage is sunlit, the α-pattern of the overhead vegetation is qualitatively the same as that of the clear sky: The α-isolines have the typical figure-8 pattern with a mirror symmetry axis along the solar–antisolar meridian, independently of the solar elevation and the sky conditions (clear or partly cloudy with visible sun's disc). Under the same sky conditions, the 8-shaped α-isolines of tree canopies (Figs. 17.2 and 17.4) are slightly expanded compared to the corresponding α-isolines of clear skies (Fig. 17.3), so that the Arago, Babinet or Brewster neutral points can disappear (Fig. 17.5): The α-pattern of the overhead vegetation resembles more the theoretical Rayleigh pattern than the real (measured) one or the theoretical pattern of Berry et al. (2004).

- *If the overhead vegetation is not sunlit*, because the sun is below the horizon, or is occluded by clouds, then the α-pattern of the foliage is extremely distorted so that there is no trace of mirror symmetry (see skies S9, S10 and S11 in Fig. 17.4) and the noisiness of α is rather large ($37\ \% \leq n_{\text{foliage}} \leq 43\ \%$).

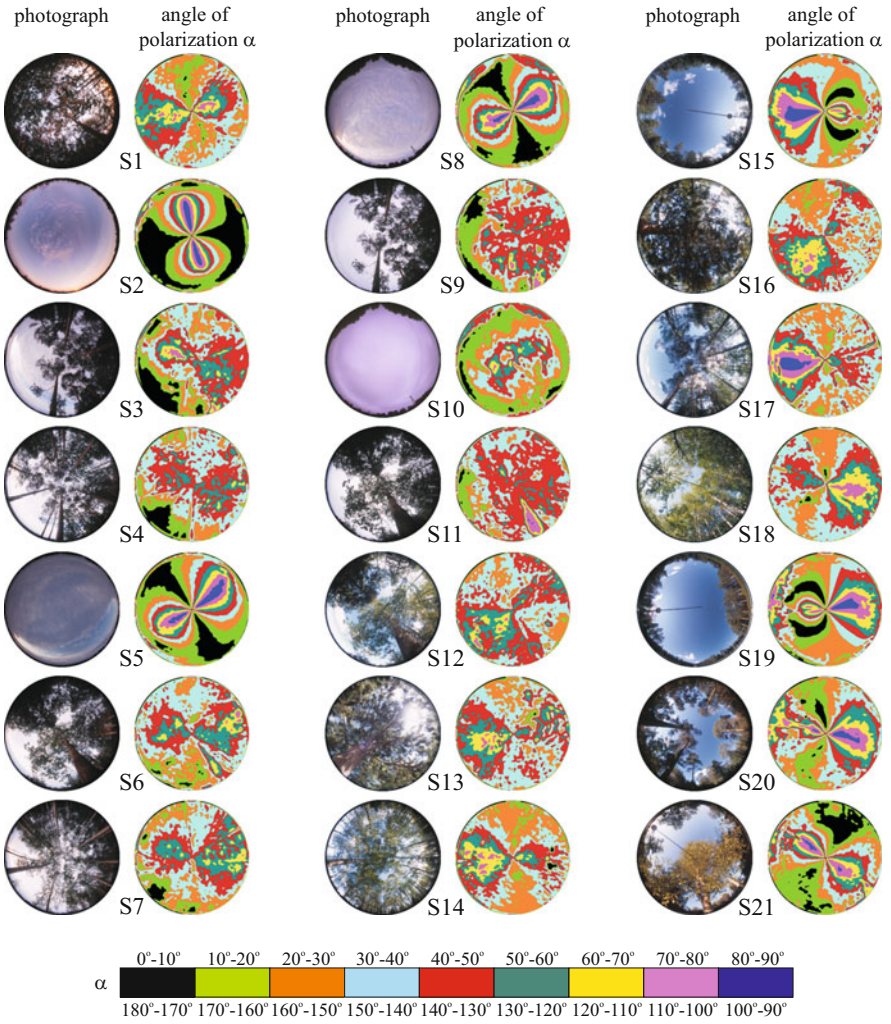

Fig. 17.4 Photographs and patterns of the angle of polarization α of skies and tree canopies measured in the *blue* (450 nm) part of the spectrum. Quite similar α-patterns were obtained in the *green* and *red* spectral ranges [after Fig. 4 on page 6027 of Hegedüs et al. (2007a)]

The surface of leaves reflects, scatters and transmits the incident light (Woolley 1971). Leaf reflectance is an intermediate between that of a perfectly diffuse Lambert reflector (reflecting the incident light uniformly into all directions) and a perfectly specular Fresnel reflector (being a smooth interface between two different dielectric media, the polarizing ability of which is described by Fresnel's laws of reflection). It is the sum of diffuse and specular components (Grant 1987). The diffuse component is unpolarized and varies little with changing angles, and its spectrum is characteristic to the (usually green) leaf tissue. The specular component

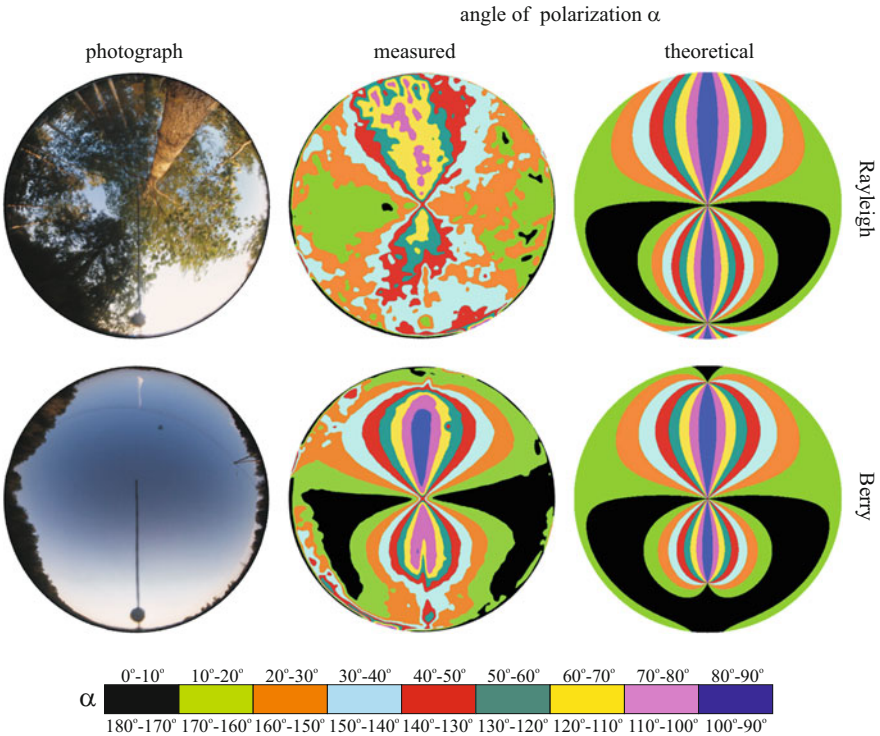

Fig. 17.5 *Left* and *middle columns*: Photographs and the patterns of the angle of polarization α of a tree canopy and a clear sky measured by full-sky imaging polarimetry in the *blue* (450 nm) part of the spectrum under the same sky conditions. *Right column*: Theoretical α-patterns calculated on the basis of the single-scattering Rayleigh model and the model of Berry et al. (2004). For the sake of easier comparisons, the *circular pictures* and *patterns* were rotated so that the solar–antisolar meridian became vertical in both cases [after Fig. 6 on page 6030 of Hegedüs et al. (2007a)]

is partially linearly polarized, is reflected from the outermost leaf surface (cuticle), spreads about the specular direction and has a spectrum that is practically the same as that of the incident light (Grant et al. 1993).

The physical reasons for the finding of Hegedüs et al. (2007a) that the pattern of the angle of polarization α (or the E-vector direction) of the sunlit foliage is qualitatively the same as that of the clear sky (Figs. 17.1, 17.2, 17.3 and 17.4), i.e. the direction of polarization of light from the sunlit overhead vegetation is approximately perpendicular to the plane determined by the observer, the sun and the leaf observed, are the following: Fig. 17.6 shows schematically the nine components (T-SU, T-SK, T-LE, S-SU, S-SK, S-LE, D-SU, D-SK, D-LE) of light from the foliage and their polarization characteristics. A particular leaf of the foliage is illuminated by sunlight (SU) and/or skylight (SK) and/or light from the neighbouring leaves (i.e. leaflight, LE). SU is unpolarized (with degree of linear polarization

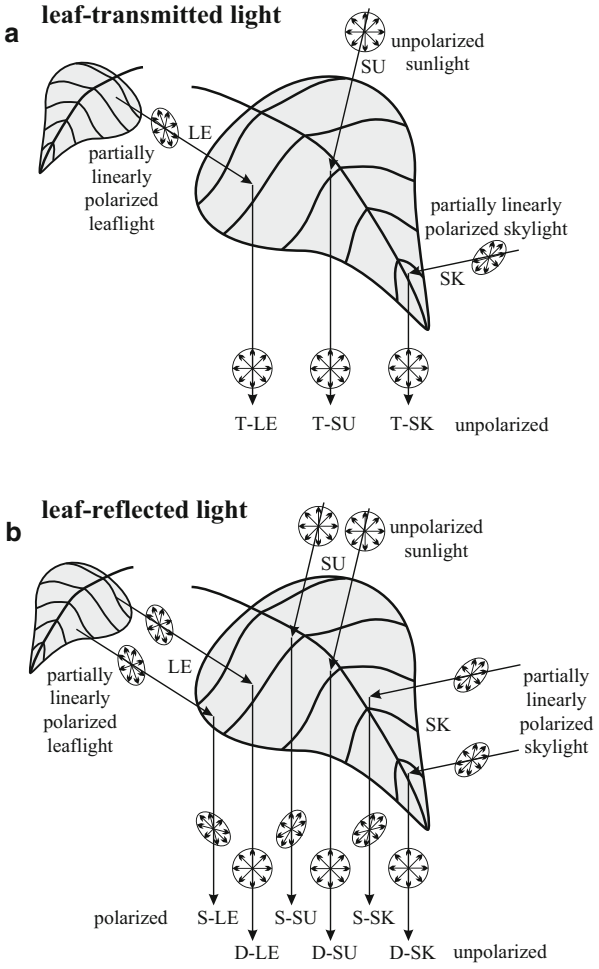

Fig. 17.6 Schematic representation of the polarization characteristics of the different components (SU, S-SK, S-LE, D-SU, D-SK, D-LE, T-SU, T-SK, T-LE) of light transmitted (**a**) and reflected (**b**) by a leaf in the foliage lit by sunlight and skylight. *Circles* and *ellipses* with *double-headed arrows* represent unpolarized and partially linearly polarized light, respectively. SU: sunlight (unpolarized); SK: skylight (partially polarized); LE: leaflight (partially polarized); S-SU, S-SK and S-LE: specularly reflected sunlight, skylight and leaflight (partially polarized); D-SU, D-SK and D-LE: diffusely reflected sunlight, skylight and leaflight (unpolarized); T-SU, T-SK and T-LE: transmitted sunlight, skylight and leaflight (unpolarized) [after Fig. 5 on page 6029 of Hegedüs et al. (2007a)]

$d = 0$), while SK and LE are partially polarized ($d > 0$) due to scattering–polarization and reflection–polarization of sunlight in the atmosphere and at the leaf blades, respectively (Können 1985; Coulson 1988; Grant et al. 1993; Horváth et al. 2002a). The leaflight has two main components: light transmitted through the leaves (Fig. 17.6a) and light reflected from the leaves (Fig. 17.6b). The former possesses three further components: the sunlight (T-SU), skylight (T-SK) and leaflight (T-LE) transmitted through the leaves. T-SU, T-SK and T-LE are practically unpolarized ($d \approx 0$) because of the diffuse scattering and multiple reflection of light (SU, SK, LE) within the leaf tissue (Können 1985; Coulson 1988; Grant et al. 1993; Horváth et al. 2002a) (Fig. 17.6a).

Light can be reflected from a leaf either diffusely by the leaf tissue and its rough outer surface (due to hairs or wax) or specularly from smooth leaf cuticle (Coulson 1988; Grant et al. 1993; Horváth et al. 2002a) (Fig. 17.6b). If the incident light (SU,

SK, LE) penetrates into the leaf tissue, it can either be diffusely reflected into all directions after multiple scattering on and reflection from the plant cells (D-SU, D-SK, D-LE) or be transmitted diffusely through the leaf (T-SU, T-SK, T-LE). The diffusely reflected components D-SU, D-SK and D-LE are practically unpolarized ($d \approx 0$) (Grant et al. 1993; Horváth et al. 2002a). The specularly reflected components S-SU, S-SK and S-LE are partially polarized (Coulson 1988; Grant et al. 1993; Horváth et al. 2002a). According to Fresnel's laws of reflection (Azzam and Bashara 1992), the direction of polarization of specularly reflected light is perpendicular to the plane of reflection determined by the incident light, reflected light and the local normal vector of the reflecting surface. Thus, the direction of polarization of S-SU is perpendicular to the plane containing the observer, the sun and the observed point of a sunlit leaf. The direction of polarization of the other two specularly reflected components S-SK and S-LE is usually tilted to this plane, because the direction of the incident skylight (SK) and leaflight (LE) is generally different from that of the sunlight (SU).

From these it follows that among the nine components of leaflight, only the sunlight reflected specularly from the smooth cuticle of leaves (S-SU) can result in directions of polarization perpendicular to the plane of reflection passing through the observer, the sun and the observed sunlit leaf of the foliage. This S-SU component is the reason for the white gloss of shiny, smooth sunlit leaves. This highly or moderately polarized, cuticle-reflected gloss often overwhelms the unpolarized green light reflected diffusely from the leaf tissue. According to Können (1985), in the foliage there can be many leaves oriented in many different directions, but the gloss of the foliage as a whole is tangentially polarized with respect to the sun, i.e. perpendicular to the plane of reflection.

The above qualitative optical model also explains why under the same sky conditions the 8-shaped α-isolines of tree canopies expand relative to those of the clear sky, so that the neutral points may disappear (Fig. 17.5): Since the S-SU component, per definition, practically corresponds to the single scattering of light, the α-pattern of sunlit overhead vegetation resembles the Rayleigh pattern. The α-pattern of the clear sky more or less deviates from the Rayleigh pattern due to multiple scattering of light in the air (see Subchapter 18.2).

Thus, if the vegetation is sunlit, the E-vector pattern of the foliage is qualitatively the same as that of the clear sky. The same holds true for moonlit scenes at night, when the main source of light is sunlight reflected by the moon, if the latter is not occluded by clouds. The main reason for this phenomenon is the polarization effect of the S-SU component of leaflight. Consequently, the illumination of the foliage by direct sunlight plays an important role, while solar elevation and sky conditions (clear or partly cloudy with visible sun's disc) are irrelevant. The deviations of the α-pattern of the sunlit vegetation from that of the clear sky are the consequences of the polarization characteristics of the other eight components T-SU, T-SK, T-LE, S-SK, S-LE, D-SU, D-SK and D-LE of leaflight. The larger the contribution of these eight components to the net leaflight, the greater these deviations. If the sun is occluded by clouds, the foliage is not sunlit; thus, the S-SU component does not exist, and consequently the α-pattern of the foliage

differs considerably from that of the clear sky (see skies S9, S10 and S11 in Fig. 17.4).

Earlier, it has been shown that the E-vector pattern of the sky during full moon at night (Gál et al. 2001) and during the day under smoky (Hegedüs et al. 2007b), foggy (Hegedüs et al. 2007c) and partly cloudy (Brines and Gould 1982; Pomozi et al. 2001; Suhai and Horváth 2004; Hegedüs et al. 2007c) as well as total overcast conditions (Hegedüs et al. 2007d) is qualitatively the same as that of the clear, sunlit sky. The polarimetric results presented in this subchapter supplement these earlier findings, demonstrating that the distribution of the angle of polarization is a very stable pattern in the optical environment encompassing both sunlit and moonlit skies and including furthermore sunlit grassland and overhead vegetation.

Since the mirror symmetry axis of the E-vector pattern of the sunlit overhead vegetation is always the solar–antisolar meridian, the azimuth direction of the sun occluded by foliage in forests can be assessed from this polarization pattern. For instance, tropical honeybees (the ancestors of all recent bees), living and dancing on exposed limbs in tropical forests, are frequently confronted with the problem of orientation underneath sunlit overhead vegetation (Wilson 1971). Hegedüs et al. (2007a) proposed the following scenario for the evolution of polarization-based navigation in bees: In the ancient bees, living in forests, the ability to perceive downwelling polarized leaflight has evolved in the UV part of the spectrum in order to assess the azimuth direction of the invisible sun (occluded by foliage) from the E-vector pattern of the sunlit overhead vegetation for navigational purposes. Later, when the descendants of these ancient bees dispersed from the tropical forests into other regions, this ability was used to perceive polarization of the skylight in the UV even under cloudy conditions in order to determine the azimuth of the sun, hidden by clouds, for the purpose of orientation. According to this hypothesis, the perception of polarized leaflight in forests for navigational purposes preceded the detection of polarized skylight and the use of direct celestial polarization for orientation purposes.

17.2 Why Do Dusk-Active Cockchafers Sense Downwelling Polarization in the Green Spectral Range?

In insects, the linear polarization of downwelling light (skylight or light from the tree canopy) is detected by upward-pointing ommatidia in the so-called dorsal rim area (DRA) of the compound eye. These ommatidia are anatomically and physiologically specialized and contain two sets of monochromatic and highly polarization-sensitive photoreceptors with orthogonal microvilli directions (Labhart and Meyer 1999). The spectral type of the DRA receptors is ultraviolet (UV) in flies, honeybees, desert ants, certain scarab beetles and spiders, for example, while blue in crickets, desert locusts and cockroaches [Table 10.1 of Horváth and Varjú (2004), p. 54; Table 1 of Barta and Horváth (2004)].

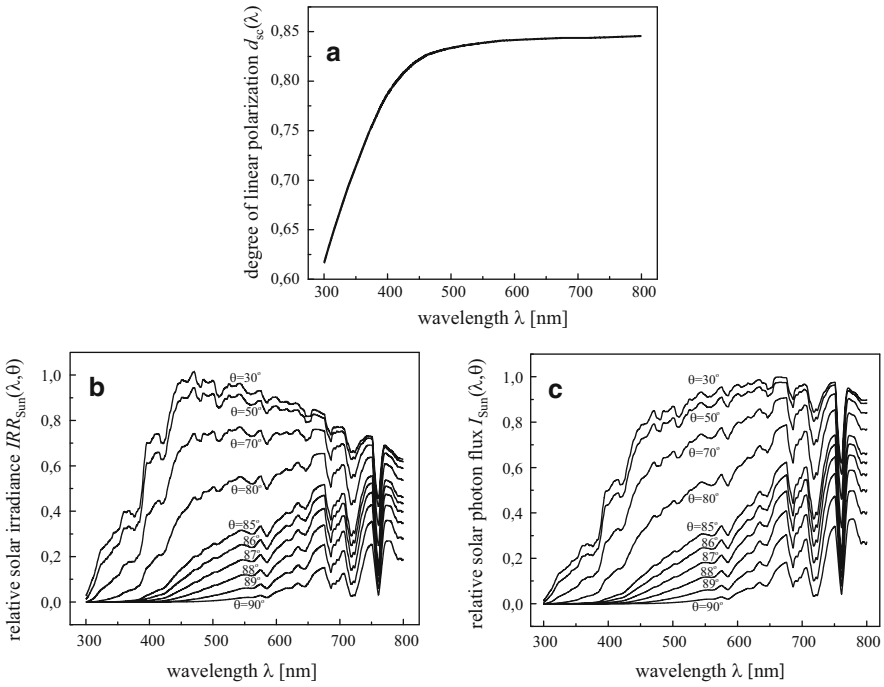

Fig. 17.7 (**a**) Degree of linear polarization d_{sc} versus wavelength λ of scattered light from clear sky measured at 90° from the sun for a solar zenith angle $\theta = 80°$ (Coulson 1988, p. 285). (**b**) Relative irradiance $IRR_{Sun}(\lambda, \theta)$ of unpolarized direct sunlight for solar zenith angles $\theta = 30°$, 50°, 70°, 80°, 85°, 86°, 87°, 88°, 89° and 90° (*top* to *bottom*), computed on the basis of the 1976 US Standard Atmosphere. (**c**) Relative solar photon flux $I_{Sun}(\lambda, \theta)$ for solar zenith angles $\theta = 30°$, 50°, 70°, 80°, 85°, 86°, 87°, 88°, 89° and 90° (*top* to *bottom*) [after Fig. 1 on page 232 of Hegedüs et al. (2006)]

Explanations for cricket preference of the blue spectral range for detection of skylight polarization have been discussed by Labhart et al. (1984), Herzmann and Labhart (1989), Zufall et al. (1989), Horváth and Varjú (2004) and Barta and Horváth (2004). The cricket *Gryllus campestris*, for instance, is active not only during the day but also during crepuscular periods (dusk and dawn) and at night, having highly polarization-sensitive blue receptors in its DRA. Horváth and Varjú (2004, pp. 53–73) and Barta and Horváth (2004) showed that the degree of linear polarization d_{cloudy} of light from cloudy parts of the sky is always relatively high in the violet and blue (400 nm $< \lambda <$ 470 nm), rendering the violet-blue the second optimal spectral range after the UV (in which d_{cloudy} is maximal) for detection of skylight polarization under partly cloudy conditions. Using the blue portion of the spectrum has a significant advantage over using UV under clear skies, when the degree of skylight polarization is sufficiently high for all wavelengths (Fig. 17.7a). The intensity I of the UV component of sunlight (Fig. 17.7b, c) and light from the clear sky is low relative to that of the blue and green components. At twilight under

clear sky, the light intensity is more likely to fall below the sensitivity threshold of a polarization-sensitive visual system operating in the UV rather than in the blue. According to Zufall et al. (1989), the combination of blue spectral and polarization sensitivity in the DRA may be a common adaptation of insects that are active at circumstances of very low light intensities, as opposed to day-active insects (e.g. honeybees, desert ants and flies) which predominantly use UV receptors as detectors for skylight polarization [see Table 10.1 of Horváth and Varjú (2004, p 54)]. However, the question is whether this argument also holds for cloudy conditions. On the one hand, detection of skylight may be more disadvantageous in the UV than in the blue, because under cloudy conditions the UV component of skylight is much weaker than under clear sky. On the other hand, perception of skylight polarization could be more advantageous in the UV than in the blue, because under cloudy skies d_{cloudy} is the highest in the UV [see Fig. 4 of Barta and Horváth (2004)]. The question is, which effect is the stronger one?

The perception of skylight polarization in the UV by several insect species is surprising, because both the degree of polarization d (Fig. 17.7a) and the intensity I of light from the clear sky are considerably lower in the UV than in the blue or green. This is the so-called UV-sky-pol paradox. Horváth and Varjú (2004, pp. 53–73) and Barta and Horváth (2004) have presented a quantitative resolution to this paradox. They proved by model calculations that if the air layer between a cloud and a ground-based observer is partly sunlit at higher solar elevations, d of skylight originating from the cloudy region is highest in the UV [see Fig. 4 of Barta and Horváth (2004)], because in this spectral range the unpolarized UV-deficient cloudlight dilutes the polarized light scattered in the air beneath the cloud the least. Similarly, if the air under foliage is partly illuminated by a high sun, d of downwelling light from the canopied region is maximal in the UV [see Fig. 5 of Barta and Horváth (2004)], because in this spectral range the unpolarized UV-deficient green canopylight dilutes the polarized light scattered in the air beneath the canopy the least. Therefore, in daylight the detection of polarization of downwelling light under clouds or canopies is most advantageous in the UV, in which spectral range the risk is smallest that d is lower than the threshold $d_{\text{threshold}}$ of polarization sensitivity in animals. On the other hand, under clear skies there is no favoured wavelength for perception of celestial polarization, because d of skylight is sufficiently high ($d > d_{\text{threshold}}$) at all wavelengths. Horváth and Varjú (2004) and Barta and Horváth (2004) have also shown that there is an analogy between the detection of UV skylight polarization and the polarotactic water detection in the UV. The atmospheric optical explanation and computational model of Barta and Horváth (2004) and Horváth and Varjú (2004, pp. 53–73)—to explain why is it advantageous for animals to detect celestial polarization in the ultraviolet—were experimentally corroborated by Wang et al. (2014), who used a sky-polarimetric approach and built a polarized skylight sensor that modelled the processing of polarization signals by insect photoreceptors in the UV, visible and near-infrared spectral ranges. They showed that light from the cloudy sky has maximal degree of polarization in the UV, and under both clear and cloudy skies

the angle of polarization of skylight can be measured/detected with a higher accuracy in the UV than in the visible spectral range.

The above-mentioned atmospheric optical reasons explain why certain insects detect the polarization of downwelling light either in the UV or in the blue part of the spectrum. There are, however, at least two insect species in which the DRA receptors are green sensitive: In the DRA retina of the European cockchafer, *Melolontha melolontha*, polarization is detected by receptors with maximal sensitivity at $\lambda_{max} = 520$ nm (Labhart et al. 1992), and in the tenebrionid desert beetle, *Parastizopus armaticeps*, at $\lambda_{max} = 540$ nm (Bisch 1999). Hegedüs et al. (2006) gave an atmospheric optical and receptor-physiological model to explain why longer wavelengths (green and red) are advantageous in the perception of the polarization of downwelling light under canopies illuminated by the setting sun. Their explanation focused on illumination situations in a canopied optical environment at sunset, because cockchafers are active at dusk and fly predominantly under canopies during their swarming, feeding and mating periods (Schneider 1952).

Brines and Gould (1982), Pomozi et al. (2001) and Suhai and Horváth (2004) have experimentally shown that the E-vector (or direction or angle of polarization) pattern of clouded celestial regions is approximately the same as that of the corresponding clear sky regions (see also Chap. 18). Pomozi et al. (2001) have also demonstrated that in the visible part of the spectrum under partly cloudy conditions, the shorter the wavelength λ, the greater the proportion k of the celestial polarization pattern suitable for animal orientation. Hence, k is determined primarily by the degree of polarization $d(\lambda)$ of skylight, for which Barta and Horváth (2004) have presented a quantitative estimation. Hegedüs et al. (2006) showed that the E-vector pattern under canopies illuminated by sunlight is nearly the same as that under clear sky at the same solar position (see Sect. 17.1). Consequently, $d(\lambda)$ of downwelling light under canopy is what determines k. However, because the detectability of light polarization also depends on the light intensity I, the polarized intensity $\mathrm{PI}(\lambda) = d(\lambda) \cdot I(\lambda)$ also has to be taken into account in the estimation of the spectral region that is optimal for orientation by means of the polarization of downwelling light under canopies.

Using three atmospheric optical models (Fig. 17.8), Hegedüs et al. (2006) computed the degree of polarization $d(\lambda)$ (Fig. 17.9) and the polarized intensity $\mathrm{PI}(\lambda) = d(\lambda) \cdot I(\lambda)$ (Fig. 17.10) of downwelling light under canopies. The at-ground direct-normal spectral solar irradiance, $\mathrm{IRR}_{Sun}(\lambda, \theta)$ (Fig. 17.7b), was calculated from MODTRAN (MODerate resolution TRANsmittance code, Berk et al. 1983), where θ is the solar zenith angle ($=0°$ for sun at the zenith and 90° for sun on the horizon). The solar irradiance spectrum $\mathrm{IRR}_{Sun}(\lambda, \theta)$ gives the energy of solar radiation per unit time, per unit area and per unit wavelength interval. Since photoreceptors respond to photon flux rather than photon energy, $\mathrm{IRR}_{Sun}(\lambda, \theta)$ was converted to solar photon flux $I_{Sun}(\lambda, \theta) = \lambda \cdot \mathrm{IRR}_{Sun}(\lambda, \theta)/hc$, where h is the Planck constant and c is the velocity of light in vacuum. $I_{Sun}(\lambda, \theta)$ (Fig. 17.7c) gives the number of photons of solar radiation per unit time, per unit area and per unit wavelength interval and is called the intensity of sunlight further on.

In the models of Hegedüs et al. (2006), the downwelling light under canopies illuminated by direct sunlight with solar spectrum $I_{Sun}(\lambda, \theta)$ had two components

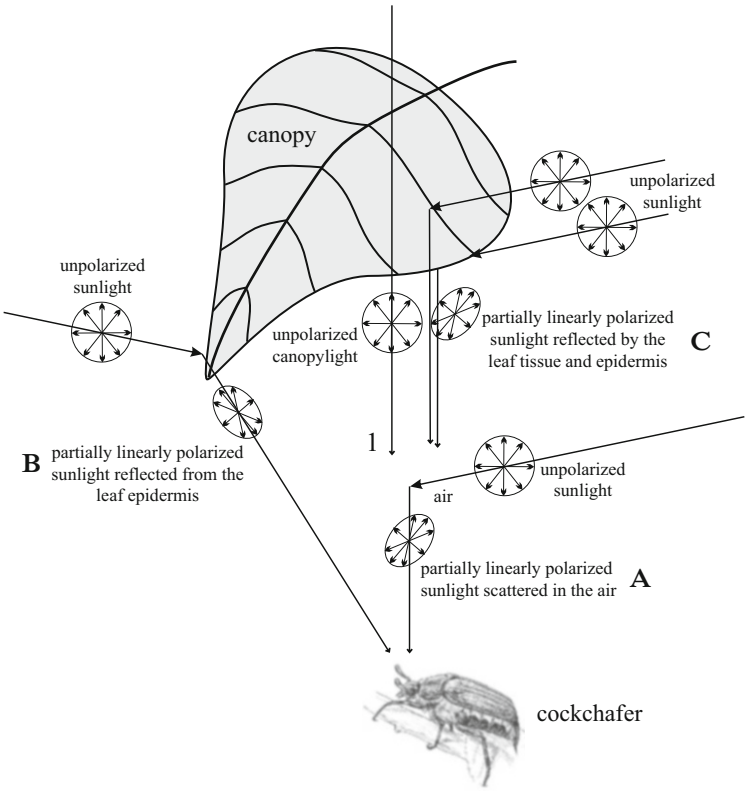

Fig. 17.8 Schematic representation of the two components of light reaching a cockchafer under a canopy in the case of the three atmospheric optical models of Hegedüs et al. (2006). In all three models the first component, called canopylight (1), is the unpolarized green light transmitted through the canopy. The second component is the partially polarized sunlight (A) scattered in the air layer between the canopy and the cockchafer or (B) reflected from the leaf cuticle or (C) reflected by both the leaf tissue and cuticle [after Fig. 2 on page 234 of Hegedüs et al. (2006)]

with a weighting factor a (control parameter) describing the ratio of the first (unpolarized) and second (polarized) components (Fig. 17.8): (1) The first component, the unpolarized green canopylight transmitted through the foliage, was the same in all three models. (2) The models differed only in the second component describing different partially linearly polarized parts of the downwelling light under various illumination conditions: (A) sunlight undergoing the first-order Rayleigh scattering in the air layer between the ground observer and the foliage; (B) light reflected from the cuticle (outer surface) of leaves, the degree of polarization of which was practically independent of wavelength λ; and (C) combination of the cuticle-reflected light and the light returned by the leaf tissue below the cuticle (where the light transmitted through the cuticle underwent diffuse scattering and then left the leaf tissue by refraction at the cuticle). For all three models the

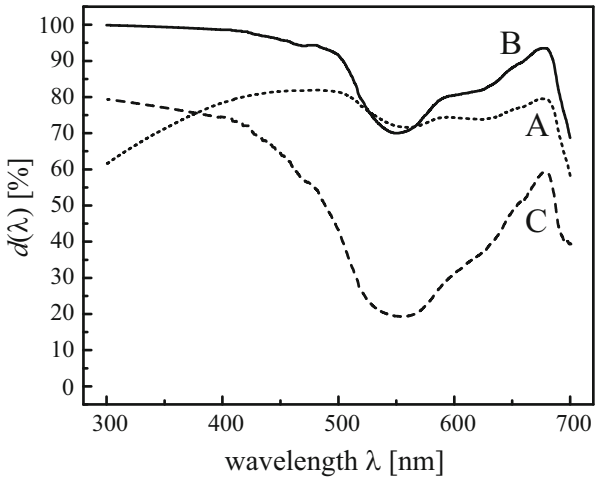

Fig. 17.9 Degree of polarization $d(\lambda, a)$ of downwelling light under a canopy calculated from the atmospheric optical models A, B and C of Hegedüs et al. (2006) for control parameter $a = 1$ at solar zenith angle $\theta = 90°$. The control parameter a is the ratio of the first (unpolarized) and second (partially polarized) components of downwelling light. Qualitatively similar results were obtained for other values of θ and a. Increasing a means increasing the proportion of partially polarized sunlight scattered underneath the canopy (model A), reflected from the leaf cuticle (model B) or reflected by both the leaf tissue and cuticle (model C) [after Fig. 3 on page 236 of Hegedüs et al. (2006)]

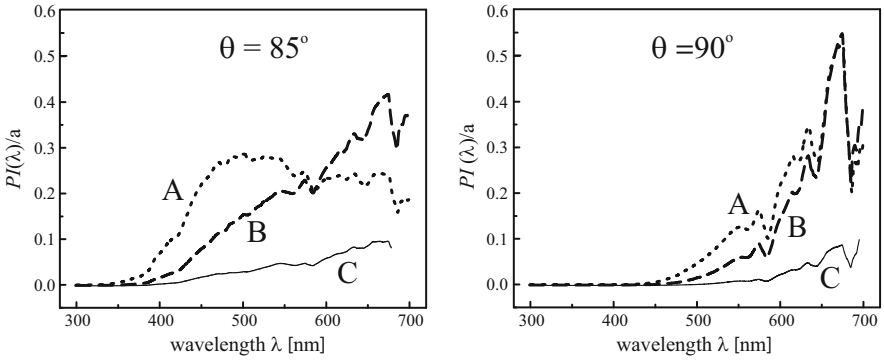

Fig. 17.10 PI$(\lambda)/a$, where PI$(\lambda) = d(\lambda) \cdot I(\lambda)$ is the polarized intensity of downwelling light under a canopy and a is the control parameter, calculated from the atmospheric optical models A, B and C of Hegedüs et al. (2006) for solar zenith angles $\theta = 85°$ and 90°. Qualitatively similar results were obtained for other values of θ [after Fig. 4 on page 237 of Hegedüs et al. (2006)]

wavelength range included the UV (300 nm $\leq \lambda \leq$ 400 nm) and visible (400 nm $< \lambda \leq$ 700 nm) parts of the spectrum.

As a receptor-physiological approach, Hegedüs et al. (2006) calculated the quantum catches $Q_{\text{par}}(\lambda_{\max})$ and $Q_{\text{perp}}(\lambda_{\max})$ and the logarithmic quantum catch

difference $\Delta\log Q(\lambda_{max}) = \log Q_{par}(\lambda_{max}) - \log Q_{perp}(\lambda_{max})$ of DRA photoreceptors with orthogonal microvilli, where Q_{par} and Q_{perp} are the amounts of light absorbed by a DRA receptor (the quantum catch) if the E-vector of partially linearly polarized light is parallel (par) or perpendicular (perp) to the receptor microvilli and λ_{max} is the wavelength where the receptor's absorption spectrum is maximal. The greater the logarithmic quantum catch difference $\Delta\log Q(\lambda_{max})$, the better the detection of polarization. Thus, maximizing $\Delta\log Q(\lambda_{max})$ is optimal for DRA receptors. In the model, the photoreceptors were stimulated by downwelling light under canopies illuminated by sunlight as a function of the wavelength λ and the solar zenith angle θ as calculated by the above-mentioned three atmospheric optical models. Hegedüs et al. (2006) focused on high values of θ, because cockchafers are active at dusk. They estimated the spectral range in which a monochromatic DRA cross analyser detecting the polarization of downwelling light under canopies would function optimally.

Considering the maximization of $d(\lambda)$, in all three atmospheric optical models (Fig. 17.9), the UV-blue and red are the first and second most advantageous spectral ranges, respectively, and green is the most disadvantageous part of the spectrum for the detection of polarization of downwelling light under canopies, independently of the solar zenith angle (Hegedüs et al. 2006). From this it follows that the green (520 nm) sensitivity of DRA receptors in cockchafers (*Melolontha melolontha*) cannot be explained by means of an adaptation to the wavelengths of maximal values of the degree of polarization d of downwelling light under canopies. High enough d of downwelling light is only one prerequisite of polarization vision under canopies. In addition, the intensity I also needs to be sufficiently high for detection of polarization, especially during sunset, when I considerably and rapidly decreases with increasing solar zenith angle. To decide whether d and I are simultaneously high enough at any given wavelength, the polarized intensity $PI(\lambda) = d(\lambda)\cdot I(\lambda)$ should be considered.

According to the three atmospheric optical models of Hegedüs et al. (2006), as the solar zenith angle θ increases from 0° to 90°, the wavelength where the polarized intensity $PI(\lambda)$ is maximal shifts from violet-blue towards the red spectral range (Fig. 17.10). Hence, prior to sunset, PI is maximal in the green, and at sunset PI is sufficiently high in the green while at the same time being very much higher than in the short (blue, violet, UV) wavelength range. From these it can be concluded that the spectral sensitivity of DRA receptors in cockchafers is tuned to the maximal or sufficiently high polarized intensity PI of downwelling light in the green part of the spectrum under canopies during sunset.

A similar conclusion can be drawn by analysing the logarithmic quantum catch difference $\Delta\log Q(\lambda)$ (Fig. 17.11) and the quantum catch $Q(\lambda)$ (Fig. 17.12): $\Delta\log Q(\lambda)$, which is the measure of the efficiency of polarization detection, is generally higher in the UV and blue than in the green. Thus, considering only the maximization of $\Delta\log Q(\lambda)$, green-sensitive DRA receptors would be less advantageous than blue- or UV-sensitive ones under canopies (Fig. 17.11). During sunset, however, $Q(\lambda)$ diminishes strongly with decreasing λ (Fig. 17.12); therefore, the quantum catch of UV- and blue-sensitive DRA receptors would certainly be too small,

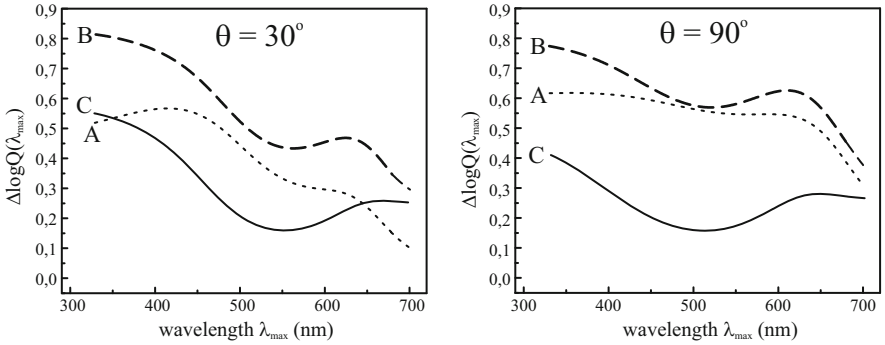

Fig. 17.11 Logarithmic quantum catch difference $\Delta\log Q(\lambda_{max}, a)$ of polarization-sensitive model receptors with orthogonal microvilli calculated from the atmospheric optical models A, B and C of Hegedüs et al. (2006) for control parameter $a = 1$ at solar zenith angles $\theta = 30°$ and 90°. Qualitatively similar results were obtained for other values of θ and a [after Fig. 5 on page 238 of Hegedüs et al. (2006)]

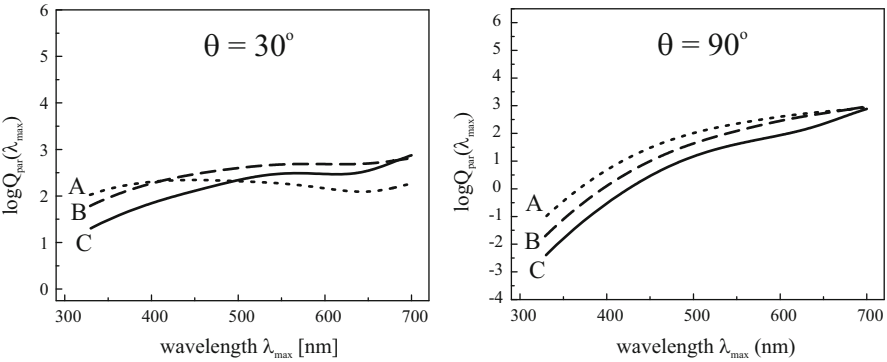

Fig. 17.12 Logarithm of the quantum catch $Q_{par}(\lambda_{max}, a)$ of a polarization-sensitive model receptor with microvilli parallel to the E-vector of downwelling light calculated from the atmospheric optical models A, B and C of Hegedüs et al. (2006) for control parameter $a = 1$ at solar zenith angles $\theta = 30°$ and $\theta = 90°$. Qualitatively similar results were obtained for other values of θ and a [after Fig. 6 on page 240 of Hegedüs et al. (2006)]

and only green-sensitive receptors have large enough quantum catch Q for the detection of polarization.

Considering atmospheric optics, the primary condition for successful detection of light polarization is that polarized intensity must be over the stimulus threshold of photoreceptors. Only if this prerequisite is fulfilled can the degree of polarization d be considered. Analogously, according to the receptor-physiological approach, receptors need to catch enough light quanta to be able to detect polarization by comparing the quantum catches of two receptor types with orthogonal microvilli (cross analyser in the DRA). Thus, the optimal strategy for achieving a successful

and efficient orientation by means of polarization of downwelling light is to select a spectral range of sensitivity for the receptors, where both $d(\lambda)$ and $\mathrm{PI}(\lambda)$ (in the atmospheric optical term, Figs. 17.9 and 17.10) and both $\Delta\log Q(\lambda_{\max})$ and $Q(\lambda_{\max})$ (in the receptor-physiological term, Figs. 17.11 and 17.12) are simultaneously maximal or at least moderately high. Hegedüs et al. (2006) showed that the green sensitivity of the polarization-sensitive DRA photoreceptors in *Melolontha melolontha* is tuned to the high polarized intensity $\mathrm{PI}(\lambda) = d(\lambda)\cdot I(\lambda)$ of downwelling light in the green resulting in an optimal compromise between simultaneous maximization of the quantum catch $Q(\lambda_{\max})$ and the logarithmic quantum catch difference $\Delta\log Q(\lambda_{\max})$ under canopies during sunset (Figs. 17.9, 17.10, 17.11 and 17.12).

Hegedüs et al. (2006) also explained qualitatively why green-sensitive polarization detectors in the DRA also function efficiently enough during the pre-feeding and egg-laying flights of cockchafers always occurring prior to sunset and under the sky. During their lifetime cockchafers fly in two significantly different optical environments during sunset (1) under clear or cloudy skies during their pre-feeding and egg-laying flights and (2) under canopies illuminated by the setting sun during their swarming flights. During the pre-feeding and egg-laying cockchafer flights at dusk, the optimal wavelength range of DRA receptors would be the blue part of the spectrum. This explains why DRA receptors in dusk-active crickets orienting under twilight skies are blue sensitive (Labhart et al. 1984; Herzmann and Labhart 1989; Zufall et al. 1989; Horváth and Varjú 2004; Barta and Horváth 2004). For the cockchafer swarming flight under canopies at sunset, however, the optimal spectral range for DRA receptors is the long wavelength segment of the spectrum. Therefore, red-sensitive DRA receptors would be the most advantageous for this task, because the degree of polarization, the polarized intensity, the quantum catch and the quantum catch difference are all simultaneously maximal or sufficiently high in the red spectral range. However, red receptors generally do not occur in beetles (Briscoe and Chittka 2001). Since the DRA receptors in *Melolontha melolontha* are green sensitive, they serve the swarming flight best (for which longer wavelengths are optimal), rather than the pre-feeding and egg-laying flights (for which shorter wavelengths are optimal). The pre-feeding and egg-laying flights occur prior to sunset when the intensity of skylight in the green is still relatively high; thus, green-sensitive DRA receptors can still serve orientation by means of skylight polarization.

All three atmospheric optical models of Hegedüs et al. (2006) assume that the canopy is illuminated by direct light from the setting sun. This condition is not satisfied if the setting sun is occluded by clouds on overcast days. However, on cloudy days cockchafers usually do not perform swarming flights.

Hegedüs et al. (2006) also explained qualitatively why the green-sensitive polarization detectors in the DRA of the dusk- and night-active beetle *Parastizopus armaticeps* (Coleoptera: Tenebrionidae) can also function efficiently enough at twilight under clear desert skies: This beetle inhabits the Kalahari desert in southern Africa (Heg and Rasa 2004) and has to orient under predominantly clear twilight skies. Considering the perception of skylight polarization under clear skies, there is

no favoured wavelength because the degree of polarization is sufficiently high (much higher than the threshold of polarization sensitivity) at all wavelengths (Fig. 17.7a). Thus, the proportion of the celestial polarization pattern useful for orientation is sufficiently large at all wavelengths, both in the UV and visible parts of the spectrum (Horváth and Varjú 2004; Barta and Horváth 2004). As we mentioned above, crickets possess blue-sensitive DRA receptors, thereby avoiding the very low intensity I of skylight in the UV at dusk, and utilize the maximal I and the relatively high degree of polarization d of skylight in the blue (Fig. 17.7a). The green-sensitive DRA receptors in *Parastizopus armaticeps* can also function efficiently enough at twilight, because they avoid the very low I in the UV at dusk, and utilize the relatively high I and the maximal d of skylight in the green (Fig. 17.7a).

Finally, it should be emphasized that beyond the atmospheric optical and receptor-physiological arguments presented here, certainly other important biological and/or environmental factors may exist which determine the optimal wavelength range for the detection of polarization of downwelling light in cockchafers.

References

Azzam RMA, Bashara NM (1992) Ellipsometry and polarized light. North-Holland, Amsterdam, NY

Barta A, Horváth G (2004) Why is it advantageous for animals to detect celestial polarization in the ultraviolet? Skylight polarization under clouds and canopies is strongest in the UV. J Theor Biol 226:429–437

Berk A, Bernstein LS, Robertson DC (1983) MODTRAN: a moderate resolution model for LOWTRAN 7, Air Force Geophysical Laboratory Technical Report GL-TR-83-0187, Hanscom Air Force Base, MA 01731-5000

Berry MV, Dennis MR, Lee RL Jr (2004) Polarization singularities in the clear sky. New J Phys 6: 162

Bisch SM (1999) Orientierungsleistungen des nachtaktiven Wüstenkäfers *Parastizopus armaticeps* Peringuey (Coleoptera: Tenebrionidae). Ph.D. thesis, University Bonn, Germany

Brines ML, Gould JL (1982) Skylight polarization patterns and animal orientation. J Exp Biol 96: 69–91

Briscoe AD, Chittka L (2001) The evolution of color vision in insects. Annu Rev Entomol 46: 471–510

Coulson KL (1988) Polarization and intensity of light in the atmosphere. A. Deepak Publishing, Hampton, VA

Endler JA (1993) The color of light in forests and its implications. Ecol Monogr 63:1–27

Gál J, Horváth G, Barta A, Wehner R (2001) Polarization of the moonlit clear night sky measured by full-sky imaging polarimetry at full moon: comparison of the polarization of moonlit and sunlit skies. J Geophys Res D 106:22647–22653

Grant L (1987) Diffuse and specular characteristics of leaf reflectance. Remote Sens Environ 22: 309–322

Grant L, Daughtry CST, Vanderbilt VC (1987a) Polarized and non-polarized leaf reflectances of Coleus blumei. Environ Exp Bot 27:139–145

Grant L, Daughtry CST, Vanderbilt VC (1987b) Variations in the polarized leaf reflectance of Sorghum bicolor. Remote Sens Environ 27:333–339

Grant L, Daughtry CST, Vanderbilt VC (1993) Polarized and specular reflectance variation with leaf surface features. Physiol Plant 88:1–9

Heg D, Rasa OAE (2004) Effects of parental body condition and size on reproductive success in a tenebrionid beetle with biparental care. Ecol Entomol 29:410–419

Hegedüs R, Horváth Á, Horváth G (2006) Why do dusk-active cockchafers detect polarization in the green? The polarization vision in *Melolontha melolontha* is tuned to the high polarized intensity of downwelling light under canopies during sunset. J Theor Biol 238:230–244

Hegedüs R, Barta A, Bernáth B, Meyer-Rochow VB, Horváth G (2007a) Imaging polarimetry of forest canopies: how the azimuth direction of the sun, occluded by vegetation, can be assessed from the polarization pattern of the sunlit foliage. Appl Opt 46:6019–6032

Hegedüs R, Åkesson S, Horváth G (2007b) Anomalous celestial polarization caused by forest fire smoke: why do some insects become visually disoriented under smoky skies? Appl Opt 46: 2717–2726

Hegedüs R, Åkesson S, Wehner R, Horváth G (2007c) Could Vikings have navigated under foggy and cloudy conditions by skylight polarization? On the atmospheric optical prerequisites of polarimetric Viking navigation under foggy and cloudy skies. Proc R Soc A 463:1081–1095

Hegedüs R, Åkesson S, Horváth G (2007d) Polarization patterns of thick clouds: overcast skies have distribution of the angle of polarization similar to that of clear skies. J Opt Soc Am A 24: 2347–2356

Herzmann D, Labhart T (1989) Spectral sensitivity and absolute threshold of polarization vision in crickets: a behavioral study. J Comp Physiol A 165:315–319

Horváth G, Varjú D (2004) Polarized light in animal vision—polarization patterns in nature. Springer, Heidelberg

Horváth G, Gál J, Labhart T, Wehner R (2002a) Does reflection polarization by plants influence colour perception in insects? Polarimetric measurements applied to a polarization-sensitive model retina of Papilio butterflies. J Exp Biol 205:3281–3298

Horváth G, Bernáth B, Suhai B, Barta A, Wehner R (2002b) First observation of the fourth neutral polarization point in the atmosphere. J Opt Soc Am A 19:2085–2099

Kong IA (1990) Polarimetric remote sensing. Elsevier, Amsterdam

Können GP (1985) Polarized light in nature. Cambridge University Press, Cambridge

Labhart T, Meyer EP (1999) Detectors for polarized skylight in insects: a survey of ommatidial specializations in the dorsal rim area of the compound eye. Microsc Res Tech 47:368–379

Labhart T, Hodel B, Valenzuela I (1984) The physiology of the cricket's compound eye with particular reference to the anatomically specialized dorsal rim area. J Comp Physiol A 155: 289–296

Labhart T, Meyer EP, Schenker L (1992) Specialized ommatidia for polarization vision in the compound eye of cockchafers, *Melolontha melolontha* (Coleoptera, Scarabaeidae). Cell Tissue Res 268:419–429

Pomozi I, Horváth G, Wehner R (2001) How the clear-sky angle of polarization pattern continues underneath clouds: full-sky measurements and implications for animal orientation. J Exp Biol 204:2933–2942

Schneider F (1952) Untersuchungen über die optische Orientierung der Maikäfer (*Melolontha vulgaris* F. und *M. hippocastani* F.) sowie über die Entstehung von Schwärmbahnen und Befallskonzentrationen. Mitteilungen der Schweizerischen Entomologischen Gesellschaft 25:269–340

Shashar N, Cronin TW, Wolff LB, Condon MA (1998) The polarization of light in a tropical rain forest. Biotropica 30:275–285

Suhai B, Horváth G (2004) How well does the Rayleigh model describe the E-vector distribution of skylight in clear and cloudy conditions? A full-sky polarimetric study. J Opt Soc Am A 21: 1669–1676

Vanderbilt VC, Grant L (1985) Polarization photometer to measure bidirection reflectance factor R(55°, 0°, 55°, 180°) of leaves. Opt Eng 25:566–571

Vanderbilt VC, Grant L, Daughtry CST (1985a) Polarization of light scattered by vegetation. Proc IEEE 73:1012–1024

Vanderbilt VC, Grant L, Biehl LL, Robinson BF (1985b) Specular, diffuse and polarized light scattered by two wheat canopies. Appl Opt 24:2408–2418
Wang X, Gao J, Fan Z (2014) Empirical corroboration of an earlier theoretical resolution to the UV paradox of insect polarized skylight orientation. Naturwissenschaften 101:95–103
Wilson EO (1971) Insect societies. Harvard University Press, Cambridge, MA
Woolley JT (1971) Reflectance and transmittance of light by leaves. Plant Physiol 47:656–662
Zufall F, Schmitt M, Menzel R (1989) Spectral and polarized light sensitivity of photoreceptors in the compound eye of the cricket (*Gryllus bimaculatus*). J Comp Physiol A 164:597–608

Chapter 18
Polarization of the Sky

Gábor Horváth, András Barta, and Ramón Hegedüs

Abstract Based on full-sky imaging polarimetric measurements, in this chapter we demonstrate that the celestial distribution of the angle of polarization (or E-vector direction) of skylight is a very robust pattern being qualitatively always the same under all possible sky conditions. Practically the only qualitative difference among clear, partly cloudy, overcast, foggy, smoky and tree-canopied skies occurs in the degree of linear polarization d: The higher the optical thickness of the non-clear atmosphere, the lower the d of skylight. We review here how well the Rayleigh model describes the E-vector pattern of clear and cloudy skies. We deal with the polarization patterns of foggy, partly cloudy, overcast, twilight, smoky and total-solar-eclipsed skies. We describe the possible influences of the changed polarization pattern of smoky and eclipsed skies on insect orientation. We consider the polarization of 'water-skies' above Arctic open waters and the polarization characteristics of fogbows. Finally, we deal with the change of skylight polarization due to the transmission through Snell's window of the flat water surface.

Electronic supplementary material is available in the online version of this chapter at 10.1007/978-3-642-54718-8_18. The supplementary figures can also be accessed at http://extras.springer.com and the videos at http://www.springerimages.com/videos/978-3-642-54717-1.

G. Horváth (✉)
Environmental Optics Laboratory, Department of Biological Physics, Physical Institute, Eötvös University, Pázmány sétány 1, 1117 Budapest, Hungary
e-mail: gh@arago.elte.hu

A. Barta
Estrato Research and Development Ltd, Mártonlak utca 13, 1121 Budapest, Hungary
e-mail: bartaandras@gmail.com

R. Hegedüs
Max Planck Institute for Informatics, Campus E1.4, 66123 Saarbruecken, Germany

INRIA Sud-Ouest Bordeaux, 200, Avenue de la Vieille Tour, 33400 Talence, France

Laboratoire Photonique, Numérique et Nanosciences (L2PN), UMR 5298, CNRS IOGS University Bordeaux, Institut d'Optique d'Aquitaine, 33405 Talence, France
e-mail: ramon.hegedus@gmail.com

G. Horváth (ed.), *Polarized Light and Polarization Vision in Animal Sciences*, Springer Series in Vision Research 2, DOI 10.1007/978-3-642-54718-8_18,

18.1 Introduction: Robustness of the Celestial E-Vector Pattern

According to full-sky imaging polarimetric measurements, the celestial distribution of the angle of polarization α is a very robust pattern being qualitatively always the same under all possible sky conditions (Fig. 18.1). Practically the only qualitative difference among clear (Fig. 18.1a, Gál et al. 2001; Suhai and Horváth 2004), partly cloudy (Fig. 18.1b, Pomozi et al. 2001a; Suhai and Horváth 2004; Hegedüs et al. 2007a), totally overcast (Fig. 18.1c, Hegedüs et al. 2007b), foggy (Fig. 18.1d, Hegedüs et al. 2007a), smoky (Fig. 18.1e, Hegedüs et al. 2007c) and tree-canopied (Fig. 18.1f, Hegedüs et al. 2007d; see Chap. 17) skies is in the degree of linear polarization d: The higher the optical thickness of the non-clear atmosphere, the lower the d-value.

The reason for this robust behaviour of the angle of polarization $\alpha = 0.5 \cdot \arctan(U/Q)$ of light (where Q and U are the second and third Stokes parameters) from the non-clear sky is that α is determined by single scattering. Single scattering by Rayleigh scatterers and by cloud and fog particles (water droplets or ice crystals) produces mainly positive polarization, i.e. perpendicular to the plane of scattering (Können 1985; Coulson 1988). The single-scattering process controls the angle of polarization α, also in the case of multiple scattering, e.g. by clouds or fog. Although the Stokes parameters U and Q become smaller themselves due to multiple scattering, their ratio U/Q remains essentially the same. The degree of polarization $d = (Q^2 + U^2)^{1/2}/I$ (where I is the intensity, i.e. the first Stokes parameter) determined by the magnitude of Q and U is more sensitive to the type of particles, especially their size.

The fact that the celestial α-pattern is so robust (Fig. 18.1), being qualitatively the same under all sky conditions, is of great biological importance for the orientation of polarization-sensitive animals based on skylight polarization: If the degree of polarization d of skylight is higher than the threshold d^* of polarization sensitivity of animals, then their orientation can be governed by the celestial angle of polarization α, from the pattern of which the direction of the solar meridian can be determined, if the sun is occluded by fog, smoke, clouds or tree canopy. Although d of light from overcast skies, for example, is usually not higher than about 16 % (Hegedüs et al. 2007b), the threshold of polarization sensitivity in field crickets (*Gryllus campestris*) and honeybees (*Apis mellifera*), for instance, is $d^* = 5$ % and 10 %, respectively (Horváth and Varjú 2004). This means that these animals could use the celestial α-pattern for navigation even under totally overcast conditions. In the future it would be worth testing this prediction.

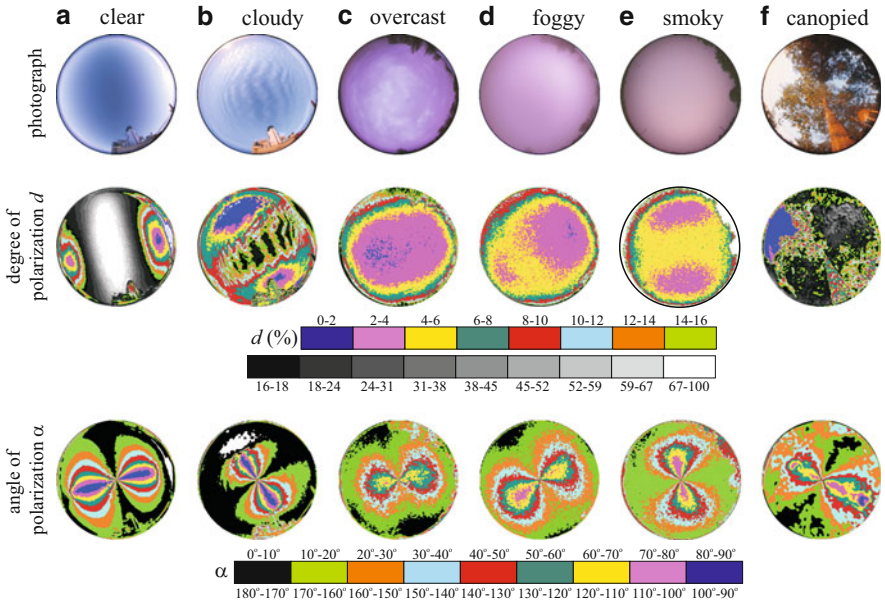

Fig. 18.1 Photograph and patterns of the degree d and angle α of linear polarization of clear, cloudy, overcast, foggy, smoky and tree-canopied skies measured by full-sky imaging polarimetry in the blue (450 nm) part of the spectrum

18.2 How Well Does the Rayleigh Model Describe the Pattern of the Direction of Polarization of Clear and Cloudy Skies?

Many animals are sensitive to the linear polarization of light, and several species can orient by means of the celestial polarization pattern (Horváth and Varjú 2004). These animals use the distribution of the direction of polarization of skylight in the ultraviolet, blue or green part of the spectrum (Barta and Horváth 2004). In the models and theories explaining the orientation behaviour of these animals, it is always assumed that in any point of the celestial hemisphere the direction of polarization of skylight is perpendicular to the scattering plane determined by the sun, the observer and the point observed (e.g. Kirschfeld et al. 1975; Wehner 1976, 1983, 1984, 1989, 1994, 1997; van der Glas 1977; Rossel et al. 1978; Brines 1980; Able 1982; Phillips and Waldvogel 1982; Rossel and Wehner 1982; Wehner and Rossel 1985; Able and Able 1990; Schmidt-Koenig et al. 1991; Hawryshyn 1992; Shashar et al. 1998; Freake 1999; Labhart and Meyer 1999). Hence, in the literature dealing with the sky compass orientation of these animals, it is hypothesized that the celestial pattern of the direction of polarization follows the rules of the first-order Rayleigh scattering of sunlight in the atmosphere (Coulson 1988; Dennis 2007; Hannay 2007). This hypothesis originates from Karl von Frisch (1967), who

supposed that this condition is realized for most areas of the clear sky, when he tried to interpret his pioneering observations on the celestial orientation of honeybees.

A widespread belief is that the Vikings were able to navigate on the open sea by means of the direction of polarization of clear (blue) patches of the sky when the sun was occluded by clouds. It is hypothesized (Ramskou 1967, 1969; Britton 1972; Schaefer 1997) that under partly cloudy conditions a Viking navigator could locate the sun, if he knew that the solar direction is perpendicular to the direction of polarization of skylight determined by a mysterious birefringent or dichroic crystal called 'sunstone' (see Chap. 25). Obviously, such navigation is practicable only if the single-scattering Rayleigh predictions are correct for the sky. Even small deviations of the direction of skylight polarization can produce large errors if used in a strictly geometrical way to locate the sun, impairing the navigator's ability to reach his actual goal. Hence, in considering how accurately a navigator could orient by this method, we must look also at how the pattern of the direction of polarization of real skies differs from the single-scattering Rayleigh pattern.

Suhai and Horváth (2004) presented the first high-resolution maps of the Rayleigh behaviour in clear and cloudy sky conditions measured by full-sky imaging polarimetry in the red (650 nm), green (550 nm) and blue (450 nm) parts of the spectrum versus the solar elevation angle θ_S (Figs. 18.2 and 18.3). Earlier, similar studies (Brines and Gould 1982; Coulson 1988) were restricted only to small numbers of celestial points, due to the use of scanning point-source polarimeters. The maps (Figs. 18.2 and 18.3) of Suhai and Horváth (2004) display those celestial areas at which the deviation $\Delta\alpha = |\alpha_{\text{measured}} - \alpha_{\text{Rayleigh}}|$ is below the threshold $\alpha_{\text{threshold}} = 5^\circ$, where α_{measured} is the angle of polarization of skylight measured by full-sky imaging polarimetry and α_{Rayleigh} is the celestial angle of polarization calculated on the basis of the single-scattering Rayleigh model (Coulson 1988). From these maps the proportion r of the full sky was derived for which the single-scattering Rayleigh model describes well (with an accuracy of $\Delta\alpha = 5^\circ$) the direction of polarization of skylight (Suhai and Horváth 2004). In the celestial maps of the Rayleigh behaviour (Figs. 18.2 and 18.3), 'Rayleigh' points with $\Delta\alpha \leq \alpha_{\text{threshold}}$ are shaded grey, 'non-Rayleigh' points with $\Delta\alpha > \alpha_{\text{threshold}}$ are white and the 'overexposed' points are black. Suhai and Horváth (2004) found the following trends (Figs. 18.2 and 18.3):

- Depending on the solar elevation angle θ_S, r is high for clear skies, especially for low solar elevations ($40\ \% < r < 70\ \%$ for $\theta_S \leq 13^\circ$).
- At a given solar position and in a given spectral range, r is always higher for the clear sky than for the cloudy sky. In the clear sky r ranges from about 13 to 69 % and from 4 to 69 % in the cloudy sky. However, when the sun is at or near the horizon and is not occluded by clouds, the r-values of cloudy skies approximate those of clear skies.
- The lower the solar elevation angle θ_S, the higher is r for both clear and cloudy skies, independently of the spectral range. Under clear sky conditions in the red part of the spectrum, r increases from 19 to 65 % as θ_S decreases from 65° (noon) to 0° (sunrise or sunset). Under cloudy sky conditions in the red, r increases from 4 to 56–65 % as θ_S decreases from its highest value to zero.

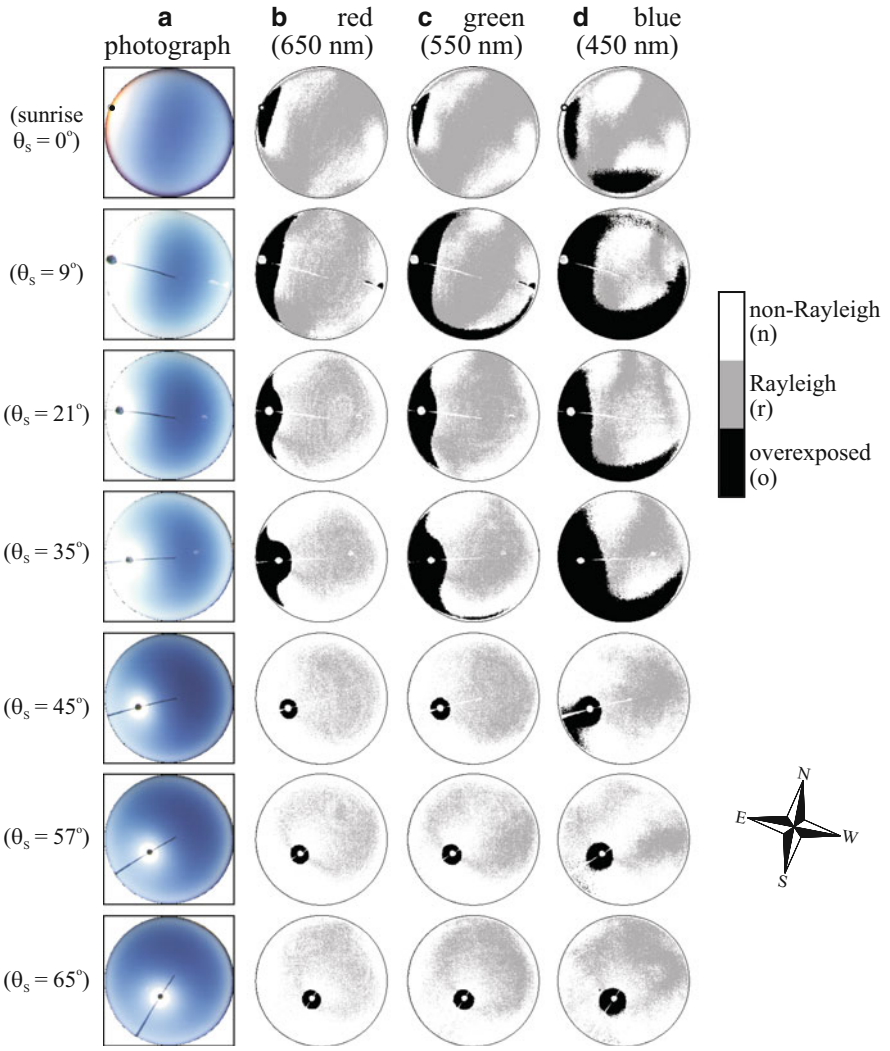

Fig. 18.2 (**a**) Distribution of the radiance of clear skies versus the solar elevation angle θ_S from the horizon. The centre of the circular pictures is the zenith, the perimeter is the horizon and the zenith angle φ is proportional to the radius ($\varphi_{zenith} = 0°$, $\varphi_{horizon} = 90°$). (**b**, **c**, **d**) Maps of the proportion r of the sky that follows the Rayleigh model for clear skies at the wavelengths 650 nm (red), 550 nm (green) and 450 nm (blue) versus θ_S. 'Rayleigh' points with $\Delta\alpha = |\alpha_{measured} - \alpha_{Rayleigh}| \leq 5°$ are shaded grey, 'non-Rayleigh' points with $\Delta\alpha > 5°$ are white and overexposed points are black. The approximately hourly positions of the sun are represented by dots or the disc of the sun occulter. The radial bar in the circular pictures is the wire of the sun occulter. The compass rose shows the geographic compass directions. Note that East and West are transposed in the compass rose, because we are looking upward at the sky-dome rather than downward at a map [after Fig. 1 on page 1670 of Suhai and Horváth (2004)]

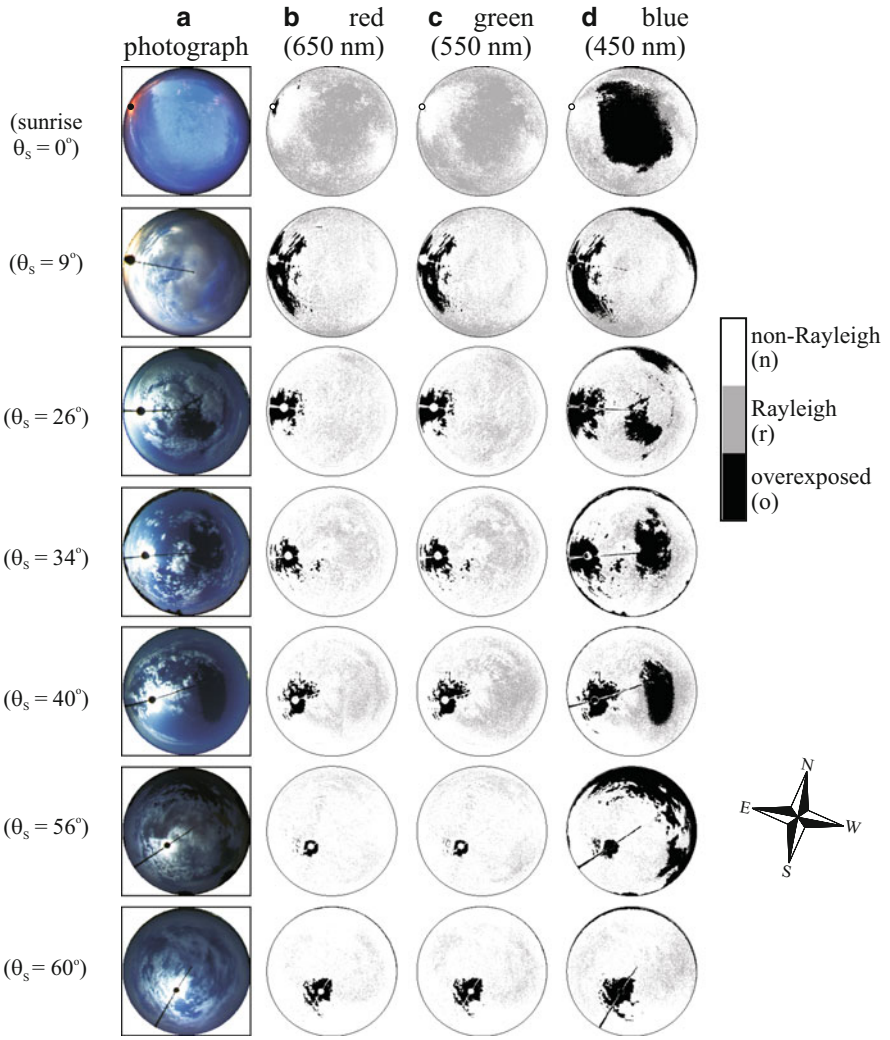

Fig. 18.3 As Fig. 18.2 for partly cloudy skies with approximately the same solar elevation angles θ_S and the same solar azimuth angles as in Fig. 18.2 [after Fig. 2 on page 1672 of Suhai and Horváth (2004)]

- For high solar elevations, r is highest in the blue part of the spectrum, lower in the green and lowest in the red under clear as well as cloudy sky conditions. This partly explains why the shorter wavelengths are generally preferred by day-active animals navigating by means of the celestial polarization (Barta and Horváth 2004). For lower solar elevations, $r_{green} > r_{red}$, but $r_{blue} < r_{green}$.
- Sometimes, a considerable part (r_{clouds}) of the pattern of the direction of polarization of the cloudy sky regions follows the Rayleigh pattern. The lower the

solar elevation θ_S, the higher the value of r_{clouds}, independently of the spectral range. Under cloudy sky conditions in the green, for example, r_{clouds} increases from about 1 to 12–34 % as θ_S decreases from its highest value to zero.

The increase or decrease of $\alpha_{threshold}$ increased or decreased the r-value but did not influence the validity of these trends. Hence, Suhai and Horváth (2004) found that the celestial pattern of the direction of polarization generally well follows the Rayleigh pattern, which is a fundamental hypothesis in the study of animal orientation and Viking navigation with the use of the celestial α-pattern.

18.3 Polarization Patterns of Foggy and Cloudy Skies

In sunshine the Vikings navigated on the open sea by sundials (Thirslund 2001). According to a widespread hypothesis (Barfod 1967; Ramskou 1967, 1969; LaFay 1970; Binns 1971; Britton 1972; Kreithen and Keeton 1974; Schnall 1975; Wehner 1976; Walker 1978; Nussbaum and Phillips 1982; Können 1985; McGrath 1991; Roslund and Beckman 1994; Schaefer 1997; Shashar et al. 1998; Thirslund 2001), when the sun was occluded by fog or clouds, the Vikings might have navigated by the skylight polarization detected with an enigmatic birefringent or dichroic crystal, called 'sunstone' (see Chap. 25). There are two atmospheric optical prerequisites for this alleged sky-polarimetric Viking navigation under foggy/cloudy skies: (1) The degree of linear polarization d of skylight should be high enough and (2) at a given sun position, the pattern of the angle of polarization α of the foggy/cloudy sky should be similar to that of the clear sky.

Using full-sky imaging polarimetry, Hegedüs et al. (2007a) measured the d- and α-patterns of Arctic clear, foggy and cloudy skies when the sun was invisible. For the same sun position, the measured α-pattern of a given sky was compared from pixel to pixel with the corresponding celestial α-pattern calculated on the basis of the model of Berry et al. (2004) based on the neutral points, later derived using multiple scattering by Hannay (2004). This model provides a very good quantitative approximation of experimental clear sky α-patterns, particularly in respect to the existence of neutral points. At a given celestial point, the measured α_m and the theoretical α_{th} were considered to be similar and dissimilar if $|\alpha_m - \alpha_{th}| \leq 5^\circ$ and $|\alpha_m - \alpha_{th}| > 5^\circ$, respectively.

Comparing the d- and α-patterns of foggy (Figs. 18.4d, g), clear (Figs. 18.4e, h) and cloudy (Figs. 18.4f, i) skies, Hegedüs et al. (2007a) established that the polarization patterns of foggy and cloudy skies are qualitatively the same as that of the corresponding clear sky. Depending on the cloudiness and the wavelength, the average degrees of polarization $d_{cloudy} = 10$–25 % and noisiness $n_{cloudy} = 4$–15 % of partly cloudy skies were between those of the clear ($d_{clear} = 16$–34 %, $n_{clear} = 3$–6 %) and foggy ($d_{foggy} = 4$–15 %, $n_{foggy} = 5$–45 %) skies. The average similarities of the clear, partly cloudy and foggy skies were $s_{clear} = 65.8$–70.7 %, $s_{cloudy} = 49.0$–61.8 % and $s_{foggy} = 41.4$–50.0 %. The similarity was usually highest

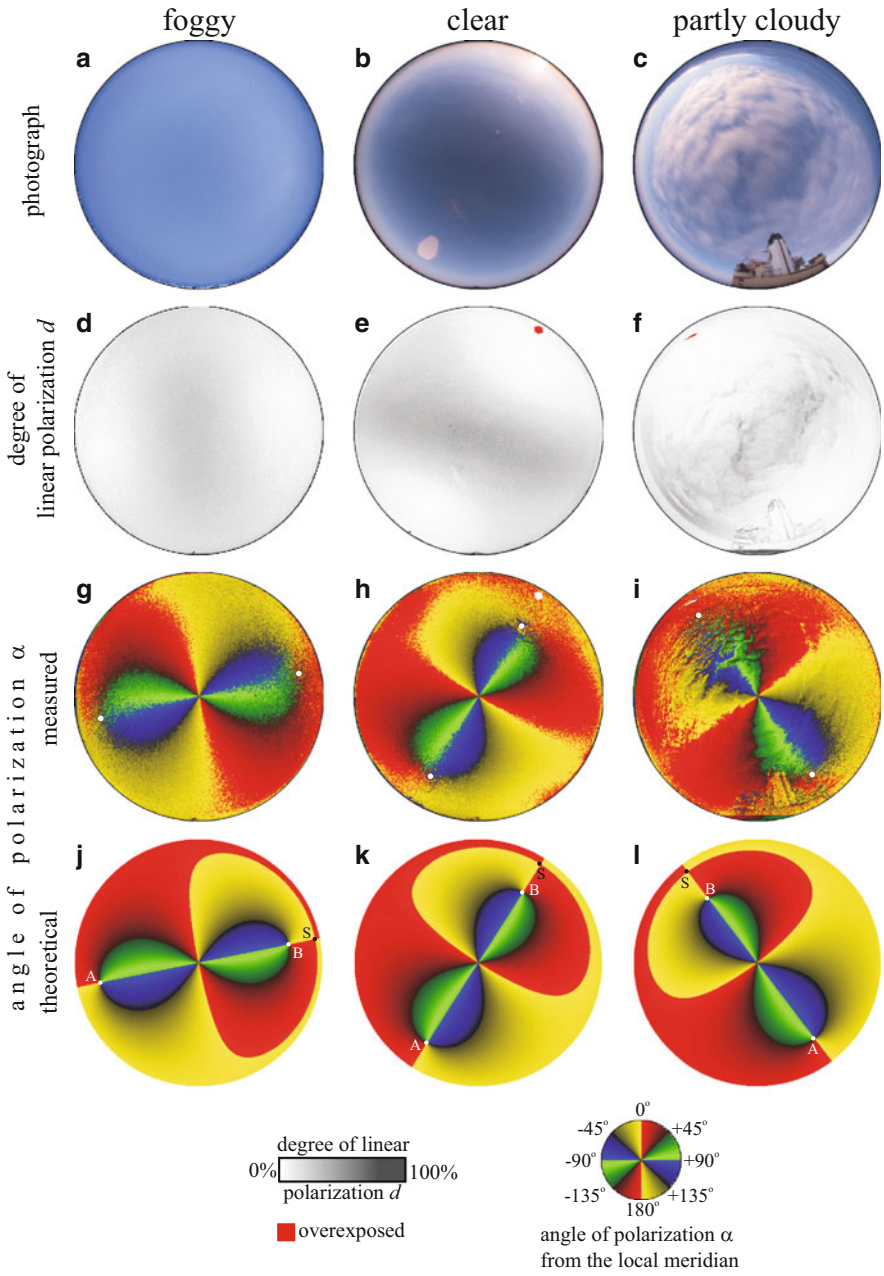

Fig. 18.4 Photographs (**a**–**c**) and patterns of the degree of linear polarization d (**d**–**f**) and angle of polarization α (**g**–**i**) of a sunlit foggy Arctic sky, a clear Arctic sky and a partly cloudy Arctic sky measured by full-sky imaging polarimetry in the blue (450 nm) part of the spectrum. The optical axis of the fisheye lens was vertical; thus, the horizon is the perimeter and the centre of the circular patterns is the zenith. (**j**–**l**) Theoretical α-patterns of the clear sky calculated on the basis of the

in the blue part of the spectrum for partly cloudy and foggy skies. The minima and maxima of s for clear, partly cloudy and foggy skies were $45\ \% \leq s_{\text{clear}} \leq 81\ \%$, $36\ \% \leq s_{\text{cloudy}} \leq 72\ \%$ and $19\ \% \leq s_{\text{foggy}} \leq 71\ \%$. This showed that if the fog is not too thick, then the celestial α-pattern can be as similar or even more similar to the theoretical α-pattern than those of certain clear skies. However, according to the preceding text, the following relations are true for the averages: $d_{\text{foggy}} < d_{\text{cloudy}} < d_{\text{clear}}$, $n_{\text{clear}} < n_{\text{cloudy}} < n_{\text{foggy}}$ and $s_{\text{foggy}} < s_{\text{cloudy}} < s_{\text{clear}}$. Figure 18.5 shows the maps of similarity of α to the theory for the foggy, clear and cloudy skies of Fig. 18.4 computed in the red (650 nm), green (550 nm) and blue (450 nm) parts of the spectrum.

According to the polarimetric measurements of Hegedüs et al. (2007a), the degree of polarization d of fog light is more or less reduced relative to the d of light from the clear sky, but the α-pattern of sunlit fog[1] remains qualitatively the same as that of the clear sky. This can be explained as follows: In the single-scattering Rayleigh model, the direction of polarization of scattered skylight is always perpendicular to the main plane of scattering determined by the observer, the sun and the celestial point observed. This type of Rayleigh polarization is called 'positive polarization' (Coulson 1988). Multiple scattering results in that the direction of polarization of scattered light has a component parallel to the main plane of scattering. This type is called 'negative polarization' (Coulson 1988). Hence, multiple scattering introduces negative polarization into the atmosphere. This depolarizes the skylight, i.e. decreases its d. The stronger the multiple scattering, the larger the amount of negatively polarized light added to the positively polarized single-scattered light, and thus the lower the net d of skylight. Neutral (unpolarized) points occur where the amounts of positively and negatively polarized skylight are equal. Apart from the neutral points, the α-pattern of multiple-scattered skylight remains similar to that characteristic of the single-scattering Rayleigh atmosphere, as long as $d > 0$.

In sunlit fog, scattering of sunlight happens on the tiny water droplets (of water fog) or ice crystals (of ice fog). On the one hand, the α-pattern of sunlit fog is not the result of light scattering in the air between the observer and the fog. Note that the observer is often within the fog layer. On the other hand, the reason for the α-pattern of sunlit fog is not that the α-pattern of the clear sky above the fog is visible through the fog layer. The α-pattern of the sunlit fog is the result of scattering of sunlight on

Fig. 18.4 (continued) model of Berry et al. (2004) for the same sun position as in skies **a**, **b** and **c**. The positions of the sun as well as the Arago and Babinet neutral points are marked by dots in the α-patterns. The abbreviations in patterns **j**, **k** and **l** are S = sun, A = Arago neutral point and B = Babinet neutral point [after Fig. 1 on page 1085 of Hegedüs et al. (2007a)]

[1] Sunlit fog means that the fog layer is illuminated by direct sunlight, because the sun is not occluded by clouds.

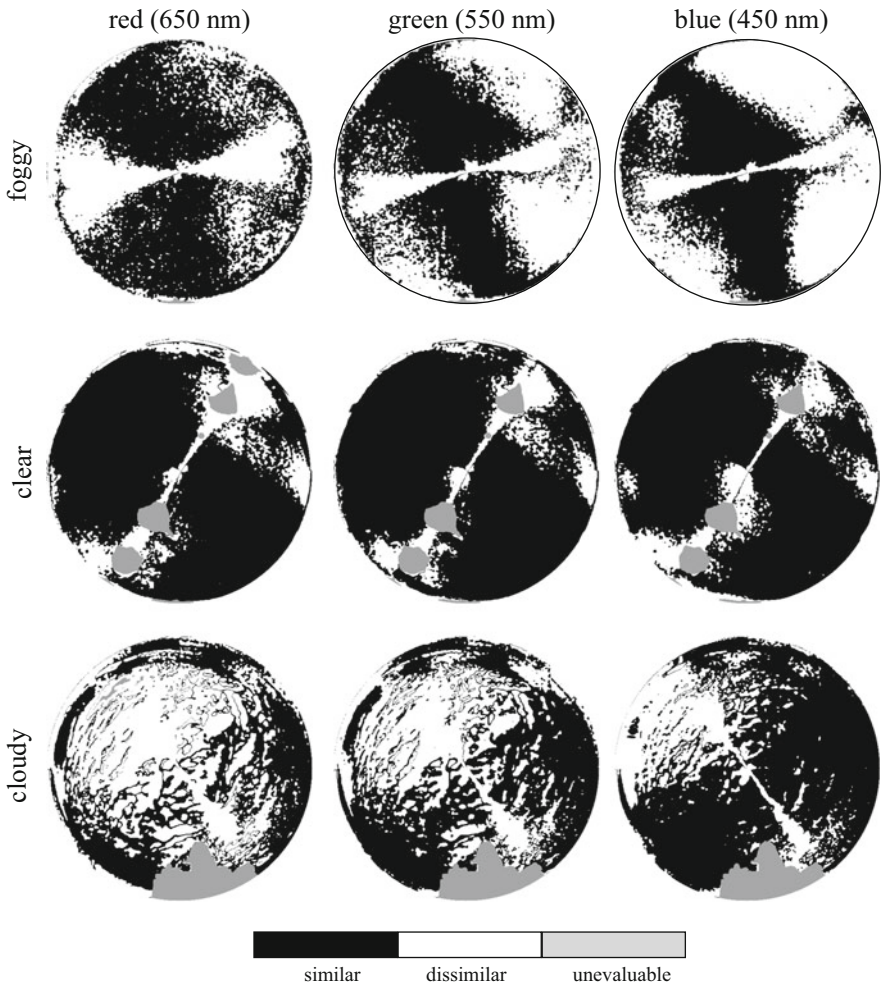

Fig. 18.5 Maps of similarity (and dissimilarity) of the angle of polarization α to the theory for the sunlit foggy, clear and partly cloudy skies shown in Fig. 18.4 computed in the red (650 nm), green (550 nm) and blue (450 nm) parts of the spectrum. Celestial regions are shaded by black and white, the α-patterns of which are similar and dissimilar, respectively, in comparison with the theoretical α-patterns calculated on the basis of the model of Berry et al. (2004) for the same sun positions. The grey sky regions were unevaluable due to under- or overexposure [after Fig. 2 on page 1091 of Hegedüs et al. (2007a)]

the fog particles rather than the transmission of polarized light from the clear sky or scattering of light below the fog layer.

Hegedüs et al. (2007a) also showed that although prerequisite (2) of the sky-polarimetric Viking navigation is always fulfilled under both foggy and cloudy conditions if the fog layer is illuminated by direct sunlight, prerequisite (1) is usually satisfied only for cloudy skies. In sunlit fog the Vikings could have

navigated by polarization only, if d of light from the foggy sky was sufficiently high (see Chap. 25).

18.4 Polarization Patterns of Overcast Skies

Earlier, the polarization of light from heavily overcast skies has been measured only sporadically in some celestial points by point-source polarimetry (Coulson 1971, 1988; Brines and Gould 1982; Können 1985; Horváth and Varjú 2004). Hegedüs et al. (2007b) measured the patterns of the degree d and angle α of linear polarization of totally overcast skies (when the sun was invisible) on the Arctic Ocean and in Hungary by full-sky imaging polarimetry in the red, green and blue parts of the spectrum. They found that depending on the optical thickness of the cloud layer, the pattern of α of light transmitted through the ice or water clouds of a totally overcast sky is qualitatively the same as the α-pattern of the corresponding clear sky with the same sun position. Under overcast conditions the value of α is determined predominantly by scattering on cloud particles themselves. Nevertheless, d of light from overcast skies is rather low ($d \leq 16$ %).

Figure 18.6 shows the patterns of the radiance I, degree of polarization d and angle of polarization α of a clear Arctic sky above the extended ice/snow cover of the Arctic Ocean in the red, green and blue parts of the spectrum. d of light from the clear sky is highest at 90° from the sun and gradually decreases towards the solar and antisolar points (Fig. 18.6b–d); furthermore, d is highest in the red ($d_{\max} = 59$ %) and lowest in the blue ($d_{\max} = 36$ %) part of the spectrum. The angle of polarization α of light from the clear sky has a characteristic pattern (Fig. 18.6e–g): The isolines with $\alpha =$ constant are always 8 shaped with a centre at the zenith and an axis of mirror symmetry coinciding with the solar–antisolar meridian in such a way that the smaller loop of the 8 figure is always in the solar half of the sky.

Figure 18.7 shows the I-, d- and α-patterns of a totally overcast sky in Hungary over an extended snow surface. d of light from the overcast sky is very low, and its pattern has approximately a rotational symmetry with a minimum near the zenith and an approximately annular maximum on the horizon (Fig. 18.7b–d). Depending on the wavelength, the maximum of d ranges between 4 and 16 %. The α-patterns of the overcast sky (Fig. 18.7e–g) are qualitatively the same as those of the clear sky (Fig. 18.6e–g): At all three (red, green, blue) spectral ranges, the α-isolines are again 8 shaped with a centre at the zenith and a symmetry axis along the solar–antisolar meridian. This was also true for all the other numerous overcast skies studied by Hegedüs et al. (2007b).

Due to the strong multiple scattering of light on the cloud particles (ice crystals or water droplets), the d of light from the overcast sky is considerably reduced in comparison with d of light from the clear sky; furthermore, the α-pattern of the overcast sky is noisier than that of the clear sky (noisiness n of an α-pattern denotes

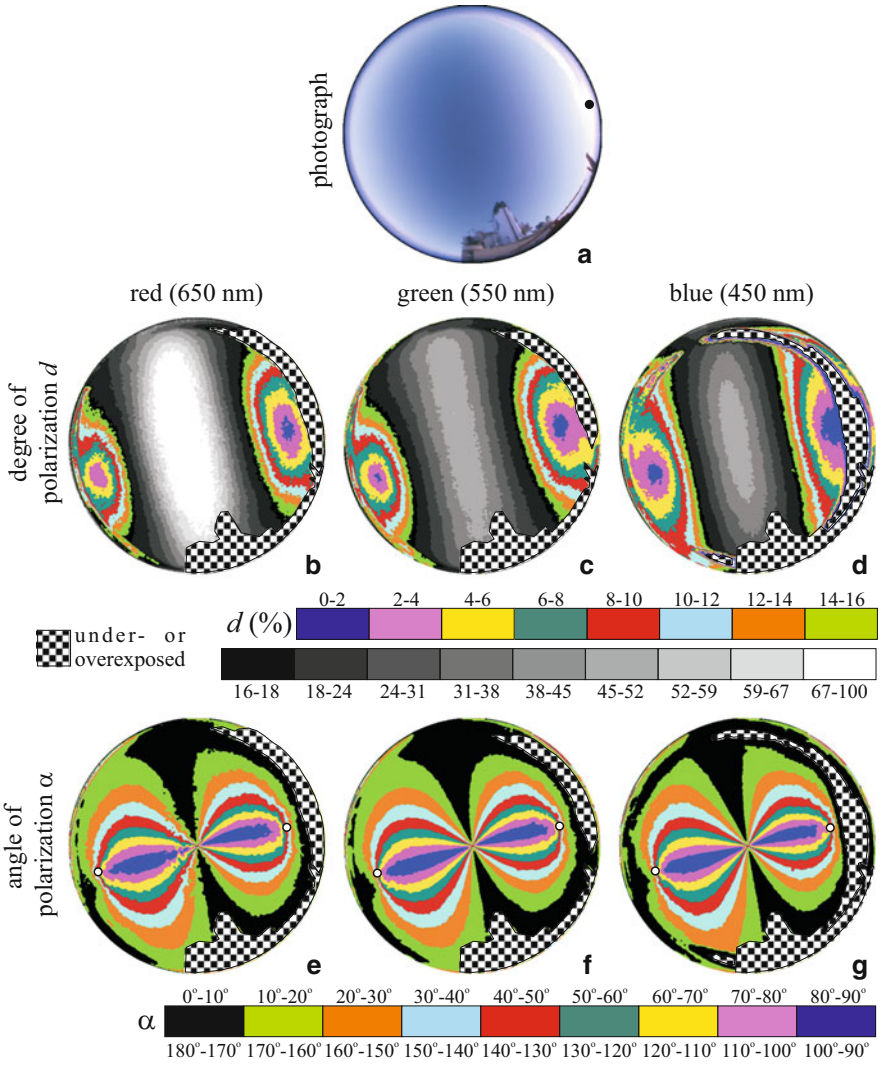

Fig. 18.6 Photograph (**a**) and patterns of the degree of linear polarization d (**b**–**d**) and angle of polarization α (clockwise from the local meridian) (**e**–**g**) of an Arctic clear sky measured by full-sky imaging polarimetry in the red (650 nm), green (550 nm) and blue (450 nm) parts of the spectrum. The optical axis of the fisheye lens was vertical; thus, the horizon is the perimeter and the centre of the circular patterns is the zenith. On the bottom of the circular photograph, the silhouette of the Swedish icebreaker Oden can be seen. In the photograph the position of the sun near the horizon is marked by a dot. In the α-patterns the positions of the Arago and Babinet neutral (unpolarized) points are marked by dots [after Fig. 1 on page 2350 of Hegedüs et al. (2007b)]

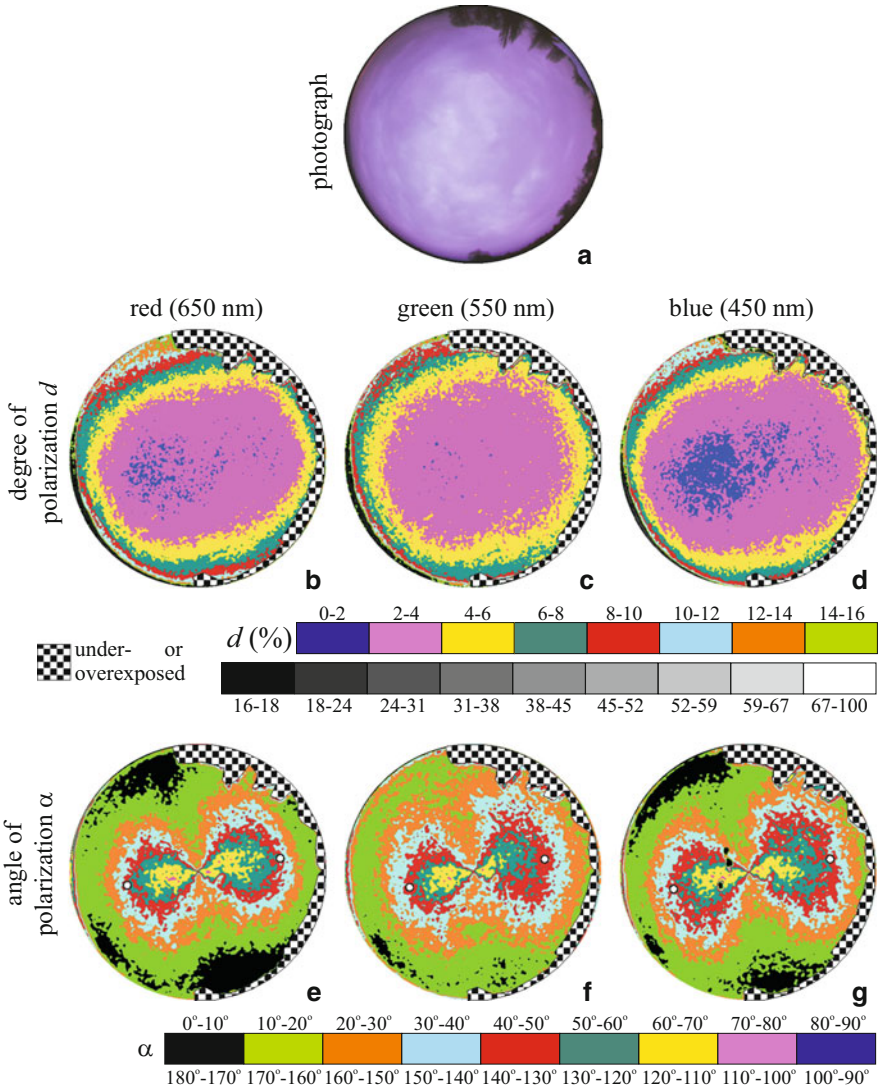

Fig. 18.7 As Fig. 18.6 for a totally overcast sky in Hungary when the ground was covered by snow. On the periphery of the colour picture, the dark silhouette of some trees can be seen [after Fig. 2 on page 2351 of Hegedüs et al. (2007b)]

how noisy it is compared to the white noise: $n = 0$ %, no noise; $n = 100$ %, white noise). The noisiness ($22\ \% \leq n \leq 43\ \%$) of the overcast skies studied by Hegedüs et al. (2007b) was about seven times higher than that of the clear sky in Fig. 18.6 ($3\ \% \leq n \leq 6\ \%$). Hence, depending on the optical thickness of the ice or water

clouds and the wavelength, the α-pattern of totally overcast skies is similar to that of the clear sky.

18.5 Celestial Polarization Pattern During Twilight

Scattering of sunlight produces patterns of partially linearly polarized light in the sky throughout the day (Brines and Gould 1982; Können 1985; Coulson 1988; Pomozi et al. 2001a; Horváth and Varjú 2004; Suhai and Horváth 2004), and similar patterns appear at night when the moon is bright enough (Gál et al. 2001). This celestial polarization pattern is used for orientation by many animal species (Horváth and Varjú 2004). But what are the characteristics of this pattern during the period of twilight, when the sun is below the horizon and the moon is not in the sky?

Astronomical twilight commences in the morning when the sun's influence is just detectable in the upper atmosphere, when the sun's centre is 18° below the eastern horizon and when the reverse situation holds in the evening. The duration of astronomical twilight depends on the inclination of the sun's path in a given situation: In the tropics, for example, where the sun moves nearly perpendicularly to the horizon most of the year, it lasts 1.25–1.5 h (Cronin et al. 2006). During the earlier parts of morning astronomical twilight, the influence of the sun is barely perceptible, but since it directionally illuminates the upper atmosphere, polarized light is scattered to the Earth's surface.

Despite the minimal illumination provided by skylight near the extremes of astronomical twilight, certain insects can navigate at these times. The halictid bee, *Megalopta genalis*, emerges from its nest in the Panamanian forest beginning approximately 1 h to 45 min before sunrise and forages for 15 to 30 min, probably on flowers in the forest canopy, before returning accurately to its home (Warrant et al. 2004). This behavioural pattern is reversed at sunset. The eyes of this tropical bee have specializations for extreme dim-light vision (Greiner et al. 2004; Warrant et al. 2004) and appear to be capable of analysing sky polarization, and it is hypothesized that this bee makes use of the upper-atmospheric polarization pattern during its foraging flights. In the tropics, the sun moves nearly perpendicularly to the horizon, so its azimuth changes very slowly over the period before twilight, making for a stable polarization pattern. Nocturnally migrating birds also require polarization cues at twilight to set their internal compasses for their flights in the dark and become disoriented when provided with a depolarized celestial pattern at this time (Muheim 2011; see also Chap. 12).

Using full-sky imaging polarimetry, Cronin et al. (2006) studied the celestial polarization pattern during the period of twilight and its changes before sunrise and after sunset. They obtained that during twilight, celestial polarized light occurs in a wide band stretching perpendicular to the location of the hidden sun and reaching maximal degrees of polarization near 80 % at wavelengths >600 nm. In the tropics, this polarization pattern appears approximately 1 h before local sunrise and

disappears nearly 1 h after local sunset (within 10 min after the onset of astronomical twilight at dawn and before its end at dusk) and extends with little change through the entire twilight period.

According to Cronin et al. (2006), animals that use polarized light for orientation during the day must solve a difficult geometric problem: While the daytime pattern of sky polarization is fully predictable and strong, it shows complex changes throughout the day as the sun travels across the sky. Similar problems are faced by animals that use nocturnal polarization patterns generated by moonlight. In contrast, during the period from near the onset of astronomical twilight to dawn (or the reverse at dusk), celestial polarization has a very constant pattern, varying little in angular distribution, degree of polarization and spectral content throughout much of this time. Hence, if an animal like *Megalopta genalis* is capable of detecting skylight polarization at very low intensities, the twilight interval provides a relatively simple orientation cue in the heavens.

18.6 Anomalous Sky Polarization Due to Forest Fire Smoke: Why Do Some Insects Disorient Under Smoky Skies?

The smoke and other combustion products of huge and long-lasting forest fires may have disadvantageous effects in triggering weather fluctuations and contributing to the global climate change (Kasischke and Stocks 2000; Bréon 2006). Apart from causing huge damage to local economy and biodiversity as well as health problems to humans, large-scale forest fires also release a huge amount of carbon to the atmosphere, contributing considerably to the annual increase in atmospheric carbon dioxide (Aldhous 2004). The most immediate consequence of forest fires is the diminution of direct solar radiation due to the absorption by smoke, which decreases the solar energy available to plant photosynthesis and solar power plants (Johnson and Miyanishi 2000). The most spectacular consequences of forest fires are some striking colour phenomena in the sky visible with the naked eye, like reddish skies, colourful rings around the sun or beautifully coloured sunset glows (Coulson 1988). These atmospheric optical phenomena induced by forest fire smoke are very similar to those caused by dust clouds produced by volcanic eruptions (Coulson 1988).

Using full-sky imaging polarimetry, Hegedüs et al. (2007c) measured the celestial polarization patterns in Fairbanks (Alaska) during several separate forest fires in the vicinity. They documented quantitatively that the celestial polarization, a sky attribute that is necessary for orientation of many polarization-sensitive animal species (Horváth and Varjú 2004), above Fairbanks on 17 August 2005 was in several aspects anomalous due to the forest fire smoke: (1) The pattern of the degree of linear polarization d of the reddish smoky sky differed considerably from that of the corresponding clear blue sky. (2) Due to the smoke, d of skylight was drastically

reduced ($d_{max} \leq 14$ %, $d_{average} \leq 8$ %). (3) Depending on wavelength and time, the Arago, Babinet and Brewster neutral points of sky polarization had anomalous positions relative to their normal positions.

Many polarization-sensitive animals (arthropods, fishes, amphibians, reptiles and birds) use the polarization pattern of skylight for orientation (Horváth and Varjú 2004). If this pattern changes drastically, as observed by Hegedüs et al. (2007c), animals orienting on the basis of sky polarization could easily go astray. An anomalous polarization pattern could also reduce the motivation to migrate, such that the invertebrate and vertebrate fauna would avoid migration and potentially be trapped in areas where their survival would be threatened by direct exposure to the fire.

Johnson et al. (2005) reported on the environmental impacts of Canadian forest fires in August 2003, when in British Columbia over 1.5 M hectares of forest burned, in over 2,000 separate fires. Aerosols, consisting of suspended ash particles, concentrated in valleys and moved east onto the Prairies. Smoke darkened the sky, and many insects reduced straight-line flying to short distances only. Flights by grasshoppers (Orthoptera: Acrididae) were greatly reduced. A previously uncommon but locally occurring seed bug (*Sphragisticus nebulosus*; Hemiptera: Rhyparochromidae) fledged, but delayed flight, building up in large numbers in southern Alberta grassland. When skies cleared, mass bug migrations invaded Medicine Hat in sufficient numbers to close stores and restaurants (Johnson et al. 2005).

Hegedüs et al. (2007c) suggested that the disorientation of insects observed by Johnson et al. (2005) under smoky skies might be the consequence of the anomalous sky polarization induced by the smoke of forest fires. Considering orientation, the most disturbing effect could be that the degree of polarization d of light from smoky skies is very low. If d is lower than the species-dependent threshold d^* of polarization sensitivity, the skylight polarization cannot be detected.

Hence, large-scale forest fires may have not only a direct negative effect on habitat availability and mortality in animal populations but also could influence the animals' ability to navigate and escape from the dangers of the fire itself. On a more regional scale, it cannot be excluded that forest fires can have a negative effect on animal migration systems in which migration between different habitats is crucial for the survival of the migrants (Alerstam et al. 2003).

Gál et al. (2001) showed that the polarization pattern of the moonlit clear night sky is practically the same as that of the sunlit clear sky, if the position of the moon and sun is the same. Thus, Hegedüs et al. (2007c) expected that forest fire smoke has similar effects on the sky polarization during day and night. Gábor Horváth and Alexandra Farkas measured the celestial polarization of sunlit and moonlit, smoky and clear skies by full-sky imaging polarimetry (Figs. 18.8, 18.9, 18.10 and 18.11). They showed that the smoke of burning vegetation reduced considerably the d of sunlit ($d_{max} \leq 19.2$–35.3 %, $d_{average} \leq 13.0$–26.3 %) and moonlit ($d_{max} \leq 16.3$–19.4 %, $d_{average} \leq 12.5$–17.6 %) skies relative to the corresponding clear sunlit ($d_{max} \leq 56.6$–61.9 %, $d_{average} \leq 34.1$–41.5 %) and clear moonlit ($d_{max} \leq 28.9$–48.5 %, $d_{average} \leq 20.4$–31.3 %) skies. Furthermore, the wavelength- and

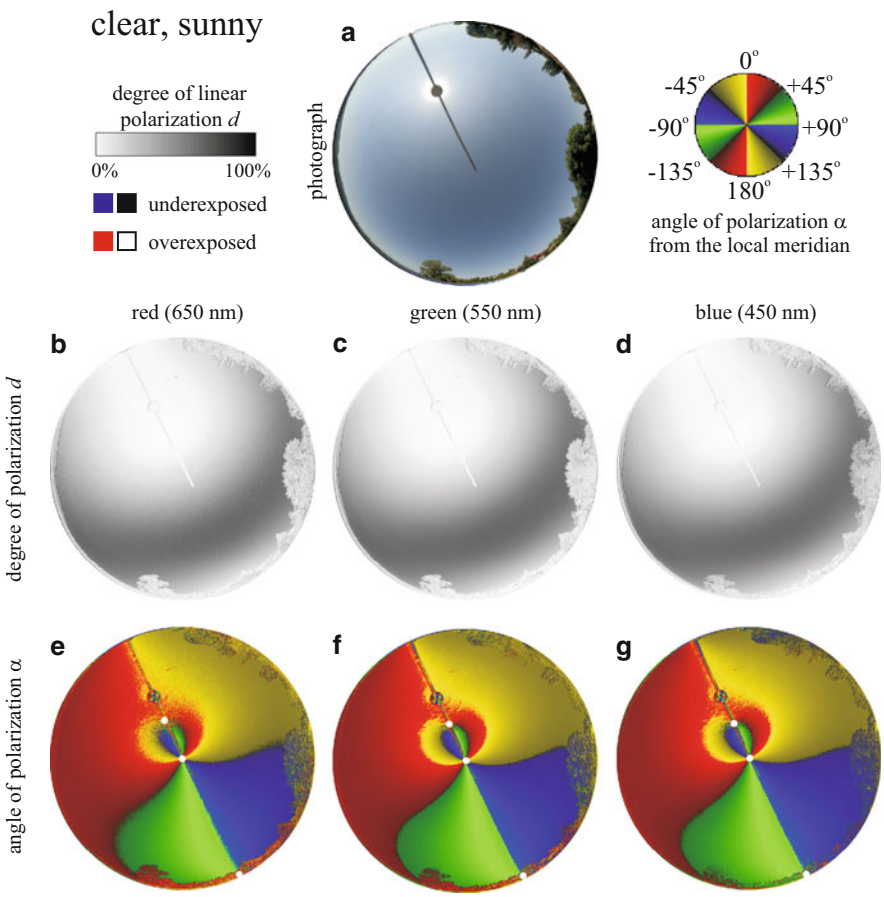

Fig. 18.8 Colour photograph (**a**) and the patterns of the degree of linear polarization d (**b**, **c**, **d**) and the angle of polarization α clockwise from the local meridian (**e**, **f**, **g**) of skylight measured in the Hungarian town Göd (47° 70′ N, 19° 15′ E) on the shore of river Danube under a clear sunlit sky on 28 August 2012 at 12:26 h (UT) by full-sky imaging polarimetry in the red (650 nm), green (550 nm) and blue (450 nm) parts of the spectrum. In the α-patterns the positions of the zenith (at the centre of the circular pattern) and the Arago (in the antisolar sky region) and Babinet (in the solar sky region) neutral points are marked by dots

time-dependent angular distance between the Arago and Babinet neutral (unpolarized) points of sunlit and moonlit skies decreased and increased due to the smoke for higher (44°–47°) and lower (19°–20°) solar/lunar elevations, respectively.

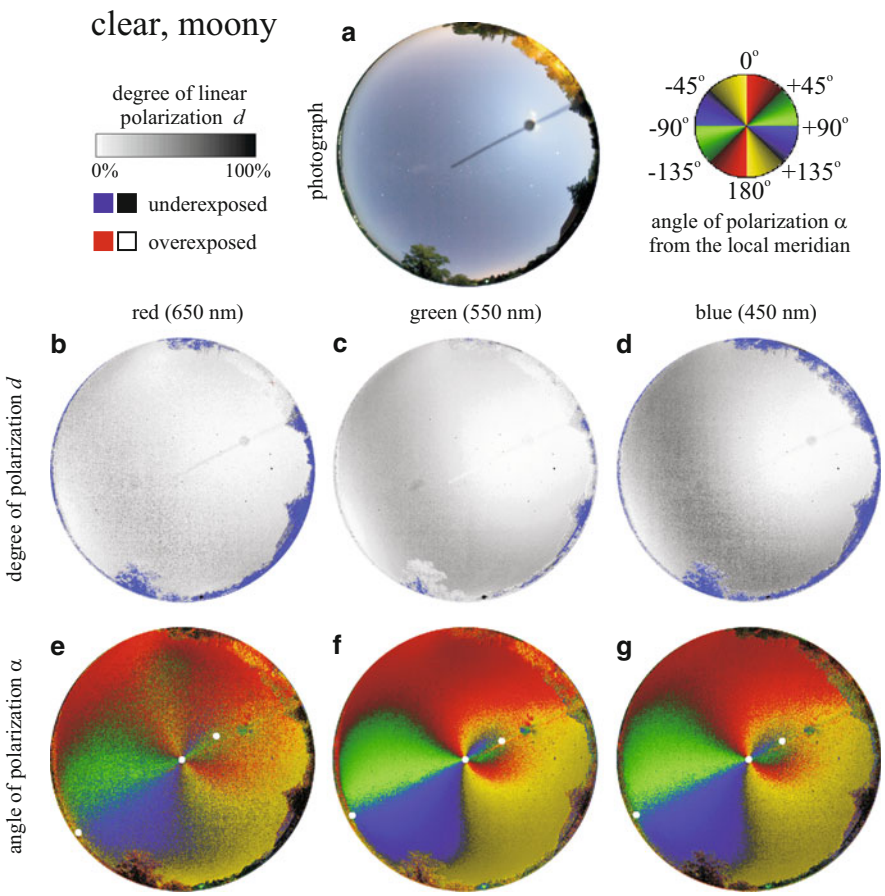

Fig. 18.9 As Fig. 18.8 for a clear moonlit sky measured on 3 October 2012 at 22:33 h (UT)

18.7 Sky Polarization During Total Solar Eclipses

Piltschikoff (1906) reported that at the beginning of the totality of a solar eclipse (30 August 1905, Philippeville, Algeria), the degree of linear polarization d of skylight decreased drastically at 90° from the eclipsed sun. de Bary et al. (1961) observed the temporal change in d of skylight at 90° from the obscured sun during the total solar eclipse on 15 February 1961 in Viareggio (Italy). Moore and Rao (1966) registered the polarization at some celestial points during the total eclipse on 30 May 1965 from an aircraft in the vicinity of Bellingshausen Atoll at an altitude of 12.3 km. Rao et al. (1972) measured the d of skylight at a few points of the sky during the total eclipse on 12 November 1966 from an aircraft flying at an altitude of 10 km above the Uruguayan coast. Dandekar and Turtle (1971) performed polarimetric measurements in the blue and red spectral ranges during the total

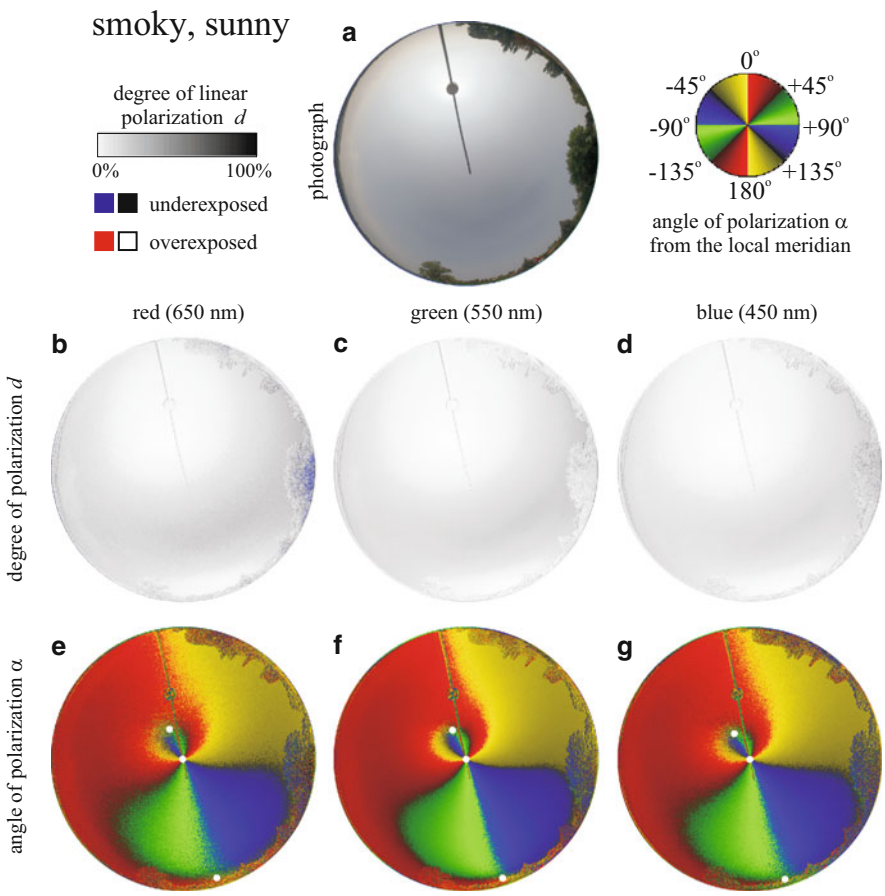

Fig. 18.10 As Fig. 18.8 for a smoky sunlit sky measured on 2 September 2012 at 11:50 h (UT)

eclipse of 7 March 1970 in Kinston (USA). Miller and Fastie (1972) observed the skylight polarization during the total solar eclipse on 30 May 1965 from an aircraft flying at an altitude of 12.2 km over the South Pacific. Shaw (1975) measured sequentially the celestial polarization along the solar–antisolar meridian and perpendicular to it in the blue part of the spectrum during the 30 June 1973 total eclipse in Kenya (Africa). Using two polarimeters oriented in the direction of the zenith and at 90° from the sun in the sun's vertical, Coulson (1988) observed a virtual lack of polarization response during a partial (80 %) eclipse of the sun at Davies (USA) on 26 February 1979. With the help of a numerical model, Können (1987) explained quantitatively several polarization characteristics of the eclipsed sky, especially the occurrence of a neutral (unpolarized, $d = 0$) point near the zenith. All these measurements of the polarization of eclipsed skies were carried out by point-source polarimeters with fields of view not wider than a few degrees.

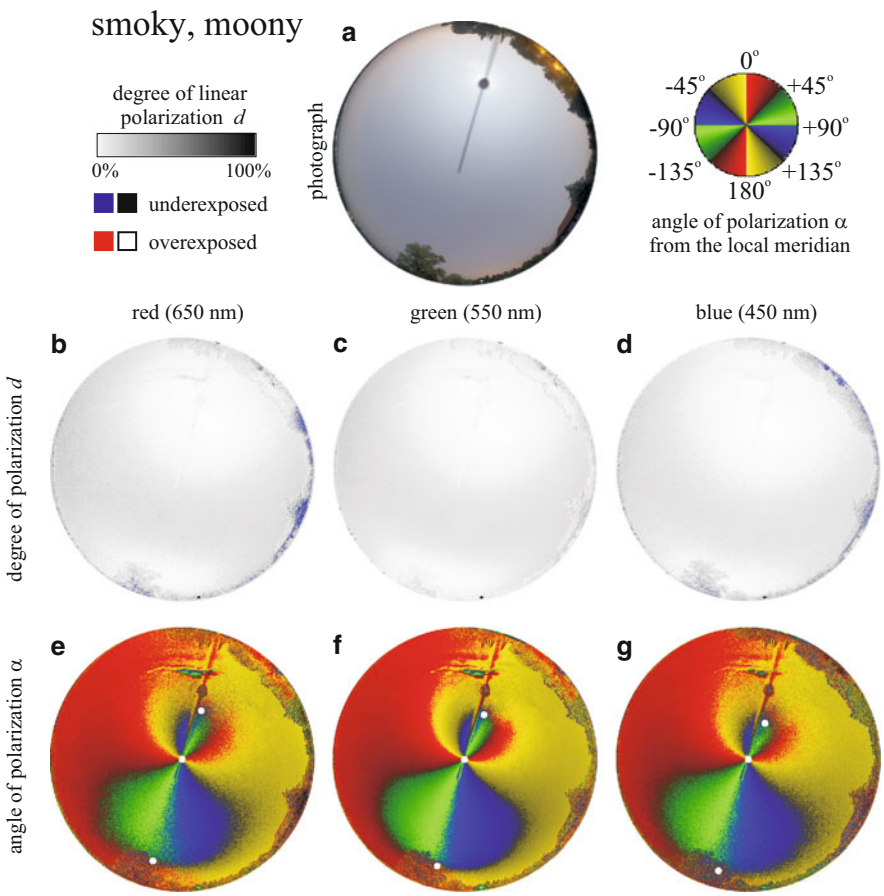

Fig. 18.11 As Fig. 18.8 for a smoky moonlit sky measured on 1 September 2012 at 23:13 h (UT)

Gerharz (1976) took photographs about the celestial circumsolar area of $12^\circ \times 15^\circ$ through a modified Savart filter and a green interference filter during the total eclipse of 7 March 1970 near Williamston (USA). From the photographed interference bands, he deduced the degree and angle of linear polarization of light scattered from the circumsolar region of the eclipsed sky. Using full-sky (180° field-of-view) imaging polarimetry, Pomozi et al. (2001b) measured the spatiotemporal change of the fine structure of the polarization pattern of the eclipsed sky during the total solar eclipse of 11 August 1999 in Kecel (Hungary). They compared these patterns with the normal celestial polarization patterns measured at the same time on the day after the eclipse. As a second control sky, they used the celestial polarization pattern measured on 26 August 1999 in Tunisia with the same solar zenith angle (32°) as that during the Hungarian eclipse. Pomozi et al. (2001b) also investigated the spectral characteristics of sky polarization during totality in the red, green and blue parts of the spectrum. They gave a qualitative explanation for the

origin of the pattern of the angle of polarization and the neutral point of skylight polarization near the zenith observed during totality. Horváth et al. (2003) reported on the observation of some neutral points and points with minimum d in the eclipsed sky during the solar eclipse on 11 August 1999 in Kecel.

Using full-sky imaging polarimetry, Sipőcz et al. (2008) measured the spatiotemporal change of the polarization of skylight during the total solar eclipse on 29 March 2006 at Side (Turkey). They observed the temporal variation of the celestial patterns of the degree d and angle α of polarization of the eclipsed sky measured in the red (650 nm), green (550 nm) and blue (450 nm) parts of the spectrum. They also reported on the temporal and spectral change of the positions of neutral (unpolarized, $d = 0$) points and points with local minima or maxima of d of the eclipsed sky. These results were compared with the observations performed by the same polarimetric technique during the total solar eclipse on 11 August 1999 in Hungary (Pomozi et al. 2001b; Horváth et al. 2003).

Figure 18.12 shows the photograph of the sky and the celestial patterns of d and α measured by full-sky imaging polarimetry in the green (550 nm) spectral range during the total solar eclipse on 29 March 2006 in Turkey from the first to the fourth contact. Scenes 1 and 2 represent the sky conditions at the beginning (first contact) and the end (second contact) of the partial pre-eclipse, while scenes 12 and 13 represent the sky conditions at the beginning (third contact) and the end (fourth contact) of the partial post-eclipse, respectively.

During the pre- and post-eclipse, both the d- and α-patterns of the sky (scenes 1–2 and 12–13 in Fig. 18.12) were essentially the same as those of the normal clear sky, if the obscuration of the sun's disc was not larger than 87.9 % (pre-eclipse) and 88.5 % (post-eclipse): d of light from the pre- and post-eclipsed sky was always highest (depending on the wavelength and time with $d_{\max} = 45$–52 %) at 90° from the sun, and it gradually decreased towards the sun and antisolar point. Depending on the wavelength and time, $d_{\text{average}} + \Delta d$ was 30–36 % for the pre- and post-eclipsed skies, where Δd is the standard deviation of d. d was zero at the Babinet and Brewster neutral points positioned along the solar meridian at an angle of about 15° from the sun. Depending on the wavelength and time, the percentage k of the α-pattern for which $45° \leq \alpha \leq 135°$ was 57–72 % during the pre-eclipse and 52–57 % at the beginning of the post-eclipse. Hence, prior to and immediately after totality, k was larger than 50 %. Both the d- and α-patterns of the pre- and post-eclipsed skies were mirror symmetric to the solar–antisolar meridian.

When the obscuration of the sun's disc was 99.5 %, considerable differences occurred between the polarization patterns of the pre-eclipsed sky and the normal sky (scene 3 of Fig. 18.12). Scene 3 with its 99.5 % obscuration of the sun's disc is an intermediate between the pre-eclipse and totality.

During totality (when the obscuration of the sun's disc was 100 %), both the celestial d- and α-patterns (scenes 4–11 in Fig. 18.12) were significantly different from those of the normal sky (scenes 1–2 and 12–13 in Fig. 18.12): The degrees of polarization of eclipsed skylight were reduced relative to the d-values of the pre- and post-eclipsed skies. Depending on the wavelength and time during totality, $d_{\text{average}} + \Delta d$ of skylight was 5–26 % (30–36 % for the pre- and post-eclipse) and

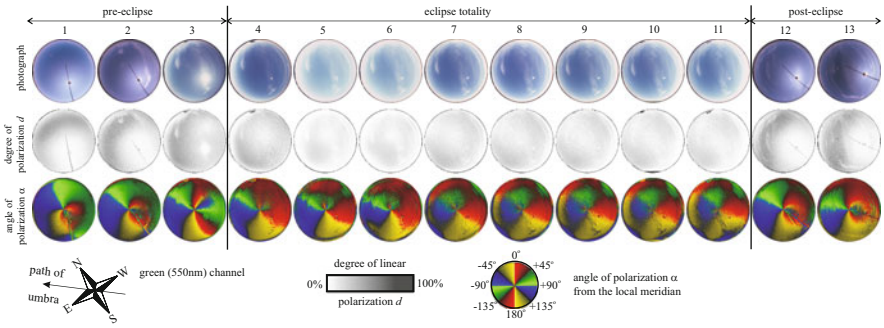

Fig. 18.12 Photograph and patterns of the degree of linear polarization d and angle of polarization α of skylight measured by full-sky imaging polarimetry in the green (550 nm) spectral range during the total solar eclipse on 29 March 2006 in Turkey. East (West) is on the left (right) rather than on the right (left) of the compass rose, because we are looking up through the celestial dome rather than down onto a map [after Fig. 2 on page H4 of Sipőcz et al. (2008)]

$d_{\max} = 4$–36 % (45–52 % for the pre- and post-eclipse), while k of the α-pattern was 33–43 % (52–72 % for the pre- and post-eclipse). Hence, during totality k was smaller than 50 %. During totality both the d- and α-patterns of the sky changed more or less temporally, and the α-pattern was approximately mirror symmetric to the solar–antisolar meridian. Contrary to the relatively great spectral dispersion of d of skylight, the wavelength dependence of α of skylight was rather modest during the entire eclipse period (from pre-eclipse through totality to post-eclipse).

During totality Sipőcz et al. (2008) observed some points with local minima or maxima of d: Figure 18.13 shows the temporal change of the positions of the celestial points with d extrema in scenes 3–11 during the eclipse in the red, green and blue spectral ranges. In scenes 3–11 in all the red, green and blue spectral ranges, there were always two or three local maxima (π_1, π_2 and/or π_3) and two local minima (η_1 and η_2) of d. Both the positions and the minimal/maximal d-values of the celestial points η_1, η_2, π_1, π_2 and π_3 depended on the wavelength of light (Fig. 18.13).

The celestial points π_1, π_2 and π_3 with local maxima of d are called ‘polarized points’ in analogy to the ‘unpolarized (neutral) points’ (Sipőcz et al. 2008). These polarized points were positioned near the horizon perpendicularly and approximately symmetrically to the solar–antisolar meridian (Fig. 18.13). The position of the polarized point π_1 changed greatly in time, while the temporal variation of the positions of the other two polarized points π_2 and π_3 was small. One of the points (η_1) with a local minimum of d was near the zenith, while the other local minimum of d (η_2) was near the horizon and the antisolar meridian (Fig. 18.13). According to Sipőcz et al. (2008), in scene 5 (Fig. 18.12) the local minimum η_2 of d (≤ 1 %) near the horizon (Fig. 18.13) might be a neutral point in all the red, green and blue parts of the spectrum. In scene 5 (Fig. 18.12) the local minimum η_1 of d (≤ 1 %) near the zenith (Fig. 18.13) could be a neutral point in the blue spectral range. Similarly, in

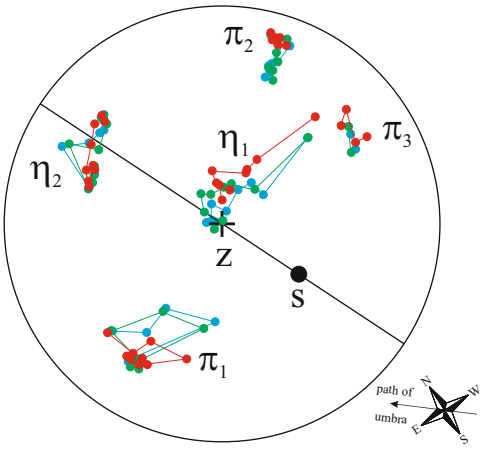

Fig. 18.13 Temporal and spectral change of the positions of the celestial points with extrema of the degree of position d measured by full-sky imaging polarimetry in the red (650 nm), green (550 nm) and blue (450 nm) parts of the spectrum during the total eclipse on 29 March 2006 in Turkey. π_1, π_2, π_3: local maxima of d; η_1, η_2: local minima of d; Z, +: zenith; S: sun; circle: horizon; diameter through the sun: solar–antisolar meridian [after Fig. 6 on page H7 of Sipőcz et al. (2008)]

scene 6 (Fig. 18.12) the local minimum η_2 of d ($\leq$1 %) might be a neutral point in the green and blue parts of the spectrum, and the local minimum η_1 of d ($\leq$1 %) could be a neutral point in the blue spectral range (Fig. 18.13). The change of α was 90° if the neutral point η_1 near the zenith was crossed along the solar–antisolar meridian (Fig. 18.12). Such a celestial point was classified as 'type 2 neutral point' by Horváth et al. (2003). On the other hand, crossing the neutral point η_2 near the horizon (Fig. 18.13), the wavelength-dependent change of α was much smaller than 90° (Fig. 18.12). Horváth et al. (2003) classified such a celestial point as 'type 3 neutral point'. The position of point η_2 changed only slightly as a function of time, while the temporal variation of the position of point η_1 was considerable (Fig. 18.13).

The reason for the complex temporal change of the celestial polarization patterns observed during totality (Figs. 18.12 and 18.13) is that as the moon's shadow (umbra) moved across the observation point, the geometry of light scattering changed due to the varying illumination conditions of the eclipsed sky.

On the basis of the comparison between the observations on 11 August 1999 in Hungary with a zenith angle of 32° of the eclipsed sun (Pomozi et al. 2001b; Horváth et al. 2003) and on 29 March 2006 in Turkey with a solar zenith angle of 46° (Sipőcz et al. 2008), the conclusion can be drawn that practically the same characteristics of celestial polarization were encountered during both eclipses. This shows that the observed polarization phenomena of the eclipsed sky seem to be

general rather than particular. The validity of this conclusion should be tested by further imaging polarimetric observations of future total solar eclipses.

18.7.1 Possible Influence of the Changed Polarization Pattern of the Eclipsed Sky on Insect Orientation

To acquire more information about the identification and use of the sun and other celestial cues in the sea–land orientation of the sandhopper *Talitrus saltator*, Ugolini et al. (2004) carried out releases in a confined environment during a partial solar eclipse with 86 % maximum obscuration of the sun's disc. The sandhoppers were unable to identify the sun (86 % covered) during this partial eclipse nor to use other celestial compass cues for orientation. In the opinion of Ugolini et al. (2004), this was probably due to the low level of light intensity (close to the minimum level for orientation recorded at sunset) and to the variations in intensity and polarization of the partially eclipsed sky. However, the sky polarization could not be the reason for the disorientation of *Talitrus saltator* observed by Ugolini et al. (2004) during the mentioned partial solar eclipse, because even at a solar obscuration of 86 % the polarization pattern of the partially eclipsed sky is the same as that of the normal (non-eclipsed) sky: Sipőcz et al. (2008) found that during the pre- and post-eclipse on 29 April 2006, the celestial polarization pattern was the same as that of the clear sky for obscurations of the sun's disc not larger than 88.5 %. On the other hand, the polarization pattern of the eclipsed sky at 99.5 % obscuration of the sun's disc (scene 3 in Fig. 18.12) was considerably different from that of the normal and pre-/post-eclipsed skies (Sipőcz et al. 2008). Similar results were obtained by Pomozi et al. (2001b) for obscurations of the sun's disc not larger than 98 % during the total solar eclipse of 11 August 1999 in Hungary. Coulson (1988) observed the same effect during the partial solar eclipse on 26 February 1979 when the maximum obscuration of the sun's disc was 80 %. This means that even if the obscuration is 98 %, the polarization pattern of the eclipsed sky is predominantly determined by the scattering of sunlight coming directly from the eclipsed sun's disc.

Hence, the polarization pattern of the sky suffers a sudden and dramatic change at the moment of the beginning and the end of the total eclipse (Piltschikoff 1906; de Bary et al. 1961; Moore and Rao 1966; Dandekar and Turtle 1971; Miller and Fastie 1972; Rao et al. 1972; Shaw 1975; Gerharz 1976; Pomozi et al. 2001b; Horváth et al. 2003; Sipőcz et al. 2008). The short event (lasting a few tens or hundreds seconds) of the totality of an eclipse is unexpected and strange for all living creatures. It raises the question how the sudden change of the celestial polarization pattern during totality affects the behaviour of animals that navigate on the basis of this pattern (Bernáth et al. 2001). Most animals use the sun as the chief navigational reference. Many polarization-sensitive animals rely on the polarization pattern of the sky only when the sun is not seen for some reason, e.g. it is

occluded by clouds, or it is below the horizon. In such situations they deduct the direction of the solar meridian from the normal pattern of the direction of polarization of skylight. During a total solar eclipse, but out of the short period of totality, the celestial polarization pattern is practically the same as that of the normal sky (Pomozi et al. 2001b; Horváth et al. 2003; Sipőcz et al. 2008); thus, animals navigating by means of skylight polarization can rely on it without losing their way. However, during totality the sky polarization pattern is significantly different from the normal pattern (Pomozi et al. 2001b; Horváth et al. 2003; Sipőcz et al. 2008); therefore, it could not be used for navigation. Thus, animals, even if they were able to perceive and tried to follow the anomalous skylight polarization pattern under the poor illumination conditions of totality, would most probably be disoriented. It is possible that the observed strange behaviour of honeybees is caused by this phenomenon in some sort (Szentkirályi and Szalay 2001; Baldavári 2001). This is significant only when the solar corona is occluded by clouds. Animals could navigate when the corona, being about as bright as the full moon, can be seen, because the corona marks the position of the sun. In this case skylight polarization would not be needed for orientation, and its altered structure could not mislead animals during totality.

Even if an animal loses its way during totality for some reasons (e.g. due to the suddenly decreasing intensity of ambient illumination or the anomalous skylight polarization pattern), this would not make a serious harm to it in most cases. Totality lasts no more than a few minutes. Then the skylight polarization pattern is restored; only the intensity of illumination needs significant time (a couple of hours) to reach its original high level. However, for certain animals, like honeybees (*Apis mellifera*) that leave their hives with precisely dosed amounts of 'fuel' (honey), these few minutes of navigation malfunction during the totality may have lethal consequences: If the bee runs out of 'fuel' during the minutes of totality, it will not be able to reach the hive and perish even under the normalized skylight polarization pattern after totality. This phenomenon could be verified only by systematic observations of the behaviour of honeybees during total solar eclipses. However, such data are very rarely published, if any. The pioneer observations during the total solar eclipse on 11 August 1999 in Hungary open a window on this rarely examined phenomenon (Szentkirályi and Szalay 2001; Baldavári 2001).

18.8 Polarization of 'Water-Skies' Above Arctic Open Waters

In the ice cover of the Arctic Ocean, there are long or short, wide or narrow, permanent or temporary open water surfaces, especially in the summer. These open waters are called 'polynya' (when permanent, long and wide) or 'leads' (when temporary, short and narrow) and are of great importance to animal life in the Arctic

(Stirling 1980, 1997; Stirling and Cleator 1981) and Antarctic (Ancel et al. 1992) regions. Polynyas rise where the warm seawater of constant currents of the Arctic Ocean streams up. Captains of icebreaker ships prefer to follow the line of such polynyas and leads, because then the ship can move easier and faster (Hegedüs et al. 2007e). The open water surfaces can be visually detected on the basis of their low albedo (reflectivity): Polynyas and leads occur as dark grey or black stripes in the high-albedo (white) ice field (Fig. 18.14a). Above the upstreaming warmer water of polynyas, rising vapour occurs frequently. If the sky is foggy, the sky above dark water surfaces is always dark grey (Fig. 18.14b–d). This phenomenon is called the 'water-sky'. On the other hand, the foggy sky above high-albedo ice/snow surfaces is always white (Fig. 18.14a–d), which is called the 'ice-sky'. Hence, at the ice–water border of polynyas and leads, there is a difference in radiance between the ice-sky and the water-sky (Fig. 18.14b, c). Thus, polynyas and leads can be remotely detected by means of this celestial radiance difference or of the dark grey band (Fig. 18.14d, e) of the water-sky, even if the water surface is not visible because of the curvature of the Earth's surface. The captains of icebreakers in the Arctic Ocean used to search for open waters in such a way (Tilzer 1994). The pilots of helicopters of icebreakers also use this information during ice reconnaissance flights above the Arctic ice cover (Hegedüs et al. 2007e).

Polar bears and several seabird species in the Arctic region are strongly dependent on the existence of open waters (leads and polynyas), because their prey (mainly seals for polar bears; fish and invertebrates for birds) originate from the seawater (McRoy and Goering 1976; Brown and Nettleship 1981; Hirche et al. 1991; Stirling et al. 1993; Born et al. 1997; Stirling 1997). Animals inhabiting the Arctic ice landscape could possibly detect open waters from a distance on the basis of the dark grey water-sky, like captains of icebreakers. This hypothesis has not been tested behaviourally until now. On the other hand, certain Arctic birds may also be sensitive to polarized light, like several other bird species using sky polarization for orientation (Horváth and Varjú 2004).

Hegedüs et al. (2007e) measured the polarization patterns of water-skies above polynyas in the Arctic ice cover (Fig. 18.15). They showed that there are statistically significant differences in the angle of polarization between the water-sky and the ice-sky radiating light with low degrees of linear polarization (Fig. 18.15). The polarization characteristics of water-skies are determined predominantly by the polarization of light reflected from the water surface, such that the polynya-reflected light is always horizontally polarized with a degree of polarization depending on the angle of reflection. This horizontally polarized polynya-reflected light is reflected/scattered from the fog cloud towards the observer, resulting in the nearly horizontal polarization ($+45^\circ < \alpha < +135^\circ$) of light from the water-sky (Fig. 18.15c). If there is a celestial bright band below the water-sky, there is a maximal difference in the direction of polarization between the ice-sky and the water-sky if the latter occurs in front of nearly vertically polarized ice-sky regions. This difference becomes smaller the more the direction of polarization of ice-sky light deviates from the vertical, and the difference diminishes if the background of the water-sky is a nearly horizontally polarized celestial area.

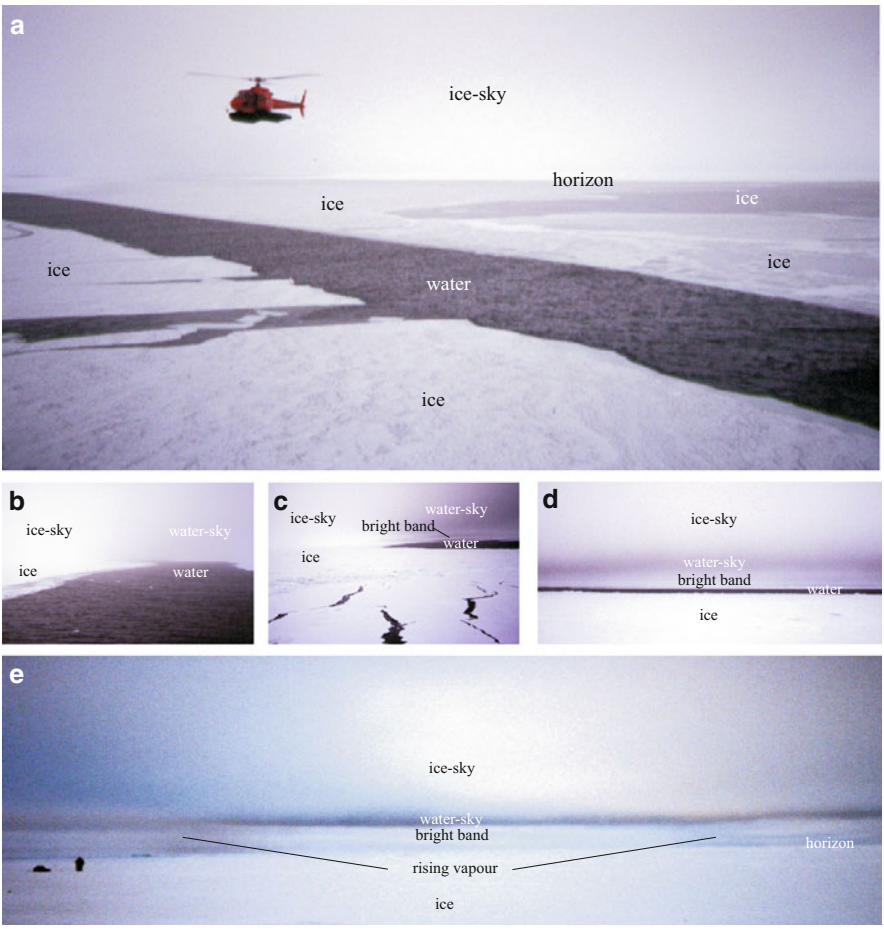

Fig. 18.14 (**a**) A typical low-albedo (dark) open water surface (polynya) in the high-albedo (white) Arctic ice cover. The helicopter was stationed on board of the Swedish icebreaker Oden and was used for ice reconnaissance flights. (**b**, **c**) Typical white 'ice-skies' and grey 'water-skies' above the Arctic ice broken with polynyas. (**d**) Above a long straight distant polynya visible near the horizon, a long water-sky occurs. (**e**) An elongated horizontal water-sky above a long straight polynya which is not visible because of the curvature of the Earth's surface. The two darker spots between the water-sky and the horizon are water vapour clouds arising from two warmer spots of the polynya's water surface. Not directly visible remote open waters can be detected from a distance on the basis of the smaller radiance of light from water-skies visible above them [after Fig. 1 on page 133 of Hegedüs et al. (2007e)]

Hegedüs et al. (2007e) suggested that the polarization phenomenon of water-skies and ice-skies could help biological (e.g. Arctic birds) and man-made sensors to detect open waters not directly visible from a distance. However, the threshold of such polarization-based detection should be rather low, because the degree of polarization of light radiated by water- and ice-skies is not higher than 10 %.

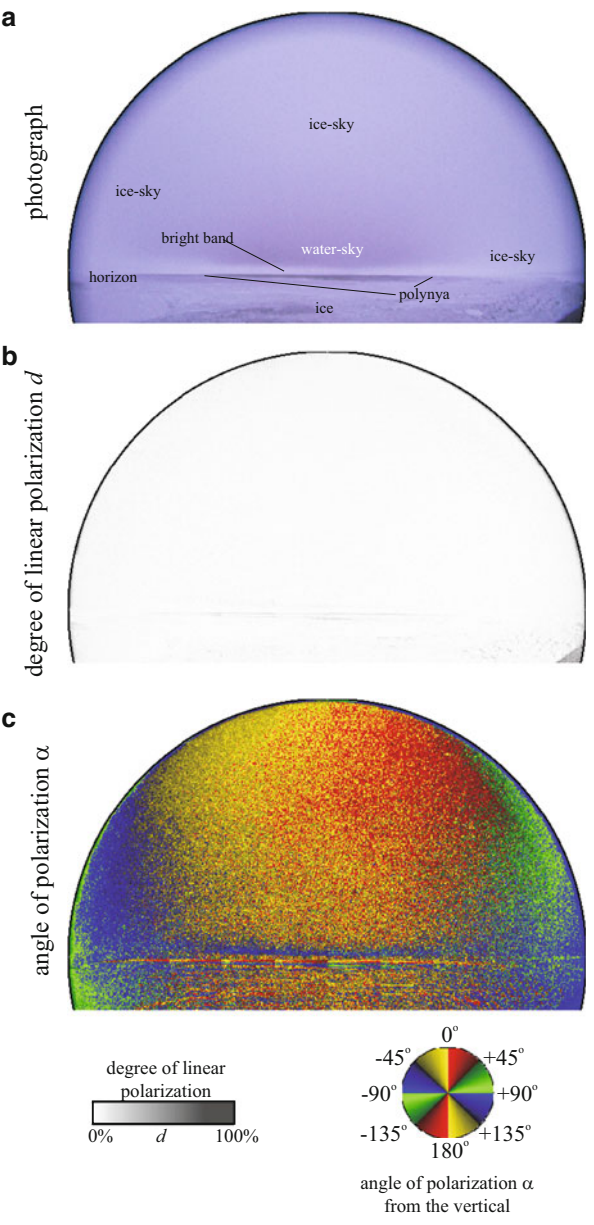

Fig. 18.15 (**a**) 180° field-of-view photograph of the sky above the Arctic ice with a polynya stretching nearly parallel to the horizon in the middle part of the picture on 11 September 2005 at 01:50 (local summer time = UTC − 8 h) at the geographical coordinates 89° 14.6′ N and 174° 2′ W. (**b**, **c**) Patterns of the degree of linear polarization d and the angle of polarization α of the sky measured by 180° field-of-view imaging polarimetry in the blue (450 nm) part of the spectrum. These patterns were very similar to those measured in the green (550 nm) and red (650 nm) spectral ranges. The optical axis of the fisheye lens was horizontal; thus, the horizon is the horizontal diameter of the circular picture, the upper and lower parts of which show the sky and the ice cover with a polynya, respectively. Only a fraction of the ice surface is shown. The horizontal celestial bright band below the grey water-sky is due to the bright ice-sky light reaching the observer through the more or less transparent rising vapour below the fog cloud. Thus, the light from this bright band has approximately the same radiance and polarization as the original ice-sky light [after Fig. 3 on page 136 of Hegedüs et al. (2007e)]

18.9 Polarization Patterns of Fogbows

One of the most spectacular atmospheric optical phenomena is the rainbow occurring when sunlight is back-scattered from water droplets falling in the air (Minnaert 1940; Dave 1969; Tricker 1970; Greenler 1980; Lee and Fraser 2001). The polarization characteristics of the rainbow have been studied both theoretically (Können and de Boer 1979; Können 1985; Coulson 1988) and experimentally (Barta et al. 2003; Horváth and Varjú 2004). A special type of the rainbow phenomenon is the fogbow (Fig. 18.16), also called as 'white rainbow', for example (Tyndall 1884; McConnel 1890; Lenggenhager 1982; Lynch and Futterman 1991), when sunlight is back-scattered from tiny water droplets slowly sedimenting in the air. The emergent sunlight is mostly deviated by 135° to 150° from its incident direction to produce the main fogbow of 30°–45° radius centred on the antisolar point. The deviation corresponds roughly to the geometric optics angle of minimum deviation of ~138° for the 42° radius rainbow (Minnaert 1940; Greenler 1980; Cowley 2011).

The optical characteristics of the fogbow depend on the size of the fog droplets (Fig. 18.17). Due to the small droplet size, the differently coloured arcs overlap considerably; therefore, the bright fogbow is white. The mean drop radius is smaller than 60 μm and usually ranges from 25 to 50 μm (Lynch and Schwartz 1991). As the droplet diameter increases, the primary bow narrows and the supernumerary bows inside the main bow move close together (Cowley 2011) (Fig. 18.17).

The polarization of fogbow light can be demonstrated with photographs (Fig. 18.16) taken through linear polarizers (von Bullrich 1963; Lenggenhager 1983). According to Können (1985), the degree of linear polarization of the fogbow is lower than that of the rainbow; thus, the fogbow usually cannot be totally extinguished with a linearly polarizing filter. Using imaging polarimetry, Horváth et al. (2011) measured the polarization characteristics of several Arctic fogbows in the red, green and blue parts of the spectrum (Figs. 18.18, 18.19 and 18.20). In the patterns of the degree of polarization d, fogbows and their supernumerary bows were best visible in the red spectral range due to the least dilution of fogbow light by light scattered in air (Fig. 18.18c–e). In the patterns of the angle of polarization α, fogbows were practically not discernible, because their α-pattern was the same as that of the sky (Fig. 18.18f–h): The direction of polarization is perpendicular to the plane of scattering that is parallel to the arc of the bow, independently of the wavelength (Horváth et al. 2011). Fogbows and their supernumerary bows were best seen in the patterns of the polarized radiance $\mathrm{PR} = dI$ (where I is the radiance) measured in the red spectral range, since the disturbing light scattering between the polarimeter and the fogbow as well as behind the fog is the weakest in the red part of the spectrum (Figs. 18.19 and 18.20). In these patterns the angular distance δ between the peaks of the primary bow and the first supernumerary bow and the angular width σ of the primary bow were determined along different radii from the centre of the bow. δ ranged between 6.1° and 13.4°, while σ changed from 5.3° to 19.5° (Horváth et al. 2011). Certain fogbows were relatively homogeneous, meaning small variations of δ and σ along their bows. Other fogbows were

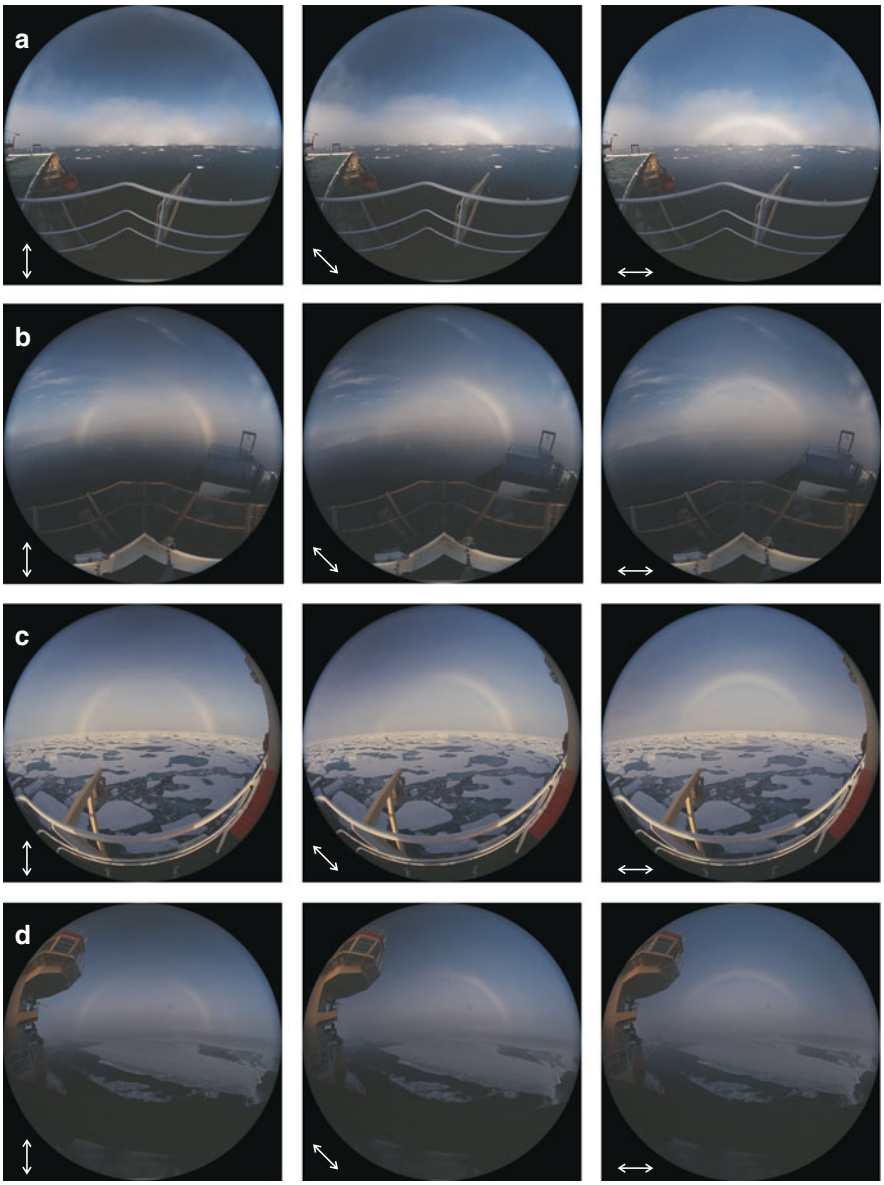

Fig. 18.16 180° field-of-view photographs of Arctic fogbows (**a**, **b**, **c**, **d**) taken through a linear polarizer. The directions of the transmission axis of the polarizer are represented by double-headed arrows. The photos were taken by Gábor Horváth during the Beringia 2005 Arctic research expedition

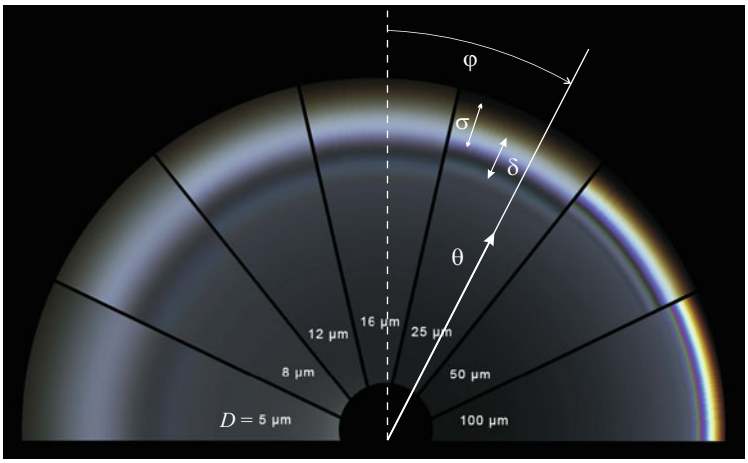

Fig. 18.17 Simulated appearance of the fogbow as a function of the droplet diameter D ranging from 5 to 100 μm. The fogbow patterns were computed by the software IRIS (Cowley 2011, http://atoptics.co.uk). φ: angle (clockwise from the vertical) of the direction of a given radius. δ: angular distance between the peaks of the primary bow and the first supernumerary bow. σ: angular width of the primary bow. θ: angular distance from the bow centre along a radius [after Fig. 1 on page F65 of Horváth et al. (2011)]

heterogeneous, possessing quite variable δ- and σ-values along their bows. This variability was the consequence of the characteristics of the high Arctic with open waters within the ice shield resulting in the spatiotemporal change of the droplet size within the fog.

Figure 18.17 shows the computed appearance of the fogbow as a function of the droplet diameter D ranging from 5 to 100 μm. According to Fig. 18.17, both the peak distance δ and the bow width σ of the fogbow decrease with the increasing diameter D of fog droplets. The value of D in fog changes both spatially and temporally in a chaotic manner due to the chaotic turbulence of air (Schumann 1940). The angular extension of the primary fogbow is about $2 \times 42°$. Within this angular region, the distribution of droplet size can drastically change spatiotemporally, resulting in the diversity of the δ- and σ-values of fogbows.

Figure 18.19a, b shows two examples of fogbows, the polarized radiance PR, angular peak distance δ and angular bow width σ of which changed only moderately along the bow. Figure 18.19c, d gives two examples of fogbows, PR, δ and σ of which substantially changed along the bow. In Fig. 18.20 six selected fogbows are compared with each other in the pattern of polarized radiance PR in a similar way as in Fig. 18.17.

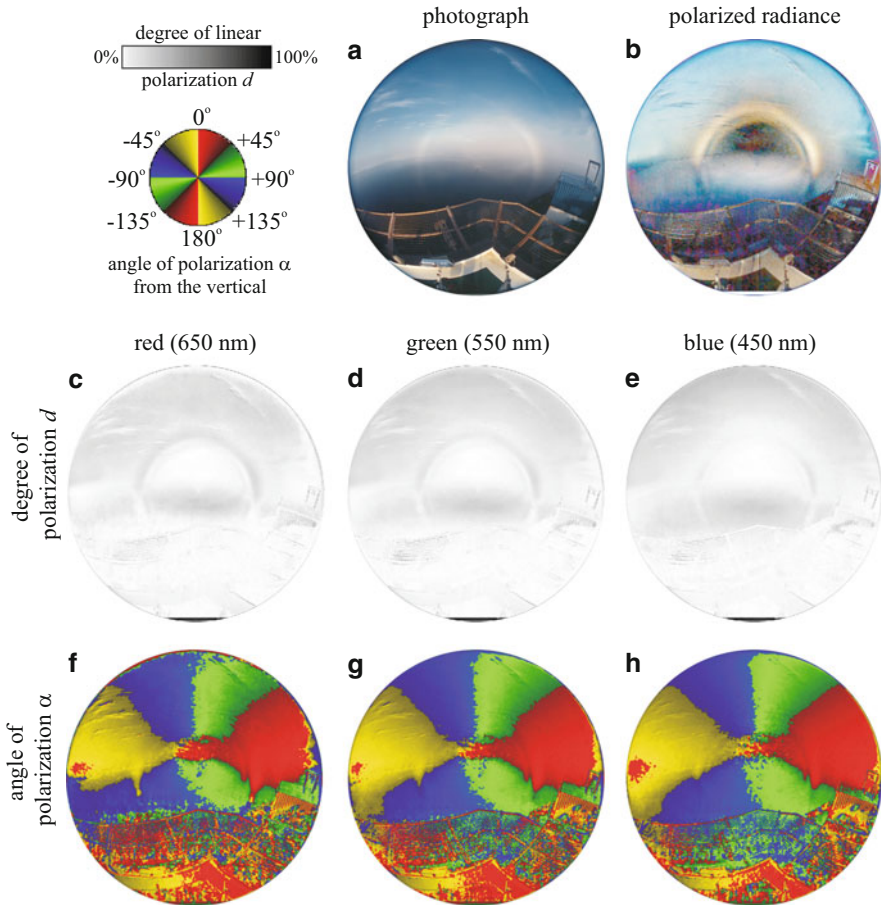

Fig. 18.18 Photograph (**a**), polarized radiance PR = dI (**b**) and patterns of the degree of linear polarization d (**c**, **d**, **e**) and angle of polarization α (**f**, **g**, **h**) of an Arctic fogbow measured by imaging polarimetry in the red, green and blue parts of the spectrum. Angle α is measured clockwise from the vertical. Figure 18.18b is a composite image of the polarized radiance PR: In the red, green and blue channels, the PR-values measured in the red, green and blue spectral ranges, respectively, are displayed [after Fig. 2 on page F67 of Horváth et al. (2011)]

18.10 Skylight Polarization Transmitted Through Snell's Window of Flat Water Surfaces

Snell's window is the circular region on the flat water surface above an underwater observer with an aperture angle of 97.5°, within which the entire celestial hemisphere above the water is compressed due to refraction (Lythgoe 1979). The underwater light field is partially linearly polarized (Waterman 1981), except for some elliptical polarization near the water surface (Ivanoff and Waterman 1958). In

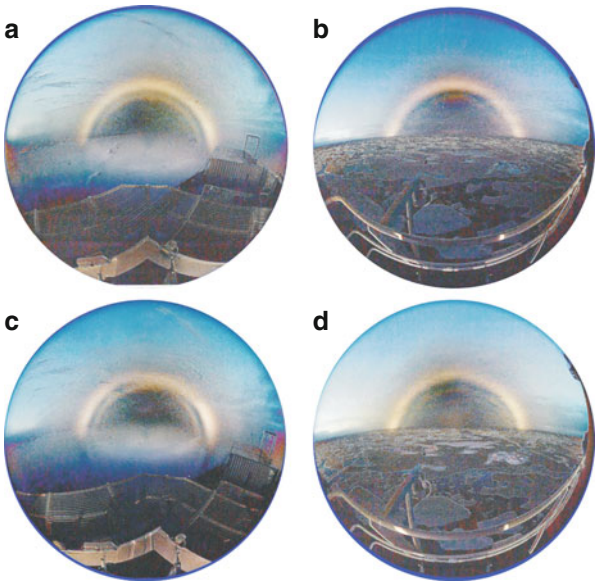

Fig. 18.19 Patterns of the polarized radiance PR of Arctic fogbows. (**a**, **b**) Along these fogbow PR, the angular distance δ between the peaks of the primary bow and the first supernumerary bow and the angular width σ of the primary bow change only moderately due to the small change of the droplet size. (**c**, **d**) Along these fogbows PR, δ and σ change strongly due to the large change of the droplet size [after Figs. 3, 4, 5 on pages F68, F69 of Horváth et al. (2011)]

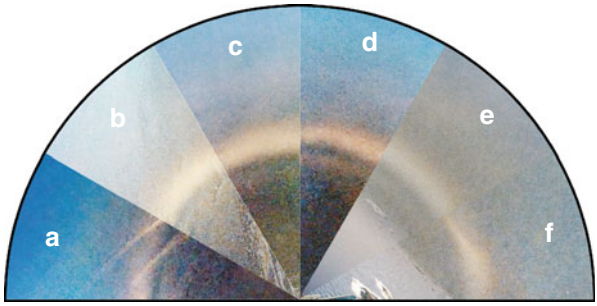

Fig. 18.20 Comparison of six Arctic fogbows (a–f) in the pattern of polarized radiance PR measured by imaging polarimetry [after Fig. 6 on page F69 of Horváth et al. (2011)]

shallow waters, the linear polarization pattern has been divided into two parts, one inside of Snell's window and the other outside of it (Waterman 1954).

Generally, the polarization pattern within Snell's window near the water surface and a few metres deep is assumed to be determined by the same factors as those influencing the skylight polarization. Therefore, sun position, cloud cover, amount of atmospheric dust and haze, the distance of the direction of observation from the zenith and multiple scattering all affect the polarization pattern within Snell's window (Waterman 1954).

Using the Fresnel theory of refraction polarization and the single-scattering Rayleigh model of skylight polarization, Horváth and Varjú (1995) computed the influence of refraction on the celestial polarization patterns visible within Snell's window of the water surface for four sun altitudes. These calculations assumed a flat water surface (no surface waves) and single-scattering Rayleigh skylight from a clear sky. However, due to the focusing of sunlight by surface waves and the

wavelength-dependent attenuation of light in water (Shashar et al. 2004), deviation from this model is likely to occur. Indeed, Cronin and Shashar (2001), measuring polarization at 15 m deep on a coral reef, did not find substantial differences between the polarization patterns within and outside Snell's window in the 350–600 nm spectral range. Additionally, neither polarization measurements conducted in an artificial turbid media (Timofeyeva 1970) nor measurements performed at sea and in freshwater lakes (Timofeyeva 1969; Novales-Flamarique and Hawryshyn 1997) reported differences between the two proposed patterns.

Polarization-sensitive animals utilize the underwater polarization pattern in various manners (Waterman 1981; Wehner 2001; Horváth and Varjú 2004), especially for body orientation and navigation (Groot 1965; Forward et al. 1972; Forward and Waterman 1973; Kleerekoper et al. 1973; Hawryshyn et al. 1990; Hawryshyn 1992; Schwind 1999). For example, the grass shrimp (*Palaemonetes vulgaris*) exploits the polarization pattern of Snell's window in its offshore escape response (Goddard and Forward 1989, 1990, 1991; Ritz 1991). Hawryshyn and McFarland (1987) as well as Parkyn and Hawryshyn (1993) suggested that fishes make use of the UV component of the polarization pattern (being abundant inside Snell's window) for body orientation and navigation. For such animal orientation tasks, the distribution of polarization of skylight is important (Horváth and Varjú 2004).

Using a rapid-sampling point-source polarimeter, Sabbah et al. (2006) examined the underwater polarization pattern within Snell's window and its dependency on the wavelength in shallow (2 m deep) waters. Using the Fresnel theory of refraction polarization, they calculated the celestial polarization patterns transmitted through Snell's window of a flat water surface. These calculations were performed using measured celestial polarization patterns (semiempirical predictions) as well as skylight polarization patterns calculated using the single-scattering Rayleigh model (theoretical predictions). Comparisons between underwater measurements and semiempirical/theoretical predictions revealed that within Snell's window, the semiempirically predicted and measured directions of polarization of transmitted skylight did not differ significantly from each other. Conversely, predicted values of degree of linear polarization d were lower than the measured values, yet were significantly correlated to them. Sabbah et al. (2006) concluded that the change in polarization of skylight transmitted through the water surface can be generally described by the Fresnel theory of refraction polarization. Within Snell's window, d was found to be wavelength dependent. This dependency varied with the sun position, and at high sun altitudes the maxima of d generally appeared at both ends of the measured spectrum (at 350–400 and 700 nm).

In the opinion of Sabbah et al. (2006), this wavelength dependency of polarization within Snell's window in shallow waters may lead to differential spectral sensitivity in polarization-sensitive visual systems of certain animals according to the task and time of activity: Many biological visual tasks require determining the natural polarization pattern in the sky within Snell's window or discriminating between the background polarization and the one arriving from an object. In such cases, improved sensitivity may be achieved if the animal's polarization sensitivity

is tuned to spectral regions where high polarization occurs. In cases where the differences in polarization between wavelengths were large, Sabbah et al. (2006) found high degrees of polarization at the short (350–400 nm) or long (700 nm) ends of the spectrum. Indeed, salmonids possessing UV polarization sensitivity (Parkyn and Hawryshyn 1993) were long suggested to orient and even navigate using the polarization pattern within Snell's window (Horváth and Varjú 1995; Novales-Flamarique and Hawryshyn 1997). Planktivorous fishes also, on occasion, use polarization sensitivity for finding transparent food items (Novales-Flamarique and Browman 2001). Other planktivorous fishes possess enhanced visual acuity and forage at the margins of Snell's window (Munk 1970). If indeed polarization sensitivity is used during daytime for plankton detection within or at the edge of Snell's window, one may predict that UV- or red-sensitive photoreceptors (Hawryshyn et al. 1990, 2003) are important for such a task. At low sun altitudes the maximal degree of polarization is attained at a wavelength of about 450 nm. Thus, Sabbah et al. (2006) suggested that for tasks performed mainly at twilight (low solar elevations), polarization sensitivity will be centred in the blue spectral region, where high light intensity penetrates the water (McFarland 1986, 1991; McFarland et al. 1999).

References

Able KP (1982) Skylight polarization patterns at dusk influence migratory orientation in birds. Nature 299:550–551

Able KP, Able MA (1990) Ontogeny of migratory orientation in the savannah sparrow, *Passerculus sandwichensis*: mechanisms at sunset. Anim Behav 39:1189–1198

Aldhous P (2004) Borneo is burning. Nature 432:144–146

Alerstam T, Hedenström A, Åkesson S (2003) Long-distance migration: evolution and determinants. Oikos 103:247–260

Ancel A, Kooyman GL, Ponganis PJ, Gendner JP, Lignon J, Mestre X, Huin N, Thorson PH, Robisson P, Le Maho Y (1992) Foraging behaviour of emperor penguins as a resource detector in winter and summer. Nature 360:336–339

Baldavári L (2001) Change of honeybee behaviour in an apiary during the total solar eclipse on 11 August 1999. Állattani Közlemények 86:137–143 (in Hungarian)

Barfod JHP (1967) Navigation. Kulturhistoriskt Lexikon Nordisk Medeltid 12:260–263

Barta A, Horváth G (2004) Why is it advantageous to perceive the polarization of downwelling light under clouds and canopies in the UV? J Theor Biol 226:429–437

Barta A, Horváth G, Bernáth B, Meyer-Rochow VB (2003) Imaging polarimetry of the rainbow. Appl Opt 42:399–405

Bernáth B, Pomozi I, Gál J, Horváth G, Wehner R (2001) Skylight polarization during the total solar eclipse of 11 August 1999 and its possible biological implications. Állattani Közlemények 86:81–92 (in Hungarian)

Berry MV, Dennis MR, Lee RL Jr (2004) Polarization singularities in the clear sky. New J Phys 6: 162

Binns AL (1971) Sun navigation in the Viking age, and the Canterbury portable sundial. Acta Archaeologica 42:23–34

Born E, Wiig O, Thomassen J (1997) Seasonal and annual movements of radio-collared polar bears (*Ursus maritimus*) in northeast Greenland. J Mar Syst 10:67–77

Bréon FM (2006) How do aerosols affect cloudiness and climate? Science 313:623–624
Brines ML (1980) Dynamic patterns of skylight polarization as clock and compass. J Theor Biol 86:507–512
Brines ML, Gould JL (1982) Skylight polarization patterns and animal orientation. J Exp Biol 96: 69–91
Britton W (1972) The Britton Viking sun-stone expedition. Nutrition Today 1972 (May/June): 14–23
Brown RGB, Nettleship DN (1981) The biological significance of polynyas to arctic colonial seabirds. In: I Stirling, H Cleator (eds) Polynyas in the Canadian Arctic. Can Wildl Serv Occas Pap 45:59–65
Coulson KL (1971) On the solar radiation field in a polluted atmosphere. J Quant Spectrosc Radiat Transf 2:739–755
Coulson KL (1988) Polarization and Intensity of Light in the Atmosphere. A. Deepak Publishing, Hampton, VA
Cowley L (2011) Software IRIS ©, http://atoptics.co.uk
Cronin TW, Shashar N (2001) The linearly polarized light field in clear, tropical, marine waters: spatial and temporal variation of light intensity, degree of polarization and e-vector angle. J Exp Biol 204:2461–2467
Cronin TW, Warrant EJ, Greiner B (2006) Celestial polarization patterns during twilight. Appl Opt 45:5582–5589
Dandekar BS, Turtle JP (1971) Day sky brightness and polarization during the total solar eclipse of 7 March 1970. Appl Opt 10:1220–1224
Dave JV (1969) Scattering of visible light by large water spheres. Appl Opt 8:155–164
de Bary E, Bullrich K, Lorenz D (1961) Messungen der Himmelsstrahlung und deren Polarisationsgrad während der Sonnenfinsternis am 15.2.1961 in Viareggio (Italien). Geofisica Pura et Applicata 48:193–198
Dennis MR (2007) A three-dimensional degree of polarization based on Rayleigh scattering. J Opt Soc Am A 24:2065–2069
Forward RB, Waterman TH (1973) Evidence for e-vector and light intensity pattern discrimination by the teleost *Demogenys*. J Comp Physiol A 87:189–202
Forward RB, Horch KW, Waterman TH (1972) Visual orientation at the water surface by the teleost *Zenarchopterus*. Biol Bull 143:112–126
Freake MJ (1999) Evidence for orientation using the e-vector direction of polarized light in the sleepy lizard *Tiliqua rugosa*. J Exp Biol 202:1159–1166
Gál J, Horváth G, Barta A, Wehner R (2001) Polarization of the moonlit clear night sky measured by full-sky imaging polarimetry at full moon: comparison of the polarization of moonlit and sunlit skies. J Geophys Res D 106:22647–22653
Gerharz R (1976) Appearance of the atmospheric scatter field during a solar eclipse. J Geophys 42: 163–167
Goddard SM, Forward RB (1989) The use of celestial cues in the offshore escape response of the shrimp *Palaemonetes vulgaris*. Mar Behav Physiol 16:11–18
Goddard SM, Forward RB (1990) The decay and learning of an y axis orientation behavior: the offshore escape response of the shrimp *Palaemonetes vulgaris* (Say). J Exp Mar Biol Ecol 142:137–150
Goddard SM, Forward RB (1991) The role of the underwater polarized light pattern, in sun compass navigation of the grass shrimp, *Palaemonetes vulgaris*. J Comp Physiol A 169: 479–491
Greenler R (1980) Rainbows, halos, and glories. Cambridge University Press, Cambridge, UK
Greiner B, Ribi WA, Warrant EJ (2004) Retinal and optical adaptations for nocturnal vision in the halictid bee *Megalopta genalis*. Cell Tissue Res 316:377–390
Groot C (1965) On the orientation of young sockeye salmon (*Oncorhynchus nerka*) during their seaward migration out of lakes. Behaviour 14(suppl)(1):198
Hannay JH (2004) Polarization of sky light from a canopy atmosphere. New J Phys 6:197

Hannay JH (2007) Radiative transfer: exact Rayleigh scattering series and a formula for daylight. Proc R Soc A 463:2729–2751
Hawryshyn CW (1992) Polarization vision in fish. Am Sci 80:164–175
Hawryshyn CW, Mcfarland WN (1987) Cone photoreceptor mechanisms and the detection of polarized light in fish. J Comp Physiol A 160:459–465
Hawryshyn CW, Arnold MG, Bowering D, Cole RL (1990) Spatial orientation of rainbow trout to plane-polarized light: the ontogeny of e-vector discrimination and spectral characteristics. J Comp Physiol A 166:565–574
Hawryshyn CW, Moyer HD, Allison WT, Haimberger TJ, Mcfarland WN (2003) Multidimensional polarization sensitivity in damselfishes. J Comp Physiol A 189:213–220
Hegedüs R, Åkesson S, Wehner R, Horváth G (2007a) Could Vikings have navigated under foggy and cloudy conditions by skylight polarization? On the atmospheric optical prerequisites of polarimetric Viking navigation under foggy and cloudy skies. Proc R Soc A 463:1081–1095
Hegedüs R, Åkesson S, Horváth G (2007b) Polarization patterns of thick clouds: overcast skies have distribution of the angle of polarization similar to that of clear skies. J Opt Soc Am A 24: 2347–2356
Hegedüs R, Åkesson S, Horváth G (2007c) Anomalous celestial polarization caused by forest fire smoke: why do some insects become visually disoriented under smoky skies? Appl Opt 46: 2717–2726
Hegedüs R, Barta A, Bernáth B, Meyer-Rochow VB, Horváth G (2007d) Imaging polarimetry of forest canopies: how the azimuth direction of the sun, occluded by vegetation, can be assessed from the polarization pattern of the sunlit foliage. Appl Opt 46:6019–6032
Hegedüs R, Åkesson S, Horváth G (2007e) Polarization of "water-skies" above arctic open waters: how polynyas in the ice-cover can be visually detected from a distance. J Opt Soc Am A 24: 132–138
Hirche HJ, Baumann MEM, Kattner G, Gradinger R (1991) Plankton distribution and the impact of copepod grazing on primary production in Fram Strait, Greenland Sea. J Mar Syst 2: 477–494
Horváth G, Varjú D (1995) Underwater refraction-polarization patterns of skylight perceived by aquatic animals through Snell's window of the flat water surface. Vis Res 35(12):1651–1666
Horváth G, Varjú D (2004) Polarized light in animal vision—polarization patterns in nature. Springer, Heidelberg
Horváth G, Pomozi I, Gál J (2003) Neutral points of skylight polarization observed during the total eclipse on 11 August 1999. Appl Opt 42:465–475
Horváth G, Hegedüs R, Barta A, Farkas A, Åkesson S (2011) Imaging polarimetry of the fogbow: polarization characteristics of white rainbows measured in the high Arctic. Appl Opt 50: F64–F71
Ivanoff A, Waterman TH (1958) Elliptical polarization of submarine illumination. J Mar Res 16: 255–282
Johnson EA, Miyanishi K (2000) Forest fires: behavior and ecological effect. Academic, New York
Johnson DL, Naylor D, Scudder G (2005) Red sky in day, bugs go astray. Annual Meeting of the Canadian Association of Geographers, Western Division, Lethbridge, Alberta, Canada, 12 March 2005, Abstracts, p 145
Kasischke ES, Stocks BJ (2000) Fire, climate change and carbon cycling in the boreal forest, Ecological studies series. Springer, Heidelberg
Kirschfeld K, Lindauer M, Martin H (1975) Problems of menotactic orientation according to polarized light of the sky. Zeitschrift für Naturforschung 30c:88–90
Kleerekoper H, Matis JH, Timms AM, Gensler P (1973) Locomotor response of the goldfish to polarized light and its e-vector. J Comp Physiol A 86:27–36
Können GP (1985) Polarized light in nature. Cambridge University Press, Cambridge, UK
Können GP (1987) Skylight polarization during a total solar eclipse: a quantitative model. J Opt Soc Am A 4:601–608

Können GP, de Boer JH (1979) Polarized rainbow. Appl Opt 18:1961–1965
Kreithen ML, Keeton WT (1974) Detection of polarized light by the homing pigeon, *Columba livia*. J Comp Physiol 89:83–92
Labhart T, Meyer EP (1999) Detectors for polarized skylight in insects: a survey of ommatidial specializations in the dorsal rim area of the compound eye. Microsc Res Tech 47:368–379
LaFay H (1970) The Vikings. Nat Geosci 137:492–541
Lee RL Jr, Fraser AB (2001) The rainbow bridge: rainbows in art, myth, and science. Pennsylvania State University Press, Philadelphia, PA
Lenggenhager K (1982) Ergänzungen zur Entstehung der Regenbogen, inneren Nebenbogen und Nebelbogen. Archiv für Meteorologie, Geophysik und Bioklimatologie A 31:147–156
Lenggenhager K (1983) Erklärung der im Vergleich zum Regen- und Nebelbogen umgekehrten Teilpolarisation der Nebelglorien. Archiv für Meteorologie, Geophysik und Bioklimatologie A 32:165–172
Lynch DK, Futterman SN (1991) Ulloa's observation of the glory, fogbow, and an unidentified phenomenon. Appl Opt 30:3538–3541
Lynch DK, Schwartz P (1991) Rainbows and fogbows. Appl Opt 30:3415–3420
Lythgoe JN (1979) The ecology of vision. Clarendon, Oxford, UK
McConnel JC (1890) The theory of fog-bows. Philos Mag (Series 5) 29:453–461
Mcfarland WN (1986) Light in the sea—correlations with behaviors of fishes and invertebrates. Am Zool 26:389–401
Mcfarland WN (1991) The visual world of coral reef fishes. In: Sale PF (ed) The ecology of fishes on coral reefs. Academic, New York, pp 16–37
McFarland W, Wahl C, Suchanek T, McAlary F (1999) The behavior of animals around twilight with emphasis on coral reef communities. In: Archer SN, Djamgoz MBA, Loew ER, Partridge JC, Vallerga S (eds) Adaptive mechanisms in ecology of vision. Kluwer Academic, Dordrecht, pp 583–628
McGrath WH (1991) The stars look down. Navigation News 3 (May/June 1991):14–15
McRoy CP, Goering JJ (1976) Annual budget of primary production in the Bearing Sea. Mar Sci Commun 2:255–267
Miller RE, Fastie WG (1972) Skylight intensity, polarization and airglow measurements during the total solar eclipse of 30 May 1965. J Atmos Terr Phys 34:1541–1546
Minnaert M (1940) Light and color in the open air. G Bell and Sons, London
Moore JG, Rao CRN (1966) Polarization of the daytime sky during the total solar eclipse of 30 May 1965. Ann Geophys 22:147–150
Muheim R (2011) Behavioural and physiological mechanisms of polarized light sensitivity in birds. Philos Trans R Soc B 366:763–771
Munk O (1970) On the occurrence and significance of horizontal band-shaped retinal areas in teleosts. Videnskabellae Meddelelser Danfra Naturhistorisk Forening 133:85–120
Novales-Flamarique I, Browman HI (2001) Foraging and prey-search behaviour of small juvenile rainbow trout (*Oncorhynchus mykiss*) under polarized light. J Exp Biol 204:2415–2422
Novales-Flamarique I, Hawryshyn CW (1997) Is the use of underwater polarized light by fish restricted to crepuscular time periods? Vis Res 37(8):975–989
Nussbaum A, Phillips RA (1982) Contemporary optics for scientist and engineers. Prentice Hall Inc., Englewood Cliffs, NJ, USA
Parkyn DC, Hawryshyn CW (1993) Polarized light sensitivity in rainbow trout (*Oncorhynchus mykiss*): characterization from multiunit ganglion cell responses in the optic nerve fibers. J Comp Physiol A 172:493–500
Phillips JB, Waldvogel JA (1982) Reflected light cues generate the short-term deflector-loft effect. In: Papi F, Wallraff HG (eds) Avian navigation. Springer, Heidelberg, pp 190–202
Piltschikoff N (1906) Sur la polarization du ciel pendant les éclipses du soleil. Comptes Rendus Acad Sci Paris 142:1449

Pomozi I, Gál J, Horváth G, Wehner R (2001a) Fine structure of the celestial polarization pattern and its temporal change during the total solar eclipse of 11 August 1999. Remote Sens Environ 76:181–201
Pomozi I, Horváth G, Wehner R (2001b) How the clear-sky angle of polarization pattern continues underneath clouds: full-sky measurements and implications for animal orientation. J Exp Biol 204:2933–2942
Ramskou T (1967) Solstenen. Skalk 2:16–17
Ramskou T (1969) Solstenen—primitiv navigation I Norden for Kompasset. Rhodos, Kobenhavn
Rao CRN, Takashima T, Moore JG (1972) Polarimetry of the daytime sky during solar eclipses. J Atmos Terr Phys 34:573–576
Ritz DA (1991) Polarized-light responses in the shrimp *Palaemonetes vulgaris* (Say). J Exp Mar Biol Ecol 154:245–250
Roslund C, Beckman C (1994) Disputing Viking navigation by polarized skylight. Appl Opt 33: 4754–4755
Rossel S, Wehner R (1982) The bee's map of the e-vector pattern in the sky. Proc Natl Acad Sci USA 79:4451–4455
Rossel S, Wehner R, Lindauer M (1978) E-vector orientation in bees. J Comp Physiol A 125:1–12
Sabbah S, Barta A, Gál J, Horváth G, Shashar N (2006) Experimental and theoretical study of skylight polarization transmitted through Snell's window of a flat water surface. J Opt Soc Am A 23:1978–1988
Schaefer BE (1997) Vikings and polarization sundials. Sky Telesc 1997(May):91–94
Schmidt-Koenig K, Ganzhorn JU, Ranvaud R (1991) The sun compass. In: Berthold P (ed) Orientation in birds. Birkhäuser, Basel, pp 1–15
Schnall U (1975) Navigation der Wikinger. Schriften des Deutschen Schiffahrtsmuseums 6: 92–115
Schumann TEW (1940) Theoretical aspects of the size distribution of fog particles. Q J Roy Meteorol Soc 66:195–208
Schwind R (1999) *Daphnia pulex* swims towards the most strongly polarized light—a response that leads to 'shore flight'. J Exp Biol 202:3631–3635
Shashar N, Cronin TW, Wolff LB, Condon MA (1998) The polarization of light in a tropical rain forest. Biotropica 30:275–285
Shashar N, Sabbah S, Cronin TW (2004) Transmission of linearly polarized light in sea water: implications for polarization signaling. J Exp Biol 207:3619–3628
Shaw GE (1975) Sky brightness and polarization during the 1973 African eclipse. Appl Opt 14: 388–394
Sipőcz B, Hegedüs R, Kriska G, Horváth G (2008) Spatiotemporal change of sky polarization during the total solar eclipse on 29 March 2006 in Turkey: polarization patterns of the eclipsed sky observed by full-sky imaging polarimetry. Appl Opt 47:H1–H10
Stirling I (1980) The biological importance of polynyas in the Canadian Arctic. Arctic 33:303–315
Stirling I (1997) The importance of polynyas, ice edges, and leads to marine mammals and birds. J Mar Syst 10:9–21
Stirling I, Cleator H (eds) (1981) Polynyas in the Canadian Arctic. Occasional Paper—Canadian Wildlife Service 45, pp 1–70
Stirling I, Andriashek D, Calvert W (1993) Habitat preferences of polar bears in the Western Canadian Arctic in late winter and spring. Pol Res 29:13–24
Suhai B, Horváth G (2004) How well does the Rayleigh model describe the E-vector distribution of skylight in clear and cloudy conditions? A full-sky polarimetric study. J Opt Soc Am A 21: 1669–1676
Szentkirályi F, Szalay L (2001) Influence of the total solar eclipse of 11 August 1999 on the behaviour and collecting activity of honeybees. Állattani Közlemények 86:115–136 (in Hungarian)
Thirslund S (2001) Viking navigation: sun-compass guided Norsemen first to America. Gullanders Bogtrykkeri a-s, Skjern, Humlebaek, Denmark

Tilzer M (1994) 125 Jahre Deutsche Polarforschung, 2nd edn. Alfred-Wegener-Institut für Polar- und Meeresforschung, Bremerhaven, Germany
Timofeyeva VA (1969) Plane of vibrations of polarized light in turbid media. Izv Atmos Ocean Phys 5:1049–1057
Timofeyeva VA (1970) The degree of polarization of light in turbid media. Izv Atmos Ocean Phys 6:513–522
Tricker RAR (1970) Introduction to meteorological optics. Elsevier Publishing Co., New York
Tyndall J (1884) Note on the white rainbow. Philos Mag (Series 5) 17:148–150
Ugolini A, Castellini C, Tiribilli B (2004) The orientation of the sandhopper *Talitrus saltator* during a partial solar eclipse. J Comp Physiol A 190:855–859
van der Glas HW (1977) Models for unambiguous E-vector navigation in the bee. J Comp Physiol A 113:129–159
von Bullrich K (1963) Der Beginn der Nebelbildung und seine optische Auswirkung. Z Angew Math Phys 14:434–441
von Frisch K (1967) The dance language and orientation of bees. Harvard University Press, Cambridge, MA, USA
Walker J (1978) More about polarizers and how to use them, particularly for studying polarized sky light. Sci Am 238(1):132–136
Warrant EJ, Kelber A, Gislen A, Greiner B, Ribi W, Wcislo W (2004) Nocturnal vision and landmark orientation in a tropical halictid bee. Curr Biol 14:1309–1318
Waterman TH (1954) Polarization patterns in submarine illumination. Science 120:927–932
Waterman TH (1981) Polarization sensitivity. In: Autrum H (ed) Comparative physiology and evolution of vision in invertebrates B: invertebrates visual centers and behavior I. Berlin, Springer, pp 281–469
Wehner R (1976) Polarized-light navigation by insects. Sci Am 235(7):106–115
Wehner R (1983) Celestial and terrestrial navigation: human strategies—insect strategies. In: Huber F, Markl H (eds) Neuroethology and behavioral physiology. Springer, Heidelberg, pp 366–381
Wehner R (1984) Astronavigation in insects. Annu Rev Entomol 29:277–298
Wehner R (1989) The hymenopteran skylight compass: matched filtering and parallel coding. J Exp Biol 146:63–85
Wehner R (1994) The polarization-vision project: championing organismic biology. Fortschritten in der Zoologie 39:103–143
Wehner R (1997) The ant's celestial compass system: spectral and polarization channels. In: Lehrer M (ed) Orientation and communication in arthropods. Birkhäuser, Basel, pp 145–185
Wehner R (2001) Polarization vision—a uniform sensory capacity? J Exp Biol 204:2589–2596
Wehner R, Rossel S (1985) The bee's celestial compass—a case study in behavioural neurobiology. Fortschritten in der Zoologie 31:11–53

Chapter 19
Polarisation Signals

Justin Marshall, Nicholas Roberts, and Thomas Cronin

Abstract Humans are fascinated by the colour vision, colour signals and 'dress codes' of other animals as we can see colour. This property of light may be useful for increasing the contrast of objects during foraging, defence, camouflage and sexual communication. New research, largely from the last decade, now suggests that polarisation is a quality of light also used in signalling and may contain information at least as rich as colour. As many of the chapters in this book detail, polarisation in animals is often associated with navigation, habitat choice and other tasks that require large-field processing. That is, a wide area of the light field, such as the celestial hemisphere, is sampled from. Polarisation vision that recognises and extracts information from objects is most likely confined to processing through small numbers of receptors. This chapter examines the latest evidence on polarised signals from animals and their environments, including both linear and circular polarisations. Both aquatic and terrestrial examples are detailed, but with emphasis on life underwater as it is here that many recent discoveries have been made. Behaviour relative to signals is described where known, and suggestions are given as to how these signals are received and processed by the visual system. Camouflage as well as signalling in this light domain is also considered, with the inevitable conclusion for this new field that we need to know more before solid conclusions can be drawn.

J. Marshall (✉)
Sensory Neurobiology Group, Queensland Brain Institute, University of Queensland, St Lucia, Brisbane, QLD 4072, Australia
e-mail: justin.marshall@uq.edu.au

N. Roberts
School of Biological Sciences, University of Bristol, Woodland Road, Bristol BS8 1UG, UK
e-mail: nicholas.roberts@bristol.ac.uk

T. Cronin
Department of Biological Sciences, University of Maryland, Baltimore County, 1000 Hilltop Circle, Baltimore, MD 21 250, USA
e-mail: cronin@umbc.edu

G. Horváth (ed.), *Polarized Light and Polarization Vision in Animal Sciences*, Springer Series in Vision Research 2, DOI 10.1007/978-3-642-54718-8_19,

19.1 Introduction

As many of the chapters in this book illustrate, our understanding of animal polarisation vision is dominated by navigation or orientation behaviours that utilise the large-field celestial E-vector pattern (Chap. 18). Both invertebrates such as ants, beetles, spiders, bees and crickets (Labhart 1980, 1988; Wehner 1989; Dacke et al. 1999, 2013) and vertebrates such as fish (Hawryshyn 1992) and birds (Muheim et al. 2009) are known to make use of linearly polarised light in this way. Typically, this involves a specialised eye region, in insects the dorsal rim area (DRA) of the compound eye or sometimes the ocelli (Wehner and Labhart 2006; Baird et al. 2013), and in the vertebrates the location of polarisation sensitivity is still not well defined.

Large bodies of water and other wet surfaces such as mudflats are highly reflective and polarising and form a second category of large-field information (Chap. 16). Polarisation has been shown to be important in the lives of both vertebrates and invertebrates living in and around water (Fig. 19.1, Chaps. 5, 7, 8, 9 and 10). Many insects, for example, hunt around, breed and lay eggs on water or wet surfaces and have visual systems adapted for this (Schwind 1984a, b; Horváth and Zeil 1996; Horváth et al. 1997; Chap. 5). Underwater, a third source of large-field polarisation is the scattered light field, and in common with the sky and water surface, one of the features of this environment is the predictable nature of the E-vector orientation during the day. For most of the day, the underwater light field is predominantly horizontally polarised. Besides enabling possible time-based orientation information, the sky, wet or shiny surfaces and the view horizontally underwater provide a predictable, polarised backdrop (Cronin et al. 2003; Shashar et al. 2004) (Fig. 19.1).

All of these sources of polarisation are large field, and identifying and interacting with these may rely on many photoreceptors in specified arrays or eye regions (Schwind 1984a). For example, there are several optical and neural adaptations of DRAs that specifically blur or low-pass filter the image, making them better suited to examine large areas of sky free from the clutter of localised objects (Wehner and Labhart 2006). Polarisation information of the kind we will discuss in this chapter most likely relies on different visual axes and photoreceptors. There may be objects of particular interest that demand foveal or at least acute-zone fixation, requiring well-defined spatial resolution to distinguish polarised information against the background. This information may be in the form of signals designed to be conspicuous against the background or in the form of camouflage, where the polarisation is designed to match the background. Animals that include polarisation content in signals or camouflage must both exploit and ‘understand’ these backgrounds. However, it is important to state right from the beginning that just as colour or intensity may not be independent in the way a signal or camouflage appears to an intended receiver, polarisation is no different. Polarisation information may or may not be an independent conspicuous or concealed channel of information. The information content must always be viewed in the context of the

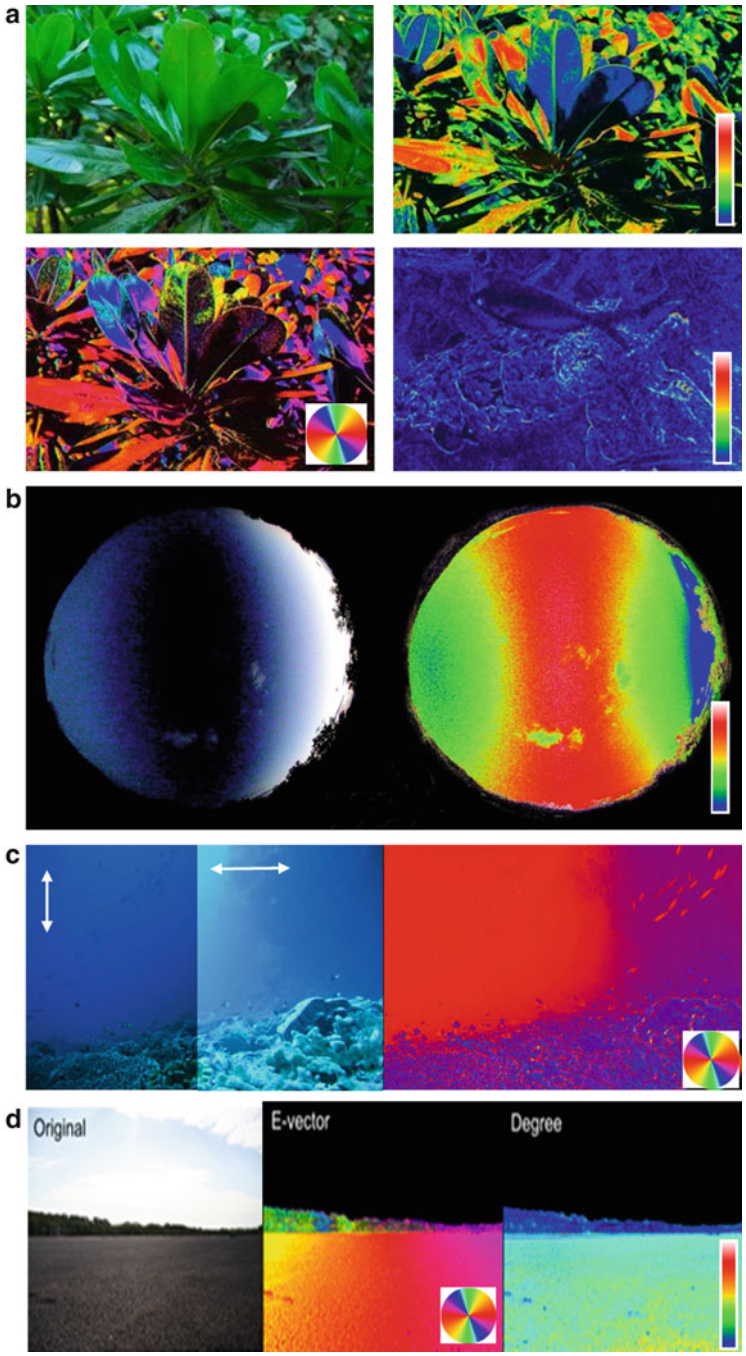

Fig. 19.1 Terrestrial and aquatic scenes and backgrounds containing polarised light and against which polarised signals might appear. (**a**) Waxy leaves from a bush (*top left*), converted to false colour images (Cronin et al. 2003), showing degree (*top right*, scale from 0 to 100 %) and angle (*bottom left*, scale encodes angle such that *red* is horizontal). The image *bottom right* shows degree

receivers' visual system, specifically whether or not it can process intensity, colour and polarisation independently.

Part of the job of this chapter is to disentangle what we know about the retinal mechanisms of polarisation sensitivity (PS) and what we are beginning to learn about the polarisation properties of animals themselves. Critical in this is a good understanding of the scale at which objects must be viewed. It has been known since the early twentieth century that body parts of animals polarise light with Michelson (1911) demonstrating its presence in reflections from butterflies, beetles and, through implication, birds. His careful quantification of the physics of iridescent thin-film and multilayer colours and polarisation has been expanded upon rapidly in the last decade as the realisation that some of the photonic attributes of animal colours and polarising parts might have applications that are useful for our own lives (Parker 1999; Vukusic et al. 2000a, b; Vukusic and Sambles 2004; Kinoshita et al. 2007, 2008). In particular, cuticles, wing scales and feather barbules all self-assemble together in different ways and with different periodicities. They may have one-, two- or three-dimensional order, producing an astonishing array of mechanisms of both colour and polarisation. The potential to mix air, keratin, chitin and dense melanin pigment granules has allowed this expansion in air, while aquatic animals must deal with a lack of refractive index difference between surfaces and the aquatic medium in constructing their polarising structures.

However, as the stomatopods (mantis shrimp) in particular demonstrate, a number of mechanisms are clearly possible and equally effective in producing highly polarised signals underwater (Chiou et al. 2005, 2008a, b, 2012; Cronin et al. 2009). This fundamental difference between signal production in aquatic and terrestrial environments is critical, however, as it reduces the possibility as well as the problems of polarisation from a specular or shiny surface (Fig. 19.1). Hand in hand with a multitude of structures comes an equally diverse range of polarisations that are reflected. As has been described previously in Chap. 7, the polarisation state of light can be defined in terms of three different properties: the angle of polarisation, the degree (or per cent) of polarisation and the ellipticity of polarisation. The angle of polarisation describes the predominant direction in

Fig. 19.1 (continued) of polarisation in an underwater shallow reef demonstrating lack of polarisation. The photograph contains a fish and a cuttlefish against a coral reef background. The polarisation signals in the arms of the cuttlefish (Fig. 19.8) may be just visible. (**b**) Celestial E-vector information shown through a fish-eye lens photograph of the sky at dusk through a linearly polarising filter arranged orthogonal to sky polarisation, producing a *dark band* running N to S (*left*) and false colour image indicating the degree of polarisation with a key as in (**a**) (*right*). Note how the depolarising clouds contrast against the 80 % polarised sky. (**c**) A reef scene around midday at 20 m through orthogonal linearly polarising filters as indicated by *double-headed arrows* (*left*) and false colour image of angle of polarisation (*right*). This shows the largely horizontally polarised background light field that predominates underwater for much of the day (Cronin and Shashar 2001). The school of fish, *top right*, contrast due to motion artefact. (**d**) Mudflat environment showing the angle and degree of polarisation in false colour produced by reflected sunlight from the wet surface (photograph and analysis by Martin How)

which the electric field vector of light oscillates; the degree of polarisation defines the extent to which waves oscillate at the same angle. The ellipticity equates to us visualising the tip of the electric field rotating along an ellipse. In the case of circularly polarised light, this ellipse is a circle. The direction of E-vector rotation defines whether the light is either left- or right-hand circularly polarised.

The covert or secret communication channel that polarisation signalling can provide makes it an attractive research subject. However, it often also leads to overenthusiastic optimism in hypotheses and correlations. Finding an animal that has or most likely has PS for navigation and that also possesses iridescent and therefore polarised body colours and patterns is not enough to prove that this animal must also use polarisation for signalling. It is always worth asking what the adaptive benefit of the polarisation dimension might be along with how the multidimensional information would be perceived by the receiver. Behavioural evidence of polarisation as a source of information is absolutely necessary, but this is an area in which, for signalling at least, we remain almost entirely ignorant. It is one thing to show PS ability and another entirely to show it in the context of a behaviour that relies on the polarising information content conveyed in the surface being examined. Unfortunately, the 'secret' nature of polarisation to our own visual system makes the careful quantification of this parameter of light all the more important when planning experiments. Without this it is hard to see where mistakes are made; imagine trying to set up a psychophysical colour discrimination test while being entirely colour blind.

Whether the receiver's visual system perceives the colour or polarisation information from an object separately or in combination is what we must address. As already indicated, one of the large questions in this emerging field is to determine the behavioural uses of this information and whether a comparison of the similarities and differences with colour is worthwhile. Bernard and Wehner (1977) (but see Hegedüs and Horváth 2004a) and more recently How and Marshall (2014) have attempted this theoretically and note the similarity between hue and E-vector angle, saturation and degree (per cent) of polarisation and intensity or luminance in each modality. Intensity of colour and polarisation can be independent, although in both cases sometimes linked to what we might term black-and-white intensity. In particular, any signal differences in luminance need careful consideration from the biological perspective. A behavioural reaction to a polarisation difference may in fact primarily be a response to a contrast perceived by the animal as brightness and have no relevance to polarisation per se (Chap. 9). Critical here is an understanding of the possible separate processing pathways of polarisation, colour and luminance, and again, this is an area ripe for investigation.

When illuminated and viewed from different angles, the hue, E-vector angle and degree of polarisation of objects constructed from pigments or three-dimensional periodic structures do not change. However, simpler specular or diffuse reflectors can polarise or depolarise and change the E-vector angle of reflected light differently, depending on the illumination direction and viewing angle. For a potential polarising signaller, this creates a problem not present in the colour dimension (see also Horváth et al. 2002 and Hegedüs and Horváth 2004b). A red apple in a

green tree is highly contrasting due to hue difference, no matter what the viewing direction; however, the polarisation information in a background can be highly variable. Figure 19.1a illustrates this for a waxy-leafed bush, where the different orientations of the leaves result in surfaces displaying differing degrees of polarisation and differing E-vector angles. This property in polarisation is in some cases likened to 'polarisation pollution' (which is different from the polarised light pollution treated in Chap. 20; Horváth et al. 2009) and may be reason for insects to degrade PS within the non-DRA ommatidia in an effort to avoid confusion (Wehner and Bernard 1993; Labhart and Meyer 1999; Kelber et al. 2001). The lack of such 'polarisation noise' underwater (Fig. 19.1) may be one factor driving the trend for aquatic invertebrates, especially the crustaceans and cephalopods, to concentrate visual investment in polarisation more than colour (Chaps. 7 and 8).

Conversely, such a high-contrast E-vector patchwork might provide effective camouflage for a leaf-shaped animal with polarisation reflection (see butterflies discussed below). In Fig. 19.1, throughout this chapter and elsewhere in the book, false colour images are used to interpret the dimensions of polarisation for our eyes (including later on intensity), and the methods to produce these are detailed in Horváth et al. (2002), Cronin et al. (2003) and Horváth and Varjú (2004). When considering coloured objects against backgrounds, we assess the three components of hue, saturation and intensity in a combined fashion, so again some caution is needed in interpreting contrasts in any one dimension. A numerical measure of contrast is useful to form hypotheses, and How and Marshall (2014) suggested a model of polarisation distance, similar to that used in chromatic colour space (Vorobyev and Osorio 1998; Kelber et al. 2003). One of the working hypotheses resulting from this is that most signals will evolve along differences in degree or per cent as this dimension is, for reasons just given, more reliable than angle or intensity.

Because this is an emerging field, it is necessary to be cautious but also open-minded. Does an animal with PS for one task, such as navigation, also use PS for signal reception? Not necessarily, but the retinal and neurophysiological capability for one PS task is a good start. It is worth asking if iridescence or specular reflections necessarily mean polarisation signalling. Again no, and both these other ways of producing polarisation must be investigated carefully. Having some polarisation reflection is again a good start, however, and it may be our human colour-biased eyes that are missing the real story. As well as a signal and receiving mechanism, the neural pathways and behaviours to interpret polarisation are critical but, as we have noted, poorly understood. Clearly, an understanding of the polarising environment within which the signal might appear is important.

To finish this introduction, we list some of the possible signalling situations or circumstances in which polarisation sensitivity might be used for object detection where polarisation is a considered contrast mechanism (Fig. 19.1). This listing of environmental circumstances naturally leads to a consideration of polarisation as factor in camouflage and object recognition, and some examples of this are discussed below:

- An intrinsically polarising object may contrast against a non-polarising background, and that background may be the environment or other parts of the animal that are non-polarising.
- An intrinsically polarising object may contrast against a polarising background of different angle and/or degree, and that background may again be environment or other animal regions.
- A depolarising or non-polarised object may contrast against a polarising background in either E-vector angle or degree of polarisation (Figs. 19.1b and 19.8).
- An intrinsically polarising object may match or mimic a polarised background or part of a polarised background through (dynamic) cryptic or disruptive camouflage [for terminology in colour camouflage, see Stevens and Merilaita (2009)].
- An object may be polarisation neutral, with the polarisation of reflected light the same as the incident light. This is specifically in the context of camouflage or breaking of camouflage in midwater silvery or transparent organisms (Johnsen et al. 2011; Johnsen and Marshall 2012; Jordan et al. 2012; Brady et al. 2013).
- A host animal (e.g. horse, cattle or zebra) of blood-sucking female tabanid flies may be weakly polarising (due to a homogeneous bright coat), strongly polarising (due to a homogeneous dark coat) or alternating weakly and strongly polarising (due to a striped or spotted fur pattern). This feature significantly influences the attractiveness of the host animal to polarotactic tabanids, independently of the direction (angle) of polarisation of coat-reflected light (Horváth et al. 2010; Blahó et al. 2012a, 2013; Egri et al. 2012a; and Chap. 22). This positive polarotaxis in female tabanids is governed by the degree of polarisation of host-reflected light and differs from the polarotaxis governed by the horizontal polarisation serving water detection by male and female tabanids (Horváth et al. 2008; Kriska et al. 2009; Egri et al. 2012b).

19.2 Terrestrial Signals

19.2.1 Butterflies

Butterflies are known to be differentially sensitive to linear polarisation based on a number of lines of evidence including anatomical, electrophysiological and behavioural data (Chap. 4; Maida 1977; Kelber et al. 2001; Sweeney et al. 2003). Some possess DRAs, and monarch butterflies are known for feats of navigation rivalling birds (Reppert et al. 2004). As well as these large-field behaviours, an object-based polarisation task is found in Papilionid butterflies that chose waxy leaves of a particular colour to lay eggs under. All of the *Papilio* eye is E-vector sensitive (Kelber 1999), and this means they encounter the problem of seeing false colours when looking at polarised objects (Chap. 13). While some insects may use disrupted rhabdom structure to maintain independent colour and polarisation vision (Chaps. 2–4), *Papilio* species deliberately mix colour and polarisation, specifically

looking for green horizontally polarising citrus leaves to oviposit under (Kelber et al. 2001). This may be ecologically sound as these leaves are oriented horizontally (and therefore reflect horizontally polarised light, Fig. 19.1), while vertically oriented or oblique leaves reflect usually non-horizontally polarised light, which is perceived as bluish colours as a result of the receptor's spectral sensitivity (Kelber et al. 2001, but see also Horváth et al. 2002; Hegedüs and Horváth 2004a, b). Horizontal undersides may provide more cover for eggs from the sun and protect them from the eyes of hungry birds. Interestingly, fish may also mix colour and polarisation information; however, the behavioural context that might benefit from such apparent confusion is less clear (Chap. 9).

Butterflies are of course known for their colours and colour signalling in a variety of contexts, including between sexes. Recent evidence suggests that polarisation also forms a component of this communication. Females of the rainforest butterfly *Heliconius cydno* show strong iridescent, polarised wing reflections, while males do not (Fig. 19.2). Mate-choice experiments, in which the polarising component was removed, indicated that males prefer polarisation displaying mates (Sweeney et al. 2003, Fig. 19.2). Polarisation components of signals may be especially effective in deep rainforest, for under the shaded canopy polarisation is relatively rare (Fig. 19.1). It may also be that a polarisation signal stands out better in the patchy light distributions of the forest where colours may suffer from strong illumination differences and become less reliable for conveying information. This measure to counteract a breakdown in colour constancy may also explain the use of polarised signals in marine environments as explained below. In open meadows, where specular polarisation confusion may abound (Fig. 19.1), polarised signals are less common among butterflies. A larger survey of 144 nymphalids like *H. cydno* found that 75 species had polarisation reflections and that the majority of these were forest dwellers (Douglas et al. 2007).

Many of the colours of butterflies are structural instead of or in combination with pigmentary colouring. The way in which the wing scales are built has fostered an evolutionary explosion of photonic mechanisms that manipulate light (Vukusic et al. 2000a, b; Vukusic and Sambles 2004; Vukusic and Hooper 2005; Stavenga et al. 2010, 2012). Alternate layers of chitin and air and a variety of precisely arrayed surface structures and internal structuring produce colours and in some cases polarise light also. As noted in the introduction, many iridescent colours may or may not be polarised also, but, especially where colour has already been exploited for communication, this may not be visually and behaviourally relevant. Especially in the case of butterflies where light is manipulated so comprehensively by scale structures, it is possible to find iridescent colours that do not polarise and also some wing areas that are circularly polarising (Marshall, unpublished). The ecological context is a very emergent field, and, as with the beetles (see on) while we are beginning to learn much about polarising and colour properties of butterfly wings, the biological interpretation of these needs careful work.

Vukusic et al. (2000a, 2002) and Wilts et al. (2011) have provided recent examples of butterfly colours that also polarise, including some of the *Papilio* species. The 'glass scales' of the swordtail butterfly, *Graphium sarpedon*, cause

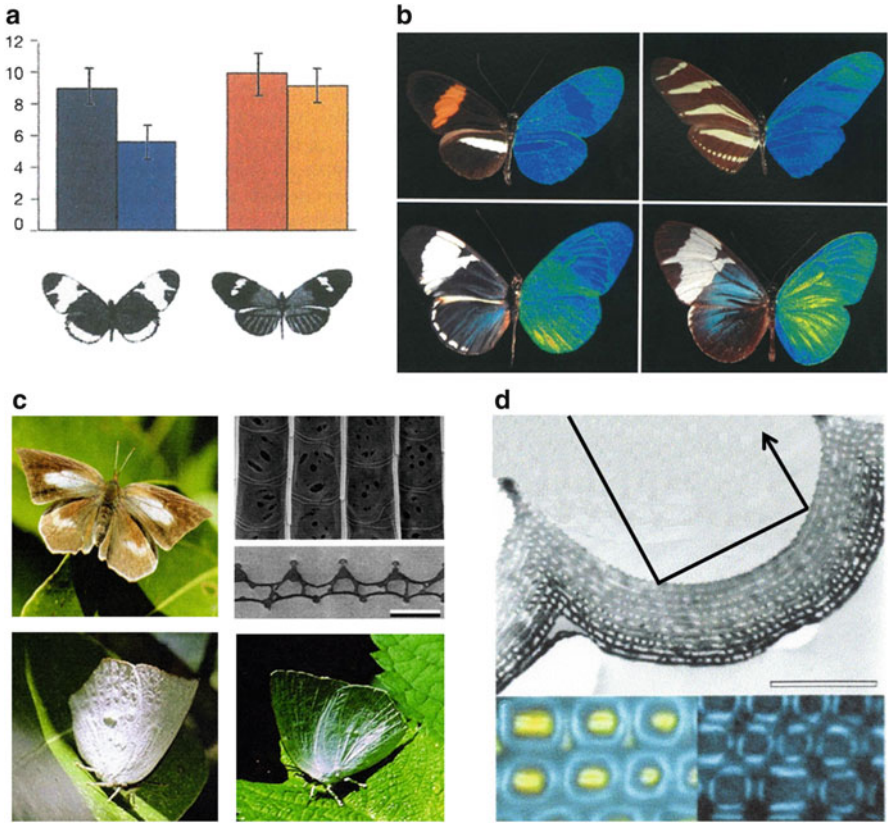

Fig. 19.2 Polarised signals from butterflies. (**a**) Comparative behavioural response of the male brush-footed butterfly, *Heliconius cydno* (*left*), that possesses strongly polarising thin-film iridescence and *H. melpomene malleti*, a closely related species that shows no iridescence. *Histograms* plot mean number of male approaches in 10 min to female wings behind filters that pass (*left*) or depolarise (*right*) polarised reflection (Sweeney et al. 2003). (**b**) *Heliconius* butterfly wings in normal (*left side*) and false colour degree of polarisation (*right side*), for open area-dwelling species *H. melpomene* (*left*) and *H. charitonius* (*right*, *top row*) and forest-dwelling species *H. cydno* (*left*) and *H. sapho* (*right*, *bottom row*). Note elevated polarisation in forest dwellers [from Douglas et al. (2007)]. (**c**) Specular colour camouflage and simultaneous polarisation signals in the sunbeam butterfly, *Curetis acuta*. Female with wings open (*top left*) and wings closed (*bottom row*) in direct sun (*left*) and shade (*right*). *Top right* shows transmission (*top*) and scanning (*bottom*) electron micrographs of the wing scales [scale bar = 2 μm, from Wilts et al. (2011)]. (**d**) Polarisation reflection through double reflection in the surface wing concavities in the swallowtail butterfly, *Papilio palinurus*. *Top*, transmission electron micrograph of concavity in iridescent scale (scale bar = 1 μm). *Bottom*, real colour image showing how *green* iridescence is produced by combining *blue* and *yellow* reflection and the removal of the *yellow* polarised component between crossed polarising filters [from Vukusic et al. (2000b)]

polarising iridescence, and Stavenga et al. (2010, 2012) suggested that they may function in intraspecific signalling. The green colours of the wings are constructed, unusually for a butterfly, using a blue bile combined with yellow carotenoid and may aid in disruptive camouflage in these strikingly patterned butterflies. The glass scales (as their name suggests) are transparent and found on the ventral wing surface. As well as enhancing the blue-green colours of the wings through reflection, they also produce polarised iridescence when illuminated obliquely (Stavenga et al. 2010, 2012). This is achieved through thin-film reflectance and is strongly angle dependent (Fig. 19.2). The result in flight might be a flashing polarised signal visible to butterflies and other insects that possess polarisation sensitivity but invisible to potential predators such as birds and other vertebrates that lack polarisation sensitivity. This combination of using colours for camouflage and polarisation for covert or 'secret' communication is a recurring theme in polarisation and as we will see below may also be useful in beetles, cephalopods, stomatopods and other crustaceans.

The sunbeam butterfly, *Curetis acuta*, is a sexually dimorphic species, the female displaying white and the male orange spots on a black/brown surround. The underwing colouration of both sexes is silvery white, caused by specular reflection from non-pigmented scales, using thin-film reflectance, similar to but more diffuse than the scales of *G. sarpedon* (Fig. 19.2, Stavenga et al. 2012). This slightly scattering mirror means that on shaded leaf and vegetation, with wings folded, the butterfly reflects its green leaf habitat and is well camouflaged. As this is a hibernating species, remaining hidden for long periods is clearly a priority. In oblique directional illumination, the wing undersides are strongly polarising and, like *G. sarpedon*, might provide a directional polarised signal to eyes with polarisation sensitivity, when the butterfly is in flight. Again, there appears to be a dual function of these specialised scales: communication in polarisation and concealment in colour or, in this case, reflected colour. The possibility that the butterflies might stand out in polarisation if illuminated directly is countered by the often waxy nature of the leaves of the Japanese Oak, *Quercus acuta*, they associate with. As demonstrated in Fig. 19.1, such leaves may form a disruptive polarising background due to different leaf angles, and a strongly polarising butterfly in such an environment may be better camouflaged than a depolarising butterfly. More careful in situ polarisation images of butterflies and indeed other animals in their natural habitat are needed to further such specular speculations.

19.2.2 Beetles, Linearly and Circularly Polarised Signals

Both cockchafer and scarab beetles are known to be sensitive to the celestial E-vector for orientation, utilising a DRA area (Chap. 2, Frantsevich et al. 1977; Labhart et al. 1992; Dacke et al. 2013). For more than a century, we have also known that the reflections from scarab beetles are elliptically polarised (Michelson 1911), and this discovery has been revisited numerous times (Neville and Caveney

1969; Goldstein 2006) including a similar helical geometry of the crustacean cuticle (Neville and Luke 1971). More recently still, within the resurgence of interest in photonic structures in nature, a variety of structures in beetles and butterflies have been revealed that in general elliptically polarise and some cases circularly polarise the reflected light (Figs. 19.3 and 19.7). Some of the known mechanisms, all resulting from cuticular microstructures, are reviewed by Vukusic and Sambles (2004), Goldstein (2006), Vukusic and Stavenga (2009) and Arwin et al. (2012). These include isotropic multilayer Bragg reflectors (in e.g. *Coptomia laevis*), a left-handed or right-handed chiral narrowband reflectors (in e.g. *Cetonia aurata*), chiral broadband reflectors (of a gold or silver appearance in e.g. *Anoplognathus aureus*) and combination of left-handed and right-handed reflectors (in e.g. *Chrysina argenteola*).

Michelson (1911) was the first to note that right-handed circular reflections were linked to the red end of the spectrum in some scarabs, while mid-wavelengths were left-handed (Fig. 19.3 and see Fig. 19.7 and a similar story for stomatopods). In these examples, the photonic mechanism relies on stacks of cuticle that form a chiral Bragg reflector that is directly analogous to cholesteric liquid crystal selective reflection (Fig. 19.3, Arwin et al. 2012). Typically, the pitch of the helix multiplied by the mean refractive index of the birefringent chitin defines the wavelength centre of the reflection band. More simply, the layers of cuticle describe azimuthally twisted nanostructures, and the spatial periodicity of the helix form determines both the colour and elliptical polarisation properties of light reflected. In *Chrysina* (then *Plusiotis*) *resplendens*, Caveney (1971) described a 1/2-wave retardation plate between helical layers. By converting one handedness of polarised light to the other, the overall reflectivity of the structure was increased. Similar optical composite layers are also known in stomatopod crustaceans (Figs. 19.5 and 19.7, Chiou et al. 2008a, b). Repeated, hexagonal surface structures may also determine the colour and polarisation of reflected light (Fig. 19.3, Jewell et al. 2007; Sharma et al. 2009). Both the detailed physics and the bio-inspired nanofabrication of man-made devices are outside the scope of this chapter but worth further investigation (e.g. Vukusic and Sambles 2004; Jewell et al. 2007).

A review of the taxonomic distribution of elliptical polarisation in 19,000 species of beetles has been attempted by Pye (2010), and the list, both among beetles and other insects, grows every day. Following the examples of Goldstein (2006), Lowrey et al. (2007) and Arwin et al. (2012) used ellipsometry (i.e. polarimetry) to make particularly careful studies of the seven subfamilies of beetles now known to possess polarisation reflections. They quantified several parameters including directionality, wavelength range, elliptical range (from circular to linear) and degree of polarisation and note that right-handed as well as left-handed circular polarisation is relatively common, dispelling previous suggestions of its rarity. In a number of beetles, ellipticity changes from linear to circular in different body areas or in single locations over the wavelength range 300–800 nm (Fig. 19.3; Hegedüs et al. 2006; Arwin et al. 2012). In truth, given the variety of beetles out there and number of species, even the extensive survey of Pye (2010) only scratches the surface.

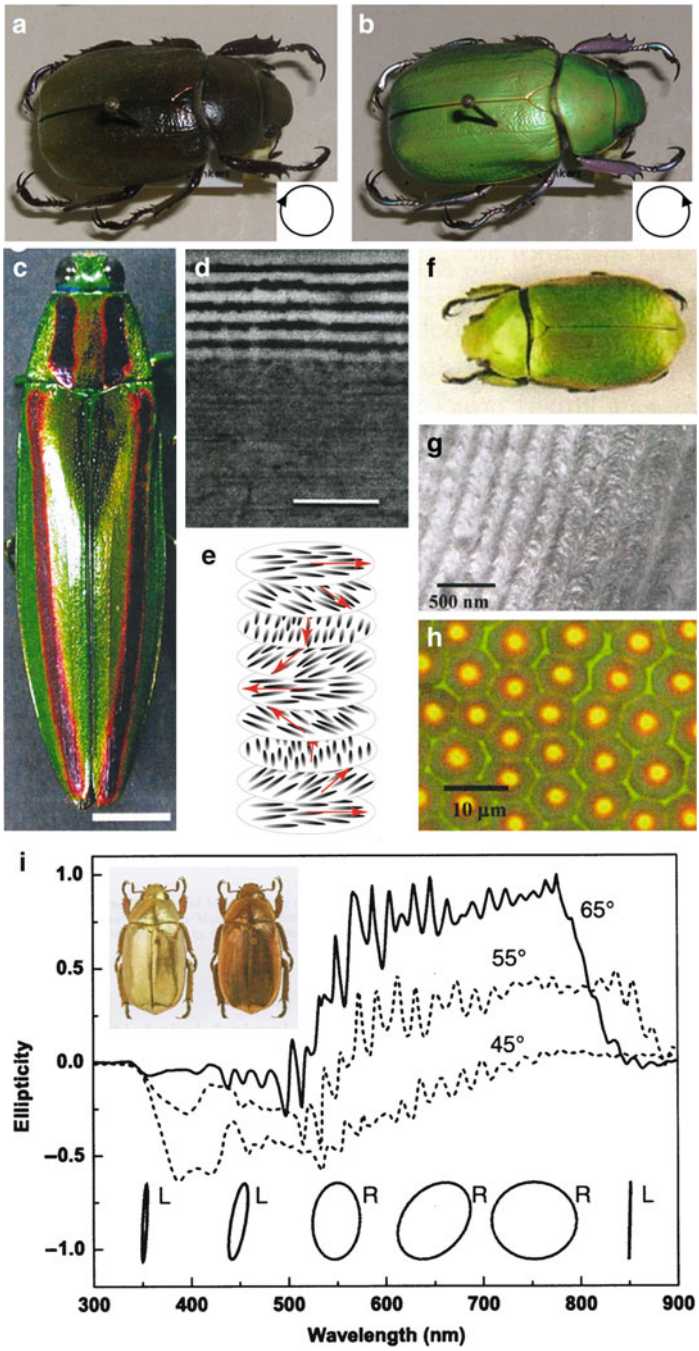

Fig. 19.3 Beetle circular and linear polarisation. (**a**, **b**) The scarab beetle, *Chrysina beyeri*, photographed through left- and right-handed circular polarisation filters, demonstrating the left-handed chiral reflection from its cuticle. Note silvered legs through left-handed filter, the beetle here appearing as it would through no filter. (**c**) Colour photograph of the Japanese

If there is any visual relevance to these polarising reflections, the distribution and directionality of the signal may be particularly important, and imaging polarimetry (Hegedüs et al. 2006) and directional ellipsometry and a scatterometric approach (Stavenga et al. 2009, 2011a, b) are useful in this respect. The colours and linear polarisation reflections of the Japanese jewel beetle, *Chrysochroa fulgidissima*, result from the beetle's iridescent elytra and are hypothesised as useful in intraspecific recognition (Fig. 19.3, Stavenga et al. 2011a).

Before getting carried away by our ability to quantify pretty things, however, it is important to ask if the animal is able to perceive circular or linear polarisation of light and, most importantly, if this is behaviourally relevant. Under some circumstances, humans may see polarised light, but, at least from an evolutionary perspective, it has rarely been behaviourally relevant (Chap. 14).

As well as the directionality of possible signals and their biological relevance, the directionality of visual axes and polarisation sensitivity is important to understand. For example, while several beetle species are known to possess a DRA for use in navigation on the basis of sky polarisation (Labhart et al. 1992; Dacke et al. 2013), whether the same eye region might be used to view polarising beetles or other small objects is not known. In fact, the DRA areas are often optically and neurally modified to perform best as low-pass filters for viewing the large-field stimulus of the celestial polarisation pattern (Chap. 18) and are not suited for distinguishing small objects (Labhart et al. 1992; Labhart and Meyer 1999). In bees there are recent suggestions that the DRA or other eye regions may process polarisation information from model flowers (Foster et al. 2013). Here it is thought that bees that must enter tunnel-shaped floral structures such as orchids or foxgloves to get a nectar reward may receive downward directed linear polarisation information from the flower, possibly using the DRA; however, the details of this story are still emerging. It is perhaps more likely, both in beetles and bees, that if polarisation signals are relevant, specific ommatidia from the main eye region are employed, as is the case in butterflies and dragonflies (Maida 1977; Gordon 1977; Laughlin and Mcginness 1978; Labhart and Nilsson 1995; Stavenga et al. 2001).

Fig. 19.3 (continued) jewel beetle, *Chrysochroa fulgidissima*. (**d**) Transmission electron micrograph through the *purple areas* of the elytra showing the layering at the surface. Layers in *green areas* are closer together, and these structures cause linear polarisation (scale bar = 1 μm, from Stavenga et al. 2011b). (**e**) Diagrammatic representation of the chiral liquid crystal stack structures causing circularly polarised reflections from the scarab *Chrysina gloriosa*. (**f**, **g**, **h**) Details of similar circular polarisation in *Chrysina boucardi*. (**g**) Transmission electron micrograph through the elytra showing curved sections through helicoid layers similar to (**e**) (scale bar = 0.5 μm). (**h**) High-magnification bright-field illuminated light micrograph of small area of elytra showing repeated hexagonal patterns within which crystal stacks are found [scale bar = 10 μm, from Jewell et al. (2007)]. (**i**) Ellipticity of light reflected from *Chrysina argenteola* for incident unpolarised light at angles indicated. Inset ellipses show state of polarisation at selected wavelengths including left- (L) or right-handed (R) polarisation. *Inset photographs above* show beetle under left-handed (*left*) and right-handed (*right*) circularly polarised light illumination [from Arwin et al. (2012)]

The current debate on whether scarab beetles possess circular polarisation sensitivity is worth briefly reviewing as it illustrates gaps in our current knowledge (a more detailed review is given in Chap. 6). Brady and Cummings (2010) used behavioural phototaxis to test whether the jewel scarab, *Chrysina gloriosa* with left-handed circularly polarising exocuticle, could distinguish linear from circular polarisation. In a flight arena, beetles were forced to choose from four containers illuminated with unpolarised (UP), linearly polarised (LP), left-circularly polarised (LCP) and right-circularly polarised (RCP) light. They were most strongly attracted to the UP source with RCP and LCP coming last, respectively, and LP between these and UP. Container brightness was not varied between stimuli, and, while some attempt was made to equate brightness between stimuli, as the receptor mechanism is also unknown in scarabs, it is not possible to determine what the beetles' choice was based on. In other words, none of the dimensions of polarisation were disambiguated from unpolarised or indeed from each other (further criticism of this study can be read in Chap. 6).

In beetles we also lack physiological, optical, anatomical and functional (circularly polarisation-sensitive eye regions do not exist terrestrially) explanations for this circular polarisation preference in *Chrysina gloriosa* suggested by Brady and Cummings (2010). Counter to the results of Brady and Cummings (2010), Blahó et al. (2012b) did not find any preferential polarotactic response to circularly polarised light in four species of also LCP-reflecting scarab beetles. In other experimental series, a range of potential attractant sources were used, including photographs of beetles on vegetation transilluminated with and without LCP, RCP, LP and UP light and the beetles themselves of similar or different sex or different species with LCP and RCP reflected light. In all cases, none of the beetles was attracted to any of the stimuli given, and as beetle retinal structure is rather similar across the species investigated (Gokan and Meyer-Rochow 1984), it is supposed the results can be generalised. To advance this field, the retinal and optical structure and the electrophysiological response of the photoreceptors to circularly polarised light must be examined.

Finally, for the beetles, interestingly, the larvae of *Photuris* fireflies emit LCP and RCP bioluminescent light from their left and right lanterns, respectively (Wynberg et al. 1980). However, any visual significance of the circular polarisation component of this light is unknown. As with perhaps all of the polarisation activity in beetle integument, circular polarisation may simply be a by-product of the exoskeletal structure and of no relevance to vision or visual behaviour (see also Chap. 6).

19.2.3 Flies, Dragonflies, Other Insects and Even Spiders?

With photoreceptors constructed from microvilli and colours that may, if resulting from structural phenomena, produce polarised light, any invertebrate might be considered 'fair game' for possible polarisation signals. As just discussed, this

correlation in butterfly and beetle has raised the possibility of polarisation signalling in these invertebrate groups, so clearly others are worth consideration and careful behavioural experimentation. Relatively little is known about possible polarisation signals in other insects or indeed other colourful arthropods such as the salticid jumping spiders. These behaviourally complex spiders show many colour and even fluorescent-based signalling systems, some of which rely on peacock-like iridescent displays (Li et al. 2007). Several spider groups also possess polarisation sensitivity, previously associated with celestial orientation (Dacke et al. 1999), and their potential for polarisation signalling has yet to be investigated.

The bodies and wings of the odonates (dragonflies and damselflies) may be coloured and used in inter- and intraspecific signals. Some of the wing structures are known to employ complex photonic structures (Prum et al. 2004; Vukusic et al. 2004), and the association of dragonflies with also polarising water surfaces (Horváth et al. 1998, 2007; Wildermuth 1998; Bernáth et al. 2002; Kriska et al. 2009) makes this group 'low-hanging fruit' for polarisation signalling or potentially camouflage. As reviewed in Chaps. 5 and 21, several flies, midges and other insects show positive polarotaxis to water, and this along with the possible 'polarisation conversation' between tabanid flies and their equine hosts (Chap. 22) is a new and interesting area.

Among the flies, Dolichopodids possess alternating rows of ommatidia that combine differently coloured corneal facets, red and yellow, and photoreceptor microvilli that are orthogonal between the rows (Trujillo-Cenoz and Bernard 1972). This design was suggested useful in prey detection through water or around specular vegetation. Given that many Dolichopodid species are strikingly adorned with metallic interference colouration, just like beetles, and are known for their complex courtship behaviours (Land 1993), it would be worth investigating the possible role that body colours play in these and other fly species known to utilise polarised light. Many flies are also now known to have sexually dimorphic compound eye regions, with the males investing large areas in female-spotting zones. Building on the observations of Trujillo-Cenoz and Bernard (1972), Land (1993) suggested that the Dolichopodid, *Poecilobothrus nobilitatus*, may have a specialised Dolichopodid detector based on both colour and polarisation signals. He even noted differential polarisation reflections associated with different interference colouration (unpolarised orange and horizontally polarised green) on the abdomen of the females.

19.2.4 Fiddler Crabs

In common with other arthropods and cephalopods, crustaceans possess microvilli within and in arrays of photoreceptors that are indicative of polarisation sensitivity (Chaps. 7 and 8). As detailed further below, the stomatopod crustaceans are known to possess complex polarisation vision and signals. Before examining polarisation signals in water, however, here we discuss crustaceans that, due to littoral or largely

terrestrial habitats, might produce polarisation signals in air. Several crab species such as the ghost crabs, land hermit crabs, coconut crabs and fiddler crabs conduct most of their vision-related activities out of water. The fiddler crabs in particular show diverse colouration and a complex social signalling system that has attracted much attention for decades (Zeil and Hofmann 2001; Zeil and Hemmi 2006). Male fiddler crabs give the animals their name with a comically enlarged claw or cheliped that is used in sexual and agonistic interactions on the mudflats where they live. Complex signalling systems involving different colours and claw-waving motions are known in different species (How et al. 2007), and Zeil and Hofmann (2001) suggested that polarisation may play a part in the display, from either the cheliped or other body parts. They also hypothesised that the degree of wetness of the crab, and the correlated degree of specular polarisation signal resulting from this, might enable other crabs to judge local from wandering individuals. As many fiddler crab battles are around burrows, it might be a selective advantage to be able to distinguish crabs that have just emerged from a wet home burrow and others that have been away from their home for a longer period. The potential attacker may be able to gauge if the intended victim can quickly retreat, whether it is near a burrow or just wandering (Zeil and Hofmann 2001).

A wet or naturally specular carapace will present a small area of polarisation with the E-vector angle dependent on the orientation of the surface or body area. This sort of front-surface specularity is distinctly different to polarisation produced by the internal cuticular mechanisms of the insects already discussed and in the aquatic animals detailed below. One advantage that largely terrestrial crabs have over their more watery counterparts is the range of refractive index difference that life in air allows. In a sense, it may not be necessary to go to elaborate lengths to construct polarising signals; however, a wet and specular polarisation signal from a surface is highly variable in both angle and degree with angle and illumination and may not make a good reliable signal. This may be why the terrestrial insects that might use polarisation for signalling do construct their signals in ways more complex than simple surface reflection. The mostly horizontal wet or shiny carapace of fiddler and other crabs may in fact be used in polarisation camouflage on an also horizontal polarising large-field wet mudflat, disguising them from potential aerial predators, for example (Fig. 19.1, Hemmi et al. 2006). Conversely, a fiddler crab erecting a vertical display claw (Chap. 7, Fig. 7.9) would present a vertically polarising specular surface against the largely horizontally polarised background, perhaps providing extra contrast to the PS systems of conspecifics. Yet again, there is unfortunately little direct evidence that suggests that polarisation is used by any crustacean other than mantis shrimps.

19.2.5 Birds

When Michelson (1911) noted polarisation from beetles, he also commented on birds and their iridescent plumage. A walk through any natural history museum

with a simple linearly polarising filter makes it clear that some bird feathers do polarise light, and Noh et al. (2010) and Stavenga et al. (2011a) have begun to quantify the photonic nature of this. However, while we know that bird feathers may produce polarised light by a number of structural mechanisms including multilayer iridescence and scattering, the visual function of this reflection, if any, remains obscure. Avian polarisation sensitivity is linked to navigation (Chap. 12), so in common with many of the insect examples, we are left with a large-field-type polarisation sensitivity, a possible polarisation signal and little knowledge on retinal, neural or behavioural mechanisms that might link the two. The retinal substrate for PS is less well understood in vertebrates, due to the intrinsically polarisation-insensitive rod and cone structure (but see Chaps. 9 and 14 for fishes and humans). Reptiles and amphibians may be equally as colourful as the birds, also producing colour via structural means (Fox and Vevers 1960; Fox 1976; Prum 1999; Chaps. 10 and 11). Little is known about correlations of signals and polarisation for these vertebrate groups also, and for the moment, due to lack of data, we are best left to dream about possibilities and substantiate them later.

19.3 Aquatic Signals

Much of our knowledge of polarisation signalling comes from work in marine animals. Underwater, polarisation signals are rapidly attenuated, largely due to beam scatter, so that even in the very clearest waters after only 3–4 m the signal strength is more than halved (Shashar et al. 2004). The most effective spectral region to place polarisation signals varies with water type and is detailed elsewhere (Horváth and Varjú 2004 and Chap. 15); however, whatever the colour, polarisation seems, like UV, to be a short-range signal. Again like UV, this supports the idea that it may be a covert or 'secret' messaging system, used by small animals at short range and hidden from the eyes of long-distance predators.

In fact, polarisation may be a more reliable signal underwater than colour, as its content remains the same at any depth. The spectrum is a strong function of depth (Jerlov 1976; Chap. 15), and signal reliability may be why the deeper-living stomatopods seem to swap colour for polarisation body adornments (Figs. 19.4, 19.5 and 19.6), although shallow species have both. It may also explain why most crustaceans and almost all the cephalopods, the ocean's most successful invertebrate predators, have remained almost exclusively colour blind (Chaps. 7 and 8, Messenger 1977; Marshall and Messenger 1996).

As already briefly mentioned, following work on scarab beetles, Neville and Caveney (1969) and Neville and Luke (1971) also described circularly polarised reflections from lobster cuticle. As these crustacean areas are hidden in the leg joints and not, as yet, found on the more calcified carapace regions, signalling using such areas remains a remote possibility. Some crustaceans do perform leg or appendage spreads as displays, and this might display the joints; however, rather

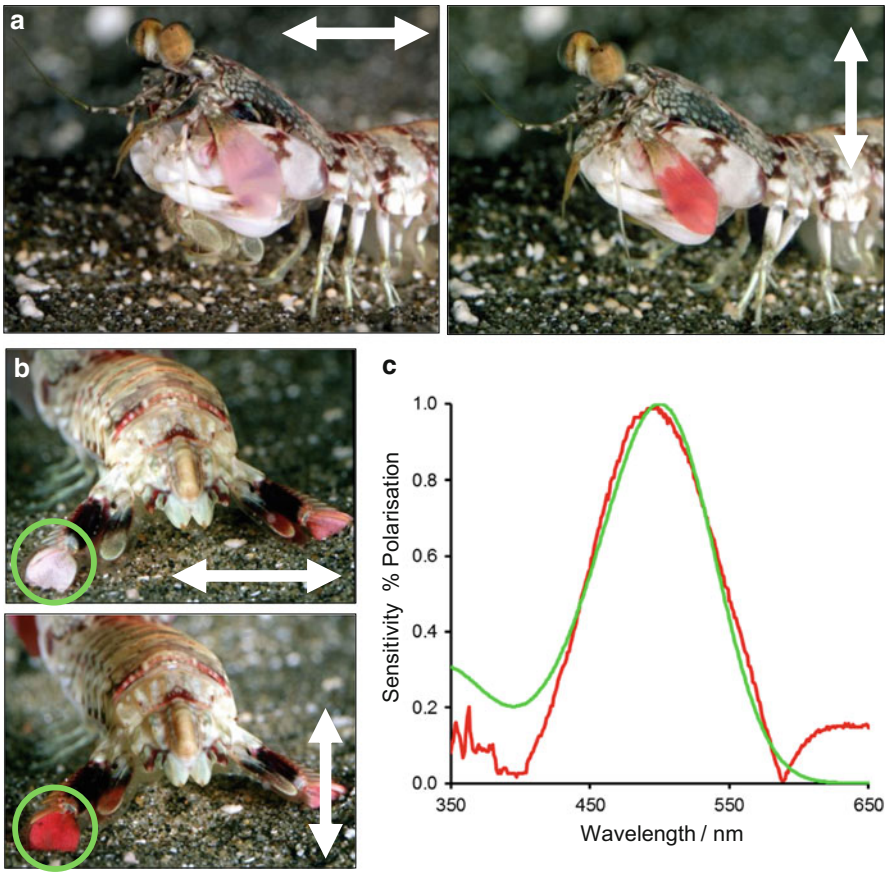

Fig. 19.4 Linear polarisation spectral tuning in the stomatopod *Odontodactylus latirostris*. (**a**, **b**) Antennal scales (**a**) and telson (**b**) showing polarising activity through horizontally and vertically polarising filters as indicated by *arrows*. (**c**) Per cent polarisation (*red line*) of telson paddle (*circled* in **b**) and spectral sensitivity (*green line*) of 500 nm visual pigment. Many of the linearly polarising reflectors of stomatopods, independent of their colour (see Fig. 19.6b), are most efficient around 500 nm. This is well matched to the spectral sensitivities of linear PS receptors in many stomatopod and cephalopod species (Cronin et al. 2000, Fig. 19.8)

than clutch at such straws, it is more profitable to concentrate on the crustaceans known to produce, receive and use polarisation signals, the stomatopods.

19.3.1 Stomatopods

Of all the polarisation signalling systems known, we probably know more about the stomatopods than any other animal. Evidence exists from behaviour, intracellular and extracellular electrophysiology, photoreceptor anatomy, optics and photonics,

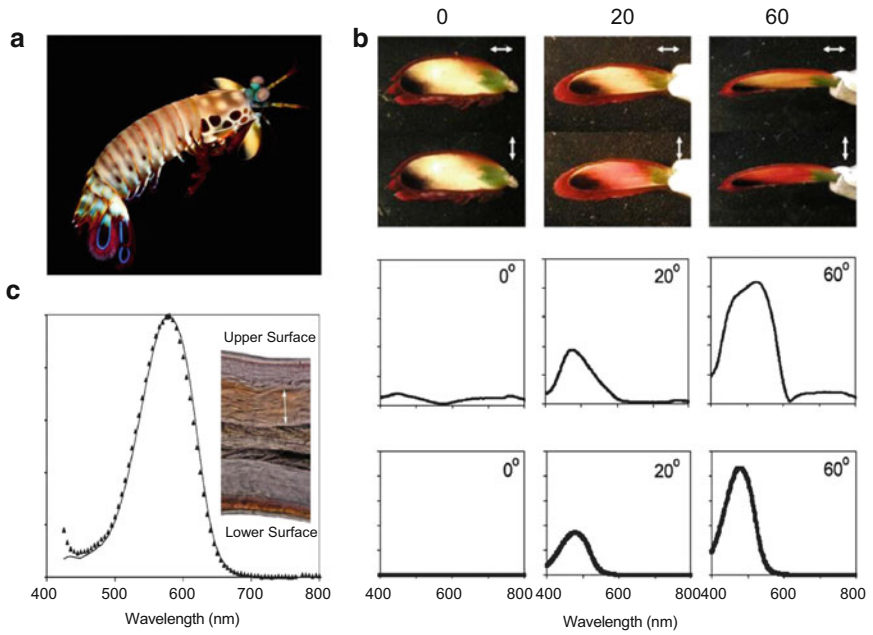

Fig. 19.5 Details of the dichroic molecule polarisation mechanism in antennal scale of *Odontodactylus scyllarus*. (**a**) Swimming *O. scyllarus* showing back surface of antennal scales (photograph, Roy Caldwell). (**b**) *Left antennal scale* photographed through horizontal (*top row*) and vertical (*bottom row*) linear polarising filters and at tilt angles of 0.20 and 60°. Note change in colour to *redder* and *darker* in vertical polarisation, similar to *O. latirostris* in Fig. 19.4. *Graphs below* show per cent polarisation from 0 to 100 % at different tilt angles (*top row*) and modelled polarisation spectra based on absorption of aligned astaxanthin molecules (*bottom row*, also 0 to 100 %). (**c**) Normalised absorption spectrum of acetone-extracted pigment from antennal scale (*triangles*) and pure astaxanthin acetone solution (*line*) [from Cronin et al. (2009) and Chiou et al. (2012)]. *Inset* shows freshly sectioned, unstained section of the antennal scale; the *arrows* mark *area of pink* dichroic tissue

and further details are provided in Chap. 7. Here we focus on the signalling mechanism. Several species of stomatopods from all superfamilies polarise light by reflection, although it is not clear if all use polarisation as a signal. Supporting the idea, polarised reflections are often situated on body parts, such as antennal scales, legs or uropods, that are used in social communication (Figs. 19.4–19.8). Also in line with these being specifically adapted for polarisation signalling, the degree of polarisation emitted is high, reaching 60–80 % (Figs. 19.5 and 19.6). Even against the up to 40 % polarisation of background space-light underwater (Fig. 19.1), these will stand out, and those seen in front of the polarisation-poor reef substrate (Fig. 19.1a) will be particularly conspicuous. Three mechanisms of polarisation signalling are known in stomatopods, two linear and one circular, the latter most likely building on one of the linear mechanisms. The two linear systems are quite different. The first described here relies on the ordered arrangement of a naturally dichroic molecule, the astaxanthin.

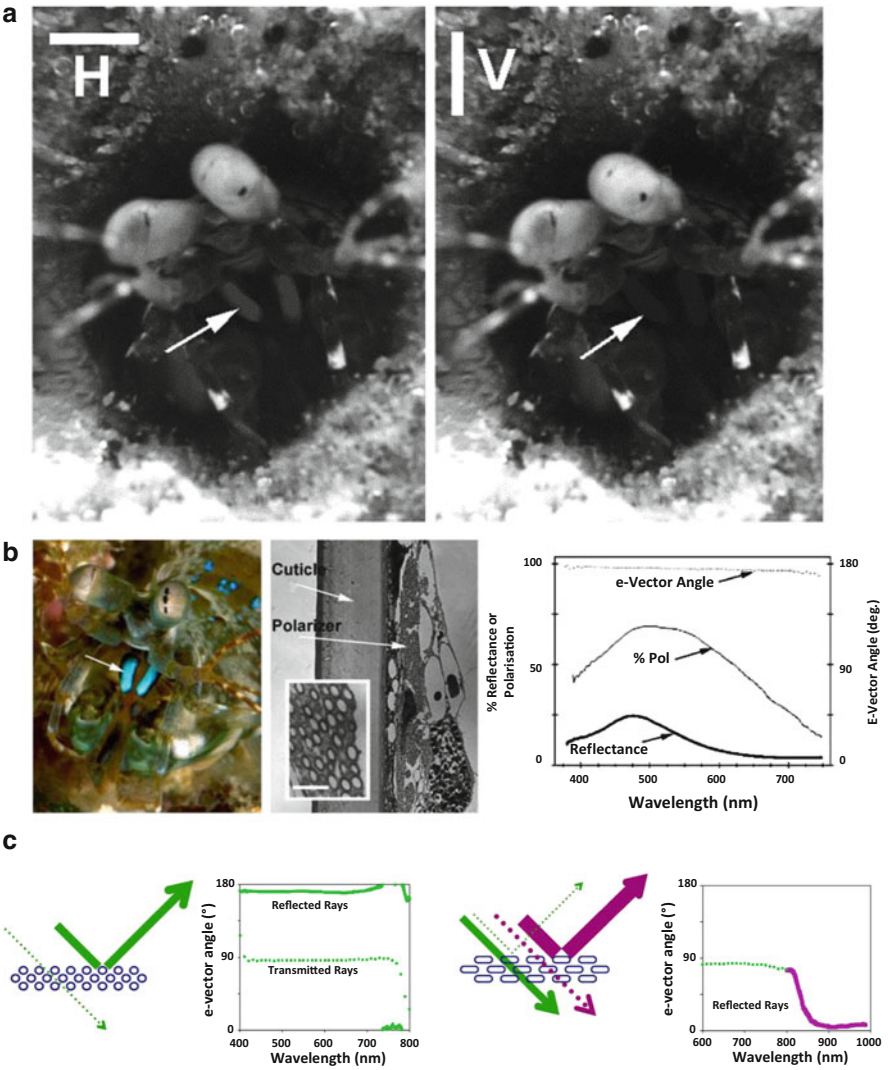

Fig. 19.6 The scattering polarised *blue* maxillipeds of the stomatopod *Haptosquilla trispinosa*. (**a**) Animal photographed in its burrow through horizontal and vertical polarisers as indicated. *Arrows* point to front plate of maxillipeds, the horizontal reflections from which are more extinguished through vertical filter. (**b**) *Left*—colour photograph of animal displaying from burrow. Note that the *blue spots* seen on carapace do not polarise. Middle—transmission electron micrographic details of the *blue* maxilliped cuticle and underlying polariser tissue, seen in *enlarged inset* to show ellipsoidal vesicles (scale 0.5μm). *Right*—spectral features of polarisation. (**c**) Diagrammatic representation of scatter caused by vesicles and measured E-vector orientation graphs showing wavelength-dependent polarised beam splitting. In diagrams, *dotted rays* are polarised perpendicular to page, and *solid lines* are polarised parallel to page. *Left side* shows transmission and reflection of medium wavelength (*green*) light with vesicles viewed end on and therefore circular in cross section. As shown by the data measured and graphed, vertically and

Astaxanthin is a ketocarotenoid found in many crustaceans imparting a pink or red colour, such as seen on the antennal scales and uropods of several species (Figs. 19.5 and 19.6, Cronin et al. 2009). Chiou et al. (2012) recently described this in detail for *Odontodactylus scyllarus* (Fig. 19.6), but it may be a relatively widespread mechanism in other *Odontodactylus* species as well as stomatopods from other genera or superfamilies (Fig. 19.4). Rather than producing polarisation through layering or other photonic structures, this molecular mechanism for polarisation reflection appears unique to the stomatopods.

Examination of the internal structure of the antennal scales of *O. scyllarus* reveals a specific pink-coloured layer containing astaxanthin molecules and showing strong dichroism (Fig. 19.6b). In common with other carotenoids, astaxanthin contains a long chain of conjugated double bonds. It is this structure that, due to preferential E-vector absorption along the chain's long axis, results in the molecule's dichroic properties. Astaxanthin is also of just the right size and molecular structure to span lipid bilayers and therefore becomes arranged vertically through cell membranes. The result is an overall dichroism perpendicular to the membrane surface, and the pink tissue shown in Fig. 19.6b must contain several membrane layers, adding up to a strong polarisation signal. Interestingly, the direction of polarisation of the signal from the overall antennal scale is not normal to its surface, but is an oblique tilt angle around 60° (Fig. 19.6c). This implies a specific internal orientation of these membranes to achieve this directionality yet to be shown.

In terms of signalling and behaviour, the observed result from this tilted polarisation reflector is a dark red, strongly polarised reflection at the correct angle (60°) to the antennal scale and is most apparent on the reverse or posterior side of the scale (Fig. 19.6c). Stomatopods wave and rotate their antennal scales during behavioural interaction, and it may be that, like butterflies, the angle-specific polarisation is flashed on and off. In truth, we know little about how this signal is used, but it is curious that it faces backwards. Other, yet to be characterised, polarisation signals are found on the uropod teeth of *O. scyllarus*, and these are both specific to males and faced forward in interspecific interaction (Chiou et al. 2005). It is known that *O. scyllarus* can learn to discriminate stimuli with different E-vectors (Marshall et al. 1999), and the eye regions probably responsible for carrying this signal are well characterised (Marshall et al. 1991 and Chap. 7). However, while we can note their presence and that (in laboratory situations) behavioural and physiological responses to polarisation, the revealing of the actual function of these polarisers in nature requires more work.

Fig. 19.6 (continued) horizontally polarised light is split and remains constant through spectrum. *Right side* again shows transmission and reflection of medium wavelength light but with vesicles viewed side-on and therefore with oval cross section. With this 90° rotated view, transmitted and reflected rays are orthogonal to those seen *Left*. Long-wavelength (*red*) light (>850 nm) interacts with the vesicle long dimension most efficiently with polarisation parallel to their long axis. As a result, in measurements graphed, observed long-wavelength polarisation is perpendicular to medium wavelengths

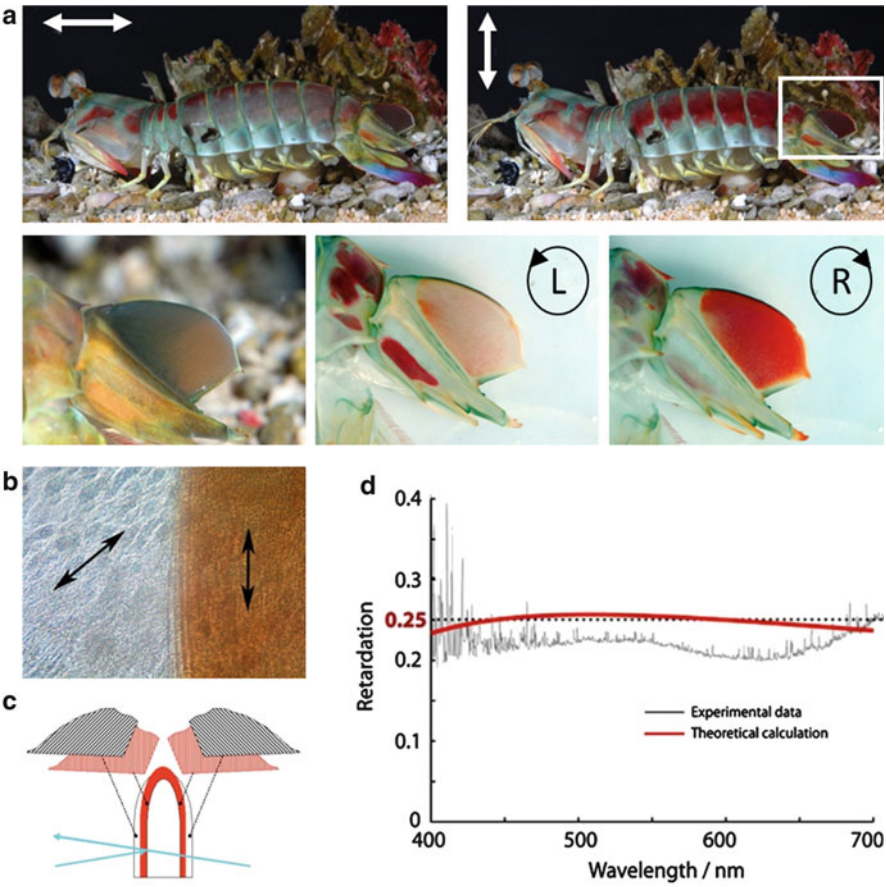

Fig. 19.7 Linearly and circularly polarised signals from *Odontodactylus cultrifer* (photographs, Roy Caldwell). (**a**) The thoracic and abdominal carapace is strongly linearly polarised with *pinkish red pigment* similar to that in Figs. 19.4 and 19.5. In males, the central carina of the telson, outlined on the *right* and *enlarged below*, is circularly polarised. Note the lack of substantial change in this area under different linear polarisations. (**b**) Surface view of one-half of the carina such that the *left half* contains only retarder layer and *right half* has both retarder and pigmented dichroic polariser. (**c**) Diagrammatic representation of the carina organisation in section and with relative placement of the layers (*grey*: retarder layer, *pink*: dichroic layer) to show how circular polarisation of opposite handedness is produced from each side in both reflected and transmitted light [from Cronin et al. (2009)]. (**d**) Measured (*thin line*) and theoretical (*red line*) retardation of R8 photoreceptor compared to ideal 1/4-wave retardation (*dotted line*). This photoreceptor's secondary function converts the circularly polarised signals from stomatopods to linearly polarised ones, a form of light the underlying photoreceptors can detect (see Fig. 7.7). Note remarkably spectrally flat retardation [from Chiou et al. (2008b)]

The second type of linear polariser described in stomatopods has received some behavioural analysis in a more natural context and relies on a quite different photonic mechanism. One subgroup of the genus *Haptosquilla* (including

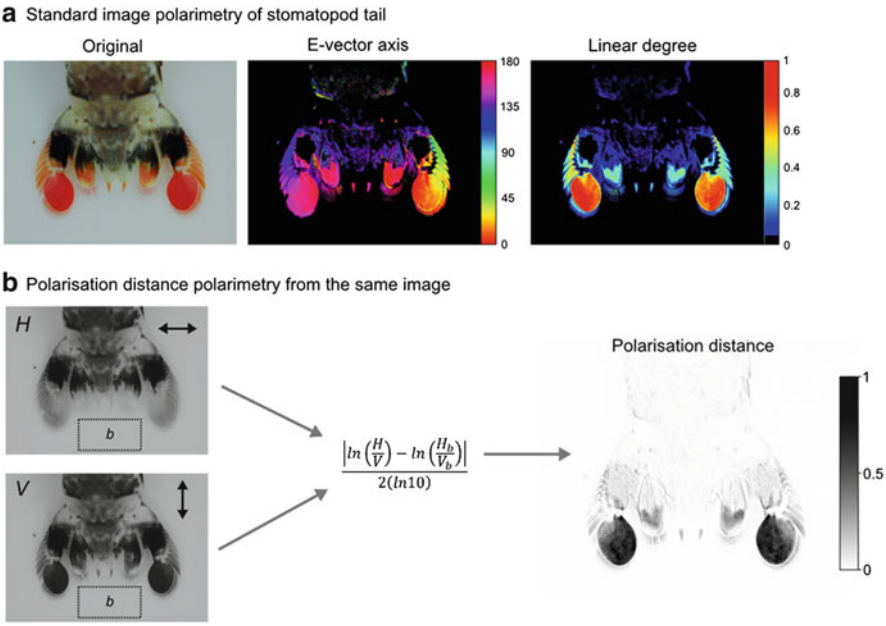

Fig. 19.8 Polarimetric analysis and false colour images (as in Fig. 19.1) and calculated polarisation distance of the linearly polarised signal in the telson of *O. latirostris* (Fig. 19.4). Polarisation distance is calculated relative to background, the boxed area marked b in (**b**). See text for details [from How and Marshall (2014)]

H. trispinosa, *H. nefanda*, *H. stoliura* and *H. pulchella*), species common in both shallow and deeper reef areas, displays a brilliant metallic-blue section of their first maxillipeds on meeting conspecifics (Fig. 19.5). As well as being blue, this is a highly polarising signal, with the E-vector direction approximately horizontal relative to the animal (Fig. 19.5). Chiou et al. (2011) removed the colour and polarisation component of this signal in males and scored the resulting reaction of females in mate-choice experiments. Females preferred males with polarising and blue maxillipeds, and while this does not distinguish between the colour and polarisation component of the signal, it clearly shows the signal is used in sexual display. More recently, Roberts et al. (unpublished) have gone on to show that several species, including *H. trispinosa*, react more to horizontally polarised than to vertically polarised signals.

Several stomatopod species also display iridescent blue spots on various body regions, including the maxillipeds, but those of various *Haptosquilla* species are the only ones known to also polarise. *H. trispinosa* also possesses other non-polarising blue spots, on the abdominal segments, for example (Fig. 19.5). Resonant scatter from a disordered three-dimensional array of ovoid vesicles in tissue below the cuticle is thought to be the underlying polarisation mechanism, interestingly with maximal degree of polarisation around 500 nm, despite the maximum reflectance

being at a shorter wavelength (<500 nm) (Fig. 19.5). Peak polarisation efficiency close to 500 nm (Fig. 19.5) is a remarkably good match to the spectral sensitivity of the linear polarisation photoreceptors known in most stomatopod species (Cronin et al. 2000 and Fig. 19.4). This suggests that it is the polarisation, not the colour, of the signal that is important and, at 500 nm, spectrally optimal for transmission in many marine waters.

While the full details remain speculative, the ovoid shape and size of the vesicles seem important for polarisation. The long axis of the vesicle strings is arranged parallel to the long axis of the maxilliped section they sit within and perpendicular to the polarisation they produce. The horizontal E-vector angle displayed is remarkably constant across the visible spectrum (Fig. 19.5b). Unlike the highly directional dichroic polarisers described for *O. scyllarus*, these scattering polarisers reflect nearly constant polarisation over a wide range of viewing angles. Another interesting property the vesicles show is that of a polarising beam splitter. Vertically polarised light is preferentially transmitted relative to the long axis of the vesicles and the overall axis of the maxilliped segment, while horizontally polarised light is reflected (Fig. 19.5c). This scattering system depends critically on the dimension of the vesicles, the short dimension preferentially backscattering medium wavelengths of light with E-vectors parallel to the shorter radius and therefore horizontally polarised. The vesicle long axis interacts preferentially with longer wavelength light, shifting the plane of polarisation from horizontal to vertical at long wavelengths (Fig. 19.5c).

The third type of polarised signals known from stomatopods is circularly polarising areas, such as the keel of the uropod in *O. cultrifer*. Figure 19.7a (top) shows photographs of a male through perpendicular linearly polarising filters, and most obvious is the difference in abdominal and thoracic regions that show dichroic reflectance, most likely via the same dichroic astaxanthin mechanism described above. Also clear in these photographs is the lack of change in the red keel region of the uropod (boxed right). As shown in three photographs in Fig. 19.7a (bottom), this lack of change between perpendicular linear analysers is expected as the keel reflects and indeed transmits circularly polarised light, shown by photographs taken through LCP and RCP filters. Chiou et al. (2008b) and Chap. 7 described the visual apparatus required to perceive this difference. Chiou et al. (2008b) also showed behavioural discrimination between LCP and RCP and hypothesised that, as males possess the signal and females do not, it is part of the complex sexual signalling repertoire of these species.

To receive circularly polarised light, stomatopods have evolved receptors (in rows 5 and 6 of their mid-band eye region) that contain a 1/4-wave retarder and underlying linear polarisation receiving mechanism at precisely the correct angle (see Chap. 7 for details and Roberts et al. 2009). To produce circular polarisation, a 1/4-wave retarder is also used, this time overlying linearly polarising cuticular tissue. In other words, a composite laminar structure exists (Fig. 19.7b, c). Importantly, this satisfies the observation that both reflected and transmitted light through the keel are circularly polarised and that on either side of the animal the handedness of the signal reverses (Fig. 19.7c). Although yet to be confirmed, most

likely the linearly polarised component of this signal is produced by the dichroic, pink astaxanthin tissue described above (Figs. 19.4 and 19.6). What turns the linearly polarised light to circularly polarised is the overlying birefringent 1/4-wave retardation layer (the structure of which is also not fully known), the fast axis of which is at 45° to the underlying linear polariser (Fig. 19.4b). This birefringent layer may contain oriented calcite crystals, a material commonly found in crustacean cuticle. Whatever the material, the production of circularly polarised light is quite different between stomatopods and insects.

Recent observations have found circularly polarised reflections on a variety of body regions in other species, including *Gonodactylaceus falcatus* and other gonodactyloid species; however, these are all left-handed no matter the side they are found on. It also appears that they may be sex-specific signals, again suggesting a role in mate choice; however, the behavioural proof of this has yet to be attempted. Also interesting is the possibility that some stomatopod species may operate both signals and receiving mechanisms in areas of polarisation between linear and circular (Chiou and Marshall unpublished). This is an exciting area for future work, but before rushing to publication we will be looking to solidify all five of the five areas of evidence required to show such circular or elliptical polarisation signalling. These are:

(a) Behaviour relative to elliptically polarised light including widely varying brightness and chromatic controls
(b) Anatomical and optical evidence that the photoreceptors are able to receive elliptically polarised light
(c) Electrophysiological evidence that photoreceptors and/or other areas of nervous system preferentially receive and process elliptically polarised light
(d) Evidence for signals or environmental elliptically polarised light that the animals might react to in nature
(e) A natural behaviour relative to (d) such as mate choice or other behaviours relative to natural and not just laboratory-produced stimuli

19.3.2 Cephalopods

Cephalopod skin is a complex structure, including specialised cells that interact with light in three categories: chromatophores, leucophores and iridophores (Hanlon 1982; Hanlon and Messenger 1988). In common with many structural colour production mechanisms, a by-product of cephalopod iridophores is that they polarise light by reflection (Shashar et al. 1996; Mäthger and Denton 2001; Chiou et al. 2007, 2008a; Mäthger et al. 2009a, b). Cephalopods are also known to be capable of polarisation sensitivity (Moody and Parriss 1961; Saidel et al. 1983, 2005; Talbot and Marshall 2010; Temple et al. 2012), and it is of course tempting to assume that the two are linked. Unlike other animals, including beetles, butterflies and stomatopods where the capacity for both colour vision and mixed colour and polarisation complicates the story, cephalopods are comfortingly colour blind

(Marshall and Messenger 1996; Mäthger et al. 2006). Their discarding of colour as a medium for information transfer and increased object contrast makes it more likely that polarisation has become their currency for signalling. This case is further strengthened by the discovery of polarising arm stripes, in both cuttlefish and squid, with properties that seem particularly convergent with signalling (Fig. 19.9). Firstly, these are directed forward and are easy to observe in inter- and possibly intraspecific interactions. Secondly, the arm stripes can be turned on and off by a combination of neural control of the iridophore itself and by being covered up by overlying and also neutrally controlled chromatophores (Mäthger and Hanlon 2007). Finally, the arm stripes appear unique among cephalopod iridophores in that their polarisation content is remarkably non-directional (Fig. 19.9, Chiou et al. 2007).

Chiou et al. (2007) investigated the arm stripes with multi-angle spectrophotometry and transmission electron microscopy in both cuttlefish and squid (Fig. 19.9). Intriguingly, although clearly constructed from iridophores (Fig. 19.9), the degree of polarisation was not highly dependent on viewing or illumination angle, as might be expected. Instead it remained close to 80 % over most angles and also with a constant spectral maximum at around 500 nm (Fig. 19.9). As a result the signal is constant at any arm orientation, in both polarisation and intensity. This mechanism relies on there being a series of packets of multilayer reflectors, with their surface orientations at different angles, rather than large areas with the same orientation (Chiou et al. 2007).

Although cephalopods are known to discriminate polarised patterns and information (Shashar et al. 1996; Pignatelli et al. 2011; Temple et al. 2012) and also can use polarisation in feeding (Shashar et al. 1998, 2000) and social contexts (Shashar et al. 1996; Boal 1997), it is still not clear what information might be carried in these signals. Boal et al. (2004) found that female *Sepia officinalis* showed more polarisation signals than males and reacted to polarised patterns. It was not clear in this study how other signals, such as the conspicuous black-and-white stripes used in social contexts, combined with polarisation. A more recent study (Cartron et al. 2012) indicated that *S. officinalis* can use E-vector information in landmark learning, but the relevance of this to the life of the animal is not clear.

Given that polarisation vision is clearly highly evolved in cephalopods, as are their complex social interactions, further study of these and indeed other likely polarising signals is clearly worthwhile, however. Interestingly, the blue rings from the *Hapalochlaena* sp. 'blue-ringed' octopus, a clear and well-known aposematic signal, are not strongly polarised other than at quite oblique angles (Mäthger et al. 2009a, b, 2012). This is remarkable as they are certainly made from beautifully ordered multilayer structures (Mäthger et al. 2009a, b, 2012). It is possible that these signals are not designed primarily for cephalopod eyes. The blue ring often displayed and indeed flashed (through neural control in interaction with chromatophores or muscles that reveal and cover up the iridophore areas; Mäthger et al. 2012) on a yellow background is very conspicuous to the colour vision systems of potential vertebrate predators, such as fish. Yellow and blue is a known effective message, travelling far in marine waters (Lythgoe 1979; Marshall

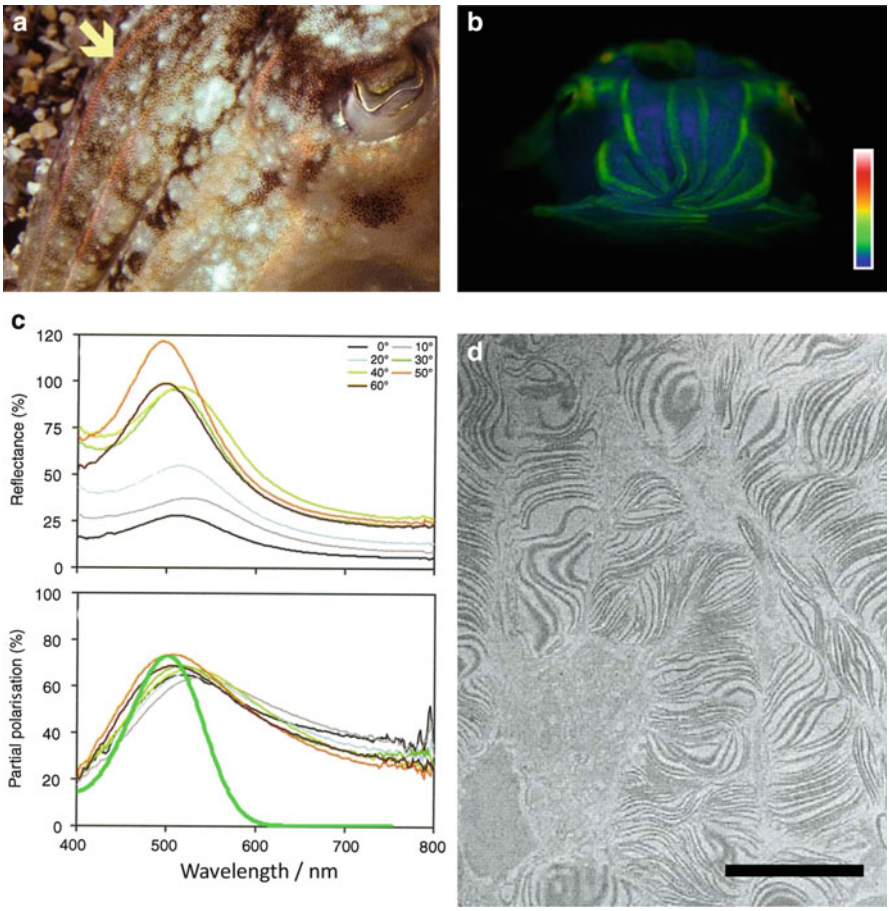

Fig. 19.9 Polarised light reflection from cephalopods. (**a**) The head and upper arm region of the cuttlefish, *Sepia officinalis*. *Arrow* indicates *pinkish arm stripes* that contain the polarising reflectors. (**b**) False colour image of per cent polarisation of cuttlefish arms and head (*scale bar* as in Fig. 19.1). (**c**) Reflectance (*top*) and per cent polarisation (*bottom*) of the arm stripes of the squid, *Doryteuthis pealeii*, measured at several tilt angles. Note how while colours change with tilt, per cent polarisation remains relatively constant. The single spectral sensitivities of cephalopods are close to 500 nm visual pigment shown below. (**d**) Transmission electron micrograph of iridophores in the arm stripes of *D. pealeii* (*scale bar*: 7.5 μm) [from Chiou et al. (2007)]

2000a, b), and is therefore effective as an aposematic signal, advertising the toxin-laden bite that blue rings are famous for.

Other iridophores around the eyes of cephalopods are also non-polarising (Mäthger et al. 2009a, b), and it may be a mistake to assume that all iridophores also show polarised reflections as a by-product. It seems that the cephalopods have evolved remarkable control over this information channel via a number of mechanisms (Mäthger et al. 2006, 2009a, b, 2012) and possibly for good reason.

19.3.3 Fish

The underwater light field in clear pelagic waters is significantly different from terrestrial and shallow water visual environments. To a good approximation the surrounding radiance distribution is cylindrically symmetric about the vertical axis (Denton and Nicol 1965a). Denton proposed that highly reflective silvery fish make use of this symmetry, where a 100 % reflection would match the background light field irrespective of the viewing angle (Fig. 19.10a, b). The vertical orientation of the reflective elements (guanine platelets) in the scales in many of these fish, despite the curvature of their bodies, fits this requirement to produce an idealised vertical mirror.

However, specular surfaces usually polarise light to varying degrees depending on the angle of illumination, with light becoming 100 % polarised at a specific angle called Brewster's angle. This has the knock on effect that at these angles, the reflectivity can be as low as 50 % for an incident unpolarised light field (see Fig. 4.47 on page 120 in Optics 3rd edn by Hecht 1998). In a separate set of measurements, Denton and Nicol (1965b) noted that in fact the reflections from the bleak (*Alburnus alburnus*) appeared not to have a Brewster's angle and that the reflected light did not become close to 100 % polarised, as would be expected from a normal specular reflector. Jordan et al. (2012) repeated some of these measurements in several other species (herring, sardine and sprat) and discovered that reflections only reached a maximum of 30 % polarisation. They found that this was due to a specific mixing of two different optical types of guanine in the multilayer stack (Fig. 19.10c; see Chap. 9). Jordan et al. (2012) proposed that this was because weakly polarising reflectors minimise the drop in reflectivity at higher angles of incidence. This allows the fish to better match the intensity of the background over all viewing angles.

More recently, Brady et al. (2013) showed that the reflective sides of another silvery-sided fish species, the lookdown (*Selene vomer*), were also a weakly polarising reflector. Both Jordan et al. (2012) and Brady et al. (2013) further suggested that a weakly polarising structure might also help camouflage a fish, which is an advantage against any polarisation-sensitive predators, such as squid. However, what needs to be considered now is how a relevant polarisation-sensitive receiver processes both intensity and polarisation information together. A two-channel polarisation detector system, as is found in the retina of many cephalopod predators, will perceive combined intensity and polarisation information reflected from a prey item compared with the background. This makes it incorrect to discuss intensity-based crypsis and 'polaro-crypsis' as independent camouflage strategies.

As a final note of caution, not all silvery fish are good specular reflectors. The diffuse component in many reflections has the effect of depolarising the information a viewer will receive. This is clearly illustrated in Fig. 19.10d showing how this silvery fish does not match the background in the degree of polarisation. This mismatch to background will persist even in the case of perfect specular reflection, where background light shows high degrees of polarisation, especially at angles

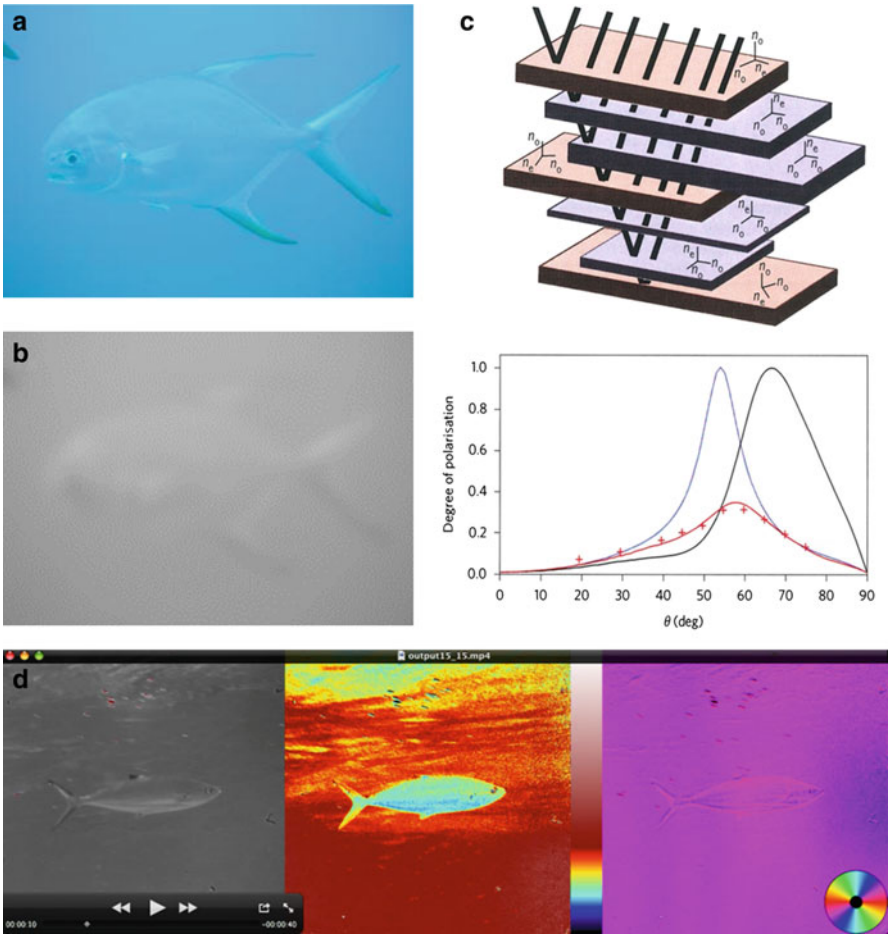

Fig. 19.10 Lack of polarisation camouflage in silvered fish. (**a**, **b**) The snub-nosed dart, *Trachinotus blochii*, in midwater. *Lower image* is colour stripped and blurred to represent resolution and spectral capability of cephalopod predator. (**c**) Optical multilayer model of silvered fish skin. *Top*: Diagrammatic representation of skin with two types of guanine crystals, Type 1 (*purple*) and Type 2 (*orange*), showing refractive index (*n*) coordinate axes. *Middle*: Simulations of the degree of polarisation at different angles of incidence for Type 1 (*black line*) and Type 2 (*blue line*) crystals. *Red line* is a mixture of crystals in ratio found in nature (in herring, *Clupea harengus*) and is an excellent fit to measured data (*red crosses*). Note how combined degree of polarisation is low but optimised at an angle around 58°, close to Brewster's angle [from Jordan et al. (2012)]. (**d**) Real-time videometric analysis of silvery fish (*Scomberoides* sp.) in midwater showing intensity, degree and angle of polarisation (*left* to *right*). *Scale bars* as in Fig. 19.1 but with first 30 % of degree of polarisation expanded over whole spectrum. Note poor camouflage in degree of polarisation, where fish is around 15 %, while background water is over 30 %, but good camouflage in intensity and angle of polarisation. This image is from an unpublished work with Viktor Gruev [and see Gruev et al. (2010)]

away from Brewster's angle. Based on our current knowledge, it is too early to say whether the control of the degree of polarisation by any silvery fish reflector is an adaptation to better camouflage that fish to the eyes of a polarisation-sensitive predator.

19.4 Conclusions and Future Research

To conclude this chapter, the following are some of the emerging ideas, caveats and hypotheses we think worth future consideration in polarisation signals:

- Polarised signals may work best in specific habitats, such as forest shade or underwater, where strong signals or polarisation clutter in the background may not be present to confuse the signal.
- Degree of polarisation rather than angle of polarisation may be a more reliable signal, as it is more invariant with illumination or the angle the polarising object is held at.
- Polarisation may work well for covert or 'secret' communication among smaller species, in the same way that UV colour might, as especially in the marine environment, the signal is rapidly degraded over distance by light scattering.
- In the marine environment, crustaceans and especially cephalopods seem to have specialised in polarisation rather than colour information, and this includes using polarisation for signals.
- Spectral tuning of polarisation receptors around 500 nm in marine environments has co-evolved or at least become co-adapted with polarisation signals that, independent of their colour, reflect polarised light most efficiently close to 500 nm.
- When looking for a polarised signal, it is more likely that specular, intrinsic photonic or pigment-based features generate polarisation.
- Circular polarisation vision is only confirmed in stomatopods using four lines of evidence: (1) anatomical and optical correlates within the eye, (2) behaviourally relevant circular polarisation signals, (3) intracellular electrophysiology and (4) behaviour. The evidence in scarab beetles is confounding (see Chap. 6).
- Polarisation camouflage as well as communication may exist. For example, animals living in the highly disruptive polarisation environment of well-lit foliage may exploit disruptive camouflage principles. Alternatively, midwater animals may seek to camouflage against the background of underwater space-light with relatively high (20–40 %) degrees of polarisation. However so far, good evidence for such 'polaro-crypsis' is still required (contrast Fig. 19.10 with Brady et al. 2013). Polarisation differences between species and their relative environments also need to be considered.
- Perhaps the most salient take-home message from this chapter is the following: Where it is found that an object may reflect or produce polarised light, while it is worth looking at this as a potential signal, the polarisation may be either redundant (as in some iridescent colour signals) or not visually relevant.

References

Arwin H, Magnusson R, Landin J, Järrendahl K (2012) Chirality-induced polarization effects in the cuticle of scarab beetles: 100 years after Michelson. Philos Mag 92:1583–1599

Baird E, Warrant EJ, Ribi W (2013) The unusual ocellar morphology of the orchid bee. Third international conference on invertebrate vision, proceedings, 1–8 August 2013, Lund, Sweden

Bernard GD, Wehner R (1977) Functional similarities between polarization vision and color vision. Vis Res 17:1019–1028

Bernáth B, Szedenics G, Wildermuth H, Horváth G (2002) How can dragonflies discern bright and dark waters from a distance? The degree of polarization of reflected light as a possible cue for dragonfly habitat selection. Freshw Biol 47:1707–1720

Blahó M, Egri Á, Báhidszki L, Kriska G, Hegedüs R, Åkesson S, Horváth G (2012a) Spottier targets are less attractive to tabanid flies: on the tabanid-repellency of spotty fur patterns. PLoS One 7(8):e41138. doi:10.1371/journal.pone.0041138 + supporting information

Blahó M, Egri Á, Hegedüs R, Jósvai J, Tóth M, Kertész K, Biró LP, Kriska G, Horváth G (2012b) No evidence for behavioral responses to circularly polarized light in four scarab beetle species with circularly polarizing exocuticle. Physiol Behav 105:1067–1075

Blahó M, Egri Á, Száz D, Kriska G, Åkesson S, Horváth G (2013) Stripes disrupt odour attractiveness to biting horseflies: battle between ammonia, CO_2, and colour pattern for dominance in the sensory systems of host-seeking tabanids. Physiol Behav 119:168–174

Boal JG (1997) Female choice of males in cuttlefish (Mollusca: Cephalopoda). Behaviour 134: 975–988

Boal JG, Shashar N, Grable MM, Vaughan KH, Loew ER, Hanlon RT (2004) Behavioral evidence for intraspecific signaling with achromatic and polarized light by cuttlefish (Mollusca: Cephalopoda). Behaviour 141:837–861

Brady PC, Cummings ME (2010) Differential response to circularly polarized light by the jewel scarab beetle *Chrysina gloriosa*. Am Nat 175:614–620

Brady PC, Travis KA, Maginnis T, Cummings ME (2013) Polaro-cryptic mirror of the lookdown as a biological model for open ocean camouflage. Proc Natl Acad Sci 110:9764–9769

Cartron L, Darmaillacq AS, Jozet-Alves C, Shashar N, Dickel L (2012) Cuttlefish rely on both polarized light and landmarks for orientation. Anim Cogn 15:591–596

Caveney S (1971) Cuticle reflectivity and optical activity in scarab beetles: the role of uric acid. Proc R Soc Lond B 178:205–225

Chiou TH, Cronin TW, Caldwell RL, Marshall J (2005) Biological polarized light reflectors in stomatopod crustacean. Proc SPIE 5888:1–9

Chiou TH, Mäthger LM, Hanlon RT, Cronin TW (2007) Spectral and spatial properties of polarized light reflections from the arms of squid (*Loligo pealeii*) and cuttlefish (*Sepia officinalis* L.). J Exp Biol 210:3624–3635

Chiou TH, Caldwell RL, Hanlon RT, Cronin TW (2008a) Fine structure and optical properties of biological polarizers in crustaceans and cephalopods. Proc SPIE 6972:1–10

Chiou TH, Kleinlogel S, Cronin T, Caldwell R, Loeffler B, Siddiqi A, Goldizen A, Marshall J (2008b) Circular polarization vision in a stomatopod crustacean. Curr Biol 18:429–434

Chiou TH, Marshall NJ, Caldwell RL, Cronin TW (2011) Changes in light-reflecting properties of signalling appendages alter mate choice behaviour in a stomatopod crustacean *Haptosquilla trispinosa*. Mar Freshw Behav Physiol 44:1–11

Chiou TH, Place AR, Caldwell RL, Marshall NJ, Cronin TW (2012) A novel function for a carotenoid: astaxanthin used as a polarizer for visual signalling in a mantis shrimp. J Exp Biol 215:584–589

Cronin TW, Shashar N (2001) The linearly polarized light field in clear, tropical marine waters: spatial and temporal variation of light intensity, degree of polarization and e-vector angle. J Exp Biol 204:2461–2467

Cronin TW, Marshall NJ, Caldwell RL (2000) Spectral tuning and the visual ecology of mantis shrimps. Philos Trans R Soc Lond B 355:1263–1267
Cronin TW, Shashar N, Caldwell RL, Marshall J, Cheroske AG, Chiou TH (2003) Polarization signals in the marine environment. Polarizat Sci Remote Sens 5158:85–92
Cronin TW, Chiou TH, Caldwell RL, Roberts N, Marshall J (2009) Polarization signals in mantis shrimps. In: Shaw JA, Tyo JS (eds) Proceedings of SPIE 7461:1–12 (Polarization Science and Remote Sensing)
Dacke M, Nilsson DE, Warrant EJ, Blest AD, Land MF, O'Carroll DC (1999) Built-in polarizers form part of a compass organ in spiders. Nature 401:470–473
Dacke M, Byrne M, Smolka J, Warrant E, Baird E (2013) Dung beetles ignore landmarks for straight-line orientation. J Comp Physiol A 199:17–23
Denton EJ, Nicol JAC (1965a) Reflexion of light by external surfaces of the herring, *Clupea harengus*. J Mar Biol Assoc UK 45:711–738
Denton EJ, Nicol JAC (1965b) Studies on reflexion of light from silvery surfaces of fishes, with special reference to the bleak, *Alburnus alburnus*. J Mar Biol Assoc UK 45:683–703
Douglas JM, Cronin TW, Chiou TH, Dominy NJ (2007) Light habitats and the role of polarized iridescence in the sensory ecology of neotropical nymphalid butterflies (Lepidoptera: Nymphalidae). J Exp Biol 210:788–799
Egri Á, Blahó M, Kriska G, Farkas R, Gyurkovszky M, Åkesson S, Horváth G (2012a) Polarotactic tabanids find striped patterns with brightness and/or polarization modulation least attractive: an advantage of zebra stripes. J Exp Biol 215:736–745 + electronic supplement
Egri Á, Blahó M, Sándor A, Kriska G, Gyurkovszky M, Farkas R, Horváth G (2012b) New kind of polarotaxis governed by degree of polarization: Attraction of tabanid flies to differently polarizing host animals and water surfaces. Naturwissenschaften 99:407–416 + electronic supplement
Foster JJ, Sharkey CR, Whitney HM, Roberts NW, Partridge JC (2013) Bees, flowers and polarization. Third international conference on invertebrate vision, proceedings, 1–8 August 2013, Lund, Sweden
Fox DL (1976) Animal biochromes and structural colours: physical, chemical, distributional and physiological features, 2nd edn. University of California Press, Berkeley
Fox HM, Vevers G (1960) The nature of animal colours. Sidgwick and Jackson, London
Frantsevich L, Govardovski V, Gribakin F, Nikolajev G, Pichka V, Polanovsky A, Shevchenko V, Zolotov V (1977) Astroorientation in *Lethrus* (Coleoptera, Scarabaeidae). J Comp Physiol 121: 253–271
Gokan N, Meyer-Rochow VB (1984) Fine-structure of the compound eye of the buprestid beetle *Curis caloptera* (Coleoptera, Buprestidae). Z Mikrosk Anat Forsch 98:17–35
Goldstein DH (2006) Polarization properties of Scarabaeidae. Appl Opt 45:7944–7950
Gordon WC (1977) Microvillar orientation in the retina of the nymphalid butterfly. Zeitschrift für Naturforschung C 32:662–664
Gruev V, Perkins R, York T (2010) CCD polarization imaging sensor with aluminum nanowire optical filters. Opt Express 18:19087–19094
Hanlon RT (1982) The functional organisation of chromatophores and iridescent cells in the body patterning of *Loligo plei* (Cephalopoda: Myopsida). Malacologia 23:89–119
Hanlon RT, Messenger JB (1988) Adaptive coloration in young cuttlefish (*Sepia officinalis* L.): the morphology and development of body patterns and their relation to behaviour. Philos Trans R Soc Lond B 320:437–487
Hawryshyn CW (1992) Polarization vision in fish. Am Sci 80:164–175
Hecht E (1998) Optics. Addison-Wesley, Reading, MA
Hegedüs R, Horváth G (2004a) How and why are uniformly polarization-sensitive retinae subject to polarization-related artefacts? Correction of some errors in the theory of polarization-induced false colours. J Theor Biol 230:77–87
Hegedüs R, Horváth G (2004b) Polarizational colours could help polarization-dependent colour vision systems to discriminate between shiny and matt surfaces, but cannot unambiguously code surface orientation. Vis Res 44:2337–2348

Hegedüs R, Szél G, Horváth G (2006) Imaging polarimetry of the circularly polarizing cuticle of scarab beetles (Coleoptera: Rutelidae, Cetoniidae). Vis Res 46:2786–2797
Hemmi JM, Marshall J, Pix W, Vorobyev M, Zeil J (2006) The variable colours of the fiddler crab *Uca vomeris* and their relation to background and predation. J Exp Biol 209:4140–4153
Horváth G, Varjú D (2004) Polarized light in animal vision—polarization patterns in nature. Springer, Heidelberg
Horváth G, Zeil J (1996) Kuwait oil lakes as insect traps. Nature 379:303–304
Horváth G, Gál J, Wehner R (1997) Why are water-seeking insects not attracted by mirages? The polarization pattern of mirages. Naturwissenschaften 84:300–303
Horváth G, Bernáth B, Molnár G (1998) Dragonflies find crude oil visually more attractive than water: multiple-choice experiments on dragonfly polarotaxis. Naturwissenschaften 85:292–297
Horváth G, Gál J, Labhart T, Wehner R (2002) Does reflection polarization by plants influence colour perception in insects? Polarimetric measurements applied to a polarization-sensitive model retina of *Papilio* butterflies. J Exp Biol 205: 3281–3298 + cover picture
Horváth G, Malik P, Kriska G, Wildermuth H (2007) Ecological traps for dragonflies in a cemetery: the attraction of *Sympetrum* species (Odonata: Libellulidae) by horizontally polarizing black gravestones. Freshw Biol 52:1700–1709
Horváth G, Majer J, Horváth L, Szivák I, Kriska G (2008) Ventral polarization vision in tabanids: horseflies and deerflies (Diptera: Tabanidae) are attracted to horizontally polarized light. Naturwissenschaften 95:1093–1100
Horváth G, Kriska G, Malik P, Robertson B (2009) Polarized light pollution: a new kind of ecological photopollution. Front Ecol Environ 7:317–325
Horváth G, Blahó M, Kriska G, Hegedüs R, Gerics B, Farkas R, Åkesson S (2010) An unexpected advantage of whiteness in horses: the most horsefly-proof horse has a depolarizing white coat. Proc R Soc B 277:1643–1650
How MJ, Marshall NJ (2014b) Polarization distance: a framework for modelling object detection by polarization vision systems. Proc R Soc B Biol Sci 281(1776):20131632
How M, Zeil J, Hemmi J (2007) Differences in context and function of two distinct waving displays in the fiddler crab, *Uca perplexa* (Decapoda: Ocypodidae). Behav Ecol Sociobiol 62:137–148
Jerlov NG (1976) Marine optics. Elsevier oceanography series. Elsevier, Amsterdam
Jewell SA, Vukusic P, Roberts NW (2007) Circularly polarized colour reflection from helicoidal structures in the beetle *Plusiotis boucardi*. New J Phys 9:1367–2630
Johnsen S, Marshall NJ (2012) Through the looking glass: are silvery fish safe from viewers with polarization vision? Integr Comp Biol 52:E87
Johnsen S, Marshall NJ, Widder EA (2011) Polarization sensitivity as a contrast enhancer in pelagic predators: lessons from in situ polarization imaging of transparent zooplankton. Philos Trans R Soc B 366:655–670
Jordan TM, Partridge JC, Roberts NW (2012) Non-polarizing broadband multilayer reflectors in fish. Nat Photonics 6:759–763
Kelber A (1999) Why 'false' colours are seen by butterflies. Nature 402:251
Kelber A, Thunell C, Arikawa K (2001) Polarisation-dependent colour vision in *Papilio* butterflies. J Exp Biol 204:2469–2480
Kelber A, Vorobyev M, Osorio D (2003) Animal colour vision—behavioural tests and physiological concepts. Biol Rev 78:81–118
Kinoshita M, Pfeiffer K, Homberg U (2007) Spectral properties of identified polarized-light sensitive interneurons in the brain of the desert locust *Schistocerca gregaria*. J Exp Biol 210:1350–1361
Kinoshita M, Takahashi Y, Arikawa K (2008) Simultaneous color contrast in the foraging swallowtail butterfly, *Papilio xuthus*. J Exp Biol 211:3504–3511
Kriska G, Bernáth B, Farkas R, Horváth G (2009) Degrees of polarization of reflected light eliciting polarotaxis in dragonflies (Odonata), mayflies (Ephemeroptera) and tabanid flies (Tabanidae). J Insect Physiol 55:1167–1173

Labhart T (1980) Specialized photoreceptors at the dorsal rim of the honeybees compound eye: polarizational and angular sensitivity. J Comp Physiol 141:19–30
Labhart T (1988) Polarization-opponent interneurons in the insect visual system. Nature 331: 435–437
Labhart T, Meyer EP (1999) Detectors for polarized skylight in insects: a survey of ommatidial specializations in the dorsal rim area of the compound eye. Microsc Res Tech 47:368–379
Labhart T, Nilsson DE (1995) The dorsal eye of the dragonfly *Sympetrum*: specializations for prey detection against the blue sky. J Comp Physiol A 176:437–453
Labhart T, Meyer EP, Schenker L (1992) Specialized ommatidia for polarization vision in the compound eye of cockchafers, *Melolontha melolontha* (Coleoptera, Scarabaeidae). Cell Tissue Res 268:419–429
Land MF (1993) Chasing and pursuit in the dolichopodid fly *Poecilobothrus nobilitatus*. J Comp Physiol A 173:605–613
Laughlin S, Mcginness S (1978) Structures of dorsal and ventral regions of a dragonfly retina. Cell Tissue Res 188:427–447
Li DQ, Lim MLM, Land MF (2007) Sex-specific UV and fluorescence signals in jumping spiders. Science 315:481
Lowrey S, Silva LD, Hodgkinson I, Leader J (2007) Observation and modelling of polarized light from scarab beetles. J Opt Soc Am A 24:2418–2425
Lythgoe JN (1979) The ecology of vision. Clarendon, Oxford
Maida TM (1977) Microvillar orientation in retina of a pierid butterfly. Z Naturforsch C 32: 660–661
Marshall NJ (2000a) Communication and camouflage with the same 'bright' colours in reef fishes. Philos Trans R Soc Lond B 355:1243–1248
Marshall NJ (2000b) The visual ecology of reef fish colours. In: Espmark Y, Amundsen T, Rosenquist G (eds) Animal signals: signalling and signal design in animal communication. Tapier, Trondheim, pp 83–120
Marshall NJ, Messenger JB (1996) Colour-blind camouflage. Nature 382:408–409
Marshall NJ, Land MF, King CA, Cronin TW (1991) The compound eyes of mantis shrimps (Crustacea, Hoplocarida, Stomatopoda) 1. Compound eye structure—the detection of polarized light. Philos Trans R Soc Lond B 334:33–56
Marshall J, Cronin TW, Shashar N, Land M (1999) Behavioural evidence for polarisation vision in stomatopods reveals a potential channel for communication. Curr Biol 9:755–758
Mäthger LM, Denton EJ (2001) Reflective properties of iridophores and fluorescent 'eyespots' in the loliginid squid *Alloteuthis subulata* and *Loligo vulgaris*. J Exp Biol 204:2103–2118
Mäthger L, Hanlon R (2007) Malleable skin coloration in cephalopods: selective reflectance, transmission and absorbance of light by chromatophores and iridophores. Cell Tissue Res 329: 179–186
Mäthger LM, Barbosa A, Miner S, Hanlon RT (2006) Color blindness and contrast perception in cuttlefish (*Sepia officinalis*) determined by a visual sensorimotor assay. Vis Res 46:1746–1753
Mäthger LM, Denton EJ, Marshall NJ, Hanlon RT (2009a) Mechanisms and behavioural functions of structural coloration in cephalopods. J R Soc Interface 6:S149–S163
Mäthger LM, Shashar N, Hanlon RT (2009b) Do cephalopods communicate using polarized light reflections from their skin? J Exp Biol 212:2133–2140
Mäthger LM, Bell GRR, Kuzirian AM, Allen JJ, Hanlon RT (2012) How does the blue-ringed octopus (*Hapalochlaena lunulata*) flash its blue rings? J Exp Biol 215:3752–3757
Messenger JB (1977) Evidence that Octopus is colour blind. J Exp Biol 70:49–55
Michelson AA (1911) On the metallic colouring in birds and insects. Philos Mag Lond 21:554–567
Moody MF, Parriss JR (1961) The discrimination of polarized light by octopus: a behavioural and morphological study. Zeitschrift für vergleichende Physiologie 44:268–291
Muheim R, Phillips JB, Deutschlander ME (2009) White-throated sparrows calibrate their magnetic compass by polarized light cues during both autumn and spring migration. J Exp Biol 212:3466–3472

Neville AC, Caveney S (1969) Scarabaeid beetle exocuticle as an optical analogue of cholesteric liquid crystals. Biol Rev Camb Philos Soc 44:531–562
Neville AC, Luke BM (1971) Form optical activity in crustacean cuticle. J Insect Physiol 17: 519–522
Noh H, Liew SF, Saranathan V, Prum RO, Mochrie SGJ, Dufresne ER, Cao H (2010) Double scattering of light from biophotonic nanostructures with short-range order. Opt Express 18: 11942–11948
Parker AR (1999) Invertebrate structural colours. In: Savazzi E (ed) Functional morphology of the invertebrate skeleton. Wiley, New York, pp 65–90
Pignatelli V, Temple SE, Chiou TH, Roberts NW, Collin SP, Marshall NJ (2011) Behavioural relevance of polarization sensitivity as a target detection mechanism in cephalopods and fishes. Philos Trans R Soc B 366:734–741
Prum (1999) The optics of feather color. Biophotonics International 1999 March/April
Prum RO, Cole JA, Torres RH (2004) Blue integumentary structural colours in dragonflies (Odonata) are not produced by incoherent Tyndall scattering. J Exp Biol 207:3999–4009
Pye JD (2010) The distribution of circularly polarized light reflection in the Scarabaeoidea (Coleoptera). Biol J Linn Soc 100:585–596
Reppert SM, Zhu H, White RH (2004) Polarized light helps monarch butterflies navigate. Curr Biol 14:155–158
Roberts NW, Chiou TH, Marshall NJ, Cronin TW (2009) A biological quarter-wave retarder with excellent achromaticity in the visible wavelength region. Nat Photonics 3:641–644
Saidel WM, Lettvin JY, Macnichol EF (1983) Processing of polarized light by squid photoreceptors. Nature 304:534–536
Saidel WM, Shashar N, Schmolesky MT, Hanlon RT (2005) Discriminative responses of squid (*Loligo pealeii*) photoreceptors to polarized light. Comp Biochem Phys A 142:340–346
Schwind R (1984a) Evidence for true polarization vision based on a 2-channel analyzer system in the eye of the water bug, *Notonecta glauca*. J Comp Physiol 154:53–57
Schwind R (1984b) The plunge reaction of the backswimmer *Notonecta glauca*. J Comp Physiol 155:319–321
Sharma V, Crne M, Park JO, Srinivasarao M (2009) Structural origin of circularly polarized iridescence in jeweled beetles. Science 325:449–451
Shashar N, Rutledge PS, Cronin TW (1996) Polarization vision in cuttlefish: a concealed communication channel? J Exp Biol 199:2077–2084
Shashar N, Hanlon RT, Petz AD (1998) Polarization vision helps detect transparent prey. Nature 393:222–223
Shashar N, Hagan R, Boal JG, Hanlon RT (2000) Cuttlefish use polarization sensitivity in predation on silvery fish. Vis Res 40:71–75
Shashar N, Sabbah S, Cronin TW (2004) Transmission of linearly polarized light in seawater: implications for polarization signaling. J Exp Biol 207:3619–3628
Stavenga DG, Kinoshita M, Yang EC, Arikawa K (2001) Retinal regionalization and heterogeneity of butterfly eyes. Naturwissenschaften 88:477–481
Stavenga DG, Wilts BD, Leertouwer HL (2009) Imaging scatterometry and microspectrophotometry of lycaenid butterfly wing scales with perforated multilayers. J R Soc Interface 6: S185–S192
Stavenga DG, Giraldo MA, Leertouwer HL (2010) Butterfly wing colors: glass scales of *Graphium sarpedon* cause polarized iridescence and enhance blue/green pigment coloration of the wing membrane. J Exp Biol 213:1731–1739
Stavenga DG, Leertouwer HL, Marshall NJ, Osorio D (2011a) Dramatic colour changes in a bird of paradise caused by uniquely structured breast feather barbules. Proc R Soc B 278: 2098–2104
Stavenga DG, Wilts BD, Leertouwer HL, Hariyama T (2011b) Polarized iridescence of the multilayered elytra of the Japanese jewel beetle, *Chrysochroa fulgidissima*. Philos Trans R Soc B 366:709–723

Stavenga DG, Matsushita A, Arikawa K, Leertouwer HL, Wilts BD (2012) Glass scales on the wing of the swordtail butterfly *Graphium sarpedon* act as thin film polarizing reflectors. J Exp Biol 215:657–662

Stevens M, Merilaita S (2009) Animal camouflage: current issues and new perspectives. Philos Trans R Soc B 364:423–427

Sweeney A, Jiggins C, Johnsen S (2003) Insect communication: polarized light as a butterfly mating signal. Nature 423:31–32

Talbot CM, Marshall J (2010) Polarization sensitivity in two species of cuttlefish—*Sepia plangon* (Gray 1849) and Sepia mestus (Gray 1849)—demonstrated with polarized optomotor stimuli. J Exp Biol 213:3364–3370

Temple SE, Pignatelli V, Cook T, How MJ, Chiou TH, Roberts NW, Marshall NJ (2012) High-resolution polarisation vision in a cuttlefish. Curr Biol 22:R121–R122

Trujillo-Cenoz O, Bernard GD (1972) Some aspects of the retinal organisation of *Sympyncus lineatus* Loew (Diptera, Dolichopodidae). J Ultrastruct Res 38:149–160

Vorobyev M, Osorio D (1998) Receptor noise as a determinant of colour thresholds. Proc R Soc Lond B 265:351–358

Vukusic P, Hooper I (2005) Directionally controlled fluorescence emission in butterflies. Science 310:1151

Vukusic P, Sambles JR (2004) Photonic structures in biology. Nature 429:680

Vukusic P, Stavenga DG (2009) Physical methods for investigating structural colours in biological systems. J R Soc Interface 6:S133–S148

Vukusic P, Sambles JR, Ghiradella H (2000a) Optical classification of microstructure in butterfly wing-scales. Photon Sci News 6:61–66

Vukusic P, Sambles JR, Lawrence CR (2000b) Structural colour: colour mixing in wing scales of a butterfly. Nature 404:457

Vukusic P, Sambles JR, Lawrence CR, Wootton RJ (2002) Limited-view iridescence in the butterfly *Ancyluris meliboeus*. Proc R Soc Lond B 269:7–14

Vukusic P, Wootton RJ, Sambles JR (2004) Remarkable iridescence in the hindwings of the damselfly *Neurobasis chinensis chinensis* (Linnaeus) (Zygoptera: Calopterygidae). Proc R Soc Lond B 271:595–601

Wehner R (1989) Neurobiology of polarization vision. Trends Neurosci 12:353–359

Wehner R, Bernard GD (1993) Photoreceptor twist: a solution to the false-color problem. Proc Natl Acad Sci 90:4132–4135

Wehner R, Labhart T (2006) Polarisation vision. In: Warrant EJ, Nilsson DE (eds) Invertebrate vision. Cambridge University Press, Cambridge

Wildermuth H (1998) Dragonflies recognize the water of rendezvous and oviposition sites by horizontally polarized light: a behavioural field test. Naturwissenschaften 85:297–302

Wilts B, Pirih P, Stavenga D (2011) Spectral reflectance properties of iridescent pierid butterfly wings. J Comp Physiol A 197:693–702

Wynberg H, Meijer EW, Hummelen JC, Dekkers HPJM, Schippers PH, Carlson AD (1980) Circular polarization observed in bioluminescence. Nature 286:641–642

Zeil J, Hemmi JM (2006) The visual ecology of fiddler crabs. J Comp Physiol A 192:1–25

Zeil J, Hofmann M (2001) Signals from 'crabworld': cuticular reflections in a fiddler crab colony. J Exp Biol 204:2561–2569

Chapter 20
Anthropogenic Polarization and Polarized Light Pollution Inducing Polarized Ecological Traps

Gábor Horváth, György Kriska, and Bruce Robertson

Abstract In the last decade it has been recognized that the artificial polarization of light can have uniquely disruptive effects on animals capable of seeing it and has led to the identification of polarized light pollution (PLP) as a new kind of ecological photopollution. In this chapter we review some typical examples for PLP and the resulting polarized ecological traps. All such polarized-light-polluting artificial surfaces are characterized by strongly and horizontally polarized reflected light attracting positively polarotactic aquatic insects, the larvae of which develop in water or mud, such as aquatic beetles (Coleoptera), water bugs (Heteroptera), dragonflies (Odonata), mayflies (Ephemeroptera), caddisflies (Trichoptera), stoneflies (Plecoptera) and tabanid flies (Tabanidae), for example. We survey here the PLP of asphalt surfaces, solar panels, agricultural black plastic sheets, glass surfaces, black gravestones and the paintwork of black-, red- and dark-coloured cars. We show how

Electronic supplementary material is available in the online version of this chapter at 10.1007/978-3-642-54718-8_20. Colour versions of the black and white figures as well as supplementary figures can also be found under http://extras.springer.com. Videos can be accessed at http://www.springerimages.com/videos/978-3-642-54717-1.

G. Horváth (✉)
Environmental Optics Laboratory, Department of Biological Physics, Physical Institute, Eötvös University, Pázmány sétány 1, 1117 Budapest, Hungary
e-mail: gh@arago.elte.hu

G. Kriska
Group for Methodology in Biology Teaching, Biological Institute, Eötvös University, Pázmány sétány 1, 1117 Budapest, Hungary

Danube Research Institute, Centre for Ecological Research, Hungarian Academy of Sciences, Karolina u't 29, 1113 Budapest, Hungary
e-mail: kriska@ludens.elte.hu

B. Robertson
Division of Science, Mathematics and Computing, Bard College, 30 Campus Drive, Annandale-on-Hudson, NY 23504, USA
e-mail: broberts@bard.edu

G. Horváth (ed.), *Polarized Light and Polarization Vision in Animal Sciences*, Springer Series in Vision Research 2, DOI 10.1007/978-3-642-54718-8_20,

the maladaptive attractiveness (PLP) of certain artificial surfaces to polarotactic insects can be reduced or eliminated. We consider how birds, spiders and bats exploit polarotactic insects trapped by different sources of PLP. We deal with the phenomenon that the vertically polarized mirror image of bridges seen at the river surface can deceive swarming polarotactic mayflies, which is an atypical kind of PLP. We explain why strongly polarizing black burnt-up stubble fields do not attract aquatic insects, which is an example for a horizontal, black polarizing surface that does not induce PLP and thus is an exception proving the rule. Finally, we show that phototaxis and polarotaxis together have a more harmful effect on the dispersal flight of night-active aquatic insects than they would have separately. This provides experimental evidence for the synergistic interaction of phototaxis and polarotaxis in these insects.

20.1 Polarized Light Pollution and Polarized Ecological Traps

Illumination of the night sky by electric lights, as in urban areas, that interferes with astronomical observation is known as 'astronomical light pollution' (Riegel 1973; Upgren 1996; Wilson 1998; Cinzano et al. 2001). This and other artificial light that has the effect of disrupting biological systems is known as 'ecological light pollution' (ELP) (Verheijen 1958, 1985; Longcore and Rich 2004, 2006; Rich and Longcore 2006). By appearing at atypical locations or times, artificial light can disorient, attract or repulse animals, disrupting critical behaviours and negatively impacting their survival or reproductive success (Rich and Longcore 2006, p. 3). ELP includes sky glow, direct glare, chronically increased illumination and temporary, unexpected fluctuations in lighting associated with lighted structures (e.g. bridges, buildings and towers), street and security lights and vehicle lights (Rich and Longcore 2006, pp. 3–4). The documented and the possible ecological consequences of all these artificial night lighting were comprehensively summarized in the monograph edited by Rich and Longcore (2006).

Attraction (positive phototaxis) or repulsion (negative phototaxis) of animals by the spatiotemporally enhanced intensity of light relative to the dark environment defines a major axis of animal responses to ELP, and researchers have historically focused on understanding animal movement in relation to the intensity and/or colour of artificial light. More recently, however, it has been recognized that the artificial polarization of light can have uniquely disruptive effects on animals capable of seeing it and has led to the identification of 'polarized light pollution' (PLP) as a new kind of ecological photopollution (Horváth et al. 2009). Two typical examples are shown in Fig. 20.1. PLP is characterized by strongly (i.e. with high degrees of linear polarization) and horizontally polarized light reflected from smooth (shiny) artificial surfaces (Figs. 20.2 and 20.3) having negative fitness on polarotactic aquatic insects which generally include all insect taxa whose larval stages require water bodies to mature into adults: aquatic beetles (Coleoptera), water bugs (Heteroptera), dragonflies (Odonata), mayflies (Ephemeroptera), caddisflies (Trichoptera), stoneflies (Plecoptera) and tabanid flies (Tabanidae), for example (Fig. 20.4).

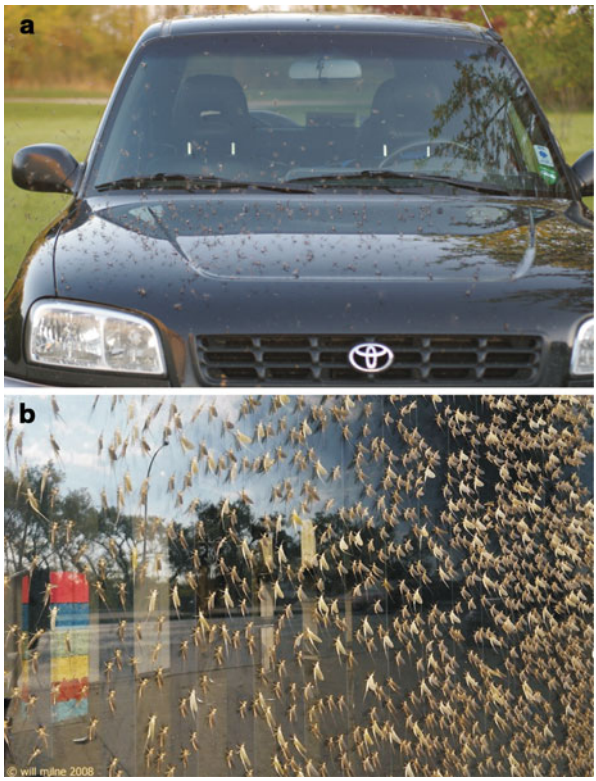

Fig. 20.1 Two typical examples for polarized light pollution. (**a**) Mayflies attracted to a shiny black car (photograph: courtesy of Rebecca Allen). (**b**) Mayflies landed on a vertical glass pane (photograph: courtesy of Will Milne)

Early understanding of the importance of polarized light to aquatic insects came from the research of Schwind (1983a, b, 1984a, b, 1985a, b). He discovered that the backswimmer, *Notonecta glauca*, detects water by means of the horizontally polarized light reflected from the water surface (Gál et al. 2001a), rather than by the intensity or colour of water-reflected light or by the glittering or mirroring of the water surface. In the ventral eye region of *Notonecta*, Schwind et al. (1984) found ultraviolet-sensitive photoreceptors with horizontal and vertical microvilli being highly sensitive to horizontally and vertically polarized light (Schwind 1983b). These orthogonally polarization-sensitive photoreceptors are able to determine whether the direction of polarization of light from the optical environment is horizontal or not. In *Notonecta* an exactly or nearly horizontally polarized light stimulus elicits a typical plunge reaction (Schwind 1984b). This attraction of *Notonecta* to horizontally polarized light is called 'positive polarotaxis'.

As a general rule, females of most aquatic insect taxa (e.g. Ephemeroptera, Odonata, Plecoptera, Trichoptera) must return to water to lay their eggs. Water bodies also often serve as rendezvous for both sexes. Orientation in aquatic insects is predominantly visual, and the eye of many aquatic insects is sensitive to the polarization of light in the visible or ultraviolet spectral ranges (Schwind 1991, 1995). These insects find their habitat largely on the basis of horizontally polarized light reflected from the water surface (Schwind and Horváth 1993; Horváth 1995;

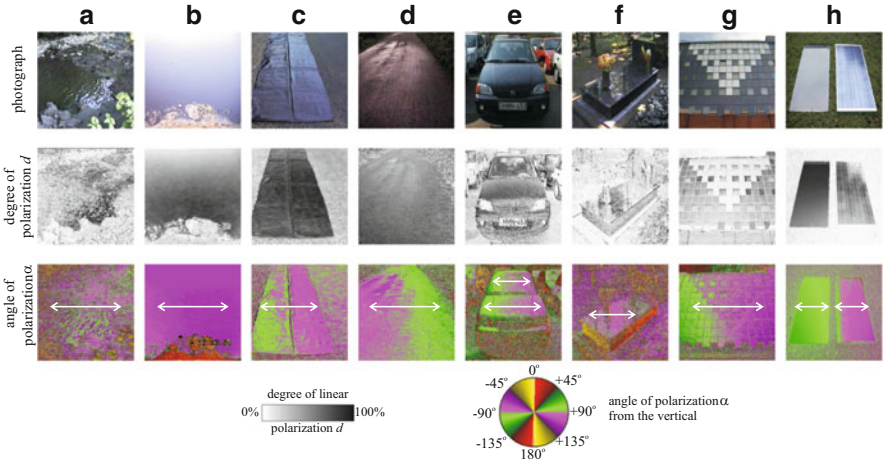

Fig. 20.2 Photographs and patterns of the degree of linear polarization d and the angle of polarization α (clockwise from the vertical) of a water surface (**a**) and different artificial surfaces (**b**–**h**) causing polarized light pollution. (**a**) Dark waterbody. (**b**) Crude oil lake in the desert of Kuwait. (**c**) *Horizontal black plastic sheet* on an asphalt road. (**d**) Dry asphalt road. (**e**) Black car. (**f**) Polished black gravestone. (**g**) Windows with *grey/black glass* ornamentation. (**h**) Two horizontal photovoltaic solar panels on the grassy ground. In the α-patterns *double-headed arrows* show the local direction of polarization [after Fig. 3 on page 319 of Horváth et al. (2009)]

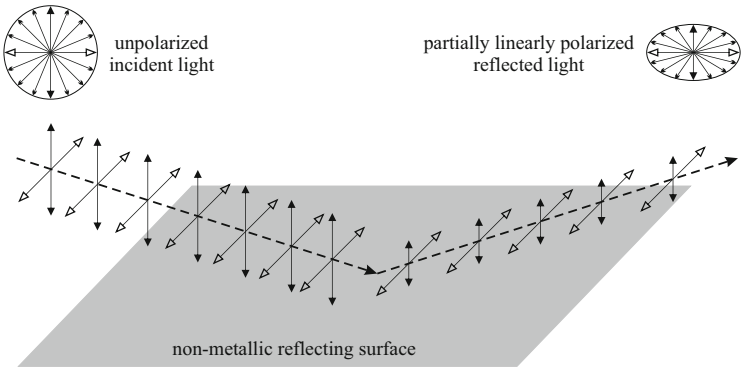

Fig. 20.3 After reflection from a non-metallic (dielectric) surface, unpolarized light becomes partially linearly polarized. After reflection the electric field vector is shorter in the plane of reflection (*double-headed arrows* with *black heads*) than in the perpendicular plane (*double-headed arrows* with *open heads*) [after Fig. 2 on page 318 of Horváth et al. (2009)]

Gál et al. 2001a). Consequently, polarization is detected in the region of the electromagnetic spectrum, which is characteristic of their preferred habitat (Schwind 1995).

Depth, turbidity, transparency, colour, surface roughness of the water and substratum composition as well as the illumination strongly influence the reflection–polarization characteristics of water bodies (Horváth and Varjú 2004;

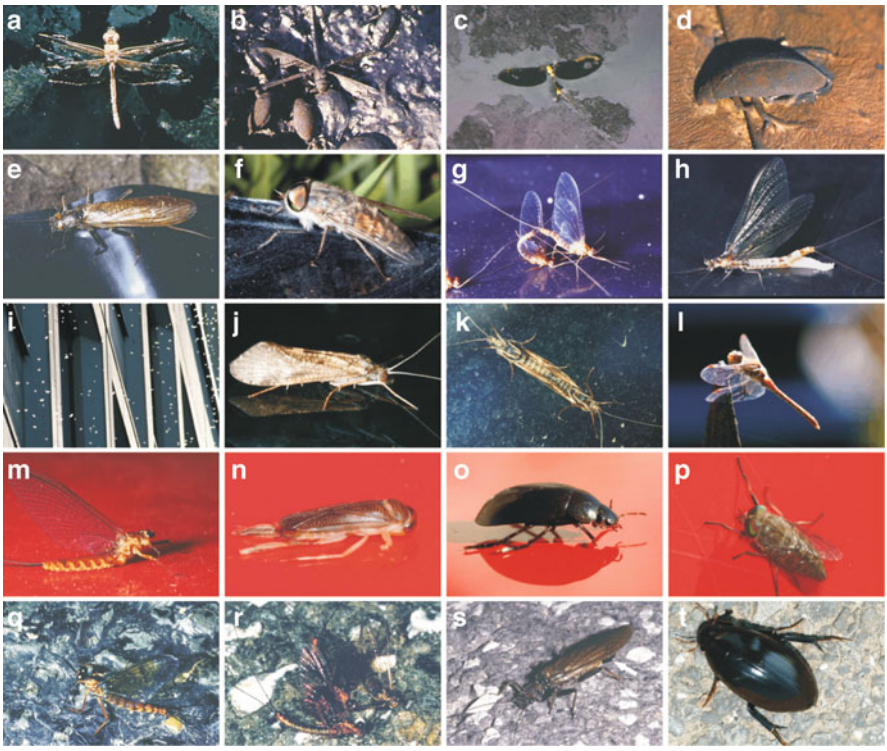

Fig. 20.4 Polarotactic aquatic insects and insects associated with water deceived by and attracted to different sources of polarized light pollution (photographs b-t taken by György Kriska). *Row 1*: Some typical representatives of insects trapped by a crude oil lake in the desert of Kuwait (**a**) and a waste oil lake in Budapest, Hungary (**b**–**d**). **a**: Hawker dragonfly (Aeshnidae) (courtesy of Jochen Zeil). **b**: An emperor dragonfly (*Anax imperator*) and scavenger beetles (Hydrophilidae). **c**: A mayfly (*Cloeon dipterum*). **d**: A great silver diving beetle (*Hydrophilus piceus*). *Row 2*: Water insects landed on *horizontal shiny black dry plastic sheets* used in agriculture. **e**: A female large stonefly (*Perla abdominalis*). **f**: A tabanid fly (Tabanidae). **g**: Copulating mayflies (*Rhithrogena semicolorata*). **h**: A female mayfly (*Ephemera danica*) laying her eggs on the *black plastic sheet*. *Row 3*: **i**: Mass swarming of *Hydropsyche pellucidula* caddisflies (*white spots*) in front of the vertical glass surfaces of a building on the bank of the river Danube in Budapest. **j**: An *H. pellucidula* landed on a pane of glass. **k**: A copulating pair of *H. pellucidula* on a glass pane. **l**: A male dragonfly (*Sympetrum* sp.) perching near a polished black tombstone. *Row 4*: Insects associated with water on the dry roof of a red car. **m**: A mayfly (Heptageniidae). **n**: A water bug (*Sigara striata*). **o**: A scavenger beetle (*Hydrochara caraboides*). **p**: A tabanid fly (Tabanidae). *Row 5*: Aquatic insects landed on dry asphalt roads. **q**: A male mayfly (*Epeorus assimilis*). **r**: Copulating mayflies (*Rhithrogena semicolorata*). **s**: Oviposition by a female large stonefly (*Perla abdominalis*), whose black egg batch at the tip of her abdomen is shown by the *tip of a white arrow*. **t**: A great silver diving beetle (*Hydrophilus piceus*)

Chap. 16). In this way, polarized light reflected by water provides important information on the quality of freshwater habitats for polarotactic insects and can aid the orientation of these insects from a distance when other cues

(e.g. atmospheric humidity, dimension and shape of the waterbody, undulation of the water surface, water plants on the surface and the shore, temperature and odour) are still ineffective (Fig. 20.2a, and see Chaps. 5 and 16).

Following Schwind's (1985a, b, 1991, 1995) finding that aquatic bugs and beetles are polarotactic, other studies (Kriska et al. 1998, 2006a, 2007, 2008; Wildermuth 1998; Horváth et al. 1998, 2007, 2008; Bernáth et al. 2001b; Wildermuth and Horváth 2005; Csabai et al. 2006; Lerner et al. 2008; Horváth et al. 2011) found that dragonflies, mayflies, tabanid flies, stoneflies, chironomids and caddisflies also exhibit positive polarotaxis when searching for water. To date, more than 300 polarotactic aquatic insect species are known that recognize their aquatic habitat by positive polarotaxis (Horváth and Kriska 2008; see also Chap. 5). Consequently, there are a remarkably broad array of water-seeking insect taxa that we know, and are predicted to be, susceptible to being deceived by and attracted to artificial surfaces that reflect highly and horizontally polarized light (i.e. PLP sources) (Fig. 20.4). This visual ecological phenomenon is the major reason for PLP, the physical, behavioural and ecological bases for which we will describe in this chapter.

Physical principles dictate the properties of both artificial and natural polarizers. According to the rule of Umow (1905), the darker a surface in a given part of the spectrum, the higher the degree of linear polarization d of light reflected from it. Since diffuse reflection from rough (matte) surfaces results in depolarization, the smoother (the shinier) a surface, the higher the d of reflected light. Since the direction of polarization of light reflected from smooth dielectric materials is always perpendicular to the plane of reflection, if this plane is exactly or nearly vertical, the reflected light is exactly or approximately horizontally polarized (Fig. 20.3). From these it follows that:

- Smooth and black artificial surfaces with exactly/nearly vertical plane of reflection mirror strongly and exactly/nearly horizontally polarized light at the Brewster angle.

The higher the d of light and the less deviated its direction of polarization from the horizontal, the more attractive it is to polarotactic aquatic insects (Horváth and Varjú 2004). Consequently:

- Smooth and black artificial surfaces with exactly/nearly vertical plane of reflection are very attractive to polarotactic insects.

In this chapter we formulate and develop the following visual ecological thesis: Smooth and dark artificial surfaces with exactly/nearly vertical plane of reflection are attractive to polarotactic aquatic insects and thus constitute polarized ecological traps for these animals, thus representing important and deleterious sources of PLP. In Sects. 20.2–20.13 we review the experimental evidence supporting this thesis. Using theoretical calculations (Schwind and Horváth 1993; Horváth 1995; Horváth and Pomozi 1997) and imaging polarimetry (Horváth and Varjú 1997, 2004; Gál et al. 2001b; Mizera et al. 2001; Horváth et al. 2002), we compare the reflection–polarization characteristics of water bodies and artificial reflectors. Excluding astronomical photopollution, Table 20.1 summarizes the major characteristics of the conventional ecological photopollution and the PLP.

Table 20.1 Major characteristics of conventional ecological photopollution and polarized light pollution

Characteristics	Conventional ecological photopollution	Polarized light pollution
Source of photopollution	Artificial night lights: sky glow, lighted structures, streetlamps, security lights, vehicle headlights, fishing boats, flares on hydrocarbon platforms, lights on undersea research vessels	Strongly and horizontally polarized light reflected from artificial surfaces: oil lakes; asphalt roads; black plastic sheets in agriculture; glass surfaces (e.g. buildings); black-, red-, dark-coloured car paintwork; black gravestones; photovoltaic panels; solar panels
Extent of photopollution	Global	Global
Cue(s) eliciting the photoreaction of animals	Intensity and colour of light	Horizontal linear polarization of light
Time of day of photopollution	Between dusk and dawn	Both day and night
Directly or indirectly affected animals	Night-active animals	Polarotactic aquatic insects and their predators (spiders, birds, bats)
Effects of photopollution	– Attraction/repulsion by lights – Disturbances of circadian rhythm – Disruption of physiological processes (moult, hormone production) – Increased deaths due to collisions with objects – Alteration of seasonal patterns of behaviour – Misdirected orientation and migration – Altered foraging pattern – Interference with intra/interspecific visual communication – Altered nest site choice – Desynchronization of mating – Disturbance of community interactions (e.g. increased competition and predation risk)	– Attraction of polarotactic aquatic insects to horizontally polarized light – Mortality due to dehydration – Mortality of the eggs laid on artificial polarizers due to dehydration – Disruption of water-associated behaviour elicited by horizontally polarized light – Inability to orient towards water and migrate between water bodies – Increased mortality associated with congregation of predators (spiders, birds, bats) near concentrations of insects on artificial polarizers

Man-made objects associated with development activities have resulted in the introduction of different sources of PLP (Figs. 20.1 and 20.2) into and around natural habitats. Throughout most of the history of the planet Earth, the primary natural source of horizontally polarized light has been the flat surface of water bodies. The degree of polarization d is higher if light is reflected from water bodies with a darker-coloured substrate and if that reflection takes place at about 37° from the horizontal, also known as the Brewster angle (Horváth and Varjú 2004). PLP is

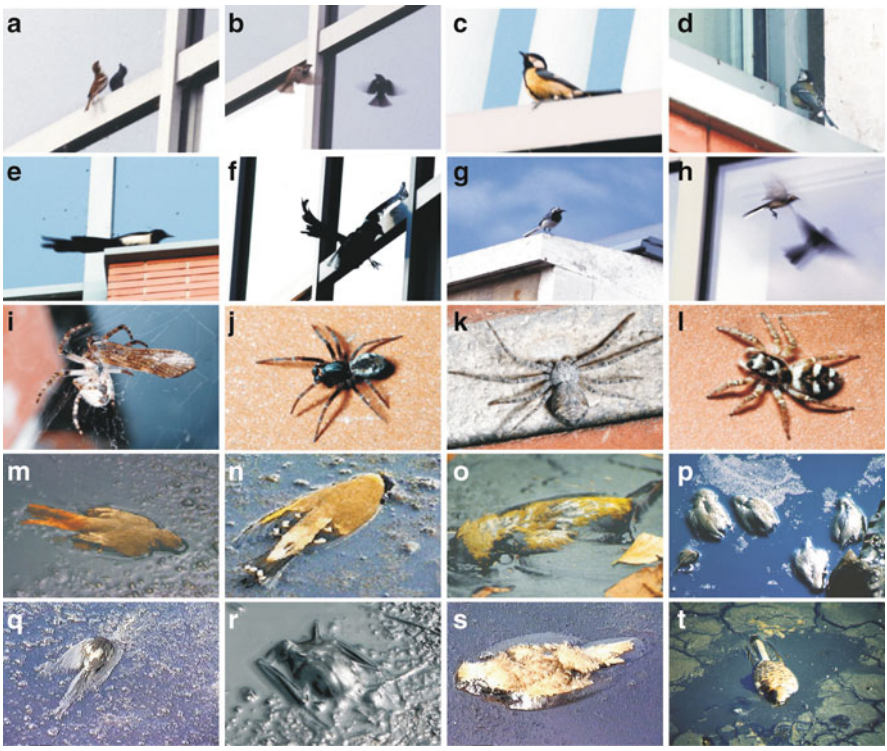

Fig. 20.5 Predators feeding on the polarotactic insects attracted to two different sources of polarized light pollution (photographs taken by György Kriska and Gábor Horváth). *Rows 1–2*: Urban birds feeding on the mass-swarming caddisflies, *Hydropsyche pellucidula*, attracted to vertical glass surfaces. **a–b**: A male house sparrow (*Passer domesticus*) hunting caddisflies at a window. **c**: A great tit (*Parus major*) standing on a window frame. **d**: A *P. major* following caddisflies with attention. **e**: A European magpie (*Pica pica*) on an edge of a building. **f**: A *P. pica* on wing capturing caddisflies from a glass pane. **g**: A white wagtail (*Motacilla alba*) perching on a protrusion of a building. **h**: A hovering wagtail gathering caddisflies from a glass pane. *Row 3*: Spiders on the wall of a building where caddisflies (*H. pellucidula*) swarmed. **i**: An *Araneus umbraticus* feeding on a caddisfly captured by its cobweb. **j**: A long-jawed spider (Tetragnathidae) on a brick. **k**: A crab spider (Thomisidae) between two bricks. **l**: A jumping spider (*Salticus zebraneus*) on a brick. *Row 4*: Carcasses of insectivorous vertebrates lured by polarotactic insects and trapped by the waste oil lake in Budapest. The insects were attracted to the polarized-light-polluting oil surface. **m**: A black redstart (*Phoenicurus ochruros*). **n**: A European goldfinch (*Carduelis carduelis*). **o**: A yellowhammer (*Emberiza citrinella*). **p**: A flock of European greenfinches (*Carduelis chloris*). **q**: A European magpie (*Pica pica*). **r**: A bat (Chiroptera). **s**: A long-eared owl (*Asio otus*). **t**: A kestrel (*Falco tinnunculus*)

mainly a by-product of the human architectural, building, industrial and agricultural technology, and it may allow to function feeding webs composed of polarotactic insects and their predators, such as spiders, birds and bats, for example (Fig. 20.5).

The phenomenon of PLP is global and new in an evolutionary sense, having increased rapidly only over the last decades, following the spread of strongly and

horizontally polarizing artificial surfaces such as oil lakes and open-air oil reservoirs, asphalt roads, plastic sheets, glass surfaces and cars, for example (Figs. 20.1 and 20.2). The mortality associated with PLP may threaten populations of endangered aquatic insect species. Aquatic insects attracted to strongly and horizontally polarizing dry artificial surfaces may perish due to dehydration or may oviposit onto these surfaces where eggs universally fail to survive (Wyniger 1955; Horváth et al. 1998, 2007, 2009, 2010a,b; Kriska et al. 1998, 2006a, 2007, 2008; Wildermuth 1998, 2007; Stevani et al. 2000a,b; Bernáth et al. 2001b; Günther 2003; Horváth and Varjú 2004; Csabai et al. 2006; Horváth and Kriska 2008; Málnás et al. 2011). Within ecological and evolutionary science, such cases in which rapid environmental changes lead organisms to prefer the worst available habitat are known as ecological traps (Dwernychuk and Boag 1972; Schlaepfer et al. 2002; Fletcher et al. 2012). In other words, artificial polarizers represent evolutionarily novel objects, the polarization characteristics of which mimic evolved behavioural cues that have historically indicated the presence of water but which now lead them to experience reproductive failure and reduced survival. Furthermore, because this kind of maladaptive behaviour is predicted to lead to population declines in affected species (Kokko and Sutherland 2001), ecological traps created by PLP are of potentially high conservation concern for aquatic insect populations and with potential to impact populations of fish and other predatory organisms that rely upon aquatic insects as a food source (Robertson et al. 2013).

PLP can occur not only in daytime but also at night, if moonlight or city light (e.g. sky glow, streetlamps) is reflected from polarized-light-polluting surfaces. In addition, vulnerability to PLP (based on positive polarotaxis) could be enhanced through synergy with conventional photopollution (based on positive phototaxis) associated with artificial night lighting. PLP could also be influenced by lunar cycles, especially in rural environment, where artificial night lighting is rare or lacking. It is important to determine and monitor the sources of PLP in order to minimize and/or replace them by artificial surfaces which are ‘aquatic insect friendly’. Since many human developments with numerous polarized-light-polluting artificial surfaces are near water bodies (Marsh and Grossa 2002), the aquatic insects living in/at lakes, rivers, ponds and streams are all subject to PLP (Fig. 20.4). Because aquatic insects are critically important as members of food webs in aquatic ecosystems, adverse effects of PLP on these animals could have serious ecological consequences.

Flight to horizontally polarized light reflected from artificial surfaces could disturb the ecology of aquatic insects and often can lead to high mortality of the adults and/or the eggs laid onto these polarized-light-polluting surfaces. Polarotactic aquatic insects frequently are not able to escape from the source of PLP. We call this behaviour the ‘polarization captivity effect’ *sensu* Eisenbeis (2006), which culminates in the death of insects due to dehydration and exhaustion. The migration, dispersal, mating and reproduction of aquatic insects can also be disturbed by sources of PLP encountered in their long-distance flight paths. We call this the ‘polarization crash barrier effect’ *sensu* Eisenbeis (2006) because of the interruption of movement across the landscape. Aquatic insects are also vulnerable to normal (unpolarized) artificial lights: Scheibe (2000), for example, documented

that streetlamps have a long-distance effect for light-susceptible mayflies and caddisflies emerging from a small mountain stream. The night-time attraction of these insects to lamps is so strong that if there were a row of streetlamps along a stream, a species could become locally extinct in a short time. This extinction can only be accelerated by PLP.

In Sects. 20.2–20.13 we review typical cases in which anthropogenic sources of polarized light affect the behaviour and fitness of polarization-sensitive animals, directly or indirectly, and discuss the potential for PLP to influence ecological interactions with other species. The knowledge on PLP slowly penetrates also into the education (e.g. Horváth 2012).

20.1.1 Suggested Remedies of PLP

Within each section we also discuss specific ways to eliminate PLP associated with various anthropogenic objects or mitigate its impacts on populations of polarotactic organisms. Because a summary of these recommendation will be particularly useful to wildlife conservationists and concerned landscape planners, road and building designers and policymakers, we summarize those recommendations here:

1. Make illuminated reflecting surfaces as rough as possible: The rougher a surface, the lower the degree of polarization d of reflected light. If the surface roughness is so large that d of reflected light is lower than the threshold d^* of polarization sensitivity of a polarotactic insect, then the surface is unattractive to this insect, because it does not perceive the polarization of reflected light.
2. Align the concerned reflector in such a way that the plane of reflection is never vertical. This should help ensure that the direction of polarization of reflected light is not horizontal which is most attractive to polarotactic insects.
3. Make the concerned surface as bright (closer to white) as possible, since due to the rule of Umow (1905) such surfaces reflect only weakly polarized (with low degrees of polarization d) or even unpolarized ($d = 0$) light.
4. Split the concerned surface into small fragments through an appropriate white grid pattern (see Sects. 20.3 and 22.3).

Intuitively, it is likely that man-made structures that produce high levels of PLP will probably attract fewer insects when they are located more distantly from natural water bodies like lakes and streams where aquatic insects are most abundant. However, anecdotal evidence suggests that artificial polarizers even miles from water bodies can attract aquatic insects *en masse*. Moreover, our understanding of the breadth of nonaquatic nocturnally active insects that use sky polarization for navigation and that may be attracted even by horizontally polarized nocturnal light pollution associated with artificial polarizers is lacking. Consequently, more specific and robust recommendations about how to disarm ecological traps associated with PLP cannot yet be made. Reducing skyward-directed light pollution via shading or other methods that direct night lighting downwards may have the effect of increasing PLP upon artificial polarizers. However, this will only

occur where night lighting falls upon man-made objects with the aforementioned shiny and dark characteristics, and such pollution can be mitigated if care is given to the placement and/or orientation of nocturnal lighting such that it does not fall upon highly polarizing surfaces.

20.1.2 Generalization and Extension of PLP

The term of polarized light pollution can be generalized by extending it to all natural sources of polarized light which are changed naturally or artificially in such a way that this change disturbs the behaviour of polarization-sensitive animals using this polarized visual cue. Here we mention examples for a natural (induced by a total solar eclipse) and a man-made (induced by forest fires) change of sky polarization that can be considered as generalized cases of PLP:

1. Not only the celestial distribution of intensity and colour but also the pattern of both the degree d and the angle α of linear polarization of skylight changes drastically during the totality of solar eclipses due to the considerably altered illumination conditions (Pomozi et al. 2001; Horváth et al. 2003; Sipőcz et al. 2008; see Sect. 18.7). d of light from the eclipsed sky is usually considerably reduced, and if it becomes lower than the threshold d^* of polarization sensitivity of a given species navigating on the basis of sky polarization, the animal can disorient. Furthermore, even if $d > d^*$ during totality, the α-pattern of the eclipsed sky differs so greatly from that of the normal sky (Pomozi et al. 2001; Horváth et al. 2003; Sipőcz et al. 2008) that polarization-sensitive animals may disorient when they try to navigate by means of this altered celestial α-pattern. Hence, the temporally altered polarization pattern of the eclipsed sky (occurring a few times every year along huge elongated areas on the Earth's surface) is a special source of PLP of natural origin. Bernáth et al. (2001a) suggested that one of the reasons of the odd disorientated behaviour of honeybees (*Apis mellifera*) observed during a total solar eclipse (Baldavári 2001; Szentkirályi and Szalay 2001) may be the unnatural polarization pattern of the eclipsed sky.
2. The polarization pattern of the smoky sky during forest fires is more or less anomalous relative to that of the normal sky (Hegedüs et al. 2007; see also Sect. 18.6). Especially d of skylight is drastically reduced because of depolarization due to multiple scattering of sunlight on smoke particles. If d of light from a smoky sky is dropped below the threshold d^* of polarization sensitivity of animals using sky polarization for orientation, they can be disoriented. Hegedüs et al. (2007) suggested that the disorientation of certain insects observed by Johnson et al. (2005) under smoky skies during the forest fire season in August 2003 in British Columbia was the consequence of the anomalously low degrees of sky polarization caused by the forest fire smoke. Thus, generally, the unnatural celestial polarization pattern induced by various natural or man-made fires is another source of PLP.

Fig. 20.6 Examples of aquatic insects attracted to and landed on a dry asphalt road in the immediate vicinity of a mountain creek near Budapest, Hungary, in June 1997 (**a**–**c**) and 2008 (**d**–**i**). (**a**) A male *Rhithrogena semicolorata* mayfly. (**b**) A female *Epeorus assimilis* mayfly. (**c**) A female and two male *Epeorus assimilis* attempting to mate. (**d**) A male *Epeorus assimilis*. (**e**) A male *Ephemera danica* mayfly. (**f**) A female *Perla abdominalis* stonefly. (**g**–**i**) Carcasses of female *Perla abdominalis* run over by cars [after Fig. 1 on page 2 of Horváth et al. (2010b); photographs taken by György Kriska]

20.2 Polarized Light Pollution of Asphalt Surfaces

20.2.1 Insects Attracted to Asphalt Roads

Ladócsy (1930) observed that mayflies (*Palingenia longicauda*) swarming above the river Tisza in Hungary were attracted to a wet asphalt road running parallel to the river. Puschnig (1926), Bromley (1928), Fraser (1936) and Whitehouse (1941) reported that different dragonfly species patrolled along dry asphalt roads instead of rivers and showed a stereotypical water-touching behaviour on the asphalt surface. Kriska et al. (1998) observed that near sunset mayflies swarmed, mated above and landed on a dry asphalt road running in the immediate vicinity of their emergence site, a mountain streamlet (Fig. 20.6a–e). After copulation females laid their eggs on the dry asphalt surface instead of ovipositing them on the water surface. Near mountain creeks, female stoneflies with their egg batches were also often seen on the asphalt road (Fig. 20.6f–i). Collectively, these observations suggest that mayflies and stoneflies were apparently deceived by and attracted to the dry asphalt surface.

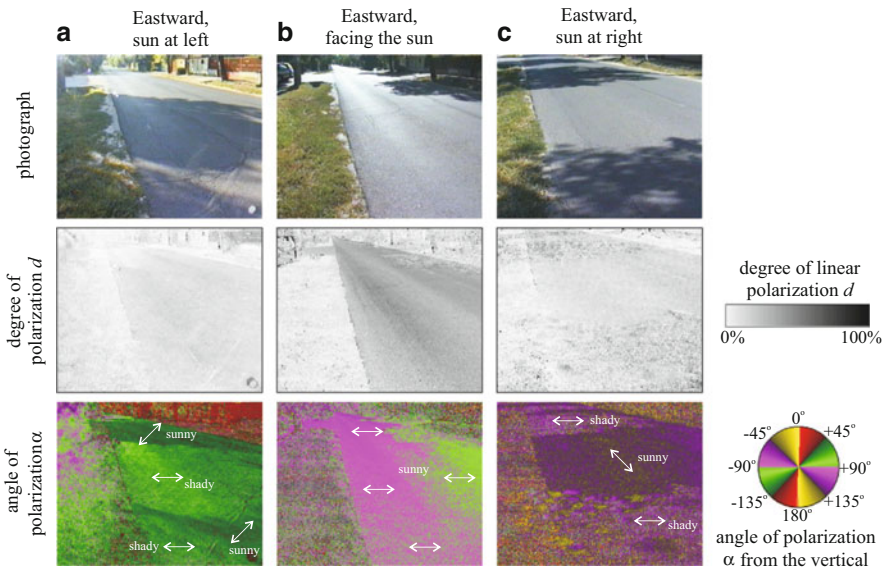

Fig. 20.7 Reflection–polarization patterns of a sunlit, partly shady dry asphalt road running eastward measured in the green (550 nm) part of the spectrum for three different solar directions. The angle of elevation of the polarimeter's optical axis was −20° from the horizontal. In the *lowermost row double-headed arrows* show the local direction of polarization of asphalt-reflected light. (**a**) The sun was shining from the *left-hand side*. (**b**) The sun was shining in the face of the polarimeter. (**c**) The sun was shining from the *right-hand side* [after Fig. 6 on page 18 of Horváth et al. (2010b)]

Kriska et al. (1998) revealed the reasons for this behaviour: In multiple-choice field experiments, they showed that mayfly species detect water by means of the horizontal polarization of water-reflected light and thus possess positive polarotaxis, i.e. they are attracted to horizontally polarized light. Imaging polarimetry revealed that when mayflies swarm at sunset, asphalt surfaces mimic a highly and horizontally polarizing water surface to water-seeking mayflies. They found that the darker and smoother the asphalt surface, the greater is its attractiveness to polarotactic mayflies, because it can reflect and polarize the incident light in such a way that the reflected light becomes a supernormal stimulus for water-seeking mayflies in comparison to the light reflected from water. The highly and horizontally polarizing asphalt roads with relatively homogeneous distributions of the degree and direction of polarization of reflected light (Figs. 20.7, 20.8, 20.9 and 20.10) are much more attractive to polarotactic mayflies than water surfaces.

The eggs laid by mayflies and stoneflies on dry asphalt roads inevitably perish within about an hour due to dehydration. These egg batches and the adults that lay them are commonly crushed by cars (Fig. 20.6g–i) and even eaten by predatory birds such as white and yellow wagtails (*Motacilla alba* and *M. flava)* that systematically search asphalt surfaces for prey (Horváth et al. 2010b). These birds either chased and captured the insects flying above the asphalt or picked up the insects landed on the

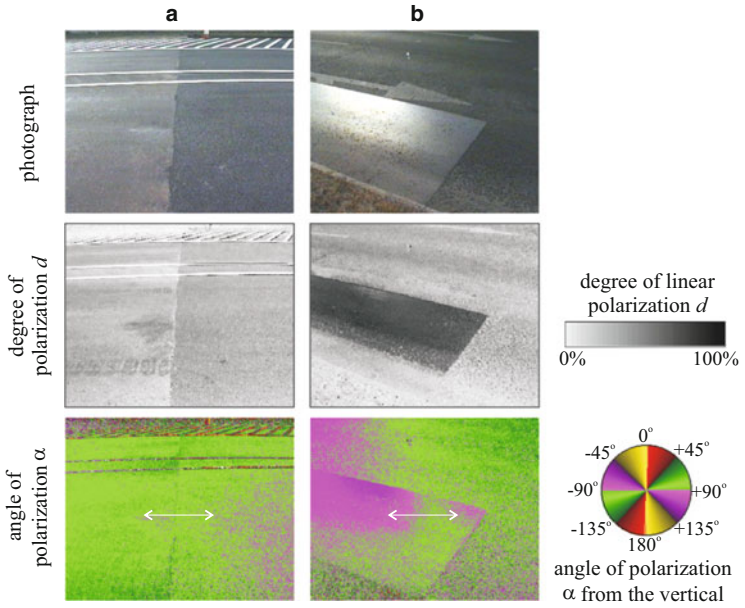

Fig. 20.8 Reflection–polarization patterns of two different sunlit dry asphalt surfaces measured in the green (550 nm) part of the spectrum. In both cases the polarimeter viewed towards the solar meridian, and the angle of elevation of its optical axis was -35° from the horizontal. In the *lowermost row double-headed arrows* show the local direction of polarization of asphalt-reflected light. (**a**) The *left half* of the asphalt surface was brighter than the *right one*, because the *left*/*right half* was composed of old/new asphalt. On the *top part* of the photograph, *white guidelines* on the road are visible. (**b**) Here a *rectangular part* of the old rough (matte) asphalt surface was replaced by new smooth (shiny) asphalt. On the *top* and *middle parts* of the photograph, *white arrows* as guide marks on the road are visible [after Fig. 8 on page 20 of Horváth et al. (2010b)]

asphalt or their carcasses, themselves sometimes becoming victims of traffic. This behaviour of wagtails on asphalt roads was quite similar to that observed on huge shiny black plastic sheets laid onto the ground and used frequently in agriculture (Bernáth and Horváth 1999; Bernáth et al. 2001c; see Sect. 20.4).

20.2.2 Reflection–Polarization Characteristics of Asphalt Surfaces

Horváth et al. (2010b) studied the polarizing characteristics of asphalt surfaces as functions of the surface features (roughness, darkness, painted with white striates or not), the illumination conditions (sunny or shady) and the direction of view relative to the solar meridian. They obtained the following typical characteristics:

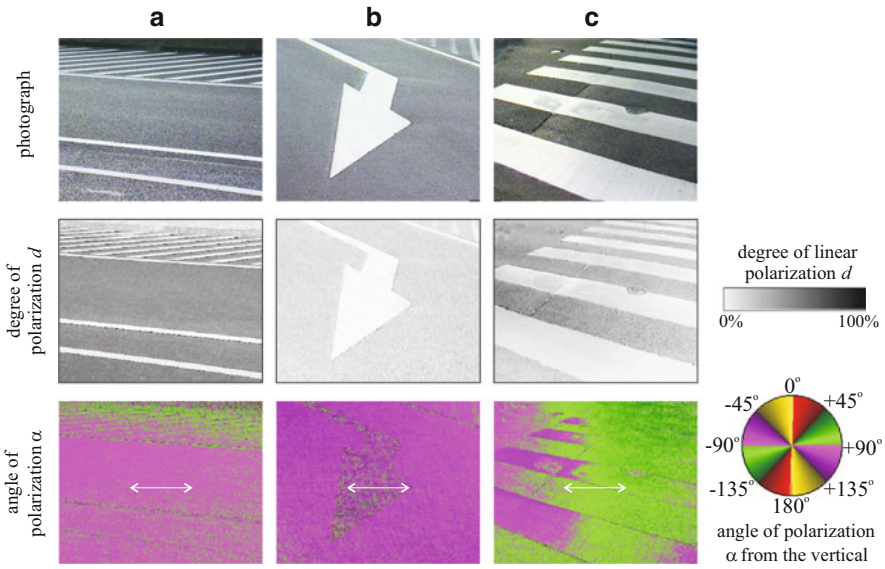

Fig. 20.9 Reflection–polarization patterns of three different sunlit dry asphalt surfaces measured in the green (550 nm) part of the spectrum. The polarimeter viewed towards the solar meridian, and the angle of elevation of its optical axis was −35° from the horizontal. In the *lowermost row double-headed arrows* show the local direction of polarization of asphalt-reflected light. (**a**) Asphalt with *white guidelines*. (**b**) Asphalt with a *white arrow guide mark*. (**c**) Asphalt with *white zebra stripes* [after Fig. 9 on page 21 of Horváth et al. (2010b)]

1. The direction of polarization of light reflected from rough sunlit asphalt surfaces is always perpendicular to the plane of reflection/scattering determined by the sun, the observer and the point observed. Since this plane is usually tilted relative to the horizontal asphalt surface, the direction of polarization of light reflected/scattered (returned) by sunlit asphalt surface is generally oblique with respect to the surface (Fig. 20.7a, c). The light returned by sunlit asphalt is (exactly or nearly) horizontally polarized only, if the asphalt is viewed towards the solar or antisolar meridian (Figs. 20.7b and 20.8).
2. The direction of polarization of light reflected from shady asphalt surfaces (illuminated by skylight only) is always (exactly or nearly) horizontally polarized (Fig. 20.7a, c).
3. The darker/brighter an asphalt surface, the higher/lower the degree of polarization of asphalt-reflected light (Figs. 20.8 and 20.9).
4. The rougher/smoother an asphalt surface, the lower/higher the degree of polarization of asphalt-reflected light (Figs. 20.8 and 20.10).
5. The degree of polarization of light reflected from wet asphalt is higher than that reflected from dry one (Fig. 20.10).

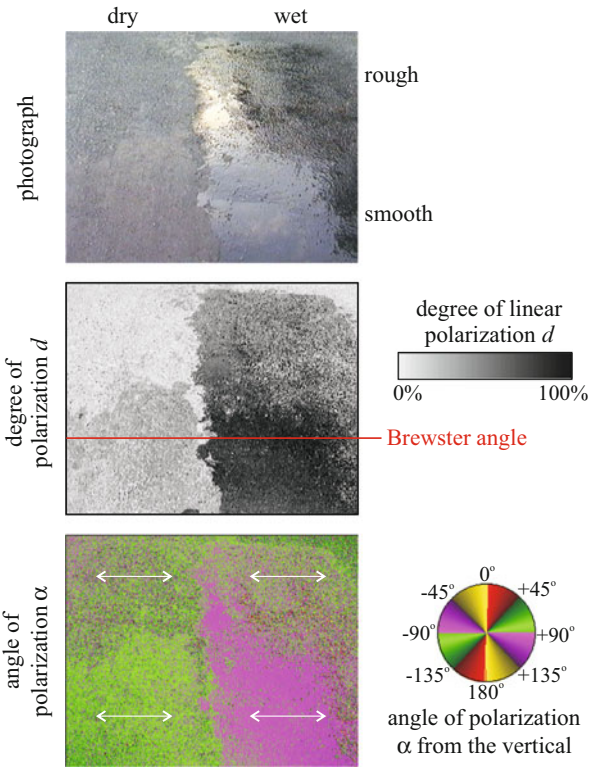

Fig. 20.10 Reflection–polarization patterns of an asphalt surface with four different characteristics (*top left quarter*, dry and rough; *top right quarter*, wet and rough; *bottom left quarter*, dry and smooth; *bottom right quarter*, wet and smooth) measured in the green (550 nm) part of the spectrum. The angle of elevation of the polarimeter's optical axis was −35° from the horizontal, and the asphalt was illuminated by skylight at sunset. In the *lowermost row double-headed arrows* show the local direction of polarization of asphalt-reflected light. Directions of view corresponding to the Brewster angle ($\theta_{\text{Brewster}} = 57.3°$ from the vertical) of asphalt are represented by a *horizontal line* [after Fig. 11 on page 24 of Horváth et al. (2010b)]

20.2.3 When Do Asphalt Surfaces Reflect Strongly and Horizontally Polarized Light?

Figure 20.11 summarizes qualitatively the directions of polarization of light reflected from a sunlit dry asphalt road as a function of the solar azimuth direction relative to the road line: If the observer is facing the solar or antisolar meridian, the asphalt-reflected light is horizontally polarized, and thus from both directions of view, sunlit asphalt surfaces can be attractive to polarotactic aquatic insects. If the sun is shining from left/right, the direction of polarization of asphalt-reflected light is tilted to right/left relative to the vertical, and thus sunlit asphalt surfaces are not attractive to aquatic insects.

Figure 20.12 shows qualitatively the directions of polarization of skylight/sunlight reflected from shady/sunlit regions of a dry asphalt road: The direction of polarization of asphalt-reflected sunlight is usually tilted relative to the horizontal road surface. If the road is shady, that is, illuminated by skylight only, the asphalt-reflected skylight is always horizontally polarized. Under this condition, light from the sky comes from all possible directions from above, and due to symmetry, the average incident direction of skylight is vertical. Thus, the average

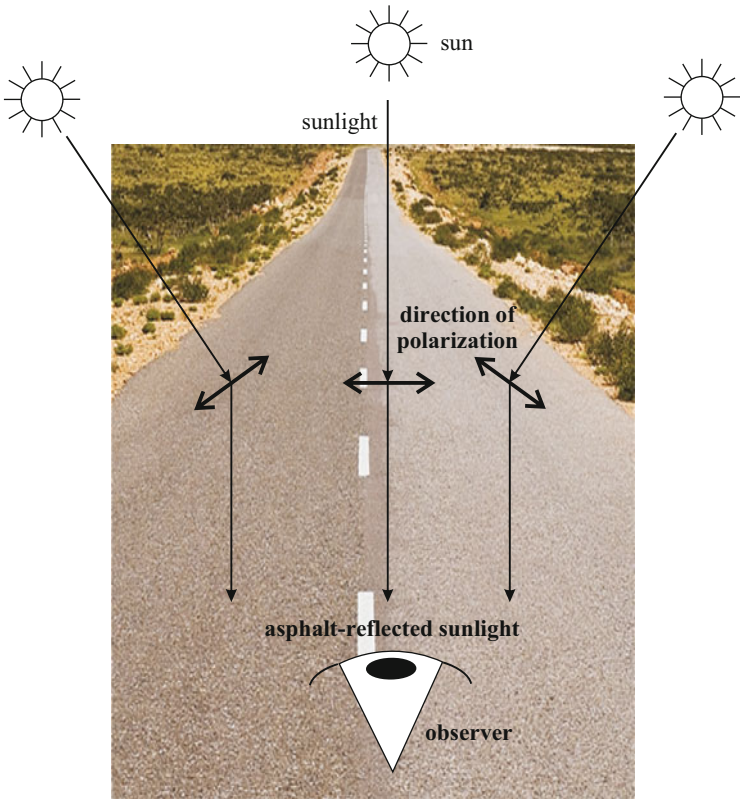

Fig. 20.11 Schematic representation of the directions of polarization (*double-headed arrows*) of light reflected from a sunlit dry asphalt road for three different solar directions [after Fig. 13 on page 28 of Horváth et al. (2010b)]

plane of reflection is vertical, and, consequently, the average direction of polarization of asphalt-reflected skylight is horizontal. For these reasons, shady asphalt surfaces can always be attractive to polarotactic water insects.

20.2.4 Reducing the Polarized Light Pollution of Asphalt Surfaces

Horváth et al. (2010b) suggested some possible strategies to mitigate the severity of PLP produced by asphalt: The PLP of asphalt surfaces can be reduced or even eliminated by constructing asphalt from materials that create a rough (less smooth) surface (Fig. 20.10) and from brighter aggregate materials (e.g. gravel) or by applying paint that creates a white-striated appearance (Fig. 20.9). Rough asphalt surfaces reflect/scatter light diffusely, and bright/white-striated asphalt surfaces reflect only weakly polarized or unpolarized light. Both treatments ensure that the

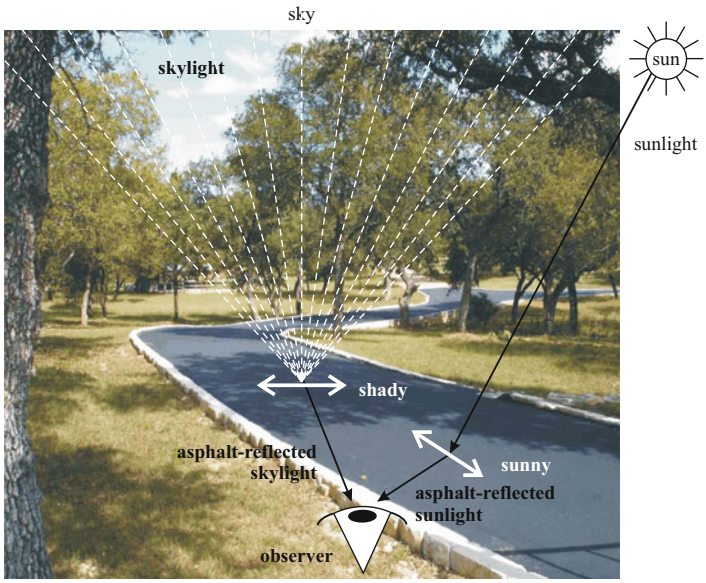

Fig. 20.12 Schematic representation of the directions of polarization (*double-headed arrows*) of skylight/sunlight reflected from shady/sunlit regions of a dry asphalt road [after Fig. 14 on page 29 of Horváth et al. (2010b)]

degree of polarization of asphalt-reflected light can be reduced below the threshold of polarization sensitivity of polarotactic aquatic insects, thus eliminating the evolutionary trap. If a shiny dark asphalt surface is covered by small-sized white gravel or painted by matte white stripes, the PLP will be minimal. In areas with gravel roads, the change of gravel to the more insect-attracting asphalt should, if possible, be avoided. White stripes painted onto the asphalt surface (Fig. 20.9) reduce or even eliminate the attraction to polarotactic insects as zebra stripes do (see Sects. 20.3 and 22.3). Such interventions will be most impactful when implemented near emergence sites of endangered aquatic insects, especially in the vicinity of wetlands, rivers and lakes.

20.3 Reducing the Maladaptive Attractiveness of Solar Panels to Polarotactic Insects by Surface Fragmentation Due to White Grid Patterns

The use of photovoltaic solar cells and solar collectors as a source of energy has increased dramatically over the last several decades and is poised to continue to do so (Camacho et al. 2007; Currie et al. 2008). The aforementioned optical characteristics (strong and often horizontal reflection–polarization) of smooth and black surfaces match those commonly exhibited by solar panels and collectors making

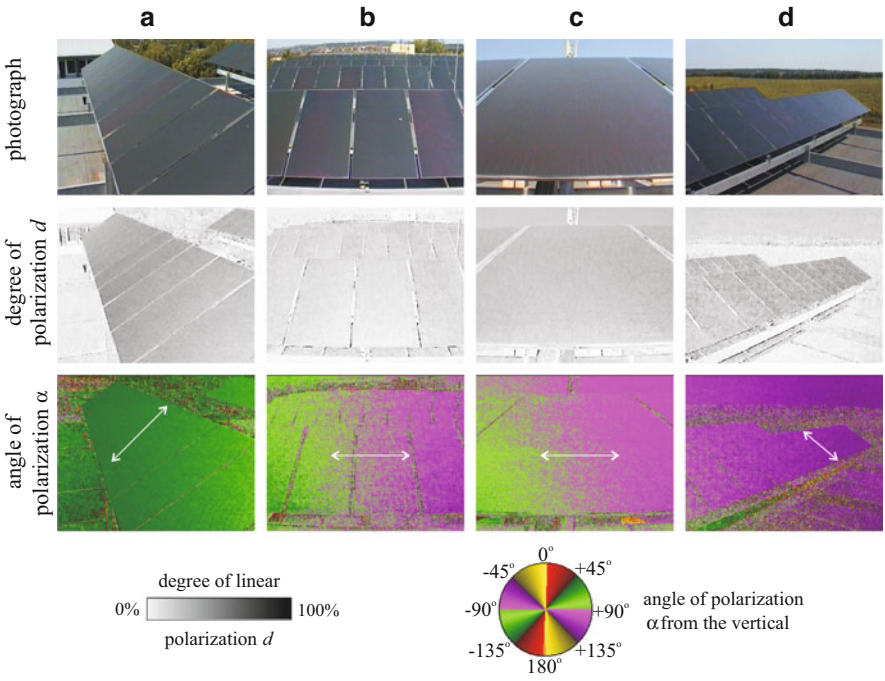

Fig. 20.13 Photographs and reflection–polarization patterns of photovoltaic solar panels with homogeneous *shiny black surface* on the rooftop of the Szent István University in Gödöllő, Hungary, measured in the green (550 nm) spectral range from four different directions of view: from *right* (**a**), from *front and above* (**b**), from *front and below* (**c**) and from *left* (**d**). In the α-patterns, the *double-headed arrows* show the local direction of polarization of reflected light [after Supplementary Fig. S2 of Horváth et al. (2010a)]

them sources of PLP (Figs. 20.13 and 20.14) that attract polarotactic aquatic insects (Fig. 20.15) (Horváth et al. 2009). The consequence of this may be that the design of solar panels and collectors and their placement relative to aquatic habitats will likely affect populations of aquatic insects that use polarized light as a behavioural cue.

Using imaging polarimetry, Horváth et al. (2010a) measured the reflection–polarization characteristics of different solar panels and collectors (Figs. 20.13 and 20.14). At the Brewster angle ($\theta_{\text{Brewster}} = 56.3°$ from the vertical), solar panels polarize reflected light almost completely (degree of polarization $d \approx 100$ %), which substantially exceeds typical polarization values for water ($d \approx 30$–70 %). They noticed, however, that white decorative frames and the white gridding of partitioned solar panels reflect weakly polarized or unpolarized light (Fig. 20.14). The direction of polarization of light reflected from solar panels and collectors is always horizontal when the plane of reflection is vertical (Figs. 20.13 and 20.14).

In multiple-choice experiments performed in a Hungarian wetland, Horváth et al. (2010a) monitored the behavioural responses of mayflies (Ephemeroptera),

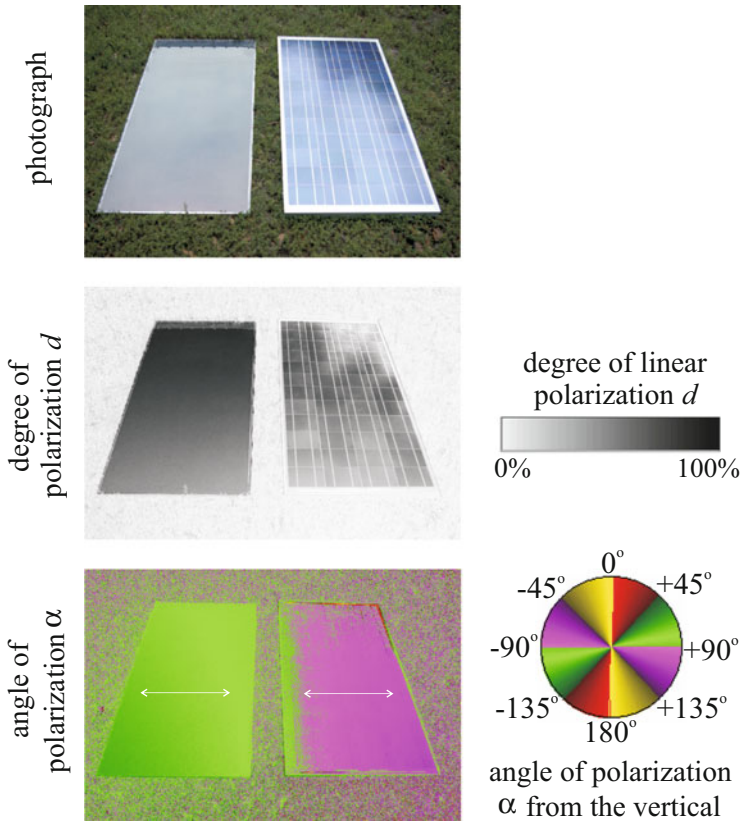

Fig. 20.14 Photograph and reflection–polarization patterns of a homogeneous black solar panel (*left*) and a black solar panel with a white grating (*right*) measured in the green (550 nm) part of the spectrum. In the α-pattern, *double-headed arrows* show the local direction of polarization of reflected light. The polarimeter viewed towards the antisolar meridian and the angle of elevation of its optical axis was -35° from the horizontal [after Fig. 2 on page 1647 of Horváth et al. (2010a)]

caddisflies (*Philopotamus*: Trichoptera), dolichopodids (Dolichopodidae, Diptera) and tabanids (Tabanidae, Diptera) to different horizontal test surfaces laid on the ground: (1) white-framed solar panels and nonpolarizing surfaces (matte black cloth, matte white cloth), (2) white- and black-framed solar panels with an underlying strongly and horizontally polarizing plastic sheeting, (3) white- and black-framed solar panels in the absence of an underlying polarizing plastic sheeting, (4) shiny black surfaces with different nonpolarizing white grid patterns on a weakly polarizing substrate (Fig. 20.16) and (5) a solar panel with a white framing versus a homogeneously black solar panel (Fig. 20.14).

Given the typically deleterious effects of habitat fragmentation on the abundance and species richness of species in natural systems (Collinge 2000; Funk et al. 2005; Moore et al. 2008), in one of their experiments Horváth et al. (2010a) tested

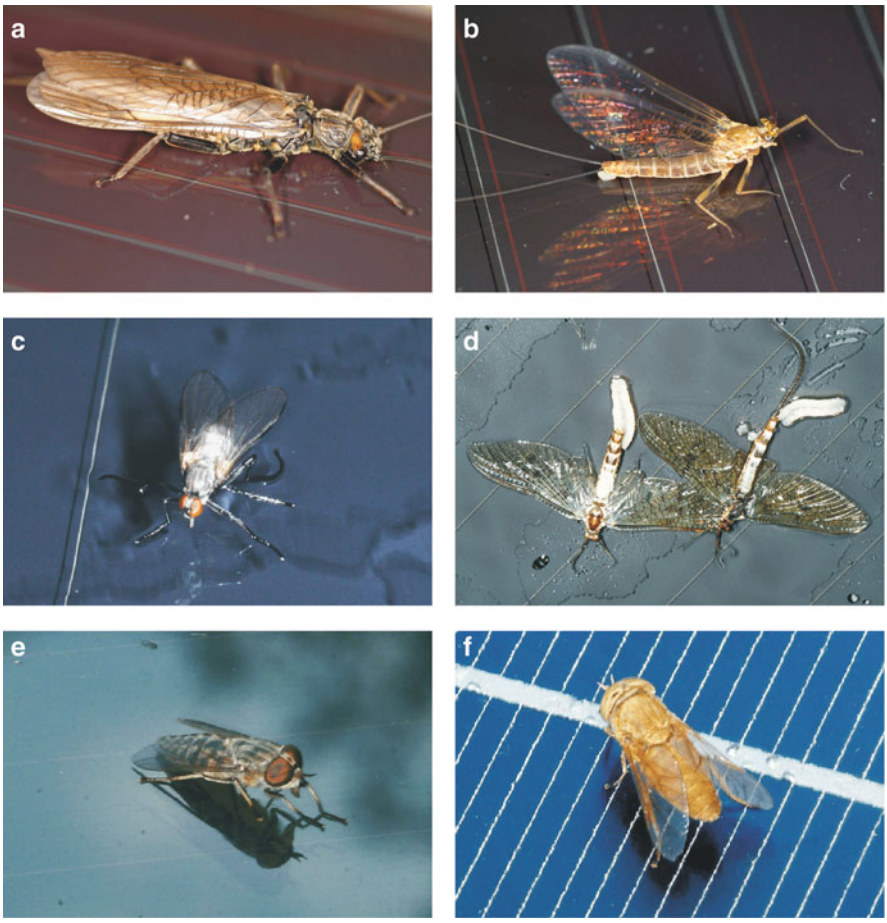

Fig. 20.15 Polarotactic aquatic insects attracted to and landed on the shiny black surface of horizontal solar panels. (**a**) Adult female stonefly (*Perla abdominalis*). (**b**) Female mayfly (*Rhithrogena semicolorata*) with a white egg batch on the end of her abdomen. (**c**) A dolichopodid fly (Dolichopodidae). (**d**) Female mayflies (*Ephemera danica*), the elongated white egg batches of which laid onto the panel are clearly seen. (**e**, **f**) Tabanid flies (Tabanidae) landed on a homogeneous black solar panel (**e**) and a white-gridded solar panel (**f**) [after Supplementary Fig. S1 of Horváth et al. (2010a)]

whether partitioning strongly and horizontally polarizing shiny black horizontal surfaces into smaller sections could make them unattractive to polarotactic insects (Fig. 20.16): Because the operative nature of attraction of all known taxa of polarotactic aquatic insects to water is its horizontally polarized light signature, sticky test surfaces of strongly polarizing smooth black plastic (2 m × 2 m) with a white frame (width 1 cm) on their outer edge were created. Three from the white-framed four test surfaces were orthogonally partitioned by white,

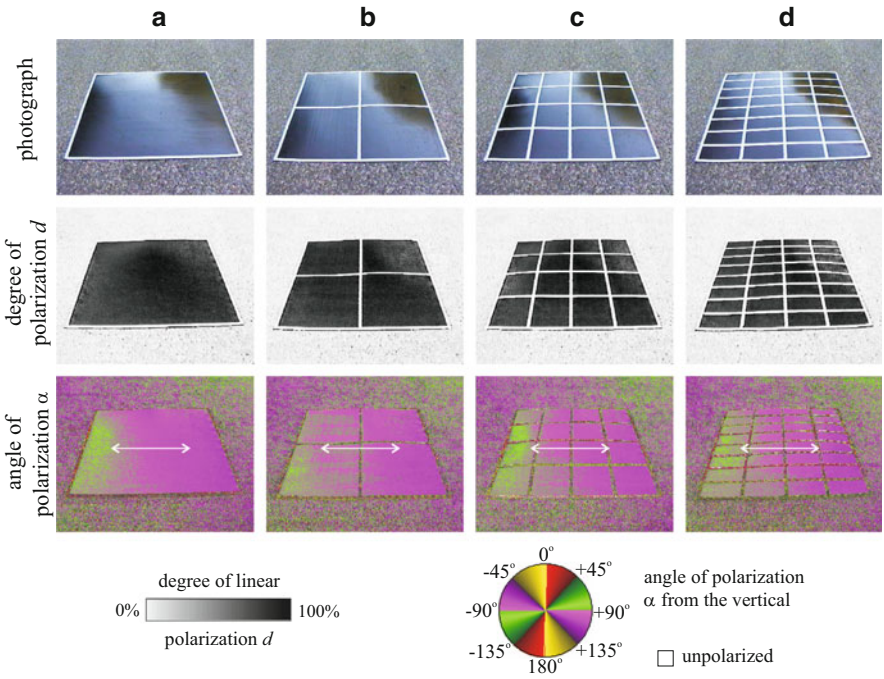

Fig. 20.16 (**a**) Photographs and reflection–polarization patterns of the four polarizing surfaces (2 m × 2 m) used in one of the experiments of Horváth et al. (2010a) with mayflies, caddisflies and dolichopodids. (**b**, **c**, **d**) The white-framed surfaces are orthogonally partitioned by nonpolarizing *white tape*. In the α-patterns, *double-headed arrows* show the local direction of polarization of reflected light. The polarimeter viewed towards the antisolar meridian and the angle of elevation of its optical axis was -35° from the horizontal [after Fig. 3 on page 1648 of Horváth et al. (2010a)]

nonpolarizing tape (width 1 cm) with a low d (<5 %) that effectively fragmented the total area of black polarizing surface into smaller panels (Fig. 20.16).

On highly and horizontally polarizing surfaces, mayflies, caddisflies, dolichopodid flies and tabanids exhibited oviposition behaviour more often than above surfaces with lower degrees of polarization (including water), but in general they avoided solar panels with nonpolarizing white borders and white grates (Horváth et al. 2010a). The strongly and horizontally polarizing surfaces that had nonpolarizing, white panel borders were significantly less attractive to these insects than the same panels without white partitions (Fig. 20.17). Polarotactic insects avoided the white-framed solar panels but were attracted to the solar panels with polarizing black frames. The relation between the number of orthogonal white stripes on a test surface and the number of attracted insects per unit black area for all investigated taxa was negative (Fig. 20.17): Captures per square metre of polarizing black surface were 10–27 times higher on the unpartitioned surface relative to the most highly partitioned surface. Captures of dolichopodids and mayflies on the homogeneous black solar panel were three and seven times higher

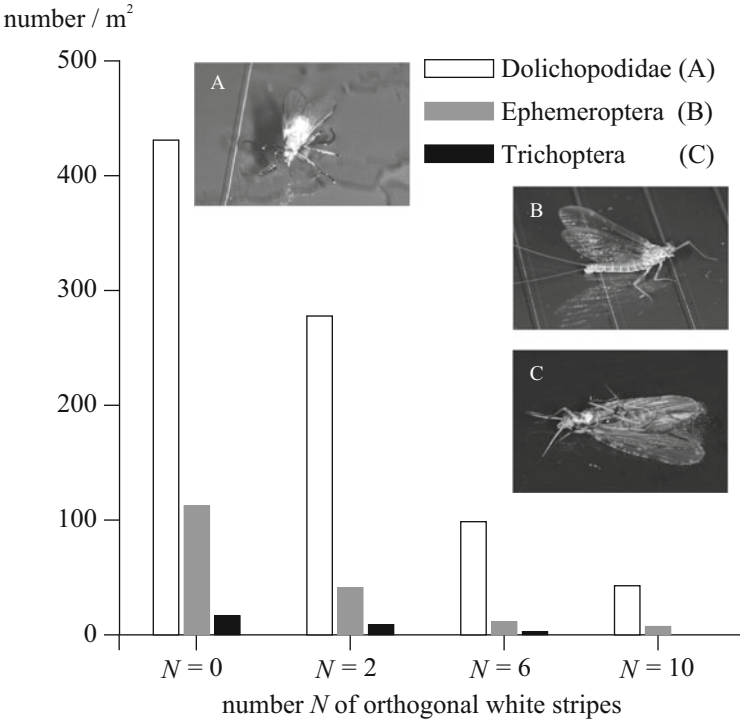

Fig. 20.17 The surface density (number/m^2) of polarotactic dolichopodids (Diptera), mayflies (Ephemeroptera) and caddisflies (*Philopotamus* sp., Trichoptera) trapped by a strongly and horizontally polarizing sticky surface with different numbers of orthogonal white strips (Fig. 20.16) [after Fig. 4 on page 1650 of Horváth et al. (2010a)]

than those on the partitioned white-gridded panel, respectively. Tabanids touched down on the homogeneous solar panel nine times more frequently than on the white-gridded panel. After landing, tabanids stayed on the homogeneous photovoltaic panel seven times longer period than on the white-gridded panel.

Though a sufficiently dense white grid of nonpolarizing strips partitioning the solar-active area of solar panels reduces or eliminates their attractiveness to aquatic insects, addition of a nonpolarizing gridding reduces the solar-active surface area which will reduce the performance of these panels in direct proportion to the total surface area of the grid (Horváth et al. 2010a). In the aforementioned experiments (Fig. 20.17), significant (10- to 27-fold) reductions of the attractiveness to polarotactic insects could be reached with an approximately 2 % loss of effective (i.e. energy-producing black) surface area in a solar panel. Thus, the cost of effectively eliminating the attractive effect of PLP on polarotactic aquatic insects amounts to a relatively small drop in performance of photovoltaic solar panels.

The exact biological mechanism underlying reduction in attraction associated with gridding remains unclear. It could be that the low spatial resolution of the insect compound eye reduces polarization contrast, rendering the appearance of a white-gridded solar panel as less polarized and therefore less attractive. Alternatively, if larger water bodies are associated with higher mating, oviposition or reproductive success, insects may prefer larger habitat patches for mating and oviposition, a preference common among terrestrial and aquatic vertebrates (Herkert 1994; Funk et al. 2005; Moore et al. 2008). Figure 20.18 summarizes this explanation: A strongly and horizontally polarizing shiny black surface is attractive/unattractive to polarotactic insects if its area s is larger/smaller than a critical area A_{critical} that may be dependent on species. The biological reason for this is the following. For a given aquatic insect species, there is a minimal and a maximal dimension of the bodies of water where the larvae can optimally develop. Thus, the adult females of this species lay their eggs only in such water bodies, the surface of which is neither smaller nor larger than these lower and upper limits:

- If there is only one black unit surface with $s < A_{\text{critical}}$ in a given optical environment, it is unattractive to water-seeking flying polarotactic insects (Fig. 20.18a).
- If there are $N \times N = N^2$ such black unit surfaces at large enough distances from each other, each of them functions further on as an individual unit surface s, thus remaining henceforward unattractive to polarotactic insects, because $s < A_{\text{critical}}$ (Fig. 20.18b).
- If, however, there are N^2 black unit surfaces contacting each other, their individual unit surfaces are summed up, functioning as a large surface with $S = N^2 s$ area, and if $S > A_{\text{critical}}$, they are attractive to polarotactic insects (Fig. 20.18c).
- If there are N^2 white-framed unit surfaces s contacting each other (Fig. 20.18d), they are separated from each other by a depolarizing white frame, and thus their individual unit surfaces s cannot be summed up in the visual system of the approaching polarotactic insect. Consequently, each of them functions as an individual unit surface s, and if $s < A_{\text{critical}}$, they remain unattractive to polarotactic insects, in spite of the fact that they contact each other (Fig. 20.18d). The prerequisites of this effect are that the depolarizing separations, i.e. the white stripes, should be wide enough, and their number has to be large enough.

The main conclusion that can be drawn from these results is that although solar panels/collectors can act as ecological traps due to their PLP, fragmenting their solar-active area does lessen their attractiveness to polarotactic insects (Horváth et al. 2010a). The potential effects of PLP associated with solar panels on populations of aquatic insects remain unclear, but they are predicted to cause rapid and potentially large population declines (Delibes et al. 2001; Donovan and Thompson 2001), especially when located near natural wetlands and water bodies. Finally, we note that new technologies such as three-dimensional solar panels that use vertically aligned arrays of carbon nanotubes (Camacho et al. 2007; Currie et al. 2008) reflect only a small amount of diffuse light with weak and not always horizontal polarization and so should produce little PLP. Nanostructured corneal

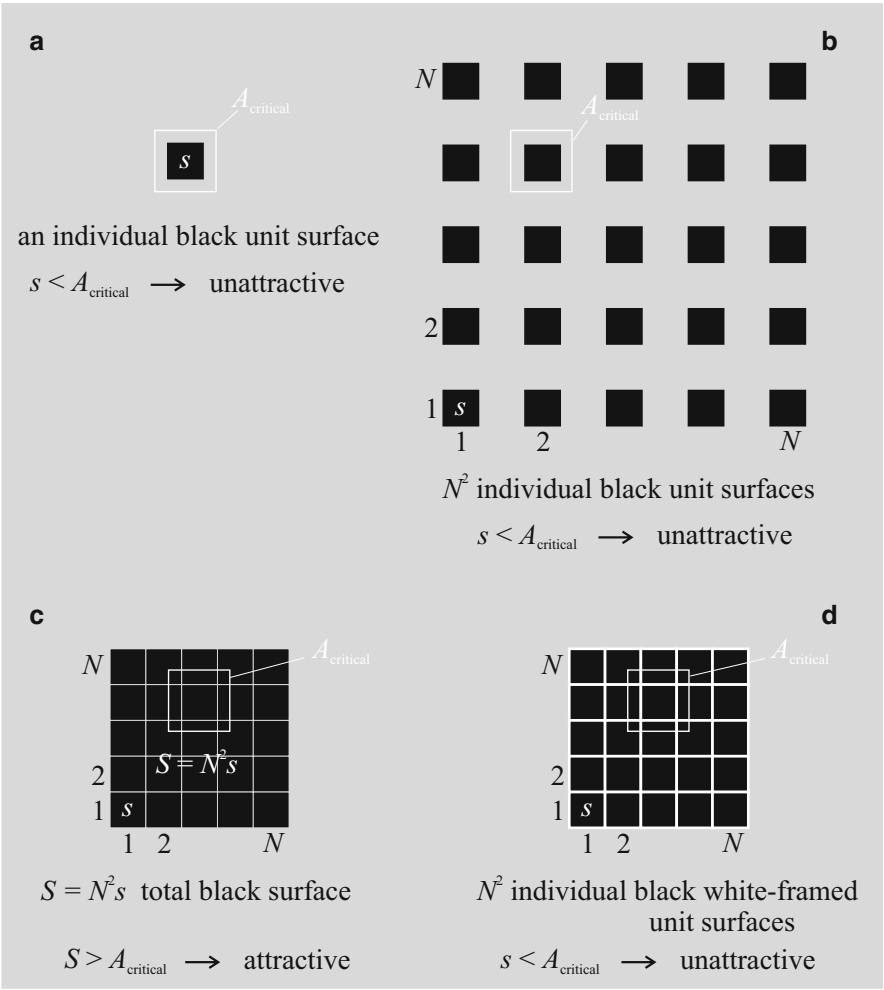

Fig. 20.18 For explanation of the attractivity/unattractivity of horizontal shiny black surfaces without/with depolarizing white grid patterns to positively polarotactic insects. A horizontal shiny black surface is attractive/unattractive to such insects, if its area s is larger/smaller than a species-specific critical area $A_{critical}$

nipple arrays of night-active moth eye facets can help to design such thin-film solar panels (Dewan et al. 2012).

The test surfaces and solar panels used by Horváth et al. (2010a) were on the ground and oriented horizontally to mimic natural water bodies. Solar panels and collectors are often elevated above the ground and tilted at an angle to maximize interception of solar radiation (Fig. 20.13). Orientation and elevation appear to be generally unimportant in mitigating behavioural responses of polarotactic insects to artificial polarizing reflectors. Vertical glass surfaces are highly effective at

horizontally polarizing light (Malik et al. 2008) and attracting polarotactic aquatic insects to oviposit *en masse* even many stories above ground level (Kriska et al. 2008). Aquatic beetles, water bugs and dragonflies are also attracted to and oviposit on the roof, hood and trunks of dark-coloured strongly polarizing automobiles that are elevated and tilted at various heights and angles (Watson 1992; Jäch 1997; Nilsson 1997; van Vondel 1998; Wildermuth and Horváth 2005). Consequently, tilted and even highly elevated solar panels may also attract these insects. Elevation may even increase the distances at which such structures can be detected. Tabanids, however, are an exception from this rule, because they are not attracted to horizontally polarizing surfaces if elevated above the ground (Blahó et al. 2012; Egri et al. 2012; 2013a, b; see Sects. 22.1 and 23.2).

20.4 *Motacilla* Wagtails as Insect Indicators on Horizontal Plastic Sheets Used in Agriculture Attracting Polarotactic Aquatic Insects

Another artificial polarizing surface that has become increasingly abundant through its use in certain types of intensive agriculture is black plastic sheeting (Fig. 20.19). Black plastic sheeting has gained favour in raised-bed farming (e.g. strawberry fields) because it suppresses the growth of weeds and can be used to keep the soil warm in order to speed up the sprouting of crop plants or to cover and protect produce from weather extremes. Unfortunately, as a horizontally oriented shiny black surface sheeting, it has great potential to produce PLP and lure and kill aquatic insects *en masse* (Csabai et al. 2006).

Bernáth et al. (2008) carried out dual-choice field experiments with a pair of black and white plastic sheets (12 m × 33 m) laid on the ground in Hungarian wetlands (Fig. 20.20). To estimate the number of insects lured to the plastic sheets, they counted the number of wagtails (*Motacilla alba*, *M. flava*) feeding in flocks on the plastic sheets (Fig. 20.21) and on water banks in the vicinity; furthermore, the number of their feeding rate. To determine the numbers of insects lured by plastic sheets, black, white, light grey and dark grey sticky insect traps (1 m × 1 m) on the ground were deployed. These four sticky traps formed a gradient of both the degree of linear polarization and the intensity of reflected light: The lower the intensity, the higher the degree of polarization. Bernáth et al. (2008) also studied the role of the plastic sheet area by comparing the feeding rates and number of wagtails on the black plastic sheet, the area of which was 400 m^2 at the beginning; then it was halved by folding in every 2 days (the smallest size was 6 m^2).

Only the black-coloured plastic sheets attracted insects associated with water (Ephemeroptera; Plecoptera; Coleoptera, e.g. Hydrophilidae, Dytiscidae; Heteroptera, e.g. Corixidae, Notonectidae, Gerridae) (Bernáth et al. 2008). All these aquatic insects showed similar behavioural elements on and above the black plastic sheet: landing, flying up, touching and crawling on the surface and egg laying; finally all of them dried out and perished within some hours. Almost at

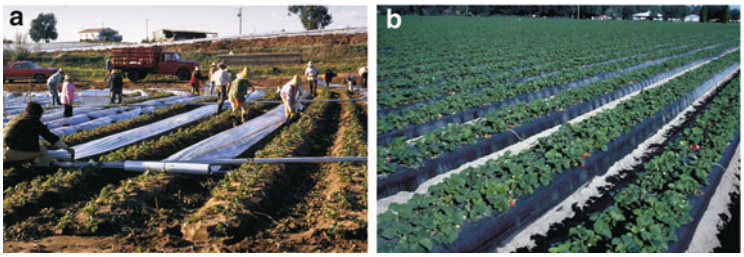

Fig. 20.19 The use of strongly and horizontally polarizing, shiny black plastic sheets on several hectares became widespread in agriculture, especially in the modern raised-bed technology of strawberry production

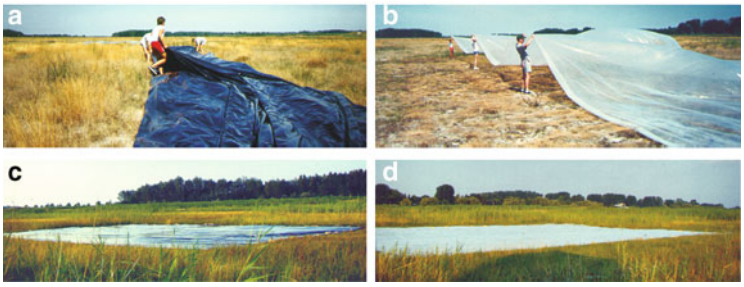

Fig. 20.20 (**a**, **b**) Laying a *black* and a *white plastic sheet* (600 m^2) onto the ground in the field experiment of Bernáth et al. (2008). (**c**, **d**) The *plastic sheets* were pinned down by bricks on their edges and restretched regularly. Their surface imitated the polarized light signature of a dark and a bright waterbody

every sunset the black plastic sheet rattled sounding like the pattering of raindrops. The reason for this was thousands of Corixidae bugs landing on and crashing into the black plastic and then jumping repeatedly up and down. They did not leave this optical trap and did not fly away from the visually attractive black plastic sheet; they remained on it throughout the night and perished due to dehydration. Thus, black plastic sheets can be dangerous mostly for aquatic insects. It is estimated that a raised-bed strawberry plantation of 10 ha covered by shiny black plastic sheets can kill about 1 t of aquatic insects every day in this way (Bernáth et al. 2008).

The number of insects trapped by the sticky traps was proportional to the surface brightness (Fig. 20.22): The white sticky trap caught the most insects. There was no significant difference between the black and the dark grey traps, and both traps captured significantly less insects than the light grey trap. The white trap captured mainly small Dipterans, while small aquatic insects and Corixidae water bugs, for example, were found exclusively on the dark grey and black traps. Dipterans were never observed to be detained and perish on the shiny white dry (nonsticky) plastic sheet.

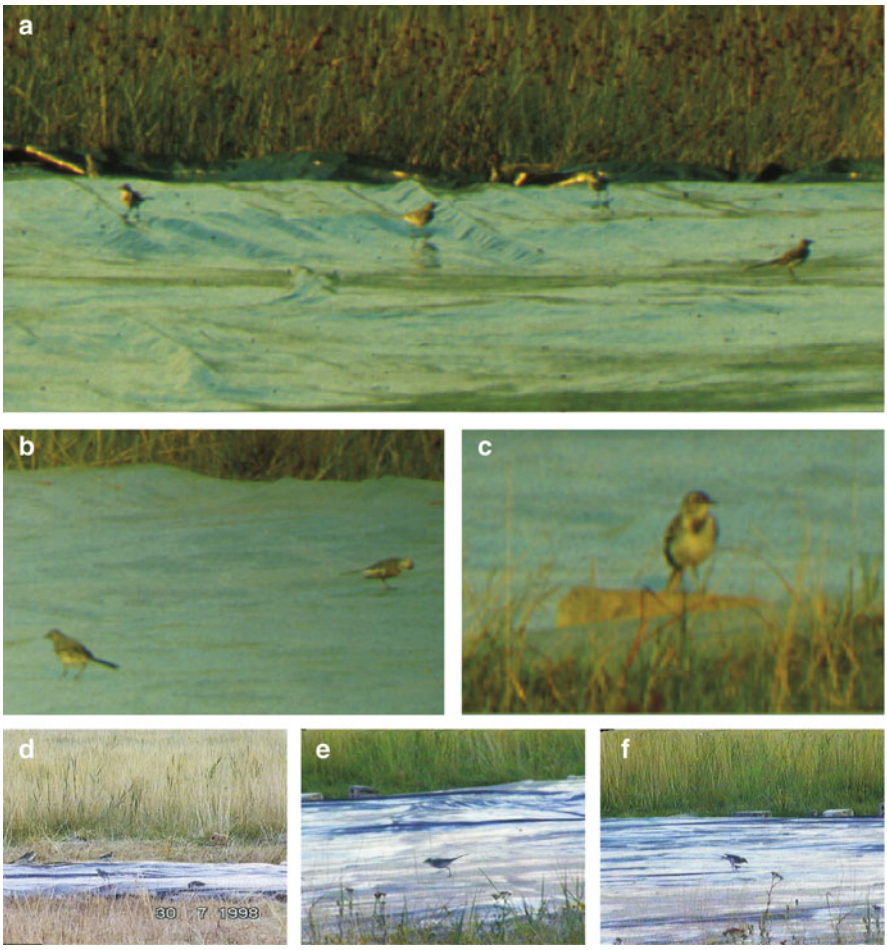

Fig. 20.21 Behaviour of wagtails (*Motacilla alba* and *M. flava*) on the *plastic sheets* used in the field experiments of Bernáth et al. (2008). (**a**) Wagtails gathered on the *plastic sheets* even in the very first evening of their deployment. (**b**) Birds fed in flocks; aggressive behaviour was rarely observed even if birds approached each other nearer than 1 m. (**c**) In the first days the birds preferred to sit on the bricks pinning down the edge of the sheets, and they frequently flew over the sheets. Later on they walked on the plastic surface (**d**) chasing (**e**) and picking (**f**) small insects attracted to and flying over the plastic

Wagtails were attracted to feed on insects lured to plastic sheeting (Bernáth et al. 2008). Most birds gathered on the black plastic sheet prior to sunset and immediately after sunrise (Fig. 20.23b, d). In the evening, the black plastic was more effective insect attractor than the white plastic: Aquatic insects arrived to the black plastic *en masse* in the dusk period.

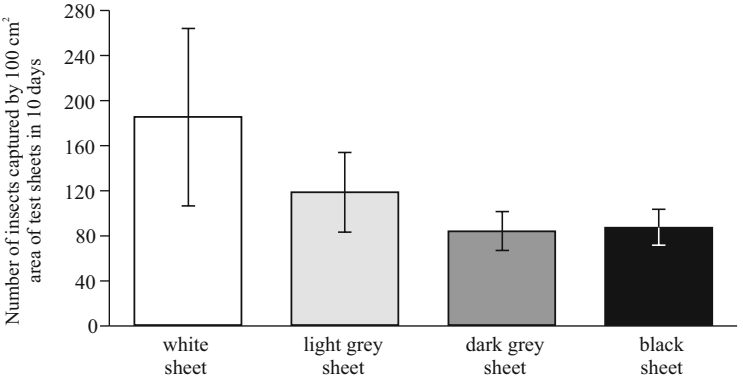

Fig. 20.22 Number of insects trapped by 1 dm^2 sampling areas of the sticky plastic sheets. *Columns* represent the average; *vertical bars* show the standard deviation of the number of insects in 12 sample areas on each sticky plastic sheet [after Fig. 2 on page 148 of Bernáth et al. (2008)]

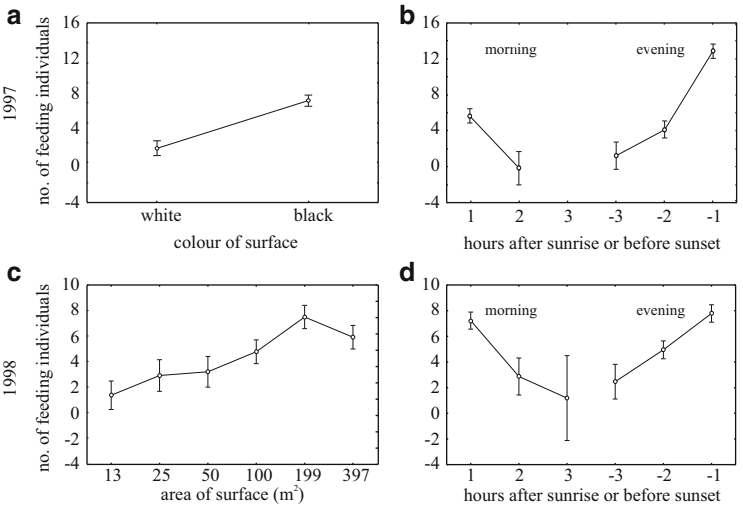

Fig. 20.23 Average number of wagtails (*Motacilla alba* and *M. flava*) feeding on natural water banks and the (black and white) plastic sheets used in the field experiments of Bernáth et al. (2008) (**a**, **c**) in the hours after sunrise and before sunset (**b**, **d**) in 1997 (**a**, **b**) and 1998 (**c**, **d**) near Kunfehértó. *Vertical bars* show 0.95 confidence intervals. In 1997 the wagtails were studied on both the black and white plastic sheets as well as on the shore of alkaline lakes. In 1998 the wagtails were investigated on a single black plastic sheet with gradually decreasing and increasing area, respectively [after Fig. 3 on page 149 of Bernáth et al. (2008)]

During the day wagtails feed primarily on larger Dipterans around dung spots protected and guarded by single individuals. However, in the morning and evening wagtails assemble on water banks to hunt for small aquatic insects flying in these periods in great numbers (Zahavi 1971; Davies 1977; Davies and Houston 1981; Houston et al. 1985; Csabai et al. 2003, 2004, 2006). Wagtails are also known to

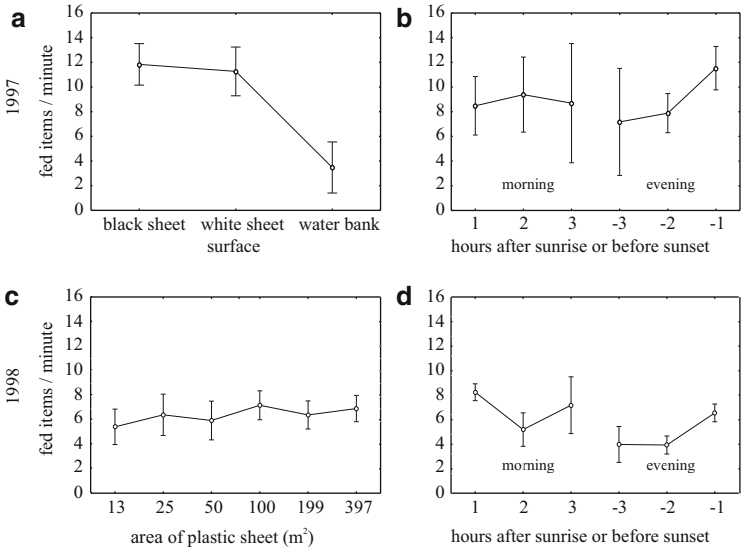

Fig. 20.24 As Fig. 20.23 for the average feeding rate of wagtails [after Fig. 4 on page 151 of Bernáth et al. (2008)]

take advantage of insect-attracting artificial surfaces like asphalt roads, for example (Rezanov 1981).

Both the black and white plastic sheets acted as a significantly much richer food source than water banks (Fig. 20.24a). The feeding rate of wagtails was not significantly higher on the black plastic sheet than that on the white one (Bernáth et al. 2008). Wagtails kept so high feeding rate on both plastic sheets, which was unreachable on the water banks (Fig. 20.24). In the hour before sunset, the feeding rate was significantly higher both on the black plastic sheet and the water bank than on the white plastic. Significantly more birds fed on the black plastic than on the white plastic, especially in the hour before sunset (Fig. 20.23).

No wagtails were observed on the black plastic sheet, if its surface was smaller than 12 m^2 (Bernáth et al. 2008). The feeding rate of wagtails did not change significantly (Fig. 20.24c) in spite of the fact that the area of the black plastic sheet was gradually reduced from 100 % (400 m^2) to 3 % (12 m^2). The number of birds was nearly proportional to the plastic area (Fig. 20.23c).

The strong attractiveness of horizontal shiny black plastic sheets to polarotactic insects makes them an efficient tool for entomologists to monitor aquatic insects (Csabai et al. 2003, 2004, 2006). Since the size, shape and optical characteristics of plastic sheets (e.g. black, strongly polarizing; grey, moderately polarizing; white, depolarizing) can be manipulated and controlled easily, even in field experiments, such plastic sheets can be applied as a useful method in future behaviour–ecological research, especially in dry habitats, where large natural water surfaces are rare or missing. However, if laid out on great areas in the field, such plastic sheets may seriously harm the local population of water-loving insects. Thus, the possible

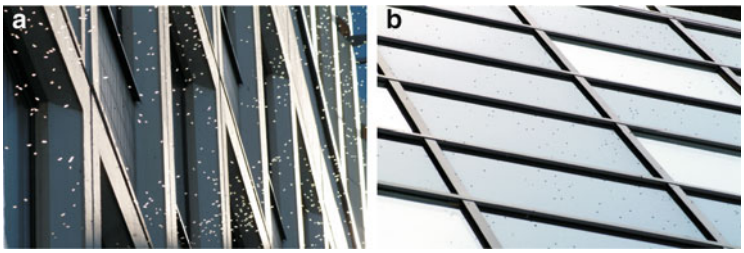

Fig. 20.25 (**a**) Mass swarming of *Hydropsyche pellucidula* caddisflies (*white spots*) in front of the vertical glass panes of a building of the Eötvös University in Budapest on 1 May 2007. (**b**) Numerous individuals of *H. pellucidula* (*black spots*) landed on the glass panes [after Fig. 1 on page 462 of Kriska et al. (2008)]

detrimental effects of such agricultural technologies may be serious and should be investigated thoroughly in the future.

20.5 Glass Buildings on River Banks as Polarized Light Traps for Mass-Swarming Polarotactic Caddisflies

Dusk-active aquatic insects, such as mayflies and caddisflies, for example, often swarm at buildings, which is generally explained by the marker effect (Brodskiy 1973; Savolainen 1978; Reich and Downes 2003): The dark silhouette of a building against the bright sky can function as a conspicuous rendezvous site for swarming insects. The caddisflies *Hydropsyche pellucidula* emerge at dusk from the river Danube and swarm around trees and bushes on the river bank under calm and warm weather conditions. After copulation, the fertilized females return to the river where they lay their eggs into water.

Kriska et al. (2008) observed that every year in April and May after emerging from the river Danube in Budapest (Hungary), *Hydropsyche pellucidula* are attracted in mass to the vertical glass surfaces of buildings standing on the river bank (Figs. 20.25 and 20.26): The individuals lured mainly to dark vertical glass panes land, move randomly, copulate and remain on the glass for hours (Fig. 20.26a–c). Through the aperture between the frame of partly open tiltable windows and the building wall, caddisflies fly into the rooms where they become trapped (Fig. 20.26d). Females often lay their eggs onto the dry glass pane (Fig. 20.26e, f). After swarming the caddisflies rest motionless on glass surfaces and red bricks of the buildings. On the next day, after sunrise the remaining insects rest motionless in the shadow of window frames and among bricks. These individuals, if survived, join to the new swarms developing again in the next afternoon. The slightly higher (by 2–5 °C) air temperature near the building walls heated up daytime due to direct sunshine, and the places around the buildings sheltered from the wind prolong by about half an hour the swarming of caddisflies relative to the swarming time observed on the cooler and windier river bank.

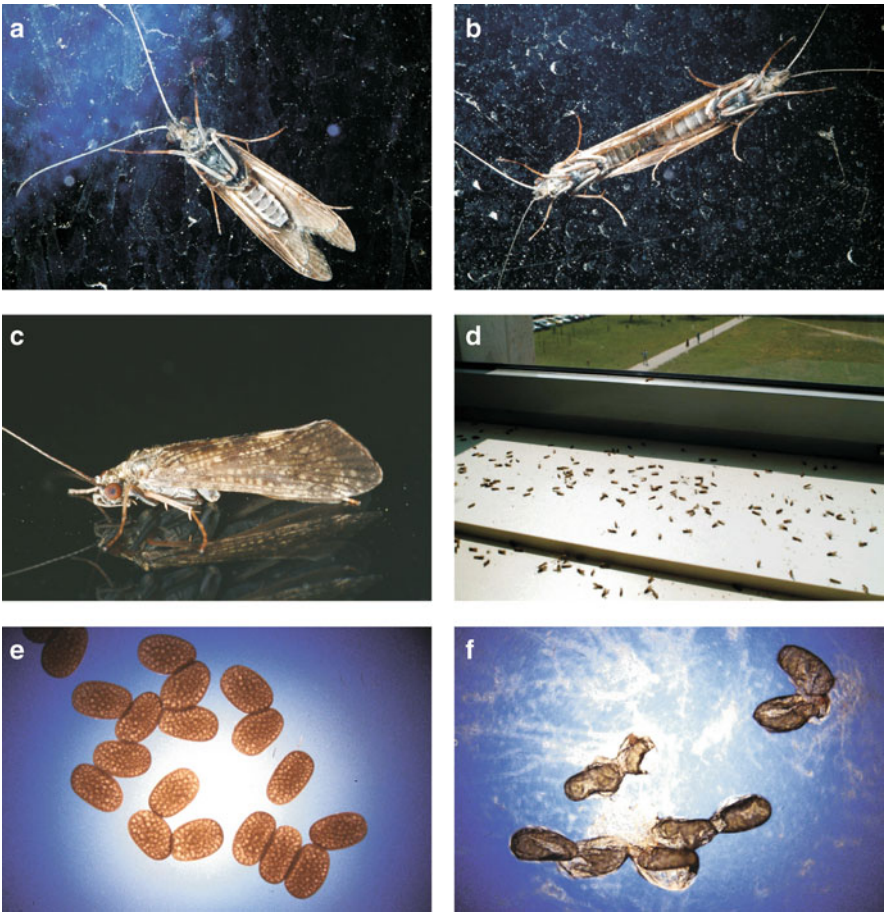

Fig. 20.26 (**a**) A *Hydropsyche pellucidula* landed on the outside surface of a glass window and photographed from inside a room. (**b**) A copulating pair of *H. pellucidula* on the outside of a glass pane and photographed from inside. (**c**) Adult *H. pellucidula* landed on the inside surface of a window (the picture is rotated by 90°). (**d**) Numerous carcasses of *H. pellucidula* trapped by a partly open tiltable window [after Fig. 2 on page 464 of Kriska et al. (2008)]. (**e**) Light micrograph of some freshly laid eggs of *H. pellucidula*. (**f**) Light micrograph of some dried-out eggs of *H. pellucidula*

In laboratory choice experiments, Kriska et al. (2008) showed that ovipositing *H. pellucidula* are attracted to strongly and horizontally polarized light stimulating their ventral eye region and thus have positive polarotaxis. In the field they documented that strongly polarizing vertical black glass surfaces are significantly more attractive to both female and male *H. pellucidula* than weakly polarizing white ones (Table 20.2, Fig. 20.25b).

Using imaging polarimetry, Kriska et al. (2008) measured the reflection–polarization characteristics of vertical glass surfaces of buildings where caddisflies swarmed (Fig. 20.27). The vertical walls of the building were partly covered by

Table 20.2 Numbers (mean ± standard deviation) of the caddisflies *Hydropsyche pellucidula* landed on black and white vertical glass panes of a building of the Eötvös University in Budapest averaged for 50 black and 50 white quadratic (2 m × 2 m) glass surfaces

		Vertical glass surface	
No.	Date (2007)	Black	White
1	19 April	*6.6 ± 3.5	2.2 ± 1.0
2	20 April	*10.1 ± 4.2	3.0 ± 1.3
3	22 April	*17.2 ± 5.3	5.3 ± 2.2
4	1 May	*28.5 ± 11.3	5.1 ± 2.1
5	5 May	*65.2 ± 24.6	9.1 ± 3.2

On a given day each counting was performed three times, at 17:30, 18:00 and 18:30 h (=local summer time = UTC + 2 h), and the counts made at each time interval within a day were averaged. Data belonging to the black vertical glass surfaces are marked by *, which are statistically significantly larger than the corresponding data belonging to the white glass surfaces [after Table 2 on page 463 of Kriska et al. (2008)]

black and white glass surfaces as ornamentation (Figs. 20.25b and 20.27). The darker a glass surface, the higher was the degree of polarization d of glass-reflected light (Fig. 20.27). Prior to landing, every flying caddisfly had to choose between a black and a white glass. According to Table 20.2, the black vertical glass surfaces attracted in average 3–7 times more caddisflies than the white ones. The pattern of the direction of polarization of a given building's wall depended on the direction of view relative to the solar meridian. However, the direction of polarization of glass-reflected light was always horizontal (Fig. 20.27) for the walls being in shadow (e.g. facing towards the antisolar meridian), if the plane of reflection was vertical (i.e. the downwelling skylight or the upwelling groundlight mirrored from the vertical glass panes was seen by flying caddisflies).

Kriska et al. (2008) proposed that after their emergence from the river, *H. pellucidula* are attracted to buildings by their dark silhouettes and the glass-reflected horizontally polarized light. After sunset this attraction could be strengthened by positive phototaxis elicited by the buildings' lights. The attraction of caddisflies to vertical glass surfaces has not been expected, because vertical glass panes do not resemble the horizontal surface of waters, from which these insects emerge and to which they must return to oviposit.

It is still unknown which parts of the eye in *H. pellucidula* are polarization sensitive. According to the laboratory experiments of Kriska et al. (2008), it is known that ovipositing female *H. pellucidula* have positive polarotaxis, if the ventral region of their eyes is stimulated by horizontally polarized light. If the eye of *H. pellucidula* had only a ventral polarization-sensitive eye region, then a flying *H. pellucidula* could be attracted by polarized light to a vertical glass surface only, if the insect approached the glass at an appropriately large (a few metres) height from the ground. Only in this case could the horizontally polarized glass-reflected light stimulate the ventral eye region: Then the light originating from the ground is reflected from the vertical glass surface towards the eyes of the flying insect. This glass-reflected groundlight is always nearly horizontally polarized, because the direction of reflection is then always approximately vertical (see

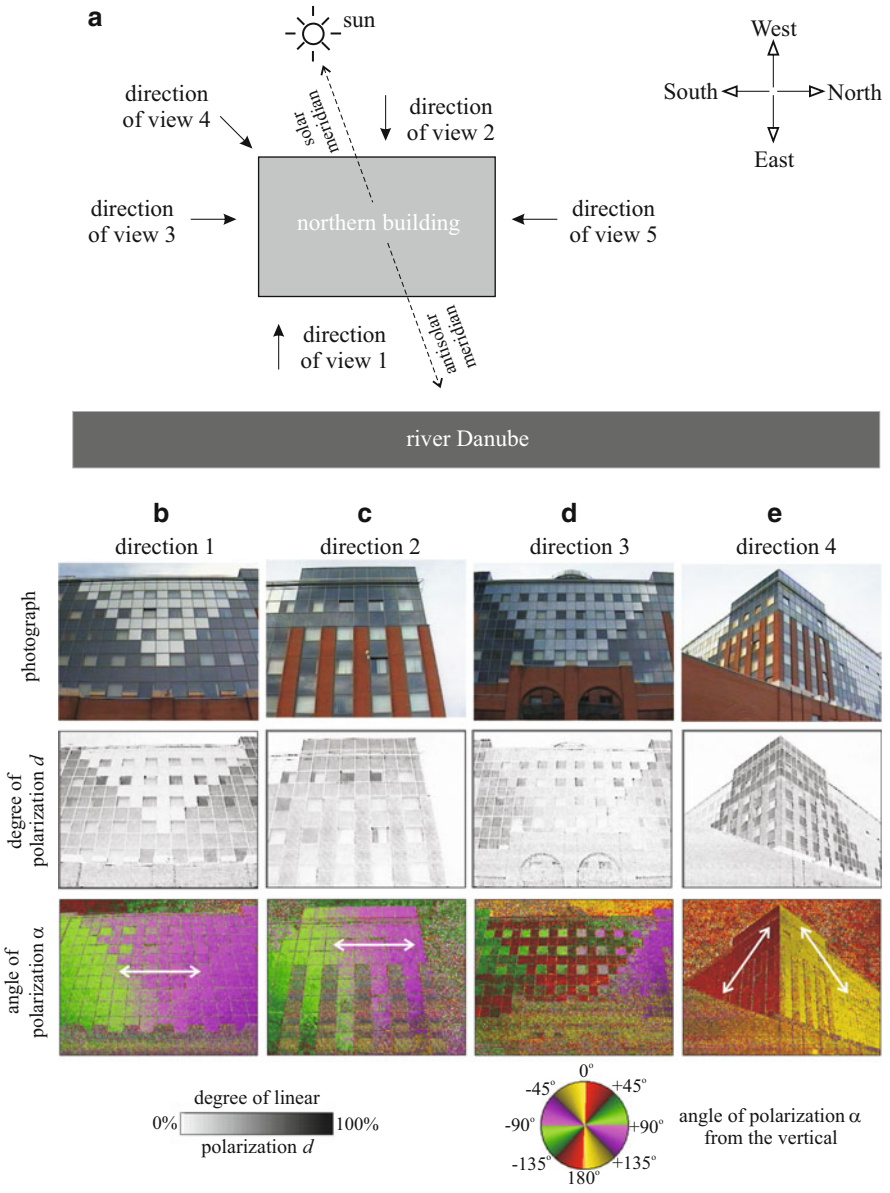

Fig. 20.27 (**a**) Geometry of the northern building of the Eötvös University on the bank of the river Danube in Budapest (Hungary) with directions of view 1, 2, 3, 4 and 5 of the polarimeter. (**b**–**e**) Photograph and patterns of the degree of linear polarization d and angle of polarization α (clockwise from the vertical) of the northern building, at the vertical glass surfaces of which *Hydropsyche pellucidula* caddisflies swarmed. In the α-patterns the *double-headed arrows* show the average directions of polarization of light reflected from the vertical glass surfaces. The reflection–polarization patterns were measured in the green (550 nm) part of the spectrum, and they were practically the same as those in the red (650 nm) and blue (450 nm) spectral ranges. During the measurements the sky was clear and cloudless, the sun was shining and the solar elevation

Sect. 20.6). Kriska et al. (2008) observed that the height of the swarms of *H. pellucidula* at the buildings was always larger than a few metres.

Caddisflies usually move away from their emergence sites only at distances from which they can see the horizontally polarized water-reflected light. However, *H. pellucidula* swarmed also on those sides of the investigated buildings, from which the river Danube was not visible (Kriska et al. 2008). The reason for this may partly be that all glass surfaces of the buildings can reflect horizontally polarized light (see above and also Sect. 20.6) and thus can be attractive to polarotactic caddisflies. Since the caddisflies swarming at the riverside of the buildings still see the river surface, there is a chance that some of the fertilized females return to the river to oviposit. On the other hand, since the caddisflies swarming at the opposite side of the buildings do not see the river, they remain near the water-imitating horizontally polarizing glass surfaces, where they necessarily dry out or become trapped by the partly open tiltable windows and perish together with their eggs (Fig. 20.26d–f).

Actually, all such glass buildings could be ecological traps (Schlaepfer et al. 2002) for all aquatic insects, which perish together with their eggs after being trapped. Tall buildings, which are attractive to polarotactic insects because of their polarizing properties, could become 'meeting points' of these insects, bringing males and females more easily together in such 'focal areas' rather than near some scattered natural meeting places. This phenomenon could be advantageous to these insects, but only, if they do not oviposit onto the glass surfaces and/or are not trapped by the partly open windows.

20.6 Why Do Vertical Reflectors Attract Polarotactic Insects?

Kriska et al. (2008) observed that after their dusk emergence from rivers, the *Hydropsyche pellucidula* caddisflies are attracted to the vertical glass surfaces of buildings, where they swarm, land, copulate, oviposit and remain on the glass for hours (Figs. 20.25 and 20.26). The attraction of *H. pellucidula* to vertical reflectors is surprising. This is because these insects are attracted only to horizontally polarized light, while depending on the direction of view, vertical glass panes can reflect light with all possible directions of polarization. In addition, the vertical orientation of such objects would seem unmistakable for a flat body of water. Why are flying polarotactic caddisflies attracted to vertical glass surfaces? Why do these insects remain on vertical panes of glass after landing?

Malik et al. (2008) showed that both questions can be partly explained by the reflection–polarization characteristics of vertical glass surfaces and by the positive polarotaxis of caddisflies. They measured the reflection–polarization patterns of

Fig. 20.27 (continued) angle was $\theta = 9.4°$. The angle of elevation of the optical axis of the polarimeter was +35° relative to the horizontal [after Fig. 3 on page 4364 of Malik et al. (2008)]

shady and sunlit, black and white vertical glass surfaces from different directions of view under clear and overcast skies by imaging polarimetry in the red, green and blue parts of the spectrum. The light reflected from the Brewster zone (an annular region, the centre line of which is a circle at an angle of $\theta_B = 56.3^\circ$ from the normal vector of the surface, where $\theta_B = \arctan n$ is the Brewster angle for the refractive index $n = 1.5$ of glass) of vertical glass surfaces is maximally polarized, and the direction of polarization of light reflected from the Brewster zone can be horizontal, tilted or vertical. The darker a glass surface, the higher is the degree of polarization d of reflected light. In Fig. 20.27 the d-pattern of building's walls is patchy, because d of reflected light depends both on the brightness and the tiltedness of the reflecting surface. Depending on the direction of view, certain parts of the skylit and/or sunlit vertical glass surfaces of the building reflect horizontally polarized light, while other regions reflect obliquely or vertically polarized light (Fig. 20.27). According to the measurements of Malik et al. (2008), buildings with vertical glass surfaces have always such parts, from which nearly horizontally polarized light is reflected for both low and high solar elevations. Thus, glass buildings near waters can attract not only aquatic insects swarming near sunset but also polarotactic insects flying during the day.

Malik et al. (2008) determined those areas of the investigated glass surfaces, which are sensed as water by a hypothetical polarotactic insect facing and flying towards (Figs. 20.28e and 20.29e) or landed on (Figs. 20.28f and 20.29f) a vertical pane of glass: The dorsoventral symmetry axis of all polarotactic aquatic insects is a distinguished reference direction, because these insects are attracted to light, whose direction of polarization is exactly or nearly perpendicular to this axis, while light with direction of polarization parallel or tilted to this axis is unattractive (Schwind 1985a, 1991, 1995; Horváth and Varjú 2004). Such polarotactic aquatic insects consider as water only those areas that reflect light with degrees of polarization d higher than the threshold d^* of their polarization sensitivity and with angles of polarization α differing from the direction perpendicular to their dorsoventral symmetry plane by less than a certain threshold $\Delta\alpha^*$ in that part of the spectrum, in which the polarization of reflected light is perceived. Therefore, a hypothetical polarotactic aquatic insect was assumed to take those areas of a vertical glass surface for water, from which light is reflected under the following two conditions: (1) $d > d^* = 10\,\%$, and (2) deviation $|\alpha - 90^\circ|$ of the angle of polarization α from the direction normal to the insect's dorsoventral symmetry axis is smaller than $\Delta\alpha^* = 5^\circ$ (Malik et al. 2008). The whole eye of this hypothetical aquatic insect was assumed to be polarization sensitive. The quantity 'percentage W of a vertical glass surface detected as water' was defined, which is the angular proportion W of the viewing directions (relative to the angular extension of the field of view containing the reflecting glass surface) for which both conditions are satisfied. In other words, W gives the proportion of the field of view in which the vertical glass surface is sensed as water by polarization. The higher the W-value for a vertical glass surface, the larger its attractiveness to water-seeking polarotactic aquatic insects. At a given glass surface, the values of W were calculated for two situations: (1) A polarotactic aquatic insect was assumed to face and fly towards the vertical glass surface (Fig. 20.30). Since in this case the dorsoventral symmetry axis of the insect's head is vertical, α was measured from the vertical (Figs. 20.28c

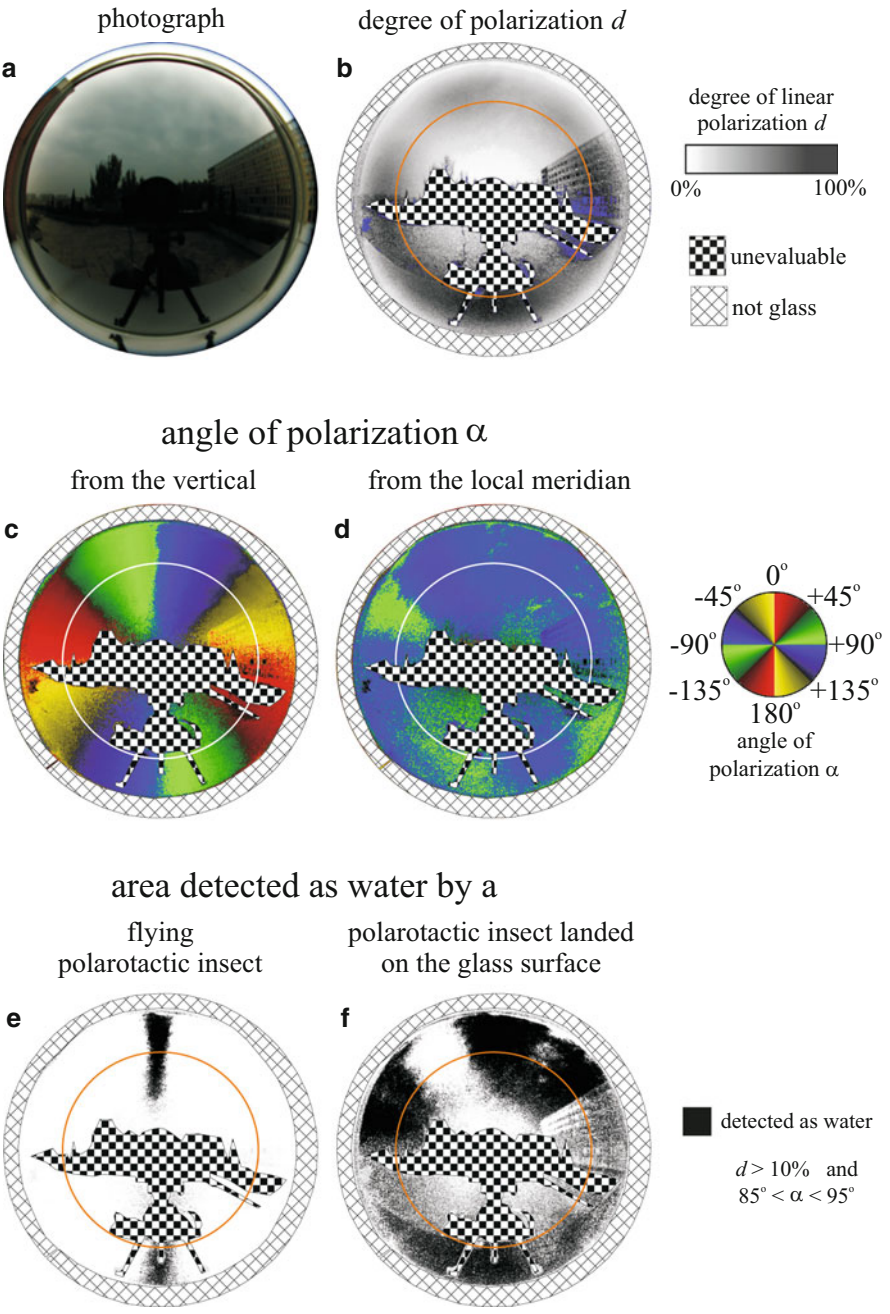

Fig. 20.28 Photograph (**a**) and patterns of the degree of linear polarization d (**b**) and the angle of polarization α (**c**, **d**) of a black vertical glass surface measured by 180° field-of-view imaging polarimetry in the blue (450 nm) part of the spectrum under a totally overcast sky. Angle α of reflected light is measured clockwise from the vertical (**c**) or from the local meridian passing through the point observed (**d**). (**e**) Area (*black*) of the vertical glass surface detected as water by a hypothetical polarotactic aquatic insect flying perpendicularly to the glass. (**f**) Area (*black*) of the

and 20.29c). (2) A polarotactic aquatic insect was assumed to be landed on the vertical glass surface, and the insect faced in an arbitrary direction parallel to the glass (Fig. 20.31). Since the dorsoventral symmetry axis of the insect's head is always perpendicular to the glass surface, α was measured from the local meridian passing through the observed point of the glass surface (Figs. 20.28d and 20.29d). This meridian is always perpendicular to the glass surface.

To a flying polarotactic aquatic insect, only the strongly and exactly or nearly horizontally polarizing areas of a vertical glass surface can be attractive. Thus, only two narrow, approximately vertical elongated patches of shady black and white vertical glass surfaces can be attractive to such an insect (Figs. 20.28e and 20.29e), because only these glass regions reflect exactly or approximately horizontally polarized light with high enough d (Fig. 20.30). The other parts of the vertical shady glass surfaces are unattractive to flying polarotactic insects, because the polarization of light reflected by them is not horizontal and/or not strong enough (Fig. 20.30).

When a polarotactic aquatic insect is landed on the vertical glass surface and looks into an arbitrary direction parallel to the glass, the insect's dorsoventral symmetry plane is always perpendicular to the glass surface (Fig. 20.31). Then the direction of polarization of light reflected from a vertical black glass surface is practically always exactly or approximately parallel to the glass (Fig. 20.28d), while the direction of polarization of light reflected from a vertical white glass surface can be perpendicular, tilted or parallel to the glass (Fig. 20.29d). The areas of vertical shady black and white glass surfaces sensed polarotactically as water by an aquatic insect landed on the glass are placed along the Brewster zone (Figs. 20.28f and 20.29f). On the other hand, almost the whole surface of sunlit white vertical glass surfaces is not detected polarotactically as water (Malik et al. 2008).

Considering the proportion W of a vertical glass surface detected as water by a hypothetical polarotactic aquatic insect flying towards or landed on the glass, Malik et al. (2008) established the following trends: (1) At a given sky condition (clear or overcast) and in a given spectral range (red, green, blue), W of a polarotactic insect is higher for a black glass than that for a white one, especially for an insect landed on the glass. (2) At a given glass surface and spectral range, W is larger under an overcast sky than under a clear sky. (3) W is lowest for sunlit white vertical glass surfaces. (4) W is much larger for a polarotactic insect landed on a given vertical glass surface (Figs. 20.28f and 20.29f) than that for an insect facing and flying towards the same glass (Figs. 20.28e and 20.29e). (5) W more or less depends on the wavelength of light under clear sky conditions due to the blueness of skylight.

Fig. 20.28 (continued) vertical glass surface detected as water by a hypothetical polarotactic insect landed on the glass. The insect was assumed to consider a surface as water, if the reflected light has the following polarization characteristics: $d > 10$ % and $85° < \alpha < 95°$. It was also assumed that the insect's entire eye is polarization sensitive. In the circular patterns **b–f**, the Brewster angle is shown by *circles*. The horizontal optical axis of the polarimeter passes through the centre of a given circular pattern, the perimeter of which represents angles of view perpendicular to the optical axis [after Fig. 6 on page 4366 of Malik et al. (2008)]

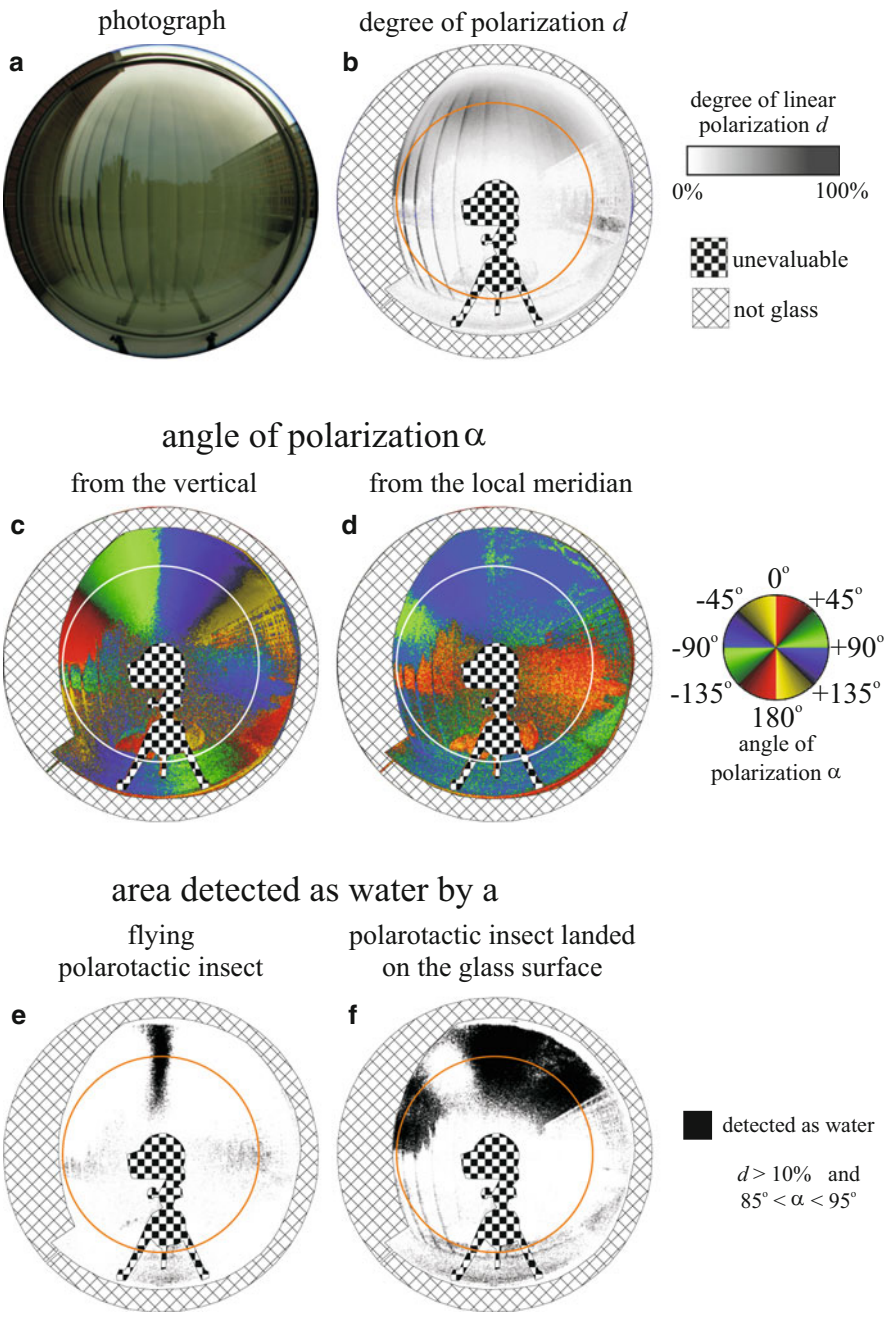

Fig. 20.29 As Fig. 20.28 for a white vertical glass surface under a totally overcast sky [after Fig. 8 on page 4367 of Malik et al. (2008)]

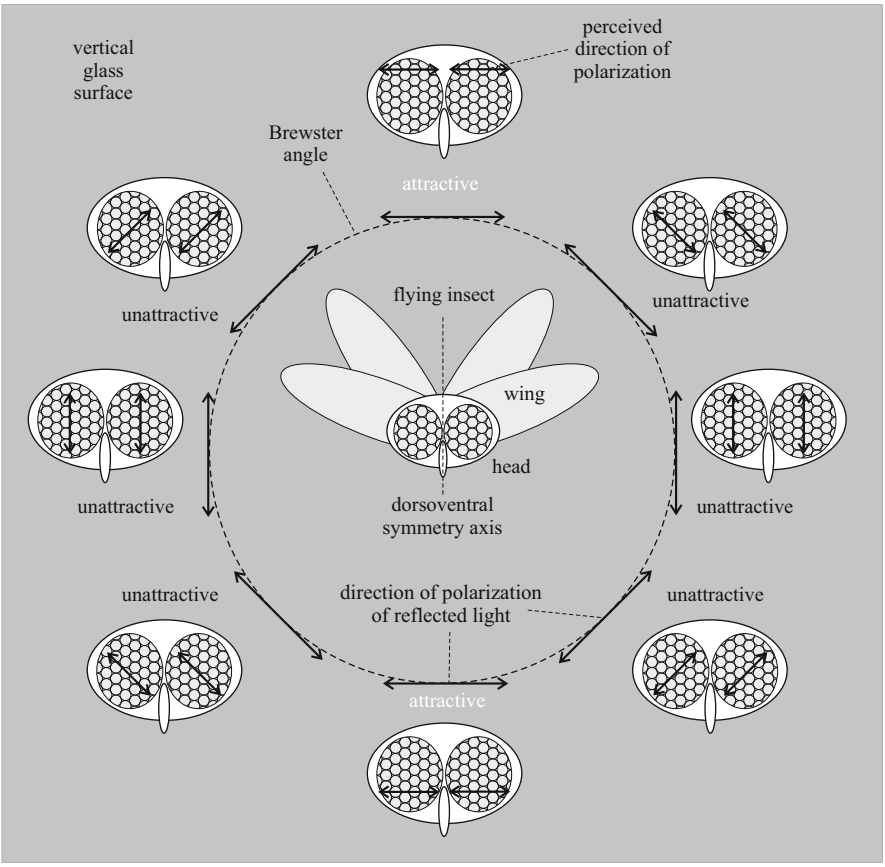

Fig. 20.30 How a flying polarization-sensitive insect approaching perpendicularly to a vertical glass surface perceives the direction of polarization (*double-headed arrows*) of light reflected from the glass at the Brewster angle (*dashed circle*). A polarotactic aquatic insect is attracted to the reflected light only, if the perceived direction of polarization is exactly or nearly perpendicular to its dorsoventral symmetry axis. If the perceived direction of polarization is parallel or tilted to this symmetry axis, the reflected light is unattractive to the insect [after Fig. 11 on page 4370 of Malik et al. (2008)]

20.6.1 Why Are Polarotactic Caddisflies Attracted to Vertical Glass Surfaces?

The black vertically elongated areas in Figs. 20.28e and 20.29e show those regions of the investigated vertical black and white glass surfaces, which are sensed as water by a flying polarotactic aquatic insect, the entire eye of which is assumed to be polarization sensitive: These black areas are very attractive to a flying polarotactic aquatic insect, if they fall within the field of view of the insect's polarization-sensitive eye region. This can be one of the reasons why after their

emergence from the river Danube, the polarotactic flying *H. pellucidula* can be lured to the glass-covered vertical walls of buildings on the river bank.

The proportion W of the vertical glass surface sensed as water by a flying polarotactic insect is higher for black glass surfaces than for white ones (Malik et al. 2008). Thus, black and dark grey vertical panes of glass are more attractive to polarotactic caddisflies than white and light grey ones. This explains the observation of Kriska et al. (2008) that strongly polarizing vertical dark glass surfaces were significantly more attractive to both female and male *H. pellucidula* than weakly polarizing bright ones (Fig. 20.25b; see Sect. 20.5).

However, the attraction of *H. pellucidula* to vertical glass surfaces can be only partly explained by the reflection–polarization characteristics of vertical glass reflectors and by the positive polarotaxis of caddisflies. The marker effect of the dark silhouettes of buildings against the bright sky and the positive phototaxis elicited by the room lights at dusk can also result in that caddisflies are lured to buildings. Other important factors may be the air temperature and humidity and furthermore the strength and direction of wind. All these environmental parameters are more or less influenced around buildings and thus surely affect the swarming of caddisflies. Kriska et al. (2008) also observed that *H. pellucidula* do not swarm at and do not stay for a longer period at/on sunlit and windy glass surfaces, because they can dry out easily and cannot fly in strong wind.

20.6.2 Why Do Polarotactic Caddisflies Remain on Vertical Glass Surfaces After Landing?

Figure 20.31a schematically shows a light beam reflected from a vertical glass surface and received by the ventral eye region of an insect landed on the glass. If the ventral eye region of this insect is polarization sensitive, it perceives the polarization patterns shown in Figs. 20.28b, d and 20.29b, d and senses more or less areas of the glass surface as water (Figs. 20.28f and 20.29f). Figure 20.31b represents how such a polarotactic insect landed on a vertical glass surface and looking into different directions senses the direction of polarization of light reflected from the glass at the Brewster angle. Since the perceived direction of polarization is always perpendicular to the insect's dorsoventral symmetry axis, independently of the direction of view, the light reflected from the Brewster angle is always attractive to the insect, if it has positive polarotaxis. The proportion W of the vertical glass surface sensed as water by a landed polarotactic insect is much higher for a black glass than for a white one, because dark glass surfaces are much stronger polarizers than bright ones (Malik et al. 2008). This is one of the reasons for why *H. pellucidula* observed by Kriska et al. (2008) remained for hours on dark vertical glass surfaces after landing and why vertical dark glass surfaces were significantly more attractive to *H. pellucidula* than bright ones (Fig. 20.25b; see Sect. 20.5).

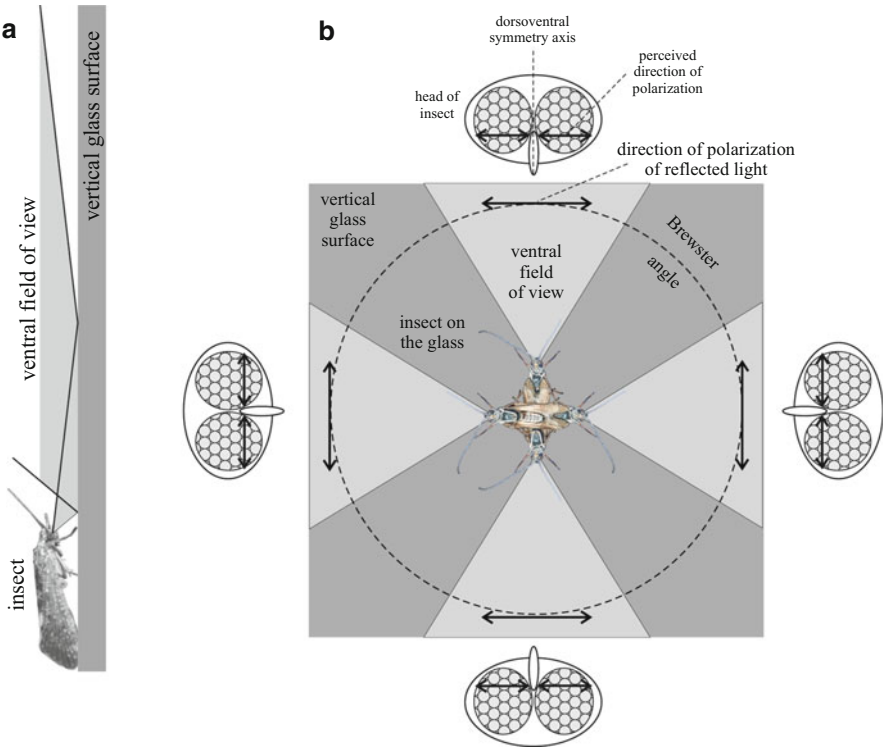

Fig. 20.31 (**a**) Side view of a light beam (*light grey*) reflected from a vertical glass surface and received by the ventral eye region of an insect landed on the glass. (**b**) How a polarization-sensitive insect landed on a vertical glass surface and looking into different directions (here only four such directions are shown) perceives the direction of polarization (*double-headed arrows*) of light reflected from the glass at the Brewster angle (*dashed circle*). Since the perceived direction of polarization is always perpendicular to the insect's dorsoventral symmetry axis (independently of the direction of view), the light reflected from the Brewster angle is always attractive to a polarotactic aquatic insect landed on the glass [after Fig. 12 on page 4371 of Malik et al. (2008)]

20.6.3 The 'Greenest' Buildings Considering Aquatic Insect Protection

Because even vertically oriented artificial polarizers like glass buildings can be ecological traps (Schlaepfer et al. 2002; Robertson and Hutto 2006; Horváth and Kriska 2008) for mass-swarming caddisflies, conservationists, planners and architects interested in 'disarming' these ecological traps or preventing their creation in the first place require some guidelines. Malik et al. (2008) recommended the following optical characteristics of 'green' buildings (those which produce minimal PLP):

- A ‘green’ building minimizes the used glass surfaces. All unnecessary panes of glass should be avoided that would have only an ornamental function. In a building practically the only necessary glass surfaces are the windows.
- A ‘green’ building avoids bricks with shiny-appearing, that is, smooth surfaces. The optimal is the use of bricks with matte surfaces.
- A ‘green’ building avoids the use of shiny (smooth) dark surfaces. The windows of dark rooms can also attract polarotactic insects. If the bright curtains are drawn in, the degree of polarization of light reflected from the window is considerably reduced, and thus the window becomes unattractive to polarotactic insects.
- A ‘green’ building avoids the use of shiny red surfaces, the attraction of which to polarotactic insects is similar to that of shiny black surfaces (see Sect. 20.9).
- The walls of a ‘green’ building must not be too bright either, because near and after sunset bright surfaces reflect a large amount of city light, which can also lure insects by phototaxis. The optimal compromise is the use of medium grey and matte surfaces, which reflect light only moderately with a weak and usually non-horizontal polarization.

20.7 Urban Birds Exploit Insects Trapped by the Polarized Light Pollution of Glass Buildings

Glass buildings can strongly and horizontally polarize reflected sunlight and skylight, fooling polarotactic aquatic insects into thinking they are exaggerated water surfaces and high-quality breeding habitat. Kriska et al. (2008) and Malik et al. (2008) have observed that caddisflies (*Hydropsyche pellucidula*) are lured to swarm *en masse* at dusk at vertical glass surfaces of buildings standing on the bank of the river Danube (Fig. 20.25). Individuals land upon the glass panes where they mate and oviposit (Fig. 20.26), actually preferring this artificial substrate to the nearby river. Eggs experience complete mortality (Kriska et al. 2008), and most adults are unable to escape by overcoming their attraction to the polarized light signature of the building’s glass surfaces and die of exhaustion, a phenomenon known as the polarization captivity effect (Horváth et al. 2009).

Robertson et al. (2010) observed that four urban generalist bird species (white wagtail, *Motacilla alba*; house sparrow, *Passer domesticus*; great tit, *Parus major*; European magpie, *Pica pica*) are able to supplement their diet by taking advantage of an atypical prey species, caddisflies (*Hydropsyche pellucidula*) caught by glass-reflected polarized light of buildings on the bank of the river Danube (Fig. 20.32). In natural environments, caddisflies emerge from bodies of water, where they swarm, copulate and lay only a single clutch of eggs on the water surface before dying (Hoell et al. 1998). Patterns of reproductive behaviour near the artificial polarizing surfaces of buildings parallel this pattern.

According to the observations of Robertson et al. (2010), white wagtails typically perched on the building’s ledges or high on the roof edge from which they

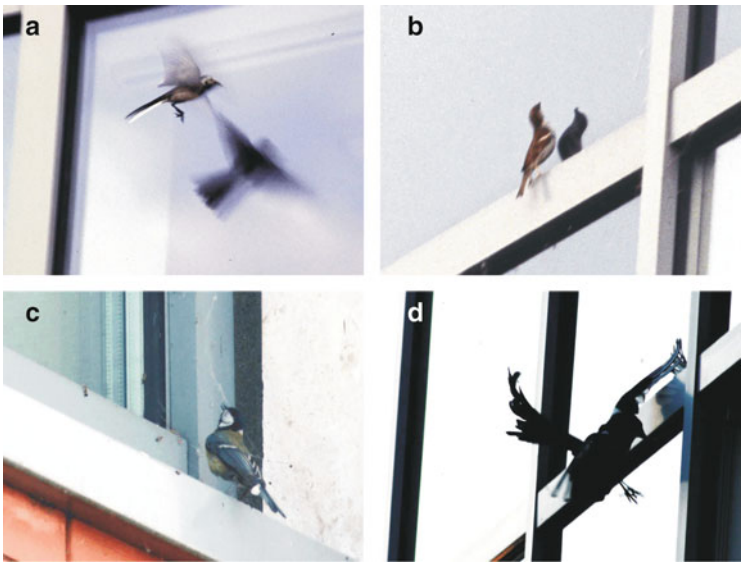

Fig. 20.32 (**a**) Hovering white wagtail (*Motacilla alba*) catching caddisflies from a window. (**b**) House sparrow (*Passer domesticus*) capturing caddisflies from a vertical glass surface. (**c**) Great tit (*Parus major*) standing on a window's edge and catching caddisflies. (**d**) European magpie (*Pica pica*) on wing capturing landed caddisflies from a window [after Fig. 2 on page 287 of Robertson et al. (2010)]

flew up to hover–glean caddisflies from window surfaces (Fig. 20.32a). Individuals appeared to move systematically to a new pane of glass after exhausting the supply of prey upon their closest pane. Wagtail individuals remained at a single location for several minutes before flying up to glean a caddisfly from the glass. House sparrows (Fig. 20.32b) and great tits (Fig. 20.32c) exhibited similar foraging techniques for capturing caddisflies. Individuals stood on the narrow metal window frames surrounding each glass pane while closely focusing their attention on caddisflies upon the glass above them (Fig. 20.32b, c). Unlike wagtails, great tits and house sparrows were never observed to catch flying caddisflies. White wagtails, house sparrows and great tits were frequently observed with their bill full of captured caddisflies, indicating that prey were being collected to provision young.

Using a web camera, Robertson et al. (2010) documented the occurrence of European magpies attracted by the caddisflies swarming at and landing on the building's glass surfaces. Magpies settled on the horizontal surface of the building edge and picked up the caddisflies from the surface of the horizontal ledge but were also observed to glean prey from the vertical glass panes while in flight (Fig. 20.32d). After repeated successful captures, magpies were often observed to move to the next adjacent windowpane before resuming foraging. The timing of magpie visits to ledges was non-random and exhibited a bimodal pattern of visits peaking around dawn and sunset (Fig. 20.33).

This daily pattern of avian foraging behaviour indicates birds regularly visit strongly and horizontally polarizing glass buildings to feed on attracted polarotactic

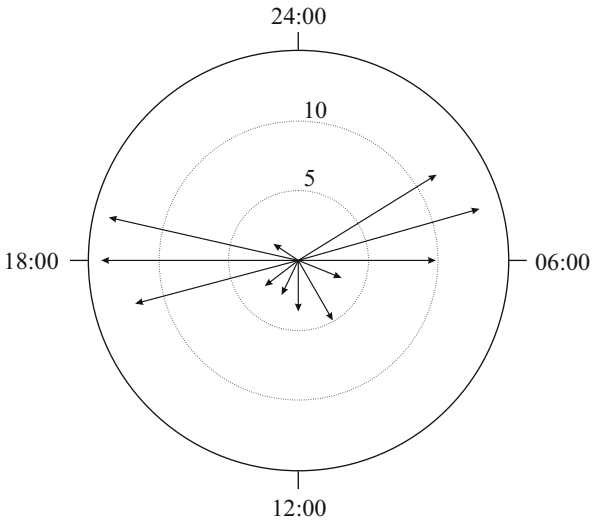

Fig. 20.33 Timing of foraging visits of European magpie (*Pica pica*) to the northern building of the Eötvös University as detected by a web camera from 17:00 h on 16 May to 20:00 h on 23 May in 2007. *Arrow lengths* represent the proportion of all visits made during a particular hour over the course of the 8-day observation time (scale = 0–15 %) [after Fig. 3 on page 288 of Robertson et al. (2010)]

caddisflies near sunrise and sunset. Foraging behaviours used by terrestrial land birds to collect caddisflies were typical of those used in more natural environments (Madge and Burn 1994; Harrap and Quinn 1996; Badyaev 2003; Anderson 2006). The link between caddisfly abundance on glass panes and the darkness of glass panes on this building (see Sect. 20.5) demonstrates that some portions of the structure are less attractive to caddisflies and so may also be to birds.

This was the first example of exploitation of a species that is victim of polarized light pollution (Horváth et al. 2009). Robertson et al. (2010) demonstrated the ability of polarized light pollution to create novel predator–prey interactions, a phenomenon that may be a common and widespread occurrence where polarizing structures are built near freshwater. Because birds are consuming prey that will eventually experience reproductive and adult mortality associated with the polarized light trap, this scenario appears to represent a clear case of compensatory mortality (Errington 1946). The predator–prey interactions observed by Robertson et al. (2010) are qualitatively similar to the hunting of insects attracted to streetlamps at night by anuran amphibians (Buchanan 2006), reptiles (Perry and Fisher 2006), birds (Eisenbeis 2006), bats (Rydell 2006) and spiders (Frank 2006), a well-known secondary effect of conventional (nonpolarized) ecological light pollution.

The findings of Robertson et al. (2010) represent a case of animal innovation: Although the birds did not use novel behavioural techniques, they exploited a novel source both in terms of prey species and foraging site. If this is a geographically widespread phenomenon, as was suggested (Robertson et al. 2010), it might be a significant factor affecting urban bird ecology and even conservation. For example, increasing densities of nest predators (e.g. magpies) could have detrimental effects on the reproductive success of other urban-nesting birds. Alternatively, higher densities of non-native cavity-nesting birds (e.g. house sparrows) could increase competition for nest sites with native birds.

20.8 Ecological Traps for Dragonflies in a Cemetery: Attraction of *Sympetrum* species by Horizontally Polarizing Black Gravestones

Horváth et al. (2007) observed that both sexes (matures or juveniles) of the dragonfly species *Sympetrum flaveolum*, *S. striolatum*, *S. sanguineum*, *S. meridionale* and *S. danae* were attracted by polished black gravestones in a cemetery in Kiskunhalas (Hungary) without any waterbody (Fig. 20.34). Tombstones preferred by these dragonflies had an area of at least 0.5 m^2 with an almost horizontal, polished, black surface, the sky was open above them and there was at least one perch in their immediate vicinity. The dragonflies displayed the same behaviour as at water surfaces (Oehme 1999): (1) They perched persistently in the immediate vicinity of the chosen gravestones and defended their perch against other dragonflies. (2) Flying individuals repeatedly touched the horizontal surface of the shiny black tombstones with the ventral side of their body. (3) Pairs in tandem position frequently circled above black gravestones.

Using imaging polarimetry, Horváth et al. (2007) found that the black gravestones, like smooth water surfaces, reflect strongly and horizontally polarized light (Fig. 20.35). Gravestones reflected strongly and nearly horizontally polarized light, if their surface was shiny (smooth), black or dark grey and approximately horizontal. The smoother and/or the cleaner was the surface of a gravestone, the higher was the degree of linear polarization d of reflected light. The direction of polarization of light reflected from a tombstone was always perpendicular to the plane of reflection, i.e. it was horizontal, if the gravestone's reflecting surface was horizontal. Vertical tombstone surfaces can reflect horizontally, obliquely and vertically polarized light. Gravestones with matte and/or bright and/or non-horizontal surfaces reflect light with low degrees of polarization and/or with non-horizontal direction of polarization.

In the cemetery, Horváth et al. (2007) performed double-choice field experiments with various horizontal test surfaces (1 m × 1 m, shiny black plastic sheet, shiny white plastic sheet, aluminium foil, matte black cloth, matte white cloth, matte light brown wooden board) laid onto the ground. At every corner of each test surface, a thin wooden stick was stuck vertically into the ground. These sticks functioned as perches for the dragonflies, the behaviour of which was observed at the test surfaces. The number, position and illumination (sunlit or shaded) of the dragonflies sitting on the ($2 \times 4 = 8$) perches at the test surfaces were recorded. The duration and the numbers of occurrence of the following five typical behavioural elements were measured: (1) *perching* (Fig. 20.34a–e), (2) *feeding*, (3) *attacking*, (4) *tandem flight* and (5) *surface touching* (Fig. 20.34f). All dragonflies definitely preferred sunny perches, independently of the underlying test surface. Ectothermic dragonflies, for thermoregulatory reasons, usually prefer sunlit places (Corbet 1999, pp. 285–291) enabling them quick starts for sallies towards prey or approaching conspecifics (Moore 1991; Oehme 1999).

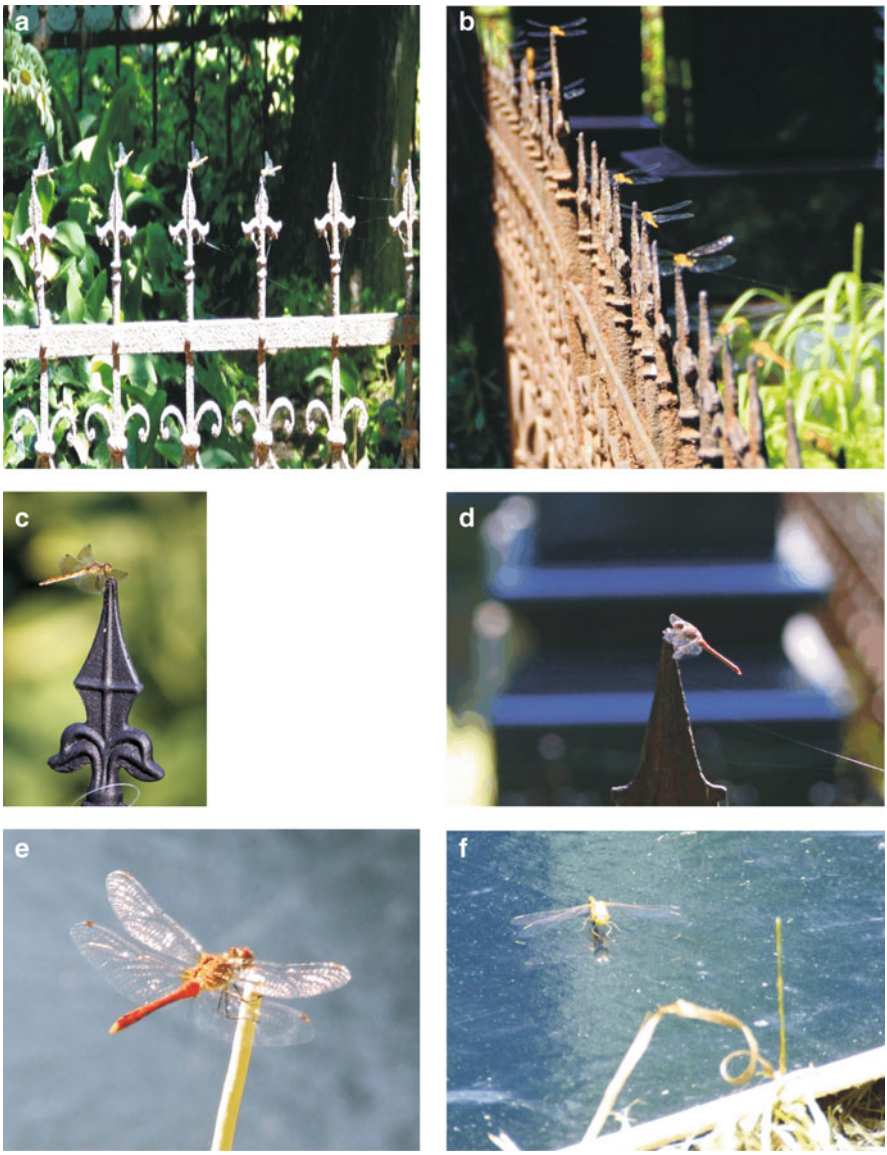

Fig. 20.34 (**a**, **b**) Male and female *Sympetrum* dragonflies perching on the tips of sunlit iron railings in a cemetery in the Hungarian town Kiskunhalas. (**c**–**e**) Male *Sympetrum* dragonflies perching near polished black tombstones. (**f**) A female *Sympetrum* dragonfly displaying touching behaviour at the shiny black plastic sheet used in the double-choice experiments of Horváth et al. (2007). The photo shows the brief moment when the female touches the test surface with her legs and ventral body side [after Fig. 1 on page 1703 of Horváth et al. (2007)]

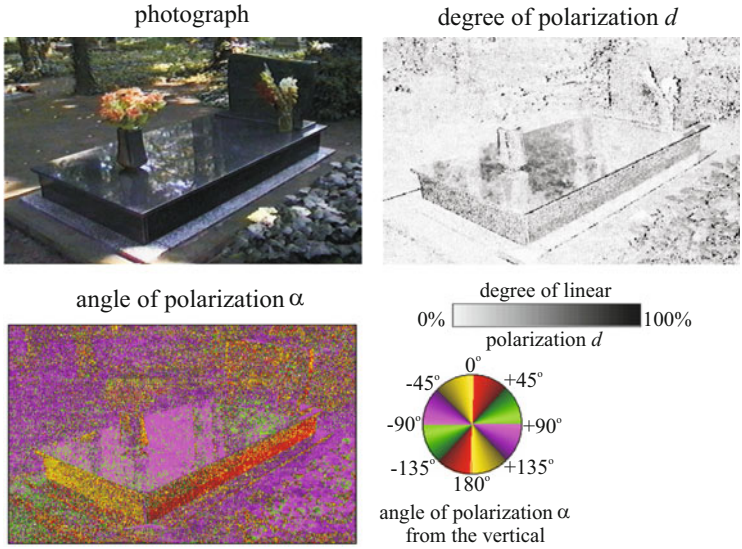

Fig. 20.35 Reflection–polarization characteristics of a horizontal black polished gravestone in the shade of trees, illuminated by light from a clear sky measured by imaging polarimetry in the green (550 nm) part of the spectrum. The angle of elevation of the optical axis of the polarimeter was −30° with respect to the horizontal [after Fig. 3 on page 1704 of Horváth et al. (2007)]

At the shiny black plastic sheet, the total perching time was 2.5–7 times (statistically significantly) longer than at all other test surfaces. There were no statistically significant differences in the number of feeding events between the shiny black plastic sheet and any other test surface. The number of attacks was 6–12 times (statistically significantly) higher at the shiny black plastic sheet than at the other test surfaces. Both tandem flights and touching were observed only at the black plastic. Dragonflies frequently touched the horizontal surface of dark grey or black gravestones, like the water surface under natural conditions (Corbet 1999, p. 19). Since this touching occurred only at shiny dark grey or black tombstones, Horváth et al. (2007) concluded that *Sympetrum* species mistook the horizontal surface of these gravestones for water.

It was obvious that the shiny black plastic sheet, the polarizing ability of which was similar to that of the horizontal parts of shiny black gravestones, was much more attractive to dragonflies than the other test surfaces. Only the shiny black plastic sheet reflected strongly and horizontally polarized light; the other test surfaces reflected unpolarized or weakly and non-horizontally polarized light. Since the shiny black plastic was much more attractive than the matte black cloth, simple negative phototaxis (i.e. an attraction to dark surfaces) could not explain the observed behaviour of dragonflies. Because the shiny black plastic was much more attractive than the shiny white plastic, the matte white cloth and the aluminium foil, positive phototaxis of dragonflies was also excluded. From these Horváth et al. (2007) concluded that the *Sympetrum* dragonflies attracted to shiny black tombstones possess positive polarotaxis, that is, they detect water by means of the horizontally polarized light

reflected from water surfaces as many other dragonfly species (Wildermuth 1998; Horváth et al. 1998). This and the reflection–polarization characteristics of black gravestones explained why these dragonflies were attracted to black tombstones. If females attracted to the black gravestones oviposit on them, the latter constitute an ecological trap *sensu* Schlaepfer et al. (2002) for dragonflies that are not close to water, thus reducing the insects' individual fitness.

Sympetrum dragonflies recognize each other or their prey most easily from below, i.e. when the target shows against the sky as a uniform and bright background (Labhart and Nilsson 1995). This explains why the dragonflies mostly choose gravestones without overhanging foliage. Another reason may be that perches near a gravestone in the open are more likely to be sunlit (and therefore desired) than those under trees. Black horizontally aligned tombstones that are surrounded by low vegetation mimic well the optical characteristics of open water bodies even not larger than a few square metres. They typically attract dragonflies such as certain *Sympetrum* species that preferentially breed in small bodies of still water. Therefore, black gravestones may elicit oviposition.

Although these dragonflies occurred in numbers and presumably stayed for longer periods in the cemetery, it should be studied in the future to what degree their reproductive success could be diminished by the described ecological trap. The deception of *Sympetrum* species by gravestones in the cemetery at Kiskunhalas is not unique. It has also been noticed in a graveyard in Sopron (Hungary) and in the cemetery of Teichland (Brandenburg, Germany) with *Sympetrum depressiusculum* involved (Tomy Gottfried, 2007, personal communication).

20.9 The 'Greenest' Car Is White and Dirty: Attraction of Aquatic Insects to Horizontally Polarizing Car Paintwork

Aquatic insects are frequently observed to land on red cars (Jäch 1997; Nilsson 1997; van Vondel 1998; Kriska et al. 1998; Bernáth et al. 2001b), which was explained by the shiny appearance and/or the red colour of the car body (Jäch 1997; Nilsson 1997) or was considered enigmatic (van Vondel 1998). Water insects (e.g. Coleoptera and Heteroptera) often swarm in large numbers, mate above and land on the roofs, bonnets and boots of black or red cars, and Ephemeroptera and Odonata females frequently lay their eggs *en masse* on these car surfaces (Fig. 20.36). Although different insect species associated with water have been observed to swarm above cars, particularly the landing of water insects on red cars drew the attention of researchers studying water insect migration (Jäch 1997; Nilsson 1997; van Vondel 1998).

To reveal the visual ecological reasons for the previously perplexing question of why do red cars lure aquatic insects, Kriska et al. (2006a) monitored the numbers of aquatic beetles and bugs (1,059 Coleoptera and 170 Heteroptera specimens, representing 30 Coleoptera and 7 Heteroptera taxa, collected manually by insect

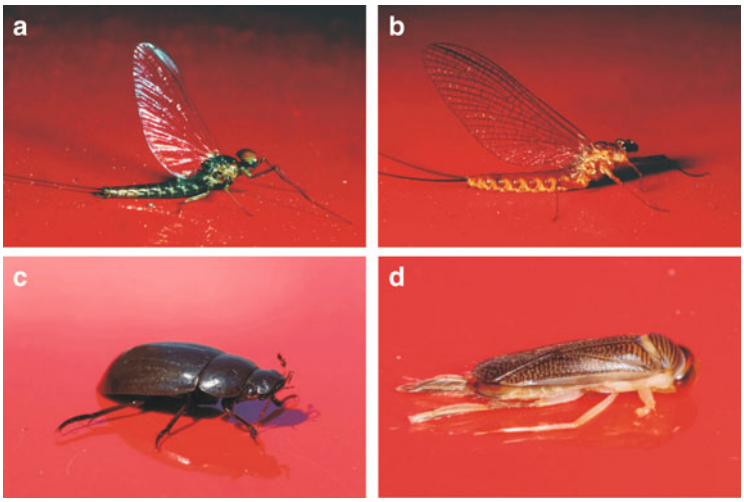

Fig. 20.36 Insects associated with water landing on the roof of a red car. (**a**) A male mayfly (*Baetis* sp.). (**b**) Another mayfly (*Epeorus assimilis*). (**c**) A scavenger beetle (*Hydrochara caraboides*). (**d**) A water bug (*Sigara striata*). The insects were observed and photographed in April and May 2005 in Hungary on the roof of the same red car [after Fig. 1 on page 1668 of Kriska et al. (2006a)]

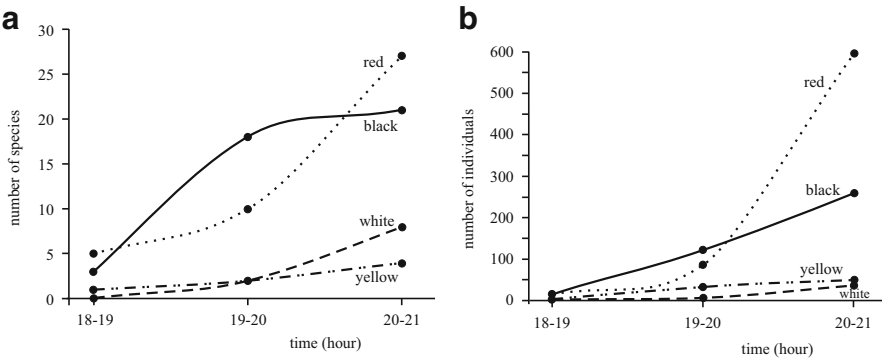

Fig. 20.37 Numbers of species (**a**) and individuals (**b**) captured on the black, red, yellow and white plastic sheets versus the time near sunset (between 18–19, 19–20 and 20–21 h = local summer time = UTC + 2 h) in the field experiment of Kriska et al. (2006a). The polynomials are fitted to the data points

aspirators and hand nets) attracted to dry horizontal shiny (smooth) red, yellow, white and black plastic sheets (9 m × 3 m) laid on the ground in a Hungarian wetland. They found that red and black reflectors are equally strongly attractive to water insects, while yellow and white reflectors are unattractive (Fig. 20.37). Since horizontal matte black, red, yellow and white clothes did not attract aquatic insects, the water insects deceived by differently coloured shiny plastic sheets were

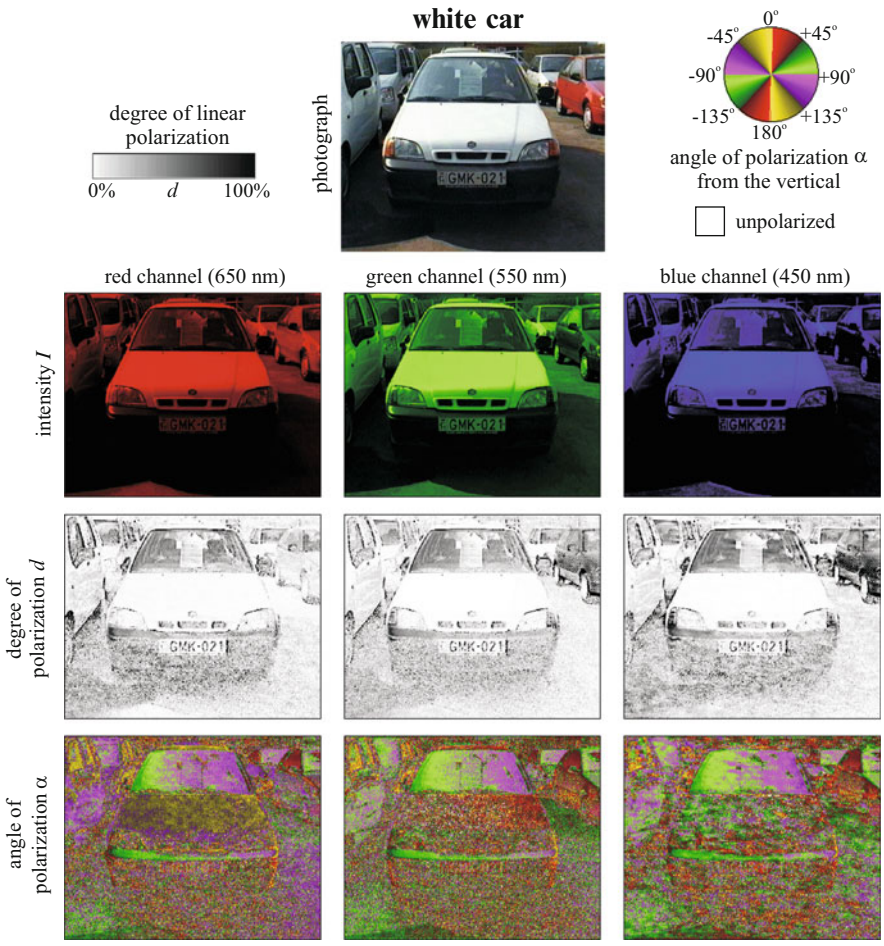

Fig. 20.38 Reflection–polarization characteristics of a white car measured by imaging polarimetry in the red (650 nm), green (550 nm) and blue (450 nm) parts of the spectrum under a clear sky at a solar zenith angle of 55°. The car was illuminated from the left-hand side by the sun. The long axis of the car and the viewing direction of the polarimeter were perpendicular to the solar meridian. The angle of declination of the optical axis of the polarimeter was −20° from the horizontal [after Fig. 3 on page 1670 of Kriska et al. (2006a)]

attracted by the horizontal polarization rather than by the colour and/or intensity of reflected light.

Kriska et al. (2006a) also measured the reflection–polarization patterns of sunlit red, yellow, white and black medium dirty (neither washed nor waxed) cars in the red, green and blue parts of the spectrum under the same illumination conditions (solar position) (Figs. 20.38, 20.39, 20.40 and 20.41). They showed that the visual deception of aquatic insects by red cars can be explained solely by the reflection–polarization characteristics of car bodies. In the blue and green part of the spectrum, the degree of linear polarization d of light reflected from red and black cars is high

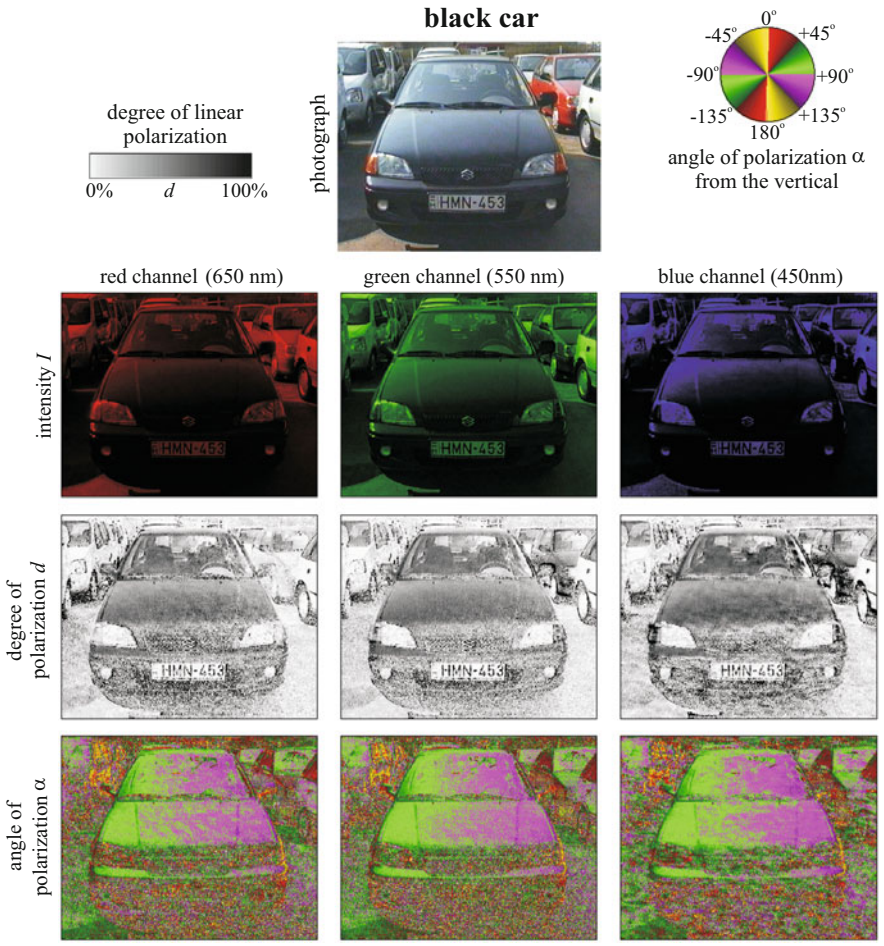

Fig. 20.39 As Fig. 20.38 for a black car

(≤42–54 %), and the direction of polarization of light reflected from red and black car roofs, bonnets and boots is nearly horizontal (Figs. 20.39 and 20.41). These parts of the bodywork mimic a water surface for the polarization-sensitive visual system of aquatic insects, for which a horizontally polarized light source is the more attractive the higher the degree of polarization (Schwind 1991, 1995; Horváth and Varjú 2004). Thus, the horizontal surfaces of red and black cars are strongly attractive to red-blind polarotactic water insects. The d of light reflected from the horizontal surfaces of yellow and white cars is very low ($d < 12$ %), and its direction of polarization is usually not horizontal (Figs. 20.38 and 20.40). Consequently, yellow and white cars are unattractive to polarotactic water insects. The direction of polarization of light reflected from the tilted windscreen and the more or less vertical side walls and windows of the cars were nearly horizontal only, if the plane of reflection was nearly vertical, that is, the incident light came from above

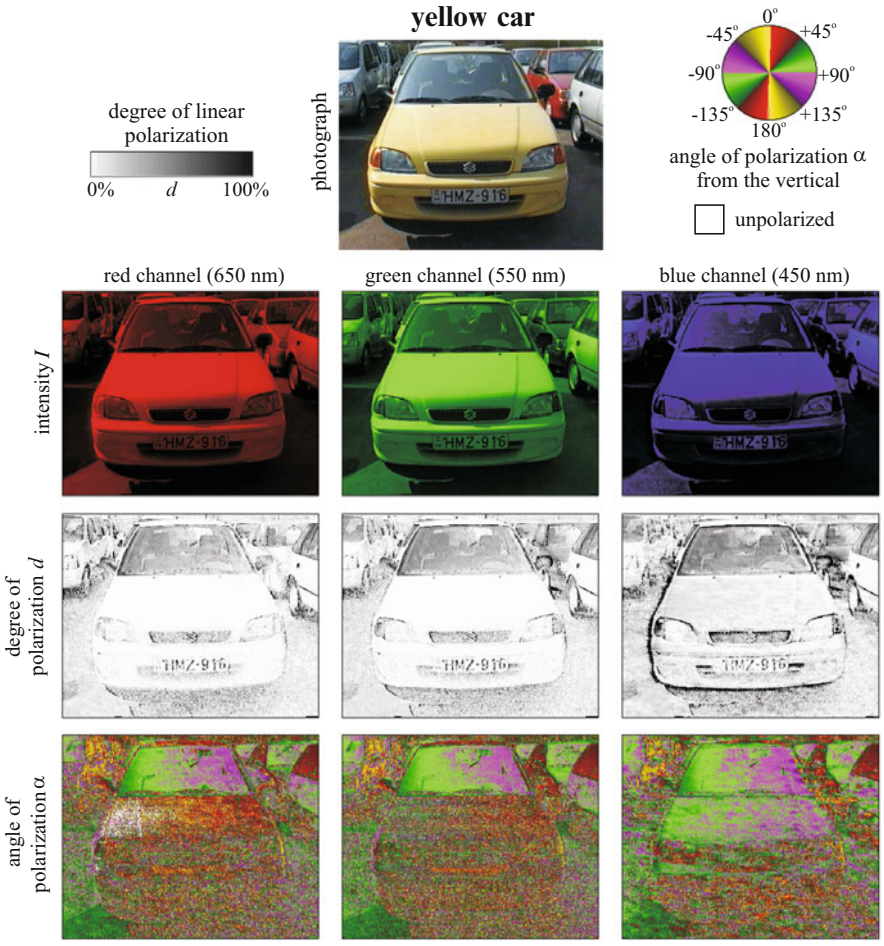

Fig. 20.40 As Fig. 20.38 for a yellow car

(Figs. 20.38, 20.39, 20.40 and 20.41). The reflection–polarization characteristics of the black, white, red and yellow horizontal plastic sheets used in the water-insect-monitoring field experiment of Kriska et al. (2006a) were similar to those of the horizontal surfaces of cars with corresponding colours.

Mizera et al. (2001) discussed the differences in the reflection–polarization between metallized and non-metallized paints of car bodies. The metallized paints influence the polarization of reflected light as do non-metallized paints because of the transparent non-metallic clearcoat. However, the reflectivity of metallized paints is high over a relatively wide spectral range, in which the d of reflected light is considerably reduced. Hence, the bodywork of cars with metallized paint possesses low d in the wide spectral region, where the metal particles reflect light efficiently.

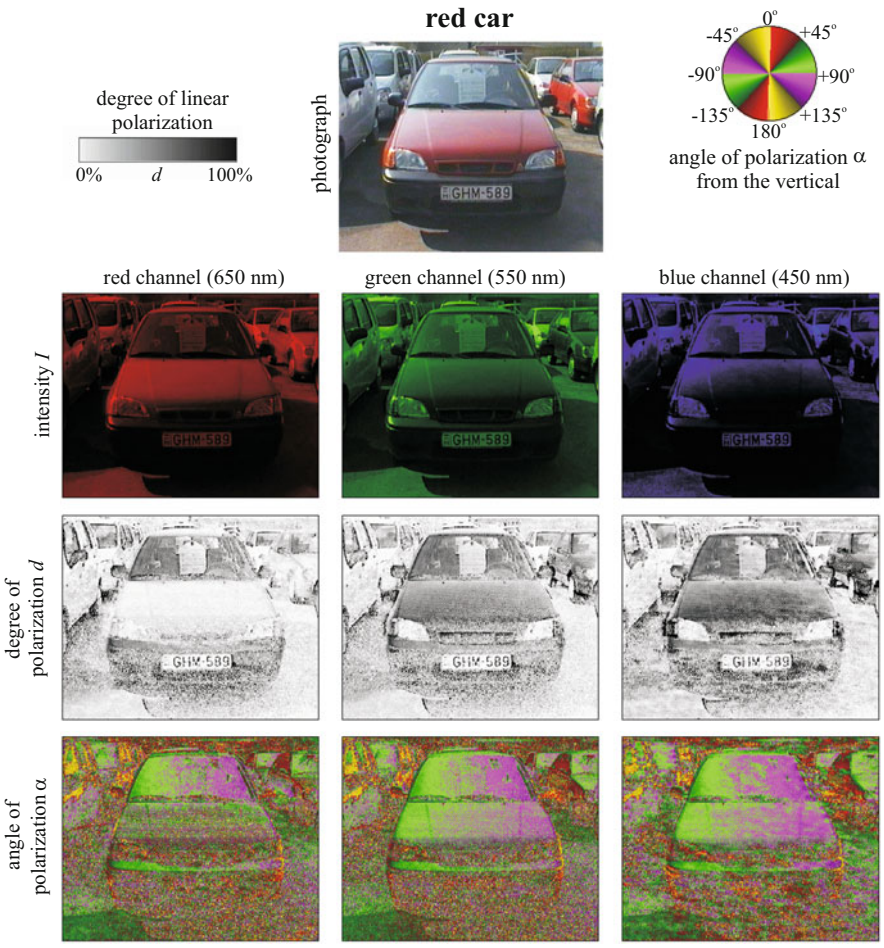

Fig. 20.41 As Fig. 20.38 for a red car

In large parking lots the visual deception of water insects by the car body can increase significantly, because the cars park close to each other and their polarizing effects are summed, thus forming an ecological trap. This phenomenon could be harmful near nature conservation areas including any kinds of wetland. An egg packet of a female mayfly, for example, contains 6,000–9,000 eggs (Kriska et al. 1998). All the eggs laid onto car surfaces perish. This also often occurs in the case of water insect imagos, due to dehydration on hot car surfaces. On the other hand, white and yellow (or more generally, brightly coloured) cars have never been observed to lure water insects. Consequently, concerning water insect protection, these bright-coloured cars can be considered as environmentally friendly (i.e. friendly to aquatic insects). Nature lovers could choose such environmentally friendly light colours for their cars to avoid egg loss by confused water insects. Due

to depolarization by diffuse reflection, dirty cars (with rough surfaces) reflect light with much lower d than recently washed and/or waxed shiny cars. Thus, the most environmentally friendly ('green') car of all would be one that never gets washed. Figures 20.38, 20.39, 20.40 and 20.41 represent the typical reflection–polarization patterns of medium dirty cars.

Summarizing the above results, the 'greenest car is white and dirty'.

20.10 Polarization-Based Visual Deception of Dragonflies by Car Bodies

Sunlit car bodies have frequently been reported to attract sexually active dragonflies. In most cases females of libellulid species oviposited on the horizontal surfaces of vehicles (Svihla 1961; Watson 1992; Günther 2003). In contrast, males are rarely seen to stay over parked cars. Torralba-Burrial and Ocharan (2003) reported on several individuals of *Crocothemis erythraea* dragonflies showing territorial behaviour over car roofs, and both sexes were deceived by the light reflected from the car surface that was mistaken for a waterbody. Choice experiments with horizontal test surfaces composed of perspex plates, plastic sheets and aluminium foils laid on the ground revealed that it is the horizontal polarization of reflected light that leads dragonflies to confuse plane artificial surfaces with water: Both sexes are attracted to such surfaces, where the males establish territories and mate and the females lay eggs onto the surface (Horváth et al. 1998; Wildermuth 1998). Some dragonfly species find waste and crude oil surfaces visually even more attractive than water, because the degree of linear polarization of oil-reflected light is higher than that of water-reflected light (Horváth and Zeil 1996; Horváth et al. 1998; Bernáth et al. 2001b). Among libellulids, *Libellula depressa* has been shown in both sexes to mistake glass panels, perspex and plastic sheets for water (Wyniger 1955; Wildermuth 1998).

Wildermuth and Horváth (2005) observed a male *Libellula depressa* to establish its territory over a dark green car (Fig. 20.42). Deducing from its behaviour what is typical only at water surfaces (perching on the antenna, patrolling with flying in loops and circles close above the bonnet and roof, chasing rivals and defending his territory against other male conspecifics in air fights), it obviously mistook the car bonnet for a waterbody, thus establishing his territory over the surface of the vehicle and using the radio antenna as a perch. The observed male *Libellula depressa* exhibited exactly the same territorial behavioural elements over the car as the species normally shows at reproductive sites. An imaging polarimetric analysis of the car body showed that the light reflected from the bonnet and the roof was strongly and horizontally polarized with similar polarization characteristics in the red, green and blue parts of the spectrum as those of stagnant waters (Horváth and Varjú 1997; Gál et al. 2001a; Bernáth et al. 2002). It was concluded that the dragonfly was deceived by the reflected horizontally polarized light resembling the corresponding pattern at a flat water surface (Wildermuth and Horváth 2005).

Fig. 20.42 A territorial male *Libellula depressa* perching on the tip of the radio antenna of a dark green car parked by a vineyard. The body axis of the dragonfly is held parallel to the steeply incident sun rays, thus minimizing heating of the body. The colour of the car roof is not clearly visible because the sky and the nearby surroundings are mirrored at the shiny surface [after Fig. 1 on page 98 of Wildermuth and Horváth (2005)]

As the surface of sunlit cars can heat up to more than 90 °C (Stevani et al. 2000b), severe problems arise for those dragonfly individuals that try to perch over the car or to touch the surface with the abdominal tip while ovipositing. Difficulties may also arise for the car industry, because eggs laid onto vehicles can damage the resin of the coachwork as does acid rain. Stevani et al. (2000a, b) showed that the eggs of *Miathyria*, *Tauriphila* and *Erythemis* dragonflies at temperatures between 50 and 92 °C produce sulfonic acids that destroy the clearcoat.

Beyond polarization, the colour of the paintwork can also influence the attractiveness to dragonflies, which, however, is still to be investigated.

20.11 Bridges as Optical Barriers for Mayflies: How the Vertically Polarized Mirror Image of Bridges Deceives Flying Female Mayflies

Freshwater biodiversity is declining at rates much faster than those of marine and terrestrial biodiversity (Dudgeon et al. 2006). Although habitat fragmentation, a leading cause for global biodiversity loss, predominantly endangers terrestrial biotas, populations inhabiting flowing waters can also become fragmented due to dams (Petts 1984; Brittain and Saltveit 1989; Zwick 1992; Dynesius and Nilsson 1994; Ligon et al. 1995). Bridges can also represent barriers, for example, by disrupting natural dispersal processes in aquatic insects. Ladócsy (1930) has reported that during a mass swarming after a rain, many female long-tailed mayflies *Palingenia longicauda* landed and oviposited on the wet asphalt road running on a bridge crossing river Tisza in Hungary, instead of laying their eggs into the river.

Male nymphs of *P. longicauda* emerge first and moult into subimagos on the water surface and then fly to the river bank, where they moult into imagos (Andrikovics and Turcsányi 2001). The male imagos then fly back above the river, where they fly horizontally at a height of 5–50 cm above the water surface along a zigzag trajectory in search of females. Female larvae emerge at this time, moult into subimagos and mate as subimagos with males on the water surface. After mating, masses of females fly up to 3–4 km upstream 5–15 m above the river midline, where they lay their eggs. This 'compensation flight' (Russev 1959) serves to compensate for the larval drift that occurs during the aquatic life and for the river flow. Some females (up to 50 %, Andrikovics and Turcsányi 2001) do not copulate with males, and their eggs develop parthenogenetically. Because males are the heterogametic sex in mayflies (Soldán and Putz 2000), unfertilized eggs develop into females. Neither males nor females feed after the emergence from the water; therefore, their energy content and body size at hatching are important in their flight capabilities.

Field experiments by Kriska et al. (2007) showed that *P. longicauda* has both water-searching and water-following flights. In the former, mayflies fly up to heights of 15–30 m in search of horizontally polarized light signals. This flight can be observed only, if the mayflies are captured and released on the river bank. *P. longicauda* shows positive polarotaxis (Kriska et al. 2007), similarly to other mayfly species (Schwind 1995; Kriska et al. 1998; Turcsányi et al. 2009). When mayflies approach surfaces reflecting weakly polarized or vertically polarized light, such as water surfaces shaded by the riverbank vegetation, they suddenly turn back towards the river midline (Kriska et al. 2007; see also Sect. 5.4).

Málnás et al. (2011) tested whether and how bridges present barriers to aquatic insects by studying mass swarmings of *P. longicauda* mayflies on the river Tisza in Hungary (Fig. 20.43). Imaging polarimetry showed that the bridge disrupted the horizontally polarizing channel guiding the flight of mayflies above the river (Figs. 20.44 and 20.45): The horizontally polarized light reflected from the river surface and sensed by mayflies as water created a 'polarization channel', which was narrower than the width of the river and elicited the water-following flight of males and the compensation flight of females. In contrast, the regions of the water surface, where the riparian vegetation and the bridge were mirrored, reflected weakly and vertically polarized light due to the vertically polarized light backscattered from the waterbody that overwhelms the horizontally polarized light reflected from the water surface. Thus, the vertically polarized mirror image of the bridge crossing the river interrupted the horizontally polarized optical channel guiding the mayflies, confusing their light perception and disrupting their compensation flight. Since mayflies turn back, if their ventral polarization-sensitive eye region perceives weakly and non-horizontally polarized light (e.g. when they approach the river bank), the depolarizing or non-horizontally polarizing water surface under the bridge elicited a similar turning-back reaction (Fig. 20.43c).

Female mayflies approaching the bridge displayed four behaviour types (Fig. 20.43): (1) Most females approaching the bridge within 0.5–2 m turned

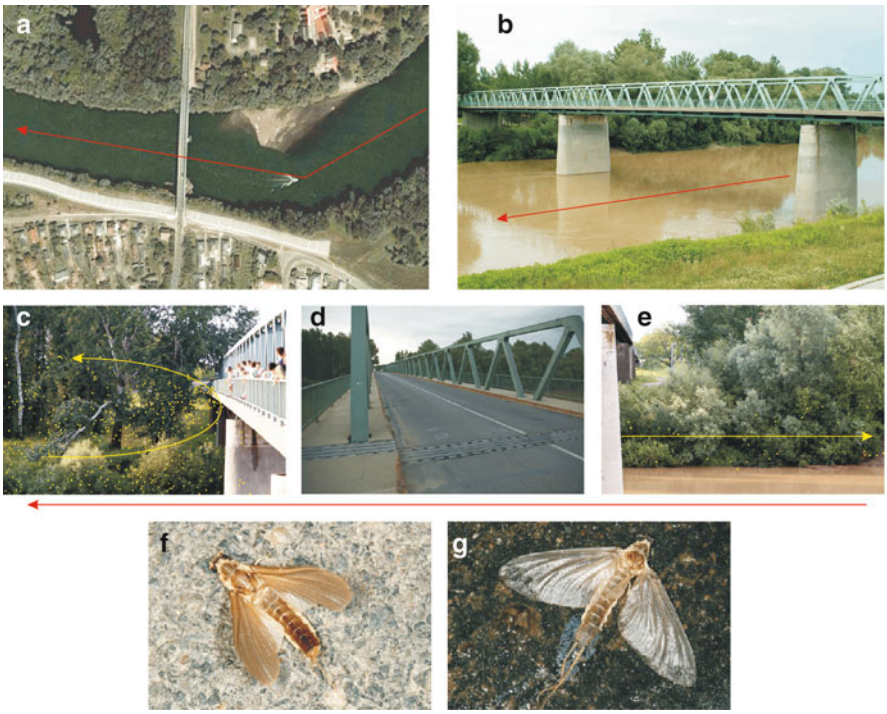

Fig. 20.43 (**a**) Aerial photograph of the bridge over river Tisza at the village Tivadar (http://maps.google.com/maps). (**b**) The bridge photographed from the left bank of Tisza. *Arrows* show flow direction. (**c**) *Palingenia longicauda* mayflies (marked by *bright dots* for visibility) at the downstream side of the bridge. The *curved arrow* shows the typical turning-back flight. (**d**) The asphalt road on the bridge. (**e**) Mayflies (*bright dots*) at the upstream side of the bridge. The *straight arrow* shows the typical horizontal flight. (**f**, **g**) Egg-laying *Palingenia longicauda* on the dry (**f**) and wet (**g**) asphalt road of the bridge [after Fig. 1 on page 825 of Málnás et al. (2011)]

back (Fig. 20.43c). (2) Some low-flying females continued to fly upstream below the bridge (Fig. 20.43e). (3) Some high-flying females flew over the bridge and continued their compensation flight. (4) Some females landed and laid eggs on the bridge's asphalt road (Fig. 20.43f, g) reflecting horizontally polarized light with moderate degrees of polarization ($30\ \% < d < 50\ \%$).

The numbers of flying individuals were estimated by counting mayflies on digital photographs taken simultaneously on both sides of a bridge (Fig. 20.43c, e). Behavioural observations showed that upon approaching the bridge, upstream-flying mayflies typically turned back and 86 % of them never crossed the bridge (Fig. 20.46). Lack of physical contact showed that the bridge was an optical, rather than a mechanical, barrier for the flying polarotactic mayflies.

Using calorimetry, Málnás et al. (2011) determined the energy content of swarming, compensation-flying mayfly females captured by hand nets near the bridge at different phases of swarming to evaluate whether the repeated turning back from the bridge caused increased energy loss in females. Energy loss and time

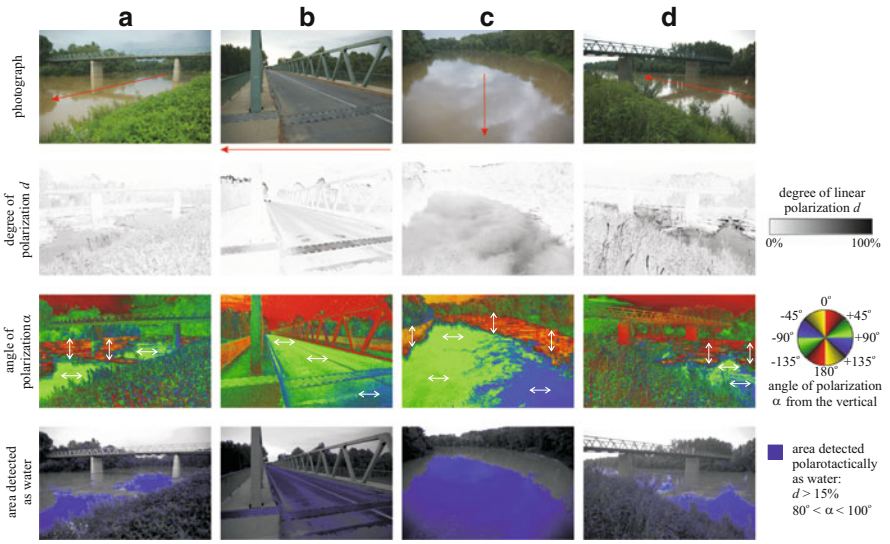

Fig. 20.44 Photographs (*row 1*), patterns of the degree d and angle α (clockwise from the vertical) of linear polarization and areas detected polarotactically as water ($d > 15$ % and $80° < \alpha < 100°$) of the bridge environment measured by imaging polarimetry in the blue (450 nm) part of the spectrum. Patterns were similar in the red and green spectral ranges. The angle of elevation of the optical axis of the polarimeter was $-15°$ from the horizontal. In *row 1 arrows* show flow direction, and in *row 3 arrows* show the local directions of polarization of light reflected by water or asphalt. (**a**) Downstream side of the bridge. (**b**) Asphalt road on the bridge. (**c**) River Tisza upstream from the bridge. (**d**) Upstream side of the bridge [after Fig. 2 on page 826 of Málnás et al. (2011)]

constraints forced females to lay eggs only downstream from the bridge: The energy content of females collected at the bridge was only 68 % of that of females collected at the same time 1 km downstream from the bridge, although there was no difference in dry body mass between the groups. Females at the bridge were energetically exhausted compared to females on their upstream way to the bridge.

Counts of larval skins shed by swarming individuals showed nearly 2 to 1 female per male (proportion of females: 56–85 %) downstream from the bridge, while sex ratio upstream from the bridge was slightly male biased (proportion of males: 21–72 %). Málnás et al. (2011) suggested that the surplus of parthenogenetic females, which produce only female larvae, downstream from the bridge may have led to the observed sex ratio bias since the construction of the bridge (1942). The study of Málnás et al. (2011) provided four key results: (1) Bridges can function as an optical barrier for female mayflies during their upstream compensation flight. (2) The environment of bridges presents a weakly and vertically polarized barrier to most female mayflies as if the bridge had been an impenetrable physical barrier. (3) 86 % of the females had their polarotactic perception confused by the bridge and did not cross the bridge. These females are energetically exhausted relative to

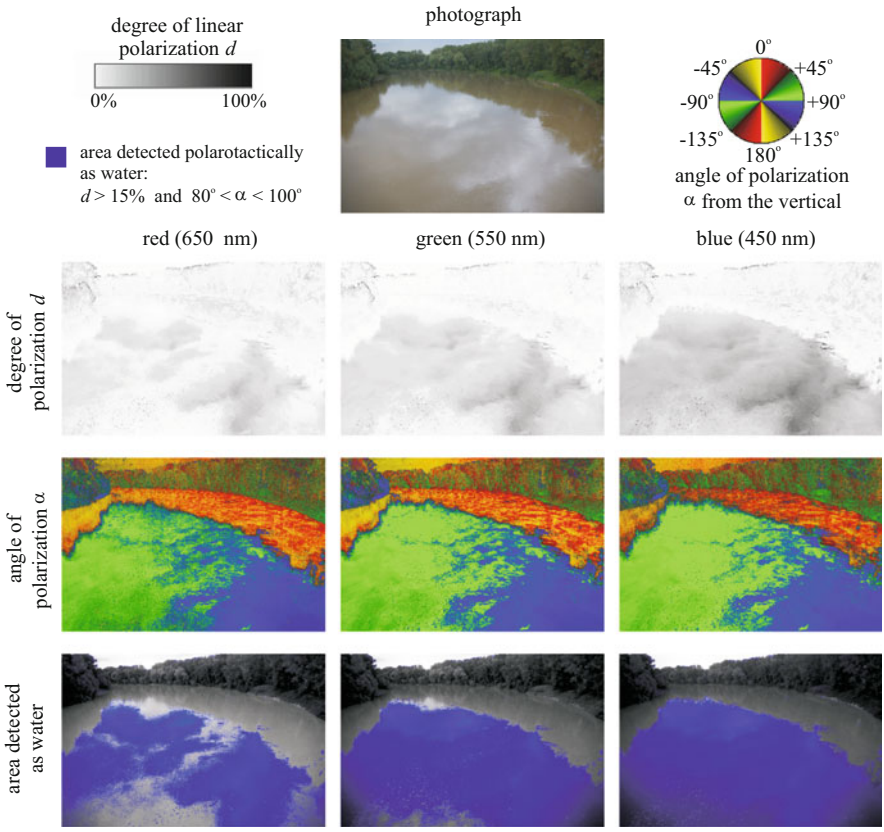

Fig. 20.45 As Fig. 20.44 for river Tisza upstream from the bridge, measured in the red (650 nm), green (550 nm) and blue (450 nm) parts of the spectrum [after Fig. 3 on page 827 of Málnás et al. (2011)]

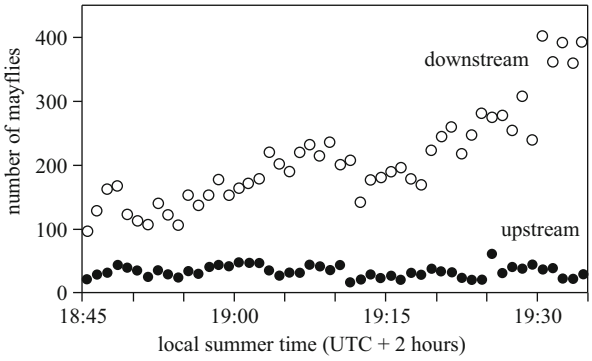

Fig. 20.46 Number of flying mayflies, *Palingenia longicauda*, counted on photographs taken at the downstream and upstream side of the bridge above the river Tisza on 25 June 2009 once every minute between 18:45 and 19:34 ($n = 50$ photos on each side). Mayfly flight ended abruptly at 19:45 at a thunderstorm [after Fig. 4 on page 828 of Málnás et al. (2011)]

females that have not yet reached the bridge. The exhaustion of females at the bridge causes them to lay their eggs in the river section just downstream from the bridge. (4) The accumulation of females, especially of those reproducing parthenogenetically, is related to female-biased sex ratios downstream from the bridge and male-biased sex ratios upstream from the bridge.

Málnás et al. (2011) showed that the bridges selectively not only removed and added polarized light signatures to riparian habitats in evolutionarily novel ways but also provided a rare example of how the behavioural responses of individual mayflies to man-made structures are linked to population-scale consequences. Sex ratio biases due to bridges may decrease effective population size and genetic variability, which may have contributed to the recent extinction of this species from most of Europe. This effect may be particularly important in species that depend on the synchronous presence of large numbers of individuals for successful reproduction, such as *P. longicauda*. This study, therefore, raises the possibility that not only chemical pollution but also polarized light pollution (Horváth et al. 2009, 2010b) due to bridges as well as possibly other artificial structures may have contributed to the rapid collapse of *P. longicauda* populations in the former European range of this species as population models of ecological traps have predicted (Kokko and Sutherland 2001).

20.12 Why Do Strongly Polarizing Black Burnt-Up Stubble Fields Not Attract Aquatic Insects? An Exception Proving the Rule

On the basis of the findings outlined so far in this chapter, one would predict that all 'black anthropogenic products' that reflect light with high degree of polarization and horizontal direction of polarization should deceive and lure polarotactic insects (Bernáth et al. 2001b,c). One notable exception is burnt-up stubble fields that result from wildfires or controlled burns used to manage wildlife habitat or reduced the risk of wildfire (Fig. 20.47). Indeed, the resulting black ash layer reflects strongly polarized light due to the effect of Umow (1905): The darker a surface in a given spectral range, the higher the degree of linear polarization of light reflected by it. In addition, flying polarotactic insects can be shown to be abundant above burnt-up stubble fields by attracting them to strongly and horizontally polarizing black plastic sheets (2 m × 2 m) (Kriska et al. 2006b). Yet, insects in these areas do not attempt to lay eggs on ash, nor do they perform other behaviours associated with aquatic habitats.

To explain this observation, Kriska et al. (2006b) measured the reflection–polarization characteristics of burnt-up stubble fields (Fig. 20.48) in the visible spectrum at three directions of view: towards the solar meridian (SM), towards the antisolar meridian (ASM) and perpendicular to the solar meridian (PSM).

Fig. 20.47 A Hungarian stubble field near Balatonszemes (46° 82′ N, 17° 78′ E) prior to burning (**a**), during burning (**b**) and after burning (**c**). (**d**) Black ash of the burnt-up stubble field [after Fig. 1 on page 4383 of Kriska et al. (2006b)]

They established the following (Fig. 20.48): (1) The degree of polarization d of light reflected from the black ash is always medium or high (average: 16–41 %). (2) The higher the d is, the darker is the ash. (3) The direction of polarization of ash-reflected light is nearly horizontal only towards the solar and antisolar meridians, and it is tilted in other directions of view. Thus, burnt-up stubble fields could be attractive to water-seeking flying polarotactic aquatic insects only from directions of view towards the SM and ASM, and from other directions of view, they are unattractive. (4) The standard deviations of the degree d and the angle α of polarization of ash-reflected light are always large (Δd: ±12–23 %, $\Delta\alpha$: ±18–44°). The latter two characteristics explain why burnt-up stubble fields are generally unattractive to aquatic insects. Thus, burnt-up stubble fields are an exception proving the rule that black anthropogenic products deceive and attract polarotactic insects.

The high standard deviation of d of light reflected from burnt-up stubble fields can be explained by the large spatial change of the darkness of the ash. The ash layer is a rough surface due to the random orientation of the charred stalks of straw. Rough surfaces possess the characteristic that the direction of polarization of reflected light is always perpendicular to the plane of reflection (Können 1985; Horváth and Varjú 2004). In the case of sunlit burnt-up stubble fields, the plane of

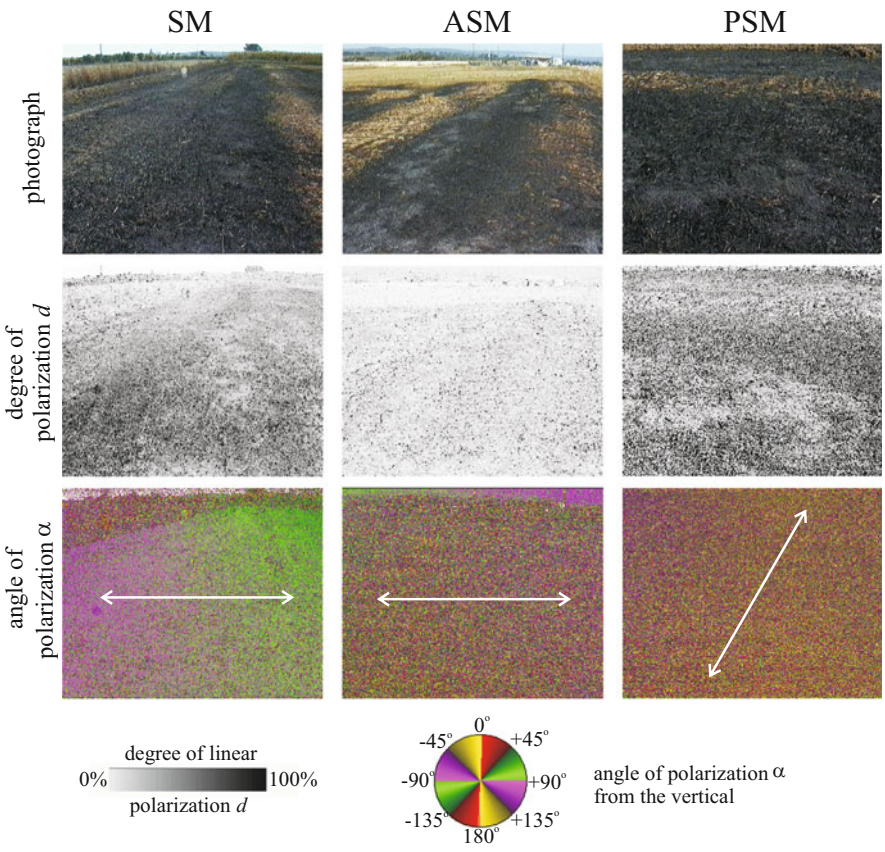

Fig. 20.48 Photographs and patterns of the degree of linear polarization d and the angle of polarization α (clockwise from the vertical) of a Hungarian burnt-up stubble field measured by imaging polarimetry under a clear sky in sunshine in the green (550 nm) part of the spectrum when the direction of view of the polarimeter was towards the solar meridian (SM) and antisolar meridian (ASM) and perpendicular to the solar meridian (PSM). The elevation angle of the optical axis of the polarimeter was $-30°$ from the horizontal. *Double-headed arrows* show the local directions of polarization of ash-reflected light [after Fig. 2 on page 4384 of Kriska et al. (2006b)]

reflection passes through the observer, the sun and the point of the ash observed. This plane of reflection is vertical towards both the SM and ASM, and it is tilted for other directions of view. This is the reason for the findings that the average direction of polarization of light reflected from burnt-up stubble fields is nearly horizontal towards the SM and ASM, and it is tilted in all other directions of view (Fig. 20.48). The reason for the large standard deviation of the direction of polarization of ash-reflected light is the random orientation of the charred stalks of straw.

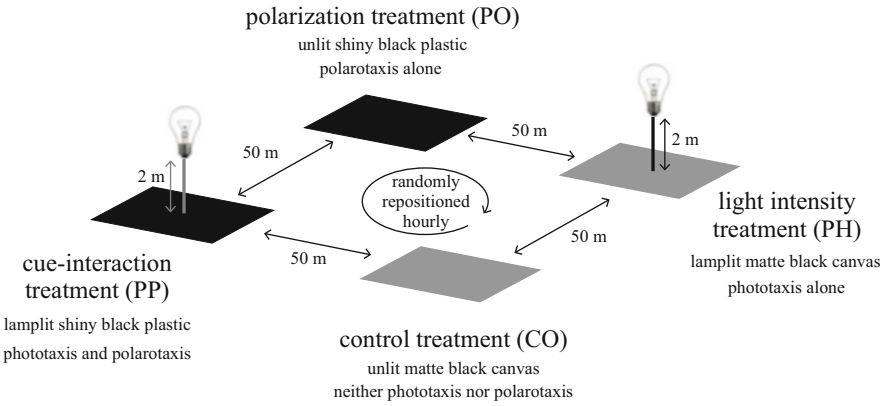

Fig. 20.49 Schematic representation of the experimental design of Boda et al. (2014) [after Fig. 1b on page 387 of Boda et al. (2014)]

20.13 Synergistic Influence of Phototaxis and Polarotaxis on the Night Flight of Aquatic Insects

Many dusk-active (crepuscular) or night-active (nocturnal) aquatic insect species possess positive phototaxis, that is, they are attracted to the intensity of unpolarized light of given spectral characteristics. It has long been observed that artificial lighting influences the flight behaviour of aquatic insects as they are lured to light (Nowinszky 2003; Choi et al. 2009). This effect is used in light traps being a classical tool of mass sampling in insect ecology (Nowinszky 2004). For example, artificial light can trigger abnormal dispersal behaviour such as disorientation (Longcore and Rich 2004; Rich and Longcore 2006). As shown in this chapter, water insects possess also positive polarotaxis; thus, strongly and horizontally polarizing artificial surfaces cause polarized light pollution (Horváth et al. 2009).

In a multiple-choice field experiment, Boda et al. (2014) showed that both phototaxis and polarotaxis simultaneously influence the dispersal flight of crepuscular and nocturnal aquatic insects: At night the spectrum (intensity and colour) of artificial light lures water-seeking flying aquatic insects from remote distances (positive phototaxis caused by photopollution), and then the horizontally polarized light reflected from a given artificial surface attracts and entraps the deceived insects (positive polarotaxis induced by polarized light pollution). It was found that phototaxis-based photopollution and polarotaxis-based polarized light pollution together have a more harmful effect on the dispersal flight of water insects than they would have separately.

During their field experiment in full darkness at night, Boda et al. (2014) offered simultaneously four visual stimuli for aerial aquatic insects (Fig. 20.49): (1) lamplit matte black canvas inducing phototaxis alone, (2) unlit shiny black plastic sheet eliciting polarotaxis alone, (3) lamplit shiny black plastic sheet inducing

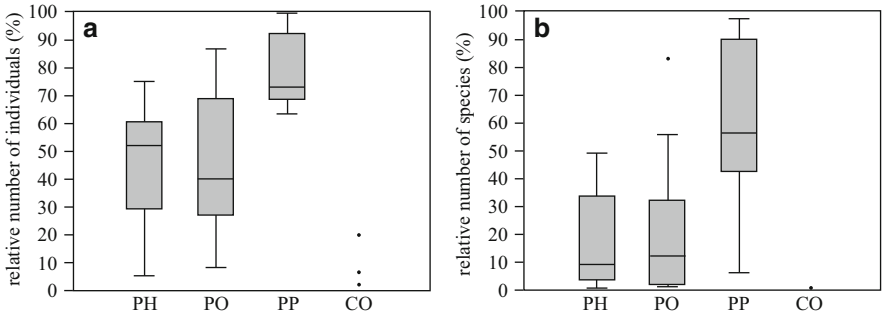

Fig. 20.50 Relative number of individuals (**a**) and species (**b**) among the experimental treatments PH (lamplit matte black canvas inducing phototaxis alone), PO (unlit shiny black plastic sheet eliciting polarotaxis alone), PP (lamplit shiny black plastic sheet inducing photo- and polatoraxis together) and CO (unlit matte black canvas as a control without phototaxis and polarotaxis) in the field experiment of Boda et al. (2014). The interaction of light intensity and horizontal polarization resulted in the most attractive test surface, the PP. *Grey box*: interquartile range. *Inner line*: median. *Dot*: outlier. *Whisker*: standard error [after Fig. 3 on page 391 of Boda et al. (2014)]

simultaneously phototaxis and polarotaxis and (4) unlit matte black canvas as a visually unattractive control. The unlit matte black canvas trapped only a negligible number (13) of water insects. The sum (16,432) of the total numbers of water beetles and bugs captured on the lamplit matte black canvas (7,922) and the unlit shiny black plastic sheet (8,510) was much smaller than the total catch (29,682) caught on the lamplit shiny black plastic sheet (Fig. 20.50). This provided experimental evidence for the synergistic interaction of phototaxis (elicited by the unpolarized direct lamplight) and polarotaxis (induced by the strongly and horizontally polarized plastic-reflected light) in the investigated aquatic insects. Thus, horizontally polarizing artificial lamplit surfaces can function as an effective ecological trap due to this synergism of optical cues, especially in the urban environment.

The flight behaviour elicited by the synergistic interaction of phototaxis and polarotaxis can occur in all aquatic insect species. Unfortunately, this phenomenon is not as rare in nature as we think at first. Lamplit car parks, solar panels near indicator lighting and illuminated glass buildings, for instance, have the potential to significantly disrupt the ecosystem by simultaneous photopollution and polarized light pollution. The follow-up investigation of the generality of this phenomenon could be an interesting and important task of future research.

References

Anderson TR (2006) Biology of the ubiquitous house sparrow: from genes to populations. Oxford University Press, Oxford, UK

Andrikovics S, Turcsányi I (2001) The long-tailed mayfly—ecology of an endangered species, vol 10. Tisza Klub, Szolnok (in Hungarian)

Badyaev AV (2003) Family Motacillidae. In: Perrins C (ed) Encyclopedia of birds. Edward Grey Institute of Field Ornithology and Andromeda Oxford Limited, Oxford, UK

Baldavári L (2001) Effects of the total solar eclipse of 11 August 1999 on behaviour of honeybees, recorded in an apiary. Zool Bull 86:137–143 (in Hungarian)

Bernáth B, Horváth G (1999) Visual deception of a great white egret by shiny plastic sheets. Ornis Hung 8–9:57–61

Bernáth B, Pomozi I, Gál J, Horváth G, Wehner R (2001a) Sky polarization during the total solar eclipse on 11 August 1999 and its possible biological implications. Zool Bull 86:81–92 (in Hungarian)

Bernáth B, Szedenics G, Molnár G, Kriska G, Horváth G (2001b) Visual ecological impact of "shiny black anthropogenic products" on aquatic insects: oil reservoirs and plastic sheets as polarized traps for insects associated with water. Arch Nat Conservat Landsc Res 40(2):89–109

Bernáth B, Szedenics G, Molnár G, Kriska G, Horváth G (2001c) Visual ecological impact of a peculiar waste oil lake on the avifauna: dual-choice field experiments with water-seeking birds using huge shiny black and white plastic sheets. Arch Nat Conservat Landsc Res 40(1):1–28

Bernáth B, Szedenics G, Wildermuth H, Horváth G (2002) How can dragonflies discern bright and dark waters from a distance? The degree of polarization of reflected light as a possible cue for dragonfly habitat selection. Freshw Biol 47:1707–1720

Bernáth B, Kriska G, Suhai B, Horváth G (2008) Wagtails (Aves: Motacillidae) as insect indicators on plastic sheets attracting polarotactic aquatic insects. Acta Zool Acad Sci Hung 54:145–155

Blahó M, Egri Á, Barta A, Antoni G, Kriska G, Horváth G (2012) How can horseflies be captured by solar panels? A new concept of tabanid traps using light polarization and electricity produced by photovoltaics. Vet Parasitol 189:353–365

Boda P, Horváth G, Kriska G, Blahó M, Csabai Z (2014) Phototaxis and polarotaxis hand in hand: night dispersal flight of aquatic insects distracted synergistically by light intensity and reflection polarization. Naturwissenschaften 101:385–395

Brittain JE, Saltveit SJ (1989) A review of the effect of river regulation on mayflies (Ephemeroptera). Regul Rivers Res Manag 3:191–204

Brodskiy AK (1973) The swarming behavior of mayflies (Ephemeroptera). Entomol Rev 52:33–39

Bromley SW (1928) A dragonfly ovipositing on a paved highway. Bull Brooklyn Entomol Soc 23: 69

Buchanan BW (2006) Observed and potential effects of artificial night lighting on anuran amphibians. In: Rich C, Longcore T (eds) Ecological consequences of artificial night lighting. Island Press, Washington, DC, pp 192–220

Camacho RE, Morgan AR, Flores MC, McLeod TA, Kumsomboone VS, Mordecai BJ, Bhattacharjea R, Tong W, Wagner BK, Flicker JD, Turano SP, Ready WJ (2007) Carbon nanotube arrays for photovoltaic applications. J Miner Mater Soc 59(3):39–42

Choi H, Kim H, Kim JG (2009) Landscape analysis of the effects of artificial lighting around wetland habitats on the giant water bug Lethocerus deyrollei in Jeju Island. J Ecol Field Biol 32:83–86

Cinzano P, Falchi F, Elvidge CD (2001) The first world atlas of the artificial night sky brightness. Mon Not R Astron Soc 328:689–707

Collinge SK (2000) Effects of grassland fragmentation on insect species loss, colonization, and movement patterns. Ecology 81:2211–2226

Corbet PS (1999) Dragonflies. Behaviour and ecology of Odonata. Harley Books, Great Horkesley

Csabai Z, Gidó Z, Móra A, Boda P, Dévai G, Király A, Szilágyi K, Varju T (2003) Migration activity patterns of aquatic beetles and aquatic bugs (Coleoptera, Heteroptera) I. Changing of the number of individuals and species richness. Hidrológiai Közlöny (J Hung Hydrol Soc) 83: 29–32 (in Hungarian)

Csabai Z, Gidó Z, Boda P, Móra A (2004) Migration activity patterns of aquatic beetles and aquatic bugs (Coleoptera, Heteroptera) III. Seasonal and daily migration of selected species. Hidrológiai Közlöny (J Hung Hydrol Soc) 84:28–30 (in Hungarian)
Csabai Z, Boda P, Bernáth B, Kriska G, Horváth G (2006) A 'polarisation sun-dial' dictates the optimal time of day for dispersal by flying aquatic insects. Freshw Biol 51:1341–1350
Currie MJ, Mapel JK, Heidel TD, Goffri S, Baldo BA (2008) High-efficiency organic solar concentrators for photovoltaics. Science 321:226–228
Davies NB (1977) Prey selection and social behaviour in wagtails (Aves: Motacillidae). J Anim Ecol 46:37–57
Davies NB, Houston AI (1981) Owners and satellites: the economics of territory defence in the pied wagtail, *Motacilla alba*. J Anim Ecol 50:157–180
Delibes M, Gaona P, Ferreras P (2001) Effects of an attractive sink leading into maladaptive habitat selection. Am Nat 158:277–285
Dewan R, Fischer S, Meyer-Rochow VB, Özdemir Y, Hamraz S, Knipp D (2012) Studying nanostructured nipple arrays of moth eye facets helps to design better thin film solar cells. Bioinspir Biomim 7:016003. doi:10.1088/1748-3182/7/1/016003
Donovan TM, Thompson FR (2001) Modelling the ecological trap hypothesis: a habitat and demographic analysis for migrant songbirds. Ecol Appl 11:871–882
Dudgeon D, Arthington AH, Gessner MO, Kawabata ZI, Knowler DJ, Leveque C, Naiman RJ, Prieur-Richard AH, Soto D, Stiassny MLJ, Sullivan CA (2006) Freshwater biodiversity: importance, threats, status and conservation challenges. Biol Rev 81:163–182
Dynesius M, Nilsson C (1994) Fragmentation and flow regulation of river systems in the Northern third of the world. Science 266:753–762
Dwernychuk LW, Boag DA (1972) Ducks nesting in association with gulls - an ecological trap? Can J Zool 50(5):559–563
Egri Á, Blahó M, Sándor A, Kriska G, Gyurkovszky M, Farkas R, Horváth G (2012) New kind of polarotaxis governed by degree of polarization: attraction of tabanid flies to differently polarizing host animals and water surfaces. Naturwissenschaften 99:407–416 + electronic supplement
Egri Á, Blahó M, Száz D, Kriska G, Majer J, Herczeg T, Gyurkovszky M, Farkas R, Horváth G (2013a) A horizontally polarizing liquid trap enhances the tabanid-capturing efficiency of the classic canopy trap. Bull Entomol Res 103:665–674
Egri Á, Blahó M, Száz D, Barta A, Kriska G, Antoni G, Horváth G (2013b) A new tabanid trap applying a modified concept of the old flypaper: linearly polarising sticky black surfaces as an effective tool to catch polarotactic horseflies. Int J Parasitol 43:555–563
Eisenbeis G (2006) Artificial night lighting and insects: attraction of insects to streetlamps in a rural setting in Germany. In: Rich C, Longcore T (eds) Ecological consequences of artificial night lighting. Island Press, Washington, DC, pp 281–304
Errington PL (1946) Predation and vertebrate populations. Q Rev Biol 21:144–177
Fletcher RJ Jr, Orrock JL, Robertson BA (2012) How the type of anthropogenic change alters the consequences of ecological traps. Proc R Soc Lond B 279:2546–2552
Frank KD (2006) Effects of artificial night lighting on moths. In: Rich C, Longcore T (eds) Ecological consequences of artificial night lighting. Island Press, Washington, DC, pp 305–344
Fraser FC (1936) The Fauna of British India. Odonata, vol 3. Taylor and Francis, London
Funk WC, Greene AE, Corn PS, Allendorf FW (2005) High dispersal in a frog species suggests that it is vulnerable to habitat fragmentation. Biol Lett 1:13–16
Gál J, Horváth G, Meyer-Rochow VB (2001a) Measurement of the reflection-polarization pattern of the flat water surface under a clear sky at sunset. Remote Sens Environ 76:103–111
Gál J, Horváth G, Meyer-Rochow VB, Wehner R (2001b) Polarization patterns of the summer sky and its neutral points measured by full-sky imaging polarimetry in Finnish Lapland north of the Arctic Circle. Proc R Soc A 457:1385–1399
Günther A (2003) Eiablage von *Sympetrum vulgatum* auf ein parkendes Auto (Odonata: Libellulidae). Libellula 22:19–23

Harrap S, Quinn D (1996) Tits, nuthatches and treecreepers. Princeton University Press, Princeton, NJ
Hegedüs R, Åkesson S, Horváth G (2007) Anomalous celestial polarization caused by forest fire smoke: why do some insects become visually disoriented under smoky skies? Appl Opt 46: 2717–2726
Herkert JR (1994) The effects of habitat fragmentation on midwestern grassland bird communities. Ecol Appl 4:461–471
Hoell HV, Doyen JT, Purcell AH (1998) Introduction to insect biology and diversity, 2nd edn. Oxford University Press, Oxford, UK
Horváth G (1995) Reflection-polarization patterns at flat water surfaces and their relevance for insect polarization vision. J Theor Biol 175:27–37
Horváth G (2012) Chapter 9: Polarized light pollution, pp 82–108. In: Csanád M, Horváth Á, Horváth G, Veres G (2012) Environmental physics methods laboratory practices. electronic text-book (Horváth Á (ed)), p 206, Typotex Kiadó, Budapest, ISBN 978-963-279-551-5
Horváth G, Kriska G (2008) Polarization vision in aquatic insects and ecological traps for polarotactic insects. In: Lancaster J, Briers RA (eds) Aquatic insects: challenges to populations. CAB International Publishing, Wallingford, Oxon, pp 204–229, Chapter 11
Horváth G, Pomozi I (1997) How celestial polarization changes due to reflection from the deflector panels used in deflector loft and mirror experiments studying avian navigation. J Theor Biol 184:291–300
Horváth G, Varjú D (1997) Polarization pattern of freshwater habitats recorded by video polarimetry in red, green and blue spectral ranges and its relevance for water detection by aquatic insects. J Exp Biol 200:1155–1163
Horváth G, Varjú D (2004) Polarized light in animal vision—polarization patterns in nature. Springer, Heidelberg
Horváth G, Zeil J (1996) Kuwait oil lakes as insect traps. Nature 379:303–304
Horváth G, Bernáth B, Molnár G (1998) Dragonflies find crude oil visually more attractive than water: multiple-choice experiments on dragonfly polarotaxis. Naturwissenschaften 85:292–297
Horváth G, Barta A, Gál J, Suhai B, Haiman O (2002) Ground-based full-sky imaging polarimetry of rapidly changing skies and its use for polarimetric cloud detection. Appl Opt 41:543–559
Horváth G, Pomozi I, Gál J (2003) Neutral points of skylight polarization observed during the total eclipse on 11 August 1999. Appl Opt 42:465–475
Horváth G, Malik P, Kriska G, Wildermuth H (2007) Ecological traps for dragonflies in a cemetery: the attraction of *Sympetrum* species (Odonata: Libellulidae) by horizontally polarizing black gravestones. Freshw Biol 52:1700–1709
Horváth G, Majer J, Horváth L, Szivák I, Kriska G (2008) Ventral polarization vision in tabanids: horseflies and deerflies (Diptera: Tabanidae) are attracted to horizontally polarized light. Naturwissenschaften 95:1093–1100
Horváth G, Kriska G, Malik P, Robertson B (2009) Polarized light pollution: a new kind of ecological photopollution. Front Ecol Environ 7:317–325
Horváth G, Blahó M, Egri Á, Kriska G, Seres I, Robertson B (2010a) Reducing the maladaptive attractiveness of solar panels to polarotactic insects. Conserv Biol 24:1644–1653 + electronic supplement
Horváth G, Kriska G, Malik P, Hegedüs R, Neumann L, Åkesson S, Robertson B (2010b) Asphalt surfaces as ecological traps for water-seeking polarotactic insects: how can the polarized light pollution of asphalt surfaces be reduced? Environmental remediation technologies, regulations and safety. Nova Science Publishers, Inc., Hauppauge, NY, p 47
Horváth G, Móra A, Bernáth B, Kriska G (2011) Polarotaxis in non-biting midges: female chironomids are attracted to horizontally polarized light. Physiol Behav 104:1010–1015
Houston AI, McCleery RH, Davies NB (1985) Territory size, prey renewal and feeding rates: Interferation of observations on the pied wagtail (*Motacilla alba*) by simulation. J Anim Ecol 54:227–239
Jäch MA (1997) Daytime swarming of rheophilic water beetles in Austria (Coleoptera: Elmidae, Hydraenidae, Haliplidae). Latissimus 9:10–11

Johnson DL, Naylor D, Scudder G (2005) Red sky in day, bugs go astray. Annual Meeting of the Canadian Association of Geographers, Western Division, Lethbridge, AB, 12 March 2005, Abstracts, p 145

Kokko H, Sutherland WJ (2001) Ecological traps in changing environments: ecological and evolutionary consequences of a behaviourally mediated Allee effect. Evol Ecol Res 3:537–551

Können GP (1985) Polarized light in nature. Cambridge University Press, Cambridge, UK

Kriska G, Horváth G, Andrikovics S (1998) Why do mayflies lay their eggs *en masse* on dry asphalt roads? Water-imitating polarized light reflected from asphalt attracts Ephemeroptera. J Exp Biol 201:2273–2286

Kriska G, Csabai Z, Boda P, Malik P, Horváth G (2006a) Why do red and dark-coloured cars lure aquatic insects? The attraction of water insects to car paintwork explained by reflection-polarization signals. Proc R Soc B 273:1667–1671

Kriska G, Malik P, Csabai Z, Horváth G (2006b) Why do highly polarizing black burnt-up stubble-fields not attract aquatic insects? An exception proving the rule. Vis Res 46:4382–4386 + cover picture

Kriska G, Bernáth B, Horváth G (2007) Positive polaritaxis in a mayfly that never leaves the water surface: polarotactic water detention in *Palingenia longicauda* (Ephemeroptera). Naturwissenschaften 94:148–154

Kriska G, Malik P, Szivák I, Horváth G (2008) Glass buildings on river banks as "polarized light traps" for mass-swarming polarotactic caddis flies. Naturwissenschaften 95:461–467

Labhart T, Nilsson DE (1995) The dorsal eye of the dragonfly *Sympetrum*: specializations for prey detection against the blue sky. J Comp Physiol A 176:437–453

Ladócsy K (1930) The mating flight of the Tisza mayfly (*Palingenia longicauda*, Oliv) in 1929 in Szeged. Part 2. Fishery 31(7–8):28–30 (in Hungarian)

Lerner A, Meltser N, Sapir N, Erlick C, Shashar N, Broza M (2008) Reflected polarization guides chironomid females to oviposition sites. J Exp Biol 211:3536–3543

Ligon FK, Dietrich WE, Trush WJ (1995) Downstream ecological effects of dams. Bioscience 45:183–192

Longcore T, Rich C (2004) Ecological light pollution. Front Ecol Environ 2:191–198

Longcore T, Rich C (2006) Synthesis. In: Rich C, Longcore T (eds) Ecological consequences of artificial night lighting. Island Press, Washington, DC, pp 413–430, Chapter 17

Madge S, Burn H (1994) Crows and jays: a guide to the crows, jays and magpies of the world. A & C Black, London

Malik P, Hegedüs R, Kriska G, Horváth G (2008) Imaging polarimetry of glass buildings: why do vertical glass surfaces attract polarotactic insects? Appl Opt 47:4361–4374 + cover picture

Málnás K, Polyák L, Prill É, Hegedüs R, Kriska G, Dévai G, Horváth G, Lengyel S (2011) Bridges as optical barriers and population disruptors for the mayfly *Palingenia longicauda*: an overlooked threat to freshwater biodiversity? J Insect Conserv 15:823–832 + electronic supplement

Marsh WM, Grossa JM Jr (2002) Environmental geography: science, land use, and earth systems, 2nd edn. Wiley, New York

Mizera F, Bernáth B, Kriska G, Horváth G (2001) Stereo videopolarimetry: measuring and visualizing polarization patterns in three dimensions. J Imaging Sci Technol 45:393–399

Moore NW (1991) Male *Sympetrum striolatum* "defends" a basking spot rather than a particular locality (Anisoptera: Libellulidae). Notulae Odonatologicae 3:112

Moore RP, Robinson WD, Lovette IJ, Robinson TR (2008) Experimental evidence for extreme dispersal limitation in tropical forest birds. Ecol Lett 11:960–968

Nilsson AN (1997) On flying *Hydroporus* and the attraction of *H. incognitus* to red car roofs. Latissimus 9:12–16

Nowinszky L (2003) The handbook of light trapping. Savaria University Press, Szombathely

Nowinszky L (2004) Nocturnal illumination and night flying insects. Appl Ecol Environ Res 2:17–52

Oehme H (1999) Jagderfolg und Jagdtaktik bei *Sympetrum striolatum* (Charpentier) (Anisoptera: Libellulidae). Libellula 18:79–87
Perry G, Fisher RN (2006) Night lights and reptiles: observed and potential effects. In: Rich C, Longcore T (eds) Ecological consequences of artificial night lighting. Island Press, Washington, DC, pp 169–191
Petts GE (1984) Impounded rivers: perspectives for ecological management. Wiley, Chichester
Pomozi I, Gál J, Horváth G, Wehner R (2001) Fine structure of the celestial polarization pattern and its temporal change during the total solar eclipse of 11 August 1999. Remote Sens Environ 76:181–201
Puschnig R (1926) Albanische Libellen. Konowia 5: 33, 113, 208, 313
Reich P, Downes BJ (2003) Experimental evidence for physical cues involved in oviposition site selection of lotic hydrobiosid caddis flies. Oecologia 136:465–475
Rezanov AG (1981) Feeding behaviour and modes of feeding in the wagtail *Motacilla alba* (Passeriformes, Motacillidae). Zool Zhurnal 60(4):548–556 (in Russian)
Rich C, Longcore T (eds) (2006) Ecological consequences of artificial night lighting. Island Press, Washington, DC
Riegel KW (1973) Light pollution: outdoor lighting is a growing threat to astronomy. Science 179:1285–1291
Robertson BA, Hutto RL (2006) A framework for understanding ecological traps and an evaluation of existing evidence. Ecology 87:1075–1085
Robertson B, Kriska G, Horváth V, Horváth G (2010) Glass buildings as bird feeders: urban birds exploit insects trapped by polarized light pollution. Acta Zool Acad Sci Hung 56:283–293
Robertson BA, Rehage J, Sih A (2013) Ecological novelty and the emergence of evolutionary traps. Trends Ecol Evol 28:552–560
Russev B (1959) Vol de compensation pour la ponte de *Palingenia longicauda* (Oliv.) (Ephem.) contre courant du Danube. C R Acad Bulg Sci 12:165–168
Rydell J (2006) Bats and their insect prey at streetlights. In: Rich C, Longcore T (eds) Ecological consequences of artificial night lighting. Island Press, Washington, DC, pp 43–60
Savolainen E (1978) Swarming in Ephemeroptera: the mechanism of swarming and the effects of illumination and weather. Ann Zool Fenn 15:17–52
Scheibe MA (2000) Quantitative aspects of the attraction of roadway lighting to insects emerging from nearby waters (Ephemeroptera, Plecoptera, Trichoptera, Diptera: Simuliidae, Chironomidae, Empididae) with consideration of the spectral emission of different sources of light. Ph.D. thesis, Fachbereich Biologie, Johannes Gutenberg Universität, Mainz (in German)
Schlaepfer MA, Runge MC, Sherman PW (2002) Ecological and evolutionary traps. Trends Ecol Evol 17:474–480
Schwind R (1983a) A polarization-sensitive response of the flying water bug *Notonecta glauca* to UV light. J Comp Physiol 150:87–91
Schwind R (1983b) Zonation of the optical environment and zonation in the rhabdom structure within the eye of the backswimmer, *Notonecta glauca*. Cell Tissue Res 232:53–63
Schwind R (1984a) Evidence for true polarization vision based on a two-channel analyser system in the eye of the water bug, *Notonecta glauca*. J Comp Physiol A 154:53–57
Schwind R (1984b) The plunge reaction of the backswimmer *Notonecta glauca*. J Comp Physiol A 155:319–321
Schwind R (1985a) Sehen unter und über Wasser, Sehen von Wasser. Naturwissenschaften 72: 343–352
Schwind R (1985b) A further proof of polarization vision of *Notonecta glauca* and a note on threshold intensity for eliciting the plunge reaction. Experientia 41:466–467
Schwind R (1991) Polarization vision in water insects and insects living on a moist substrate. J Comp Physiol A 169:531–540
Schwind R (1995) Spectral regions in which aquatic insects see reflected polarized light. J Comp Physiol A 177:439–448

Schwind R, Horváth G (1993) Reflection-polarization pattern at water surfaces and correction of a common representation of the polarization pattern of the sky. Naturwissenschaften 80:82–83
Schwind R, Schlecht P, Langer H (1984) Microspectrophotometric characterization and localization of three visual pigments in the compound eye of *Notonecta glauca* L. (Heteroptera). J Comp Physiol A 154:341–346
Sipőcz B, Hegedüs R, Kriska G, Horváth G (2008) Spatiotemporal change of sky polarization during the total solar eclipse on 29 March 2006 in Turkey: polarization patterns of the eclipsed sky observed by full-sky imaging polarimetry. Appl Opt 47(34):H1–H10
Soldán T, Putz M (2000) Karyotypes of some Central European mayflies (Ephemeroptera) and their contribution to phylogeny of the order. Acta Soc Zool Bohem 64:437–445
Stevani CV, Faria DLA, Porto JS, Trindade DJ, Bechara EJH (2000a) Mechanism of automotive clearcoat damage by dragonfly eggs investigated by surface enhanced Raman scattering. Polym Degrad Stab 68:61–66
Stevani CV, Porto JS, Trindade DJ, Bechara EJH (2000b) Automotive clearcoat damage due to oviposition of dragonflies. J Appl Polym Sci 75:1632–1639
Svihla A (1961) An unusual ovipositing activity of *Pantala flavescens* Fabricius. Tombo 4:18
Szentkirályi F, Szalay L (2001) The impact of total solar eclipse of 11 August 1999 on behaviour and foraging activities of honeybees. Zool Bull 86:115–136 (in Hungarian)
Torralba-Burrial A, Ocharan FJ (2003) Coches como hábitat para libélulas? Algunos machos de *Crocothemis erythraea* creen que sí. Boletin de la Sociedad Entomologia Aragonesa 32:214–215
Turcsányi I, Szentkirályi F, Bernáth B, Kádár F (2009) Flight of mayflies towards horizontally polarised and unpolarised light. Aquat Insects 31(Suppl 1):301–310
Umow N (1905) Chromatische Depolarisation durch Lichtzerstreuung. Physikalische Zeitschrift 6:674–676
Upgren AR (1996) Night blindness: light pollution is changing astronomy, the environment, and our experience of nature. Amic J 17(4):22–25
van Vondel BJ (1998) Another case of water beetles landing on a red car roof. Latissimus 10:29
Verheijen FJ (1958) The mechanisms of the trapping effect of artificial light sources upon animals. Arch Néerl Zool 13:1–107
Verheijen FJ (1985) Photopollution: artificial light optic spatial control systems fail to cope with. Incidents, causations, remedies. Exp Biol 44:1–18
Watson JAL (1992) Oviposition by exophytic dragonflies on vehicles. Notulae Odonatologicae 3:137
Whitehouse FC (1941) A guide to the study of dragonflies of Jamaica. Bulletin of the Institute of Jamaica Science Series No. 3:1–69
Wildermuth H (1998) Dragonflies recognize the water of rendezvous and oviposition sites by horizontally polarized light: a behavioural field test. Naturwissenschaften 85:297–302
Wildermuth H (2007) Polarotaktische Reaktionen von *Coenagrion puella* und *Libellula quadrimaculata* auf Erdbeerkulturen als ökologische Falle (Odonata: Coenagrionidae, Libellulidae). Libellula 26(3/4):143–150
Wildermuth H, Horváth G (2005) Visual deception of a male *Libellula depressa* by the shiny surface of a parked car (Odonata: Libellulidae). Int J Odonatol 8:97–105
Wilson A (1998) Light pollution: efforts to bring back the night sky. Environ Build News 7(8): 8–14
Wyniger R (1955) Beobachtungen über die Eiablage von *Libellula depressa* L. (Odonata, Libellulidae). Mitteilungen der Entomologischen Gesellschaft Basel NF 5:62–63
Zahavi A (1971) The social behaviour of the white wagtail (*Motacilla alba alba*) wintering in Israel. Ibis 113:203–211
Zwick P (1992) Stream habitat fragmentation: a threat to biodiversity. Biodivers Conserv 1:80–97

Part III
Practical Applications of Polarization Vision and Polarization Patterns

Chapter 21
Polarization as a Guiding Cue for Oviposition in Non-biting Midges and Mosquitoes

Amit Lerner

Abstract Recently, a new utilization for light polarization has been demonstrated: the use of reflection polarizations from water surface to assess habitat quality and choose oviposition sites for water-living insects. While contradicting results were shown in the laboratory and at the natural habitat of long-living mosquitoes, their short-living, non-biting relatives, the chironomids (Chironomidae, midges, which serve as the host of the *Cholera* pathogen among many other species of bacteria), have shown clear response both under confined and unconfined conditions. The understanding of the advantage of following reflection polarizations to detect suitable reservoirs for oviposition opens a new research field of controlling pest insects using reflection-polarization traps, which has not been addressed to date.

21.1 Introduction: Purposes for Polarotaxis in Dipterans

Sensitivity to light polarization is very common among two-winged flies (Diptera) as apparent from behavioural studies showing polarotaxis [see reviews in Horváth and Varjú (2004) and in Part I]. Species in this order contain photoreceptive retinula cells with orthogonal microvilli, and in some species even cells with a third orientation of 45° exist, which allows for a full and most accurate detection of the two polarization components: the partial linear polarization and the orientation (E-vector) of polarization. Nonetheless, the purpose for detecting light polarization by dipteran insects was somewhat vague. As the dorsal rim area (DRA) of their compound eyes was found to be more polarization sensitive than other eye regions in some species (Labhart 1980; Nilsson et al. 1987; Labhart et al. 1992, 2009;

A. Lerner (✉)
Ocean BioOptics and Vision Laboratory, Israel Oceanographic and Limnological Research, National Institute of Oceanography, Tel-Shikmona, P.O.B. 8030, Haifa 31080, Israel
e-mail: amit.lerner@ocean.org.il

G. Horváth (ed.), *Polarized Light and Polarization Vision in Animal Sciences*, Springer Series in Vision Research 2, DOI 10.1007/978-3-642-54718-8_21,

Labhart and Meyer 1999), it was suggested that dipterans are using the polarization pattern of the sky as a sun compass for navigation. This purpose was shown in the field in the desert ants (Wehner and Müller 2006), but not yet in any dipteran species. Another use suggested for polarization sensitivity in dipterans is the detection of water bodies. Water and horizontal wet surfaces reflect highly and horizontally polarized light. In migrating desert locusts, it was suggested that the detection of water is important to avoid flying over the water (Shashar et al. 2005; see also Sect. 5.6). The purpose of water detection probably requires the special orthogonal microvilli architecture of the photoreceptive retinula cells that allows polarization vision in the ventral part of the insect eye.

21.2 Polarization as a Guiding Cue for Oviposition in Non-biting Midges

Chironomids (non-biting midges; Chironomidae) are dipterans including thousands of species globally dispersed in the world. They are aquatic insects that complete their developmental stages from egg to pupa underwater. The adults that emerge from the water surface live a very short time from a few hours to 2 days, in which they mate only once during sunset and die soon after. Before dying, each female oviposit only once, one gelatinous sac containing hundreds of eggs (egg batch) in the air-water-substrate interface. The larvae emerge from this sac and descend to the bottom of the water reservoir while feeding on the organic carbon in the water in all its forms (dissolved, particulate, etc.). After few weeks the pupa ascends to the water surface, and the adult emerges from the water body to the air (Armitage et al. 1995). Chironomids are a nuisance to humans as they may appear in water supply systems and as the carriers of the *Cholera* pathogen (Broza et al. 1998, 2005; Broza and Halpern 2001; Halpern et al. 2004); hence the importance of studying their reproductive behaviour.

Past studies (Danthanarayana and Dashper 1986; Schwind 1991) showed positive polarotaxis (attraction to horizontally polarized light) of chironomid adults using polarized light traps and reflective surfaces. Meltser et al. (2008) showed that the chironomid female does not oviposit randomly, but prefers dark water/wet surfaces. They also showed that this choice is guided by a visual, rather than an olfactorial, cue. These specularly reflecting (shiny) dark surfaces are usually highly polarizing (Umow 1905). Therefore, it was unclear whether the attraction of chironomid females was to the low light intensity (negative phototaxis) or the high polarization (positive polarotaxis), as these two cues were not carefully separated and controlled. Lerner et al. (2008), in a couple of multiple-choice experiments, separated and controlled these two visual cues to check which one is guiding the females to oviposition sites. One experiment was conducted indoors in a closed tent, where the females were lured to fly in, while the other was conducted outside on the edge of the midges' natural pond. In the indoor

experiment in the tent, four egg traps, transmitting high-intensity unpolarized light, high-intensity polarized light, low-intensity polarized light and low-intensity unpolarized light, were offered to the females. The amount of egg batches laid in the unpolarized and polarized traps was 40 and 60 %, respectively, showing preference to highly polarizing oviposition sites. However, this was not enough to determine if the polarization and not the intensity is the guiding cue.

Therefore, Lerner et al. (2008) conducted a second experiment outdoor. In this experiment four tubs (40 litre each) were deployed at the edge of a natural pond, where the chironomid population thrive. Two of the tubs were painted matte white to increase their reflectivity and reduce their reflection polarizations, while the other two tubs were left matte black. Two tubs of each brightness (white and black) were filled with tap (clear) water, while the other two were filled with pond water (from the natural reservoir of the chironomids, which was turbid by high concentration of dissolved and particulate organic carbon in water). This way the white tap-water-filled tub reflected high-intensity unpolarized light, the white tub with the pond water reflected low-intensity light with 20 % linear polarization and the two black tubs reflected low-intensity light with ~40 % polarization (there was a little difference in polarization and intensity between the two black tubs). In this case, the chironomid females followed the oviposition cue only as no egg batches (on average) were found in the high-intensity unpolarized tub, while their amount increased with increase of partial polarization. Therefore, Lerner et al. (2008) concluded that the polarization and not the intensity of light reflected from water surfaces is the cue guiding chironomid females to their oviposition sites.

This finding was further confirmed by Lerner et al. (2008) anatomically as a triple orientation arrangement of the microvilli (three retinula cells with their microvilli oriented at 0°, 45° and 90° to each other) in the ventral part of the female eye was demonstrated. This study quantified (in means of egg counting) the use of polarization for choosing oviposition site by chironomids, a phenomenon that was previously qualitatively described (as pre-oviposition behaviour) in other dipteran families (e.g. Horváth et al. 2007; Kriska et al. 2007). Following the study of Lerner et al. (2008), eight more European chironomid species were found to show pre-oviposition behaviour towards highly and horizontally polarizing surfaces (Horváth et al. 2011).

21.3 Why Chironomids Use Polarization to Detect Oviposition Sites?

In trying to understand why chironomid females prefer polarization over intensity as their guiding cue to oviposition sites, Lerner et al. (2008) measured the intensity and polarization of light reflected from the surface of tubs filled by water with varied turbidity levels as resulted by different total organic carbon (TOC) concentrations in water. They showed that while the reflected intensity is decreasing with

increasing water turbidity and TOC concentrations, the partial polarization increases. This, however, does not rule out the negative phototaxis (attraction to low light intensity) as a guiding cue. Therefore, Lerner et al. (2008) measured the light reflected from the pond surface at sunset, when chironomids swarm and mate and the females descend to oviposit. The intensity of light reflected from the chironomid natural reservoir was rapidly decreasing with time after sunset, while the partial polarization remained constant and high close to 70 %. This is because the polarization of pond-reflected light predominantly depends on the water turbidity and the particulate concentrations, while the intensity of reflected light depends on the main light source (setting sun in the sky). Lerner et al. (2008) concluded that the reason for using polarization rather than intensity of reflected light to detect water bodies suitable for oviposition is because it is a stable optical cue which provides a hint about the habitat quality, as high partial polarization of reflected light means more organic carbon in the water on which chironomid larvae feed, which may be interpreted by the females to be highly survival-success habitat for their offspring.

21.4 Egg Density Mediates Polarization-Guided Oviposition

In the indoor experiment (in the tent) of Lerner et al. (2008), the chironomids did not ignore the traps reflecting unpolarized light. This bothered the researchers as the expectation was that if the polarization is the only guiding cue, then unpolarized sites should be completely ignored, as resulted in the outdoor experiment. This difference in the chironomid oviposition behaviour between confined and unconfined conditions was further investigated by Lerner et al. (2011). The counts of egg batches were reanalysed to check for an effect of egg density and habitat availability on the choice of females. It was shown that under the confined condition of the tent, where egg density was in an order of magnitude higher and habitat availability (egg traps) was limited, the female preference to highly polarizing sites was weaker than in the unconfined experiment outdoor, where the egg density was in an order of magnitude lower and habitat availability was high (as females were free to oviposit along the pond bank in addition to the egg traps). Lerner et al. (2011) concluded that in the lack of suitable habitats, since chironomid females are short-living insects with only one cycle of oviposition, they will lay their eggs even in unsuitable low-quality habitats, as long as wet surfaces are available (the females do not oviposit onto dry surfaces and may die without laying their egg sac; personal communication by N. Meltser). This study revealed the change in oviposition behaviour between confined and unconfined conditions, which is highly important to understand and correctly interpret oviposition behaviour in natural and confined environments.

21.5 Is Mosquito Oviposition Guided by Polarization?

In their study, Meltser et al. (2008) used the mosquito *Culex pipiens* (Culicidae) as a control species to show that this mosquito does not oviposit by a visual but rather by a chemical cue. They offered a decaying material that provided a chemical cue and changed the water turbidity by growing algae which served as the visual cue. Unlike the chironomids that ignored completely chemical cues, the *Culex pipiens* mosquitoes chose their oviposition site by the chemical cue and ignored the visual one. This result was confirmed by Bernáth et al. (2008), who reported that in a dual-choice experiment in the laboratory, another mosquito species, *Aedes aegypti* (Culicidae), might also be non-polarotactic. However, later on, Bernáth et al. (2012) repeated their experiment, but then they controlled the chemical cues by rinsing the water offered in the experimental chamber. They showed that without the chemical cues of the water, *Aedes aegypti* females preferred highly and horizontally polarizing sites twice more than unpolarizing sites. It remains questionable, whether mosquitoes actually use polarization to detect water bodies in their natural habitat, as the above-mentioned studies were conducted in the laboratory only. As neither anatomical nor electrophysiological evidences support the use of polarization by mosquitoes, polarization sensitivity in this group remains to be reinforced in future studies.

21.6 Concluding Remarks and Future Studies

Chironomids and mosquitoes provide us an exceptional window to explore polarization-guided oviposition behaviour. On one hand, these two insect groups resemble in their seeking for a suitable water reservoir that includes organic carbon in water as food for their offspring. On the other hand, they differ dramatically in their lifespan which may make the difference in the primary cues that they use to choose a proper habitat for oviposition. Mosquitoes, as long-living creatures with multiple cycles of oviposition, can wait for organic matter to deteriorate and produce its smell which is a strong indicator for the amount and quality of the organic matter in water on which their larvae feed. Unlike mosquitoes, chironomids, as very short-living insects, do not have time to spend and wait for the organic matter to deteriorate and its smell to develop. Alternatively, they must rely on an optical cue, the polarization of light reflected from the water body, as it is the most stable and reliable cue in the time frame of their life. There is a good chance that mosquitoes, as aquatic dipterans, may possess the anatomical structures in their retinula cells that are able to perceive polarization and use this optical cue as a backup, in case sensing the water is not optimal for some reasons. However, as polarization-guided oviposition was demonstrated in mosquitoes only in the laboratory, further investigations should be carried out to determine in the field if reflection polarization is indeed used by mosquitoes as chironomids do.

Another indication for the need of field experiments on mosquitoes is the fact that the preference in the laboratory experiments to polarizing surfaces was in the ratio of 1:2. In the case of chironomids, in the confined experiment in the tent, the exact ratio was measured. However, in the field experiment, the chironomid preference was very clear and strong as the ratio stood on 1:10 in favour of the polarizing sites. This may indicate that in the laboratory, the behavioural response may be mediated by other factors than the investigated cue, masking the importance of the latter to the females. This holds another reason to conduct experiments on mosquitoes in their natural environment in the future.

Acknowledgements Our interdisciplinary chironomid project could not have been done without the guidance of experts of different disciplines. I am deeply grateful to O. Shoer for providing access to the study site, to J. Martin for species identification, to N. Meltser and M. Broza for introducing me to the chironomid biology, to M. Halpern for guiding me through the chironomid microbiology, to N. Sapir and E. Peltzer for their statistical assistance and to R. Jeger and Y. Lichtenfeld for their microscopy work. The chironomid project was funded by the Israel Science Foundation (grant no. 1527/07) to N. Shashar.

References

Armitage PD, Cranston PS, Pinder LCV (1995) The Chironomidae: the biology and ecology of non-biting midges. Chapman & Hall, New York, NY

Bernáth B, Horváth G, Gál J, Fekete G, Meyer-Rochow VB (2008) Polarized light and oviposition site selection in the yellow fever mosquito: no evidence for positive polarotaxis in *Aedes aegypti*. Vis Res 48:1449–1455

Bernáth B, Horváth G, Meyer-Rochow VB (2012) Polarotaxis in egg-laying yellow fever mosquitoes *Aedes* (*Stegomyia*) *aegypti* is masked due to infochemicals. J Insect Physiol 58:1000–1006

Broza M, Halpern M (2001) Pathogen reservoirs—Chironomid egg masses and *Vibrio cholerae*. Nature 412:40

Broza M, Halpern M, Teltsch B, Porat R, Gasith A (1998) Shock chloramination: potential treatment for chironomidae (Diptera) larvae nuisance abatement in water supply systems. J Econ Entomol 91:834–840

Broza M, Gancz H, Halpern M, Kashi Y (2005) Adult non-biting midges: possible windborne carriers of *Vibrio cholerae* non-O1 non-O139. Environ Microbiol 7:576–585

Danthanarayana W, Dashper S (1986) Response of some night flying insects to polarized light. In: Danthanarayana W (ed) Insect flight: dispersal and migration. Springer, Heidelberg, pp 120–127

Halpern M, Broza YB, Mittler S, Arakawa E, Broza M (2004) Chironomid egg masses as a natural reservoir of *Vibrio cholerae* non-O1 and non-O139 in freshwater habitats. Microb Ecol 47:341–349

Horváth G, Varjú D (2004) Polarized light in animal vision—polarization patterns in nature. Springer, Heidelberg

Horváth G, Malik P, Kriska G, Wildermuth H (2007) Ecological traps for dragonflies in a cemetery: the attraction of *Sympetrum* species (Odonata: Libellulidae) by horizontally polarizing black gravestones. Freshw Biol 52:1700–1709

Horváth G, Móra A, Bernáth B, Kriska G (2011) Polarotaxis in non-biting midges: female chironomids are attracted to horizontally polarized light. Physiol Behav 104:1010–1015

Kriska G, Bernáth B, Horváth G (2007) Positive polarotaxis in a mayfly that never leaves the water surface: polarotactic water detection in *Palingenia longicauda* (Ephemeroptera). Naturwissenschaften 94:148–154

Labhart T (1980) Specialized photoreceptors at the dorsal rim of the honeybees compound eye—polarizational and angular sensitivity. J Comp Physiol 141:19–30

Labhart T, Meyer EP (1999) Detectors for polarized skylight in insects: a survey of ommatidial specializations in the dorsal rim area of the compound eye. Microsc Res Tech 47:368–379

Labhart T, Meyer EP, Schenker L (1992) Specialized ommatidia for polarization vision in the compound eye of cockchafers, *Melolontha melolontha* (Coleoptera, Scarabaeidae). Cell Tissue Res 268:419–429

Labhart T, Baumann F, Bernard G (2009) Specialized ommatidia of the polarization-sensitive dorsal rim area in the eye of monarch butterflies have non-functional reflecting tapeta. Cell Tissue Res 338:391–400

Lerner A, Meltser N, Sapir N, Erlick C, Shashar N, Broza M (2008) Reflected polarization guides chironomid females to oviposition sites. J Exp Biol 211:3536–3543

Lerner A, Sapir N, Erlick C, Meltser N, Broza M, Shashar N (2011) Habitat availability mediates chironomid density dependent oviposition. Oecologia 165:905–914

Meltser N, Kashi Y, Broza M (2008) Does polarized light guide chironomids to navigate toward water surfaces? Boletin do Museu Municipal do Funchal (História Natural) 13:141–149

Nilsson DE, Labhart T, Meyer E (1987) Photoreceptor design and optical-properties affecting polarization sensitivity in ants and crickets. J Comp Physiol A 161:645–658

Schwind R (1991) Polarization vision in water insects and insects living on a moist substrate. J Comp Physiol A 169:531–540

Shashar N, Sabbah S, Aharoni N (2005) Migrating locusts can detect polarized reflections to avoid flying over the sea. Biol Lett 1:472–475

Umow N (1905) Chromatische depolarisation durch lichtzerstreuung. Phys Z 6:674–676

Wehner R, Müller M (2006) The significance of direct sunlight and polarized skylight in the ant's celestial system of navigation. Proc Natl Acad Sci USA 103:12575–12579

Chapter 22
Linearly Polarized Light as a Guiding Cue for Water Detection and Host Finding in Tabanid Flies

Gábor Horváth, Ádám Egri, and Miklós Blahó

Abstract In this chapter we show that tabanid flies are attracted to horizontally polarized light stimulating their ventral eye region. Female and male tabanids use this polarotaxis governed by the horizontal E-vector to find water, while another type of polarotaxis based on the degree of polarization serves host finding by female tabanids. We show that female tabanids are less attracted to bright than dark hosts, the reason for which is partly that dark hosts reflect light with higher degrees of polarization than bright hosts. We also demonstrate that the use of a striped fur pattern has the advantage that such coat patterns attract far fewer tabanids than either homogeneous black, brown, grey or white equivalents. The attractiveness of striped patterns to tabanids is also reduced if only polarization modulations (parallel stripes with alternating orthogonal directions of polarization) occur in homogeneous grey surfaces. The attractiveness to tabanids decreases with decreasing stripe width, and stripes below a certain width threshold are unattractive at all to tabanids. Further, the stripe widths of zebra coats fall in a range where the striped pattern is most unattractive to tabanids. Tabanids are strongly attracted by CO_2 and ammonia emitted by their hosts. We show here that the poor visual attractivity of stripes to tabanids is not overcome by olfactory attractiveness. Finally, we show that dark spots on a bright coat surface also disrupt the visual attractiveness to tabanids. The smaller and the more numerous the spots, the less attractive the host is to tabanids. The attractiveness of spotty patterns to tabanids is also reduced if the target exhibits spottiness only in the angle of polarization pattern, while being homogeneous grey with a constant high degree of polarization. This could be one of the possible

Electronic supplementary material is available in the online version of this chapter at 10.1007/978-3-642-54718-8_22. Colour versions of the black and white figures as well as supplementary figures can also be found under http://extras.springer.com. The video clip can be accessed at http://www.springerimages.com/videos/978-3-642-54717-1.

G. Horváth (✉) • Á. Egri • M. Blahó
Environmental Optics Laboratory, Department of Biological Physics, Physical Institute, Eötvös University, Pázmány sétány 1, 1117 Budapest, Hungary
e-mail: gh@arago.elte.hu; adamp39@gmail.com; majkl2000@gmail.com

G. Horváth (ed.), *Polarized Light and Polarization Vision in Animal Sciences*, Springer Series in Vision Research 2, DOI 10.1007/978-3-642-54718-8_22,

evolutionary benefits that explains why spotty coat patterns are so widespread in mammals, especially in ungulates, many species of which are tabanid hosts.

22.1 Polarotaxis in Tabanid Flies

22.1.1 Ventral Polarization Vision in Tabanids: Attraction to Horizontal Polarization

The tabanid flies (Diptera: Tabanidae, including horseflies of the genus *Tabanus* and deerflies of the genus *Chrysops*, as the economically two most important tabanid genus) are distributed worldwide (Baldacchino et al. 2014). Adult tabanids feed on nectar and pollen, and the females usually feed also on (mainly mammalian) blood which aids the development of their eggs (Hayakawa 1980; Hall et al. 1998; Lehane 2005; Krcmar and Maric 2006). Tabanid females usually lay their eggs on marsh plants next to freshwater bodies, because after egg hatching the larvae must drop down into water or onto mud, where they develop (Tashiro and Schwardt 1953). The haematophagous female tabanids can find their host animals by odours, heat and visual cues (Thorsteinson et al. 1965; Allan et al. 1987; Krcmar 2005a, b, 2013; Krcmar et al. 2005; Lehane 2005). With multiple-choice experiments in the field, Horváth et al. (2008) showed the attraction to horizontally polarized light stimulating the ventral eye region in both males and females of 27 tabanid species. This behaviour is called positive polarotaxis.

The positive polarotaxis in water-seeking tabanids was discovered in a Hungarian cemetery (in the town of Kiskunhalas) where tabanids were abundant, because there was a horse school in the immediate vicinity. In this cemetery the reasons for attraction of *Sympetrum* dragonflies to polished black gravestones were studied (Horváth et al. 2007). During these experiments it was observed that tabanid flies are also lured to the strongly and horizontally polarizing shiny smooth surfaces of black tombstones (Fig. 22.1). This accidental observation inspired the subsequent systematic field experiments (Horváth et al. 2008). Hansruedi Wildermuth (Rüti, Switzerland; personal communication, 2008) observed similar reactions of *Tabanus* species to horizontal black plastic and dark brown perspex sheets during field experiments designed for the examination of dragonfly responses to shiny surfaces (Wildermuth 1998).

Horváth et al. (2008) experienced that among white, black and aluminium (colourless) horizontal, smooth or matte test surfaces laid on the ground, both female and male tabanids preferred only the strongly and horizontally polarizing smooth (shiny) black surfaces against weakly and not horizontally polarizing surfaces (positive or negative phototaxis; furthermore, colour, temperature and odour preferences were excluded). The female-to-male ratio of the attracted tabanids was about 1.7, but this ratio differed slightly from site to site and was also species specific. The attracted tabanids touched the black surface 2–50 times. They landed on the surface directly, or prior to landing, they performed a typical

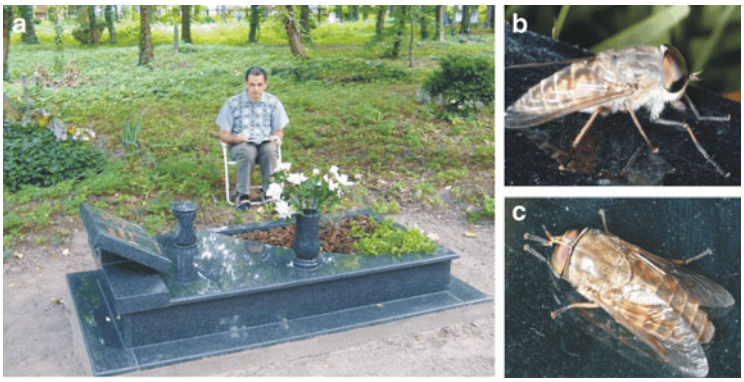

Fig. 22.1 (**a**) A polished dry black gravestone in a cemetery of Kiskunhalas (Hungary), where the positive polarotaxis of tabanid flies was discovered. (**b**, **c**) Tabanids landed on the horizontal surface of the gravestone

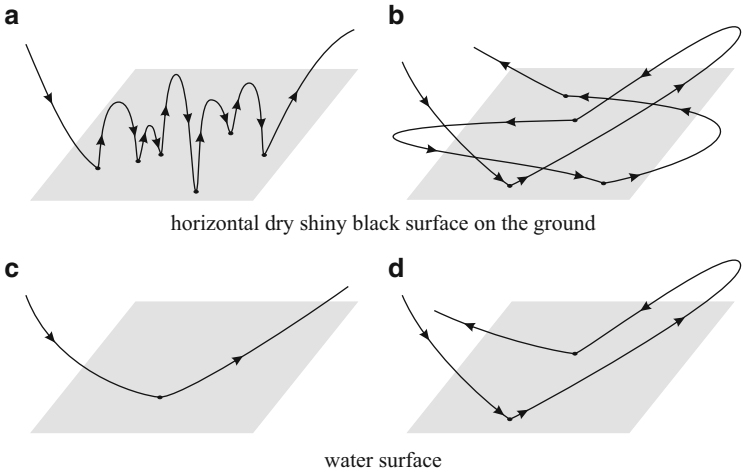

Fig. 22.2 (**a**, **b**) Schematic drawings of the trajectories of two typical types (**a**: vertical, **b**: horizontal) of the touching flight of tabanids displayed prior to landing on horizontally polarizing dry shiny black surfaces on the ground. *Dots* represent the sites where the insect touches the surface, and arrowheads show the direction of flight. (**c**, **d**) Typical flight trajectories of tabanids touching a water surface one (**c**) or two (**d**) times

touching flight with nearly vertical (Fig. 22.2a) or approximately horizontal (Fig. 22.2b) loops flying down and up or to and fro above the surface and touching it at several points. Such touchdowns are typical when tabanids are drinking or bathing (Fig. 22.2c, d).

Although Burakova and Mazokhin-Porshnyakov (1982) studied the ultrastructure of the compound eye in the tabanid species *Haematopota pluvialis*, they did not investigate the ventral eye region. Smith and Butler (1991) studied the ultrastructure of the retina of female tabanid flies of 14 different species. They

investigated five ommatidia from the equatorial eye region and one dorsal ommatidium near the eye margin. They found closely spaced rhabdomeres in the distal retina and twisting of the peripheral rhabdomeres R1–R6 only in the proximal half of the ommatidium, while the central rhabdomeres R7 and R8 do not twist, and their microvilli are orthogonal to each other. From these they hypothesized that "*unlike other flies, the dorsal margin of tabanid eyes may not be specialized for polarized light detection, but instead horse flies and deer flies may have some polarization sensitivity across the entire eye*". Although there is no overlapping among the tabanid species studied by Smith and Butler (1991) and those investigated by Horváth et al. (2008), the validity of the cited hypothesis is supported by the finding of Horváth et al. (2008) that tabanids have ventral polarization vision and positive polarotaxis. Behavioural experiments with *Hybomitra hinei wrighti* performed by Smith and Butler (1991) indicated that males of this species may use polarized light for orientation during mating flights: males, exhibiting mating flights only during times when direct sunlight is available, changed their direction of hovering orientation when a linearly polarizing filter was positioned over them and rotated. The lack of enough information on the retina in tabanid flies warrants further anatomical and electrophysiological studies on the polarization sensitivity of different eye regions in tabanids.

Horváth et al. (2008) proposed that ventral polarization vision in tabanids has an adaptive significance in the following four biological contexts:

1. It guides both male and female tabanids to water bodies, which they need for drinking and temperature control (Fig. 22.3a).
2. It provides females with an increased probability of finding hosts, because social herbivores regularly visit bodies of freshwater (Fig. 22.3b, c). Tabanid females lie in wait in shady areas under bushes and trees for a blood host to happen by. Sight is the main host-finding mechanism, but carbon dioxide and odour also play a role, and moving objects, especially if dark coloured, are most prone to attack (Lehane 2005). The commonest host animals of haematophagous tabanid females are large social herbivores that regularly visit freshwater bodies to drink and/or bath (Duncan and Vigne 1979). Consequently, female tabanids can easily and regularly meet the herd of these hosts for blood-sucking purposes (Rutberg 1987). Thus, one of the functions of polarotaxis in female tabanids could be the indirect host-seeking: first detecting a water body from a distance by horizontally polarized water-reflected light, then seeking drinking/bathing host animals at the water (Fig. 22.3b, c). The strategy of indirect host search by polarization remote sensing of the water surface (Fig. 22.4b) may be more efficient than the direct random visual search of the blood host (Fig. 22.4a).
3. It guides both sexes of tabanids to locations where the probability of encountering a mate is high (Fig. 22.3d).
4. It attracts females to potential egg-laying sites (Fig. 22.3e, f), from which larvae can descend into water or moist mud (Fig. 22.3g).

Finally, we mention that the positive polarotaxis in both sexes of tabanids offers new methods for trapping these economically important insects (see Sect. 23.2).

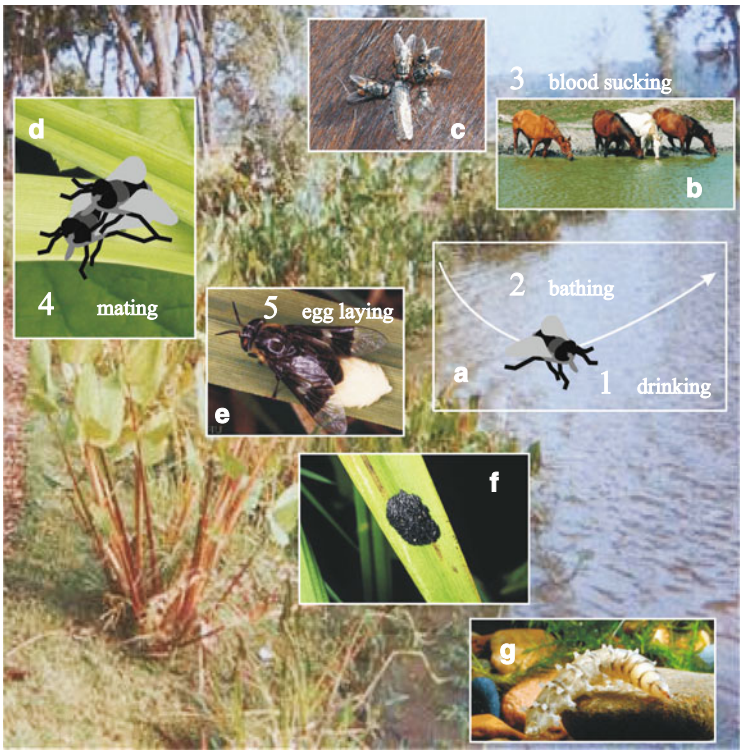

Fig. 22.3 Tabanid flies can search water by positive polarotaxis in order to drink (1), to bath (2), to find blood-host drinking/bathing at freshwater bodies (3), to find a mate near water (4), and to lay the eggs onto marsh plants near water (5). (**a**) Tabanids touch the water surface when they drink or bath to cool their body. (**b**) The host animals (e.g. horses or cattle) of tabanids gather periodically at freshwater bodies to drink or bath. (**c**) A tabanid fly (*bottom*, with vertical body) sucking the blood of a horse together with other non-tabanid dipterans. (**d**) Female and male tabanids (schematic drawings) often mate on the leaves of marsh plants near waters. (**e**) Female tabanids usually oviposit on marsh plants leaning over water or mud (Photograph E by Dr. Jerry Butler, University of Florida, USA; the other photos are taken by Dr. György Kriska). (**f**) After oviposition the originally bright eggs become dark-coloured. (**g**) After egg hatching the tabanid larvae drop into the underlying water or mud, where they usually develop

22.1.2 Two Kinds of Polarotaxis in Tabanids: The Degree and the Direction of Polarization Govern the Attraction of Tabanids to Differently Polarizing Host Animals and Water Surfaces

Orientated motion of animals towards a spatial source governed by a particular cue is called taxis. One of the most well-known taxes is phototaxis (Menzel 1979; Jékely 2009). In the early 1980s Schwind (1983, 1984, 1985a, b) discovered the phenomenon of polarotaxis: He found that the water bug *Notonecta glauca* is

Fig. 22.4 Two possible strategies of host search by female tabanids. (**a**) Direct visual and/or olfactorial random search of the blood host being somewhere in the optical environment. (**b**) Indirect search of the host drinking/bathing at water bodies with water detection by polarization remote sensing

attracted to horizontally polarized light, if this optical cue stimulates its ventral eye region. The function of this positive polarotaxis is to help the detection of aquatic habitats by means of the horizontally polarized light reflected from the water surface. Later, this kind of polarotaxis governed by the horizontal direction of polarization (E-vector) of reflected light has been found in many other aquatic insect species (Schwind 1989, 1991, 1995, 1999; Wildermuth 1998; Horváth and Varjú 2004; Csabai et al. 2006; Kriska et al. 2006, 2007, 2008; Horváth et al. 2007, 2010a, b, 2011; Lerner et al. 2008; Horváth and Kriska 2008).

Tabanid flies also detect water by this kind of polarotaxis (Horváth et al. 2008; Kriska et al. 2009). Females of many tabanid species have to find a host animal to obtain a blood meal that ensures egg development. The host choice of these tabanids is partly governed by the linear polarization of light reflected from the host's coat (Horváth et al. 2010b; Egri et al. 2012a). This polarization-based behaviour of female tabanids, however, should be different from the polarotaxis governed by the horizontal E-vector direction, because the coat-reflected light is not always horizontally polarized (Horváth et al. 2010b; Egri et al. 2012a).

Using aerial and ground-based visual targets with different degrees of polarization (changing from unpolarized through weakly and moderately polarized to strongly polarized at the Brewster angle) and directions of polarization (changing from vertical through tilted to horizontal as functions of the angle of reflection and viewing direction) in multiple-choice field experiments, Egri et al. (2012b) discovered a second kind of polarotaxis in tabanids being governed by the degree of polarization of reflected light. They showed that both female and male tabanids use

polarotaxis governed by the horizontal direction of polarization to find water. In this polarotactic water detection, the degree of polarization d plays only a marginal role: it should be higher than a species-specific threshold d^* (Kriska et al. 2009). If $d > d^*$, the polarotaxis is governed by the direction of polarization: if the deviation of the angle of polarization α from the horizontal is smaller than a threshold $\Delta\alpha^*$, a polarotactic aquatic insect is attracted to the partially linearly polarized light. The reason for the phenomenon that horizontally polarizing surfaces on the ground attract more females than males is that females have more motivation to seek water surfaces: Male and female tabanids are attracted to horizontally polarized light, if they look for mates or for water to drink or to bath; furthermore, females are also attracted to such light, if they want to lay their eggs into/near water/mud.

On the other hand, the polarotaxis based on the degree of polarization serves host finding by female tabanids, independently of the direction of polarization of light reflected from the host's coat. Since the different body parts of a host animal reflect light with different E-vector directions, this second polarotaxis cannot be elicited exclusively by horizontally polarized light. In this case the E-vector direction of host-reflected light is irrelevant, and only d of reflected light is important. Earlier studies (Horváth et al. 2010b; Egri et al. 2012a) showed that the darker the coat of the host, i.e. the higher the d of host-reflected light, the larger its attractiveness to tabanids.

Although differently coloured hosts should equally be appropriate as blood sources for female tabanids, these insects prefer darker (black, brown) hosts against brighter (light grey, white) ones partly due to the higher degrees of polarization of light reflected from darker fur coats, as shown by Horváth et al. (2010b) (see Sect. 22.2). The sense of polarotaxis governed by the degree of polarization serving host choice may be the following: Host animals cannot be unambiguously detected by means of their brightness and colour. Although dark/bright hosts in front of a bright/dark background can be easily detected, dark/bright hosts in front of a dark/bright background can be recognized only with difficulty. However, since the (usually vegetation) background reflects only weakly polarized light, a dark host animal can be easily detected by means of the strongly polarized light reflected from its coat. This may be the reason why female tabanids prefer host animals with strongly polarizing darker coats (Horváth et al. 2010b) aside from the fact that the blood of darker or brighter hosts would be equivalently appropriate for female tabanids to ripen their eggs.

The probably species-dependent spectral range where the polarization vision of tabanids functions should be determined in future studies.

22.2 An Advantage of Bright Coats of Tabanid Hosts

In nature light grey or albino ungulates are rare because of their great vulnerability. White (termed "grey" in the equestrian literature) horses, for example, have a higher sensitivity to solar radiation often leading to malign skin cancer and deficiency of the visual system (Pielberg et al. 2008). A white-coated animal is easily

detected by predators; thus individuals with white coats have been selected out from wild populations during evolution. On the other hand, humans have bred a bloodline of white horses just because of their rarity in the wild. To humans the white horse became an icon for dignity, a status symbol demonstrating wealth (Tresidder 2005).

Horváth et al. (2010b) observed the reactions of a brown (termed "bay" in the equestrian literature) and a white horse to tabanid attacks on a sunny warm day on a field in Hungary. They also measured the time periods spent by both horses in the sunny field and the shady forest bordering the field. When horses are attacked by tabanids (Fig. 22.5), they perform typical defensive reactions by which they try to drive away the tabanids from their bodies with tail swishing, kicking of legs, rolling about on the ground, shuddering of the skin, swinging the head and biting and licking the blood-sucking tabanids on their coats (Fig. 22.6). Due to the intense tabanid attacks, the observed horses shuttled between the sunny field and the shady surrounding forest. After a period spent grazing, the horses escaped from the aggressive tabanids into the shady forest refuge, where they suffered tabanid annoyance only rarely,[1] and thus they could rest and wait there quietly. After a certain period the horses ventured out from the forest shade to graze again in the sunny field, from which they were soon again driven into the forest by tabanids. This shuttling was repeated by the horses periodically until mid day, when the tabanid attacks became so intense that the horses could not graze any further in the field. It was always the brown horse that was first driven into the forest by attacking tabanids. The brown horse spent 2.2 times longer in the tabanid-free shady forest than in the sunny field, while the white horse stayed 1.2 times longer in the sunny field, where it was able to continue to graze, than in the forest.

[1] It is well known among horse keepers that in shady refuges, in forests or in stables, horses suffer tabanid annoyance only rarely. Tabanid flies do not follow horses and other host animals in large numbers to such shady places more or less surrounded by vegetation or artificial walls. The reasons for this are the following (Horváth et al. 2010b): (1) Tabanids need enough free, open space to fly. (2) Many tabanid species need a higher body temperature to start flying so quickly that they can successfully escape from the defensive reactions of a host animal (e.g. tail swishing, biting, licking), by which the host tries to drive them away from its body. In shady refuges the wing muscles of tabanids may not function rapidly enough for such an escape. Therefore, tabanids attack host animals usually under sunny conditions. For the same reason, tabanids usually do not fly and attack hosts on overcast days and under rainy or too windy conditions. However, certain small-sized tabanids prefer periods prior to rain, because the lower air temperature and the higher air humidity are advantageous to these insects, whose body has a large surface/volume ratio, and thus they can easily become dehydrated under sunny, dry and windy conditions. (3) The forest vegetation, as a structured background, makes more difficult the visual recognition of host animals.

On the other hand, when looking for water by means of the horizontally polarized water-reflected light, tabanids can quickly fly through shady areas and touch the water surface to drink and/or bath, for example. This water-seeking behaviour of male and female tabanids is quite different from the blood-sucking behaviour of tabanid females. The former can happen under both shady and sunny conditions, while the latter is usually performed in sunshine.

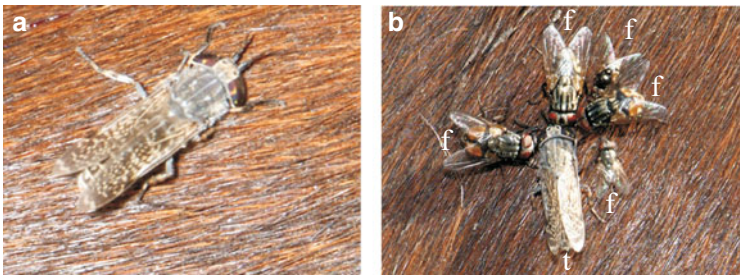

Fig. 22.5 (**a**) A blood-sucking female tabanid on the coat of a brown horse. (**b**) A blood-sucking female tabanid (t) and other non-tabanid flies (f) on the coat of a brown horse. The flies consumed the blood bubbling out from the wound cut by the tabanid [after Fig. 1a on page 1645 of Horváth et al. (2010b)]

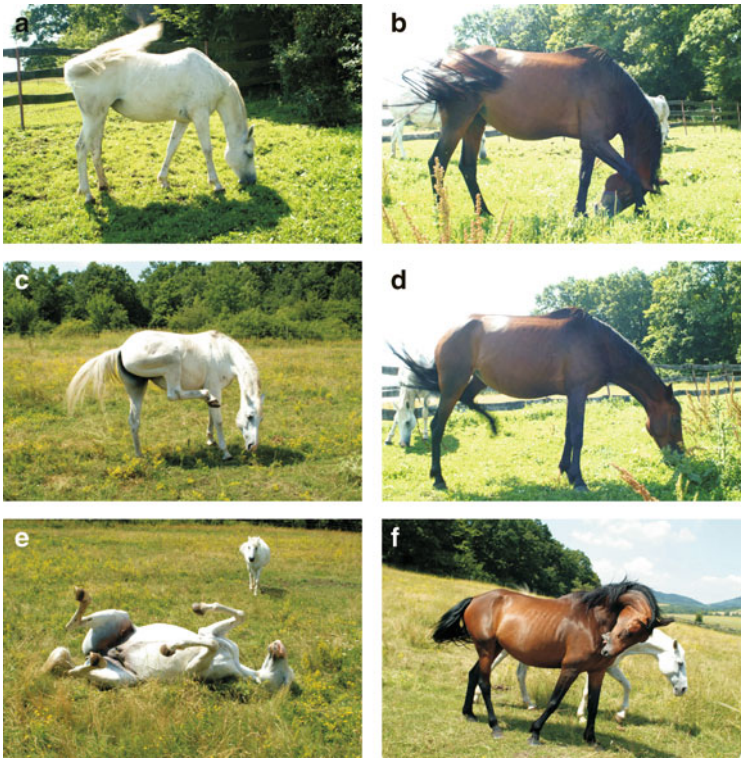

Fig. 22.6 Typical defensive reactions of a white horse (**a**, **c**, **e**) and a brown horse (**b**, **d**, **f**) to attacking tabanids observed by Horváth et al. (2010b): tail swishing (**a**, **b**), kicking of the fore leg (**b**) or the hind leg (**c**, **d**), rolling about on the ground (**e**), biting and licking the blood-sucking tabanids on the coat (**f**) [after Fig. 1b-d on page 1645 of Horváth et al. (2010b)]

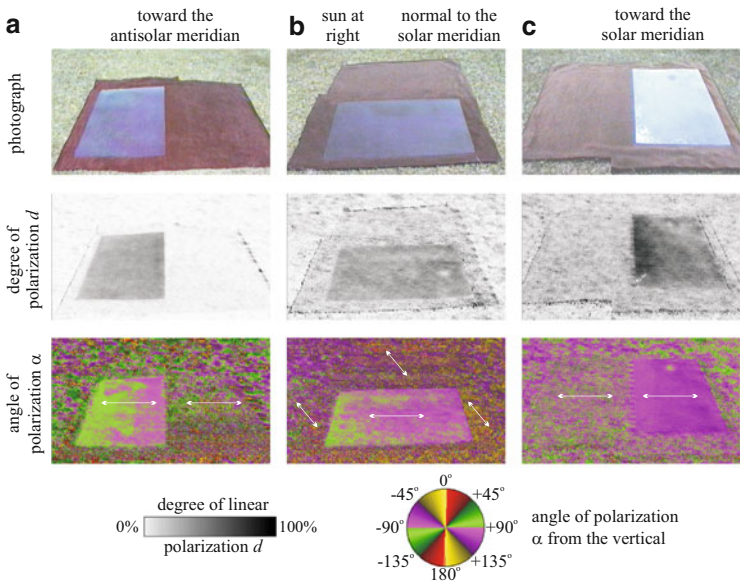

Fig. 22.7 Reflection-polarization characteristics of the shiny brown (*left*) and matte brown (*right*) sunny test surfaces used in one of the experiments of Horváth et al. (2010b) measured by imaging polarimetry in the blue (450 nm) part of the spectrum from three different directions of view relative to the solar meridian. The elevation angle of the polarimeter's optical axis was −35° from the horizontal. In the α-patterns double-headed arrows show the local directions of polarization of reflected light. When the test surfaces were shady, their polarization patterns were quite similar with the only difference that the direction of polarization of reflected light was always horizontal [after Fig. 2 on page 1646 of Horváth et al. (2010b)]

Counting the numbers of tabanids in numerous high-resolution picture pairs taken of a brown and a white horse, Horváth et al. (2010b) found that there were about four times more tabanids near to or sitting on the brown horse compared to the white one. The higher attractiveness of darker horses to tabanids relative to that of white horses was corroborated in another experiment, in which one black, one brown and one white sticky horse model was used. The black and brown horse models trapped 26 and 15 times more tabanids than the white horse model, respectively.

Horváth et al. (2010b) performed also multiple-choice field experiments, in which the attraction of tabanid flies to dry and sticky test surfaces with different reflection-polarization characteristics was studied. For example, on the ground a dry matte brown cloth was laid, the half of which was covered by a transparent, colourless plastic sheet, and the number of tabanids and their landings on both test surfaces was counted. Independently of the viewing direction relative to the solar meridian, the shiny brown surface reflected always horizontally polarized light with high degrees of polarization *d*, while the matte brown surface reflected only weakly polarized light with direction of polarization depending on the direction of view relative to the sun (Fig. 22.7). The dry matte brown cloth was unattractive to tabanids, while the plastic sheet on it attracted numerous tabanids, independently

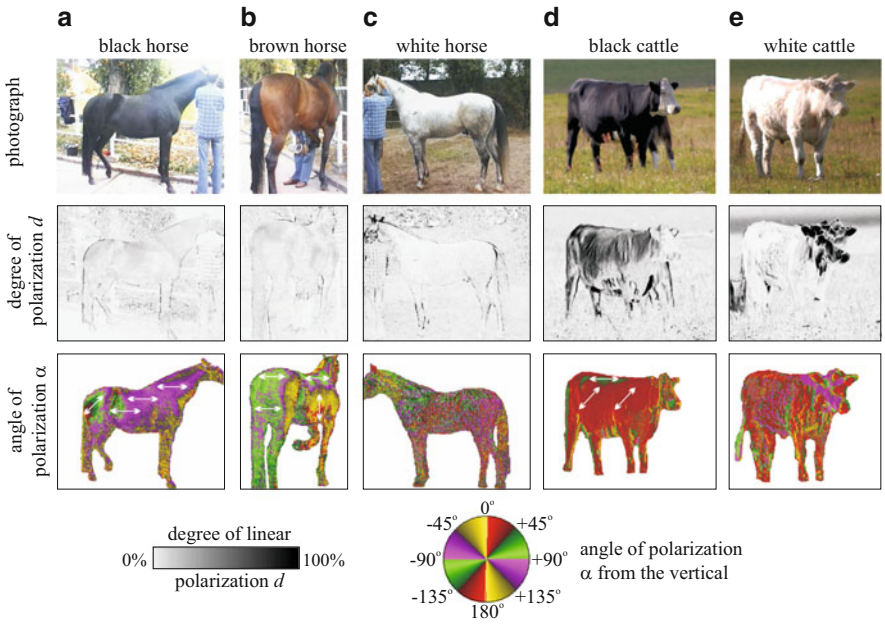

Fig. 22.8 Reflection-polarization characteristics of black (**a**), brown (**b**, bay) and white (**c**, grey) horses, and black (**d**) and white (**e**) cattle measured by imaging polarimetry in the blue (450 nm) part of the spectrum. In **d** and **e** the sun was shining from the top left corner. The optical axis of the polarimeter was horizontal. In the α-patterns double-headed arrows show the local directions of polarization of light reflected from the horse/cattle coat, and the background of the horses is white for the sake of a better visualization. In **e** the bull moved its head during polarimetry, resulting in motion artefact, which is the reason for the artificially (unreal) high degrees of polarization *d* of its head. In reality, the head of the bull reflected unpolarized or weakly polarized light as its whole body surface [after Fig. 3 on page 1647 of Horváth et al. (2010b)]

of the illumination conditions (sunny or shady) due to the positive polarotaxis governed by the direction of polarization.

In another experiment of Horváth et al. (2010b), five vegetable-oil-filled trays with different greyness (white, light grey, medium grey, dark grey, black) were laid on the ground, and the tabanids trapped by them were counted. There was a positive correlation between the darkness of a colourless, shiny, horizontally polarizing test surface and its attractiveness to tabanids: the white, light grey and medium grey oil-filled trays trapped only 1–3 % of the total number of tabanids, the dark grey tray captured 20 %, while the black tray trapped 75 %. This difference can be explained by the fact that the darker the trap surface, the higher the degree of polarization *d* of reflected light in all spectral ranges (see Fig. 5.13).

To compare the polarizing characteristics of their horse models and test surfaces with those of typical host animals of tabanids, Horváth et al. (2010b) measured the reflection-polarization patterns of living horses and cattle by imaging polarimetry. Black, brown and light grey/white fur coats reflect strongly, moderately and weakly polarized or unpolarized light, respectively (Fig. 22.8). The direction of

Fig. 22.9 A cartoon (composed by Miklós Blahó) demonstrating that black horses attract much more horseflies than white horses

polarization of coat-reflected light depends on the body part from which the light is reflected (Fig. 22.8). These polarizing characteristics are general and valid for all host animals of tabanids.

Hence, white/bright host animals are less attractive to blood-sucking tabanids than dark hosts (Fig. 22.9). The reasons for this are partly the polarizing properties of the darker coat (Fig. 22.8), rather than only the darker colour and/or higher surface temperature. The stronger attraction of tabanids to darker hosts can partly be explained by positive polarotaxis governed by the degree of polarization. Since horses and other mammals suffer considerably from tabanids, the tabanid-proof feature of host animals is advantageous.

Finally, we mention that since tabanids are usually drab and darkish in colour, it is imaginable that in order to be less visible and to protect themselves from insectivorous birds, they prefer hosts that have more or less the same brightness, colour and polarization as the tabanid flies themselves.

22.3 Visual Repellency of Zebra Stripes to Host-Seeking Tabanids

22.3.1 An Advantage of Zebra Stripes

The most striking characteristics of zebras are their black and white stripes (Fig. 22.10). Zebras occur in Central and South Africa, where three species live:

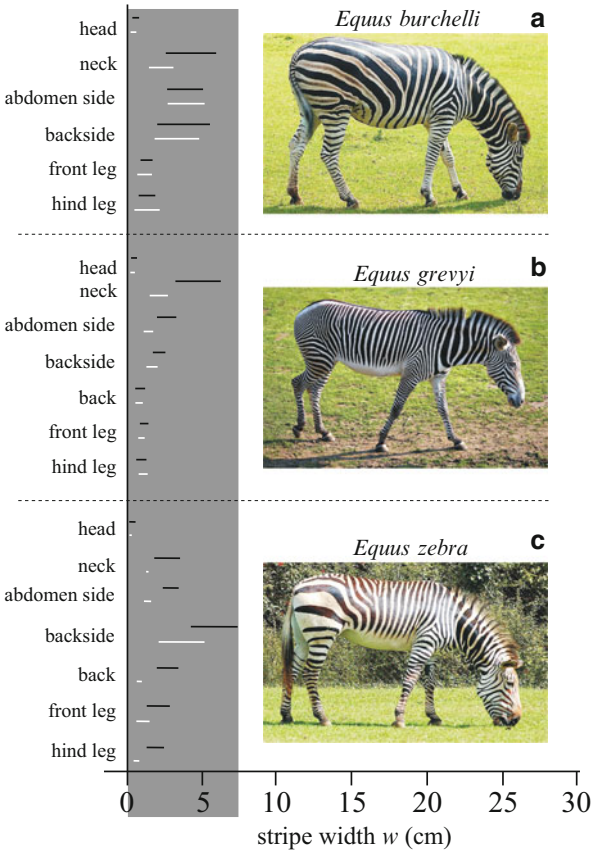

Fig. 22.10 Photographs of the three extant zebra species: (**a**) plains zebra, *Equus burchelli* (http://www.shoarns.com/ZebraGallery.html); (**b**) Grevy's zebra, *E. grevyi* (http://www.easypedia.gr/el/images/shared/4/48/Equus_grevyi_(aka).jpg); and (C) mountain zebra, *E. zebra* (http://www.shoarns.com/ZebraGallery.html). The horizontal black and white bars represent the ranges of the width w (average $\pm$ standard deviation) of the black and white stripes, respectively, measured by Egri et al. (2012a) on different body parts (head, neck, abdomen side, backside, back, front leg, hind leg) of *E. burchelli* (13 coats), *E. grevyi* (5 coats) and *E. zebra* (1 coat). Vertical grey column: range of w (0.23 cm $< w <$ 7.47 cm) measured on zebra coats (minimum of average $-$ standard deviation $\leq w \leq$ maximum of average + standard deviation) [after Fig. 1 on page 740 of Egri et al. (2012a)]

the plains zebra, *Equus burchelli* (Fig. 22.10a); the Grevy's zebra, *E. grevyi* (Fig. 22.10b); and the mountain zebra, *E. zebra* (Fig. 22.10c). The extinct quagga, *E. quagga* (Fig. 22.11), also had stripes on the head, neck and front half of its body (Bard 1977). The reason for the striped coat pattern in zebras has long been debated. Wallace (1867, 1879), for example, suggested that zebras evolved striped coats as camouflage against carnivores in tall grass. Darwin (1871) criticized this

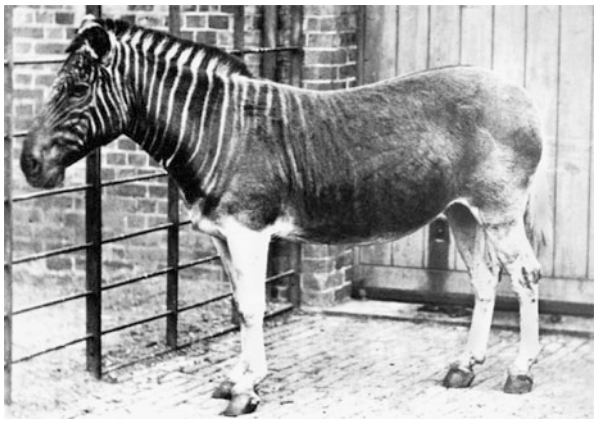

Fig. 22.11 The quagga (*Equus quagga*), a subspecies of the plains zebra (*E. burchelli*). This female quagga, formerly of the London Zoo in Regent's Park, is the only one ever photographed alive (http://en.wikipedia.org/wiki/Quagga)

hypothesis, since zebras do not occur in areas with dense vegetation, but rather prefer open savannah habitats with short grass. Since the nineteenth century, numerous alternative hypotheses have been proposed to explain the possible functions and evolutionary significance of the striped coat pattern of zebras:

- **Apparent size increase**: The stripes may create a visual illusion that increases the apparent size of the zebra. This illusion could afford zebras an advantage over their predators (Cott 1966; Cloudsley-Thompson 1984; Vaughan 1986; Morris 1990).
- **Visibility in poor light**: Near dusk and dawn or in moonlight, the stripes might be difficult to make out even when being quite close to zebras (Galton 1851; Kipling 1908; Cott 1966; Cloudsley-Thompson 1984; McLeod 1987; Morris 1990).
- **Moving stripes may dazzle predators**: The moving stripes of fleeing zebras might make it difficult for predators to single out an individual zebra from the herd (Cott 1957; Kruuk 1972; Eltringham 1979). The stripes of even a single individual may be enough to dazzle and confuse a predator (Morris 1990).
- **Camouflage**: The stripes may allow zebras to blend in with their background (e.g. tall grass or savannah vegetation) by dissolution of their contour (Wallace 1867, 1879; Thayer 1909; Marler and Hamilton 1968).
- **Social benefits**: Since the stripe pattern is individual as a fingerprint, zebras may recognize each other on the basis of their stripes (Morris 1990; Prothero and Schoch 2003). This might be especially important in the visual communication between mothers and their foals or in reinforcing the bond between male and female in courtship (Cloudsley-Thompson 1984; Becker and Ginsberg 1990). Stripes might also be visual markers for group bonding or to direct companions to particular parts of the body for grooming (Kingdon 1984).
- **Fitness indication**: Irregularities in the stripe pattern due to hurts, injuries or any kind of acute dysfunction might be a visual signal about the poor physical condition (fitness) of the individual for mate-seeking zebras (Ruxton 2002).

- **Thermoregulation**: The fat pattern in the skin may correlate with the pattern of black stripes, which might function as heat absorbers, and thus may play a role in the thermoregulation of the body. Furthermore, the black and white stripes may work together (inducing rotary breezes by thermal convection of air) to keep the animal cooler than without stripes (Cloudsley-Thompson 1984; Kingdon 1984; Morris 1990; Louw 1993).
- **Protection from tsetse flies**: Zebras seem to be unfavoured hosts for tsetse flies (Jordan 1986). According to Harris (1930), Waage (1981) and Gibson (1992), the purpose of zebra stripes may be protection from tsetse flies being vectors of dangerous pathogens, especially the trypanosomes of nagana and sleeping sickness (Foil 1989). Tsetse flies avoid striped surfaces and congregate on solid objects (Vale 1974). They usually need a large plainly coloured subject to see and land on; therefore, they do not bite zebras as often as other, homogeneously coloured animals (Estes 1992).

These explanations have been thoroughly discussed and criticized by Ruxton (2002) and Caro (2009), who concluded that the majority of these hypotheses are experimentally unconfirmed, and thus the exact reason for the evolution of a striped coat in zebras is still unknown. Nevertheless, the explanation of Waage (1981) for the benefit of zebra stripes (i.e. protection from tsetse flies) has been the only experimentally partially supported hypothesis (Turner and Invest 1973; Brady and Shereni 1988; Gibson 1992; Ruxton 2002; Lehane 2005; Caro 2009).

In six field experiments, Egri et al. 2012a studied the attractiveness of striped and homogeneous dark and white horse models, of black-and-white-striped test surfaces and of homogeneous, grey surfaces with polarization modulation (composed of parallel stripes of linear polarizers with alternating orthogonal directions of polarization) to tabanid flies as a function of the stripe width. Egri et al. (2012a) measured the stripe width in different parts of zebra coats (Fig. 22.10) as well as the reflection-polarization characteristics of zebra coats (Fig. 22.12) and their test surfaces (Figs. 22.13, 22.14 and 22.15), using imaging polarimetry. The reflection-polarization characteristics of the zebra model used in one of the field experiments (Fig. 22.14) were practically the same as those of the coat of real zebras (Fig. 22.12). Egri et al. (2012a) used the following test targets in their field experiments:

1. In experiment 1 three horizontally polarizing white-framed black trays filled with vegetable oil and placed on the ground were used. The first tray was homogeneous black, while the second and third trays had 2 and 6 orthogonal white stripes (Fig. 22.16a).
2. In experiment 2 five trays filled with vegetable oil on the ground were used (Figs. 22.13 and 22.16a). The first tray was black, the second was white and the other three trays had 1-1, 3-3 and 6-6 black-and-white parallel stripes.
3. In experiment 3 three sticky horizontal black-and-white-striped test surfaces with 1-1, 2-2 and 4-4 black-and-white parallel stripes were placed on the ground (Fig. 22.16a).
4. In experiment 4 a brown, a black, a white and a black-and-white zebra-striped sticky horse model was used (Figs. 22.14 and 22.16a).

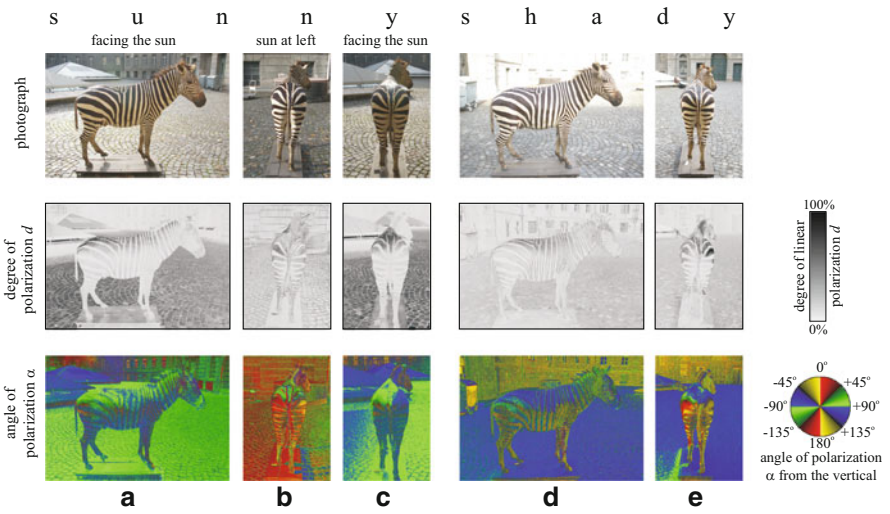

Fig. 22.12 Reflection-polarization characteristics of a real-size zebra model covered by an *E. burchelli* coat measured by imaging polarimetry in the blue (450 nm) part of the spectrum under different lighting conditions. **a**, **b**, **c**: Sunlit; **d**, **e**: shady; **a**, **c**: the polarimeter faced the sun; **b**: the sun was to the left. The optical axis of the polarimeter was horizontal [after Fig. 2 on page 741 of Egri et al. (2012a)]

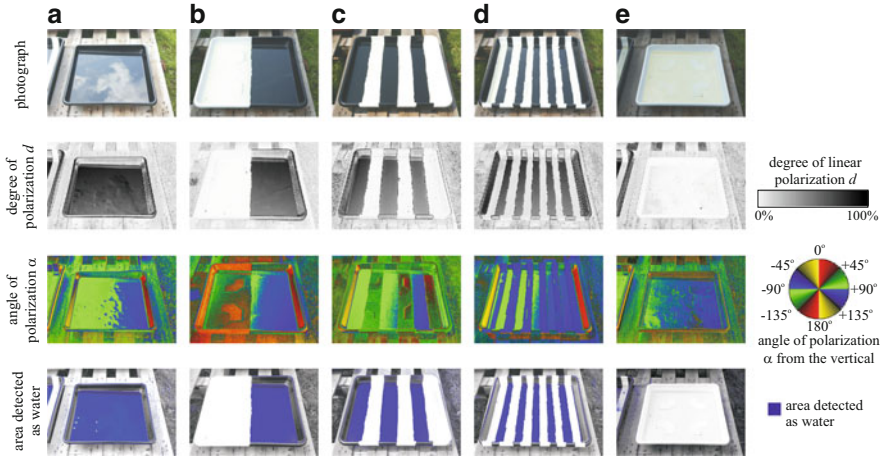

Fig. 22.13 Reflection-polarization characteristics of the black (**a**), white (**e**) and black-and-white-striped (**b**–**d**) trays filled with vegetable oil used in experiment 2 of Egri et al. (2012a). *Row 4*: Areas detected as water by polarotactic tabanids (for which the degree d and angle α of polarization of reflected light are in the following intervals: $10\ \% < d < 100\ \%$, $80^\circ < \alpha < 100^\circ$) (after Supplementary Fig. S2 of Egri et al. (2012a)]

5. In experiment 5 six sticky different vertical test surfaces were used (Fig. 22.16a): one chequered, one white, one grey and three striped. The chequered surface had two white and two black equal squares. The three black-and-white-striped surfaces were composed of four equal squares with the same stripe width but with four different stripe orientations: vertical, horizontal, +45° and −45° relative to the vertical. The first, second and third striped test surface had 13×4, 5×4 and 2×4 black stripes with a width $w = 2.0$, 6.0 and 12.5 cm, and the total area of their black and white stripes was the same.
6. Experiment 6 was performed to test the role of polarization in the attractiveness of striped patterns to polarotactic tabanids. Three sticky striped test surfaces were used (Figs. 22.15 and 22.16a): Surface Z9+ was composed of 9 linearly polarizing neutral grey parallel stripes with alternating orthogonal transmission directions (Fig. 22.15a). Surface Z17+ was made of 17 linearly polarizing parallel stripes with alternating orthogonal transmission directions (Fig. 22.15b). Surface Z17− was composed of 17 linearly polarizing parallel stripes with parallel transmission directions (Fig. 22.15c). The stripe widths of test surfaces Z17+, Z9+ and Z17− were 2.5, 4.8 and 43 cm, respectively. Z17− had a homogeneous (constant) direction of polarization. The substrate of the linearly polarizing stripes was a wooden board painted matte white. The polarizing stripes were fixed parallel to each other contacting at their margins as tightly as possible on the white substrate. One pair of each surface type was used: the first surface was laid horizontally on the ground, and the second one was fixed at a height of 1 m above the ground. The brightness, colour and degree of polarization of the test surfaces were the same (greyness = 25 %), but the patterns of the direction of polarization were different due to the different transmission directions of the polarizing stripes (Fig. 22.15). Surfaces Z9+ (Fig. 22.15a) and Z17+ (Fig. 22.15b) presented striped patterns only in the direction of polarization, while surface Z17− (Fig. 22.15c) displayed a homogeneous pattern in brightness, colour and polarization.

In all these field experiments, the ratio of the black and white surface regions of the striped test surfaces was 1:1, and the tabanids trapped by the oily/sticky test surfaces were counted and removed periodically.

Figure 22.16b shows the number N of tabanids trapped by these test surfaces as a function of the widths w of the black and white stripes for the above six experiments. The catch number N decreases monotonously with decreasing w. For example, in experiment 6 the horizontal sticky test surface H-Z17+ (Fig. 22.15b) trapped the least tabanids (17.8 %), the horizontal sticky test surface H-Z9+ (Fig. 22.15a) captured more tabanids (30.9 %), while the horizontal test surface H-Z17− (Fig. 22.15c) caught the most tabanids (51.3 %) (Fig. 22.16b). Similar results were obtained for the vertical sticky test surfaces V-Z17+ (17.3 %), V-Z9+ (30.2 %) and V-Z17− (52.5 %) used in experiment 6 (Fig. 22.16b). From this one can conclude that (horizontal or vertical) stripes with the same brightness and colour but with alternating orthogonal directions of polarization are less attractive to tabanids than similar polarizing surfaces with homogeneous (constant) direction

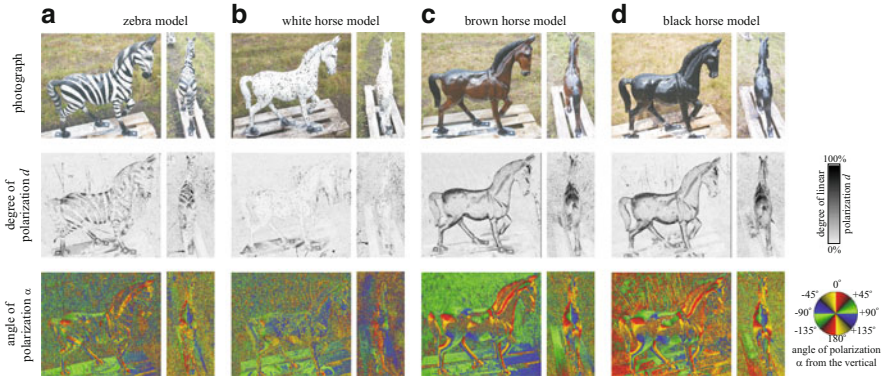

Fig. 22.14 Reflection-polarization characteristics of the black-and-white zebra-striped (**a**), white (**b**), brown (**c**) and black (**d**) sticky horse models used in experiment 4 of Egri et al. (2012a) and measured from the side (*left panels*) and from behind (*right panels*) by imaging polarimetry in the blue (450 nm) part of the spectrum. The mock horses were sunlit, and the optical axis of the polarimeter was −20° from the horizontal [after Fig. 4 on page 1648 of Horváth et al. (2010b)]

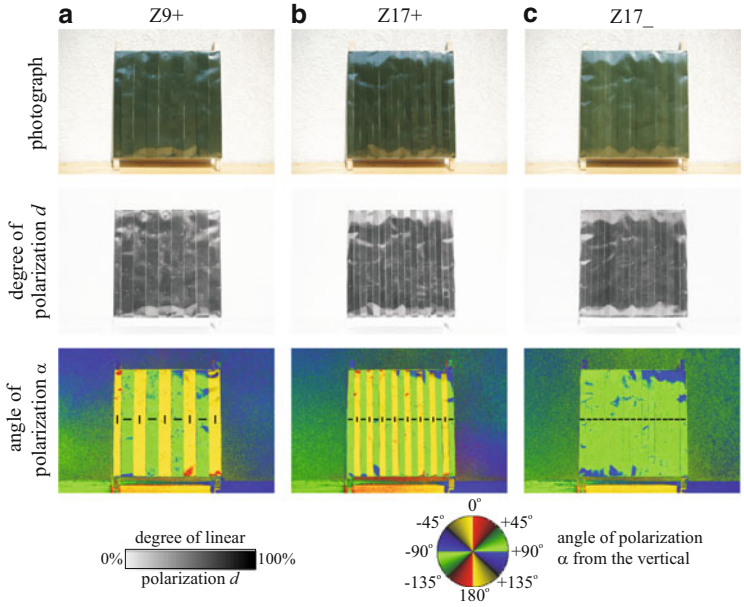

Fig. 22.15 Reflection-polarization characteristics of the linearly polarizing test surfaces used in experiment 6 of Egri et al. (2012a). In the α-patterns the short bars represent the transmission direction of the stripes of the linear polarizers [after Supplementary Fig. S3 of Egri et al. (2012a)]

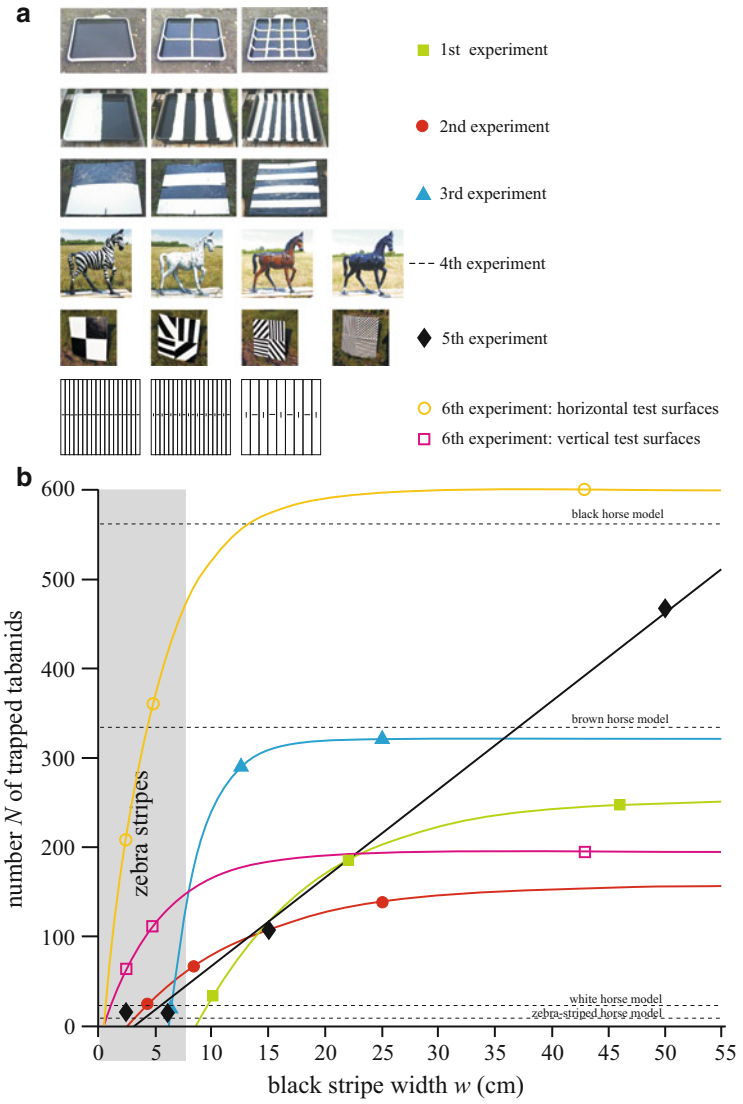

Fig. 22.16 (**a**) Stimuli used in the six experiments of Egri et al. (2012a). (**b**) Total number N of tabanids trapped by the sticky striped test surfaces in experiments 1–6 as a function of the width w (cm) of the black and white stripes (experiments 1–5) and the linearly polarizing stripes (experiment 6). The continuous exponential curves pass through the corresponding three data points of experiments 1–3 and 6, while the straight line is fitted to the four data points of experiment 5 by means of the method of least squares. The four horizontal dashed lines show the numbers of tabanids captured by the sticky black, brown, white and zebra-striped horse models used in experiment 4. The vertical grey bar represents the range of w (0.23 cm $< w <$ 7.47 cm) measured on zebra coats (minimum of average − standard deviation $\leq w \leq$ maximum of average + standard deviation). In experiment 5 the chequered test surface composed of two black squares and two white squares was considered as a pattern with a stripe width $w = 50$ cm [after Fig. 3 on page 742 of Egri et al. (2012a)]

of polarization. This shows the important role of polarization in the reduced attractiveness of striped patterns to polarotactic tabanids. Furthermore, similarly to surfaces with black and white stripes, the attractiveness of (horizontal or vertical) homogeneously coloured surfaces with alternating orthogonal directions of polarization to tabanids decreases as the width of polarizing stripes decreases. According to Fig. 22.16b, horizontal, vertical or zebra-shaped striped surfaces with brightness and/or polarization modulation have only a neglectable attractiveness to tabanids for stripe widths $0.23\ \text{cm} < w < 7.47\ \text{cm}$ (represented by a vertical grey bar in Figs. 22.10 and 22.16b) falling in the range of the average stripe width in *Equus burchelli*, *E. zebra* and *E. grevyi* zebras.

Hence, the attractiveness of striped patterns to tabanids decreases with decreasing stripe width, and the stripe widths of zebra coats fall in a range where the striped pattern is most disruptive to horseflies (Fig. 22.16b). In other words, the denser a white stripe/grid pattern on a black target, the smaller the number of attracted tabanids. The white stripes reflect unpolarized light, while the black surface areas reflect strongly linearly polarized light (at the Brewster angle) which is attractive to polarotactic tabanids. The strongly polarizing black stripes attract 3–5 times more tabanids than the weakly polarizing or unpolarizing white stripes. Egri et al. (2012a) also demonstrated that a zebra-striped horse model attracts far fewer tabanids than either homogeneous black, brown, grey or white equivalents (Fig. 22.16): the black and brown mock horses were the most attractive to tabanids, the white one was much less attractive and the black-and-white zebra-striped horse model was the least attractive. Besides brightness, one of the most important mechanisms underlying this protection is the polarization of light reflected from the host animal. It has also been shown that the attractiveness of striped patterns to tabanids is also reduced if only polarization modulations (parallel stripes with alternating orthogonal directions of polarization) occur in horizontal or vertical homogeneous grey surfaces (Figs. 22.15 and 22.16). Tabanids respond strongly to linearly polarized light, and light and dark stripes of a zebra's coat reflect very different polarizations of light (Fig. 22.12) in a way that disrupts the attractiveness to horseflies (Fig. 22.17). Egri et al. (2012a) suggested that striped coat patterns of several other large mammals (Fig. 22.18) may also function in reducing exposure to tabanids by similar mechanisms of differential brightness and polarization of reflected light.

Although there are many different hypotheses proposed to explain the possible benefits of zebra stripes, the majority of these hypotheses are unconvincing and suffer from lack of supporting experimental evidence (Ruxton 2002; Caro 2009). Waage (1981) and Egri et al. (2012a) presented the first experimentally supported explanation for the underlying mechanism for one of the possible advantages of zebra stripes. The reduced attractiveness to tabanids of other biting insects (e.g. tsetse flies and mosquitoes) alone might not explain the striped coat pattern in zebras, but they demonstrated its important role in parasite avoidance.

All three zebra species have the narrowest stripes and the thinnest skin on their head and legs (Figs. 22.10, 22.12 and Supplementary Fig. 22.21), where the stripe widths are so small that they effectively do not attract tabanids (Fig. 22.16b). This

Fig. 22.17 This cartoon illustrates the finding of Egri et al. (2012a) that a zebra-striped pattern repels polarotactic tabanids. The background colour of zebras is black, and the white stripes and bellies (where the production of dark pigmentation is inhibited) appear only in a later embryonic developmental stage (Prothero and Schoch 2003)

phenomenon may reflect an evolutionary adaptation: In the head there are several sensory organs (eyes, ears, tongue, muzzle), the efficient functioning of which is most important for survival. The legs also are indispensable to escape from predators. Consequently, head and legs must be protected in the best possible way from blood-sucking parasites (e.g. tabanids and tsetse flies), since any injury to these body parts due to aggressive biting insects might result in their insufficient functioning, undermining the escape and survival of the animal. Furthermore, in head and legs the blood vessels can more easily be reached through the thin hide, and a more efficient protection is therefore urgently needed for these body parts. Egri et al. (2012a) suggested that the numerous narrow stripes on the head and legs of zebras may serve such a visual protection.

Zebra stripes might also make it difficult for tabanid flies to be camouflaged when sitting on the host. Tabanids are usually dark brown or grey with different brightness and colour patterns. These characteristics are advantageous when they land on dark-coated host animals, because they can be more difficult to detect visually by insectivorous birds, which often follow larger herbivores, the major host animals of tabanids. However, this camouflage of tabanids is likely to be broken when they land on a zebra coat, due to the large and spatially frequent brightness and colour contrasts between the tabanid body and the underlying black or white coat.

Fig. 22.18 Some striped African mammal species being host animals of tabanids. (**a**) Brindled gnu, *Connochaetes taurinus* (http://www.wildlife-pictures-online.com/image-files/wildebeest_knp-9120-g.jpg). (**b**) Bongo, *Tragelaphus eurycerus* (http://content2.eol.org/content/2009/04/19/17/26040_large.jpg). (**c**) Male nyala, *Tragelaphus angasi* (http://www.theanimalfiles.com/images/nyala_2.jpg). (**d**) Female nyala, *Tragelaphus angasi* (http://www.iantaylor.org/sa_nyala04a.jpg). (**e**) Adult (behind) and juvenile (ahead) Lesser kudu, *Tragelaphus*

22.3.2 Stripes Disrupt Odour Attractiveness to Host-Seeking Tabanids

Similarly to other ungulates, zebras are also smelly due to the emission of carbon dioxide (CO_2) by breath and to the ammonia odour of their urine (ammonia originates from the decay of urine). Tabanid flies are strongly attracted to CO_2 and ammonia. These chemical attractants are therefore frequently used in tabanid traps (Wilson et al. 1966; Hribar et al. 1992; Hall et al. 1998; Mihok 2002; Lehane 2005; Mihok and Mulye 2010; Mihok and Lange 2012). Thus, the question arises whether the optical tabanid repellency of the striped coat pattern of zebras is or is not overwhelmed by the olfactorial attractiveness of zebras to tabanids. Could the attractive zebra smell (CO_2, ammonia, sweat) over-compensate the visual unattractiveness of zebra stripes to tabanids, resulting in the loss of the selective advantage of striped coat patterns? To answer this question, in field experiments Blahó et al. (2013) studied the attractiveness of sticky homogeneous white, black and black-and-white-striped three-dimensional targets and horse models provided with CO_2 and ammonia to tabanid flies.

In their first experiment Blahó et al. (2013) trapped tabanids with host-imitating sticky spheres and cylinders. There were two identical groups of visual targets. Each target group was composed of a white, a black-and-white-striped and a black sphere and two white, two black-and-white striped and two black plastic cylinders. One of the target groups was provided continuously with ammonia, while at the other group no ammonia was released. The two target groups were at a large enough distance from each other, so that the ammonia originating from the smelly group could not influence the area of the odourless group. In the second experiment of Blahó et al. (2013), two pairs of sticky horse models were used. Each pair was composed of a black-and-white zebra-striped mock horse and a black mock horse. Each mock horse of one of the pairs was continuously provided with ammonia and CO_2. 500 m from these smelly mock horses, another mock horse pair without ammonia and CO_2 was set at a large enough distance from each other, so that the ammonia and CO_2 originating from the smelly mock horses could not influence the area of the odourless mock horses. The emission rate of CO_2 was steadily 0.5 litre/min, which corresponded to the rate of CO_2 exhalation by horses (Marlin and Nankervis 2002; Brega 2005). Thus, the carbon dioxide concentration was similar to the natural situation around breathing zebras. In both experiments, the tabanids trapped by the sticky targets were counted and removed periodically.

Blahó et al. (2013) showed that zebra-striped targets (spheres, cylinders, mock horses and zebras) are significantly less attractive to host-seeking female tabanids

Fig. 22.18 (continued) imberbis (http://www.quantum-conservation.org/ESB/LesserKudu.gif). (**f**) Striped hyena, *Hyaena hyaena* (http://www.dkimages.com/discover/previews/813/20085902.jpg). (**g**) Okapi, *Okapia johnstoni* (http://www.pbase.com/giuss95/image/32049164). (**h**) Giraffe, *Giraffa camelopardalis* (http://www.veeriku.tartu.ee/~ppensa/giraffe3.jpg)

than homogeneous white or black targets, even if they emit tabanid-luring CO_2 and ammonia. Although CO_2 and ammonia increased the number of attracted tabanids, they neither neutralized nor quelled the visual unattractiveness of zebra stripes to host-seeking female tabanids. For example, although the combined emittance of ammonia and CO_2 enhanced the attractiveness of black horse models and mock zebras to tabanids, the mock zebra kept its visual tabanid unattractiveness in spite of the emittance of these smelly tabanid attractants. This result demonstrates the importance of visual tabanid unattractiveness of zebra-striped coat patterns and suggests that the striped pattern may have evolved as a protection against attacks from blood-sucking dipterans, such as horseflies, known to transmit lethal diseases to ungulates.

Wearing a striped coat has the evolutionary benefit that such a coat pattern disrupts the olfactorial attraction of blood-sucking female tabanids by host-specific odours, such as ammonia and CO_2, for instance. By this visual trick, zebras and other more or less striped animals (Fig. 22.18) reduce their optical attractiveness to tabanids. Other ungulates (e.g. horses), bearing non-striped coat patterns, possess other behavioural responses to tabanid attacks: (1) Hiding in shade. When possible, this is a successful tactic for hosts as tabanids prefer direct sunlight and avoid shady areas (Lehane 2005), because their flight muscles need a higher air temperature to facilitate fast escape responses in order to be quick enough to escape from the body surface of a host animal when it tries to remove (e.g. by tail hits) them when biting. (2) Grazing between sunset and sunrise. Tabanids do not fly and thus do not attack their hosts between sunset and sunrise, when the air temperature is too low for them to fly. (3) Grazing for a short time in sunshine and then running into the shade periodically. Such a typical behaviour of horses attacked by numerous tabanids on a sunlit meadow near a forest has been described by Horváth et al. (2010b).

Recently, Caro et al. (2014) studied the match of variation in striping of equid species and subspecies to geographic range overlap of environmental variables in multifactor analyses controlling for phylogeny to test the five major explanations for the striped colouration of zebras: (1) They tested whether black and white stripes are a form of crypsis, matching the background of light and dark produced by tree trunks and branches in woodland habitats. (2) To investigate an antipredator function that subsumes several mechanisms including crypsis, disruptive colouration of the body's contour and increased apparent size, making individuals difficult to single out in a herd and confusing a predator in some way or advertising jump ability, they examined whether striping in equids is associated with the presence of sympatric large predators, such as spotted hyaena (*Crocuta crocuta*), lion (*Panthera leo*), tiger (*P. tigris*) and wolf (*Canis lupus*). (3) To explore heat management, they examined associations between striping and living in habitats with average maximum annual temperatures between 25 and 30 °C. (4) They used average group size and maximum herd size as indicators of the involvement of striping in social interactions. (5) To investigate the importance of biting flies, they matched tsetse fly distributions to equid distributions and used environmental proxies for the distribution of tabanid abundance.

At the species and/or subspecies level, Caro et al. (2014) found significant associations (1) between tabanid annoyance and most striping measures (facial and neck stripe number, flank and rump striping, leg stripe intensity and shadow striping), as well as between belly stripe number and tsetse fly distribution. On the other hand, they found no consistent support for (2) camouflage, (3) predator avoidance, (4) heat management or (5) social interaction hypotheses. Thus, among the five relevant explanations for the evolutionary benefit of zebra stripes only that was supported by the data analysis of Caro et al. (2014) which argues with the visual unattractiveness of striped coat patterns to tsetse flies (Vale 1974; Waage 1981; Gibson 1992) and tabanid flies (Horváth et al. 2008, 2010a, b; Kriska et al. 2009; Egri et al. 2012a; Blahó et al. 2013).

22.4 Tabanid-Repellent Spotty Fur Patterns

The coat pattern of cattle (*Bos primigenius*) has a remarkably large diversity ranging from homogeneous black and brown, through brown-white or black-white spotty, to homogeneous grey or white (Fig. 22.19). These coat patterns are specific to species and races and are the result of domestic breeding. The different coat patterns have some advantages and disadvantages. The darkness of the coat influences the thermoregulation of the animal (Glenn 1983; Finch et al. 1984), for example. The visibility of the animal depends strongly on the brightness and colour of the coat in contrast to the background. During breeding the brightness, colour and spottiness of the coat in cattle (Fig. 22.19) and horses (Fig. 22.20) are usually of marginal importance and are the by-product of cross-breeding aiming to maximize other economically more important characteristics of the animal, e.g. the milk or meat production, weatherproofness or the shape or size of the animals.

In field experiments Blahó et al. (2012) studied the influence of the size and number of spots on the attractiveness of different test surfaces to tabanids: In experiments 1 and 2, four vertical and four horizontal (laid on the ground) sticky white plastic boards with 1, 4, 16 and 64 brown spots (Fig. 22.21) were used. The ratio of the white and brown areas of the test surfaces was 50:50 %. In experiment 3, one dark brown, one white and three spotty sticky cattle models were used (Fig. 22.22). The spotty mock cattle had a white surface with 8, 16 and 64 dark brown spots, the size of which decreased with increasing number.

To separate the effect of intensity and polarization of light reflected from the test surfaces, in their experiment 4, Blahó et al. (2012) tested the role of polarization alone in the attractiveness of spotty targets to tabanids using three different sticky and spotty test surfaces (Fig. 22.23): S4+ was a surface with 4 neutral grey, linearly polarizing squares, the transmission direction of which was perpendicular to that of their surroundings. S16+ was a surface with 16 linearly polarizing squares, the transmission direction of which was perpendicular to that of their surroundings. S16− was a surface with 16 linearly polarizing squares, the transmission direction of which was parallel to that of their surroundings. The intensity and colour of these dark grey test surfaces were homogeneous. Test surface S16− had also a

Fig. 22.19 The diversity of the coat pattern in domestic cattle ranges from homogeneous black (**a–c**) and brown (**d–f**), through spotty brown-white (**g–i**) and black-white (**j–l**), to homogeneous grey or white (**m–o**) (source: http://FreeFoto.com)

homogeneous pattern of the degree and the direction of polarization. The degree of polarization reflected both from the 4 and 16 rectangles of test surfaces S4+ and S16 + was the same as that reflected from their surrounding regions, while the direction of polarization of light reflected from these rectangles was perpendicular to that

Fig. 22.20 Spotty horses. (**a**, **b**) American paint horses. (**c**) Hungarian spotty horse

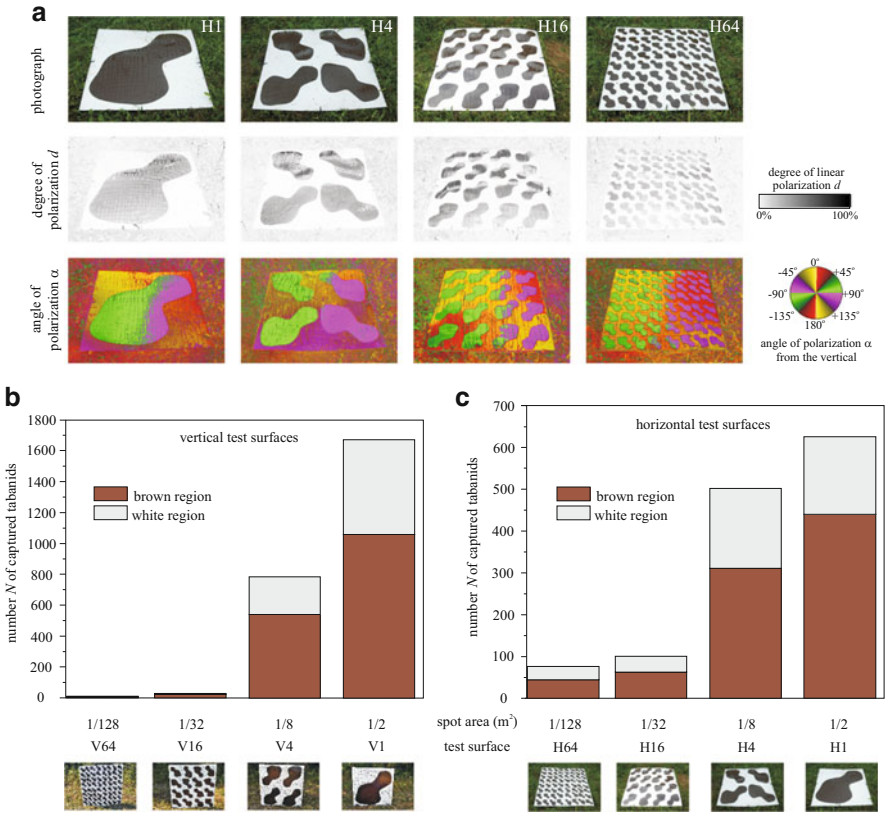

Fig. 22.21 (**a**) Reflection-polarization characteristics of the shady brown-and-white spotty horizontal sticky test surfaces with 1 (H1), 4 (H4), 16 (H16) and 64 (H64) brown spots used in experiment 2 of Blahó et al. (2012) and measured by imaging polarimetry in the blue (450 nm) part of the spectrum when the optical axis of the polarimeter was −30° from the horizontal. (**b**, **c**) Number N of tabanids captured by the brown and white regions of the vertical and horizontal spotty and sticky test surfaces in experiments 1 and 2 of Blahó et al. (2012) as a function of the area (m^2) covered by one brown spot [after Fig. 1 on page 3 of Blahó et al. (2012)]

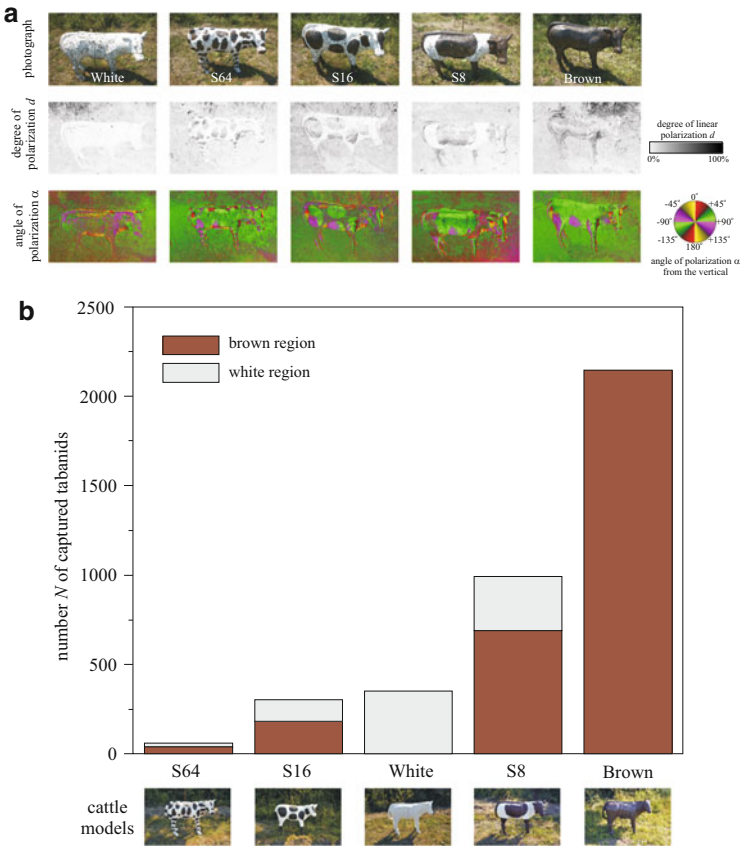

Fig. 22.22 (**a**) Reflection-polarization characteristics of the sticky cattle models used in experiment 3 of Blahó et al. (2012) when the optical axis of the polarimeter was −35° from the horizontal. White: white cattle; S64, white cattle with 64 brown spots; S16, white cattle with 16 brown spots; S8, white cattle with 8 brown spots; brown, brown cattle. (**b**) Number N of tabanids captured by the brown regions (if any) and the white areas of the sticky cattle models [after Fig. 2 on page 4 of Blahó et al. (2012)]

reflected from their surroundings. The substrate of the linearly polarizing sheets was a wooden board painted matte white. One pair of each surface type was used: the first surface was laid horizontally onto the ground, and the second one was fixed at a height of 1 m above the ground. Hence, the intensity and colour (dark grey), furthermore the degree of polarization ($d \approx 100$ %) of these test surfaces, were the same, but the direction of polarization varied due to the differing transmission directions of the polarizing squares. Surfaces S4+ and S16+ presented spotty patterns only in the direction of polarization, while surface S16− displayed a homogeneous pattern in intensity, colour and polarization (Fig. 22.23).

In all these experiments the tabanids trapped by the sticky test surfaces were counted and removed periodically. Blahó et al. (2012) experienced that the smaller

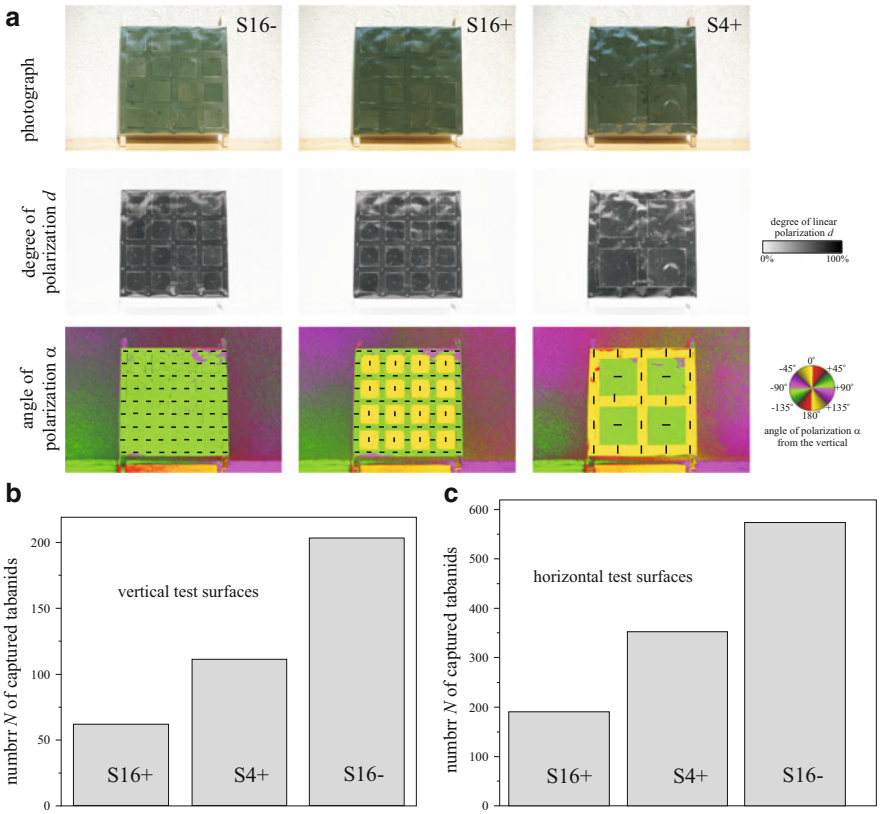

Fig. 22.23 (**a**) Reflection-polarization characteristics of the test surfaces used in experiment 4 of Blahó et al. (2012) when the optical axis of the polarimeter was horizontal. In the α-patterns the short bars represent the local transmission direction of the linear polarizer. (**b**, **c**) Number *N* of tabanids captured by the vertical and horizontal test surfaces. S16+: test surface with 16 linearly polarizing squares, the transmission direction of which is perpendicular to that of their surrounding regions. S4+: test surface with 4 linearly polarizing squares, the transmission direction of which is perpendicular to that of their surrounding regions. S16−: test surface with 16 linearly polarizing squares, the transmission direction of which is parallel to that of their surrounding regions [after Fig. 3 on page 6 of Blahó et al. (2012)]

and the more numerous were the spots, the less attractive was the target (host) to tabanids (Figs. 22.21, 22.22 and 22.23). For instance, the homogeneous brown mock cattle was the most attractive; the cattle model S8 with 8 spots was less attractive than the brown model, but more attractive than the white one. The least attractive were the spotty mock cattle S16 and S64 with 16 and 64 spots, respectively (Fig. 22.22). The attractiveness of spotty patterns to tabanids was also reduced, if the target exhibited spottiness only in the direction of polarization pattern, while being homogeneous grey with a constant high degree of polarization (Fig. 22.23). This demonstrates the important role of polarization in the reduction of

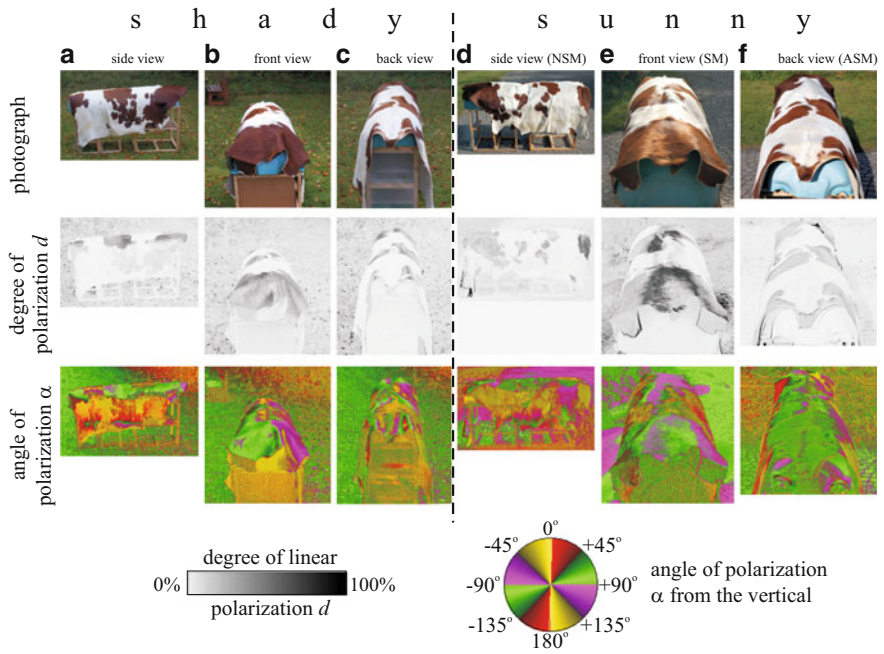

Fig. 22.24 Reflection-polarization characteristics of a shady (**a**–**c**) and a sunny (**d**–**f**) cattle coat with white and brown patches measured by imaging polarimetry in the blue (450 nm) part of the spectrum. In **d**, **e**, **f** the polarimeter viewed normally to the solar meridian (NSM), towards the solar meridian (SM) and towards the antisolar meridian (ASM), respectively. The elevation angle of the polarimeter's optical axis was −20° from the horizontal [after Supplementary Fig. S4 of Blahó et al. (2012)]

the attractiveness of spotty patterns to polarization-sensitive tabanids. In the case of real spotty coats, intensity-colour differences are associated with polarization differences, because bright regions reflect weakly polarized light while dark areas reflect strongly polarized light, and the directions of polarization of light reflected from the bright and dark areas are also different (Fig. 22.24). These intensity, colour and polarization differences of spotty patterns synergistically disrupt the attractiveness to polarotactic tabanids.

Furthermore, the brown spots were more attractive than the white surface regions (Figs. 22.21 and 22.22). The reason for this may be the following: It is important for haematophagous flies to be as cryptic as possible in order to increase their foraging abilities and decrease their predation risk. Flying around or towards larger brown spots could convey an ecological advantage (camouflage) to brown tabanids as they will evade longer the swatting of cattle or the foraging of insectivorous birds.

Blahó et al. (2012) suggested that the unattractiveness of spotty coat patterns to blood-sucking tabanids could be one of the possible evolutionary benefits why spotty coats are so widespread in mammals, especially in ungulates, many species of which are tabanid hosts. Hence, the spottiness of the coat is of not marginal

significance, since it strongly determines the attractiveness of cattle (and other host animals) to tabanids, which has been shown to have severe influence on disease transmission, as well as reduction in milk production and growth due to reduced feeding (Majer 1987; Foil 1989; Lehane 2005). Thus, coat colouration could be considered in domestic cattle breeding.

Unattractiveness to tabanids and other biting insects alone might not explain the evolution of spotty coat patterns in mammals. An appropriately spotty coat pattern can also serve as camouflage in a structured optical environment, providing protection against predators (Godfrey et al. 1987; Stevens and Merilaita 2009; Allen et al. 2010). Camouflage seems to be one of the main reasons for spots or stripes in wild animals. There are a number of examples for this theory: Tigers, leopards and many smaller cat species have a striped or spotted coat which makes them hard to detect in the wild (Ortolani and Caro 1996). Even an animal as big as a giraffe is well camouflaged by its patterned coat in its natural environment (Caro 2009).

In earlier studies (Egri et al. 2012a) it has been shown that black-and-white-striped targets are unattractive to tabanids, and this is an advantage of the zebra stripes. Blahó et al. (2012) demonstrated a similar effect, namely, the unattractiveness of spotty patterns to tabanids. In both cases, the narrower the stripes and the smaller the spots, the less is their attractiveness to tabanids. This principle could practically be used also for human clothing: by wearing appropriately stripy or spotty cloths in areas with large tabanid load, the attraction to blood-sucking female tabanids could be avoided.

References

Allan SA, Day JF, Edman JD (1987) Visual ecology of biting flies. Annu Rev Entomol 32:297–316

Allen WL, Cuthill IC, Scott-Samuel NE, Baddeley R (2010) Why the leopard got its spots: relating pattern development to ecology in felids. Proc R Soc B 278:1373–1380

Baldacchino F, Desquesnes M, Mihok S, Foil LD, Duvallet G, Jittapalapong S (2014) Tabanids: Neglected subjects of research, but important vectors of disease agents! Infection, Genetics and Evolution (in press). doi:10.1016/j.meegid.2014.03.029

Bard JBL (1977) A unity underlying the different zebra striping patterns. J Zool (Lond) 183:527–539

Becker CD, Ginsberg JR (1990) Mother-infant behaviour of wild Grevy's zebra: adaptations for survival in semi-desert East Africa. Anim Behav 40:1111–1118

Blahó M, Egri Á, Báhidszki L, Kriska G, Hegedüs R, Åkesson S, Horváth G (2012) Spottier targets are less attractive to tabanid flies: on the tabanid-repellency of spotty fur patterns. PLoS One 7 (8):e41138. doi:10.1371/journal.pone.0041138 + supporting information

Blahó M, Egri Á, Száz D, Kriska G, Åkesson S, Horváth G (2013) Stripes disrupt odour attractiveness to biting horseflies: battle between ammonia, CO_2, and colour pattern for dominance in the sensory systems of host-seeking tabanids. Physiol Behav 119:168–174

Brady J, Shereni A (1988) Landing responses of the tsetse fly *Glossina norsitans norsitans* Weidemann and the stable fly *Stomoxys calcitrans* (L.) (Diptera: Glossinidae and Muscidae) to black and white patterns: a laboratory study. Bull Entomol Res 78:301–311

Brega J (2005) Essential equine studies: anatomy and physiology. JA Allen and Co Ltd, London

Burakova O, Mazokhin-Porshnyakov G (1982) Electron microscopy of the compound eye in *Haematopota pluvialis* L. (Diptera: Tabanidae). Ent Rev 61:26–33
Caro T (2009) Contrasting coloration in terrestrial mammals. Philos Trans R Soc B 364:537–548
Caro T, Izzo A, Reiner RC, Walker H, Stankowich T (2014) The function of zebra stripes. Nature Communications 5:3535. doi:10.1038/ncomms4535
Cloudsley-Thompson JL (1984) How the zebra got his stripes—new solutions to an old problem. Biologist 31:226–228
Cott HB (1957) Adaptive colouration in animals. John Dickens, Northampton
Cott HB (1966) Colouration in animals. Methuen, London
Csabai Z, Boda P, Bernáth B, Kriska G, Horváth G (2006) A 'polarisation sun-dial' dictates the optimal time of day for dispersal by flying aquatic insects. Freshw Biol 51:1341–1350
Darwin CR (1871) The descent of man, and selection in relation to sex, vol 2. John Murray, London, p 302
Duncan P, Vigne N (1979) The effect of group size in horses on the rate of attacks by blood-sucking flies. Anim Behav 27:623–625
Egri Á, Blahó M, Kriska G, Farkas R, Gyurkovszky M, Åkesson S, Horváth G (2012a) Polarotactic tabanids find striped patterns with brightness and/or polarization modulation least attractive: an advantage of zebra stripes. J Exp Biol 215: 736–745 + electronic supplement
Egri Á, Blahó M, Sándor A, Kriska G, Gyurkovszky M, Farkas R, Horváth G (2012b) New kind of polarotaxis governed by degree of polarization: Attraction of tabanid flies to differently polarizing host animals and water surfaces. Naturwissenschaften 99:407–416 + electronic supplement
Eltringham SK (1979) The ecology and conservation of large African mammals. Macmillan, Basingstoke
Estes RD (1992) The behavior guide to african mammals including hoofed mammals, carnivores, primates. University of California Press, Los Angeles, CA
Finch VA, Bennett IL, Holmes CR (1984) Coat colour in cattle: effect on thermal balance, behaviour and growth, and relationship with coat type. J Agric Sci 102:141–147
Foil LD (1989) Tabanids as vectors of disease agents. Parasitol Today 5:88–96
Galton F (1851) South Africa. Minerva Library, New York
Gibson G (1992) Do tsetse-flies 'see' zebras? A field study of the visual response of tsetse to striped targets. Physiol Entomol 17:141–147
Glenn EW (1983) Coat color and solar heat gain in animals. Bioscience 33:88–91
Godfrey D, Lythgoe JN, Rumball DA (1987) Zebra stripes and tiger stripes: the spatial frequency distribution of the pattern compared to that of the background is significant in display and crypsis. Biol J Linn Soc 32:427–433
Hall MJR, Farkas R, Chainey JE (1998) Use of odour-baited sticky boards to trap tabanid flies and investigate repellents. Med Vet Entomol 12:241–245
Harris RHTP (1930) Report on the bionomics of the tsetse fly. Provincial Administration of Natal, Pietermaritzburg, South Africa
Hayakawa H (1980) Biological studies on *Tabanus iyoensis* group of Japan, with special reference to their blood-sucking habits (Diptera, Tabanidae). Bull Tohoku Nat Agric Exp Station 62:131–321
Horváth G, Kriska G (2008) Polarization vision in aquatic insects and ecological traps for polarotactic insects. In: Lancaster J, Briers RA (eds) Aquatic insects: challenges to populations. CAB International Publishing, Wallingford, Oxon, pp 204–229, Chapter 11
Horváth G, Varjú D (2004) Polarized light in animal vision—polarization patterns in nature. Springer, Heidelberg
Horváth G, Malik P, Kriska G, Wildermuth H (2007) Ecological traps for dragonflies in a cemetery: the attraction of *Sympetrum* species (Odonata: Libellulidae) by horizontally polarizing black gravestones. Freshw Biol 52:1700–1709

Horváth G, Majer J, Horváth L, Szivák I, Kriska G (2008) Ventral polarization vision in tabanids: horseflies and deerflies (Diptera: Tabanidae) are attracted to horizontally polarized light. Naturwissenschaften 95:1093–1100

Horváth G, Blahó M, Egri Á, Kriska G, Seres I, Robertson B (2010a) Reducing the maladaptive attractiveness of solar panels to polarotactic insects. Conserv Biol 24:1644–1653 + electronic supplement

Horváth G, Blahó M, Kriska G, Hegedüs R, Gerics B, Farkas R, Åkesson S (2010b) An unexpected advantage of whiteness in horses: the most horsefly-proof horse has a depolarizing white coat. Proc R Soc B 277:1643–1650

Horváth G, Móra A, Bernáth B, Kriska G (2011) Polarotaxis in non-biting midges: female chironomids are attracted to horizontally polarized light. Physiol Behav 104:1010–1015 + cover picture

Hribar LJ, LePrince DJ, Foil LD (1992) Ammonia as an attractant for adult *Hybomitra lasiophthalma* (Diptera: Tabanidae). J Med Entomol 29:346–348

Jékely G (2009) Evolution of phototaxis. Philos Trans R Soc B 364:2795–2808

Jordan AM (1986) Trypanosomiasis control and African rural development. Longman, New York

Kingdon J (1984) The zebra's stripes: an aid to group cohesion. In: MacDonald D (ed) The encyclopaedia of mammals. Equinox, Oxford, pp 486–487

Kipling R (1908) Just so stories. Macmillan, London

Krcmar S (2005a) Seasonal abundance of horse flies (Diptera: Tabanidae) from two locations in eastern Croatia. Journal of Vector Ecology 30:316–321

Krcmar S (2005b) Response of horse flies (Diptera, Tabanidae) to different olfactory attractants. Biologia Bratislava 60:611–613

Krcmar S (2013) Comparison of the efficiency of the olfactory and visual traps in the collection of horseflies (Diptera: Tabanidae). Entomologia Generalis 34:261–267

Krcmar S, Maric S (2006) Analysis of the feeding sites for some horse flies (Diptera, Tabanidae) on a human in Croatia. Collegium Antropologicum 30:901–904

Krcmar S, Merdic E, Kopi M (2005) Diurnal periodicity in the biting activity of horsefly species in the Kopacki rit Nature Park, Croatia (Diptera: Tabanidae). Entomologia Generalis 28:139–146

Kriska G, Csabai Z, Boda P, Malik P, Horváth G (2006) Why do red and dark-coloured cars lure aquatic insects? The attraction of water insects to car paintwork explained by reflection-polarization signals. Proc R Soc B 273:1667–1671

Kriska G, Bernáth B, Horváth G (2007) Positive polarotaxis in a mayfly that never leaves the water surface: polarotactic water detection in *Palingenia longicauda* (Ephemeroptera). Naturwissenschaften 94:148–154 + cover picture

Kriska G, Malik P, Szivák I, Horváth G (2008) Glass buildings on river banks as "polarized light traps" for mass-swarming polarotactic caddis flies. Naturwissenschaften 95:461–467

Kriska G, Bernáth B, Farkas R, Horváth G (2009) Degrees of polarization of reflected light eliciting polarotaxis in dragonflies (Odonata), mayflies (Ephemeroptera) and tabanid flies (Tabanidae). J Insect Physiol 55:1167–1173

Kruuk H (1972) The spotted hyena. University of Chicago Press, Chicago, IL

Lehane MJ (2005) The biology of blood-sucking in insects, 2nd edn. Cambridge University Press, Cambridge, UK

Lerner A, Meltser N, Sapir N, Erlick C, Shashar N, Broza M (2008) Reflected polarization guides chironomid females to oviposition sites. J Exp Biol 211:3536–3543

Louw GN (1993) Physiological animal ecology. Longman, New York

Majer J (1987) Tabanids—Tabanidae. In: Szekessy V (ed) Fauna Hungariae, vol 14(9). Akadémiai Kiadó, Budapest, pp 1–57 (in Hungarian)

Marler P, Hamilton WJ (1968) Mechanisms of animal behavior. Wiley, New York

Marlin D, Nankervis KJ (2002) Equine exercise physiology. Wiley-Blackwell, New York

McLeod DNK (1987) Zebra stripes. New Sci 115:68

Menzel R (1979) Spectral sensitivity and colour vision in invertebrates. In: Autrum H (ed) Comparative physiology and evolution of vision in invertebrates, vol VII/6A. Springer, Berlin, pp 503–580

Mihok S (2002) The development of a multipurpose trap (the Nzi) for tsetse and other biting flies. Bull Entomol Res 92:385–403

Mihok S, Lange K (2012) Synergism between ammonia and phenols for *Hybomitra* tabanids in northern and temperate Canada. Med Vet Entomol 26:282–290

Mihok S, Mulye H (2010) Responses of tabanids to Nzi traps baited with octenol, cow urine and phenols in Canada. Med Vet Entomol 24:266–272

Morris D (1990) Animal watching. A field guide to animal behaviour. Jonathan Crape, London

Ortolani A, Caro TM (1996) The adaptive significance of color patterns in carnivores: phylogenetic tests of classic hypotheses. In: Gittleman J (ed) Carnivore behaviour, ecology and evolution, vol 2, Cornell University Press. Ithaca, NY, pp 132–188

Pielberg GR, Golovko A, Sundström E, Curik I, Lennartsson J, Seltenhammer MH, Druml T, Binns M, Fitzsimmons C, Lindgren G, Sandberg K, Baumung R, Vetterlein M, Strömberg S, Grabherr M, Wade C, Lindblad-Toh K, Pontén F, Heldin CH, Sölkner J, Andersson L (2008) A cis-acting regulatory mutation causes premature hair graying and susceptibility to melanoma in the horse. Nat Genet 40:1004–1009

Prothero DR, Schoch RM (2003) Horns, tusks, and flippers: the evolution of hoofed mammals. Johns Hopkins University Press, Baltimore, MD

Rutberg AT (1987) Horse fly harassment and the social behaviour of feral ponies. Ethology 75:145–154

Ruxton GD (2002) The possible fitness benefits of striped coat coloration for zebra. Mammal Rev 32:237–244

Schwind R (1983) A polarization-sensitive response of the flying water bug *Notonecta glauca* to UV light. J Comp Physiol 150:87–91

Schwind R (1984) Evidence for true polarization vision based on a two-channel analyser system in the eye of the water bug, *Notonecta glauca*. J Comp Physiol A 154:53–57

Schwind R (1985a) A further proof of polarization vision of *Notonecta glauca* and a note on threshold intensity for eliciting the plunge reaction. Experientia 41:466–467

Schwind R (1985b) Sehen unter und über Wasser, Sehen von Wasser. Naturwissenschaften 72:343–352

Schwind R (1989) A variety of insects are attracted to water by reflected polarized light. Naturwissenschaften 76:377–378

Schwind R (1991) Polarization vision in water insects and insects living on a moist substrate. J Comp Physiol A 169:531–540

Schwind R (1995) Spectral regions in which aquatic insects see reflected polarized light. J Comp Physiol A 177:439–448

Schwind R (1999) *Daphnia pulex* swims towards the most strongly polarized light—a response that leads to 'shore flight'. J Exp Biol 202:3631–3635

Smith WC, Butler JF (1991) Ultrastructure of the Tabanidae compound eye: unusual features for Diptera. J Insect Physiol 37:287–296

Stevens M, Merilaita S (2009) Animal camouflage: current issues and new perspectives. Philos Trans R Soc B 364:423–427

Tashiro H, Schwardt HH (1953) Biological studies of horseflies in New York. J Econ Entomology 46:813–822

Thayer AH (1909) Concealing coloration in the animal kingdom. Macmillan, New York

Thorsteinson AJ, Bracken GK, Hanec W (1965) The orientation behaviour of horseflies and deerflies (Tabanidae: Diptera). III. The use of traps in the study of orientation of tabanids in the field. Entomol Exp Appl 8:189–192

Tresidder J (ed) (2005) The complete dictionary of symbols. Chronicle Books, San Francisco, CA

Turner DA, Invest JF (1973) Laboratory analyses of vision in tsetse flies (Dipt. Glossinidae). Bull Entomol Res 62:343–357

Vale GA (1974) The response of tsetse flies (Diptera, Glossinidae) to mobile and stationary baits. Bull Entomol Res 64:545–588
Vaughan TA (1986) Mammology, 3rd edn. North Arizona University, Flagstaff, AZ
Waage JK (1981) How the zebra got its stripes—biting flies as selective agents in the evolution of zebra coloration. J Entomol Soc South Afr 44:351–358
Wallace AR (1867) Mimicry and other protective resemblances among animals. Westm Foreign Q Rev 32:1–43
Wallace AR (1879) The protective colours of animals. Science 2:128–137
Wildermuth H (1998) Dragonflies recognize the water of rendezvous and oviposition sites by horizontally polarized light: a behavioural field test. Naturwissenschaften 85:297–302
Wilson BH, Tugwell NP, Burns EC (1966) Attraction of tabanids to traps baited with dry-ice under field conditions in Louisiana. J Med Entomol 3:148–149

Chapter 23
Applying Polarization-Based Traps to Insect Control

Gábor Horváth, Miklós Blahó, Ádám Egri, and Amit Lerner

Abstract Following the new findings described in Chap. 21 regarding the use of polarization cues by chironomids to detect water bodies suitable for oviposition, an effort was initiated to apply reflection-polarization traps to divert chironomid females from laying their eggs in the natural reservoir and by this to control the chironomid population. In this chapter we first review this effort and its outcome and suggest insights into the future development of chironomid reflection-polarization oviposition traps and population control. Then we present three different types of polarization-based tabanid trap: a liquid trap, a sticky horseflypaper and a photovoltaic trap. All three trap types share the common feature that they lure positively polarotactic tabanid flies with strongly and linearly polarized light reflected from special shiny black visual targets. Due to their horizontally polarizing bait surface, the liquid and the photovoltaic traps as well as the horizontally aligned horseflypaper capture water-seeking male and female tabanids attracted to the horizontal polarization of bait-reflected light. If the surface of the horseflypaper is vertical, it catches host-seeking female tabanids lured to the strongly polarized trap-reflected light. The tabanid-capturing efficacy of all three trap types has been proven in field experiments. The scientific basis of these traps

Electronic supplementary material is available in the online version of this chapter at 10.1007/978-3-642-54718-8_23. Colour versions of black and white figures as well as supplementary figures can also be found at http://extras.springer.com

G. Horváth (✉) • M. Blahó • Á. Egri
Environmental Optics Laboratory, Department of Biological Physics, Physical Institute, Eötvös University, Pázmány sétány 1, 1117 Budapest, Hungary
e-mail: gh@arago.elte.hu; majkl2000@gmail.com

A. Lerner
Ocean BioOptics and Vision Laboratory, Israel Oceanographic and Limnological Research, National Institute of Oceanography, Tel-Shikmona, POB 8030, Haifa 31080, Israel
e-mail: amit.lerner@ocean.org.il

G. Horváth (ed.), *Polarized Light and Polarization Vision in Animal Sciences*, Springer Series in Vision Research 2, DOI 10.1007/978-3-642-54718-8_23,

is the two kinds of positive polarotaxis in tabanid flies. The advantages and disadvantages of these different tabanid traps are also discussed here; furthermore, it is described how these traps could be improved in the future, and how they can be combined with the traditional canopy trap, for instance. These studies demonstrate well how basic scientific knowledge, i.e. the positive polarotaxis in chironomids and tabanids, can be applied in the design of new insect traps.

23.1 Polarization Chironomid Traps

Amit Lerner

23.1.1 Field Experiment to Divert Ovipositing Chironomid Females to Artificial Sites (Egg Traps)

As described earlier in Chap. 21, chironomid females are strongly directed by reflection polarization during oviposition and choose to lay eggs in highly and horizontally polarizing wet surfaces. This is raising the opportunity to use such traps to lure the females from egg laying in their natural sites and collect their eggs in a trap to control the population. Such an attempt was conducted, where highly polarizing traps were placed on the ground nearby the chironomids' natural pond (Lerner et al. 2012). The traps were 40 litre black tubs filled with very turbid pond water, which were shown to be effective in a previous experiment (see details in Chap. 21). The tubs were placed along the bank of the chironomid natural pond. In the first two weeks, the oviposition rates in the pond (on floating Styrofoam rafts) and in the tubs were monitored. Then the bank was covered with a white plastic sheet to reduce natural oviposition sites and direct the females to oviposit in the tubs. The eggs were counted and removed each day. Once the number of natural egg-laying sites (the pond bank in this case) was reduced, the traps' effectiveness increased, as increasing numbers of egg batches of chironomids were found. Such a response suggests that egg traps reflecting highly and horizontally polarized light should effectively lure the females to oviposit in them and therefore may be useful to control the pest population. However, polarization egg trapping is still in its infant stage to date.

A. Lerner
Ocean BioOptics and Vision Laboratory, Israel Oceanographic and Limnological Research, National Institute of Oceanography, Tel-Shikmona, POB 8030, Haifa 31080, Israel

23.1.2 Requirements for an Effective Polarization Egg Trap

One of the requirements for a polarization egg trap is that it should reflect higher partial polarization than the natural cue as perceived by the chironomids (a "super stimulus"). The partial polarization values should exceed 70 %, as this is approximately the highest percentage available in nature. Reflection from surfaces, e.g. water surface in the chironomid case, may exceed this value at directions of view close to the Brewster angle; however, it seems that chironomids do not follow this cue. The females showed a differential oviposition rate which was correlated with the partial polarization of light reflected from the surface of waters with different turbidity, although all of them should be maximally and horizontally polarizing at the Brewster angle (Lerner et al. 2008). Neglecting polarization cue at the Brewster angle makes sense from the point of view of the female, as it is only weakly correlated with the water turbidity and carbon concentrations on which the chironomid larvae feed. Thus, it is less useful as a cue to assess the habitat quality and offspring success. The fact that female chironomids follow the reflection polarization as measured in other angles, which do not exceed 70 % in nature, gives an advantage of using polarization as a cue to trap animals, as traps can be set to reflect higher partial polarization values than the natural habitats by using manufactured strongly polarizing black sheets or liquids that will provide higher partial polarization of reflected light, and therefore are more attractive to chironomid females.

Another important requirement that increases the traps' effectiveness is to decrease the amount of natural habitats available for chironomid females for oviposition. As discussed in Chap. 21, this factor affects the egg density in the traps, as the females distribute their eggs among the available habitats according to their quality as they assess it by the reflection-polarization characteristics (Lerner et al. 2011). So if, for example, we provide a trap reflecting 100 % partial polarization nearby the natural habitat which reflects only 70 % partial polarization, the females will oviposit in both habitats in a ratio of 10:7 in favour of the trap. To increase the attractiveness to 100 %, the natural habitat should be removed or made completely unattractive by lowering the partial polarization of reflected light (Lerner et al. 2012). This can be done by making the water surface brighter, which for natural reflectors means lowering the partial polarization of reflected light as stated by the law of Umow (1905).

23.2 Polarization Tabanid Traps: New Techniques of Horsefly Control

Gábor Horváth, Miklós Blahó, and Ádám Egri

23.2.1 Introduction: Need for Tabanid Traps

Tabanid flies (Tabanidae, e.g. horseflies and deerflies) can cause severe problems for humans and animals because of the diseases vectored by the haematophagous females (Foil 1989; Luger 1990; Maat-Bleeker and Bronswijk 1995; Hall et al. 1998; Sasaki 2001; Lehane 2005). Livestock, especially cattle and horses, can be so strongly annoyed by the continuous attacks of blood-sucking tabanids that they cannot graze enough, and consequently, their meat and milk production is drastically reduced (Hunter and Moorhouse 1976; Harris et al. 1987; Lehane 2005). Furthermore, tabanid bites cause visible scars on the skin of host animals. The bigger the scarless area of cattle hides, for example, the higher their value. As a consequence, the numerous bites of blood-sucking female tabanids can drastically lower the value of cattle bred for hide. Because of these serious problems, effective tabanid traps are in large demand, especially for stock breeders to control tabanids. Scientists studying tabanid flies also have to capture them by special traps.

Historically, traps based on the flight interception principle and the attraction to black targets have been routinely used to capture tabanids (Malaise 1937; Gressitt and Gressitt 1962; Catts 1970; Chvala et al. 1972; von Kniepert 1979; Wall and Doane 1980; Hribar et al. 1992). Blue-black cloth traps, such as the Nzi trap (Mihok 2002; van Hennekeler et al. 2008; Mihok and Lange 2012), for example, which rely on different attraction principles, are also frequently used for trapping tabanids. Nowadays, the most widespread tabanid trap type is the canopy trap (Fig. 23.1). It is essentially a conical/pyramidal canopy resting on a tripod/tetrapod or hanging from a large vertical hook stuck into the ground with an insect collector fitted at its apex (Muirhead-Thomson 1991, p. 215). Usually, suspended beneath the canopy is the visually attractant decoy target in the form of a shiny, smooth, black sphere (Fig. 23.1d–h) (Bracken et al. 1962; Thorsteinson et al. 1965). The function of the black sphere is to lure tabanids from a remote distance by means of optical cues (intensity and colour of target-reflected light, shape and motion of the visual target). It is generally believed that such black structures may imitate the dark silhouette of a host animal, and if they are flapping in the wind, their motion might mimic that of the host and attract female tabanids that want to suck blood (Thorsteinson et al. 1965, 1966; Lehane 2005). When the attracted female tabanids land on the

G. Horváth (✉) • M. Blahó • Á. Egri
Environmental Optics Laboratory, Department of Biological Physics, Physical Institute, Eötvös University, Pázmány sétány 1, 1117 Budapest, Hungary

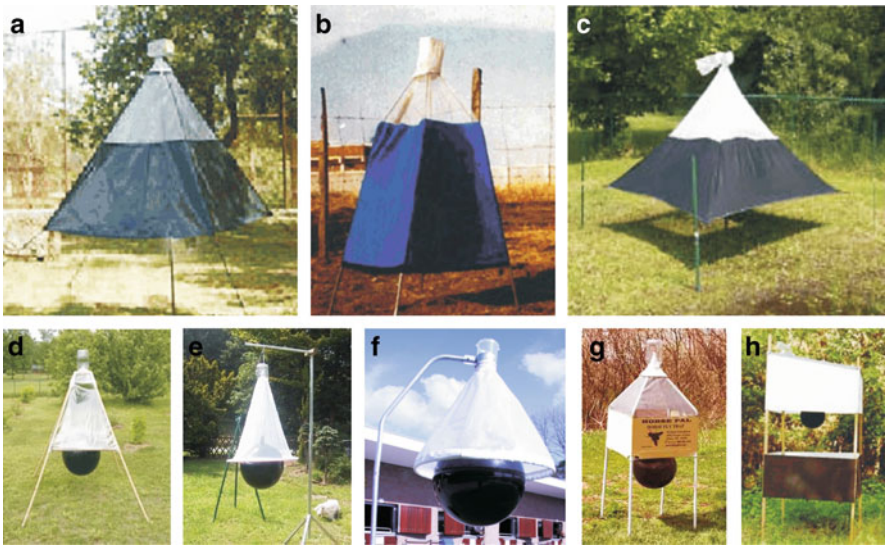

Fig. 23.1 Various canopy traps designed to catch tabanid flies. *Row 1*: Chemically baited canopy traps without black spherical visual decoys. (**a**) A grey-black canopy trap (Veer et al. 2002). (b) A white-black canopy trap (Rahman 2005). (**c**) A white-black canopy trap (http://www.nzitrap.com). *Row 2*: Canopy traps with a *shiny black sphere* functioning as a visual bait. (**d**) Manitoba trap with a pyramidal transparent *white plastic canopy* (http://www.nzitrap.com). (**e**) Manning trap with a hanging funnel-like *white netting* (http://www.bokt.nl/forums/viewtopic.php?f=149&t=789683). (**f**) H-trap having a *conical white net canopy* (http://www.h-trap.net). (**g**) HorsePal trap possessing a canopy composed of a *beige box* and a *pyramidal white netting* (http://bitingflies.com). (**h**) A white-black box trap (http://entnemdept.ufl.edu/creatures/livestock/deer_fly.htm)

black sphere and experience that a potential blood meal is not available, a proportion of them fly upward into the funnel-like end of the canopy, where they are trapped by a glass/plastic container. The tabanid-capturing efficiency can be enhanced by the addition of CO_2 or certain other chemical attractants, e.g. ammonia, phenol, octenol or acetone (Hribar et al. 1992; Mihok 2002; Mihok and Mulye 2010; Mihok and Lange 2012). Although the performance of canopy traps has been frequently demonstrated, their disadvantage is that they capture only host-seeking female tabanids attracted to the shiny black sphere (Muirhead-Thomson 1991, p. 216; Lehane 2005).

Horváth et al. (2008, 2010a, b) showed that male and female tabanids are attracted to horizontally polarized light, just like many other aquatic insect species (Schwind 1991, 1995; Wildermuth 1998, 2007; Horváth and Varjú 2004; Csabai et al. 2006; Kriska et al. 2006, 2007, 2008a, b, 2009; Horváth and Kriska 2008; Lerner et al. 2008; Malik et al. 2008; Horváth et al. 2009). The reason for this adaptive behaviour is that tabanids lay their eggs onto marsh plants near freshwater bodies or mud; thus, they have to find water, which is performed by means of the horizontal polarization of light reflected from the water surface. It has been

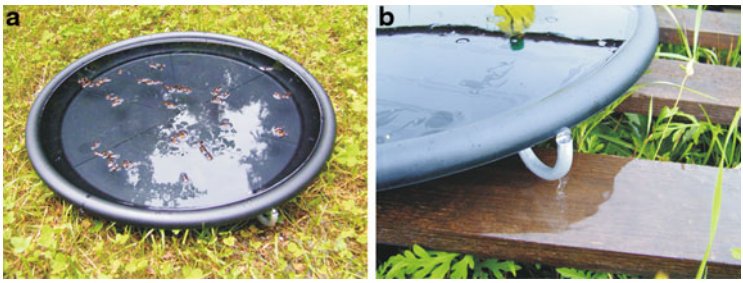

Fig. 23.2 (**a**) A new polarization liquid trap composed of a *circular black plastic tray* (with a diameter of 50 cm) possessing an aluminium overflow tube. The tray is filled with 2 litre tap water until the surplus water flows out through the overflow tube. Then 1 litre (transparent or black) vegetable oil is poured onto the water. (**b**) Close-up photograph of the overflow tube, through which the surplus water is flowing out [after Fig. 1 on page 666 of Egri et al. (2013a)]

suggested that this positive polarotactic behaviour in tabanids could be used to develop new tabanid traps (Horváth et al. 2008; Kriska et al. 2008a). In the next sections three different types of polarization-based tabanid traps are presented. The high tabanid-capturing efficiency of all three trap types has been proven in field experiments (Kriska et al. 2008a; Blahó et al. 2012; Egri et al. 2013a, b). The scientific basis of these traps is the two kinds of positive polarotaxis in tabanid flies (Horváth et al. 2008; Egri et al. 2012; see also Chap. 22).

23.2.2 Tabanid Trap Combining the Classic Canopy Trap with a Polarization Liquid Trap to Catch Host- and Water-Seeking Tabanid Flies

Host-seeking female tabanid flies, that want to suck blood to develop and ripen their eggs, can be captured by the classic canopy trap with an elevated shiny black sphere as a luring visual target (Fig. 23.1d–h). Egri et al. (2013a) showed that water-seeking male and female tabanids can be caught by a weatherproof, polarization liquid trap (Fig. 23.2) laid on the ground, because the strongly and horizontally polarized light reflected from the black liquid surface (Fig. 23.3) attracts water-seeking polarotactic tabanids. The darker a colourless (white, grey, black), shiny, horizontally polarizing liquid surface, the higher the degree of polarization d of the liquid-reflected light, and thus, the larger the attractiveness to tabanids (Kriska et al. 2009). Consequently, black is the ideal colour of the liquid surface.

The polarization liquid trap is essentially a black plastic tray (with a diameter of about 50 cm) possessing an overflow tube (Fig. 23.2). The tray is filled with 2 litre tap water; then 1 litre common, transparent vegetable oil is poured into the water. Because oil is less dense than water, the former swims in a thin layer on the latter. In rain the surplus rainwater fallen into the tray flows out through the overflow tube.

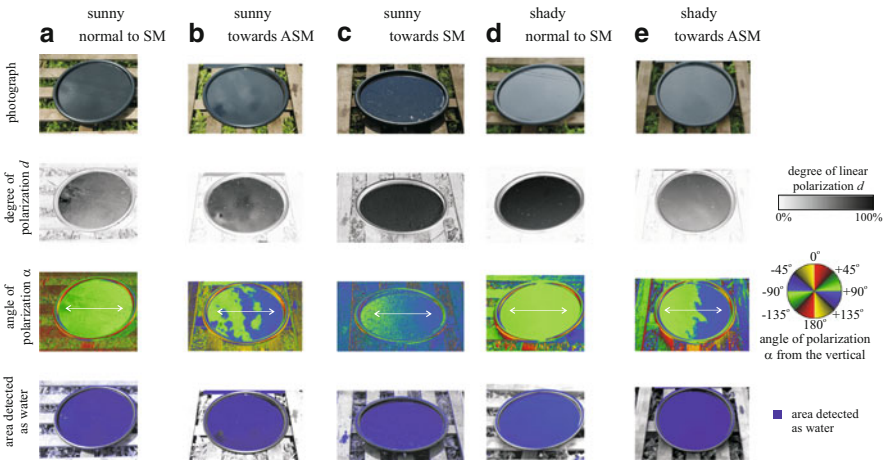

Fig. 23.3 Photograph, patterns of the degree of linear polarization d and the angle of polarization α (clockwise from the vertical) and areas detected as water (for which the liquid-reflected light has the following characteristics: $d > 20$ %, $80° < \alpha < 100°$) of a polarization liquid trap measured in the blue part of the spectrum when it was sunny (**a**, **b**, **c**) or shady (**d**, **e**) for different directions of view relative to the solar meridian. The *double-headed arrows* in the α-patterns show the local directions of polarization of reflected light. Towards SM: the polarimeter saw towards the solar meridian. Towards ASM: the polarimeter saw towards the antisolar meridian. Normal to SM: the polarimeter saw normal to the solar meridian. In the shady situation (**d**, **e**) the trap was illuminated by light from the totally overcast sky. The angle of elevation of the optical axis of the polarimeter was always nearly $-35°$ from the horizontal [after Fig. 4 on page 670 of Egri et al. (2013a)]

The result is an always ideally flat, horizontal, black liquid surface. If wind blows dust into the liquid-filled tray, the dust sediment on the bottom of the black tray can more (if the dust is bright) or less (if the dust is dark) depolarize the tray-reflected light, the consequence of which is reduction of the tabanid-attracting ability. To avoid this depolarizing effect of wind-blown sediment, the oil can be mixed with an appropriate black paint, resulting in an ideal black oil surface in the tray.

According to Fig. 23.3, the light reflected from the horizontal black oil surface of the liquid trap is always horizontally polarized. The degree of polarization d of oil-reflected light is higher or lower, depending on the reflection angle, but it is always high enough to attract water-seeking polarotactic tabanids. Light with $d > 20$ % and angles of polarization $80° < \alpha < 100°$ mean water for polarotactic tabanids (Kriska et al. 2009). As seen in the last row of Fig. 23.3, the whole oil surface of the liquid trap is sensed as water by tabanids; thus, the trap is strongly attractive to water-seeking tabanid flies. From these reflection-polarization characteristics, Egri et al. (2013a) concluded that the polarization liquid trap functions well under all illumination conditions.

In field experiments (Fig. 23.4) Egri et al. (2013a) compared the tabanid-capturing efficiencies of three different traps: (1) the classic canopy trap, (2) the polarization liquid trap and (3) the combination of these two traps. They conducted two different types of field experiments: height experiments

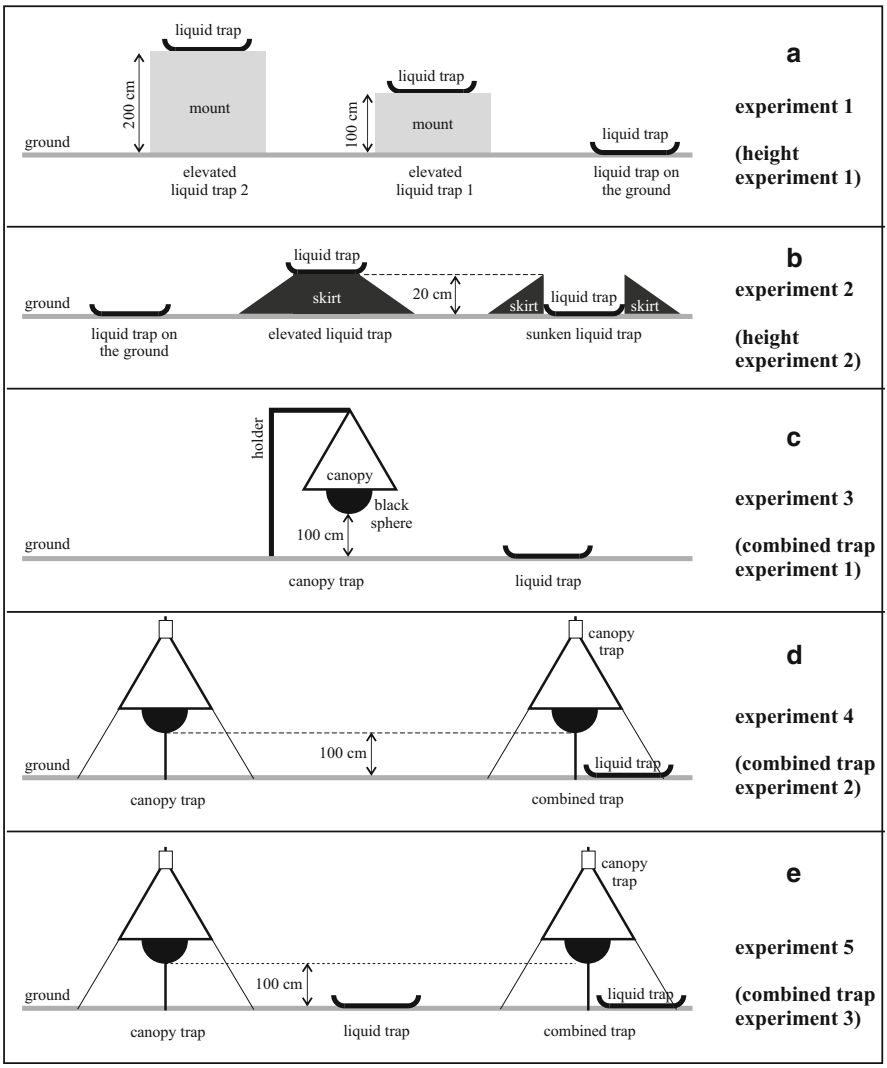

Fig. 23.4 Arrangements of the different tabanid traps used in the field experiments of Egri et al. (2013a) studying the influence of height of the trap on the tabanid-catching efficiency (**a**, **b**) and comparing the tabanid-capturing efficacies of the classic canopy trap, the polarization liquid trap and the combination of these two traps (**c**, **d**, **e**) [after Fig. 2 on page 667 of Egri et al. (2013a)]

(Fig. 23.4a, b) and combined trap experiments (Fig. 23.4c–e). In the height experiments the influence of elevation of the liquid trap on the tabanid-capturing efficacy was studied, because in earlier field studies (Horváth et al. 2008; Kriska et al. 2009; Blahó et al. 2012; Egri et al. 2012) it has been experienced that tabanids may ignore horizontally polarizing surfaces above the ground level, since this is an unnatural

situation. In the combined trap experiments, the tabanid-catching efficiencies of canopy traps, liquid traps and their combination were compared.

The advantage of the polarization liquid trap is that it attracts both male and female water-seeking tabanids by means of the horizontally polarized light reflected from the liquid surface. The reflection-polarization characteristics of the smooth black liquid surface are independent of the meteorological conditions: the trap reflects always strongly and horizontally polarized light under shady as well as sunlit illumination conditions (Fig. 23.3). The ideal height of this trap to capture maximal number of tabanids is the ground level. If the trap is elevated or sunken ($\geq \pm 20$ cm), its tabanid-capturing efficiency is drastically reduced. Although there are also elevated water surfaces in nature, filled rain barrels, for example, according to the many-year field experience of Horváth and co-workers, these do not attract tabanid flies. The mechanical trapping of tabanids touching the liquid surface is performed by a thin oil layer being hydrophilic to the chitinous body of flies. The weatherproofness of the trap is ensured by an overflow tube (Fig. 23.2). Furthermore, the oil layer on the water hinders the evaporation of water.

The reason for the finding that the liquid trap captures tabanids practically only, if its oil surface is on the ground, is that the polarization liquid trap imitates a horizontally polarizing water surface to polarotactic tabanids, seeking for water always at the ground level, which is the natural situation. Non-biting midges (chironomids) as polarotactic aquatic insects (Lerner et al. 2008) can be trapped by elevated polarization liquid traps placed on the roof of a car at a height of about 1.5 m (Horváth et al. 2011). Another example is the case of dragonflies, which are also polarotactic (Wildermuth 1998, 2007) and are lured by horizontally polarizing elevated roofs of dark or red cars (Wildermuth and Horváth 2005).

Hence, the polarization liquid trap has to be settled on the ground to keep its large tabanid-capturing efficiency. Thus, this trap must be installed in places where livestock cannot tread on it or drink the liquid (vegetable oil and water). Unfortunately, this trap cannot be installed on an elevated mount in hurdles of cattle or horses. The advantage of such an elevated mount would be that the animals could not step or drink into the liquid trap.

Egri et al. (2013a) found that the combination of the canopy and liquid traps results in a combined trap that captures 1.5–8.2 times more tabanids than the canopy trap alone. The reason for the larger efficiency of the combined trap is that it captures simultaneously the host-seeking female and the water-seeking male and female tabanids. Therefore, it is worth supplementing the traditional canopy trap with the new polarization liquid trap in order to enhance the tabanid-capturing efficacy.

In the combined trap, the liquid trap component can be replaced by a horizontal sticky black trap surface, which reflects also strongly and horizontally polarized light and catches all tabanids touching its sticky surface as the horizontal black liquid surface. Such a polarization sticky trap, the so-called horseflypaper (see below), has been designed and successfully tested by Egri et al. (2013b).

Egri et al. (2012) have also revealed the reason for the attractiveness of black spheres used in canopy traps to catch tabanids. In their experiments canopy traps

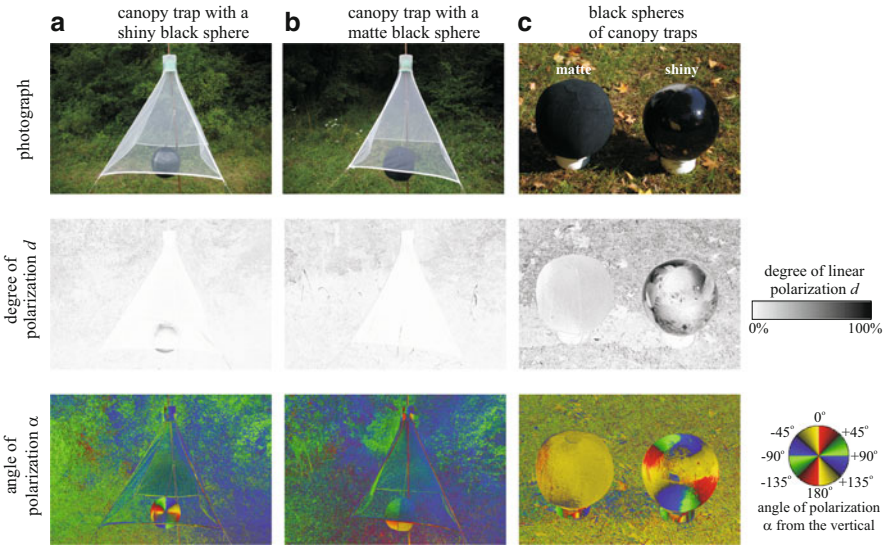

Fig. 23.5 Photograph and patterns of the degree of polarization d and angle of polarization α of light reflected from canopy traps and their visual targets (*matte* and *shiny black spheres*) measured by imaging polarimetry in the blue (450 nm) spectral range under shady (**a**, **b**) and sunlit (**c**) conditions. The elevation angle of the polarimeter's optical axis was $-15°$ (**a**, **b**) and $-45°$ (**c**) from the horizontal [after Fig. 1 on page 409 of Egri et al. (2012)]

with shiny black spheres captured significantly (9–12 times) more (exclusively female) tabanids than those with matte black spheres, because the attractiveness of the shiny spheres to tabanids was much larger than that of matte spheres due to the much higher degree of polarization d of target-reflected light, independently of the E-vector direction (Fig. 23.5). Hence, it is very important that the black decoy spheres must be highly polarizing in order to attract tabanids maximally. This can be ensured only by a smooth, shiny black surface. Consequently, weakly polarizing matte black spheres are disadvantageous for this purpose.

23.2.3 Sticky Polarization Horseflypaper Applying the Modified Concept of the Old Flypaper to Capture Host- and Water-Seeking Tabanids

It is a well-known fact that certain flies can be trapped by a sticky drab/white paper strip hanging vertically from the ceiling. This ancient trap is called the "flypaper" and is used from the beginning of the history of mankind (Beavis 1988). Several different types of such flytraps are used to catch various insect species/groups for scientific purposes (Jactel et al. 2006; Kamarudin and Arshad 2006; Chadee and

Fig. 23.6 (**a**) A classic flypaper (with numerous fly carcasses) used in households. (**b**) A traditional flypaper (covered by fly carcasses) used in equerries. (**c**) A horizontal sticky black test surface (100 cm × 100 cm) on the ground used in a field experiment by Egri et al. (2013b). The trapped tabanids (987 within a week) can be well seen. The tabanid-capturing efficacy of such test surfaces inspired the development of the polarization horseflypaper [after Supplementary Fig. S5 of Egri et al. (2013b)]

Ritchie 2010; Faiman et al. 2011) or for practical aims in the agriculture (Coli et al. 1985; Stejskal 1995; Cross et al. 2006; Moreau and Isman 2012). Depending on their application, the material (paper or plastic), colour (colourless or differently coloured), shape (e.g. rectangular or circular), stickiness (more or less gluey), alignment (vertical, tilted, horizontal or three dimensional) and position (e.g. laid on the ground, or onto an elevated substrate, or hanging high in the air) of these flytraps are different.

The classic flypaper (Fig. 23.6a, b) has four typical characteristics: (1) its sticky paper is bright (drab or white), (2) it has an elongated shape (frequently a strip), (3) it hangs vertically and (4) it is positioned high (several meters) above the ground level not to disturb people and/or animals in their vicinity. Such flypapers, however, do not trap tabanid flies. Based on the positive polarotaxis in tabanids and modifying the concept of the old flypaper (Fig. 23.6a, b), Egri et al. (2013b) designed a new tabanid trap called as "horseflypaper" (Figs. 23.6c and 23.7). In field experiments (Fig. 23.8) they showed that the ideal horseflypaper (1) is shiny black, (2) has an appropriately large (75 cm × 75 cm) surface area, (3) has sticky black vertical and horizontal surfaces in an L-shaped arrangement and (4) its horizontal surface part should be on the ground, while its vertical surface part has to be at 1–1.5 m above the ground to be the most efficient. The horizontal part of the trap captures

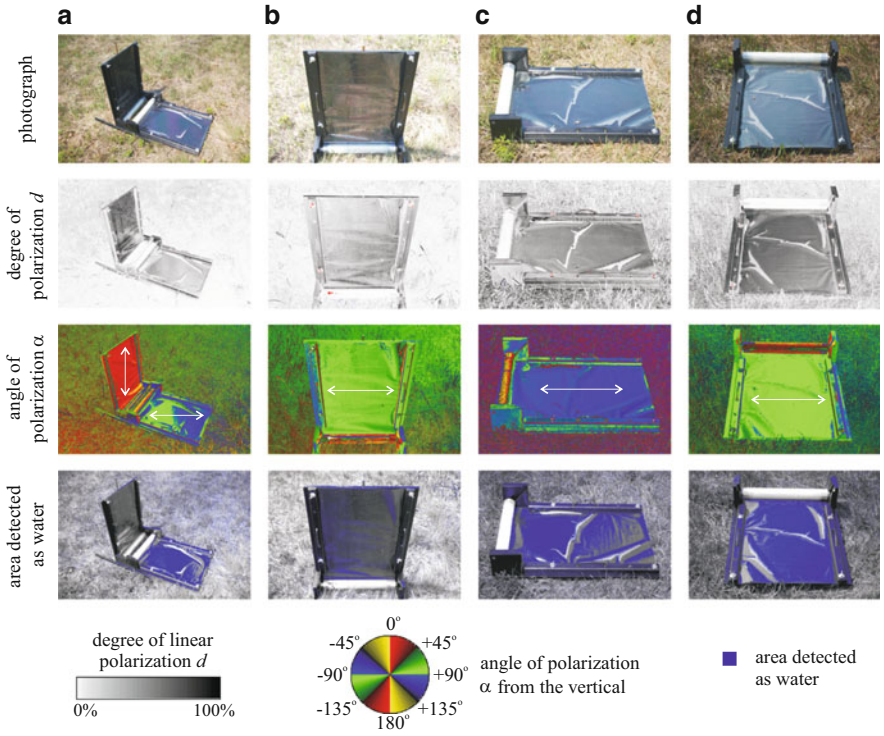

Fig. 23.7 Photograph, patterns of the degree of polarization d and the angle of polarization α (clockwise from the vertical) and areas detected as water (for which the reflected light has the following characteristics: $d > 20$ %, $80° < \alpha < 100°$) of the horizontal and vertical sticky black surfaces of a prototype of the new polarization horseflypaper tested by Egri et al. (2013b) in the field. The *double-headed arrows* in the α-patterns show the local directions of polarization of reflected light. The patterns were measured in the blue (450 nm) part of the spectrum by imaging polarimetry from different directions of view relative to the trap surfaces. The traps were illuminated by direct sunlight and skylight from the clear sky. The angle of elevation of the optical axis of the polarimeter was $-35°$ from the horizontal [after Fig. 2 on page 558 of Egri et al. (2013b)]

water-seeking male and female tabanids, while the vertical part catches host-seeking female tabanids. Egri et al. (2013b) demonstrated that this horseflypaper is an effective tool to catch polarotactic male and female tabanid flies.

From their field tests (Fig. 23.8) Egri et al. (2013b) concluded that a sticky horizontal or vertical surface captures the most tabanids if it is black; furthermore, a horizontal black sticky surface on the ground can trap more than 15 times as much tabanids as a vertical one of the same size. A horizontal sticky black surface captures the most tabanids if it is on the ground, when it can trap more than 20 times as much tabanids as a vertical sticky black surface of the same size at a height of 1–1.5 m from ground. The larger a horizontal or vertical sticky black surface, the greater the number of captured tabanids, and the ideal dimensions of horizontal and vertical sticky traps are 75 cm × 75 cm possessing maximum surface

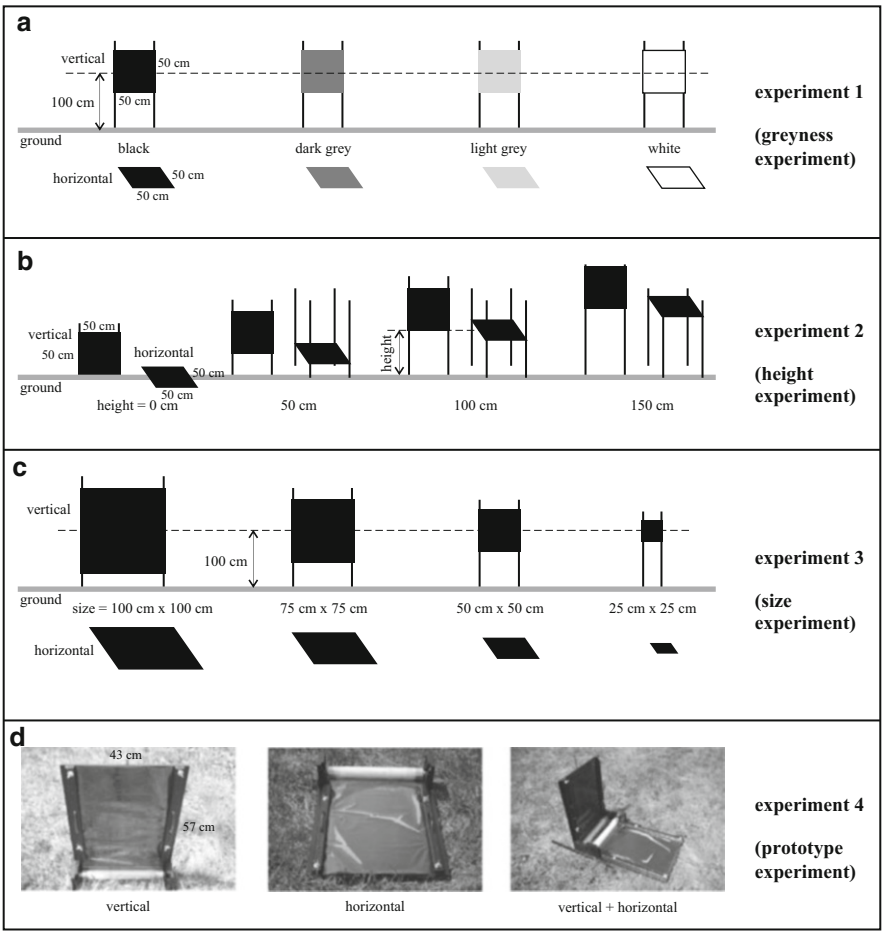

Fig. 23.8 Arrangements of the different sticky tabanid traps used in the field experiments of Egri et al. (2013b) studying the influence of greyness (**a**), height (**b**), size (**c**) and alignment (**d**) of horizontal and vertical trap surfaces on the tabanid-capturing efficacy [after Fig. 1 on page 557 of Egri et al. (2013b)]

density of tabanid catches. On the basis of these results, Egri et al. (2013b) constructed a patented prototype of the polarization horseflypaper.

The prototype of the horseflypaper (Figs. 23.7 and 23.8d) uses a roll of sticky, transparent insect-monitoring plastic sheet. It has a base plate (43 cm × 57 cm) which must be shiny black to maximize the degree of polarization of trap-reflected light. If the plastic sheet is black, the base plate should not be black. At one short side of this base plate, two perpendicular holders are mounted that have symmetrical engravings so that they can hold the roll of the sticky plastic sheet. The sheet should be rolled out with the sticky side upside along the base plate until it covers the whole plate. Then the sticky sheet is fixed with four screws along its

two non-sticky long margins by two black wooden battens to the base plate. There are two optional supporting sticks that can be mounted to the trap in a way that the sticky sheet stands vertically instead of horizontally. Egri et al. (2013b) tested three different trap arrangements (Fig. 23.8d): (1) one vertical sticky black plate standing on the ground, (2) one horizontal sticky black plate laid on the ground and (3) an L-shaped combined trap with a vertical and a horizontal sticky black plate on the ground.

The combined trap captured more tabanids (56.3 %) than the single vertical (5.4 %) and horizontal (38.3 %) traps together (43.7 %). The horizontal trap surfaces captured about 7 and 10 times more tabanids than the vertical ones. From the results of their field tests, Egri et al. (2013b) concluded that the new polarization horseflypaper functions excellently under field conditions, and it is worth combining both the vertical and horizontal sticky black trap surfaces in an L-shaped arrangement to maximize the tabanid catches. Due to practical reasons, the vertical part of the prototype trap stands on the ground (it would be difficult to fix it at an elevated position above the ground).

Hence, changing the colour of the classic vertically hanging flypaper from drab/white to black, its narrow strip shape to a 75 cm × 75 cm square, its height from several metres to 1–1.5 m above ground and its surface orientation from vertical to horizontal laid on the ground, an effective tool is obtained, the horseflypaper.

According to Fig. 23.7, the degree of polarization d of light reflected from the vertical and horizontal sticky black surfaces of the horseflypaper depends on the direction of view, but it is always high ($70\ \% < d < 90\ \%$) near the Brewster angle.[1] The direction of polarization of surface-reflected light is horizontal, if the plane of reflection is vertical. Thus, the horizontal surface part of the combined trap reflects always horizontally polarized light. If the plane of reflection is horizontal or tilted, the reflected light is vertically or obliquely polarized. The consequence of these reflection-polarization characteristics is that a predominant percentage (>90 %) of the horizontal trap surface is always detected as water by water-seeking polarotactic tabanid flies (Fig. 23.7). On the other hand, depending on the direction of view, the vertical trap surface reflects light with horizontal, oblique or vertical direction of polarization with high degrees of polarization near the Brewster angle. Thus, the vertical horseflypaper attracts only host-seeking female tabanids.

The reason for the phenomenon that horizontal sticky black surfaces on the ground trap much more tabanids than vertical ones can be the following: Vertical sticky black trap surfaces capture only those host-seeking female tabanids which want to suck blood for the development of their eggs. This host-finding period of female tabanids falls mainly on the beginning of the tabanid season. On the other hand, the horizontal sticky black trap surfaces catch all male and female tabanids that want (1) to drink water, and/or (2) to cool their body in water, and/or (3) to mate at water, and/or (4) to lay eggs into/near water (females only). Motivations (1) and

[1] $\theta_{\text{Brewster}} = \text{arc tan}(n) = 56.3^\circ$ from the normal vector of the plastic surface with a refractive index of $n = 1.5$.

(2) are characteristic for the whole tabanid season, while motivations (3) and (4) are typical for the beginning-middle and the middle-end of the tabanid season, respectively. Due to these more or less permanent motivations, the horizontal trap surfaces keep their high attractiveness to male and female tabanids throughout the entire season; thus, they capture much more tabanids than the corresponding vertical trap surfaces.

Egri et al. (2013b) experienced that the ideal size of both the vertical and horizontal surface components of the L-shaped combined horseflypaper is about 75 cm × 75 cm. Smaller or larger surfaces trap less tabanids per unit area (surface density). As mentioned above, vertical dark surfaces mimic host animals for host-seeking female tabanids. A given tabanid species may prefer a vertical dark surface with a particular size, which corresponds with the average size of the preferred or most abundant host animals. This preferred/optimal size may be tabanid species specific. In the habitat of the field experiments of Egri et al. (2013b), the following tabanid species occurred: *Tabanus tergestinus*, *T. bromius*, *T. bovinus*, *T. autumnalis*, *Atylotus fulvus*, *A. loewianus*, *A. rusticus* and *Haematopota italica*. To these species the vertical size of 75 cm × 75 cm was the most attractive, since perhaps this is the most typical average size of host animals (horses, cattle, sheeps, dogs, humans) in their biotope.

On the other hand, the horizontal surface of the L-shaped combined horseflypaper imitates a water surface for water-seeking tabanids by the horizontal polarization of reflected light. Considering drinking or body cooling by bathing, male and female tabanids may not prefer any water body of a particular size: tabanids could drink or bath practically in all water bodies. However, female tabanids may prefer an optimal size of water bodies as their egg-laying sites: too small water bodies can dry out quickly, hindering the development of tabanid larvae, while in too large water bodies fishes as predators can be dangerous to tabanid larvae. According to Egri et al. (2013b), on average the optimal size of oviposition sites seems to be about 75 cm × 75 cm for the tabanids investigated. This optimal size may, however, be species specific.

The insect carcasses on the sticky horseflypaper (Fig. 23.6c) may lure and perish small-sized insectivorous birds which try to catch the trapped tabanids from the trap surface. This can be avoided with the use of bird-repelling flags, the vertical holder of which is stuck into the ground at the corners of the rectangular horseflypaper. These flags frighten away the birds approaching the trap to capture the trapped tabanids (Gábor Horváth and György Kriska, unpublished data, 2009–2011, Eu-FP7 TabaNOid research and development project: Trap for the Novel Control of Horse-flies on Open-air Fields, No. 232366).

It has been well documented that tabanids are generally attracted to dark, especially black objects, rather than bright ones (Jones 1922; Roth and Lindquist 1948; Blickle 1955; Granger 1970; Roberts 1970; Thompson and Pechuman 1970; von Kniepert 1979; Anderson 1985; Taylor and Smith 1989; Moore et al. 1996; Hall et al. 1998). Although these sticky black surfaces are the precursors of the

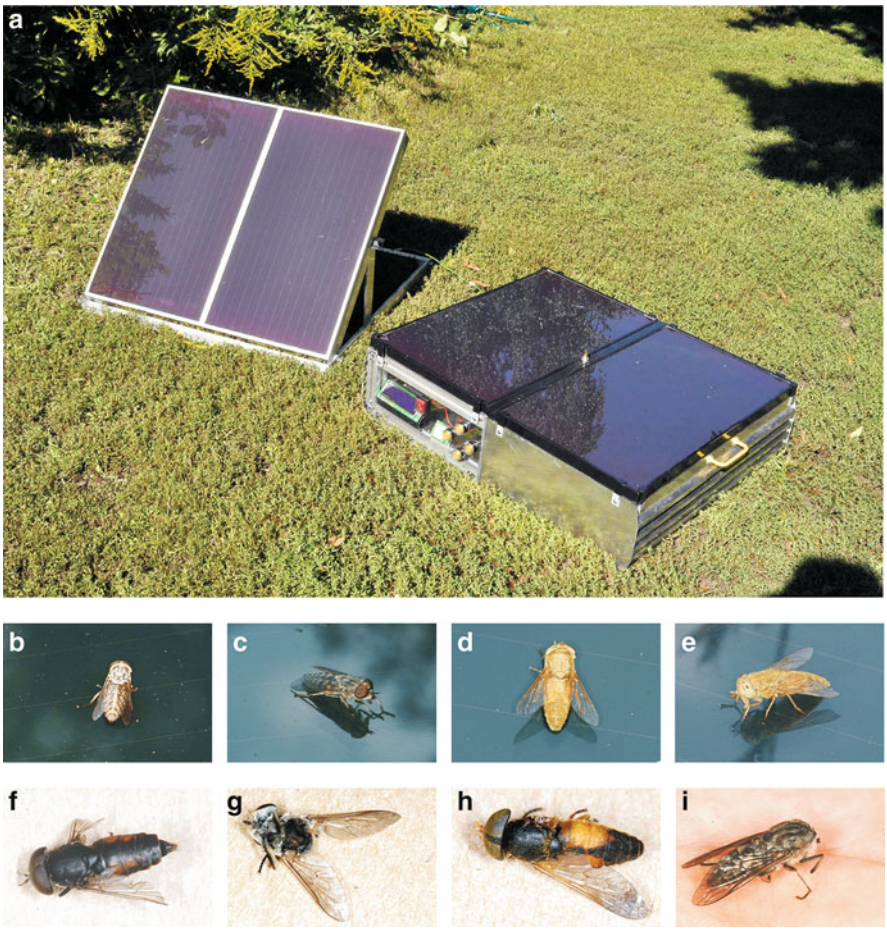

Fig. 23.9 (**a**) Photovoltaic polarization tabanid trap. *Right*: The trap is composed of two horizontal solar panels and a wire rotating above the photovoltaic surface. *Left*: Two supplementary solar panels with a tilted surface. (**b–e**) Tabanid flies landed on the horizontal photovoltaic trap surface. (**f–i**) Carcasses of tabanids hit by the rotating wire. Both female and male tabanids hit suffered so serious injuries that they perished. This demonstrates well the tabanid-trapping efficiency of this technique [after Fig. 2 on page 355 of Blahó et al. (2012)]

polarization horseflypaper, the cited researchers did not know the exact reason for the attractiveness of their shiny dark test surfaces to tabanids. In all these earlier experiments, the horizontal polarization of reflected light attracted water-seeking tabanids, in which polarotactic behaviour was discovered by Horváth et al. (2008).

23.2.4 Polarization Photovoltaic Trap to Capture Water-Seeking Tabanids

Blahó et al. (2012) developed a photovoltaic tabanid trap (Fig. 23.9a) based on two novel principles: (1) The visual target of the trap is a horizontal solar panel (photovoltaics) that attracts water-seeking polarotactic tabanids (Fig. 23.9b–e) by means of the highly and horizontally polarized light reflected from the photovoltaic surface. (2) The tabanids trying to touch or land on the photovoltaics are perished (Fig. 23.9f–i) by the mechanical hit of a wire rotated quickly with an electromotor supplied by the photovoltaics-produced electricity. Hence, the photovoltaics is bifunctional: its horizontally polarized reflected light signal attracts water-seeking, polarotactic tabanid flies, and it produces the electricity necessary to rotate the wire.

The vertical axis of rotation of the electromotor gets through the centre of the horizontal solar panel (60 cm × 60 cm). The thin (0.5 mm) metal wire rotates horizontally around its centre parallel to and a few cm above the photovoltaic trap surface. Electronics ensure that after it is switched on, the rotating wire can reach gradually its maximal angular velocity. Without such a slow spinning up, the wire would coil onto the rotation axis of the electromotor. At full sunshine and at higher solar elevation angles (>29°) above the horizon, the direct current produced by the horizontal solar panel can rotate the wire with large enough angular velocities to perish all tabanid flies attracted to the horizontally polarizing photovoltaic trap surface hitting them mechanically by the wire (Fig. 23.9f–i). When the solar elevation angle is lower than about 29°, an additional solar panel is necessary to rotate the wire with high enough angular velocities to capture tabanids. The power needed to rotate the wire of this trap is (Blahó et al. 2012):

$$P = \left(k\rho a\omega^3 R^4\right)/4, \tag{23.1}$$

where R is the half of the wire length, a is the wire thickness, ω is the angular velocity of the rotating wire, ρ is the air density and k is the shape coefficient of drag (being equal to the shape coefficient of a cylinder, if the wire has a circular cross section). This power P is necessary to compensate the full torque of the drag force acting to the rotating wire. The area of the solar panel necessary to rotate the wire with a given angular velocity ω can be calculated from Eq. (23.1).

Blahó et al. (2012) tested whether (1) the motion of the wire and (2) the buzz and/or the air motion (weak wind) produced by the rotating wire can disturb and thus repel tabanids lured to the horizontally polarizing trap surface (Fig. 23.9b–e). They found that the motion of the wire and/or the buzz and/or the air motion induced by the rotating wire repelled less than about 6–7 % of tabanids attracted to the horizontally polarizing photovoltaic trap surface, and the rotating wire could hit the attracted tabanids so strongly that they perished (Fig. 23.9f–i).

Blahó et al. (2012) observed and counted the following three typical events when tabanids approached the horizontal shiny black surface of the photovoltaics: (1) Touching the trap surface. In nature this is a typical reaction of tabanids when

they touch the water surface to drink or bath in order to cool their heated-up body. (2) Landing (and occasionally walking) on the trap surface. Tabanids neither land nor walk on the water surface. These are their typical reactions on strongly and horizontally polarizing artificial surfaces (Horváth and Kriska 2008; Horváth et al. 2008, 2009, 2010a, b). (3) Hitting the tabanids that try to touch down onto the trap surface by the rotating wire. The tabanid-capturing efficiency of the trap is defined as

$$Q_{\text{capture}} = N_{\text{H}}/(N_{\text{H}} + N_{\text{T}} + N_{\text{L}}), \tag{23.2}$$

where N_{H}, N_{T} and N_{L} are the numbers of hitting (H), touching (T) and landing (L) on the horizontal photovoltaic trap surface, respectively, when the wire is rotating. In spite of the wire rotation, a few tabanids are able to touch or land on the photovoltaic trap surface; thus $Q_{\text{capture}} < 100$ %.

Blahó et al. (2012) showed that a supplementary solar panel (Fig. 23.9a) tilted at 45° from the horizontal (with its symmetry axis oriented hourly toward the azimuth direction of the sun moving along its celestial arc) can enhance by a few hours the time period when the photovoltaic trap functions efficiently. They concluded that if the solar elevation angle is not lower than about 29°, the horizontal photovoltaic trap functions well in full sunshine and it can capture tabanid flies attracted to its horizontal photovoltaic surface with an efficiency of $Q_{\text{capture}} > 92$ %. They found that if the solar elevation angle is not lower than about 10°, the horizontal photovoltaic trap with an oblique (45° from the horizontal) supplementary photovoltaics functions excellently in full sunshine, and it can perish tabanids lured to its horizontal photovoltaics with an efficiency of $Q_{\text{capture}} > 94$ %. If the normal vector of the additional photovoltaics does not follow the direction of the solar meridian, the efficient tabanid-capturing period inevitably decreases by a few hours. Since the abundance of tabanids is usually highest in early afternoon, it is worth orienting the fixed supplementary photovoltaics towards the South or South-West on the northern hemisphere.

According to Fig. 23.10, the degree of polarization d of light reflected from the horizontal photovoltaic trap surface is approximately 90 % and the direction of polarization of reflected light is horizontal ($\alpha \approx 90°$ from the vertical) at the Brewster angle (–34° from the horizontal). Thus, the horizontal, shiny, black photovoltaic trap surface reflects strongly and horizontally polarized light, which is sensed as water by water-seeking polarotactic tabanids. This is the reason for the large attractiveness of the horizontal photovoltaics to tabanid flies. On the other hand, depending on the azimuth direction of view, the tilted supplementary photovoltaics reflects light with moderate degrees of polarization ($d < 25$ %) and not always horizontal, but also tilted directions of polarization (Fig. 23.10). All these polarization characteristics are practically independent of the wavelength of light, because the photovoltaic surfaces are colourless (black).

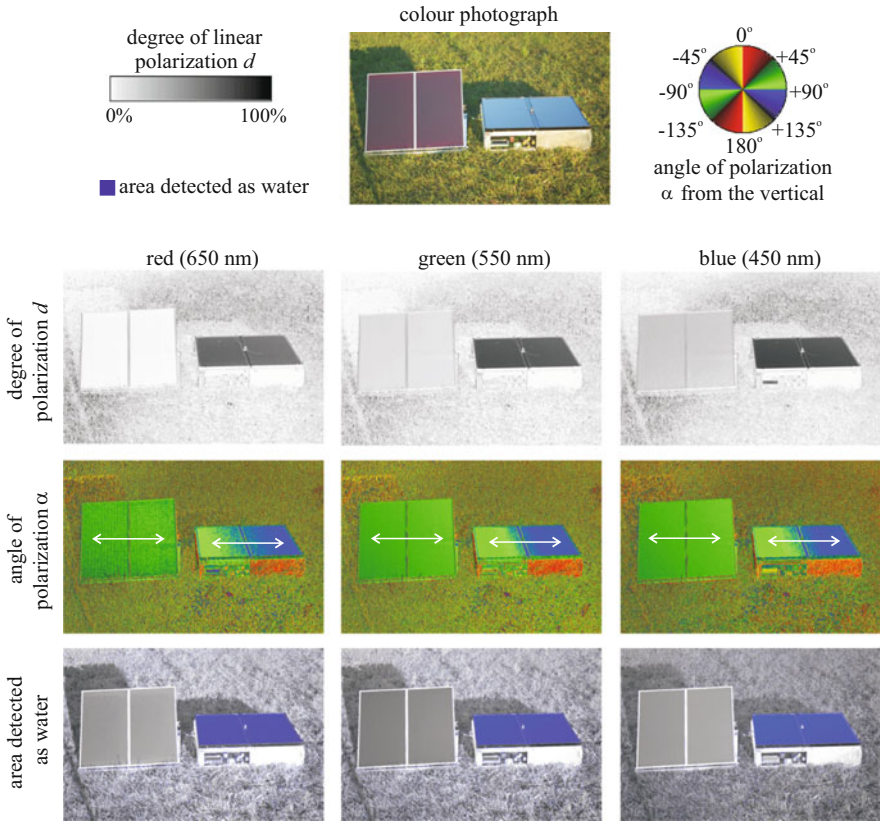

Fig. 23.10 Photograph, patterns of the degree of polarization d and the angle of polarization α (clockwise from the vertical) and areas detected as water (for which the reflected light has the following characteristics: $d > 20$ %, $80° < \alpha < 100°$) of the horizontal photovoltaic polarization tabanid trap with supplementary tilted photovoltaics measured by imaging polarimetry in the red (650 nm), green (550 nm) and blue (450 nm) parts of the spectrum. The *double-headed arrows* in the α-patterns show the local directions of polarization of light reflected from the photovoltaic surfaces. The angle of elevation of the optical axis of the polarimeter was –34° (Brewster angle) from the horizontal. The photovoltaics were illuminated by skylight and sunlight [after Fig. 6 on page 360 of Blahó et al. (2012)]

23.2.4.1 Disadvantages and Advantages

If the sun is occluded by clouds, or the photovoltaic trap surface gets into the shade of vegetation or buildings, the photovoltaics produces so small electricity that the wire cannot rotate with a large enough angular velocity to hit and perish tabanids touching or landing on the horizontal photovoltaics. Thus, one of the prerequisites of an efficient functioning of this tabanid trap is that its photovoltaics must be exposed to full sunshine. However, the reduction of the tabanid-capturing

efficiency due to the occlusion of the sun by clouds is not a serious problem, because tabanids usually do not fly when the sun is hidden by clouds (Horváth et al. 2008, 2010a, b; Kriska et al. 2009; Egri et al. 2012).

A disadvantage of the photovoltaic tabanid trap is that it may also attract and perish other, non-tabanid polarotactic insects, such as water beetles, aquatic bugs and dragonflies, for example. However, on the one hand, aquatic insects are usually not protected animals due to their abundance. On the other hand, a horizontal photovoltaic trap surface of 60 cm × 60 cm is too small to lure many aquatic insects, which require a species-specific minimal surface area of the water bodies into which their eggs are laid and where their larvae can develop successfully (Bailey and Ridsdill-Smith 1991; Williams and Feltmate 1992).

A further disadvantage of the photovoltaic tabanid trap is its complexity relative to the conventional tabanid traps. Due to the electronics and the rotating wire, the electronic and moving components can go wrong. The price of this trap is also larger than that of normal traps because of the necessary photovoltaics and waterproof electronics.

When the photovoltaic tabanid trap is used in the field, it could hurt animals and humans with its rotating wire. To avoid such injuries, the trap should be settled on the ground in such places, where animals or humans cannot approach it. Otherwise, the trap has to be enclosed by an appropriate fence (e.g. a wire grid) to hinder animals and humans to touch the rotating wire.

In comparison to sticky tabanid traps, an advantage of the photovoltaic tabanid trap is that the carcasses of the captured tabanids (Fig. 23.9f–i) do not remain on the tabanid-attracting horizontal trap surface, since the hit tabanids are thrown away by the rotating wire to the neighbouring ground areas. Thus, the photovoltaic trap does not lure (and perish) insectivorous birds attracted by tabanid carcasses, not like sticky insect traps.

23.2.4.2 Improvement Possibilities

The attraction and capture principles of the photovoltaic tabanid trap are fundamentally different from those of the existing tabanid traps (Fig. 23.1) (Malaise 1937; Gressitt and Gressitt 1962; Catts 1970; Chvala et al. 1972; von Kniepert 1979; Wall and Doane 1980; Hribar et al. 1992; Mihok 2002; van Hennekeler et al. 2008; Mihok and Lange 2012). The concept of photovoltaic tabanid traps is patented in Hungary (patent number U-11-00276: Insect-perishing construction, especially tabanid trap using photovoltaics and a wire rotated with the electricity produced by the photovoltaics). The attractivity of the photovoltaic trap to tabanids can be enhanced with the use of certain chemicals (e.g. ammonia, carbon-dioxide, phenols) preferred by tabanid flies (Hribar et al. 1992; Mihok and Lange 2012). In principle, the photovoltaic trap surface and the plane of rotation of the wire can also be vertical. In this case the trap captures only host-seeking female tabanids. Using a combined trap composed of two photovoltaic traps one with a horizontal and the other with a vertical photovoltaic surface, male and female, water- and host-seeking tabanids can be caught.

References

Anderson JF (1985) The control of horse flies and deer flies (Diptera: Tabanidae). Myia 3:547–598
Bailey WJ, Ridsdill-Smith J (1991) Reproductive behaviour of insects: individuals and populations. Chapman and Hall, London
Beavis IC (1988) Insects and other invertebrates in classical antiquity. Exeter University Press, Exeter
Blahó M, Egri Á, Barta A, Antoni G, Kriska G, Horváth G (2012) How can horseflies be captured by solar panels? A new concept of tabanid traps using light polarization and electricity produced by photovoltaics. Vet Parasitol 189:353–365
Blickle RL (1955) Observations on the habits of Tabanidae. Ohio J Sc 55:308–310
Bracken GK, Hanec W, Thorsteinson AJ (1962) The orientation behavior of horseflies and deerflies (Tabanidae: Diptera). II. The role of some visual factors in the attractiveness of decoy silhouettes. Can J Zool 40:685–695
Catts EP (1970) A canopy trap for collecting Tabanidae. Mosq News 30:472–474
Chadee DD, Ritchie SA (2010) Oviposition behaviour and parity rates of *Aedes aegypti* collected in sticky traps in Trinidad. Acta Trop 116:212–216
Chvala M, Lyneborg L, Moucha J (1972) The horse flies of Europe (Diptera: Tabanidae). Entomological Society of Copenhagen, Copenhagen
Coli WM, Green TA, Hosmer TA, Prokopy RJ (1985) Use of visual traps for monitoring insect pests in the Massachusetts apple IPM program. Agric Ecosyst Environ 14:251–265
Cross JV, Hesketh H, Jay CN, Hall DR, Innocenzi PJ, Farman DI, Burgess CM (2006) Exploiting the aggregation pheromone of strawberry blossom weevil *Anthonomus rubi* Herbst (Coleoptera: Curculionidae): Part 1. Development of lure and trap. Crop Prot 25:144–154
Csabai Z, Boda P, Bernáth B, Kriska G, Horváth G (2006) A 'polarisation sun-dial' dictates the optimal time of day for dispersal by flying aquatic insects. Freshw Biol 51:1341–1350
Egri Á, Blahó M, Sándor A, Kriska G, Gyurkovszky M, Farkas R, Horváth G (2012) New kind of polarotaxis governed by degree of polarization: attraction of tabanid flies to differently polarizing host animals and water surfaces. Naturwissenschaften 99:407–416 + electronic supplement
Egri Á, Blahó M, Száz D, Kriska G, Majer J, Herczeg T, Gyurkovszky M, Farkas R, Horváth G (2013a) A horizontally polarizing liquid trap enhances the tabanid-capturing efficiency of the classic canopy trap. Bull Entomol Res 103:665–674
Egri Á, Blahó M, Száz D, Barta A, Kriska G, Antoni G, Horváth G (2013b) A new tabanid trap applying a modified concept of the old flypaper: linearly polarising sticky black surfaces as an effective tool to catch polarotactic horseflies. Int J Parasitol 43:555–563
Faiman R, Kirstein O, Moncaz A, Guetta H, Warburg A (2011) Studies on the flight patterns of foraging sand flies. Acta Trop 120:110–114
Foil LD (1989) Tabanids as vectors of disease agents. Parasitol Today 5:88–96
Granger CA (1970) Trap design and color as factors in trapping the salt marsh greenhead fly. J Econ Entomol 63:1670–1673
Gressitt JCL, Gressitt MK (1962) An improved Malaise trap. Pac Insects 4:87–90
Hall MJR, Farkas R, Chainey JE (1998) Use of odour-baited sticky boards to trap tabanid flies and investigate repellents. Med Vet Entomol 12:241–245
Harris JA, Hillerton JE, Morant SV (1987) Effect on milk production of controlling muscoid flies, and reducing fly-avoidance behaviour by the use of Fenvalerate ear tags during the dry period. J Dairy Res 54:165–171
Horváth G, Kriska G (2008) Polarization vision in aquatic insects and ecological traps for polarotactic insects. In: Lancaster J, Briers RA (eds) Aquatic insects: challenges to populations. CAB International Publishing, Wallingford, Oxon, pp 204–229, Chapter 11

Horváth G, Varjú D (2004) Polarized light in animal vision—polarization patterns in nature. Springer, Heidelberg

Horváth G, Majer J, Horváth L, Szivák I, Kriska G (2008) Ventral polarization vision in tabanids: horseflies and deerflies (Diptera: Tabanidae) are attracted to horizontally polarized light. Naturwissenschaften 95:1093–1100

Horváth G, Kriska G, Malik P, Robertson B (2009) Polarized light pollution: a new kind of ecological photopollution. Front Ecol Environ 7:317–325

Horváth G, Blahó M, Kriska G, Hegedüs R, Gerics B, Farkas R, Åkesson S (2010a) An unexpected advantage of whiteness in horses: the most horsefly-proof horse has a depolarizing white coat. Proc R Soc B 277:1643–1650

Horváth G, Blahó M, Egri Á, Kriska G, Seres I, Robertson B (2010b) Reducing the maladaptive attractiveness of solar panels to polarotactic insects. Conserv Biol 24:1644–1653 + electronic supplement

Horváth G, Móra A, Bernáth B, Kriska G (2011) Polarotaxis in non-biting midges: female chironomids are attracted to horizontally polarized light. Physiol Behav 104:1010–1015 + cover picture

Hribar LJ, LePrince DJ, Foil LD (1992) Ammonia as an attractant for adult *Hybomitra lasiophthalma* (Diptera: Tabanidae). J Med Entomol 29:346–348

Hunter DM, Moorhouse DW (1976) The effects of *Austrosimulium pestilens* on the milk production of dairy cattle. Aust Vet J 52:97–99

Jactel H, Menassieu P, Vétillard F, Barthélémy B, Piou D, Frérot B, Rousselet J, Goussard F, Branco M, Battisti A (2006) Population monitoring of the pine processionary moth (Lepidoptera: Thaumetopoeidae) with pheromone-baited traps. For Ecol Manag 235:96–106

Jones H (1922) Some notes on the habits of male Tabanidae. The Entomologist 55:40–42

Kamarudin N, Arshad O (2006) Potentials of using the pheromone trap for monitoring and controlling the bagworm, *Metisa plana* Wlk (Lepidoptera: Psychidae) on young oil palm in a smallholder plantation. J Asia Pac Entomol 9:281–285

Kriska G, Csabai Z, Boda P, Malik P, Horváth G (2006) Why do red and dark-coloured cars lure aquatic insects? The attraction of water insects to car paintwork explained by reflection-polarization signals. Proc R Soc B 273:1667–1671

Kriska G, Bernáth B, Horváth G (2007) Positive polarotaxis in a mayfly that never leaves the water surface: polarotactic water detection in *Palingenia longicauda* (Ephemeroptera). Naturwissenschaften 94:148–154

Kriska G, Majer J, Horváth L, Szivák I, Horváth G (2008a) Polarotaxis in tabanid flies and its practical significance. Acta Biol Debrecina Suppl Oecol Hung 18:101–108

Kriska G, Malik P, Szivák I, Horváth G (2008b) Glass buildings on river banks as "polarized light traps" for mass-swarming polarotactic caddis flies. Naturwissenschaften 95:461–467

Kriska G, Bernáth B, Farkas R, Horváth G (2009) Degrees of polarization of reflected light eliciting polarotaxis in dragonflies (Odonata), mayflies (Ephemeroptera) and tabanid flies (Tabanidae). J Insect Physiol 55:1167–1173

Lehane MJ (2005) The biology of blood-sucking in insects, 2nd edn. Cambridge University Press, Cambridge

Lerner A, Meltser N, Sapir N, Erlick C, Shashar N, Broza M (2008) Reflected polarization guides chironomid females to oviposition sites. J Exp Biol 211:3536–3543

Lerner A, Sapir N, Erlick C, Meltser N, Broza M, Shashar N (2011) Habitat availability mediates chironomid density-dependent oviposition. Oecologia 165:905–914

Lerner A, Haspel C, Sapir N, Meltser N, Broza M, Shashar N (2012) Insights from chironomid oviposition is useful to visual pest control. Fauna Norvegica 31:65–70

Luger SW (1990) Lyme disease transmitted by a biting fly. N Engl J Med 322:1752–1759

Maat-Bleeker F, Bronswijk van JEMH (1995) Allergic reactions caused by bites from blood-sucking insects of the Tabanidae family, species *Haematopota pluvialis* (L.) [abstract]. Allergy 50 (Suppl 26):388

Malaise R (1937) A new insect-trap. Entomologisk Tidskrift Stockholm 58:148–160

Malik P, Hegedüs R, Kriska G, Horváth G (2008) Imaging polarimetry of glass buildings: why do vertical glass surfaces attract polarotactic insects? Appl Opt 47:4361–4374
Mihok S (2002) The development of a multipurpose trap (the Nzi) for tsetse and other biting flies. Bull Entomol Res 92:385–403
Mihok S, Lange K (2012) Synergism between ammonia and phenols for *Hybomitra* tabanids in northern and temperate Canada. Med Vet Entomol 26:282–290
Mihok S, Mulye H (2010) Responses of tabanids to Nzi traps baited with octenol, cow urine and phenols in Canada. Med Vet Entomol 24:266–272
Moore TR, Slosser JE, Cocke J, Newton WH (1996) Effect of trap design and color in evaluating activity of *Tabanus abactor* Philip in Texas rolling plains habitat. Southwest Entomol 21:1–11
Moreau TL, Isman MB (2012) Combining reduced-risk products, trap crops and yellow sticky traps for greenhouse whitefly (*Trialeurodes vaporariorum*) management on sweet peppers (*Capsicum annum*). Crop Prot 34:42–46
Muirhead-Thomson RC (1991) Trap responses of flying insects: the influence of trap design on capture efficiency. Academic, London
Rahman AHA (2005) Observations on the trypanosomosis problem outside the tsetse belts of Sudan. Rev Sci Tech Off Int Epiz 24:965–972
Roberts RH (1970) Color of malaise trap and collection of Tabanidae. Mosq News 29:236–238
Roth AR, Lindquist AW (1948) Ecological notes on the deer fly at Summer Lake, Oregon. J Econ Entomol 41:473–476
Sasaki H (2001) Comparison of capturing tabanid flies (Diptera: Tabanidae) by five different color traps in the fields. Appl Entomol Zool 36:515–519
Schwind R (1991) Polarization vision in water insects and insects living on a moist substrate. J Comp Physiol A 169:531–540
Schwind R (1995) Spectral regions in which aquatic insects see reflected polarized light. J Comp Physiol A 177:439–448
Stejskal V (1995) The influence of food and shelter on the efficacy of a commercial sticky trap in *Tribolium castaneum* (Coleoptera: Tenebrionidae). J Stored Prod Res 31:229–233
Taylor PD, Smith SM (1989) Activities and physiological states of male and female *Tabanus sackeni*. Med Vet Entomol 3:203–212
Thompson PH, Pechuman LL (1970) Sampling populations of *Tabanus quinquevittatus* about horses in New Jersey, with notes on the identity and ecology. J Econ Entomol 63:151–155
Thorsteinson AJ, Bracken GK, Hanec W (1965) The orientation behaviour of horseflies and deerflies (Tabanidae: Diptera). III. The use of traps in the study of orientation of tabanids in the field. Entomol Exp Appl 8:189–192
Thorsteinson AJ, Bracken GK, Tostawaryk W (1966) The orientation behaviour of horseflies and deerflies (Tabanidae: Diptera). VI. The influence of the number of reflecting surfaces on attractiveness to tabanids of glossy black polyhedra. Can J Zool 44:275–279
Umow N (1905) Chromatische Depolarisation durch Lichtzerstreuung. Phys Z 6:674–676
van Hennekeler K, Jones RE, Skerratt LF, Fitzpatrick LA, Reid SA, Bellis GA (2008) A comparison of trapping methods for Tabanidae (Diptera) in North Queensland, Australia. Med Vet Entomol 22:26–31
Veer V, Parashar BD, Prakash S (2002) Tabanid and muscoid haematophagous flies, vectors of trypanosomiasis or surra disease in wild animals and livestock in Nandankanan Biological Park, Bhubaneswar (Orissa, India). Curr Sci 82:500–503
von Kniepert FW (1979) Eine leistungsfähige Methode zum Fang männlicher Bremsen (Diptera, Tabanidae). Zeitschrift für angewandte Entomologie 88:88–90
Wall WJ, Doane OW (1980) Large scale use of box traps to study and control saltmarsh greenhead flies (Diptera: Tabanidae) on Cape Cod, Massachusetts. Environ Entomol 9:371–375
Wildermuth H (1998) Dragonflies recognize the water of rendezvous and oviposition sites by horizontally polarized light: a behavioural field test. Naturwissenschaften 85:297–302

Wildermuth H (2007) Polarotaktische Reaktionen von *Coenagrion puella* und *Libellula quadrimaculata* auf Erdbeerkulturen als ökologische Falle (Odonata: Coenagrionidae, Libellulidae). Libellula 26(3/4):143–150

Wildermuth H, Horváth G (2005) Visual deception of a male *Libellula depressa* by the shiny surface of a parked car (Odonata: Libellulidae). Int J Odonatol 8:97–105

Williams DD, Feltmate BW (1992) Aquatic insects. CAB International, Wallingford

Chapter 24
Polarization Cloud Detection with Imaging Polarimetry

András Barta, Bence Suhai, and Gábor Horváth

Abstract In this chapter we show some practical applications of 180° field-of-view (full-sky) imaging polarimetry. The concept and structure of some full-sky imagers (Total Sky Imager, Whole Sky Imager, All Sky Imager) widely used in environmental optics are presented. Some algorithms dealing with photometric cloud detection, a hot topic in meteorology, are described. A brief summary of the satellite-borne PARASOL/POLDER imaging polarimeter is given. Two versions of full-sky imaging polarimetry are described. Both use the measured extra polarization information of skylight. Their advantageous features are (1) enhancement of accuracy and reliability of cloud detection, (2) estimation of the relative cloud-base distance distribution in the sky and (3) applicability in solar forecasting, a very special current topic.

Electronic supplementary material is available in the online version of this chapter at 10.1007/978-3-642-54718-8_24. The colour versions of the black and white figures can also be found under http://extras.springer.com

A. Barta (✉) • B. Suhai
Estrato Research and Development Ltd, Mártonlak utca 13, 1121 Budapest, Hungary
e-mail: bartaandras@gmail.com; suhai.bence@gmail.com

G. Horváth
Environmental Optics Laboratory, Department of Biological Physics, Physical Institute, Eötvös University, Pázmány sétány 1, 1117 Budapest, Hungary
e-mail: gh@arago.elte.hu

G. Horváth (ed.), *Polarized Light and Polarization Vision in Animal Sciences*, Springer Series in Vision Research 2, DOI 10.1007/978-3-642-54718-8_24,

24.1 Full-Sky Photometric Imagers

Cloud detection is an important part of meteorological observations. It can be used as an input parameter of climatic models or for estimation of the total cloud cover and parametrization of fluctuations of sea surface insolation (Kalisch and Macke 2008), as well as for the energy transfer models of the atmosphere. Until a few years ago, these measurements could be performed only by human observers, by looking at the sky with the naked eye and making the necessary estimations. These measurements were unreliable, infrequent, inaccurate and expensive (by calculating the cost of the observer for one measurement). By the appearance and spread of commercial imaging devices, such as compact digital cameras and cell phones with integrated cameras, the CCD and CMOS devices became cheaper. This tendency made it possible to appear digital imaging cloud detectors based on the intensity and colour distribution of the sky. As a new approach, clouds can also be detected with the use of the information in the polarization of scattered skylight measured by full-sky (180° field-of-view) imaging polarimetry (Horváth et al. 2002; Hegedüs et al. 2007; Estrato; Sects. 24.3−24.5).

The first step to perform cloud detection is to take images of the sky. This can be done by sky imagers. In the following subsections we briefly describe the basic concepts of the typical sky imagers currently used for cloud detection.

24.1.1 Total Sky Imager (TSI-880, TSI-440)

The Total Sky Imager (TSI-880 and its predecessor, TSI-440) is a fully automatic field-operable photometric full-sky imager (Yankee Environmental Systems, Fig. 24.1). It consists of a case containing the controlling electronics and an embedded computer to store the measurements. The case is covered with a spherical mirror dome. A stand is mounted to one side of the case that holds a CCD camera above the mirror. The camera points downward onto the centre of the mirror dome. The full image of the sky is reflected into the optics of the camera by the spherical mirror. The image of the Sun is occulted by a radial wide black stripe glued onto the mirror dome, which can be rotated in a way that the image of the Sun on the mirror is hidden by the black stripe.

24.1.2 Whole Sky Imager (WSI)

The Whole Sky Imager (WSI) was developed by the Scripps Institute (WSI Handbook) as a standard instrument for cloud detection. WSI is equipped with a

Fig. 24.1 A TSI-880 instrument at the Baseline Measurement System site of the National Renewable Energy Laboratory. The TSI-880 and its predecessor, the TSI-440, consist of a CCD camera pointing downward to the centre of a *spherical mirror dome*. The latter is responsible for the formation of the image of the whole sky dome. Underneath the mirror the *controlling unit* is placed inside a *rectangular housing*. The mirror has a radial dark band on it, and the mirror itself is rotatable by an embedded motor, so the dark band can be placed in a way that it occludes the image of the Sun from the detector (source of the photograph: http://www.nrel.gov/midc/srrl_bms/pictures.html)

180° field-of-view (full-sky) fisheye Nikkor lens with a focal length of 8 mm and a relative aperture of $f = 2.8$. It uses spectral filters with 70-nm passband widths centred at 450, 650 and 800 nm, as well as neutral density filters with 0, 2 and 3 log units. The spectral and neutral density filters are mounted on two independent filter wheels in the optical path that can be operated independently. The CCD detector has a 16-bit depth and is cooled below −35 °C by using cascaded Peltier elements. The CCD is protected from direct sunlight by an external occulter trolley and arc system (Fig. 24.2).

24.1.3 All Sky Imager

The All Sky Imager (ASI) was developed by the Atmospheric Physics Group of the University of Granada, Spain (Cazorla et al. 2008). The instrument's main parts are a digital camera, a fisheye lens and an external Sun occulter (Fig. 24.3). The camera is a RETIGA 1300C CCD camera from QImaging. The CCD detector (Sony

Fig. 24.2 A Whole Sky Imager with the solar occulter trolley and arc system (source of the photograph: http://www.arm.gov/instruments/wsi)

ICX085AK) has a resolution of 1280×1024 pixels and a 2/3″ optical format. The maxima of the transmission spectra of the colour filters of the CCD detector are at the wavelengths of 470 (blue), 540 (green) and 620 (red) nm. The camera itself is equipped with a Peltier cooler to reduce noise during low light measurements. Each pixel of the CCD is digitized with a 12-bit resolution. The fisheye lens is a FE185C057HA-1 from Fujinon. It has a full 185° field-of-view with a 5.7 mm diameter image circle that is optimized for 2/3″ detector format. The focal length of the lens is 1.8 mm with a relative aperture $f = 1.4$. The camera and the fisheye lens are placed in a weatherproof casing that has polyurethane insulation. The inner space is air-conditioned by a Peltier heater/cooler. The upper side of the casing is covered by an acrylic dome to enable full-sky view for the fisheye lens. The CCD detector is protected from direct sunlight by an external Sun tracker from Kipp & Zonen. This ensures that the fisheye lens is in full shadow at all times. Sun occlusion is important, because direct sunlight can shorten the lifetime of the detector and can cause overexposed stripes along the full width of the detector making those areas of the picture impossible to evaluate (Fig. 24.4).

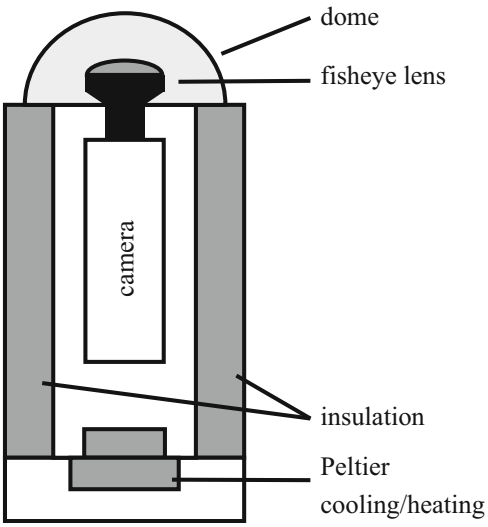

Fig. 24.3 Schematic drawing of the All Sky Imager [after Fig. 1a of Cazorla et al. (2008)]

Fig. 24.4 An All Sky Imager (ASI) installed on a rooftop at Grupo de Física de la Atmósfera, Granada, Spain. The *black arms* with *three black spheres* compose the Sun tracker. The *biggest central sphere* shades the fisheye lens of the ASI, while the *two smaller ones on the sides* shade two other optical instruments placed nearby the ASI on the same platform (source of the photograph: http://atmosfera.ugr.es/inv/index.php/es/instrumentacion/76-all-sky-imager.html)

24.2 Photometric Cloud Detection Algorithms

24.2.1 Fixed Red–Blue-Ratio Threshold

The fixed red–blue-ratio detector (Long and DeLuisi 1998; Bumke 2011) uses the red and blue intensity patterns of the sky and recognizes a given pixel as clear sky, if the ratio $I_r/I_b < c_{frbr}$, and as cloud otherwise, where I_r and I_b are the intensities of the given pixel in the red and blue parts of the spectrum, respectively, and c_{frbr} (where frbr stands for fixed red–blue ratio) is a parameter to be optimized. The clear sky is typically blue leading to smaller I_r/I_b ratios, while clouds are typically white/grey or red leading to larger I_r/I_b ratios.

24.2.2 Fixed Red–Blue-Difference Threshold

The fixed red–blue-difference detector (Heinle et al. 2010) uses the celestial red and blue intensity patterns and recognizes a given pixel as clear sky, if the difference $\Delta I_{r-b} = I_r - I_b < c_{frbd}$, and as cloud otherwise, where I_r and I_b are the intensities of the given pixel in the red and blue parts of the spectrum, respectively, and c_{frbd} (where frbd stands for fixed red–blue difference) is a parameter to be optimized. The clear sky is typically blue leading to smaller ΔI_{r-b} differences, while clouds are typically white/grey or red leading to larger ΔI_{r-b} values.

24.2.3 Adaptive Red–Blue-Ratio Threshold

The adaptive red–blue-ratio threshold detector is similar to the fixed red–blue-ratio threshold detector; however, in the case of the former, a given pixel is recognized as clear sky, if the ratio $I_r/I_b < c_{arbr}(d)$, and as cloud otherwise, where I_r and I_b are the intensities of the given pixel in the red and blue parts of the spectrum, respectively, and $c_{arbr}(d)$ (where arbd stands for adaptive red–blue ratio) is a parameter that is a function of the geometric distance d between the given pixel and the Sun in the sky picture. This algorithm is used by the TSI-880 (Pfister et al. 2003).

24.2.4 Fixed Saturation Threshold

This thresholding algorithm uses a pixels saturation value in the hue–saturation–lightness (HSL) colour space and recognizes a given sky pixel as cloudy, if its saturation value is lower than a given threshold (Souza-Echer et al. 2006). Clouds

are typically colourless features on the blue clear sky, leading to lower saturation values compared to the blue sky.

24.2.5 Euclidean Geometric Distance

The Euclidean Geometric Distance algorithm (Mantelli-Neto et al. 2010) is based on the fact that clouds are usually colourless (white, grey), and so their colours represented as points in the red–green–blue colour cube are close to the main diagonal. On the contrary, points of the clear sky are blue, so the points representing sky colours are closer to the blue edge of the colour cube.

24.2.6 Hybrid Thresholding Algorithm

The Hybrid Thresholding Algorithm (Li et al. 2011) is a mixture of a fixed thresholding and an adaptive minimum cross-entropy-thresholding algorithm. As the first step, the algorithm decides which of the two methods to use. For this purpose the colour intensity image of a cloudy or clear sky scene is converted into a greyscale normalized B/R ratio image. The normalized B/R ratio is:

$$\lambda_{\mathrm{N}} = (I_b - I_r)/(I_b + I_r), \tag{1}$$

with $-1 \leq \lambda_{\mathrm{N}} \leq +1$. The second step is to calculate the histogram of the normalized B/R ratio image. On the histogram a decision is made whether the image is unimodal or bimodal. The image is considered to be unimodal, if the standard deviation T_{s} of the histogram is less than 0.03 (optimized by the authors for the performance of the algorithm), and bimodal otherwise. For unimodal images a fixed thresholding algorithm is used. A given sky pixel is considered as cloudy, if $\lambda_{\mathrm{N}} < T_{\mathrm{f}}$, where $T_{\mathrm{f}} = 0.25$ is a threshold optimized by evaluating several unimodal images. For bimodal images an adaptive minimum cross-entropy-thresholding algorithm is used to separate cloudy and clear sky pixels. Let I_{N} be the normalized B/R ratio image. Let $h(i)$ $(i = 1, 2, \ldots, L)$ be the histogram bins, where L is the number of distinct histogram levels. The segmented image B_t with an arbitrary threshold t is defined as $B_t(x, y) = \mu(1, t)$, if $I_{\mathrm{N}}(x, y) < t$ and $B_t(x, y) = \mu(t+1, L)$, if $I_{\mathrm{N}}(x, y) \geq t$ for a given pixel at the coordinates (x, y), where $\mu(a, b) = \sum_{i=a}^{b} ih(i) / \sum_{i=a}^{b} h(i)$. The cross entropy between two probability distributions is defined as

$$D(F, G) = \sum_{i=1}^{N} f_i \log(f_i / g_i), \tag{2}$$

where $F = \{f_1, f_2, \ldots, f_{\mathrm{N}}\}$ and $G\{g_1, g_2, \ldots, g_{\mathrm{N}}\}$ are two discrete probability distributions on a given set. The cross entropy between the normalized B/R ratio image I_{N} and the thresholded image B_t for a given threshold t is

$$D(t) = \sum_{i=1}^{t} ih(i)\log\left(\frac{i}{\mu(1,t)}\right) + \sum_{i=t+1}^{L} ih(i)\log\left(\frac{i}{\mu(t+1,L)}\right). \quad (3)$$

At the optimal threshold t* the cross entropy between I_N and B_t is minimal:

$$t^* = \arg_t \min \{D(t)\}. \quad (4)$$

Pixels with $\lambda_N < t^*$ are considered as cloudy, otherwise as clear sky.

24.2.7 Neural Networks

A lot of information is encoded in a measurement that needs to be incorporated into the optimal algorithm that detects cloudiness with the lowest possible error. There is so-called local optical information, e.g. the red intensity of the investigated pixel. Furthermore, there is global optical information, like the average intensity of the measurement in the green channel, for example, or the variance of the intensity of the blue channel in the whole measurement. There is also non-optical information, like the solar elevation angle, or the azimuth distance between the Sun and the investigated sky pixel in the sky picture. Some of this information can be easily taken into account in a given algorithm to improve the accuracy; others give challenges to find the way how they can optimally improve the accuracy of a given algorithm. The difficulties come from the fact that it is hard to define why a human observer thinks that a light originating from a given point of the sky belongs to a cloud or the clear sky. It is even possible that a human observer recognizes a light with given optical properties as cloud in one sky situation and a light with the same optical properties as clear sky in another one. To overcome these issues, a multilayer perceptron-type neural network can be implemented, an algorithm capable of supervised learning with the use of the sigmoid activation function (Rumelhart et al. 1986):

$$S(x) = 1/(1 + e^{-x}), \quad (5)$$

where x is the sum of all the inputs of the perceptron. The network has to have at least three layers (Gardner and Dorling 1998). Each layer has to be fully connected to the previous layer, i.e. each neuron of a given layer has to be connected to every neuron in the previous layer. There is only one exception from this rule: each layer has a special neuron, the so-called bias neuron that does not have any input, and always has an output of 1. The bias neuron can give an offset to the inputs of the neurons of the next layer. The output layer contains only one perceptron, the target output value of which is 0 in case the investigated pixel is to be recognized as clear sky and 1 if it belongs to a cloud. During evaluation the investigated sky pixel is detected as clear sky, if the output value of the output perceptron is less than 0.5 and

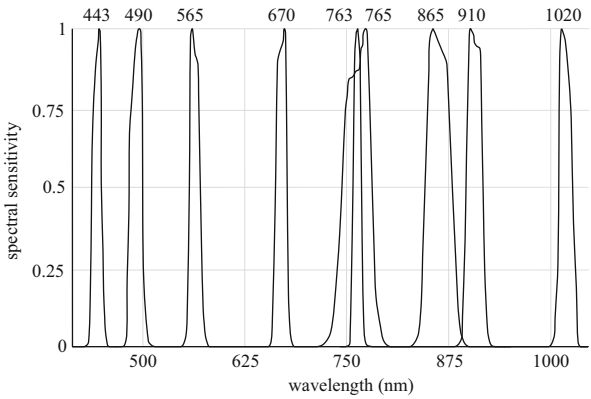

Fig. 24.5 Spectral sensitivity diagram of the PARASOL/POLDER satellite-borne imager (source of the data: http://www.icare.univ-lille1.fr/parasol/?rubrique=mission_parasol)

as cloudy otherwise. Backpropagation can be implemented as the learning algorithm with a sufficiently small learning rate to avoid oscillation of the input weights of the perceptrons.

24.3 PARASOL/POLDER

The Polarization and Anisotropy of Reflectances for Atmospheric Sciences with Observations from a Lidar (PARASOL), or earlier the Polarization and Directionality of the Earth's Reflectances (POLDER), is a satellite-borne polarimetric imager (Deschamps et al. 1994; Fougnie et al. 2007). It provides wide field-of-view measurements of spectral, directional and polarized properties of the solar radiation reflected by the Earth or the atmosphere. The PARASOL/POLDER satellite is the third of its kind orbiting the Earth. PARASOL was designed and built by the French Centre national d'études spatiales (CNES). The satellite was launched on 2 December 2004 from Kourou, French Guiana. This third version was planned to deorbit during the autumn of 2013. The detector is sensitive in the visual and near infrared (VIS/NIR) spectral range. The resolution of the CCD detector is 274×242 pixels and has a telecentric optics with $\pm 43^\circ$ field-of-view along the track and $\pm 51^\circ$ field-of-view across the track. The instrument has an embedded rotating filter wheel mounted in the optical path. The filter wheel contains nine different spectral filters (Fig. 24.5). There are three spectral bands (443, 670 and 865 nm), where polarization measurements are possible. Polarimetric measurements are used, among others, to separate water clouds from ice clouds. This can be done by seeking for the rainbow backscattering of a water cloud. If a highly linearly polarized band at about 42° from the antisolar point is registered, it is caused by rainbow scattering of water droplets. If the band with high degrees of linear polarization is not perceivable, then the cloud contains ice crystals. For further details, see Chap. 2 of Horváth and Varjú (2004, pp. 15–17).

24.4 Ground-Based Polarimetric Cloud Detectors

24.4.1 One-Camera Polarimetric Cloud Detector with Rotating Filter Wheel

In 2004 two students (András Barta and Bence Suhai) of the Environmental Optics Laboratory of the Department of Biological Physics of the Eötvös University (Budapest, Hungary) founded the Estrato Research and Development Ltd. Since then it is the basis of an ongoing effort to utilize the results obtained during research projects conducted by the Environmental Optics Laboratory. The aim of the concept was to develop a fast full-sky cloud detection system based on the patterns of skylight polarization measured by 180° field-of-view imaging polarimetry. The primary outputs of the system are:

- The probability distribution of clouds (from which the cloud existence can be estimated at any celestial point)
- Detection of the cloud-base height on the whole sky dome

Using both primary outputs, we could derive different kinds of cloud-clustering algorithms to meet the requirements of the end user.

Light is a transversal electromagnetic wave that can be characterized by its wavelength (colour), intensity (brightness), direction (or angle) of linear polarization (direction of the oscillation plane of the wave's electric field vector perpendicular to the direction of propagation), degree of linear polarization (proportion of light with the major direction of linear polarization) and degree of circular polarization (proportion of light with left- or right-handed circulation of the electric field vector around the direction of propagation). The polarized skylight has a characteristic polarization pattern that depends on the position of the Sun, the albedo of the Earth's surface, the aerosol concentration in the air, the existence of clouds and the height of the cloud base. Skylight is predominantly linearly polarized (Können 1985; Coulson 1988). Its circularly polarized component is usually negligible and depends on the composition and concentration of atmospheric aerosols (Hannemann and Raschke 1974). The traditional photographic techniques can only be used for measuring the spectrum (intensity as a function of wavelength) of skylight. For the measurement of the celestial polarization pattern, a full-sky imaging polarimeter is required that is composed of a photographic camera equipped with appropriate (linear and optionally circular) polarization filters (Horváth et al. 2002).

The basis of our instrument (Fig. 24.6) is a wide (180°) field-of-view imaging polarimeter that can take pictures of the whole sky through 3 linearly and optionally 1 circularly polarizing filters. From these measured data, a computer program can calculate the intensity, direction of polarization, linear and optionally circular degrees of polarization of skylight in the red (650 nm), green (550 nm) and blue (450 nm) spectral ranges pixel by pixel of the full-sky image. An appropriate computer algorithm can detect the clouds with the use of these polarization patterns

Fig. 24.6 Full-Sky Imaging Polarimetric Cloud Detector (FSIPCD) developed by the Estrato Ltd tested in the expedition ANT-XXVII-1-2010 from Bremerhaven (Germany) through the Atlantic Ocean to Capetown (South Africa) onboard the research vessel Polarstern organized by the German Alfred Wegener Institute for Polar and Marine Research (Barta et al. 2014). Underneath the transparent dome, the fisheye lens and the arbitrarily adjustable solar occulter are visible

(two-dimensional distributions), because the clouds more or less modify the polarization pattern characteristic to the clear sky (Horváth et al. 2002; Chap. 7 of Horváth and Varjú 2004, pp. 41–46).

Using the measured celestial polarization patterns, another algorithm can enhance the intensity and colour contrasts of the colour picture of the sky by reducing the blurring effect of atmospheric scattering. The contrast of clouds relative to the clear sky regions is naturally reduced by the partially linearly polarized light scattered in the air layer between the observer (cloud detector) and the clouds that is added to the weakly polarized or unpolarized cloudlight. This disturbing partially polarized scattered light component can be subtracted from the skylight, resulting in a contrast-enhanced colour picture as if there were no scattering air layer ("haze") between the observer and the clouds.

The polarization data measured by full-sky imaging polarimetry can also be used to determine the relative heights of the cloud base (Fig. 24.8), because the deviation of the degree of linear polarization in a cloudy sky from that of a clear sky is proportional to the cloud-base height causing the reduced degree of linear polarization of skylight. The relative cloud-base heights combined with the contrast-

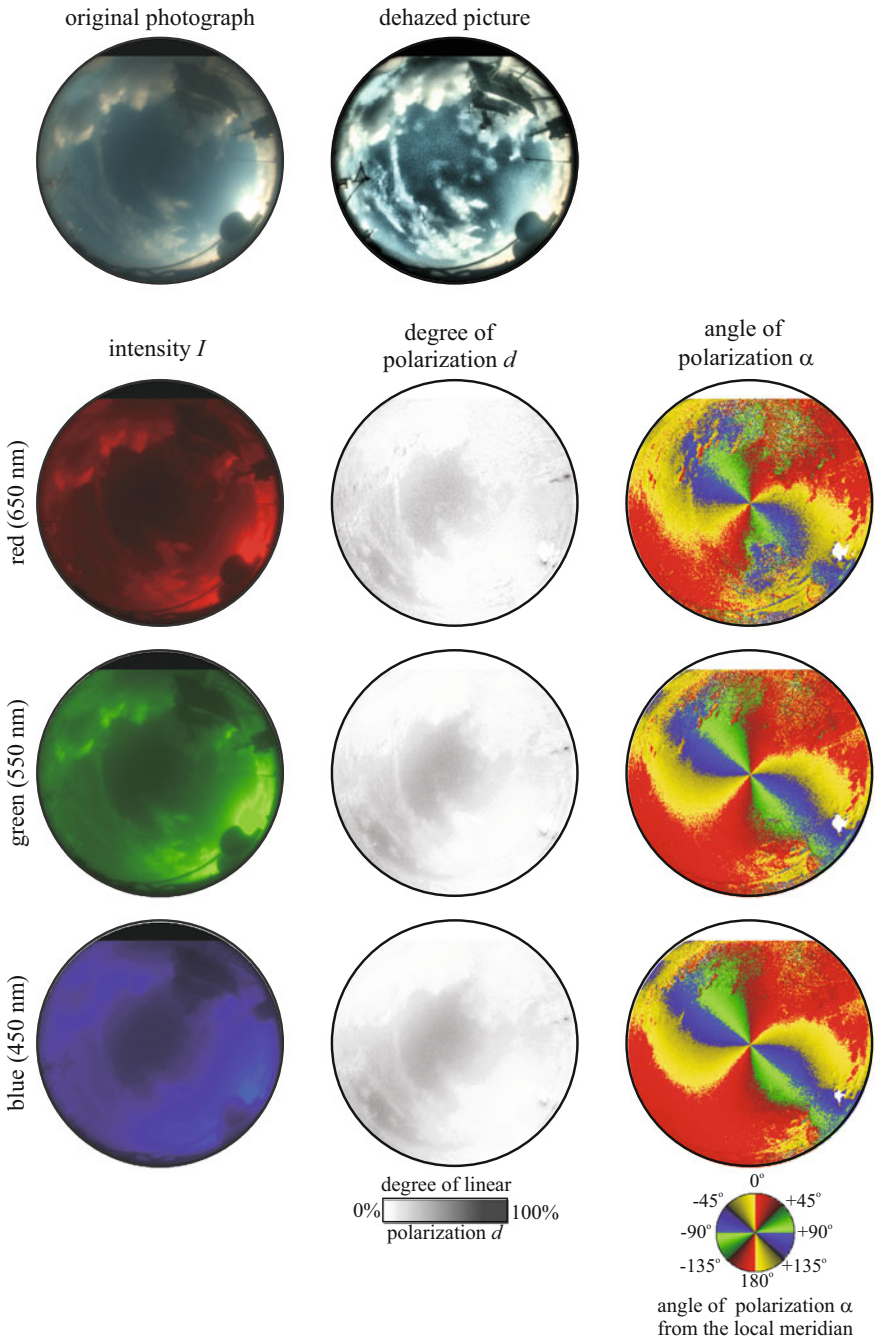

Fig. 24.7 A dehazed picture (row 1, right) of a partly cloudy sky (row 1, left) with higher colour contrasts. The dehazing algorithm is based on the intensity and polarization information (rows 2–4) in each pixel of the original photograph by assuming that haze in the air polarizes light due to scattering. Thus, the dehazed picture is practically the unpolarized part of the celestial scene

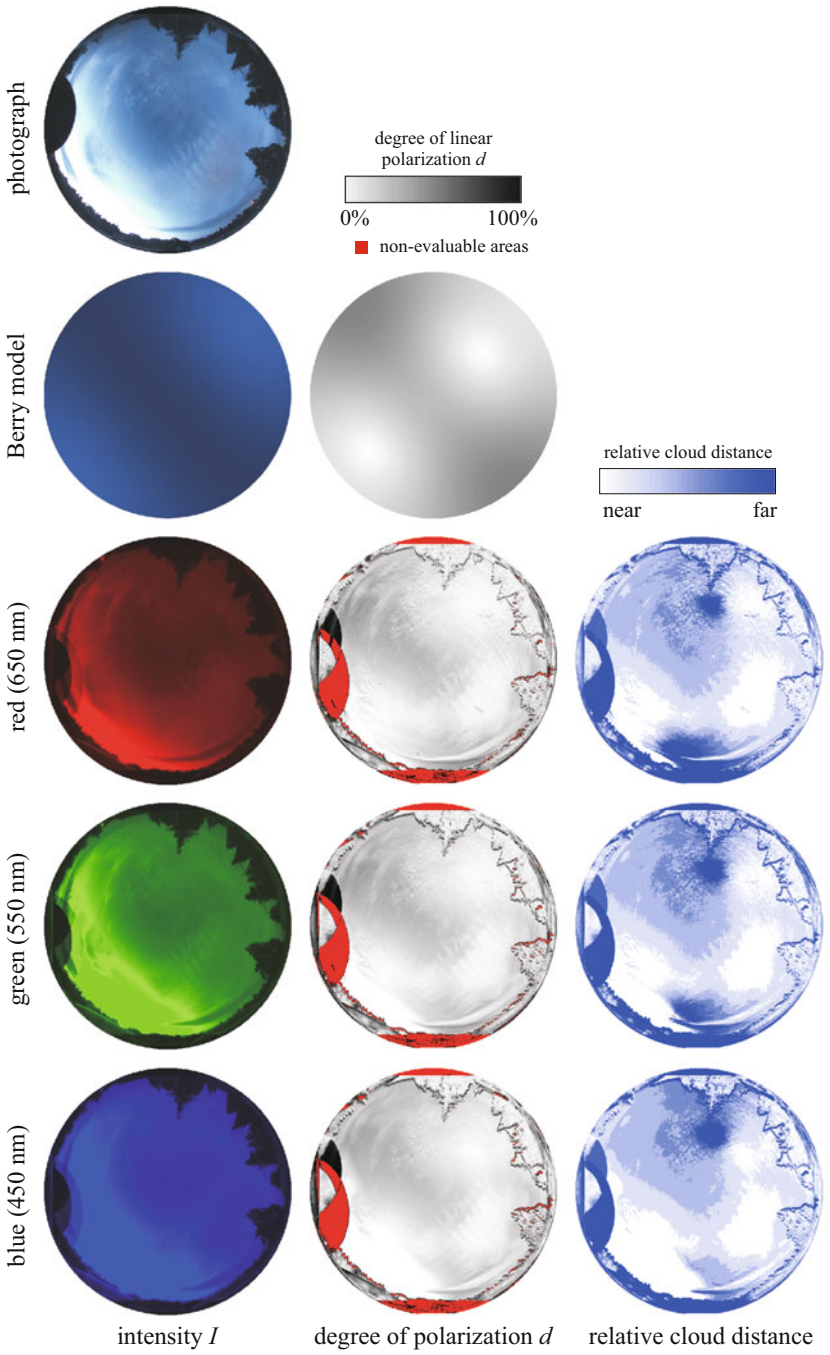

Fig. 24.8 Relative cloud-base distance pattern of a partly cloudy sky in the Gothard Observatory of the Eötvös University, Szombathely, Hungary (47° 15′ 27.594″ N, 16° 36′ 10.962″ E) on 4 July 2013 in 4:10 AM (UTC + 2 h). *Row 1*: Intensity pattern of the sky. The centre of the *circular image* corresponds to the zenith, while the perimeter is the horizon. *Row 2*: Berry model of the

enhanced "dehazed" colour images from two or more different cloud detectors can also be converted into a three-dimensional cloud scene.

Based on the patterns of cloud probability and cloud-base height, we can develop a cloud-clustering algorithm by which the type (cirrus, cumulus, etc.) of clouds can also be determined beyond the existence, size, shape, colour, texture and base height of clouds.

During our previous measurement campaigns in Budapest (Hungary) and the international ANT-XXVII-1-2010 expedition from Bremerhaven (Germany) through the Atlantic Ocean to Cape Town (South Africa) onboard the research vessel Polarstern organized by the German Alfred Wegener Institute for Polar and Marine Research, we showed that exploiting polarization information from skylight usually improves the accuracy of cloud detection (Barta et al. 2014). Note that cloud-base height measurements for the whole celestial hemisphere can be performed only by full-sky imaging polarimetry.

24.4.2 Three-Camera Polarimetric Cloud Detector

The three-camera cloud detector is a new version based on the one-camera model. The difference is that instead of using only one camera with an integrated rotating filter wheel to take the three linear polarization pictures required for linear polarimetry, the 3-camera model uses three distinct cameras each equipped with a fixed linearly polarizing filter with different transmission angles. The main advantage of the 3-camera model against the 1-camera model is that the three required linear polarization pictures can be taken at the same time, thus eliminating motion artefact introduced by the displacement of clouds during the rotation of the filter wheel in the 1-camera model.

24.5 Applications

24.5.1 Cloud Distribution

Currently, the cloud detectors available from the market are exclusively based on the measured intensity of skylight in different (usually red, green and blue) parts of the spectrum (Pust and Shaw 2008). This means that for a given direction in the sky, only the intensity of skylight is measured in the red, green and blue spectral ranges.

Fig. 24.8 (continued) intensity I and degree of linear polarization d of the clear sky with the same solar position as in the photograph. *Rows 3–5*: Patterns of the intensity I, degree of linear polarization d and calculated relative cloud-base distance in the red (650 nm), green (550 nm) and blue (450 nm) spectral ranges. The cloud base in a given celestial point is considered farther (*darker blue*) if the ratio of the measured and calculated d of a given point is closer to 1 and nearer (*lighter blue*) if that is closer to 0

Using these data, a simple algorithm calculates the colour of skylight coming from a given celestial direction. If the sky colour deviates from the white smaller than a threshold, the algorithm assumes that in the investigated celestial point a colourless cloud exists; otherwise the sky pixel is considered clear. One of the disadvantages of this method is that the sky regions around the Sun and anti-Sun as well as near the horizon are usually whitish, i.e. more or less colourless; thus, they may be detected as colourless clouds by an algorithm based exclusively on a colour picture of the sky. On the other hand, clouds illuminated by the red-orange rising or setting Sun are reddish; thus, they are not recognized as clouds by an algorithm looking for colourless celestial points. A similar problem occurs for high-altitude or far clouds, which are bluish due to the Rayleigh scattering (Suhai and Horváth 2004; Hannay 2007, 2009) in the air layer between the clouds and the observer (cloud detector). The chance of such misdetections can be decreased with the use of additional optical data, namely, the state of polarization of skylight, which can be measured by full-sky imaging polarimetry.

LIDAR is a laser-based RADAR equipment used to measure the cloud profile. It measures the backscattering of the emitted laser beam and derives the water content distribution along the direction of the laser beam. The disadvantage of this instrument for cloud detection is that it can measure the cloud profile only in one direction of the sky (usually in the zenith) at a given point of time. The so-called scanning LIDAR measures cloud profiles along a line or even in a small area of the sky. These measurements performed by periodical rotating/turning of the laser beam requires some time, during which the sky scene can change. Thus, clouds can be detected and cloud-base height can be measured by a LIDAR only in a very limited sky region.

A polarimetric cloud detector based on full-sky imaging polarimetry can detect clouds and can also measure the relative cloud-base height in numerous celestial directions, the number of which depends only on the spatial resolution of the digital camera used. By using four times more information (degrees of linear and circular polarization, direction of polarization and intensity in the red, green and blue spectral ranges) of skylight in a given celestial direction (relative to the traditional method using only the intensity of skylight in the red, green and blue parts of the spectrum), more accurate algorithms can be developed to detect clouds. The reliability of this approach is evident in comparison to the subjective cloud detection by human observers. The higher accuracy of a polarization-based cloud detection relative to the intensity- and colour-based traditional method has been shown experimentally (Barta et al. 2014).

24.5.2 Cloud-Base Height

Measuring the cloud-base height in numerous celestial directions (by scanning LIDAR) is a time-consuming procedure. With a polarization-based method, the distribution of the relative cloud-base height can be easily measured in the full sky

(Fig. 24.8). Although this method provides a lower vertical resolution relative to a LIDAR measurement, this resolution is high enough for cloud-clustering purposes. Using an absolute value of the cloud-base height measured by a LIDAR in a given celestial direction, the numerous relative cloud-base heights obtained by full-sky imaging polarimetry can also be converted to absolute values of the cloud-base height.

24.5.3 Solar Forecasting

Ultra-short-term weather forecasting is a special area of meteorology, in which very accurate and reliable short-term (0–4 h) predictions are needed for a limited geographical area. Such forecasts are used by airports, sports and other open-air events, but improvements in the accuracy and reliability of forecasts can open up new applications. For photovoltaic power plants and grids relying on solar energy sources, accurate forecast of photovoltaic output 0–4 h in advance could bring considerable benefits in terms of economic, environmental and operational costs. This output is largely determined by cloud coverage over the solar plant area. Hail suppression operations, addressing an extremely local and small-scale weather phenomenon, could also benefit from faster, more precise and better localized forecasts.

With the integration of high penetrations of renewable energy sources quickly becoming a reality for many utilities, and increases in rooftop and distribution solar energy systems, it is now being examined how to improve the accuracy of solar forecasting models. Accurate solar forecasts are essential for the power system operator to ensure grid reliability and also important for solar power plant owners to minimize deviations from bids made in the power market and reduce operating costs. The problem is, as clean as these forms of energy are, intermittency can make them difficult to rely on. Technology is being developed to pre-emptively alert energy providers of meteorological changes, allowing them to switch to alternate forms of energy during times of low output. This is a completely novel area, where operational practices, the adoption of consistent codes, standards and regulatory procedures are partial or non-existent. A novel device, the full-sky polarimetric cloud detector (Fig. 24.6), delivering fast, ultra-short-time cloud coverage forecast for a limited geographical area, has the potential to be a vital component of such services.

A polarimetric cloud detector constantly monitoring cloud coverage and cloud-base height distribution can make ultra-short-term forecasts of cloud development based on recent tendencies. Accurate solar forecasts delivered by the use of data provided by the polarimetric cloud detector systems are essential in the renewable energy sector.

24.5.4 Studying Animal Orientation and Viking Navigation

A polarimetric cloud detector (Fig. 24.6) is principally a full-sky imaging polarimeter. Apart from their above-mentioned meteorological applications, the celestial polarization patterns measured by this instrument in the visible spectrum (see Chap. 18) can also be used for pure scientific purposes, such as to study the orientation of polarization-sensitive animals by means of sky polarization [Pomozi et al. 2001; reviewed by Horváth and Varjú (2004)] as well as to investigate the sky-polarimetric navigation of Vikings (see Chap. 25).

24.5.5 Aerosol Characterization

Full-sky imaging polarimeters (which are the basis of polarimetric cloud detectors) can also be used to calculate aerosol characterization in the atmosphere. Kreuter and Blumthaler (2013) described a method, where the patterns of the Stokes parameters Q and U (or the degree of linear polarization) obtained from a full-sky imaging polarimetric measurement are decomposed to their Zernike polynomials and can be represented by the Zernike coefficients. The high-dimensional space of these representations can be transformed into a two-dimensional space obtained by principal component analysis based on model data, where the different types of aerosols (industrial, biomass burning, desert dust, oceanic) are distinguishable. The calculations based on realistic models of certain aerosol types proved to be robust against noise, aerosol optical depth, solar zenith angle and aerosol microphysical properties.

References

Barta A, Horváth G, Horváth Á, Egri Á, Blahó M, Barta P, Bumke K, Macke A (2014) Testing a polarimetric cloud imager aboard research vessel Polarstern: Comparison of ten different cloud detection algorithms. Appl Opt (in press)

Bumke K (2011) The expedition of the research vessel "polarstern" to the Antarctic in 2010 (ANT-XXVII/1). In: Bumke K (ed) Berichte zur Polar- und Meeresforschung (Reports on polar and marine research), vol 628. Alfred Wegener Institute for Polar and Marine Research, Bremerhaven, Germany, pp 1–82

Cazorla A, Olmo F, Alados-Arboledas L (2008) Development of a sky imager for cloud cover assessment. J Opt Soc Am A 25:29–39

Coulson KL (1988) Polarization and intensity of light in the atmosphere. A. Deepak Publishing, Hampton, VA

Deschamps PY, Bréon FM, Leroy M, Podaire A, Bricaud A, Buriez JC, Seze G (1994) The POLDER mission: instrument characteristics and scientific objectives. IEEE Trans Geosci Remote Sens 32:598–615

Estrato (Research and Development, Ltd) http://www.estrato.hu/

Fougnie B, Bracco G, Lafrance B, Ruffel C, Hagolle O, Tinel C (2007) PARASOL in-flight calibration and performance. Appl Opt 46:5435–5451
Gardner MW, Dorling SR (1998) Artificial neural networks (the multilayer perceptron)—a review of applications in the atmospheric sciences. Atmos Environ 32:2627–2636
Hannay JH (2007) Radiative transfer: exact Rayleigh scattering series and a formula for daylight. Proc R Soc A 463:2729–2751
Hannay JH (2009) Radiative transfer: exact Rayleigh scattering series and a daylight formula. J Opt Soc Am A 26:669–675
Hannemann D, Raschke E (1974) Measurements of the elliptical polarization of sky radiation: preliminary results. In: Gehrels T (ed) Planets, stars and nebulae studied with photopolarimetry. University of Arizona Press, Tucson, AZ, pp 510–513
Hegedüs R, Åkesson S, Horváth G (2007) Polarization patterns of thick clouds: overcast skies have distribution of the angle of polarization similar to that of clear skies. J Opt Soc Am A 24:2347–2356
Heinle A, Macke A, Srivastav A (2010) Automatic cloud classification of whole sky images. Atmos Meas Tech 3:557–567
Horváth G, Varjú D (2004) Polarized light in animal vision—polarization patterns in nature. Springer, Heidelberg
Horváth G, Barta A, Gál J, Suhai B, Haiman O (2002) Ground-based full-sky imaging polarimetry of rapidly changing skies and its use for polarimetric cloud detection. Appl Opt 41:543–559
Kalisch J, Macke A (2008) Estimation of the total cloud cover with high temporal resolution and parametrization of short-term fluctuations of sea surface insolation. Meteorol Z 17:603–611
Können GP (1985) Polarized light in nature. Cambridge University Press, Cambridge, UK
Kreuter A, Blumthaler M (2013) Feasibility of polarized all-sky imaging for aerosol characterization. Atmos Meas Tech 6:1845–1854
Li Q, Lu W, Yang J (2011) A hybrid thresholding algorithm for cloud detection on ground-based color images. J Atmos Ocean Technol 28:1286–1296
Long C, DeLuisi J (1998) Development of an automated hemispheric sky imager for cloud fraction retrievals. In: Proceedings of 10th symposium on meteorological observations and instrumentation, American Meteorological Society, Phoenix, AZ, January, 1998
Mantelli-Neto SL, von Wangenheim A, Pereira EB, Comunello E (2010) The use of Euclidean geometric distance on RGB color space for the classification of sky and cloud patterns. J Atmos Ocean Technol 27:1504–1517
Pfister G, McKenzie RL, Liley JB, Thomas A, Forgan BW, Long CN (2003) Cloud coverage based on all-sky imaging and its impact on surface solar irradiance. J Appl Meteorol 42:1421–1434
Pomozi I, Horváth G, Wehner R (2001) How the clear-sky angle of polarization pattern continues underneath clouds: full-sky measurements and implications for animal orientation. J Exp Biol 204:2933–2942
Pust NJ, Shaw JA (2008) Digital all-sky polarization imaging of partly cloudy skies. Appl Opt 47: H190–H198
Rumelhart DE, Hintont GE, Williams RJ (1986) Learning representations by back-propagating errors. Nature 323:533–536
Souza-Echer MP, Pereira EB, Bins LS, Andrade MAR (2006) A simple method for the assessment of the cloud cover state in high-latitude regions by a ground-based digital camera. J Atmos Ocean Technol 23:437–447
Suhai B, Horváth G (2004) How well does the Rayleigh model describe the E-vector distribution of skylight in clear and cloudy conditions? A full-sky polarimetric study. J Opt Soc Am A 21:1669–1676
WSI Handbook. https://www.wmo.int/pages/prog/gcos/documents/gruanmanuals/Z_instruments/wsi_handbook.pdf
Yankee Environmental Systems, Inc. http://www.yesinc.com

Chapter 25
Sky-Polarimetric Viking Navigation

Gábor Horváth, Alexandra Farkas, and Balázs Bernáth

Abstract It is a widely discussed and regularly cited theory that Viking navigators might have been able to locate the position of the sun occluded by clouds or below the horizon with a mysterious birefringent or dichroic crystal, the sunstone, on the basis of the pattern of skylight polarisation. In this chapter we describe the steps and the experimentally tested efficiency of this sky-polarimetric navigation method, and we show modern navigation instruments that operate in a similar principle. We investigate the atmospheric optical prerequisites of sky-polarimetric Viking navigation, looking for the ideal weather conditions, under which sunstones could be used for this navigational task. We also discuss other hypothesised Viking navigation instruments, like the horizon board and the sun compass or twilight board. Finally, we consider the Medieval Norse sailing routes and some alternative atmospheric optical navigation cues, which also could help during the long-time marine voyage of Viking seafarers.

25.1 Introduction

It is a frequently cited theory that Vikings—seafaring Norse people flourishing from the eighth to the twelfth century—might have been able to navigate by means of the polarisation pattern of the sky. The theory was first outlined by Ramskou (1969) as an analogy of a modern polarimetric navigational instrument (the Kollsman's polarised

G. Horváth (✉) • A. Farkas
Environmental Optics Laboratory, Department of Biological Physics, Physical Institute, Eotvos University, Pazmany setany 1, 1117, Budapest, Hungary
e-mail: gh@arago.elte.hu; kfarkasalexandra@gmail.com

B. Bernáth
Institute of Biology, University of Neuchatel, Rue Emile-Argand 11, CH-2000, Neuchatel, Switzerland
e-mail: bbernath@angel.elte.hu

G. Horváth (ed.), *Polarized Light and Polarization Vision in Animal Sciences*, Springer Series in Vision Research 2, DOI 10.1007/978-3-642-54718-8_25,

skylight compass, type no. 2029B-01) used through the preceding decades on airplanes flying above the North Pole. The alleged medieval tools for it are the mysterious 'sunstones', but their role in the Viking navigation discipline is rather a disputed theory than a proven fact. The sole written source founding the theory is a scene in the Rauðúlfs þáttur, that is, a saga on Olaf II Haraldsson (995–29 July 1030), also known as King Olaf, the Holy. A Viking named Sigurður claims that he is '*able to discern the motion of heavenly bodies, those which he sees, and to know the stars which mark the hours, so that he will know time length at day and night although he does not see the celestial bodies, and still he knows how to discern all hours both day and night*'. Later on he is tried by King Olaf: '*The king made people look out and they could nowhere see a clear sky. Then he asked Sigurður to tell where the sun was at that time. He gave a clear assertion. Then the king made them fetch the solar stone and held it up and saw where light radiated from the stone and thus directly verified Sigurður's prediction*' (Vilhjalmsson 1997). Although interpreting this scene as a poetic description of a medieval polarimetric navigation procedure was inspired by reliable modern navigation methods, and later on we cite dedicated field experiments proving the functionality of such methods, evidences for its actual use during the Viking era are scarce.

Roslund and Beckman (1994) emphasised the lack of evidence for the hypothesis that Viking navigators used skylight polarisation. They also treated the usefulness of skylight polarisation for orientation with pronounced scepticism. One of their qualitative counter-arguments was the assumption that solar positions or solar azimuth directions could be estimated quite accurately by the naked eye, even if the sun is behind clouds or below the sea horizon. Barta et al. (2005) tested quantitatively the validity of this qualitative counter-argument. Their data, obtained in psychophysical laboratory experiments, did not support the common belief that the invisible sun can be located quite accurately from the celestial brightness and/or colour patterns under partly cloudy or twilight conditions. Thus, the mentioned counter-argument of Roslund and Beckman (1994) cannot be taken as a valid criticism of the hypothesis of sky-polarimetric Viking navigation.

Neither a description of the nature of sunstones nor that of the use of sunstones is known from contemporary sources; only their high value is marked by their mentioning in treasure inventories. Ramskou (1969) hypothesised that sunstones might have been dichroic or birefringent crystals used to analyse the direction of polarisation of skylight, a long forgotten and then reinvented solar navigation method. The sole archaeological artefact supporting his theory is a calcite crystal, which was found decades later at Alderney between navigational tools in the wreck of a sixteenth-century Elizabethan ship that carried a great load of iron weaponry (Bound and Monaghan 2001; Le Floch et al. 2013). While it is tempting to associate this crystal with navigation tasks, it cannot be known whether it served as an optical compass used to calibrate the hardly trusted magnetic compass or simply was a precious cargo item secured on the quarterdeck. Until now archaeological surveys produced no such sunstones at any known Viking localities. But calcite is a quite soft and fragile mineral that does not resist heat. Thus, if it was the material of sunstones, original pieces could hardly survive Viking cremation ceremonies and mechanical weathering of millennia on the sea floor (Le Floch et al. 2013).

The Viking sunstones are frequently mentioned as the first artificial counterparts of the polarisation compass of polarisation-sensitive animals. In the last decade, several field tests and theoretical studies pointed out that sunstones surely could not guide Viking navigators under overcast skies. But, they could have been used for appointing the sun below the horizon more precisely and reliably than most atmospheric optical phenomena. According to the newest interpretation of a tenth-century artefact Viking compass dial, this information could have been used to derive true direction, which hardly can be overvalued during the long and bright Nordic twilights. Sunstones were not magic items providing their users with 'polarisation vision' in any case. Today we think of them as a key element of a hypothesised forerunner of modern twilight compasses, a possibly forgotten fascinating technical achievement that was reinvented only in the middle of the twentieth century.

25.2 Modern Sky-Polarimetric Navigation

The polarisation pattern of the sky was already discovered and studied in the eighteenth century, and it was utilised by meteorologists long before it entered into modern navigation (Können 1985; Coulson 1988). But after World War II, when trans-Arctic shortcut flight routes gained strategic and economic importance, sky-polarimetric navigation instruments proved to be an asset. The Scandinavian Airlines prepared charter flights even over the Antarctic from Australia to South America to serve the 1956 Summer Olympics in Melbourne. Difficulties of large-scale Arctic operations, which were parts of military doctrines during the starting Cold War era, were experienced during the Operation High Jump of US Navy in 1947 in Antarctica. In the unkindly and uncharted polar territories, the magnetic compass is quite unreliable due to the great magnetic deviations. Gyrocompasses were not sufficiently precise to use on long polar routes before 1952 (Pedersen 1955). Stars near the celestial poles that normally guide sailors are seen inconveniently close to the zenith and are outshone by the midnight sun during the polar summer. The sun compass was a good old alternative to use. This instrument allows the navigator to derive true directions from the cast shadow of gnomons and pre-drawn hyperbolic gnomonic lines. Its versions were standard equipments of long-range aircrafts and even of desert forces in World War II and later on. It functioned also over the polar circles, but the long shadows caused by ever-low solar elevation angles and the non-hyperbolic form of gnomonic lines rendered it less practical.

A reliable Arctic navigation method was developed at Johns Hopkins University by A.H. Pfund and adopted by the US National Bureau of Standards in 1948. It was the skylight compass, an instrument used for appointing the solar meridian, even if the sun was under the horizon. As a rule of thumb, skylight has a linear polarisation perpendicular to the plane of scattering, which is the plane defined by the sun, the observer and the observed celestial point. The degree of polarisation of skylight is

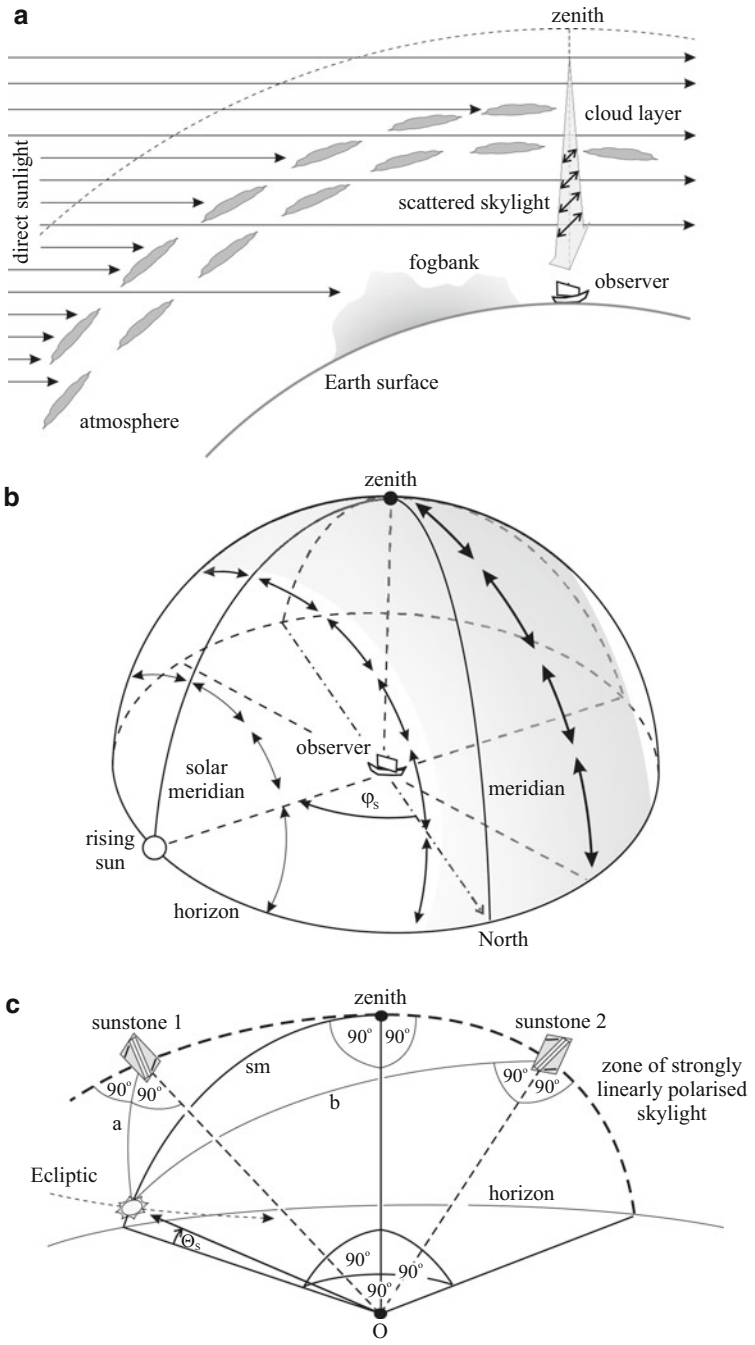

Fig. 25.1 (**a**) The setting or rising sun may be obscured from surface observers by nearby fogbanks, but even thin distant clouds may obscure it due to the curvature of the Earth surface. However, partially linearly polarised skylight produced by scattering in the high atmosphere will reach the observer on the surface, unless thick cloud layers are present. (**b**) Skylight is produced by

highest at 90° away from the sun (see Chap. 18). Thus, at low solar elevations skylight is highly polarised in the vicinity of the zenith, and its direction of polarisation, which can easily be identified by a linear polariser, is perpendicular to the solar meridian (Fig. 25.1). If appropriate astronomical tables are available, this information may be converted into true directions. Very soon, biological analogies of the skylight compass were discovered in the honeybee (*Apis mellifera*) and then in several other animals (von Frisch 1949; Horváth and Varjú 2004; see Part I). Advanced versions of the skylight compass were used for decades on board of military and civil aircrafts over Arctic regions (Kollsman Instruments 1960).

25.3 Medieval Norse Sailing Routes

The Viking age traditionally refers to the period from ca. 800 to 1100, when Scandinavian-origin people, primarily from territories of modern-day Sweden, Denmark and Norway, left their homes and travelled far to plunder, but also to settle and trade in new areas. They sailed westward through the unknown seas and colonised the North Atlantic islands. They settled on Iceland and Greenland and set up permanent bases and trade outpost on the eastern shores of North America (Arneborg 2000; Pringle 2012).

Obviously, Norse mariners roaming the vast waters of the North Atlantic Ocean had to come up with their own solutions for the problems of Arctic navigation. The magnetic compass was not introduced into Europe until the thirteenth century, so they could rely only on characteristic landmarks, marine currents and swells, sighting marine animals (whales and sea birds), bright stars, atmospheric optical phenomena and the sun. Today it is accepted by the scientific community that principles of the ancient astronomy were not available in North Europe during the Viking age, but primitive sun compasses (stone direction finders) were used long before.

In the Norse literature, several sailing directions are preserved (Fig. 25.2). Coastal navigation was preferred, but Vikings also were able to cross open seas. Their favoured method was latitude sailing, which means sailing directly to west or to east along latitudes marked by prominent settlements or coastal landmarks.

Fig. 25.1 (continued) the Rayleigh scattering of direct sunlight on air particles forming a characteristic linear polarisation pattern being mirror symmetrical to the solar and antisolar meridians. This feature allows sky-polarimetric navigation. (**c**) The position of the sun can be estimated using two linear polarisers or two calcite crystals (sunstones). At low solar elevation angles, the degree of linear polarisation of skylight is the highest in a zone (*thick dashed line*) passing perpendicular to the solar meridian (sm) at 90° from the sun across the zenith. The direction of polarisation is normal to the plane of scattering defined by the observed celestial point, the sun and the observer *O*. Two sunstones can be used to determine the direction of skylight polarisation and marking out the great circles *a* and *b* lying in the plane of scattering. The intersection of *a* and *b* estimates the position of the sun [after Bernáth et al. (2014)]

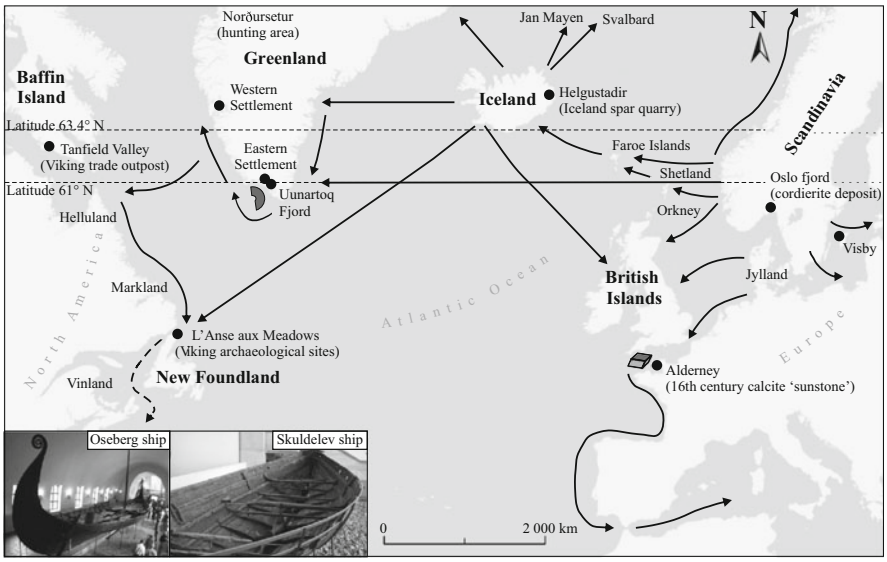

Fig. 25.2 The main Viking sailing routes and archaeological sites. Localities where the artefacts supporting the sky-polarimetric Viking navigation theory were found are separated both by great distances and long time [after Thirslund (2001)]

Vikings did not have magnetic compass; however, they divided the horizon to eight named sections forming the 'attir' system, a primitive analogue of modern compass points. It served as an independent reference to record bearings, but it was also used for coding azimuths of celestial bodies to provide directional and temporal references. Prominent stars, first of all the Pole Star was used as a nightly navigation cue, although it was located 6° 14′ off the celestial pole during the Viking era. The navigation season covered the summer months characterised by almost perpetual daylight on northern latitudes; thus, solar navigation was important as well. The Sagas and the Grágás record at last seven main sailing routes of exceptional socio-economic relevance between the latitudes of South Ireland and Svalbard (Fig. 25.2). Even the southern tip of Greenland was connected to Norway by merchant ships sailing more than 2,500 km (1,350 nautical miles) along the 61st latitude (Ramskou 1969; Thirslund 1997, 2001; Karlsen 2003).

25.4 Climatic Conditions in the Viking Era

Theories on the use of sunstones with solar navigation tools outline various and sometimes quite short sailing seasons; thus, it is important to recognise that Viking-age navigators had to face other sea conditions than that of our time. The spread of Norse people and the establishment of their colonies have been taken as a proof that the Viking-age climate of this region was probably similar to the warmest years of

the twentieth century (Hughes and Diaz 1994; Bradley et al. 2003). This so-called Medieval Warm Epoch (from the period 650–880 until 1030–1220) was first described by Lamb (1965), who based his argument mainly on historical anecdotes. In addition, many palaeoclimatological measurements have been carried out; nonetheless, well-calibrated temperature and sea ice data sets with decadal or higher resolution are still only available for a few locations. Both types of evidence suggest a low sea ice interval with prevailing warmer water and a climate in the North Atlantic region, which created favourable conditions for sailing and trading. The settlers, who travelled from Iceland to Greenland in the late tenth century, probably first travelled west from Iceland, then south along the Greenland coast (Fig. 25.2). This route runs across the Denmark Strait, which is known for high variability in sea ice extent. The presence of ice could be a potential hazard to travellers and traders, but during the Medieval Warm Epoch, sea ice possibility would less adversely affect sailing in this area (Ogilvie et al. 2000; Miller et al. 2010; Ribeiro et al. 2012).

After the Medieval Warm Epoch, a cold period began around 1270. A transition from less to more sea ice had been a major threshold shift with serious implications for both marine organisms and the North Atlantic Norse society. The earliest detailed account of sea ice is found in 'The Kings' Mirror' composed in Norway most probably around 1250. The unknown author clearly had first-hand information from someone familiar with Norse Greenland and the surrounding seas, but it is unclear that this is perceived as a new or a persistent threat to navigation (Larson 1917). A geographical description from ca. 1350 also contains notes on the presence of much sea ice along the Icelandic coasts. A description of Greenland originating about 1360 included that the old route from Iceland to Greenland has become difficult due to the presence of sea ice (which is also an indirect indication of the more favourable sailing conditions during the Medieval Warm Epoch). There is some further evidence from Iceland that the latter part of the thirteenth century experienced a relatively harsh climate (Ogilvie et al. 2009).

The increase of sea ice disrupted fisheries, and the ice coverage of fjords blocked landing stages and cut off communities for a long time. Moreover, the colder climate hindered cultivation. The most immediate impacts of the onset of regular summer drift ice adjacent to the eastern settlement area would have been on the maritime components of the Norse economy, local and international seafaring and maritime subsistence activities. The multiple problems and hazards imposed on small boat traffic in increasingly ice-filled waters would also have impacted the long-distance voyaging to the Norðursetur hunting grounds (Fig. 25.2) and prevented the hunting activities. The dramatic climate changes in the fourteenth century were extremely serious for a society living as precariously as did the Greenlanders; the abnormally cold summers finally triggered the abandonment of Norse settlements (Grove 2001; Ogilvie et al. 2009).

Contemporary written sources should be interpreted with great caution when it comes to exact dates and climate. Most written sources regarding the Viking age origin from later times; even the known forms of the Sagas were written down only in the thirteenth century and might have been updated in accordance with the cooling climate and decay of mercantile activities in the region (Larson 1917;

Arneborg 2000). Another possible source of discrepancies was the asynchronous calendar systems (primarily Julian and old Nordic) referred in the original narratives (Vilhjalmsson 1997). Reconciling calendars, astronomical constellations and the possible climatic background is a most complicated task that can hardly be solved without the tools of astronomy.

25.5 The Presumed Nature of the Legendary Sunstone

The operation of the sunstone is described only in the Saga of King Olaf, and it hardly can be identified with any known physical phenomenon. The King holds up the sunstone to see where light radiates from it and to verify the presumed position of the sun, but no known material would gleam just from holding it towards the occluded sun. Ramskou (1969) suggested that this is the description of a crude sky-polarimetric method applying a chiselled crystal, e.g. dichroic cordierite, or tourmaline. Such crystals can be used as rough linear polarisers. Although they are not common, naturally polished transparent cordierite pebbles occur on the shore of the Oslo Fjord, for example.

By rotating such a crystal to and fro and looking at the sky through it, the sky appears to brighten and fade periodically, because, with the exception of the principal neutral points (Horváth et al. 2002), the skylight is partially linearly polarised. Looking through the crystal, the Viking navigator could calibrate the sunstone by adjusting it in such a way that a patch of the clear sky appears brightest or darkest. A line pointing to the true position of the sun would then be scraped into the crystal. After such a calibration, the direction of the sun hidden by clouds can be determined by looking at a clear patch of sky through the crystal and rotating it until the sky appears the brightest or darkest. The scratch on the sunstone shows the direction of the invisible sun with an accuracy of about 5° (Ramskou 1969), if the direction of polarisation of skylight corresponds to the Rayleigh theory of first-order light scattering, i.e. the direction of polarisation of light from an arbitrary point of the clear sky is perpendicular to the plane of scattering determined by the observer, the sun and the celestial point observed (Suhai and Horváth 2004; see Sect. 18.1). Such a scratch or an equivalent marking would also unquestionably identify an excavated crystal as a sunstone.

However, it is more plausible that sunstones were pieces of Icelandic spar (Fig. 25.3), which is a transparent birefringent variety of calcite occurring in raw form in eastern Iceland (Karlsen 2003; Horváth et al. 2011; Ropars et al. 2012). Such a crystal was found in a sixteenth-century shipwreck at Alderney (Fig. 25.2) (Le Floch et al. 2013). If a small dark dot is put on the crystal, ordinary and extraordinary rays will form two images of it on the opposing face. Since the rays are totally linearly polarised and their directions of polarisation are perpendicular to each other, the brightness of the images will depend on the direction and degree of polarisation of incident skylight. The crystal can be rotated to reach equal brightness of the images. At this arrangement that is called ‘isotropy point’, the direction of

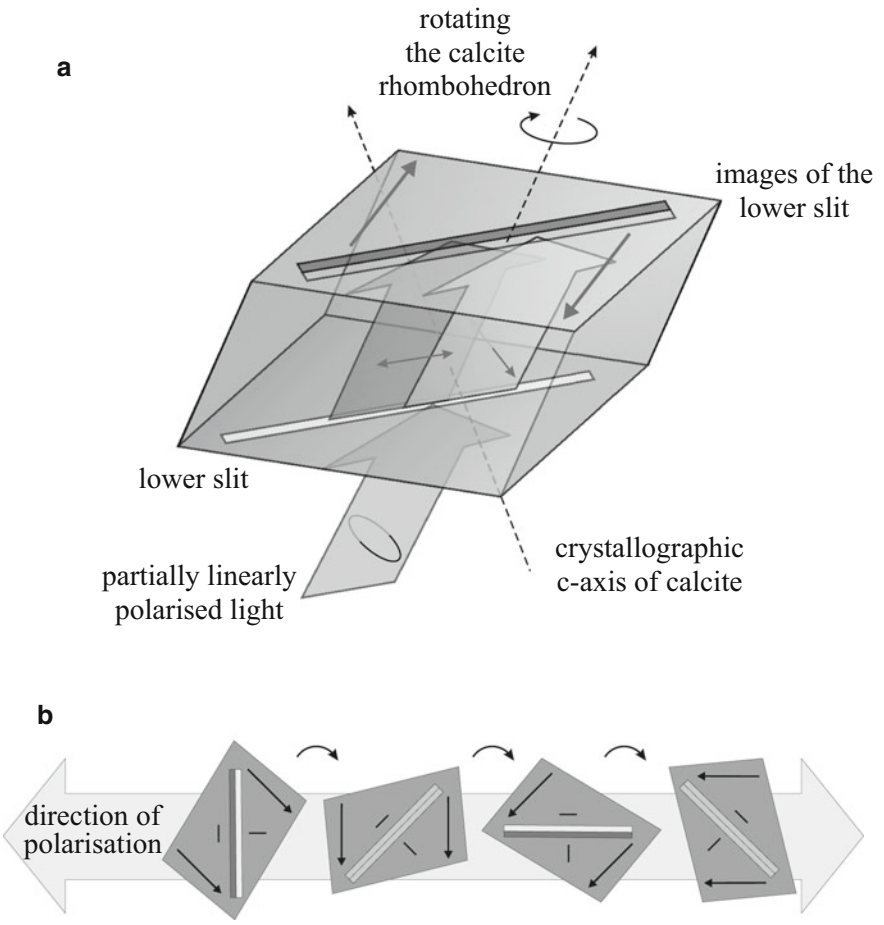

Fig. 25.3 (**a**) A calcite rhombohedron can be used to measure the direction of polarisation of transmitted skylight. All faces of the crystal are covered, and only two narrow slits perpendicular to the crystallographic *c*-axis of the calcite remain open. Partially linearly polarised skylight entering the lower slit is separated into totally linearly polarised ordinary and extraordinary rays, and two images of the lower slit are formed in the exit face. (**b**) The brightness of the slit images are equal, if the axis of the slit encloses 45° with the direction of polarisation of incident skylight. One specific slit image is the *brightest*, while the other image is the *darkest* when the slit is parallel to the direction of polarisation of incident skylight. The brightness ratio of the slit images is transposed when the rhombohedron is rotated by 90°. Should the degree of polarisation of incident skylight be high enough, could the direction of polarisation be unambiguously identified with rotating the rhombohedron [after Bernáth et al. (2013b)]

polarisation of both the ordinary and the extraordinary rays closes 45° with that of the incident light. Since the human eye is highly sensitive to intensity contrast (Hubel 1988), the direction of polarisation of skylight can be measured with such

prepared calcite crystals with an accuracy of 1°, provided the degree of polarisation is high enough (Karlsen 2003; Ropars et al. 2012).

To gain images that are larger and easier to perceive, the crystal should be covered in such a way that only slits perpendicular to the crystallographic *c*-axis of the calcite are left clear on the two greatest faces (Fig. 25.3) (Bernáth et al. 2013b, 2014). Ordinary and extraordinary rays diverting apart while crossing the crystal form two parallel images of the entrance slit on the exit face. Slit images are equally bright when the axis of the entrance slit encloses 45° with the direction of polarisation of entering light.

But irrespective of the material composition of his sunstone, the movements of King Olaf, as described in the Rauðúlfs þáttur, are clearly inappropriate for sky-polarimetric navigation, seemingly the scene cannot refer to such a measurement at all. If one intends to estimate the position of the obscured sun, he should measure the angle of polarisation in sky regions away from it (Fig. 25.1c). Two measurements would provide two celestial great circles, the intersections of which are the position of the sun and anti-sun. Then, one may convert this data into true directions with a sun compass, for example, but nothing like that is mentioned in the Saga. In modern sky-polarimetric navigation, the azimuth angle of the sun is used; true directions are looked up in astronomical charts on the basis of known time and appropriate position. The first known Nordic astronomical chart appropriate for such a conversion is part of the Icelandic book Oddatala originating from the twelfth century, the end of the Viking age (Roslund 1989).

However, King Olaf only intends to verify the position of the sun appointed by Sigurður, and the sunstone scene shows a perfectly logical way of it: measuring the degree of polarisation of skylight. A polariser or a sunstone would transmit unpolarised light with a constant intensity irrespective of its rotation; thus, it would not darken if rotated in front of unpolarised or very weakly polarised points in the sky. This is characteristic of only the principal neutral polarisation points located right above and below the sun and anti-sun (Können 1985; Horváth et al. 2002). Unpolarised light emanates from the Babinet and Brewster neutral points (approximately, 20° above and below the sun, respectively), or from the Arago neutral point (about 20° above the anti-sun), and the direct sunlight is also unpolarised. Low degrees of polarisation are characteristic for the regions around the sun and anti-sun including these neutral points.

Should Sigurður be right, would King Olaf hold his sunstone towards the sun disc or a nearby neutral point? His sunstone would be transilluminated by unpolarised skylight; thus, it would gleam continuously when rotated. But should the stone blink, the bragging Viking would be confuted and ashamed instantly. A wise and dramatic way of probing the boaster, worth to be sung of! It is worth to note that the continuous gleam of the stone could easily be associated with the gleam of the sun itself by an untrained observer or an inspired poet. Such a quick test could be logical for someone knowing and practising sky-polarimetric navigation; in fact, it could be a perfect way of verifying the estimated position of the sun after a routine measurement. But not under all weather conditions could this method function with birefringent or dichroic crystals. Would have it been a reliable test or

would measurement errors give to Sigurður a fat chance to get away with a bold guess? The only clue the Saga gives us is that *they could nowhere see a clear sky* at that time.

25.6 The Possibility of Sky-Polarimetric Navigation by Vikings Under Various Weather Conditions

The sky-polarimetric Viking navigation method can be used only if two atmospheric optical prerequisites are satisfied: (1) the direction of polarisation of skylight must follow the predictions of Rayleigh theory, and (2) the degree of linear polarisation of skylight must be high enough to produce perceivable periodic brightening and darkening of the sky when seen through a rotating sunstone, and the direction of skylight polarisation can be determined with a sufficient accuracy (Horváth et al. 2011). Early attempts to determine whether skylight polarisation obeyed Rayleigh theory were limited to a few directions of the sky owing to the usage of point-source polarimeters (Brines and Gould 1982). Pomozi et al. (2001) and Suhai and Horváth (2004) measured directions of polarisation of skylight for the whole celestial hemisphere under clear and partly cloudy conditions with full-sky imaging polarimetry, computed their differences from theoretical values and determined which parts of the sky followed Rayleigh theory with an accuracy of 5° threshold for both clear and cloudy celestial regions (see Sect. 18.2). They concluded that at a given solar elevation, the proportion of the sky that is usable for sky-polarimetric Viking navigation is always higher for a clear sky (13–70 %) than for a partly cloudy sky (4–69 %). Multiple scattering of the light in clouds can result in directions of polarisation of cloudlight different from those of the Rayleigh sky based on first-order scattering (Roslund and Beckman 1994; Horváth et al. 2011). If the sun is near or on the horizon, then almost equally large proportions of partly cloudy skies are suitable for sky-polarimetric Viking navigation as those of the clear sky. The lower the solar elevation, the higher the ratio of the sky that is appropriate for this navigation method both under clear and partly cloudy skies, which justify the use of sunstones with twilight boards and horizon boards (Bernáth et al. 2014; see Sect. 25.7.3). Sometimes the direction of polarisation of skylight follows Rayleigh theory in relatively large cloudy regions of the sky (12–34 %), and these areas increase with the decrease of solar elevation (Pomozi et al. 2001; Suhai and Horváth 2004). The sky regions near the sun and the neutral points are inadequate for sky-polarimetric navigation in most cases, because their polarisation pattern considerably differs from the Rayleigh pattern and their degrees of polarisation are too low (Horváth et al. 2002).

According to Horváth et al. (2011), usually large parts of the clear and partly cloudy skies follow Rayleigh theory quite accurately. But Vikings sailing the North Atlantic must often have encountered poor visibility with fog so dense that even the sun's disc would have been invisible to them (Roslund and Beckman 1994),

particularly with the sun near the horizon. According to Hegedüs et al. (2007a), the pattern of the direction of polarisation of foggy skies (when the fog is lit from above by direct sunlight, but the sun is absolutely indiscernible) is quite similar to that of the clear sky. Thus, the above-mentioned first condition of sky-polarimetric navigation is met for foggy situations nearly as well as for clear skies. However, the degrees of polarisation of foggy skies are often very low (4–15 %) (Hegedüs et al. 2007a). Therefore, in this case the limiting factor of the sky-polarimetric navigation method is the low degree of sky polarisation (Horváth et al. 2011; see Sect. 18.3).

Vikings probably often sailed also under completely overcast skies, so we must briefly consider the polarisation characteristics of light under this meteorological condition. According to Hegedüs et al. (2007b), the patterns of the direction of polarisation under totally overcast skies are also very similar to those of clear skies (see Sect. 18.4). Thus, the first prerequisite of sky-polarimetric Viking navigation mentioned above is also met under overcast skies. But again, the degrees of polarisation of overcast skies are so low (3–8 %) (Hegedüs et al. 2007b) that it is very unlikely that Viking navigators were able to use this sky-polarimetric method for navigation under overcast conditions (Roslund and Beckman 1994). Horváth et al. (2011) proposed that under overcast conditions, the direction of skylight polarisation could be determined only very inaccurately. Field tests with calcite sunstones justified this prediction (Bernáth et al. 2013b; see Sect. 25.7.2).

25.7 Hypothesised Viking Solar Navigation Instruments and Sunstones

Sources on Viking culture offer only a few clues about marine navigation. Today it is accepted by the scientific community that Vikings used primitive solar navigation instruments. Written sources and archaeological artefacts inspired the ideas of the horizon board (Karlsen 2003) and Viking sun compass (Thirslund 2001), instruments looking similar, but being fundamentally different. A combination of them called twilight board was suggested recently by Bernáth et al. (2014). They also raised the possibility that Vikings rather used a sophisticated sun-shadow board providing data on current latitude and not directions (Bernáth et al. 2013a). Some of these instruments could have been used with sunstones, others not.

25.7.1 The Horizon Board

The horizon board is a primitive but effective tool (Fig. 25.4a) suggested by Karlsen (2003) for interpreting directional references of the Grágás, the old Icelandic law book. It consists of a flat board wearing marks that represent characteristic

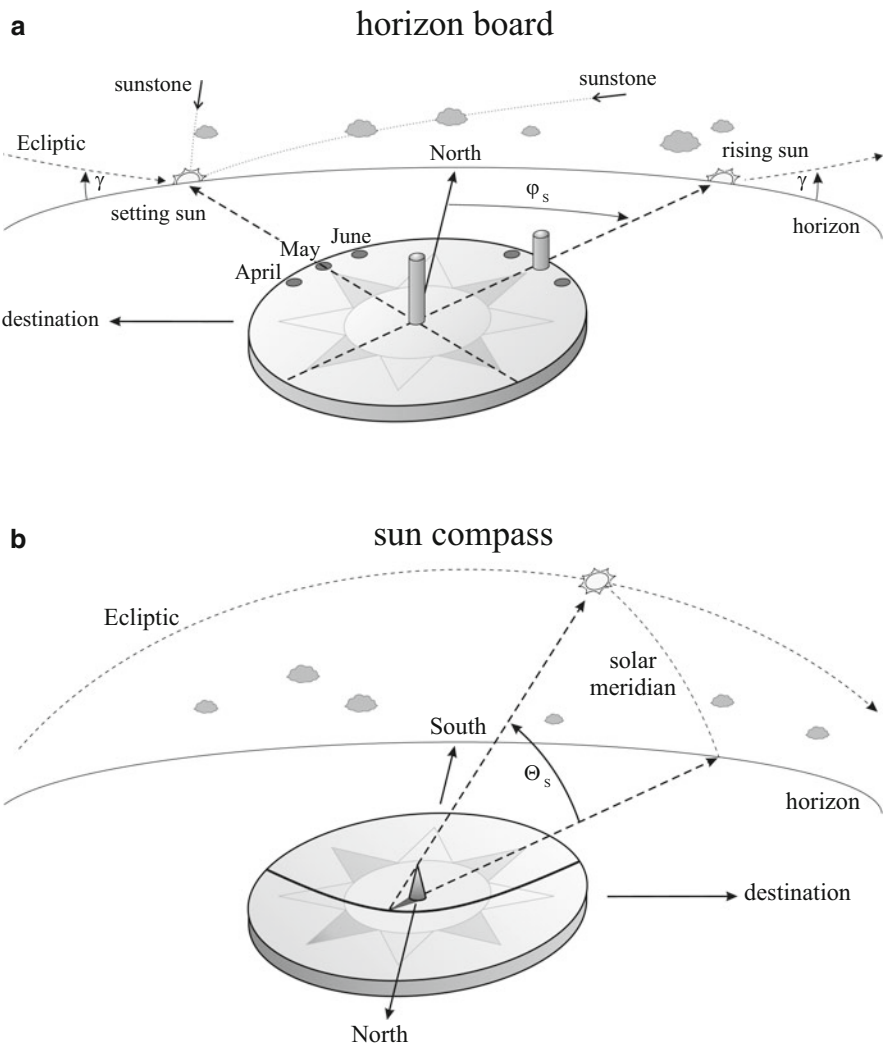

Fig. 25.4 (**a**) A horizon board wears holes on its perimeter coding the azimuth angles φ_S of the rising and setting sun at a given latitude. Shift of the rising and setting sun during the whole navigation season can be followed by choosing appropriate holes along the perimeter. Pecks inserted into the holes help reading bearings. The navigator can derive true directions at sunrise and sunset by aiming the sun with the central and the peripheral pecks and also at noon by recording the direction of the shortest shadow. Seasonal change of φ_S can be followed by using different holes. The accuracy of orientation is limited by exact timing of readings that is difficult at northern latitudes due to the small angle γ enclosed by the path of the sun and the horizon. (**b**) A sun compass wears a thin and high central gnomon and one or more matching gnomonic lines. During the day the navigator can derive true directions by fitting the tip of the shadow to the gnomonic line. At low solar elevation angles θ_S, the shadow tip falls off the horizontal circular board; thus, orientation is not possible [after Bernáth et al. (2014)]

directions according to the attir system, a central hole and a series of holes on the perimeter coding seasonal azimuth angles φ_S of the rising and setting sun at the latitude chosen for crossing the sea. The seasonal shift of the rising and setting sun during the whole navigation season can be followed by choosing appropriate holes along the perimeter. Pecks inserted into the holes help reading bearings. True directions can be read on a horizon board three times a day: (1) at sunrise and (2) sunset by aiming at the sun with the central and the peripheral pecks and (3) possibly at noon, if the direction of the shortest shadow of the central peck can be recorded. Considering the average cruising speed of mere 6 knots (11 km/h) of Viking ships, such rare reading of direction is not a serious hindrance. Navigators could maintain course for several hours steering by wind, waves and cast shadows of ship parts until a correction could be made (Lewis 1972; Severin 1978). However, accurate orientation is essential, especially if reference bearings are rarely available and no fix on location can be achieved.

Using a horizon board requires performing readings in the very moments of sunrise, noon and/or sunset. Reading a false solar azimuth due to missing the right moment transforms directly to a navigation error. Appointing the moment of sunrise, sunset and noon without a chronometer and nautical tables is not trivial at northern latitudes. People of temperate and tropical countries are accustomed to rapid sunsets, but in sub-Arctic regions the rising and setting sun seems to roll along the horizon. On the day of the summer solstice at the 61st latitude, the sun disc subtending an arc of mere 0.52° needs 10 min to cross the horizon, while its azimuth angle changes by 2°. In clear weather navigators may follow a convention like modern astronomers and define sunset or sunrise by the moment when the upper limb of the sun disc seems to touch the horizon. But, when the setting or rising sun is obscured by fogbanks lying over the sea surface or by distant cloud layers seen behind the horizon, the time of sunset and sunrise can be identified with a significant bias (Fig. 25.1a).

Karlsen (2003) suggested that calcite sunstones could be used under such circumstances for deriving the solar meridian from the polarised skylight emanating from around the clear zenith (Figs. 25.1 and 25.3). But neither this specific technique nor other polarimetric methods involving sunstones could provide the exact value of the solar elevation angle. In field tests calcite sunstones allowed assessing the solar elevation with a bias of 9° and with a clear tendency of overestimation in the period of sunset and civil twilight in the equinoctial period (Bernáth et al. 2013b, 2014). This means that the azimuth angle of the obscured setting and rising sun could be detected with an error of 10°. The moment of sunset could be appointed only with about 45 min bias in the time of Equinox and about 90 min bias in the time of summer solstice.

To guess the moment of noon is even more dubious! Length of the noon shadow is the shortest, but it will hardly change while the sun seems to travel parallel with the horizon. On the day of summer solstice, the solar elevation varies less than 0.5° within 75 min around noon characterised by a practically constant shadow length, while the solar azimuth changes by 30°. This period is perfect for observing the shortest length of the shadow to estimate current latitude, but it is hardly possible to

appoint south without a reference for local solar time. Consequently, only a rough guess on the direction of south can be made.

25.7.2 The Viking Sun Compass

Based on a dial fragment artefact found under the ruins of an eleventh-century Benedictine convent in Uunartoq in Greenland (Figs. 25.2 and 25.5a), Vikings are thought to use hand-held sun compasses during the long Nordic days (Sølver 1953; Taylor et al. 1954; Thirslund 2001; Karlsen 2003). A sun compass is an inverted horizontal sundial: Instead of following the cast shadow of a central gnomon on a fixed dial, one rotates a levelled compass dial to fit its pre-drawn hyperbolic gnomonic line right under the tip of the shadow. In this position the major (mirror-symmetry) axis of the hyperbola aims at true north (Fig. 25.4b). The Uunartoq artefact is a half of a round dial wearing deliberately incised lines (Fig. 25.5a) that were interpreted as gnomonic lines valid on days of Equinox and summer solstice at the 61st latitude, which was the transatlantic Viking route between Norway and Greenland (Fig. 25.2).

Theoretically, sun compasses can provide true directions from sunrise to sunset. In practice, their operation period is limited by their dimensions to distinct sections of the day. In the case of solar navigation, a relevant source of error is disregarding the seasonal shift of the ecliptic in the sky. Gnomonic lines and azimuth angles of the setting and rising sun are valid only on given days of the year at given latitude. Luckily, deviations originating from using inappropriate curve in the forenoon and in the afternoon compensate each other (Thirslund 2001). On the other hand, a sun compass can be oriented only when the shadow tip falls on the dial; thus, it cannot be used when the sun is below a minimum solar elevation angle defined by the height of the gnomon and the radius of the dial. Even at the 61st latitude, the sun ascends to 52.4° above the horizon at noon on the day of the summer solstice; thus, a thin and high gnomon should be used that sets well-visible cast shadow at such high solar elevations. Around noon the shadow length hardly changes, while the solar azimuth changes quickly, so small sun compasses are quite unreliable in this period. Since instruments of the Vikings must have been small enough to be carried by the navigators, their hand-held sun compasses most probably were useless for hours at noon, before sunset and after sunrise.

A further serious hindrance of sun compasses is their sensitivity to the changing lighting conditions. Thin cloud layers, dust, smoke and atmospheric haze scatter or absorb direct sunlight. Shadows are poorly contrasted when the intensity of direct sunlight is comparable to or lower than that of scattered skylight. Under such circumstances, a Viking navigator could easily underestimate the shadow length and derive compass directions with significant errors. When the sun is occluded, cast shadows do not appear at all; thus, sun compasses cannot be used.

According to the interpretation of Thirslund (2001), the Uunartoq find is the dial of a hand-held sun compass that was used at the 61st latitude. A series of notches is

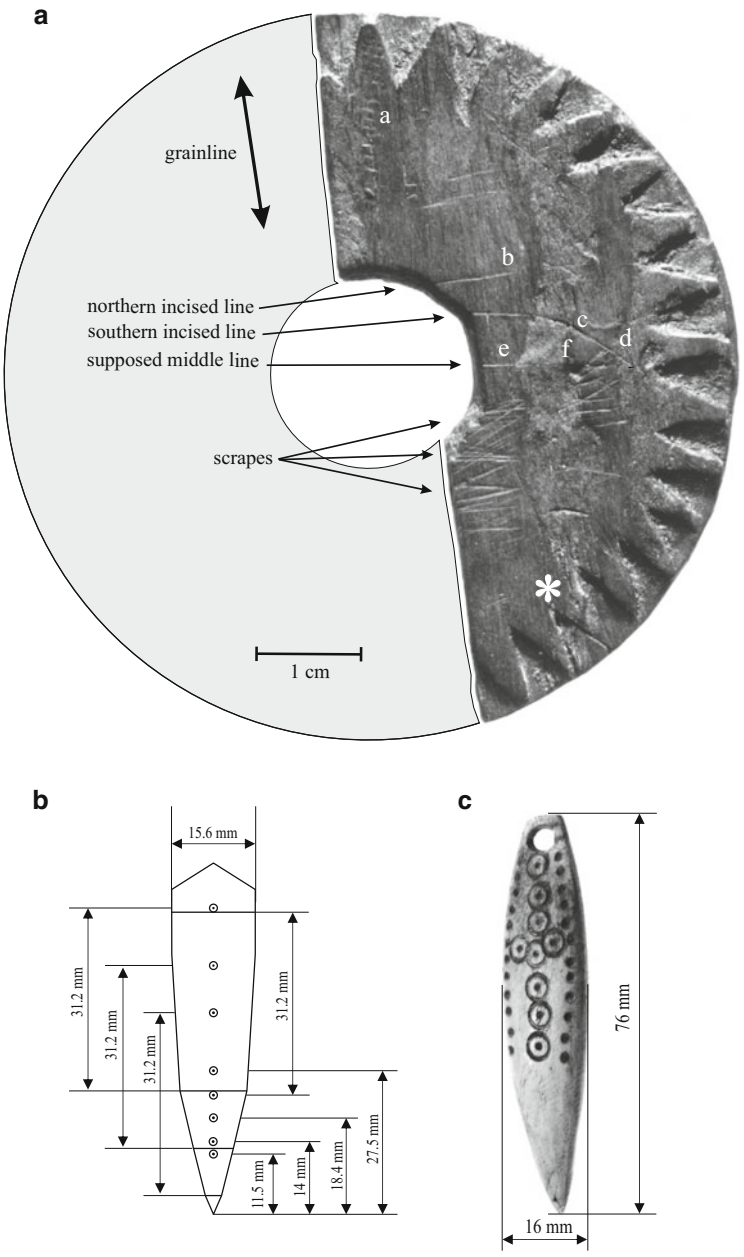

Fig. 25.5 (**a**) Photograph of the eleventh-century sundial artefact fragment found by C.L. Veabek in Uunartoq in Greenland in 1948. (The photograph was kindly provided by the Maritime Museum of Denmark.) The dial is shown in 2:1 scale and oriented according to the twilight board interpretation. Supposed outline of the missing part is symbolised by *grey shading*; *double-headed arrow* shows the grainline of the timber. Studiers during the twentieth century identified two deliberately incised lines that were interpreted as gnomonic lines (*b* and *c*). A series of 16 notches in the *upper segment* (*a*) was considered to be a loose marking of north, a depression about 81° from it (*d*) was taken as marking of east. One cog of the alleged irregular compass division was

the loose mark of the direction of north; a well-visible depression roughly marks the direction of east, while the straight incised line represents the equinoctial line that is the straight path of the shadow on the day of Equinox (Fig. 25.5a). The loose marking of cardinal directions was attributed to the erroneous division of the compass rose. The dial has a diameter of 70 mm and a large central hole with a diameter of 17 mm, probably a socket for a grip, beside which its incised gnomonic lines terminate. These assumptions demand a gnomon with a height of about 4.3 mm that would cast shadow on the dial only at solar elevations between 7° and 27°. It is not surprising that those who studied in more detail the Uunartoq dial hypothesised a lost central part with a pin-like gnomon and a complement of the gnomonic lines. Despite the above problems, sun compasses of sizes commensurable with that of the Uunartoq dial but wearing series of complete gnomonic lines were found to be remarkably efficient on board of small sailing ships under favourable weather conditions.

A shadow stick could have replaced the missing shadow and allowed orientation using a sun compass with satisfying accuracy in weather situations when shadows were not formed (Fig. 25.5b), but the sun position could reliably be estimated (Fig. 25.6) (Bernáth et al. 2013b). It is a small acute object provided with a series of sockets representing shadow length at chosen solar elevation angles. The appropriate socket should be fitted to the gnomon tip, and the narrower tapering end of the stick should aim at the antisolar meridian (Fig. 25.9b,c). Distances between the tips of the gnomon and the shadow could easily be calculated or found empirically. Since the sockets should not overlap, the smallest resolution of elevation angles is determined by the dimensions of the shadow stick and the diameter of the sockets.

Theoretically, sunstones could be used with a sun compass and a shadow stick practically under any weather condition, but this was questioned by sky-polarimetric measurements (Horváth et al. 2011) and was confuted by psychophysical experiments (e.g. Bernáth et al. 2013b). Calcite sunstones are quite efficient when clear patches of the sky are visible, but they are practically useless under overcast skies characterised with low degrees of polarisation (see Sect. 25.6). The navigators should perceive the weak contrast between the ordinary and extraordinary rays before the bright sky background. Since the human retinal cells are nonlinear receptors, distinguishable differences in light intensity depend on the eye adaptation. Unlike under steady laboratory lighting, in the field the eyes of the observers continuously adapt to the ever-changing intensity of the background skylight and

Fig. 25.5 (continued) corrected by the woodcarver (*asterisk*). Some markings in the *middle* and *lower segments* could be interpreted as *construction lines* added during a trigon-based geometrical construction while producing the compass. One intersection of these lines is even marked by the depression (*f*). (**b**) Characteristic sizes of the hypothesised shadow stick to be used with the Uunartoq artefact dial shown in 1:1 scale. (**c**) A Viking bone pendant of a *circular design* from Estonia, tenth to eleventh century AD shown in 1:1 scale (source: http://www.icollector.com). Its markings do not form a pattern coding evenly distributed elevation angles, but naive imitations of 'navigator pendants' and genuine shadow sticks are supposed to take similar form, shape, size and decorations [after Bernáth et al. (2014)]

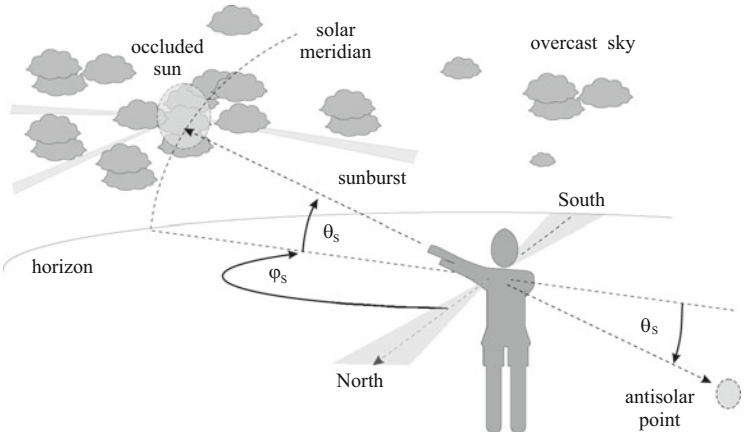

Fig. 25.6 Under clear skies the gnomon casts a clear sharp shadow on the horizontal dial of a levelled sun compass, but it cannot be seen when the sun is occluded. The navigator must estimate the elevation θ_S and azimuth angle φ_S of the sun. These data can be gained also by estimating the position of the anti-sun [after Bernáth et al. (2013b)]

not to the intensities of the spots seen in the sunstone. Consequently, the minimum contrast levels distinguishable for the observers are higher and change continuously. When the navigator rotates the sunstones to reach equal brightness of the ordinary and extraordinary rays, he marks out only an eligible angular range but not a specific direction. This causes a great error in estimating the direction of skylight polarisation. Under such conditions, the observers are greatly influenced by their sense of direction. The derived directions considered as north were found to have even greater dispersion than blind-guessed directions (Bernáth et al. 2013b); thus, sky polarimetry with sunstones under overcast skies should not be treated as a measurement, but rather as a sophisticated representation of the sense of directions (Fig. 25.7).

No genuine shadow sticks were identified by archaeologists until now. Such small items would badly conserve, and their true identity would be hard to recognise without a concept. But one can unquestionably rule whether a given wooden stick, a carved fang of a boar or a metal pendant could have been used as a shadow stick. Candidate objects should be straight and acute, 40–50 mm long, and should wear a series of sockets (Fig. 25.5b). Distances between the sockets and the tip should follow the ratios given by the function $f(\alpha, n) = 1/\sin(n \cdot \alpha/4)$, where n is a natural number and α is the angle seen subdued by the extended fist of the navigator (about 9–11°). Some genuine examples or naive imitations may easily lay in collections without recognising their true purpose and registered as pendants or clasps (Fig. 25.5c).

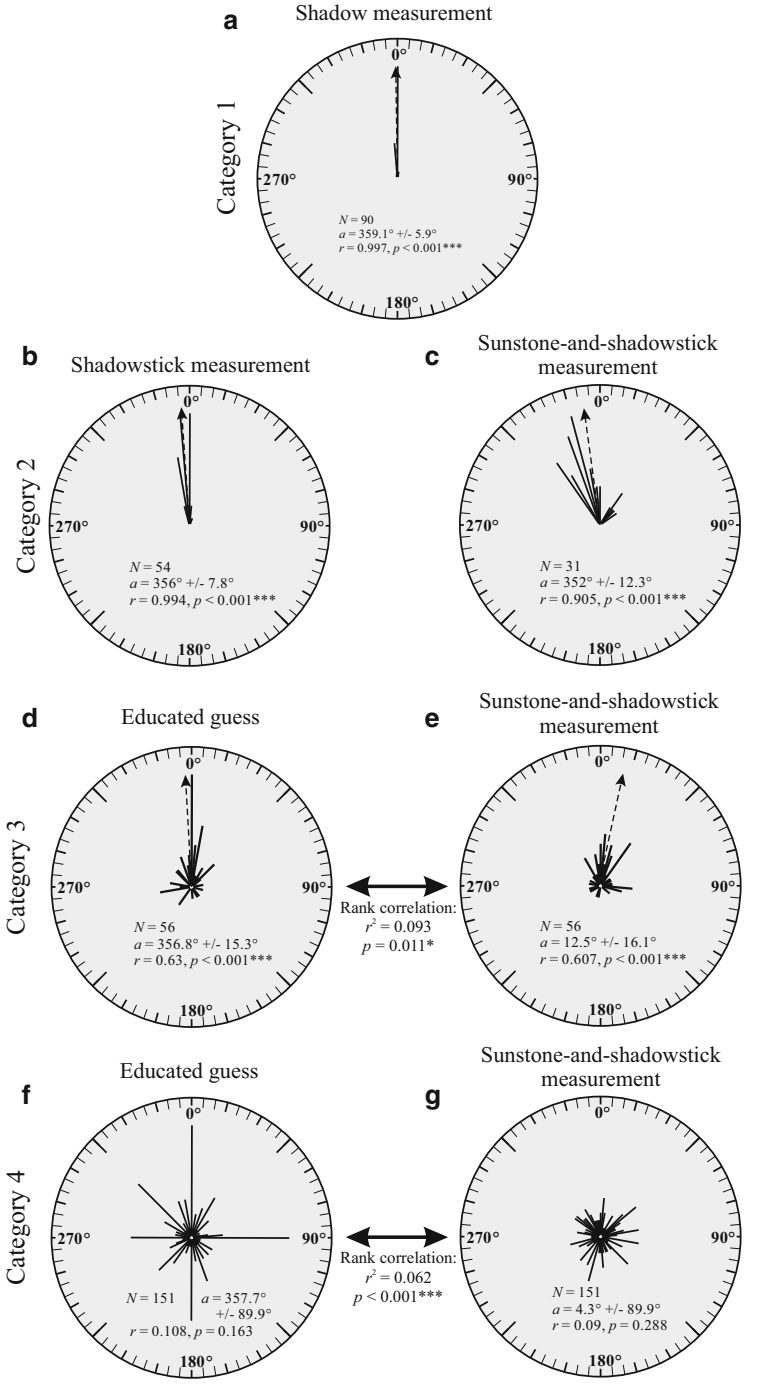

Fig. 25.7 Histograms of directional angles considered to be true north (0°) under clear skies (**a**, category 1), under partially overcast skies (**b**, **c**; category 2), under total but inhomogeneous overcast skies (**d**, **e**; category 3), and under totally overcast homogeneous skies (**f**, **g**; category 4)

25.7.3 The Twilight Board

Bernáth et al. (2013a, 2014) have thoroughly analysed the lines and scratches seen on high-resolution photographs of the Uunartoq artefact (Fig. 25.5a) and associated it with alternative functions. If the find was part of a sun compass, its dimensions are puzzling. Since the dial fragment lacks the central section, the shape and exact position of its gnomon can only be conjectured. The large central hole is unexpected, although central sections of the gnomonic lines on a small sun compass are quite useless, and one may choose to use this space for more practical functions. It is more puzzling that both gnomonic lines terminate well before the perimeter. In the case of a dedicated sun compass, a larger dial with complete gnomonic lines would be rational. The southern incised line resembles a hyperbola, but it does not fit to the real path of the shadow of a central gnomon on any date at the 61st latitude. Fair, but no good fit could be achieved about three weeks after Equinox. One may also note that the supposed marking of north does not point to 0°, but to 8.7°. Puzzling details may simply be flaws originating from the primitive production environment, and the fragment may even be a discarded shoddy piece, but some unaddressed details may be purposeful elements. The artefact can be reconstructed also as a twilight board, a combination of a horizon board and a sun compass that is ideal to be used in the matutinal and crepuscular periods (Bernáth et al. 2014).

The large central hole might have housed a broad and short conical gnomon optimised for using at low solar elevation angles (Fig. 25.8a). If the base of the gnomon is nearly or perfectly tangential to the asymptotes of the gnomonic lines, at low solar elevations the edge of the cast shadow of such a gnomon will lay on the asymptotes. Thus, the navigator could orient himself by aligning the straight edge of the metre-long shadow of the gnomon to the outmost visible point of the gnomonic line. Unlike the dials of sun compasses, the dial of a twilight board may be small and may wear only the inner section of the gnomonic line that significantly deviates from its asymptote. The broad gnomon unavoidably covers the central sections of gnomonic lines, but at intermediate solar elevation angles, the shadow tip falls on the compass dial and the instrument can function as a sun compass. It is worth to note that the asymptotes point towards the setting and rising sun, and they are marked out by the outmost point of the gnomonic line and the base

Fig. 25.7 (continued) using a sun compass, two calcite sunstones and a shadow stick. *Dashed arrows* mark the directions of the mean vectors. The number of individual orientations N, the direction of the mean vector with 95 % confidence limits, the length of the mean vector $\underline{\boldsymbol{r}}$ and the significance level p of the Rayleigh test for uniformity of distribution of the measured directions are given in the lower half of the dials. The distributions of direction considered as north are significantly directional under weather situations 1–3 (**a**–**e**), while they are uniform under weather situation 4 (**f**, **g**). The test values r^2 and significance levels p of circular rank correlation tests mark significant correlations between directional angles identified as true north by the operator using the sunstone and the shadow stick (**e**, **g**) and between their unaided guesses (**d**, **f**) [after Bernáth et al. (2013b)]

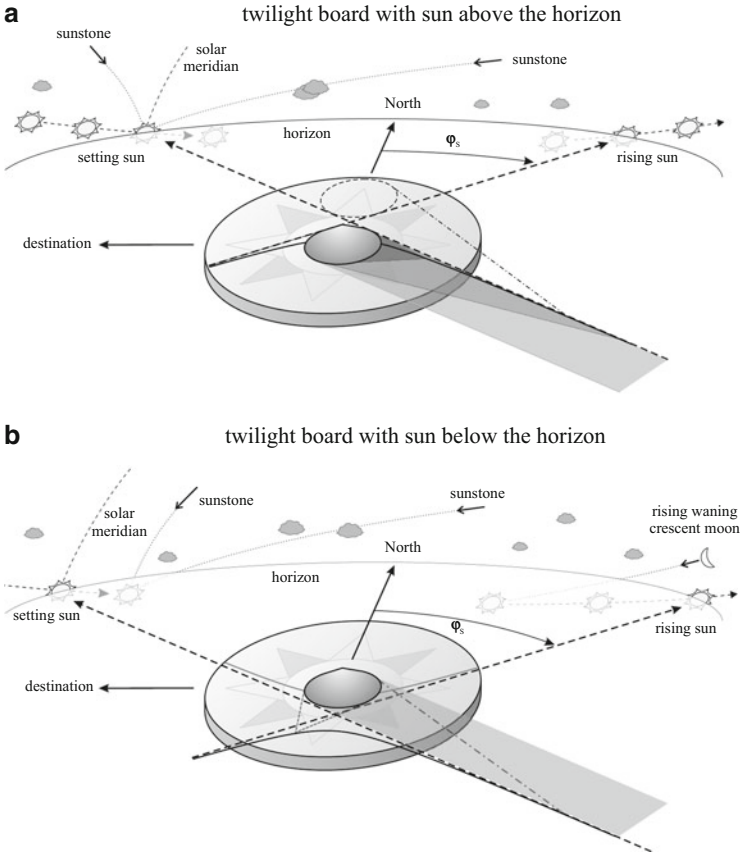

Fig. 25.8 (**a**) A twilight board is the combination of a horizon board and a sun compass wearing a short conical gnomon and a matching gnomonic line (*thick solid line*); the base of the gnomon is tangential to the asymptotes (*dashed arrows*) of the gnomonic line. At low solar elevation angles Θ_s, the edge of the shadow lies on an asymptote of the gnomonic line. The navigator can derive true directions by fitting the edge of the shadow to the outer section of the gnomonic line. The 'cast' shadow (*dash-dot line*) of an imaginary down-pointing gnomon (*dashed circle*) when 'illuminated' by the set sun from below the horizon would act likewise. (**b**) If the pair of appropriate gnomonic lines is marked in the twilight board, it can be turned by 180 degrees and used after sunset and before sunrise with a shadow stick. Position of the sun under the horizon must be estimated on the basis of atmospheric optical phenomena or the moon crescent or by using sunstones [after Bernáth et al. (2014)]

of the gnomon. Thus, this instrument can double as a horizon board (Fig. 25.4a). Astronomical records and historical documents underpinning the possible use of the horizon board fit to the twilight board as well (Karlsen 2003). Neither instrument is affected by atmospheric refraction, which increases the perceived elevation of celestial bodies close to the horizon by about 0.5°. Atmospheric refraction should

be regarded in modern navigation, but it only slightly affects the width of the gnomon shadow and causes a negligible error.

No existing circle is tangential to asymptotes of all gnomonic lines valid on different days, but an optimal base diameter of the conical gnomon could be calculated for any combination of dates and latitudes. Applying a single gnomon with a given base diameter results in a navigation error that changes during the year and may limit the period in which that gnomon could be effectively used. On the 61st latitude, the traditional Viking sailing route between Norway and Greenland, a single gnomon could serve from 24 February until 15 April (Bernáth et al. 2014). At southern latitudes the operation season is significantly longer: at the 46th latitude, the supposed position of Vinland (Fig. 25.2), a single gnomon could be used for more than 2 months. However, in the Mediterranean region rapid sunsets and short civil twilight would constrain the usability of a twilight board to those of simple horizon boards.

Skylight polarisation patterns tend to be the most appropriate for sky-polarimetric Viking navigation during the matutinal and crepuscular periods, the ones for which the twilight board is optimised. It can effectively be used with sunstones and an appropriate shadow stick when the sun is low above the horizon and is obscured by distant clouds or fogbanks, but the sky is clear around the zenith (Bernáth et al. 2014). The twilight board requires a special shadow stick that codes also the width of the shadow at the edge of the compass dial (Fig. 25.5b). Distances between the stick tip and the sockets corresponding to low solar elevations may be arbitrarily chosen, because the shadow tip would fall off the dial anyway. However, the width of the stick at a distance from the socket equalling with that between the gnomon tip and the dial edge must be the same as the shadow width at this point. Since at zero solar elevation the shadow tip lies in infinity, corresponding width of the shadow stick equals with the base diameter of the gnomon. These requirements and practical arrangement of the sockets dictate a characteristic arrowhead shape for the shadow stick (Fig. 25.5b).

Although the underlying geometrical principles may seem to be very complicated, observing the shadow of various gnomons can easily inspire the idea of a twilight board. Its great advantage to the horizon board is its extended periods of daily operation. Serial reading is possible by utilising the shadow edge that shows the azimuth of the setting or rising sun for a long period in spite of the continuously changing actual solar azimuth angle. This allows navigators to read accurate bearings of the setting or rising sun during a longer period, not only in a few moments, and reduce bearing errors by averaging the frequent readings. Under heavily overcast skies, accuracy would significantly decrease, but the instrument could be efficiently used together with sunstones, when clear patches around the zenith are visible (Barta et al. 2005; Hegedüs et al. 2007a, b).

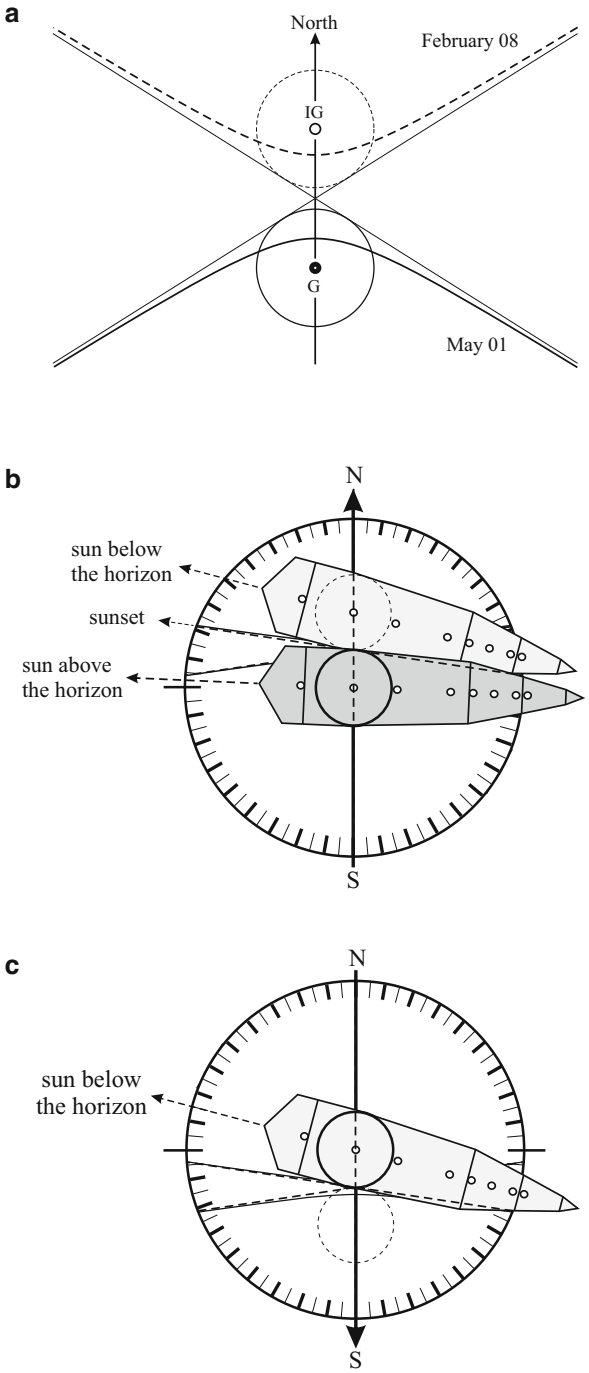

Fig. 25.9 (**a**) Geometrical arrangements of gnomons, gnomonic lines and their asymptotes. In summer in the northern hemisphere, the shadow of a conical gnomon (*solid circle*) follows the southern branch of a hyperbola (*thick solid line*) with the gnomon in its focus G. The shadow of the

25.7.4 A Possible Medieval Twilight Navigation Toolkit

For symmetry reasons, a kit composed of a twilight board, a shadow stick and two sunstones could be adopted for using during the twilight period, when the sun is below the horizon, forming a true twilight compass (Figs. 25.8b and 25.9). This hypothetical toolkit is a true functional analogue of the twentieth-century twilight compasses, and the artefact compass dial found in Uunartoq could have been used in this role as it is. On the other hand, developing this navigation method requires abstraction and significant knowledge on geometry, on the apparent movement of the sun and on atmospheric optics that may raise doubts about its medieval use (Bernáth et al. 2014). However, one should never underestimate the power of thorough observation, experience and expert instructions.

The shadow of the conical central gnomon, which is positioned in the southern focal point of the hyperbolic gnomonic line, will disappear from the twilight board in the moment of sunset. But one may imagine that from this moment, an imaginary conical gnomon pointing downward in the northern focal point of the gnomonic line is 'illuminated' by the already set sun from below the horizon and casts an imaginary shadow on the underside of the dial. The tip of this imaginary shadow would follow the gnomonic line that was used with the real shadow (Fig. 25.8a). Thus, when the sun is just a few degrees below the horizon, also the edge of this imaginary shadow lays on the asymptote of the real gnomonic line. One may intend to use the shadow stick for visualising the imaginary shadow on the upper surface of the dial (Fig. 25.9b). To find the appropriate socket on the shadow stick, one should take the absolute value of the now negative solar elevation angle. The socket corresponding to this value should be fitted to the centre of the imaginary gnomon

Fig. 25.9 (continued) same gnomon would approximate the northern branch (*thick dashed line*) with IG in its other focus on the day when the azimuth of the setting sun is 180° away from that of the rising sun on the given summer day. Corresponding dates can be found by the span between Equinox and them. For symmetry reasons, the 'cast shadow' (*dash-dot line*) of an imaginary down-pointing gnomon (*dashed circle*) placed in IG and 'illuminated' by the set sun would approximate that of the real shadow of the real gnomon. If the base of the conical gnomon is tangential to the asymptote, one edge of the real and imaginary shadows will lay on the same asymptote in the periods around sunset and sunrise. (**b**) At low positive and negative solar elevation angles, when the shadow is not visible but the sun position can be estimated, the appropriate socket of the stick is fitted to the tip of the central gnomon (shown in *dark shade*). After sunset the shadow stick could represent the shadow of an imaginary gnomon 'illuminated' from below the horizon (shown in *light shade*). The side point of the stick representing the edge of the shadow at the given solar elevation should be fitted to the asymptote; the matching socket should be fitted to the centre of the imaginary gnomon, and the dial should be rotated until the stick points towards the solar meridian. (**c**) When the sun is below the horizon, it is an easier way of navigating with the twilight compass to turn it by 180°. Now the real gnomon plays the role of the imaginary one, only it still points upward. The shadow stick can be used to represent the imaginary shadow below the compass dial. The northern incised line represents the imaginary gnomonic line. The kit functions as an efficient twilight compass as long as the azimuth and elevation angle of the set sun can reliably be estimated [after Bernáth et al. (2014)]

positioned along the north-south line, while the edge point of the stick representing the matching width of the shadow should be aligned with the asymptote. This is possible only if the place of the second gnomon is previously marked on the compass; otherwise, the appropriate position of the shadow stick is ambiguous. Since the place of the imaginary gnomon shifts day by day, the task is hardly achievable.

Luckily, one can take further advantage of symmetry and utilise the northern branch of the above-mentioned hyperbola (Fig. 25.9a). This branch may be drawn even without a sophisticated geometrical construction: it is simply the path of the shadow tip on the day when the sun is seen to set 180° away from the rising sun of the date of the southern gnomonic line. Positions of the shadow tip may easily be marked on the corresponding days to gain the northern and southern branches of the hyperbola. Such pairs of days can be appointed by counting matching numbers of days ahead and back from the day of Equinox and can be verified with the aid of the attir system. If both branches are marked on the compass, it should simply be rotated by 180° when the sun is below the horizon (Figs. 25.8b and 25.9c). Now the real and imaginary gnomons switch places, and the northern branch of the hyperbola will move to the right position and may be used with the shadow stick. A pair of sunstones could be used for estimating the solar azimuth and elevation by performing skylight polarimetry. Like the tip of the real shadow during the day, also the tip of the imaginary shadow deviates from the asymptote as the sun moves deep below the horizon and follows a path nearly identical with that of the real shadow of the real gnomon. It is worth to note that the sun may be followed below the horizon without the aid of sunstones, because several atmospheric optical phenomena and even the crescent moon provides clues (see Sect. 25.8). Thus, the twilight compass could have been developed independent of the sunstones, and it could have even been a motivation to develop sky-polarimetric navigation.

The Uunartoq compass dial can be interpreted as a twilight board used as a twilight compass. The series of notches in its northern part should be considered to precisely mark true north, while the equinoctial line should be considered unmarked. This means that the northern incised line deviates from the equinoctial line at about 8.7° and approximates the gnomonic line valid on 10 March. Gnomonic lines valid on the last days of March fit to the southern line. According to the twilight compass concept, it should represent 30 March, and indeed, the gnomonic line calculated for this day fits well to the southern incised line on the artefact dial. The asymptotes of these gnomonic lines are nearly tangential to a gnomon with a base diameter of 15.7 mm fitting into the large central hole of the artefact (Bernáth et al. 2014).

Bernáth et al. (2014) tested the reconstructed medieval twilight compass in the field, and they proved that it is functional even during civil twilight, when the sun is below the horizon, but not lower than −8° (Fig. 25.10). Its accuracy is comparable to that of modern pocket-size magnetic compasses or sighting the Pole Star during the Viking age. During the twilight period, the intensity of skylight is high enough and its polarisation characteristics can be analysed using birefringent or dichroic crystals. When the sun is lower than −6° below the horizon, nautical twilight begins.

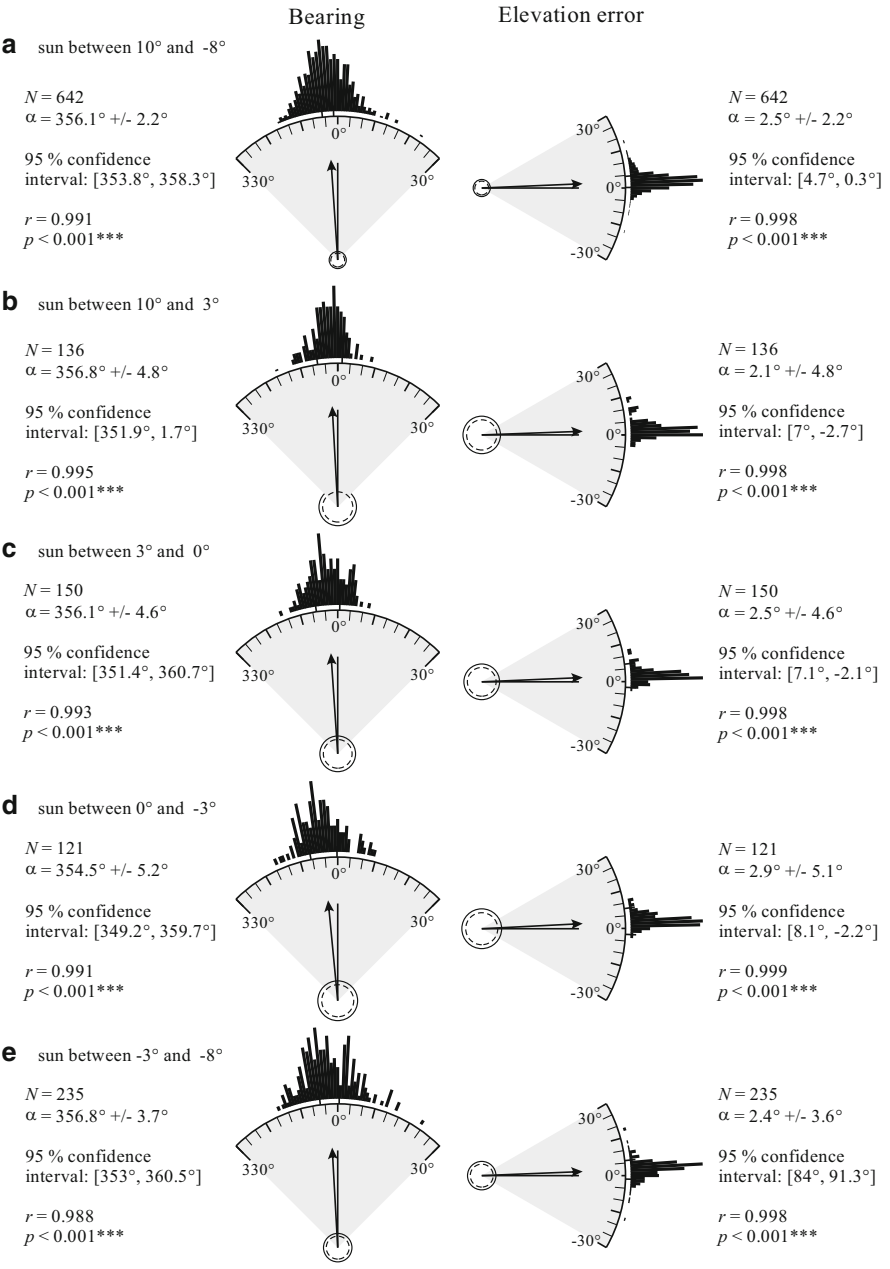

Fig. 25.10 Histograms of bearings considered to be true north and error of solar elevation angles estimated by six test persons equipped with a twilight compass kit consisting of a twilight board, a shadow stick and two calcite sunstones in Budapest (47° 28′ N, 19° 4′ E) in clear weather during the autumnal equinoctial period. The 642 trials (**a**) were performed at solar elevation angles between 10° and −8°. Sky polarimetry gets more difficult with the darker zenith region. Accuracy in periods before sunset or after sunrise with the sun above the horizon (**b**, **c**) should be compared with that during periods after sunset or before sunrise with the sun below the horizon (**d**, **e**). The

Then, the sky is dark enough to take reliable sightings of well-known stars and use the still visible horizon for reference until the sun is not lower below the horizon than −12°. Then, stars can be taken as directional and latitude reference until civil dawn, when the twilight compass can be used again. Civil twilight lasts long in the Arctic countries in the summer, rendering twilight compasses most valuable.

The twilight board (or twilight compass set) is the most viable medieval instrument that could be used with sunstones and would reliably provide significant plus information to the navigator under weather conditions when the sunstone is usable. It is in coherence with the existing few archaeological evidences as well. Its possible role and constrains are strikingly similar to that of modern sky-polarimetric navigation instruments developed during the twentieth century. The modern and the medieval twilight compass could be independent solutions for the same navigational problem. However, the actual use of the latter in the Viking age is far from proven.

25.7.5 An Alternative Navigation Method: A Sun-Shadow Board with a Sundial

It is worth to mention that scrapes on the Uunartoq find allow it to be interpreted also as a sophisticated marine sundial produced by geometrical construction and used to appoint local solar noon and read the noon shadow length to derive current latitude (Bernáth et al. 2013a). Sunstones do not play any role in this interpretation, which outlines a most practical nautical instrument that has functional counterparts in the medieval era: Arabian sailors regularly checked the elevation angle of circumpolar stars with the kamal, and late-medieval Europeans measured the noon solar elevation angle with cross-staffs and backstaffs to sail along chosen latitudes (Mörzer-Bruyns 1994). Arrangement of the scrapes indicated (Bernáth et al. 2013a) that the Uunartoq instrument probably was intended to be used around the latitude 63.43° N, the southernmost tip of Iceland, and could serve well in the whole region roamed by sailors from Iceland and Greenland (Fig. 25.2).

However, the design of such a combined sun compass and sun-shadow board surmises advanced knowledge on astronomy and geometry, as does developing the twilight compass kit described above. While gnomonics and astronomy were assets of ancient European civilisations, they are thought to be unavailable in North Europe

Fig. 25.10 (continued) numbers of individual trials *N*, the direction of the mean vector $\underline{\boldsymbol{a}}$, width of the 95 % confidence interval, value of the Rayleigh *r* statistics and its level of significance *p* are given. *Straight lines* mark the expected direction, and *arrows* mark the found direction and length of the average vectors. *Solid circles* mark the length of average vectors required for 1 % significance of Rayleigh statistics. Likewise, *dashed circles* mark the length of average vectors required for 5 % significance of Rayleigh statistics. Positive deviation marks overestimation of the solar elevation angle [after Bernáth et al. (2014)]

in the tenth century. On the other hand, unexpected occurrences of advanced technologies in contemporary Nordic localities mark that mercantile connections with southern cultures could provide Norse people with developed instruments and significant practical knowledge (Schmidt et al. 1999). Still little is known about how advanced navigation instruments Vikings could produce and would they have needed sunstones to extend their operation period or not. Future archaeological excavations should produce further fragments of dials or instruments to decide how solar navigation was performed in the Viking age.

25.7.6 A Millennium-Old Carved Schedule

Atmospheric optical and astronomical considerations render navigation with sunstones to be viable, but also the contemporary climate and economy should be regarded when one judges the plausibility of sky-polarimetric Viking navigation. While solar navigation instruments are constrained by gnomonic lines that are valid only at given latitudes and on given dates, such lines provide information on the season of intended operation. All interpretations of the Uunartoq artefact dial dictate that it was used in the equinoctial period. Should the northern incised line be either the equinoctial line as suggested by Thirslund (2001) or the gnomonic line used solely during the twilight period (Bernáth et al. 2014), it could serve navigation at the end of March as latest. Markings referring to dates months away from the start of the nautical season would have been pointless.

If one accepts that the Uunartoq find was a twilight board used with sunstones and a shadow stick at the 61st latitude, then one also accepts a schedule. The gnomonic line of 10 March is unambiguously marked out by the asymptotes of the northern gnomonic line, while the southern one must be valid on 30 March. Since the lines can swap the role before and after Equinox, this interpretation links outbound sail to 10 March and inbound sail to 30 March. Considering the cruising speed of replica Viking ships, crossing the North Atlantic Ocean with a good wind could take about 2–3 weeks. A departure on the first day of March would predict landing in Greenland around the day of Equinox, marked by the feast of Eostre, the ancient Nordic feast of spring. Repairs and trading could take several days, but the ship could be ready to leave by the end of March. The twilight compass is accurate only until the middle of April at the 61st latitude, but it allows a safe return by the end of March. The artefact dial is equally functional during the autumn equinoctial period defining the dates of 1 and 30 September, when sea ice is the least expansive.

A North Atlantic crossing in September is less justified by mercantile considerations; an early spring crossing could augur much better if climatic conditions allowed it in the tenth century. In springtime the Greenland colony was hungry for fresh supplies of metal wares, timber and textiles and was ready to pay in hides, skin ropes and walrus ivory. These commodities were highly appreciated luxuries throughout northern Europe, but every day of the navigation season might be needed to deliver them and take the profit home before winter froze lines of

communication. Since the arrival of Equinox is easy to perceive from any continents, commodities could wait embarkation at prominent farms.

Altogether, the theory of sky-polarimetric Viking navigation is plausible, but many pieces of this puzzle are missing. It is possible to define a functional and reliable twilight navigation method that applies sunstones for polarimetry, could be performed with the existing archaeological artefacts, provides excess information to navigators, is usable in seasons when an Atlantic crossing is economically viable and does not contradict today accepted climatic models. But still it remains only a theory that can be either justified or confuted by future evidences.

25.8 Atmospheric Optical Phenomena Providing Alternative Navigation Cues

How and why could Norse people discover the use of sunstones is a mystery for us, as is the origin of several impressive ancient inventions. In our time more than 80 % of the human population lives in densely populated closed cities. When travelling great distances, we are accustomed to follow road signs, to use maps, to rely on sophisticated navigation instruments and to ask for direction. Medieval people moved much more confidently in nature, and they knew and surely utilised several signs that are seldom even sighted by the modern city-dwelling population (Lewis 1972). There are several atmospheric optical phenomena also in the Arctic territories that offer reliable navigation cues, which could be used beside sun compasses and sunstones.

The atmospheric conditions of polar marine regions are prosperous for the formation of upper mirages, which extend the visual range far over the horizon. Coastal mountains, rocks or trees or even whole islands can float in the air when the light rays pass through layers of different temperatures and densities. The temperature inversion causes light to bend downward to the colder, denser layers; it produces an abnormal visual effect, which bears no resemblance to real things. Upper mirages occur frequently during the sailing seasons, although one must also consider that temperature inversion and helpful mirages probably formed less frequently over the warmer seawater during the Medieval Warm Epoch. Viking navigators probably had ample opportunity to see distorted or dislocated land images. These observations might provide views from beyond the normal horizon and help their westward expansion across the North Atlantic. They could easily correlate this effect with subsequent land sightings and legends about charmed islands (Sawatzky and Lehn 1976; Lehn and Schroeder 1979). But the polar upper mirage often occurs only as an unrecognisable narrow horizontal band in or near the horizon, so it can help to discover a new land, but can be misleading during scheduled voyages.

Sunstones may seem to be the only tool to locate the sun under the horizon, but nature offers alternatives. Fanlike crepuscular or anti-crepuscular rays are

sometimes visible in the twilight sky when remote high mountains or clouds cast their shadows on the air. The aerial dust particles, aerosols or small water droplets themselves scatter the sunlight and make the rays visible. These rays radiate from the imaginary point below the horizon where the sun is, and the rays converge towards the anti-sun on the opposite side of the sky (Lynch and Livingston 2010). These phenomena indicate the position of the sun during twilight, so they may also have helped Viking navigators when the sun had been below the horizon, but the brightest stars were not yet visible. For instance, the Icelandic volcanoes could provide enough aerosols which led to formation of crepuscular rays.

A very similar phenomenon can frequently be seen under overcast skies during the day, when direct sunlight shines through holes between the clouds and forms sunbursts in the less illuminated air below the clouds. These rays also converge towards the occluded sun and may be seen from great distances. Viking navigators could use such sunbursts like crepuscular rays to locate the occluded sun and estimate its azimuth and elevation angles (Fig. 25.6). The appropriate position of the sun above the clouds may be estimated also on the basis of the intensity pattern of the clouds, but this pattern is greatly influenced by the thickness of the cloud layers and is therefore quite misleading (Barta et al. 2005).

The disc of the moon is a further cue that tends to be visible even when prominent stars and constellations are obscured by clouds and haze. Mariners regard the moon for ages to forecast ebb and flood, but its path in the sky is most complicated, and building a reliable lunar compass is troublesome. However, the waning and waxing moon crescent acts like a celestial arrowhead: it unambiguously codes the direction and angular distance of the sun disc with respect to the moon disc. This simple relationship could easily be observed in daytime before and after new moon and allows the observer to reliably estimate the position of the sun even far below the horizon during the long moonlit Arctic nights.

Some specialists argue that even the polarisation pattern of the clear sky can be perceived with unaided eyes utilising Haidinger's brush (see Sect. 14.1) (Ropars et al. 2012). This entoptic phenomenon of human eyes forms an orthogonal blue and yellow double 8-shaped pattern when one glimpses on a linearly polarised light source. Indeed, most people see this phenomenon and can be trained to observe its form while looking at the zenith at sunset or sunrise, but it could hardly be used for reliably estimating the position of the sun.

These atmospheric optical phenomena may seem to reduce the value of sunstones and render their use to be unsubstantiated, but in fact they could have facilitated the development of this unique sky-polarimetric navigation method. Since the Norse seafarers must have been familiar with their natural environment, the main advantage of any navigation instrument could not be its exclusiveness, but being much more reliably available than occasional natural phenomena. Expanding the use of sun compasses must have been a natural desire at latest when long-range sailing gained a central role in the Norse society. Knowledge of natural signs showing the occluded sun above or below the horizon must build up and primitive techniques of utilising this information unquestionably were developed. Such knowledge and the rise of marine activity in the Nordic seas could form a drive

to search for new technical solutions of locating the occluded sun, as it happened also in the middle of the twentieth century. Using birefringent or dichroic crystals (sunstones) could have been a sound solution. However, archaeological evidences should justify their actual use.

References

Arneborg J (2000) Greenland and Europe. In: Fitzhugh WF, Ward E (eds) Vikings: the North Atlantic Saga. Smithsonian Books, Washington, pp 304–317

Barta A, Horváth G, Meyer-Rochow VB (2005) Psychophysical study of the visual sun location in pictures of cloudy and twilight skies inspired by Viking navigation. J Opt Soc Am A 22: 1023–1034

Bernáth B, Blahó M, Egri Á, Barta A, Horváth G (2013a) An alternative interpretation of the Viking sundial artefact: an instrument to determine latitude and local noon. Proc R Soc A 469 (2154): Article no. 20130021. doi:10.1098/rspa.2013.0021

Bernáth B, Blahó M, Egri Á, Barta A, Kriska G, Horváth G (2013b) Orientation with a Viking sun-compass, a shadow-stick, and two calcite sunstones under various weather conditions. Appl Opt 52:6185–6194

Bernáth B, Farkas A, Száz D, Blahó M, Egri Á, Barta A, Akesson S, Horváth G (2014) How the Viking sun-compass could be used with sunstones before and after sunset? Twilight board as a new interpretation of the Uunartoq artefact fragment. Proc R Soc A 470:20130787. doi:10.1098/rspa.2013.0787

Bound M, Monaghan J (2001) A ship cast away about Alderney: investigations of an Elizabethan shipwreck. Alderney Maritime Trust, Alderney

Bradley RS, Hughes MK, Diaz HF (2003) Climate in medieval time. Science 302:404–405

Brines ML, Gould JL (1982) Skylight polarization patterns and animal orientation. J Exp Biol 96: 69–91

Coulson KL (1988) Polarization and intensity of light in the atmosphere. A. Deepak Publishing, Hampton, VA

Grove JM (2001) The initiation of the "little ice age" in regions round the North Atlantic. Clim Chang 48:53–82

Hegedüs R, Åkesson S, Wehner R, Horváth G (2007a) Could Vikings have navigated under foggy and cloudy conditions by skylight polarization? On the atmospheric optical prerequisites of polarimetric Viking navigation under foggy and cloudy skies. Proc R Soc A 463:1081–1095

Hegedüs R, Åkesson S, Horváth G (2007b) Polarization patterns of thick clouds: overcast skies have distribution of the angle of polarization similar to that of clear skies. J Opt Soc Am A 24: 2347–2356

Horváth G, Varjú D (2004) Polarized light in animal vision—polarization patterns in nature. Springer, Heidelberg

Horváth G, Bernáth B, Barta A, Suhai B, Wehner R (2002) First observation of the fourth neutral point in the atmosphere. J Opt Soc Am A 19:2085–2099

Horváth G, Barta A, Pomozi I, Suhai B, Hegedüs R, Åkesson S, Meyer-Rochow B, Wehner R (2011) On the trail of Vikings with polarized skylight: experimental study of the atmospheric optical prerequisites allowing polarimetric navigation by Viking seafarers. Philos Trans R Soc B 366:772–782

Hubel DH (1988) Eye, brain, and vision. WH Freeman, New York, NY

Hughes MK, Diaz HF (1994) Was there a 'medieval warm period', and if so, where and when? Clim Chang 26:109–142

Karlsen LK (2003) Secrets of the Viking navigators. One Earth Press, Seattle

Kollsman Instruments (1960) Installation, operation and service instructions: polarized sky light compass Type No. 2029B-01. Kollsman Instrument Corporation, New York
Können GP (1985) Polarized light in nature. Cambridge University Press, Cambridge
Lamb HH (1965) The early medieval warm epoch and its sequel. Palaeogeogr Palaeoclimatol Palaeoecol 1:13–37
Larson LM (1917) The King's Mirror (Speculum Regale-Konungs Skuggsjá). Translated from the Old Norse with introduction and notes by Laurence Marcellus Larson. Twayne Publishers, Inc., The American-Scandinavian Foundation, New York
Le Floch A, Ropars G, Lucas J, Wright S, Davenport T, Corfield M, Harrisson M (2013) The sixteenth century Alderney crystal: a calcite as an efficient reference optical compass? Proc R Soc A 469:2153
Lehn WH, Schroeder II (1979) Polar mirages as aids to norse navigation. Polarforschung 49: 173–187
Lewis D (1972) We, the navigators. University Hawaii Press, Honolulu
Lynch DK, Livingston W (2010) Color and light in nature. Thule Scientific, Topanga, CA
Miller GH, Brigham-Grette J, Alley RB, Anderson L, Bauch HA, Douglas MSV, Edwards ME, Elias SA, Finnei BP, Fitzpatrick JJ, Funder SV, Herbert TD, Hinzman LD, Kaufman DS, MacDonald GM, Polyak L, Robock A, Serreze MC, Smol JP, Spielhagen R, White JWC, Wolfe AP, Wolff EW (2010) Temperature and precipitation history of the Arctic. Quat Sci Rev 29:1679–1715
Mörzer-Bruyns WFJ (1994) The cross-staff: history and development of a navigational instrument. Vereeniging Nederlandsch Historisch Scheepvaart Museum, Amsterdam
Ogilvie AEJ, Barlow LK, Jennings AE (2000) North Atlantic climate c. ad. 1000: millennial reflections on the Viking discoveries of Iceland, Greenland and North America. Weather 55:34–45
Ogilvie AEJ, Woollett JM, Smiarowski K, Arneborg J, Troelstra S, Kuijpers A, Pálsdóttir A, McGovern TH (2009) Seals and sea ice in medieval Greenland. J N Atl 2:60–80
Pedersen ES (1955) Polar airline navigation. Navigation 4:270–274
Pomozi I, Horváth G, Wehner R (2001) How the clear-sky angle of polarization pattern continues underneath clouds: full-sky measurements and implications for animal orientation. J Exp Biol 204:2933–2942
Pringle H (2012) Vikings and native Americans. National Geographic online http://news.nationalgeographic.com/news/2012/10/121019-viking-outpost-second-new-canada-science-sutherland/
Ramskou T (1969) Solstenen. Skalk 2:16–17
Ribeiro S, Moros S, Ellegaard M, Kuijpers A (2012) Climate variability in West Greenland during the past 1500 years: evidence from a high-resolution marine palynological record from Disko Bay. Boreas 41(1):68–83. doi:10.1111/j.1502-3885.2011.00216.x
Ropars G, Gorre G, Le Floch A, Enoch J, Lakshminarayanan V (2012) A depolarizer as a possible precise sunstone for Viking navigation by polarized skylight. Proc R Soc A 468:671–684
Roslund C (1989) Sun tables of Star-Oddi in the Icelandic sagas. In: Aveni AF (ed) World archeoastronomy. Cambridge University Press, Cambridge, p 498
Roslund C, Beckman C (1994) Disputing Viking navigation by polarized skylight. Appl Opt 33: 4754–4755
Sawatzky HL, Lehn WH (1976) The Arctic mirage and the early North Atlantic. Science 192: 1300–1305
Schmidt O, Wilms KH, Lingelbach B (1999) The Visby lenses. Optom Vis Sci 76:624–630
Severin T (1978) The Brendan voyage. Hutchinson and Co. (Publishers) Ltd, London
Sølver CV (1953) The discovery of an early bearing-dial. J Navig 6(3):294–296
Suhai B, Horváth G (2004) How well does the Rayleigh model describe the E-vector distribution of skylight in clear and cloudy conditions? A full-sky polarimetric study. J Opt Soc Am A 21:1669–1676
Taylor EG, May WE, Motzo RB, Letherbridge TC (1954) A norse bearing-dial? J Navig 7:78–84

Thirslund S (1997) Sailing directions of the North Atlantic Viking age (from about the year 860 to 1400). J Navig 50:55–64

Thirslund S (2001) Viking navigation: sun-compass guided Norsemen first to America. Gullanders Bogtrykkeri a-s, Skjern, Humlebaek, Denmark

Vilhjalmsson T (1997) Time and travel in the old norse society. In: Poster C, Utz R (eds) Disputatio. An international transdisciplinary journal of the late middle ages, vol 2, Constructions of time in the late middle ages. Northwestern University Press, Evanston, IL, pp 89–114

von Frisch K (1949) Die Polarisation des Himmelslichtes als orientierender Faktor bei den Tänzen der Bienen. Experientia 5:142–148

Index

G. Horváth (ed.), *Polarized Light and Polarization Vision in Animal Sciences*, Springer Series in Vision Research 2, DOI 10.1007/978-3-642-54718-8,